DTIC File Copy

Proceedings of the
Thirty-Eighth

IWCS

AD-A216 023

INTERNATIONAL WIRE AND CABLE SYMPOSIUM

November 14 thru 16, 1989

DTIC
ELECTE
DEC 12 1989
S D
B

DISTRIBUTION STATEMENT A
Approved for public release;
Distribution Unlimited

SPONSORED BY
US ARMY COMMUNICATIONS—
ELECTRONICS COMMAND (CECOM)
FORT MONMOUTH, NEW JERSEY

PROCEEDINGS OF 38TH INTERNATIONAL WIRE AND CABLE SYMPOSIUM

Sponsored by
US Army Communications-Electronics Command
(CECOM)
Fort Monmouth, New Jersey

HYATT REGENCY HOTEL
ATLANTA, GEORGIA
NOVEMBER 14, 15 and 16, 1989

APPROVED FOR PUBLIC RELEASE: DISTRIBUTION UNLIMITED

89 12 11 045

38TH INTERNATIONAL WIRE AND CABLE SYMPOSIUM

SYMPOSIUM COMMITTEE

Elmer F. Godwin, *Director*
GEF Associates
3A Buttonwood Drive
Shrewsbury, NJ 07702
(201) 741-8864 (Home)
(201) 544-4615 (Office)

Dr. C. Ronald Simpkins, *Chairman*
E. I. DuPont de Nemours & Co., Inc.
Little Falls Centre 1
P.O. Box 80810
Wilmington, DE 19880-0810
(302) 996-8564

Dr. Ken-ichi Aihara
NTT America, Inc.
One Landmark Square Rm 700
Stamford, CT 06701
(203) 967-9379

Dr. Peter R. Bark
Siecor Corporation
P.O. Box 489
489 Siecor Park
Hickory, NC 28603
(704) 323-6205

David Fallowfield
Alberta Government Telephone
EDTNABCS (17)
17th Flr [illegible]065 Jaspe[illegible]
Edmon[illegible]berta T5J-3D1
Canada
(403) 42[illegible]

Dr. Reiner J. Gerdes
Contel Laboratories
270 Scientific Drive Suite 10
Technology Park/Atlanta
Norcross, GA 30092
(404) 448-2206

Patrick Hart
Pacific Bell
2600 Camino Ramon
Room 3S850
San Ramon, CA 94583
(415) 823-7157

Hans A. Mayer
Olex Cables Division of
Pacific Dunlop Ltd.
207 Sunshine Road
Tottenham, 3012
Melbourne, Australia
61-3-316-2222

James J. Pickering
Union Carbide Corp.
Weston Canal Center
CN 450
Somerset, NJ 08873
(201) 271-7908

Richard Rossi
General Cable Company
One Cragwood Road
South Plainfield, NJ 07080
(201) 412-3807

Peter Stahl
General Electric Company
Plastic Group
1 Plastic Avenue
Pittsfield, MA 01201
(413) 448-7644

Robert Streich
AT&T Network Systems
505 North 51st Avenue
P.O. Box 13369
Phoenix, AZ 85043
(602) 233-5100

George Webster
1660 Manhasset Drive
Dunwoody, GA 30338
(404) 394-0598

ADVISORY GROUP

Leo Chattler
DCM Industries, Inc.
13666 East 14th Street
San Leandro. CA 94578
(415) 352-5330

Michael A. DeLucia
David Taylor Research Center
Energy R&D Office, Code 2759
Annapolis, MD 21402-5067
(301) 267-3825
Autovon 281-3825

Marta Farago
Northern Telecom Canada Ltd.
P.O. Box 6122, Station A
Montreal, Quebec H3C-3J4 Canada
(514) 634-3511

Irving Kolodny
Consultant
80-56 230th Street
Bellerose Manor, NY 11427
(718) 464-9197

Frank Short
B.I.C.C. Cables Limited
Helsby, Warrington, WA6 00J England
011-44-9282-2727

MISSION

The International Wire and Cable Symposium provides a forum for the exchange of technical information amongst suppliers, manufacturers, and users on technological advancements in materials, processes, and products used for voice, data and video signal transmission systems.

TECHNICAL SESSIONS

Tuesday, November, 14, 1989

9:30 a.m.	SESSION I	Tutorial—How and When Will Fiber Optics Expand into the Subscriber Loop Telephone Network?
1:30 p.m.	SESSION II	Copper Cable Design/Applications I
1:30 p.m.	SESSION III	Fiber Optic Cable Installation and Field Test Methods
1:30 p.m.	SESSION IV	Cable Materials

Wednesday, November 15, 1989

8:30 a.m.	SESSION V	Subscriber Network I
8:30 a.m.	SESSION VI	Military Applications I
8:30 a.m.	SESSION VII	Fiber Optic Splices and Connectors
2:00 p.m.	SESSION VIII	Subscriber Network II
2:00 p.m.	SESSION IX	Copper Cable Design/Applications II
2:00 p.m.	SESSION X	Fire, Smoke and Toxicity Technology
3:45 p.m.	SESSION XI	Poster Session

Thursday, November 16, 1989

8:30 a.m.	SESSION XII	Building Cabling and Wiring Distribution Design
8:30 a.m.	SESSION XIII	Fiber Optic Cable Design
8:30 a.m.	SESSION XIV	Testing of Cable, Components and Materials
1:00 p.m.	SESSION XV	Military Applications II
1:00 p.m.	SESSION XVI	Processing and Testing of Fibers Cables

PAPERS

The papers in this volume were printed directly from unedited reproducible copies prepared by the authors. Responsibility for contents rests upon the authors and not the symposium committee nor its members. After the symposium, all the publication rights of each paper are reserved by their authors, and requests for republication of paper should be addressed to the appropriate author. Abstracting is permitted, and it would be appreciated if the symposium is credited when abstracts or papers are republished. Requests for individual copies of papers should be addressed to the authors.

Accession For	
NTIS GRA&I	☑
DTIC TAB	☐
Unannounced	☐
Justification	
By	
Distribution/	
Availability Codes	
Dist	Avail and/or Special
A-1	

PROCEEDINGS
INTERNATIONAL WIRE AND CABLE SYMPOSIUM

Bound—Available at Fort Monmouth

30th International Wire & Cable Symposium Proceedings—1981—$8.00
31st International Wire & Cable Symposium Proceedings—1982—$8.00
32nd International Wire & Cable Symposium Proceedings—1983—$8.00
33rd International Wire & Cable Symposium Proceedings—1984—$10.00
34th International Wire & Cable Symposium Proceedings—1985—$15.00
35th International Wire & Cable Symposium Proceedings—1986—NOT AVAILABLE
36th International Wire & Cable Symposium Proceedings—1987—NOT AVAILABLE
37th International Wire & Cable Symposium Proceedings—1988—NOT AVAILABLE
38th International Wire & Cable Symposium Proceedings—1989—$30.00

Extra Copies: 1-3, $30.00 per copy; 4-10, $25.00 per copy; 11 and above $20.00 per copy.

Make a check or bank draft payable in US dollars to the INTERNATIONAL WIRE & CABLE SYMPOSIUM and forward request to:

International Wire and Cable Symposium
P.O. Box 7597
Shrewsbury, NJ 07702

Telephone inquiries may be directed to Darla Henry (201) 544-3163.

NOTE: Proceedings shipped by surface mail can not be traced in the event they are not delivered. Overseas air mail will be an additional $30.00 per copy for Europe and $35.00 per copy for Asia.

Photocopies are available for complete sets of papers for 1964 thru 1989. Information on prices and shipping charges should be requested from the:

US Department of Commerce
National Technical Information Service (NTIS)
Springfield, Virginia 22151
USA
Telephone: (703) 487-4650
Include Title, Year and "AD" Number

13th Annual Wire & Cable Symposium (1964)	—AD 787164
15th Annual Wire & Cable Symposium (1966)	—AD A006601
16th International Wire & Cable Symposium (1967)	—AD 787165
17th International Wire & Cable Symposium (1968)	—AD 787166
18th International Wire & Cable Symposium (1969)	—AD 787167
19th International Wire & Cable Symposium Proceedings 1970	—AD 714985
20th International Wire & Cable Symposium Proceedings 1971	—AD 733399
21st International Wire & Cable Symposium Proceedings 1972	—AD 752908
22nd International Wire & Cable Symposium Proceedings 1973	—AD 772914
23rd International Wire & Cable Symposium Proceedings 1974	—AD A003251
24th International Wire & Cable Symposium Proceedings 1975	—AD A017787
25th International Wire & Cable Symposium Proceedings 1976	—AD A032801
26th International Wire & Cable Symposium Proceedings 1977	—AD A047609
27th International Wire & Cable Symposium Proceedings 1978	—AD A062322
28th International Wire & Cable Symposium Proceedings 1979	—AD A081428
29th International Wire & Cable Symposium Proceedings 1980	—AD A096308
30th International Wire & Cable Symposium Proceedings 1981	—AD A110859
31st International Wire & Cable Symposium Proceedings 1982	—AD A125662
32nd International Wire & Cable Symposium Proceedings 1983	—AD A136749
33rd International Wire & Cable Symposium Proceedings 1984	—AD A152119
34th International Wire & Cable Symposium Proceedings 1985	—AD A164384
35th International Wire & Cable Symposium Proceedings 1986	—AD A180828
36th International Wire & Cable Symposium Proceedings 1987	—AD A189610
37th International Wire & Cable Symposium Proceedings 1988	—AD A200903
Kwic Index of Technical Papers, International Wire & Cable Symposium (1952-1975)	—AD A027588

MESSAGE FROM THE DIRECTOR

Welcome to the 38th International Wire and Cable Symposium (IWCS). I am pleased to report that last year's symposium (37th) was a tremendous success, both in attendance and in the favorable responses received on the technical presentations. The international representation continues to increase each year and represents more than 25% of the total attendance.

The response this year to the call for papers was extremely good, with many abstracts submitted for consideration. To utilize many of the excellent abstracts received, the program was expanded and includes over one hundred technical and poster papers. The poster session which was received with such great enthusiasm each of the two previous years, was greatly expanded this year. The tutorial session entitled "How and When Will Fiber Optics Expand Into the Subscriber Loop Telephone Network," should provide the interest for an exciting and interesting symposium beginning.

The committee held one of its regular planning meetings in West Germany this year and met with representatives of the Germany Wire and Cable Association. During the trip, several manufacturers of Cable-Wire and connective devices were also visited. The visit's were extremely informative and provided the committee members the opportunity to see and discuss with their Germany counterparts, various Cable-Wire developments and manufacturing concepts. It was an interesting and exciting trip.

Committee members Dr. Peter Bark, Siecor Corp.; Dr. Reiner Gerdes, Contel Laboratories; Dr. Keiji Tachikawa, NTT America, Inc.; and Mr. Patrick Hart, Pacific Bell, are retiring from the committee. Each member by their efforts and specialized knowledge, contributed significantly to the success of the symposium. On behalf of the sponsor and the committee, I extend to each, a very special thanks for their sincere dedication, cooperation and support of the symposium's objectives.

The committee solicits and needs the continued support of all members of the Wire and Cable industry. For the 39th Symposium, a new two-tier plan is offered to contributors. The plan consist of Gold Sustaining Contributors ($500.00) and Silver Sustaining Contributors ($300.00). Hospitality Suites will only be available for Gold Sustaining contributors.

The 1990 symposium (39th) will return to the Bally's Reno Hotel, in Reno, Nevada. The 1991 (40th) symposium will be in St. Louis, Missouri at the Adam's Mark Hotel.

Elmer F. Godwin

ELMER F. GODWIN
Director, IWCS

FREDERIC S. TOPOR
Tutorial Session

DR RAINER J. GERDES
Chairman IWCS

TERRY APPENZELFER
Tutorial Speaker

DR. R. RAMAN
Accepting Award for
DR. STEPHEN PIERCE
For Outstanding Technical Paper

LELAND SCHMIDT
Tutorial Speaker

WILLIAM WOOD
Receiving Award for Best Poster Paper

L. J. Gadwin
Director, IWCS

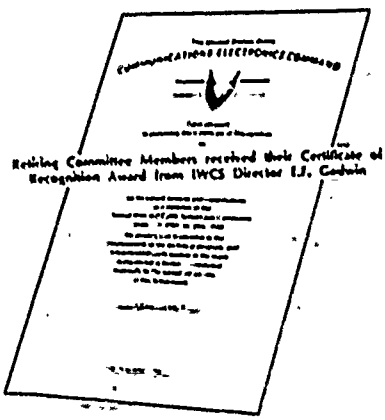

Retiring Committee Members received their Certificate of Recognition Award from IWCS Director L.J. Gadwin

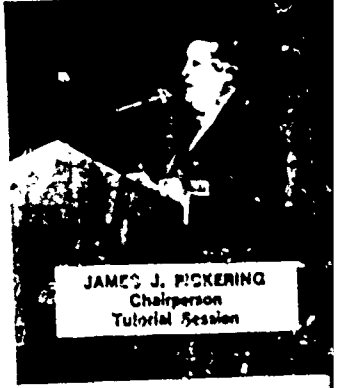

JAMES J. PICKERING
Chairperson
Tutorial Session

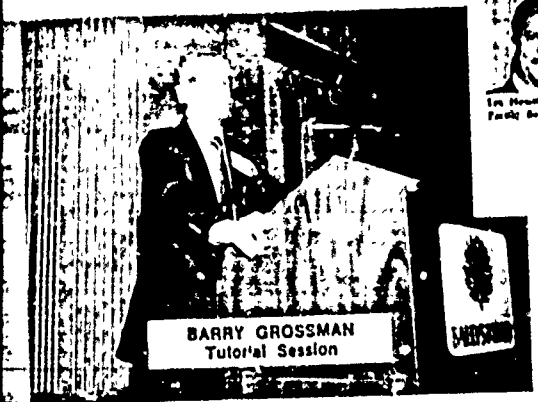

BARRY GROSSMAN
Tutorial Session

HIGHLIGHTS OF THE 1988 IWCS SYMPOSIUM

SPEAKERS AND AWARDS

BRIAN R. MOIR
Tutorial Session

RICHARD ROSSI
Receiving Award for Best Presentation

DAVID G. THOMA
Luncheon Speake

IWCS
SESSION II: MATERIALS
SESSION IN PROGRESS

37th INTERNATIONAL
WIRE & CABLE
AWARD LUNCHEON

INTERNATIONAL
WIRE AND CABLE
SYMPOSIUM

IWCS SYMPOSIUM
1988
BALLY'S RENO HOTEL
RENO, NEVADA

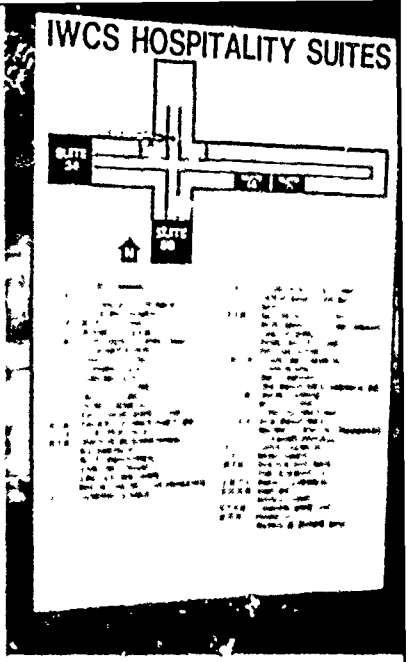

37th WIRE & CABLE
SYMPOSIUM

Reception

FREE TO ALL REGISTRANTS
(ADMITTANCE BY TICKET ONLY)

GRAND BALLROOM
BALLY'S RENO HOTEL

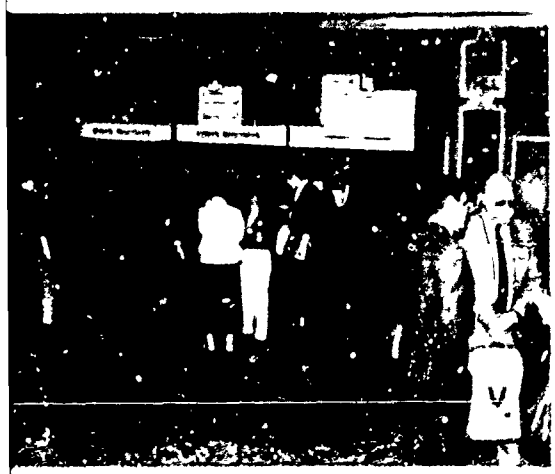

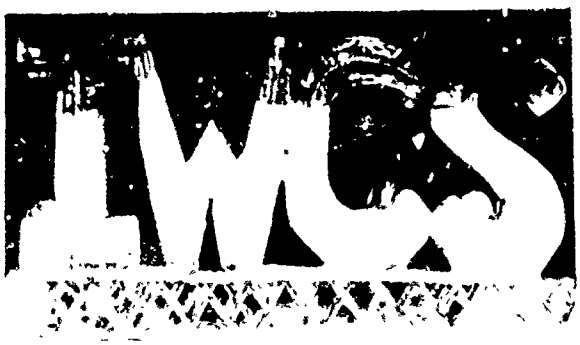

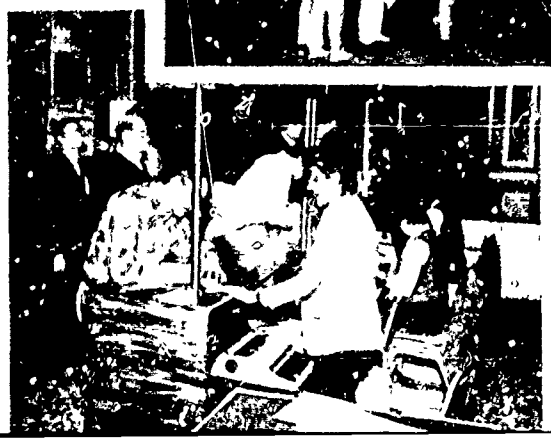

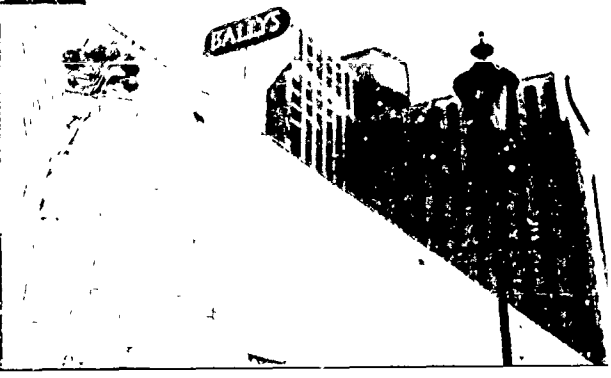

I W C S
DISPLAYS
THE PROBLEM

AWARDS

	Outstanding Technical Paper	*Best Presentation*
1968	H. Lubars and J. A. Olszewski, General Cable Corp.—"Analysis of Structural Return Loss in CATV Coaxial Cable"	N. Dean, B.I.C.C.—"The Development of Fully Filled Cables for Distribution Network"
1969	J. P. McCann, R. Sabia and B. Wargotz, Bell Laboratories—"Characterization of Filler and Insulation in Waterproof Cable"	J. D. Kirk, Alberta Government Telephones—"Progress and Pitfalls of Rural Buried Cable"
1970	D. E. Setzer and A. S. Windeler, Bell Laboratories—"A Low Capacitance Cable for the T2 Digital Transmission line"	Dr. O. Leuchs, Kable and Metalwerke—"A New Self-Extinguishing Hydrogen Chloride Binding PVC Jacketing Compound for Cables"
1971	R. Lyenger, R. McClean and T. McManus, Bell Northern Research—"An Advanced Multi-Unit Coaxial Cable for Toll PCM Systems"	S. Nordblad, Telefonaktiebolaget L. M. Ericsson—"Multi-Paired Cable of Nonlayer Design for Low Capacitance Unbalance Telecommunications Network" N. Kojima, Nippon Telegraph and Telephone—"New Type Paired Cable for High Speed PCM Transmission"
1972	J B. Howard, Bell Laboratories—"Stabilization Problems with Low Density Polyethylene Insulations"	S. Kaufman, Bell Laboratories—"Reclamation of Water-Logged Buried PIC Telephone Cable"
1973	Dr. H. Margin, Kabelmetal—"High Power Radio Frequency Coaxial Cables, Their Design and Rating"	R. J. Oakley, Northern Electric Co., Ltd.—"A Study Into Paired Cable Crosstalk"
1974	D Doty, AMP Inc.—"Mass Wire Insulation Displacing Termination of Flat Cable"	G. H. Webster, Bell Laboratories—"Material Savings by Design in Exchange and Trunk Telephone Cable"
1975	T. S. Choo, Dow Chemical U.S.A.—"Corrosion Studies on Shielding Materials for Underground Telephone Cables"	J. E. Wimsey, United States Air Force—"The Bare Base Electrical Systems"
1976	N J. Cogelia, Bell Telephone Laboratories and G. K. Lavcie and J. F. Glahn, US Department of Interior—"Rodent Biting Pressure and Chemical Action and Their Effects on Wire and Cable Sheath"	Michael DeLucia, Naval Ship Research and Development—"Highly Fire-Retardant Navy Shipboard Cable"
1977	T K. McManus, Northern Telecom Canada Ltd. and R. Beveridge, Saskatchewan Telecommunications, Canada—"A New Generation of Filled Core Cable"	William L. Schmacher, AMP Inc.—"Design Considerations for Single Fiber Connector"
1978	F. Suzuki, S. Sato, A. Mori and Y. Suzuki; Sumitomo Electric Industries, Ltd. Japan—"Microcoaxial Cables Insulated with Highly Expanded Polyethylene By Chemical Blowing Method"	Richard C. Mondello, Bell Labs.—"Design and Manufacture of an Experimental Lightguide Cable For Undersea Transmission Systems"
1979	S. Masaki, Y. Yamazaki and T. Ideguchi, Nippon Telegraph and Telephone Public Corporation, Japan—"New Aluminum Sheath Cable Used for Electromagnetic Shielding"	I. Wadehra, IBM Corporation—"Performance of Polyvinyl Chloride Communication Cables in Modified Steiner Tunnel Test"
1980	P Kish and Y. BeBorgne, Northern Telecom Canada Limited, Montreal, Canada—"General Crosstalk Model For Paired Communication Cables"	J J. Refi, Bell Laboratories—"Mean Power Sum Far-End Crosstalk of PIC Cables as a Function of Average Twist Helix Angle"
1981	C J Arroyo, N. J. Cogelia, Bell Laboratories, and B. J. Darsey, Western Electric—"Thermal Behavior of Experimental Plenum Cable Sheaths Determined in a Radiant Heat Chamber"	G. S. Anderson, Belden Corporation—"Installation of Fiber Optic Cable on 457 Meter Tower"
1982	R. H. Whiteley, Raychem Ltd.—"A Comprehensive Small Scale Smoke Test"	A. Yoshizawa, The Furukawa Electric Co., Ltd.—"Structure and Characteristics of Cables for Robots"
1983	V A Fentress, Raychem Corp. and D. V. Nelson, Stanford University—"Fracture Mechanics Evaluation of the Static Fatigue Life of Optical Fibers in Bending"	J. R. Bury, Standard Telecommunication Laboratories, Ltd., Hallow, England—"Development of Flame Retardant, Low Aggressivity Cables"
1984	M Fujise and Y. Iwamoto, KDD Research & Development Laboratories, Tokyo, Japan—"Self-Core-Alignment Arc-Fusion Splicer Based on a Simple Local Monitoring Method"	William E. Dennis, Dow Corning Corporation, Midland, Michigan—"Hydrogen Evolving Tendencies of Cable Fillers and Optical Fiber Coatings"
1985	James A. Krabec and John W. Kincaid, Jr., Belden Technical Research Center—"Advances In the Optimization of Multi-Layer Shield Design"	Stephen Hornung, British Telecom Research Laboratories—"Manufacture and Performance of Fibre Units for Installation by The Viscous Drag of Air"
1986	Simon D. Dadakarides and Bruce B. Lusignam, Stanford University—"Magnetically Loaded Cables"	Dave Fischer, Superior Cable Corp.—"Progress Towards the Development of Lightning Test for Telecommunication Cables" John C. Chamberlain, Siecor Corp.—"Zero Halogen Fire Retardant Fiber Optic Shipboard Cable"

	Outstanding Technical Paper	*Outstanding Poster Paper*	*Best Presentation*
1987	Stephen B. Pierce—Contel Laboratories—"Digital Transmission on Customer Premises Wiring"	William Wood—Bell Communication Research "Performance Analysis of Optic Fiber Cleavers"	Richard Rossi—General Cable Company Cable Sheathing Design and Performance Criteria"
1988	Martin C. Light Jr., James A. Moses, Mark A Sigmon and Christopher A. Story—Siecor Corp.—"Design and Performance of Telecommunication Cable Optimized for Low Fiber Count"	Dr. R. Raman - Contel Laboratories—"Loss at Dissimilar Fiber Splices"	Janice B. Haber - AT&T Laboratories Single-Mode Media and Apparatus for Fiber to the Home"

CONTRIBUTORS

AEG Kabel AG
Monchengladbach,
Federal Republic of Germany
AFA Industries
Garfield, NJ
Akzo Engineering Plastics, Inc.
Neshanic Station, NJ
Alberta Government Telephones
Edmonton, Canada
Alcave
Caracas, Venezuela
Allied-Signal Inc.
Morristown, NJ
Amoco Chemical Company
Naperville, IL
Anixter Bros., Inc.
Skokie, IL
AT Plastics Inc.
Brampton, Ontario, Canada
AT&T Network Systems
Phoenix, AZ
AT&T Technologies
Phoenix, AZ
Ausimont U.S.A.
Morristown, NJ
Barcel Wire & Cable Corp.
Irvine, CA
Belden Engineering Center
Richmond, IN
Belden Wire and Cable
Richmond, IN
Bell Canada
Montreal, Quebec, Canada
Bellcore
Morristown, NJ
BICC Cables Ltd.
Warrington, England
BICSI
Tampa, FL
BP Performance Polymers Inc.
Hackettstown, NJ
Breen Color Concentrates Inc.
Lambertville, NJ
Brintec Brand-Rex
Willimantic, CT
Camdan Wire Co., Inc.
Camden, NY
Canada Wire & Cable Ltd.
Manitoba, Canada
Cary Chemicals Inc.
Farmingdale, NJ
CasChem Inc.
Bayonne, NJ
Chengdu Cable Plant
Chengdu, China
Ciba-Geigy
Hawthorne, NY
Contel Corporation
Norcross, GA
Continental Wire & Cable Co.
York, PA
Corning Glass Works
Corning, NY
Corning Inc.
Corning, NY
DeSoto Inc.
Des Plaines, IL
DuPont Canada Inc.
Ontario, Canada
E.I. DuPont de Nemours & Company
Wilmington, DE
Dussek Campbell Limited
Belleville, Ontario, Canada
Dussek Campbell Limited
Crayford, Kent, United Kingdom
EB Norsk Kabel a.s
Asker, Norway
EMS-Chemie AG
Domat/Ems, Switzerland
Engineered Yarns America Inc.
Fall River, MA
Essex Group, Inc.
Decatur, IL
Facile Technologies, Inc.
Paterson, NJ
Fitel General Inc.
Carrollton, GA
Fujikura Ltd.
Tokyo, Japan
The Furukawa Electric Co., Ltd.
Tokyo, Japan
Gelok International Park
Dunbridge, OH
GEM Gravure Co., Inc.
West Hanover, MA
General Cable Company
South Plainfield, NJ
GTE Telephone Operations
D/FW Airport, TX
GTE Testmark Laboratories
Lexington, KY
Hargo Industrial Packaging
Cedar Grove, NJ
Himont U.S.A. Inc.
Wilmington, DE
Hong Kong Telephone Co., Ltd.
GPO Hong Kong
Huls AG
Marl, West Germany
ICI Fluoropolymers
Exton, PA
International Wire & Machinery Assoc.
Leamington Spa, England
Judd Wire Inc.
Turners Falls, MA
Kabelmetal Electro North America Inc.
Larchmont, NY
Kroschu-Kabelwerke Kromberg & Schubert
GmbH u. Co.
West Germany
KT Industries Ltd.
Winnipeg, Manitoba, Canada
Laribee Wire Mfg. Co., Inc.
Jordan, NY
Lonza Inc.
Fair Lawn, NJ
Mach-1 Compounding
Macedonia, OH
MM Cables—Telecommunications
Australia

Mohawk Wire and Cable Corp.
Leominster, MA
NEK Cable, Inc.
Ronkonkoma, NY
NEPTCO Inc.
Pawtucket, RI
Neste Chemicals, Inc.
New Brunswick, NJ
Neste Polyeten AB
Stenungsund, Sweden
Nokia-Maillefer
Ecublens-Lausanne, Switzerland
Nokia-Maillefer, Inc.
South Hadley, MA
Nokia Telecommunications Cables
Vantaa, Finland
Northern Telecom Canada
Lachine, Quebec, Canada
Northern Telecom Canada Ltd.
Saskatoon, Saskatchewan, Canada
NTT America Inc.
Stamford, CT
NTT Transmission Systems Laboratories
Tokai-Mura, Ibaraki-Ken, Japan
Olex Cables, Div. of Pacific Dunlop Ltd.
Victoria, Australia
Omega Wire Inc.
Camden, NY
Pacific Bell
San Ramon, CA
Pennwalt Corp.
Philadelphia, PA
Penreco-Div. of Pennzoil Products Company
Butler, PA
Phelps Dodge International Corp.
Coral Gables, FL
Philips Kommunications Industrie AG
Koln, West Germany
Phillips Cables Ltd.
Ontario, Canada
PPG Industries, Inc.
Pittsburgh, PA
Quantum Chemical Corp.
Cincinnati, OH
Raychem Corp.
Fuquay-Varina, NC
RXS Schrumpftechnik-Garnituren GmbH
Hagen, West Germany
Siecor Corp.
Hickory, NC
Siemens Aktiengesellschaft
Munchen, Germany
Sigma Cable Co. (PTE Ltd.)
Singapore, Republic of Singapore
Solem Industries
Norcross, GA
Soltex Polymer Corp.
Houston, TX
The Stewart Group Ltd.
Markham, Ontario, Canada
Sumitomo Electric Industries, Ltd.
Yokohama, Japan
Superior Teletec Inc.
Atlanta, GA
Swedish Telecom
Farsta, Sweden
The Swiss Insulating Works Ltd.
Switzerland
Syarikat Telekom Malaysia Berhad
Kuala Lumpur, Malaysia
Telecom Australia
Australia
Teledyne Thermatics
Elm City, NC
Tensolite Company, Subsidiary of Carlisle Corp.
St. Augustine, FL
Texas Instruments
Attleboro, MA
Toray Plastics (America) Inc.
North Kingstown, RI
UBE Industries (America), Inc.
New York, NY
Union Carbide-Polyolefins
Danbury, CT
Weber & Scher Mfg., Company, Inc.
Newark, NJ
Wire Industry
Surrey, England

TABLE OF CONTENTS

TUESDAY MORNING—9:30 AM-12:00 Noon
Regency Ballroom · The Falcon and Condor Rooms · Terrace Level

Greetings
Dr. Ron Simpkins, E.I DuPont de Nemours and Co., Inc., Wilmington, DE, IWCS Chairman

SESSION I: TUTORIAL, HOW AND WHEN WILL FIBER OPTICS EXPAND INTO THE SUBSCRIBER LOOP TELEPHONE NETWORKS?

Chairperson: Dr. Reiner J. Gerdes, Contel Laboratories, Norcross, GA

Panelists (Invited Presentations):
Mr. Frank D. Reece, President and General Manager, North Pittsburgh Telephone Co., Gibsonia, PA
Mr. Jim Chiddix, Senior Vice President, Engineering and Technology for American Television and Communication Corp., Stamford, CT
Mr. Richard K. Snelling, P.E. Executive Vice President - Networks and Director of Southern Bell Telephone and Telegraph Co., Atlanta, GA
Mr. Jess Chernak, Executive Director, Loop Technology Division, AT&T Bell Laboratories, Whippany, NJ

TUESDAY AFTERNOON—1:30 PM-5:00 PM
Regency Ballroom · Falcon Room · Terrace Level

SESSION II: COPPER CABLE DESIGN/APPLICATIONS

Chairperson: Mr. Leo Chattler, DCM Industries, Inc., San Leandro, CA

An Ultraminiature Flexible Hook-up Cable for Interconnecting High Bit Rate Digital Transmission Equipment—*C. Blanco, S. Camara, F. Santos, C. G. Cortines,* Alcatel-Standard Electrica S.A., Cantabria, Spain 6

Active Under-Carpet Cabling System for IEEE 802.3—*S. Ueda, K. Yokoi, K. Takenaka, A. Mori, Y. Sasatani, A. Nakamura,* Sumitomo Electric Industries, Ltd., Konohana-Ku Osaka, Japan 21

High Performance Twisted-Pair Cable for LAN Systems—*M. Plasse, L. Desroches, P. A. Guilbert,* Northern Telecom Canada, Lachine, Quebec, Canada 27

New Generation of Indoor Cables—*F. Shaikhzadeh, K. Fukui, N. Ishizaki, J. C. Souza,* Furukawa Industrial S.A., Sao Paulo, Brazil 38

Shielding Efficiency of Communications Wire and Cable for High Speed Transmission—*Lal Hore,* Bellcore, Morristown, NJ 46

Test and Measurement Parameters for Multipair Telephone Multipair Copper Cables—*E. Esposito,* Teleco Cavi, Abruzzi, Italy 56

TUESDAY AFTERNOON—1:30 PM-5:00 PM
Regency Ballroom · Condor Room · Terrace Level

SESSION III: FIBER OPTIC CABLE INSTALLATION AND FIELD TEST METHODS

Chairperson: Dr. Peter Bark, Siecor Corp., Hickory, NC

Developments and Experience in the Installation of the Perth to Adelaide Optical Fibre Route—*P. Hulbert, M. McKiernick, R. Schuster,* Telecom Australia, Victor ., Australia 64

Development of Optical Fiber Units for Air Blown Fiber (ABF) Cabling System—*H. Sano, K. Hayashi, Y. Terasawa, S. Tanaka, Y. Masuda,* Sumitomo Electric Industries, Ltd., Yokohama, Japan 69

Construction of Continuous Optical Cable to 10 km-long Waterway of Hydraulic Power Plant—*H. Sawada, S. Hasegawa,* Hokkaido Electric Power Co., Asahikawa, Japan and *T. Amano, H. Horima,* Sumitomo Electric Industries, Ltd., Yokohama, Japan 76

Universal Fiber Identification Test Instrument—*S. Morrison, C. Sarevanos,* Northern Telecom Canada Ltd., Saskatoon, Canada 84

A Method for Identifying Single-mode Fibers in an Operating Fiber Cable System—*K. Arakawa, K. Yoshida, H. Ikeya,* NTT Technical Assistance and Support Center, Tokyo, Japan 88

"Clip-on"—A Possible Measurement Technique for Future Optical Networks—*S. M. James, D. A. Ferguson, D. Drouet,* British Telecom Research Labs, Ipswich, England 94

TUESDAY AFTERNOON—1:30 PM-5:00 PM
Continental Ballroom North · International Tower

SESSION IV: CABLE MATERIALS

Chairperson: Mr. James Pickering, Union Carbide Corp., Somerset, NJ

Analysis of Stabilizer Concentrations in Polyolefin Cable Materials—*K. D. Dye,* AT&T Network Systems, Phoenix, AZ, *V. J. Kuck, F. C. Schilling, M. G. Chan, L. D. Loan,* AT&T Bell Laboratories, Murray Hill, NJ 98

A Lifetime Prediction Method for Thermoplastic Polymers—*D. R. Parris,* Siecor Corp., Hickory, NC 105

Effect of Chemical Structure of Polyimide on the Property of Polyimide and Polyimide Enamelled Wire—*H. Inoue, T. Inaike,* UBE Industries, Ltd., Osaka, Japan 111

Polybutylene Terephthalate (PBT) with Improved Hydrolysis Resistance and Low Post Shrinkage for Loose Buffer Tubes—*J. Eickholt, R. Schuler,* Huls AG, Marl, West Germany 120

Factors That Influence PIC Degradation of Filled Foamskin Telephone Cable—*L. P. Beltz,* 3M Co., Austin, TX. 123

WEDNESDAY MORNING—8:30 AM-12:00 NOON
Regency Ballroom · The Phoenix Room · Terrace Level

SESSION V: SUBSCRIBER NETWORKS I

Chairperson: Dr. George Webster, AT&T Bell Laboratories, Norcross, GA

Results on a Large Scale Installation of a Fiber Optic Distribution Network—*JP. Boinet, M. de Vecchis, C. Vergez,* Les Cables De Lyon, Clichy, France 132

An Optical Bus Architecture in the Last Mile—*D. Wong, R. Narciso,* Raynet Corp., Menlo Park, CA 136

Development of Passive Optical Networks for Subscriber Loop Application in Australia—*J. McCarter, T. MacGregor, G. Nicholson, B. Smith, G. J. Semple* and *S. Rozental,* Telecom Australia, Melbourne, Australia 141

Fiber-To-The-Home Update: Drop Installation Flexibility—*G. Cobb, W. H. Bensel, J. B. Haber,* AT&T Bell Laboratories, Norcross, GA; and *M. Dixit,* AT&T Bell Laboratories, Whippany, NJ 149

A SZ Slot Ribbon Fiber Cable for Subscriber Network—*N. Okada, A. Mogi, N. Misono,* Fujikura Ltd., Chiba, Japan; *T. Hayakawa,* Fujikura, Ltd., Tokyo, Japan; *K. Niikura,* Sumitomo Electric Industries, Ltd., Yokohama, Japan; *M. Miyazaki,* Tokyo Electric Power Co., Ltd., Tokyo, Japan; and *M. Kurokawa,* Furukawa Electric Co., Ltd., Tokyo, Japan 155

WEDNESDAY MORNING—8:30 AM-12:00 NOON
Continental Ballroom North · International Tower

SESSION VI: MILITARY APPLICATIONS I

Chairperson: Mr. Michael DeLucia, David Taylor Research Center, Annapolis, MD

Moderator: Mr. Vasilios E. Katomiris, CECOM, Ft. Monmouth, NJ

Low/No Halogen Thermoplastic Fiber Optic Cables for Shipboard Application—*K. Kathiresan,* AT&T Bell Laboratories, Norcross, GA; *J. B. Fluevog,* and *L. Sherrets,* AT&T Network Systems, Norcross, CA 162

Optical Fiber Design Challenges for Tactical System Applications—*H. Hsu,* Hughes Aircraft Co., Canoga Park, CA and *V. Katomiris,* U.S. Army CECOM, Fort Monmouth, NJ 172

Optical Fibers for Underwater Sensing—*N. Lagakos, T. R. Hickman, J. Bucaro,* and *A. Dandridge,* Naval Research Laboratory, Washington, DC 179

Development and Application of Low-Smoke, Flame-Retardant Flexible RF Cable—*A. Fedor,* Brand-Rex Cable Systems Division, Willimantic, CT 183

Manufacturing and Inspection Methods for High Strength Optical Fiber for Missile Payout Applications—*F. I. Akers, T. E. Wilson,* Alcatel Cable Systems, Roanoke, VA 188

WEDNESDAY MORNING—8:30 AM-12:00 NOON
Continental Ballroom South · International Tower

SESSION VII: FIBER OPTIC SPLICES AND CONNECTORS

Chairperson: Dr. C. Ronald Simpkins, E.I. DuPont de Nemours & Co., Inc., Wilmington, DE

Optical Fiber Cable Transfer Splicing System Using Optical Fiber Connectors—*I. Watanabe, M. Shimizu, H. Kobayashi,* NTT Network Systems, Ibaraki, Japan 191

Degradation of Fiber Strength During Coating Stripping—*T. Wei,* GTE Laboratories, Inc., Waltham, MA, *H. H. Yuce, H. C. Hasz,* Bellcore, Morristown, NJ, *P. Key,* Bellcore, Red Bank, NJ 199

Analysis of Mass Fusion Splice Loss for Optical Fiber Ribbons—*K. Osaka, T. Watanabe, M. Fukuma, Y. Asano,* Sumitomo Electric Industries, Ltd., Yokohama, Japan 205

Field Trials on Mass Splicing of Subscriber Loop Application—*W. Zell, J. A. Becker, P. Deusser, W. Eutin, J. M. Schneider,* Philips Kommunikations Industrie AG, Koeln, West Germany 212

Pre-Connectorized 1000-Fiber Cable—*H. Yokosuka, S. Togo, H. Hosoya, H. Hirao,* Fujikura Ltd., Chiba, Japan 218

Fully Automatic Mass-Fusion Splicer for Single-Mode Optical Fiber Ribbon—*M. Matsumoto, T. Haibara, M. Kawase,* NTT Network Systems Development Center, Ibaraki, Japan 225

AWARDS LUNCHEON
12:00 NOON-2:00 PM
Regency Ballroom · Terrace Level

Guest Speaker: Dr. William B. Macurdy, Vice President Transmission Systems AT&T Bell Laboratories, Holmdel, NJ

WEDNESDAY AFTERNOON—2:00 PM-5:45 PM
Regency Ballroom · The Phoenix Room · Terrace Level

SESSION VIII: SUBSCRIBER NETWORK II

Chairperson: Mr. Patrick Hart, Pacific Bell, San Ramon, CA

High Fiber Count Cable for Subscriber Loop Applications—*S. Grant, W. Bernard,* Siecor Corp., Hickory, NC 233

One-Thousand-Fiber Optical Cable Composed of Eight Fiber Ribbons—*H. Sawano, Y. Kikuchi, K. Kobayashi, N. Okada, M. Misono, H. Suzuki* and *N. Sato,* Fujikura Ltd., Chiba, Japan 240

A Composite Optical and Metallic Subscriber Connection Cable for Overhead Installation—*C. S. Pegge, S. T. Spedding, W. W. Thomas, D. J. Walker* and *G. Thambythurai,* BICC Cables Ltd., Helsby, England 246

Development of Optical and Power Feeder Composite Cables and Their Connectors for Home Automations—*K. Ishikawa, S. Ohira,* Tohoku Electric Power Co., Inc., Sendai, Japan; *K. Niikura, H. Igarashi, H. Horima,* Sumitomo Electric Industries, Ltd., Yokohama, Japan; and *K. Ogata, A. Kurosawa,* Kitanihon Electric Cable Co., Ltd., Koriyama, Sendai, Japan 251

WEDNESDAY AFTERNOON—2:00 PM-5:45 PM
Continental Ballroom North · International Tower

SESSION IX: COPPER CABLE DESIGN/APPLICATIONS II

Chairperson: Mr. Leo Chattler, DCM Industries, San Leandro, CA

Electrical Characteristics of a Metallic Digital Subscriber Line (DSL) for the Integrated Services Digital Network (ISDN) Basic Rate Interface (BRI)—*R. C. Pepe, J. Poulsen,* General Cable Co., South Plainfield, NJ 259

Loop Survey in Taiwan and Some Follow-up Proposals for ISDN Basic Rate Access—*Wu-Jhy Chiu, Ming-Jung Wu, Wen-King Hwang, Guy-Ren Luh,* Telecommunication Laboratories, Taiwan, Republic of China 274

Leaky Coaxial Cables for Mobile Communications—*H. G. Haag, G. Thönnessen, K. Schulze-Buxloh,* AEG Kabel, Mönchengladbach, Federal Republic of Germany 286

WEDNESDAY AFTERNOON—2:00 PM-5:45 PM
Continental Ballroom South · International Tower

SESSION X: FIRE, SMOKE AND TOXICITY TECHNOLOGY

Chairperson: Ms. Marie Farago, Northern Telecom Canada Ltd., Montreal, Quebec, Canada

Development of Flame Retardant Halogen-Free Jelly-Filled Non-Metallic Optical Cable—*H. Horima, K. Niikura, N. Akasaka, T. Yamanishi,* Sumitomo Electric Industries, Ltd., Yokohama, Japan 295

The 1990 National Electrical Code—Its Impact on the Communications Industry—*S. Kaufman,* AT&T Bell Laboratories, Norcross, GA 301

Development of Low Halogen and Non Halogen Fire Resistant Low Smoke Cable Sheathing Compounds Based on Functionalized Polyolefins PVC Blends—*L. K. Sanghi, A. Bhattacharyya, B. Mukherjee, A. Sen,* Fort Gloster Industries Ltd., Howrah, India; *P. P. De* and *A. K. Bhowmick,* Rubber Technology Centre, Kharagpur, India 306

Flash and Ignition Characteristics of Flame Retardant Materials—*S. Yoshida, K. Ito, Y. Tamamoto, F. Aida, E. Hosokawa,* Showa Electric Wire & Cable Co., Ltd., Kawasaki, Japan 318

WEDNESDAY AFTERNOON—3:45 PM-5:45 PM
Hanover Hall · Exhibit Level

SESSION XI: POSTER SESSION

Chairperson: Mr. Peter Stahl, General Electric Company, Pittsburgh, MA

Reparation of a Fiber Optic Ground Wire on an UHV Overhead Power Line—*M. de Vecchis,* Les Cables de Lyon, Clichy, France; *JP. Bonicel, G. Couvrie, O. Tatat,* Les Cables de Lyon, France; and *P. Kouteynikoff,* Electricite de France, Clamart, France 326

Development of the Standard FRP and Its Application to Optical Cable—*S. Matsuno, M. Okada,* Ube-nitto Kasei, Ltd., Gifu, Japan; *A. Saito, K. Ogata,* Kitanihon Electric Cable Co., Ltd., Sendai, Japan; *H. Horima, K. Niikura,* Sumitomo Electric Industries Ltd., Yokohama, Japan 331

Feasible Optical Cable Designs with Additional Functions for LAN Applications—*K. Ogata, A. Saito, T. Shishido,* Kitanihon Electric Cable Co., Ltd., Sendai, Japan; and *H. Horima, K. Kuwata, H. Igarashi,* Sumitomo Electric Industries, Ltd., Yokohama, Japan 338

New Composite Cable Applying the Air Blown Fiber Technique—*S. Konno, K. Kikuchi,* East Japan Railway Co., Tokyo, Japan; *A. Ona, G. Morikawa, K. Yamashita, M. Ryuto,* Sumitomo Electric Industries, Ltd., Yokohama, Japan 344

Low Smoke, Fire Retardant Cable Jackets Based on Ethylene Vinylacetate and Hydrogenated Nitrile Rubber—*H. Meisenheimer,* Bayer, AG, Leverkusen, Federal Republic of Germany 351

Design and Measurement of Constructing Tensile Force in Aerial Cable Suspension Line—*T. S. Lai, G. T. Tzeng, H. K. Peng, C. T. Chang, Y. J. Huang,* Telecommunication Laboratories, Taiwan, Republic of China 357

Fiber Strain During Cable Pulling, An Important Factor in Cable Design—*W. Wenski, B. Menze, J. Schulte,* Kabelmetal Electro GmbH, Hannover, Federal Republic of Germany 368

Automated Test System for Optical Fiber Cable Plants—*S. Heckmann, V. Riech,* Philips Kommunikations Industrie AG, Koln, West Germany 374

Reliability and Environmental Performance of Cabled Single-Mode Optical Fibers—*J. Kurki, L. Stormbom, L. Oksanen, T. Räsänen,* and *E. Leino,* Nokia Telecommunication Cables, Vantaa, Finland 380

The Finger Splice—A Toolless Mechanical Splice for Optical Fibers—*L. Finzel* and *M. Heier,* RXS Schrumpftechnik-Garnituren, GmbH, Hagen, Federal Republic of Germany 390

A Novel, Easy Entry, Aerial Splice Closure—*K. Rebers,* 3M Co., Austin, TX 395

Fiber Optic Drop Cables in the Subscriber Loop—*W. Bernard* and *S. C. Grant,* Siecor Corp., Hickory, NC 402

New Fiber Optic Pulling Grip Installation Procedure—*M. E. Conner, S. L. Hassell, R. Wagman,* Siecor Corp., Hickory, NC 408

Integrated Family of Joining Products for High Density Fiber Optic Networks—*J. Huber,* 3M Co., Austin, TX 420

Fiber Optic Terminating Units with Low-Loss Mechanical Splicing—*R. Keith,* 3M Co., Austin, TX 422

Effect of Sheath Processing Parameters on Cable Performance—*W. F. Busch, K. E. Bow* and *D. G. Pikula,* Dow Chemical USA, Granville, OH 427

Some Recent Developments in High Temperature Composite Materials for Tape Wrapped Wire and Cable Constructions—*E. C. Lupton, M. N. LaTorra, J. A. Effenberger, K. G. Koerber,* and *J. Petriello,* Chemical Fabrics Corp., Merrimack, NH 434

Plastic Cladding Fiber Cable and Its Fusion Splicing for Indoor and Outdoor Installation—*S. Shimizu, K. Komura, T. Sato, Y. Matsuda,* The Furukawa Electric Co., Chiba, Japan 438

Development of Novel Multiple Single-Mode Fiber Connector Composed of V-Grooved Silicon Chip and Guide-Pins—*K. Saito, T. Kakii, H. Ishida, S. Suzuki,* Sumitomo Electric Industries Ltd., Yokohama, Japan 444

Development of a Non-Destructive Test for Microbend Loss Mechanisms in Cabled Fibre—*P. A. Sutton, J. L. L. Roberts, A. T. Summers,* STC Telecommunications, Newport, England; and *A. Phoenix, D. Rees,* Polytechnic of Wales, Mid Glamorgan, UK 450

Low Loss Single-Mode Multi-Fiber Plastic Connector—*T. Ohta, T. Sigematsu, Y. Kihara, H. Kawazoe,* The Furukawa Electric Co., Chiba, Japan 45[illegible]

Development of Dry-Type Water-Blocking Optical Fiber Cable Using Swelling Material—*H. Hiramatsu, N. Ishi, K. Nagai,* The Furukawa Electric Co., Chiba, Japan 463

Low-Temperature Loss Stabilized Cables with Optical Fibers Coated by UV Curable Resins—*K. Maeda, S. Okagawa, M. Mikami, S. Sentsui,* The Furukawa Electric Co., Chiba, Japan 469

A New Analytical Method of Hydrogen Evolution from Optical Fiber Cable—*T.-C. Chang, J.-C. Lin, Y. Liu,* Telecommunication Laboratories, Taiwan, Republic of China 475

Highly Accurate Backscatter Measurement in the Quality Control of the Cabling of Single Mode Fibers—*R. Girbig, M. Hoffart,* AEG Kabel, Moenchengladbach, Federal Republic of Germany 480

Rigid PVC As Thin Wall Insulation for Indoor Telephone Exchange Cables—*C.-G. Ekroth, S. Halvarsson, E. Nilsson,* Ericsson Cables AB, Hudiksvall, Sweden 486

Design and Performance of Single-Mode Plug-In Type Optical Fiber Connectors—*S. Iwano, E. Sugita, K. Kamayama, R. Nagase,* NTT Opto-electronics Laboratories, Ibaraki, Japan and *K. Nakamo,* NTT Applied Electronics Laboratories, Tokyo, Japan 492

A Small Diameter High Fiber Count Overhead Optical Groundwire—*G. B. Anderson,* Alcoa Fujikura Ltd., Spartanburg, SC 500

A Unique Approach to Air Pressurized Optical Cable Employing Standard Fiber Tubes—*R. J. Smith* and *N. E. Felske,* Northern Telecom Canada Ltd., Saskatchewan, Canada 505

Factors Affecting Mechanical Stripping of Polymer Coatings from Optical Fibers—*J. R. Toler, C. K. Chein,* Corning Glass Works, Corning, NY 509

An Environmentally Sealed Terminal Block With Rotary Connection—*E. DeBruycker, J. Pinyan,* Raychem Corp., Fuquay-Varina, NC; and *G. Shimirak,* Raychem Corp., Menlo Park, CA 513

Ageing Effects in Submarine Cables—*J. N. Russell, P. Worthington,* STC Submarine Systems, Southampton, U.K.; *G. J. Cannell,* STC Technology, Harlow, U.K. 518

On the Choice of Single-Mode Fibers in Loose Tube Cables with Repect to Bending Performance—*S. Stuefloten, L. Bjerkan, E. Nessel,* EB Cables, Asker, Norway, and *S. Hopland,* Norwegian Telecommunication Administration, Oslo, Norway 526

Heat Shrinkable Composite Splice Closures—*M. R. Read,* Raychem, N.V., Kessel-Lo, Belgium 533

Fire Properties of Silicones for the Electrical and Optical Fiber Cabling Industry—*R. R. Buch, W. E Dennis, C. M. Monroe, R. G. Challee,* Dow Corning Corp., Midland, MI 542

New Nitrogen Gas Extrusion Process For Highly Expanded Polyethylene Insulated Coaxial Cables—*M. Ishikawa, Y. Suzuki, Y. Ito, S. Kawabata, S. Takaki,* Sumitomo Electric Industries, Yokohama, Japan 549

Rheology of a Polymer Blend for Cable-Filling Compounds—*S. A. Khan,* Bellcore, Red Bank, NJ; and *E. E. Hershkowitz,* Bellcore, Morristown, NJ 556

Reflectionless Mechanical Interconnection Components for Analog Systems—*J. A. Aberson, G. A. Alameel, G. F. DeVeau, K. M. Yasinski,* AT&T Bell Laboratories, Norcross, GA 564

DAY MORNING—8:30 AM-12:00 NOON
Continental Ballroom North · International Tower

SESSION XII. BUILDING CABLING AND WIRING DISTRIBUTION DESIGN

Invited Presentations

Chairperson: Mr. Richard Rossi, General Cable Co. South Plainfield, NJ

Moderator: Mr. O. Wes Summers, Southern Bell Telephone Co., Atlanta, GA

Service Entrance and Termination—Space and Design Considerations, Appropriate Codes—*R. Jensen,* New Jersey Bell Telephone Co., Linden, NJ

Building Backbone Systems via Twisted Pair, Fiber or Coaxial Cable—*D. Davila,* Siecor Corp., Hickory, NC

Grounding, Bonding and Electrical Protection of Cabling Systems—*E. Cantwell,* ECOS Electronics Corp., Oak Park, IL

Wire and Cable Distribution Systems—Alternative Methodologies—*G. Loveren,* Dutile & Loveren Communications, Long Beach, CA

Decreased Risk Hazards through Firestopping—*P. Shepard,* Firestop Division Heavy Duty/Nelson, Lilburn, GA

Other Distribution Concerns Including LAN's, Life Safety Systems, Security and Paging Systems—*F. Bisbee III,* Communications Planning Corp., Jacksonville, FL

The Distribution Design Professional and BICSI—*H. Plister,* GTE Telephone Operations—South Area, Tampa, FL

THURSDAY MORNING—8:30 AM-12:00 NOON
Regency Ballroom · Falcon Room · Terrace Level

SESSION XIII: FIBER OPTIC CABLE DESIGN

Chairperson: Mr. David Fallowfield, Alberta Government Telephone, Alberta, Canada

An Enhanced Ribbon Structure for High Fiber Count Cables in the Home—*K. W. Jackson, P. D. Patel, M. L. Pearsall, J. R. Petisce,* AT&T Bell Laboratories, Norcross, GA; and *G. A. Lochkovic,* AT&T Network Systems, Norcross, GA 569

New Generation of Self-Supporting Optical Fibre Aerial Cables—*H. G. Haag, G. Hög, P. E. Zamzow,* AEG Kabel, Monchengladbach, Federal Republic of Germany 575

Dispersion-Flattened Single-Mode Fibers for the Subscriber Loop: Design, Properties, Cabling and Passive Components—*J. Schulte, W. Stelb,* Kabelmetal Electro GmbH, Hanover, Federal Republic of Germany; and *T. M. Hauff, A. Oehler, M. Moratzky, W. E. Heinlein,* University of Kaiserlautern, Kaiserlautern, Federal Republic of Germany 583

Development of the Optical Fiber Cable Installed in the Sewer Pipe Network—*M. Nilima, K. Komiyama,* and *S. Sentsui,* The Furukawa Electric Co., Tokyo, Japan 591

On the Crest of a New Wave in Optical Submarine Cable Technology—*W. Giebel,* Seimens AG, Munich, Federal Republic of Germany 597

A One-Hundred-Fiber Submarine Cable Composed of Hermetically Coated Fiber Ribbons Inserted Into Slots—*N. Yoshizawa, Y. Miyazima, Y. Katsuyama,* NTT Transmission Systems Laboratories, Ibaraki, Japan 603

THURSDAY MORNING—8:30 AM-12:00 NOON
Regency Ballroom · Condor Room · Terrace Level

SESSION XIV: TESTING OF CABLE, COMPONENTS AND MATERIALS

Chairperson. Mr. Frank Short, BICC Cables Ltd., Helsby, Warrington, England

Post-mortem Failure Analysis of Optical Fiber Cables—*H. H. Yuce, A. DeVito, C. J. Wieczorek, W. T. Anderson, J. P. Verachi Jr.,* Bellcore, Morristown, NJ 611

Fiber Optic Connector Geometry Test Station—*Z. Pasturcyk, B. Wong, C. Saravanos,* Northern Telecom Canada Ltd., Saskatoon, Canada 623

Core Filling Assessment and Performance of Filled Cables in Duct Installations—*J. Olszewski* and *R. Rossi,* General Cable Co., Edison, NJ 627

THURSDAY AFTERNOON—1:00 PM-4:00 PM
Regency Ballroom · Falcon Room · Terrace Level

SESSION XV: MILITARY APPLICATIONS II

Chairperson: Mr. Irving Kolodny, Consultant—Telecommunications, Bellerose Manor, NY

Moderator: Mr. Vasilios R. Kalomiris, CECOM, Ft. Monmouth, NJ

Strength and Static Fatigue of Optical Fibers at Different Temperatures—*D. Biswas,* SpecTran Corp., Sturbridge, MA 634

High Strength, Fatigue Resistant, Singlemode Optical Fibers with Unique Thin Hard Coatings for Special/Severe Applications—*B. J. Skutnik, M. H. Hodge, J. P. Clarkin,* Ensign-Bickford Optics Co., Avon, CT 638

An Overview of the Development of a New Generation of Aerospace Wire and Cable Insulation Systems—*R. E. Hawkins,* Champlain Cable Corp., Winooski, VT 644

Single and Multimode Tactical Cable Assemblies—*B. V. Darden, K. Kathiresan, B. LeFevre,* AT&T Bell Laboratories, Norcross, GA; *J. B. Fluevog,* AT&T Network Systems, Norcross, GA; *V. E. Kalomiris,* U.S. Army CECOM, Ft. Monmouth, NJ 648

Fiber Optic LAN for Military Applications—*F. Halloran, J. Martinez,* U.S. Army CECOM, Fort Monmouth, NJ; *R. Hartmayer, L. A. Bergman,* Jet Propulsion Laboratory, Pasadena, CA 658

A Small Diameter, High Strength, Single Channel Fiber Optic Aircraft Cable Family for Use with 38999 Contacts—*W. B. Beck, R. E. Hille, P. O. Scadding,* Ensign-Bickford Optics Co., Avon, CT 665

Interface Components for High Performance Bidirectional Transmission Over Single Fiber Cable—*T. Leonard, J. Eide, C. Mueller,* Alcatel Cable Systems Inc., Roanoke, VA 672

THURSDAY AFTERNOON—1:00 PM–4:00 PM
Regency Ballroom · Condor Room

SESSION XVI: PROCESSING AND TESTING OF FIBERS CABLES

Chairperson: Mr. Hans Mayer, Olex Cables Division of Pacific Dunlop Ltd., Melbourne, Australia

Field Measurements of the Effects of Hydrogen Gas on Installed Submarine Single-Mode Fiber Cables—*W. T. Anderson, A. J. Johnson, A. DeVito,* Bellcore, Morristown, NJ 675

Investigation of Total and Distributed Hydrogen Levels in Installed Fiber Optic Submarine Cables—*S. Hopland,* Norwegian Telecommunications Administration, Cables Division, Oslo, Norway 684

Corrosion-Resistant Armor to Prevent H_2-Induced Loss in Underwater (Wire-Armored) Fiber Optic Cable—*N. E. Hardwick III, L. C. Hotchkiss, J. J. Bloe,* and *D. L. Philen,* AT&T Bell Laboratories, Norcross, GA 689

Fibre Reliability Considerations in Future Low Cost Submarine Systems—*E. S. R. Sikora, J. M. Scott, J. V. Wright, C. A. Gould,* British Telecom Research Laboratories, Martlesham, U.K. 696

Will a Reduced Bend Loss Sensitivity Affect the Lifetime of Optical Fibers?—*T. Svensson,* Swedish Telecom, Farsta, Sweden 705

Dr. Reiner J. Gerdes
Contel Corporation
Norcross, Georgia

Dr. Gerdes is the Director of Contel Laboratories, an organization within the Telephone Operations Sector of Contel Corporation.

During the past two decades, he has been involved in the development and investigation of a wide range of materials and products used in the telecommunications industry. He is the author or coauthor of more than 150 technical papers and reports. He received his college education in the U.S., France, and Germany where he received a Ph.D. in physical chemistry.

Frank D. Reese
Vice President
and General Manager
North Pittsburgh Telephone Co.
Gibsonia, PA

Mr. Reese, who is currently President and General Manager of North Pittsburgh Telephone Company, has 50 years of telephone company experience. Graduating from Cornell University with a B.S. AME in 1939 he started as an Equipment Engineer for General Telephone Company of Pennsylvania. He subsequently became Engineering Director of GTE Service Corporation, and President of GTE Automatic Electric Laboratories prior to assuming the position of Executive Vice President of North Pittsburgh Telephone Company in 1973, General Manager in 1975, and President and General Manager in 1979.

He is a Professional Engineer licensed in the State of Pennsylvania and is extremely active in professional and industry organizations. Mr. Reese is a Senior Member of the Institute of Electrical and Electronics Engineers, Inc. and has been Chairman of the Communications Switching Committee, the Communications Technology Group and the Communications Society's Advisory Council. He is also Director and Past Chairman of the Board of the National Engineering Consortium, Inc; Vice-Chairman, Board of Directors and Member of the Executive Committee of the Exchange Carriers Association; Member and Past Chairman Board of Directors, Pennsylvania Telephone Association; Member, Board of Directors and its Executive Committee, Chairman Operations & Engineering Committee and Past Chairman, Manufacturer Subcommittee for Technical Liaison of the United States Telephone Association.

Jess Chernak
Executive Director
Loop Technology Division
AT&T Bell Laboratories
Whippany, NJ

Mr. Chernak was appointed to his current position as Executive Director of the Loop Technology Division at AT&T Bell Laboratories, Whippany, New Jersey in 1979. He is responsible for the design and application of transmission media, loop apparatus, and optical and electronic system design.

Mr. Chernak joined AT&T Bell Labs in 1960 and initially was active in exploring the use of computers for designing transmission systems. He was promoted to supervisor in 1963, responsible for work on such applications of computers. Five years later, he was made head of the Computer-Aided Analysis Department. In 1970, he was appointed director of the Transmission Technology Laboratory, responsible for the design of equipment used in transmission systems, including magnetic components and microwave filters.

In 1976, he became director of the Digital Transmission Laboratory, in North Andover, Massachusetts, responsible for the design of all digital transmission facilities in the local exchange area of the Bell Operating Companies.

A Native of New York City, Mr. Chernak received his B.E.E. degree for the Polytechnic Institute of Brooklyn, where he graduated Summa Cum Laude in 1960. He received his M.E.E. degree from New York University in 1961. Both degrees were in electrical engineering.

Mr. Chernak has published a number of articles on computer-aided design and transmission system design. He is a member of the Institute of Electrical and Electronics Engineers, Eta Kappa Nu and Tau Beta Pi honor societies.

He currently resides in Short Hills, New Jersey, with his wife Barbara.

Jim Chiddix
Senior Vice President
American Television
and Communications Corp.
Stamford, CT

Mr. Chiddix is Senior Vice President, Engineering and Technology, for American Television and Communications Corporation, the country's second largest cable television operator, headquartered in Stamford, Connecticut. ATC, a publicly owned corporation, serves 3.9 million subscribers in 32 states. Mr. Chiddix is responsible for corporate engineering activities as well as research and development.

ATC leads the cable industry in exploring the use of optical fiber technology in cable television systems. Their "fiber backbone" concept for optical trunking has gained wide acceptance as an evolutionary approach, offering the prospect of improved performance and increased channel capacity from existing cable systems. In recognition of his pioneering role in exploring the use of fiber, Mr. Chiddix was named Man Of The Year by Communication Engineering and Design Magazine in January, 1989.

Mr. Chiddix, 43, has been in the cable television business for 17 years. He spent seven years as General Manager at Cablevision, Inc. in Waianae, Hawaii, and eight years as Engineering Vice President at Oceanic Cablevision in Honolulu, an ATC division. In September, 1986, he joined ATC's corporate office.

Mr. Chiddix is a Senior Member and former Director of the Society of Cable Television Engineers (SCTE). In 1983 he received the National Cable Television Association's Engineering Award for Outstanding Achievement in Operations, reflecting, in part, his role in introducing addressable converter technology.

Mr. Chiddix also has an extensive background in the development of videotape automation systems. As a founder of CRC Electronics in Honolulu, he contributed to the development and manufacture of control systems for pay television playback, automated videotape delay, and automated commercial insertion. CRC Electronics was sold to Texscan-Compuvid in 1982.

Mr. Chiddix was born in Easton, Pennsylvania, taught courses in computer and radar electronics in the U.S. Army, and attended Cornell University.

Richard Snelling
Executive Vice President
Networks/Director
Southern Bell Telephone &
Telegraph Company
Atlanta, GA

Mr. Snelling is Executive Vice President-Network and a Director of Southern Bell Telephone and Telegraph Company at its headquarters in Atlanta, Georgia.

He is a native of St. Petersburg, Florida, and graduated from the University of Florida. He joined Southern Bell's Jacksonville training program in 1956, followed by several engineering positions in West Palm Beach, Orlando, Cocoa, Jacksonville, and Ft. Lauderdale.

Mr. Snelling returned to Jacksonville in 1969 as plant extension engineer and became division engineer in Ft. Lauderdale during 1971. He was named engineering director at company headquarters on December 1, 1972 and became Atlanta general plant manager in June, 1976. Two years later on February 1, Mr. Snelling was elected vice president-Georgia-network, and later was named vice president- network at company headquarters on October 1, 1979. He was elected to his current title at company headquarters on November 1, 1982 and was elected a member of the board of Southern Bell in December, 1983.

He is a senior member of the Institute of Electrical and Electronic Engineers and a member of the Georgia and National Engineering Societies of Professional Engineers. He is also past chairman of the board-Consumer Credit Counseling Service in Atlanta; past chairman of the Applied Research Council of Bell Communications Research, Incorporated; member of the Board of Trustees for National Foundation for Consumer Credit; Advisory Council member-Southeastern Consortium of Minorities in Engineering; honorary director-Georgia Engineering Foundation; member, Engineering Advisory Council, University of Florida; member, Georgia Tech National Advisory Board; member, Eastern Communications Forum Executive Advisory Council; chairman, International Conference on Communications '90; registered professional engineer, State of Florida; member, elder and Sunday school teacher at Shallowford Road Presbyterian Church, Atlanta; Advisory Board Member, Atlanta Presbytery Campaign Leadership.

AWARDS LUNCHEON

Dr. Ron Simpkins - (Chairman IWCS)
E.I. DuPont de Nemours and
Company Inc.
Wilmington, DE

Dr. William B. Macurdy
Vice President of
Transmission Systems
AT&T Laboratories
Holmdel, NJ

Dr. C. Ronald Simpkins received undergraduate degrees from The University of Tennessee and Ph. D. in Chemical Engineering from the University of Delaware.

In his twenty-five year career with DuPont, he has managed technical, manufacturing, research, and process computer engineering groups. During the last five years, he was responsible for fiber optic technology development in the DuPont Wire & Cable Group. He is currently Optoelectronics Networking Business Manager in the DuPont Electronics Department.

Dr. Simpkins is the 1989 Chairman of the International Wire and Cable Symposium.

Dr. Macurdy is Vice President of Transmission Systems at AT&T Bell Laboratories. He is responsible for planning and development of transmission and media products for AT&T Network Systems and the AT&T and User organization.

Dr. Macurdy joined Bell Labs. in 1957 as a member of the Switching Systems Engineering organization. Initially, he worked on plans to convert Bell System telephone equipment to Touch-tone service. His later duties included planning for electronic control of switching systems, engineering of video telephone switching systems, and mobile telephone services.

In 1969, he was appointed Director of the Switching Engineering Center, the following year became Director of the Traffic Network Planning Center and, in 1975, Director of the Digital Terminal Laboratory. His responsibilities in this position included development of transmission terminals for 4ESS™ and the development of equipment used in digital transmission systems. In 1977,

he became Executive Director of the Switching Systems Engineering Division. In 1979, he was appointed Vice President of Transmission Systems and became Vice President of Operations Systems and Network Planning in August, 1981. He was appointed Vice President, Manufacturing of Transmission Equipment and Cable and Wire Products in October, 1984 at AT&T Network Systems. He assumed his present position in October 1985.

Dr. Macurdy received Bachelor's and Master's degrees in Engineering from Dartmouth College in 1955 and 1957, respectively. Two years later he received a Master's degree in Electrical Engineering from New York University, and a Ph.D. in Electrical Engineering from the Massachusetts Institute of Technology in 1962. He is presently a member of the Dartmouth Society of Engineers and of the Institute of Electrical and Electronics Engineers.

AN ULTRAMINIATURE FLEXIBLE HOOK-UP CABLE FOR INTERCONNECTING HIGH BIT RATE DIGITAL TRANSMISSION EQUIPMENT

C. BLANCO, S. CAMARA, F. SANTOS, C.G. CORTINES

ALCATEL STANDARD ELECTRICA, S.A.
Maliaño, Cantabria, Spain

SUMMARY

The use of VLSI technology in high data rates digital multiplexers has allowed such a high packing density of the electronic equipment that the hook-up cables connecting the multiplexers and distribution frames have had to be miniaturized, but which at the same time do not lose their excelent electrical performance nor the inherent properties of the materials.

The following paper describes a cable specially designed for this purpose which along with a very small final diameter, exibits high electrical performance such as SRL, cross talk and transfer impedance as well as good flame retardant and ageing properties of the material that forms the cable jacket.

The paper describes the mathematical routine followed to design the cable as well as the electrical transmission and material testing usually carried out on the finished prototype.

INTRODUCTION

The high degree of miniaturization that is taking place in digital transmission equipment, due to the extensive use of VLSI techniques, is increasing the packing density of the equipment to such a degree that the hook-up cables that are used to connect the digital multiplexers to the main distribution frames need also to be reduced in size accordingly.

The cables used to interconnect the transmission equipment need to be bound together in bundles of up to 160 cables per rack and each of these bundles, in turn, need to be housed in a duct where space is also limited.

The geometrical reduction in size of a flexible coaxial cable can, in principle, be pushed up to limits in which only the mechanical procesability of the materials are the final bounds. However, before that theoretical limit is actually reached, other considerations impose higher boundaries that cannot be ignored if the cable is to perform adequately.

Among these considerations are:

- Maximum attenuation allowed at the higher bit data rate.
- Connectorization of the cable ends.
- Solderability of both center and outer conductor.
- Signal cross-talk between two cables running together.

Digital equipment operating at bit rates of 2 and 8 Mbits/sec. do not impose such a stringent requirement on cable attenuation as the equipment, which operate at bit rates of 34 and 140 Mbits sec. Bearing in mind that the average distances separating the racks that contain the digital multiplexers from the main distribution frames have a range of 50 m, an attenuation figure of less that 8 dB/100 m at 10 Mhz can be considered as satisfactory.

The distances over which these cables run parallel to one another, on the other hand, pose a more serious issue as regards the transfer of energy from cables lying adjacent to each other.

To obtain a high Near End Cross Talk figure between two parallel cables at the transmission frequencies in question a single copper braid has been found to be insufficient. Consequently we were obliged to screen the leakage of energy out of the cable core using a very thin metal foil placed underneath the conventional copper braid.

In order to obtain a low standing wave ratio coefficient in the cable, the cable impedance regularity in the whole frequency spectrum of interest had to be controlled. Particularly critical

is the impedance deviation due to the systematic repetition of regularly spaced irregularities. These variations are produced during the dielectric extrusion process and are mainly due to the lack of uniformity of the insulation diameter of the coaxial capacitance. Special attention was paid, during the extrusion process, to these two parameters in order to minimize the final Return Loss figure of the cable.

To facilitate the soldering operation of the outer copper braid to the connector body a thin drain wire was laid between the metallic screen and the braid that forms the outer conductor. This, in turn, ensures continuity even if there is a breakage in the metallic screen. Nevertheless this wire has the drawback of giving the cable a certain degree of ovality which is maintained as low as possible by using a drain wire of the same diameter as the cable center conductor.

As the cable is for indoor use, the material chosen for the cable's outer jacket is a type of PVC, which combines good mechanical, fire resistant and aging properties, at a reasonable cost. Due to the thin wall thickness of the outer jacket and the inherent ovality of the cable, obtaining good aging properties has proved to be particularly demanding. The new material has been fully evaluated and found satisfactory for the required application.

CABLE DESIGN

As mentioned above the final cable diameter is a critical parameter; therefore cable dimensioning was of primary concern in the cable design process.

After some preliminary trials, a diameter of 0.25 mm, which roughly corresponds to the 20 AWG, was chosen for the central conductor of the coaxial cable.

The dimensioning of the dielectric was carried out based on the fact that the cable's final impedance should match that of the digital multiplexers ie. 75 ohms.

The diameter over dielectric (DOD) in a coaxial cable is determined by the following expression: (1)

$$D_1 = K_1\, d\, 10^{\frac{z_o \sqrt{\varepsilon r}}{138.2}} - 1.5\, d_w \qquad (1)$$

where,

K_1 = Effective diameter factor (K_1 = 1.05 for bare conductors and very thin cables)

d = Over-all diameter of inner conductor

z_o = Characteristic impedance

εr = Relative permitivity of dielectric

d_w = Diameter of the wires of the braid

In order to maintain the optimum control of the diameter and coaxial capacitance of the dielectric, solid polyethylene was chosen as insulating material. Based on this, the following values were entered in the above expresion,

z_o = 75 ohms

εr = 2.28

d_w = 0.1 mm

The resulting DOD is then D_1 = 1.6 mm.

The cable's mutual capacitance can be calculated using the following expression,

$$C = \frac{\sqrt{\varepsilon r}}{c\, z_o} \qquad (2)$$

where,

c = 3 10^8 m/sec.

Entering into this expression the values mentioned previously we obtain, for the cable's mutual capacitance, a value of

C = 67 pF/m

The cable phase velocity can, in turn, be calculated using the equation,

$$v_p = \frac{c}{\sqrt{\varepsilon r}} \qquad (3)$$

and using for εr the value of 2.28 we obtain

v_p = 66.22 %

Cable attenuation can be predicted using the following equation (1)

$$\alpha = \alpha_{c1} + \alpha_{c2} + \alpha_{c3} =$$

$$\alpha = \frac{2.287\ 10^{-3}\ \sqrt{\varepsilon_{rl}}}{\log_{10}\frac{D_1}{k_d}}\left[\frac{k_3 k_t\sqrt{c_1}}{d} + \frac{k_b k_t\sqrt{c_2}}{D_1}\right] + 1.047\ 10^{-4}\sqrt{\varepsilon_r}\ f\ tg\delta\ (nep/cm) \quad (4)$$

where,

f = frequency in Mhz.

k_3 = voltage factor ($k_3 = 1$ for bare conductors).

k_t = coating factor ($k_t = 1$ for pure copper).

k_b = braiding factor (it is a function of the diameter of the dielectric).

For small diameters of dielectric the following formula can be used.

$$k_b = 0.078\ D_1 + 1.6$$

C_1 = resistivity of inner conductor.

C_2 = resistivity of outer conductor.

$tg\ \delta$ = tangent of loss angle of the dielectric

If we introduce, into the above equation, the values,

$$C_1 = C_2 = 1.7241\ \ 10^{-6}\ \text{ohms/cm}$$

$$tg\ \delta\ \ = 5\ \ 10^{-4}$$

we can predict what the cable attenuation will be at a certain frequency. If we take $f = 10$ Mhz, we obtain,

$$\alpha = 7.88\ \text{dB/100 m}$$

In order to obtain a high NEXT value between two cable lengths bound together a combination of an aluminium polyester film applied longitudinally and overlapped plus an outer tinned copper braid was chosen for the outer conductor.

Although the radial leakage of energy is mainly controlled by the metallic foil, the outer braid provides the necessary conductivity to maintain the cable attenuation at a low value.

In the wake of this the outer braid was designed so as to ensure a high coverage percentage and consequently a low transfer impedance and high frequency resistance.

The corresponding filling factor and percentage coverage of a braid are given by the following expressions: (2) (3)

$$\text{Filling factor: } K_f = \frac{m \times n \times d_w}{2\pi D}\sqrt{1 + \frac{n^2 p^2}{L^2}} \quad (5)$$

$$D = D_1 + 2d_w \quad (6)$$

where,

m = Total number of spindles applying braid in both directions.

n = Number of ends of wire per spindle.

d_w = Diameter of one braiding wire.

L = Lenth of lay.

$$\text{Coverage factor } B = 2K_f - K^2_f \quad (7)$$

After some elementary algebraic manipulations we obtain,

$$K_f = 1 - \sqrt{1 - B} \quad (8)$$

and the length of lay necessary to be applied so as to obtain a certain coverage factor,

$$l = \frac{\pi(D_1 + 2d_w)}{\sqrt{\left[\frac{(1-\sqrt{1-B})\ \ 2\pi(D_1 + 2d_w)}{m \times n \times d_w}\right]^2 - 1}} \quad (9)$$

entering into this expression the following parameters,

m = 16

n = 5

D_1 = 16 mm

d_w = 0.1 mm

we obtain a coverage factor of 93% for lengths of lay of 20 mm.

A very critical parameter in high bit rate digital transmissions over coaxial cables is the return loss or the energy returned by the cable in the whole frequency spectrum. This parameter is particularly relevant as the distances between the two pieces of transmission equipment are in the order of 100 m.

The Return loss in a coaxial cable is related to the impedance uniformity of the whole length of the cable or its standing wave ratio. As we will see this impedance uniformity must be controlled by a careful monitoring of the diameter of the insulation and the uniformity of the coaxial capacitance of the cable.

The structural return loss of a coaxial cable is produced by the distribution of uniformly spaced irregularities and is dependent upon the length of the irregularities, the number of irregularities, the reflection coefficient of each irregularity, and the transmission frequency. (4) (5)

The worst peak level of the returned signal is produced at a certain critical frequency, and assuming a perfect symmetry of the irregularities and that the reflection coefficient of each irregularity is significantly lower than 1 we obtain, for this reflection coefficient, a value of,

$$\rho_{12} = \frac{(1 - e^{-\alpha L})\ 10^{-PR/20}}{e^{-\alpha L}\ (1 - e^{2\alpha nL})} \qquad (10)$$

where,

ρ_{12} = reflection coefficient of each irregularity.

L = Length of each irregularity.

PR = Return loss at the critical frequency (in dB).

n = Number of irregularities.

Combining now expressions (1) and (2) we obtain,

$$dZ_o = -69.1 \log_{10} \frac{D_1}{d} (\varepsilon_r)^{-3/2}\ d\varepsilon_r \qquad (11)$$

we can also obtain that,

$$\partial C = -\frac{\sqrt{\varepsilon_r}}{c} Z_o^{-2}\ \partial Z_o \qquad (12)$$

$$\partial C = \frac{1}{2c Z_o} (\varepsilon_r)^{-1/2}\ \partial \varepsilon_r \qquad (13)$$

whereas,

$$dZ_o = \rho_{12}\ 2\ Z_o \qquad (14)$$

we can obtain,

$$|dC| = 4 \frac{\sqrt{\varepsilon_r}}{c Z_o} \rho_{12} \qquad (15)$$

and taking into account (10) we finally get (1)

$$dC = 4 \frac{\sqrt{\varepsilon_r}}{c Z_o} \frac{(1-3^{-\alpha L})\ 10^{-PR/20}}{e^{-\alpha L}\ (1-e^{-2\alpha nL})} \qquad (16)$$

This expression gives us the variation allowed to the coaxial capacitance in a coaxial cable provided we want to obtain a certain value of return loss at a certain critical frequency.

In a similar way we can obtain from expression (1)

$$\partial D_1 = \frac{D_1 + 1.5\ d_w}{60.02} \sqrt{\varepsilon_r}\ \partial Z_o \qquad (17)$$

and,

$$\partial D_1 = \frac{D_1 + 1.5\ d_w}{60.02} \sqrt{\varepsilon_r}\ 2\ Z_o\ \rho_{12} \qquad (18)$$

and taking into account (10) we can write (1)

$$dD_1 = \frac{D_1 + 1.5\ d_w}{60.02} \sqrt{\varepsilon_r}\ 2\ Z_o \frac{(1-e^{-\alpha L})\ 10^{-PR/20}}{e^{-\alpha L}\ (1-e^{-2\alpha nL})} \qquad (19)$$

This expression gives us the variations allowed to the diameter of the insulation of the coaxial cable if we want to obtain a certain figure of return loss at a specific critical frequency.

Expression (16) and (19) were calculated in a computer for the coaxial cable we are studying and the following set of values were obtained (TABLE I).

TABLE I

f (Mhz)	PR (dB)	r	ρ_{12}	ΔD_1 (mm)	Δc (pF)
1	15	0.7525	0.1341	0.8101	35.9581
	20	0.7525	0.0754	0.4555	20.2210
	25	0.7525	0.0424	0.2561	11.3711
	30	0.7525	0.0238	0.1440	6.3944
20	15	0.9378	0.0127	0.0769	3.4168
	20	0.9378	0.0071	0.0432	1.9214
	25	0.9378	0.0040	0.0243	1.0804
	30	0.9378	0.0022	0.0136	0.6076
40	15	0.9554	0.0085	0.0514	2.2821
	20	0.9554	0.0047	0.0289	1.2833
	25	0.9554	0.0027	0.0162	0.7216
	30	0.9554	0.0015	0.0091	0.4058
60	15	0.9633	0.0058	0.0413	1.8355
	20	0.9633	0.0038	0.0232	1.0322
	25	0.9633	0.0022	0.0130	0.5804
	30	0.9633	0.0012	0.0073	0.3264
80	15	0.9680	0.0059	0.0356	1.5819
	20	0.9680	0.0033	0.0200	0.8896
	25	0.9680	0.0018	0.0112	0.5002
	30	0.9680	0.0010	0.0063	0.2813
100	15	0.9712	0.0052	0.0318	1.4130
	20	0.9712	0.0029	0.0179	0.7946
	25	0.9712	0.0016	0.0100	0.4468
	30	0.9712	0.0009	0.0056	0.2512

To simplify the use of equations (16) and (19), the above table has been expressed in graphical terms as can be seen in Figures 1 and 2.

A direct consequence of the smallness of the diameter of the cable being designed is that the maximum power rating which the cable is able to withstand is also relatively small.

As is already very well known, the maximum power transmitted by a cable is a function of the frequency of the signal and as regards the cable in question calculations were carried out for the frequencies of 10 and 100 Mhz.

The total temperature rise of the inner conductor above ambient temperature is given by the expression (1)

$$T_c = H_o \left[\frac{\alpha_{c_1} + \frac{1}{2}\alpha_d}{\alpha} \frac{G_d}{2\pi} \ln \frac{D_1}{k_1 d} + \frac{G_c}{2\pi} \ln \frac{D_s}{D_o} \right] + \left[\frac{H_o}{10\pi D_s k_h} \right]^{4/5} \qquad (20)$$

where,

G_d, G_c = Thermal resistivities of dielectric and sheath.

D_o, D_s = Inner and outer diameter of the jacket.

k_h = Thermal dissipation constant for cable surface exposed to the air.

In our cable, $k_h = 8.2 \times 10^{-4}$

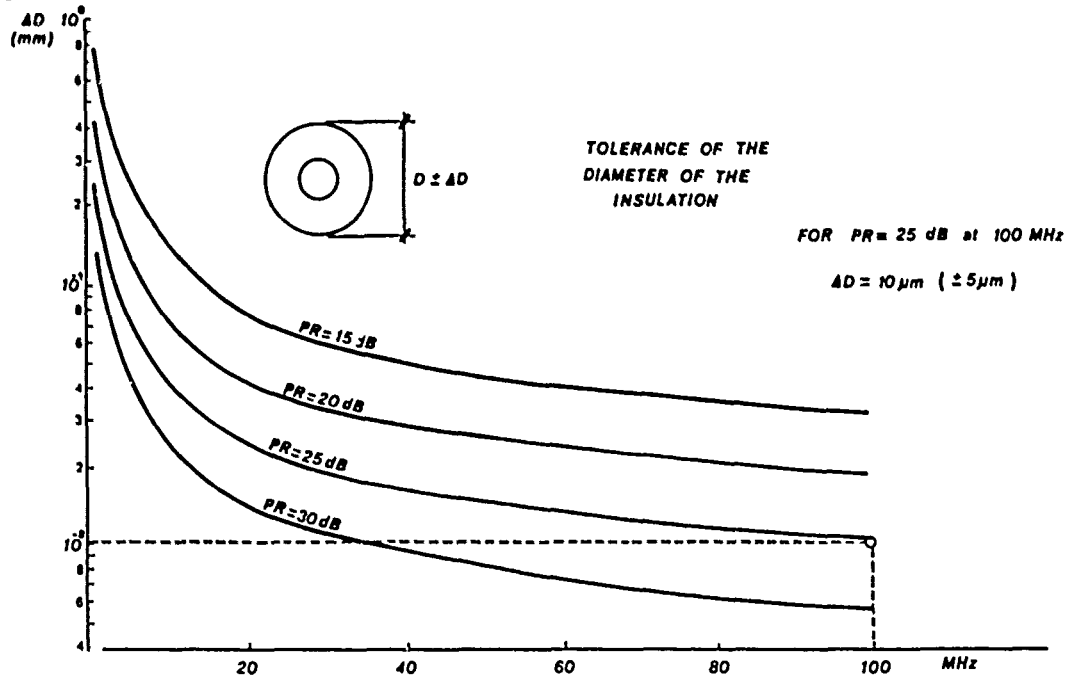

Fig. 1: Maximum absolute deviation of the insulation resist. vs. critical frequency

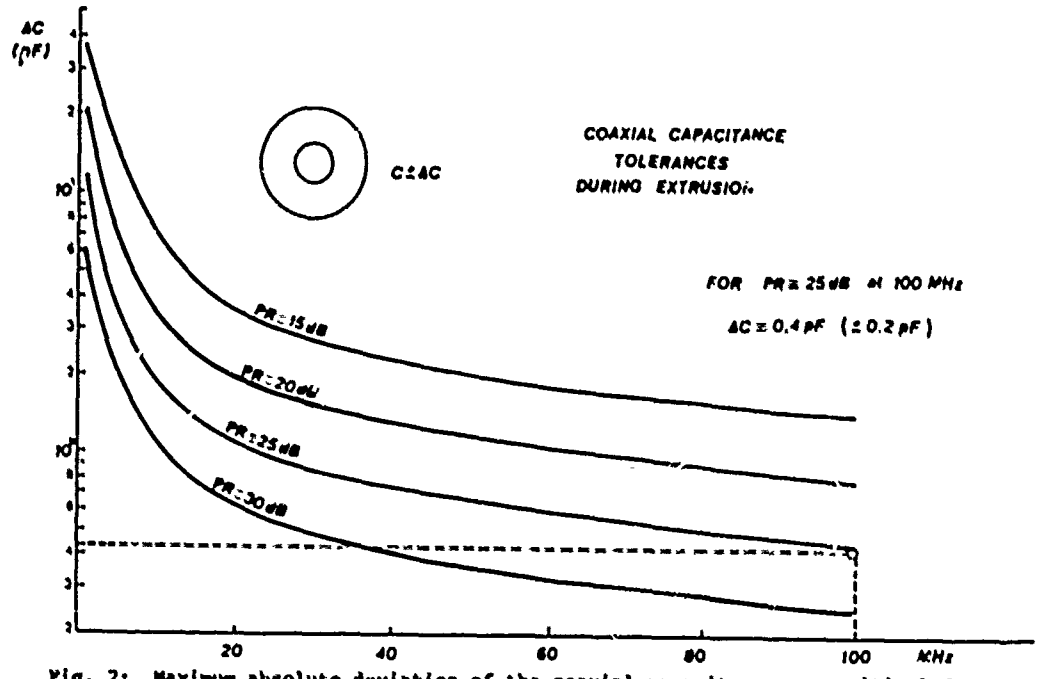

Fig. 2: Maximum absolute deviation of the coaxial capacitance vs. critical frequency

Replacing the corresponding values of these parameters in equation (20) we obtain

$$S_d = 1.28 \log_{10} \frac{1.6}{0.25} = 1.0319$$

$$S_c = 2.56 \log_{10} \frac{2.94}{2.34} = 0.25$$

f	α c1 (dB/m)	α c2 (dB/m)	α d (dB/m)
10 Mhz	0.0618	0.0166	0.000686
100 Mhz	0.19	0.052	0.00686

The following equation can then be obtained,

$$f = 10 \text{ Mhz};\ T_c = 1.0634\ H_o + \left[\frac{H_o}{0.0602}\right]^{4/5}$$

$$f = 100 \text{ Mhz};\ T_c = 1.2459\ H_o + \left[\frac{H_o}{0.0602}\right]^{4/5}$$

whose solutions are respectively,

f = 10 Mhz $H_o = 5.9$

f = 100 Mhz $H_o = 5.7$

The maximum power rating can finally be obtained using the expression,

$$P_o = 8.686 \frac{H_o}{2(\alpha T_c)}$$

where,

αT_c = Cable attenuation at T_c with a temperature coefficient of 0.20% per degree celsius.

Based on this we obtain,

f = 10 Mhz $P_o = 263$ Watts

f = 100 Mhz $P_o = 101$ Watts

Other intermediate values can easily be obtained by means of a computer, which can be programmed to follow the above routine.

The results are shown in a graph in Figure 3.

To summarize the design process used so far, the following table sets out the details of the construction of the cable.

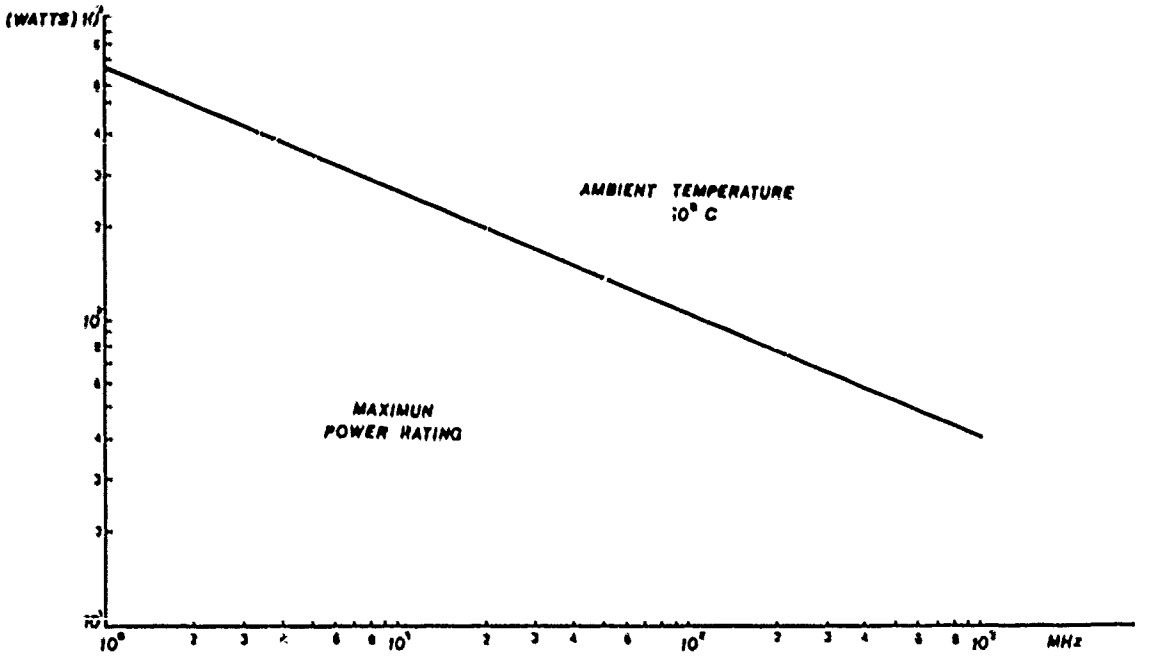

Fig. 3: Maximum power rating vs. frequency

TABLE II

1. CENTER CONDUCTOR

- Material	Tinned copper
- Diameter (mm)	0.25

2. DIELECTRIC

- Material	Solid polyethylene
- Diameter (mm)	1.60
- Tolerance of the diameter (µm)	± 5
- Tolerance of the coaxial capacitance (pF)	± 0.2

3. OUTER CONDUCTOR

3.1. Foil tape

- Material	Aluminium polyester
- Width (mm)	6
- Thickness (mm)	0.031

3.2. Braid

- Material	Tinned copper
- Groups	16
- Wires / Group	5
- Wire diameter (mm)	0.1
- Lay length (mm)	20
- Coverage (%)	>90

3.3. Drain wire

- Material	Tinned copper
- Diameter (mm)	0.25

4. OUTER JACKET

- Material	PVC
- Outer diameter (mm)	2.7 - 2.9

Figure 4 is a schematic design of the cross section of the cable.

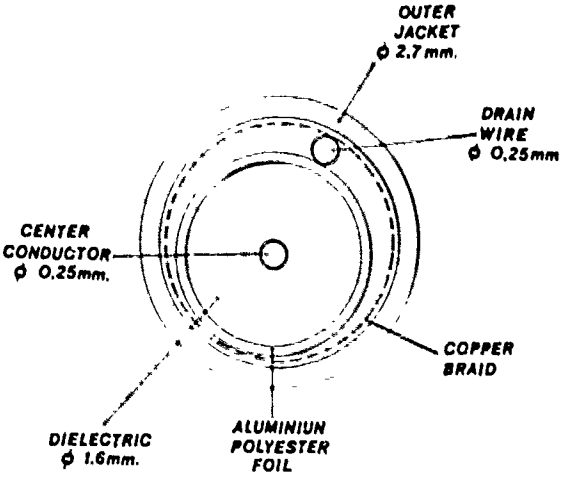

Fig. 4: Cross section of the cable

RESULTS OF THE CABLE TESTING

1. PROCESS MEASUREMENTS

During extrusion of the cable both the cable diameter and the coaxial capacitance were constantly monitored.

The aim of this monitoring was to ensure that throughout the whole process both parameters were closely kept within the required limits, in order to ensure that the final Structural Return Losses of the cable were kept above a reasonable value compatible with the high frequency and high data rate the cable is supposed to transmit.

The graphic plot of this continuous monitoring is given in Figure 5.

The following Table III summarizes the results obtained.

So as to make sure that the measurements were completely accurate and were not made inaccurate because of pigtails or connecting pins, both cable ends, were soldered to the test equipment connectors.

The coaxial terminating loads were also soldered to the free cable ends and screened from outer interferences.

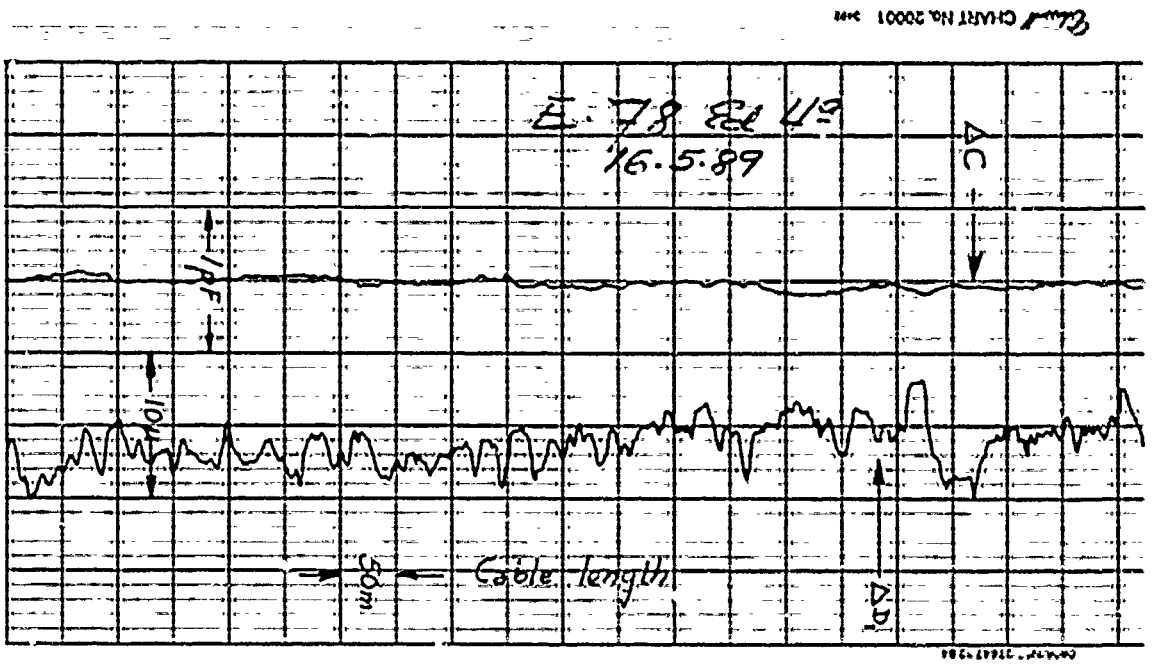

Fig. 5: Continuous monitoring of the capacitance and diameter of the insulation

As can be seen, the variations of the cable's coaxial capacitance are kept within the $\pm$ 0.2 pF and the variations of the dielectric diameter are kept within the limits of $\pm$ 5μm.

2. ELECTRICAL AND TRANSMISSION MEASUREMENTS

Once the cable was finished it was subjected to a complete series of electrical and transmission measurements in order to assure its performance at frequencies of up to 100 Mhz.

Near End Cross Talk measurements were carried out on two 10 meter cable lengths bound together.

The braids of the two cables were connected to each other and to the earth of the equipment. The object of this measurement was to simulate an actual installation in which a group of cables run parallel to one another in a common bundle along distances in the order of 10 m.

The rest of the tests were carried out using standard procedures and their results as shown in Figures 6 to 12.

TABLE III

1.	D.C. Resistance (ohms/km)	
	- Inner conductor	336.8
	- Outer conductor	25.6
2.	Mutual Capacitance (nF/km)	64
3.	Dielectric Strength (V: (1 min. 50 Hz)	3000
4.	Insulation Resistance (Mohms/km) (1 min. 500 V_{DC})	100,000
5.	Characteristic Impedance	Fig. 6,7,8
6.	Attenuation (L = 100 m)	Fig. 9
7.	Return Loss (L = 100 m)	Fig. 10
8.	Near End Cross Talk (L = 10 m)	Fig. 11
9	Time domain reflection (L = 100 m)	Fig. 12

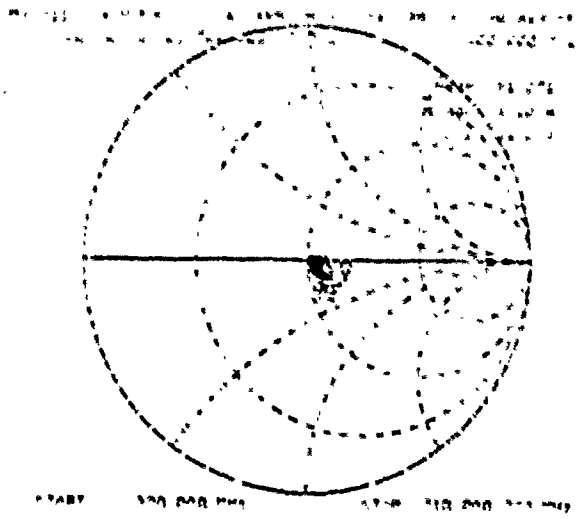

Fig. 7: Cable impedance vs. frequency Smith diagram (ρ = 1 full scale)

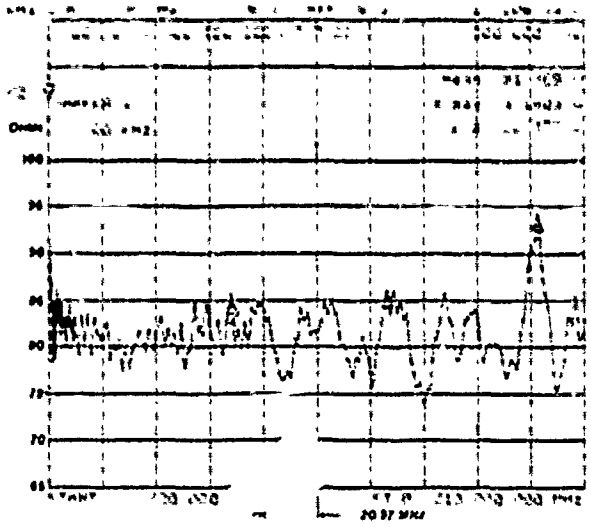

Fig. 6: Linear representation of the cable impedance vs. frequency

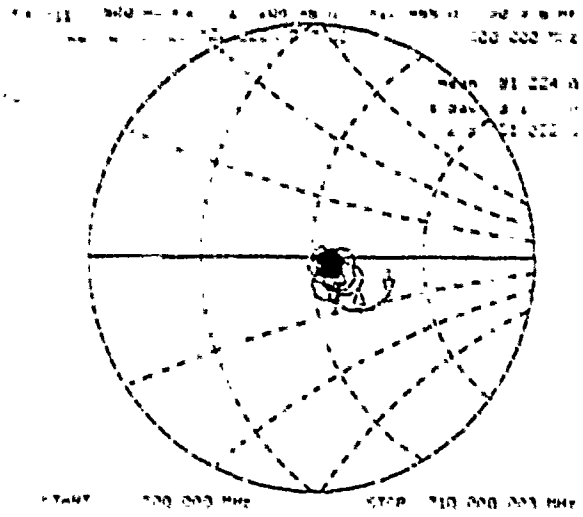

Fig. 8: Cable impedance vs. frequency Smith diagram (ρ = 0.5 full scale)

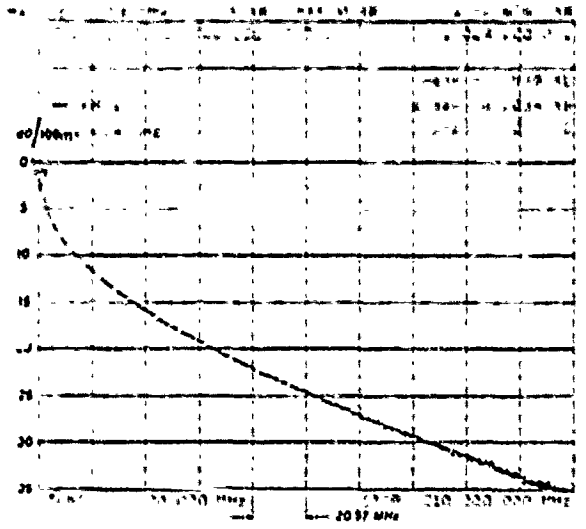

Fig. 9: Cable attenuation vs. frequency

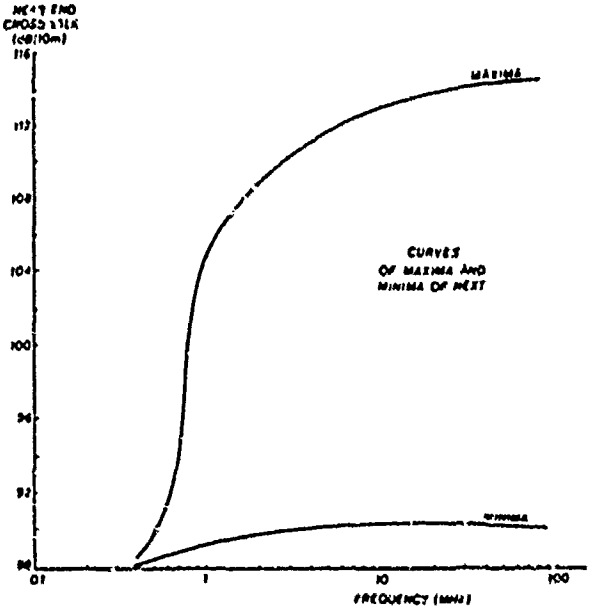

Fig. 11: Maximum and minimum curves of cable near end cross talk

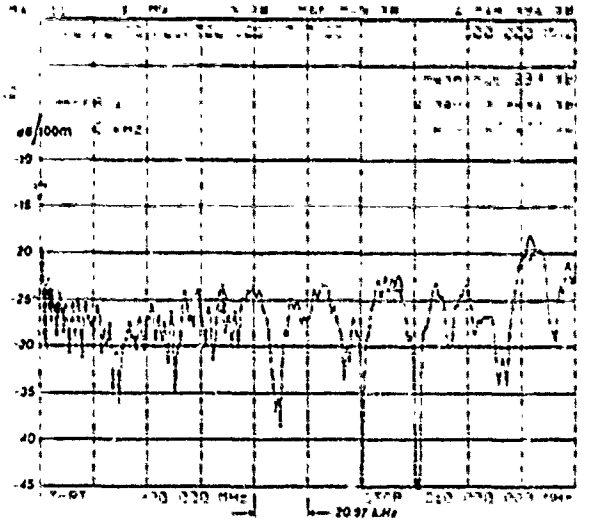

Fig. 10: Cable structural return loss vs. frequency

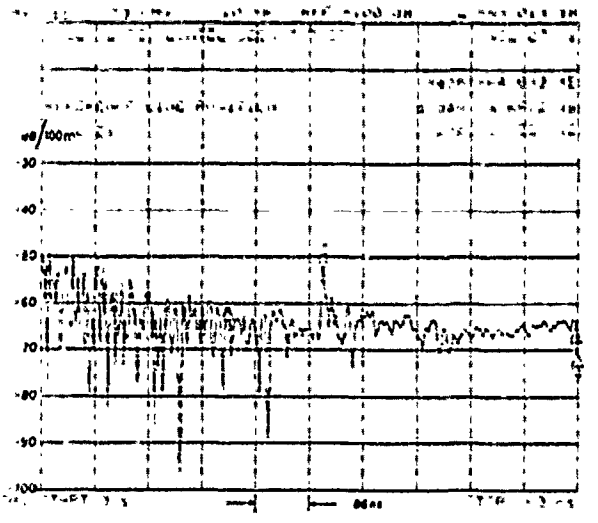

Fig. 12: Cable reflexion coefficient in the time domain

SHEATHING COMPOUND

The material used as the cable jacket is a dielectric compound of polyvinyl chloride with a K = 70, having plastification (DIDP) and stabilization degrees adequate to provide the material with good characteristics at a reasonable cost.

The following mechanical, electrical and thermal properties have been studied in the material.

1. DENSITY

The test was carried out in a gradient column at 20°C according to ASTM D-1505. The value obtained for the material density is 1.26 g/cm^3.

2. TENSILE STRENGTH AT BREAK

It was carried out following BS 6469-84 using dumb-bell test specimens 75 mm long obtained from molded plates having a thickness of 1.27 mm. The samples were subsequently subjected to temperature conditioning at 23 ± 2°C during 24 hours.

The average tensile strength obtained is 185 kgf/cm^2.

3. ELONGATION AT BREAK

The test was carried out according to BS 6469-84 using similar samples to the ones used in the previous paragraph.

The elongation at break obtained is 330%.

4. TENSILE STRENGTH AND ELONGATION AT BREAK AFTER AGEING

Test samples similar to the previously mentioned in paragraphs 2 and 3 were subjected to ageing treatment in an air oven with flow under pressure. The oven, of a Wallace Type, had a temperature regulator and an air flow meter graduated for 8 complete changes of air per hour.

The ageing was performed at 80, 90 and 100°C during time periods of 5, 10, 15, 20 and 30 days.

After each ageing period, the samples were tested and the results are shown in Fig. 13 and 14.

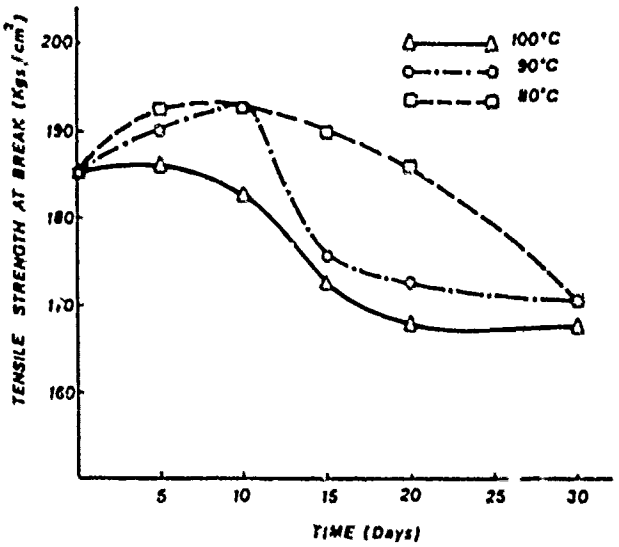

Fig. 13: Sheathing compound tensile strength after aging

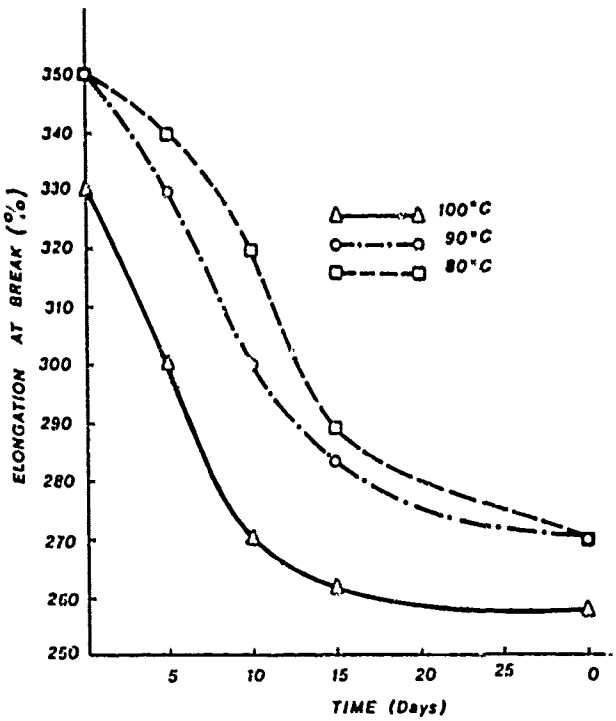

Fig. 14: Sheathing compound strain after aging

5. LOSS OF MASS TEST

New dumb-bell test pieces were subjected to the same ageing treatment as before. The percentage of loss of weight obtained are indicated in Fig. 15.

6. BENDING TEST AT LOW TEMPERATURE AND HEAT SHOCK TEST

Both tests were carried out following the procedure indicated by BS 6469-84. Visual examination of the samples did not show any indication of cracks or deterioration of the specimens.

7. HEAT DEFORMATION TEST

This test was again carried out according to BS 6469-84 using temperatures of 80, 90 and 100ºC and using weights of 250, 350 and 500 g during 4 hours.

The results are shown in Fig. 16.

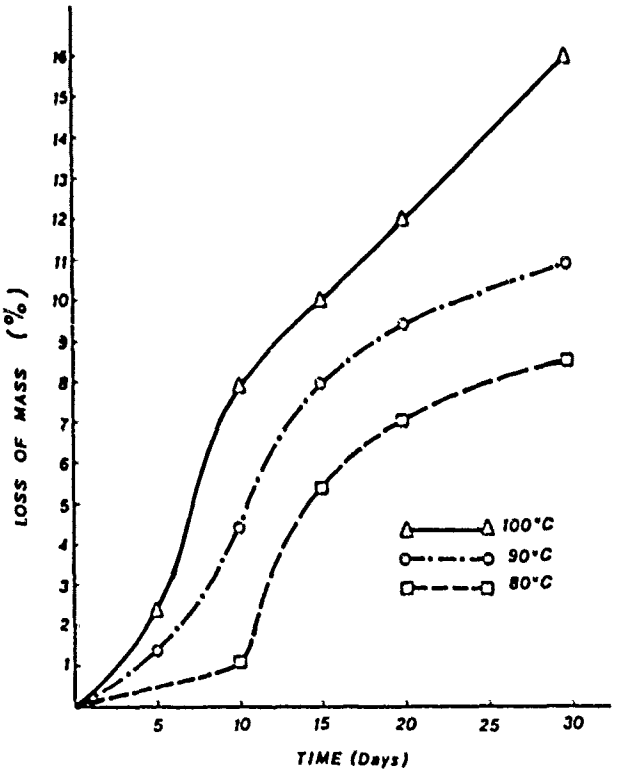

Fig. 15: Loss of mass of the sheathing compound after aging

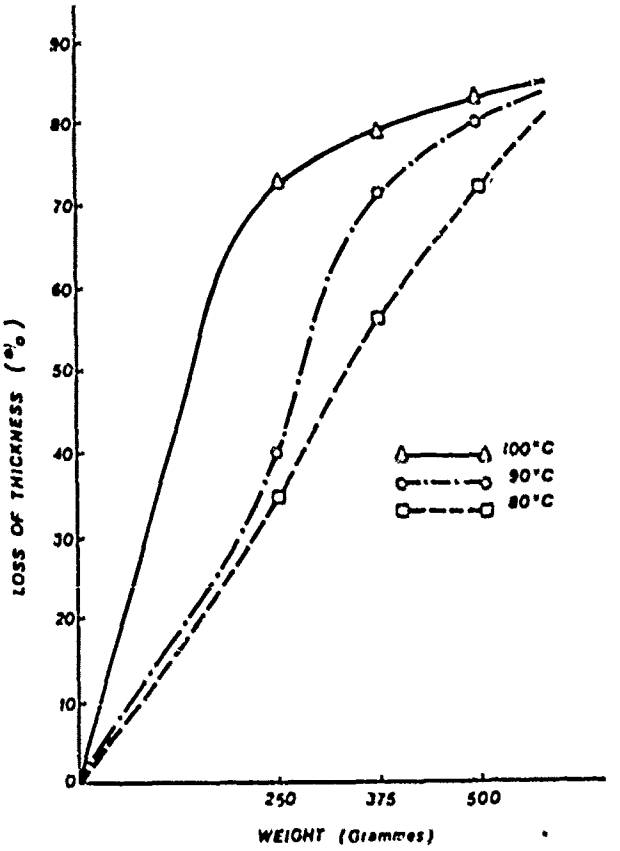

Fig. 16: Loss of thickness of the sheathing compound

8. OXIDATIVE INDUCTION TIME

The thermal stability of the material was tested using a differential scanning calorimeter (DSC) in a N_2/O_2 atmosphere. The procedure and the results are shown in Fig. 17.

9. ASH CONTENT

This test was performed using a thermogravimetry technic (TG), employing nitrogen as purging gas. The loss of mass during the test in the temperature range of 50 to 950ºC is of 95% as can be seen in Fig. 18.

10. FLAME SELF-EXTINCTION

It was tested according to IEC-189-1 using samples of 260x10x3 mm. The extinction time is lower than 30 sec and the burn out area shorther than 15 cm.

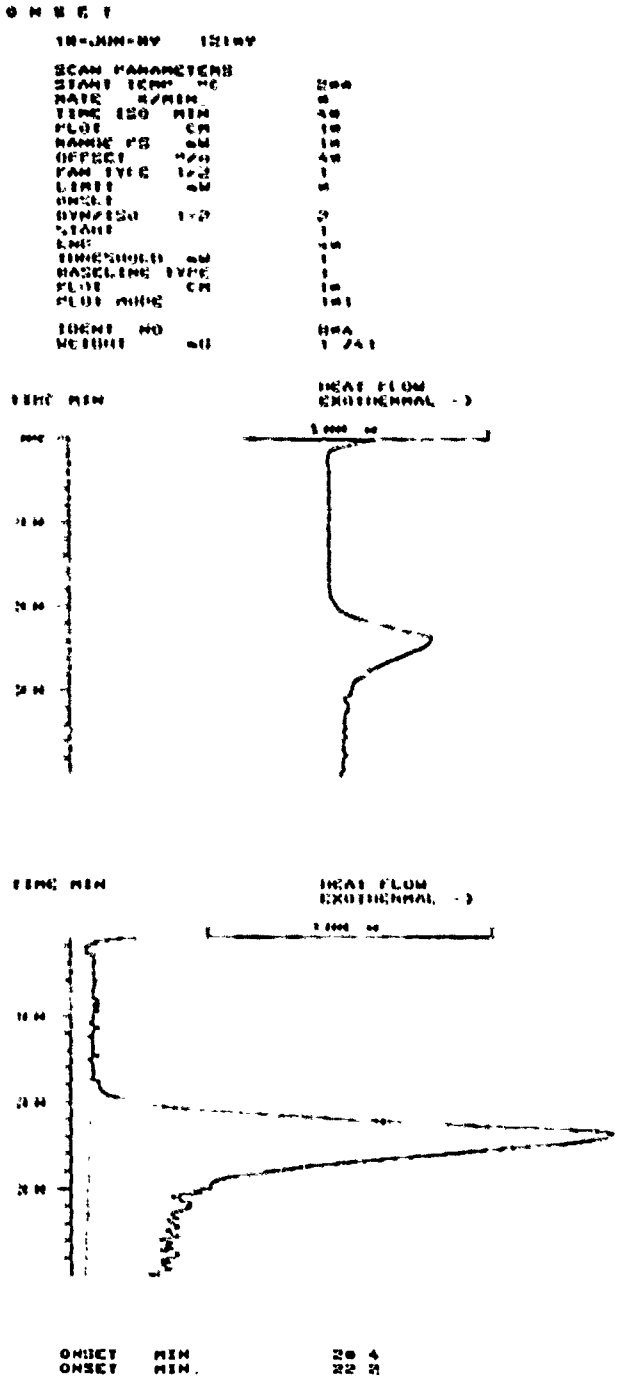

Fig. 17: Oxidative induction time (OIT)

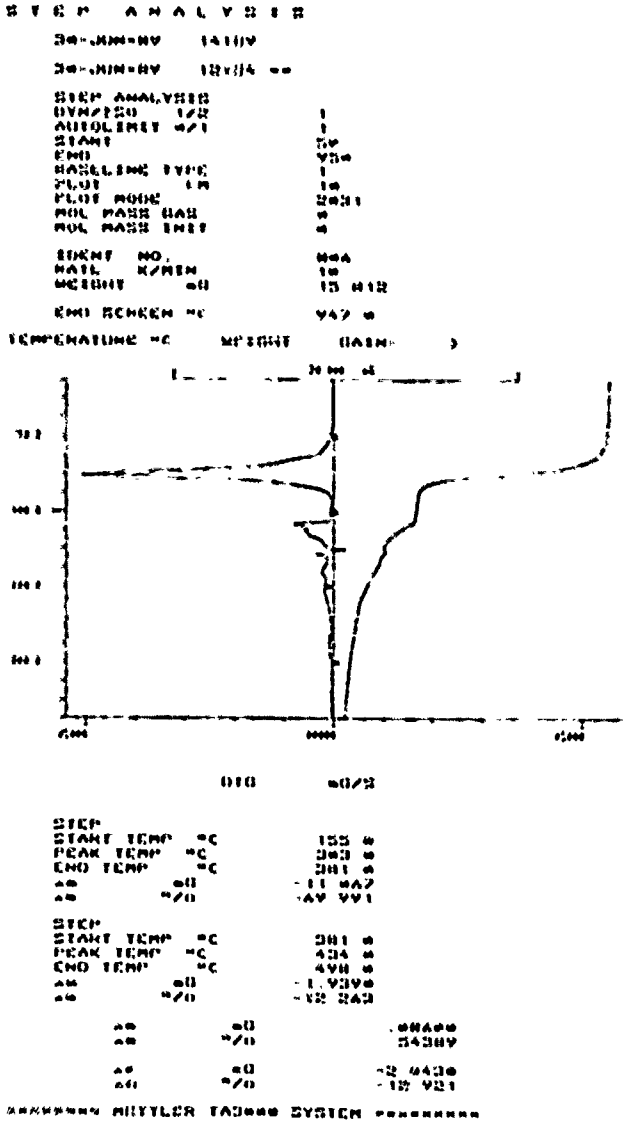

Fig. 18: Thermogravimetric analysis

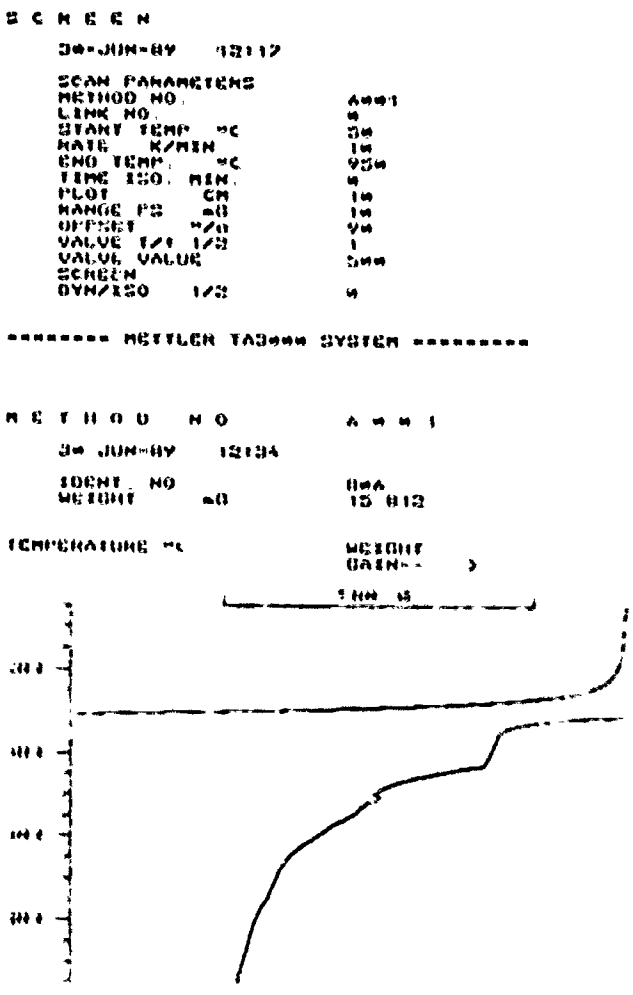

Fig. 19: Screen of thermogravimetric analysis

11. LIMITING OXYGEN INDEX

The test was carried out following ASTM D-2863 using samples of 200x6x4 mm. The limiting oxygen index (LOI) obtained has been of 24%.

12. DIELECTRIC CONSTANT AND DISSIPATION FACTOR

The tests were performed using a Q-Meter HP-4342-A and a liquid displacement cell according to ASTM D-1531 at a frequency of 10 Khz. The obtained results are,

- Dielectric constant 4.39
- Loss tangent 0.0922

13. VOLUME RESISTIVITY

Carried out following ASTM D-257, the test samples used had a radial thickness of 1.27 ± 0.13 mm and a diameter of 330 mm. The samples previous to the test were soaked in distilled water during 24 hours.

14. HARDNESS

The compound has a hardness in the scale Shore A of 82 - 83º.

CONCLUSION

A miniature flexible coaxial cable intended as hook up for digital transmission has been designed, manufactured and tested showing good transmission and electrical properties and good agreement with the predicted results.

The characteristic impedance of the cable has resulted in a value slightly higher than initially anticipated by theoretical calculations indicating that the equation used for calculations is no longer valid when the cable dimensions are reduced to limits such as those considered here.

REFERENCES

R.1 C. Blanco, S. Cámara, C.G. Cortines. "A microcoaxial cable for highly packed high bit rates digital multiplexers". IWCS. 1988, pag. 335-347.

R.2 L.R. Spicer. "Relationship between attenuation and wire-braid design for flexible radio-frequency cables". Electrical Communication, Volume 40, Number 4, 1965, pag. 4 7-492.

R.3 J. Spergel. "Computer aided design of braid parameters for coaxial cable". IWCS. 1966, pag. 319-326.

R.4 J.A. Olszewski and H. Lubars. "SRL phenomenon in coaxial cables". Proceedings of the IEEE, Vol. 58, No. 7, July 1979, pag. 1036-1050.

R.5 C. Blanco. "Perturbations in a wide band transmission over coaxial cables due to regularly spaced irregularities". E.T.S.I.T. Madrid 1972, pag. 90-147.

CARLOS BLANCO received his Doctorate Degree in Telecommunications Engineering from Madrid University in 1972. He also received his Master Degree in Physics from Santander University in 1976. He joined ITT, STANDARD ELECTRICA in Spain in 1971 as R & D Manager of the Telephone Cable Division.

During 1982-1984 he joined ITT, ELECTRO OPTICAL PRODUCTS DIVISION in Roanoke, Virginia as Senior Scientist in the Optical Fiber R & D Department.

During 1987 he joined TELCOR (TELEFONICA CORNING GLASS) as Technical Director of the Optical Fiber Manufacturing Plant.

Since 1972 he has acted as part time Professor of the Electrical Engineering Department of the Santander University.

During 1983 he was nominated Adjunct Professor of the Electrical Engineering Department of the Virginia Politechnic Institute and State University, in Blacksburg, Virginia, lecturing on Optical Fibers and Optical Communications.

Presently, Dr. Blanco is with ALCATEL STANDARD ELECTRICA in Spain as Manager of the New Products Development Department.

SUSANA CAMARA received her Master Degree in Chemistry from Oviedo University in 1984, where she specialized in Organic Chemistry.

She joined ALCATEL STANDARD ELECTRICA in 1987 where she presently works in the R & D Materials Department.

FRANCISCO SANTOS was born in 1945. He graduated as a B.S. in 1964 at Santander Technical University. He joined ALCATEL STANDARD ELECTRICA in 1971 where he is at present responsible of Industrial Applications of New Materials Development.

He has participated in the development of various telecommunication cable products mainly those concerned with the use of special PVC compounds.

CARLOS G. CORTINES was born in 1944. In 1968 he graduated from Valladolid University with a Degree in Physics. He joined STANDARD ELECTRICA, ITT, today ALCATEL, and worked in the Engineering Department of the Telecommunication Cable Division. From 1982 he is the head of the Optical Fiber Development Group in ALCATEL STANDARD ELECTRICA, Cable Factory in Maliaño-Cantabria.

ACTIVE UNDER-CARPET CABLING SYSTEM FOR IEEE 802.3

S.Ueda , K.Yokoi , K.Takenaka , A.Mori , Y.Sasatani , A.Nakamura

Sumitomo Electric Industries , LTD.
Osaka , Japan

Summary

In this paper we describe a new active under-carpet cabling system for IEEE 802.3. We have developed three main components for this system.

(1)Thin coaxial trunk cable which has suitable shape for placement under carpet.
(2)Thin and compact transceiver unit which can be set on the floor and lies flush with the carpet.
(3)Transceiver cable which is thinner and more flexible than conventional cable.

By application of high density surface mounting technology, the transceiver unit is reduced in height to only 8 mm. We can set it on the floor as part of the carpet. Cables are reduced in size by using our original highly expanded polyolefin insulation technology. This system is easy to construct, expand or rearrange, and special processes are not necessary to keep modern offices free of visible cables.

1.Introduction

Recently, local area networks (LANs) have been widely used in laboratories, factories and offices. For cabling systems, the following characteristics are desirable:

(A)A network configuration that can be easily expanded and/or rearranged.
(B)No visible cumbersome cables.

IEEE 802.3 is one of the most popular types of LAN. But it has several inconveniences:

(1)Cables are thick and inflexible.
(2)Drilling is necessary to attach the transceiver unit to the coaxial cable.
(3)Transceiver unit is large.
(4)Cables running on the floor, wall or ceiling are unattractive.

In any modern office, a wire-free environment and technical convenience are especially important, and expansion and rearrangement of network configuration is often necessary. But conventional cabling systems for IEEE 802.3 are not suitable for expansion or rearrangement because of the above mentioned reasons. Special processes are necessary to keep modern offices free of visible cables.

To solve these problems, we have developed a new active under-carpet cabling system for IEEE 802.3. In designing this new cabling system, we had paid much attention to keep the fine appearance of the environment and to maintain user-friendliness. To accomplish this, we have developed several new components:

(1)Flat coaxial trunk cable with suitable shape for placement under carpet.
(2)Ultra-thin and compact transceiver unit using high density surface mounting technology.
(3)Transceiver cable which is thinner and more flexible than conventional cable.

With these developments, a new active under-carpet cabling system can be implemented. We call this system "active" because the transceiver unit forms part of the coaxial trunk cable. We have named this system "8023UCCS (Under Carpet Cabling System)".

2.System overview

Fig.1 shows an application example of 8023UCCS. From fig.1, you can see that there are no visible, cumbersome cables and big transceiver units on the floor and/or beside the desks. They are concealed by carpets so that there is no need for special processes to conceal them, such as a free access floor. 8023UCCS consists of three main parts: a flat coaxial trunk cable, a thin and compact transceiver unit and a thin transceiver cable. Below, we describe each component.

3.Flat thin coaxial trunk cable

The conventional yellow coaxial cable

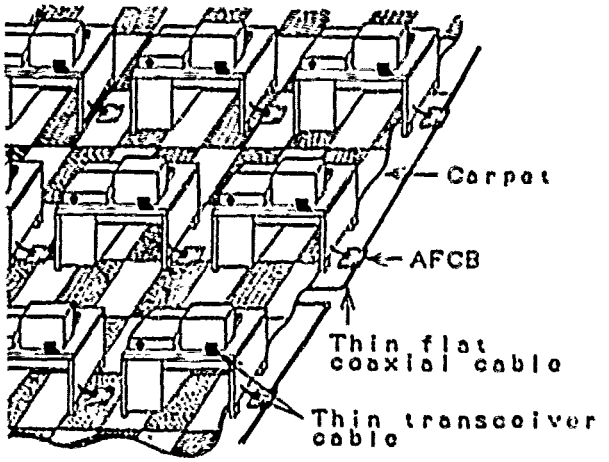

Fig.1 An application example of 8023UCCS

Item		Unit	Contents
Inner Conductor	Material Nom. O. D.	mm	Tinned annealed copper wire 0.51
Insulator	Material Nom. O. D.	mm	Highly expanded irradiated polyolefin 1.4
Outer Conductor	Material Composition Nom. O. D.	mm mm	Tinned annealed copper wire Spiral sheald of 0.08 tinned copper wire 1.36
Drain Wire		mm	Tinned annealed copper wire 0.5mm
Sheath	Material Nom. O. D.	mm	PVC 5.0×12.0×2.5
Conductor Resistance		Ω/km	Max 92.4
Insulation Resistance		MΩ-km	Min 100000
Dielectric Strength		AC V/min	1000
Capacitance		pF/m	Typ. 90 (at 1KHz)
Characteristic Impedance		Ω	50±3 (at 10MHz)
Attenuation Constant		dB/km	23 (at 1MHz) 100 (at 30MHz) 36 (at 4MHz) 120 (at 30MHz) 77 (at 10MHz) 187 (at 70MHz)
Velocity of Propagation		%	77

table 1 Electrical characteristics of flat thin coaxial cable

for IEEE 802.3 is approximately 10 mm in diameter and has poor flexibility due to its rigid construction. It is not easy to handle and unattractive if it runs on the floor, wall or ceiling. Certain environments, such as modern intelligent offices or model shop computing rooms, require a fine appearance and easy cable installation. When a conventional cable system is used in such rooms, much attention is needed to keep them wire-free. To achieve this, usually two wiring method can be used. One of them is a free access floor and the other is an under carpet cabling system. Now we had developed a new flat coaxial cable which is only 2.5 mm thick and has a trapezoid shape suitable for placement under carpet. In the case of conventional coaxial cable and free access floor, it is hard for users to construct, expand or rearrange the network configuration. Usually, installation workers will do it. But our flat thin coaxial cable is so easy to handle that users can do it by themselves. Only a few easy procedures are needed. First, turn over the carpet, next, place the cable on the floor, and then cover the floor with the carpet.

To reduce the size without sacrificing mechanical strength, we used highly expanded insulation technology. In addition, we considered maximum segment length due to the increase of cable attenuation caused by reduction in size. Fig.2 and fig.3 show the structure and appearance, respectively. Table 1 shows the electrical characteristics. Attenuation constant vs frequency characteristics is shown in fig.4. The attenuation constant of this flat cable is approximately 4.2 times as great as that of the conventional yellow coaxial cable. So we established the maximum segment length at 117 m. As for the connecting method of the transceiver units to the thin flat coaxial cable, a conventional tap connector can not be used

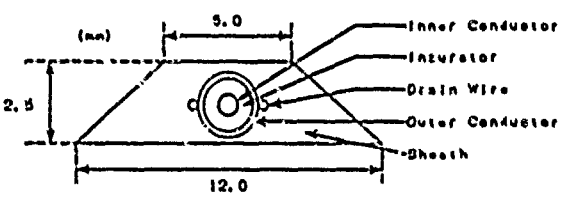

Fig.2 Cross sectional view of flat coaxial cable

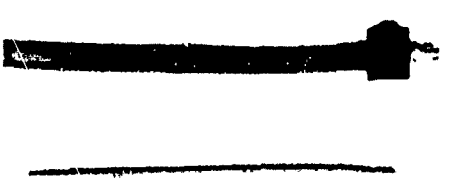

Fig.3 Appearance of flat thin coaxial cable
upper:flat thin coaxial cable
lower:conventional coaxial cable

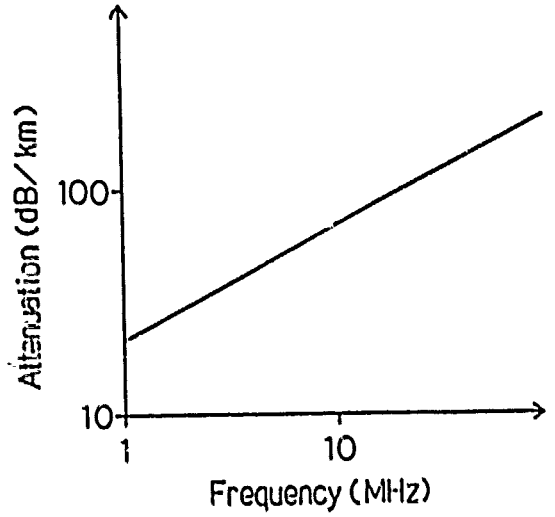

Fig.4 Attenuation constant vs. frequency of flat thin coaxial cable

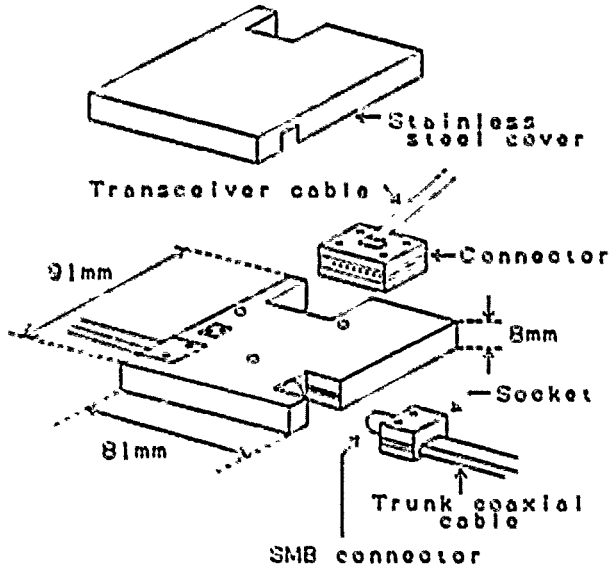

Fig.5 Appearance of AFCB

because of the reduced size of the cable and the transceiver unit. Therefore we developed original SMB connectors specifically fitted for this cable and transceiver unit.

4.Thin and compact transceiver unit

The next new component of 8023UCCS is the ultra-thin and compact transceiver unit which lies flush with the carpet. Fig.5 shows the appearance and fig.6 shows the block diagram. Its height is reduced to only 8 mm, almost the same as that of carpet. To achieve this, the total thickness of all components in the transceiver unit must not exceed 5.5 mm. If they exceed the limit, the case become so thin that it does not have sufficient strength to withstand the pressure of being stamped on. The most difficult component to adapt to this limit was the DC-DC converter. We redesigned the circuitry and applied high density surface mounting technology to create a new compact, high performance DC-DC converter. The specifications of the DC-DC converter are as follows:

(1)Wide range input regulation from 9.5 V to 15.5V with stable output of -9±5%V.
(2)Maximum output current of -200 mA with a conversion efficiency of over 70 %.
(3)Dielectric strength between input and output terminal of over 500 ACV/min.

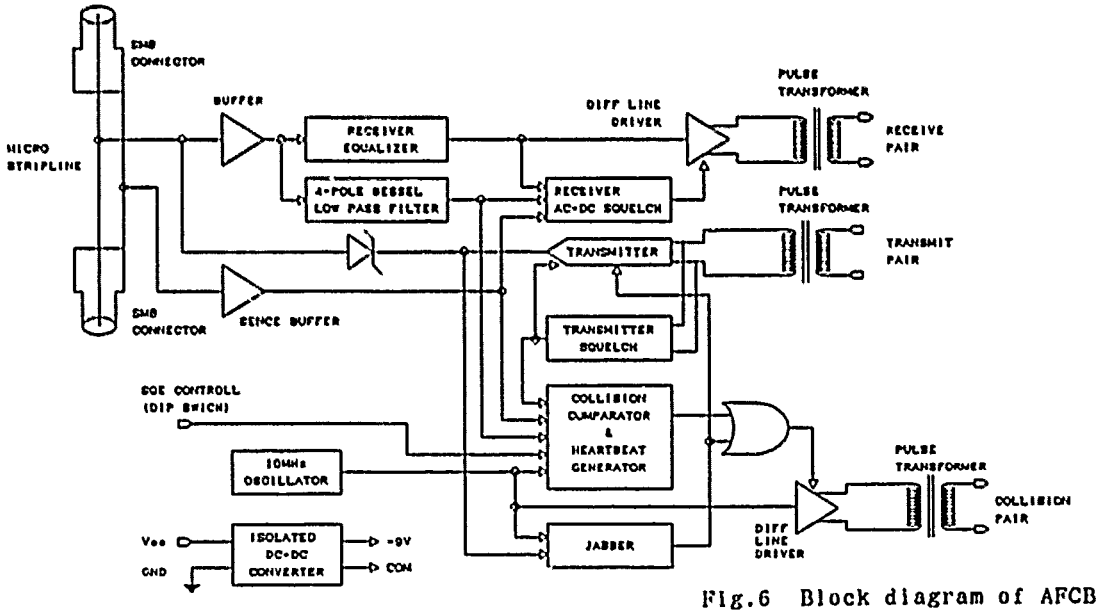

Fig.6 Block diagram of AFCB

(4)Isolation resistance between input and output terminal of over 100 Mohm at 500 DCV.
(5)L*W*T = 31*19.5*5.5 (mm)

As mentioned above, the transceiver unit will be attached to the flat thin coaxial trunk cable by using SMB connectors. When we use connecting methods other than a tap connector, we must consider impedance matching between the cable and the connecting portion. If it is not sufficiently matched, distortion of the signal will be greater as the number of connection becomes greater. But IEEE 802.3 standard does not mention signal distortion level in the case of type N connectors. Therefore we formed a micro-strip line inside the transceiver unit which has the same characteristic impedance of the flat coaxial trunk cable to minimize signal distortion. Because of this, the transceiver unit forms a part of the flat coaxial cable and we call this system an "active cabling system". We have named this transceiver unit an "Active Flat Connector Box (AFCB)".

To maintain the strength of the case against the pressure of being stamped on, we designed a reinforced structure including crossbeams, posts, and a stainless steel cover. This cover also protects against Electromagnetic Emission (EMI) and disconnection. For EMI, we took the additional countermeasure of painting the outside of the case with conductive paint.

There is no need for drilling process to attach AFCB to the flat thin coaxial cable. It is necessary only to cut the carpet and set AFCB on the floor.

5.Thin and flexible transceiver cable

The final new component is a miniature transceiver cable. Conventional transceiver cable for IEEE 802.3 is about 9 mm in diameter and has poor flexibility. Our new transceiver cable is reduced in size to 6 mm and is more flexible compared to conventional cable. Conventional transceiver cable can be up to 50 m long. But 50 m long transceiver cable is not necessary in general and it becomes cumbersome if it is excessively long, because of poor flexibility. In our cabling system, the transceiver unit will be set close to the Data Terminal Equipment (DTE), so cable length of 5 m is sufficient. In designing the miniature transceiver cable, we must

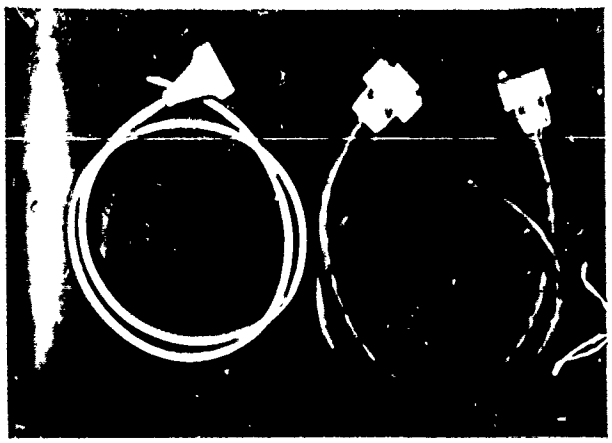

Fig.7 Cross sectional view of transceiver cable
left :flexible thin transceiver cable
right:conventional transceiver cable

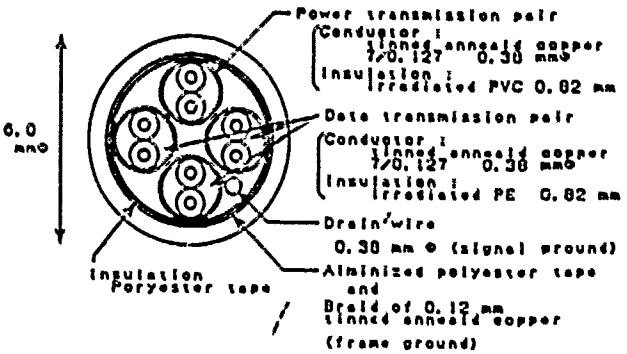

Fig.8 Cross sectional view of transceiver cable

Item	Units	IEEE STD.	Power Pair	Signal Pair
Conductor Resistance	Ω	Max 1.75	Max 1.27	Max 1.27
Isolation Resistance	MΩ-Km	-	Min 50	Min 10000
Characteristic Impedance	Ω	78±5	-	78±5
Attenuation Constant	dB	Max 3	-	Max 0.75
Velocity of Propagation	-	0.65C	-	Typ. 0.65C
Crosstalk Constant	dB	Max -40	Max -40	Max -40

table 2 Electrical characteristics of flexible thin transceiver cable

consider voltage drop in the power transmission pair and signal attenuation in the data transmission pairs. To provide electrical characteristic assurance in maximum length and mechanical strength, we selected AWG28 for the inner conductors. Fig.7 and fig.8 show the cable's appearance and cross section, respectively. Table 2 shows the electrical characteristics.
This transceiver cable has a conventional D-sub connector for DTE and on the other side a flat connector for AFCB. Because of the reduced size of AFCB, we designed a special flat connector.

6.Conclusion

We have developed a new active under-carpet cabling system for IEEE 802.3. In designing this system, we paid much attention to keep fine appearance of the environments and user-friendliness. It has a flat coaxial cable which is only 2.5 mm thick and has a trapezoid shape suitable for placement under carpet. The transceiver unit is small and only 8 mm thick, so it can be set on the floor as part of the carpet. The transceiver cable is also reduced in size and is more flexible than conventional cable. It is easy to construct or expand this system, or to rearrange the configuration of the network. Additionally it does not need special processes to keep modern offices free of visible cables. So users can do it all by themselves.

Seiji Ueda

Sumitomo Electric
Industries,Ltd.
1-3,Shimaya 1-Chome,
Konohana-ku Osaka,
Japan

Seiji Ueda received his M.E. degree in electronic engineering from Kobe university in 1985. He then joined Sumitomo Electric Industries,Ltd., and engaged in development and design of hybrid integrated circuits. Mr. Ueda is now a member of Application Specific Devices R&D Department.

Yukihiro Sasatani

Sumitomo Electric
Industries,Ltd.
1-3,Shimaya 1-Chome,
Konohana-ku Osaka,
Japan

Yukihiro Sasatani received his M.E. degree in electronic engineering from Osaka university in 1974. He then joined Sumitomo Electric Industries,Ltd., and engaged in development and design of hybrid integrated circuits. Mr. Sasatani is now Cheaf Reserch Associate, Application Specific Devices R&D Department.

Akihiko Nakamura

Sumitomo Electric
Industries,Ltd.
1-3,Shimaya 1-Chome,
Konohana-ku Osaka,
Japan

Akihiko Nakamura received his M.E. degree in mechanical engineering from Tokyo university in 1969. He then joined Sumitomo Electric Industries,Ltd., and engaged in development and design of hybrid integrated circuits. Mr. Nakamura is now Manager, Application Specific Devices R&D Department.

Kiyonori Yokoi

Sumitomo Electric
Industries,Ltd.
3-3,Satsuki-Cho,
Kanuma-city,
Tochigi-prefecture
Japan

Kiyonori Yokoi received his B.S. degree in electric engineering from Keio university in 1985. He then joined Sumitomo Electric Industries,Ltd., and engaged in development and design of plastic cables. Mr. Yokoi is now a member of Engineering Section, Electronics Wire Division.

Akinori Mori

Sumitomo Electric
Industries,Ltd.
3-3,Satsuki-Cho,
Kanuma-city,
Tochigi-prefecture
Japan

Akinori Mori received his B.S. degree in mechanical engineering from Kyushu university in 1970. He then joined Sumitomo Electric Industries,Ltd., and engaged in development and design of plastic cables. Mr. Mori is now Manager,Engineering Section, Electronics Wire Division.

Kaku Takenaka

Sumitomo Electric
Industries,Ltd.
1-3,Shimaya 1-Chome,
Konohana-ku Osaka,
Japan

Kaku Takenaka received his M.E. degree in electric engineering from university of Osaka prefecture in 1974. He then joined Sumitomo Electric Industries,Ltd., and engaged in design and development of information systems of new traffic. Mr. Takenaka is now Manager, Vehicle Communcation and Information Systems Section, Systems & Electronics Division.

HIGH PERFORMANCE TWISTED-PAIR CABLE FOR LAN SYSTEMS

by

M. Plasse, L. Desroches, P.A. Guilbert

Northern Telecom Canada Limited
Communication Cable Division

ABSTRACT

The use of twisted pairs for high speed data transmission in the premises wiring application is now common. Local area networks are currently using twisted pairs at data rates of up to 16 Mbps.

The design of inside wiring cables must be evaluated for system reach and EMI emissions as well as compliance with NEC and FCC requirements for optimum system performance.

Measurement methods assessing the performance of cables on digital systems were developed and results of analog and digital measurements are given. Using this data, new cable designs providing substantial reach improvements over conventional wiring are presented.

INTRODUCTION

Local Area Networks (LANs) and other high speed digital systems are now common place in the office environment. Traditionally these systems were designed with coaxial cables as the principal transmission media. With the evolution of technology both in data transmission and digital signal processing, the transmission media used for high speed data networks must be reconsidered.

The use of impedance matching devices and/or baluns has permitted the migration of coax based networks to twisted pairs providing a more cost effective and space efficient solution. The variety of twisted pair cabling designs combined with the increasing data rates highlight the need for proper characterization of the transmission media in its intended environment.

To the cable designer the desired conventional cable properties are low loss and reduced signal to noise ratio. However, to the network engineer and end user the transmission capacity, reduced signal distortion and low electromagnetic interference (EMI) are important. Preferably at low cost and compact size.

The focus of this paper is on the development of an optimal cable design based on measurements made of both analog and digital parameters. Cable types with different design features such as characteristic impedance, shield type (if applicable), insulation material, pair balance, and gauge were selected for evaluation.

Analog measurements were made using S-parameters. New test methods were developed for the study and the evaluation of digital transmission characteristics and factors affecting EMI. Actual system reach was established and supports the digital measurement results. Using the data collected an optimal cable design was derived.

1 - TRANSMISSION CHARACTERISTICS

Seven (7) cable types having different generic design features were selected for the evaluation. The description of the cable types is given in Table 1.1

TYPE	IMP	SHIELD	GAUGE	REMARKS
1	100 Ω	No	24	DIW
2	100 Ω	No	24	Low loss ins.
3	100 Ω	No	22	Low loss ins.
4	150 Ω	Individual	22	IBM type I
5	150 Ω	No	24	Cellular ins.
6	150 Ω	Overall	24	Cellular ins.
7	100 Ω	No	24	Low loss ins. (Opt Bal)

Table 1.1: Cable type evaluated

Throughout this paper measurements are reported on a selection of these cable types depending on the parameter of interest.

1.1 ANALOG CHARACTERIZATION

Methods for measuring attenuation and crosstalk have evolved from bridge measurements. The speed and automation of data acquisition providing more data through the frequency spectrum of interest. The use of S-parameter instruments has also increased the frequency bandwidth of the measurement.

The apparatus used for the measurement is shown in Figure 1.1.1. It is composed of a network analyzer, the accompanying S-parameter test set, baluns, and a computer connected via a GPIB interface (see appendix A). The frequency bandwidth of interest is 100 kHz to 20 MHz well within the capability of the instrument which is limited to 200 MHz and of the baluns which are limited to approximately 30 MHz. Both attenuation and crosstalk are two port measurements done in a balanced mode. Proper transformers are used to adapt the 50 Ω unbalanced

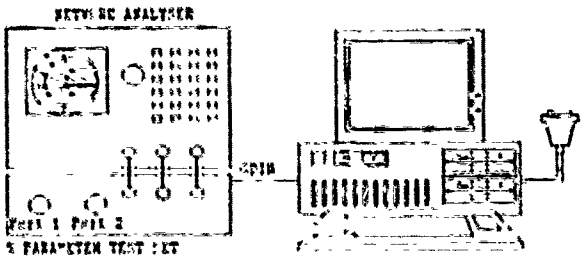

Figure 1.1.1: Analog Setup

impedance of the instrument to the balanced impedance of the cable. This technique of measuring the secondary parameters at higher frequency (attenuation, phase shift, impedance) is referenced in outside publications[1].

Using this measuring technique, four cables were compared for attenuation. As mentioned previously in Table 1.1, cable 1 represents the unshielded twisted pairs (DIW) which complies with the draft TIA Standard[2] for horizontal wiring and cable 4 represents shielded twisted pairs which complies with the IBM Type I specification[3].

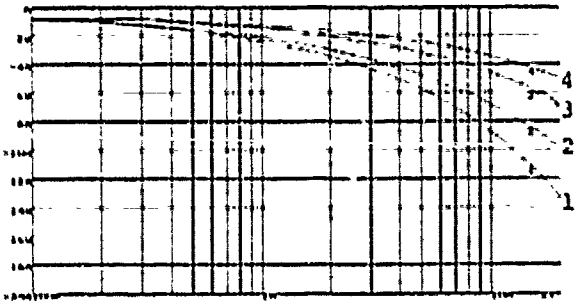

Figure 1.1.2: Attenuation characteristics

As seen in Figure 1.1.2, the performance of cables 2 and 3 falls in between the two specifications. This would be expected due to a less lossy insulation material used in cables 2 and 3. All three cables 1, 2 and 3 have the same impedance of 100 ohms. Cables 3 and 4 are 22 AWG cables which explains the lower attenuation.

The results of crosstalk measurements can be seen in Figure 1.1.3, cables 2 and 3 have a 10 dB advantage over cable 1. The optimal twist lays and the well balanced pairs are the reasons for this improvement.

The crosstalk for the IBM type I standard is almost at the ambient noise level since its two pairs are individually shielded.

From the above data it can be seen that significant gains can be made on cable transmission losses by the choice of insulation material and/or design

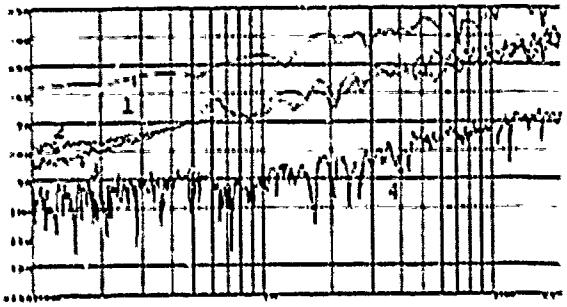

Figure 1.1.3: Crosstalk comparison

characteristic impedance. Signal to noise ratio on the other hand can be controlled using individually shielded pairs or a proper selection of twist lengths.

1.2 DIGITAL CHARACTERISTICS

In a digital environment, the cable cannot be dissociated from the system on which it is operating: its performance will be dependent on the transmitted frequency, the encoding technique, the presence / absence of filtering etc.. The method used for the study of the cable types is the analysis of the eye pattern through which the effect of the transmission parameters on the signal can be seen for various bit patterns

Two Local Area Networks having different properties were studied: the IBM Token Ring (IEEE 802.5[4]) and Ethernet by Lattisnet (IEEE 802.3[5]). The differences between the two are given in Table 1.2.1.

	IBM TOKEN RING	SYNOPTICS Ethernet
OPERATING FREQUENCY	4 MHz	10 MHz
ENCODING TECHNIQUE	Differential Manchester	Manchester
ARCHITECTURE	Star-Ring	Star
DRIVING SIGNAL	Not filtered	Filtered

Table 1.2.1: IBM Token Ring and Synoptics Ethernet systems

The "eye pattern" is the result of superimposing all possible pulse sequences during a defined period of time. Since a random signal is fed through the pairs, a large selection of combinations are recorded. For that reason it was found that the "eye pattern" is the most efficient method to evaluate a cable for a given system. Not only is the strong influence of the analog parameters visible but the decision area for a given system can easily be defined.

For error free transmission and/or regeneration, the eye must be open, meaning a decision area must exist.

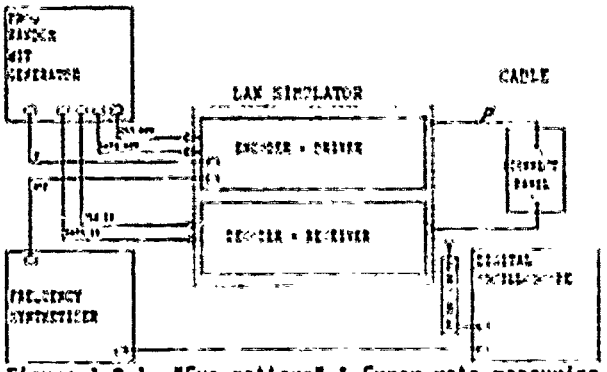

Figure 1.2.1: "Eye pattern" & Error rate measuring setup

Figure 1.2.1 depicts the measurement setup used for the evaluation of eye patterns. It is composed of a Frequency Synthesizer (FS), a Programmable Random Bit Generator (PRBG), a LAN simulator which is a replica of the final stage of a network card (encoder/decoder, driver/receiver), and the cable under test. The LAN simulator circuits were designed and developed for Ethernet and Token Ring systems providing the capability to inject a known bit stream from the PRBG.

The FS provides a square wave signal to an oscilloscope and the LAN simulator which after conditioning returns it to the PRBG. The PRBG then returns the clock and a data signal to the LAN simulators to be encoded and driven along the cable through an interconnect panel and back to be received and decoded. The data along with the clock are sent back to the PRBG to be compared to the original data and analyzed. This allows the original transmission to be compared with the received signal and the error rate monitored.

A digital oscilloscope with a differential probe is used to analyze the signal at the receiving end of the interface. The oscilloscope, connected to a PC, transfers the data via a GPIB bus. An application software controls the instrument and compiles the data. A minimum of a thousand traces were stored for one test. The superimposition of these traces are used to make up the "eye pattern". The different shades in the traces are a function of the density of points accumulated at this particular position: The darkness of the lines is proportional to the number of occurrences of the same measured value.

In the following section eye pattern traces are shown for measurements made on Token Ring (4 Mbps) and Ethernet. Data is presented for identical lengths of cables 1, 2 and 3 and at the reach limit of each cable for the two systems. The effect of crosstalk on eye pattern is also shown.

Note: all graphs use the same scale.

TESTS AT 500 FEET

Token Ring 4 MHz - Differential manchester

The encoding technique used by the Token Ring is the differential Manchester. Its signalling scheme follows three rules: a signal transition always occurs in the centre of the bit time; a zero bit has a transition at the beginning of the bit time contrarily to the one bit which has no transition. The DC level is around 0 V.

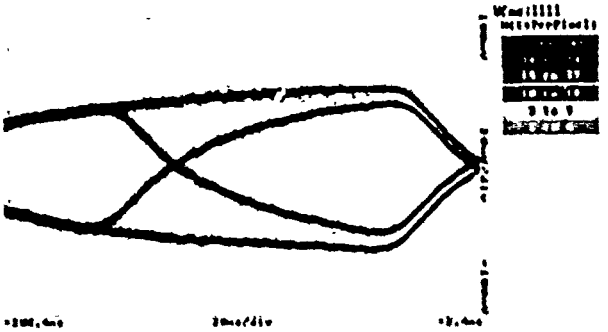

Figure 1.2.2: CABLE TYPE 1, 24 AWG, 500 feet

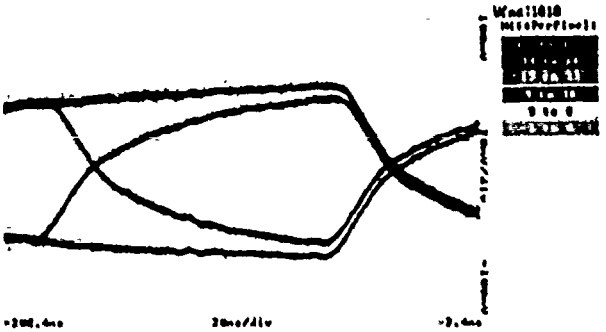

Figure 1.2.3: CABLE TYPE 2, 24 AWG, 500 feet

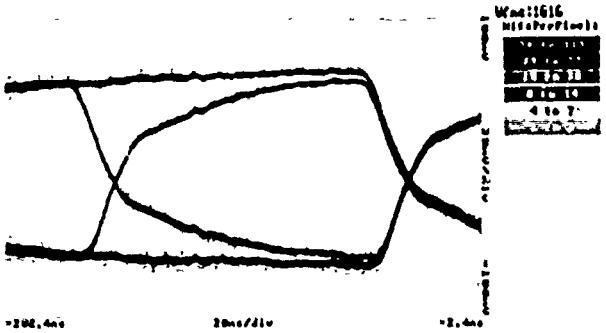

Figure 1.2.4: CABLE TYPE 3, 22 AWG, 500 feet

Ethernet 10 MHz - Manchester

The encoding technique used by the Ethernet system is the Manchester. It's signalling scheme follow two rules; each bit symbol is split into two halves with the second half containing the binary inverse of the half; the first half contains the complemented and the second half contains the uncomplemented signal of the bit value. Like the differential Manchester, a transition always occurs in the middle of each bit-symbol.

Figures 1.2.5 to 1.2.7 show equal lengths of 500 feet for cable types 1, 2 & 3 but on the Ethernet LAN.

Ethernet systems transmit at a much higher frequency (10 MHz). As seen on the graph, the amplitudes have decreased significantly.

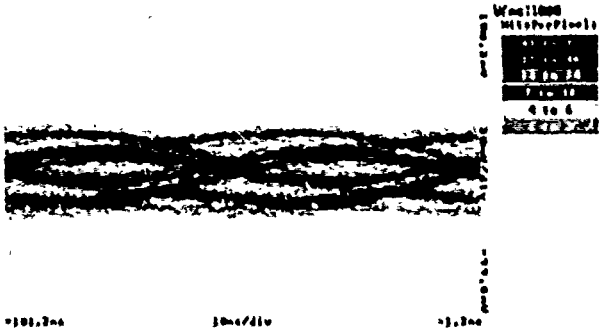

Figure 1.2.5: CABLE TYPE 1, 24 AWG, 500 feet

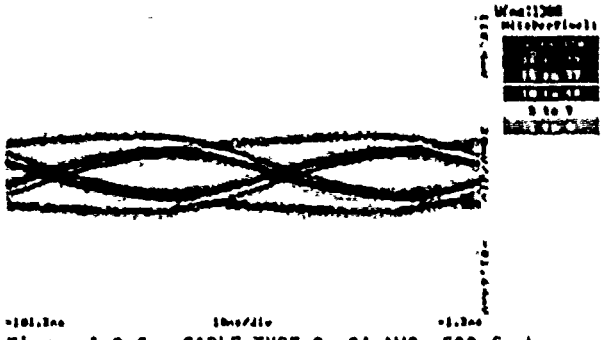

Figure 1.2.6: CABLE TYPE 2, 24 AWG, 500 feet

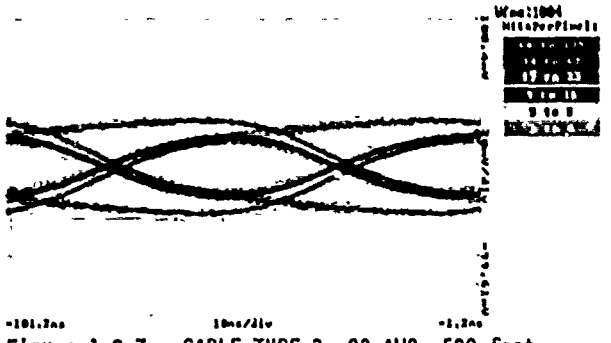

Figure 1.2.7: CABLE TYPE 3, 22 AWG, 500 feet

TESTS AT REACH LIMIT

The performance of a system is evaluated by the tolerance margin available to make a decision on the received signal. This parameter is defined at the aperture of the eye. The openness of the eye can be affected by a decrease in signal level or an irregular shift in time of the incoming bit sequence known as jitter. The system electronics set the maximum jitter and signal attenuation in the form of a minimum aperture required for proper system operation. These are sometimes given in the form of a template with well defined height and width. In the case of cable type 1, the length studied is very close to the reach limit of 600 feet for the Ethernet LAN (fig 1.2.5). The eye is almost closed, the system has reached its operational limit.

When looking at any "eye pattern" two discrete traces can easily be seen for the binary levels. Two amplitudes are observed for each trace, one corresponding to a series of 1's or 0's and the other to a series of alternating 0's and 1's. The latter has the lowest amplitude since the apparent frequency is higher and therefore the signal more attenuated. When a series of continuing 1's or 0's are transmitted, i.e. there is more time for the cable to charge or discharge , thus the voltage amplitude can reach a higher or lower steady state amplitude than when alternating 0's and 1's are sent.

Of the three cable types, the signal on cable 3 has the highest amplitude and the steepest rise time, hence a larger eye opening and a larger decision tolerance for the system (fig 1.2.4).

Jitter measurements are made by measuring the width in time of the trace at the zero crossing point.

In order to identify the minimum decision levels that exist for the two systems, amplitude and time, measurements were performed at the reach limit.

TOKEN RING - REACH LENGTH

The three cable types measured at the maximum reach limit for the IEM Token Ring system gave identical values of 19 ns for timing jitter. A minimum amplitude of 2 V peak to peak is measured.

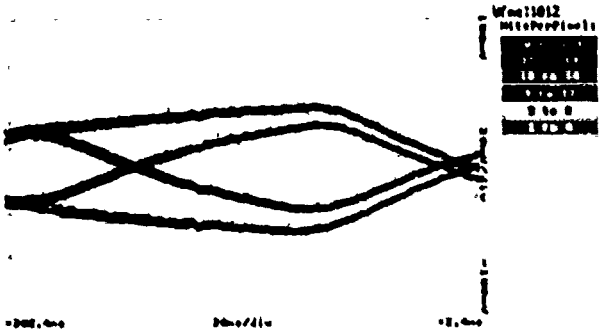

Figure 1.2.8: CABLE TYPE 1, 24 AWG, 800 feet

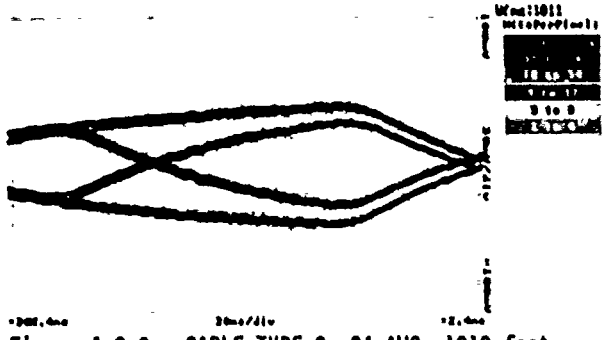

Figure 1.2.9: CABLE TYPE 2, 24 AWG, 1010 feet

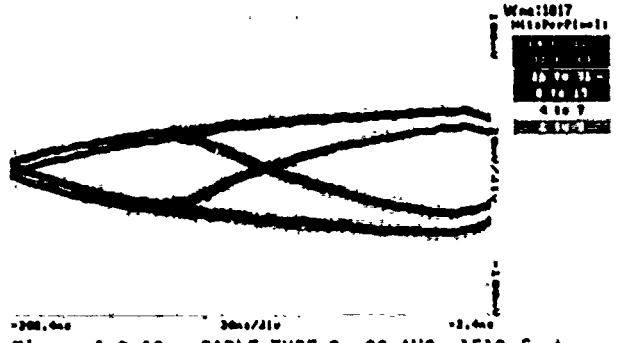

Figure 1.2.10: CABLE TYPE 3, 22 AWG, 1510 feet

ETHERNET - REACH LENGTH

Measurement on Ethernet systems are presented in figures 1.2.11 to 1.2.13 where scale and gain has been changed to focus on the decision area since the minimum amplitude is around 200 mV.

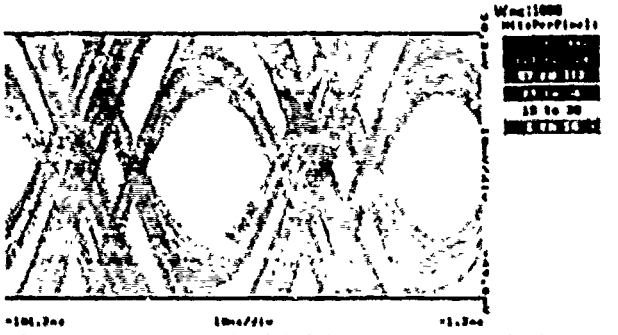

Figure 1.2.11: CABLE TYPE 1, 24 AWG, 600 feet

Figure 1.2.12: CABLE TYPE 2, 24 AWG, 800 feet

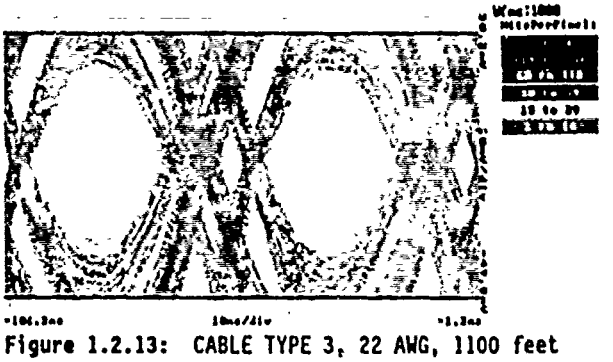

Figure 1.2.13: CABLE TYPE 3, 22 AWG, 1100 feet

In the case of the Ethernet network, the system can tolerate a much smaller aperture. The eye is almost closed before the system fails to transmit error free. Again the limit in voltage amplitude is the same for all three cable types at their maximum operating length.

It is clear that the effect of attenuation is significant; the degradation of the signal causes the eye to shrink to a certain limit. Once encoded, the frequency of the data varies in time, and the different amplitudes of these frequencies are well seen in the graphs

CROSSTALK CONSIDERATIONS

Another factor affecting the digital performance of a cable is crosstalk. Tests with two systems operating within the same cable were performed. The objective was to determine if the crosstalk of pair 1 and 2 from the first system was disturbing pair 3 and 4 of the second system.

The setup used was with Ethernet because of its higher bit rate. The LAN simulators were connected to the disturbing pair and actual LAN signals were connected to two other pairs. The result in Figure 1.2.14 shows the influence is not visible on the eye pattern.

To magnify the effect of crosstalk, an RF generator was used to induce noise in the adjacent pairs. With an output signal of 20 dB, the result is more visible (Figure 1.2.15): the ripples induced account for almost 15% of the amplitude of the original signal. Knowing the crosstalk level of cable 2 at 10 MHz is -45 dB, the induced noise level using the RF Generator is close to -25 dB.

In reality it is unlikely a system with that much power would run on an adjacent pair. The objective of this exercise was to show the effect of strong crosstalk on system performance.

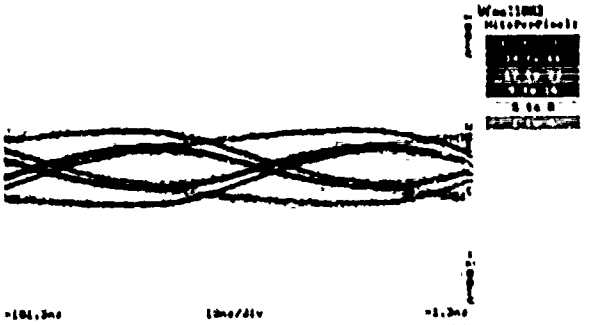

Figure 1.2.14: CABLE TYPE 2, Crosstalk: 10 Mbps Ethernet

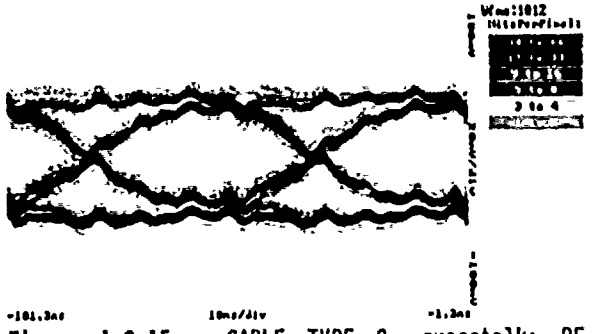

Figure 1.2.15: CABLE TYPE 2, crosstalk: RF Generator

2 - EMI CONSIDERATIONS

In 1968 the Federal Communication Commission was mandated to enforce legislation controlling electro magnetic interference from electronic devices at frequencies between 30 MHz and 1000 MHz. Harmonics from systems having much lower frequencies, digital systems in particular, can easily generate interference in this bandwidth.

With the evolution of higher bit rate systems (10 and 16 Mbps), radiated EMI from the transmission media is of serious concern to the system designer. Parameters affecting radiation must be evaluated in the design of a cable for digital transmission.

In this section the effect on radiated emissions were studied for cables 1 to 7. These cables have different design parameters which can affect EMI such as different types of shield or pair balance.

Two methods were used to evaluate the cable performance. In the first instance a method was developed to increase the sensitivity of measurements by isolating the cable from all other electronic equipment. Development of this test method was required since all recognized standards specify that measurements be made on the complete system including the electronic equipment, cables and other peripheral devices. Once the tests were completed, measurements were made in accordance to the FCC MP4 standard for verification that discrete frequency components do not exceed the FCC limits. In this case the cable is tested as an accessory to a computing device.

Both measurements were made in an open field environment. This was done to eliminate reflections in the 30 to 200 MHz bandwidth. Anechoic cones in a shielded room cannot fully absorb reflections in this bandwidth. No data was recorded at frequencies above 230 MHz due to the low level of the harmonics at these frequency.

2.1 CABLE EMI TESTING

The test procedure developed for measurements on the cable alone is a derivation of the FCC MP4 procedure. The cable sample is placed on a rotating boom and configured to expose a length of 10 ft horizontal and two vertical lengths of 7 ft each. It is energized with a broadband signal to obtain measurement over a wide frequency spectrum. A schematic of the test set-up is given in Fig 2.1.1.

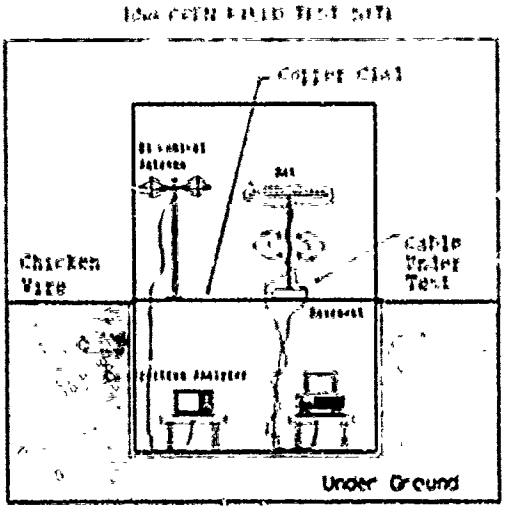

Figure 2.1.1: EMI Test Setup

This configuration fulfils two functions; it maximizes the field in a single direction and is a good simulation of an actual installation. With the cable transmitting the antenna is oriented to find the maximum field intensity. The antenna is then set in this position. Measurements are taken on a spectrum analyzer synchronized to the broadband source. Data is collected in the 30 MHz to 230 MHz frequency range and is tabulated in a field strength vs frequency plot with the field strength given in $dB_\mu V/m$

Measurements were made in a balanced mode using impedances matched to a broadband source and the cable terminated with its characteristic impedance. Return to ground for shielded products was provided through the wall outlet earth protection which was verified to be a good ground.

The results observed show the significant impact of design parameters with respect to EMI compatibility. Measured data is summarized in figs 2.1.2 and 2.1.3 where it can be seen that cable type 4 having a foil/braid shield radiates the least energy when properly terminated. However when the shield on this cable is no longer terminated to ground, emissions become much greater and much worse than for unshielded cable types tested.

It is also seen that the frequency response of cables is an irregular function of frequency i.e. higher frequency signals will not necessarily radiate more.

Another observation made was that the emissions from the higher impedance cable were much greater. This can be explained by the closer coupling of the cable to free space which has a characteristic impedance of 377 ohms.

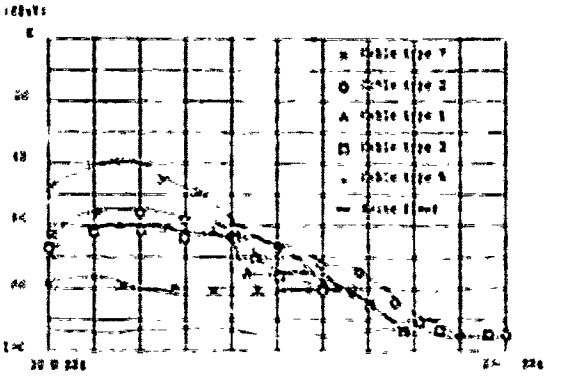

Figure 2.1.2: Measured emission for sample set 1

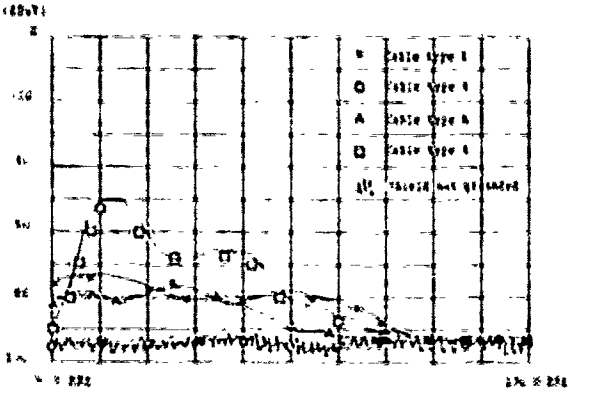

Figure 2.1.3: Measured emission for sample set 2

Sample set 1 is mostly 150Ω cables. Sample set 2 is mostly 100Ω cables. Cable 7 is in both sets as a reference point

2.2 SYSTEM MEASUREMENTS TO FCC

Having evaluated the performance of different cable designs subjected to a broadband source, actual system tests are needed to verify compliance with the FCC requirements.

It is important to note that the intent of the FCC regulations is to protect the customer from radio interference, implying that all LAN environments must be free from interference. Interference can originate at the computing device, along the cable path and at the cable concentrator.

FCC states that the measurements must be made on the worst case. The method adopted here was to include the maximum cable loop length as an accessory to the device under test combining the computing and cable path environment. Measurements on the cable

concentrator were not performed since the signal on the cable is the strongest at the computer (regenerator) end of the cable.

Using this setup, tests were performed on three systems with different cable types. The test results are summarized in Table 2.2.1.

The FCC MP4 measurement procedure is based on a unit under test which is placed on a rotating table three meters from a biconical antenna adjustable in height and polarity. The angle of the antenna is adjusted to obtain a worse case measurement for each unit under test. Appropriate software is used so that there is a traffic load between computers.

As for the previous measurements the results are plotted for field intensity vs frequency. The FCC field strength limit set for certain bandwidth is also shown in Figure 2.2.1. Under these test conditions peaks at discrete frequencies were observed at harmonics of the transmission base rate. Emission levels of different cable types at these harmonics represent the maximums and are summarized in Table 2.2.1. This data is for system measurements made without media filters. It shows that it is possible to meet the FCC limits at 16 Mbps using unshielded cable designs.

	Ethernet	Token Ring 4	Token Ring 16
Cable 1	10.0	20.4	35.0 *
Cable 2	10.3	21.8	35.8 *
Cable 3	9.6	21.0	28.4
Cable 4	N.A.	Noise floor	Noise floor
Cable 4 (No grnd)	N.A.	24.3	37.5 *
Cable 7	7.6	19.0	27.5

Table 2.2.1: Verification results

Notes: Values are dBμV/m at 30 meters
FCC Limit = 30 dBμV/m
* = Exceeding limits

This data agrees well with that observed in section 2.1. It is clear the higher characteristic impedance of the cable has a negative impact on radiation.

As observed earlier it can also be seen that radiation is not necessarily a function of frequency or bit rate. In the case of system tests however other parameters come into play such as signal levels, signal shaping, coding and filtering.

It is important to note that significant EMI improvements can be made on unshielded designs through design and process optimization.

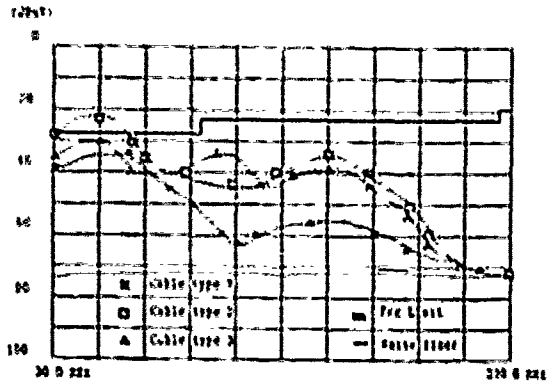

Figure 2.2.1: Cable radiated emission VS ambiant noise.

3 - SYSTEM TEST

There are many reasons for developing a better inside cable. Ultimately, it will be connected to a data network to enhance performance such as: providing a safety margin for actual equipment as well as planning for future improvements in technology, extending the reach of the actual system to connect workstations placed further from the wiring closet, simplification of the cabling system by using only a few types of cables.

System tests have been performed to evaluate the performance of the cables for particular LAN systems. Three LAN systems (IBM Token Ring® 4 Mbps Ethernet by Lattisnet® 10 Mbps and IBM Token Ring® 16 Mbps) operating with various cabling solutions were evaluated for the setup. The goal was to observe the difference of reach attainable by changing the type of wiring used.

Figure 3.1 depicts the setup used for system tests. The list of hardware and software used can be found in appendix C.

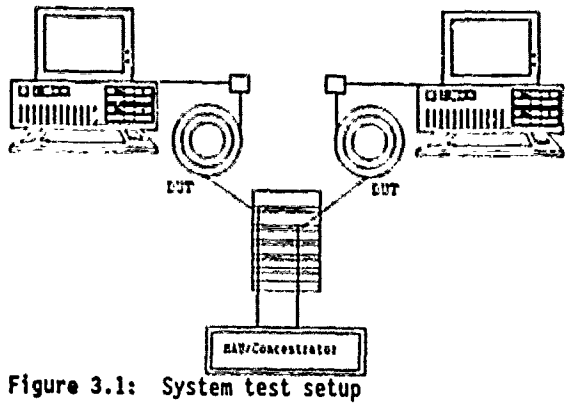

Figure 3.1: System test setup

The PC's are connected to the wall outlet with a short length of patch cord (10 feet). From the wall outlet, the cable to be tested is connected to the concentrator/access unit.

One PC was configured as a file server. The PC's were then switched on and diagnostic tests were performed. An error-free communication with the file server was the criterium for accepting the link as valid. The length of the cable was increased to the point where the system was unable to communicate correctly. This yielded the system reach values shown in Table 3.1. These can then be compared on a relative basis.

SYSTEM	Token Ring 4 Mbps	Lattisnet 10 Mbps	Token Ring 16 Mbps
Cable 1	790	610	300
Cable 2	1010	790	500
Cable 3	1530	1105	800
Cable 4	1880	1340	1040

Table 3.1: System reach values in feet between PC and MAU/Concentrator

It is to be noted that the value obtained for the token ring system as measured is the maximum ring length. The reach for the Lattisnet system is the length of the drop between the concentrator and the transceiver.

The analysis of the attenuation values for different cables yields results which are consistent with previously observed data in terms of the attenuation budget for the cabling system are as follows:

IBM Token Ring 4 Mbps: 12.5 dB
Lattisnet 10 Mbps: 15.0 dB
IBM Token Ring 16 Mbps: 13.0 dB

It was observed that the improvement in transmission characteristics of unshielded twisted pair cables, particularly the attenuation, yields enhanced reach for LAN systems. This also demonstrates that it is possible to operate 16 Mbps systems on unshielded twisted pair cables of suitable design.

CONCLUSION

Seven cable types have been studied in this paper ranging from the traditional inside wire (DIW) to shielded cable such as the IBM type I (Table I).

The development of measurement methods towards characterization of digital transmission characteristics was presented. Findings on analog, EMI and digital parameters considered for the design of an improved cable were given. The results of system tests using these new designs corroborate that test methods are available for the system performance evaluation of new cable designs.

Analog and digital characterization performed on the cable types have enabled us to pinpoint the parameters which must be taken into account in the design of a better cable.

Attenuation was shown to be the dominant factor for system reach. Significant improvements can be realized through an optimal choice of materials.

The EMI tests showed that a properly constructed unshielded cable can have excellent EMI properties and meet FCC limits as well as outperform a shielded cable that is not well terminated.

The optimal cable design choice to the end user must be cost effective and provide ease of installation. It is these considerations which have brought the standard practice to using unshielded 24 AWG twisted pairs.

The data presented here shows that it is possible to push the performance of unshielded twisted pairs towards higher bit rates while providing installation advantages. Actual system tests showed that improvement of 70 % at 16 MHz, 30% at 10 MHz and 27% at 4 MHz for reach are attainable.

REFERENCES

1. R. B. Hobgood, 1983 IWCS Proceedings, pp 271-276.
2. TIA/EIA Commercial Building Wiring Standard PN-1097, Draft 8.0, July 1989.
3. IBM Cabling System, Technical Interface Specifications, second edition, International Business Machine 1987.
4. ANSI/IEEE Std 802.5-1985 ISO/DP 8802/5 Institute of Electrical and Electronics Engineers Inc., New York, NY.
5. ANSI/IEEE Std 802.3-1985 ISO/DIS 8802/3, Institute of Electrical and Electronics Engineers Inc., New York, NY.

* IBM Token Ring is a Trademark of Internation Business Machine Corporation.

* Lattisnet is a Trademark of Synoptics Communications.

APPENDIX A

ANALOG MEASUREMENT EQUIPMENT

1- Network Analyzer
1- S-Parameter Test Set
2- Baluns (50Ω unb/ 100Ω bal, 50Ω unb/ 150Ω bal)
1- AT compatible computer

APPENDIX B

DIGITAL MEASUREMENT EQUIPMENT

1- Frequency Synthesizer
1- Digital Transmission Analyzer
2- Ethernet LAN simulator (inhouse design)
2- Token Ring LAN simulator (inhouse design)
1- Digital Oscilloscope
1- Differential Probe

APPENDIX C

REACH TEST MATERIAL

HARDWARE

2 - PC's, AT's or good compatible
1 - Cross-connect panel

(Token Ring)
2- Token ring adapter 16/4
1- Token ring Media Access Unit
2- Media Filters
2- RJ11 Baseboard jack
Misc: Data connectors, patch cords,

(Lattisnet)
2- Ethernet adapter card
1- Lattisnet 1010 concentrator
1- Lattisnet 405 UTP host
2- Lattisnet 505 UTP transceiver
2- RJ11 baseboard receptacle
Misc: patch cords, adapter cables

SOFTWARE

Microsoft DOS 3.3

(Token Ring)
IBM LAN program
IBM LAN support program

(Lattisnet)
Novell Advanced Netware
Etherlink diagnostics

Michel Plasse received his B.E. in Electrical Engineering from Ecole Polytechnique de Montréal. He joined Northern Telecom Canada Limited Communication Cable Division's Research & Development department in 1987 where he is responsible for systems characterization and electrical test methods.

Lise Desroches received her B.E. in Electrical Engineering from Ecole Polytechnique de Montréal. She joined Northern Telecom Canada Limited Communication Cable Division's Research & Development department in 1986 where she is responsible for cable design and characterization.

Paul-André Guilbert received his B.E. in Electrical Engineering from Université de Sherbrooke. He joined Northern Telecom Canada Limited Communication Cable Division's Research & Development division in 1985 where he is responsible for shields design and EMI measurements.

NEW GENERATION OF INDOOR CABLES

F. Shaikhzadeh K. Fukui N. Ishizaki J. C. M. Souza

Furukawa Industrial S.A. Produtos Elétricos
Rua Afonso Brás, 413 - 04511 - São Paulo - SP - Brazil

Abstract

Historically, indoor distribution cables in telephone exchanges and buildings have been PVC insulated. However, with the introduction of the ISDN, the use of digital transmission mode is increasing rapidly as well as transmission rates. As a result of this, conventional indoor cables present some problems for digital transmission, such as: (1) impedance unbalance between the indoor and the outside cable causes return losses and pulse distortions (2) transmission characteristics change according to room temperature; and (3) the signal attenuation increases proportionately to the transmission rate.

To reduce or eliminate these problems, a new generation of indoor cables was developed, which keeps the electrical and transmission characteristics close to those of the outside plant cables. Besides, these characteristics do not change with temperature and frequency variations.

Introduction

In the last few years, there has been a great increase in the utilization of optical fiber cables in telecommunications networks. Now, many countries have a great number of optical trunk cables (exchange to exchange), but the distribution network is nearly always built with metallic cables and it has resisted the introduction of optical fiber cables due to, mainly, economic reasons.

Thus, we can foresee that in many countries and for a long time, the distribution network will continue being metallic, and trunk cables will gradually be replaced with optical cables. However, investments in outside plants are very expensive and at present, many now-installed metallic cables will only reach the end of their life-time in one or two decades. This fact does not allow the substitution of all metallic cables with optical cables. It is only possible in the three following cases:

(1) New installations;
(2) Substitution of defective cables or cables at the end of their life-time;
(3) Substitution of cables installed in high-density telephone regions, where ducts are full.

Because of this, metallic and optical cables will continue to coexist in the same outside plants in many places and for a long time. This coexistence constituting a hybrid network and beyond any doubt, the distribution network will continue with metallic cables.

At present, most metallic outside plants are made up of both paper-insulated and foam-polyethylene insulated cables, while most indoor cables (both on the subscriber side, and on the exchange side) are made up of PVC insulations.

Insulation materials and also the design of outside cables are different from the materials and designs often used in indoor cables. Consequently, the electrical and transmission characteristics of both families can be very different, and the cables do not react to the transmitted signal the same way.

Outside plant cables and also distribution cables have a characteristic impedance and propagation velocity greater than PVC-insulated cables. This fact causes a distortion in the transmitted signal from a type of cable to another, which is known as impedance unbalance. When the signal propagates from an indoor cable to an outside cable, there is a signal loss in the joint point. Furthermore, there is also a distortion in the transmitted signal at this point. Throughout the line, a distortion and a signal loss happen at least twice in the output of the subscriber line and in the input of the telephone exchange.

In the conventional telephone transmission for voice telephony, this signal unbalance has little importance. But, with the introduction of the ISDN (Integrated Service Digital Network), more services are added to the network such as: Data Transmission, Facsimile, Videotext Service, etc. In this case, the transmitted signals are not analogic, but digital, and there is an increase in the transmission rate and, consequently, in the signal frequency.

The signal unbalance and the pulse distortion that occur in the joint of indoor cable with the outside cable in a digital transmission can cause many problems. Digital pulses might be very atennuated and very distortioned, and in this case, they will be read by the signal listener as transmission errors. Then, all the pulse package must be retransmitted. This reduces the transmission speed, and, consequently, the final efficiency of the Digital Network.

Another problem that occurs with the PVC-insulated cables (especially in tropical areas) is the variation of their electrical and transmission characteristics due to frequency or room-tempera-

ture changes. In a PVC-insulated cable, when the room temperature rises, the cable capacitance increases drastically. Consequently the impedance, the attenuation and the propagation velocity become variable.

In an analogic signal transmission, this fact does not cause a significant alteration in the transmission quality, but for Digital Pulses at high frequency, the temperature effect alters the signal and the transmission rate, which worsens the losses and distortions that occur in the joint of indoor and outside cables.

To reduce or eliminate these problems, a New Family of indoor cables was developed to be used in telephone exchanges and internal subscriber lines. This new family reduces the impedance unbalance that occurs in the joint of indoor cables and outside cables. Moreover, they have very good stability in their electrical and transmission properties with temperature or frequency variations.

This New Family of cables was developed according to the following premises:

(1) Electrical and transmission properties as close as possible to the common cables used in outside plants.

(2) High flexibility and good mechanical strength assuring an easy and safe installation.

(3) Elevated thermal class assuring a good level of safety in installations with high-density wiring.

(4) Excellent flame-retardant properties in conformity with the UL and CSA standards.

All these objectives were reached through the use of precise design parameters and the development of a new type of insulation material. This material is a modified polyolefin with properties very similar to the polyethylene or polypropylene. This material results from a polyolefin basis added with brominated alycyleic flame retardant plus a metal oxide to get improved flame retardant properties. In this formulation is added a proper filler to increase certain properties of the insulation and so helping the flame-retardancy. Stabilizer, color concentrate and other additives are used to reach the final required properties of insulation.

Insulation Material

The insulation material of the New Family of indoor cables is made with a modified polyolefin, which has similar properties (especially electrical properties) to those of the polyolefins often used for insulation of outside plant telecommunication cables. Besides, it is a flame-retardant material, and consequently, suitable to internal use.

Table 1 presents the main properties of this insulation material. In this table, one can see a comparison with other materials commonly used as insulation of conventional telecommunication cables.

The following advantages are possible with the use of the new material in relation with PVC insulations:

(1) The density of the modified polyolefin is about 25% bellow the density of the typical PVC insulation. This allows reduction in the cables weight of products made with this new material.

(2) The volume resistivity of the new material is approximately one million times superior to the volume resistivity of conventional PVC insulated cables. This results in insulation resistances quite superior to that of PVC-insulated cables, thus offering higher safety for the user.

(3) The break elongation of the new material is also superior, which contributes to a greater flexibility of the cables insulated with the new

PROPERTIES OF INSULATION MATERIAL

Property	PVC	Paper	Polyolefin	New Material
Dielectric Constant at 1 MHz	4 ~ 6	1.7	2.3	2.3
Volume Resistivity, Ohm/cm	10^{11}	10^{13}	10^{17}	10^{17}
Specific Gravity	1.2 ~ 1.5	0,73	0,93	1,05
Elongation at Break (%)	200 ~ 400	–	500 ~ 700	700
Flame Retardancy	Yes	No	No	Yes

TABLE 1

modified polyolefin.

(4) At last, the dielectric constant of the new material is half of a typical PVC compound used in the insulation of indoor cables. This factor allows designing and manufacturing of indoor cables with similar transmission properties to those of outside-plant cables, because the capacitance is proportionate to the dielectric constant, and the characteristic impedance, the attenuation and the propagation velocity are strongly dependent on the cable capacitance.

In addition to these advantages, the modified polyolefin has exceptional stability in relation to the dielectric constant with variations of temperature and measuring frequency, which is the contrary of what happens with PVC-insulated cables (figures 1 and 2). Therefore, the transmission characteristics of the cables insulated with the new material will not change with variations of room temperature and signal frequency.

Design of the Family of Cables

The conductors of this new family of cables are made of fully-annealed copper, usually tinned. These conductors are solid when the cable is used in telephone exchanges or in internal distribution of buildings. They may be flexible if the cable is used in equipment connections or when the installation requires high-flexibility cables.

The conductors are insulated with the new modified polyolefin, as explained in the last topic. A suitable thickness is used to reach the appropriate cable capacitance.

The insulated wires are identified by using a color code or by ring-marking printing. These wires are twisted in pairs and are concentrically cabled to form a cable core. This core is covered with a non-woven tape and shielded with an aluminum/polyester laminated tape, spiral wrapped around the cable core. A drain wire of tinned copper is spiral-wrapped around the aluminum/polyester tape in continuous contact with the aluminum for the grounding of the cable.

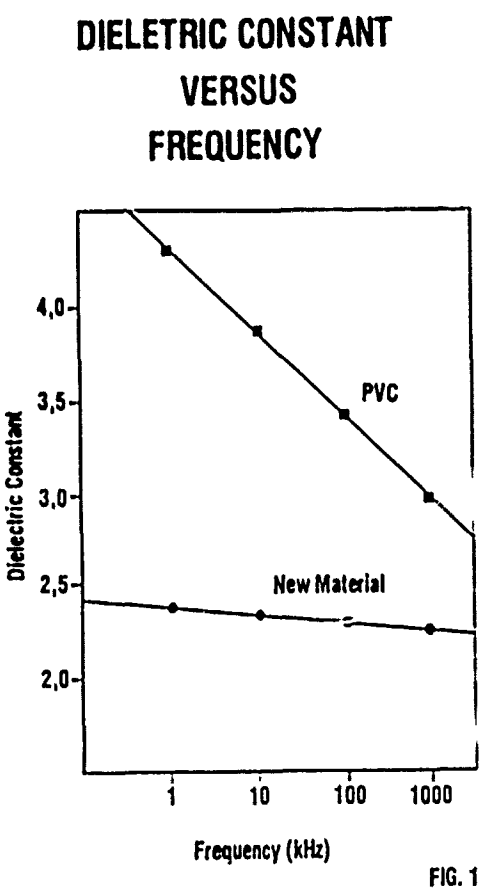

FIG. 1

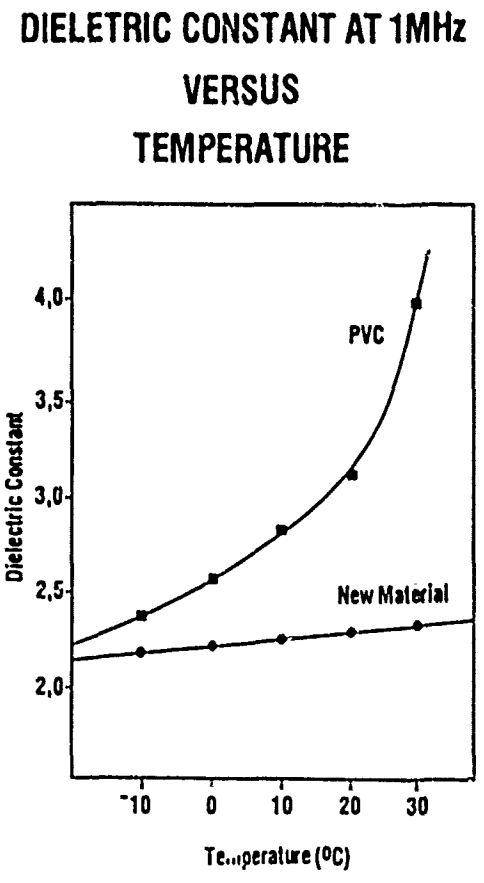

FIG. 2

A jacket of UL-approved flexible PVC is applied around the core to form the complete cable.

Evidently, many cable constructions can be made according to the above parameters. Because of this, only one type of cable arrangement will be analyzed in the following topics. This cable arrangement has a conductor diameter of 0.50 mm and a thirty-pairs core. This is a very common cable configuration in the Brazilian Telephone Network, both in the subscriber side and in the exchange side. The same cable construction, but with PVC insulation, is also analyzed for comparison.

Main Features of the New Family of Indoor Cables

Table 2 shows the main characteristics of the different types of cables. In this table, we can see the following features of the new family of cables:

(1) The new insulation material allows capacitances close to the capacitances of the outside-plant cables.

(2) Therefore, the new cables have transmission characteristics very similar to those outside-plant cables.

(3) The new cables have superior insulation resistance and, therefore, they are safer.

(4) The transmission properties of the new cables do not change with temperature and frequency.

Table 3 shows some characteristics of the new family of cables in comparison with the same cable construction insulated with polyvinyl chloride. The characteristics are shown for cables with diameter of 0.50 mm and a 30-pair core.

First of all, we can observe a 10% weight reduction in relation to the conventional cables. This allows for a decrease in the cable pull-tension and easier handling. Moreover, the cable diameter is 11% smaller than that of conventional cables which allows for an easier duct installation and a higher number of cables put in a duct.

The insulation resistance is increased greatly, and the dielectric strenght between conductors or between conductors and shield is twice as much as in conventional cables. These two advantages of the cables allow for a safer cable operation even in installations with a very large number of cables, because the resistance to damages from lightning and short-circuit is increased.

The transmission characteristics of the new cables, such as impedance, attenuation and propagation velocity, have been greatly improved if compared with conventional cables. This improvement allows for a better signal transmission, with less distortion of pulse and signal attenuation.

Moreover, these characteristics are very close to those of the outside-plant cables. This reduces or even eliminates the impedance unbalance that occurs in the joint of the indoor and outside-plant cables. With this, we can have much less digital-pulse distortion and much fewer signal losses in this joint.

Electrical Characteristics in Relation to Temperature

Figure 3 shows the variation that occurs with the capacitance of PVC-insulated cables when the temperature changes. The same figure shows the excellent capacitance stability of the new cables.

The capacitance of conventional cables ranges from 77 nF/km at 0 degrees to 118 nF/km at 40 degrees, while the new cables have a practically stable capacitance in this temperature range. Thus, the new cables have very stable transmission characteristics and their impedance, attenuation and propagation velocity do not vary in this temperature range.

The variation of the transmission characteristics of the conventional cables is big problem in tropical areas or in air-conditioned buildings, where the cables frequently pass from warm or cool rooms to room-temperature places. This can cause variations in the transmitted signal, especially in case of a digital signal in high-transmission rate.

COMPARISON BETWEEN TYPES OF CABLES

Property	Paper Insulated	Polyethylene Insulated	PVC Insulated	New Cable
Capacitance (nF/km)	56	54	100	54
Propagation Speed (%)	77	66	48	66
Insulation Resistance (MΩ . km)	5,000	15,000	600	15,000
Temperature Dependency	No	No	Yes	No

TABLE 2

CHARACTERISTICS OF THE NEW CABLE

Property	Conventional Indoor Cable	New Cable
Conductor Resistance (Ω/km)	97.8*	97.8*
Insulation Resistance (MΩ. km)	600*	15.000
Dielectric Strength (Volts)	1.500	3.000
Characteristic Impedance (Ohms) at 1 kHz	600*	750
Attenuation (dB/km) at 1 kHz	1.9*	1.4
Propagation Speed (%)	48*	66
Mutual Capacitance (nF/km)	100*	54
Cable Diameter (mm)	13.5	12.0
Cable Weight (kg)	230	209

* Variable with temperature

TABLE 3

Another characteristic which varies with the temperature is the insulation resistance. For conventional PVC-insulated cables, the insulation resistance decreases very rapidly with temperature increases, as shown in figure 4. This fact may cause low insulation between the conductors of these cables. Problems with low insulation will not occur with the new cables, because the volume resistivity of the new material is very stable with temperature changes and the insulation resistance of the new cables is pratically constant in the room-temperature range.

Electrical Characteristics in Relation of Frequency

In conventional PVC-insulated cables, the mutual capacitance decreases with the increase of the transmission frequency, as shown in figure 5. This way, other characteristics also vary. For example, the attenuation of the cable is greatly increased, as shown in figure 6. This limits the maximum frequency that can be transmitted by the cable. This fact is very important in large buildings, where distribution cables are very long and, in these cases, the transmission rate and the signal quality can be affected by the internal-cable attenuation.

MUTUAL CAPACITANCE VERSUS TEMPERATURE

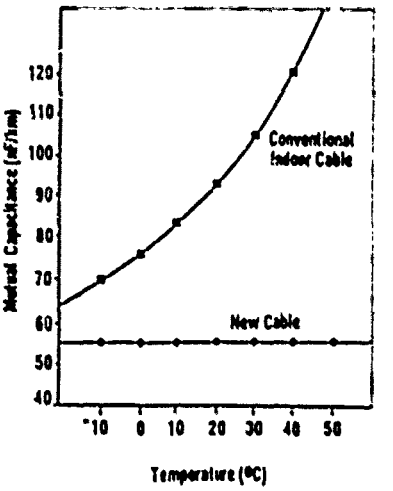

FIG. 3

INSULATION RESISTANCE VERSUS TEMPERATURE

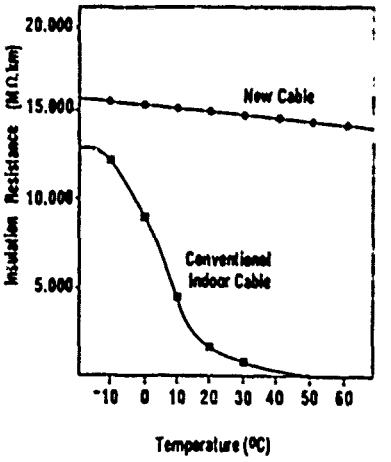

FIG. 4

MUTUAL CAPACITANCE
VERSUS
FREQUENCY

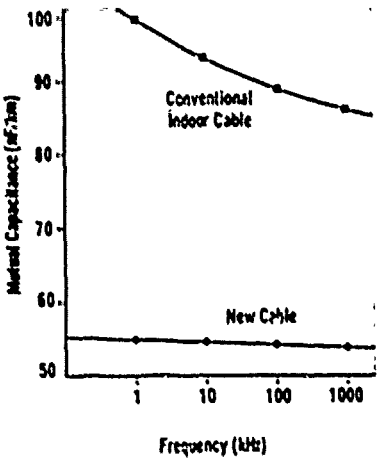

FIG. 5

The newly-developed indoor cables show an excellent mutual-capacitance stability in relation to the frequency increase. Thus, their signal attenuation increases much more smoothly than that of the conventional cables. Thus, these cables offer a signal transmission in much higher frequencies than the PVC-insulated cables. They also improve significantly the signal quality and the transmission rates.

Safety and Fire Protection

The new cables have excellent fire-retardant properties, because they are used inside buildings, and, in this case, superior safety is required. The new family of cables was designed to comply with UL standards, especially the "Vertical Flame Test" and the "Vertical-tray Flame Test" specified by UL-1581 (Figures 7 and 8).

In the former, a vertically-suspended sample of insulation shall not flame longer than 60 s following five 15 s applications of a standard gas flame. Also, the insulation burn shall not ignite combustible material in its vicinity.

In the "Vertical-tray Test" six samples of cable, with 96-in length, are fastened in a vertical steel ladder (cable tray type). A standard-test flame, supplied by means of propane-gas burner (ribbon type), is applied to the cable samples for 20 minutes. After this time, the burner flame is to be extinguished and the two following measures are recorded:

(1) The time that the samples continue to flame after removal of burner.

(2) The total length of damage to the cable on each sample.

ATTENUATION
VERSUS
FREQUENCY

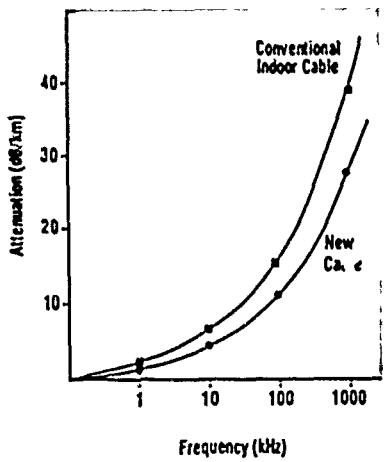

FIG. 6

UL1581
VERTICAL
TRAY
FLAME
TEST

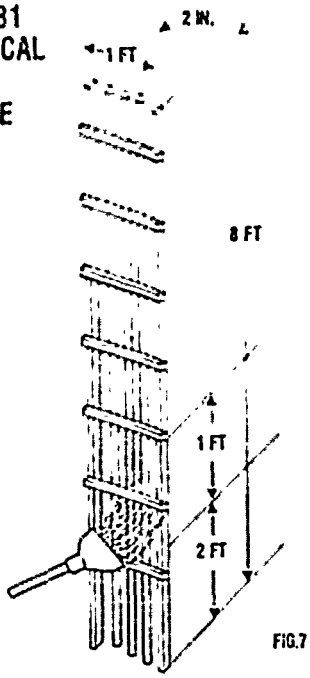

FIG.7

UL VERTICAL FLAME TEST

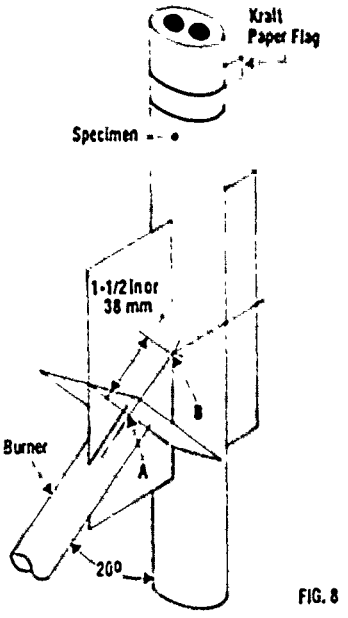

FIG. 8

The new cables are self extinguished in a few seconds after the removal of the burner flame and the length of damage in the "Vertical-tray Test" is not greater than 0.80 m for all samples.

Thus, the newly-developed cables comply, integrally, this two flame tests and others fire tests that are recognized by cable manufacturers and consumers.

Conclusion

The new family of cables is suitable for internal use in telephone-exchange distribution networks, and in commercial, residential or industrial buildings. And they are manufactured with flexible conductors, they may be used in installation of telecommunication or data equipment offering the following advantages, if compared to the conventional PVC-insulated cables:

- Their transmission characteristics are very similar to those of the outside-plant cables, which avoids the impedance unbalance between indoor and outside-plant cables, and, therefore it also avoids signal losses and pulse distortions in the joint of these cables.

- Their transmission characteristics do not change with the temperature. Thus, they may be used in tropical areas and in large air-conditioned buildings without any variations in the transmitted signal.

- The new cables present an excellent transmission stability with signal-frequency changes, which allows for the high-frequency attenuations to become much smaller than that of the conventional PVC-insulated cables. This causes higher transmission rates.

- The insulation resistance of these new cables is practically independent of the temperature changes, which contributes for safer cable operation and fewer damages to the cables.

- They are flame retardant and comply totally with the UL-standards for its cable class.

- They have a final cost equivallent to that of the conventional cables.

Foad Shaikhzadeh

Furukawa Indl. S.A.
Produtos Elétricos
São Paulo, SP
Brazil

Foad Shaikhzadeh received a B.S. degree in Electronics Engineering from the University of São Paulo in 1978. He joined Furukawa Industrial S.A. in 1979 and has worked on sales engineering, quality control and product engineering of metallic and optical telecommunications and electronics cables. He is presently the General Manager of the Technical Department.

Kingo Fukui

Furukawa Indl. S.A.
Produtos Elétricos
Curitiba, PR
Brazil

Kingo Fukui joined Furukawa Industrial S.A. after receiving the B.S. degree in Chemistry from São Paulo State University in 1975. He has been engaged in development of materials for telecommunication and eletronics cables. Mr. Fukui is currently Deputy General Manager of Research & Development activities of Furukawa Indl. S.A.

Nobuo Ishizaki

Furukawa Indl. S.A.
Produtos Elétricos
Campinas, SP
Brazil

Nobuo Ishizaki received a B.S. degree in Telecommunications Engineering from INATEL - Instituto Nacional de Telecomunicações in 1978. He joined Furukawa Industrial S.A. in 1979 and worked in the development of telephone networks, product and process engineering. He is now Industrial Manager of the computer cable assemblies plant.

João Carlos M. Souza

Furukawa Indl. S.A.
Produtos Elétricos
Curitiba, PR
Brazil

João Carlos M.Souza joined Furukawa Industrial after receiving his B.S. degree in Chemical Engineering from Federal University of Paraná in 1981. He has been engaged in development of plastic materials, irradiated polymers, optical cable design and fire protection technology. Mr. Mariano is presently Assistant Manager of the Materials Group in the Research and Development Department.

SHIELDING EFFICIENCY OF COMMUNICATIONS WIRE AND CABLE FOR HIGH SPEED TRANSMISSION

Lal M. Hore

BELLCORE, NEW JERSEY, USA

ABSTRACT

Relationship between surface transfer impedance and radiation from coaxial wires with longitudinally folded metal tapes, braid and metal/poly/metal laminated tapes is discussed. Also presented is a discussion of the measurement of surface transfer impedance with a Triaxial Cavity and radiation leakage by the Absorbing Clamp technique. Effects of flexures on the shielding effectiveness are also discussed.

The effect of shielding on twisted pair wires is established by measuring various transmission parameters of which near end crosstalk (NEXT) is of significant importance. Contained herein are also discussions on signal-to-noise ratio (SNR) and margins for various transmission impairments and their effects in limiting the distances of high speed transmission. The frequency-distance guidelines for shielded and unshielded wires are compared.

INTRODUCTION

The present day telecommunications systems intended for use in large commercial buildings, between buildings in college campus environment and central offices (C.O.) include voice, data, FAX, computer and other telecommunications applications. For these systems the distances with different types of transmission media may extend up to 10,000 feet, cover approximately 10,000 to ten million square feet of office space and for a population of between 100 and 50,000 individual users.[1]

At present three different types of telecommunications media are commonly used for both horizontal and backbone (riser) wiring within commercial premises and also within a central office environment. These media are,[1,2]

(1) Unshielded Twisted Pair

(2) Shielded Twisted Pair

(3) Coaxial

In addition to the above, 62.5/125μm Optical Fiber cable is recognized as a suitable media for use in the backbone section of the wiring. This paper will not cover the use of optical fiber media.

For use in electronically sensitive locations up to giga-hertz range, coaxial wires require adequate shielding. Proper shielding minimizes the effects of electromagnetic interference (EMI) by containing radiation and by keeping out external interference. For high speed transmission through unshielded twisted copper pairs, a trade-off between signal frequency and transmission distance has been investigated by researchers including the author of this paper. A definite need has been realized to study shielded twisted copper pairs and estimate the effect of shielding on signal frequency versus transmission distance.

This paper presents an overview of the present state of the art and the experimental results of the surface transfer impedance measurement by Triaxial Cavity Technique, and the radiation leakage measurement by Absorbing Clamp for coaxial wires. The transmission characteristics of shielded and unshielded twisted pair wires are measured, and from the near end crosstalk (NEXT) and attenuation data, a relationship between the signal frequency and transmitted distance has been estimated and presented in this paper.

EXPERIMENTAL SAMPLES

Samples used for various shielding and/or transmission measurements are,

Twisted Pair

Sample No. 1 - 25 pair 24 AWG Shielded Wire
Sample No. 2 - 25 pair 22 AWG Shielded Wire
Sample No. 3 - 12 pair 22 AWG Shielded Pair Wire
Sample No. 4 - 25 pair 24 AWG Unshielded Inside Wire
Sample No. 5 - 25 pair 24 AWG Unshielded Inside Wire
Sample No. 6 - 25 pair 24 AWG Unshielded Inside Wire
Sample No. 7 - 25 pair 24 AWG Unshielded Inside Wire

Coaxial

Sample No. 8 - RG-6 Coaxial (laminated tape and corrugated aluminum shield)
Sample No. 9 - RG-6 Coaxial (laminated tape and braid)
Sample No. 10 - RG-6 Coaxial (laminated tape and braid)
Sample No. 11 - RG-59 Coaxial (laminated tape and braid)
Sample No. 12 - RG Type Coaxial (double braided shield)

Construction and dimensional analysis of the twisted pair wires are given in Table No. 1. Of these, sample numbers 1 and 2 are covered with aluminum laminated shield over the core; whereas in sample number 3, all pairs are individually shielded with braid. Sample numbers 4, 5, 6 and 7 have no shield either on individual pair or over core. For the coaxial sample numbers 8, 9, 10, 11 and 12, Table numbers 2 and 3 provide the pertinent construction and dimensional data. Figure 1 is the actual photograph of the coaxial wires without jacket after the flexure test.

TEST METHODS OF COAXIAL WIRES

Absorbing Clamp Technique:

The Rohde & Schwartz Model MDS-20 Absorbing Clamp is used in Europe to determine acceptable radiation levels from power cords of household electrical devices according to the recommendation of the Comite International Special des Perturbations Radioelectriques.[3,4] In reference 4, it is also suggested that the absorbing clamp could be used to test shield efficiency of coaxial cables.

Table 1: CONSTRUCTION AND DIMENSIONAL ANALYSIS OF TWISTED PAIR WIRE

Sample No.	Pair/AWG	DOD* Average	Insulation Material	Shield	Jacket Material
1	25/24	0.032	semi rigid PVC	Aluminum/Mylar	Grey PVC
2	25/22	0.036	PVC	Aluminum/Mylar	Grey PVC
3	12/22	0.059	Polyethylene	Tinned Copper Braid (90% coverage)	Grey PVC
4	25/24	0.032	PVC	None	Grey PVC
5	25/24	0.031	PVC	None	Grey PVC
6	25/24	0.033	PVC	None	Grey PVC
7	25/24	0.032	PVC	None	Grey PVC

* DOD: Diameter Over Dielectric

Table 2: CONSTRUCTION ANALYSIS OF COAXIAL
(All dimensions are in inches)

	RG-6 Sample #8	RG-6 Sample #9	RG-6 Sample #10	RG-59 Sample #11	RG Type Double Braid Sample #12
Center Conductor	Cu/steel	Cu/steel	Cu/steel	Cu	Cu
Dielectric	Expanded PE	Expanded PE	Expanded PE	Expanded PE	Solid PE
Velocity of Propagation (%)	76	81.5	78	78	66
First Shield*	Al Poly/Al (corrugated type) bonded to core	Al/PVA/PE bonded to core	Al/PVA/PE bonded to core	Al/PVA/PE bonded to core	Copper Braid 0.0036 dia. of wire Picks (P) = 12/inch Strand (N) = 3-carrier Carrier (C) = 24
Coverage (%)	100	100	100	100	90
Thickness	0.0016	0.0023	0.0026	0.0026	--
Overlap	0.125	0.125	0.125	0.125	--
Second Shield	4 mil Al (corrugated type) glued to jacket	Copper Braid	Copper Braid	Copper Braid	Copper Braid
Dia. of wire	--	0.006	0.006	0.006	0.0036
Picks/inch (P)		8	8	4.5	16
Strands/Carrier (N)		4	4	4	3
Number of Carriers (C)		16	16	16	24
Coverage (%)	100	61	59	63	85
Jacket	Black PVC	Black PVC	Black PVC	Black PVC	Beige PVC

* Plastic used in making the shield laminate was not analyzed for confirmation. The plastic materials indicated above were noted from product brochures.

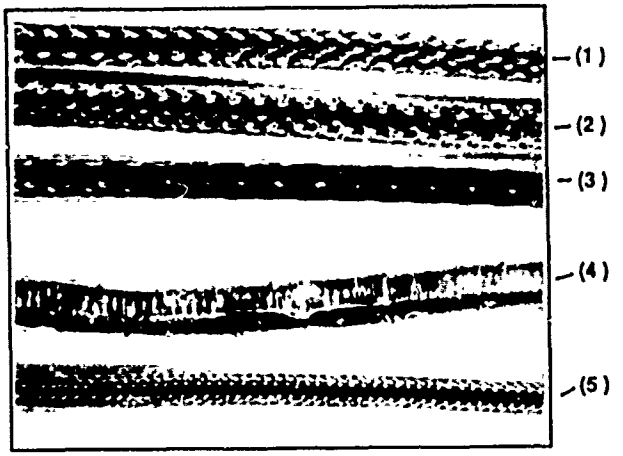

FIGURE 1: PHOTOGRAPH OF CABLE SHIELD AFTER FLEXURE

(1) RG-6, NO. 9 (AL. LAMINATE AND BRAID)

(2) RG-6, NO. 10 (AL. LAMINATE AND BRAID)

(3) RG-59, NO. 11 (AL. LAMINATE AND BRAID)

(4) RG-6, NO. 8 (AL. LAMINATE AND CORRUGATED AL. SHIELD)

(5) RG TYPE, NO. 12 (DOUBLE BRAID)

Table 3: DIMENSIONAL ANALYSIS
(All dimensions are in inches)

	RG-6 Sample #8	RG-6 Sample #9	RG-6 Sample #10	RG-59 Sample #11	RG Type Double Braid Sample #12
Diameter of center conductor	0.040	0.040	0.0376	0.0314	0.0137
Diameter over dielectric	0.174	0.175	0.182	0.145	0.099
Diameter under outer shield	0.176	0.179	0.187	0.150	0.134
Diameter over outer shield	0.199	0.203	0.211	0.168	0.146
Diameter over jacket	0.297	0.264	0.270	0.230	0.184

The absorbing clamp MDS-20 consists of an oblong plastic case fitted with a hinged lid so that the cable to be measured can be inserted. Fitted inside the top and bottom halves of the case is a row of spring supported ferrite half-rings which, when the hinged case is closed, form a closed magnetic circuit. The two rings nearest to the test item carry the secondary windings of the current transformer, the output of which is connected by coaxial cable to the output socket of the device and from there to the output of the receiver.

A coaxial cable under test was excited by a well shielded signal generator providing a known input signal level and was properly terminated. The ratio of the output signal level to the cable input signal level provides a measure of shielding. In the laboratory tests, cable samples used were 12 feet (3.7 m) in length and stretched out on a wooden table 34 inches (86 cms) in height (Figure 2). The input signal was set at 100 mv after the 50 Ω/75 Ω converter. The absorbing clamp was moved from one end of the sample to the other and the highest signal level received at the voltmeter was recorded.

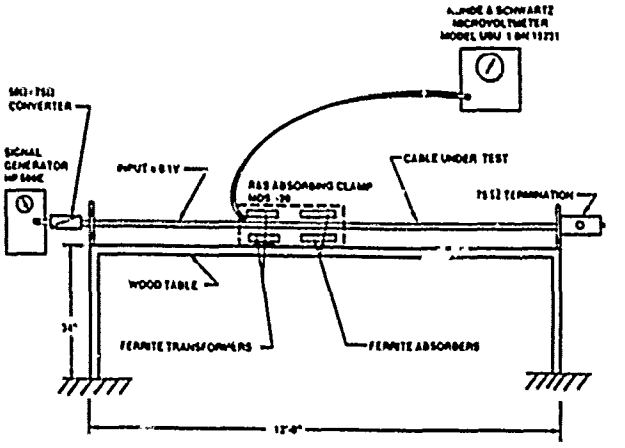

FIGURE 2: ROHDE & SCHWARTZ MDS-20 ABSORBING CLAMP TEST

From the data taken with the MDS-20 Absorbing Clamp certain conclusions can be drawn. From 50 MHz to 200 MHz, all samples have the radiation level of 10 μv, and below (Figure 3). With the exception of RG type No. 12 with double braid, all the rest of the samples reached around 25 μv at 250 MHz, and then dropped to around 15 μv at 300 MHz. Double braided sample No. 12 showed the lowest overall radiation at only 14 μv across the frequency band, 50 MHz to 300 MHz. It is worth mentioning that the noise level of the generator as measured by the microvoltmeter was less than 2 microvolts which is the minimum level the receiver can measure.

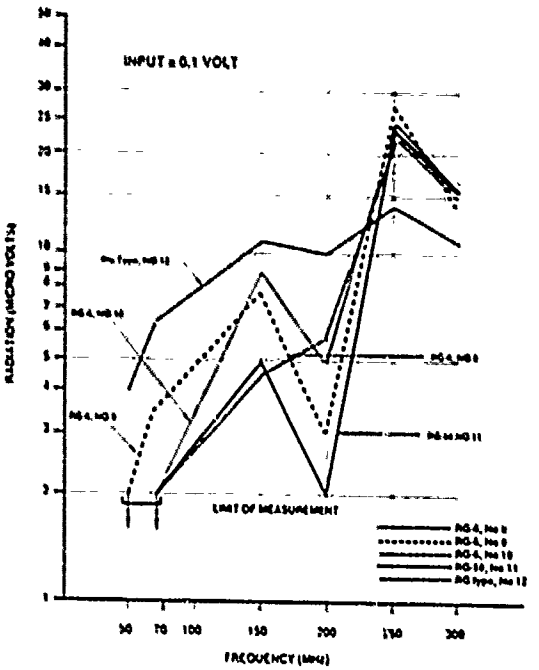

FIGURE 3 RADIATION LEAKAGE VERSUS FREQUENCY OF COAXIAL WIRES EMPLOYING RHODE & SCHWARTZ MDS-20 ABSORBING CLAMP

Flexure Test:

Shielding efficiency of the coaxial wire can degrade in service as a result of flexure. To evaluate the flexure characteristics, therefore, the shielding efficiency was measured by the Absorbing Clamp technique both before and after flexure. The area showing the maximum radiation was marked prior to flexure. Next, with a circular mandrel five times the outer diameter of the coaxial wire the sample was bent to form a semi-circle as shown in Figure 4, at the location of the worst radiation. Using a motor driven Flexure Test Equipment similar to one used by Smith[5], the sample was flexed through 10,000 cycles.

After flexure, the coaxial samples were tested for radiation leakage. The results presented in Figures 5 through 10 show that the radiation leakage increased significantly from coaxial sample No. 8 and the shielding efficiency of the same sample degraded by about 20 dB at 300 MHz. Coaxial sample Nos. 9, 10 and 12 by comparison, degraded by 3 dB to 6 dB only at the same frequency of 300 MHz. The best performer in the Flexure Test is RG-59 sample No. 11 which improved its shielding efficiency by about 10 dB at 300 MHz.

After the Flexure Test, jacket of each sample was removed to examine the effect of flexing. As clearly seen in Figure 1, sample No. 8 showed multiple kinks and breaks on the outer aluminum tape. The braided samples did not show any noticeable physical change on the outer braid due to flexure.

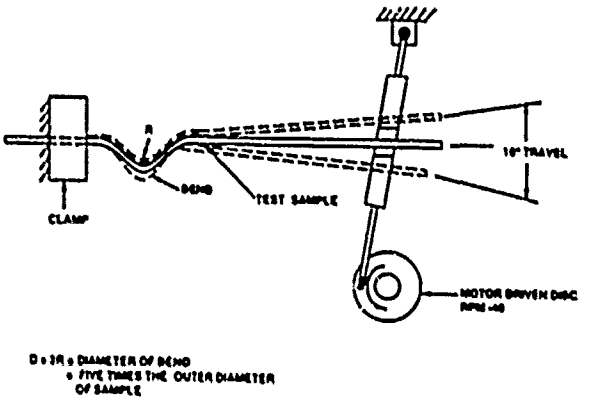

D = 5R = DIAMETER OF BEND = FIVE TIMES THE OUTER DIAMETER OF SAMPLE

FIGURE 4: FLEXURE TEST EQUIPMENT

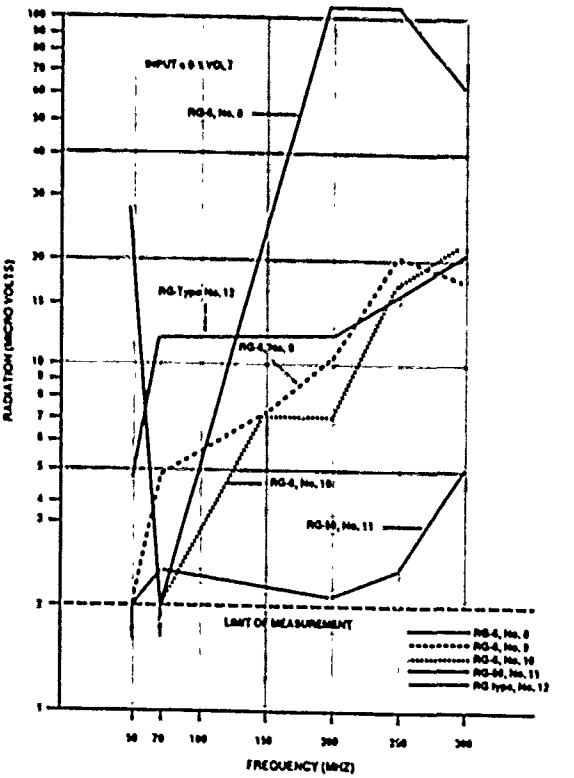

FIGURE 5: RADIATION LEAKAGE VERSUS FREQUENCY OF COAXIAL WIRES EMPLOYING RHODE & SCHWARTZ MDS-20 ABSORBING CLAMP AFTER10,000 FLEXURES

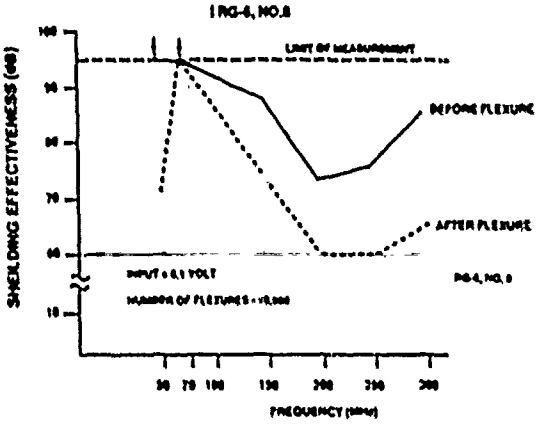

FIGURE 6: SHIELDING EFFECTIVENESS VERSUS FREQUENCY OF COAXIAL WIRES ROHDE & SCHWARTZ MDS-20 ABSORBING CLAMP TECHNIQUE

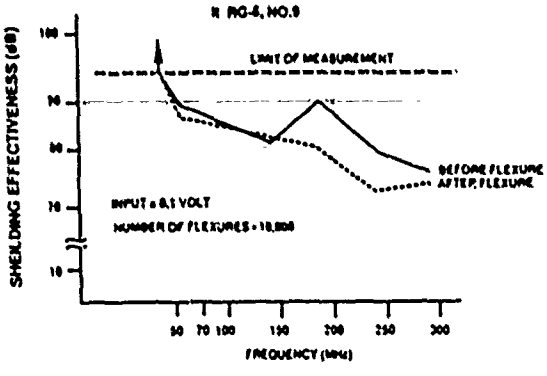

FIGURE 7: SHIELDING EFFECTIVENESS VERSUS FREQUENCY OF COAXIAL WIRES ROHDE & SCHWARTZ MDS-20 ABSORBING CLAMP TECHNIQUE

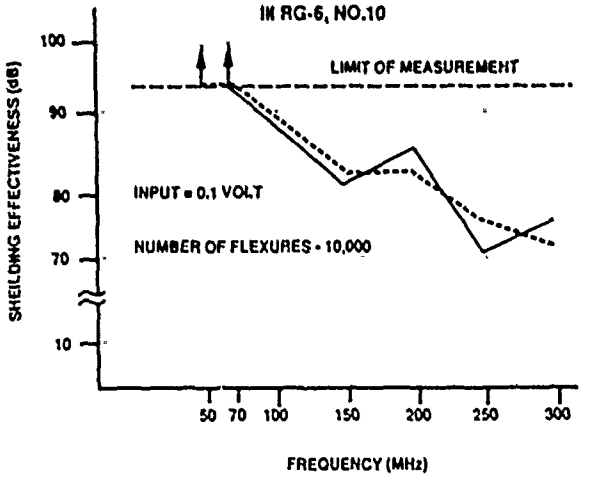

FIGURE 8: SHIELDING EFFECTIVENESS VERSUS FREQUENCY OF COAXIAL WIRES ROHDE & SCHWARTZ MDS-20 ABSORBING CLAMP TECHNIQUE

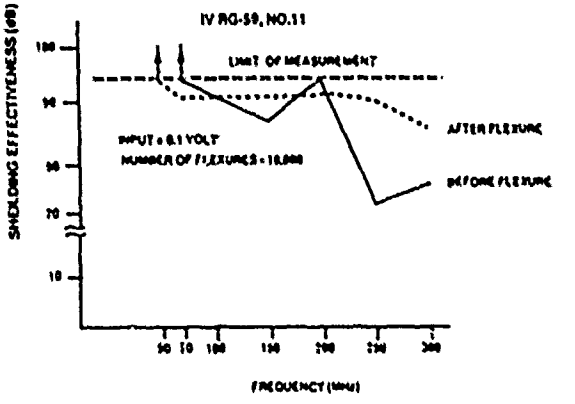

FIGURE 9: SHIELDING EFFECTIVENESS VERSUS FREQUENCY OF COAXIAL WIRES ROHDE & SCHWARTZ MDS-20 ABSORBING CLAMP TECHNIQUE

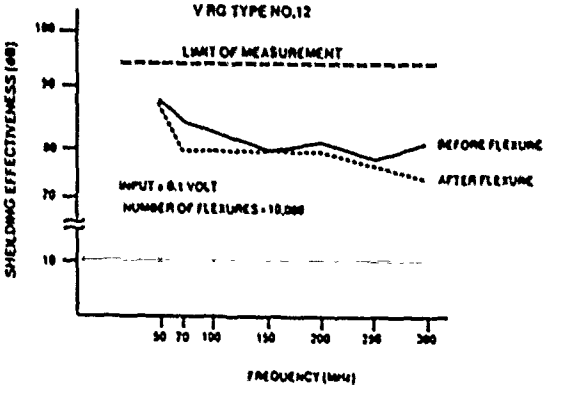

FIGURE 10: SHIELDING EFFECTIVENESS VERSUS FREQUENCY OF COAXIAL WIRES ROHDE & SCHWARTZ MDS-20 ABSORBING CLAMP TECHNIQUE

Surface Transfer Impedance by Triaxial Cavity Method:

Many papers have been published on the surface transfer impedance measurements. Of these, papers presented by Simons[6], Oakley[7], and Simons[8] are particularly referenced here. The schematic cross-section of Triaxial Cavity and Test Set Up for the present measurement are shown in Figures 11 and 12. The coaxial sample under test was terminated by a carbon resistor matching its characteristic impedance. A signal generator providing a known input current excited the sample. The imperfect shield, in turn, excited a signal in the outer coaxial system whose resultant output voltage was detected by a terminating voltmeter. The left end of the outer shell was shorted by a metal disc to the cable shield. The magnitude of surface transfer impedance, Z_t, was calculated from the output voltage V, input current I, and sample length ℓ, from the following expressions. The derivation of equations 1a and 1b is found in Appendix.

The Triaxial Cavity which was designed in the laboratory is suitable for measurement on a sample length of 30 cm only. The various samples measured in the Triaxial Cavity did not exceed 1/3 λ at 300 MHz. International Electrotechnical Commission (IEC) recommends that the cavity exterior system have a maximum length of 0.35 λ[9] where λ_{min} is the shortest wavelength measured. Thus with the existing length

of the cavity, measurement was limited to 300 MHz. The surface transfer impedance (Z_t) in milli-ohms/meter was computed for various samples from the measured data at a number of frequencies, see Figure 13 and Table 4.

$$Z_t = \left|\frac{V}{I}\right| F \quad \text{Ohms per unit length} \tag{1a}$$

$$F = \left| \frac{\left(\frac{m^2-1}{m}\right)\frac{1}{K}(\cos\chi + j\alpha \sin\chi)}{\sin\chi\cos\chi - \frac{1}{m}\cos\alpha\chi\sin\chi + j\left(\cos\alpha\chi + \frac{1}{m}\sin\alpha\chi\sin\chi - 1\right)} \right| \tag{1b}$$

where,

χ = $\beta\ell$ (phase shift in outer system).

m = B/Ba = λ_a/λ (ratio of wavelengths of outer to inner systems).

Z_1 = impedance termination of output voltage V.

K = characteristic impedance of outer system.

α = K/Z_1

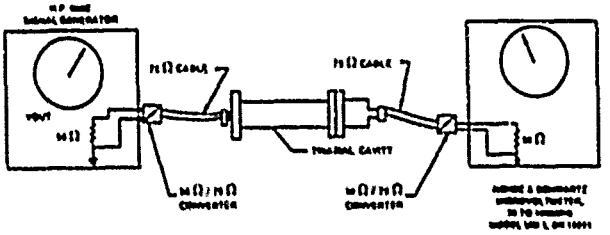

NOTE: I = VOUT / 12Ω

FIGURE 11: CAVITY TEST SET-UP (SIMPLIFIED)

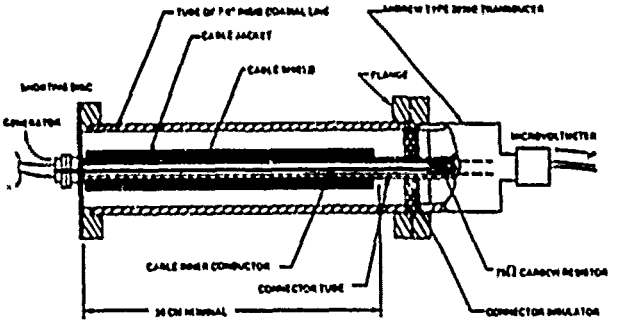

FIGURE 12: SCHEMATIC CROSS-SECTION OF TRIAXIAL CAVITY

Table 4: SURFACE TRANSFER IMPEDANCE (milli-ohm/meter) @ MHz

Sample	50	100	150	200	250	300
i) RG-6, No. 8	42.2	154.1	34.2	24.1	35.8	138.7
ii) RG-6, No. 9	27.0	37.5	21.9	22.2	48.2	96.5
iii) RG-6, No. 10	16.8	29.7	18.0	16.6	38.1	78.6
iv) RG-59, No. 11	10.9	24.7	42.9	112.2	140.3	583.6
v) RG Type, No. 12	9.0	14.6	30.6	23.2	27.7	127.3

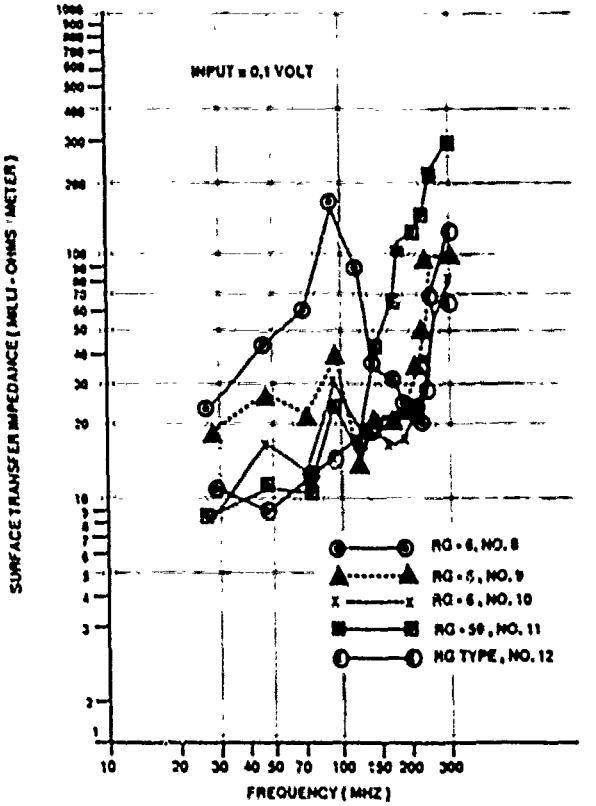

FIGURE 13: SURFACE TRANSFER IMPEDANCE VERSUS FREQUENCY TRIAXIAL CAVITY TECHNIQUE

SHIELDING RESULTS OF COAXIAL WIRES

The input voltage used to excite all wire samples in both the Triaxial Cavity and the Absorbing Clamp techniques was 100 mv. The peak signal of coaxial drop wire in one of the applications i.e., CATV system is 1.26 mv, so that data should be multiplied by 0.0126 to check compliance with the radiation limits allowed for this system. In Table 5 the measured radiation corrected for 1.26 mv signal level in the Triaxial Cavity shows that all cable samples fall well below the FCC limits of radiation[10]

The above correction was made by using the following simple expression:

$$\textit{Radiation}\,(\mu v/\text{meter}) = \frac{\text{Microvoltmeter reading } (\mu v) \times 1.26(mv)}{\text{Length of Triaxial Cavity (meter)} \times \text{Excitation voltage (mv)}}$$

$$= \frac{\text{Microvoltmeter reading } (\mu v) \times 1.26}{0.3 \times 100}$$

$$= 0.042 \times \text{microvoltmeter reading } (\mu v/\text{meter}) \tag{2}$$

Surface transfer impedance values measured by the Triaxial Cavity Method on unflexed samples as presented in Table 4 and Figure 13 up to 300 MHz, showed increasing values as frequency increased with few ups and downs in between. Sample No. 8 with double aluminum tapes showed a high value of surface transfer impedance at 100 MHz, meaning

high leakage at this frequency. The reason for this increase could not be explained. Sample No. 11 also showed an unusually higher rate of increase of impedance between 150 MHz and 300 MHz. Analyzing the measured radiation shown in Table 5 (after correction for 1.26 mv signal level), sample No. 11 also showed a very high radiation leakage at 300 MHz. 0.79 μv/meter radiation at this frequency is more than double the value measured for most of the remaining samples. However, after the same sample was flexed 10,000 times, the shielding effectiveness improved (Figure 9).

Table 5: MEASURED RADIATION CORRECTED FOR 1.26 mv SIGNAL LEVEL (by Triaxial Cavity Technique)

Freq. (MHz)	FCC Radiation Limits (μv/meter)	Measured Radiation Corrected for 1.26 mv Signal Levels (μv/meter) RG-6 No. 8	RG-6 No. 9	RG-6 No. 10	RG-59 No. 11	RG-Type No. 12
50	15	0.39	0.25	0.15	0.10	0.08
175	20	0.15	0.10	0.08	0.28	0.08
300	15	0.44	0.30	0.25	0.79	0.32

With the exception of sample Nos. 8 and 12, all other wires have aluminum/poly/aluminum laminate as the inner shield and approximately 60% coverage of copper wire braid as the outer shield (Table 2). Sample No. 8 has aluminum/poly/aluminum laminate as inner shield and aluminum tape as outer shield. Sample No. 12 has 90% and 81% coverage for both inner and outer copper braid respectively.

Triaxial cavity method is considered more reliable compared to the Absorbing Clamp Technique, since the latter test is influenced both from the external ingress of radiation through the shield of cable sample which acts as an antenna and also due to the variation in sample length.

Comparing the results of both Triaxial Cavity method and Absorbing Clamp technique, sample No. 10 appeared to have provided the best shielding up to 300 MHz possibly due to the existence of least gap at the overlap of the inner shield. Because of the cracks on outer aluminum shield and the formation of kinks on the inner aluminum/poly/aluminum laminate, sample No. 8 showed the worst shielding effectiveness after flexure.

TRANSMISSION CHARACTERISTICS OF SHIELDED AND UNSHIELDED TWISTED PAIR WIRE

Margin Consideration

In Hore and Thuraisamy's paper[11], it has been shown that Near End Crosstalk (NEXT) and loss characteristics are dominant factors for high speed transmission through twisted copper pairs. In the same paper, various impairments i.e., inductive noise, echo, intersymbol interference, impulse noise, etc. were discussed and their effects in limiting the transmission distance were presented in Table 6. By applying a quasi-statistical method, i.e., adding half of the dB values allotted to each class of impairment to the RMS combination of the other half, a margin of 12.67 dB can be obtained. Thus, based on engineering judgement, a margin of 12 dB is considered acceptable for various impairments.

In digital transmission for a Bit Error Ratio (BER) of one error in ten million (10^7), a signal having binary code requires a peak Signal-to-Noise Ratio (SNR) of 14.3 dB[12]. For engineering computation this margin for SNR may be considered 14.5 dB.

Table 6: MARGIN REQUIREMENTS

SOURCE	EXPLANATION	ALLOCATION
Cable	Temperature, Aging, Manuf. Variations, Water, Splices	3 dB
CO or Customer Bldg. Wire	Crosstalk, Loss, Bridged Taps, Noise	3 dB
Noise	Impulse: Switching, Elevators Low Frequency: Power Influence Broadband: ?	3 dB
Receiver	Nonlinearity, Jitter, Unbalance, Manuf. Variations, Mis-Equalization, Mis-Cancellation of Echo	3 dB
Receiver	Residual Intersymbol Interference, Echo	3 dB
Unknowns	Unexpected Items not listed above	3 dB

$$\text{MARGIN} = 3 + 3 + 3 + 3 + 3 + 3 + \sqrt{3^2 + 3^2 + 3^2 + 3^2 + 3^2 + 3^2} = 12.67$$

In addition to the above margin, it is shown in Reference 11 that a bridged tap could produce significant increase in attenuation, particularly at higher frequencies. In real world situations, bridged taps are commonly provided in customer premises wiring as well as in Central Office environments. It may happen that the bridged taps are provided without knowing the magnitude of their effects. From experimental measurements shown in Reference 11, it was clearly established that a bridged tap having its length the same as the quarter wave length of the transmitted signal produced significant increase in attenuation. At 772 KHz one bridged tap was shown to produce an increase of 8.6 dB average on 25 pair/24 gauge inside wire. The corresponding increase was about 10 dB at 1.6 MHz.

Considering all the factors, i.e., impairments, Signal-to-Noise Ratio and bridged taps, it is appropriate to classify the following three categories of margins:

(1) SNR of 14.5 dB for binary code + 6dB margin = 20.5 dB

(2) SNR of 14.5 dB for binary code + 12 dB margin = 26.5 dB

(3) SNR of 14.5 dB for binary code + 18 dB margin = 32.5 dB

Measurement of Transmission Parameters

Samples of both shielded and unshielded inside wires from different vendors were used in our measurements to characterize inside wiring cables. The construction and dimensional analyses of these wires are shown in Table 1. Mutual capacitance, capacitance unbalance, characteristic impedance, attenuation and near end crosstalk (NEXT) were measured and shown in Table 7 using a DCM model CMS - 2 PCX Computerized Automatic Cable Measuring System. The measurement technique employed using the DCM test set can be found in Chattler's paper[13].

Table 7: TRANSMISSION CHARACTERISTICS OF SHIELDED INSIDE WIRE

	Sample No. 1 25/24 (Shielded Core)	Sample No. 2 25/22 (Shielded Core)	Sample No. 3 12/22 (Shielded Pr.)
Cm (nF/mile), Avg.	120.3	120.0	83.4
Max.	125.6	138.1	84.2
Cap. Unbalance			
Pair-to-Ground Avg. (pF/kft)	173	234	444
Max. (pF/kft)	413	827	1292
Pair-to-Pair Avg. (pF/kft)	14.3	6.7	0
Max. (pF/kft)	84.8	23.3	0
Characteristic Impedance (Z o)			
Ohms, Avg. @ 64 kHz	100.3	100.3	100.0
128 kHz	98.5	98.4	100.5
256 kHz	98.2	98.1	98.0
1000 kHz	96.4	96.4	96.9

RESULTS OF SHIELDED AND UNSHIELDED PAIRS

It has been mentioned earlier that both sample Nos. 1 and 2 are covered with aluminum/mylar laminate over the core; whereas, sample No. 3 has copper braided shield over each pair. Sample Nos. 4, 5, 6 and 7 have no shield at all. Transmission measurements on these unshielded samples were reported in Reference 11 and therefore the results are not included in this paper. However, for comparison of crosstalk behavior of both shielded and unshielded wires, sample No. 7 has been chosen. This sample was found to have the worst power sum near end crosstalk behavior of all the unshielded samples. The test results of the sample is therefore tabulated along with three shielded samples in Table 8 for comparison.

1% NEXT values for each of the sample Nos. 1, 2, 3 and 7 are computed by three equations provided under Table 8. DCM test set computes the average NEXT values in dB/ kft by using the first equation. Using this value, total average NEXT is computed from the second equation and finally, 1% NEXT value from the 3rd equation. One explanation may be necessary for the total average NEXT value which is defined as the worst average crosstalk coupling expected in a measured unit of pairs for an infinite length. 1% NEXT values thus computed for the measured frequencies of 150, 772, 1600, 3150 and 6300 KHz for sample Nos. 1, 2, 3 and 7 show the following:

- 25/22 gauge shielded core (sample No. 2) shows 2 to 4 dB improvement of 1% NEXT values over the 25/24 gauge shielded core (sample No. 1).
- 12/22 gauge shielded pair wire (sample No. 3) shows 34 to 38 dB improvement of 1% NEXT values over 25/24 gauge shielded core (sample No. 1) in the frequency range of 772 KHz to 6,300 KHz.
- 25/24 gauge unshielded core (sample No. 7) shows the similar 1% NEXT values as that of 25/24 gauge shielded core (sample No. 1).

For our measurement program sufficient number of samples were not available. However, the above results may be considered as indicative of the typical crosstalk characteristics of the shielded and unshielded inside wires manufactured by the industry.

Table 8: 1% PS NEXT CHARACTERISTICS OF SHIELDED INSIDE WIRE

	Sample 1 (25/24 Sh. Core)			Sample 2 (25/22 Sh. Core)			Sample 3 (12/22 Sh. Pair)			Sample 7 (25/24 Unsh. Core)		
Freq. (kHz)	Att. dB/kft	$NEXT_m$ dB/kft	1% NEXT dB	Att. dB/kft	$NEXT_m$ dB/kft	1% NEXT dB	Att. dB/kft	$NEXT_m$ dB/kft	1% NEXT dB	Att. (dB/kft)	$NEXT_m$ (dB/kft)	1% NEXT (dB)
150	3.68	$\bar{x}$: 55.61 Worst: 53.18 σ: 1.77	50.61	3.03	$\bar{x}$:61.66 Worst: 56.62 σ: 3.25	52.85	3.03	$\bar{x}$: 83.44 Worst: 81.09 σ: 2.38	76.65	3.79	$\bar{x}$:54.3 Worst: 51.9 σ:1.5	50.9
772	7.86	$\bar{x}$: 44.84 Worst: 42.41 σ: 2.3?	39.29	7.81	$\bar{x}$: 51.15 Worst: 46.0 σ: 3.13	43.74	5.74	$\bar{x}$: 82.35 Worst: 78.02 σ:2.29	76.69	7.08	$\bar{x}$: 42.9 Worst: 40.9 σ:1.1	40.1
1600	11.70	$\bar{x}$: 41.31 Worst: 38.70 σ: 2.07	36.49	12.56	$\bar{x}$:46.91 Worst: 40.90 σ: 3.27	39.29	9.54	$\bar{x}$: 81.18 Worst: 76.49 σ: 2.87	74.44	10.94	$\bar{x}$:38.6 Worst: 36.9 σ: 1.1	36.0
3150	17.23	$\bar{x}$: 36.76 Worst: 33.22 σ: 2.09	31.89	18.87	$\bar{x}$: 44.00 Worst: 37.52 σ: 3.36	36.17	14.72	$\bar{x}$: 76.55 Worst: 69.47 σ: 4.14	66.90	16.17	$\bar{x}$:34.7 Worst: 32.9 σ: 1.3	31.7
6300	[illegible]	$\bar{x}$: 32.80 Worst: 29.39 σ: [illegible]	28.09	26.65	$\bar{x}$: 39.40 Worst: 34.86 σ: 2.93	32.57	19.67	$\bar{x}$: 68.89 Worst: 64.09 σ: 2.76	62.46	24.21	$\bar{x}$: 30.9 Worst: 28.4 σ: 1.1	28.3

$$NEXT_m(dB/kft) = \text{next} + 10 \log \left[\frac{1 - 10^{-\frac{\alpha}{\ell}}}{1 - 10^{-\frac{1}{\ell}}} \right]$$

$$\text{Total Avg. } NEXT\ (dB) = NEXT_m - 10 \log \left(\frac{1}{1 - 10^{-\frac{1}{\ell}}} \right)$$

$$1\%\ NEXT\ (dB) = \text{Total Avg. } NEXT - 2.33\sigma$$

where,

next = Measured value of NEXT in dB

α = Average attenuation in dB/kft

$\bar{x}$ = Average value of 25 pairs

σ = Standard Deviation

ℓ = Length of cable

DISCUSSION ON TRANSMISSION FREQUENCY VERSUS DISTANCE

Results of 1% NEXT characteristics for sample Nos. 1, 2, 3 and 7 from Table 8 are plotted in Figure 14. These results do not take into consideration the effect of SNR, impairments and bridged taps, or reflection for impedance mismatches due to gauge and/or other changes.

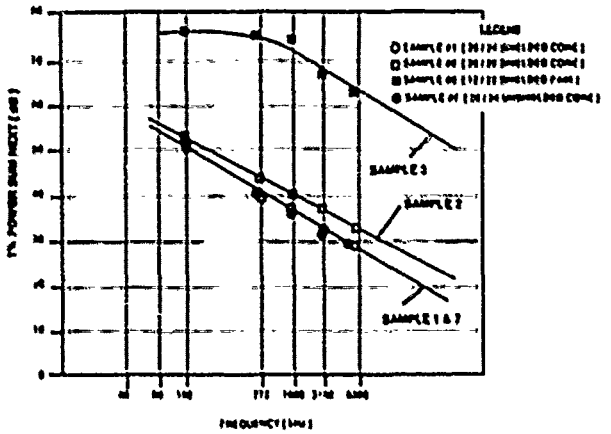

FIGURE 14 : NEXT MODELS FOR SHIELDED AND UNSHIELDED PAIR

The NEXT model in Figure 14 can be used to estimate the relative transmitted distance at the frequencies of interest within the acceptable bit error ratio of 10^{-7}. In the earlier discussions, 20.5, 26.5 and 32.5 dB were considered for three appropriate values for SNR plus margin. While these SNR values apply to the composite signal (all frequencies) at a point inside the receiver, we use them here as in reference 11 to estimate relative transmitted distance for the signal. By subtracting SNR and margin from 1% PS NEXT values, a corresponding set of curves are drawn and displayed. Figure 15 shows such curves for shielded pair. The dB loss values of these curves are taken as the maximum attenuation of the transmitted signal, and converted to wire length at the frequency of interest. The distances thus computed for various frequencies are plotted for the three of SNR plus margin values. Figure 16 refers to the shielded pair and Figure 17 refers to the shielded or unshielded core.

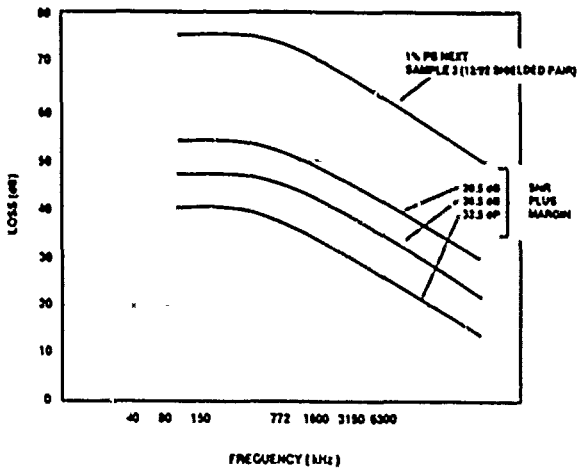

FIGURE 15 : NEXT MODEL AND SNR PLUS MARGINS FOR SHIELDED PAIR

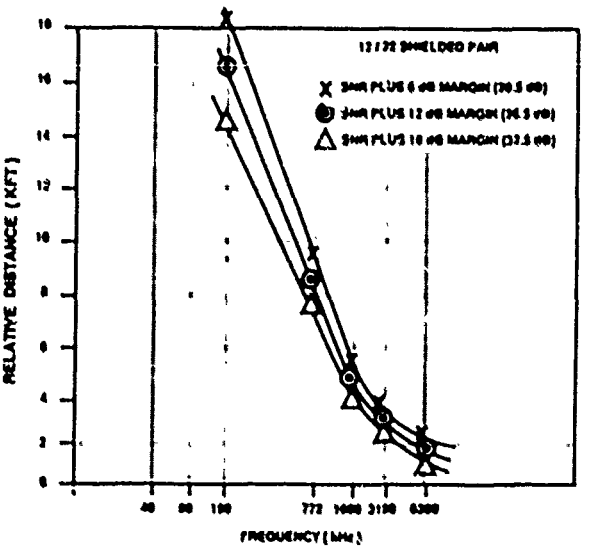

FIGURE 16 : DISTANCE Vs. FREQUENCY FOR SHIELDED PAIR

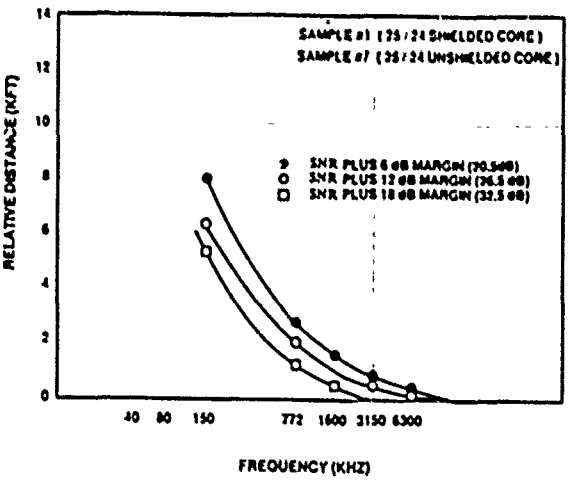

FIGURE 17: DISTANCE VS. FREQUENCY FOR SHIELDED AND UNSHIELDED CORE

The above set of plots are guidelines for relative transmission range for both shielded and unshielded inside wires. Actual distances for a specific system depend on many factors, including the details of the transceiver technology, the other impairments besides NEXT, bandwidth, etc. The frequency versus distance plots in figures 16 and 17 are not clearly related to bit rate because any digital signal covers a band of frequencies rather than just one frequency.

SUMMARY

The present study on shielding efficiency of communications wire and cable was divided into two sections - coaxial wires and twisted pairs. For coaxial wires various shielding designs considered for the study included,

- aluminum/poly/aluminum laminate for inner shield and corrugated aluminum for outer shield,
- aluminum/poly/aluminum laminate for inner shield and copper braid of different coverages for outer shield, and
- double braided shield of different coverages.

The shielding effectiveness of these samples were measured by using (1) Rohde & Schwartz Model MDS-20 Absorbing clamp and (2) Triaxial Cavity Method for determining the surface transfer impedance. Both the above methods were used before flexure and after on the coaxial samples. The results show that the sample with aluminum/poly/aluminum laminated inner shield and corrugated aluminum outer shield (sample No. 8) did not perform as well as the other samples because of cracks on the outer shield and kinks developed on the inner shield. Sample No. 10 with aluminum/poly/aluminum laminated inner shield and 60% copper braided outer shield provided the best shielding up to 300 MHz possibly due to the existence of the least gap at the overlap of the inner shield. This study is not intended to recommend any particular shield design for a desired application, rather to suggest methods of determining the shielding effectiveness in the range of frequencies of interest.

The shielding effectiveness of twisted pair wires was determined by measuring near end crosstalk (NEXT) loss of various samples of wire. These included,

- unshielded inside wire,
- inside wire with shielded core, and
- inside wire with shielded pair.

The data clearly shows that individually shielded pair design has the best NEXT performance as compared with the wires with or without shielding over core. Depending on the signal bandwidth, the signal-to-noise ratio may vary and also the effects of impairments on loss consideration. To transmit high speed data and other signals, determination of NEXT performance at the frequencies of interest, and SNR and margin requirements are of significant importance. Based on these data, relative transmitted distances are estimated for a goal of one error in 10^7 bits per second. Figures 16 and 17 provide guidelines of the trade-off between frequency and transmitted distance of the inside wires with and without shield. The two sets of curves clearly show that shielded pairs have distinct advantage in transmitting much longer distances over the unshielded pairs of either shielded core or unshielded core. For example, at 772 kHZ, the shielded pairs are capable of transmitting between 7.7 kft and 9.8 kft for the three categories of SNR plus margin requirements of 20.5, 26.5 and 32.5 dB. The corresponding transmitted distances at 772 kHZ for unshielded core and shielded core range between 1.1 kft and 2.8 kft. At other frequencies there is also a significant increase in transmitted distances using the wires with shielded pairs over the wires with or without shielded core.

APPENDIX

RESPONSE OF A TRIAXIAL CAVITY - DERIVATIONS OF EQUATIONS

Much has been written on derivations of equations relating voltage output from a triaxial cavity to the surface transfer impedance of the cable under test which forms its inner coaxial system[3,4].

Figure 14 illustrates schematically a transmission line of length ℓ with a series point source of emf located in the bottom conductor. The line parameters are, as shown, K and Γ; line terminations at left and right ends are Z and Z_1, respectively. Let the emf be of unit voltage ($e = 1$) and its location from the origin at the left be $x = \xi$. Schelkunoff[3] has shown that the transverse voltage at some point $x > \xi$ is

$$V(x, \xi) = \frac{K}{D}\left[\cosh \Gamma \xi + Z_1 \sinh \Gamma \xi\right]\left[K \sinh \Gamma(\ell - x) + Z_1 \cosh \Gamma(\ell - x)\right] \tag{I-1}$$

where,

$$D = K\left[(K^2 + Z_1 Z) \sinh \Gamma \ell + K(Z_1 + Z) \cosh \Gamma \ell\right]. \tag{I-2}$$

If we are interested only in the output voltage across Z_1 at $x = \ell$ we have for $V(\ell, \xi)$:

$$V = V(\ell, \xi) = \frac{KZ_1}{D}\left[K \cosh \Gamma \xi + Z_1 \sinh \Gamma \xi\right]. \tag{I-3}$$

Suppose that along the bottom leg there exists a distribution of sources $e(\xi)$; then the output voltage V at $x = \ell$ becomes

$$V = \int_0^\ell e(\xi) V(\ell, \xi) d\xi. \tag{I-4}$$

If the bottom leg is the outer conductor of a coaxial cable excited from the left end by input current $I(0)$ and match-terminated at the right, then (Figure 14b)

$$e(\xi) = I(0)\, Z_t\, e^{-\gamma \xi}, \tag{I-5}$$

where Z_t and γ are the surface transfer impedance and propagation constant, respectively. This is the condition which obtains in the test set-up shown in Figure 11 with $Z_1 = 0$ and $Z_2 = 50$ ohms. With $Z_1 = 0$ the expression for D simplifies to

$$D = K^2\left[K \sinh \Gamma \ell + Z_1 \cosh \Gamma \ell\right] \tag{I-6}$$

Inserting I-3, I-5, and I-6 into I-4 and carrying out the integration there results:

$$V = \frac{I(0) Z_t}{\cosh \Gamma \ell + \left(\frac{K}{Z_1}\right)} \left(\frac{1}{\Gamma^2 - \gamma^2}\right)\left\{e^{-\gamma \ell}(\gamma \cosh \Gamma \ell + \Gamma \sinh \Gamma \ell) - \gamma\right\} \tag{I-7}$$

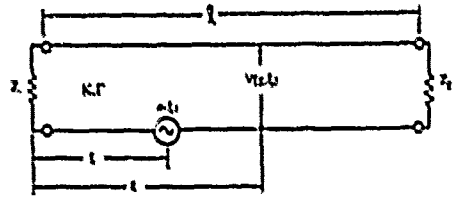

FIGURE 16a: SERIES POINT SOURCE IN A TRANSMISSION LINE

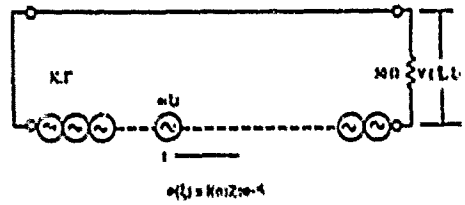

FIGURE 16b: EXCITATION OF OUTER SYSTEM IN TRIAXIAL CAVITY

Since the tube and cable lengths are short it is convenient to ignore attenuation in $\Gamma\ell$ and $\gamma\ell$ so that $\Gamma \approx j\beta_0$ and $\gamma \approx j\beta$.

$$V \approx \frac{I(0)Z_t}{\cos\beta_0\ell + j\left(\frac{K}{Z_t}\right)\sin\beta_0\ell}\,\frac{1}{(\beta^2-\beta_0^2)}\left(e^{-j\beta\ell}(j\beta\cos\beta_0\ell - \beta_0\sin\beta_0\ell) - j\beta\right) \qquad (1\text{-}8)$$

Setting $\beta_0\ell = \chi$, $m = \beta/\beta_0$, $n = K/Z_t$, and solving for Z_t, equation (1) is obtained.

ACKNOWLEDGEMENTS

The author would like to thank Messrs. A. J. Gambardella and A. Stephenson of Bellcore for their help in measuring the transmission parameters of shielded wires, and Messrs. G. Galiotti and H. Simon, former employees of General Cable Company in helping the author in measuring the shielding effectiveness of coaxial wires and developing the equation for the surface transfer impedance of coaxial wire by using the Triaxial Cavity Method. The author very much appreciates the management of General Cable Company in permitting him to publish the experimental results of the shielding effectiveness of coaxial wires using different techniques while the author was working in the Research and Development Laboratory of the company.

REFERENCES

1. Electronics Engineering Association Standard PN 1907, Draft 7, May 1989.
2. Bellcore Technical Advisory, TA-TSY-000139, Issue 1, July 1986, "Central Office Coaxial Cable".
3. J. M. DeStadelhofen and R. Bersier, "La Pince Absorbanteuse Nouvelle Methodede Measure Pour L'Antiparasitage en Ondes Metrique", Technische Mitteilugen PTT, March 1969.
4. H. Goldmann, "Absorbing Clamp MDS-20 for Interference Measurements in VHF Range", News from Rohde & Schwartz, No. 46.
5. Kenneth L. Smith, "Analysis and Measurement of CATV Drop Cable R. F. Leakage", IEEE Transactions on Cable Television, Vol. CATV, No. 4, October 1979.
6. K. A. Simons, "Relating Transfer Impedance to Coaxial Cable Radiation", Twenty Third International Wire and Cable Symposium, 1974.
7. R. J. Oakley, "Surface Transfer Impedance Measurements - A Practical Aid to Communication Cable Shielding Design", Eighteenth International Wire and Cable Symposium, 1969.
8. K. A. Simons, "A Review of Measuring Techniques for Determining the Shielding Efficiency of Coaxial Cables", Jerrold Electronics Corp., May 22, 1973.
9. International Electrotechnical Commission, Radio Frequency Cables, Part 1, General Requirements and Measuring Methods, Publications 96-1, Second Edition, Geneva, 1962.
10. Federal Communications Commission No. 47, Part 76, Revised as of October 1, 1988.
11. L. M. Hore and V. Thuraisamy, "High Speed Transmission Through Twisted Pair Wire", Thirty-Seventh International Wire and Cable Symposium, 1988.
12. "Transmission Systems for Communications", 5th Edition, Published by Bell Telephone Laboratories, 1982.
13. L. M. Chattler, "A Guide to Electrical Specification Requirements for Multipair Telephone Cables", Presented at WIRE ASIA 82, Singapore, October 1982.
14. S. A. Schelkunoff, "Electromagnetic Waves", Van Nostrand, Princeton, 1943.

Lal M. Hore

Bellcore
445 South Street
Room MRE-2K171
Morristown, NJ 07960

Lal M. Hore received the B.Sc (Hons.) degree with Physics major, M.Sc. (Tech.) degree in Applied Physics, both from the University of Calcutta and Dr. Tech. degree from the Technical University of Budapest in Electrical Engineering. He was with Bell Northern Research, Canada as Member of R&D staff in design and development of communications cables from 1970 to 1972 and next with General Cable Company's Telecommunications Cable Division from 1972 to 1987 - first eight years in the R&D Laboratories as Research Manager in the Communications Cable Section and next as Staff Project Manager in the Applications Engineering. Since 1987, he has been with Bellcore (Bell Communications Research, Inc.) and currently, he is responsible for the preparation of Technical References for Outside Plant Cables and also the development of transmission requirements of all wire products for high speed transmission.

Dr. Hore has authored numerous technical papers on dielectric properties of electrical insulation materials and telecommunications wire and cable. He holds three patents on communications cables.

TEST AND MEASUREMENT PARAMETERS FOR TELEPHONE MULTIPAIR COPPER CABLES

Ernesto Esposito

TELECO CAVI SPA
Via Nazionale Adriatica 2D - Roseto degli Abruzzi, Italy

SUMMARY

Following the common tendency toward the introduction of new telecommunication services,the most industrialized countries are implementing the digitalization of the network.

In order to cope with the future request of ISDN and high speed data links (2 Mbit/s) from the subscribers,high quality transmission carriers must be available.

For that reason in Italy, besides the implementation of a optical fibre network for long distance and trunk applications,a familiy of multipair copper cables with improved high frequency characteristics in order to meet the SIP (Italian Telecommunication Operating Company) specifications has been developed for the subscriber network.

1. INTRODUCTION

This paper describes the manufacturing process, the main electrical parameters under measurement (both high and low frequency) and the tests developed for a new family of multi-pair copper cables for the Italian Distribution Network.

In addition the results of the above tests for two different cables, 2400 copper pairs unfilled and 400 pairs jelly filled, both polyethilene insulated are reported.

The acceptance limits, the tolerances and the high number of parameters under measurement, insure high quality transmission characteristics, also for high frequency applications.

Moreover, in order to work in compliance with the Quality Assurance Process, it is possible to statistically control the production trend in term of electrical as well as mechanical and geometrical parameters.

2. MANUFACTURING PROCESS

The cross section of a typical multipair copper cable is shown in Fig.1.

The cable is manufactured utilizing a high speed industrial process. This process is controlled by continuously monitoring the primary cable parameters, R,L,G,C, where R and L are respectively the resistance and the inductance of the conducter, while C and G are respectively the capacitance and the conductance between two conductors (1).

The manufacturing process is summarized as follows:

a) The copper wire is drawn, annealed and insulated at a very high speed (about 2500 m/minute);

b) The insulated wires are twisted in pairs;

c) The pairs are combined together to form the 10 pairs units and simultaneously the 100 pairs units;

d) To make the different cables ranging from 200 to 2400 pairs the 100 pair units are stranded together;

e) At last jelly (for m filled solution only) and different internal/external protections are extruded at a speed of 25m/minute.

During this process the following parameters must be controlled:

- Copper wire diameter and circularity.
- Wire/insulator concentricity.
- Faults number: the maximum acceptance limit is one fault for 150 km of insulated wire.
- Control on the geometry of the pair during the twisting and the stranding stages of manufacture.
- Accuracy in the manufacturing of the internal/external cable protections.

In order to guarantee the final product quality and performances with such a high speed process,it is of fundamental importance to continuously monitor and control the above parameters during all the stages of manufacturing.

3. ELECTRICAL PARAMETERS

In this paragraph are considered the most important electrical parameters for the behaviour of the telephone network , i.e. the R,L,G,C characteristics (1,2).

The telephone line characteristics are related to the following parameters (1):

-Capacitance unbalance to ground;
-Resistence unbalance;
-Capacitance and inductance coupling;
-Crosstalk coupling;
-Variation of the impedance characteristics;
-Variation of the dielectric constant.

All the above quantities depend upon the cable design as well as the manufacturing processes.

To control the R,L,G,C, characteristics the measurement of the following electrical parameters are required (1):

-wire electrical resistance;
-pair resistive unbalances;
-pair mutual capacitances;
-pair capacitive ground unbalances;
-pair capacitive unbalances for any combination;
-pair conductance;
-**pair attenuation;**
-**near end crosstalk for any pair combination (NEXT);**
-**far end crosstalk for any pair combination (FEXT);**
-**characteristic impedance;**
-insulating resistance for any wire;
-dielectric rigidity for any pair;

(In bold the parameters statistically measured are shown.)

3.1 Electrical Characteristic Values

In order to ensure the maximum utilization of the pairs inside the cable even at high frequency,the following values must be met:

Electrical wire resistance:

wire diameter(mm)	max (ohm/km)	mean
0,4	150,0	144,0
0,6	66,6	63,9

Mutual capacitance:

The mutual capacitance for any pair in the frequency range between 800 and 1000 Hz must be lower than:

- non filled cables	mean	50 nF/km
	max	55 nF/km
- filled cables	mean	55 nF/km
	max	60 nF/km

Unbalance capacitance:

The unbalance capacitance measured (for a 500 m cable length) in the frequency range between 800 and 1000 Hz, must be lower than:

- pair to pair	max (95%)	100pF
	max	150pF
- pair to ground	max (95%)	700pF
	max	1200pF

Dielectric Rigidity Test

Any pair must withstand for 3 seconds, without any electrical discharge, the following D.C. values:

wire (mm)	DC(kV) wire	DC(kV) wires/shield
0,4	2,5	6
0,6	3,5	6

High frequency characteristics

The attenuation and impedance values, at 20 degrees C, must be:

f(kHz)	Impedance(ohm)		Atten.(dB/km)	
	0,4mm	0,6mm	0,4mm	0,6mm
0,8	<1150	<850	<2	<1,5
80	<160	<150	<12	<7
1000	<140	<135	<27	<19

In order to determine NEXT and FEXT mean values distribution, a statistical analysis (at 1MHz) on the following combinations is required:

Near end crosstalk:

A among all pairs within unit (10 pairs)
B among all pairs between adjacent units (10 pairs)

Far end crosstalk:

C among all pairs within unit
D among all pairs between adjacent units
E among all pairs between alternate units

The mean and minimum (98%) values measured for any 100 pairs unit must not be less than the following:

	A	B	C	D	E
x(dB)	60	66	63	69	78
x 98%(dB)	45	50	50	55	62

These values apply for 500m cable length; for different lengths it is possible to calculate NEXT and FEXT with the following equation:

$$K\ (dB/km) = K_0 - 10\log_{10}(L/L_0)$$

where K_0 is the measured NEXT value, L =1000m, L_0 is cable length under measurament

4. STATISTICAL EVALUATION

The effectiveness of both the design and the manufacturing process is in the final measurement results on the finished cable.

A statistical analysis of the resulting values help in the evaluation of the cable performances as well as the process quality.

The parameters under statistical control are listed below:

Measured Parameters	Statistical Evaluation
Resistance	Maximum Individual Average Standard Deviation Histogram
Mutual Capacitance	Minimun Individual Maximum Individual Average Standard Deviation Histogram
Capacitance Unbalance	Min Ind Pair to Pair Max ind Pair to Ground Average Standard Deviation Histogram RMS
Attenuation 1MHz	Maximum Individual Average Standard Deviation Histogram RMS
FEXT & NEXT	Maximum Individual Average Standard Deviation Histogram RMS

The minimum and maximum individual values control the range of the particular measurement. The average value takes under control the quantity of high and low values; the magnitude of the high and low values is controlled by the RMS value. The standard deviation, on the other hand, controls the magnitude of the variation around the average, thereby controlling the dispersion of the data. The desirable situation is to have the smallest standard deviation possible. The histogram is a means of showing the manufacturer and the user the dispersion of values on a frequency distribution basis.

In Tables 1 and 2 some typical results of the electrical measurements for two different cables are shown.

All the measurements described above and shown are obtained by an integrated and computerized system that performs all tests for both high and low frequency on 100 pairs units (Fig.2). A total of 26500 measurements can be performed in 90 minutes. In Figs. 3 to 10 are shown the statistical results for attenuation, impedance, NEXT and FEXT at 1MHz. Furthermore the maximum, minimum and mean values as well as standard deviation (S) are indicated.

5. CONCLUSIONS

In order to ensure the quality of the network in view of the request of new services by the subscribers, a family of multipair copper cables with improved low and high frequency performances has been developed.

These cables meet the requirements imposed by the SIP Specifications, in particular for crosstalk, attenuation and impedance performances.

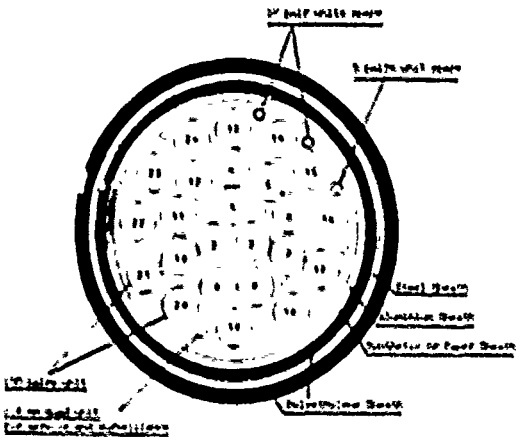

Fig.1 Typical multipair (2400 pairs) copper cable structure.

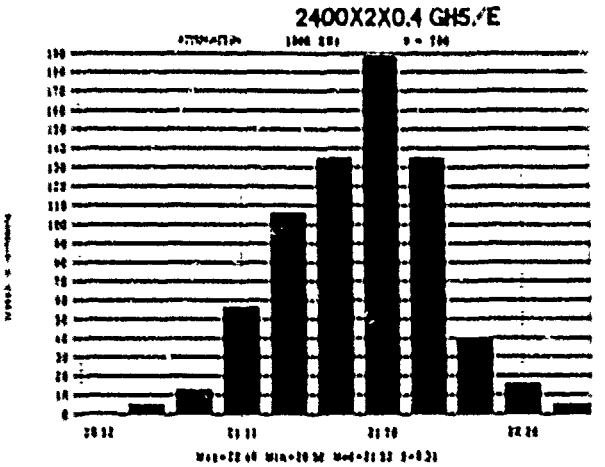

Fig.3

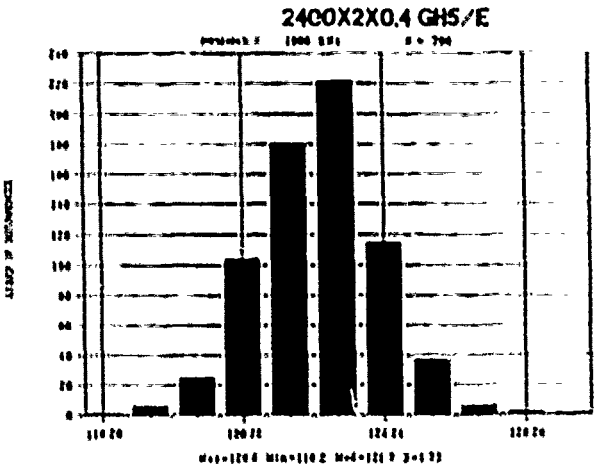

Fig.4

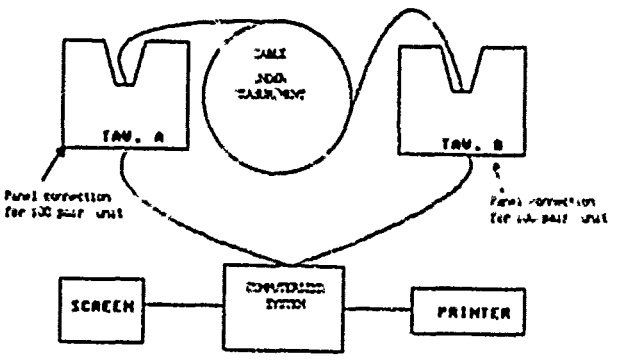

Fig.2 Electrical (high and low) measurement set up.

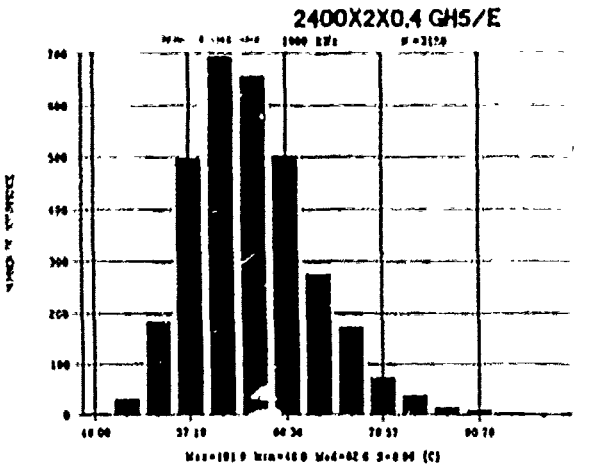

Fig.5

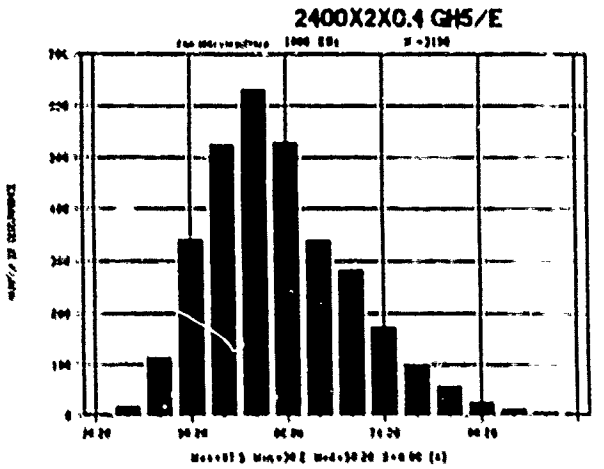

Fig.6

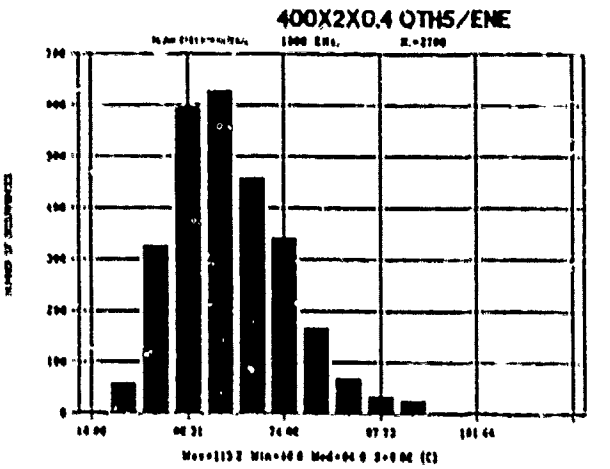

Fig.9

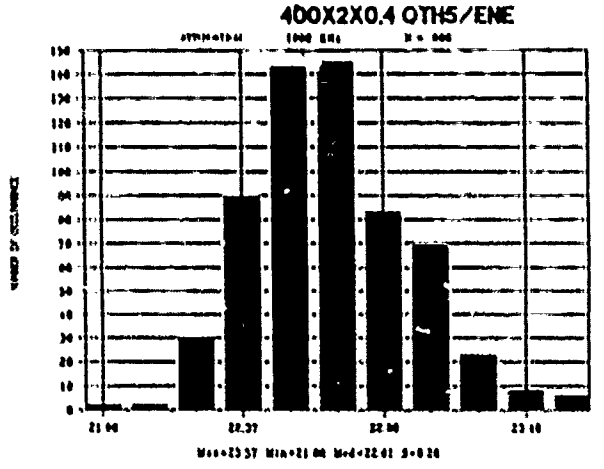

Fig.7

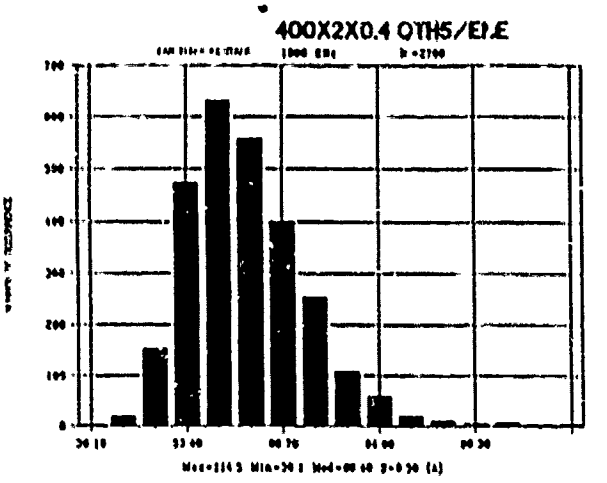

Fig.10

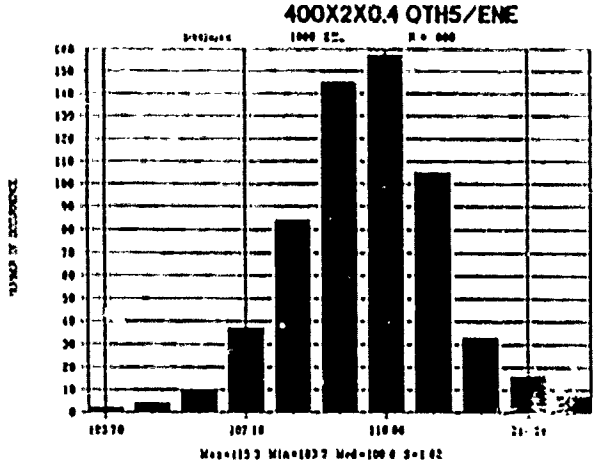

Fig.8

LOW FREQUENCY

UNIT	CABLE TYPE : TE 2400X2X0.4 GH5/E					
	Conductor Resis. Ohm/Km. a 20 °C		Mutual Capacity nF/Km		Unbalance C. pF/500 mt. P/P	P/T
	Mean	Max.	Mean	Max.	Max.	Max.
Ø1	138.55	142.79	46.63	47.94	82.4	661
Ø6	138.55	142.79	46.63	47.94	82.4	661
Ø7	138.55	142.79	46.63	47.94	82.4	661
14	138.55	142.79	46.63	47.94	82.4	661

HIGH FREQUENCY

UNIT	CABLE TYPE : TE 2400X2X0.4 GH5/E					
	IMPEDANCE Ohm			ATTENUATION dB/Km a 20 °C		
	Ø.8 KHz MAX.	80 KHz MAX.	1000 KHz MAX.	Ø.8 KHz MAX.	80 KHz MAX.	1000 KHz MAX.
Ø1	998.20	144.60	129.60	1.76	9.42	22.34
Ø6	997.50	145.20	128.52	1.75	9.43	22.36
Ø7	1012.20	138.52	127.42	1.76	9.45	22.35
14	1008.50	139.56	126.52	1.75	9.48	22.75

UNIT	CABLE TYPE : TE 2400X2X0.4 GH5/E														
	Far End Crosstalk dB/Km a 1 MHz.						Near End Crosstalk Attenuation dB a 1 MHz.								
	Comb. A			Comb. B			Comb. C			Comb. D			Comb.E		
	%	Min.	Mean	%	Min.	Mean	%	Min.	Mean	%	Min.	Mean	%	Min.	Mean
Ø1	1.4	39.2	58.9	Ø.4	43.3	70.6	1.6	46.0	62.5	Ø.6	52.0	76.1	Ø.0	76.3	92.7
Ø6	Ø.8	39.9	59.6	Ø.6	42.9	70.8	1.4	46.5	63.5	Ø.4	52.1	77.5	Ø.0	77.2	93.5
Ø7	Ø.4	42.2	59.7	Ø.8	42.9	70.5	1.2	46.5	64.5	Ø.6	51.9	77.8	Ø.0	77.5	94.2
14	Ø.6	41.9	60.1	Ø.6	41.9	70.1	Ø.8	47.1	64.6	Ø.6	51.8	76.9	Ø.0	77.3	94.5

Tab. 1 Low and High frequency results for electrical measurement (2400 cp.)

LOW FREQUENCY

UNIT	CABLE TYPE : TE 400X2X0.4 QTH5/ENE					
	Conductor Resis. Ohm/Km. a 20 °C		Mutual Capacity nF/Km		Unbalance C. pF/500 mt. P/P P/T	
	Mean.	Max.	Mean.	Max.	Max.	Max.
01	133.29	133.54	53.86	54.57	49	181
02	133.66	134.00	54.10	54.52	48	167
03	134.14	134.43	54.02	54.58	50	178
04	134.96	135.30	54.00	54.56	52	163

HIGH FREQUENCY

UNIT	CABLE TYPE : TE 400X2X0.4 QTH5/ENE					
	IMPEDANCE Ohm			ATTENUATION dB/Km a 20 °C		
	0.8 KHz MAX.	80 KHz MAX.	1000 KHz MAX.	0.8 KHz MAX.	80 KHz MAX.	1000 KHz MAX.
01	925.60	136.60	103.70	1.84	9.05	21.92
02	924.50	135.90	105.80	1.83	9.07	21.86
03	925.50	136.50	115.30	1.84	9.06	22.01
04	925.30	136.20	106.20	1.84	9.08	23.57

CABLE TYPE : TE 400X2X0.4 QTH5/ENE															
UNIT	Far End Crosstalk dB/Km a 1 MHz.						Near End crosstalk Attenuation dB a 1 MHz.								
	Comb. A			Comb. B			Comb. C			Comb. D			Comb.E		
	%	Min.	Mean	%	Min.	Mean	%	Min.	Mean	%	Min.	Mean	%	Min.	Mean
01	0.2	41.6	62.2	0.1	45.3	71.9	0.6	48.2	64.1	0.2	46.5	76.5	0.0	77.6	93.4
02	0.2	41.6	61.3	0.2	45.1	71.5	0.3	49.3	65.2	0.2	46.6	77.2	0.0	77.2	92.9
03	0.1	41.5	61.2	0.2	45.2	71.2	0.3	49.2	65.3	0.1	47.6	78.5	0.0	76.8	91.5
04	0.2	38.1	60.4	0.2	45.5	72.1	0.2	46.6	64.0	0.2	47.3	78.2	0.0	77.2	92.5

Tab. 2 Low and High frequency results for electrical measurement (400 cp.)

Acknowledgements: The author wish to thank the SIP Management for the permission to publish this paper; moreover thanks are due to Mr. Morè of Teleco Cavi Q&A Division for useful discussions and cooperation.

REFERENCES

[1] Leo M. Chattler :" A Guide to Electrical Specification Requirements for Multipair Telephone Cables", Wire Asia 82, Singapore, October 1982
[2] Chipman, Robert A.: " Transmission Lines", Schaum's Outline Series; Mc Graw Hill Book Comp. 1968

Ernesto Esposito was born in 1951 in Roseto degli Abruzzi (Italy).
Received his Doctorate in Telecomunication Engineering in Bologna in 1976.
After a short experience in teaching, from 1978 is employed in Teleco Cavi where, after being involved in the design of optical and copper telecomunication cables, is now in charge of the "Research and Development Departement".

DEVELOPMENTS AND EXPERIENCE IN THE INSTALLATION OF THE PERTH TO ADELAIDE OPTICAL FIBRE ROUTE

P Hulbert, M McKiterick, R Schuster

Telecom Australia - Melbourne, Australia

ABSTRACT

This paper describes the installation of a 2600 km cable route from Perth to Adelaide across some of the most isolated and difficult terrain in Australia. Most of the cable was installed by direct burial using Telecom developed techniques, although to help overcome approximately 200 km of unrippable rock, it was necessary to develop alternative rock sawing equipment. Unseasonal weather conditions were another challenge for what proved to be a highly successful project.

INTRODUCTION/BACKGROUND.

A high capacity broadband bearer was required to upgrade the existing radio bearer between Perth and Adelaide and to provide for growth for television bearers, telephony and other digital traffic. Capacity requirements, cost, maintenance and reliability considerations led Telecom Australia to choose a single mode optical fibre cable solution. Direct buried optical fibre cable presented challenges during installation, which are described in this paper, but it was considered that this would provide the most reliable solution in the long term. Since reliability and availability are prime considerations of Telecom's major customers, the route selected has the added advantage of being physically diverse from the existing radio route and from the planned second cable route. Figure 1 shows the planned cable route and the existing radio route.

Cable Design. The cable design was based on the standard configurations used by Telecom Australia to install over 14,000 km of the interexchange network. The main features of the design are light weight, non metallic and small size. Both slotted core and loose tube cables were installed on this project with all cables filled to prevent water ingress, and a nylon jacket for insect protection for plough cables and lower hauling friction for duct hauled cables was included.
The small diameter and low weight of these cables has enabled up to 20 km lengths to be successfully installed on this route. Table 1 gives the range of physical and optical

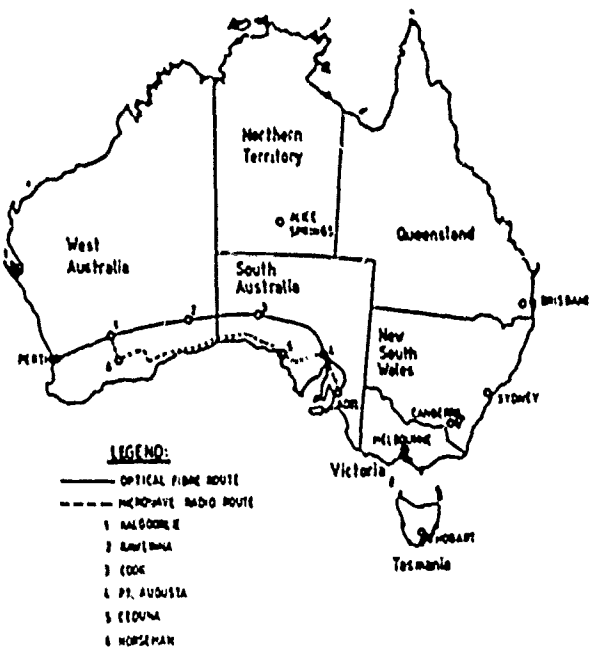

Figure 1 Perth - Adelaide Transmission Routes.

characteristics for cable supplied to this project.

It is Telecom Australia's experience that, provided the route is prepared properly, the selected strength and crush characteristics allow a very economic cable design and total cost effective solution for the installed cable. Figure 2 shows the basic cross sectional features of the cables.

System Design. Based on estimated statistics of the power budget parameters involved (Ref 1) Telecom Australia has developed a design regenerator spacing of 50 km for 565 Mbit/s systems at 1310 nm and this allows for a possible upgrade to 2.55 G bit/s systems at 1550 nm. A total of 14 fibres were included in the design with two of these provided exclusively for the Australian National Railways for a train control and communication system (also supplied by Telecom Australia).

A total of 50 regenerators and 3 line terminal stations were required typically at spacings of 50 km and feature a 1 + N protection system. The equipment is accommodated in underground chambers which control the local environment without the need for active air conditioning. The transmission equipment uses relatively low cost and maintenance free solar power provided by ground mounted arrays at 34 of the regenerator sites where mains power is not available.

CHARACTERISTICS			QUANTITY
CABLE FIBRE ATTENUATION AT	1300 nm		0.35 – 0.40 dB/Km
	1550 nm		0.21 – 0.30 dB/Km
CABLE OUTSIDE DIAMETER			11 – 13 mm
CABLE WEIGHT			90 – 110 Kg/Km
BEND RADIUS	A) NO LOAD	– PLOUGH	150 mm
		– DUCT	225 mm
	B) FULL LOAD	– PLOUGH	300 mm
		– DUCT	450 mm
CRUSH RESISTANCE	(DURING INSTALLATION)		20KN/m
	(WHILST INSTALLED)		10KN/m
RATED TENSILE STRENGTH FOR		A) PLOUGH	500 N
		B) DUCT	1200 N

TABLE 1.

PERTH TO ADELAIDE, SINGLE MODE OPTICAL FIBRE CABLE PHYSICAL AND OPTICAL CHARACTERISTICS

ROUTE CHARACTERISTICS

Route Selection - The route selection analysis was based on maintenance and economic considerations and resulted in the 14 fibre single mode optical cable being laid in the Railway Reserve for the majority of the route. Additional factors are that it provides a physically diverse route from the existing high capacity digital radio route and the drop-offs required by the Australian National Railways for a train control and communication system could be readily included.

Route Survey - The final route selected travelling east out of Perth traverses through State Forest in hilly country, then through farming country and along minor roads for about 250 km. The route then uses the Energy Commission's power line easement to Kalgoorlie and from there, east along the Australian National railway reserve to Port Augusta. At Port Augusta, the route travels south through private property and along roadway easements to Adelaide. Wherever possible, towns and built up areas were bypassed.

The State forest east of Perth suffers from Dieback disease which is a fungus that attacks the roots of Eucalyptus trees. Special precautions had to be taken to prevent the spread of this fungus on the wheels and tracks of vehicles. Precautions included waiting for dry weather windows and regular disinfecting of tractor tracks and car wheels.

Sand hills, extending east of the Nullarbor plain are reasonably stable but are held by a light covering of desert flora which is easily disturbed. A great deal of care was required in route selection, preparation and cable installation and route re-instatement to prevent erosion.

The Nullarbor plain, extending 700 km east of Rawlinna, consists of a desert landscape with very hard limestone rock that rises to the surface in waves making about 20% of this section un-rippable (approx 200 km).

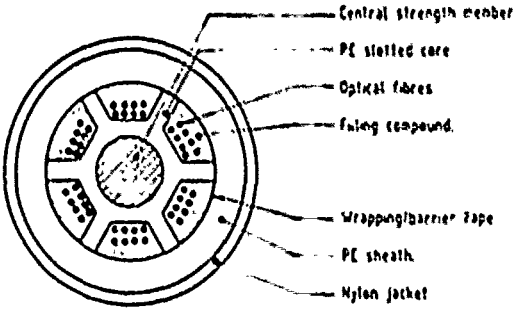

SLOTTED CORE DESIGN

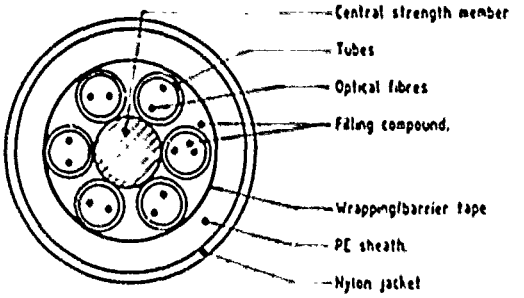

LOOSE TUBE DESIGN

FIG. 2 CABLE DESIGNS

INSTALLATION METHODS

The cable was installed by directly ploughing it into a prepared slip line or in the case of rocksawing, a trench, using a crawler tractor with suitable modifications for essentially zero tension installation (ref 2). This is the installation technique used extensively by Telecom Australia using light weight, low tensile

strength (500 N) non metallic cables. In built up areas, the cable design calls for a minimum tensile strength of 1200N and the cable is hauled into conduits or polyethylene subducts using tension controlled winches.With the appropriate level of route preparation, the cable is readily installed with the on-drum cable characteristics unchanged.

Route Preparation Options. It was the route preparation phase of this project that presented the major challenge to installation and support staff. In "normal" conditions the ground is prepared by ripping, perhaps by a number of passes, and then the cable is directly buried using the tractor described in references 1 and 2.

Across the Nullarbor Plain, because of the quantity of rock and the need to adopt the most cost effective solution Telecom Australia was forced to very closely examine the three route preparation options, ripping, blasting and rock sawing. Ripping is the most cost effective and the fastest method, however, in rocky terrain reinstatement can prove expensive because of the large boulders dragged up by the process. Furthermore, approximately 200 km of the route, on the Nullarbor plain, proved to be un-rippable even with a 100 tonne ripping tractor.

Drilling and blasting is a proven and viable alternative in hard rocky areas. It is not the preferred method because it is expensive and does not generate "fines" in the bottom of the trench for subsequent cable installation. Top soil must be bladed over the trench which must then be proof ripped before installation. On the Nullarbor Plain, the top soil is very thin and in some cases, soil would have to be carted for some distance. Even with these limitations, blasting was used on the Nullarbor plain. Rocksawing appeared to be the preferable alternative to blasting because fine soil is generated in the trench bed and there are no restoration problems. Telecom Australia had not had a great deal of experience with rocksaws. After testing and purchasing a number of machines for work on the Nullarbor Plain, there was concern over the ability of commercially available rocksaws to penetrate the hard rock. It was therefore considered advantageous to develop and trial a local machine.

Rocksaw Comparison.

Conventional rock cutting machines are dedicated to the task of cutting rock by typically rotating a chain or a wheel fitted with tungsten carbide teeth at high speed (approx. 4.5 m/s). Any rock encountered will then be pulverised into fine particles. This results in a substantial amount of friction between the teeth and the rock face which generates heat and may lead to early failure of the teeth. This conventional rock excavation leaves a trench of rectangular transverse cross section which requires a significant amount of energy to form the corners (as the rock adjacent to the corners is more difficult to remove). Those teeth placed furthest from the chain (or wheel) centre line are placed under considerable strain which results in high wear rates and breakages. Also, conventionally mounted rock cutting teeth wear rapidly in hard rock because they are mounted with a negative rake angle with respect to the rock face (see figure 3)

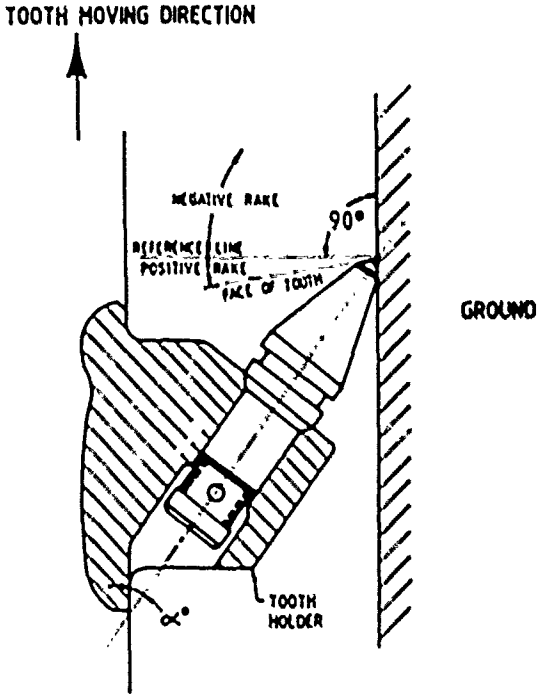

- NEGATIVE RAKE ANGLE INCREASES ∝°(>45°)
- POSITIVE RAKE ANGLE DECREASES ∝°(<45°)
- POSITIVE RAKE IN COMBINATION WITH THE ROTATION OF THE TOOTH HAS A SHARPENING EFFECT ON THE TOOTH TIP.

Fig.3: ROCK CUTTING TEETH WITH RAKE ANGLES.

The Telecom designed machine (see figure 4) consists of a cutting chain mounted on the rear of a crawler tractor with the blade facilities retained for versatility. The principle of operation is to chisel the rock into fragments rather than pulverising it into a powder and is achieved by using a slower chain speed (1.4 m/s) with a correspondingly higher torque. Fewer teeth are fitted to the chain, resulting in much higher tooth loads which induce shear strains behind the exposed surface of the rock, dislodging it in small fragments. The teeth are arranged so that they cut a curved cross section, with the teeth grouped closer together at the edge of the chain where the loading is highest. The teeth are oriented on the chain such that they have a positive rake angle with respect to the rock face.

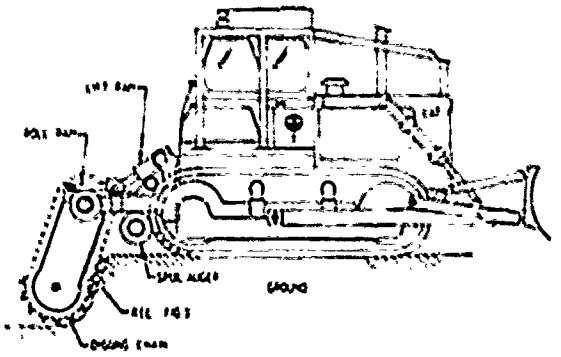

FIELD TRIALS.

To confirm the suitability of Telecom Australia's standard cable designs in this type of environment, three field trials were undertaken.

Ripping.

Concern existed over the placement of cables in rocky areas that had been prepared by standard ripping techniques. The limestone rock on the Nullarbor was rippable in some places, however, due to the large amount of rock present in some localised areas it generated fragments of rock with the potential to cause cable bending problems and possibly sharp enough to penetrate the non-metallic cable. If sufficient "fines" are generated at the bottom of the trench then the cable will be protected from this type of damage. A field trial was conducted at Rawlina on the Nullarbor Plain, which was considered to be typical of the worst terrain but was still rippable. The trial consisted of ploughing a length of standard cable to a depth of 600 mm in a trench prepared by ripping to a depth of 750 mm. After the ploughing operation, the trench was reinstated by blading surrounding rock fragments over the trench and compacting the mound using the tracks of the tractor weighing approximately 60 tonnes.

The cable was tested immediately after ploughing and again after the reinstatement operation using an OTDR and no change in characteristics was confirmed. The cable was also tested six months later and it was confirmed that no changes had occurred due to natural subsidence/compaction. The trial demonstrated that, even though it was not apparent, sufficient "fines" were generated by the ripping operation to adequately bed the cable and protect it from large and sharp rock fragments.

Blasting.

Drilling and blasting, although proven and reliable, is the most expensive option, and since it does not produce sufficient 'fines' in the bottom of the trench, it is the least preferred option.

Trialling on the Nullarbor could not be arranged to confirm the suitability of Telecom's standard cable design. Therefore the installation of a 120 km of fibre cable in mid Western Australia in a rocky area, which was considered to be at least as severe as the Nullarbor, was closely monitored. In some areas the rock was so extensive that suitable top soil had to be brought to the site and then proof ripped before the cable could be installed.

After acceptance testing of the cable no faults due to cable palacement were found. This cable has since been in operation for approximately two years and confirmed that provided adequate precautions are taken with trench preparation, the standard cable design is suitable.

Rocksawing.

In the un-rippable areas, the Nullarbor limestone rock has a compressive strength ranging from 200 to 300 MPa and a laboratory seismic velocity of approximately 6000 m/s. Concern existed that rock of this hardness would present productivity and potentially cable reliability problems in the harsh conditions. A field trial was established to evaluate the production capability and maintenance requirements of a Telecom designed saw and a commercial unit.

The evaluation procedure for the trial was to have a ripping tractor make one or two passes at the required depth without cross ripping. The rocksaws were then required to saw the length of the trench that were not able to be ripped to depth. The trial was carried out at Cook (point 3 on figure 1) on the Nullarbor Plain with one machine working westward and the other eastward.

The initial results of the trial confirmed expectations that the locally designed rocksaw performed well in comparison with the commercial model in this type of rock. The length of the trench cut was greater, the number of teeth used was less and the amount of fuel used was also less. On the basis of this trial it was decided to proceed with construction of several more rocksaw units. It was also decided to continue with the commercial model since in both cases, the trenching rate was low due to the hardness of the rock and all available machines would be needed to meet targets. Another consideration was long term reliability which could not be assessed in a limited trial. The local machine was still an unproven quantity.

CABLE INSTALLATION PERFORMANCE AND TEST RESULTS

The construction phase of the project began in June 1987 and was completed in August 1989 using an average of approximately 60 field personnel. Cable was supplied to the project in lengths up to 20 km and plough rates varied from 5 km/day up to 20 km/day.

Productivity was hampered significantly in December 1988 when rainfall reached seven times the monthly average making access impossible.

Figure 4 shows the typical distribution of regenerator section insertion loss, normalised back to a loss coefficient per km. These results are considered excellent given the difficulty of the route preparation phase.

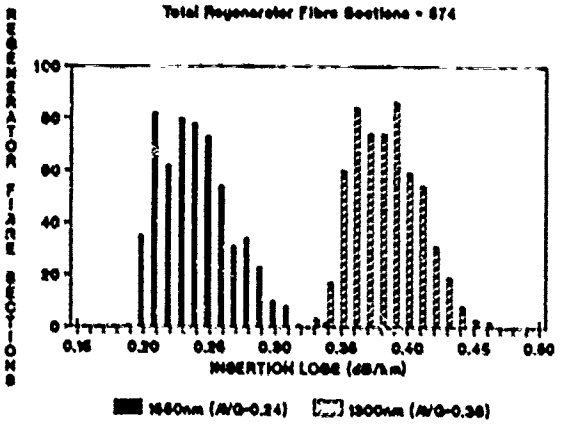

FIG 5 DISTRIBUTION OF REGENERATOR SECTION INSERTION LOSS

Conclusion.

A very light weight, relatively low strength cable design has been succesfully installed and commissioned in harsh conditions by applying properly engineered installation practices.

Experience gained on the current project is being applied to the design and construction of more robust rocksaws of both the local type and the commercially available machines. These units will be used on a physically diverse cable route which is planned to follow the coast road where more limestone rock will be negotiated. The expectation is that while the conditions will be more difficult, the installation will proceed at a higher productivity rate than achieved on this project.

Acknowledgements

The editorial assistance of Mr Kiss, Dr Johansen and Mr Guerra is gratefully appreciated. The permission of the D M D Telecom Australia to publish this paper is acknowledged.

References

1. "Installation, Evaluation and Future Design of Optical Fibre Long Haul Routes in Australia" - E Johansen, B M Faulks, B T de Boer, 35th International Wire and Cable Symposium, Reno, Nevada, November 1986.

2. Cable Designs and Installation Technique for Direct Buried Non-Metallic Optical Cables - B T de Boer, R W A Ayre, R B Schuster, 34 th International Wire and Cable Symposium, Cherry Hill, New Jersey November 1985.

Authors.

P HULBERT

Optical Cable Networks Branch
Telecom Network Engineering
Telecom Australia
10/ 518 Little Bourke Street
Melbourne, Victoria
Australia 3000

Phil Hulbert joined Telecom Australia in 1972 as a Cadet Engineer and subsequently graduated in Science ('74) and Electrical Engineering ('75) from the University of Adelaide. He has 9 years experience in the fields of Quality Assurance and Material provisioning. The last three years he has been involved in the design, manufacture and testing of optical fibre cables and is currently Manager of the Optical Cable Design Section.

M McKITERICK

Optical Cable Networks Branch
Telecom Network Engineering
Telecom Australia
10/ 518 Little Bourke Street
Melbourne, Victoria
Australia 3000.

Michael McKiterick graduated in 1970 from the Royal Melbourne Institute of Technology in Civil Engineering and joined Telecom Australia in 1974. Currently, he has national oversight for the development of external practices associated with optical fibre cable installation and jointing.

R SCHUSTER

Telecom Automotive Plant
Project Section
Telecom Australia
54 Postle Street
Coopers Plains, Queensland
Australia 3000.

Richard Bryan Schuster joined Telecom Australia in 1982 after graduating form the University of Queensland with honors in Mechanical Engineering. He has had substantial experience in external plant installation practices associated with cable ploughing equipment and procedures. Richard has been involved in the design of Telecom Australia's patented Zero Tension Cable Laying System as well as the Telecom Rock Ditcher, which won an Institution of Engineer's Engineering Excellence award.

Development of Optical Fiber Units for Air Blown Fiber (ABF) Cabling Systems

H. Sano K. Hayashi Y. Terasawa S. Tanaka Y. Masuda

Sumitomo Electric Industries, Ltd.
Yokohama, Japan

ABSTRACT

ABF cabling system is a new optical fiber cabling system that has special merits and applications. Recent reports of optical fiber unit for this system, however, showed attenuation increase under 0°C, and the further attenuation increase at low temperature after heat aging. We have investigated design of the unit, and clarified that the extrusion stress of skin layer is one of the important factor of the behavior of transmission properties. Skin layer material of small melt index, has been chosen and has shown good transmission properties in wide temperature range. Some variations of unit including easy strippable type and fiber ribbon unit type, have also been developed and shown good transmission properties and good blowing properties.

1. INTRODUCTION

A new optical cable installing system, called Air Blown Fiber cabling system, has been proposed by British Telecom Research Laboratories in 1983 [1]. They have also reported the design of optical fiber unit of 7 fibers, and temperature performance of multi-mode fiber unit as the change of attenuation was less than 0.2dB/km between -10°C and+40°C [2].

We have been trying to modify this cabling system to meet Japanese applications. In Japan, optical fiber cables are installed not only as under-ground cables but as aerial ones or as special combined ones. Therefore we had to develop the cable's design with high performance of attenuation in more wide temperature range, from -40°C to 80°C. On the other hand, many types of optical fiber units such as optical

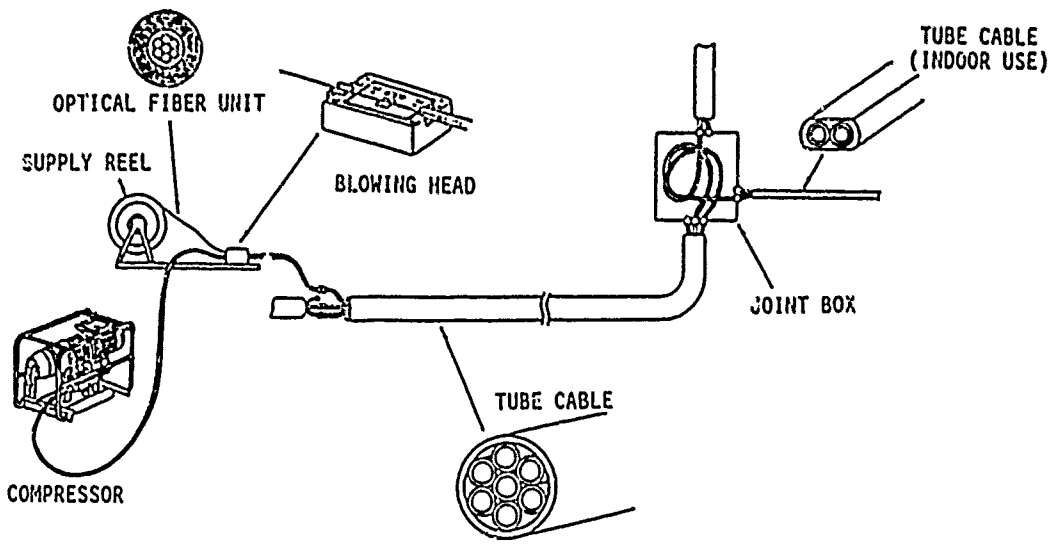

FIGURE 1 CONSTRUCTION OF ABF CABLING SYSTEM

fiber ribbons of different number of fibers, are used in Japan. We have strong requirement to keep a rich assortment of unit variations.

In this paper, we report 7-fiber unit design with good transmission properties between -40 °C and 80 °C, and new variations of optical fiber units.

2. Construction of ABF System

Construction of ABF system is shown in Figure 1. Optical fibers are packaged as optical fiber units with expanded polyethelene coating. Optical fiber unit is payed of from a supply reel into a pre-installed tube cable by blowing head. Drag force of compressed air supplied at the head, blows the unit through the tube. this procedure has some special merits caused by the process, as follows:

1. After installing of tube cables, optical fiber units can be installed, only after optical network will be required. Therefore the first investiment can be minimized.

2. With jointing tubes of pre-installed cables, branching or connecting are easily done without optical fiber splicing. Therefore splicing points at every junction are not required, so that installing cost is reduced and cable reliability is increased.

3. By this procedure, drawing out is easily done as blowing into a tube cable. Therefore, with changing tube junctions and unit types, enlargement or alternation of the fiber networks are suported.

4. Installing stress are distributed all the length, because drag force by fluid is generated on the all surface of the units.

For the merits ABF cabling system is mainly used for applications of local area networks or combined cables with metal cables.

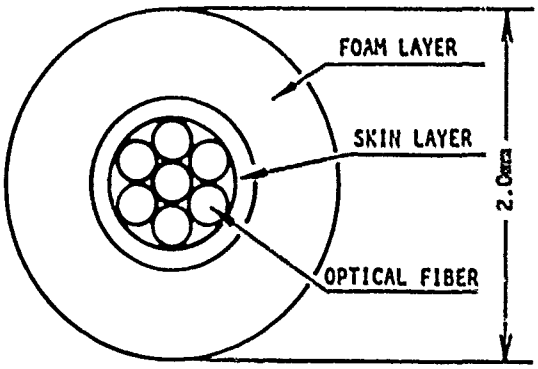

FIGURE 2 CROSS-SECTION OF OPTICAL FIBER UNIT

3. NEW DESIGN OF 7-FIBER UNIT

1) ATTENUATION INCREASE OF CONVENTIONAL UNIT AT LOW TEMPERATURE

The optical fiber unit of ABF cabling system, has large cross section of polyethylene foam layer and skin layer as shown in Figure 2. This foam layer performs enlargement of its surface for improved blowing properties. The skin layer is coated to package optical fibers and to give suitable stiffness of unit.

Figure 3 shows the changes of attenuation of multi-mode fiber unit and single-mode fiber unit against temperature in a heat cycle test, when material A (Table 1) was used for skin layers. Attenuation were measured at the wavelength of 0.85 μm for multi-mode fiber and at 1.30 μm for single-mode fiber. The attenuation increase took place at temperatures less than 0°C, and expended after first high temperature aging. We confirmed that the attenuation increase at low temperature, dose not extend after the second or third high temperature aging.

This behavior was considered that release of the extrusion stress at high temperature induces strain on optical fibers beyond adding the attenuation above 0°C, but the stress was added to the shrinkage stress at low temperature of the coating layers and showed the extension of attenuation after heat aging. In order to confirm and to take measures to the above problem, we have investigated the skin coating material, because foam layer material is not easy to change for the large effectiveness on the blowing properties.

Table 1 shows the physical properties of skin coating materials, and Figures 4 and 5 show the changes of attenuation between -40°C and 80°C for material B and C as skin coating material respectively.

TABLE 1 PROPERTIES OF SKIN MATERIALS

PROPERTY	TEST CONDITION	MATERIAL for SKIN COATING		
		A	B	C
Melt index (g)	230°C/2.16kg	2.0	9.0	8.0
Thermal expansion coefficent (K^{-1})	—	1.1×10^{-4}	1.6×10^{-4}	1.0×10^{-4}
Tensile modulus (kg/cm^2)	23°C	44	48	15
Optical fiber strain caused by skin and form coating (%)	Optical phase delay technique	0.09	0.05	0.06

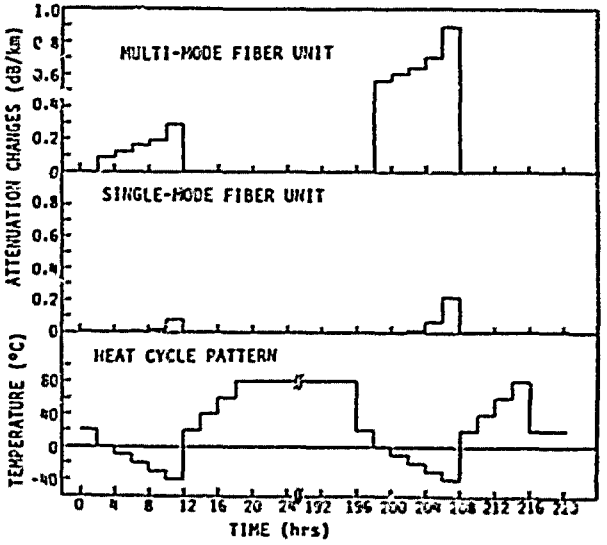

FIGURE 3 THE CHANGE OF ATTENUATION AGAINST TEMPERATURE (Material A as skin layer)

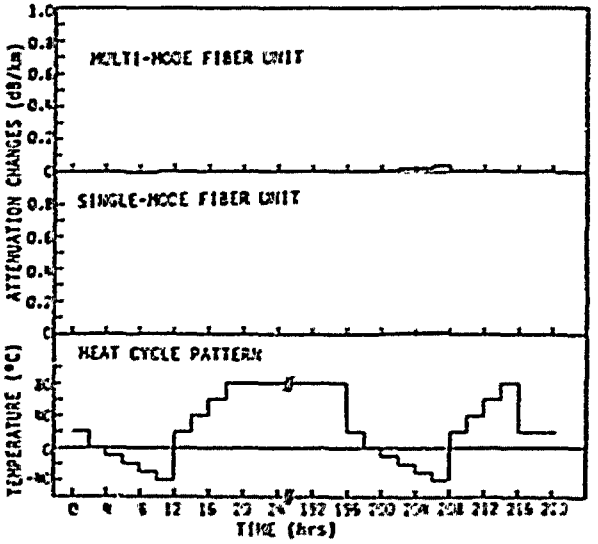

FIGURE 4 THE CHANGE OF ATTENUATION AGAINST TEMPERATURE (Material B as skin layer)

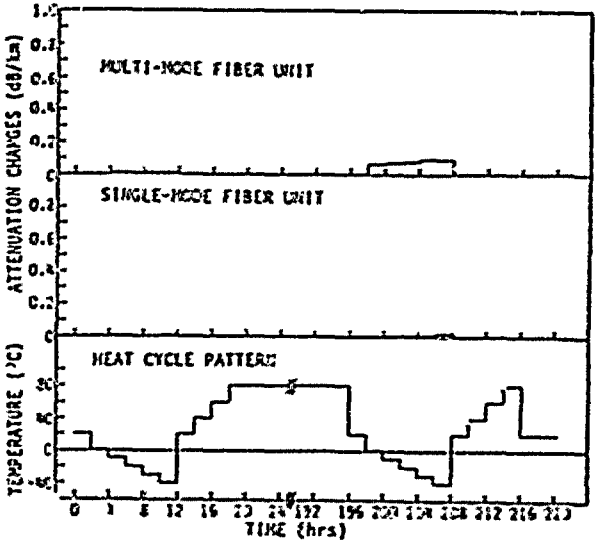

FIGURE 5 THE CHANGE OF ATTENUATION AGAINST TEMPERATURE (Material C as skin layer)

2) EFFECT OF EXTRUSION STRESS

Material A has small melt index, and it means the large extrusion stress is expected to remain. Material B, on the other hand, has almost the same tensile modulus as material A but larger melt index, therefore we expected that the extrusion stress of skin layer could be decreased, and the further attenuation increase at low temperature after heat aging could be reduced, if the extrusion stress was responsible to the extension. Residual extrusion stress of all coatings were directly measured as strain release of optical fibers by removing the unit coatings by optical phase delay technique, as shown in Table 1. The values of extrusion stress were in expected relationship to the melt index. On the other hand, the further attenuation increase at temperatures below 0°C after heat aging, could not be observed. In this case, the residual extrusion stress of skin layer was considered to induce considerable strain on optical fibers after heat aging, as compared with that of foam layer. Therefore melt index, as a parameter of extrusion stress, is concluded to be one of the most important property to choose a skin layer material of optical fiber unit of this system.

3) LOW TEMPERATURE SHRINKAGE

To decrease the strain on optical fibers at low temperature, the soft material C was chosen for skin layer material. Material C had almost the same melt index as material B. The extrusion stress, shown in Table 1, was a little less than the value of material B, for tensile strength of material C was less than that of material B. For the same reason, a skin layer of material C generated smaller strain on optical fiber at low temperature, than the skin of material B. Figure 5 shows the changes of attenuation when material C was used as skin layer.

The attenuation increase of this unit at low temperature was, contrary to our expectation, a little larger than that of the unit which used material B.

We considered the reason for above result that the soft skin layer could not level the irregularity of the foam layer shrinkage.

Among these three materials, we have concluded material B was the best as the skin layer material of A8F cabling system.

4) EVALUATION OF NEW DESIGN UNIT OF 7 FIBERS

Transmission properties and blowing property of new design unit of 7 fibers was evaluated as Table 2.

The attenuation changes were sufficiently small for both units of multi-mode and single-mode fibers. Attenuation increase at low temperature was less than 0.05dB/km for each fiber types and for each observing wavelength between -40°C and 80°C. The values were small enough to apply these units not only to local area networks but to long distance transmission use.

Using compressed air in 5kg/cm², the unit could be blown into 500m tube cable which was wound on a drum of 1m in diameter within 17 minutes. Then there was no problem to install this new design unit. The installation performance is as good as our conventional units.

4. NEW VARIATIONS OF A8F UNITS

To meet the demand of wider applications, we have developed new variations of units.

Table 3 shows structures of unit variations with some special properties. Type 1 and type 2 have a rip code for the purpose of pulling out fibers from unit easily. Type 3 to type 6 were fiber ribbon unit especially for connecting ordinary fiber ribbon cables.

Outer diameter of these units were controlled to be 2.0mm without type 6, so that the existing equipments can be used.

Attenuation increase at low temperature were evaluated by the same procedure of the previous chapter. All types of multi-mode fiber units showed good properties, such as attenuation increase less than 0.20dB/km at -40°C. Also all types of single mode fiber units similarly showed good properties, less than 0.05dB/km at the same condition.

Blowing properties of these units were also evaluated by measuring time for blowing the unit through 500m length tube cable wound on a drum of 1m in diameter using compressed air in 5kg/cm². Blowing the type 5 and type 6 units needed more minutes than other units. The reason for the result is considered that these units had inclination to keep the given figure, such as a curve of reel, resulting the increased friction between units and tubes. However the times were less than 25 minutes, hence, there is still no problem to practical use.

TABLE 2 PROPERTIES OF NEW DESIGNED 7-FIBER UNIT

Multi-mode fiber unit		Wavelength		Test conditions
		0.85μm	1.30μm	
Attenuation (dB/km)		2.45	0.37	Unit on reel of 30cm in diameter
Attenuation increase of unit (dB/km)	-20°C	0.02	0.02	Unit in coil of 30cm in diameter Maximum attenuation increase in 3 times Temperature cycles between -40°C and 80°C
	-40°C	0.04	0.03	
Single-mode fiber unit		Wavelength		Test conditions
		1.30μm	1.55μm	
Attenuation (dB/km)		0.38	0.28	Unit on reel Of 30cm in diameter
Attenuation increase of unit (dB/km)	-20°C	< 0.01	0.01	Unit in coil of 30cm in diameter Maximum attenuation increase in 3 times Temperature cycles between -40°C and 80°C
	-40°C	< 0.01	0.01	
Blowing properties (min)	300m tube	8.30		Blowing time through correspondent length tube Using compressed air in 5kg/cm²
	500m tube	17.00		

5. CONCLUSION

We have investigated the optical fiber unit design for ABF cabling system to extend the applications. We have clarified that the residual extrusion stress of skin layer is responsible for the attenuation increase at low temperature after heat aging.

Based on these results, we have developed new designed unit coated by a material with large melt index, as the ABF unit for the wide temperature range use. This type of unit shows good transmission properties between -40°C and 80°C and good blowing properties.

We have also developed several ABF units for special applications.

REFERENCES

[1] S. A. Cassidy and M. H. Reeve, "A radically new approach to the installation of optical fibre using the viscous flow of air", Proc. IWCS, pp.250-253, November 1983.

[2] S. Horning, S. A. Cassidy, P. Yennadhiou and M. H Reeve, "The blown fiber cable", IEEE, J. on Selected Area in Commun., Vol.sac-4, No.5, August 1986.

TABLE 3 DEVELOPED UNIT VARIATIONS

Type		Structure (without foam layer)	Outer diameter of foam layer (mm)	Attenuation increase at -40°C (dB/km)		Blowing property (min) **
				Multi-mode 0.85μm	Single-mode 1.30μm	
7-fiber unit (Standard)	0	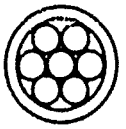	2.0	0.04	< 0.01	17 *
6-fiber unit (with rip code) ▨:rip code	1		2.0	0.04	< 0.01	17 *
	2		2.0	0.05	< 0.01	17 *
Fiber ribbon unit (2-fiber ribbon with rip code) ▨:rip code	3		2.0	0.13	0.02	18
	4		2.0	0.13	< 0.01	17 *
	5	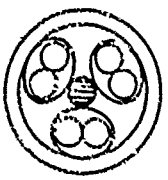	2.0	0.08	< 0.01	19
	6	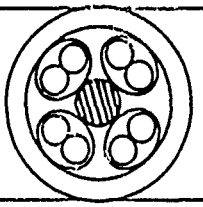	2.6	0.03	0.01	24

* Maximum suplying speed of blowing head = 17m/min
** Blowing time through 500m length tube using compressed air in 5kg/cm²

Hiroaki Sano

Sumitomo Electric Industries, Ltd.

1, Taya-cho, Sakae-ku, Yokohama, Japan

Hiroaki Sano was born in 1960 in Osaka, Japan, and received his M.E. degree in Polymer Science from Kyoto Univ. in 1984. He then joined Sumitomo Electric Industries and has engaged in development of optical fiber manufacturing process and cables. Mr. Sano is a member of Communication R&D Dept. in Yokohama Research Laboratories.

Kuni Hayashi

Sumitomo Electric Industries, LTd.

1, Taya-cho, Sakae-ku Yokohama, Japan

K. Hayashi was born in Shanghai, China on August 21, 1958. He received his B.S. degree in Electrical engineering from Chiba Univ. in 1986. He then joined Sumitomo Electric Industries and has been engaged in research and development of optical fiber and cables. Mr. Hayashi is a member of Communication R&D Department in Yokohama Research Laboratories.

Yoshiaki Terasawa

Sumitomo Electric Industries, Ltd.

1, Taya-cho, Sakae-ku Yokohama, Japan

Yoshiaki Terasawa was born in Hokkaido, Japan, on August 10, 1961. He received the B.S. and M.S. degree in applied physics from Hokkaido University in 1985 and 1987, respectively. He joined Sumitomo Electric Industries, Ltd., in april 1987 and engaged in research and development of optical fiber cable. Mr. Terasawa is a member of Communication R&D Development in Yokohama Research Laboratories.

Shigeru Tanaka

Sumitomo Electric Industries, Ltd.

1, Taya-cho, Sakae-ku, Yokohama, Japan

Shigeru Tanaka was born in Tokyo, Japan, on December 2, 1951. He received the B.S. and M.S. degree from Tokyo University, Tokyo, Japan, in 1974 and 1976, respectively.
He joined Sumitomo Electric Industries, Ltd. in 1976, and has been engaged in the design and characterization of optical fibers and fiber cables. He is a Chief Research Associate of the Communication R&D Department.
Mr. Tanaka is a member of the Institute of Electronics and Communication engineers of Japan.

Yuichi Masuda

Sumitomo Electric Industries, LTd.

1, Taya-cho, Sakae-ku Yokohama, Japan

Yuichi Masuda received his M.S. degree in Electrical Engineering from Kyoto Univ. in 1970. He then joined Sumitomo Electric Industries and has been engaged in development of optical fiber and cables. Mr. Masuda is now manager of Communication Research Department, and a member of the Institute of Electronics and Communication Engineers of Japan.

CONSTRUCTION OF CONTINUOUS OPTICAL CABLE TO 10 KM-LONG WATERWAY OF HYDRAULIC POWER PLANT

H. Sawada*, S. Hasegawa*, H. Horima**, T. Amano**

* The Hokkaido Electric Power Co., Inc. Asahikawa, Japan

** Sumitomo Electric Industries, Ltd. Yokohama, Japan

ABSTRACTS

Recently the electric power company utilities are actively constructing optical communication networks over a wide range. As the applicable range of optical cable expands, installation of optical cable in severe environment has been examined. One example is that the Hokkaido Electric Power Co. applied on optical cable to the waterway in its Setose hydraulic power plant for monitoring the buildings and water level and remotely controlling the water gate of the dam. On the other hand, the waterway incessantly receives a rapid water flow or substantial hydraulic pressure. For achieving higher reliability the Hokkaido Electric Power Co. introduced a continuous long length joint-free optical cable for the waterway. In this report the cable construction and installation techniques are discussed for the said continuous optical cable used in the waterway and the measured cable characteristics and the result of installation are introduced.

1. Foreword

Nowadays, electric power company utilities are active in construction of optical communication network over an extensive range, utilizing the excellent features of optical fiber such as low loss, wide bandwidth characteristics and non-inductive characteristics.

Typical optical cables employed by such utilities are classified into OPGW (composite fiber-optic ground wire) to be laid along the overhead power transmission line route, self-supporting type optical cable to be installed along the overhead power distribution line route and plane sheath-provided ordinary optical cable to be laid in duct, though this depends on cable laying environment. In addition, there are indoor optical cables.

Along with expansion of applicable range of optical cable, its introduction is now under study in severe environment.
This is exemplified by the application of optical cable to the waterway in a hydraulic power plant of a power utility, which is introduced here. Focusing on the superb characteristics of optical cable, the Hokkaido Electric Power Co. recently determined to adopt an optical communication system for monitoring the buildings and the water level of the dam up the river in the mountains, and for remotely controlling the opening and closing of the water gate from the dam down the river located in the city area.

A dam is of course constructed in a mountain. If optical cable is laid along a foot-way or road on behalf of its construction and maintenance, transmission line will become extremely long. Hence, installation of a repeater will increasingly be unavoidable for transmitting ITV color images. For achieving the duplication of transmission line, it is requested to lay optical cable along the route where there is the smallest chance of damage occurring due to guns, birds and insects.

Needless to say, the shortest installation route from a dam to the power plant lies in the waterway of that plant. Besides, in the waterway, there is no possibility of the above-mentioned damage due to guns, birds and insects. Furthermore, the waterway has been designed so as not to allow a large substance to float through in except for sand and pebbles. On the other hand, the waterway incessantly receives a rapid water flow, or substantial hydraulic pressure. And water cannot be stopped immediately, signifying a rather hard installation environment. Therefore, a higher reliability is required for introducing optical cable. Recently the Hokkaido Electric Power Company introduced optical cable in the waterway of about 9.1 km, which is located in the Muri dam on the Yubetsu river system belonging to its Engaru Power Station. This paper reports examinations made by the authors on the structure and installation engineering of optical cable for waterway, and the installation situation of this cable on site.

2. Overview of System

This system has been built up intended to remotely supervise from the downstream Yubetsu river dam the upstream Muri dam for gathering water to be used by the Setose hydraulic power plant belonging to the Engaru Power Station of the Hokkaido Electric Power Co.

Figure 1 outlines this system and Figure 2 shows its route diagram. The intended remote control scheme can be outlined as follows. Two ITV units have been installed in the Muri dam. From these

3. Cable Installation Environment

The present cable route is shown in Fig. 2. It spans a section from the Muri dam of the Hokkaido Electric Power Company's Engaru Power Station to the Yubetsu river dam. Cable is laid in the waterway for the relevant hydraulic power plant and directly buried over some range.

The waterway is a tunnel shaped as shown in Fig. 3. During generation of hydraulic power, the waterway is always filled with water. Moreover, hydraulic pressure and flow reach approximately 3.6 kg/cm^2 and 3m/sec., respectively. It was observed that sand, pebbles, wood pieces and others flowed, which has entered through the water inlet of dam together with water.

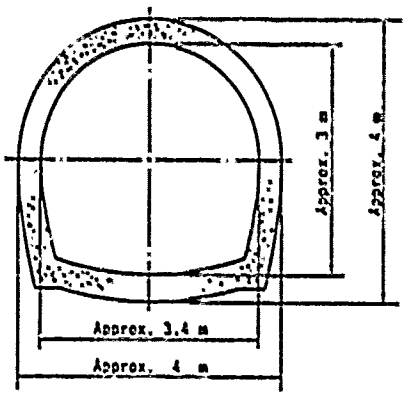

Cross Section of the Waterway

The reason why the waterway was selected as a cable route despite such hard conditions in its inside is summed up as follows.

(1) An aerial copper communication cable has already been installed over mountains. For duplication with this cable, namely preventing simultaneous occurrence of damage, the new communication cable need be laid on a different route.

(2) For another aerial cable, a new foot-way must be constructed because it is absent.

(3) Aerial cable cannot be said to be free from damage due to guns, birds and insects.

(4) The use of waterway in the relevant hydraulic power plant allows the shortest course possible which runs the section of interest. It is advantageous from the viewpoint of system.

For the above reasons, the waterway has been determined as a cable route.

4. Optical Cable Design

The design of optical cable has been examined in consideration of such a special cable environment as mentioned above.
First of all, for the environmental reasons enumerated below, we have decided to employ a continuous joint-free optical cable without providing a cable joint in the dam waterway.

(1) For cable installation, water must be discharged completely from the waterway. However, spring water, etc. will always flow into the waterway to increase humidity up to an extremely high level. Therefore, fiber splicing with a splicing machine is expected to be difficult in the waterway.

(2) Transmission line must have a high reliability against flowing water, water pressure or external force given from floating materials.

(3) The waterway has a curvature radius of several ten meters or more only at a few locations. Besides, its grade approximates merely 1/1000. These characteristics are suited for laying a long cable without a joint.

For introduction as a continuous joint-free optical cable with a long length, optical cable has been designed as follows in order to be laid under a high tension at installation and endure a rapid water flow at about 3 m/sec after installation; an iron wire of 1.2 mm dia. and outer polyethylene (PE) sheath for preventing corrosion of the iron wire are wound on the inner sheath. The inner sheath has employed a LAP sheath as a moisture barrier, and the cable core has adopted a slot structure which excels in compressive characteristics. Figure 4 shows the construction of the optical cable laid in the waterway of this dam. The construction, as it is, has also been used for the burial cable.

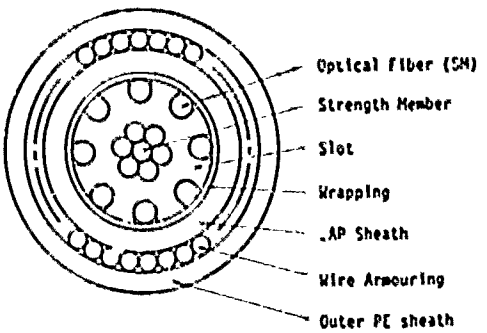

Fig. 4 Construction of the Optical Cable

Table 1 lists the characteristic requirements of the optical cable employed for this system. The optical fiber has 6 fibers in total; 2 fibers for transmitting ITV signal from the Muri dam and remotely controlling the open/close status of dam gate, and spare 4 fibers for future cable extension to upstream dam, etc.

units,video and voice signals, which represent water level in the dam and the conditions of buildings, are transmitted to the Yubetsu riber dam administration office for supervision on the TV screen (color moving pictures). The Yubetsu river dam side sends the open/close signal of the Muri dam gate for the purpose of remote control.

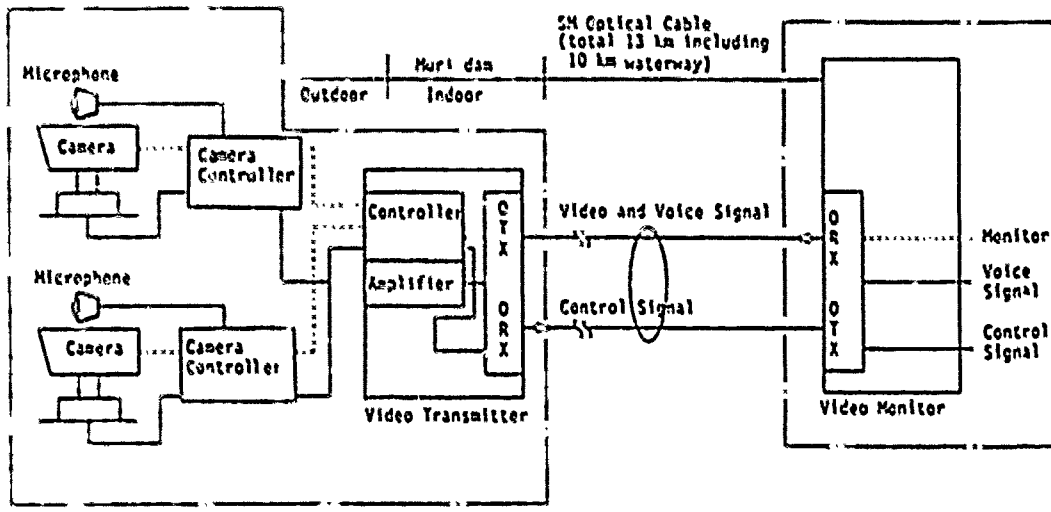

Fig. 1 Outline of System

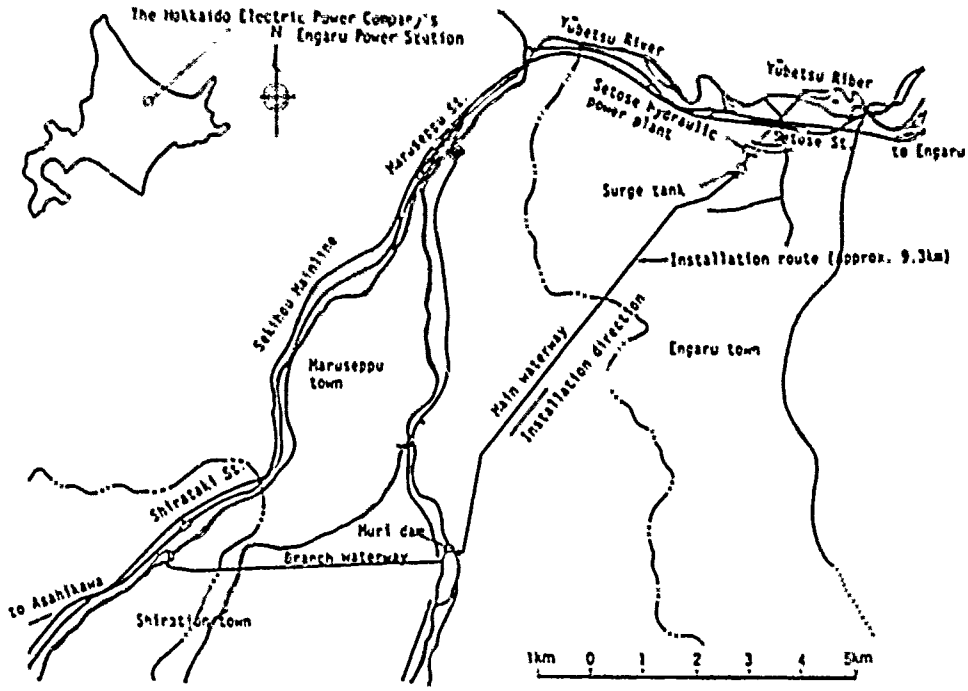

Fig. 2 Route Diagram

Table 1 Optical Fiber Characteristics

Item		Requirements	Characteristics of fibers in cable
Fiber type		Single mode	Single mode
Number of fiber		6	6
Attenuation	1.3 μm	Less than 0.6 dB/km	Less than 0.37 dB/km
	1.55 μm	—	Less than 0.23 dB/km
Cut off wavelength		1.10 ~ 1.29 μm	1.18 ~ 1.24 μm

5. Examination of Installation Method in Waterway

For laying a continuous joint-free optical cable of slightly less than 10 km, application of the installation methods below has been examined in particular.

(1) Upon laying the cable, it is predicted that cable tension would exceed a few tons at maximum if hauled only by its pulling end. To circumvent this, we should employ 8 intermediate pulling machines at intervals of about 1 km.

(2) Each intermediate pulling machine should be provided with a single telephone set in order to control the cable tension while exchanging information at the installation site of each machine.

(3) To minimize external force to be applied to the optical cable while it is laid out, a pulley should be arranged at intervals of 2 to 10 m in response to curvature.

(4) Workman should always be beside the pulling end of optical cable while it is pulled for installation so that the cable can pass the pulleys smoothly.

6. Characteristics of Optical Cable

We produced a wire armoured optical cable shown in Fig. 4 whose length is 9.6 km including the waterway of about 9.1 km from Muri dam to Setose Power Station. This section details the result of characteristic evaluations of this cable.

6.1 Transmission Characteristic

Although this optical cable is used at a wavelength of 1.3 μm, transmission characteristics at a wavelength of 1.55 μm have also been evaluated because a high cable reliability need be secured. Average loss of 6 fibers was 0.36 dB/km at 1.3 μm and 0.22 dB/km at 1.55 μm. That is, deterioration of optical characteristics in manufacturing process has not been observed particularly.

6.2 Mechanical Characteristics

Mechanical characteristics have been investigated, assuming a pulling tension in long length optical cable installation, application of hydraulic pressure of 3.6 kg/cm² and external force due to floating materials such as pebbles. Every results indicate stable characteristics with a proper safety factor. Table 2 summarizes the result of test. Figs. 5 and 6 detail each result of tensile and compression tests.

Table 2 Methods and Results of Tests

Methods	Results
Tensile 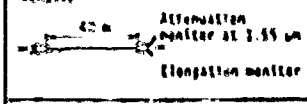	No attenuation change up to 800 kgf of tensile load
Compression 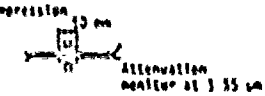	No attenuation change up to 700 kgf/50 mm of compression load Deformation is approx. 18% at the same time
Impact	No fiber snapping at 10 kg of impact load
Bending 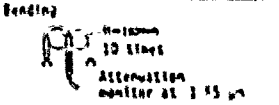	No attenuation change while 10 times bending at 180 mm of bending radius
Torsion 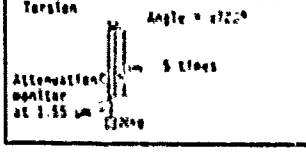	No attenuation change while ±720° of torsion angle

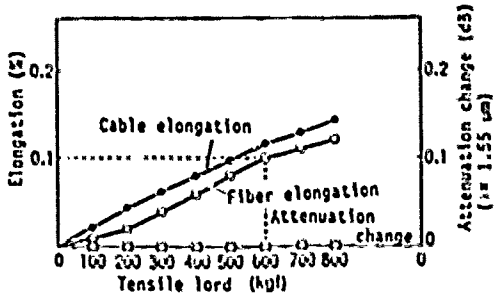

Fig. 5 Tensile Test

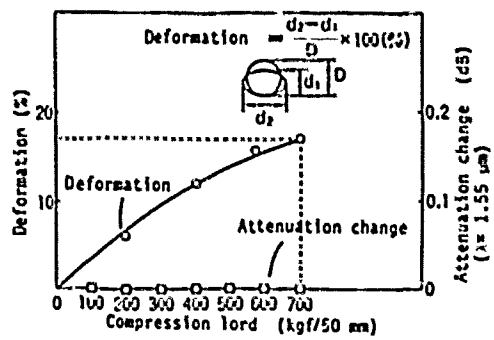

Fig. 6 Compression Test

6.3 Temperature Characteristics

In the Engaru district of Hokkaido, temperature drops to even -30°C in winter excluding the inside of dam waterway. To cope with this, the optical cable has been designed within a wide temperature range of -40 to + 60°C. The result of measurement is shown in Fig. 7. At both wavelengths, loss fluctuation was within 0.05 dB/km. This proves that characteristics are stable even at a low temperature.

7. Installation Work

Cable installation work was undertaken taking the opportunity of the sand/soil discharge from waterway and equipment check which is carried out once every several years. Because water feed into the waterway was stopped for only one month, installation was required to be completed within that period of time including preparations. This meaned a rather tough condition.

The installation work is outlined in Fig. 8.

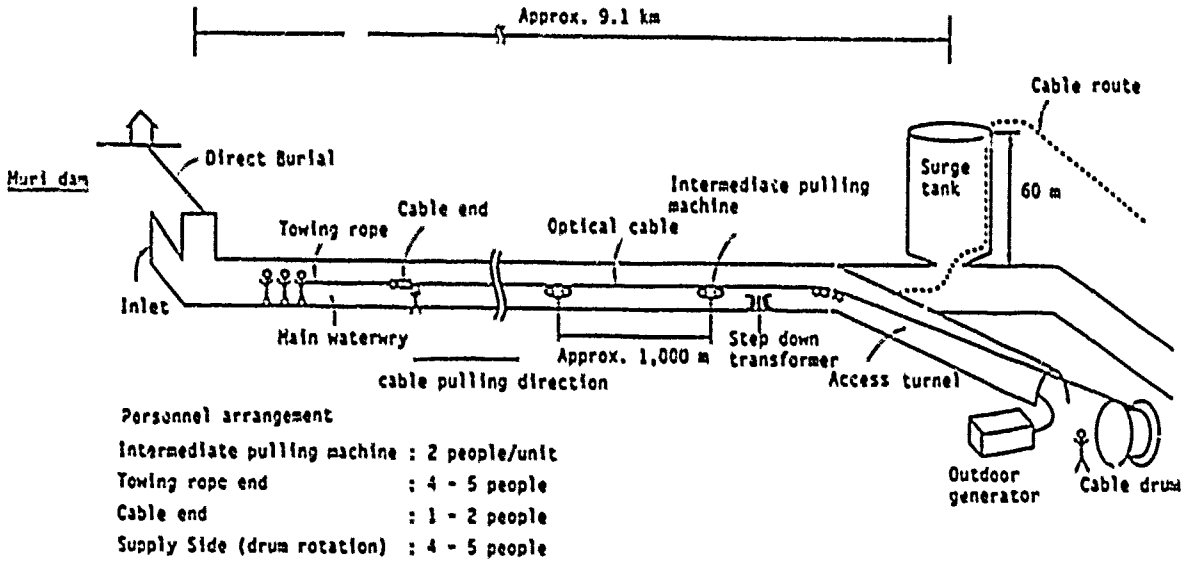

Fig. 8 Outline of The Installation Work

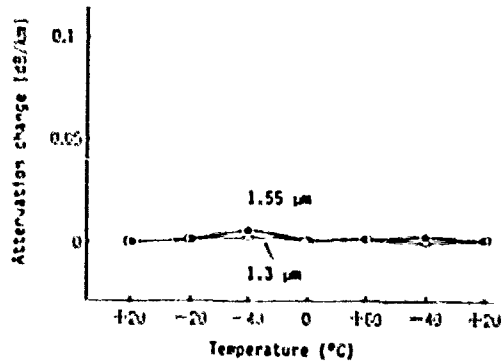

Fig. 7 Temperature Test

Due to problem on synchronization with the intermediate pulling machines and reason on the location for installation, a full-fledged drawing machine was not used on the supply side of optical cable. Instead, the cable have been paid out manually by use of a manual roller.

The optical cable was wound on an iron drum with a flange diameter of 2.5 m and an outer width of 1.2 m. It was 9.6 km long and weighed about 6 tons in the wound status. But 4 to 5 persons were adequate for paying out the cable.

This can be said to be one of the proofs which verify that this installation work was dependent on the small diameter and light weight characteristics inherent to optical cable.

Figure 9 shows the optical cable paid out manually.

Fig. 9 Supply Side of Optical Cable

The installation site lies in waterway and underground. It is matter of course that there is no equipment like power source or lighting in the waterway subjected to continuous long length joint-free optical cable installation. Furthermore, use of an internal combustion engine must definitely be avoided in the waterway because of poor ventilation. With regard to the construction equipment, therefore, the on-site measures listed below have been taken.

(1) For power source, an outdoor generator was installed at the inlet of waterway so as to supply 200 V into it. The voltage was dropped to 100 V by the transformer provided in the waterway to minimize voltage drop.

(2) To light the inside of waterway, 500 working lights were installed at intervals of 10 to 20 m.

(3) Bicycles were used for movement of both workers and materials because it excels in mobility and does not cause environmental pollution. Only for transportation of heavy objects or urgent purposes, motorbikes were driven.

Under the above-mentioned situation, installation was carried out. As a result, the cable was laid over a distance of 9.3 km in essential 2 days with maximum installation tension about 200 kgf and average installation speed approx. 10 m/min. After installation, the characteristics of cable were checked over the entire length by means of OTDR. In consequence, there was no change before and after installation, so we have confirmed that installation was successful. Figure 10 shoots the situation of construction in the waterway.

Fig. 10 Situation of Installation (in the waterway)

Then the cable was fastened to the wall face of waterway with the aid of a saddle. Fastening was made at intervals of 2 m to counter rapid water flow. Because even 9,000 saddle screws had to be tightened, the saddle was installed at 1.5 m above the bottom of waterway in order to facilitate screw tightening work. Figure 11 snaps saddle fastening work.

Equipments used for this construction are listed in Table 3.

Table 3 List of Equipments Used in The Work

Equipments	Number of units used	Remarks
Intermediate pulling machine	8 (1 km apart)	Reduction of the install tension of the optical cable
Pulley	Approx. 1700 (2-10 m apaprt)	Reduction of the install tension of the optical cable and guide for the optical cable
Working light	Approx. 500	Lighting in the waterway
Telephone	9	Communication between pulling machines
Bicycle	17	Travel in the waterway
Motorbike	4	Transportation of the tools or emergency use
Rearcart	6	Transportation of the tools

Fig. 11 Cable Fastened to The Wall of The Waterway

8. Conclusion

In order to introduce optical cable into a hard and special installation environment, namely a dam waterway, its structure and installation method have been examined, and the characteristics have been tested. As a result, laying a continuous joint-free optical cable of nearly 10 km has been completed in the dam waterway.

In the future, there may be the growing number of cases where electric power company utilities introduce optical cable in a special environment as represented by the waterway in a hydraulic power plant. This project can be said to be an epoch-making answer to diverse needs taking place along the expansion of application range of optical cable.

In the end, we would like to express our gratitude to the people concerned inside and outside our company for their hearty guidance and assistance over a time period from the manufacture to installation of this cable.

Reference

(1) Self-Controlling Puller Instruction Manual.

Hiroshi Sawada
Hokkaido Electric Power Co., Inc.
1, 3-jou, Toukou,
Asahikawa, 078-11,
Japan

Hiroshi Sawada joined the Hokkaido Electric Power Co., Inc. in 1970, and was engaged in the Nayoro Power Office. He is now in Hydro Power Stations and Substations Section, the Asahikawa Central Power Office.

Shinichi Hasegawa
Hokkaido Electric Power Co., Inc.
514, Aza Toyosato,
Engaru-cho, Monbetsu-gun,
099-04, Japan

Shinichi Hasegawa joined the Hokkaido Electric Power Co., Inc. in 1972, and was engaged in the Kushiro Power Office. He is now in Hydro Power Stations and Substations Section, the Engaru Power Office.

Hiroaki Horima
Sumitomo Electric Industries, Ltd.
1, Taya-cho, Sakae-ku,
Yokohama, 244, Japan

Hiroaki Horima joined Sumitomo Electric Industries, Ltd. in 1972, and worked on the development of CATV coaxial cables, multipair PEF-insulated junction cables and low loss unbalanced type cables. Thereafter, he concentrated on the development of optical fiber cables. He is now Section Manager of the Fiber Optics Division at Sumitomo Electric Industries, Ltd. He is a member of the Institute of Electronics and Communication Engineers of Japan.

Tsuguo Amano
Sumitomo Electric Industries, Ltd.
1, Taya-cho
Yokohama, 244, Japan

Tsuguo Amano joined Sumitomo Electric Industries, Ltd. in 1987. He has been engaged in the development and design of optical fiber cables in the Fiber Optics Division.

UNIVERSAL FIBER IDENTIFICATION TEST INSTRUMENT

S. MORRISON and C. SARAVANOS

NORTHERN TELECOM CANADA LIMITED, OPTICAL CABLE DIVISION

SASKATOON, SASKATCHEWAN, CANADA

ABSTRACT

A universal fiber identification test instrument has been developed. The instrument is capable of detecting traffic or test signals which may be present in a fiber by inducing a small loss which does not disturb the transmission system. The universality of the instrument results from a bend configuration which reduces the bend loss dependance on fiber design and operating wavelength. This bend configuration was also optimized to improve collection of the extracted signal. The result is an instrument which can be used with all fiber types and at all wavelengths commonly used in the telecommunications industry and which induces no more than 3.0 dB loss with measurement sensitivity as low as -62 dBm.

INTRODUCTION

Signal extraction from an optical fiber by some form of fiber bending mechanism has been utilized to detect the presence of traffic and prevent costly disruptions caused by mistaken fiber identification.[1] Until now this technique has been limited by the significant variability in the amount of signal extracted from the fiber since the amount of loss induced by a specific bend configuration depends both on the fiber design parameters and the operating wavelength. Currently available instruments are often based on bend configurations designed around nominal values for a specific fiber type at a single wavelength. If these conditions change, the loss induced by the bend can vary greatly, causing system alarms for excessive loss or no signal detection for insufficient loss.

By understanding the fiber bending principles and developing a bend geometry which has minimum dependance on signal wavelength and fiber parameters, a universal fiber identification test instrument can be offered.

LOSS INDUCED BY FIBER BENDING

There are a number of causes of variation in the amount of loss induced in a fiber for a given bend configuration. Of primary importance is the dependance of loss on the optical wavelength and fiber characteristics. Mathematical modelling was undertaken to determine the sensitivity of various configurations to wavelength and to singlemode fiber parameters such as mode field diameter and cutoff wavelength. From this analysis the design for a bend configuration which greatly reduced loss dependencies resulted.

Experimental results for three different bend configurations are shown in figures 1, 2 and 3. Each bend configuration is tested on three different single mode fiber types of varying bend sensitivity designated as A, B and C in order of increasing mode field diameters. Figure 1 is for a bend configuration commonly used with large mode field diameter fibers. Figure 2 is for a bend configuration found in instruments intended for small mode field diameter fibers. Figure 3 results from the use of the mathematically optimized bend configuration.

It can be easily seen that neither of the two conventional bend configurations can be used on all three fibers over their normal operating wavelength region. A similar example could be presented for variations in the fiber's cutoff wavelength.

A second important cause for variation in the induced loss is believed to be due to constructive and destructive recoupling of light traveling in whispering gallery modes with the fundamental mode of single mode fibers.[2] This phenomenon is exhibited as oscillations in the loss versus wavelength graphs for the traditional bend configurations shown in Figures 1 and 2. These oscillations will also appear for small dimensional variations in the fiber bend radius at a constant wavelength. Further mathematical analysis allowed the authors to determine the specific conditions under which this effect can be eliminated. Figure 4 shows again the induced loss versus wavelength for a conventional bend mechanism along with the theoretically predicted maxima and minima of the interference. From Figure 3 it can be seen that this phenomenon has been eliminated in the universal bend mechanism.

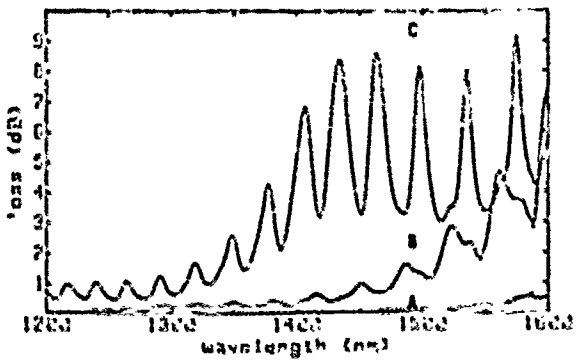

Figure 1: Loss induced by a bend mechanism intended for large mode field diameter fibers.

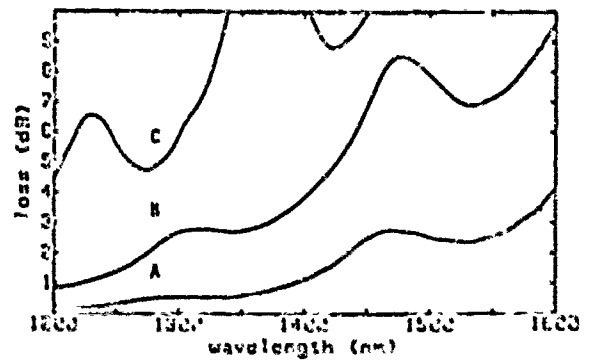

Figure 2: Loss induced by a bend mechanism intended for small mode field diameter fibers.

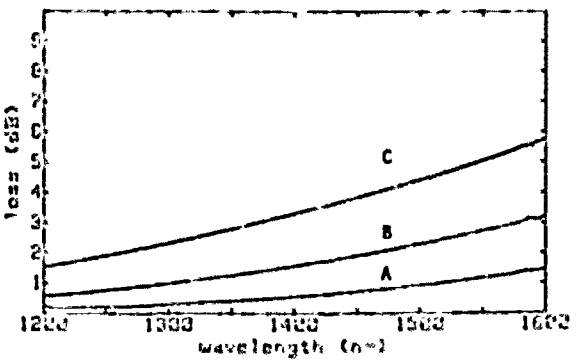

Figure 3: Loss induced by the universal bend mechanism.

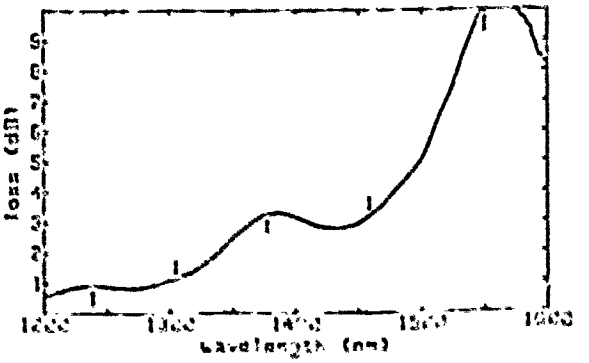

Figure 4: Theoretically predicted interference points for a conventional bend mechanism compared with experimental results.

COLLECTION OF EXTRACTED SIGNAL

Since in rare cases absorption of the extracted signal by the colorings applied to the fiber coating can be as high as 15 dB, it is of great importance that the maximum amount of the extracted signal be collected. Also of concern is the instance where, with uncolored fibers, optical radiation extracted from the fiber core can be guided in the acrylate coating through the bend mechanism, greatly reducing coupling efficiency.

By using a rigid optical element of predetermined refractive index, a number of desirable characteristics can be obtained. First, it is possible to precisely define the fiber bend geometry which results in highly repeatable loss values. Second, it is possible to obtain coupling efficiency exceeding 50%. Third, the refractive index of the element can be chosen to allow light bound by unpainted fiber sections to escape at the bending region.

PERFORMANCE REPORT

Table 1 shows the results from use of the instrument on six common fiber design types at their commonly used wavelengths.
Figure 5 shows the fiber identification test instrument containing the universal bend mechanism.

Fiber Type	Wave-length (nm)	Insertion Loss (dB)	Sensitivity (dBm)
Singlemode Design A	1310	0.44	-54.1
	1550	1.56	-58.7
Singlemode Design B	1310	1.05	-56.3
	1550	2.66	-61.1
Singlemode Design C (Large MFD fiber)	1310	2.82	-59.8
Singlemode Design D (Dispersion shifted fiber)	1550	0.29	-51.7
Multimode 50 um	850	1.71	-50.0
	1300	1.65	-53.9
Multimode 62.5 um	850	1.03	-46.2
	1300	0.93	-50.3

Table 1: Summary of instrument performance

Figure 5: Fiber identification test instrument containing the universal bend mechanism.

CONCLUSION

A new bend technique has been developed where loss dependance on wavelength and fiber design is minimized. As a result, the fiber identification test instrument incorporating this design has the same performance specification for a broad range of fiber designs and wavelengths. This includes depressed and matched cladding singlemode fibers, dispersion shifted fibers and multimode fibers, all within their normal operating wavelength windows. The induced loss is specified not to exceed -3.0 dB, while maintaining a detection sensitivity below -50 dBm. This allows for 15 dB of margin for signal absorption due to fiber coloring while still maintaining a minimum sensitivity of -35 dBm. In addition, the testing of a fiber requires less than 3 seconds and less than 1 mm of excess fiber slack, allowing for "in cable" fiber testing. Finally, in addition to detecting traffic signals, the instrument is also capable of identifying test tones at 270 Hz, 1 KHz or 2 KHz modulation frequencies.

REFERENCES

1. I. Finvers, D.D. Clegg, V. So, P.J. Vella, "Live Fiber Identifiber", Proceedings of the 35th IWCS.

2. Alun J. Harris, Peter F. Castle, "Bend Loss Measurements on High Numerical Aperture Single-Mode Fibers as A Function of Wavelength and Bend Radius", JLT, Vol. LT-4, No. 1, Jan. 86.

Shawn Morrison received his B.Sc. in Electrical Engineering in 1984 from the University of Saskatchewan, and joined the Optical Cable Division of Northern Telecom the same year. He is currently a member of the Research and Development group responsible for fiber optic installation products.

Costas Saravanos was born in Makrakomi, Greece, in 1951. He received the B.Sc. degree in physics from the University of Athens in 1973, and the M.Sc. degree in solid-state physics from the South Dakota School of Mines and Technology in 1980 and is currently completing the Ph.D. degree in electrical engineering at the University of Ottawa.

Following a year with the Digital Transmission Division of Northern Telecom, Canada, he joined the Optical Cable Division in 1982 where he was engaged in single-mode fiber process optimization. Since 1985 he has been a Manager in the Fiber Research Laboratories in Ottawa and Saskatoon responsible for fiber design optimization, fiber characterization and installation products development.

A Method for Identifying Single-mode Fibers in an Operating Fiber Cable System

Koji ARAKAWA, Koji YOSHIDA and Hiroji IKEYA

NTT Technical Assistance and Support Center
Musashino, Tokyo, 180, Japan

ABSTRACT

This paper discusses a method of identifying optical fibers in an operating transmission system by bending the fibers and then detecting in specific fibers an extra identification light which has a longer wavelength than the transmission signal. The identification light is injected into a non-operating fiber, which is to be identified. The optimum wavelength and bending shape for fiber identification are studied experimentally and theoretically for concatenated single-mode fibers. The resulting apparatus can identify fibers without disturbing signal transmission.

1. Introduction

Optical fiber cables containing many single-mode fibers[1] are used for subscriber loops[2] and trunk communication lines. The large number of fibers in a cable makes it difficult to identify fibers by color coding alone.

In optical fiber maintenance, such as cable re-routing or branching, an optical fiber is cut inside a mechanical closure. Therefore, a method of identifying the fiber to be cut is needed to avoid cutting the wrong fiber in the closure, which contains operating optical fibers. However, an identification method that does not disturb an operating optical fiber transmission system has not been developed until now.

This paper discusses an optical fiber identifier design and the related experimental and theoretical studies on concatenated single-mode fibers, along with the optimum wavelength and bending shape associated with fiber identification.

2. Fiber identification and cable re-routing

Transmission lines which use optical fiber cables sometimes have to be partially re-routed after installation for reasons such as road construction. The method of optical fiber cable re-routing is shown in Fig.1. The procedure is: (1) Install the new cable between existing man-holes. (2) In the existing cable, cut the non-operating fibers at both man-holes, after fiber identification. (3) At both ends, prepare the optical fibers of the newly-installed cable. (4) Splice an existing fiber and a new fiber, and prepare a new transmission channel. (5) Exchange the channel of previous operating system with the new transmission channel prepared in step (4). (6) Repeat steps (2) through (5) until all the fibers in the existing cable are spliced with fibers in the new cable.

In step (2), confirmation of the non-operating status of the fiber should be made so as to prevent an operating fiber from being cut. However, confirmation using only the color of the fiber coating material may result in human error such as mistaking the color or unit. Therefore, a fiber identification method which detects the optical power radiated from a bent fiber and does not disturb the signal transmission is proposed.

The concept of fiber identification method is illustrated in Fig.2. Light power injected into the non-operational fiber to be identified is detected from the bent fiber.

3. Selection of reference light source wavelength

3.1 Wavelength dependence on fiber bending loss

The wavelength dependence on the bending loss is shown in Fig.3 for a single-mode fiber having a mode-field diameter of 9.5 μm, a coating diameter of 0.25 mm and a cut-off wavelength of 1250 nm. The increase in loss for a radius of 9 mm is very small at the 1300 nm wavelength used for signal transmission, but loss increases as the wavelength increases. The results also indicate that the power radiated is greater at longer wavelengths.

3.2 Calculation of the optimum wavelength for a reference light source

The optical power radiated from a single turn with a radius of 9 mm is calculated as follows. Fiber loss factors, namely, ultraviolet absorption loss α_{uv}, infrared loss α_{ir}, and Rayleigh scattering loss α_{rl} were estimated relative to the silica glass material comprising the fiber. Total fiber loss α_T, relative to GeO_2-doped silica glass, is given by [3]

$$\alpha_T = \alpha_{uv} + \alpha_{ir} + \alpha_{rl} \qquad (1)$$

$$\begin{cases} \alpha_{uv} = \dfrac{154.4X}{44.6X + 60} \times 10^{-2} \cdot e^{4.63/\lambda} & (dB/km) \\ \alpha_{ir} = 7.81 \times 10^{11} \cdot e^{-48.48/\lambda} & (dB/km) \\ \alpha_{rl} = \dfrac{A}{\lambda^4} & (dB/km) \end{cases}$$

where λ is wavelength, X is GeO_2 content, and A is the Rayleigh scattering coefficient determined by the slope of the curve.

Radiated optical power, P, from a bent fiber at the fiber identification point is given by

$$P = S \cdot P_0 \cdot 10^{-(\alpha_T \times L/10)} \cdot (1 - 10^{-\alpha_l/10}) \qquad (2)$$

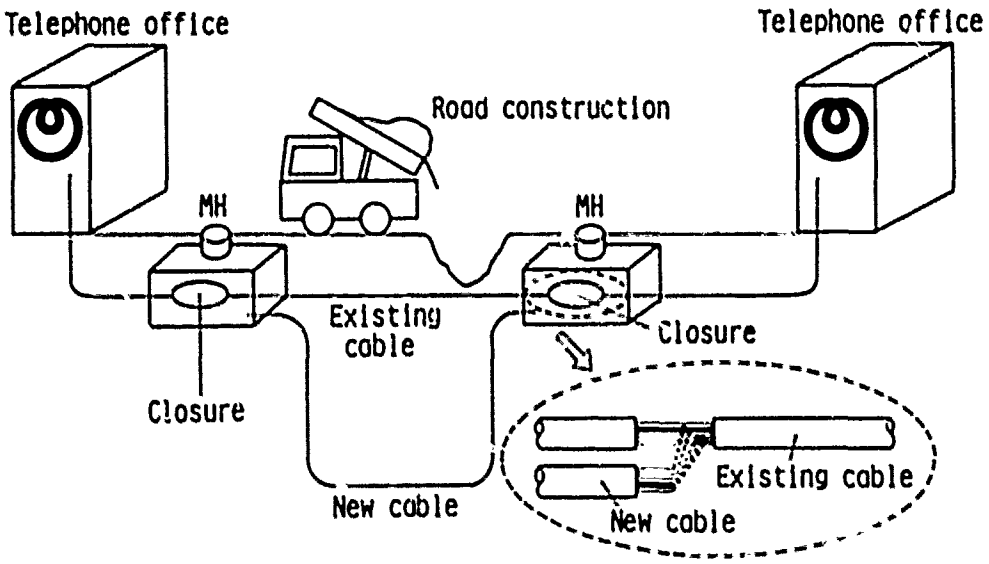

Fig.1 Re-routing method for optical fiber cables

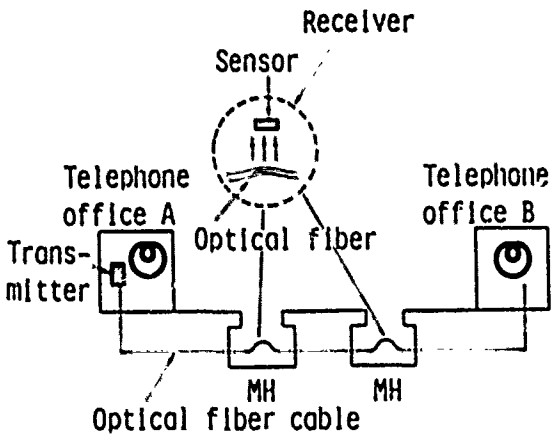

Fig.2 The concept behind the method for identifying optical fiber cables

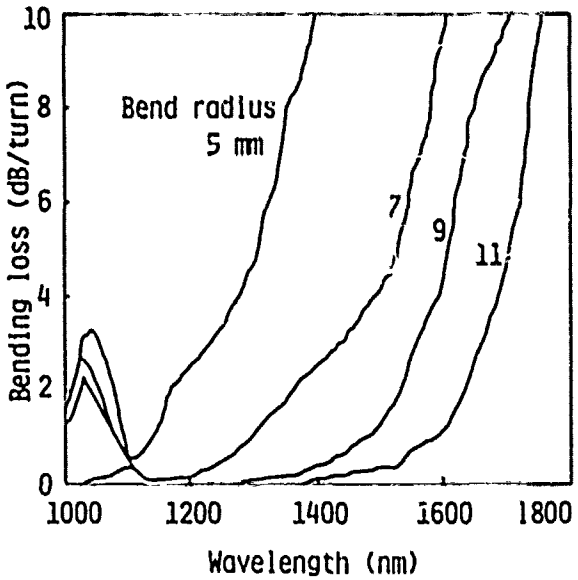

Fig.3 Wavelength dependence on bending loss

where P_0 is the input optical power, S is the coupling efficiency for detecting the radiated power, L is the distance between the light source and the fiber bend, and α_L is the bending loss at each wavelength.

The optical power radiated from a single turn with a radius of 9 mm is calculated for concatenated single-mode fibers, and is shown in Fig.4 as a function of the distance between the light source and the fiber bend. The calculation was carried out using the mean value of measured spectral losses in commercially installed optical fiber cables, and equations (1) and (2). Sufficient light can be detected at around the cut-off wavelength for short distances, but the radiated optical power is uncertain due to the higher mode in this region. Though the optimum wavelength of around 1700 nm, which is longer than the water-peak, changes with the distance, sufficient radiated light can be detected at 1550 nm, a wavelength for which laser-diodes are commercially available. Therefore, the 1550 nm laser diode was chosen as the reference light source for the identifier.

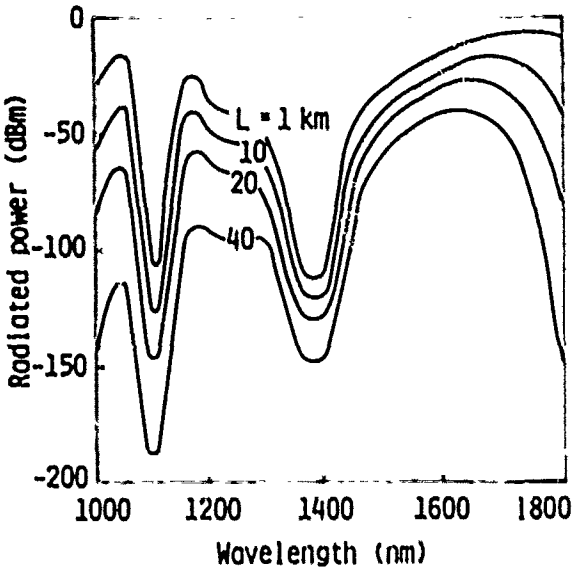

Fig.4 Wavelength dependence on power radiated from a bent fiber

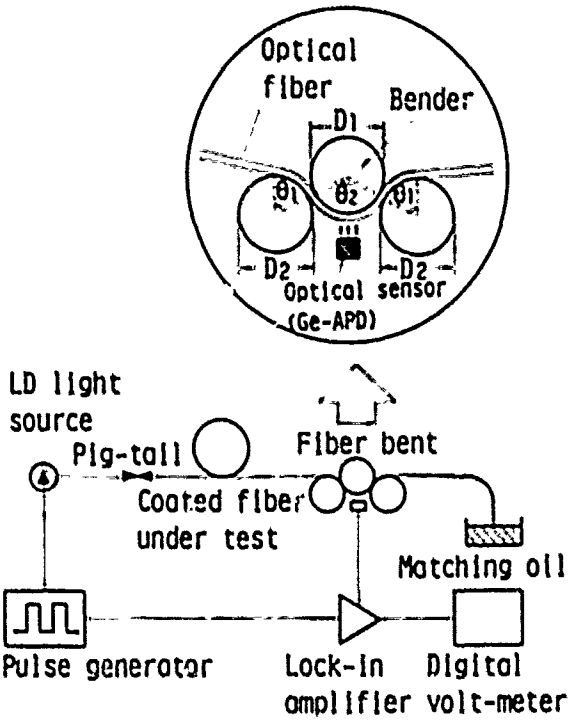

Fig.5 Experimental set-up

4. Fiber bend shape

The shape of the fiber bend was studied, using the experimental set-up shown in Fig.5, with regard to the optical power radiated from a bent fiber, the insertion loss caused by fiber identification at a given signal transmission wavelength, and the handling ease of the optical fiber identifier. A typical distribution of detected optical power levels from bent fibers, including one with approximately the optimum bend, are shown in Fig.6 for bending radius of 9 mm. The best bending shape is obtained by measuring the power level dependence on bending radius and angle.

5. Wavelength dependence of light power transmitted through a colored coating

To clarify the influence of the coating material on the radiated power, the wavelength dependence on the coating material transparency is measured by spectrum meter. The wavelength dependence on the power ratio of light transmitted through a 0.2 mm colored coating film is shown in Fig.7. The marked absorption by the color coating is not observed at wavelengths around 1550nm. These results indicate that the coating material has no influence on power radiation.

6. Measured splicing loss and fiber loss

In design of an optical fiber identifier, the relation between optical losses at 1300 nm and 1550 nm for conventional single-mode fibers is one of the most important characteristics. Therefore, splicing loss for concatenated fibers was measured with an OTDR at 1300 nm and 1550 nm. The relation between fusion splicing loss for the above-mentioned wavelengths is shown in Fig.8. The measured fusion splicing loss indicated no wavelength dependence. The fiber loss in existing cables, of approximately 20 km in

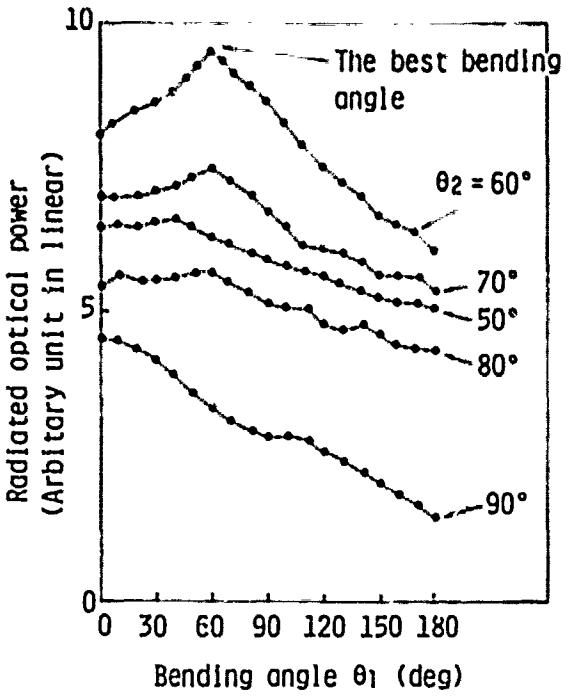

Fig.6 Distribution of detected optical power levels from bent fibers

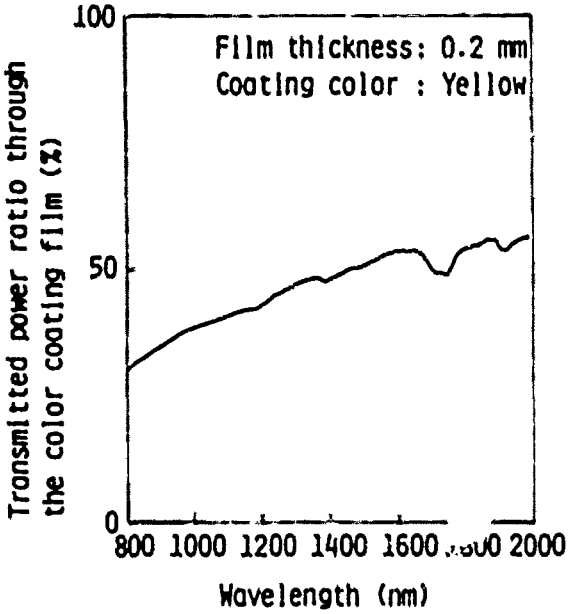

Fig.7 The wavelength dependence on the power ratio of light transmitted through a colored coating film

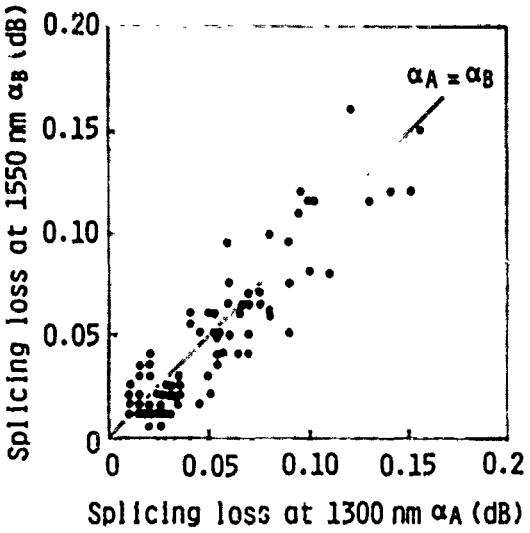

Fig.8 Measured splicing loss for fibers at 1300 nm and 1550 nm

length, for the 1300 nm wavelength region was also measured at both wavelengths. The results are shown in Fig.9 as a function of the fiber loss ratio at 1300 nm and 1550 nm. Those results show that the mean fiber loss value at 1550 nm is about 80 percent that at 1300 nm, and that there is no problem of loss when the 1550 nm wavelength for identification light source is applied to in the existing cable, including splicing points and residual fiber strain after installing a cable.

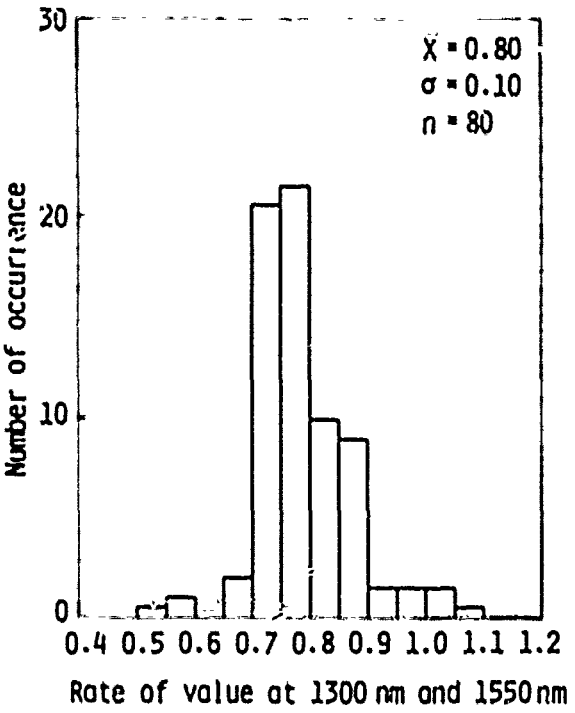

Fig.9 Measured fiber loss ratio between 1300 nm and 1550 nm for conventional fibers in the field

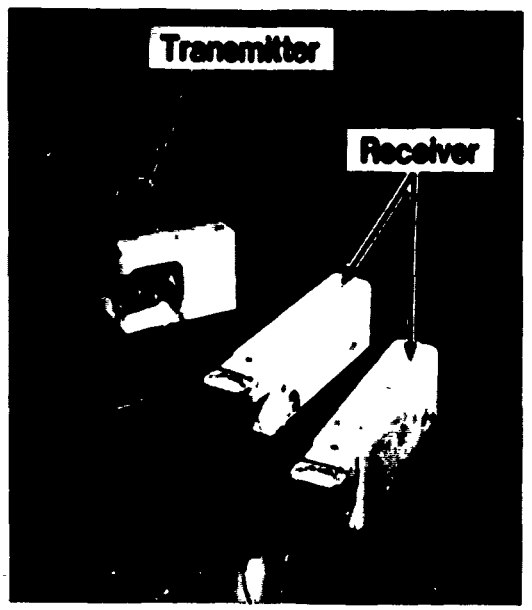

Fig.10 Optical fiber identifier configuration

Table 1. Specifications for the optical fiber identifier

Cable type	Single-mode fiber cable
Optical light source	Laser diode (1550 nm Operating wavelength)
Coupling Efficiency	≦ 42 dB (using conventional fibers)
Insertion loss	≦ 0.2 dB (using conventional fibers)
Dimensions	Transmitter (20 × 10 × 6 cm) Receiver (20 × 4 × 6 cm)
Weight	Transmitter 800 grams Receiver 400 grams
Power source	9 V Internal rechargeable battery or AC charging adapter

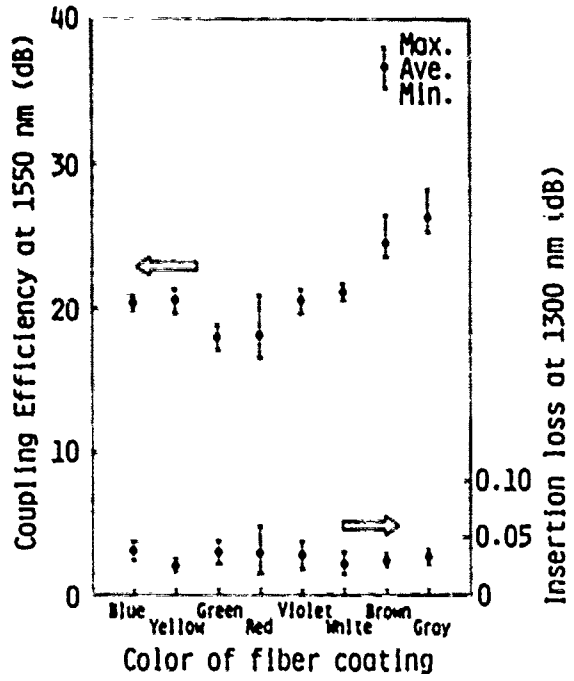

Fig.11 The dispersion of coupling efficiency at 1550 nm and insertion loss at 1300 nm for conventional fibers as measured using the identifier

7. Optical fiber identifier performance

An optical fiber identifier was designed and manufactured according to the concept described above. Its performance in the field showed that fiber identification did not disturb the operating transmission system. No bit-errors were observed when live fibers operating at 400 Mbit/s[4] were bent by the equipment. The configuration of the equipment for optical fiber identification is shown in Fig.10.

The dispersion of coupling efficiency at 1550 nm and insertion loss at 1300 nm for conventional fibers, as measured using the fiber identifier equipment, is shown in Fig.11. These characteristics are not influenced by the colored coating. These results show that the optical fiber identifier does not disturb operating signal transmission, and is highly practical for use on lines in the field. The specifications for the optical fiber identifier are shown in Table 1.

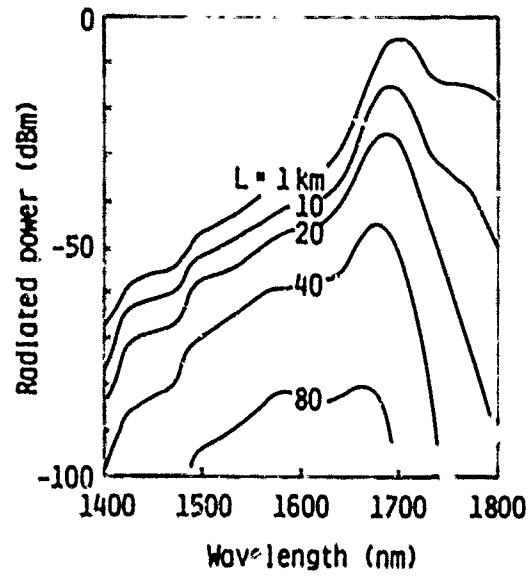

Fig.12 Wavelength dependence on power radiated from a bent fiber

8. Application of dispersion-shifted fibers

A similar technique can be applied to the identification of 1550 nm dispersion-shifted fibers by using a laser diode operating at a longer wavelength. The optical power radiated from a single turn with a radius of 8 mm was calculated for a dispersion-shifted fiber using equations (1) and (2). The results are shown in Fig.12 as a function of the distance between the source and the fiber bend. Sufficient radiated optical power can be detected at 1650 nm, for which experimental laser diodes are now available.

9. Conclusion

A new method for identifying fibers in operating optical fiber systems using single-mode fiber cables has been presented. Experimental field tests show that the optical fiber identifier does not disturb active signal transmission, and is highly practical for use in optical fiber maintenance.

Acknowledgement

The authors would like to thank Shigemi Kodera and Masataka Hirai for their helpful discussions and suggestions.

Reference

(1) H. ISHIHARA, A. HIROOKA, and K. SATO: 'Commercialized single-mode optical fiber cable techniques', ECOC 83, 1983, pp. 533-538.
(2) M. KAWASE, T. FUCHIGAMI, T. HAIBARA, S. NAGASAWA, and S. TAKASHIMA; 'Loop-Network Configuration For Subscriber Loops and Single-Mode Optical Fiber Ribbon Cable Technologies Suitable For Mid-Span Access', IWCS, 1988, pp. 144-149.
(3) T. MIYA, A.KAWANA, Y. TERUKUNI, and T. HOSAKA: 'Fabrication of Single-mode Fibers for 1.5 μm Wavelength Region', Trans. IECE, E63, No.7, 1980.
(4) K. AIDA, and S. NAKAGAWA: 'F-400M Optical Fiber Transmission System Design and Experiment', GLOBE COM 85', 23, 1.1-1.4, 1985.

Koji Yoshida

NTT Technical Assistance and Support Center

Midori-cho, Musashino-shi, Tokyo, 180 Japan

Koji Yoshida is a Senior Engineer at the Technical Assistance and Support Center, NTT Telecommunications Service Support Headquarters, Musashino, Tokyo, Japan. He received his B.E. degree in communications engineering from Osaka University in 1973. He joined NTT in 1973. He is engaged in the development of optical testing instrument and in research on optical fiber cable reliability. Mr.Yoshida is a member of the Institute of Electronics, Information and Communication Engineers of Japan.

Koji Arakawa

NTT Technical Assistance and Support Center

Midori-cho, Musashino-Shi, Tokyo, 180 Japan

Koji Arakawa is a Senior Engineer at the Technical Assistance and Support Center, NTT Telecommunications Service Support Headquarters, Musashino, Tokyo, Japan. He received his B.E. degree in electronics engineering from Osaka Prefecture University in 1978. He joined NTT in 1978. He is engaged in research on optical fiber cable reliability and in the development of optical fiber maintenance equipment. Mr.Arakawa is a member of the Institute of Electronics, Information and Communication Engineers of Japan.

Hiroji Ikeya

NTT Technical Assistance and Support Center

Midori-cho Musashino-shi, Tokyo, 180 Japan

Hiroji Ikeya is an Engineer at the Technical Assistance and Support Center, NTT Telecommunications Service Support Headquarters, Musashino, Tokyo, Japan. He received his B.E. degree in mechanical engineering from Meijo University in 1983. He joined NTT in 1983. He is engaged in the design of subscriber optical fiber cable systems and in the development of optical fiber maintenance equipment.

"CLIP-ON" - A POSSIBLE MEASUREMENT TECHNIQUE FOR FUTURE OPTICAL NETWORKS

S M James D A Ferguson D Drouet

British Telecom Research Laboratories
Martlesham Heath, Ipswich, IP5 7RE, United Kingdom

Summary

A small fraction of light in an optical fibre is couple[illegible]rough the 'side' of the fibre using one of two possible [illegible] taps. These taps can then be incorporated [illegible] field measurement instruments which may [illegible] installation, commissioning and maintenance network. In this paper we will describe the applic[illegible] technology to produce a "Clip-on" optical power meter.

Introduction

Optical fibre has to date been used extensively in long distance, high capacity trunk and international routes but has yet to penetrate the local loop to any significant extent. Various local network topologies have however been recently proposed and these are expected to initiate the transformation from copper to fibre: an operation which is expected to show a rapid upward trend. To reduce the cost of a local fibre system British Telecom has proposed a fibre and equipment sharing network (1). It uses passive splitters to divide the signal on a single exchange fibre up to 32 ways to carry telephony and broadband services. The telephony service uses a TDM protocol in the exchange to customer direction with a TDMA structure in the return direction. In this and other shared networks a problem occurs during maintenance or network rearrangements affecting a single customer. It is desirable to undertake such work with the system live, without jeopardising the integrity of the remaining customers. Any measurements which are made on the live networks must therefore not cause a significant increase in system loss. It is worth noting however that at the commisioning stage of a network such constraints need not apply and the measurement can be fully intrusive.

In this paper we discuss two "Clip-on" optical taps which are capable of extracting varying fractions of light from a signal propagating in a fibre. We compare and contrast various characteristics of each tap (insertion loss, collection efficiency, mechanical performance and spectral response). We then describe two "Clip-on" optical power meters using these taps, one of which is non-intrusive and may be used for live testing whilst the other is intrusive.

Optical Taps

It is well known that light is coupled to a radiative mode if a fibre is subjected to a localised perturbation (2). Several commercially available "Clip-on" type devices rely on a tight bend to couple out light and a large area detector to sense it. Typically these devices exhibit low coupling efficiency from fibre to detector with effective losses in excess of 20dB.

For operation under the non-intrusive regime insertion losses need to be low and coupling efficiencies need be higher to offer usable performance. The light eminating from a more gently bent fibre is distributed and therefore some form of focussing or collecting optics is required.

We report two tap configurations using macrobending or microbending and employing simple bulk optical components to yield high coupling efficiencies with contrasting spectral and mechanical performance.

Bend Loss

"Clip-on" instruments using macrobending or microbending need to be able to deal with two factors, over and above the geometry of the bend, which will affect the light coupled from the fibre and hence sensed by the detector. They are:-

- fibre propagation parameters i.e mode field radius (MFR) and cut-off wavelength
- system wavelength

These variables affect all "Clip-on" devices and effectively determine the overall accuracy of an instrument. The dependance on fibre parameters and system wavelength is given by a simplified pure bend loss expression (3):-

$$2\alpha = \frac{C}{\sqrt{R}} \exp\left[-\frac{4\Delta w^3 R}{3aV^2} \right]$$

where 'R' denotes bend radii, 'V' is a function of wavelength and cut-off wavelength and 'a' denotes MFR.

Fibre supplied by a manufacturer will show a spread in its propagation constants. The extent to which these parameters vary is defined in British Telecom's case by a specification 'window' which sets the following limits, MFR 9.2um - 10.2um, and cut-off wavelength 1150nm - 1280nm. Within this 'window' fibres display differing bend loss characteristics, and we may identify two distinct regions at the extreme corners of the 'window'. We have termed these the 'Bend Sensitive' region (short cut-off, large MFR) and the 'Bend Insensitive' region (long cut-off, small MFR). A manifestation of this varying fibre bend sensitivity is illustrated in figure 1a/b which shows loss as a function of wavelength for fibres at these extremes of the specification 'window' for a 180 degree bend of 15mm radius.

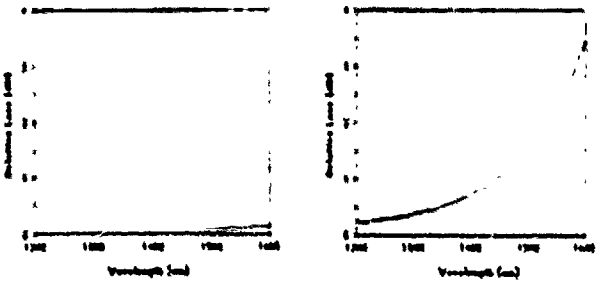

Figure 1a/b. Bend loss for bend insensitive and bend sensitive fibres respectively

Fibre Coating and Colouring

Whilst the propagation parameters and system wavelength affect the amount of light coupled out of the fibre, an additional factor, the absorption of fibre coatings, introduces a loss between fibre and detector. Typically the fibre will have a one or two layer acrylate primary coating and a coloured ink coating for protection and identification respectively.

We have measured typical losses introduced by the primary/coloured coating for fibres in the British Telecom network (table 1).

COLOUR	LOSS (dB@1300nm)	SD (dB)
Brown	11.5	0.75
Red	2.7	0.33
Orange	0.1	0.02
Yellow	1.3	0.25
Green	5.6	1.5
Blue	1.5	0.4
Grey	12.6	1.2

Table 1. Loss Penalties of Coloured Coatings

The loss represents a mean of recorded measurements in differing positions along the same length of fibre. The variation observed could introduce some inaccuracies when making "Clip-on" measurements. Further measurements for individual colours have shown variation from batch to batch and also from manufacturer to manufacturer. We believe this is due to the uneveness of the coating and variation in the constituents of the ink. It is envisaged that in future the coatings and inks may need to be controlled with regard to their performance in the IR spectrum, with an eventual move to IR transparent inks and coatings.

Optical Tap Configuration

We now compare two types of optical tap concentrating on the following parameters:-

- system insertion loss
- collection efficiency
- spectral response i.e flatness
- mechanical repeatability
- dependance of insertion loss on fibre propagation parameters

Macrobend Tap:

Fibre is bent round a fixed mandrel. The light which is coupled out is collected around the circumference by a secondary waveguide (figure 2). The insertion loss of this arrangement depends not only on the radius and duration of the bend but also on the fibre propagation parameters (figure 1a/b). We have experimented with radii from 3mm to 15mm and achieved up to 30% efficiency of light collection.

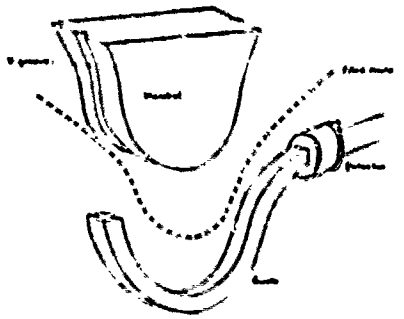

Figure 2. Macrobend Tap

This tap is mechanically repeatable since the alignment of fibre with waveguide is not critical, and as shown in figure 3 once a threshold is exceeded efficiency is independant of application pressure.

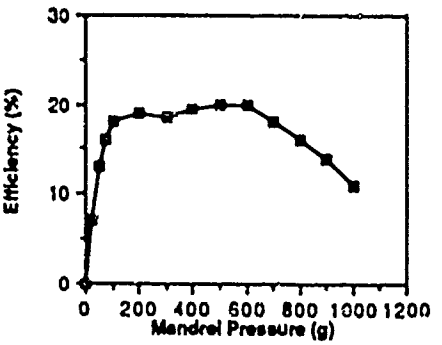

Figure 3. Efficiency v Pressure for Macrobend Tap

Single sharp bend tap

May be regarded as a single microbend (figure 4). Insertion loss is dependant upon the geometry of the bend as before, but this tap is less sensitive to the position of the fibre in the specification 'window'. Its spectral performance (figure 5) increases uniformly with wavelength. This makes it ideal for accurate non-intrusive power measurements. It is apparent that the wavelength dependance of insertion loss is significantly reduced from the macrobend tap.

This tap can be tuned to extract large amounts of power by selecting the appropriate bend geometry.

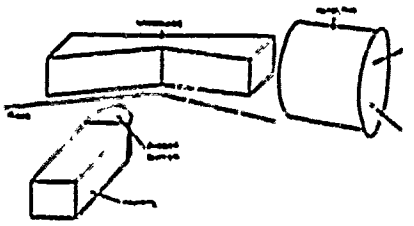

Figure 4. Single sharp bend tap

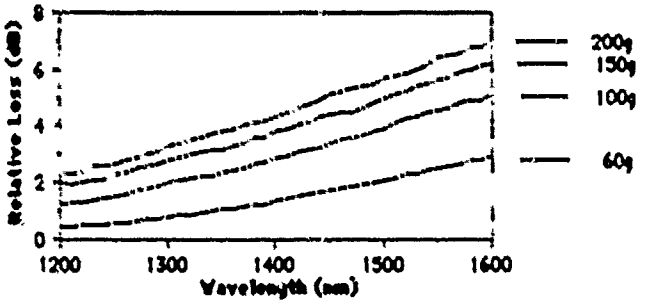

Figure 5. Single sharp bend tap spectral response for bend sensitive fibre

The fibre is pressed against the waveguide (which sets the bend geometry) with a soft rubber mandrel. As a result the insertion loss is a function of pressure (figure 5). The collection efficiency is only weakly dependant on waveguide geometry.
Owing to the almost point source nature of the light propagating from the fibre at the bend, collection efficiency is high, up to 60% has been measured. The repeatability is dependant on fibre to waveguide alignment to a small extent and on the repeatability of mandrel pressure to a greater extent.

Instruments

"Clip-on" taps can be utilised in a variety of field instruments (4,5,6). The tap selected would depend on the instrument characteristics, network topology and the particular testing need. The fundamental tool is an optical power meter which is analagous to a multimeter. The multimeter however is able to test on a 'through' basis whereas the conventional optical power meter operates in 'term' mode. The "Clip-on" taps therefore represent the equivalent of the high impedance input of the multimeter and permit true non-intrusive or 'through' power measurements to be made.

Clip-on Power Meter

British Telecom is currently preparing a field trial of a shared fibre, local network (7). The trial system will make use of signals at three wavelengths, these being 1300nm, 1550nm and 1575nm for telephony, broadband services and test purposes (8) respectively. It is envisaged that initial commisioning tests will be intrusive at 1300nm and 1550nm with subsequent live maintenance carried out non-intrusively at 1575nm. Owing to the significant mechanical differences between the intrusive and non-intrusive taps, we have demonstrated seperate instruments for each type of measurement and wavelength.
It is possible to write a basic, common specification for the power meters, the requirements are:-

- accurate and repeatable measurement
- insensitivity to the position of the fibre in the specification 'window'.
- insensitivity to the fibre coating/colouring.
- operation over a wide temperature range.
- sympathy with the fibre coating
- rejection of all unwanted signals on the fibre.
- handheld, rugged, field usable device

To comply with this specification we can select a tap which is most applicable to each type of instrument and yields the most accurate and repeatable measurement.
Intrusive Power Meter: The macrobend tap was selected on the grounds of good mechanical repeatability, ease with which the majority of the core power could be extracted, minimal wavelength dependance at small radii and similarly, low sensitivity to the position of the fibre in the specification 'window' at small radii (i.e since nearly all of the power in the core has been extracted).
At a radius of approximately 3mm and arc of 120 degrees the insertion loss is always in excess of 18dB even in the most bend insensitive fibre at 1300nm. The collection efficiency was approximately 10% at 1300nm.
Non-intrusive Power Meter: For this instrument the single sharp bend tap was used on the basis of its high coupling efficiency and low sensitivity to the position of the fibre in the specification 'window'. The single bend subtends an angle of 174 degrees and at a pressure of 150 grams the insertion loss was a maximum of 2dB at 1550nm in the most bend sensitive fibre. At 1300nm the loss was less than 0.6dB and overall collection efficiency was approximately 48%.

Accuracy

In both power meters we have identified four elements contributing to accuracy of power measurements:-
- mechanical repeatability
- variation in fibres propagation parameters
- absorption of fibre coatings/colourings
- temperature variation

Considering each in turn.
Mechanical repeatability: is due to improper fibre handling and alignment, mandrel pressure and mechanical tolerances. For a repeated measurement of waveguide collected power for constant fibre core power we have attained a SD of 5.3% for the intrusive device and 5.8% for the non-intrusive device.
Propagation parameters: is due to variation in the position of the fibre in the specification 'window' which results in variable bend losses. For the intrusive device the effect is minimal since in excess of 90% of the core power is extracted. The non-intrusive device typically displays a standard deviation of 8% from a fibre in the centre of the 'window'.
Colour variation: as a result of the fibre colouring process the losses from fibre through coating to detector vary significantly (table 1). Between one batch of colours a 12.5dB variation is typically observed. To minimise both this and propagation parameter variation a fibre calibration facility has been incorporated. In this a measurement can be made against a recorded calibration parameter.
Temperature variation: will mainly affect the optical receiver since a DC coupled design is employed. A temperature monitoring facility is included which recalibrates accordingly.

A summary of standard deviations for the four sources in error is given in table 2.

	Intrusive Instrument	Non-Intrusive Instrument
Mechanical variation (σ_m)	5.3%	5.8%
Fibre specification (σ_f)	2%	8%
Coloured coatings (σ_c)	4%	4%
Temperature drift (σ_t)	2%	2%

Table 2. SD of error sources

Instrument Performance: The overall accuracy is then given by:-

$$\sigma_{mean} = \sqrt{\sum_{1}^{n} \sigma_n^2}$$

$$= \sqrt{\sigma_m^2 + \sigma_f^2 + \sigma_c^2 + \sigma_t^2}$$

The resulting overall accuracies and mean sensitivities are given in table 3.

	Sensitivity	Accuracy
Intrusive Instrument	-45dBm	0.3dB/7%
Non-Intrusive Instrument	-37dBm	0.5dB/11%

Table 3. Overall accuracies

Conclusions

We have demonstrated two types of optical taps with contrasting optical and mechanical performance. Their characteristics have been examined in relation to three operational variables; fibre propagation parameters, system wavelength and fibre coatings. Two types of power meter have been demonstrated for use during the commisioning and maintenance stages of a shared fibre network. Four major sources of measurement error were quantified along with an overall accuracy for each type of instrument.

The variability of bend loss and fibre coatings have been identified as error sources. In future it may be advantageous to more tightly control these parameters by a revision of the fibre specification.

Acknowledgements

The authors would like to thank Paul Botham for theoretical studies, Phil Steward and Roland Downing for mechanical development and the Director of Research for permission to publish this paper.

References

1. J R Stern et al: Passive optical local networks for telephony applications and beyond. Elec Lett, Nov 87, Vol 23, No 24, pp 1255-7.
2. Gambling et al: Radiation from curved single mode fibres.Elec Lett, Vol 12, No 21, Oct 76, pp567-9.
3. D Marcuse: Curvature loss formula for optical fibres. J Opt Soc Am, Vol 66, No 3, Mar 76, pp216-220.
4. S M James: Non intrusive optical fibre identification using a high efficiency macrobending optical component. Elec Lett, Sept 88, Vol 24, No 19.
5. S Hornung et al: Non-intrusive measurement instruments for live optical systems. IOOC, Kobe, Japan, July1989.
6. S M James et al: Clip-on optical fibre power measurements. IEE colloquium LAN's and techniques for the local loop, E13, C14, 1989/44.
7. T R Rowbotham: Plans for a British trial of fibre to the home. IEE Conference on Telecommunications, April 1989.
8. P J Keeble: Maintenance of passive optical networks. OFC 90, to be published.

ANALYSIS OF STABILIZER CONCENTRATIONS IN POLYOLEFIN CABLE MATERIALS

K. D. Dye*, V. J. Kuck**, F. C. Schilling**, M. G. Chan**, and L. D. Loan**

*AT&T Network Systems-Phoenix, AZ **AT&T Bell Laboratories-Murray Hill, NJ

ABSTRACT

Two analytical techniques, a new high resolution nuclear magnetic resonance (NMR) method, and high performance liquid chromatography (HPLC) have been used to develop procedures for the analyses of the antioxidant tetrakis[methylene(3,5-di-tert-butyl-4-hydroxy-hydrocinnamate) methane (AO-1) and the metal deactivator N,N'-bis[3-(3',5'-di-tert-butyl-4-hydroxyphenyl)-propanyl]hydrazine (MD-1) in polyolefin cable materials. Agreement between the two methods is excellent and they have been used to measure the effects of manufacturing processes and aging on the depletion of stabilizers from DEPIC (Dual Extruded Plastic Insulated Conductor) cable insulation.

Depletion of stabilizers from the insulation is shown to be due to three mechanisms: thermal-oxidative degradation processes, chemical reaction with the blowing agent used to expand the insulation, and extraction of the additives by the cable filling compound. The most significant reduction in stabilizer concentration is observed after aging of the insulation in filling compound.

INTRODUCTION

Polyethylene cable materials are susceptible to thermal oxidative degradation during both processing and end use[1]. Protection from this degradation may be achieved by the incorporation of suitable stabilizer systems into the materials. The stabilizer system most commonly employed in wire and cable materials consists of an antioxidant and a metal deactivator, at concentrations of about 0.1-0.2% by weight[2]. Measurement of stabilizer concentrations is an essential component in the development of an understanding of degradation mechanisms; unfortunately, the quantitative analysis of polyolefin stabilizers is difficult. Most of the problems can be traced to the following three factors; the presence of the stabilizers in a relatively insoluble polymer matrix, the high reactivity and low stability of the stabilizers, and the low stabilizer concentrations[3].

Several "insitu" spectroscopic analytical schemes have been proposed in attempts to overcome the difficulties caused by the insoluble polymer matrix. These methods consist of preparation of a thin film of the polymer, followed by either UV or IR analysis. Most of the commonly used antioxidants absorb strongly in the UV spectrum; however, the absorption bands of many stabilizers overlap and this method is rarely applicable to multicomponent systems[4]. IR analysis is more functional group specific than UV, but quantitation depends on the presence of unique interference-free bands for each component to be measured[5]. This criterion is usually difficult to meet in cable materials, as they contain more than one stabilizer in addition to various blowing agents and pigments.

These observations suggest two courses of action: development of a more sensitive analytical technique to allow analysis in the presence of the polymer or extraction of the stabilizers from the polymer matrix. Following the first approach, a new high resolution nuclear magnetic resonance (NMR) method for the direct determination of stabilizer levels has recently been introduced[3]. This method employs selective signal suppression to allow the direct determination of stabilizer levels. Several authors have presented methods based on extraction followed by quantitation using high performance liquid chromatography (HPLC)[2,4,5]. These two techniques have been used in this work to study the effect of the manufacturing process and of aging on stabilizer levels in DEPIC (Dual Extruded Plastic Insulated Conductor) cable materials[6].

EXPERIMENTAL

Materials

The stabilizers in this study were used as received and included the following. Irganox 1010, tetrakis[methylene(3,5-di-tert-butyl-4-hydroxy-hydrocinnamate)]methane (AO-1), Irganox 1024, N,N'-bis[3-(3',5'-di-tert-butyl-4-hydroxyphenyl)propanyl]hydrazine (MD-1), and Irganox 1035, thiodiethylene bis[3,5-di-tert-butyl-4-hydroxy-hydrocinnamate) (AO-2). The polyethylenes used in the standard samples were high density solid (PE1-10) and expandable (EPE1-11) base resins obtained from the cable insulation manufacturers. The DEPIC cable materials examined were solid and expanded polyethylene insulations and extended thermoplastic rubber (ETPR) filling compounds[6]. The insulations were stabilized with AO-1 and MD-1 and the filling compounds were stabilized with AO-2. The expandable insulation resins also contained an azodicarbonamide blowing agent.

Analytical Techniques

NMR Analysis -The NMR data were recorded on a JEOL GX-500 Spectrometer. The materials were studied in an 80:20 (by volume) mixture of *cis*-decalin:*p*-dioxane-d_8 at 115°C. This mixture is a good solvent for the additives and cable materials and provided a stable deuterium lock signal for the NMR spectrometer. Hexamethyldisiloxane (HMDS) was used as the internal reference. The standard solution used in this study contained 0.2 wt % of AO-1 and MD-1 and 10.0 wt % of polyethylene base resin. To determine additive concentration, ten percent by weight solutions of the various polymeric materials were prepared. Sample solutions were made in a nitrogen atmosphere and the tubes were sealed with paraffin film. An NMR pulse sequence was used for selective signal suppression of the polymer and solvent resonances and the intensity of the resonances after 500 scans was taken as the measure of additive concentration.

HPLC Analysis -HPLC analysis consisted of two steps: extraction of the stabilizers from the polymer matrix, followed by HPLC quantitation. Extraction was performed by a modified version of the method presented by Fech and DeWitt in 1980[7]. Samples were ground to -20 mesh in a Wiley mill, and one gram of the ground polymer was then heated under nitrogen in 100 ml of

refluxing toluene until dissolution occurred. The solution was removed from heat, and 100 ml methanol was added (under nitrogen) to precipitate the polyethylene. After cooling to room temperature, the mixture was filtered using a 0.45 μm polytetrafluoroethylene filter. The filtrate was taken to dryness under nitrogen, and the residue was brought up to 10 ml with methanol. The sample was filtered with a 0.2 μm syringe filter and an injection volume of 50 μl was used. HPLC analysis was performed at room temperature on a Waters system consisting of a model 510 pump, model 700 WISP injector, and a Maxima 820 data station. A Waters model 440 UV detector was used for detection at a fixed wavelength of 280 nm. The column set consisted of a 3.9 mm x 30 cm Waters μBondapak C_{18} reverse-phase column, fitted with a Guard Pak precolumn filter. An isocratic mobile phase of methanol with 1% acetic acid and 1% water was used, at a 1.0 ml/min flow rate. Mixed liquid standards were prepared in methanol, at concentrations corresponding to 0.05%, 0.10%, 0.15%, 0.25%, 0.40%, and 0.50% each of AO-1 and MD-1.

Film Preparation

NMR Analysis - Laminates of expandable and nonexpandable HDPE containing standard concentrations of AO-1 and MD-1 were prepared by molding pellets between chemically cleaned copper or aluminum sheets. The sheets were cleaned by immersion in an alkaline detergent electro-cleaner with application of a 5 A current for 5-10 s, a deionized water rinse and immersion in a 50% HCl solution for 20-30 s, and then a second water rinse. These procedures were repeated until the metal surface wet evenly. Sheets were dried with nitrogen and suspended in air to prevent contamination. Pellets (2 grams) were sandwiched between the metal sheets and molded for one minute under pressure (250 lbs sq in) in an electric press at 200-215°C. The sandwich was removed and cooled under pressure to ambient temperature. The laminates were separated and the polyethylene films (7 mils) used for NMR analysis. Foaming of the expandable polyethylene was confirmed by visual examination.

RESULTS AND DISCUSSION

Analysis

Phenolic stabilizers can readily be identified using a high-resolution NMR spectrometer operated at high magnetic fields. The proton spectra of three common stabilizers, AO-1, MD-1 and AO-2, are shown in Figure 1. For AO-1, the resonance of the 3-methylene protons at 3.92 ppm is unique to that stabilizer and for AO-2 both the 3-methylene protons at 4.08 ppm and the 4-methylene protons at 2.59 ppm permit identification. The 2-methylene protons of AO-1 and AO-2 resonate at 2.44 ppm, while those protons in MD-1 generate peaks at 2.33 ppm, thus providing identification of that stabilizer. The spectrum of a stabilized polyethylene sample shows that the resonances unique to each additive are observed (Figure 2). By comparison with spectra for samples with known amounts of the additives, the peak intensities of the methylene protons were used to determine additive concentration.

Identification and quantitation of the stabilizers was also straightforward with the HPLC method. No interference was found between AO-1, AO-2, or MD-1. The chromatograms were stable and reproducible with good peak separation for both liquid standards and polymer extracts (Figure 3). Quantitation was performed from peak areas by comparison of sample peaks to calibration curves. Accuracy of the retention times and quantitation routine were verified by frequent injection of standard solutions.

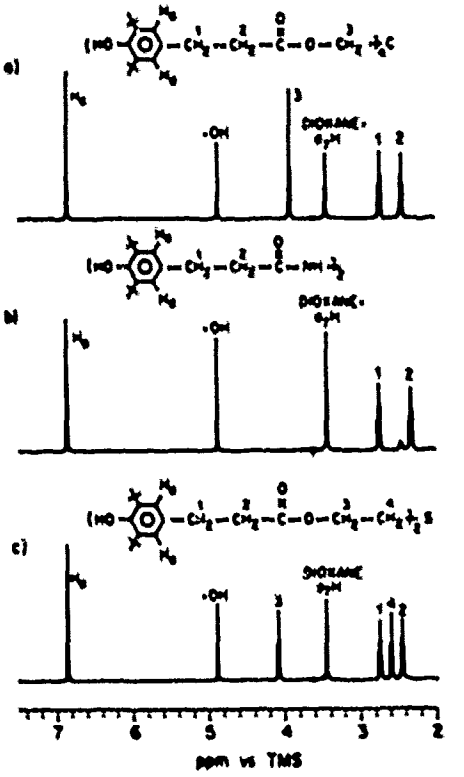

Figure 1 500 MHz ^1H NMR spectra of (a) AO-1, (b) MD-1, and (c) AO-2 in 80:20 (by vol) mixture of *cis*-decalin / *p*-dioxane-d_8 at 115°C

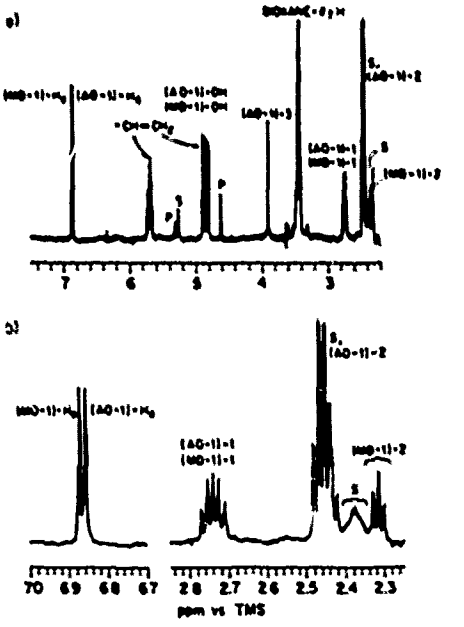

Figure 2 500 MHz ^1H NMR spectra of a commercial stabilized polyethylene product, solvent and temperature as in Figure 1, see Figure 1 for structural designations (s and p refer to solvent and polymer respectively)

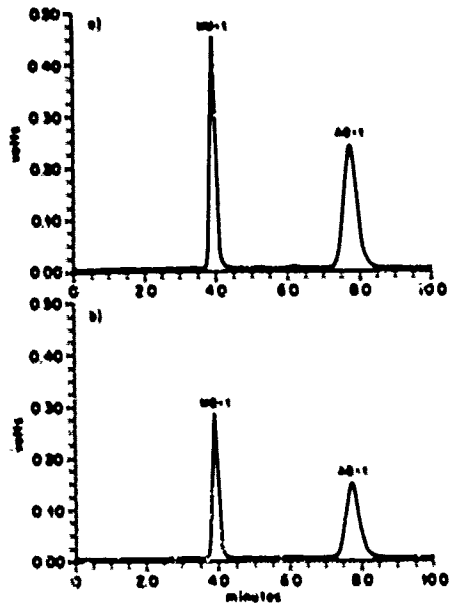

Figure 3 Chromatograms of (a) mixed standard solution (0.25% each of AO-1 and MD-1) in methanol, and (b) polymer extract from PE8

Reproducibility of the extraction method was found to be excellent. Twenty three duplicate samples of a solid polyethylene raw material (PE3) were analyzed, and the range, mean, and standard deviation determined for each additive (Table 1). The accuracy of the HPLC method was verified by comparison with values obtained by NMR and excellent agreement was found (Table 2).

Table 1.
REPRODUCIBILITY OF HPLC RESULTS

		%AO-1		
0.22	0.21	0.21	0.19	0.18
0.18	0.19	0.19	0.19	0.19
0.18	0.20	0.18	0.19	0.18
0.18	0.19	0.18	0.19	0.18
0.18	0.18	0.18		
Mean	0.183			
Range	0.18-0.22			
σ	0.020			
		%MD-1		
0.20	0.19	0.19	0.19	0.19
0.19	0.20	0.18	0.17	0.19
0.18	0.19	0.18	0.20	0.19
0.18	0.18	0.18	0.18	0.18
0.18	0.18	0.18		
Mean	0.186			
Range	0.17-0.20			
σ	0.008			

Analysis of solid and expandable polyethylene raw materials from two suppliers showed lot to lot variation in stabilizer content (Table 2). Supplier B tended to furnish material that was consistently lower in stabilizer content. Material from both suppliers was lower in MD-1 concentration than AO-1 concentration.

Table 2.
CONCENTRATION (%) OF STABILIZERS IN RAW MATERIALS

	NMR		HPLC	
Material	AO-1	MD-1	AO-1	MD-1
Supplier A				
PE1	0.20	0.20	0.21	0.20
PE2	0.18	0.20	0.22	0.21
PE3			0.18	0.19
PE4			0.19	0.19
PE5			0.23	0.16
PE6			0.21	0.16
PE7			0.18	0.21
EPE1	0.20	0.20		
EPE2			0.19	0.15
Supplier B				
PE8			0.15	0.12
PE9			0.21	0.15
EPE3	0.13	0.13		
EPE4			0.13	0.13
EPE5			0.14	0.13
EPE6			0.15	0.11
EPE7			0.21	0.15
EPE8			.15	0.12

Stabilizer Loss

Processing affected the concentration of both additives. After extrusion the concentration of the additives was about 18% lower in the insulation than in the raw materials (Table 3), based on the assumption that 24 AWG wire is composed of about 45% solid and 55% foam. The cabling and filling process slightly decreased the additive concentrations in the insulation (Table 4).

Table 3.
CONCENTRATION (%) OF STABILIZERS AFTER EXTRUSION[a]

	SOLID		FOAM		INSULATION	
Material	AO-1	MD-1	AO-1	MD-1	AO-1	MD-1
PE4/EPE4	0.19	0.19	0.13	0.13	0.14	0.11
PE5/EPE5	0.23	0.16	0.14	0.13	0.16	0.11
PE6/EPE6	0.21	0.16	0.15	0.11	0.09	0.15
PE8/EPE7	0.21	0.15	0.15	0.12	0.17	0.13
PE7/EPE8	0.21	0.18	0.15	0.12	0.15	0.12

[a]Determined by HPLC

Table 4.
CONCENTRATION (%) OF STABILIZERS AFTER CABLING[a]

	INSULATION		CABLE	
Material	AO-1	MD-1	AO-1	MD-1
PE9/EPE10	0.10[b]	0.08[b]	0.08[b]	0.08[b]
PE10/EPE11	0.13[b]	0.12[b]	0.07[b]	0.07[b]

[a] Determined by NMR [b] Determined by HPLC

Aging in filling compound at elevated temperatures dramatically reduced the concentration of the additives. The results of two different aging studies are shown in Table 5. When insulation was aged in air for 28 days at 70°C, there was slight reduction in AO-1 and MD-1. However aging the insulation in a large excess of filling compound for 28 days at 70°C, resulted in a significant loss of AO-1 and MD-1. Similar results were obtained when a cable was aged for 28 days at 70°C. Chromatograms of cabled material before and after aging are shown in Figure 4.

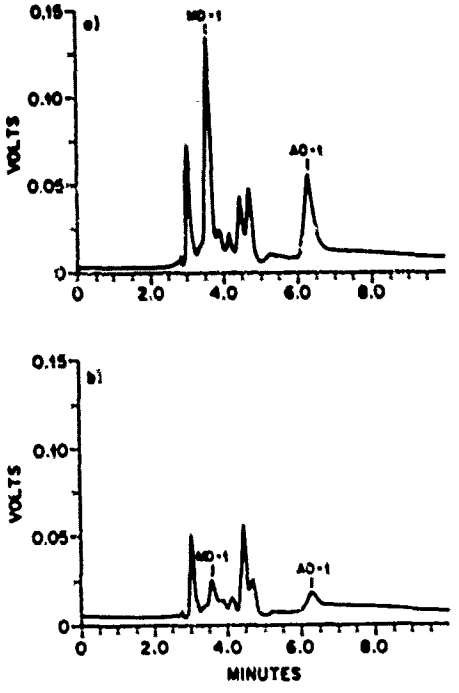

Figure 4 Chromatograms of (a) stabilizer extract from standard cable insulation (PE10/EPE11) and (b) cable insulation after aging at 70°C for 28 days

Table 5.
EFFECT OF AGING ON CONCENTRATION (%) OF STABILIZERS[a]

	PE10/EPE11		PE4/EPE4	
	AO-1	MD-1	AO-1	MD-1
Insulation				
•initial	0.13	0.12	0.14	0.11
•after 4 weeks at 70°C in air	0.12	0.10	0.13	0.10
•after 4 weeks at 70°C in filling cpd	•	•	0.04	~0.01
Cable				
•initial	0.07	0.07	•	•
•after 4 weeks at 70°C in filling cpd	0.02	~0.01	•	•

[a] Determined by HPLC

Analysis of the filling compound from aged cables explains the low concentration of AO-1 measured in the insulation samples. NMR spectra (Figure 5) of unused filling compound and of filling compound from a cable manufactured in 1985 show that during storage a significant amount of AO-1 had been extracted from the insulation. However, little MD-1 was found in the filling compound, confirming previous studies[12,13] that have shown AO-1 to be extracted by hydrocarbon materials more readily than is MD-1. HPLC analysis of a filling compound extract from an aged cable gives similar results. For the HPLC analysis of the filling compound, the extraction technique was the same as that used with polyethylene. This method must be considered to be semiquantitative, as the oily fraction is only partially soluble in methanol, and complete separation is impossible. Figure 6 gives the chromatograms of the filling compound extracts of a standard cable before and after aging for 28 days at 70°C. Peaks for AO-1 and MD-1 are clearly evident, and correspond to concentrations of about 0.05 and 0.02%, respectively.

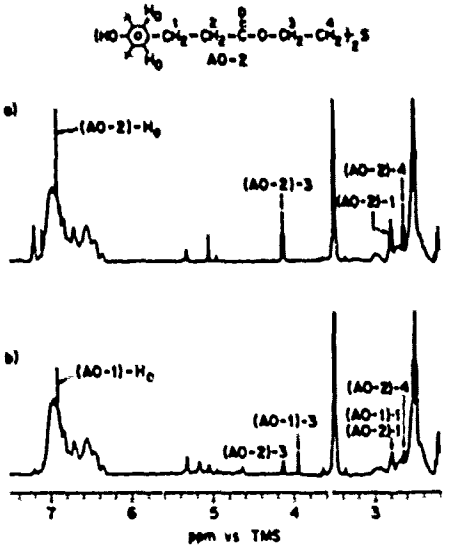

Figure 5 500 MHz ^{1}H NMR spectra of (a) ETPR filling compound and (b) filling compound removed from a cable manufactured in 1985

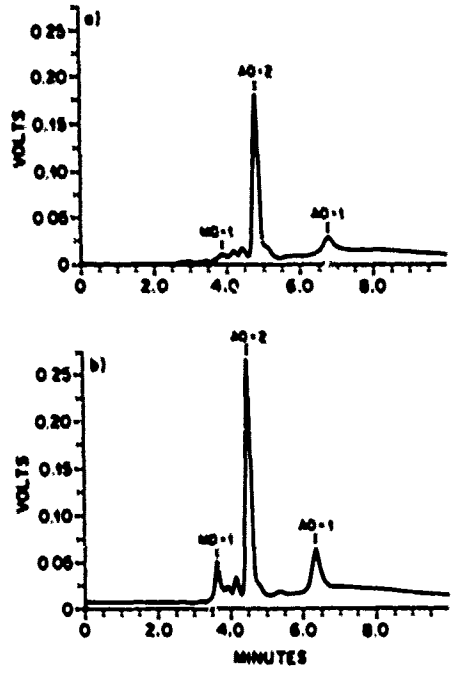

Figure 6 Chromatograms of (a) extract from filling compound in a recently manufactured cable (PE10/EPE11) and (b) extract from filling compound in the same cable aged at 70°C for 28 days

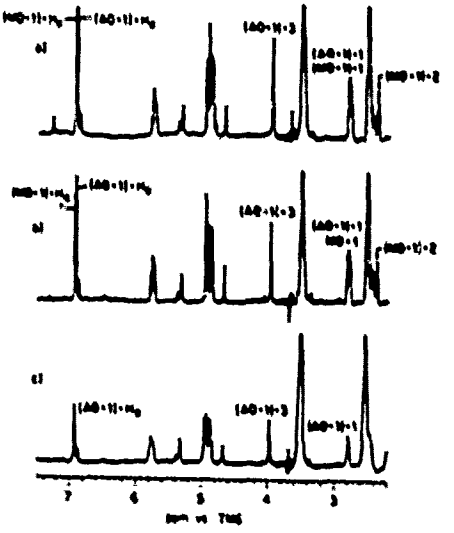

Figure 7 500 MHz ^{1}H NMR spectra of (a) polyethylene pellets, (b) polyethylene molded on aluminum, and (c) polyethylene molded on copper

Film Studies

The loss of MD-1 from the insulation during aging cannot be attributed to extraction only, since little MD-1 was found in the filling compound. Other processes must be contributing to depletion of the metal deactivator. Analysis of insulation after extrusion showed a decrease in the concentration of MD-1, indicating that interactions between the azodicarbonamide blowing agent, MD-1 and the copper may occur. To test this theory, polyethylene pellets with and without blowing agent were molded against electrochemically cleaned sheets of copper and aluminum. The molding conditions were similar to those used in the manufacture of expanded insulation, however, the metal to polyethylene ratio was significantly greater than that found in an insulated wire.

Analysis of the polyethylene films showed that the residual concentrations of the additives were significantly affected by the molding conditions. Molding polyethylene against copper substantially decreased the concentration of MD-1 and the addition of blowing agent completely destroyed the deactivator in the foamed polymer (Figure 7 and Table 6). This depletion is considerably less in insulation, which has a lower copper to polyethylene ratio (Table 3).

Molding against aluminum had less effect on the deactivator level. The loss of AO-1 during molding was not as severe. On aluminum the decrease in antioxidant concentration was similar to that of the deactivator and was not accelerated by addition of the blowing agent. On copper there was less loss of AO-1 than MD-1.

Table 6.
CONCENTRATION (%) OF STABILIZERS[a] IN POLYETHYLENE FILMS

MATERIAL	AO-1	MD-1
PE Pellets	0.20	0.20
PE on Al	0.13	0.15
PE on Cu	0.14	0.09
PE and AZO Pellets	0.20	0.20
PE and AZO on Al	0.15	0.15
PE and AZO on Cu	0.11	0.00

[a]Determined by NMR

Cables

Additive concentrations were also measured in DEPIC cables manufactured earlier (Table 7). The concentrations of AO-1 and MD-1 in the insulation had roughly decreased to the same level, with one exception, and were higher than the values measured after aging cable for 28 days at 70°C (Table 5). Analysis of the filling compound showed that both of the additives had been extracted, with the AO-1 present at a greater concentration that the MD-1. No AO-2 was found in the insulation samples.

Table 7.
CONCENTRATION (%) OF STABILIZERS IN CABLE MATERIALS[a]

INSULATION		
Date of Manufacture	AO-1	MD-1
1984	0.04	0.04
1985	0.04	0.04
1986	0.05	0.03

FILLING COMPOUND			
Date of Manufacture	AO-1	MD-1	AO-2
1984	0.08	~ 0.02	0.20
1985	0.15	~ 0.05	0.10

[a]Determined by NMR

CONCLUSIONS

Two analytical techniques: a new, high resolution NMR method, and HPLC analysis, have been used to determine stabilizer levels in polyolefin cable insulations. Excellent agreement between the two methods has been found and they have been used to measure the the effects of manufacturing processes and of aging on the depletion of stabilizers from DEPIC cable insulation.

Three mechanisms contributing to the depletion of stabilizers from DEPIC cable materials were identified: thermal-oxidative processes, chemical reaction with the azodicarbonamide blowing agent and copper, and extraction by the filling compound. During extrusion both antioxidant (AO-1) and metal deactivator (MD-1) concentrations are diminished. The depletion of antioxidant is due mainly to thermal-oxidative processes, while the depletion of metal deactivator is a result of thermal oxidation and interaction with the blowing agent at the copper interface. Stabilizer loss during the cabling operation is attributed primarily to dissolution of the stabilizers in hot filling compound, although some depletion by thermal-oxidative degradation may occur.

The most significant reduction in stabilizer concentration is observed after aging insulation at elevated temperatures in the presence of filling compound. All three depletion mechanisms operate during aging. With unfilled cable cores, thermal-oxidative processes lower stabilizer concentration slightly; however, with filled cables extraction of the stabilizers, particularly AO-1, by the filling compound is the major cause of stabilizer loss. Extraction by filling compound can not completely explain MD-1 depletion. Chemical reaction of the deactivator with the blowing agent and copper conductor is also a major contributor to metal deactivator depletion.

ACKNOWLEDGEMENTS

We thank Kent Connole for his excellent technical advice and assistance in obtaining samples; Dave McCall for suggesting and encouraging the NMR studies; and Gail Peins for help in preparation of the metal sheets.

REFERENCES

1. Hawkins, W. L., *Polymer Degradation and Stabilization*, Springer- Verlag, Berlin, (1984)
2. Gächter, R. and Müller H., *Plastics Additives*, Hanser Publishers, New York, (1985)
3. Wheeler, D. A., *Tantala*, 15:1315, (1968)
4. Scholl, F., *Atlas of Polymer and Plastics Analysis Vol. 3*, Carl Hanser Verlag, Munich, (1981)
5. Wheeler, D. A., ibid
6. Schilling, F. C. and Kuck, V.J., paper presented at 20th Annual Eastern Analytical Symposium, New York, Sept. 1989.
7. Fech, J. and De Witt A., *Proceedings of the International Wire and Cable Symposium*, 327 (1980)
8. Schabron, J. F. and Fenska, L. E., *Anal. Chem.*, 352, 1411 (1980)
9. British Standard 2782, Part 4, Method 405D (1985)
10. Mitchell, D. M., *Proceedings of the International Wire and Cable Symposium*, 216, (1974)
11. Mitchell, D. M., *Proceedings of the International Wire and Cable Symposium*, 500, (1988)
12. Chan, M. G. and Powers, R.A., *Soc. Plast. Eng. Pap.*, 21, 292, (1975)
13. Brown, G. D., *Proceedings of the International Wire and Cable Symposium*, 337, (1987)

K. D. Dye
AT&T Network Systems
505 N 51st Avenue
Phoenix, AZ 85043

Karen D. Dye graduated from New Mexico Institute of Mining and Technology in 1982 with a B.S. in Chemistry. She joined AT&T Network Systems (Phoenix Works) in 1985, where she is an Engineer in the Materials Laboratory. She is involved in analysis of raw materials, final product evaluations, and development work. Her area of special interest is analytical methods development.

V. J. Kuck
AT&T Bell Laboratories
600 Mountain Avenue
Murray Hill, N. J. 07974

M. G. Chan
AT&T Bell Laboratories
600 Mountain Avenue
Murray Hill, N.J. 07974

Valerie J. Kuck joined AT&T Bell Laboratories, Murray Hill, N.J. in 1967 and is currently a Member of Staff in the Plastics and Chemistry Research and Engineering Department. In 1961 she received a B.S. in Chemistry from Saint Mary-of-the Woods College and a M.S. in Chemistry in 1964 from Purdue University. Presently she is doing research on coatings for optical fibers and on the degradation and stabilization of polymers.

Maureen G. Chan is Supervisor of the Chemical Stabilization Group in the Plastics Chemistry Research and Engineering Department at AT&T Bell Laboratories, Murray Hill, N. J. She joined AT&T Bell Laboratories in 1982 where her research has concentrated on studies of the degradation and stabilization of polymers used in telecommunications cables. She received a B.S. in Chemistry from Chestnut Hill College (1981) and a M.S. in Chemistry from Stevens Institute of Technology (1985).

F. C. Schilling
AT&T Bell Laboratories
600 Mountain Avenue
Murray Hill, N.J. 07974

L. D. Loan
AT&T Bell Laboratories
600 Mountain Avenue
Murray Hill, NJ 07974

Fred Schilling graduated from Wayne State University, Detroit, Michigan in 1973 with a B.S. in Chemistry. In that same year he began working in the Polymer Chemistry Research Department at AT&T Bell Laboratories, Murray Hill, N.J. where he is a Member of the Technical Staff. His research has concentrated on the application of NMR spectroscopy in the study of synthetic polymers. Current research interests include the solid state NMR analysis of isolated polymer chains in crystalline organic matrices; the study of molecular structure and chain dynamics of polysilanes; the relationship between the carbon and silicon chemical shift and bond conformation; and the effects of crystal packing interactions on the chemical shift.

Don Loan is currently Head of the Plastics Chemistry Research and Engineering Department at AT&T Bell Laboratories, Murray Hill, N. J. He was educated in England, and after completing his primary and secondary education in the Greater London area received B. Sc. (1951) and Ph.D (1954) degrees from the University of Birmingham. His graduate work focussed on the chemistry of polymers and he has worked in this general area to the present time. His current responsibilities include work in the area of polymer stabilization, the synthesis and chemistry of polymers suitable for use at high temperature, and in general problems in polymer chemistry. He is author of more than thirty papers in the scientific literature.

A LIFETIME PREDICTION METHOD FOR THERMOPLASTIC POLYMERS

Donald R. Parris

Siecor Corporation
489 Siecor Park
Hickory, NC 28603

ABSTRACT

The hydrolytic stability of polybutylene terephthalate (PBT) and polycarbonate resins was evaluated. Rates of reaction were monitored through changes in elongation to break and melt flow index (MFI). Due to the continuous nature of the MFI vs. time curves, the time to lifetime endpoint could be extrapolated before the material had degraded to that point. This significantly reduces the time to make a lifetime prediction.

BACKGROUND

Long term prediction of polymeric material behavior is of particular importance in the cable industry. Cables are commonly expected to have field lifetimes of up to 40 years while exposed to many possible combinations of temperature and humidity.

It is desirable to predict a material's useful lifetime in a relatively short period of time. The prediction is typically made by placing a material in an environment similar to actual field conditions and increasing the temperature to accelerate any reactions between the material and its environment. A lifetime endpoint is chosen based on the time to reach some limiting value of a critical property such as tensile strength or elongation to break. The time to the "lifetime endpoint" as a function of temperature is then extrapolated (via Arrhenius) to predict lifetimes at lower temperatures.

Polymeric materials in cables will almost always react with something in their environment. How fast anything reacts is a function of the availability of reactants (quantity and mobility), the activation energy for the reaction and the temperature. The predicted lifetime must therefore be stated as valid at a certain temperature in the presence of a certain reactive specie(s) (e.g. 40°C/water).

Since the polymer molecules are relatively bound in the solid state, one must typically depend upon the mobility of some non-polymeric (small) chemical species to make any reactions physically possible. Water and oxygen are two relatively small chemical species that all cable materials will see throughout their lifetime. Additionally, cable materials may come in contact (and possibly react) with internal cable filling and flooding compounds and with various chemicals from the external environment.

PBT (polybutylene terephthalate) has been used in fiber optic cable buffer tubes for many years. It is known that hydrolysis is a primary degradation mechanism for such polyesters (Ref 1,2,3 & 4). The activation energy for the hydrolysis of PBT has been reported by Kelleher et al (Ref 4) to be 25.1 kcal/mol. This study indicates that this activation energy is not applicable to all PBTs as several different reaction rates have been observed for PBTs from different manufacturers.

The elongation to break for these PBT's was found to be the most sensitive mechanical property to monitor as a function of aging time in water. The tensile strength has been followed by others in similar studies (Ref 1 & 3) but was found by this author to be degradation insensitive until the material became brittle. A typical plot of PBT elongation to break as a function of aging time in water at 60, 80 and 100°C is shown in Figure 1. A typical plot of PBT tensile strength as a function of aging time in water at 60, 80 and 100°C for the same material is shown in Figure 2. The elongation to break here is clearly a more sensitive indicator of the effects of degradation.

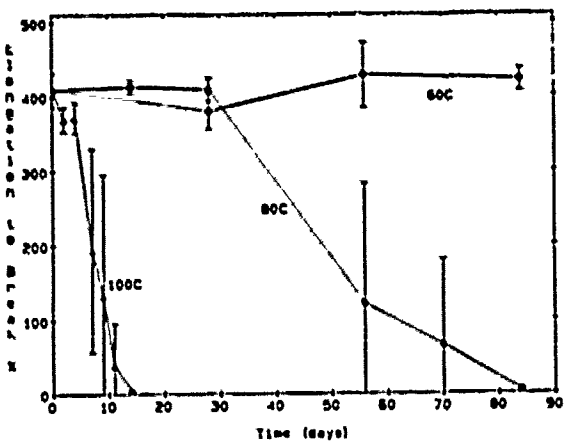

Figure 1: Elongation to break as a function of aging time in water for a typical PBT

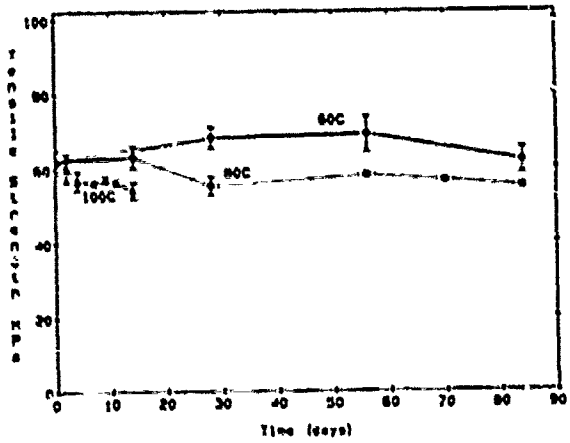

Figure 2: Tensile strength as a function of aging time in water for a typical PBT

The elongation to break as a degradation monitor, however, is far from perfect. In an aging study the elongation to break values between the initial elongation and zero elongation often have extremely high standard deviations. This is a consequence of the increasing flaw sensitivity of the material as it degrades. Flaws could be surface flaws from the extrusion of test strips or from imperfect edges created when the "dumbbell" tensile test sample is die cut. Flaws could also be internal to the polymer as impurities/inclusions.

- Unaged materials are relatively flaw insensitive. As a material degrades, the critical flaw size necessary to cause failure in tensile testing decreases. As the critical flaw size decreases, the number of flaws of critical size or larger increases and the distance between these flaws becomes smaller. This will result in small standard deviations for elongation to break values early in the degradation process (relatively flaw insensitive), large standard deviations for intermediate stages of degradation (large distances between flaws of critical size) and smaller standard deviations as the material further degrades (increasingly smaller distances between flaws of critical size). The region of highest standard deviation in an elongation to break versus time curve will be approximately between 15 and 85% of the original elongation to break. In this region is is important to note that the material is still deforming plastically; that is, at this stage of degradation all of the material's elastic performance is still available and being used to resist the stress being applied.

Because of the high standard deviations for such elongation to break data and the non-continuous nature of most elongation to break vs. time curves, the curves cannot be curvefitted to predict future values with confidence. Graphical and numerical methods to optimize such data evaluations have been described by Nelson (Ref 5,6 & 7) and Hahn (Ref 8), but continuous curves and data with low standard deviations would always be best.

A typical lifetime prediction study based on presently accepted methods could be carried out as follows. The lifetime endpoint for any material is established as a minimum absolute value of elongation to break or as a maximum allowable percentage loss in elongation to break. The elongation to break is charted as a function of aging time and the time to the endpoint is determined with some accuracy for any set of environmental conditions. The material lifetime is then plotted as a function of temperature in an Arrhenius diagram from which lifetimes at lower service temperatures are extrapolated. The practical problem that one faces with this approach is that it may require extremely long times in the lower temperature environments for a material to reach its endpoint (up to 3 years or more for a PBT in 60°C water). Additionally, for an accurate lifetime prediction using this method, due to the inability to accurately extrapolate mechanical property data, the sample should be removed from the aging environment on exactly the day that it reaches its lifetime endpoint. This means that a large number of samples must be prepared so that samples can be removed relatively often for testing. This also means that it may be three years before one can make a lifetime prediction based on aging in lower temperature (e.g. 60°C) water.

METHODOLOGY OF LIFETIME PREDICTION

Various PBT's were evaluated in several separate studies by monitoring the elongation to break and the Melt Flow Index (MFI) as a function of aging time in water at 60, 80 and 100°C. Monitoring MFI here is very convenient because water, the most aggressive species for these resins in the normal cable environment, can be removed from the polymer by drying and will therefore not interfere with the MFI measurement. The MFI value also gives an indirect but accurate idea of the extent of degradation that has occurred.

All testing (tensile and MFI) was conducted on PBT strips that were identically extruded and aged. After aging, the tensile samples were allowed to condition at room temperature and 50% r.h. for a minimum of 24 hours prior to testing at a crosshead speed of 20 mm/min. After removal from the aging water, the MFI test strips were dried in a vacuum oven at 100°C and 25" mercury for 16 hours and then measured for MFI at 250°C with a 2.16 kg load. Eight grams of extruded sample were used for each MFI measurement. From these data an elongation to break and a MFI versus time curve was generated. The elongation to break curves are discontinuous with coefficients of variance (standard deviation / average) as high as 200% (see Figure 1). The MFI curves, however, are continuous with average coefficients of variance of about 5%. MFI vs. aging time curves for PBTs aged up to 60 days in 60, 80 and 100°C water are shown in Figures 3, 4 and 5. Figures 3 and 4 show the actual data points and the best fit exponential regression curves. Little change in MFI was observed for any material in 60°C water in this time frame and thus the data points are shown connected and not curvefitted in Figure 5.

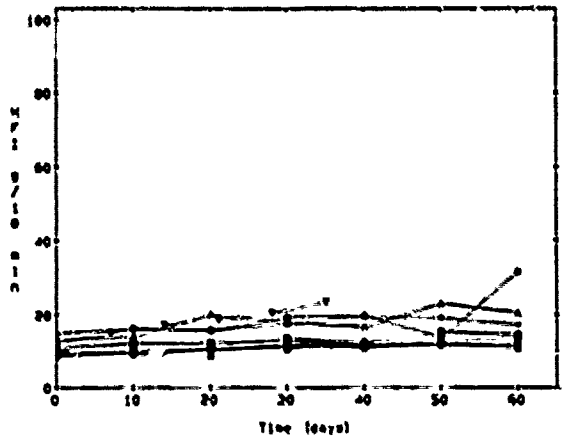

Figure 3: MFI as a function of time in 60°C water for 9 different PCTs

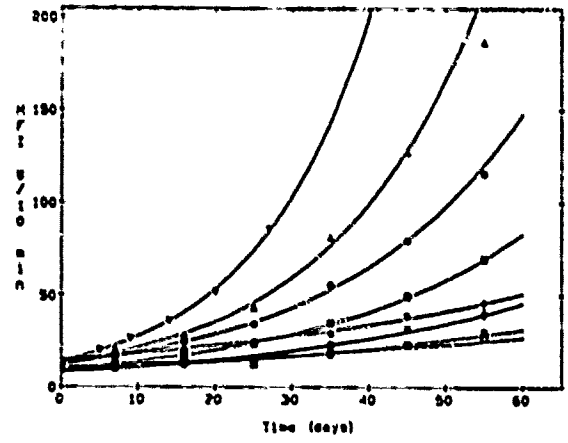

Figure 4: MFI as a function of time in 80°C water for 9 different PBTs

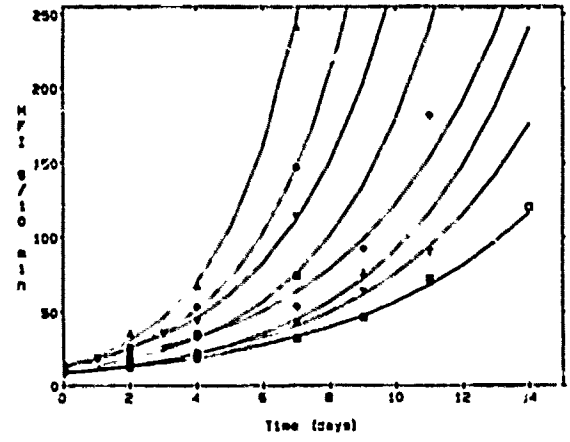

Figure 5: MFI as a function of time in 100°C water for 9 different PBTs

This same method was used to evaluate different polycarbonates. Here, hydrolysis of the ester linkage in the polycarbonate chain will result in polymer degradation. The MFI vs time relationship for a representative polycarbonate aged in 60, 80 & 100°C water is shown in Figure 6.

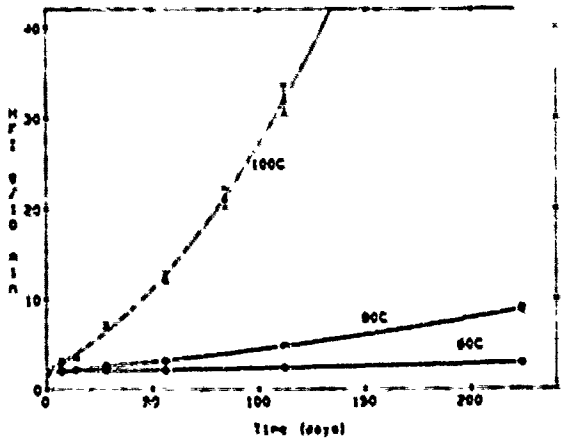

Figure 6: MFI as a function of time in water at 60, 80 and 100°C for a typical polycarbonate

The MFI was also found in this work to be indicative of the mechanical state of the material, that is, a certain MFI value was found to correspond with a certain elongation to break value regardless of the water aging temperature for the PBT. This too was reported by Kelleher et al. A plot of MFI vs elongation to break for a typical PBT is shown in Figure 7. An interesting point here is that although all of the PBT's had similar initial MFI values of 8 - 15 g/10 min, the MFI values at their lifetime endpoint varied greatly from 60 - 250 g/10 min at ~10% elongation to break.

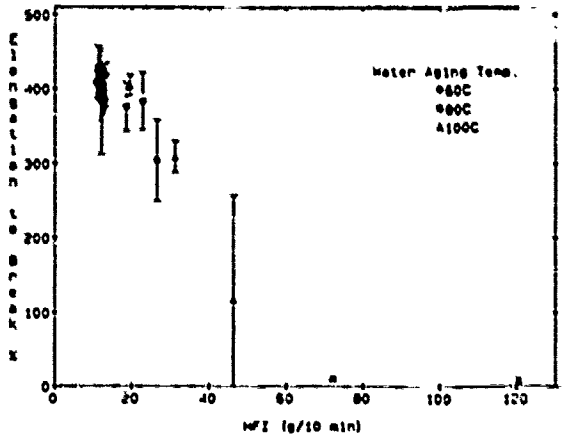

Figure 7: Elongation to break as a function of MFI for a typical PBT

Kelleher et al (Ref 4) reported that there was a relationship between the MFI and aging time for PBTs in water and that as the MFI increased, so did the rate of reaction. They attributed this behavior to a possible catalysis by polymer end groups but went no further to characterize this relationship.

Nine different PBTs were aged in water at 60, 80 and 100°C for up to 60 days. Endpoint MFIs were determined from the 100°C data on MFI and elongation to break as a function of time. In all of the environments where the MFI had reached or exceeded the endpoint, the MFI vs time curves were curvefitted and the

time to endpoint MFI as a function of aging time was calculated. [No PBT aged in 60°C water reached its endpoint during this evaluation.] This data is represented in Figure 8 where the percent difference between the predicted and actual time to the endpoint MFI is plotted as a function of the percent of time to the endpoint that has already passed. Here, more than 90% of the predicted times to the endpoint MFI lie within 10% of the actual value when the materials have been aged for only 40% of the total time that is required to reach their endpoint.

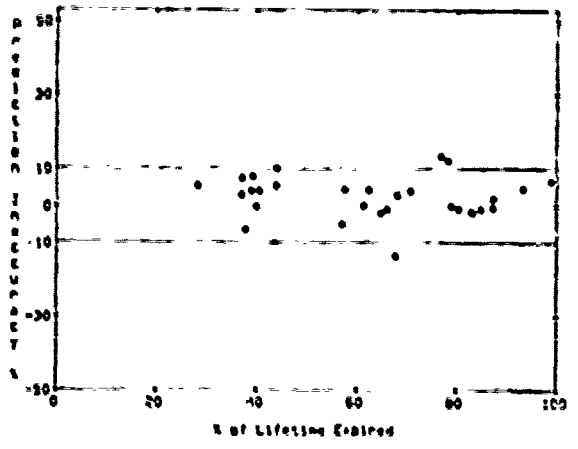

Figure 8: Percent difference between actual and predicted MFI values as a function of percent of lifetime expired

With this information, material lifetime predictions can be made before the actual lifetime endpoint is reached. This is because one can determine the endpoint elongation to break and corresponding endpoint MFI from higher temperature aging results in a short period of time. The lower temperature, longer term test samples can also be monitored for their MFI over time. These data can then be curvefitted and the time to endpoint MFI extrapolated. The more data acquired, the higher the confidence level of the prediction.

LIFETIME PREDICTION EXAMPLE

Extruded strips ~ 1 x 5 x 150 mm and tensile test dumbbells die cut from the same extruded strips of PBT A were placed in distilled water at 60, 80 & 100°C. Samples were removed according to the following schedule.

PBT A TEST SCHEDULE

Aging Time	Temperature (°C)		
(Days)	60	80	100
0	X	X	X
2			X
4			X
7	X	X	X
9			X
10		X	
14	X	X	
28	X	X	
42		X	
56	X		
113	X		

At each removal date, 5 tensile test samples and 8 grams of extruded strips to conduct an MFI measurement were removed. Plots of elongation to break and MFI versus time are shown in Figures 9 & 10. The relationship between elongation to break and MFI is shown in Figure 11. The lifetime endpoint for this example was chosen to be that point at which the material loses all ability to exhibit plastic deformation, that is, when the plastic will only elongate as far as its original strain at yield (~10 - 15% strain). This occurs in 100°C water in about 8 days as shown in figure 10. The tensile strength is reduced at this point only by about 10%, but the material is actually to the point of becoming brittle.

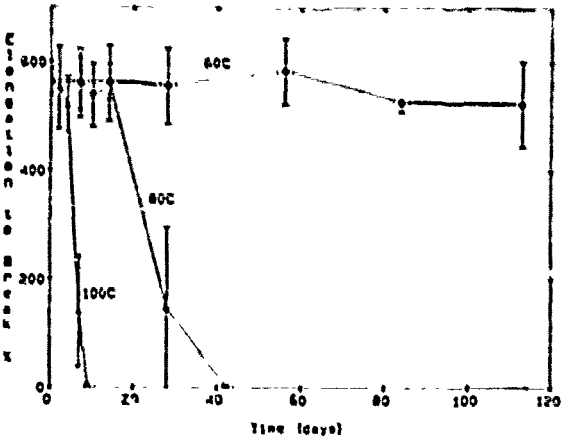

Figure 9: Elongation to break as a function of aging time in water at 60, 80 and 100°C for PBT A

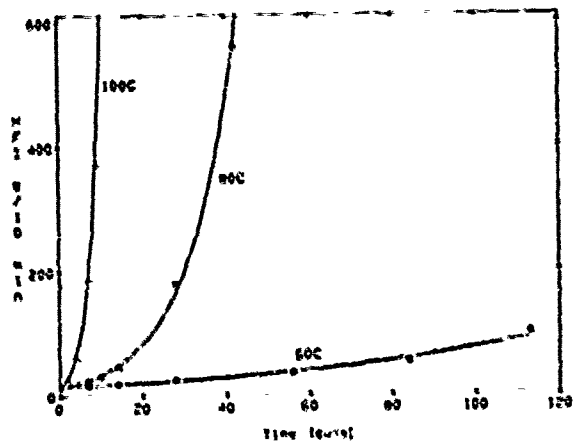

Figure 10: MFI as a function of aging time in water at 60, 80 and 100°C for PBT A

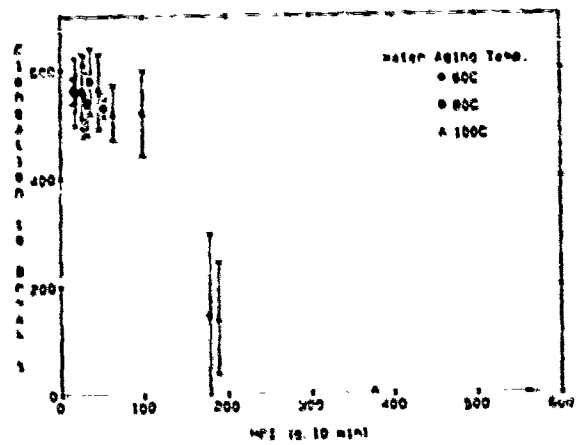

Figure 11: Elongation to break as a function of MFI for PBT A

The MFI vs. time results at this temperature (Figure 10) are curvefit. The best curvefit is an exponential regression equation:

$$MFI = 13.13\ (1.21)^{X}$$

The MFI value ("endpoint MFI") at 8 days is calculated from this equation to be ~250 g/10 min. Subsequent data collected from the lower temperature environments is curvefit with each new data point and the time to MFI = 250 g/10 min is calculated. Using the Arrhenius method, the logarithm of the time to the lifetime endpoint is plotted against the reciprocal temperature in Kelvin to form what should be a straight line. This plot is used to interpolate or extrapolate lifetimes at any other temperature.

The resulting lifetime predictions as a function of aging time are listed below.

Aging Time (days)	Time to Endpoint in 100°C Water (days)	Time to Endpoint in 80°C Water (days)	Time to Endpoint in 60°C Water (days)	Lifetime Prediction ($40°C/H_2O$) (days/years)
14	8	36.3	202	1400/3.8
28	8	32.5	163	1000/2.7
42	8	32.7	163	1000/2.7
56	8	32.7	183	1150/3.2
84	8	32.7	191	1250/3.4
113	8	32.7	177	1100/3.0

Here one can see that the lifetime prediction after only 14 days is almost the same as the prediction after 113 days. Confidence in the 113 day prediction is high because the material has completely degraded in 80 and 100°C water and is about halfway degraded in 60°C water. Earlier predictions are in excellent agreement with later ones.

PBT has a glass transition temperature (Tg) of about 55°C, above which all of this accelerated testing is conducted. The reaction rates below the Tg will be slowed to some extent and therefore predictions made here for temperatures below this Tg would represent a worst case.

NOTE: The most hydrolytically stable PBTs evaluated will have lifetimes in 60°C water of around 3 years. This example is of a relatively hydrolytically unstable PBT but it was used here to illustrate the method because significant degradation was observed at all water temperatures within 4 months

CONCLUSION

This work was originally undertaken to evaluate PBTs for fiber optic applications. It was observed during the course of the program that by simultaneously monitoring the melt flow index (MFI) as well as some mechanical property such as elongation to break, one could make lifetime predictions with more confidence and in less time than was previously possible. The circumstances that make this possible are:

- Hydrolysis is known as a major degradation mechanism for polyesters.
- Polyesters (like PBT) can be hydrolyzed in water, dried to remove all unreacted water and then measured for MFI values.
- Elongation to break as a function of time curves for degrading polymers are typically discontinuous and have a large region of high standard deviation. Thus they are not curvefittable and values cannot be extrapolated with confidence
- MFI as a function of time curves for polyesters degrading in water are continuous and curvefittable. Measured values have low standard deviations and values can be extrapolated with confidence.
- A relationship between MFI and elongation to break has been established for PBTs degrading in water.

Utilization of this method is based on a unique set of circumstances and assumptions and is only applicable under those conditions. Under the right circumstances, however, this method can be applied to evaluate 1 material or to compare several materials to one another.

ACKNOWLEDGMENT

The author wishes to thank Herr Helmut Seller and Herr Gerhard Lange of the Siemens A.G. Fiber Optic Materials Lab in Munich, West Germany for their ideas and suggestions which laid the groundwork for this study. The author would like to thank Siecor Materials Lab technicians, K.Tedder, R.Peterson and C.Topping for performing hundreds of measurements with painstaking attention to detail.

REFERENCES

1. Grune, G.L. and Talarico, T.L., "Accelerated Aging of Polyethylene Terephthalate (PET) Film in Elevated Temperature and Humidity Environments," Coil Winding Proceedings, Oct. 1985, pp. 210 - 220.
2. Kishore, K. and Sankarallingam, S., "Kinetic Analysis of the Data on the Effect of Humidity on the Stability of Poly(Butylene Terephthalate)," Polym. Engr. and Science, 24, 13, (1984), pp. 1043 - 1046.
3. Gardner, R.J. and Martin, J.R., "Effect of Relative Humidity on the Mechanical Properties of Thermoplastic Polyesters," SPE ANTEC, Tech. Papers, 25, (1979), pp. 831 - 834.
4. Kelleher, R.P., Wentz, R.P. and Falcone, D.R., "Hydrolysis of Poly(butylene terephthalate)," Polym. Engr. and Science, 22, 4, (1982), pp. 260 - 264.
5. Nelson, W., "Analysis of Accelerated Life Test Data - Part I: The Arrhenius Model and Graphical Methods," IEEE Trans. on Electrical Insulation, EI-6, 4, (1971), pp. 165 - 181.
6. Nelson, W., "Analysis of Accelerated Life Test Data - Part II: Numerical Methods and Test Planning," IEEE Trans. on Electrical Insulation, EI-7, 1, (1972), pp. 36 - 55.
7. Nelson, W., "Graphical Analysis of Accelerated Life Test Data with the Inverse Power Law Model," IEEE Trans. on Reliability, R-21, 1, (1972), pp. 2 - 11.
8. Hahn, G.J. and Nelson, W., "Graphical Analysis of Incomplete Accelerated Life Test Data," Insulation/Circuits, Sept. 1971, pp. 79 - 84

Donald R. Parris

Siecor Corporation
489 Siecor Park
Hickory, NC 28603

Donald Parris was born in Shelbyville, Kentucky in 1958. He served in the U.S.Air Force from 1976 to 1980. He attended Virginia Polytechnic Institute where he received his B.S. and M.S. degrees in Materials Engineering in 1984 and 1986 respectively. He joined Siecor Corp in January 1986, left to work at the Siemens Fiber Optic Materials Lab in Munich, West Germany for 18 months in 1987 & 1988 and is currently supervisor of the Materials Laboratory at Siecor R,D&E in Hickory N.C..

EFFECT OF CHEMICAL STRUCTURE OF POLYIMIDE ON THE PROPERTY OF POLYIMIDE AND POLYIMIDE ENAMELLED WIRE.

Hiroshi Inoue, Toshihiro Inaike

UBE Industries, LTD., Hirakata, Osaka, Japan

ABSTRACT

Polyimides and polyimide enamelled wires from two types of acid anhydrides (pyromellitic dianhydride (PMDA) and 3,3',4,4'-biphenyltetracarboxylic dianhydride (BPDA)) and two types of diamines (4,4'-oxydianiline and p-phenylenediamine) have been prepared and their properties have been investigated. It has been revealed that BPDA based polyimides and polyimide enamelled wires are superior in thermal, chemical, and radiation resistance to PMDA based polyimides. Further, we have developed enamelled wires of polyimide containing inorganic filler (boron nitride) which have a longer life under impressed test at 1-3 KV than that of unfilled polyimide. The difference in these properties of BPDA and PMDA based polyimides is due to the difference of the reactivity of the imide groups of BPDA and PMDA.

1.INTRODUCTION

At first polyimide was developed for military and space industries, however, it has been widely adopted in the electric and electronic industries for it's high chemical and heat resistance, and superior mechanical and electrical properties. The most well-known polyimide is obtained from pyromellitic dianhydride (PMDA) and 4,4'-oxydianiline (ODA). However, 3,3',4,4'-biphenyltetracarboxylic dianhydride (BPDA) has been commercialized starting from phthalic acid through a coupling reaction, and a number of polyimides have been derived from BPDA. Thanks to the biphenyl structure, BPDA was found to be promising as a basic material for polyimide production.[1-4,6-10,17-19]

This paper discusses the characteristics of homopolymer and copolymer of polyimide from two types of acid dianhydrides (PMDA and BPDA) and two types of diamines (ODA and p-phenylenediamine (PPD)), and polyimide enamelled wires and enamelled wires made of filled polyimide.

2.EXPERIMENTAL

2.1.Sample

(1) The films presented in Table 1 were prepared in the usual way. The thickness of the films was 25 μm. (2) Polyimide enamelled wires shown in Tables 5 and 6 were prepared in the usual way. The diameter of copper wire was 1 mm. Filled polyimide enamelled wires consisted of two layers, an inner layer made of filled polyimide and an outer layer made of unfilled polyimide. The thickness ratio of the two layers was 7/3 (inner/outer). The thickness of the insulating layer was about 40 μm.

2.2. Thermal aging test

The procedure was carried out according to IEC 216

2.3. Irradiation

Samples were irradiated by ^{60}Co γ-ray with a dose rate of 10 KGy/h at room temperature in air atmosphere.

2.4. Hydrolysis

Films were immersed in boiling water. Deionized water was used.

2.5. Viscosity stability

Polymer solid of polyamic-acid varnishes was 20 wt%. Varnishes were stored at 50°C, and occasionally withdrawn and their viscosities were measured.

2.5. Analysis

(1) Thermogravimetric analysis (TGA). Thermograms were obtained in air atmosphere with a Shimadzu TGA-1 Thermogravimetric Analyzer at a heating rate of 10°C/min. Films of 25 μm thick were used.

(2) Thermal mechanical analysis (TMA). TMA spectra were measured with a Rigaku CN8098A1 Thermomechanical Analyzer. Glass transition temperatures were measured using a penetration prove on 25 μm thick films at a heating rate of 10°C/min under a load of 10 g. The linear expansion coefficients were measured using attachment for tensile mode on film of 5 mm width, 10 mm length (between chucks) at a heating rate of 10°C/min under a load of 2 g.

(3) Tensile property. Tensile properties were obtained with a Shimadzu Autograph IM-100 according to the ASTM method D882-67.

(4) Enamelled wire. The evaluation of enamelled wires were carried out according to JIS C3003. Impressed tests were conducted on twist-pair wires.

(5) Viscosity. Viscosities of varnishes were measured with a Tokyokeiki Visconic EHD Viscometer at 30°C

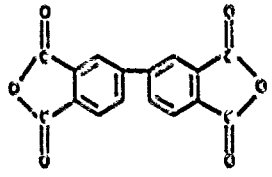

BPDA

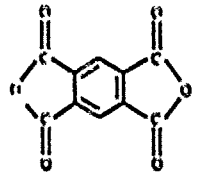

PMDA

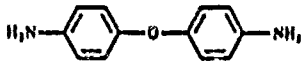

ODA

PPD

3.RESULTS AND DISCUSSION

3.1. Tensile property

The chemical composition and tensile properties of polyimides investigated in this paper are summarized in Table 1. Polyimides from ODA have a high elongation of over 70% and a rather low strength of below 25 Kg/mm² independent of their acid anhydrides. On the other hand, polyimides mainly from PPD have a rather low elongation of below 40% and a high strength of over 38 Kg/mm². ODA has a flexible ether linkage at which bending and rotation of the molecular chain is possible, but PPD has a rigid structure. Polyimides made from ODA are more flexible and have a higher elongation than that mainly made from PPD, but the former films have a lower strength and modulus of elasticity.

3.2. Thermal property

The thermal property may be used in two ways: physical and chemical properties. The former is such as glass-transition temperature (Tg) and expansion coefficient, and the latter is such as thermal decomposition and degradation. Thermal properties of polyimide are shown in Tables 2 and 3. It is said that Tg is connected with the rigidity of polymer, and then generally increases with increasing rigidity of polymer. In addition, it is also said that Tg is affected by molecular aggregation.[7]

The order of rigidity of acid anhydride and diamine is thought to be PMDA > BPDA and PPD > ODA. Therefore, with respect to homopolymer, Tg of polyimide from PMDA and PPD must be the highest, but this polyimide is very brittle and is not practical. Next, Tg of polyimide from PMDA and ODA or BPDA and PPD must be higher. In practice, both Tg's of polyimides II and III are higher, and Tg of polyimide II is higher than that of polyimide III. As we would expect, Tg of polyimide I from BPDA and ODA is the lowest. With respect to copolymer, the order of Tg approximately follows the order of the total amount of rigid component, i.e. PMDA and PPD.

Recently, the thermal expansion coefficient of polyimide has become of interest. At the time of forming a polymer material and a metal, glass or ceramics into one body, the thermal stress is produced by the difference between the thermal expansion coefficients. This results in problems of warping, peeling, and cracking. Thermal expansion is also said to be related to the linearity of polymer molecular skeletons.[8,9] BPDA, PMDA,

Table 1.The chemical structure and tensile properties of polyimide

Polyimide	Component		Tensile property		
	Acid dianhydride	Diamine	Modulus of elasticity (kg/mm²)	Strength (kg/mm²)	Elongation (%)
I	BPDA	ODA	380	25	130
II	BPDA	PPD	900	40	35
III	PMDA	ODA	300	18	70
IV	BPDA/PMDA(7/3)	ODA	320	21	77
V	BPDA/PMDA(5/5)	ODA	310	22	85
VI	BPDA/PMDA(7/3)	PPD	790	38	32
VII	BPDA	ODA/PPD(7/3)	410	25	68
VIII	BPDA/PMDA(5/5)	ODA/PPD(3/7)	650	40	40

Table 2.Thermal property of polyimide

Polyimide	Tg (°C)	T_{TG} (°C)	TGI (°C)	Linear expansion coefficient (x10⁻⁶cm/cm/°C)
I	285	577	612	4.0
II	>400	578	621	1.4
III	385	566	607	4.2
IV	253	571	607	4.7
V	330	567	609	4.5
VI	370	572	613	1.4
VII	290	576	616	3.2
VIII	360	570	611	1.9

Table 3. Long-term heat resistance of polyimide

Polyimide	Half reduction temperature(°C)	
	Tensile strength	elongation
I	270	235
II	290	265
III	265	225

and PPD do not have any flexible linkage, such as ether, and polyimides II, VI, and VIII have a low thermal expansion coefficient. However, polyimides from ODA having a flexible linkage have a higher thermal expansion coefficient.

Several attempts have been made to develop more rapid methods of estimation of the decomposition temperature and thermal life based on TGA[12-14] The temperature determined from these methods would serve as an accurate prediction of the results of long-term thermal life tests. T_{TG} is the temperature at which 5% of the total weight loss occurs. TGI is calculated by the formula: TGI = (A+B)/2, where A = the temperature at which a straight line, drawn through the 50 and 20 % weight loss points, intercepts the 0% weight loss line; B = the temperature at which the curve intercepts the 50% weight loss line.

The order of the thermal stability (decomposition temperature) with respect to aromatic skeleton of acid dianhydride and diamine component is benzene (593°C) > biphenyl (543°C) > diphenyl ether (538°C)[15] As diamines of polyimides I and III are the same, the difference in T_{TG} and TGI results from the difference in the structure of the acid dianhydride component. The order of the thermal stability of polyimide with respect to the structure of the acid dianhydride component is BPDA > PMDA. The order of the thermal stability of BPDA and PMDA is the reverse order of the thermal stability of benzene and biphenyl. This is due to the fact that PMDA is more reactive than BPDA, and with regard to this we shall discuss a little subsequently. The results of T_{TG} and TGI of polyimides I and II are in accord with the expectations based on the aromatic skeleton of diamine. we consider that polyimide from BPDA and PPD is the most stable. The order of the thermal stability of copolymer could be understood through considering the polymer component.

The long-term heat resistance of polyimides I, II, and III was carried out (Table 3). The half reduction temperatures in tensile properties at 20000 h are obtained from extrapolation by Arrhenius plots for over 3000 h. The order of the half reduction temperature is polyimide II > I > III and is in the same manner as the results of TGA. Kawamura et al[2] performed a similar test of polyimides I and III on the dielectric breakdown voltage and tensile strength, and reported that the half reduction temperature of polyimide I is 20°C higher than III.

3.3. Hydrolysis

Resistance to boiling water of polyimides I, II, and III is shown in Fig.1. From this result it is found that the BPDA based polyimides I and II are more stable than PMDA based polyimide III. Korshak et al[17] studied the hydrolytic stability of polyimides, and reported the same result that polyimide from PMDA had the lowest resistance to hydrolysis, and that the one from BPDA had the highest. The difference in the hydrolysis

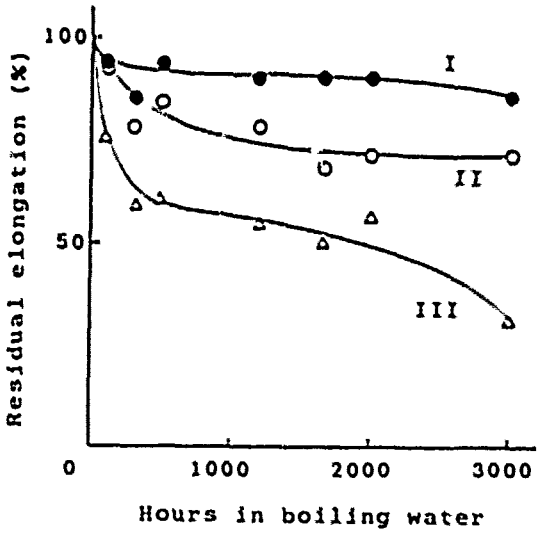

Fig.1. Residual elongation after immersion in boiling water.

Table 4. Acidity constants[11]

Acid	pKa
benzoic	4.17
phthalic	3.00
trimellitic	2.52
pyromellitic	1.92

resistance of these polyimides is due to the difference of the acid anhydride component of the polymer chain; thus, that of polyimides I and II is biphenyl skeleton (BPDA), while that of polyimide III is benzene skeleton (PMDA). The carbonyl groups in PMDA are on the same nucleus, and both carbonyl groups are conjugated to each other. On the other hand, the carbonyl groups in BPDA are attached to different nuclei, separated from one another, and both benzene rings of biphenyl are not coplanar to each other, so they are not conjugated to each other. Namely, BPDA could be thought to consist of two phthalic anhydrides. Acidity of benzoic acid to pyromellitic acid is shown in Table 4. Here, pKa shows the first ionization constant. The pKa value decreases as the number of carboxylic substituents increases. The carboxylic group has a strong electron-withdrawing inductive effect, so pKa becomes lower with the increasing of the number of carboxylic groups. In the case of alkaline hydrolysis of ester, it is very sensitive to induction effects of polar substituents, and esters substituted by polar groups are easily hydrolyzed. The reactivities of imide and ester in hydrolysis are not exactly the same, but PMDA based polyimide substituted by two polar imide groups could be naturally thought to be more easily hydrolyzed than the phthalimide type substituted by one polar imide group such as BPDA. The partial positive character on the carbon of the imide group of PMDA is stronger than that of BPDA, so the imide group of PMDA is more easily subject to nucleophilic attack, and the imide group is converted to amic-acid and leads to a rupture of the main chain. Koton et al[19] studied the kinetics of acylation of diamines by dianhydrides in detail and reported that the reactivity of diamines and dianhydrides were explained by using the parameters of the electronic structure of them caluculated by the methods of quantum chemistry and the rate constant for the acylation by PMDA is much faster than the one for the acylation by BPDA. The reactivity in both hydrolysis and the acylation is explicable to be largely dependent on the electronic structure of the components. The difference in the

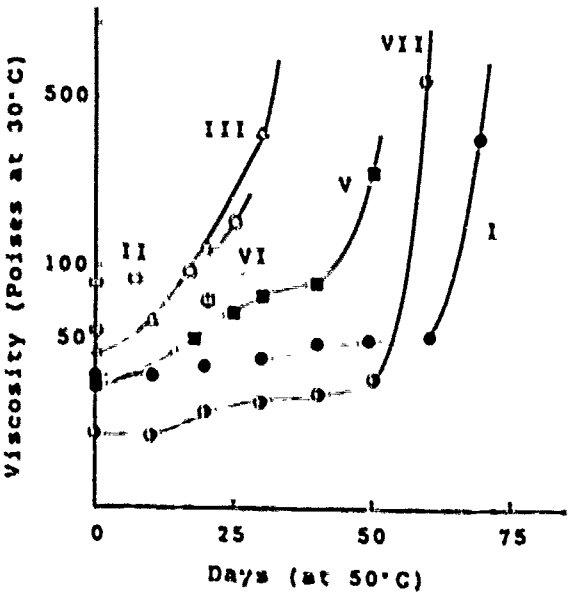

Fig.2. Viscosity stability of polyamic-acid varnishes.

thermal stability of the BPDA based polyimides and PMDA based polyimide is naturally due to the difference of the acid dianhydride component of the polymer chain. Thermal decomposition is a more complicated reaction, so we must consider not only the factor considered in the case of hydrolysis, but other factors. However, the order of the thermal stability could be predicted only by the reactivity of the imide group.

3.4. Viscosity stability of polyamic-acid varnish

Viscosity stabilities of polyamic-acid varnishes are shown in Fig. 2. The viscosity of varnishes increased and followed by gelation upon storage at 50°C. The reason for this increase in viscosity is thought to be as follows. The conversion of amic-acid to imide partially takes place upon storage, and this imidation lowers the solubility of polymer. We observed the presence of imide bond in polyamic-acid varnishes upon storage by IR and NMR. Imide ring formation is facilitated by the presence of conjugated bonds in the chain[9,19]. PMDA and PPD have conjugated functional groups; thus, the imidation rate of polyamic-acid from PMDA or PPD is faster than that from BPDA or ODA. On the other hand, the solubility of polyimide from BPDA or ODA is better than that from PMDA or PPD. Polyimide from BPDA and ODA is soluble in chlorophenol. From these view points it could be understood that polyamic-acid I is the most stable and polyamic-acid III is the least stable followed by II and VI.

Table 5. Properties of polyimide enamelled wires

Item	Polyimide I	III	IV	V	VI	VII
Film thickness(micron)	40	38	38	40	41	39
Mandrel test	1d pass	1d pass	1d pass	1d pass	1d pass	1d pas
Elongation and mandrel(%)	100	>100	>100	>100	88	>100
Dielectric breakdown(KV)	11.5	14.0	12.3	13.5	13.5	13.8
Abrasion test						
Repeated scrape(strokes)	41	25	66	58	7	83
Unidirection abrasion test(g)	1765	1480	1670	1860	1670	1780
Cut through temperature(°C)	>400	>400	387	398	>400	380
Elongation and mandrel test(%)						
after heat aging 200°Cx24h	60	73	>95	>88	60	>95
Mandrel test after						
heat aging 200°Cx6500h		1d pass	1d pass	1d pass	2d pass	
240°Cx580h		1d pass	1d pass	1d pass	3d pass	
Heat shock 250°Cx24h	1d pass	1d pass	1d pass	1d pass	1d pass	1d pas
Impressed test(AC200V) in						
0.4%NaCl aqueous solution						
at 30°C	120h	>1000h	>1000h	>1000h		470h
at 60°C		460h	1680h	1520h		

thermal stability. As to the impressed test in 0.4% NaCl aqueous solution, polyimides IV and V are the best, III is medium and I and VII are the worst. Enamelled wires of polyimides I and VII have a little turbidity, but films of the same component as I and VII are clear. Films were prepared at a slow heating rate of 10-30°C/min, but enamelled wires were prepared at a heating rate of 100-200 °C/min. The rapid heating was thought to result in turbidity. This turbidity, i.e. ununiformity is responsible for a short life under the impressed test. If the polyimide consists of the combination BPDA and PMDA, this turbidity disappears. The difference in the life under the impressed test of polyimides IV, V, and III is explained by the difference of the fraction of PMDA which is more reactive to water.

The changes of elongation and mandrel of enamelled wires of polyimides III, IV, and VI by irradiation are shown in Fig. 5. In the low dose region three enamelled wires reveal no apparent differences, but in the high dose region polyimides IV and VI are more stable than III. As to the enamelled wire of polyimide III irradiated over 20 MGy, poor adhesion between copper wire and the coated layer took place, while with the enamelled wires of IV and VI they showed good adhesion even at 60 MGy. Enamelled wires of polyimides III and IV after irradiation are shown in Figs. 6 and 7. It is not possible to estimate the accurate elongation and mandrel when poor adhesion occurs, since elongation and mandrel of III over 20 MGy is not accurate. Accordingly, it could be thought that the

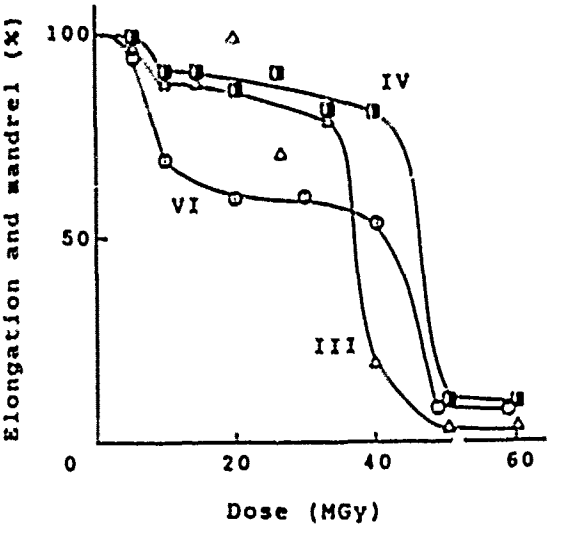

Fig.5. The change of elongation and mandrel of polyimide enamelled wire by irradiation.

enamelled wires of IV and VI are more stable than that of III even in the low dose region. These results are the same as those of films.

We prepared filled enamelled wires to expect the electrical and heat conducting properties to improve. The properties of filled enamelled wires are shown in Table 6. In this case, polyimide V component was chosen for varnish of enamelled wire. If the outside of enamelled wire is a filled

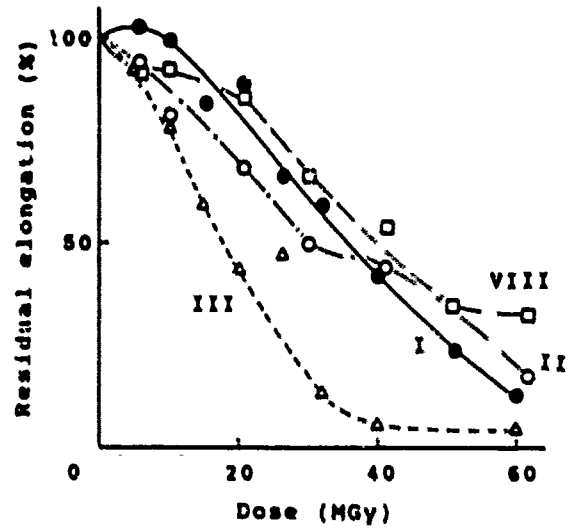

Fig.3. The change of residual elongation of polyimide by irradiation.

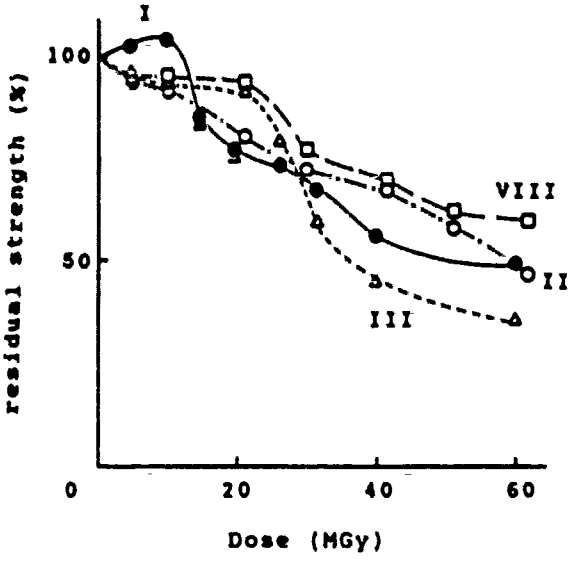

Fig.4. The change of residual strength of polyimide by irradiation.

3.5. Irradiation

It is well-known that polyimide has not only the highest heat resistance, but also the highest radiation resistance. We examined the radiation resistance of polyimides I, II, III, and VII. The changes of the retention ratio of the tensile properties are shown in Figs. 3 and 4. As to the tensile property, the decrease in elongation is pronounced even in a low dose region in film III compared with films I, II, and VIII. Namely, the dose of a 50% reduction of the initial value in film III is about 20 MGy, while those in the films from BPDA are 35-45 MGy. As the tensile strength is not very much more sensitive to degradation than elongation, the difference in decrease in strength between III and BPDA based polyimides is not pronounced. BPDA based polyimides possess higher radiation resistance as well as higher thermal stability than III. Sasuga[6,8,9] and Morita[3,10] studied radiation resistance of polyimides in detail, and reported the results to be similar to our studies. In spite of the radiation-induced changes described above, no remarkable change is observed in Tg and modulus of elasticity after 31.7 MGy irradiation to I and III. This reveals that chain scission mainly occurs by radiation, but a crosslinking reaction which influences modulus and Tg rarely occurs. This is also borne out by the fact that all irradiated polyimides were easily dissolved in a hydrazine based etchant. This chain scission could be thought to comprise to some extent of the conversion of imide to amic-acid which leads to a rupture of the chain, because the tensile properties of polyimides I, II, and III after 60 MGy irradiation were restored to a slight degree by heat treatment at 400°C, for example the restoration of elongation was from 6% to 11% for polyimide II and from 4% to 12% for polyimide III. This restoration could be thought to be owing to the imide formation of the cleavage part. We measured ATR spectra (FT-IR) of polyimides I and III after 40 MGy irradiation, but no remarkable change was observed. It is noteworthy that polyimide VIII from both BPDA and PMDA (the ratio is 5/5) has the same resistance as polyimides I and II from only BPDA. The stability of polyimide incorporated with BPDA is greater than that predicted by the simple additivity of component contribution. The difference in radiation resistances of BPDA based polyimides and PMDA based polyimide is naturally due to the difference of the acid dianhydride component. Degradation by irradiation is a more complicated reaction as well as thermal decomposition, but it is almost certain that the radiation resistance is largely dependent on the reactivity of the imide groups of BPDA and PMDA.

3.6. Enamelled wire

The properties of enamelled wires are shown in Table 4. Enamelled wires of polyimides II and VIII were not produced. There are not large differences in general properties among polyimides except for polyimide VI. Polyimide VI lacks flexibility to a degree. Polyimide III has lower strokes in a repeated scrape. A heat aging test (200°C x 6500 h) of polyimides was carried out. After a heat aging test their mandrel properties almost were unchanged, and these polyimides have good

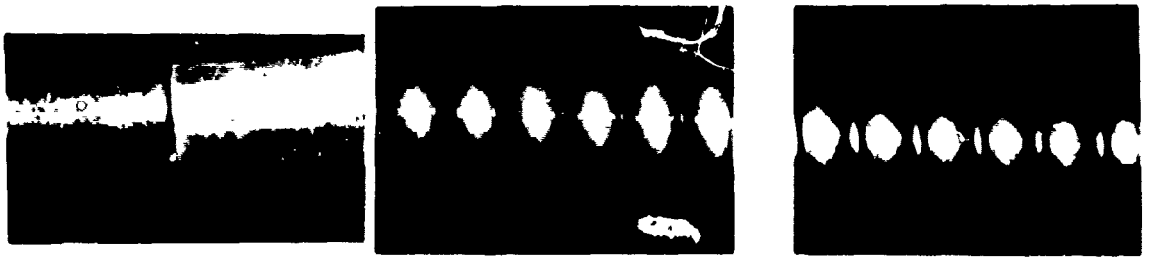

Elongation(39%) Elongation(39%)+1d Elongation(39%)+1d

Polyimide III Polyimide IV

Fig.6. Enamelled wires after 20 MGy irradiation.

Elongation(5%) Elongation(5%)+1d Elongation(10%) Elongation(10%)+1d

Polyimide III Polyimide IV

Fig.7. Enamelled wires after 52.5 MGy irradiation.

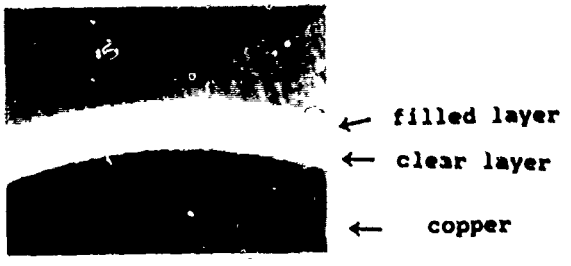

Fig.8. Vertical sectional view of BN filled enamelled wire.

layer, the outer unevenness may influence the properties of enamelled wire. Therefore, filled enamelled wires should consist of two layers; i.e. an inner filled layer and an outer clear layer (the thickness ratio of inner/outer is 7/3). Fig. 8 is a vertical sectional view of BN filled enamelled wire. The general properties of these filled enamelled wires are not much different from those of clear enamelled wire except repeated scrape. Filled enamelled wires have a longer life under the impressed test at 3 KV than clear enamelled wire. These filled enamelled wires are thought to have good heat conductivity. For example, the heat conductivity of film containing 30wt% BN is about three times that of clear film. These BN filled enamelled wires have very good properties. We prepared other filled enamelled wires, such as mica, Al_2O_3, and Si_3N_4, but their properties were not so good.

4. CONCLUSION

The thermal property, hydrolysis, and radiation resistivity of polyimides with different structures obtained from two acid dianhydrides and two diamines were studied. The results obtained in this study are summarized below.

(1) Tg is connected with the rigidity of the monomer component, since polyimides

Table 6. Properties of enamelled wires of polyimide V containing BN

Item	Enamelled wire A	B	C
Varnish(V component)			
Filler	—	BN	BN
Filler particle size(μ)		1-6	1-6
Filler content against polyamic acid(wt%)	—	10	30
Filler content in polyimide of enamelled wire(wt%)	—	10.2	29.0
Film thickness(μ) (thickness ratio of outer clear layer and inner filled layer=3/7)	40	41	43
Mandrel test	1d pass	1d pass	1d pass
Elongation and mandrel(%)	>100	>100	>100
Dielectric breakdown(KV)	13.5	12.0	12.1
Abrasion test			
Repeated scrape(strokes)	58	18	15
Unidirection abrasion test(g)	1860	1680	1650
Cut through temperature(°C)	398	>400	>400
Elongation and mandrel test(%) after heat aging 200°Cx24h	>88	>88	>88
Heat shock 200°Cx1h	1d pass	1d pass	1d pass
Impressed test in air			
at 3KV(AC)	22h	35h	52h
at 1KV(AC)	245h		310h

from monomer components rich in PMDA and PPD components have higher Tg.

(2) Thermal and viscosity stability,and hydrolysis and radiation resistivity are mainly connected with the chemical reactivity of the acid dianhydride component; i.e. PMDA is more reactive than BPDA, hence polyimides from BPDA are more stable.

(3) Enamelled wires of polyimide using BPDA as one component, have good radiation resistance, and a long life under the impressed test in a NaCl aqueous solution.

(4) Enamelled wire of polyimide containing BN has a longer life under the impresed test.

The results of our study provide evidence that not only homopolymers from BPDA, but copolymers incorporated with BPDA are superior in thermal, chemical, and radiation resistance.

5.Acknowledgment

The authors wish to thank Mr. Yukio Hiraoka of Mitsubishi Cable Industries, LTD., for the enamelled wire preparation and measurements and Dr. Toyoaki Kimura of Nagoya University for irradiation of the samples. We also wish to thank Mr. Yoshikazu Sasaki, general manager of Corporate Reseach & Development of UBE Industries, Ltd., for his continuing valuable advice and helpful discussions, and Mr. Tadashi Muramatsu, a co-worker, for preparation of polyimide and measurements.

6.REFERENNCES

(1)N.A.Adrova, M.I.Bessonov, L.A.Laius and A.P.Rudakov, Polyimides, A New Class of Thermally Stable Polyimides, Prog. Sci., VII, Tecomic, 1970.

(2)Y.Kawamura and M.Minami, Denki gakkai Zenkoku Taikai Koen Ronbunshu, 1983, 372.

(3)Y.Morita, T.Seguchi, K.Yoshida, Y. Yamamoto and H.Yagyu, Denki Gakkai Zetuen Zairyo Kenkyuukai Shiryo, 1984, EIM-84-129.

(4)H.Inoue, H.Okamoto and Y.Hiraoka, Radiat. Phy. Chem., 1987, 29, 283.

(5)A.M.Sheila and R.L.Edward, IEEE trans. Nuclear Sci. 1984, 31, 1293.

(6)T.Sasuga, M.Hayakawa, K.Yoshida and M. Haggiwara, Polymer 1984, 26, 1039.

(7)M.Kochi, T.Horigome and I.Mita, "Proceedings of second International Conference on Polyimides", 1985, 454.

(8)T.Sasuga and M.Hagiwara, Kobunshi Ronbunshu 1985, 42, 283.
(9)T.Sasuga, Polymer 1988, 29, 1562.
(10)Y.Morita, K.Watanabe and H.Yagyu, Denki Gakkai Zetuen Zairyo Kenkyuukai Shiryo,1988, EIM-88-129, 109.
(11)Encyclopedia of Polymer Science and Technology,Interscience Publisher (a division John Wiley and Sons, Inc.) 1964, 1, 139.
(12)T.Sunoi a and T.Kaneko, Netsu Sokutei, 1983, 66; Denki Gakkai Gijutsu Hokoku 1982, 11, No. 134.
(13)G.P.Brown, et al., Proc. Elect. Insulation Conf. 1971, 10, 132.
(14)NEMA Standard Publication, 1974, No. RE-1.
(15)P.M.DiCerbo, Insulation/Circuits, 1975, Feb., 21.
(16)J.H.Freeman, L.W.Frost. G.M.Mower and E.J.Traynor, Spe Transations, 1965, April, 75.
(17)V.V.Korshak, S.V.Vinogradova, Ya.S. Vygodskii, Z.V.Graschenko and N.I. Lushkina, Polym. Sci. USSR, 1972, A14, 2153.
(18)S.Numata and N.Kinjo, Polym. Eng. Sci., 28, 906, 1988.
(19)M.M.Koton, V.V.Kudriavtsev and V.M. Svetlichy, "Investigation of the of aromatic diamines and dianhydrides of tetracarboxylic acids in the synthesis of polyamic acids", in POLYIMIDE Synthesis, Characterization, and Applications, K.L.Mittal, Ed., Plenum Press, New York, pp171-187 (1984).

Hiroshi Inoue

UBE Industries, Ltd.,Hirakata Laboratory
3-10,Nakamiya kitamachi,Hirakata Osaka,Japan

Mr.Inoue received the B.S.degree (1969) and the M.S.degree (1971) in Organic Chemistry from Nagoya University. He joined UBE industries Ltd., and his work has been research and development of polyamide and polyimide. His Current research is concerned with thermosetting polyimide.

Toshihiro Inaike

UBE Industries, Ltd.,Hirakata Laboratory
3-10,Nakamiya kitamachi,Hirakata Osaka,Japan

Mr.Inaike recieved the B.S. degree (1964) and the M.S.degree (1966) in Chemistry from Osaka Prefecture University. He joined UBE Industries, Ltd., and his work has been research and development of epoxy resin, phenol resin, and polyimide. He is a member of the society of polymer science, Japan.

POLYBUTHYLENE TEREPHTHALATE (PBT) WITH IMPROVED HYDROLYSIS RESISTANCE AND LOW POST SHRINKAGE FOR LOOSE BUFFER TUBES

Jürgen Eickholt, Dr. Ralf Schüler

HÜLS AKTIENGESELLSCHAFT, 4370 Marl, West Germany

Abstract

Polybutylene terephthalate (PBT) has become the material of choice in the majority of fiber optic loose tube cable designs. This is due to the good mechanical properties and chemical resistance coupled with the good processability of this material. The thermal hydrolysis resistance, as well as the post extrusion shrinkage can be improved by modifying the material. This paper describes the unique characteristics and capabilities of these new VESTODUR resins.

1. Introduction

Loose buffer tube fiber optic cable construction has been employed now for many years and the resulting cables have performed successfully under a wide variety of conditions. Loose buffer tubes provide maximum protection for the fiber against compression and tension, provided the selected buffer materials are of a satisfactory quality. Polyamide 12 and polybutylene terephthalate (PBT) are widely used for loose buffer tubes. Although both polymers tend to post crystallize and PBT is sensitive to hydrolysis at higher temperatures, these polymers have represented the best cost-performance ratio for buffer tubes until today. Since more and more cables are being installed in environments of high temperature and high humidity, the development of materials with improved hydrolysis resistance and low post shrinkage became necessary.

2. Loose buffer tube materials

Buffer materials for loose tubes have to meet the following reqirements:

- easy processing with high melt strength
- low coefficient of thermal expansion
- low post crystallization
- high flexural modulus with good kink resistance
- low moisture absorption
- good hydrolysis and chemical resistance

In order to give a broad picture of the different properties, several PBT grades have been included in this paper for comparison. One thermoplastic polyester elastomer, used in the market, has been included as well.

3. Hydrolysis resistance

All thermoplastic polyesters and polyester elastomers lack a good thermal hydrolysis resistance. Commonly available materials have a lifetime of approximately 1 000 hours at 80 °C in water. The elongation at break and the change in viscosity number are two suitable creteria to determine degredation of polyesters due to moisture exposure.

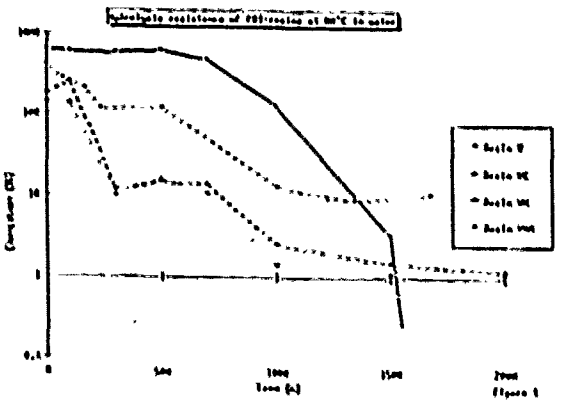

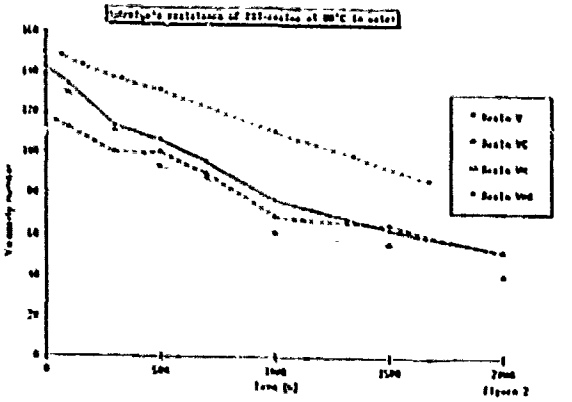

As shown in Figure 1, resin VHR is superior to the other resins in water at 80 °C. We consider a residual elongation of 5 % as the minimum elongation to keep a fiber optic cable in function. From figure 2 follows that an elongation of 5 % relates to a viscosity number of approx. 70 cm³/g. Below this viscosity number, most thermoplastic polyesters start to embrittle.

4. Post extrusion shrinkage

Most of the loose buffer tube materials are semicrystalline in nature with the tendency to post crystallize. It is known, that equilibrium crystallinity is not achived by normal quenching. Further crystallixation can therefore occur as a function of temperature and time. This post crystallization is prevalent above the glass transition temperature, a temperature above which many cables are cycled during testing or exposed to in some applications. Thy crystallinity of PBT loose buffer tubes can be influenced by the cooling rate of the melt.

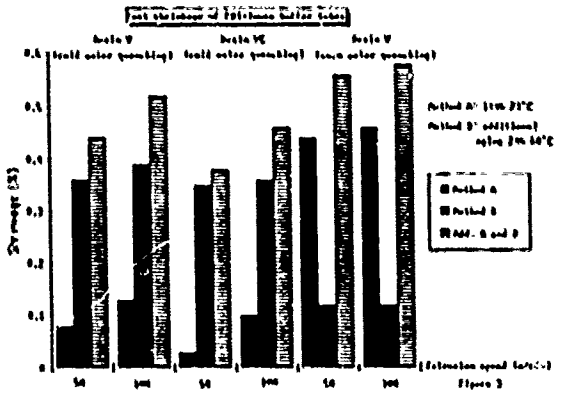

* As shown in figure 3, cold water quenching yields in a low crystalline material, resulting in a low post extrusion shrinkage of approximately 0,1 %. Heat aging this tube above the glass transition temperature (24 hours at 60 °C) will result in further crystallization causing an additional shrinkage of 0,35 %.

* Quenching the tube in warm water (70 °C) will result in a higher crystalline material, with a post extrusion shrinkage of 0,45 % and an additional shrinkage of 0,15 % after heat aging.

All data were determined on 2,5 x 1,7 mm tubes, extruded at a speed of 50 respectively 100 m/min and stored for one week at 23 °C with 50 % relative humidity (standard climate). Loose buffer tubes spooled onto a reel would not show this high levels because of a hindered shrinkage. Nevertheless many processors wind and store the tubes on plates, where a free shrinkage can occur. In a strain free position, the contraction must therefore remain smaller than 0,1 % to prevent the fiber form being pressed against the inner wall of the tube or attenuation increases will occur.

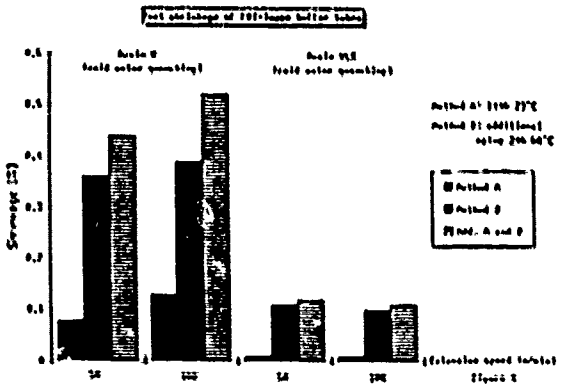

Figure 4 shows the post shrinkage of the newly developed resin VLS compared to that of a commonly available PBT quenched in cold water. Even after 2 month storage at standard climate resin VLS reveals no post extrusion shrinkage. This behavior does not change substantially when the tube is aged for 24 hours at 60 °C. The total shrinkage of tubes prepared from this resin was only 0,1 %.

5. General properties

The next table (figure 5) shows the typical property values of the new resin in comparison to conventionally available PBT's. It is worth noting, that resin VLS exhibits a much lower coefficient of thermal expansion above 50 °C as compared to resin V, as shown in figure 6.

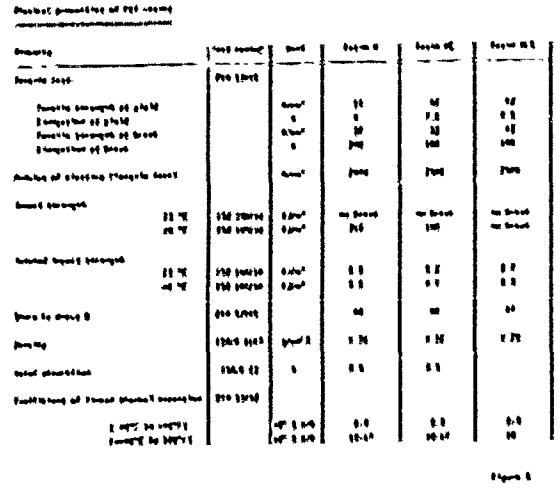

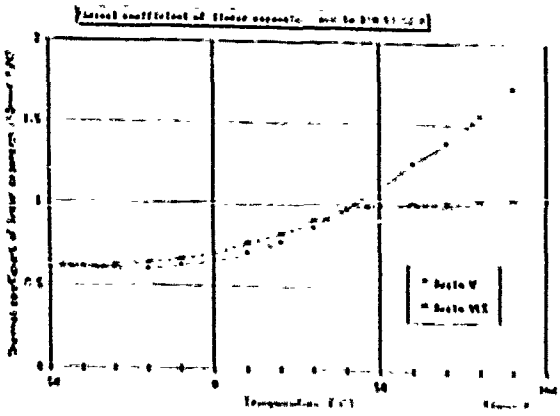

Conclusions

1. A new modified polybutylene terephthalate resin has been developed to fulfil the requirements for optical fiber loose jacketing in environments with high temperature and humidity.

2. By modifying polybutylene terephthalate in a suitable manner, the post extrusion shrinkage can be minimized to meet all requirements of fiber optic loose tube cable designs.

Jürgen Eickholt is a member of the technical service and marketing staff for engineering plastics at Hüls AG, Marl, West Germany. His current responsibilities include the world wide technical service and marketing of materials for fiber optic jacketing and technical support to the research and development group within Hüls AG.

Ralf Schüler is member of the research and development staff at Hüls AG, Marl, West Germany. He is the Technical Supervisor of the VESTODUR(R) group and responsible for the development of PBT- and Copolyester resins. He holds a. Ph. D. in chemistry from the university of Münster.

FACTORS THAT INFLUENCE PIC DEGRADATION OF FILLED FOAMSKIN TELEPHONE CABLE

Linwood P. Baltz

JM

ABSTRACT:

This paper will show some of the consequences of aging PIC foamskin insulation under various conditions. One of the most deleterious conditions will be shown to be insulation that has not been cleaned of filling compound, and is then exposed to air at elevated aging temperatures. The data indicates that cleaning the conductors before aging gives superior aging characteristics. Yet it is a commonly held belief in the industry that not cleaning the conductors is more beneficial. This paper gives ample evidence that this view is false, at least in the case of foamskin covered conductors.

INTRODUCTION:

The investigation of plastic insulated conductors (PIC) and the mechanisms of its degradation has been going on in some form or other for over 20 years.[1] During this time the industry has moved from low density to high density polyethylene insulation, has briefly used polypropylene, and has most recently invested heavily in foam and foamskin insulations.[2,3,4] With each passing year experimentation yields new facts about the plastic insulation and the factors that affect its longevity. The general consensus in the telephone industry is that PIC degradation is primarily caused by the loss of antioxidants from the polyethylene insulation that is extruded onto the copper conductors.[6] Filled cables are particularly susceptible to this loss of antioxidant, evidently because of solubility considerations between the filler and the antioxidant, and recently there has been more and more data indicating that foamed insulations are more likely to show early degradation than solid insulations.

Much effort has been expended to determine how fast various antioxidants and combinations of antioxidants lose their effectiveness when exposed to the pedestal environment.[7] Research has shown that dry heat aging either in a pedestal or in a laboratory air-circulating oven will eventually lead to cracking of PIC insulation.[5] These cracking tests have been supplemented with the so-called OIT, or oxygen induction time, which measures how much antioxidant is left in a sample of insulation. While OIT measurements can be very accurate, they are generally acknowledged to be only indicators of susceptibility of conductors to cracking, not accurate predictors of when cracking will occur. Nevertheless, The OIT measurement is a valuable tool to determine what kinds of changes are occurring in a particular insulation sample under a given set of conditions.[8]

Several other factors besides the loss of antioxidant are also suspected to be important.[10] Certainly excessive handling and re-working of PIC is a problem in pedestals that are re-entered often. Likewise, the specific chemical environment in any given location may have a bearing on the amount of degradation that occurs. Fertilizers, insecticides, decomposition products, etc. will all have an effect. Many of these factors are difficult to control unless the PIC insulation is given extra protection from its surroundings.

The purpose of this research is to discover still more details about some of the factors that affect PIC, especially foamed insulations in filled cable. One of the surprising results of the current study is the clear relationship that has emerged between the cleaning of filled cable and the subsequent life expectancy of foamed insulation. This paper will show that, contrary to what has often been assumed, when some filled cables are exposed to a warm oxidizing environment,

such as a telephone pedestal, cleaning can make a major difference to the expected lifetime of the insulation. Data will be shown to support the contention that, while cleaning may cause an initial lowering of certain electrical insulation test values due to removal of the surface layer of filling compound, in fact not cleaning the conductors will in the long run lead to faster cracking due (presumably) to the absorption of antioxidants into the filling compound. This effect occurs even with the ETPR (extended thermoplastic rubber) type of filling compounds.[12]

In addition, we will investigate the effect of water on the loss of antioxidants from PIC insulations. Although there have been speculations about the effects of water in pedestals, especially water due to atmospheric condensation,[9] there is very little real data to quantify what those effects might be. Based on our research water does have a definite deleterious effect on foamed PIC insulations.

EXPERIMENTAL DESCRIPTION:
The major part of this work involved the aging of twisted wire pairs in hot air circulating ovens at several temperatures. All pairs were looped around a half inch rod and twisted to give a uniform mechanical stress to the insulation. All color wires were used except black because there was some initial thought that black conductor insulation might be inherently more stable than the other colors. In general, six conductors or three pairs were tested for any one condition and length of time. This means that test samples were not removed from the test environment, tested, and then replaced into the test environment. Once samples were removed for testing they were out of the test and aging sequence. This allowed us to run destructive tests such as the dielectric breakdown value.

All samples unless otherwise noted were made from 16 inch lengths of 24-gauge foamskin insulated conductors taken from a Western Electric cable filled with Flexgel (I) that had been manufactured in late 1986 or early 1987. This particular cable was found to have OIT values between 20 and 30 minutes. In other words its OIT was on the edge of the current acceptability requirement for filled telephone cables.[13] This gave us a good model system that in effect was "pre-aged" and would give results within a reasonable time frame and at reasonably low aging temperatures. (Although it should be made clear that for the aging tests described below this cable was not actually pre-aged in the sense of heating for a specific time and temperature before oven testing was begun). It was recognized that the conclusions from this particular cable would have to be shown to be applicable to the more heavily stabilized systems that the cable industry was moving towards. This subject will be expanded upon in the latter portions of this paper.

Samples were aged that were cleaned and that were not cleaned. The cleaning agents used were 3M's 4413 Cable Cleaning Kit, a blend of solvents designed to dissolve grease and filling compounds, yet be gentle to the antioxidant system, and lamp oil, a common solvent used by some craftsmen. In addition, various sprays that were formulated to enhance the life of PIC insulation were tested on both cleaned and uncleaned conductors. The three types of sprays, a urethane, a drying oil coating, and a silicone, are described in more detail in a later section.

Several tests were run on the samples when they were removed from testing. The first to be discussed will be the visual observations. All the conductors were examined with a 7x handheld magnifier to determine if cracking had occurred. Based on numerous observations, visual cracking was divided into four numerical severity categories; samples were assigned a one if there was no visual evidence of cracks using a 7x magnifier; two if there were one or two cracks per pair with little or no copper showing through; three was moderate cracking, if there were more than two cracks and if the copper conductor was obviously exposed; and four was severe cracking, if the sample showed general cracking (usually a crack at each twist of the twisted pair) and exposed copper at every break in the insulation. In addition to the visual observations, insulation resistance tests were run on each wire and the dielectric breakdown was measured between each pair of conductors. Insulation resistance is measured in ohms and was run in salt water at 250 volts applied potential. Dielectric breakdown strength was run in air at a rise rate of 500 volts per second and is measured in kilovolts. In almost every instance dielectric failure occurred between the two conductors in the twisted area of the samples. Table one lists the data

collected for control samples that were aged for three to twenty-three weeks at 180°F. These samples were not cleaned. Unless otherwise noted, "not cleaned" means that the bulk of the filling compound was removed from the conductor insulation with a clean dry rag, similar to what commonly would be done in a field situation. The amount of filling compound left on these samples was estimated to be typical for filled cable installations that commonly can be found in service.

TABLE 1
TEST RESULTS FOR FILLED PIC CABLE CONDUCTORS AGED AT 180F

DRY SAMPLES, NOT CLEANED

	Cracking (1-none, 4-severe		Insul. Resist. (ohms)	Dielect. Brkdown. (kvolts)
		3 WEEKS		
	1	1	1.5E+11	12.1
	2	1	1.5E+11	
	3	1	1.5E+11	9.1
	4	1	1.5E+11	
	5	1	1.5E+11	10.8
	6	1	2E+11	
AVE		1	1.6E+11	10.7
		12 WEEKS		
	1	1	1E+12	8.7
	2	1	1E+12	
	3	1	1E+12	6.2
	4	1	1E+12	
	5	1	1E+12	8.9
	6	1	1E+12	
AVE		1	2.5E+12	7.9
		23 WEEKS		
	1	4	0	2.1
	2	4	0	
	3	4	0	1.1
	4	4	0	
	5	4	0	1.1
	6	4	0	
AVE		4	0	1.4

Table two lists the data from similar samples, aged exactly the same as the uncleaned samples in table 1, except that these samples were cleaned with 3M's 4413 cleaning solvent. Note the great differences between these two sets of data after 23 weeks aging. Through 12 weeks there were very few differences noted between the cleaned and uncleaned specimens. At 23 weeks aging at 180°F, however, the uncleaned samples had degraded very significantly. Insulation resistance readings fell to zero due to exposed copper, and dielectric breakdown voltages fell sharply. Additional samples were run that were cleaned with lamp oil that gave very similar results to those that were cleaned with 4413.

TABLE 2
TEST RESULTS FOR FILLED PIC CABLE CONDUCTORS AGED AT 180F

DRY SAMPLES, CLEANED

	Cracking (1-none, 4-severe		Insul. Resist. (ohms)	Dielect. Brkdown. (kvolts)
		3 WEEKS		
	1	1	1E+10	7.7
	2	1	1E+10	
	3	1	1E+11	8.5
	4	1	1E+11	
	5	1	1E+11	7.5
	6	1	1E+11	
AVE		1	7.0E+10	7.9
		12 WEEKS		
	1	1	8E+11	6.8
	2	1	7E+11	
	3	1	7E+11	7.5
	4	1	5E+11	
	5	1	4E+11	7.5
	6	1	5E+11	
AVE		1	6.0E+11	7.3
		23 WEEKS		
	1	1	4E+13	9.9
	2	1	2E+13	
	3	1	4E+13	7.9
	4	1	8E+13	
	5	1	3E+13	6.1
	6	1	9E+13	
AVE		1	5E+13	8.0

Charts one through four attempt to show the data in an easily visualized form. The first two charts show the insulation resistance (on a logarithmic y scale) and the dielectric breakdown voltages for cleaned and uncleaned samples during the aging process. In most of the testing, cleaning gives a somewhat lower initial value for electrical tests such as the dielectric breakdown, but over the long run the uncleaned samples begin to lose their advantage and deteriorate badly compared to the cleaned samples. Chart 2 is a good example. The uncleaned specimens actually start at a significantly higher value, 10.7 KV vs 7.9 KV, but at 12 weeks aging at 180°F the values are very close and at 23 weeks aging the cleaned samples have proven to be superior.

CHART 1
PIC CONDUCTOR INSULATION RESISTANCE - CLEANED VS UNCLEANED FILLED DEPIC CABLE AGED AT 180F

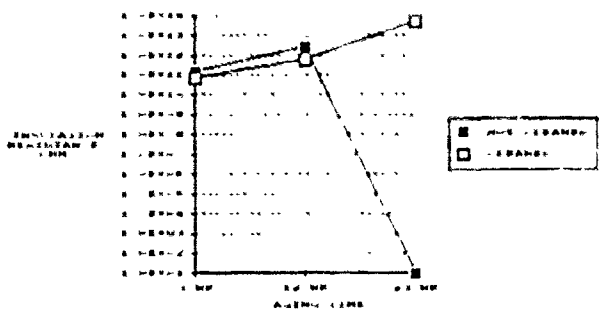

CHART 2
DIELECTRIC BREAKDOWN =
CLEANED VS UNCLEANED FILLED DEPIC CABLE

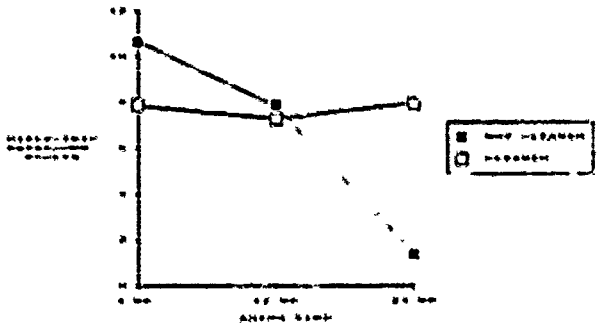

Samples identical to those above were run at exactly the same aging times and conditions except that these samples were washed twice per week for 15 seconds in tap water. This was done in order to test for the effects of water washing such as might occur in a pedestal due to condensation. The results of these tests are shown in the next two tables, table 3 describing the data for uncleaned water washed samples and table 4 for cleaned water washed samples.

Charts 3 & 4 describe the relationship between cracking and dielectric breakdown by combining these two data series on the same graph. Note the different appearances of these charts depending upon whether the conductors were cleaned or not.

CHART 3
CRACKING VS DIELECTRIC BREAKDOWN
FOR UNCLEANED DEPIC CABLE AGED AT 180F

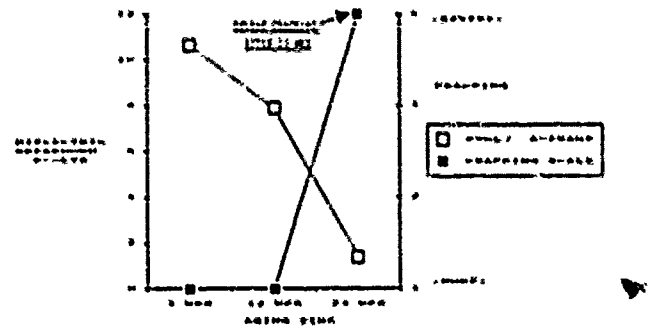

CHART 4
CRACKING VS DIELECTRIC BREAKDOWN
FOR CLEANED DEPIC CABLE
AGED AT 180F

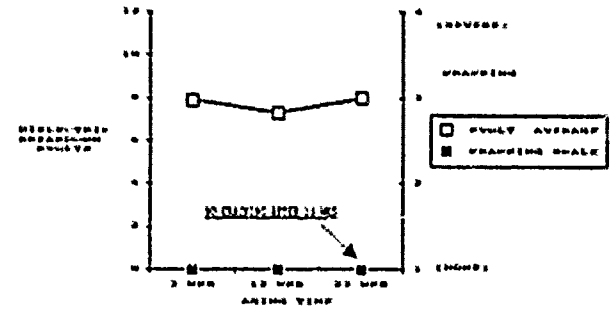

TABLE 3
TEST RESULTS FOR FILLED PIC CABLE
CONDUCTORS AGED AT 180F

WASHED SAMPLES, NOT CLEANED

		Cracking (1-none, 4-severe)	Insul. Resist. (ohms)	Dielect. Brkdown. (kvolts)
		3 WEEKS		
	1	1	2.5E+11	9
	2	1	2.5E+11	
	3	1	2.5E+11	10.5
	4	1	2.5E+11	
	5	1	3.5E+11	11.6
	6	1	4E+11	
AVE		1	2.9E+11	10.4
		12 WEEKS		
	1	1	1.5E+12	1.9
	2	2	0	
	3	1	2E+12	6
	4	1	2E+12	
	5	1	2E+12	8.4
	6	1	2E+12	
AVE		1.17	1.6E+12	5.4
		23 WEEKS		
	1	4	0	0.6
	2	4	0	
	3	4	0	1.1
	4	4	0	
	5	4	0	0.8
	6	4	0	
AVE		4	0	0.8

TABLE 4
TEST RESULTS FOR FILLED PIC CABLE
CONDUCTORS AGED AT 180F

WASHED SAMPLES, CLEANED

	Cracking (1-none, 4-severe)	Insul. Resist. (ohms)	Dielect. Brkdown. (kvolts)
		3 WEEKS	
1	1	1.5E+11	8.9
2	1	1.5E+11	
3	1	2E+11	9.5
4	1	2E+11	
5	1	2.5E+11	7.4
6	1	3.5E+11	
AVE	1	2.0E+11	8.6
		12 WEEKS	
1	1	2E+12	7.5
2	1	2.5E+12	
3	1	2.5E+12	10.8
4	1	2E+12	
5	1	3E+12	9
6	1	3E+12	
AVE	1	2.5E+12	9.1
		23 WEEKS	
1	1	4E+13	6.2
2	2	4E+13	
3	2	5E+13	5.7
4	2	5E+13	
5	2	3.5E+13	3.9
6	1	7.5E+13	
AVE	1.67	4.8E+13	5.3

Once again the uncleaned samples fared poorly in all test areas after 23 weeks aging compared to the cleaned samples. Comparing the uncleaned water washed samples with the uncleaned dry samples (table 1) revealed that there was a constantly diminished performance from the washed specimens. Signs of degradation occurred at only 12 weeks for the uncleaned washed samples. One of the conductors had slight cracking and gave a low insulation resistance reading and the average dielectric breakdown value was lower than for the corresponding dry samples. This is a smaller effect than the effect of cleaning but it is nevertheless significant. The following charts make this clearer.

CHART 5
CRACKING VS DIELECTRIC BREAKDOWN FOR
UNCLEANED, WASHED DEPIC CABLE
AGED AT 180F

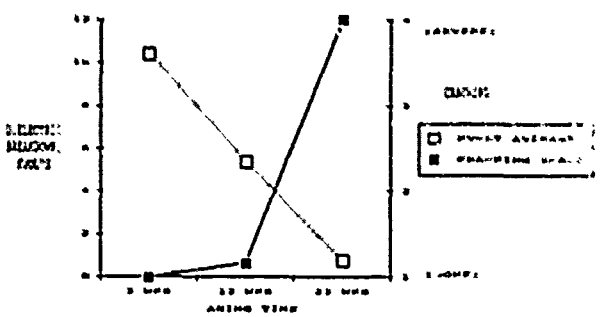

CHART 6
CRACKING VS DIELECTRIC BREAKDOWN FOR
CLEANED, WASHED DEPIC CABLE
AGED AT 180F

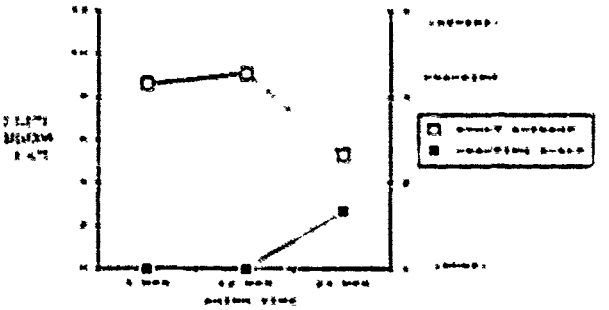

These charts illustrate the degradation that started to occur at 12 weeks aging. Chart 5 again reveals the degradation of uncleaned PIC but at a somewhat faster rate than was seen in chart 3 (the dry samples). At 12 weeks there was evidence of cracking starting to occur in the washed, uncleaned conductors. The data at 12 weeks for the washed uncleaned samples is similar to the data at 23 weeks for the washed cleaned samples (dielectric breakdown in the low 5 KV region and evidence of slight cracking). This might indicate that, under these conditions, one could expect about a doubling of the life of the insulation if it were cleaned. Comparison of charts 5 and 6 show substantial differences in the behavior of the insulation dependent on cleaning, but the effect of the water washing is perhaps more clear when comparing charts 4 and 6, which represent the data for cleaned conductors. It is evident that the effect of the water washing is to shorten the lifetime of the insulation.

In every one of these comparison tests, the cleaned samples out-performed the uncleaned conductors. In some conditions or parts of the country, however, one might wish for additional protection for the wireworks in a pedestal environment beyond what can be gained through cleaning alone. For this reason we also looked at several of the sprays that are on the market and that are used to coat PIC for [illegible] reason or another. Tests were also [illegible] up to determine the usefulness of [illegible]mentary inner pedestal closures, which have lately been used to protect the conductors in pedestals from casual handling and environmental exposure.

Three types of sprays were tested. Spray A is a urethane coating produced by 3M known as PIC Spray 5301. It was originally developed for use on low density insulations but is effective in repairing insulation breaks in all types of polyethylene coated conductors. Spray B is an electrical varnish/phenolic type spray that is made for the purpose of coating PIC that is at risk of cracking. Spray C is a silicone-fluoride copolymer that is intended to be used as a protective coating for outside plant connectors and as such will certainly coat the conductors around those connectors.

The three types of sprays were tested on both cleaned and uncleaned PIC insulation and in both dry and water washed conditions. Three coats of each spray were used on the samples. The coatings were allowed to air dry between sprayings, 3 minutes for spray A, 30 minutes for sprays B and C (sprays B and C were much slower drying than A). Spray head application speed was one foot/second at a distance of nine inches. Tables 5 and 6 show a synopsis of the data of the sprays for the uncleaned sample condition. (Note that, for brevity's sake, the data for tables 5 and 6 are actually averages of six samples for each data point shown. Under insulation resistance, rather than showing the data in ohms for each reading, the percent of "good" samples are shown. In other words, for sprays A and B at 23 weeks aging, all of the samples showed the desired high resistance, while two of the six samples for spray C failed the insulation resistance test. The column on table 5 marked "controls" is simply a restatement of table 1 in a condensed form and the similar column on table 6 corresponds to table 3.)

TABLE 5
TEST RESULTS FOR MAINTENANCE SPRAYS
AFTER AGING AT 180F ON FILLED
PIC CABLE CONDUCTORS

DRY SAMPLES, NOT CLEANED

CRACKING (1=NONE, 4=SEVERE)

	Controls	Spray A	Spray B	Spray C
3 WKS	1	1	1	1
12 WKS	1	1	1	1
23 WKS	4	1	1	1.33

INSULATION RESISTANCE (ohms)*

	Controls	Spray A	Spray B	Spray C
3 WKS	100%	100%	100%	100%
12 WKS	100%	100%	100%	100%
23 WKS	0%	100%	100%	67%

DIELECTRIC BREAKDOWN (kvolts)

	Controls	Spray A	Spray B	Spray C
3 WKS	10.7	10.5	10.2	10.1
12 WKS	7.9	9.1	8.4	9.6
23 WKS	1.4	9.3	10.6	3.4

*% OF SAMPLES SHOWING HIGH RESISTANCE(>1E+10 OHMS) (6 SAMPLES)

NOTE: THIS TABLE SHOWS AVERAGES FOR SIX SAMPLES PER DATA POINT.

TABLE 6
TEST RESULTS FOR MAINTENANCE SPRAYS
AFTER AGING AT 180F ON FILLED
PIC CABLE CONDUCTORS

WASHED SAMPLES, NOT CLEANED

CRACKING (1=NONE, 4=SEVERE)

	Controls	Spray A	Spray B	Spray C
3 WKS	1	1	1	1
12 WKS	1.17	1	1	1
23 WKS	4	2.33	2.17	4

INSULATION RESISTANCE (ohms)*

	Controls	Spray A	Spray B	Spray C
3 WKS	100%	100%	100%	100%
12 WKS	83%	100%	100%	100%
23 WKS	00%	50%	33%	00%

DIELECTRIC BREAKDOWN (kvolts)

	Controls	Spray A	Spray B	Spray C
3 WKS	10.4	9.7	10.2	11.3
12 WKS	5.4	10.8	8.6	7.7
23 WKS	0.8	0.7	11.1	6.6

*% OF SAMPLES SHOWING HIGH RESISTANCE(>1E+10 OHMS) (6 SAMPLES)

NOTE: THIS TABLE SHOWS AVERAGES FOR SIX SAMPLES PER DATA POINT.

One of the surprising results of this test series was the effect of the various sprays on uncleaned filled PIC. It is generally assumed that spraying any kind of coating on a greasy surface is ineffective. However all of our data indicates that, especially for sprays A and B, this can be an effective technique for retarding degradation. One might postulate that this was due to the cleaning effect of the sprays, that is, that in spraying the greasy conductors most of the grease was washed off and in effect the same result could have been obtained through cleaning alone. There seems to be more to the sprays, effectiveness than that, however. Consider the cleaned, water-washed samples that were not sprayed (table 4). At 23 weeks these samples showed evidence of degradation starting to occur both in the observed cracking and in the lowered dielectric breakdown voltage. When similar samples were sprayed, on the other hand, (table 8) they continued to look very good to 23 weeks aging even with water washing. (See tables 7 and 8 for the data for cleaned and sprayed conductors. Note also in table 8 that, for water washed samples, spray C actually seems to be detrimental to the PIC and gives worse results than the controls with no spray at all.)

TABLE 7
TEST RESULTS FOR MAINTENANCE SPRAYS
AFTER AGING AT 180F ON FILLED
PIC CABLE CONDUCTORS

DRY SAMPLES, CLEANED

CRACKING (1=NONE, 4=SEVERE)

	Controls	Spray A	Spray B	Spray C
3 WKS	1	1	1	1
12 WKS	1	1	1	1
23 WKS	1	1	1	1

INSULATION RESISTANCE (ohms)*

	Controls	Spray A	Spray B	Spray C
3 WKS	100%	100%	100%	100%
12 WKS	100%	100%	100%	100%
23 WKS	100%	100%	100%	100%

DIELECTRIC BREAKDOWN (kvolts)

	Controls	Spray A	Spray B	Spray C
3 WKS	7.9	9.1	9	8.4
12 WKS	7.3	8.1	8.2	8.4
23 WKS	8	8.4	8.4	7

*% OF SAMPLES SHOWING HIGH
RESISTANCE(>1E+10 OHMS) (6 SAMPLES)

NOTE: THIS TABLE SHOWS AVERAGES
FOR SIX SAMPLES PER DATA POINT.

TABLE 8
TEST RESULTS FOR MAINTENANCE SPRAYS
AFTER AGING AT 180F ON FILLED
PIC CABLE CONDUCTORS

WASHED SAMPLES, CLEANED

CRACKING (1=NONE, 4=SEVERE)

	Controls	Spray A	Spray B	Spray C
3 WKS	1	1	1	1
12 WKS	1	1	1	1
23 WKS	1.67	1	1	4

INSULATION RESISTANCE (ohms)*

	Controls	Spray A	Spray B	Spray C
3 WKS	100%	100%	100%	100%
12 WKS	100%	100%	100%	100%
23 WKS	100%	100%	100%	17%

DIELECTRIC BREAKDOWN (kvolts)

	Controls	Spray A	Spray B	Spray C
3 WKS	8.6	9.4	9.1	8.4
12 WKS	9.1	10.1	9.7	8.1
23 WKS	8.3	9.8	8.4	1.7

*% OF SAMPLES SHOWING HIGH
RESISTANCE(>1E+10 OHMS) (6 SAMPLES)

NOTE: THIS TABLE SHOWS AVERAGES
FOR SIX SAMPLES PER DATA POINT.

Clearly, the initial cleaning of filled cable when it is brought up into a pedestal is of primary importance, even with the ETPR type of filling compounds. Spraying those conductors with one of the two effective sprays adds an extra measure of safety, especially if the conductors will be exposed to condensation or if the cleaning step was not done well. There is one other line of defense that was alluded to before, and that is the supplementary inner pedestal closure concept. This not only protects the conductors from the effects of condensation and other transitory environmental factors, but also discourages casual handling and re-working of the conductors while at the same time allowing access for legitimate needs.

A series of tests was carried out that compares the relative cracking times for various PIC cables that were aged in both an "exposed" condition in a hot air aging oven and a "protected" condition in the same oven. This test was carried out at both 180°F and 200°F. The protected samples were aged in glass containers sealed with foam tape and 3M's PST (pre-stretched tubing) to give an air-tight seal. This experimental arrangement was chosen to give the best visual access to the samples so that they could be observed without continually disturbing the experiment. Control samples of 3M brand PST pedestal closures of similar internal volume were also included in the test to verify that what was happening in the glass closure was similar to the actual pedestal closure. The exposed samples were aged in both the cleaned and uncleaned condition. The results of this test are summarized in chart 7. Again the trends are similar to what we have seen before. After only 12 weeks aging the uncleaned exposed samples are cracking significantly faster than the cleaned exposed samples. However, the protected samples have shown no cracking, even at 200 degrees.

CHART 7
RELATIVE CRACKING OF PIC CONDUCTORS FOR THREE AGING CONDITIONS AFTER 12 WEEKS AT 180F AND 200F

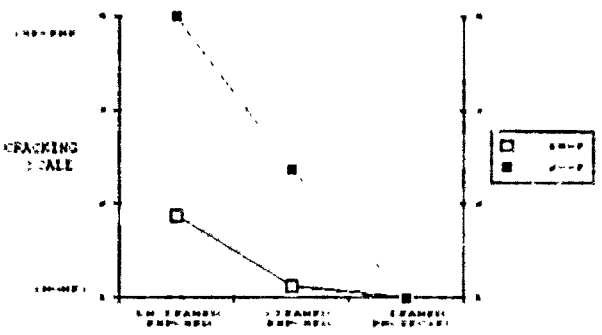

Finally, there is the question of whether the results gathered on a cable manufactured two and a half to three years ago, and that has an OIT on the lower end of the acceptance scale, can predict what will happen to the newer cables. To answer this question we gathered samples of cable from three different manufacturers, all of 1988 or early 1989 vintage, that used various filling compounds. We started aging them early in 1989. No pre-aging at elevated temperature was done on these cables since this was not done on the original cable studied. Several interesting facts emerged. First, all these samples had substantially higher OIT's than the original cable tested. They also aged better than that original cable. However, they also began to crack on a basis consistent with the trends we have already noted. That is, the uncleaned foamskin cables filled with ETPR (Flexgel) began to crack first. In fact, there seems to be a definite correlation so far with the OIT obtained on a specific cable and the endurance with which it ages. Based on the results obtained to date, filled foamskin cable will continue to experience field failures. See table 9 with a list of the cable types and the data for each.

TABLE 9
CABLES USED IN AGING TESTS

CABLE NO.	MANUFACTURER	TYPE*	MANUFACTURED
1	A	FS, ETPR	EARLY 1988
2	B	FS, ETPR	LATE 1986
3	B	FS, ETPR	MID 1988
4	C	FS, ETPR	EARLY 1989
5	C	FS, PEPJ	EARLY 1989
6	C	SO, PEPJ	EARLY 1989

*FS-FOAMSKIN
SO-SOLID

The samples that were aged in a protected environment to simulate a pedestal closure were also consistent with previously obtained results. In other words, there is every reason to believe that, even with the new cables with improved antioxidant systems, cleaning the cables where they are brought up into a pedestal, using an effective spray coating, and employing a secondary closure within the pedestal will all work to significantly prolong the life of foamskin filled PIC cables.

In conclusion, based on the aging tests performed, the data is very consistent in supporting the importance of cleaning filled cable. There is evidence that water-washing of PIC can have a deleterious effect on its aging characteristics, and the use of sprays and pedestal closures provide effective ways of minimizing the risks of premature failure of the PIC in a pedestal. Aging tests are continuing in this and other laboratories. Undoubtedly the final word has not yet been spoken on the subject of PIC degradation; however, as the knowledge base expands around this highly visible topic there will emerge more and more ways to cope with the problem, utilizing both better cable and plastics technology and more effective installation and maintenance procedures.

REFERENCES

1. Shea, J.W., "Treatment of Degraded PIC Insulation in Pedestal Closures Associated with Buried Plant", 21st International Wire and Cable Symposium, 1972

2. Malower, E.G., Kiss K.D., "Oxidative Stability of Polypropylene Compared to High Density Polyethylene", 27th International Wire and Cable Symposium, 1978

3. Biskeborn, M.C., Kiss K.D., "The Effect of Filling Compound Migration on Cellular Insulation", 27th International Wire and Cable Symposium, 1978

4. O'Rell, D.D., Patel, A., "Oxidative Stability Studies on Cellular High Density Polyethylene Insulation for Communications Wire", 24th International Wire and Cable Symposium, 1975

5. Davis, L.E., "A Global Test Method for Long Term Stability of Solid and Foam-Skin Insulation", 36th International Wire and Cable Symposium, 1987

6. Board, B.L., Ruddell, H.J., "Investigation of Premature Depletion of Stabilizers from Solid Polyethylene Insulation", 31st International Wire and Cable Symposium, 1982

7. Meyer, F.K., Linhart, H., "New Data on Long Term Stabilization of Polyethylene for Telecommunication Wire Insulation", 32nd International Wire and Cable Symposium, 1983

8. Bowmer, T.N., "Cracking of Foam-Skin Polyethylene Insulations in Pedestals", 37th International Wire and Cable Symposium, 1988

9. Havens, B., "Moving Away From a Disposable Network", Outside Plant, January-February, 1988

10. Schmidt, G.A., "Life Predictions of Insulations for Filled Cables in Pedestal Terminals", 26th International Wire and Cable Symposium, 1977

11. Wight, F.B., "A Method for Restabilization of Antioxidant Depleted Low Density Polyethylene Conductor Insulation", 28th International Wire and Cable Symposium, 1979

12. Mitchell, D.M., Sabia, R., "Development, Characterization, and Performance of an Improved Cable Filling Compound", 29th International Wire and Cable Symposium, 1980

13. Bellcore Technical Advisory, TA-TSY-000421, Issue 1, September 1988

3M Company
TelComm Products Division
PO Box 2963
Austin, Texas 78769-2963

Linwood P. (Bud) Beltz - Mr. Beltz received a B.S. degree in Chemistry from Lehigh University in 1966 and an M.S. degree from Northwestern University in Evanston, Illinois, in 1968. He has been employed with 3M for twenty years studying materials and formulating products for industrial use.

RESULTS ON A LARGE SCALE INSTALLATION OF A FIBRE OPTIC DISTRIBUTION NETWORK

JP. BOINET - M. de VECCHIS - C. VERGEZ

LES CABLES DE LYON - BP 309 - 92111 CLICHY CEDEX - FRANCE

ABSTRACT

Results on a very large scale installation of a fibre optic distribution network are given. When writing this paper, quantities installed were about the following : Number of connectable subscribers : 300000 Quantity of fibre : 70000 km Number of connections (individual fibres) : 700000.
This is a part of a more important project that will lead within some years to a network for about 900000 connectable subscribers.
Evolutions on some constitutive components of the network, compared to a previous description, are also detailed.
As a general conclusion, it appears that the results in terms of characteristics (i.e. power budget) and implementation time are perfectly in line with preliminary evaluations.

1 - INTRODUCTION

The installation of a large scale fibre-to-home project started in France in 1986. A first phase of the project designed for CATV distribution and implemented in more than ten different locations, corresponds to a fibre optic network for 420000 subscribers. Considering the following phases, we are now involved in a project corresponding to a total of about 900000 connectable subscribers (1).
A joint venture has been established between Alcatel CIT and Les Câbles de Lyon to deliver turn-key systems. Câbles de Lyon is responsible of the complete cable plant including engineering, development and production of cables and accessories, installation and on-site measurements.
The development of the network is done at a speed of about 100000 connectable subscribers / year. It means that at the end of 1989, more than 80 % of the first phase will be in operation.

2 - DESCRIPTION OF THE NETWORK

The network is of the "double star switched" kind. Switches or selectors are housed in distribution centers that can serve 960 subscribers.

The distribution network has been described in details previously (2) It is a star network and five fibres are used for the 10 homes : wavelength multiplexing is used to serve the sixth to tenth subscribers at 1300 nm since the first five subscribers are connected using the first window (around 840 nm).

The figure 1 shows a typical configuration of the distribution network.

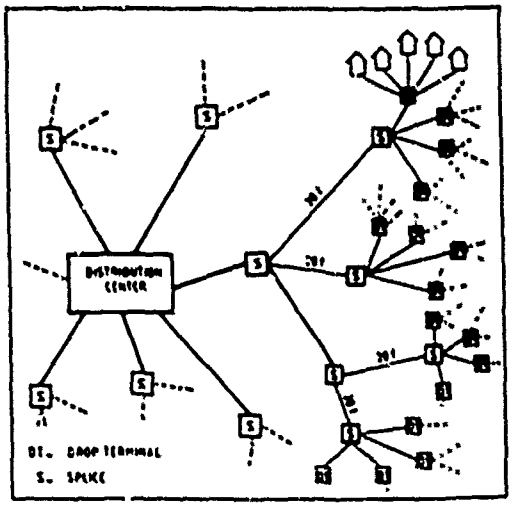

Figure 1

3 - CABLES

Cables use a reverse helix slotted core structure. They are produced by stranding basic units with 10 grooves (one fiber per groove) (see figure 2). This design has been selected considering the importance of splice -related considerations (2).
The range of standard cables is 20 - 30 - 50 - 70 - 90 -120 - 150 and 210 fibres The 210 fibre cable has been used for the first installations. Now, considering the safety aspect and possibilities of network optimization, the largest used is the 150 fibres.

Figure 2

Physical parameters of the cables are given in Table I

Main physical characteristics	Number of fibres						
	20	30	50	70	90	120	150
Maximum O.D. (mm)	16	18	20	21	27	30	30
Approximate weight (kg/km)	210	230	320	450	500	720	720
Maximum Tensile Strength (daN) (corresponding to a fibre elongation < 1,5%)	140	150	270	300	350	400	450
Crush resistance (daN/cm)	15	15	15	15	15	15	15
Minimum bending radius static (mm)	200	200	230	230	230	300	300
dynamic (mm)	200	200	250	250	250	300	300

Table I

For linking the drop terminals, 5 fibre cables are used with three different versions :

- duct type with laminated aluminium and high density polyethylene sheath (O.D. 7,5 mm)

- wall mounted, outside use : jelly filled cable (O.D. 7,5 mm)

- aerial : Optical core similar to the previous one - 8 - shaped structure with a 19 x 9,8 mm galvanized steel messenger.

4 - ACCESSORIES

Cable accessories, which have been developed in parallel with the cable structures in order to obtain the best fitting all along the line, have been described in details in a previous paper (2) and we just recall here the more important points.

Splice selection : a careful selection has been done taking into account the specific conditions of a distribution network and including quality of splice, easy field installation and costs.
The ATI Placoptic system has been selected (3)

Semi permanent splices : these devices are intermediate between a permanent splice and a connector, as they offer a limited number of reinterventions, compatible with the network operation (4).

Splice housing : the design uses a cassette splice organizer that can store on its periphery extra lengths of cable units wounded like on a drum, in order to leave the possibility to perform the splice few meters off its final location without having to loop the complete cable.

Drop terminals : it realizes the fanning out of the distribution cables and the connection to the single fibre drop cables.
Furthermore the drop terminal houses the frequency demultiplexers on the subscriber's side.

5 - EVOLUTIONS ON THE COMPONENTS

Since the last presentation in 1987, some evolutions have been done in some constitutive components of the network.

Splice housing : the first version of the splice housing was using for the outer box a reinforced moulded plastic. This version is still used for example in buildings.
For underground applications, a new version has been developed, which is waterproof under 4 m of water instead of 1 m for the first version. The outer box is made of passivated cast aluminium alloy. The internal design is not changed and, in particular, cassette splice organizers are the same for both versions (figure 3).

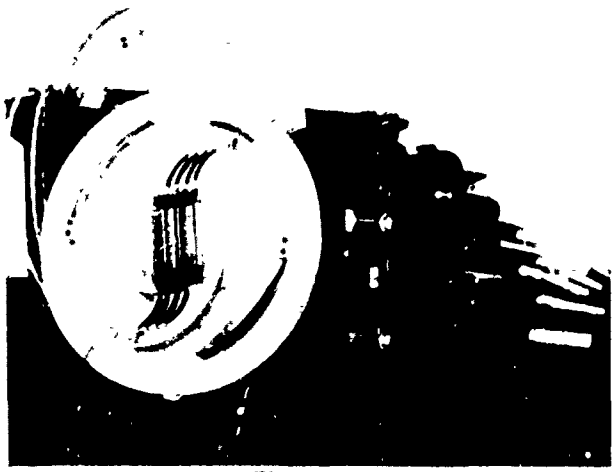

Figure 3

Boxes for 3,9 or 15 cassettes (10 fibre splices each) are available.

Drop terminals

First subscriber's connections in drop terminals were made by using splices as the characteristics of the first semipermanent splices were not convenient for outdoor operation.
Improvements have been made on these characteristics in order to qualify these semipermanent splices for use in the drop terminals. This new component, called OPTOCLIP, is manufactured by the company DEUTSCH.

It is composed of :

- two contacts each allowing fibre and cable retention through a crimping ferrule, as fibre end protection when unmated.

- one receptacle allowing contact retention direct alignment of two fibres, end to end through an index matching liquid premounted inside the center, and fixation on a stand.

The figure 4 shows a drop terminal equipped with semi permanent splices and frequency demultiplexers. It corresponds in the shown configuration to seven connected subscribers (two demultiplexers).

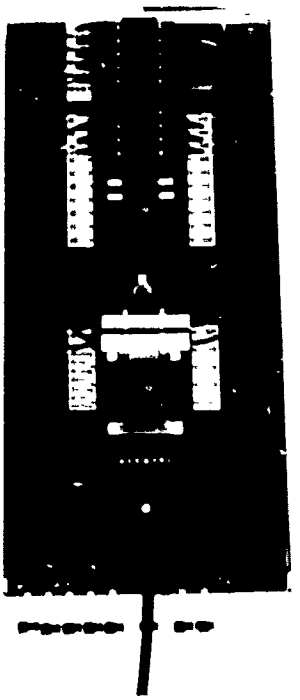

Figure 4

6 - RESULTS ON INSTALLATION

The following results correspond to the situation at mid-89 as given in Table II. The table summarizes the evolution of the installation and the quantities involved for the main components of the distribution network.

The quantities corresponding to subscriber's connection to the drop terminals (i.e. drop cable) are not included.

	End 87	End 88	Mid 89	End 89 (estimate)
Number of connectable subscribers	130000	240000	290000	340000
Fibre (km)	32000	57000	68000	81000
Cable (km)	1900	3000	3600	4300
Splice boxes	3100	5500	6700	8100
Drop terminals	12000	28000	34000	40000
Unitary splices	130000	300000	360000	430000
Semipermanent splices	156000	280000	340000	400000

Table II

Situation of distribution network installation.

The power budget for the distribution line between the distribution center and the drop terminal has been found between 1.5 and 5.5 dB at 850 nm. It includes the connecting losses at both ends (distribution center and drop terminal) a length of cable between 200 m and 1 km and 1 to 3 splices.
The average attenuation of splices at 850 nm is 0.15 dB and the standard deviation is 0.145. The figure 5 shows an histogram of the attenuation of line splices.

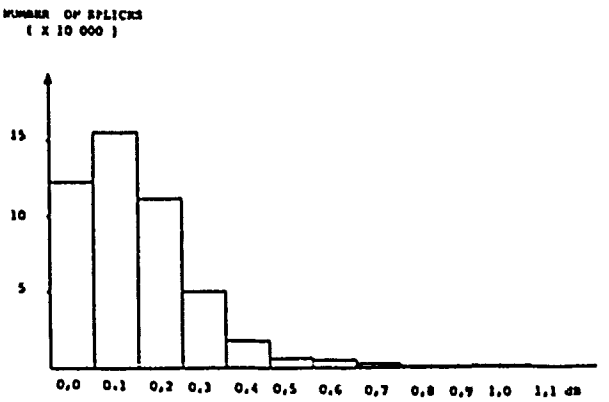

Figure 5

The semipermanent splices show an average insertion loss of 0.3 dB and a standard deviation of 0.15 dB.

CONCLUSIONS

The results obtained in term of transmission characteristics (power budget, individual attenuations, bandwidth) are perfectly in line with the preliminary evaluations used for designing the system.

Practical experience gained during a 3 year period on installation of cables and accessories shows that their functional parameters are well fitted to the specific aspects of a distribution network.

A large experience on network engineering and optimization of an optical distribution network has also been obtained.

The implementation schedule is also perfectly in line with the preliminary evaluations. It is the consequence of several points that have been correctly controlled :

- Optimization of production flaws.
- Engineering of the network.
- Training of people for installation.

REFERENCES

(1) Fiber Optics Local Distribution in France. C. VEYRES FOC/LAN 1988 and Fibers Optics Magazine - Jan/Feb 1989.

(2) Fiber Optic Subscriber Networks using 85/125 fibers.
JP. BOINET - M. de VECCHIS - JP. BONICEL - JP. BREGEON - I.W.C.S. 1987.

(3) A new multimode optical fiber splicing technique - Y. RUELLO - F.L. MALAVIEILLE - I.W.C.S. 1986.

(4) Lowloss splices and special tool kit for multimode optical fibers.
M.C. SOSTER - JL. MALINGE - SPIE, Sept. 86.

JP. BOINET - LES CABLES DE LYON
39 Rue des Chasses - 92111 CLICHY - FRANCE

Jean Pierre BOINET was born in 1944. He is graduated from Ecole Nationale Supérieure des Arts et Métiers (1967). He joined LTT in 1969 and has been involved in the construction of the French Interurban Network.
He has been in charge of the development of installation procedures for optical cables. Since the merging of LTT cable activities with Les Câbles de Lyon he is Project Manager for Videocommunications activities in the Network Engineering and Installation Department.

M. de VECCHIS - LES CABLES DE LYON
39 Rue des Chasses - 92111 CLICHY - FRANCE

Michel de VECCHIS was born in 1946. He is graduated from Ecole Nationale Supérieure des Télécommunications (1969). He joined LTT in 1970 where he worked on microwave components. He started to work on fiber optics in 1974 and has been Technical Director of the cable Division until the merging of LTT cable activities with Les Cables de Lyon in 1986. He his now Director of Technical International Marketing at Les Cables de Lyon Telecommunications Branch.
He is involved in International Standardization of Optical Fibers and Cables (Chairman of CECC WG 28 and Secretary of IEC SC 86 A).

C. VERGEZ - LES CABLES DE LYON
39 Rue des Chasses - 92111 CLICHY - FRANCE

Christian VERGEZ was born in Paris in 1952. He received the degree of Dipl. Ing. in Electronics Engineering in 1975 from "Ecole Spéciale de Mécanique et d'Electricité" Paris. In 1977 he joined LTT Outside Plant Division. He is now at Les Cables de Lyon Network Engineering and Installation Department, responsible for the design and development of cable accessories.

AN OPTICAL BUS ARCHITECTURE IN THE LAST MILE

David Wong and Ralph Narciso

Raynet Corporation
Menlo Park, California

ABSTRACT

Telephone companies are carefully evaluating several techniques for installing optical fiber into the last mile. Most fiber to the home systems have failed to provide sufficient cost reductions to justify their use, but a fiber-to-the-curb system based on a bus architecture which is economically feasible is now being demonstrated. This system is cost-effective because it allows for significant resource sharing, which divides the cost of electronic components and fiber among numerous subscribers. This fiber-to-the-curb system is being demonstrated in Lynnfield, Massachusetts. This system provides a transparent link with existing telephone company equipment and a convenient and flexible pathway to future telephone and video systems.

SHARED RESOURCES IN A BUS ARCHITECTURE

Bringing fiber to the subscriber is the current challenge facing telephone companies. Some early fiber-to-the-home systems have replaced dedicated copper wires from the central office to the home with dedicated optical fibers. Raynet Corporation, a subsidiary of Raychem Corporation, is now demonstrating a fiber-to-the-curb system based on a bus architecture. This system answers the need for economy by dividing the cost of the electronics and fiber among several subscribers.[1] It also provides flexibility by minimizing the need for splices and by incorporating the ability to support enhanced services in the future.

The extensive sharing of resources while maintaining the compatibility with existing telephone company equipment are the keys to cost reduction.[2] Both fiber and electronics costs are minimized due to the bus architecture. Instead of dedicating one or two optical fibers per subscriber this system utilizes two optical fibers from a central office or remote location which can then be shared by up to 192 subscribers. The office interface unit (OIU) is the primary interface between the telephone company equipment and the fiber-to-the-curb system. The OIU provides telephone service for up to 192 subscribers. The subscriber interface unit (SIU) is shared by up to 8 subscribers. The SIU functions as an intelligent, field-deployed electro-optics terminal. The subscriber's copper drops terminate directly to the SIU. Utilizing the existing copper drop cables provides a significant cost savings in comparison to the installation of a fiber drop cable at the subscriber's residence.

This fiber-to-the-curb system interfaces transparently with the telephone companies existing equipment and operational support systems. It also meets the telephone company's needs for detailed maintenance and trouble shooting capability by identifying and sending alarms to indicate both service-affecting and potentially service-affecting conditions and by accurately pinpointing the location of the trouble.

DEMONSTRATION SITE

The first demonstration of this fiber-to-the-curb system is being conducted at a New England Telephone Company location in Lynnfield, Massachusetts with system turn-up scheduled for the fall of 1989. The Lynnfield site is a mature subdivision of approximately 100 homes in which rehabilitation construction is being used to replace the existing underground copper system with an underground fiber-to-the-curb system which provides POTS (plain old telephone service).

The system is being installed as this paper is being written. Major portions of the installation are already complete. The Controlled Environmental Vault (CEV), (which is utilized to house the office interface units), the fiber optic cables, the power cable and the handholes for the subscriber interface units have all been installed. All of the fiber cables have been spliced and fiber pigtails have been spliced to the end of each four-Kilometer fiber bus in order to facilitate test access. The fiber pigtails have been stored in standard splice closures. Two four-Kilometer fiber buses, two office interface units and 37 subscriber interface units will be utilized for the trial.

SYSTEM DESCRIPTION

This fiber optic voice and data telecommunications system was designed for use in the local loop environment. The fiber-to-the-curb system is composed of an operational support system (OSS) called the Remote Intelligent Distribution Element Support (RIDES),[3] a System Administration Module (SAM), an Office

Interface Unit (OIU), a fiber optic bus of a length up to four Kilometers and up to 24 subscriber interface units (SIU). The system also utilizes a remote power subsystem to supply power to all of the subscriber interface units. The fiber-to-the-curb system is illustrated in Figure 1.

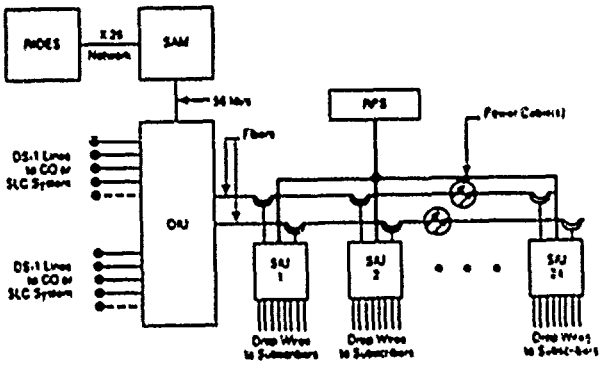

Figure 1
Fiber-to-the-Curb System

The RIDES system and SAM computers establish a user interface that efficiently administers and controls the fiber-to-the-curb systems located throughout a telephone company operating area. (See Figure 2.) The RIDES system consists of a minicomputer and resident software that provides an interface to existing telephone company operational support systems. Its primary functions are provisioning, alarms, maintenance and test and administration of one or more fiber-to-the-curb systems. The fiber-to-the-curb OSS is typically located in a centralized telephone company computer center such as the minicomputer maintenance and operations center (MMOC). One RIDES system can support up to 200 SAMs.

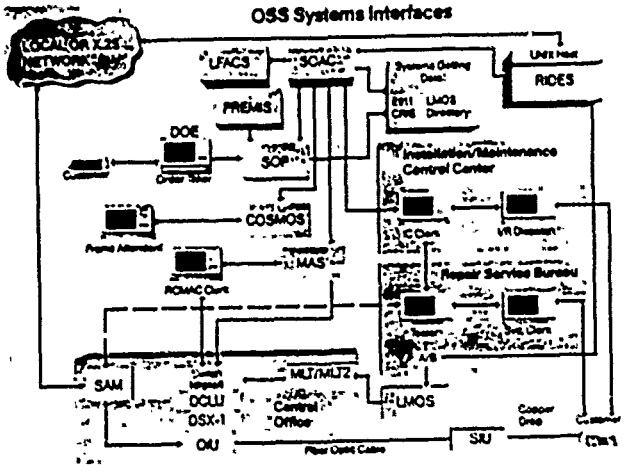

Figure 2

The SAM consists of a microcomputer and software capable of administering up to 96 OIUs. It is usually located in the telephone company's central office and its major functions are for provisioning, testing, alarm surveillance and the collection of historical data for the fiber-to-the-curb system.

The OIU (See Figure 3) intelligently connects either the central office switch, central office terminals or channel banks with the fiber-to-the-curb system. The OIU can reside in a central office or in a controlled environmental vault. The OIU controls the flow of customer traffic and configures and monitors each subscriber interface unit. It can control up to 24 SIUs and download new software releases to them when necessary. The OIU accepts up to eight primary and two protection DS-1 lines from the central office to support a maximum of 192 subscriber lines (equivalent to two SLC-96 systems or eight D4 digroups). Software in the OIU is utilized to establish the initial provisioning of the system, to add subscribers and to perform time slot interchange functions.

OFFICE INTERFACE UNIT

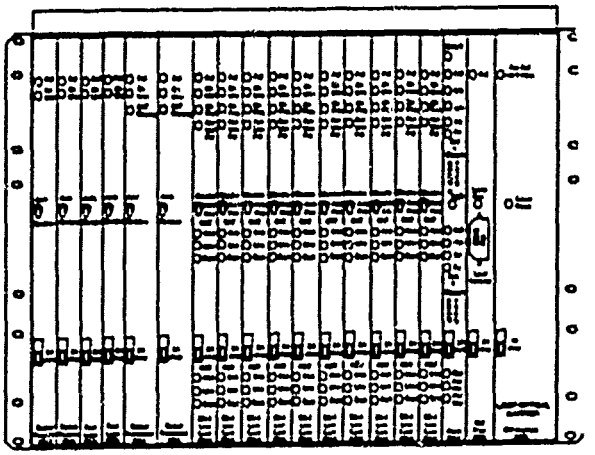

Figure 3

The fiber optic bus carries optical signals between the OIU and the SIUs on two multimode fibers. The initial trial locations will utilize multimode fiber. However, the technology is changing and future fiber-to-the-curb systems will utilize singlemode fiber. Signals on the fiber optic bus are sent in packets of information. Each packet is coded to ensure that only the correct cross connection can be made. Maximum utilization of the optical fiber is achieved through a time slot interchange function which eliminates the need for dedicated lines; instead, software enables any DS-0 channel from any DS-1 line to serve any subscriber line on any connected subscriber interface unit. This time slot interchange function allows for the grooming of circuits. Telephone company personnel can change the assigned time slots by entering commands (via common OSS screens) from a RIDES terminal.

The bus architecture is composed of two unidirectional buses; a read bus and a write bus. The read bus transports data from the optical transmitter in the OIU to the various SIUs. Data is transmitted to each SIU in a synchronous format on the read bus and each SIU extracts its subscriber data and commands. The write bus carries data in an asynchronous format from the SIUs to the optical receiver in the OIU. The data is interpreted by the OIU, mapped to the appropriate DS-1 lines and then transmitted on to the central office.

The fiber optic cable used at the Lynnfield site is a slotted core cable design with a maximum fiber count of 16. One 16 and two 8-fiber cables were installed at the field trial location. This cable design was originally selected due to the relative ease of removing the fibers in a mid-span access procedure. Raynet has subsequently developed mid-span access procedures for alternate cable designs so that future fiber-to-the-curb systems will be capable of utilizing any cable design.

The SIU intelligently interfaces between the OIU and the subscriber (See Figure 4). It is designed to be buried near the customer premises and its primary purpose is to provide narrowband communication services to customers served by the fiber-to-the-curb system.

SUBSCRIBER INTERFACE UNIT

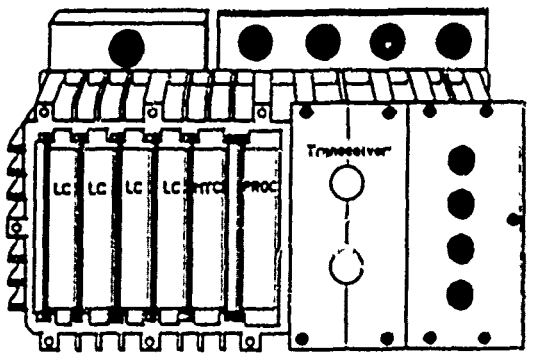

Figure 4

Each SIU can provide telephone service for up to eight subscribers. The SIUs are equipped with non-invasive couplers which permit light to be launched into or extracted from a fiber without splicing. The non-invasive couplers can be installed quickly and inexpensively. Because they require no splicing, additional subscribers can be added to the system without causing service interruptions. Two types of optical couplers are being utilized; one to serve the read bus and another to serve the write bus.

The remote power subsystem consists of a rectifier, backup batteries, power cables, power pigtails and an alarm link to the nearest subscriber interface unit. Alarm conditions occurring at the remote power supply are monitored by the designated subscriber interface unit and reported to the office interface unit, the system administration module, and the operational support system. The remote power subsystem supplies -48 volt dc power to the SIUs which then power the individual telephones. A power cable from the remote power subsystem is placed in the trench along with the fiber optic cable. The power pigtails which are used to tap the main power bus are connected to the individual SIUs.

FIBER OPTIC CABLE MID-SPAN ACCESS PROCEDURE

In order to install the SIUs for the fiber-to-the-curb system, the fiber must be removed in a mid-span access procedure. Typical mid-span access procedures require cutting and splicing fibers at each access point. The non-invasive couplers in the fiber-to-the-curb system do not require that the fibers be spliced. The fibers are simply removed from the cable and then placed into the read and write couplers. This technique is illustrated in Figures 5 through 10 and described below.

To achieve mid-span access of the fibers, the craftperson first grasps the pre-installed loop of optical cable at the SIU and uses a ring cutter to remove the outer jacket and score the armor. The outer jacket and the armor are then removed and the craftperson then gains access to the aramid ripcord (See Figure 5). After cutting one end of the now-visible aramid ripcord, the ripcord is pulled to expose the inner jacket (See Figure 6). The inner jacket is ring cut and removed with the polyester ripcord (See Figure 7). A layer of plastic tape and the binder thread are removed. All of the fibers are removed from the slotted core of the cable and then the slotted core is cut with side cutters (See Figures 8 and 9). The craftperson then installs the exposed fibers into an optical organizer tray in the subscriber interface unit (See Figure 10). The fibers are routed around the tray in a similar fashion to routing fiber in a splice tray. The cut edges of the cable are then water blocked with an optical cable seal and the entire optical cable seal is heat shrunk to the cable port on the SIU. The fibers are identified by colored bands. The craftperson selects the fiber with the correct color and places it into the coupler in the fiber organizer tray. The fiber is placed into the groove in the coupler and then the coupler slide mechanism is closed.

FUTURE ENHANCEMENTS

Future fiber-to-the-curb systems will utilize singlemode fiber and will include an environmentally hardened office interface unit capable of being installed directly in the field. The demonstration system at

Lynnfield is an underground installation with subscriber interface units installed in handholes, but in future systems there will be SIUs suitable for underground, pedestal or aerial applications. Future OIUs will be capable of providing service for up to 384 subscribers and SIUs which support special services and larger numbers of lines will also be available.

Subsequent fiber-to-the-curb system installations will also include video capability. By dividing the cost of video electronics among many subscribers, such systems also provide economic advantages over typical dedicated fiber star networks.[4]

CONCLUSION

The fiber-to-the-curb system being demonstrated at the New England Telephone Company location in Lynnfield, Massachusetts provides the key to the successful use of fiber in the last mile. This system, with its bus architecture, eliminates the need for dedicated fiber from the central office or remote terminal to each subscriber. The headend electronics can already be shared among 192 subscribers (with a future capability for 384 subscribers) and the electronics at the subscriber's end of the loop can be shared by 8 users with greater sharing possible in future products.

ACKNOWLEDGEMENTS

The authors would like to thank Margo Keeley and Elaine Null for their assistance and contributions to the work presented in this paper.

REFERENCES

1. Garbanati, L.F., and M.F. Shirley: Bell Communications Research, Inc., "Preliminary Analysis of Providing Optical Fiber to Residential Customer Premises," pp. 1-9.

2. Purkey, R.C., et al: "Architecture and Technology for the All-Fiber Loop," IEEE, 1988, pp. 0190-0196.

3. Skinner, S, et al: "RIDES™: Gateway Software to Support Raynet's New Loop Fiber Optics," FOC/LAN '88, pp. 247-254, (Sept. 12-16, 1988).

4. Large, D: "The Star-bus Network: Fiber Optics to the Home," CED Magazine, January, 1989, pp. 61-73.

Accessing the ripcord

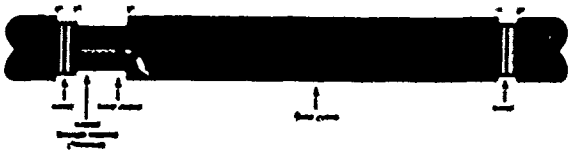

Figure 5

Removal of outer jacket/armor

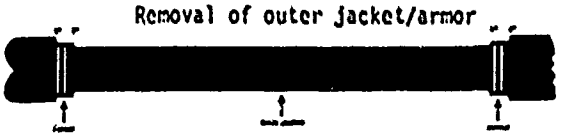

Figure 6

Removal of inner jacket

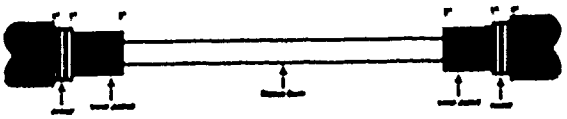

Figure 7

Removal of optical fibers

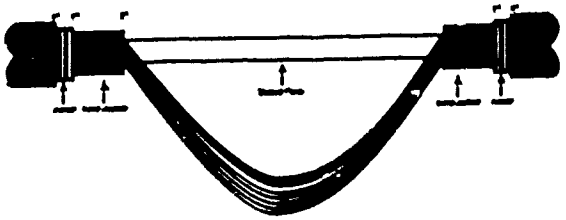

Figure 8

Removal of slotted core

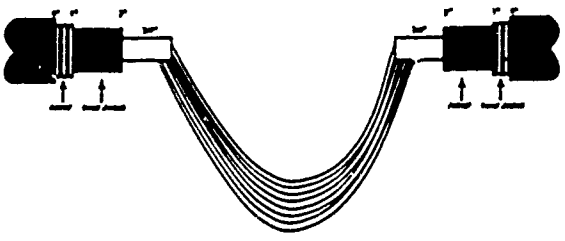

Figure 9

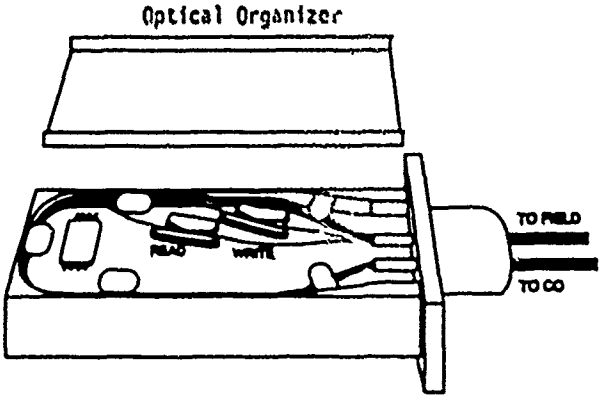

Figure 10

David P. Wong
Raynet Corporation
230 Constitution Drive
Menlo Park, CA

David P. Wong graduated from Georgia Institute of Technology in 1983 with a B.S. degree in Mechanical Engineering. Prior to joining Raynet Corporation (a subsidiary of Raychem Corporation), Mr. Wong was associated with Siecor Corporation where he worked in Applications Engineering as well as in Telephony Marketing as a Subscriber Loop Marketing Product Specialist. He was primarily involved with fiber optic cable testing and the design of fiber optic cables and hardware for the subscriber loop. Mr. Wong is currently working in Applications Engineering where he has been primarily involved with field trial support as well as documenting system installation and testing procedures. He is a member of IEEE.

Ralph A. Narciso
Raynet Corporation
230 Constitution Drive
Menlo Park, CA

Ralph Narciso is a member of the Applications Engineering Group for Raynet Corporation (a subsidiary of Raychem Corporation). He joined Raychem Corporation in 1974 after working for 6 years in central office switching with N. Y. Telephone. While at Raychem, Mr. Narciso worked primarily in product development. First, in advanced electrical interconnect systems and later in fiber optic emerging technologies, which included work with plastic clad fibers, temperature sensitive claddings, radiation hardened fiber, high and low temperature fiber cable constructions and fiber optic sensors. In 1985 Mr. Narciso joined the core development group of what was to become Raynet Corporation.

Development of Passive Optical Networks for Subscriber Loop Application in Australia

J. McCarter S. Rozental G. Nicholson I. MacGregor
G.J. Semple B.M. Smith

TELECOM AUSTRALIA
MELBOURNE, AUSTRALIA

ABSTRACT

The development of an experimental shared fibre passive optical system for subscriber loop applications is described. The paper considers the economic benefits of shared fibre architectures and discusses proposals for the further development of the experimental system to the field trial stage. The upgradeability of the system to carry future broadband services is also discussed.

1. Background

Single mode optical fibre systems have been installed extensively by Telecom Australia in the inter-exchange and long distance networks throughout Australia with in excess of some 200,000 fibre kilometres now installed. To date there has been only limited application of optical fibre in the Customer Access Network (CAN) i.e. the subscriber loop. Optical fibre systems have been used to serve large business customers with dedicated optical fibre cables linking the customer to the local exchange (central office). In addition, 120 line, remote customer multiplexers (RCMs) are being deployed in the CAN using optical fibre links to the local exchange.

Over the last two years, Telecom Australia has been conducting a trial in both Melbourne and Sydney of single mode fibre to the home. One of the main reasons for this trial was to uncover problems that may be encountered in the installation of fibre in an external plant environment that was designed for copper pair cable, and also discover any operational and maintenance difficulties associated with co-existent copper cable and fibre networks. The trial afforded the opportunity to test a number of splice enclosures and splicing techniques. Approximately ninety customers were connected in each city, with two fibres being used to provide each customer initially with a Plain Old Telephone Service (POTS). A small number of customers were then provided with five channels of distributive video. AM video transmission was used for compatibility with domestic TV sets. The AM video was transmitted over one fibre and the POTS equipment was modified using single mode biconical tapered couplers to operate over the second fibre. Passive splitting enables the output of the laser transmitter in the exchange video equipment to feed up to eight customers, thereby sharing the cost of this equipment.

Against this background of relatively limited use of fibre in the CAN due to economic considerations, Telecom Australia Research Laboratories conceived the idea of a MACNET system (Multiple Access Customer NETwork) which exploits a passive shared fibre network architecture for the provision of a mix of telecommunications services. [1,2]. An experimental MACNET system, developed under a contract placed with Australian industry was completed in October, 1988. This passive optical network development has paralleled similar developments reported by British Telecom Research Laboratories on their TPON system [3,4], although the two developments were independent.

2. Network Architecture

There are a number of network architectures, based on the use of optical fibre, that are potentially applicable to customer access networks in the next five year timeframe. The choice of the "optimum" network architecture(s) and associated transmission technique(s) is the subject of active investigation and field trials around the world. The different optical fibre network architectures can be broadly classified as:

(1) an active network which involves the use of outposted electronic equipment at a remote distribution point, such as multiplexing and/or switching equipment

(ii) a passive network (such as the MACNET system), which involves the use of optical combiners and splitters at the distribution point

(iii) a full star network, which involves dedicated (or direct) optical fibre links between the exchange and the customer

(iv) a physical loop network, which involves an optical fibre cable passing a number of customers, connected to individual fibres in the cable, in a loop arrangement from the exchange

(v) a metropolitan area network, utilising optical fibres, to support a particular metropolitan area network product such as the proposed IEEE 802.6 standard on DQDB. (Distributed Queue Dual Bus).

The choice of network architecture will depend on the application; the first two network options above, for example, are evolving from the use of optical fibre initially in the feeder cable sector (with RCM equipment) and subsequently for optical distribution to the customer. Longer term, all of these network architectures may well be implemented for different applications and customer sectors.

In Australia, in the case of the corporate business sector, where larger capacities are required and/or security is paramount, dedicated optical fibres or physical loops are considered the best approach. However, in most other applications where cost minimisation is an important issue, a shared passive optical network is an attractive alternative to active or full star networks. The choice between these three basic alternatives is not expected to become clear for at least one to two years and differ for different countries with their different regulatory and operational environments.

This paper discusses in some detail developments in Telecom Australia relating to shared fibre accesses.

3. The Experimental MACNET

The experimental MACNET system is based on the use of a single fibre which links the local exchange to a multiport optical coupler located in the street near a cluster of sixteen customers. Separate drop fibres connect each customer to the coupler. Customer information is contained in channel timeslots using continuous time division multiplexing downstream and sequential burstmode transmission upstream. Service access flexibility is achieved by microprocessor control of the number of time slots allocated to each customer.

A schematic of the experimental MACNET is shown in Fig. 1. Bi-directional access is achieved by the use of Wavelength Division Multiplexing (WDM) involving two closely spaced wavelengths in the 1300 nm window. Downstream transmission (towards the customer) is at a wavelength of 1320 nm, while the upstream transmission (towards the exchange) is at 1280 nm. The couplers used in the experimental MACNET have a nominally equal coupling ratio at 1300 nm and due to wavelength dependance, closely spaced wavelengths are used to minimise the variation in received power levels. The 16-port optical coupler can be located any distance up to 9 km from a local exchange; with each customer being located within 1 km of the coupler. The MACNET system was designed to address the problem of churn in the Customer Access Network (CAN), and incorporates flexible multiplexers which control the number of independent services allocated to a customer-end without the need to change any portion of the optical network. The primary access can be switched to any customer along with up to three of the basic accesses; the broadcast channel is available to all customers. Although there are no broadcast services carried in the Australian telecommunications network, it was envisaged that this channel could carry background music, stock reports, weather information, etc.

The experimental MACNET uses only one fibre for both directions of transmission as shown in Fig. 1.

3.1 Multiplexing

Time Division Multiplexing is used for both directions of transmission in the experimental MACNET.

From the separate customer-ends the upstream transmission of data associated with a particular service is transmitted as a data burst. The burst is triggered by the receipt of downstream data for that service. Because the drop fibres (i.e. the fibres from the multiport coupler to the customer-ends) are of variable lengths, the exchange receiver needs to be able to adjust its clock phase to cater for the variable transmission delays to achieve error free reception from each customer end. A header is added to each upstream data burst to facilitate this synchronization operation.

In the downstream direction, a header is also added which contains destination information - customer-end and port number. A portion of the broadcast data is inserted between each downstream data burst to separate the transmit times of the upstream data bursts, and thereby avoid collisions between upstream data bursts in the sixteen port passive optical coupler (see Fig. 2). The bit rate of the continuous downstream signal and the upstream signal bursts from each customer is 8192 kbit/s. Synchronization of the MACNET equipment is obtained from an exchange 2048 kbit/s clock.

3.2 Security

As the downstream data is available at all customer ends, precautions need to be taken to ensure adequate service security to each customer. In the experimental MACNET the directivity of the couplers guarantees security of the upstream data bursts. To ensure downstream security, an encryption key, generated by a random process in each customer-end is added to the header of each upstream data burst. At the exchange end this key is used to encrypt the subsequent downstream data signal.

3.3 Laboratory upgrade for broadcast video

To demonstrate the possible provision of a distributive video service as well as the provision of primary and basic access services, an eight channel frequency modulated (FM), super-trunk Sub-Carrier Multiplexed (SCM) video system was overlayed on the experimental MACNET as shown in Fig. 3. Because the optical couplers used in the experimental MACNET are wavelength dependent, the distributive video service had to be added at a wavelength close to 1300 nm - the wavelength at which all the couplers have a nominal equal split. As a consequence, the distributive video service was added by filtering the electrical drive signal to the exchange-end laser diode associated with the digital services so that the detected optical signal at a customer-end was free of harmonics above 100 MHz. The video signal was then restricted to the electrical band above 100 MHz. In this way eight channels of video were overlayed on the experimental MACNET.

4. Proposed System Development

Following a review of the technical viability and network application of the experimental MACNET system, Telecom Australia is currently considering the possibility of a significant-size field trial of a MACNET system of the configuration shown in Fig. 7. The system is based on the passive optical network supporting digital signals, at multiples of 2 Mbit/s, transmitted between the exchange and a maximum of 16 separate optical line transmission equipment (OLTE) terminals. The basic bit rate of 2 Mbit/s, based on CCITT Rec. G.703 interfaces, is chosen to avoid the MACNET system being service specific.

The two major applications identified for MACNET are catered for by:

- an outdoor OLTE terminal, with a 4x2 Mbit/s capacity; and
- an indoor OLTE terminal, with a 2x2 Mbit/s capacity.

Field trial experience may dictate other OLTE terminal options, although it is planned at this stage to have the option of partially-equipping OLTE terminals. The MACNET system is planned to incorporate a number of network maintenance and operations facilities, as well as the ability to interface control of these facilities to a network management system.

The passive optical network is based on separate fibres for each direction of transmission and 1300 nm operation. The use of separate fibres for each transmission direction is different to the experimental MACNET, described in Section 3. The choice of separate fibres is to ease constraints on system design, although in the longer term the choice between the dual or single fibre options is unclear. The MACNET system design calls for up to 20 km maximum transmission distance. The maximum differential distance between the exchange and any terminal is at least 1 km, although increasing this figure is being considered for rural applications. Also, while Fig. 7 indicates 1x16 optical couplers located at one site, in practice, the optical couplers may be deployed at more than one location, eg two stages of 1x4 optical couplers.

5. Economic Studies

In determining the potential economic application of a MACNET system, of the configuration proposed in Section 4, its use has been compared with alternative transmission methods available, in a least cost study for the two major applications identified. These cost studies relate to the proposed field trial equipment and not the experimental MACNET.

(a) use with field mounted RCM equipment for circuit growth.

(b) use in customer sites to provide 2 Mbit/s access (e.g. PABX access).

The transmission alternatives considered are:

(i) using existing copper pair cable and 2 Mbit/s line systems (denoted as "Free Cu" in Figures)

(ii) using new copper pair cable and 2 Mbit/s line systems (denoted as "New Cu" in Figures)

(iii) using direct optical fibre provision and 8 Mbit/s OLTE's (denoted as "Direct O/F" in Figures)

(iv) using a MACNET system (denoted as "MACNET" in Figures)

Cost relativity graphs for the various transmission alternatives are shown in Fig. 4 (Duct Costs Included) and in Fig. 5 (No Duct Costs), in the case of 2 Mbit/s access to customer sites. Fig. 6 demonstrates the component breakdown of relative cost at fixed distance of 3.5 kilometres from the exchange.

The major areas identified for MACNET application are:

- In urban residential and business areas, with moderate to high circuit growth requiring circuit relief or in new areas. MACNET is economic with RCM equipment for distances in excess of 1-4 km, depending on the growth rate and the comparative duct work required for Cu pair alternatives.

- In urban areas to provide digital access (based on 2 Mbit/s) to larger business customers or residential/business sites with a high number of services, such as a multi-tenant building. MACNET is economic, where existing copper pairs are not available for 2 Mbit/s access, for distances in excess of 1-3 km depending on the duct space available.

6. Evolution of a Passive Optical Network

In considering the use of a passive optical network it was seen as important to address the longer term options for evolving such a network to support broadband services or changing customer requirements. A key attribute of the proposed system is the use of CCITT Rec. G. 703, 2 Mbit/s interfaces for maximum service flexibility.

Passive optical networks are suited, compared with other optical network architectures, for low-cost provision of distributive video services such as Pay TV and interactive video. The proposed system development under consideration is designed to facilitate the provision of such services in the future, by

- including a 1550 nm wavelength optical blocking filter at the customer end in the equipment, to ensure future services can use the 1550 nm wavelength region in a network overlay arrangement without affecting existing services at 1300 nm

- including a 64 kbit/s channel to support the control and signalling of distributive video services, e.g. video channel selection, charging and access control.

As well, the proposed optical network design is based around a 16-way optical split and the use of wavelength-flattened optical couplers. This enables the entire wavelength range from about 1250 to 1550 nm to be used in the future. Services which could be simultaneously supported on such a network include

- Distributive video services, including HDTV
- Interactive and switched business video services
- Broadband ISDN

using analogue or digital transmission techniques as appropriate, with a mix of sub-carrier multiplexing and wavelength division multiplexing technology. In the very long term (post 2000), a passive optical network might provide the foundation for an all-optical (photonic) network.

It is also possible with a passive network, by utilising a separate fibre pair in the main cable, to provide at a later stage a dedicated fibre link to a particular customer. Such an example, could be a business initially served by a passive shared fibre optical network, whose service requirements change, favouring the migration to a dedicated link. Such a change does not require any re-working of the distribution plant, other than bypassing the optical couplers and direct connection to a feeder cable fibre pair.

7. Conclusion

This paper has described the development of an experimental passive optical network for subscriber loop applications. The cost effectiveness of such a system has been demonstrated against transmission alternatives. The possible development of an enhanced version of a passive optical system to a full scale field trial has been foreshadowed. The ability of such a system to simultaneously support future services such as Broadband ISDN has also been shown.

8. Acknowledgements

The authors wish to acknowledge the contributions of the numerous individuals who have played a part in the physical realisation of the experimental MACNET system.

The permission of the National General Manager Network & Consumer Services, Telecom Australia to publish this paper is hereby acknowledged.

References

(1) I.M. McGregor et al., "Optical Fibre Systems for the Customer Access Network"., Proceedings of 11th Australian Conference on Optical Fibre Technology, Geelong, Australia, December 1986, pp. 97-100.

(2) I.M. McGregor et al., "Implementation of a TDM Passive Optical Network for Subscriber Loop Applications", accepted for publication in IEEE J. Lightwave Technology.

(3) J.R. Stern et al., "Passive Optical Local Networks for Telephony Applications and Beyond", Electronics Letters, Vol. 23, November 1987, pp. 1255-1257.

(4) K.A. Oakley et al., Passive Fibre Loop for Telephony with Broadband Upgrade", Proceedings ISSLS'88, Boston, USA, September 1988, pp. 179-183.

JOHN C. McCARTER joined Telecom Australia as a cadet engineer in 1965. He graduated with a B.E. in Electrical Engineering from the University of Western Australia in 1968 and after a brief period with a regional administration joined the Telecom Australia National Office in Melbourne. Including a period of 12 months with Pacific Telephone & Telegraph Co in San Francisco Ca in 1968, Mr McCarter's career has been oriented towards outside plant and in particular, subscriber loop planning and design. He is currently Manager, Optical, Wideband & Implementation Planning Branch, Customer Access Network Unit.

IAN MacGREGOR joined Telecom Australia as a cadet engineer in 1961. At the completion of his B.E. degree he commenced work in the Telecom Australia Research Laboratories, but decided to return to Melbourne University to continue formal studies firstly towards a M.Eng.Sci. degree and then a Ph.D. In 1968 he returned to the Telecom Research Laboratories and worked in the field of Circuit Theory. From 1974 to 1984 he was Section Head of the section whose primary responsibility was circuit and system theory. In 1984 he joined the Optical Systems Section, and became interested in the application of optical fibre to the Customer Access Network. This work led to the development of MACNET. His primary Telecom interests now are centered around shared fibre architectures for the Customer Access Network, and their upgradeability for the delivery of high capacity services.

BERNARD M. SMITH was born in South Australia in 1943. He received the B.E. and Ph.D. degrees in electrical engineering from the University of Adelaide, Australia in 1964 and 1969 respectively.

He joined the Research Laboratories of Telecom Australia in 1968 and has been involved with various investigations into line transmission systems, digital data transmission and digital networks. He is currently Head, Optical Networks Section, Telecom Australia Research Laboratories. This Section is responsible for Telecom's research into optical fibre systems for the long distance and local applications, and studies in metropolitan area networks and broadband ISDN access techniques.

He is a senior member of the IEEE.

G. JOHN SEMPLE received the degrees of Bachelor of Engineering and a Master of Engineering Science from the University of Melbourne in 1966 and 1968 respectively. He joined the new Telecom Australia Research Laboratories in January 1967 and was initially concerned with problems associated with the application of primary level PCM and high capacity digital transmission systems. In 1980 Mr Semple became involved with the investigation of the local digital reticulation systems required for the delivery of basic rate ISDN services. Since 1985 John has been involved with the application of optical fibre in the customer access network. This work involves the study of new optical fibre network architectures and systems that will not only facilitate the introduction of new wideband customer services such as distributive and interactive video services but will also, in the near future, permit the cost effective delivery of the existing range of telecommunication services.

GRANT NICHOLSON was born in Hobart, Tasmania, Australia in 1955. He received the B.E. (Honours) degree and the M.Eng.Sc. degree from the University of Tasmania, Australia in 1976 and 1978 respectively.

Since 1978 he has been with the Transmission Networks and Standards Branch of the Telecom Australia Research Laboratories. He is presently leading a project group, within the Optical Networks Section, concerned with optical fibre systems for the customer access part of the telecommunications network. His research interests include modelling direct-detection and coherent, optical fibre communication systems.

SYMON ROZENTAL joined Telecom Australia in 1969 after completing his Bachelors Degree in Communications Engineering from Royal Melbourne Institute of Technology. His background experience covers planning of digital transmission in interexchange networks including economic studies relating to the application of optical fibre transmission systems. Mr. Rozental is currently Manager, Optical Fibre Implementation Planning Section, responsible for the formulation of planning guidelines for the introduction of optical fibre infrastructure into the Customer Access Network.

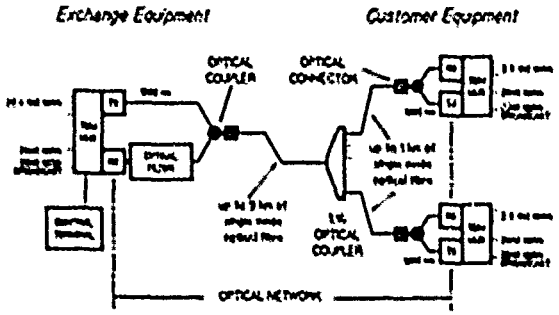

Fig. 1 The Experimental MACNET

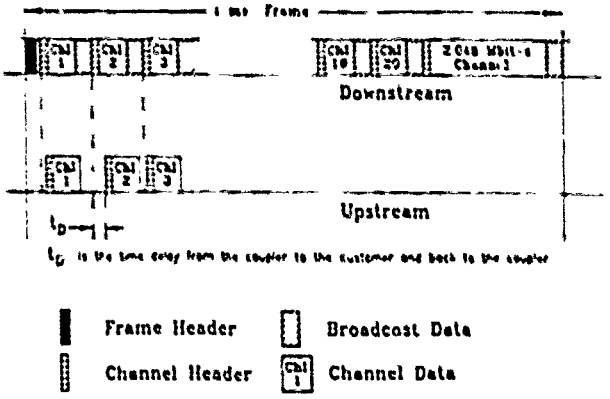

Fig. 2 Frame Structure - The Experimental MACNET

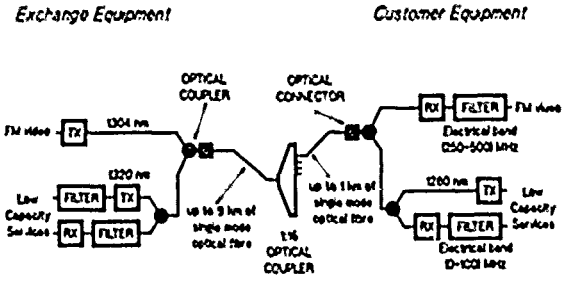

Fig. 3 Distributive Video - Experimental MACNET

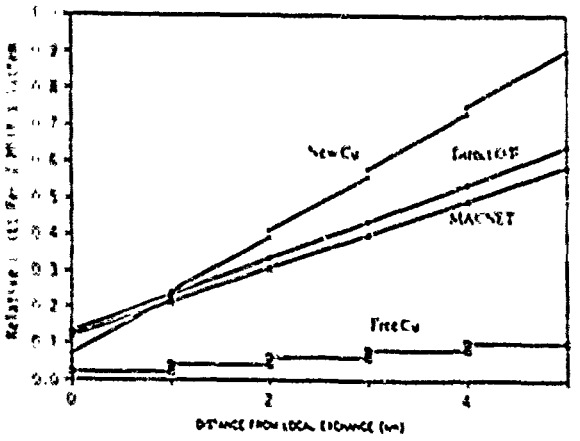

Fig. 4 Present Value Cost of Transmission for 2 Mbit/s Access (Duct Costs Included)

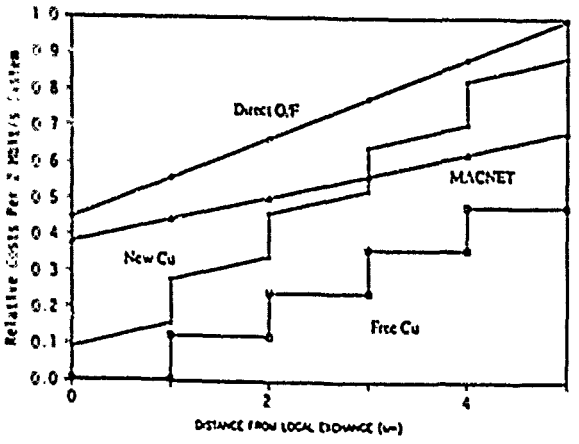

Fig. 5 Present Value Cost of Transmission for 2 Mbit/s Access(No Duct Costs)

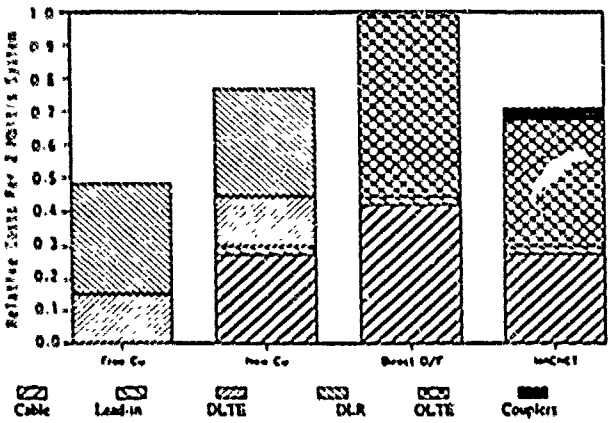

Fig. 6 Component Breakdown of Cost per 2 Mbit/s Access (3.5 km, No Duct and Pipe Costs)

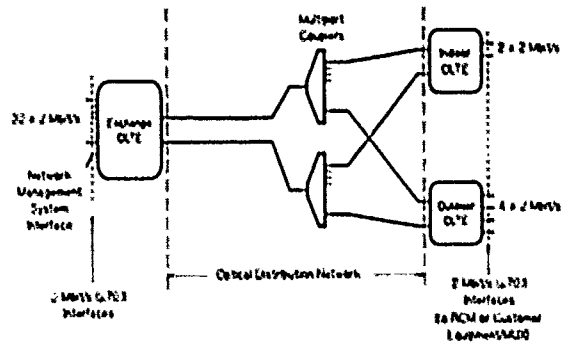

Fig. 7 Proposed Configuration for Passive Optical Network System

FIBER-TO-THE-HOME UPDATE: DROP INSTALLATION FLEXIBILITY

G. S. Cobb, W. H. Bensel and J. B. Haber

AT&T Bell Laboratories
Norcross, Georgia 30071

M. M. Dixit

AT&T Bell Laboratories
Whippany, New Jersey

ABSTRACT

In 1988, AT&T was among the first system suppliers to introduce a single-mode fiber-to-the-subscriber system with its SLC® Series 5 Digital Loop Carrier System Fiber-to-the-Home feature package. The early installations used a network of cables, splices, connectors and closures to supply a one fiber drop cable to each subscriber in a star-type architecture from a Remote Terminal to the subscriber's home. This year, preconnectorized service cables and lightguide terminals with connector ports have been introduced that offer new options which can substantially reduce service cable installation times. Preterm, the name given to a copper distribution/drop assembly manufactured off-site, has also been demonstrated in a fiber distribution/drop application with the initial installation in Charleston, South Carolina. An enhanced lightguide pedestal closure has been designed, built upon experience from early installations. A self-supporting aerial drop cable and a new lightguide aerial terminal are also being developed to allow the fiber optic system to be used in new and rehabilitation aerial applications. This paper describes the products and their design criteria that support the new, preconnectorized, preterminated plant applications, giving the telco a high degree of flexibility in methods and configurations.

1. Introduction

The year 1988 will be remembered as the year of many first Fiber-to-the-Subscriber (FITS) applications for many telephone companies. No longer were we in the "trial" stage, but an architecture was established and systems designed to deliver optical signals to the customer's premise. Service was turned up over fiber in upscale communities across the country in places like Princeton Gate in New Jersey; the Grove of Riveredge in TN, in Hallbrook Farms, a golf course community in KS; and in Ridgecrest, CA in a new housing development near the China Lake Naval Facility. Much was learned during these first applications, especially about the economic issues that must be solved if the potential of fiber is to be fully realized in the distribution plant.

It is this intense interest in economics that has lead many telephone companies to experiment with the very last component used in connecting the customer with fiber - the drop cable. As the year 1988 will be remembered for its large scale deployment of FITS systems, 1989 might be remembered as the year of Drop Cable Installation Trials.

2. Basic Architecture

AT&T's FITS offering shown schematically in Figure 1 is based on the SLC Series 5 Digital Loop Carrier system which has been extended from a feeder-only system to include loop distribution. Typically, in the feeder portion of the network, a DDM 1000 lightwave multiplexer provides high capacity digital service from the central office to a remote terminal. This type of feeder arrangement is used today with conventional copper distribution. The modifications to the SLC® Series 5 carrier system that allow all-fiber distribution begin at the RT. New channel units allow up to 4-lines of POTS service to a subscriber; these new channel units are connected to optical units that deliver DS1 optical signals over a single-mode fiber to a distant terminal either on the side of a subscriber's home (for fiber-all-the-way-to-the-home) or to one of a group of distant terminals located in a pedestal at the subscriber's property line (fiber-to-the-curb). The distant terminal is equipped with an optical unit and a channel unit and can both receive and transmit 1.5 Mbps optical signals over the single-mode fiber. Optical splitters at each end of the fiber allow bidirectional transmission over the fiber at 1310 nm.

FIGURE 1. FIBER TO THE HOME FEATURE ON SLC® SERIES 5 CARRIER SYSTEM

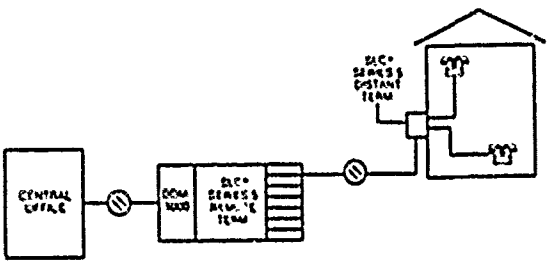

The media architecture for FITS is essentially a double star. Feeder cables emanate out from a CO to several RTs, and distribution cables fan out from the RTs into the distribution areas they serve. Typically, high fiber count backbone cables are used to branch out from the RTs, and at various branching points, groups of the backbone fibers are spliced to fibers in lower count lateral cables to carry service farther into the neighborhoods. When service is carried over fiber all the way to the subscriber's home, a fiber service cable is spliced to the distribution cable at the subscriber's property line, and a single-mode connector is used to join the service cable fiber to the distant terminal optical card. In applications where it is more economical to share the distant terminal among two or more subscribers, the distant terminals are "clustered" into a pedestal, and service to individual subscribers is completed with standard twisted pair cables. Most of the 1988 and 1989 installations have been fiber-all-the-way-to-the-home. A small number of applications (where lot sizes are relatively small and line demand is low) are being approached with shared electronics arrangements this year. The future probably holds a fair mix of both types of installations. The focus of this paper is, as was mentioned earlier, on options that help cost reduce fiber-all-the-way-to-the-home installations.

3. Curb to Premise Flexibility

3.1 Standard Lightguide Solutions

In all plant types, the final link must connect the customer to the distribution cable. Over the past year or so, this has been accomplished by splicing the service cable(s) (i.e., drops) into the distribution cable and enclosing the splice with lightguide splice closures, most of which were originally designed for trunk and long haul applications. The customer end of the drop was terminated with a field-installed ST® connector which was plugged into the Distant Terminal (DT) at the premise. This operation required the services of a skilled splicer, considerable capital investment in tools, and a splicing van or trailer. In many cases, where homes were not completed, it required multiple visits of the splicer.

3.2 New Methods

Driving new methods for the "last 100 feet" - or the drop - were the customers' concern over:

1. The diminishing number of skilled splicers and the need to have installers "connect" customers.
2. The need to install drop cables on an "as needed basis".
3. The need for fast restoration times, again using installer level skill and tools.

In response to these customers' concerns, new approaches including the introduction of preconnectorized drop cable, easy access terminals, a new drop closure and an approach similar to a former copper plant configuration, preterm, are being developed.

3.3 Preconnectorized Drop Cable Hardware

As previously described, the standard FTTS drop cable installation required the field installation of a ST connector to connect the drop cable to the DT. It was a relatively small step to consider connectorizing both ends of the drop in a controlled manufacturing environment. The manufacturing site could be a factory, a service center, or even a work center location, provided the ability to accurately test the product is available.

3.3.1 Design Criteria

There are installation circumstances that might require one end of a preconnectorized drop cable to be stored, either directly buried or in a hand hole, for periods up to two years before being put into use. Thus, it is not only necessary to properly install the ST connectors on the drop cable end, but also to package the connectorized end assembly for storage in an adverse environment. In other words, a temporary closure that can withstand the rigors of direct burial or immersion in a handhole for prolonged periods of time is required. The design criteria for such a temporary closure follow. The design must:

- Accommodate either dielectric or metallic service cables
- Accommodate one or two fibers per service cable
- Withstand a 10-foot external water head
- Withstand a 10-foot water head through a sheath fault
- Have a tensile pullout of 50 lbs.
- Allow a compression load of 200 lbs.
- Withstand an impact load of 120 inch-lbs.
- Resist chemicals typically found in soils
- Be available in single and double ended lengths of 100 ft. to 300 ft.
- Allow adequate buffered fiber length to mate with all termination devices at either premise or curb.
- Be flexible enough to store in meter boxes with less than 12 inch diameter
- Require no special tools or skills to install in field
- Achieve insertion loss ≤ 0.7 dB
- Achieve return loss ≤ -35 dB

3.3.2 Resulting Design

The most difficult design problem to solve is water entry due to a sheath fault. Much attention has recently been placed on distribution cable design, and tremendous progress has been made in water-blocking. This same kind of effort is now taking place with drop cable designs, but currently available water blocking techniques are not 100% perfect. For closure design work, a sheath fault is defined as a 2-inch length of all cable members, except core tube, which is removed six inches from the closure. A 10-foot water head is injected into the fault. The closure design must not allow water to enter the splice space, or in this situation, the space where the ST connectors are stored.

The design problem for dielectric drop cable hardware was solved by placing water-blocking tape over the sheath and core tube and holding it in place with shrink tubing. The water-blocking tape is the same material that is used to water-block lightguide cable. The tape contains a polymer which swells when it contacts water and thus blocks the water path. Laboratory test cable samples, blocked by this technique have been able to withstand 25-ft. water heads over extended periods of time.

Solving the water-blocking problem for the metallic drop cable was not as straightforward because a #14 gauge conductor attached to the drop cable shield must pass through the water-block. As shown in Figure 2, water-blocking tape was used over the sheath in the same manner as used in the dielectric design. To accommodate the irregular shapes of the electrical connection, a cured urethane elastomer material was used to fill the interstices between the core tube and the #14 gauge conductor. Heat shrink tubing was used to contain both water blocking materials. This design also passed the extended 25 ft. water head test.

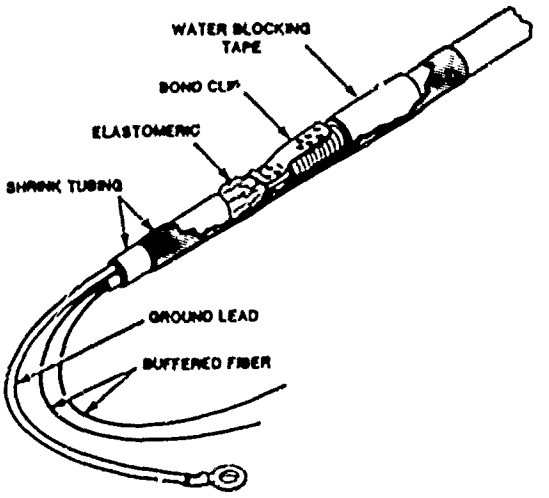

FIGURE 2. WATER BLOCK, METALLIC DROP CABLE

Figure 3 shows a complete preconnectorized drop cable end inside its protective tube assembly. The protective tube assembly was made from commercially available flexible PVC electrical conduit and solvent glued to a PVC cap on one end and a PVC adapter on the other end. The result is a very robust structure. A commercially available connector forms the seal to the drop cable sheath, provides the 50 lb. tensile pull capability and attaches to the tube assembly via

a water tight pipe thread. A length of plastic strap and a clear tube are used to support the buffered fiber and connectors during shipment and storage. The design is not only simple in concept, but it is also relatively inexpensive because it uses existing materials or parts.

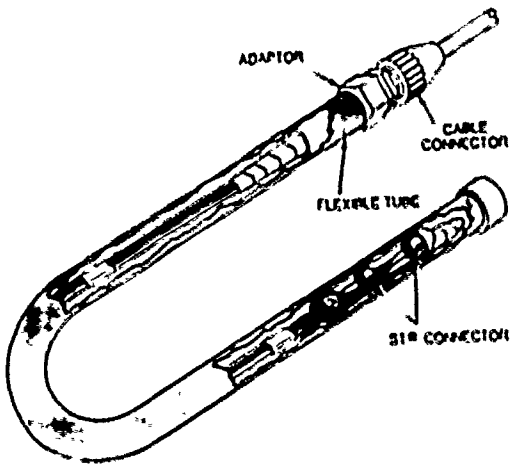

FIGURE 3. DROP CABLE PROTECTOR

3.4 Curbside Apparatus

To fully exploit the preconnectorized drop concept, a curbside (this could also be a rear lot line) facility that readily accepts the preconnectorized drop assembly with a minimum of skill and tools is required. Two options appear feasible for this facility. The best option for a particular application depends on plant type, the type of construction (new or rehab), construction timing, and the availability of craft.

The first option includes a drop closure or terminals that are specifically designed to accept the preconnectorized drop. The closure or terminal must cover a range of possible applications: direct burial, above-ground pedestal, below ground handholes and aerial installations. The drop closure must not only accommodate a number of customer drops; the design should provide a protective environment for expressed fibers, be very easy to enter and close, and not require the use of encapsulants except for the initial installation of distribution cables.

3.4.1 Drop Closure

The 2500LG/DC drop closure shown in Figure 4 was designed specifically to mate with the preconnectorized drop cable in buried or handhole environments. Four dielectric or four metallic drops can be accommodated in the cable ports. Eight ST connectors can be stored in the organizer tray. Expressed fibers, either ribbon or individual, are stored below in the distribution tray. Distribution cables with diameters up to 0.60 inch and drop cables with diameters up to 0.30 inch can be used. Easy access is achieved with five stainless steel overcenter fasteners. The primary seal is a gasoline resistance O-ring. Bonding and sheath retention are performed upon initial installation in a small compartment which is encapsulated to prevent water accumulation. This compartment is not entered or disturbed on subsequent re-entry for drop cable installation. The drop entry port mates with the preconnectorized connector.

If the drop cables are not preconnectorized, the 2500LG/DC is furnished with kits to field terminate the drop and splice it to the distribution fiber with rotary splices or fusion methods. The maximum number of splices the 2500LG/DC closure can accommodate is eight. The 2500LG/DC therefore functions as either a terminal or a splice closure.

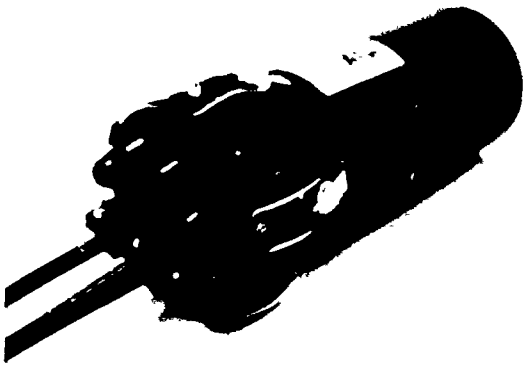

FIGURE 4. 2500LG/DC DROP CLOSURE

3.4.2 Buried Terminal

A second closure/terminal configuration to accommodate preconnectorized drops employs a cable stub that runs from a direct buried distribution splice to a terminal located in a handhole. The terminal provides a fiber appearance for each of several customers. In this approach, the expressed fibers are stored in a splice closure that need not be accessed by the drop cable installer. Design criteria for the buried terminal were established as follows. The terminal should:

- Be easily entered and closed with no special tools.
- Withstand 10-foot external waterhead.
- Withstand 10-foot waterhead sheath fault.
- Accommodate up to twelve drop cables.
- Accommodate up to twenty-four ST Connectors.
- Accommodate metallic and dielectric drop cables.
- Easily accept preconnectorized drop cables.

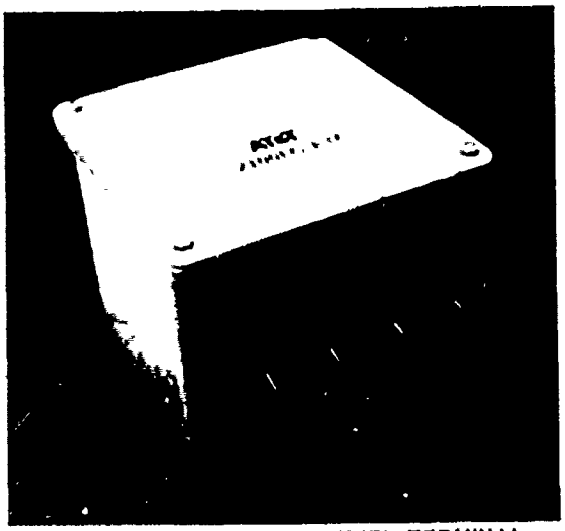

FIGURE 5. 2100LG/BT BURIED TERMINAL

Figure 5 shows the 2100LG/BT terminal. Two sizes were actually designed; the first handles up to six drops and the second to handle up to twelve drops. A PVC utility box houses a panel that acts as a coupling field. The stub cable and the drop cable terminations are attached and sealed to the terminal housing using a cable connector

and an O-ring. The terminal top is sealed using an elastomeric gasket and B-Sealant. Electrical bonding of all metallic members, when required, is achieved with a common copper bus. The preconnectorized drop cable is installed by placing an O-ring over the connector pipe thread inserting it through the appropriate port, and fastening it with a lock nut on the inside of the terminal.

3.4.3 Pedestal Terminal

In areas where buried lightguide cable is used but the distribution splices are not buried or placed in handholes, a pedestal terminal can be utilized. Design criteria for a pedestal terminal were established as follow. The terminal should:

- Protect of the fibers and splices from the environment.
- Accommodate a minimum of six metallic or dielectric drop cables
- Accommodate up to twelve ST connectors or 12 rotary splices.
- Provide safe storage of express fibers.
- Easily accept preconnectorized drop cables.
- Use the same splice tray(s) that are used in other AT&T Lightguide Closure Products.
- Require no special tools for installation.

One such terminal, shown in Figure 6, meeting these criteria is the newly designed 2300LG/PT. The terminal, molded from rugged plastic, is housed within a standard 6-inch pedestal enclosure. It consists of three major parts, a housing, a cover, and a grommet. Not shown in Figure 6 is the splice tray. The pedestal terminal can accommodate either an ST connector tray, the 12 or 24 fiber splice tray or an array splice tray used with ribbon cable. Electrical bonding of the distribution and drop cables is done external to the terminal but inside the 6-inch pedestal enclosure with standard techniques. The one piece elastomeric grommet accommodates two distribution cables and up to eight drops. Drop cable ports are a "punch out" design which do not require plugs when they are not being used. Unlike grommets in buried apparatus, the pedestal grommet does not have to form a water tight seal. It must, however, provide a barrier to insects. Slits in the grommet permit the use of preconnectorized drop cables. While the 2300LG/PT functions primarily as a terminal in FTTS applications, it can also be used for above ground cable-to-cable splices having up to twenty-four fibers.

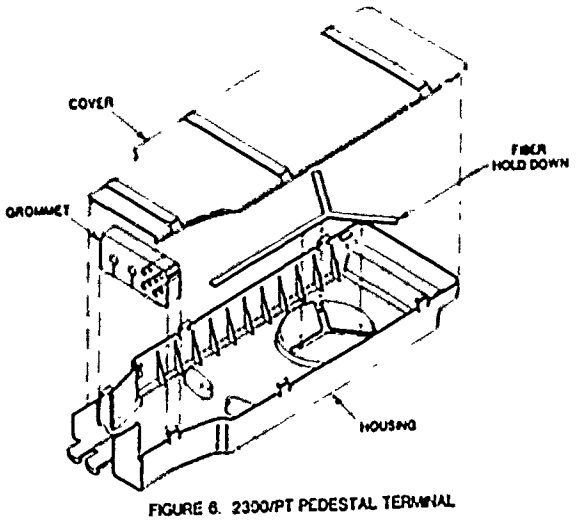

FIGURE 6. 2300/PT PEDESTAL TERMINAL

3.4.4 Aerial Terminal

The last closure/terminal option to be described is that for aerial applications. Design criteria established for the pedestal terminal are also applicable to an aerial terminal. The 2200LG/AT was designed to meet these criteria. Hung from an aerial strand, the 2200LG/AT consists of an injection molded rugged plastic housing and cover. Eight drop cables can be accommodated by individual grommets, four on each end of the terminal. The grommets are slit to allow the use of preconnectorized drop cables. Electrical bonding and grounding to the strand is facilitated by a ground bar which runs on the bottom of the terminal and connects to the support hangers on either end. As was the case in the pedestal terminal, the aerial terminal can be fitted with an ST connector tray, an array splice tray or a mechanical splice tray holding up to twenty-four splices.

3.5 Preterm - Preterminated Distribution Facilities

Thus far, we have discussed closures and terminals that were designed specifically to provide facilities for the terminating drop cable at the street. The 2500LG/DC and 2100LG/BT are used in buried or handhole environments. The 2300LG/PT is used in pedestal applications and the 2200LG/AT is to be used in aerial applications.

The second option for providing easier drop cable installation is to use the preterm concept. People familiar with copper plant construction methods will recognize the name. This concept has been used quite successfully in copper plant when applied to the appropriate outside plant conditions. Preterm, as shown in Figure 7, simply includes pre-installation joining of the drop cable fibers to the appropriate distribution fibers, splice encasement in a closure, and organization of the cable network on a cable reel. The cable reel assembly is taken to the field after the distribution trench is opened and the cable is rolled out into the trench. If drop trenches are already present, the drop cable is laid in the trench. If the drop cable trenches are not open, the drop is stored at the street for later installation. Connector protection is advisable for Lightguide Preterm Installation. The end of the drop cable that goes to the DT and is preconnectorized with ST® connectors, should have a cover installed to protect the connectors during reel storage, shipment and possible onsite storage. Connectorization and water blocking techniques similar to those used with the preconnectorized drop cable product can achieve the required level of protection.

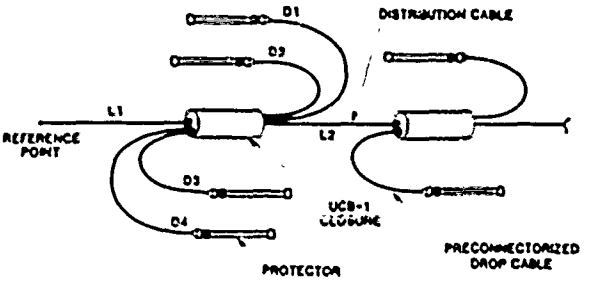

FIGURE 7 PRETERM

Crowfield Plantation, a riverfront community west of Charleston, South Carolina, was the first application of Lightguide Preterm. Eighty-four homes were served by four reels of preterm. The majority of the distribution points provided drop cables for four homes while a few served two homes. All distribution splice points were enclosed in the UCB-1 Universal Closures in an assembly that took place at the manufacturing site. End-to-end testing of all drop connection were made as they were built. Once installed in the field, the UCB-1 closure is placed in a 51D3 outer closure and encapsulated. Because most of the homes would not be completed at

the time of cable placement, the connectorized DT end of the drop cable was to be stored at the street and protected with the previously described methods.

The approach used at Crowfield allowed fast initial installation but not the easiest reentry for replacement of drops or for testing. Using the knowledge gained in the building Crowfield installation, a second preterm project is being planned that will combine the best of the preterm approach used in Crowfield with the accessibility of the 2100LG/BT Terminal and the cost effectiveness of the 2500LG/DC Closure. This architecture is shown in Figure 8. A stub cable containing the appropriate number of fibers to serve customers will be spliced at each distribution point. The splice will be enclosed in a 2500LG/DC and the other end of the stub will be connectorized with ST connectors and a protective package. The assembly will be organized on a reel as was done for the Crowfield installation. When the assembly is installed in the field, the 2100LG/BT will be installed on the connectorized stub and stored in a handhole. As homes are built, an installer will bring a double-ended connectorized drop to the field. The drop will be placed in a trench and the preconnectorized ends will be plugged into the 2100LG terminal and in the DT on the customer's premise.

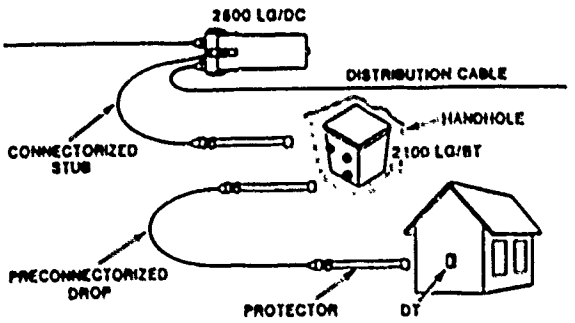

FIGURE 8. ENHANCED PRETERM

4. Testing Requirements

4.1 Optical Testing

Optical testing of the installed ST connectors is required on preconnectorized drop and preterm drops. Two measurements, Insertion Loss and Return Loss, are made. Both measurements are made against a reference assembly consisting of a length of fiber jumper, having ST connectors on both ends and a coupling on one end. Measurements are typically made at 1310 nm. Test requirements are set usually by the customer.

Preterm projects can result in some very long lengths of fiber to be tested along with the ST connector. In this case, a method is agreed to with the customer, to either alter the test requirement, or subtract out a known cable loss.

4.2 Mechanical & Environmental Testing

4.2.1 Buried Terminal

To determine the suitability of the PVC terminal housing for outside plant use, a number of mechanical, material and environmental tests were performed. To date, a Bellcore specification has not been released for lightguide terminal applications. However, since these terminals are intended for handhole and buried applications, Bellcore type tests were conducted in accordance with their specification TR-TSY-000771 dated 10/88. Results were as follows:

MECHANICAL	
Cable Pullout	
Distribution Cable	100 lbs
Drop Cable	50 lbs.
Compression	400 lbs., 15 minutes
Impact	10 ft-lb, 0°F & 100°F
ENVIRONMENTAL	
Water Immersion	10 Foot Water Head
Cable Fault	10 Foot Water Head
Freeze-thaw	40 Cycles (In Progress)
Salt-Fog Corrosion	30 Day Exposure (In Progress)
MATERIAL	
Chemical Resistance	30 Day Exposure (In Progress)
Fungus Resistance	30 Day Exposure (In Progress)

4.2.2 Splice Closure

The 2500LG/DC4 closure functions both as a splice closure and as a terminal. Bellcore has establish a uniform set of functional design and performance criteria in the recently released TR-TSY-000777. The 2500LG/DC4 closure is presently undergoing mechanical, electrical and environment testing required by this specification.

4.2.3 Preconnectorized Drops

Preconnectorized drops are not permanently installed in the outside plant environment. However, temporary storage in a buried and handhole environment could last up to two years. A number of mechanical tests and resistance to water entry are necessary to insure meeting the design intent of the product. Typical tests and their results are:

MECHANICAL TEST	
Impact	10 ft-lb
Static Load:	
Distribution Cable	100 lbs, 15 minutes
Drop Cable	50 lbs, 15 minutes
Compression	200 lbs
ENVIRONMENTAL TESTS	
Water Immersion	10 Foot Water Head
Sheath Fault	10 Foot Water Head

5. Summary

Fiber is now moving into the "last 100 feet". The architecture, fiber-all-the-way-to-the-home, requires low-cost, easy-to-install drop components. A need for flexibility in drop cable design, configuration and installation methods is required by the telcos. To accommodate the many types of drop cables, different OSP approaches, connectorized and non-connectorized cables and variable craft skill levels, new kinds of drop apparatus have been designed. A series of products were developed that accommodate either splices or preconnectorized ST connectors for buried, pedestal, handhole, and aerial plant. The fiber drop cable can be preconnectorized in a factory environment, enhancing reliability and substantially decreasing field installation time. The complementary closures and terminals to accept the preconnectorized drops have readily available connector ports that allow fast, easy installation by installer level craft.

GARY S. COBB
AT&T Bell Laboratories
Norcross, GA

Gary S. Cobb is a Distinguished Member of Technical Staff in the Lightguide Apparatus Department of AT&T Bell Laboratories, located in Norcross, Georgia. He is presently responsible for the design and development of Lightguide Closures. Prior to this assignment, he was the Project Engineer for various copper splice closures and for CONECS. Mr. Cobb was active in the development of Sea Plow IV, a vehicle for burying ocean cable. Before that he was involved in the design and development of ocean cable and associated hardware. Mr. Cobb received his BSME degree from Virginia Polytechnic Institute and State University and an MSME from the University of Maryland.

JANICE B. HABER
AT&T Bell Laboratories
Norcross, GA

Janice B. Haber is Technical Supervisor of the Lightguide Systems Engineering Group at AT&T Bell Laboratories, Norcross, Georgia. Her group provides technical support for AT&T's fiber-to-the-customer applications as well as long distance and trunking networks. Janice holds a BSEE degree from the University of Maryland and an MSEE degree from the Georgia Institute of Technology.

WILLIAM H. BENSEL
AT&T Bell Laboratories
Norcross, GA

William H. Bensel is a Member of Technical Staff-I in the Lightguide Apparatus Department at AT&T Bell Laboratories, Norcross, Georgia. He joined Bell Laboratories in 1969 after receiving an Associate Degree in Electrical Engineering from Baltimore Junior College. Since 1980, he has been engaged in the development, testing and evaluation of fiber optic closure sealing systems.

M. M. DIXIT
AT&T Bell Laboratories
Whippany, NJ

M. M. Dixit received his B.E. in Mechanical Engineering from Maharaja Sayajirao University, India in 1979 and his M.E. in Mechanical Engineering from the City College of City University of New York in 1985. He began work at AT&T Bell Laboratories in 1985 where he is a member of the Distribution Apparatus Group. For the past two years, he has been involved with the development of terminals and closures for the Fiber-to-the-Subscriber System.

A SZ SLOT RIBBON FIBER CABLE FOR SUBSCRIBER NETWORK

N. Okada [*1], A. Mogi [*1], N. Minono [*1], T. Hayakawa [*2]
M. Miyazaki [*3], M. kurokawa [*4], K. Nilkura [*5]

*1 Fujikura Ltd. Chiba, Japan
*2 Fujikura Ltd. Tokyo, Japan
*3 Tokyo Electric Power Co.,Inc. Tokyo, Japan
*4 Furukawa Electric Co.,Ltd. Tokyo, Japan
*5 Sumitomo Electric Industries, Ltd. Yokohama, Japan

Abstract

A newly designed optical fiber cable for the subscriber network has been successfully developed. The new cable has a SZ slotted structure specially designed and can accommodate up to sixty four 2-fiber ribbons. The cable has excellent properties on mid span access as well as excellent optical and mechanical characteristics under severe environmental conditions.

1. Introduction

As optical fiber cable systems begin to spread to subscriber networks, from the economical view point of the optical cable networks, it is very important for growing subscriber networks to have capability of mid span access from a laying cable. The key technology is how to joint the cable with another to be branched without disturbing the service of the other live lines.[1),2)]

For easy operation on mid span access. the following criteria have to be taken into account on the cable design.

1)How to get the sufficient excess fiber length to splice.
2)How to make fiber identification easy.
3)How to splice the target fibers easily without disturbing the service of the other live lines.

The newly developed cables are composed of a SZ slotted rod and 2-fiber ribbons. The SZ slotted structure makes it possible to get the excess fiber length, so target fibers can be easily taken out from the slots. And the ribbon structure is effective for easy fiber handling and fiber identification.

Now these optical cables have been in commercial service in Japan for one year.

2. Cable design

2-1.Cable structure

On mid span access, a cable is required a certain amount of excess fiber length to take the target fibers out and to splice the fibers.

One of the solution to the requirement is to adopt a SZ technology to fiber stranding.

Determining a cable structure, a lateral force resistance have to be taken into one of the considerations. A slotted core structure is the best choice for that requirement.

Therefore, a SZ slotted core cable was newly developed for a mid span access application.

For easy mid span operation, there must be an excess fiber length as much as possible. From the experimental results, the necessary slack for mid span operation is at least 15mm. This amount of slack has to be got from 500mm cable length which is equivalent to the length of jointing closure.

On the basis of these criteria, the parameters of the SZ slotted rods, such as the SZ lay length, the SZ reverse angle, the pitch diameter and etc., have been determined. Fig.1 shows the cable structure.

2-2.Optical fiber structure

Optical fiber structure is designed to satisfy following criteria for easy operation on mid span access.

1)Fiber identification
It is desirable that the cables for subscriber networks can accommodate a large number of fibers. Therefore, the easy identification of fibers is important.

2)Fiber handling

On mid span access, the target fibers have to be taken out from the laying cable without disturbing the service of the other live line. In another word, the optical loss increase exceeding the system limit is not allowed for the fibers in service during a mid span operation. So the optical fiber must have a suitable mechanical resistance in terms of loss increase.

On the basis of these criteria, the 2-fiber ribbon structure is used. Fig.2 shows the cross sectional view of the newly developed 2-fiber ribbon.

Generally, a pair of fibers are used for bi-directional signal transmission in subscriber networks. Therefore the 2-fiber ribbon structure is convenient for fiber handling, such as mid span access and fiber splicing , because of unity. Furthermore, the structure produces the moderate stiffness compared with mono-fibers to suppress the excess loss due to fiber bending.

The 2-fiber ribbons can be easily identified from the coloring of fibers as shown in Fig.2, so it is possible to identify many fibers in a slot.

The 2-fiber ribbons can be divided to individual fibers, as a result, the 2-fiber ribbon can be also spliced to each mono-fibers as shown in Fig.3.

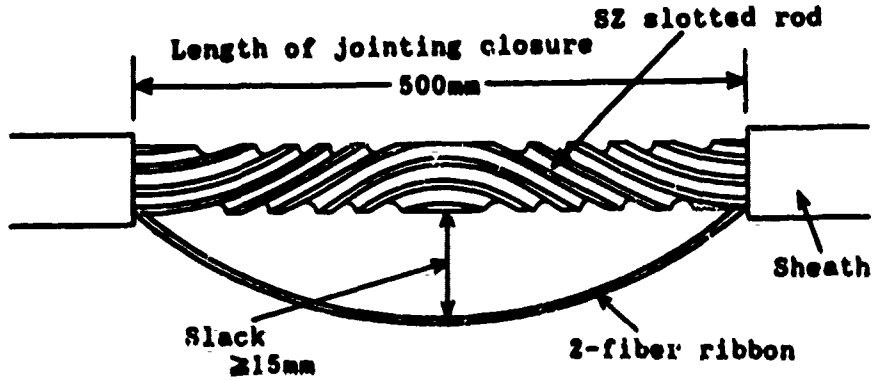

Fig.1 Cable structure

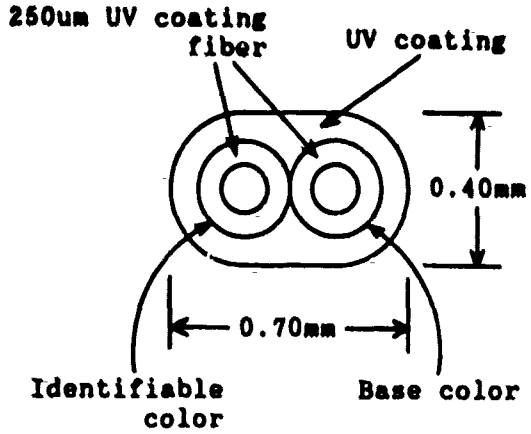

Fig.2 2-fiber ribbon structure

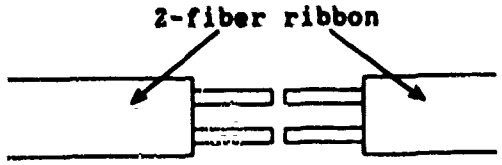

Splice of 2-fiber ribbon

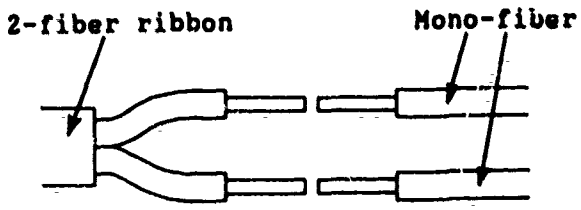

Divided into two fibers

Fig.3 Splice of fiber

We have developed three types of the SZ slot 2-fiber ribbon cables so as to meet several needs and the environments. These cables are following.

1)48-fiber type metallic cable
2)48-fiber type non-metallic cable
3)128-fiber type metallic cable

The cross sectional views of these cables are shown in Fig.4.

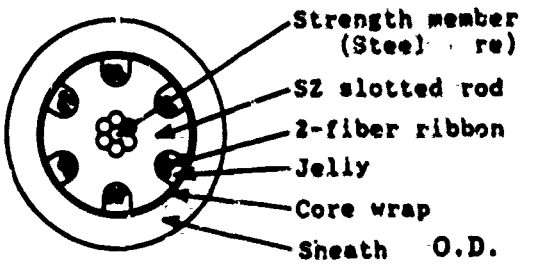

48-fiber type metallic cable

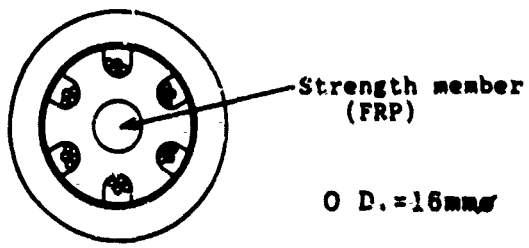

48-fiber type non-metallic cable

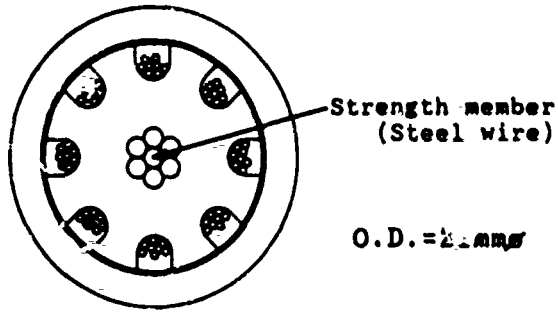

128-fiber type metallic cable

Fig.4 Cross section of cable

3. Cable properties

The cable properties are mainly described in a 128-fiber type metallic cable. The cable was manufactured experimentally and subjected to several tests. The fibers used for the experimental cable were single-mode fibers. The parameters of the fibers are shown in Table 1. The cable properties were investigated by the measuring of loss changes at 1300nm wavelength.

Table 1 Fiber parameters

Items	Parameters
Fiber	Single mode fiber
Attenuation	Less than 0.40dB/km at 1.30μm
MFD	10±1μm
λc	1.10~1.26μm

3-1.Attenuation in cable manufacturing

Fig.5 shows the loss of the optical fibers measured at each manufacturing processes. The loss changes through cabling are less than 0.02dB/km. It is verified that this cable can be manufactured easily without attenuation changes through cabling.

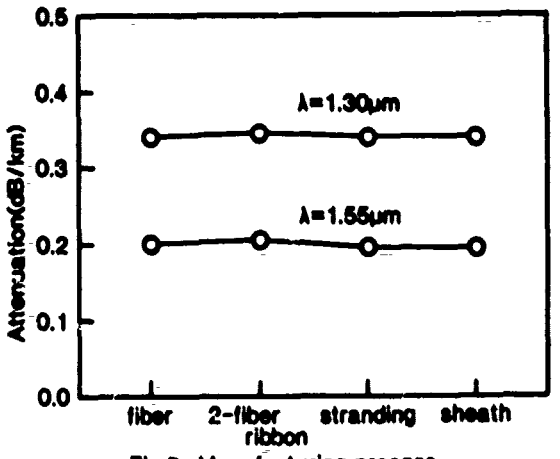

Fig.5 Manufacturing process
Attenuation of optical fibers in cable manufacturing

3-2.Temperature characteristics

The cable was subjected to temperature tests. The temperature range was -40c through +60c. Fig.6 shows the temperature characteristics in terms of loss change. The loss changes are less than 0.02dB/km. This cable can be applied to over a wide temperature range.

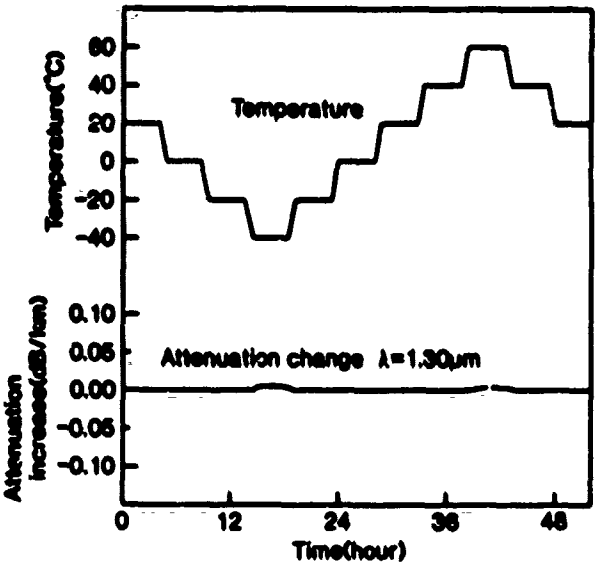

Fig.6 Temperature dependence of attenuation change

3-3.Several mechanical tests

The cable was subjected to the mechanical tests shown in Table 2. In each test, the loss changes were not observed. As a result, it was verified that this cable has an excellent mechanical characteristics.

4. Mid span access

The mid span joint was tried in a laboratory while monitoring attenuation loss changes and bit error rate. The experiment was performed with a 128-type metallic coble. Fig.7 shows the process of mid span joint. The test conditions and results are listed in table 3.

As a result, the maximum attenuation loss change was under 1.0dB at 1.3um and no bit error was observed at 100Mbits clock frequency. It was verified that the cable structure is available to do mid span joint very easily.

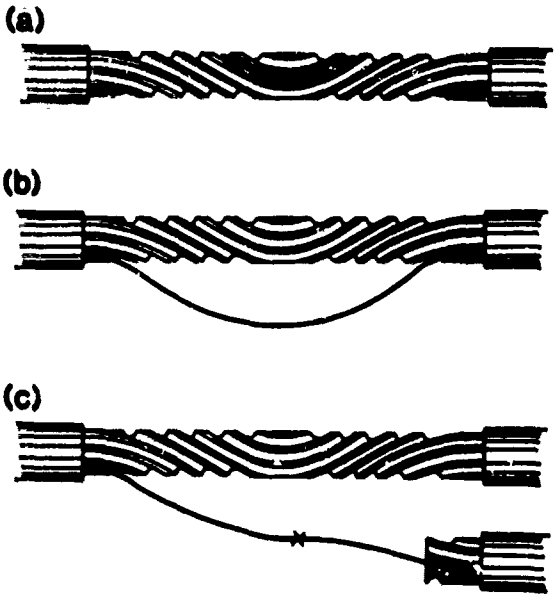

Fig.7 Process of mid span joint

a)Removing the sheath
The sheath is removed the splicing closure's length of 500mm.

b)Taking out the fibers
The fibers are taken out from the cable. The SZ slotted structure makes it easy to take out the fibers.

c)Cutting and splicing the fibers
The needed fiber are cut and spliced to the other cable. For these operation, the sufficient excess fiber length is got because of the SZ slotted structure.

Table 3 Mid span joint test conditions and results

Test items	Test conditions	Results
Slack of fibers	Cable length 500mm	More than 20mm
Attenuation change	Wavelength 1.30μm	Less than 1dB
Bit error rate	Clock frequency 100Mbits Wavelength 1.30μm	No bit error

Table 2 Mechanical test methods and results

Test items	Test methods	Results
Tensile test	Tensile strength : 360kg	Less than 0.02dB
Bending test	Bending dia. : 210mm Bending angle : ±180° 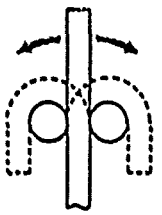	Less than 0.02dB
Compression test	Compression length : 50mm Compression load : 150kg 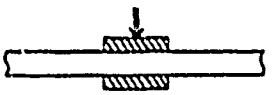	Less than 0.02dB
Impact test	Column dia. : 25mm Column weight : 500g Impact height : 1m 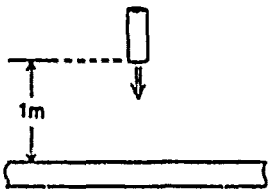	Less than 0.02dB
Twist test	Twist angle : ±90°/m Tensile strength : 25kg 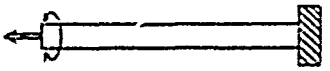	Less than 0.02dB
Squeezing test	Squeezing wheel radius : 250mm Tensile strength : 150kg 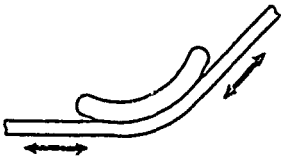	Less than 0.02dB

Conclusion

Newly designed optical cables for the subscriber networks were successfully developed. The cables consist of a SZ slotted rod and 2-fiber ribbons. The structure is suitable for mid span access from a laying cable because of the sufficient excess fiber length to access to the other cable.

The experimental cable was subjected to several tests and trials of mid span access. As a result, it was verified that the cable showed sufficient properties for practical application and the structure was available to do mid span joint very easily. The new cable could be the key technology to establish the cost minimum subscriber networks. Now this optical cables have been in commercial service in Japan for one year.

References

1) M. Aizawa, N. Miyazaki, M. Kurokawa and M. Okubo, "The development of optical fiber cable", CHN-88-25, pp.47-52, 1988.
2) M. Mizutani, M. Kurokawa, K. Niikura, T. Hayakawa and N. Misono, "Characteristics of SZ-slotted structure optical cable", IEEE Trans, B-651, 1989.

Akio Mogi

Fujikura Ltd.

1440 Mutsuzaki, Sakura, Chiba, 285, Japan

Mr. Mogi was born in 1946. He joined Fujikura Ltd. after his graduation from Haneda Institute High School in 1967 and has been engaged in research and development of the metallic cables and optical cables. He is now a chief engineer of optical cable section and a member of the Institute of Electronics, Information and Communication Engineers of Japan.

Nobuyuki Misono

Fujikura Ltd.

1440 Mutsuzaki, Sakura, Chiba, 285, Japan

Mr. Misono was born in 1949. He joined Fujikura Ltd. after his graduation from Chiba University with a B.E. degree in 1973 and has been engaged in research and development of metallic cables and optical cables. He is now an assistant chief engineer of optical cable section and a member the Institute of Electronics, Information and Communication Engineers of Japan.

Naoki Okada

Fujikura Ltd.

1440 Mutsuzaki, Sakura, Chiba, 285, Japan

Mr. Okada was born in 1964. He joined Fujikura Ltd. after his graduation from Chiba University with a B.E. degree in 1986 and has been engaged in research and development of optical cables. He is now an engineer of optical cable section and a member of the Electronics, Information and Communication Engineers of Japan.

Toshiyuki Hayakawa

Fujikura Ltd.

1-5-1 Kiba, Koto-ku, Tokyo, 135, Japan

Mr. Hayakawa was born in 1948. He joined Fujikura Ltd. after graduation from Yokohama National University with a B.E. degree in 1971 and has been in the development and design of coaxial cables, millimetric waveguides and optical cables. He is now a chief of fiber optic cable engineering section in telecommunication cable division and a member of the Institute of Electronics, Information and Communication Engineers of Japan.

Mitsuo Miyazaki

Tokyo Electric Power
Co., Ltd.

Mr. Miyazaki received M.E. degree from Erectronic Communication University. He has been in charge of development on a telecommunication fascility for power transmission control. He is a member of IEICE and IEE of Japan.

Michitoyo Kurokawa

Furukawa Electric
Co., Ltd.

6-1, Marunouchi
2-chome, Chiyoda-ku,
Tokyo, 100, Japan

Mr. Kurokawa received B.E. degree in Control Engineering from Osaka University in 1960 and has been engaged in development of telecommunication cables. He is now Manager of optical cable system development department.

Koji Niikura

Sumitomo Electric
Industries, Ltd.

1, Taya-cho,
Sakae-ku,
Yokohama, 244, Japan

Mr. Niikura recieved B.E. degree in engineering from Waseda University in 1984 and joined Sumitomo Electric Industries, Ltd. He has been engaged in the development and design of optical fiber cables in the Fiber Optics Division.

LOW/NO HALOGEN THERMOPLASTIC FIBER OPTIC CABLES FOR SHIPBOARD APPLICATION

K. Kathiresan
AT&T Bell Laboratories, Norcross, Georgia

J. B. Flunvog and L. R. Sherrets
AT&T Network Systems, Norcross, Georgia

ABSTRACT

The overwhelming advantages of fiber-optic technology for shipboard application are many and are well known. In addition to providing weight and space savings, it also offers immunity from electromagnetic interference, accommodation of future technological growth, etc. Application of fiber-optic technology for shipboard systems poses a very challenging and difficult task of the development of transmission cables. Fiber-optic cables for shipboard application are one of the most complex and demanding to design and manufacture. The stringent design specification is primarily derived from the considerations of safety of personnel aboard ship, and the operation, reliability and survivability of the shipboard systems. Shipboard fiber-optic cables with a low/no halogen thermoplastic jacket material have been developed. Cable designs with different fiber counts were manufactured and evaluated for performance to the existing specifications. This paper presents the cable designs and performance results.

INTRODUCTION

Fiber-optic technology, the medium of choice for transmission in commercial communication applications, is now becoming a medium of choice in military applications. Fiber-optics is currently being used and/or experimented with in several military and specialty applications, such as in tactical, aircraft, fiber-optic guided missiles and other weapon systems, control systems, computers and telecommunications. The U. S. Navy is also working very intensely to efficiently integrate fiber optics in both shipboard systems and shore facilities. With regard to shipboard systems, the U.S. Navy has recognized the overwhelming advantages fiber optic systems can provide to enhance a ship's operational capability. It should be noted that fiber optics affords the opportunity:

- to remove tens of thousands of pounds from a ship's weight and reduce cable space requirements by providing cables that are light in weight and have small diameters (volume), yet increase the information carrying capability compared to present copper cable systems, thereby enhancing the ship's operational capability.
- to integrate all of a ship's systems and sub-systems, i.e., control (machinery), sensors, alarms, weapons, surveillance, telecommunications, administration, video, etc., into a single survivable network aboard a ship
- to be assured that this network is capable of sustaining technological and capacity growth, and that the components are designed to last for the life of the ship
- to implement a cable plant that provides immunity against electromagnetic pulse (EMP), electromagnetic interference (EMI), and radio frequency interference (RFI) and that requires no sheath grounding
- to achieve cost effectiveness when compared to similar functional systems and to enhance the overall reliability, survivability, and capability of a new class of warships

In ships today, copper coaxial cables are used extensively to connect radar and other surveillance systems to a ship's main computers and processors distributed throughout the ship. Figure 1 illustrates typical system locations aboard a ship. Most of the sensory equipment is generally interconnected and clustered in the superstructure while the computers and displays are located below deck. This causes a high concentration of copper cable weight in the superstructure which must be balanced by ballast below. Since modern ships no longer have heavy boilers, piping, etc. below deck (lighter weight gas turbines are the main propulsion units), the added compensating ballast reduces the weight advantage originally gained by installing gas turbines. Fiber-optic cable can drastically reduce the weight of the transmission media aboard a ship and restore some of the weight reductions sought. It is estimated that as much as 90% weight and space reduction of transmission media can be achieved by replacing copper cables with fiber-optic cables. Furthermore, because the volume of the fiber cables is less than their copper counterparts, usable space inside a ship is increased.

In order to achieve all of the above advantages, fiber-optic cables for shipboard application are being developed. The design, development and manufacture of the shipboard cables are one of the most demanding and difficult, because of the stringent performance requirements. This stringent design specification is primarily derived from the considerations of safety of

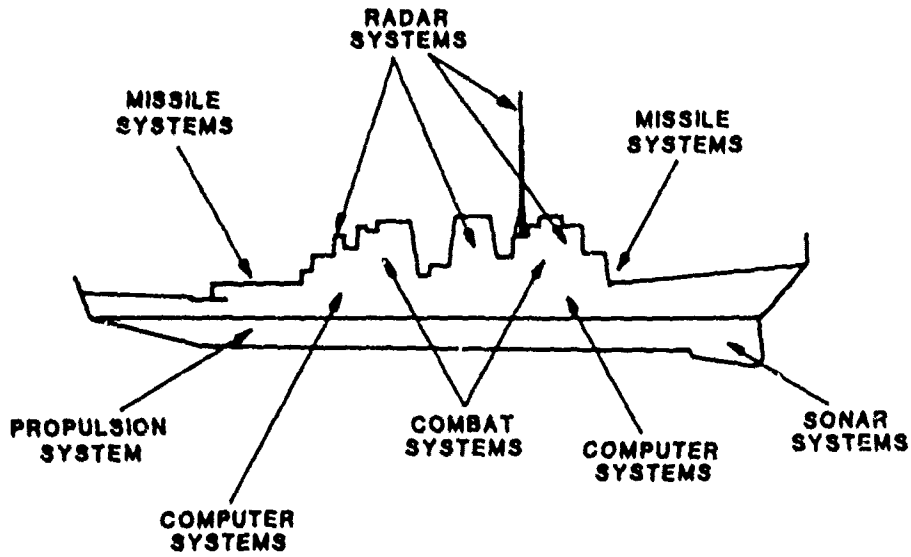

Figure 1. Typical System Locations Aboard a Navy Ship

personnel aboard ship, and the operation, reliability, and survivability of the shipboard system. In the following, the shipboard cable specifications, cable designs and the results of evaluation of the cables are presented.

SHIPBOARD CABLE SPECIFICATIONS

Currently, there are three military specifications, namely DOD-C-85045C, PMS-400-XYZ-1, and MIL-C-0085045(NAVY) (Draft), which can govern the shipboard cable design. The DOD-C-85045C specification is used at present for tactical cable designs. This specification also includes requirements pertinent to shipboard cable designs. However, this specification is not currently being used for shipboard cables. PMS-400-XYZ-1 is the specification which has been used until recently for shipboard cable designs. This draft specification, which specifies a 100/140μm multimode fiber, was considered not comprehensive enough for shipboard application. Thus, a new specification was recently developed for shipboard cables by the U. S. Navy called MIL-C-0085045(NAVY) (Draft), along with new specifications for fibers, connectors, splices, and inter-connection equipment. This new specification is currently being specified for procurements of fiber optic cables for shipboard application. The performance of the cables described later has been evaluated against this new specification.

These specifications, in general, require that the cables have low toxicity, contain low or no halogen, generate low smoke and acid gas, be flame retardant, operate under extreme operating and storage temperature ranges, withstand stringent mechanical requirements and very high water pressure, survive hostile fluids at high temperature, and meet other demanding criteria. All the above requirements, individually and in most combinations thereof, can be met with appropriate material selection and cable design features. Meeting all of the requirements simultaneously without any exceptions may be very difficult and/or may result in quite expensive cables. For example, meeting the high temperature fluid exposure requirement may call for radiation crosslinking or continuous vulcanization of jacketing materials. There are some thermoplastic materials available which will meet the fluid requirements, but are too stiff for shipboard applications. These aspects make the design, development, and manufacture of shipboard cables most difficult and challenging. The design, development, and performance evaluation of four and single fiber cables for shipboard application have been completed and are presented below.

FIBER DESIGN

Early trials aboard ships used 100/140μm multimode fiber. However, the present trend is towards radiation-hardened 62.5/125μm graded index multimode fiber. The new draft fiber specification, MIL-F-0049291(NAVY) (Draft), specifies this multimode fiber, along with single-mode fibers. The 62.5/125 multimode fiber offers the best combination of low loss, low microbending and macrobending loss sensitivity, good source-to-fiber coupling efficiency, and high bandwidth as well as compatibility with existing connectorization and splicing technologies and components. In the future, as data transmission capacity requirements increase, it appears that single-mode fibers will find more applications in shipboard fiber-optic systems. The new draft specification for fiber also covers the requirements for single-mode fibers, for such high transmission rate applications.

CABLE DESIGNS

Development of a four fiber shipboard cable has been completed. The cable cross-section is presented in Figure 2, and an isometric view is presented in Figure 3. The cable uses radiation-hardened 62.5/125 μm multimode fiber. The cable consists of a central waterblocking yarn with four optical fiber cable components (OFCC) stranded over it along with

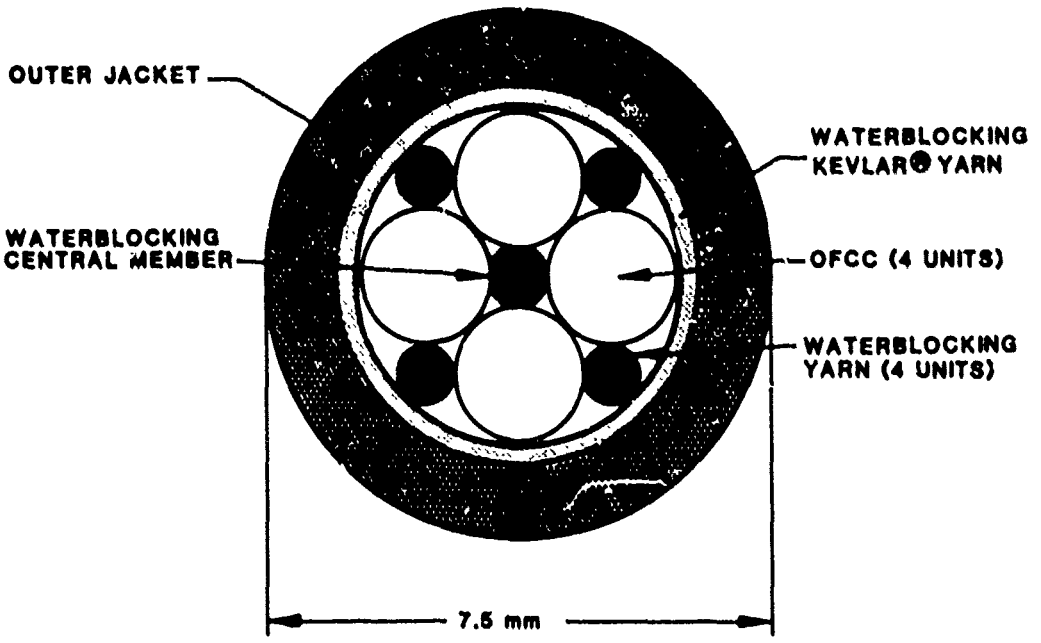

Figure 2. Cross-Section of 4-OFCC Shipboard Cable

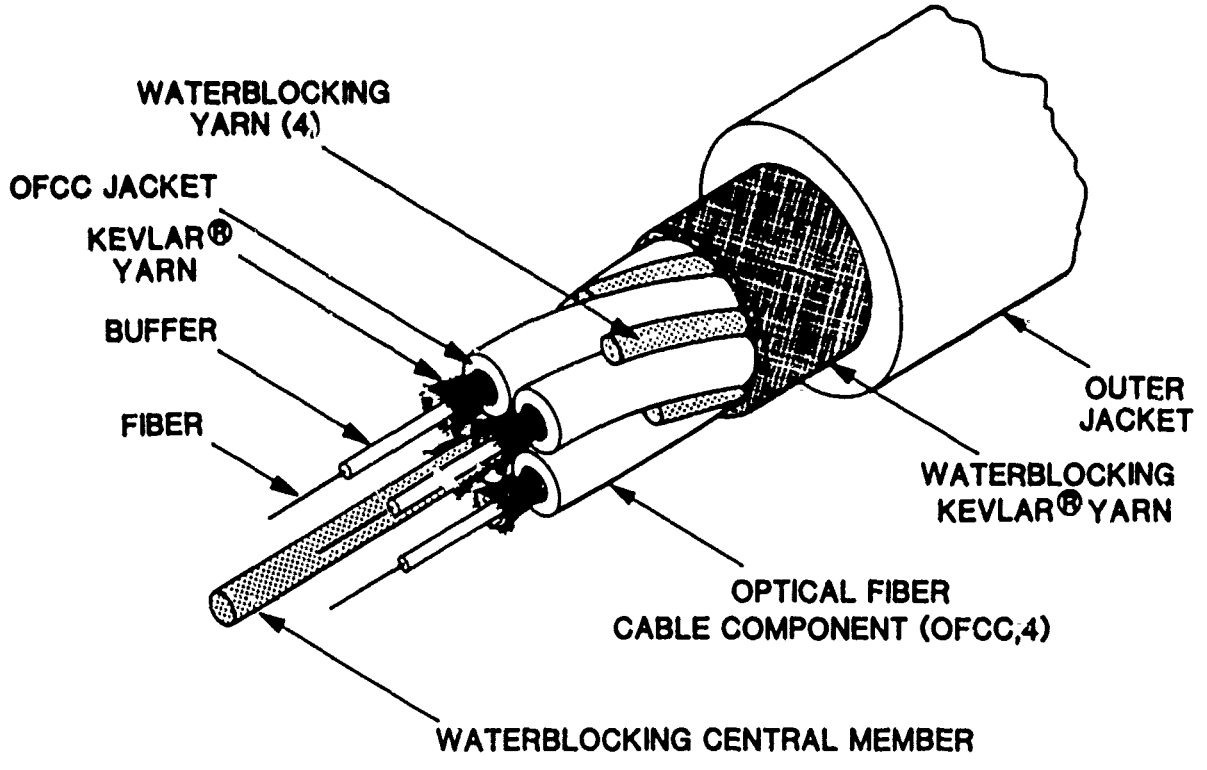

Figure 3. Isometric View of 4-OFCC Shipboard Cable

waterblocking yarn. The cross-section of the OFCC is given in Figure 4. The OFCC contains a 900 μm polyester elastomer buffered fiber, surrounded by Kevlar® yarn and a low halogen jacket. Over the OFCC units, two layers of Kevlar® yarn strength members are stranded in opposing lays. These Kevlar® yarn strength members are treated with polymers which are water swellable, eliminating the need for separate waterblocking members. The use of such waterblocking Kevlar® yarn also minimizes the cable size, in addition to providing a uniform waterblocking structure. A low halogen outer jacket is then extruded over the Kevlar® yarn strength members. The components and the cable were designed such that the cable is very flexible, compact, and meets the waterblocking requirement more than adequately.

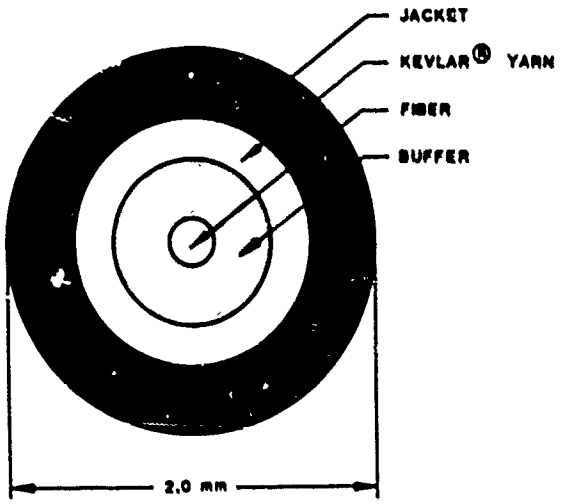

Figure 4. Cross-Section of Optical Fiber Cable Component (OFCC)

The OFCC has been evaluated as a single fiber cable by itself. Thus, in the following section, the performance results of the four fiber cable as well as the single fiber cable (OFCC) are presented.

PERFORMANCE RESULTS

The shipboard cable performance evaluation consists of optical, chemical, environmental and mechanical tests. Optical properties of attenuation rate, bandwidth and numerical aperture along with numerous other dimensional and mechanical requirements are checked at the fiber stage, and fibers which meet all the specifications are then used for cabling. Fibers used were proof tested to 690 MPa. The wavelength of operation for these cables is 1300 nm. The cables can also be operated at 850 nm. The mean attenuations of the finished cable at 1300 nm and 850 nm were 1.4 dB/km and 4.3 dB/km, respectively. The general properties of the cables are given in Table I.

The chemical tests consist of acid gas generation, halogen content, toxicity index, and fire and smoke properties. The results of these tests and the requirements are presented in Table II. The finished cables meet the acid gas generation, halogen content, and toxicity index requirements with good margin. The halogen content results correspond to the total of the four halogens, namely fluorine, chlorine, bromine and iodine.

The cables pass the IEEE-383 flame test. The IEEE-383 test is not required by MIL-C-0085045(NAVY) specification. The cables were tested and the results are reported for information only. The MIL-C-0085045(NAVY) specification requires the UL-910

TABLE I. GENERAL PROPERTIES OF SHIPBOARD CABLES

PARAMETER	CABLE PROPERTY
Cable Designs (No. of OFCCs)	4 and 1
Fiber Type	62.5/125 μm Rad-Hard
Specification	MIL-C-0085045 (NAVY) (Draft)
Material	Thermoplastic
Typical/Maximum Cabled Fiber Loss	1.4/2.0 dB/km @ 1300 nm
Typical/Maximum Cabling Added Loss (from Fiber), Δ	0.6/1.0 dB/km @ 1300 nm
Wavelengths of Operation	1300 and 850 nm

TABLE II. CHEMICAL PROPERTIES OF SHIPBOARD CABLES

TEST	REQUIREMENT FOR 4-OFCC / 1-OFCC	CABLE PERFORMANCE	
		4-OFCC	1-OFCC
Acid Gas Generation	MIL-C-0085045 ≤ 2.0% / 2.0%	= 0.19%	= 0.02%
Halogen Content	MIL-C-0085045 ≤ 0.2% / 0.2%	= 0.04%	= 0.01%
Toxicity Index	NES 713 ≤ 5.0 / 5.0	= 3.02	= 3.36
Fungus Resistance	MIL-STD-810, Method 508 Grade I / Grade I	Cable & Components Grade I	Use 4-OFCC Result
Limiting Oxygen Index temperature (For Information Only)	NES 715, ≥ 250 °C / 250 °C Not Required by MIL-C-0085045	= 306 °C	-
Oxygen Index (For Information Only)	Not Required by MIL-C-0085045	NES 715 = 43.5% @ 23 °C	-

plenum cable fire test, with two modifications to the requirements. The first modified requirement is that the flame travel time product value for the cable for the first ten minutes of the test using the ASTM-E-84 procedure shall be less than or equal to 27.5 m.min (the standard UL-910 requirement is that the flame travel should be less than or equal to 1.52 m for the total test duration of 20 minutes). The second modified requirement is that the cable should meet the standard UL-910 smoke requirements (average optical density ≤ 0.15 and maximum optical density ≤ 0.5) or the cable's specific optical density under flaming combustion (D_m) using ASTM-E-662 procedure be ≤ 225. The above modified requirements are applicable for multi-fiber (≥2) cables only. The single fiber cable (OFCC) is not required to meet any of the above requirements, except the ASTM-D-662 specific optical density under flaming combustion requirement. Table III shows that both the cables meet the specified fire and smoke requirements.

TABLE III. FIRE AND SMOKE PROPERTIES OF SHIPBOARD CABLES

TEST	REQUIREMENT FOR 4-OFCC / 1-OFCC	CABLE PERFORMANCE	
		4-OFCC	1-OFCC
Specific Optical Density Under Flaming Combustion	ASTM-E-662 D_m ≤ 225 / 225	= 50.2	= 56.0
Flame Propagation and Smoke Generation	IEEE-383 Flame Spread ≤ 2.4 m / 2.4 m Not Required by MIL-C-0085045 (For Information Only)	= 1.3 m	= 2.2 m
	UL-910 Average Optical Density ≤ 0.15 / None	= 0.11	= 0.02
	Maximum Optical Density ≤ 0.5 / None	= 0.5	= 0.25
	Flame Spread Time Product for First 10 Minutes ≤ 27.5 m.min / None	= 12.8 m.min	= 40.5 m.min

Three of the most important environmental tests are temperature cycling at ambient and high humidities, and accelerated aging. For shipboard cable evaluation, the temperature cycling at ambient and high humidities have been combined to a temperature-humidity cycling (95%RH above 20°C and uncontrolled below 20°C) as shown in Figure 5. The first three cycles correspond to the required temperature range of -28°C to 65°C. In the next two cycles, the cables were evaluated for an extended cold temperature of -55°C. The results of the temperature-humidity cycling performance of the cables are given in Figure 6. In the accelerated aging test, the cables were subjected to a constant temperature of 100°C for 240 hours. The results of the accelerated aging performance of the cables are given in Figure 7. The cables meet and surpass the requirements for these environmental tests showing excellent performance.

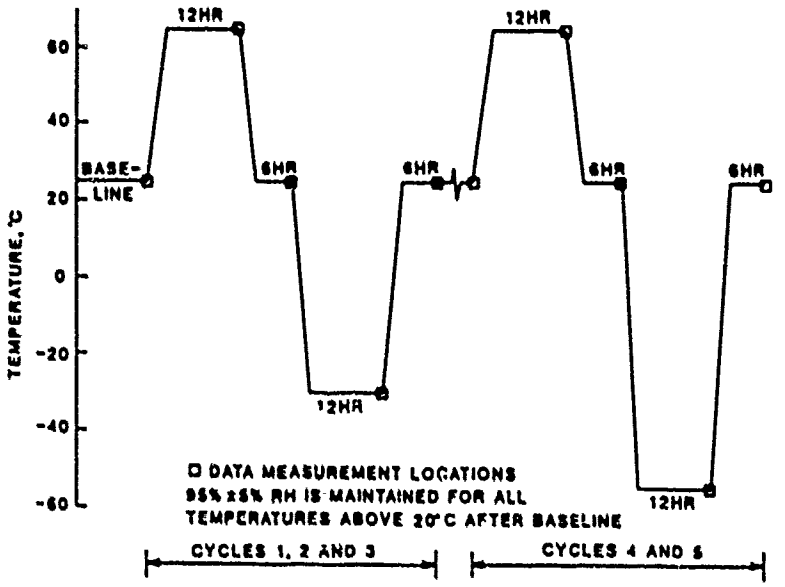

Figure 5. Temperature-Humidity Cycle for Shipboard Cables

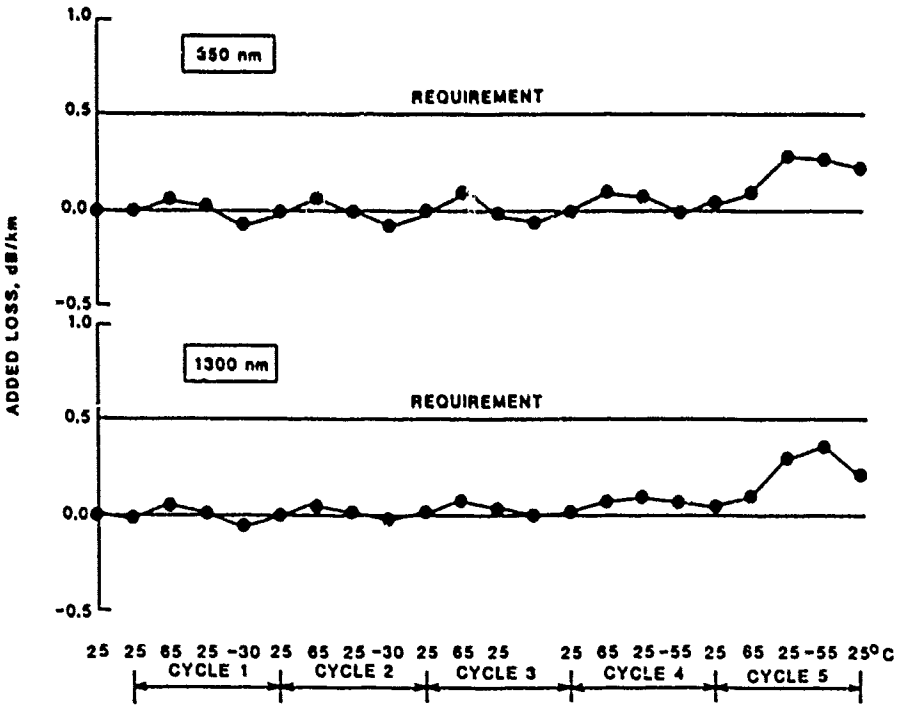

Figure 6. Temperature-Humidity Cycling Test Results for Shipboard Cables

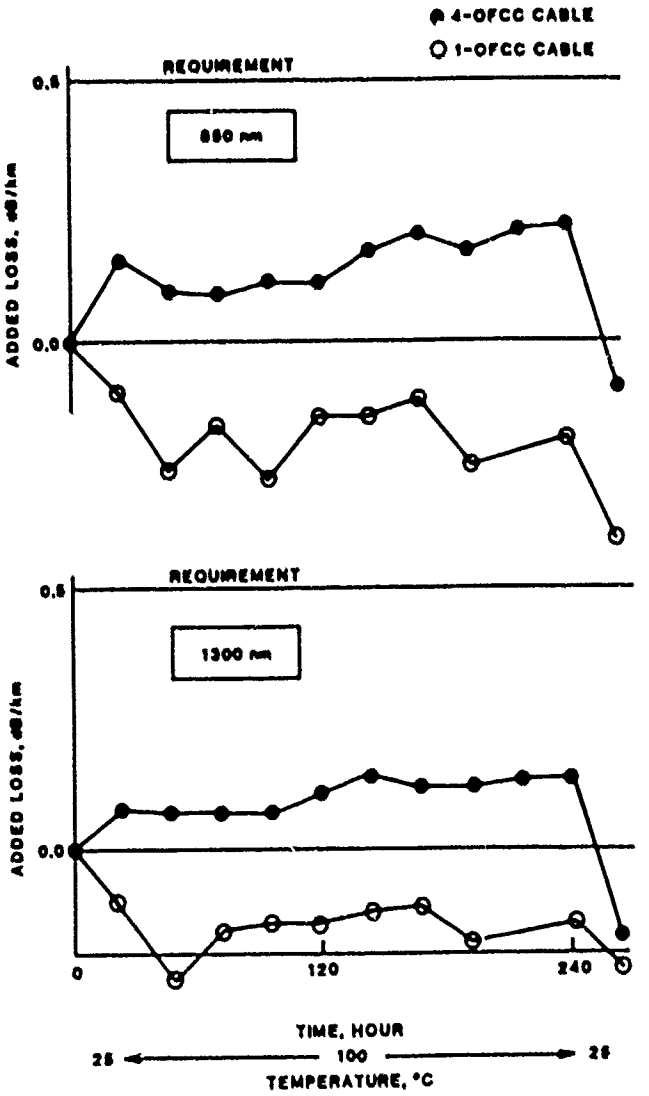

Figure 7. Accelerated Aging Test Results for Shipboard Cables

The cables were then subjected to a long list of environmental and mechanical tests. The results of these tests along with the specified requirements are given in Tables IV and V. The cables' environmental and mechanical performance exceeds that of the specification requirements in terms of test loading, number of cycles, and/or attenuation change. During these tests, for the 4-OFCC cables, two of the fibers were monitored at 850 nm wavelength, and the other two fibers at 1300 nm. The increase in attenuation (Δ) reported in Tables IV and V corresponds to the maximum of the four fiber values.

The cable jacket material and the cables were subjected to fluid immersion tests using several fluids at different temperatures. The results of tensile strength and elongation retention of dumbbell specimens of the jacket material, and the outer diameter swell of the cables due to fluid immersion at the required temperatures are given in Table VI.

CONCLUSIONS

The design, development, and performance evaluation of fiber-optic cables with four and single fibers for shipboard systems were presented. The cables either meet or surpass the requirements specified in MIL-C-00850-15 specification.

ACKNOWLEDGEMENTS

The authors gratefully acknowledge the support and contributions of several members of AT&T Bell Laboratories and AT&T Network Systems.

TABLE IV. ENVIRONMENTAL PROPERTIES OF SHIPBOARD CABLES

TEST	REQUIREMENT FOR 4-OFCC / 1-OFCC	CABLE PERFORMANCE	
		4-OFCC	1-OFCC
Thermal Shock	EIA-455-180 $\Delta^{*} \leq$ 0.5 dB/km / 0.5 dB/km Diameter Change** $\leq$ Abs($\pm$ 10% / 10%) Tensile Strength Retension*** - None	Δ = 0.15 dB/km = 1.04% = 101.5%	Δ = 0.00 dB/km = 3.04% = 101.5%
Temperature-Humidity	EIA-455-182 $\Delta \leq$ 0.5 dB/km / 0.5 dB/km Diameter Change $\leq$ Abs($\pm$ 10% / 10%) Tensile Strength Retension $\geq$ 75%	See Figures 5 & 6 = 0.2% = 96.9%	Use 4-OFCC Results = 1.9% = 96.9%
Gas Flame	EIA-455-92 $\Delta \leq$ 0.5 dB / None	Δ = 0.14 dB	Not Applicable
Weathering	ASTM-D-2565 $\Delta \leq$ 0.5 dB / None Tensile Strength Retension $\geq$ 75%	Non-Acquirable Data = 93.8%	Not Applicable
Fluid Immersion	MIL-C-0085045 For Dumbbell, FED-STD-228, 3021 & 3031 Tensile Strength Retension $\geq$ 50% Elongation Retension*** $\geq$ 50% For Cable, EIA-455-12 Diameter swell $\leq$ 10% / 10%	See Table. VI	See Table VI
Water Absorption	ASTM-D-470 $\leq$ 3.9 mg/cm^2 / 3.9 mg/cm^2	= 2.7 mg/cm^2	= 3.6 mg/cm^2
Salt Spray	EIA-455-16, 35 °C, 96 hrs No Damage / No Damage	No Damage	Use 4-OFCC Results
Accelerated Aging	FED-STD-228, 4031 $\Delta \leq$ 0.5 dB/km / 0.5 dB/km Tensile Strength Retension $\geq$ 75% Diameter Change $\leq$ Abs($\pm$ 10% / 10%)	See Figure 7 = 116.0% = 0.63%	See Figure 7 = 116.0% = 1.08%
Jacket Self-Adhesion or Blocking	EIA-455-84, 71 °C, 48 hrs No Adhesion / No Adhesion	No Adhesion	No Adhesion
Ultraviolet Radiation	MIL-STD-810, 505, Procedure II	Not Applicable	Not Applicable
Oxygen Pressure Exposure	MIL-C-0085045	Not Applicable	Not Applicable
Vibration	MIL-STD-167-1, Type I Any Transient Attenuation With $\Delta \geq$ 0.5 dB / 0.5 dB $\Delta t^{****} \geq$ 50 μsec / 50 μsec	None $\Delta \geq$ 0.5 dB and $\Delta t \geq$ 10 μsec	Use 4-OFCC Results
Shock	MIL-S-901, Grade A, Type A, Class I Any Transient Attenuation With $\Delta \geq$ 0.5 dB / 0.5 dB $\Delta t \geq$ 50 μsec / 50 μsec	None $\Delta \geq$ 0.5 dB and $\Delta t \geq$ 10 μsec	Use 4-OFCC Results

* Δ - Increase in Attenuation
** Diameter Change Values are Obtained Using Cable Samples
*** Tensile Strength and Elongation Values are Obtained Using Dumbbell Specimens
**** Δt - Time Duration

TABLE V. MECHANICAL PROPERTIES OF SHIPBOARD CABLES

TEST	REQUIREMENT FOR 4-OFCC / 1-OFCC	CABLE PERFORMANCE	
		4-OFCC	1-OFCC
Tensile Loading	EIA-455-33 ≥ 1875 N / 270 N @ 0.67% Strain Δ* ≤ 0.5 dB / 0.5 dB	≈ 3560 N, ≥ 0.97% Strain Δ ≈ 0.32 dB	≈ 500 N, ≥ 0.97% Strain Δ ≈ 0.17 dB
Dynamic Bend	MIL-C-0085045, 8x**, 650 N Δ ≤ 0.5 dB / 0.5 dB	Δ ≈ 0.20 dB	Δ ≈ 0.02 dB
Cyclic Flexing	EIA-455-104, 4.5 kg / 1.5 kg, 8x Δ ≤ 0.5 dB / 0.5 dB 500 Cycles @ 25 °C 100 Cycles @ -28 °C	Δ ≤ 0.5 dB / 0.[illegible] Δ ≈ 0.06 dB, 2[illegible] Cycles, 10.0 kg Δ ≈ 0.08 dB, [illegible] Cycles, 5.0 kg	Δ ≈ 0.02 dB, 2000 Cycles, 2.0 kg Δ ≈ 0.06 dB, 100 Cycles, 2.0 kg
Torsion	EIA-455-63, 220 N / 55 N, 10 Cycles Δ ≤ 0.5 dB / 0.5 dB	10 Cycles Δ ≈ 0.02 dB	10 Cycles Δ ≈ 0.01 dB
Flexure (Cold Bend)	EIA-455-85, 8x, -28 °C 10.0 kg / 5.0 kg, 3 Turns Δ ≤ None / 0.5 dB	Δ ≈ 0.28 dB	Δ ≈ 0.13 dB
Twist Bend	EIA-455-81, 4.5 kg / 1.5 kg, 8x Δ ≤ 0.5 dB / 0.5 dB 500 Cycles @ 25 °C 100 Cycles @ -28 °C	Δ ≈ 0.10 dB, 2000 Cycles, 10.0 kg Δ ≈ 0.10 dB, 100 Cycles, 10.0 kg	Δ ≈ 0.01 dB, 2000 Cycles, 2.0 kg Δ ≈ 0.00 dB, 100 Cycles, 2.0 kg
Crush	EIA-455-41, ≥ 1500 N / 550 N Δ ≤ 0.5 dB / 0.5 dB Crosstalk ≤ -40 dB	2000 N Δ ≈ 0.08 dB ≈ -82.5 dB	500 N Δ ≈ 0.01 dB Not Applicable
Radial Compression	MIL-C-0085045 Δ ≤ 0.5 dB / None	Torque ≈ 17.3 kg.cm Δ ≈ 0.02 dB	Not Applicable
Impact	EIA-455-25, 1.0 kg / 0.5 kg Δ ≤ 0.5 dB / 0.5 dB 50 Cycles @ 25 °C 20 Cycles @ -28 °C 20 Cycles @ 65 °C	Δ ≈ 0.04 dB, 100 Cycles, 2.0 kg Δ ≈ 0.01 dB, 20 Cycles, 2.0 kg Jacket Split @ 3 Cycles Δ ≈ 0.04 dB, 20 Cycles, 1.0 kg	Δ ≈ 0.01 dB, 100 Cycles, 0.65 kg Δ ≈ 0.02 dB, 50 Cycles, 0.65 kg Jacket Split @ 35 Cycles Δ ≈ 0.03 dB, 50 Cycles, 0.65 kg Jacket Split @ 35 Cycles
Corner Bend	MIL-C-0085045, 8x, ≥ 378 N / 100 N Δ ≤ 0.5 dB / 0.5 dB	900 N Δ ≈ 0.05 dB	200 N Δ ≈ 0.06 dB
Pressure Cycling	MIL-C-0085045	Not Applicable	Not Applicable
Hydrostatic Pressure	MIL-C-0085045	Not Applicable	Not Applicable
Dripping	FED-STD-228, 5111, 150 °C, 6 hrs No Drip / No Drip	No Drip	No Drip
Waterblocking (Distilled Water)	MIL-C-0085045, 0.102 MPa, 6 hrs Leakage ≤ 33 ml / None	0.175 MPa ≈ 18.0 ml	Not Applicable
Cable Jacket Tear Strength	FED-STD-228, 3111 ≥ 80 N/cm	≈ 88.7 N/cm	≈ 88.7 N/cm
Jacket Material Tensile Strength and Elongation	FED-STD-228, 3021 & 3031 ≥ 900 N/cm² ≥ 150%	≈ 1134 N/cm² ≈ 142%	≈ 1134 N/cm² ≈ 142%
Cable Abrasion Resistance	MIL-C-0085045 Scraping 100 Cycles, No Electrical Contact Cable-to-Cable 100 Cycles, No Electrical Contact	No Electrical Contact No Electrical Contact	Use 4-OFCC Results
Cable Shrinkage	MIL-C-0085045, 150 °C, 6 hrs ≤ 0.63 cm / 0.63 cm	≈ 0.13 cm	≈ 0.05 cm
Cable Element Removability	MIL-C-0085045 Easily Removable	Easily Removable	Easily Removable
Durability of Identification Marking	MIL-C-0085045 500 Cycles, No Erasure/Obliteration	No Erasure/Obliteration	No Erasure/Obliteration
Ribbon Delamination	MIL-C-0085045	Not Applicable	Not Applicable

* Δ - Increase in Attenuation
** Mandrel Diameter to Cable Outer Diameter Ratio

TABLE VI. FLUID IMMERSION PROPERTIES OF JACKET MATERIAL

FLUID AND SPECIFICATION	TEST TEMP., °C	0.125 inch DUMBBELL		O. D. SWELL, %	
		STRENGTH RETENTION, %	ELONGATION RETENTION, %	4-OFCC	1-OFCC
REQUIREMENT	-	≥ 50	≥ 50	≤ 10	≤ 10
Fuel Oil (Diesel) Mil-F-16884	35	69	116	5	6
Turbine Fuel (JP-5) Mil-T-5624	25	69	62	5	0
Isopropyl Alcohol TT-I-735	25	86	110	0	0
Hydraulic Fluid Mil-H-5606	50	51	96	9	8
Lubricating Oil Mil-L-17331	75	68	110	7	6
Lubricating Oil Mil-L-23699	75	76	109	5	10
Coolant	25	105	113	0	0
Seawater	25	91	87	0	0

Kris Kathiresan is a Member of Technical Staff in the Lightguide Technology Department at AT&T Bell Laboratories in Norcross, Georgia. He is responsible for the design and development of specialty cables, including military applications.

Dr. Kathiresan joined AT&T Bell Laboratories in 1985. He has a B. E. Hons in Mechanical Engineering from University of Madras, India, an M. E. in Aerospace Engineering from Indian Institute of Science, India, and a Ph. D. in Engineering Science and Mechanics from Georgia Institute of Technology, Atlanta, Georgia.

Dr. Kathiresan is a Senior Member of American Institute of Aeronautics and Astronautics and a Member of American Society of Mechanical Engineers. He is a registered Professional Engineer (Mechanical) in States of Georgia and Florida.

Jill B. Fluevog is a Development Engineer in the Lightguide Cable Engineering Department at AT&T Network Systems, Norcross, Georgia. She joined AT&T in 1985 after receiving a Bachelors Degree in Chemical Engineering from Georgia Institute of Technology. She is responsible for the development of lightguide cable products and processes for military applications. Ms. Fluevog is a member of American Institute of Chemical Engineers, Institute of Electrical and Electronics Engineers and Society of Plastic Engineers.

Larry R. Sherrets is a Senior Product Manager (Federal Market) in the Lightguide Fiber and Cable Department at AT&T Network Systems, Norcross, Georgia. He joined AT&T at the Omaha Works in 1969. He attended the University of Nebraska (Engineering/Psychology). He currently is responsible for planning, development, and marketing of Fiber Optic Products for Military Applications for the U. S. Government.

OPTICAL FIBER DESIGN CHALLENGES FOR TACTICAL SYSTEM APPLICATIONS

H. P. Hsu
Hughes Aircraft Company, Missile Systems Group
8433 Fallbrook Avenue, Canoga Park, CA. 91304

V. E. Kalomiris
U. S. Army Communications-Electronics Command
Fort Monmouth, N. J. 07703

ABSTRACT

This paper discusses the technical challenges in optical fiber design for tactical systems. The relationships between the performance concerns and various fiber design parameters are reviewed along with the state-of-the-art fibers which are optimized to meet conflicting performance requirements of tactical systems.

I. Introduction

Large signal bandwidth, low transmission loss, electromagnetic interference (EMI) or electromagnetic pulse (EMP) immunity, and light weight have made optical fiber an attractive transmission medium for both commercial and tactical communication systems. All fiber optic communication systems use similar components for signal generation/detection and transmission, however the severe operational conditions encountered by tactical systems often lead to new performance requirements on fiber-optic components. A tactical system fiber must provide a reliable signal transmission medium that meets the system performance requirements on both optical transmission capacity and mechanical integrity under all specified operational conditions. Low optical transmission loss, low signal dispersion and high strength are the common design goal for optical fibers. A tactical fiber system must also survive extreme temperature, excessive vibration/shock, rough handling, severe bending and nuclear radiation exposure.

Technical challenges often arise in developing a new fiber design for a specific tactical system, which require fiber parameter optimization and fabrication process control to ensure the fiber performance. Table 1 summarizes the relationship between the performance concerns of tactical system fiber and the key fiber design parameters. This paper discusses the technical challenges encountered in optical fiber design for the tactical systms. The impact of optical waveguide design and fabrication on fiber characteristics, such as optical attenuation, dispersion, and mechanical strength, will be reviewed. The emphasis will be on single mode fiber for long range fiber optic tactical systems that include battlefield data links, ship-board/aircraft avionics, and a new class of tethered weapon systems.

II. Optical Transmission Loss

The optical loss of fiber in tactical systems is comprised of four components, namely, intrinsic attenuation, environment-induced loss, interconnection loss and bend induced loss. The first two loss components depend strongly on the glass material and to a lesser extent on the optical waveguide design and fabrication process. The last two loss components are more sensitive to the optical waveguide design and the physical handling of fiber in the system. The mechanisms underlining these optical losses and the fiber design for loss performance optimization will be addressed in the following subsections.

Intrinsic Attenuation

The advance in fiber fabrication techniques and glass material processing in the past two decades have eliminated most of material related intrinsic attenuation problems associated with transition metal ions impurities and hydroxyl (OH) ions absorption. It is known that these contaminants in fiber must be kept below one part per billion (ppb) level to ensure a less than 0.1 db/km intrinsic attenuation. The attenuation of the state-of-the-art fiber already approaches the intrinsic Rayleigh scattering loss limit of fused silica over 800-1600 nm wavelength range. The Rayleigh scattering loss decreases inversely with the fourth power of optical wavelength while its value varies slightly with the actual dopant material in fiber. The lowest fiber attenuation, of 0.15 db/km observed at 1550 nm, was obtained with a silica core fiber produced by a vapor deposition process with special dehydration provision.[1] The attenuation of commercially available fibers are routinely quoted around 0.5 db/km and 0.3 db/km at 1300 nm and 1550 nm respectively. Technical challenge still exists in developing long length fiber for long range tactical systems, which must consider glass materials and fabrication processes with the lowest possible intrinsic attenuation without disregarding other fiber performance concerns.

PERFORMANCE CONCERNS	DESIGN PARAMETERS
OPTICAL ATTENUATION	
- INTRINSIC ATTENUATION	GLASS MATERIAL FABRICATION PROCESS
- ENVIRONMENT-INDUCED LOSS o HYDROGEN-INDUCED LOSS o RADIATION EFFECTS	GLASS MATERIAL COATING DESIGN
- INTERCONNECTION LOSS	MODE FIELD DIAMETER FIBER DIMENSION TOLERANCE
- BEND-INDUCED LOSS o MACROBEND LOSS o MICROBEND LOSS	MODE FIELD DIAMETER REFRACTIVE-INDEX PROFILE FIBER DIMENSIONS COATING MATERIAL
DISPERSION	REFRACTIVE-INDEX PROFILE GLASS MATERIAL
FIBER STRENGTH	FABRICATION PROCESS GLASS MATERIAL PROOF-TEST AND HANDLING COATING DESIGN

TABLE 1
OPTICAL FIBER DESIGN FOR TACTICAL FIBER SYSTEMS

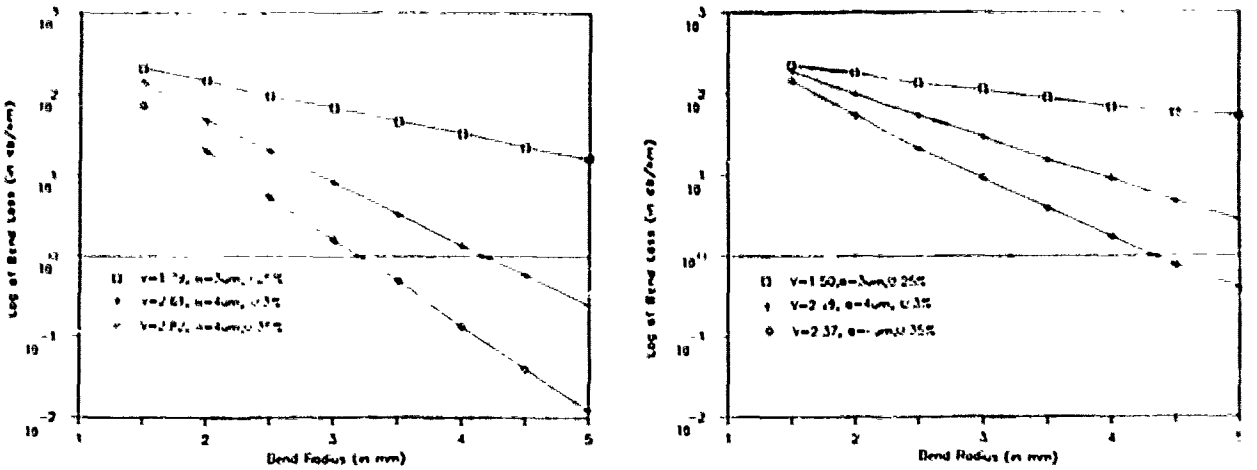

a) 1300 nm b) 1550 nm

Figure 1 Constant Curvature Bend Loss
This figure shows the constant curvature bend loss of step index fibers as a function of bend radius. Fiber design is the parameter. The bend loss is calculated in db/km.

Environment-Induced Losses

The two environment-induced losses critical to the fiber loss performance in tactical systems are hydrogen-induced loss and radiation-induced loss. Long term exposure to low level of hydrogen gas and various defects inducing radiation in nature can result in an accumulation of optical loss that can significantly impact the optical power budget of fiber optic data link (FODL) and affect the long-term reliability of tactical systems. In contrast, high dose rate and high total dose of defect inducing radiation in nuclear environment can cause an acute fiber loss increase that in effect blacks out the fiber and causes instant system failure. Studies on these environment-induced losses are still in progress, nevertheless results from this effort have already identified many loss mechanisms and fiber design alternatives.

The hydrogen-induced loss was generally considered as an aging phenomenon caused by the release of hydrogen from the silicone fiber coating and cabling structures. The two basic loss mechanisms are the permeation of hydrogen into a silica glasses network that introduces infrared absorption and the chemical reaction between hydrogen molecules and reactive defects in silica network to form absorptive hydroxyl (OH) ions. The loss depends on the ambient temperature, the hydrogen's partial pressure, the exposure time and the fiber material. Beales et al. had reported a room temperature loss increase, induced by hydrogen molecular diffusion, of 0.3 and 0.6 db/km/atm-hydrogen at 1300 nm and 1550 nm respectively.[2] Tomita and Lemaire have shown that the hydrogen pressure must be maintained below a tolerable level of a few tenths of atm to limit the hydrogen-induced fiber loss below 0.1 db/km for a 20 yer system.[3] Recent development on hermetic fibers have shown that a tight dielectric coating on glass surface can suppress the hydrogen permeation and reduce the hydrogen-induced loss.[4] However, further study is still needed to improve the understanding on hydrogen-induced loss mechanisms associated with different glass and coating materials as well as its effect on long-term fiber loss.

Radiation-induced loss, especially the high dose rate and high total dose case, represents a genuine threat to the operation of many tactical fiber optics systems. Radiation-induced defects, often referred as color centers, in glass network can absorb optical signal in fiber and interrupt FODL signal transmission. The loss depends on a large number of variables that includes the fiber design, the total dose and the dose rate of radiation, the ambient temperature and the optical signal level in fiber. Extensive works based on cobalt 60 radiation study have shown that glass material play an important role in determining the loss behaviors on both initial loss increase and subsequent recovery after the exposure.[5] The study results show the loss is lower at longer optical wavelength in 1300 nm - 1600 nm range, because the UV absorption by radiation-induced defects tends to tail off at long wavelength. Nagel reported the radiation-induced loss of germanium-doped core single mode fiber at 1300 nm exhibits a linear dependence on exposure time at low dose rate environment of 2.3 rad/hr. But the loss will exceed 1 db/m and saturate in value at the high total does (Mrad) and dose rate (100 Krad/hr) extreme.[6] The recovery of fiber loss can be accelerated by high ambient temperature or by high intensity optical power, known as "photobleaching" effect. In practice, the radiation-induced loss can be reduced by avoiding phosphorous-doped fiber design and operating a FODL at longer wavelength of 1550 nm instead of 1300 nm. The best radiation hardened fiber reported today uses pure silica core with fluorine-doped cladding fiber design.[5] The technical challenge here is to use rad-harden glass material to develop a fiber design that meets other tactical system performance requirements.

Interconnection Loss

Interconnection loss in a FODL includes connector loss, splicing loss and coupling loss to optical source and photodetector. These losses all depend on the fiber alignment at the interconnection and to a lesser extent on the light guiding capacity of fiber. The alignment tolerance of multimode fiber interconnections can be relaxed by using fibers with larger core size and core-cladding refractive index difference at the expense of higher dispersion. In the case of single mode fiber, the fiber alignment demands sub-micron accuracy for low loss interconnections. The tolerance can be relaxed by designing fiber with large mode field diameter (MFD).[7] Unfortunately, a large MFD fiber often incurs serious bend loss problem in operation. The technical challenge here is to design fiber with sufficient bend loss resistance without imposing undue constraint on alignment tolerance at the interconnections.

Bend-Induced Loss

An optical fiber also experiences many bend related losses which include cabling loss, bobbin winding losses, deployment and payout bend loss. These bend losses can change, and sometimes dominate the optical power budget of FODL in system design. Many commercial fibers have proven to be inadequate for tactical applications due to bend related losses introduced by severe operation environments. One of the prominent examples is a tethered FODL with fiber deployed from a tightly packed bobbin at high speed where the winding loss and the payout bend loss often represents the dominant losses in optical power budget consideration.

The bend-induced fiber loss can be divided into two categories based upon the bend profile: macrobend and microbend. Macrobends generally refer to a physical bend with a bend radius in thousands of wavelengths, such as mandrel winding

and peel-point bend in payout. On the other hand, microbends refers to the microscopic random deviation of fiber axis from its natural straight condition as a result of cabling, winding and environmental changes. In reality, it is often difficult to separate these two bend loss types.

The study on the macrobend loss of single mode fiber with constant bend curvature has shown the bend loss increases approximately exponentially with the decrease of the bend radius R. Figure 1 shows a family of bend loss curves, calculated by using a formula given in Ref. (8), expressed in db per unit length against the bend radius R with fiber normalized frequency V as the parameter. For a step-index fiber,

$$V = 2\pi a(n_1^2 - n_2^2)^{\frac{1}{2}}/\lambda \qquad (1)$$

The V value relates directly to the wave-guiding capability of fiber which combines all fiber design quantities including: optical wavelength λ, the fiber core radius a, the refractive index of core and cladding n_1 and n_2 respectively. A step-index single mode fiber maintains $V < 2.405$ according to the waveguide theory. Figure 1 also shows that fiber design with larger V value has lower bend loss. Figure 2 shows the calculated bend loss against the optical wavelength with different fiber design and loop radius as parameters. It shows that the bend loss increases with increasing optical wavelength and decreasing bend radius. This is consistent with the measured spectral loss curves shown in Figure 3.

When a fiber is paid outat high speeds from a precision wound bobbin, the fiber forms a whirling helix after lifting from the peel point. It is known that the sharp peel point bend, caused by a concentrated force used to rupture the winding adhesive in payout, is a non-uniform bend curve that can inflict severe bending stress and optical signal loss to risk the FODL reliability. A bend loss analysis, which is carried out by integrating the constant curvature bend loss in increment along the bend curve generated by a separated mechanical model, shows the loss increases exponentially around the peel-point and approaches its final value 1 to 2 mm from the peel-point. The calculated bend loss, expressed in terms of the cumulative bend loss along the bend curve, are shown in Figure 4 with fiber V-value as the parameter. The cumulative bend loss again critically depend on the fiber V-value similar to the case of constant curvature bend loss.

Study on microbend loss conducted with fiber cables and precision wound fiber bobbins shows that the loss depends on a large number of variables that include the fiber and coating design, the cabling and winding conditions, the deployment environment, and the ambient environment.[9] The effect of fiber design on microbend loss has been the subject of many theoretical studies. A rigorous treatment, which is rather complicated, considers the loss in terms of the coupling between the guided and radiation modes of fiber. Petermann and Kuhne have derived a simple loss formula which connects the loss directly to the MFD of single mode fiber. The loss increases approximately with the 2(p+1)th power of the fiber MFD and p is the curvature power spectrum parameter of the microbend with a value in the order of 4 or larger.[10] Besides a small MFD fiber design, a fiber embedded in a soft coating can prevent high spatial frequency deformations in fiber and thereby provide a better microbend loss protection in cabling and in operation environment. A dual coating design, which is comprised of a low module (soft) primary inner coating and a high module (hard) outer coating, has been widely used by fiber manufacturers as a practical design for controlling the fiber microbend loss and providing toughness for fiber handling.

A strong mode field confinement, which means a small MFD and operates the data link at a wavelength closest to the fiber cut-off wavelength, can reduce both the macrobend and microbend losses of single mode fiber. This leads to a fiber design with a large core-cladding index difference and a fiber V-value close to its single mode cutoff value, e.g., 2.405 for step-index fiber and a higher value for non-uniform index profile fiber. However, there is a practical limit on the amount of core-cladding index difference based on the glass materials used in fiber design. The increase also leads to the increase of the Rayleigh scattering loss and therefore increase the fiber intrinsic attenuatin. A bend loss study on a small MFD bend insensitive single mode fibers clearly illustrated the inter-dependence of bend loss vs. intrinsic loss.[11] In addition, the increase of core-cladding index difference reduces the fiber core size of single mode fiber and its MFD. This will tighten the alignment tolerance and increase connection loss at the interconnections. The technical challenge here is to design a fiber with sufficient bend loss resistance without disregarding fiber intrinsic attenuation and interconnection loss.

III. Dispersion

Dispersion introduces temporal broadening on optical pulses transmitted through an optical fiber. It will impair the integrity of the optical signal and cause transmission error at the optical receiver of FODL. Intermodal dispersion due to the difference of propagation time delay among different waveguide modes is the dominant dispersion in multimode fibers. Such dispersion can be reduced by modifying the refractive index profile of fiber core to minimize the time delay difference of guiding modes. A graded-index fiber with a parabolic index profile is known to improve the dispersion performance over a step-index fiber with the same core-cladding and core size by several orders of magnitudes. The improvement increases with the decrease of actual core-cladding index difference.

For the case of single mode fiber, the

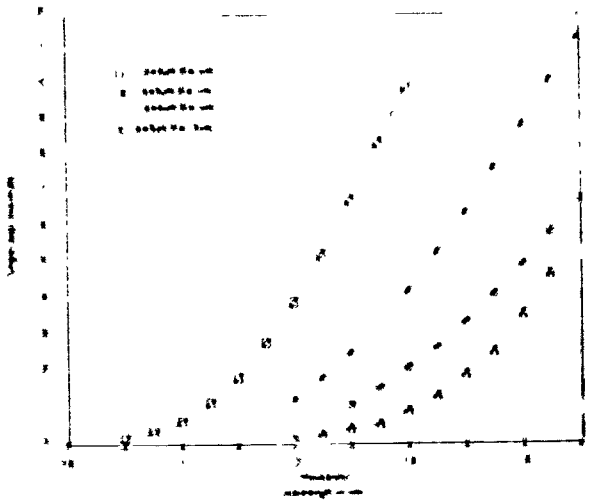

Figure 2 Single Loop Loss Against Wavelength
The bend loss of single 1 cm curvature fiber loop is shown as a function of optical wavelength. Fiber parameters a equal 0.2%, fiber core radius, a, and bend radius, R, are the calculation parameters.

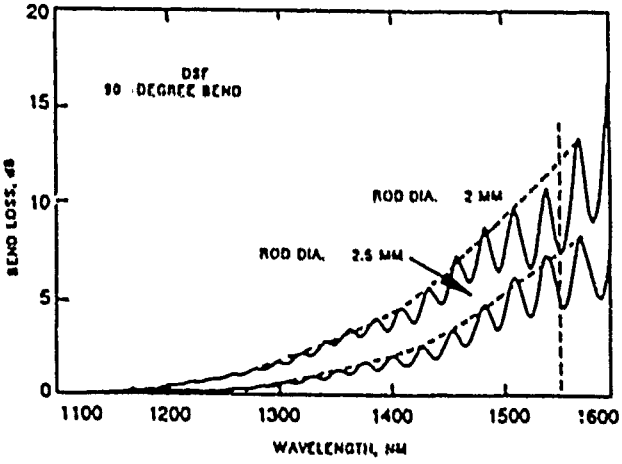

Fig. 3 Spectral Insertion Loss of Wound Fiber
This figure shows spectral insertion loss of DSF fiber subjected to 90-degree bends around 4 and 5 mm rods.

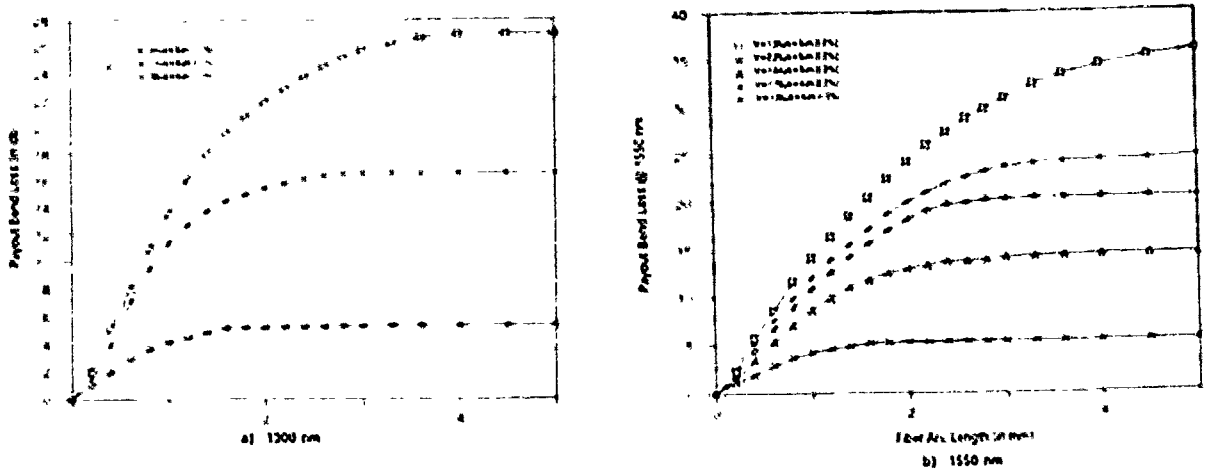

Figure 4 Payout Bend Loss

lowest-order propagation mode still experiences finite intramodel dispersion due to the transmission time delay difference among the spectral components of its optical source. This dispersion can be loosely divided into two elements: the material or chromatic dispersion and the waveguide dispersion. The former depends on the glass material while the latter depends on the refractive index profile of fiber. The wavelength dependence of these two dispersion elements are known to be opposite in effect in the wavelength range of 1300-1600 nm. The zero-dispersion wavelength of step-index silica fiber occurs around 1310 nm. By selecting a refractive index profile to offset the two dispersion elements, one can design an optical fiber with zero total dispersion at any given wavelength in 1300-1600 nm range.[12] For a long range tactical system fiber, it is desirable to shift the zero-dispersion wavelength of single mode fiber into the 1550 nm window for both low loss and low dispersion. Such dispersion-shifted fibers can be realized in several different index profiles.[13] For a wavelength division multiplexing FODL that requires both 1300 nm and 1550 nm in transmission, a fiber with low dispersion at both wavelengths is necessary. The index profile of fiber can also be modified to minimize the dispersion at both wavelengths and yields a dispersion flattened fiber.[14] It is known that the index profile design for the dispersion-shifted fiber and the dispersion-flattened fiber often adversely affect the bend loss and the intrinsic attenuation of the fibers. Design tradeoff on the exact index profile for various fiber performances is imperative for the tactical system fibers.

IV. Fiber Strength

Many tactical system fibers must withstand high bend stress or tensile load, sometimes, over several hundred thousand pounds per square inch (kpsi), under severe operation environment. The technical challenge is to develop a fiber with sufficient strength to provide a reliable signal transmission over the entire system life. The strength of optical fiber is dictated by the microscopic flaws in glass with the breaking stress inversely proportional to the flaw size. The flaw size grows under influence of stress, time and ambient environment. A Weibull analysis reported by Krause et al. shows that the cumulative failure probability of fiber is dominated by the presence of extrinsic flaws.[15] The elimination of extrinsic flaws such as drawing defects is imperative to the long range tactical system fibers.

The initial strength of fiber depends mainly on the fiber fabrication process control and the surface quality of the starting silica tube used in the case of the inside chemical vapor deposition (CVD) process. Clean heat source and drawing environment are essential to eliminate draw-induced flaws and to achieve high initial strength. Fiber manufacturers can use a proof-test process, which applies a short duration (<1 second) loading on a fiber at a specified stress level, to screen out the weak spots due to extrinsic flaws and to ensure a minimum working strength. In practice, it has been established that high humidity, high temperature and certain chemical agents, such as water and methanol, are all detrimental to the preservation of fiber strength in operation. A hermetic coating on glass surface has been shown as an effective means for improving the fiber fatigue resistance by preventing moisture from reaching and attacking the silica surface of fiber. Technical challenges remain in the areas of fabrication process control for long length high strength fiber production and understanding of flaw creation and growth process.

V. Conclusions

The breakthroughs in fiber design and fabrication techniques in the past two decades have greatly improved the performance of optical fibers. Fibers with intrinsic attenuation approaching the Rayleigh scattering loss limit and zero total dispersion at a specified wavelength have been reported. Significant improvements on the environment-induced loss, the bend-induced loss and the strength of fiber have also been achieved through an intense effort on researching their physical mechanisms and developing engineering solutions. It was found that the fiber design optimization for various performance concerns often leads to conflicting fiber design requirements. This presents an acute problem in tactical system fiber design where the fiber must survive severe operation environment. Careful design tradeoffs on glass material, refractive index profile, fiber dimensions and coating material, for a balanced fiber performance, are imperative to the development of tactical system fiber. In practice, the fiber must be thoroughly tested and meet each tactical system requirement in order to ensure its performance and reliability.

REFERENCES

1. Kanamori, H., Yokota, H., Tanaka, G., Watanabe, M., Ishiguro, Y., Yoshida, I., Kakii, T., Itoh, S., Asano, Y., and Tanaka, S. "Transmission characteristics and reliability of pure-silica-core single-mode fibers", IEEE J. Lightwave Tech. vol. 4, p. 1144, 1986.

2. Beales, K. J., Cooper, D. M., and Rush, J. D., "Increased attenuation in optical fibers caused by diffusion of molecular hydrogen at room temperature", Electron Lett. vol. 19, p. 917, 1983.

3. Tomita, A., and Lemaire, P. J., "Hydrogen induced loss increases in germanium doped single mode fibers", Electron Lett. vol. 21, p. 71, 1985.

4. Blyler, L. L., and DiMacello F. V. Jr., "Influence of coating on fiber reliability", Technical Digest, OFC'89, Paper WA1, Houston, 1989.

5. Friebele, E. J., Long, K. J., Askins, C. G., Gingerich, M. E., Marrone, M. J., and Griscom, D. L., "Overview of radiation effects in fiber optics", SPIE, Radiation Effects in Optical Materials, vol. 541, p. 70, 1985.

6. Nagel, S. R., "Reliability issues in optical fibers", SPIE Proceeding, Vol. 717, p. 8, 1986.

7. Nemoto, S., and Makimoto, T., "Analysis of splicing loss in single-mode fibers using Gaussian field approximation", Opt. and Quant. Elect. vol. 11, p. 447, 1979.

8. Marcuse, D., "Curvature loss formula for optical fibers", J. Opt. Soc. Am., vol. 66, p. 216, 1976.

9. Gloge, D., "Optical-fiber packaging and its influence on fiber straightness and loss", Bell Syst. Tech. J. vol. 54, p. 243, 1975.

10. Petermann, K., and Kuhne, R., "Upper and lower limits for the microbending loss in arbitrary single-mode fibers", J. Lightwave Tech. vol. LT-4, p. 2, 1986.

11. Tangonan, T. L., Hsu, H. P., Jones, V., and Pikulski, J., "Bend loss measurements for small mode field diameter fibers", Electron. Lett. vol. 25, p. 142, 1989.

12. Gambling, W. A., et al., "Mode dispersion, material dispersion, and profile dispersion in graded-index single-mode fiber", Microwave optics and Acoustics, vol. 3, p. 239, 1979.

13. Jeunhomme, L., "Single-mode fiber desing for long haul trnsmission", IEEE J. Quant. Electr. vol. QE-18, p. 727, 1982.

14. Kalish, D., and Cohen, L. G., "Single-mode fiber: from research and development to manufacturing", AT&T Tech. J. vol. 66, p. 19, 1987.

15. Krause, J. T., Meade, D. A., and Shapiro, S., "Assuring mechanical reliability of high strength fiber and cable for SL", Proc., Suboptic Intern. Conf., Opt. Fiber Sub. Telecomm. System, p. 117, Paris, 1986.

BIOGRAPHY

H. P. Hsu is currently a senior scientist at Missile Systems Group, Hughes Aircraft Company with responsibility in fiber-optics guided missile development. Prior to joining Hughes he worked for Bell Laboratories at Allentown PA as a member of technical staff for fiber-optic component research and development. His previous assignment was with the U.S. Naval Research Laboratory as a research associate where he conducted research on fiber-optics and integrated optics projects.

Education: BS in Electrophysics from National Chiao Tung University, Hsinchu, Taiwan. M.S. and D.Sc. both in Electrical Engineering from Washington University, St. Louis MO. He is a member of IEEE and OSA.

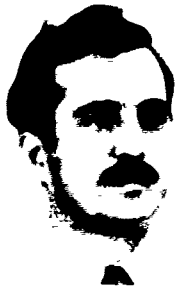

Vasilios E. Kalomiris is currently acting branch chief for Local Area Network and Fiber Optics at CECOM. Previously, his responsibilities were as a project leader for fiber optic cables, connectors, and fiber optic system development. Prior to joining CECOM, he worked for ITT-EOPD as a project engineer for the air-layable fiber optic cable program. His previous assignment was with General Cable Corp. R&D as a research engineer where he was involved with the design, development and manufacture of a prorotype power cable with flexible core.

Education: B.A. in Mathematics, B.S. in Electrical Engineering, M.S. in Electrical Engineering all from New York University and an MBA from Fairleigh Dickinson University. He is a member of AFCEA, IEEE and the Technical Chamber of Greece (Society of Professional Engineers). He received the 3rd annual Engineering Excellence Award for 1986 from CECOM; served for three years as chairman of the Tri-service Group on fiber cables and connectors; currently is chairing the point-to-point systems group.

OPTICAL FIBERS FOR UNDERWATER SENSING

N. Lagakos, T.R. Hickman, P.Ehrenfeuchter
J.A. Bucaro, and A. Dandridge

Naval Research Laboratory
Washington, D.C. 20735-5000

ABSTRACT

Optimization of single mode fibers for phase modulated interferometric sensors is considered for underwater acoustic detection. The fiber glass must be hermetically sealed for long term protection and polymers compatible with water should be used as fiber coatings. Good bonding between the fiber layers is also necessary for effectively transferring the strains from the outer coating to the fiber glass. Optimization geometry of the fibers is presented and appropriate polymer coating selection is given. An example of an underwater acoustic sensor is studied.

I. Introduction

Phase modulation of light in single mode fibers has been successfully utilized for detecting acoustic fields.[1, 2] In these sensors, the fiber coatings play a very important role in determining the fiber acoustic sensitivity.[3] So far, the emphasis has been directed towards the development of sensors for linear arrays where the fiber is immersed in organic fluids. Most of the commercial polymers used as fiber coatings, (such as U.V. curable, nylon, and Hytrel) are compatible with those fluids. In general, however, these polymers are not compatible with water. This presents a major limitation since for many applications the sensor would be immersed in water.

A systematic study has been carried out to optimize single mode fibers for phase modulated interferometric sensors for underwater acoustic detection. The fiber glass must be hermetically sealed for long term protection and polymers compatible with water should be used as fiber coatings. Tight bonding between the fiber layers must be maintained for effectively transfering the strains generated by the external field from the outer coating to the fiber glass. In this article, approaches for optimizing the composition and geometry of the fibers is presented and appropriate polymer coating selection is discussed. An example is also given of an underwater acoustic sensor.

II. Acoustic Sensitivity of Fibers

A typical Mach-Zhender interferometric sensor for detecting phase modulation in single mode fibers is shown schematically in Figure 1. Any phase modulation in the sensing fiber can be detected by comparing the phases in the sensing and reference fibers. Fiber couplers are used to split and recombine the light beams. The pressure sensitivity of the optical phase in a fiber is defined as $\Delta\phi/\phi\Delta P$ where $\Delta\phi$ is the shift in the phase ϕ due to a pressure change ΔP. If the given pressure change $\Delta\phi$ results in a fiber core axial strain ϵ_z and radial strain ϵ_r, then it can be shown that [4]

$$\frac{\Delta\phi}{\phi} = \epsilon_z - \frac{n^2}{2}[(P_{11} + P_{12})\epsilon_r + P_{12}\epsilon_z] \qquad (1)$$

Here P_{11} and P_{12} are the elastooptic coefficients of the core and n is its refractive index. The first term in (1) is the part of $\Delta\phi/\phi\Delta P$ which is due to the fiber length change, while the second and third terms are due to the refractive index modulation of the core, which is related to the photoelastic effect[4].

In order to calculate the sensitivity as given in Equation (1), the strains in the core ϵ_z and ϵ_r must be related to the properties of the fiber layers. The strains in a given layer are related to the stresses through the elastic moduli of that layer[3] while the displacements are expressed in terms of the strains. The constants involved in these calculations are found from the appropriate boundary conditions. Having calculated the various constants, the strains in the core are determined and the sensitivity is calculated using Equation (1)[3].

In general, the acoustic sensitivity is a very strong function of the elastic moduli of the outer hard polymeric coating of the fiber. High sensitivity can be achieved with coatings of low bulk modulus and high Young's modulus materials. This can be understood from the next

two figures. Fig. 2 shows the acoustic sensitivity of a fiber as a function of coating thickness for different coating Young's moduli. All other parameters of the fiber were kept constant. As can be seen from this figure, for thick coatings the sensitivity is determined by the bulk modulus which governs the fiber dimensional change. For typical fibers, however, both the bulk modulus and the Young's modulus are important. As can be seen from Fig. 3, high sensitivity requires low bulk modulus and high Young's modulus coatings. In this case, the bulk modulus determines the "maximum" fiber dimensional changes, while the Young's modulus governs the fraction of these changes, or strains, which can couple to the fiber core. A close examination of Eq. (1) reveals that the axial strain controls the acoustic sensitivity, as can be seen from Fig. 4. In this figure, the sensitivity and its contributing terms (Eq. 1) are plotted as a function of the radius of a typical single-mode fiber. As can be seen from Fig. 4, the major contribution comes from ϵ_z^1 which is the direct fiber length modulation term (first term in Eq. 1) A typical optical fiber consists of a core, a cladding, and a substrate fabricated from glasses having similar properties. Typically, this glass waveguide is first coated with an inner soft elastomer and then with an outer plastic, or metal jacket to preserve the fiber strength. If the bonding between fiber layers is not good the axial strain cannot be transferred to the glass, significantly reducing the fiber sensitivity (Fig. 4).

III. Polymers Compatible With Water

For underwater sensing all the fiber coatings should be materials compatible with water. We have studied the compatibility of many commercially available polymers (a detailed description of these polymers is given in Reference 5) with water. The study has indicated that Teflons, polyethylene, polypropylene, polystyrene, rexolite, polysulfone, and Noryl have excellent water resistance with very good dimensional stability. Nylon has a rather poor dimensional stability while Hytrel 6346 splits into large pieces after 6.5 months in water (at 75°C). As for polyurethanes, some have good water resistance and some very poor. Therefore, for underwater sensing, a careful fiber coating selection must be made for long term stability.

IV. Planar Underwater Fiber Optic Sensing

An example of an underwater, flexible, planar, fiber optic sensor is given in this section[6]. The planar fiber-optic sensor was fabricated by first forming a planar fiber spiral in which adjacent fiber loops were physically touching. The basic fiber used was a high-numerical-aperture (0.17) single-mode fiber with an 80-μm outside diameter and a 100-μm buffer jacket of silicone. The 34-m-long sensing fiber had an additional 350-μm coating of polyester (Hytrel 7246), making its total diameter 1 mm. This fiber spiral was then embedded in the center of a polyurethane layer, the overall size of which was 30 cm X 30 cm X 6 mm. The acoustic sensitivity of the planar fiber-optic sensor was studied in the frequency range of 250-2500 Hz utilizing an available low-frequency pool facility. The flexible sensor was weakly attached to a 3-mm-thick Al plate using double-sided tape and then immersed in the 9-m-diameter, 6-m-deep acoustic measurement pool. Fig. 5 shows the measured acoustic response. (This response was found to be stable for an immersion time longer than a month.) As can be seen, the sensitivity is frequency independent over the band, and the relative optical phase shift per unit of applied acoustic pressure is

$$\Delta\phi/\phi\Delta P = 8.6 \times 10^{-11}/(\text{dyn/cm}^2)$$
$$= -321 \text{ dB re} \frac{1}{\mu\text{Pa}}.$$

This sensitivity appears to be the largest reported to date for fiber acoustic sensors. The extra sensitivity is provided by the polyurethane encapsulant, as is explained below. In calculating the sensitivity (solid line in Fig. 5) an approximate model has been used in which the polyurethane layer was taken to be an additional fiber coating[6]. Fig. 6 shows the calculated fiber sensitivity as various layers are added to the fiber. As can be seen from this Figure, for a fiber radius less than 80μm (glass only) the sensitivity is very low due to the high bulk modulus of the glass[3]. When the silicone coating is added (up to 110μm radius) the sensitivity increases slightly due to the very low Young's modulus of the silicone[3]. As the polyester (Hytrel) starts building up, however, the sensitivity of the fiber increases very rapidly due to the low bulk and high Young's moduli of the polyester. The sensitivity increases even further when the polyurethane (Uralite 3140) coating is added due to its low bulk modulus (lower than that of polyester) and its relatively large thickness.

V. Conclusions

Single mode optical fibers have been considered for underwater phase modulated interferometric sensing. The fiber glass must be hermetically sealed for long term protection. Good bonding between the fiber layers is also necessary for effectively transferring the strains generated by the external field from the outer coating to the glass. The fiber coatings must be compatible with water. Teflons, polyethylenes, polypropylenes, polystyrenes, rexolite, and polysulfone have excellent water resistance and, therefore, can be used as fiber coatings for underwater sensing. Finally, an example of an

underwater fiber optic sensor was given. The sensor is flexible, planar and has shown very promising performance.

References

1. J.A. Bucaro, H. P. Dardy, & E. F. Carome, J. Acoust. Soc. Am. 62 1302 (1977).
2. J.A. Bucaro, N. Lagakos, J.H. Cole, and T.G. Giallorenzi, *Physical Acoustics* (Academic, New York, 1982), Vol. 16, p. 385.
3. N. Lagakos, E. Schnaus, J. Cole, J. Jarzynski, and J. Bucaro, IEEE J. Quantum; Electron. QE-18, 683 (1982).
4. B. Budiansky, D.C. Drucker, G.S. Kino, and J.R. Rice, Appl. Opt. 18, 4085 (1979).
5. N. Lagakos, J. Jarzynski, J.H. Cole, and J.A. Bucaro, J. Appl Phys. 59, 4017 (1986).
6. N. Lagakos, P. Ehrenfeuchter, T.R. Hickman, A. Tveten, and J.A. Bucaro, Opt Lett. 13, p. 788, 1988.

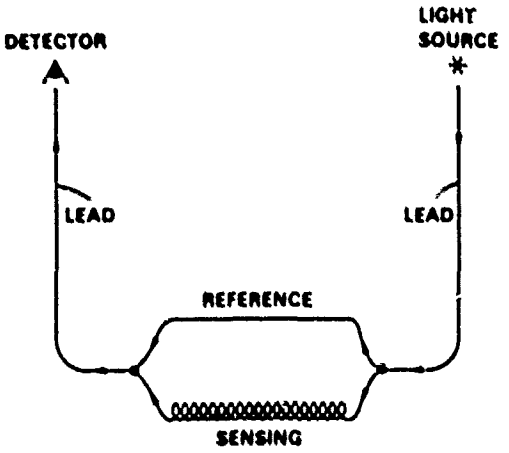

Fig. 1 Fiber Optic Interferometric (Mach-Zehnder) Sensor

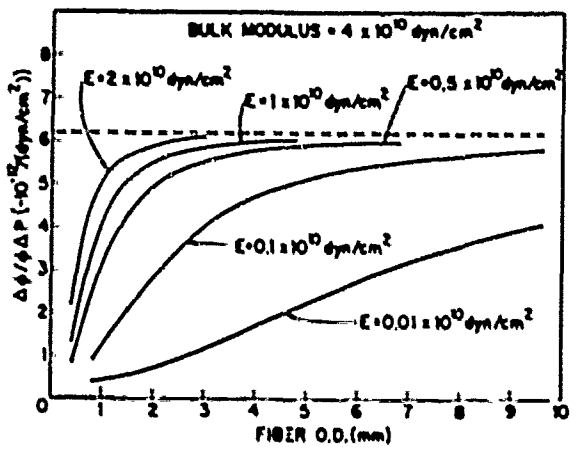

Fig. 2 Calculated Acoustic Sensitivity vs Fiber Outer Diameter for Different Young's Moduli of the Outer Coating. (bulk modulus: 4 X 10^{10} dyn/cm^2)

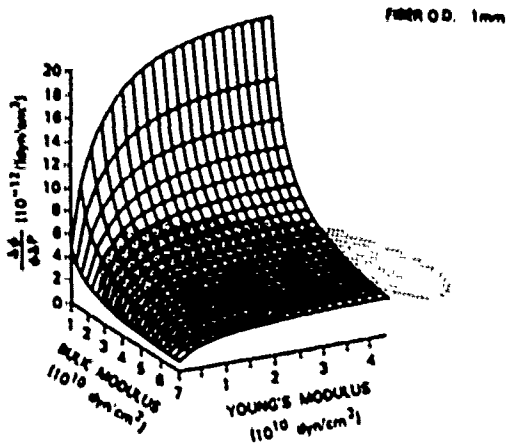

Fig. 3 Calculated Acoustic Sensitivity vs Bulk and Young's Moduli of the Fiber Outer Coating

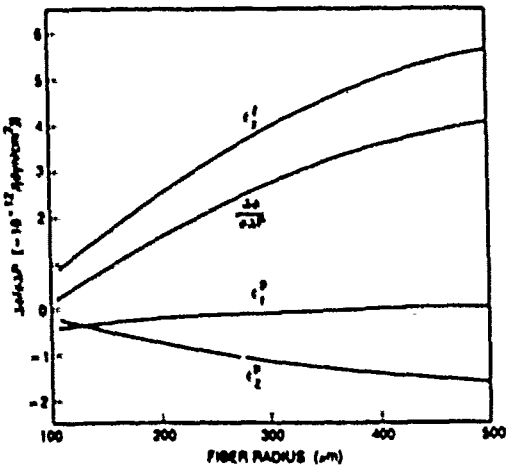

Fig. 4 Calculated Low-Frequency Acoustic Sensitivity of a Fiber vs Fiber Radius. ϵ_z^1 Shows the Phase Change due to the Length Change; ϵ_r^p and ϵ_t^p Show the Refractive Index Modulation Term

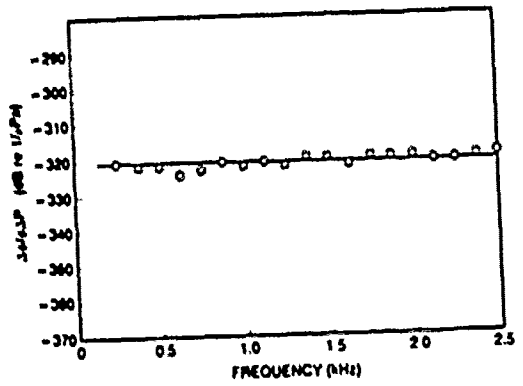

Fig. 5 Acoustic Response of the Planar Fiber Sensor

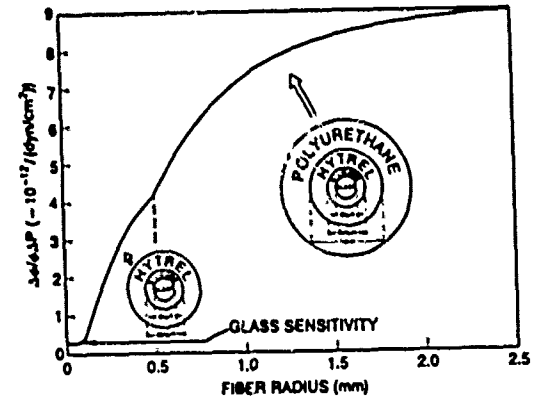

Fig. 6 Calculated Acoustic Sensitivity of a Fiber vs Fiber Radius.

DEVELOPMENT AND APPLICATION OF LOW-SMOKE, FLAME-RETARDANT FLEXIBLE RF CABLE

Anthony R. Fedor
Brand-Rex Cable Systems Div.
1600 West Main Street
Willimantic, CT 06226-1128

Abstract

The U.S. Navy's Surface Shipbuilding Program set the standard for developing requirements for low-smoke, fire-retardant multiconductor cables and extended these requirements to flexible RF cables. In response to General Electric's direction to try and replace PVC jacketed cable from surface vessels, an analysis was undertaken in 1986 to define a set of requirements for those cable types not using low-smoke, flame-retardant materials. Approximately 23% of combat system cables used per ship were found to be flexible RF types, which would have to be replaced. A general specification was developed that defined the basic and overall requirements for RF cable constructions. The major obstacle to hurdle was that of passing the IEEE-383 flame propagation test. Following engineering analysis, materials were used to create a suitable cable construction capable of passing the flame test and satisfying the physical and electrical requirements needed for a shipboard installation. To date, seven cable constructions have been tested and qualified to the drawings and are planned for shipboard installation.

Introduction

In 1981, the US Navy Shipbuilding Program Office initiated work for replacement of multiconductor PVC-jacketed cables with Low Smoke/Low Toxicity (LS/LT) jacketed cables. These cables were designed to be lighter in weight, have LS/LT characteristics and inhibit the propagation of flame. The first Advanced Marine Cables were procured to NAVSEA PMS 400-881, the predecessor to MIL-C-24640, and installed on the CG 49 (Ticonderoga-class ship) and subsequent ships of the class. In 1985, the Navy officially directed the implementation of Advanced Marine Cable and other LS/LT multiconductor cable by superseding MIL-C-915 cables with MIL-C-24640 and MIL-C-24643 cables. No RF cables were addressed at this time. GE-GESD (formerly RCA Corporation) received authorization from the Navy which provided for the development of procurement specifications and drawings for interconnecting cables having LS/LT properties that were not specified in the newer multiconductor cable specifications. Digital processing equipment required increased use of flexible RF cables. Therefore the goal was to replace MIL-C-17 type cables with similar cables having LS/LT characteristics and enhanced shielding capabilities.

The first cable designed and developed by Brand-Rex Cable Systems was the one required for compatibility with the 75-ohm Navy Tactical Data System type "D" interfaces per MIL-STD-1397. This cable was originally specified in MIL-C-17 (RG-12). RCA (at the time) generated NAVSEA Drawing 6322493, which replaced RG-12. This NAVSEA drawing specified a triaxial cable having enhanced shielding, a more ruggedized jacket, and incorporating materials that either met or exceeded the flame and LS/LT requirements of MIL-C-24640. Following a successful development, other cable types were selected for replacement. These included, but were not limited to, RG-213, RG-214, RG-216, RG-108, RG-59 and 50 ohm triaxial (M17/134 and /135) constructions. Examples of the new replacement cables (three different constructions) are shown in Figure 1.

(a) Double Optimized Shielded 50 Ohm Coaxial Cable, Foamed PE Core, 19-Strand AWG 12 Center Conductor

(b) Single Optimized Braid Shield, 78 Ohm Twinaxial Cable, Foamed PE Core, 19-Strand AWG 20 Conductors

(c) Single Optimized Braid Shield, 50 Ohm Triaxial Cable, Foamed PE Core, 19-Strand AWG 20 Center Conductor

Figure 1. Sample Constructions Qualified to NAVSEA Drawing Number 6323050 Requirements

Specification Development

GE-GESD created procurement documentation that defined the criteria for these to RF cables. Common (general) requirements are resident in a general specification and individual and unique requirements were separated into satellite (procurement) drawings. These procurement drawings cross-reference the general specification requirements applicable to a particular construction.

The general requirements specification, NAVSEA Drawing 6323050, seemed to be based upon much of the information specified in MIL-C-17, MIL-C-24640 and MIL-C-24643. New tests were not developed. Those tests specified in the above specifications were used to the maximum extent. A high degree of confidence was required to be achieved prior to cable delivery so system level performance parameters would not be degraded.

Program Discussion

Achievements

The program was divided into four distinct levels of effort that helped Brand-Rex Cable Systems Division focus on successfully developing cables superior to those currently available in the industry. These four objectives were:

1. Retardation of flame propagation.
2. Cable abrasion resistance.
3. Optimum shielding effectiveness.
4. Enhanced electrical performance.

Flame Propagation: A flame propagation test (IEEE-383) was invoked to qualify each cable construction. The IEEE-383 test was set up and completed in a relatively short period of time and yielded reproducible results. Specifically, the goal was to minimize heat buildup in the cable so it would not be consumed by the fire. Results of the development provided GE and the Navy with qualified cables that would not propogate a vertical flame. This characteristic would help confine a fire within a compartment and provide more time for a damage control team to arrive at the scene and fight the fire.

Abrasion Resistance: Cable abrasion tests were invoked on both finished cable samples (as a lot acceptance test) and on jacket material samples (as a material qualification test). Both test procedures used the same set-up and equipment as specified in MIL-C-17, Rev. F, Amendment 3, for an AWG 16 jacket/wire sample. An 8-inch rotating wheel having two abrading edges 180 degrees apart and turning at 17 RPM was used for the test. Each test sample had a 1-pound weight attached to its end and was drooped over the abrading wheel.

The goal was to have a finished cable use a jacket material that would be capable of withstanding the rigors of installation at the shipyard. Since some of the RF cable lengths were expected to exceed 500 feet, pulling these cables around corners could degrade or destroy the jacket. Not only did material type have to be reviewed, but jacket thickness also.

The material qualification test performed on the jacket/wire sample was used to evaluate jacket materials. Since the dimensions and procedures were strictly controlled, this test could be used to compare different products and get a good indication if the material would perform to the level required.

The test on the finished cable samples was invoked to specify a minimum level of performance to ensure that the cable being provided would be similar to that previously qualified. This assured the customer with a level of confidence that the cable would be capable of withstanding the shipboard environment.

Jacket thicknesses were varied for each construction to allow a minimum level of 500 cycles on the abrading wheel to be achieved by each different cable. The results proved better than those for similar cables using PVC jacket material.

Shielding Effectiveness: Shielding effectiveness criteria were specified to ensure the survivability and operation of equipment in an EMI/EMP environment. Presently, the cable specified for surface ships must have, as a minimum, an overall braid shield that meets or exceeds a level of performance of 60 dB for the attenuation of an impinging electromagnetic field over a frequency range from 30 kHz to 400 MHz. In lieu of invoking a percent coverage for the braid (which is traditionally found in specifications for the design of a braid shield), an electrical performance value was specified.

Surface transfer impedance was specified to measure the cable's shielding effectiveness and replace the physical parameters defined by the percent coverage in MIL-C-17. Samples of this type of construction were evaluated by NSWC-White Oak, Maryland. The results demonstrated the feasibility of this design and test method. The data showed a direct correlation between surface transfer impedance results obtained using the test set-up specified in 6323050 and that found of the cable's shield in the attenuation of free-field energy. The surface transfer impedance test is similar to that specified in MIL-C-24640. The test uses a triaxial configuration, having an extra braid applied over a sample cable one meter in length. The surface transfer impedance is measured using a sweep frequency signal generator and network analyzer.[1] The ratio of induced voltage measured inside of the applied braid shield to the driving current on the shield is the surface transfer impedance (Z_t) of the braided shield at a given frequency. This is mathematically described below.

$$Z_t = \frac{\Delta V}{I_s} \cdot \frac{1}{\Delta X} \text{ (ohm/m)}$$

where I_s = the uniform current flowing on the braided shield,

ΔX = the length of the cable sample,

ΔV = the leakage voltage across ΔX.

The lower the surface transfer impedance, the better the cable's shielding effectiveness.[2] A typical graph generated from one of the RF cable's surface transfer impedance tests is shown in Figure 2.

The EMP response, which gives a relative performance of a braid shield over frequency, is calculated using the following formula:

$$\text{EMP response (dB)} = -185 - 10 \log \int_{a}^{(1\times10^{9})} \frac{(Z_t(f))^2\, df}{(\alpha^2+f^2)(\beta^2+f^2)}$$

where $Z_t(f)$ = surface transfer impedance (ohm/m) at a frequency (f);
$\alpha = 2.39 \times 10^{3}$;
$\beta = 4.12 \times 10^{7}$;
f = frequency (Hz);
df = change in frequency.

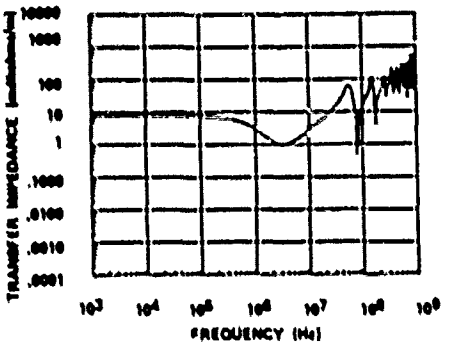

Figure 2. Typical Single Optimized Braid Surface Transfer Impedance Results

A minimum of 100 points per decade are taken and calculated to arrive at an average for the boundary units identified. Figure 3 shows a plot of the EMP response for the same cable sample tested in Figure 2.

It is assumed that every cable core diameter has an optimum braid configuration.[1] Double braided shields will generally improve a cable's shielding effectiveness but since an area of coverage is generally used in lieu of transfer impedance to quantify shielding effectiveness, there is no assurance that one cable will perform to the same level as another. Therefore, the shielding effectiveness test as defined herein is invoked as a lot acceptance test to verify the quality of shielding for each cable used. All cable constructions exhibited an average value above 60 dB for a single "optimized" shield. Two of the coaxial constructions had two optimized shields applied, and when tested together exhibited an average level of performance above 70 dB.

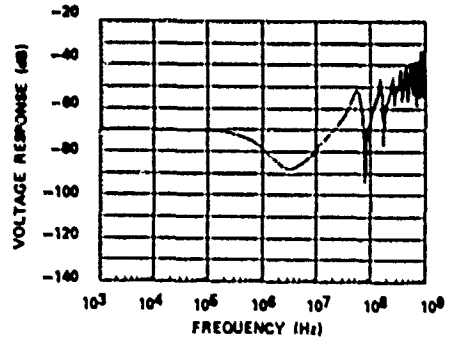

Figure 3. EMP Response Plotted at Frequency for Same Cable Sample as Shown in Figure 2. Minimum of 100 Points per Decade

Enhanced Electrical Performance: Matching or improving the electrical performance was a goal of this effort. Cable was not evaluated as an RF transmission line but as a medium for data transmission. As a result of foaming the core material, velocity of propagation was increased, attenuation at the higher frequencies was decreased, and capacitance was decreased, compared with similar cabling having solid polyethylene cores (those found in MIL-C-17). Since most uses for these cables are that of signal/data transmission, a compromise in power handling capability was not an issue. The newly developed cables are not capable of handling the same voltages and currents as those of similar cables qualified to MIL-C-17.

Fundamental Constraints

When considering the design objectives for these cables, it was necessary to keep this development compatible with existing RF connectors in use. Equipment delivered to the shipyards is provided by many sources. Since the cables directly interface with a large variety of equipment and are supplied as Government Furnished Equipment (GFE), the customer required compatibility since the plug end of the connector had to mate with those equipments. Therefore, maintaining the outside diameter and center conductor dimensions for each cable type was of extreme importance. One essential parameter was the RF cable outer jacket thickness. A minimum level of abrasion resistance (as previously discussed) was designed and specified in the procurement drawings so a level of confidence for the overall integrity of the cable would be obtained. This goal was achieved because the foaming of the cable core resulted in a decrease in core diameters which allowed for an increase in jacket thickness. Jacket thicknesses that averaged 25 to 30 mils in MIL-C-17 type cables averaged 40 to 50 mils for the newly designed cables.

All the cables developed have either maintained or decreased their overall diameters when compared with MIL-C-17 "equivalents," except for the small 50 ohm triaxial cable, NAVSEA Drawing 6323056. For this one, a conscious decision was made by the customer not to be compatible with the present connector. A tradeoff study showed a high probability of material failure during installation if the outside dimension was limited to the given connector configuration. To resolve this issue, the customer redesigned the existing connector.

The primary concern expressed by the installation activity (the shipyards) was that of flexibility. This characteristic has always been a concern, especially for new cable developments. Pulling and terminating cables onboard a ship in areas crowded with equipment is always difficult. Sometimes the installation results in compromising the performance of the cable. It is not uncommon for a cable to be bent at a radius less than 10 times its diameter. Since the increase in jacket thickness was assumed to stiffen cable constructions, the design had to compensate by allowing more flexibility from the components underneath the jacket. For almost all the cable constructions, a 19-strand versus 7-strand design was chosen

for the the center conductors. Also, a foamed polyethylene (PE) core was used for all the cables. Foamed PE tends to be more flexible than the solid PE counterparts defined in MIL-C-17. As a result, both the cores and center conductors had attributes that helped compensate for the increase in jacket thickness, thereby creating a cable with no increase in stiffness.

A cold bend test was invoked for each cable construction, specified to be run at −40 degrees Celsius over a mandrel no more than 10 times the cable's diameter. This requirement helped convince the shipyards that the quality of the cable would be maintained in the harsh shipboard environment.

Cable Development

Core

In considering various design alternatives, the material used in the core of the cable (the material that fills in around the center conductor and under the first braid or outer conductor) was deemed critical with respect to the outcome of the flame propagation test. The idea was to either minimize material in the core so it would not melt and feed the flame, or find a new material that would not burn. The two basic materials used in the cores of Mil-C-17 type RF cables are polyethylene (PE) and Teflon/FEP type products. Each pose a number of potential problems. The Teflon-type products need to be handled and installed with special care so the core maintains its designed dimension and is not squeezed down. Teflon-type products also have higher than acceptable levels of halogen content. During a fire, the material would exceed the acceptable levels of products of combustion. PE has the tendancy to readily support combustion. Adding flame retardants to PE increases the halogen content, thereby increasing toxicity levels when subjected to a flame.

An attempt was made earlier in the program to produce a dual composite core construction using two materials; a thin flame retardant skin over a foamed PE core. Flame propagation testing of this type of core showed promising results, but because of the negative factors associated with this option (the addition of halogenated flame retardants and a special tandem extrusion line needed for its manufacture), this alternative was soon abandoned.

The material finally chosen for the cores was irradiated (cross-linked) foamed PE. The degree of foaming varied with the diameter constraints and various electrical requirements for a given cable construction. A dielectric constant of 1.65 was selected as a design goal. This value is considerably lower than that of solid PE, which allowed for flexibility in the design of the core sizes. The foamed PE provided for a suitable flexible structure that would maintain its geometry and not chip or flake. As previously stated, the attempt was to decrease the cores of the MIL-C-17 type cables so the increase in jacket thickness would not enlarge the cables to a point where they would not fit into their assigned connectors.

Cross-linking the core toughened it and extended its physical properties in higher temperatures but not to the point of being "thermoset." Some of the new constructions passed the IEEE-383 test readily, but others (usually the coaxial types) did not.

Tapes/Barriers

Brand-Rex felt that a barrier material should be provided over the core to seal out both the direct flame and air, thereby reducing heat build-up in the cable. The idea was to prevent the core from melting, dripping and fueling a fire. Preliminary attempts seemed to have merit. The burner used in the IEEE-383 test produces a flame that reaches temperatures above 1500 degrees Fahrenheit. The focus during the test was on the samples, at a height approximately 3 to 4 feet above the flame source. Flame test failures tended to be similar in that the flame would break away fairly rapidly from the initially applied flame and propagate up and consume the cable. All cables tested were totally burned and charred at the base of the ladder (used to hold the cables vertical) where the initial flame source was located. Most of the specimens that passed the test had self-supporting flame break away very slowly from the original flame source but would only propagate up 1 to 3 additional feet before extinguishing itself. The final constructions utilized a barrier material in the form of a tape. Mica-fiberglass, 3-mils thick, was selected to be wrapped around the inner braids, or outer shield braid, depending on configuration. The barrier tape helped to isolate the core from the heat and allowed the constructions to pass the IEEE-383 test by not letting the core material melt and wick down the cable.

Jacket

The jacket applied to all constructions was a cross-linked polyolefin material, modified with nonhalogenated flame retardants similar to that used in MIL-C-24640 cables. Jacket material equaled less than 0.02% halogen content when measured by the X-ray fluorescence test specified in the general requirement drawing. When the jacket was burned, it did not support combustion. It charred and had the characteristic of being thermoset. In some of the triaxial constructions, the jacket was able to withstand the heat and flame to a point where no other flame barriers needed to be added. This phenomenon could be attributed to the fact that both the inner and outer jackets were of the same material and provided a heat and flame barrier.

The jacket was also tested against the specified products of combustion requirements; NES 713 for Toxicity Index, NES 715 for Oxygen Index, and NES 711 for Smoke Index. A test procedure was used to ensure that no strong acids resulted from the breakdown of the material when burned. All test results demonstrated compliance with that specified in the general requirements specification.

Implementation

It is estimated that approximately 10,000 pounds of PVC jacket material (roughly 160,000 feet of RF cable) could be used onboard a Navy Destroyer-class ship. In a fire scenario, PVC-jacketed RF cables emit toxic and acidic fumes many times greater than that of the polyolefin jacket material. In addition, PVC accelerates the flame and causes it to totally consume the cables, leaving a deadly thick blackish smoke as

a by-product. It was important to make the cables available so that they could be installed onboard the Navy Destroyer ships as soon as practical.

Incorporation of the LS/LT RF cable into the shipbuilding program documentation represented the final phase prior to purchase. In the US Navy shipbuilding program, the Program Manager has to incorporate the change into the proposal process for new ship acquisition. The selection of candidates to be included in the proposal is based on need, cost, and availability. Brand-Rex had to prove that these factors were complete for the change to be considered viable.

The first step toward incorporation was the preparation of a technical briefing paper. This paper included a description of the RF cable as a material with emphasis on the significant attributes, such as meeting the IEEE-383 flame propagation test, optimized shielding, and increased velocity of propagation. The features of an inherent low smoke / low toxicity design were also identified. The technical brief was presented to both our customer and proposed future customers (the shipyards).

A full presentation was prepared to inform the shipbuilders of the program details, including a review of both electrical and mechanical characteristics. Various RF cable designs were presented (See Figure 1 for photos of finished cables) to familiarize the shipbuilders with this development. The majority of the shipbuilders' questions were directed to the area of physical handling and installation characteristics. A major concern of the shipbuilders was the introduction of installation problems not associated with the materials presently in use. Disclosing the design and test data and supplying material samples resolved the matter.

Synopsis

A number of significant design improvements have been accomplished for the Navy program. The initial goal of PVC removal and the incorporation of an LS/LT material was successfully introduced. Incorporation of the IEEE-383 burn test further enhanced the design against the propagation of flame as a result of the use of new materials. A significant design change included the incorporation of optimized overall shielding for protection from EMI/EMP. In this area, a shielding effectivity of greater than 60 dB was achieved from E-field coupling. The use of a 19-strand center conductor resulted in greater flexibility and, with the specification of an abrasion resistance test for the LS/LT jacket material, enhanced cable installation and handling will be obtained. Combining the electrical and mechanical property gains with environmental and physical attributes resulted in a significantly improved cable design that can be effectively utilized by the US Navy.

References

(1) "Cable's Braid is Optimized to Meet EMP Threat," by J. Dennis Chalk, Electronic Packaging and Production, Cahners Publishing Company, August 1985.

(2) Ibid.

(3) Ibid.

Acknowledgement

The author wishes to thank J. Dennis Chalk for his assistance with this program. Also, thanks to all the production and process personnel involved in the development project. Finally, a special acknowledgement of appreciation to the the General Electric Company. The implementation of low-smoke cable on Navy ships would not have reached its present level without the tireless efforts of GE people in the development of the standards and specifications.

Biography

Anthony R. Fedor
Brand-Rex Cable
Systems Division
1600 W. Main St.
Willimantic, CT
06226-1128

Anthony Fedor is presently a product engineer in the Military Market Division of Brand-Rex Cable Systems Division, where he has been employed since 1985. Prior to this he was employed as a product engineer with the Tensolite Company in Buchanan, NY.

MANUFACTURING AND INSPECTION METHODS OF HIGH STRENGTH OPTICAL FIBER FOR MISSILE PAYOUT APPLICATIONS

FRANK I. AKERS AND THOMAS E. WILSON

ALCATEL CABLE SYSTEMS, INC., ROANOKE, VIRGINIA

SUMMARY

The manufacturing of high strength optical fiber for missile payout applications requires new and improved methods of processing, inspection, handling, and storage. This paper addresses some of the techniques needed to guarantee the highest probability of success during high speed payouts. The requirements for testing of fibers for payout exceed those for commercial applications.

INTRODUCTION

Optical fiber was first proposed for use in fiber guided weapons in the mid-1970's[1]. The feasibility of using fiber optics in guided weapons applications was proven in several far-sighted programs sponsored by USA CECOM and USA MICOM. The IFOCL program showed conclusively that the fiber optic guided missile could work if the system could be made reliable. Since the early efforts, numerous programs have been conducted by CECOM, MICOM, NOSC, NUSC, NWC, and others again proving the feasibility and stretching the horizon of technology. The programs have been technology drivers, initiating research into fiber design and materials[2-6]. The underlying concern for optical fiber in these applications has always been and continues to be ... reliability. As the industry has learned more about the manufacturing of optical fiber, it has become clear that there is much still to be discovered in the areas of ultra-high strength fiber, tactical applications, long term storage, and hostile environments.

MANUFACTURING TECHNIQUES

The first step in the manufacture of high strength optical fiber is the control of the raw materials used to fabricate the optical preform. It is imperative that the base materials used be tested or, at a minimum, certified by the vendor for purity, trace elements, particulates, and other contaminants. It is just as important to maintain proper control over the handling and storage of the materials prior to their use in manufacturing product. Studies[7] have repeatedly shown that particles greater than six microns can cause proof test breaks at or above 100,000 psi. Any particle incorporated into the optical preform can cause stress concentration points or actual fractures that could develop into break sources given sufficient time and stress. Laser-aided visual inspection techniques are typically used to inspect the ultra-pure quartz substrate tubes used in the MCVD process as the outer glass cladding. The liquid halides that are deposited to form the core and cladding are purified by sophisticated chemical processing techniques and are tested for contaminants by methods such as gas chromatography, infrared spectroscopy, etc.

During the process of manufacturing an optical preform, cleanliness of the environment around the manufacturing equipment is imperative. It is particularly important to control particulate matter in the vicinity of the hot preform. The MCVD process lends itself to keeping the exterior of the optical preform clean by the ability to flood the area with ultra-pure air and by flame-polishing the preform after collapse. After the preform has been produced, it is kept in a clean, inert environment to cool, then inspected for optical performance. It is also visually inspected for possible strength reducing defects, such as bubbles, inclusions, de-vitrification, etc. The preform is then stored in a dry, inert atmosphere to await drawing into fiber.

Just prior to drawing the optical preform into fiber, several proprietary operations are performed to minimize flaws in the surface of the glass. The draw process is extremely important in producing long lengths of high strength fiber, since this is the only time the fiber will exposed to atmosphere without a protective buffer coating. The tip of the preform is heated in a graphite resistance or RF induction furnace to approximately 2400 degrees Celsius and allowed to drop off, pulling a section of the preform down to a relatively small diameter. This fiber is

directed through measurement devices and coating applicators to a capstan drive which starts to pull the fiber at the present final diameter. Contamination from the draw furnace must be controlled by proper purge procedures and flow dynamics since the glass is exposed from the furnace to the coating applicators. Because the glass is still very hot, it is prone to attract minute particles of air-borne dust and furnace contaminants, such as zirconia and graphite. The fiber should be protected by shields, inert gas showers, clean air showers, and/or clean rooms[8]. Particle counters are used to measure the level of contamination near the fiber and in the general room area to check for potential strength degradation. The fiber diameter is controlled by control loops from laser measuring devices to the speed and temperature controllers. The buffer coating diameter is also measured and controlled using similar high speed laser measuring techniques and a proprietary coating diameter control device. These control loops allow the glass diameter and the coating diameter to be controlled to the extremely tight tolerances needed for payout applications. The measurement equipment is set to alarm any out-of-tolerance condition (typically set at 60-70% of the allowable tolerance) to alert the operator that a potential problem could occur. This allows the operator to make manual corrections or determine the cause of the problem before out-of-specification fiber is produced. It should be remembered that the coating diameter control for payout fiber ($\leq \pm 6$ microns) is significantly tighter than for commercial telecommunications fiber (typically $\leq \pm 15$ microns) due to precision winding requirements. The fiber is also tested by on-line proof test to weed out any major strength flaws in the fiber and to detect potential production problems. After drawing the fiber, an off-line proof test is performed at slower speed to allow additional inspection of the buffer coating to inspect for small defects that may have been missed by the on-line test equipment. This is typically done with laser diffraction techniques in multiple planes to find very small perturbations in the buffer coating. These techniques can typically detect surface changes less than 5 microns in height and , depending on the speed of the fiber, less than 1 cm in length. The size where a buffer coating perturbation becomes critical has not yet been determined. The fiber draw should be a Class 10,000 or better clean room with strict adherence to clean room practices and additional static charge elimination. Static charge can be reduced by humidity control, general room ion neutralization, localized ion neutralization or a combination of all three. The next operation is optical test. Ideally, the fiber should not be removed from a clean room after it is drawn to prevent the attraction of particulate contamination that could cause buffer damage during the rewinding or bobbin winding steps. It is best to minimize the handling and transportation of the fiber to prevent damage to the buffer coating. Standard EIA approved methods should be utilized to check the fiber for optical performance, such as attenuation, cut-off wavelength, mode field diameter, dispersion, etc., and for physical parameters, such as core concentricity, eccentricity, ovality, core/clad ratio, etc. One very important parameter for successful fiber payout is the ability of the fiber to be insensitive to both micro and macro bending force. Alcatel's single mode, bend insensitive fiber, that has been supplied on the FOG-M contract for nearly two years, is tested for bend performance prior to being accepted as a candidate for winding.[9] Even if the fiber remains in the clean room, a clean, static-free bag should be used to protect the fiber from any airborne contamination that might be attracted by static charge.

After the fiber has been tested and accepted for optical and physical characteristics, it must be either spliced to form longer lengths or prepared for precision winding. High strength fiber splicing techniques have improved significantly in the last few years. Splice strengths in excess of 300 kpsi are routine and strengths in excess of 400 kpsi can be achieved with little additional effort. Arc fusion splicing is the most common technique being used for splicing payout type fibers, with flame fusion being used by some manufacturers. Arc fusion techniques can produce splices up to approximately 500 kpsi while flame fusion is be able to exceed this level. The flame fusion technique is inherently more hazardous due to the use of hydrogen and chlorine gases in the process. The most difficult process in splicing is the recoating of the buffer coating material. Much research has been done at Alcatel to develop a consistent, reliable recoating method. The actual process is proprietary, but does consist of using precision molds and injection methods to reconstitute the buffer with the same diameter tolerance as the original buffer. The splices are tested for strength by a tensile test to insure they exceed the requirement of the product. The buffer recoat area is measured using a laser measuring device to insure the diameter is within specification and examined under a microscope to check for voids, splits, or separations. The fiber is then respooled in the clean room onto a single spool in preparation for winding. During this operation, the fiber is again checked for diameter variation and buffer damage by using two laser measuring devices set at a 90 degree angle to each other. This insures that the fiber has not been damaged in the measurement or splicing operations. If there are no damaged areas, the fiber is again placed in a clean, static-free bag and sent to the winding area, along with a diameter trace of the entire link.

Precision winding of the high strength fiber is key to successful payouts of high strength fiber. Alcatel's experience has been that much damage can be done to the fiber prior to, during, and immediately following the precision winding. It is extremely important that the fiber be wound in a clean, static controlled area that minimizes the chance of contamination. Once the fiber has been wound, only gross damage can be found with

techniques like laser illumination or OTDR. Subtle contact with the fiber can result in microscopic damage to the buffer that will cause the fiber to fail due to fatigue from the coil winding radius.

CONCLUSIONS AND CREDITS

The reliability of optical fibers used for payout depends on purity of raw materials, careful manufacturing methods, and extreme care in handling subsequent to processing. This means that reliability is built-in rather than inspected in. The successful production and protection of payout fiber depends on a new culture that rewards great attention to detail.

The authors recognize the fine ef[illegible] people of the Alcatel Defense [illegible] and thank the management of A[illegible] this work.

REFERENCES

1 Fox, D., F. I. Akers and G. Gasparian. "Optimization of an Optical Fiber for Missile Guidance Applications," presented at the Society for Optical Engineering Los Angeles Technical Symposium, Los Angeles, CA, January 1982.

2 Akers, F. I., A. R. Asam and M. S. Maklad. "Optical and Mechanical Performance of 0.1 and 0.2 NA Single Mode Fibers," presented to the International Wire and Cable Symposium, Cherry Hill, NJ, November 1979.

3 Maklad, M. S., A. R. Asam and F. I. Akers. "Recent Advances in High Strength Optical Fibers Having Surface Compression," presented to the International Wire and Cable Symposium, Cherry Hill, NJ, November 1979.

4 Schlef, C., P. Narasimham and S. M. Oh. "UV Cured Coating for Optical Fiber/Cable, presented to the International Wire and Cable Symposium, Cherry Hill, NJ, November 1979.

5 Maklad, M. S., A. R. Asam and F. I. Akers. "Bending and Microbending Losses in Single-Mode Fibers and Cables," presented at the Topical Meeting on Optical Fiber Communication, Washington, D.C., March 1979.

6 Oh, S. M., C. L. Schlef, F. I. Akers and R. E. Thompson. "Long Length, High Strength, and Low Loss Fibers," presented at the American Ceramic Society Glass Division Fall Meeting, Bedford, PA, October 1980.

7 Huff, R. G., and Frank V. Dimarcello, "Critical Particle Size of Contaminants in High and Low Modulus Coatings for High-Strength Optical Lightguides," Journal of Lightwave Technology, LT-3 No.5, October 1985.

8 Khuanghlawn, W., D. Biswas and S. White. "Particle Interaction Effects on the Strength of Optical Fibers," presented to the American Ceramic Society Annual Meeting, Chicago, IL, April 1986.

9 Biswas, D., K. Karbassiyoon and L. Hodges. "Single Mode Bend Insensitive Fiber," presented to the International Wire and Cable Symposium, Reno, NV, November 1988.

Frank Akers is the Director of Business Development at Alcatel Cable Systems. Located in Roanoke, Virginia, he is responsible for the Military and Components business units as well as the research and development activities associated with Alcatel's optical fiber plant in Roanoke. Mr. Akers has been involved with high strength fiber for payout since 1977, when he joined ITT as a process engineer.

OPTICAL FIBER CABLE TRANSFER SPLICING SYSTEM USING OPTICAL FIBER CONNECTORS

Ichiro WATANABE, Masatoshi SHIMIZU and Hideo KOBAYASHI

NTT Network Systems Development Center
Tokai, Ibaraki, 319-11, Japan

Abstract

An optical fiber cable transfer splicing system for use in removing or changing optical fiber cables is developed. This system is realized using optical fiber connectors, fiber transfer splicing equipment, synchronous control equipment and fiber identification equipment incorporating a local injector and a local detector.

With this system cable transfer is carried out with only a slight interruption to working transmission systems and mis-transfer is avoided. A mean transfer time of 12.2 ms is obtained.

1. Introduction

With increased demands on optical fiber cable networks, maintenance has become increasingly important. There is particular need for a system which has minimum influence on working transmission systems when optical fiber cables are removed or changed. During such operations, the optical fiber cable transfer splicing system[1] plays an important role. This system enables the efficient transfer splicing of existing cables to newly-installed ones when optical fiber cables at two different points, such as manholes, are removed or changed.

2. System architecture and function of components

The system architecture is shown in Fig.1. This system is composed of optical fiber connectors, fiber transfer splicing equipment, synchronous control equipment and fiber identification equipment incorporating a local injector (LI) and a local detector (LD). This equipment is explained below.

2.1 Optical fiber connector

A Mechanically Transferable (MT) Connector[2] is used for the sake of endurance, relinbility, low insertion loss and cost saving (Fig.2).

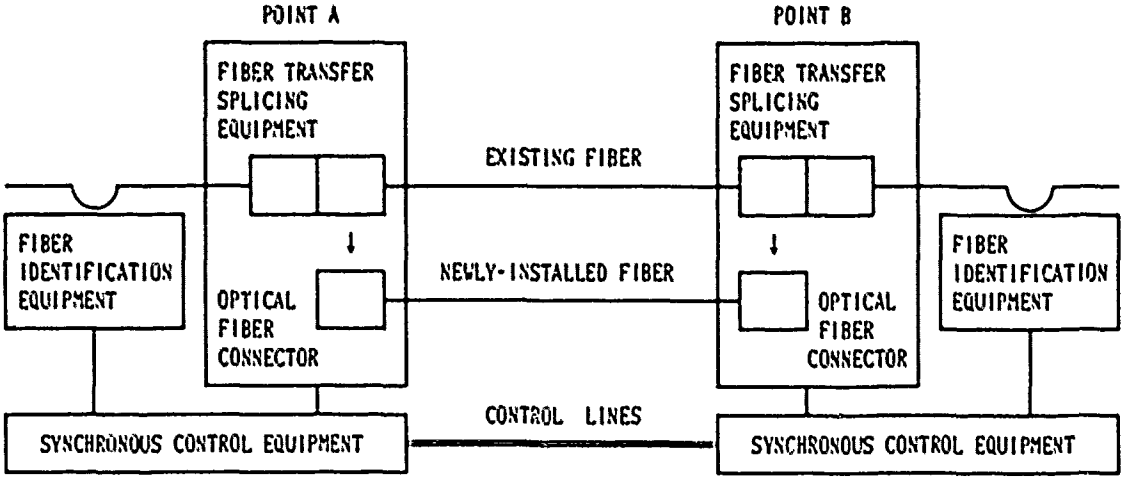

FIG. 1 -SYSTEM ARCHITECTURE

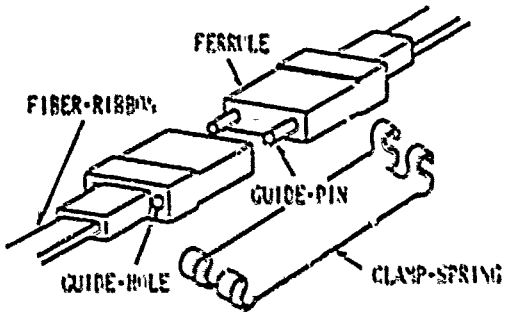

FIG. 2 -CONNECTOR STRUCTURE

2.2 Fiber transfer splicing equipment

This equipment makes it possible to transfer from existing optical fiber cables to newly-installed ones. Fig.3 shows a block diagram of this equipment. Connectors are already installed at the splicing points of each fiber. Fiber transfer splicing equipment is not usually installed at the points and is only used during transfer splicing.

The transfer mechanism is shown in Fig.4. Transfer splicing is performed as follows.

(a)move guide pins with solenoid 1

(b)release mated faces of existing ferrules with solenoid 2

(c)reposition ferrule with solenoid 3

(d)mate faces

(e)move pins with solenoid 4

During (a), (d) and (e), longitudinal pressure is required to mate the ferrule faces. Without this, excess loss would occur during transfer splicing. It is also necessary to release the mated faces to avoid damaging them. In all these operations, a matching fluid is applied to reduce connector loss and avoid Fresnel reflection.

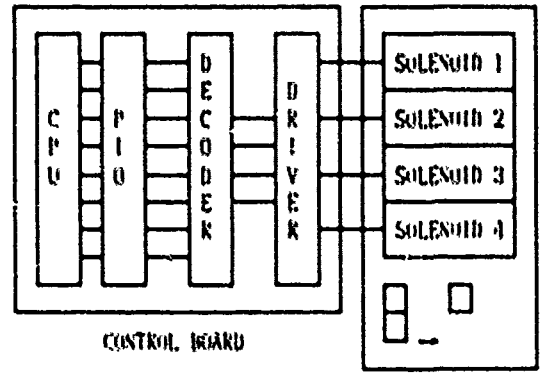

FIG. 3 -BLOCK DIAGRAM OF FIBER TRANSFER SPLICING EQUIPMENT

2.3 Synchronous control equipment

This equipment is used for synchronous control between two points. Fig.5 shows a block diagram of this equipment. Because an S/P (serial to parallel) converter is used, it is necessary to compensate for the time required for conversion. Without this compensation, the driving trigger would be delayed at point B. The time to be compensated for is calculated as follows. The transmission speed is 1200 bps. The trigger command word is composed of 10 bits including a start and a stop bit. So it takes 1/1200x10 s to convert from a serial word to a parallel word.

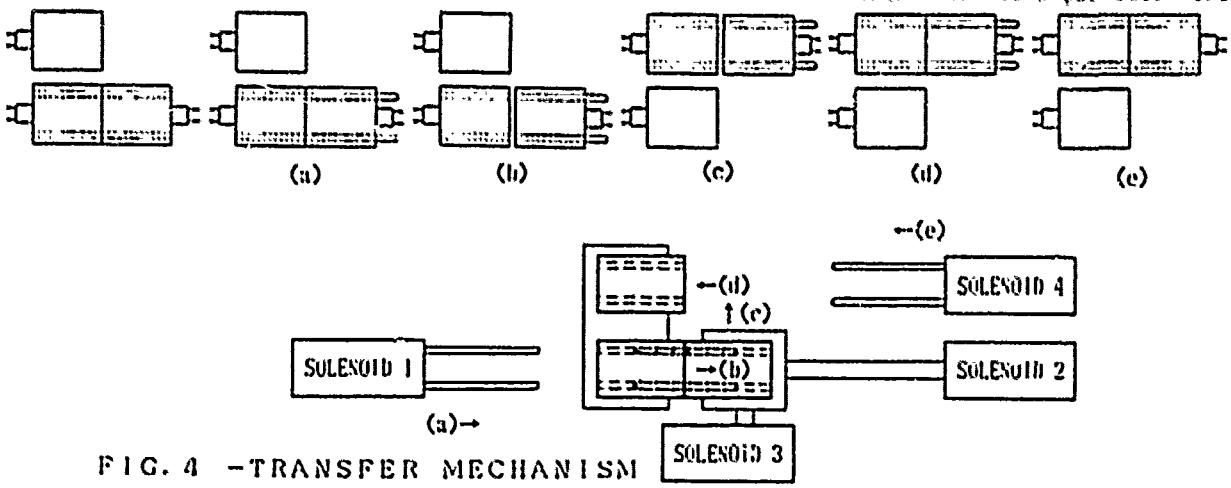

FIG. 4 -TRANSFER MECHANISM

Compensating for this time, the deviation in synchronous control can be less than (1/1200)x(1/2) s even in an asynchronous mode.

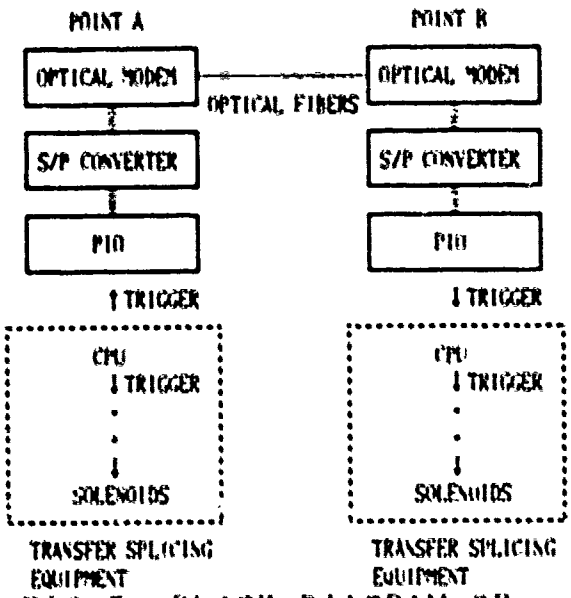

FIG. 5 -BLOCK DIAGRAM OF SYNCHRONOUS CONTROL EQUIPMENT

2.4 Fiber identification equipment

This equipment enables the identification at two points of the fiber ribbon to be transferred. Fig.6 shows an outline of the fiber identification equipment. The LI injects an identification signal into a fiber ribbon by bending it. The LD picks up the signal from the fiber ribbon also by bending it.

The requirements for fiber identification are explained as follows. In order not to disturb the working transmission system, the identification signal power must be controlled to an optimum level. For example, a high speed digital transmission system has a minimum receiving power of -43.0 dBm and a bit error rate of less than 10^{-9}. Here, the following equation is established between the S/N ratio and the bit error rate.

$$BER=(2/\pi)^{1/2}\cdot(S/N)^{-1}\exp[(-1/8)(S/N)^2]$$

With this equation, the S/N ratio at a bit error rate of 10^{-9} is calculated as 10.8 dB. To satisfy this bit error rate, the identification signal power injected into a fiber ribbon must be less than -51.8 dBm.

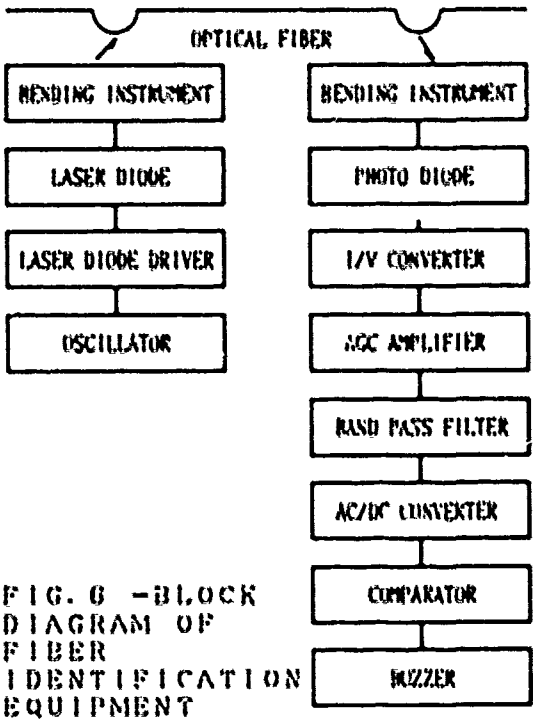

FIG. 6 -BLOCK DIAGRAM OF FIBER IDENTIFICATION EQUIPMENT

3. Experimental results

3.1 Optical fiber connector

Fig.7 shows the splicing loss after transfer. Due to the use of the MT connector, the mean insertion loss is 0.34 dB. This value is nearly equal to that obtained for hand splicing.

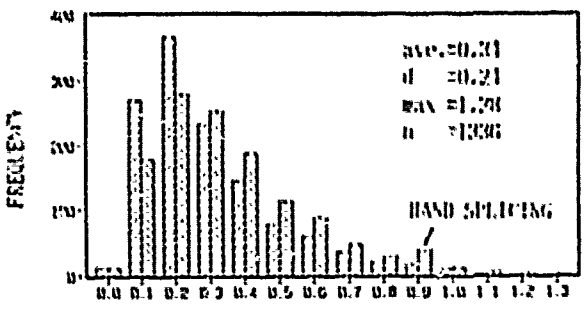

FIG. 7 -SPLICING LOSS

3.2 Transfer splicing equipment

3.2.1 Transfer time

Fig.8 shows the current wave of solenoid 1. It took about 3.4 ms from the start of the trigger to the end position of the solenoid's full stroke. So the drive timing for the solenoid was set as shown in Fig.9. Based on this timing, the mean transfer time was 12.2 ms and the maximum transfer time was 15.1 ms as shown in Fig.10. The upper graph in Fig.11 shows the transfer waveform.

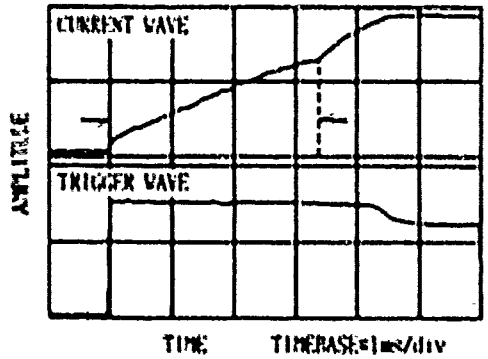

FIG. 8 -CURRENT WAVE OF SOLENOID 1

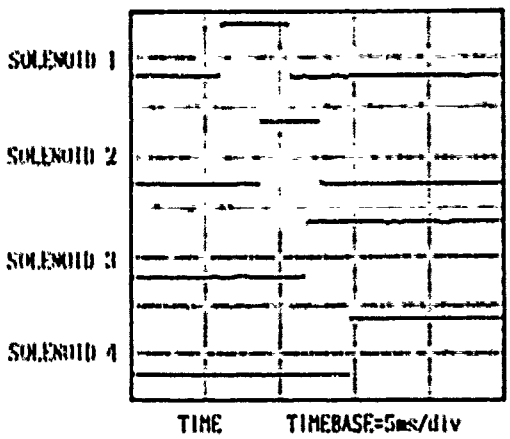

FIG. 9 -TIMING CHART OF EACH SOLENOID

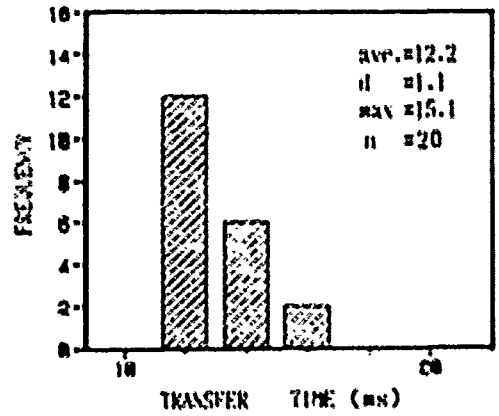

FIG. 10 -TRANSFER TIME

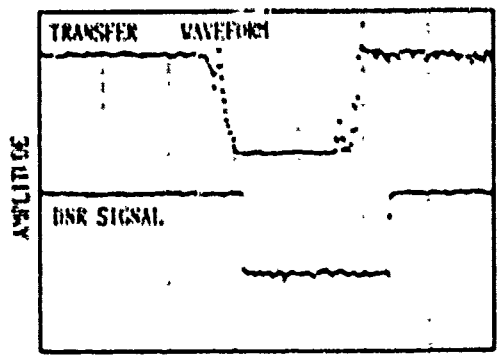

FIG. 11 -TRANSFER AND DNR SIGNAL WAVEFORMS

3.2.2 Influence on a working transmission system

The influence of transfer on a transmission system, with a transmission speed of 6.3 Mb/s and a keying of CMI (Coded Mark Inversion), was measured. To evaluate the influence on the system, it is most appropriate to observe the DNR (DCE Not Ready) signal. The DNR signal is inactive when the transmission system is working and becomes active when the system goes down. The lower graph in Fig.11 shows the DNR signal. In this graph, the lower level corresponds to an active DNR, the higher level corresponds to an inactive DNR. The mean time for the active DNR was 16.0 ms and the maximum time was 28.2 ms.

3.3 Synchronous control equipment

Deviations of the transfer trigger were measured and are shown in Fig.12. These are less than (1/1200)x(1/2) s, and agree with the estimation described in section 2.3.

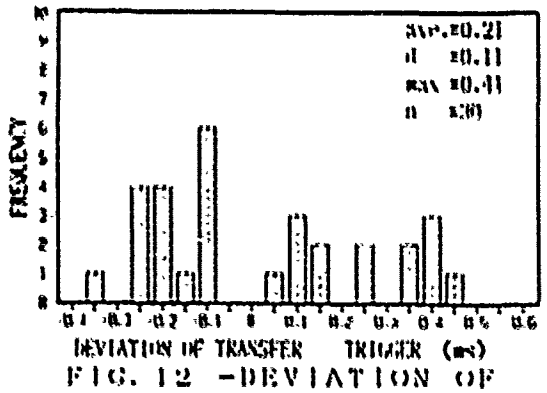

FIG. 12 -DEVIATION OF TRANSFER TRIGGER

3.4 Fiber identification equipment

3.4.1 Injection efficiency and detection efficiency

First, the injection efficiency was measured and is shown in Fig.13. It can be seen that the maximum efficiency was -52 dB and the minimum efficiency was -55 dB. Here, the injection efficiency is calculated by subtracting the injection efficiency signal power from the propagation signal power.

Next, the detection efficiency was measured and found to have a maximun value of -17 dB and a minimum value of -21 dB.

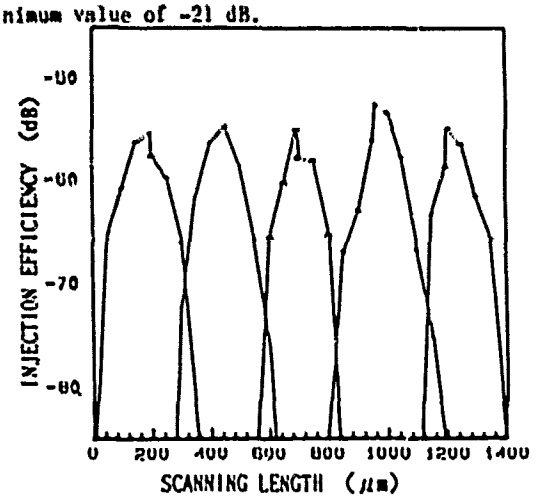

FIG. 13 -INJECTION EFFICIENCY

3.4.2 Transfer function and detector sensitivity

First, the transfer function of the LD was measured. This is shown in Fig.14. The input power to the LD was -80 dBm. It can be seen that a spectrum power of 270 Hz clearly appears.

Second, the coherence was measured at an input power of -80 dBm. This is shown in Fig.15, which reveals that the output power at 270 Hz is caused wholly by input.

Finally, the detector sensitivity was measured. Fig.16 shows the probability density function at an input power of -80 dBm, Fig.17 shows the same function at an input power of -84 dBm. It was also measured at input powers of -77 dBm, -81 dBm, -82 dBm, -83 dBm, -85dBm and -86 dBm. From these experiments, the cumulative distribution function was calculated by integrating the probability density function along the amplitude-axis. The output variations of the detecter, which have a probability of 99.9%, were also calculated as shown in Fig.18. From this figure, it can be seen that the minimum receiving power is about -83 dBm.

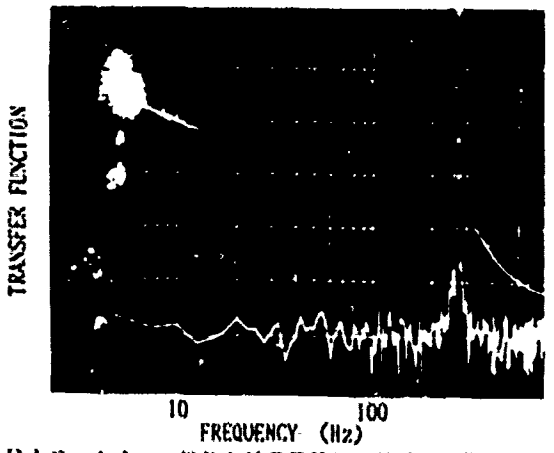

FIG. 14 -TRANSFER FUNCTION

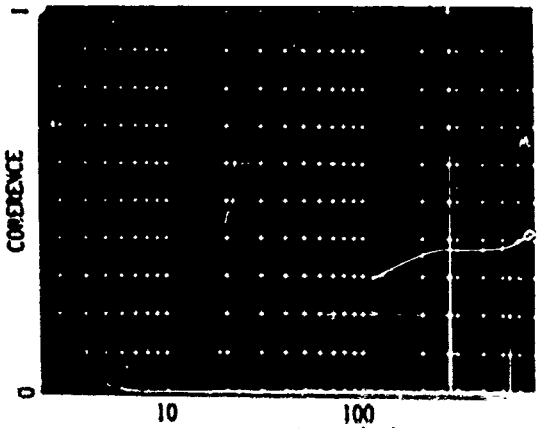

FIG. 15 -COHERENCE

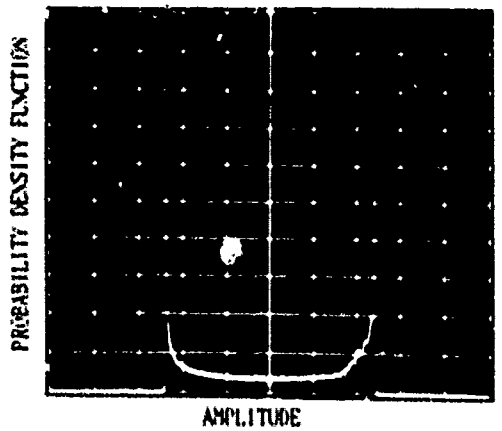

FIG. 16 -PROBABILITY DENSITY FUNCTION AT INPUT POWER OF -80dBm

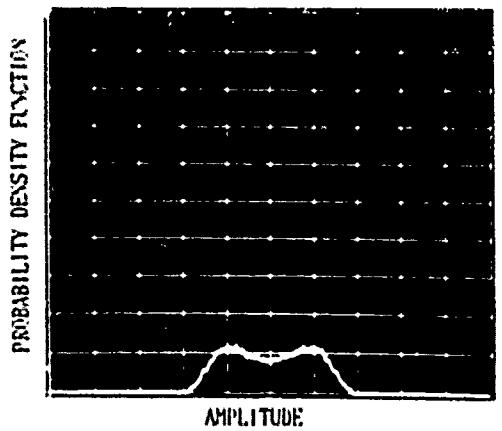

FIG. 17 -PROBABILITY DENSITY FUNCTION AT INPUT POWER OF -84dBm

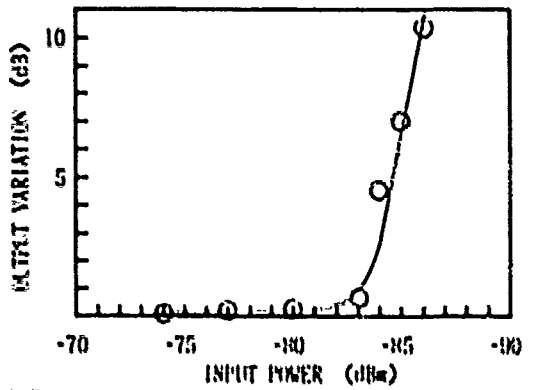

FIG. 18 -OUTPUT VARIATION OF LOCAL DETECTOR

4. Discussion of experimental results

4.1 Influence on a working transmission system

The time during which DNR is active is longer than the transfer time described earlier. The experimental result is explained as follows. It takes about 0.5 ms for DNR to become active when the optical input goes down at the receiving unit of the working transmission system for its frame composition, and it takes 4 ms to become inactive when an optical signal enters the receiving unit of the system for its frame recovery flow. For these reasons, the total time during which DNR is active is calculated by

$$T_{DNR}=T_T-0.5+4.0 \text{ (ms)}$$

Here, T_{DNR} is the time during which DNR is active, and T_T is the transfer time. With this equation and experimental result, the mean time while DNR is active is estimated to be 15.7 ms. The experimental result agrees with this estimation .

4.2 Capacity of fiber identification equipment

The power of the laser diode used in the experiment was -3 dBm and the maximum injection efficiency was -52 dBm. So the maximum power of the injection signal injected into a fiber is -55 dBm and the injection signal has no disturbance on a working transmission. It was found experimentally that the minimum injection efficiency was -55 dB, the minimum detection efficiency was -21 dB and the minimun receiving power was about -83 dBm. The power of the laser diode used in the experiment was -3 dBm. So the loss margin is calculated as 4 dB (-3-55-21-(-83)) and should be assigned to transmission loss. Assuming that the fiber loss is 1.0 dB/km including splicing loss, the identification equipment can be applied to a fiber of 4 km. Next, as the output variations of the detector described in section 3.4.2 had a probability of 99.9 %, the dispersion d_{OUT} at an input power of -83 dBm is calculated as 0.15 (0.51/3.3) dB. Here, d_{OUT} is the dispersion of the output variation. Setting the reference power of comparator at -80 dBm, the margin for identification is 3 dB, and this value corresponds to $20d_{OUT}$. From all these values, the error probability of the fiber identification equipment at -83 dBm is calculated at less than 10^{-21}. Using this equipment, it will be possible to estimate any difference in splicing loss before and after transfer splicing.

5. Conclusions

An optical fiber cable transfer splicing system has been developed. In this system, transfer splicing was performed using transfer splicing equipment and optical fiber connectors, synchronous control was achieved using synchronous control equipment and fiber identification was realized using a local injector and a local detector.

In addition to the above functions, a splicing loss estimation function using an LI and an LD is currently being laboratory tested.

Finally, the whole system is now being tested in the laboratory and will be introduced commercially in 1990 in order to improve actual specifications.

Acknowledgements

The authors would like to acknowledge S.Takashima, H.Shimoda, T.Uenoya and J.Mizusawa for their helpful suggestions and iank S.Nagasawa for valuable discussio and assistance.

References

[1]I.Watanabe et al., 'Optical fiber cable transfer splicing system,' 1989 Spling Natl. Conv. Rec. IEICE Japan.

[2]S.Nagasawa et al.,'MECHANICALLY TRANSFERABLE MULTIFIBER CONNECTORS,' IOOC'89, paper 21C2-1, 1989.

Ichiro Watanabe

NTT Network Systems
Development Center

Tokai, Ibaraki,
319-11, Japan

Ichiro Watanabe received his B.E. degree in electrical engineering from Chiba University in 1983.

He joined NTT in 1983. Since 1987 he has been in the Fiber Optics Local Network Systems Project Group, where he has been engaged in the development of the optical fiber cable transfer splicing system. He is a member of IEICE of Japan.

Masatoshi Shimizu

NTT Network Systems
Development Center

Tokai, Ibaraki,
319-11, Japan

Masatoshi Shimizu received his B.E. and M.E. degrees in electrical engineering from Ibaraki University in 1981 and 1983, respectively.

He joined NTT in 1983. Since 1987 he has been in the Fiber Optics Local Network Systems Project Group, where he has been engaged in the development of the optical fiber cable transfer splicing system. He is a member of IEICE of Japan.

Hideo Kobayashi

NTT Network Systems
Development Center

Tokai, Ibaraki,
319-11, Japan

Hideo Kobayashi received his B.E. degree in mechanical engineering from Yamanashi University in 1968.

He joined NTT in 1968. Since 1987 he has been in the Fiber Optics Local Network Systems Project Group, where he has been engaged in the development of the optical fiber cable transfer splicing system. He is a member of IEICE of Japan and the Japan Society of Mechanical Engineers.

DEGRADATION OF FIBER STRENGTH DURING COATING STRIPPING

T. Wei
GTE Laboratories Incorporated
Waltham, MA 02254

H. H. Yuce, C. H. Hasz
Bellcore
Morristown, NJ 07960

P. L. Key
Bellcore
Red Bank, NJ 07701

SUMMARY

The use of fiber optic cables in telecommunications has quickly broadened from long distance transmission to include subscriber loops and customer premises installations. As fiber cables are brought closer to the customer, the number of connectors or splices in the fibers increases dramatically and so does the concern over the mechanical reliability of such interconnections. The preparation of either mechanical or fusion splices or the installation of connectors normally includes several steps which may damage the fiber including removal of the cable structure (sheath, jacketing, and buffer tubes), stripping of the coating, cleaning the fiber, cleaving the fiber end, the splicing or connector installation operation itself, and fiber recoating procedures. In this study, we have investigated the coating stripping and fiber cleaning steps in detail. Comparing the strength of stripped and unstripped fiber, we found that the normal stripping and cleaning operations caused significant damage as evidenced by large strength reductions.

INTRODUCTION

Optical fibers are being rapidly deployed for telecommunications applications. Early concerns about the mechanical reliability of this medium because of the brittle nature of glass have been largely overcome by the remarkable progress of the industry in increasing the strength of optical fibers. Fiber strength is controlled by the presence of small surface flaws which can be introduced during fabrication by even minor contact of the fiber surface with a solid object or by incorporation of inclusions from the manufacturing environment into the fiber. Current commercial fibers have strengths in excess of 700,000 psi when tested in short lengths (about 1 to 5 feet). These strengths have been achieved by carefully avoiding surface damage and inclusions during fiber drawing and by protecting the fiber surface with a polymer coating.

However, like any communications cable, fiber cable must be spliced and connectorized. In the process of splicing fibers or installing connectors, the coating must be removed thus exposing the glass surface to damage and degrading environments[1]. Installation of either mechanical or fusion splices or various types of connectors involve several steps which may induce surface flaws including removal of the cable structure (sheath, jacketing, and buffer tubes), stripping the coating, cleaning the stripped fiber end, cleaving the fiber end, splicing or connector installation, and fiber recoating.

The development of processes to produce high strength fusion splices has been the subject of several recent papers[2-5]. In this paper, we examine the effects of the stripping and cleaning steps on the strength of fiber. Specifically, to prepare a fiber for either splicing or connectorization, the craftsperson must remove the coating on a short length of fiber. The most common technique for removing the coating involves the use of a mechanical stripping tool with a sharp knife edge not too dissimilar from tools used to strip insulation from copper wire. During this operation, parts of the stripping tool and coating debris can contact the glass surface leading to damage. We have concentrated on mechanical stripping since it is more likely to damage the fiber than chemical stripping and, because of safety regulations on chemical usage, mechanical strippers are more commonly used in the field.

After stripping the coating, the craftsperson normally wipes the fiber clean with a tissue soaked in alcohol or acetone to remove coating debris or dirt that might interfere with the subsequent cleaving, splicing, or connectorization steps. We shall show that these processes, even when carefully done, can cause significant strength reductions.

EXPERIMENTAL

The objective of this study was to characterize the degree of strength degradation introduced by stripping of the coating and by cleaning the stripped fiber. One of the problems with such a study is that the individual technique of the operator would appear to be a significant parameter. To include operator effects in this study, we split the testing between the authors' laboratories to determine if consistent results could be obtained by following similar test procedures. The results from each lab are designated as either Lab 1 or 2. Five UV-cured, epoxy acrylate coated, commercial silica-based fibers with a nominal 125 μm core and 250 μm coated diameter were obtained for testing; the fibers are designated herein as Fibers A, B, C, D, and E. Seven mechanical stripping tools manufactured by four different vendors were used; the tools are designated in this study by manufacturer as Tools 1, 2, 3, and 4. Finally, two commercial chemical strippers were evaluated which are designated as Chemical Stripper 1 and 2.

A similar stripping procedure was used at the two labs in which a stripping tool (or chemical stripper) was used to strip a section about 1/2 inch long in the middle of the test sample. The tensile strength of the sample was then measured on a screw driven universal testing machine. Samples were gripped on 10 cm diameter capstans covered with a soft elastomeric sleeve. The tensile strengths of similar unstripped sections from each of the five fibers were also measured to provide reference strength levels. Designations of fibers and stripping tools and other test parameters used by the two labs are listed below:

Parameter	Lab 1	Lab 2
Fibers	A, B	C, D, E
Stripping Tools	1, 2, 3	1, 2, 3, 4
Gage length	0.5 m	0.5 m (Fiber E) 1 m (Fibers C & D)
Strain rate	10 %/min	50 %/min (Fiber E) 25 %/min (Fibers C & D)
Test Environment	22 °C, 45% RH	25 °C, 50% RH
Number of Samples	31	23 (Fiber D) 15 (Fibers C & E)

Since coating debris can affect the operation of stripping tools, we also examined the effect of cleaning the stripping tool before stripping. This was done by using a cotton swab soaked in isopropyl alcohol to clean the cutting edges of the stripping tool and then blowing the edges dry with an air duster. Samples were divided into two groups; those stripped with a clean tool and those stripped with an uncleaned tool.

The second major area examined in this study was the effect of cleaning the fiber after stripping. This study was carried out by first stripping a 1/2 inch long section in each test sample using a cleaned stripping tool. Then, four different "cleaning" procedures were used on groups of stripped samples:

(a) wiped once with bare fingers

(b) wiped once with a lint-free tissue soaked in isopropyl alcohol

(c) wiped twice with a lint-free tissue soaked in isopropyl alcohol

(d) wiped five times with a lint-free tissue soaked in isopropyl alcohol

After "cleaning", the tensile strength of the test samples was determined by the same procedure outlined above.

RESULTS AND DISCUSSION

The effect of stripping on tensile strength is shown in Table 1 where the minimum, median, and maximum strengths are listed for each fiber for the various stripping conditions. All of the stripping conditions have a very significant effect on both the median strength as well as the spread in the strength distribution. Generally, the maximum observed strength values do not decrease as much as either the median or minimum strength values. There appear to be significant differences in the strength-impairing effect between the mechanical strippers tested. However, cleaning the stripping tool before stripping doesn't significantly affect the strength reduction observed. The chemical strippers behaved similarly to the better mechanical strippers. Although the results from both laboratories showed significant strength degradation, results with similar tools were not comparable.

The strength of optical fibers normally can be fitted to a Weibull distribution. However, the strengths of the stripped samples do not fit a Weibull distribution very well as shown in Figures 1 - 2. The strength of a chemically stripped fiber also shows significant deviations from Weibull behavior (Figure 3).

The effect of the various cleaning procedures on the strength of stripped fibers is shown in Table 2 where the minimum, median, and maximum strengths are listed for the various cleaning procedures. It is clear from this Table that cleaning procedures also have an effect on fiber strength but one that is less than that of stripping.

Table 1 - Effect of Stripping on Fiber Strength

Fiber, Lab	Stripping Condition	Strength, ksi		
		Minimum	Median	Maximum
Fiber A, Lab 1	Unstripped	764	810	828
	Chemical Stripper 1	352	751	792
	Tool 1, uncleaned	109	347	811
	Tool 1, cleaned	110	358	768
	Tool 2, uncleaned	307	742	773
	Tool 2, cleaned	188	751	788
	Tool 3, uncleaned	436	740	777
	Tool 3, cleaned	436	747	784
Fiber B, Lab 1	Unstripped	715	746	768
	Chemical Stripper 1	288	700	735
	Tool 1, uncleaned	107	335	751
	Tool 1, cleaned	114	347	621
	Tool 2, uncleaned	209	578	720
	Tool 2, cleaned	232	585	730
	Tool 3, uncleaned	186	705	770
	Tool 3, cleaned	188	665	724
Fiber C, Lab 2	Unstripped	723	729	738
	Chemical stripper 2	234	707	728
	Tool 1, uncleaned	6	114	250
	Tool 1, cleaned	67	145	657
	Tool 4, uncleaned	167	661	734
	Tool 4, cleaned	294	693	735
Fiber D, Lab 2	Unstripped	724	731	742
	Tool 1, cleaned	125	100	525
	Tool 2, cleaned	99	239	625
	Tool 3, cleaned	95	256	306
	Tool 4, cleaned	130	256	728

Table 2 - Effect of Cleaning on Fiber Strength

Fiber, Lab	Condition	Strength, ksi		
		Minimum	Median	Maximum
Fiber A, Lab 1	Unstripped	764	810	828
	As stripped, Tool 1, cleaned	110	358	768
	Tool 1, wiped once with fingers	111	238	734
	Tool 2, wiped once with fingers	106	554	776
	Tool 3, wiped once with fingers	107	554	774
	Tool 1, wiped once with tissue	76	210	743
	Tool 1, wiped twice with tissue	52	246	716
	Tool 1, wiped 5 times with tissue	65	198	725
Fiber B, Lab 1	Unstripped	715	746	768
	As stripped, Tool 1, cleaned	114	347	621
	Tool 1, wiped once with fingers	98	221	545
	Tool 2, wiped once with fingers	109	365	720
	Tool 3, wiped once with fingers	106	374	723
	Tool 1, wiped once with tissue	114	338	630
	Tool 1, wiped twice with tissue	83	222	555
	Tool 1, wiped 5 times with tissue	91	219	547
Fiber E, Lab 2	Unstripped	679	693	701
	As stripped, Tool 2, cleaned	274	586	686
	Tool 2, wiped once with tissue	274	586	649
	Tool 2, wiped twice with tissue	179	316	603
	Tool 2, wiped 5 times with tissue	111	371	638

In fact, the various cleaning procedures all had similar effects on strength. Typical Weibull plots for the strength of cleaned fibers are illustrated in Figures 4 and 5 showing a distinctively non-Weibull behavior.

The results of this study show that current fiber stripping and cleaning practices cause significant damage to the stripped section of fiber and consequent strength reduction. It would appear that improved procedures and stripping tools are desirable. In addition, it would be very desirable to design fiber connectors to minimize any stress on the stripped length of fiber. Many fiber connectors are supposed to provide strain relief to the stripped section but, as reported by Wagner[6], fiber failures have been observed in temperature-humidity testing of such connectors. It was concluded that stresses are imposed on the fiber in such tests because of the mismatch of the thermal expansion coefficients of the various materials in the connector.

CONCLUSIONS

Stripping tools and cleaning procedures used in preparing the ends of optical fibers for splicing or connectorization can significantly reduce the strength of the stripped section of fiber. This suggests that splices and connectors may be the "weak-link" in a deployed fiber.

REFERENCES

1. T. Wei and F. S. Leong; "Friend or Foe"; **Telephony**; 216(24); 32-33 (1989).
2. J. T. Krause, C. R. Kurkjian, and U. C. Paek; "Strength of Fusion Splices for Fibre Lightguides"; **Electronics Letters**; 17(6); 232-233 (1981).
3. J. T. Krause, C. R. Kurkjian, and U. C. Paek; "Tensile Strengths > 4 GPa for Lightguide Fusion Splices"; **Electronics Letters**; 17(21) 812-813 (1981).
4. Y. Negishi et al; "High-Strength Fiber Splice Applied for Submarine Optical Fiber Cable"; **J. Optical Communications**; 6(4) 122-126 (1985).
5. J. T. Krause; "Ultrahigh-Strength Fibre Splices by Modified H_2/O_2 Flame Fusion" **Electronics Letters** 22(20) 1075-1076 (1986).
6. W. R. Wagner; "Failure Analysis of Fiber Optic Components"; in **Fractography of Glasses and Ceramics**; Advances in Ceramics; 22; 389-402 (1988).

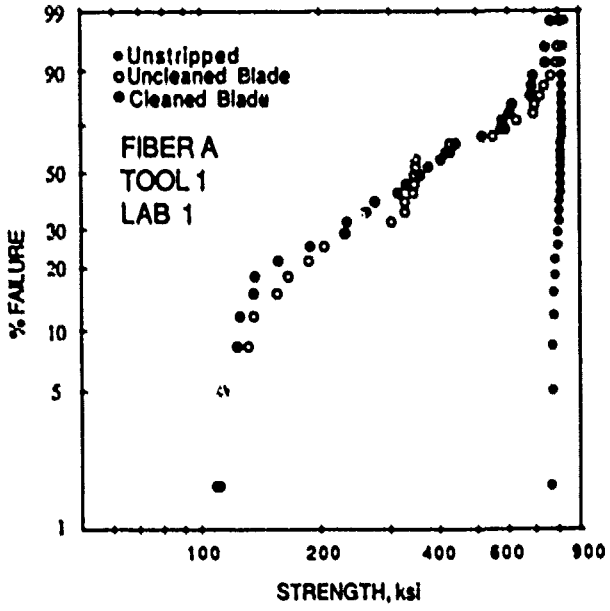

Figure 1: Effect of stripping procedure on liber strength.

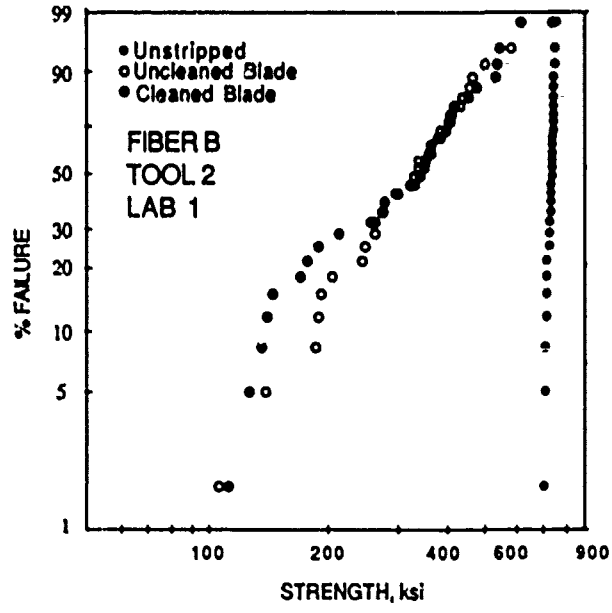

Figure 2: Effect of stripping procedure on fiber strength.

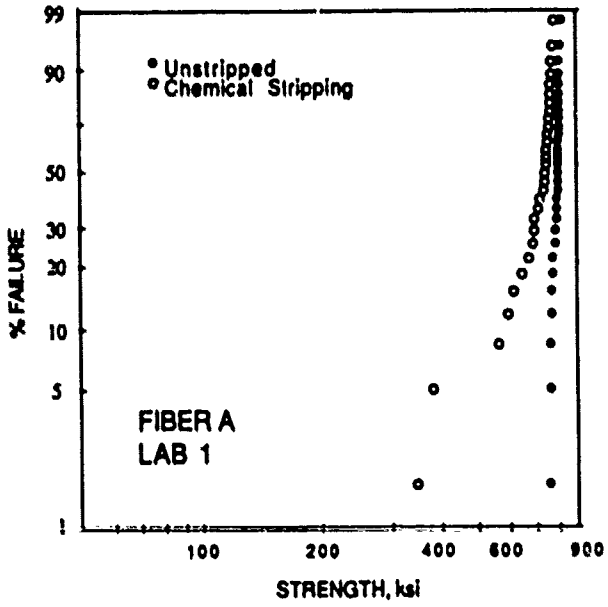

Figure 3: Effect of stripping procedure on fiber strength.

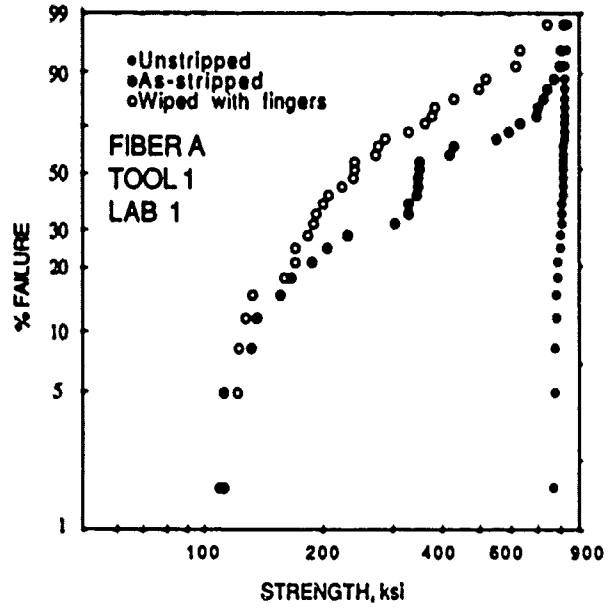

Figure 4: Effect of cleaning procedure on fiber strength.

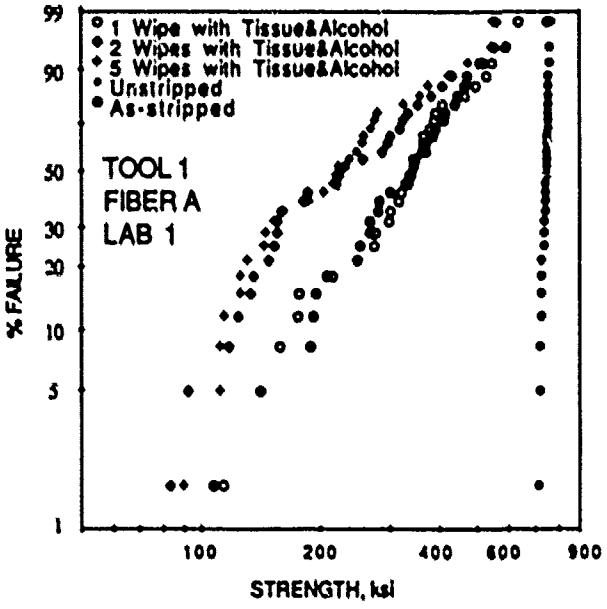

Figure 5: Effect of cleaning procedure on fiber strength.

T. (Mike) Wei is a Research Supervisor in the Optical Fiber and Components Department of GTE Laboratories in Waltham, Massachusetts. After receiving a PhD in physics from the University of Pennsylvania, Mr. Wei joined 3M Company where he conducted research on fiber optics and polymer physics. In 1984, he joined GTE where he is responsible for fabrication, characterization, and reliability studies of optical fibers.

Hakan H. Yuce is a Member of Technical Staff in the Fiber Distribution and Reliability Research District at Bellcore in Morristown, New Jersey where he is involved in failure analysis and reliability studies of optical fibers. He received a B.S. in mechanical engineering from the Technical University of Istanbul, Turkey; an M.S. from MIT; and a PhD from Stanford.

P. Leland Key is District Manager of the Metallurgical Science and Engineering Research District at Bellcore in Red Bank, New Jersey. After receiving a PhD from the University of California at Berkeley, Mr. Key joined Bell Labs where he conducted research on the mechanical behavior of metals. In 1983, he joined Bellcore where he is responsible for metals research.

Charles H. Hasz is a Senior Staff Technologist in the Fiber Distribution and Reliability Research District at Bellcore in Morristown, New Jersey. Mr. Hasz began his career at Bell Labs in 1956 where he worked on acoustic research. In 1983, Mr. Hasz joined Bellcore where he is involved with deployment procedures for fiber optics. Mr. Hasz has attended RCA Institutes and Newark College of Engineering.

ANALYSIS OF MASS FUSION SPLICE LOSS FOR OPTICAL FIBER RIBBONS

Keiji OSAKA Tsutomu WATANABE Masumi FUKUMA Yasuo ASANO

Communications R&D Dept., Yokohama Research Laboratories,
Sumitomo Electric Industries, LTD.

Abstract

Using numerical simulations, relations between geometrical parameters and the splice loss of mass fusion were statistically made clear.

The calculation consists of several steps. In these steps, two major factors were taken into consideration. One is a lateral offset of the core and the other is self-alignment effect due to surface tension of melted silica during fusion. The offset decrease was formularized through experiments.

Various groups of parameters were compared. The comparison suggests the probable achievements of mass fusion splice loss. Corresponding experimental splices were made using 12-fiber ribbons, and the average loss of 0.13 dB were obtained. The simulation was proven to be reasonable.

1.Introduction

Recently a quick and economical way of connecting fiber-optic cables is a point of interest especially for the construction of subscriber networks. In constructing subscriber networks or local area networks, the number of splice points may be large and the cost per splice should be much lower. Therefore, more economical technique is preferrable.

To satisfy such demands, mass fusion splice technique is one of the solutions. Fusion splice technique has been widely applied to trunk lines where the splice loss should be attained as low as possible. Fusion splice has been developed starting from single fiber splice to twelve-fiber splice, keeping its consistent characteristics such as lower splice loss, higher reliability and higher efficiency. Actually it was reported that 12-fiber SM ribbons were splicable with less than 0.1 dB in a laboratory (1) or 10-fiber SM ribbons were spliced with average loss of 0.11 dB in 4 minutes in the field.(2)

But many researchers or engineers referred to limited combinations of different fibers or identical fibers. Our major interest is the achievable splice loss in the field construction where fibers are chosen from certain groups which have certain distribution of geometrical parameters.

In analizing this problem, some mechanisms that enable lower splice loss will be presented.

FIG.1 SCHEMATIC VIEW OF BUTT JOINTED FIBERS

2.Background

Conventionally in order to splice single-mode fibers (SMFs), both ends of the two fibers to be spliced needed to be aligned to meet the core because both cores had eccentricities from the centers of the cladding ('clad center'). For the purpose core alignment mechanisms and eccentricity detection methods such as LID system or direct core monitoring system were developed.(Fig. 1-1)

But apparently to splice ribbon fibers (Fig. 1-2), to apply and extend such alignment system (individual alignment) is too complex and too impractical. Moreover, owing to the manufactures' efforts, core eccentricity or other parameter mismatches are improving. In this case it is unnecessaty to detect the core position. Usually each pair of the mating fibers have lateral offsets between their cladding centers (clad offset), due to the fact that the fibers have different cladding diameters or positioning of the fibers onto the V-grooves is improper. However, small clad offsets can be minimized with the help of surface tension effect of the fused fibers. Such misaligned fibers have a clad offset before splice and it will decrease during fusion. In these situation, there still remain some core offsets. These phenomenon including core deformation are schematically illustrated in Fig. 2. In case of mass fusion splice, clad offsets are different due to fiber pairs and can be minimized after splice (Fig. 3). According to the published papers mass fusion technique is superior in achieving stablly low loss.

This technique is performed under the condition :

(A)Stable fusing area over a wide range,
(B)Longer fusing period excites self-alignment force, resulting in a minimized axis offset,
(C)Fusion compensates endface defects such as cleaved length variance or endface inclination.

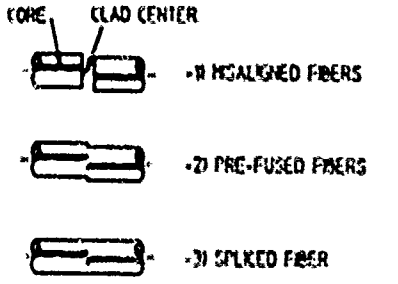

FIG.2 SURFACE TENSION EFFECT (SCHEMATIC FIGURE)

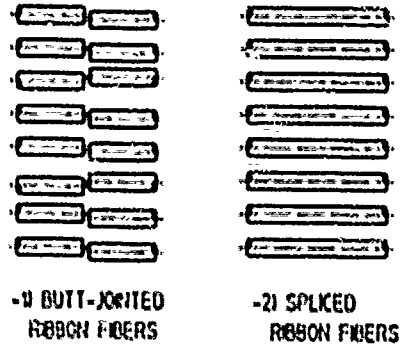

FIG.3 APPEARANCE OF MASS FUSION SPLICE

Splice loss is assumed to be caused by two major factors --- intrinsic and extrinsic.

$$\alpha Total = \alpha I + \alpha E \quad \text{----- (1)}$$

Intrinsic factor αI results from fiber parameter mismatch. Extrinsic factor αE results from endface qualities or endface separation and they are under the control of splice craftsmen. In case of above mentioned mass fusion process, cladding diameter mismatch or core eccentricity is treated as or[illegible]trinsic factors.

To pr[illegible], the advantages of longer fusing period, a relation of clad offset between before splice and after splice was investigated. Fig. 4 shows the results, where tendency seems linear, thus obtaining a following formula: ---

$$Pb = C \cdot Pa \quad \text{----- (2)}$$

Here Pa denotes clad offset before fusion, Pb: clad offset after fusion, C: experimental constant. The decreased ratio was 0.7 for 4-second fusion and 0.1 for 10-second fusion. The data suggest, if the core eccentricity is low, a core offset before splice can be minimized by taking advantages of surface tension, thereby core alignment mechanisms can be omitted.

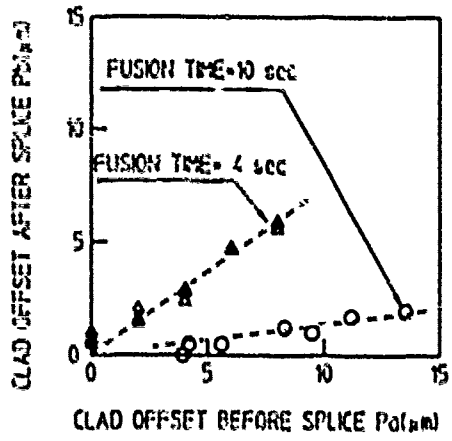

FIG.4 RELATION OF CLAD OFFSET BETWEEN BEFORE SPLICE AND AFTER SPLICE

3.Numerical analysis

3-1.Assumption

In order to obtain intrinsic loss αI, the relations between geometrical parameters and the splice loss of mass fusion was analized using numerical simulations. For the purpose not a single parameter but a group of parameters subject to different distributions that represent fiber geometry was considered in the simulation. To estimate the splice loss in the field and to simplify the discussion, the following assumptions were made: ---

(A)One pair of mating fibers is chosen at random from a certain fiber group, that is defined with independent parameters which are subject to predetermined distributions.
(B)Fiber geometry is repesented with minimum number of independent parameters.
(C)As an intrinsic cause of splice loss, only a core axis offset is considered.
(D)An extrinsic cause is represented by an empirical splice loss of identical fibers.
(E)In mass fusion splice, any difference due to fiber position are negligible.
(F)Self-alignment effect can be formularized simply by core axis offset reduction.

Using this simulation method, various groups of parameters were calculated and statistically compared. The comparison suggests the probable achievements of the splice loss.

To determine the extrinsic loss of mass fusion, identical 12-fiber ribbons were spliced. Fig. 5 shows the splice loss histogram and the average loss is 0.05 dB. This figure means the probable loss in mass fusion splice including a variance due to endface qualities or craftsmen's skill at present.

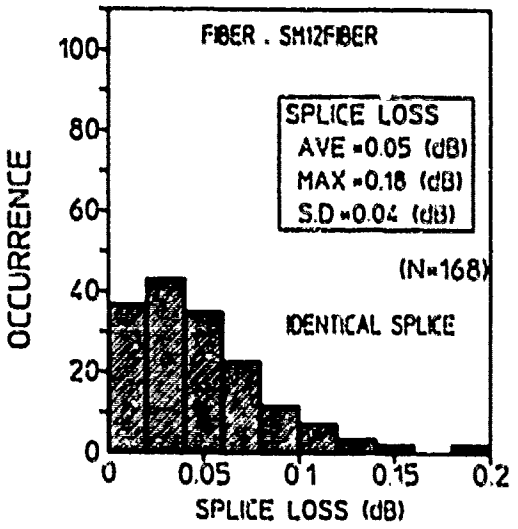

FIG.5 EXPERIMENTAL RESULTS
(IDENTICAL 12 FIBER RIBBON)

3-2.Geometrical model

Four independent parameters that would affect the splice loss were chosen. They are listed in Table 1 and illustrated in Fig. 6. (cladding diameter D, mode field diameter W, cladding non-circularity κ , core eccentricity c) An endface of a SMF is represented by an ellipse with long radius of Xa and short radius of Xb. Cladding diameter D is defined as (Xa+Xb)/2 and cladding non-circularity κ is defined as $|Xa-Xb|/D$. Core eccentricity c is the distance between clad center and MFD center.

3-3.Procedure of the simulation

As is shown in Fig. 7, the simulation starts from preparation of groups of parameters according to real data. The splice loss is represented by the next equation.

$$\alpha I = f(D, W, \kappa, c) \quad \text{----- (3)}$$

To simulate the reality, normal distribution was chosen for cladding diameter, mode field diameter. Rayleigh distribution was chosen for cladding non-circularity and core eccentricity. To avoid extreme values, upper and lower limits were set for normal distribution and upper limit was set for Rayleigh distribution.

In the second step clad offset P1 is calculated. (Fig. 6-2) Here two tangents are generated at the angle of θ degree (the bottom angle of the V-groove). The angle ϕ from the long radius to one tangent is chosen at random between -180 to +180 degrees. P1 is defined as the distance between two centers of the cladding ellipses and derived equation is: ---

$$P1 = \overrightarrow{V_1} - \overrightarrow{V_2} \quad \text{----- (4)}$$

TABLE 1 DEFINITION OF PARAMETERS

PARAMETER NAME	DISTRIBUTION TYPE	DISTRIBUTION PARAMETER	UPPER LMT	LOWER LMT
CLADDING DIAMETER	NORMAL	AVERAGE	128 (μm)	122 (μm)
		STANDARD DEVIATION		
CLADDING NON-CIRCULARITY	RAYLEIGH	AVERAGE	77 (%)	—
		MAXIMUM 77		
CORE ECCENTRICITY	RAYLEIGH	AVERAGE	C (μm)	—
		MAXIMUM C		
MFD	NORMAL	AVERAGE	10 (μm)	9 (μm)
		STANDARD DEVIATION		

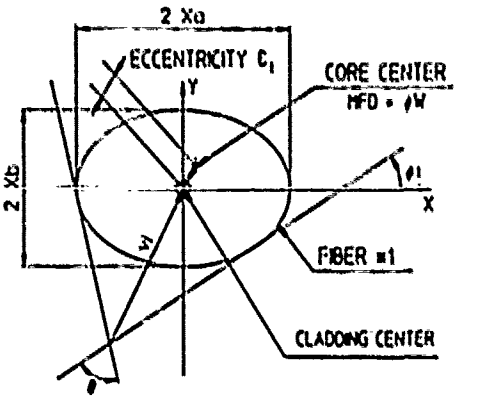

-1) GEOMETRICAL MODEL

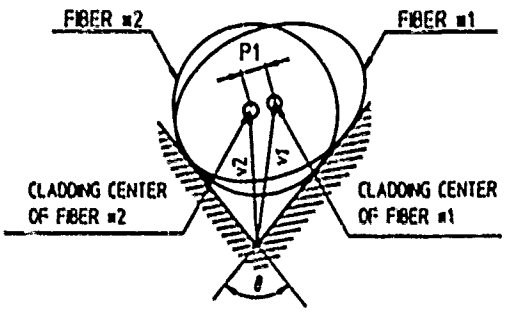

-2)CALCULATION OF CLAD OFFSET

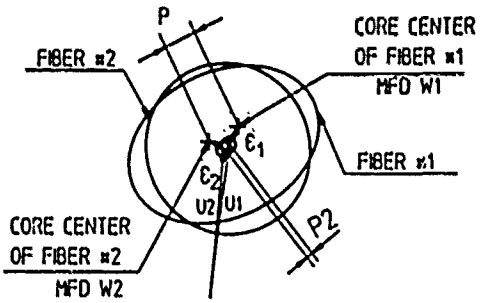

-3)CALCULATION OF CORE OFFSET

FIG.6 PARAMETERS OF FIBERS

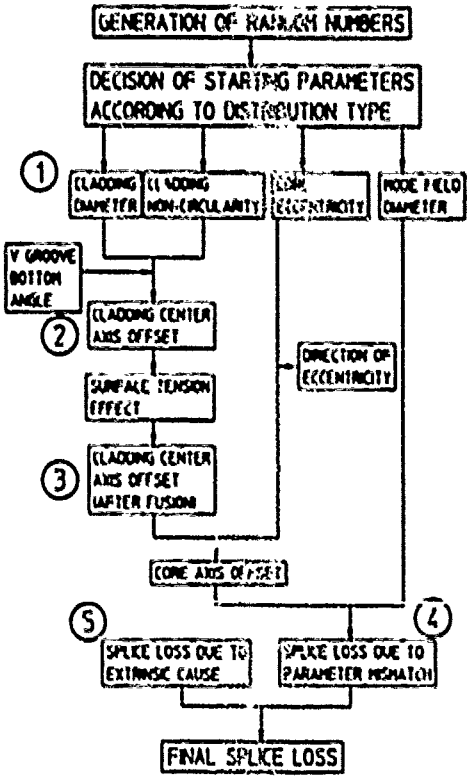

FIG.7 PROCEDURE OF CALCULATION

Here, $\vec{v_i}$ means a position vector from the bottom of the V-groove.(See Appendix 1)

In the third step, taking surface tension effect into consideration,

$$P2 = K \cdot P1 \quad (0<K<1) \text{ ----- } (5)$$

Here the same value is substituted to K as C in equation (2).

In the fourth step, the core position is generated at the distance c from the cladding center to the direction of the angle ß (0< ß<360) from the line connecting two clad centers. Thus core offset P is calculated.(Fig. 6-3)

$$\vec{P} = (\vec{u_1} + \vec{c_1}) - (\vec{u_2} + \vec{c_2}) \text{---- } (6)$$

Here, $\vec{ui}$: clad center position after fusion, $\vec{ci}$: core position vector from clad center. Using generated MFDs, splice loss is calculated by substituting these values into Marcuse's formula: ---

$$\alpha I = -10 \log \left(\frac{2W_1W_2}{W_1^2+W_2^2}\right) \exp \left(\frac{P^2}{W_1^2+W_2^2}\right) \text{ ---(7)}$$

In the last step, extrinsic loss due to fusion αE should be added. From the splice results of identical fiber ribbon shown in Fig. 4, Rayleigh distribution of average loss 0.05 dB was generated for αE. Final total splice loss was obtained by adding αE to αI as in equation(1).

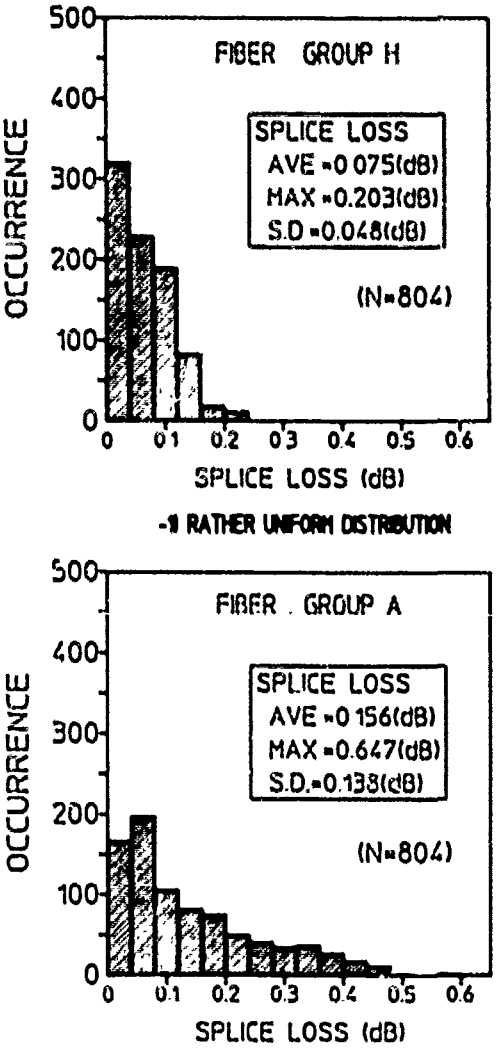

FIG.8 SIMULATED RESULTS

3-4.Starting parameters and the final results

Two different groups of starting parameters were chosen. Fig. 8-1) and -2) show two different histograms of simulated 804 splices from different groups of parameters. Before these trials, 1608 fibers were generated that were subject to predetermined distribution. The number of trials (804) were found enough to bare reproducibility. Table 2 shows their starting parameters. Fig. 8-1 shows the result from rather uniform distributions (similar to one manufacturer's typical data) and the average loss is very low, whereas Fig. 8-2 shows the result from rather scattered distributions (taken from CCITT recommendation and modified), where the average loss is a little bit higher. But still the loss is low enough compared with conventional mechanical connectors.

TABLE 2 INITIAL VALUE OF THE PARAMETERS AND THE SIMULATED SPLICE LOSS

PARAMETER NAME / GROUP	CLADDING DIAMETER		CLADDING NON-CIRCULARITY		CORE ECCENTRICITY		MFD		SPLICE LOSS	
	AVERAGE	S.D.	AVERAGE	MAXIMUM	AVERAGE	MAXIMUM	AVERAGE	S.D.	AVERAGE	S.D.
A	125	1.0	0.7	2.0	0.5	1.0	9.5	0.24	0.156	0.138
H	125	0.35	0.51	2.0	0.22	0.8	9.52	0.14	0.075	0.048

4.Discussion of the methods

4-1.Reasonability of the simulation

Actual splice experiments were performed with various fiber ribbons. The parameters are listed in Table 3. They are expected to represent a "rather scattered" distribution. Fig. 9 shows the result of the splice loss, where average loss is around 0.13 dB. The value is very close to the estimated loss shown in Fig. 8-2.

4-2.Analysis of intrinsic splice loss factors

To clarify the dependency of the splice loss on each parameter, average loss were compared by changing starting parameters one by one. From the results, it was found that the average and maximum of the core eccentricity affected most to the splice loss. Fig. 10-1 and -2 show the tendency. From these figures it will be said that in order to attain lower average splice loss less than 0.1 dB. the average and the maximum value of core eccentricity should be less than 0.3 um, 0.6 um, respectively. These values are not impractical ideal, but are within our reach as listed in Table 2, group H.

5.Conclusion

Using numerical simulation method, mass fusion splice achievements of SMFs were discussed and statistically obtained. A mechanism that self-alignment force due to surface tension minimizes clad offset were presented and it was clarified the linear decrease of clad offset can explain the loss achievements.

The simulation was proven probable by the comparison between actual splice results and the simulated results. The simulation taught us that core eccentricity is the most important factor. Mass fusion splice loss was less dependent on other parameters such as cladding diamater, cladding non-circularity and MFD.

In other words, good results will be obtained by the combination of mass fusion splice technique and the conventional fiber geometries. But better results will be obtained by combining mass fusion technique with better fibers.

This simulation method was found valid to 12-fiber ribbon splices but can be applied to any number of fiber ribbons. In practical aspects, this analysis supports the mass fusion splice technique without individual core alignment.

We would like to express our thanks to our

TABLE 3 PARAMETERS OF THE SAMPLE FIBERS

PARAMETER NAME	MAXIMUM VALUE	MINIMUM VALUE
CLADDING DIAMETER (μm)	126.5	124.1
CLADDING NON-CIRCULARITY (%)	1.6	0.3
CORE ECCENTRICITY (μm)	0.8	0.2
MFD (μm)	9.8	9.2

(N=168)

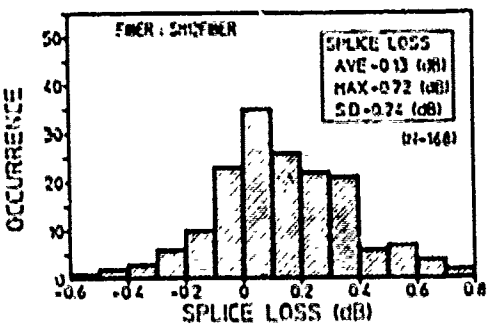

FIG.9 EXPERIMENTAL RESULTS (DIFFERENT 12 FIBER RIBBON)

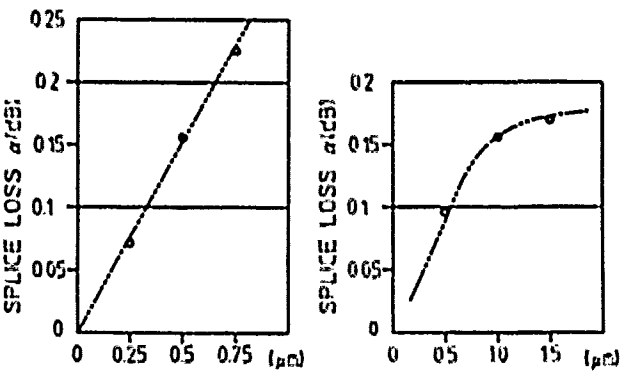

-1)EFFECT OF AVERAGE CORE ECCENTRICITY

-2)EFFECT OF MAXIMUM CORE ECCENTRICITY

FIG.10 EFFECT OF PARAMETERS ON SPLICE LOSS

colleagues involved in the experiment and discussion.

REFERENCES

(1)T. Yanagi et al., "Low Loss Mass-Fusion Splicing Technique for 12-Fiber Ribbon" OFC/OFS '88.

(2)T. Haibara et al., " Single-Mode Multifiber Jointing Technique for High-Density, High-Count Subscriber Cables" p.576-585, IWCS'88.

(3)I. Hatakeyama et al., "Fusion Splice Loss for Single-Mode Optical Fibers" IEICEJ p.803-810, Vol. J62-C No.12, '79/12.

<Appendix>

1.The position vector is defined as

$$\vec{V_i} = \left(\frac{\sqrt{Xa_i^2 \tan^2\phi_i + Xb_i^2} - \sqrt{Xa_i^2 \tan^2(\phi_i+\theta) + Xb_i^2}}{\tan(\phi_i+\theta) - \tan\phi_i} , \right.$$

$$\left. \tan\phi_i \left(\frac{\sqrt{Xa_i^2 \tan^2\phi_i + Xb_i^2} - \sqrt{Xa_i^2 \tan^2(\phi_i+\theta) + Xb_i^2}}{\tan(\phi_i+\theta) - \tan\phi_i} \right) + \sqrt{Xa_i^2 \tan^2\phi_i + Xb_i^2} \right)$$

2.Equation (6) is derived from the figure below.

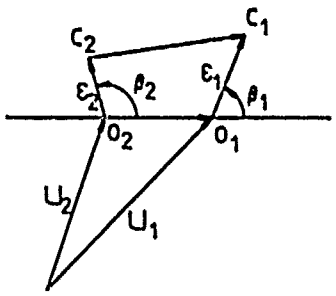

Here, O_i ; clad center, C_i ; core center.

Keiji Osaka

Sumitomo Electric
Industries, Ltd.

1, Taya-cho, Sakae-ku
Yokohama, Japan

Keiji Osaka was born in 1955 and received his M.S. degree in precision mechanical engineering from Kyoto University in 1981. He joined Sumitomo Electric Industries the same year and has been engaged in research and development of high NA optical fiber fabrication and fusion splice technology. He is now a staff member of Communications R&D Dept. Yokohama Research Labs. and a member of the Institute of Electronics, Information and Communication Engineers of Japan.

Yasuo Asano

Sumitomo Electric
Industries, Ltd.

1, Taya-cho,Sakae-ku,
Yokohama, Japan

Yasuo Asano received his B.S. degree in mechanical engineering from Waseda University in 1968. He joined Sumitomo Electric Industries in 1971 and has been engaged in development of jointing technologies for coaxial cables and fiber optic cables. He is now a chief research associate of Communication R & D Dept. Yokohama Research Laboratories and a member of Japan Society of Mechanical Engineers and the Institute of Electronics, Information and Communication Engineers of Japan.

Tsutomu Watanabe

Sumitomo Electric
Industries. Ltd.

1, Taya-cho, Sakae-ku,
Yokohama, Japan

Tsutomu Watanabe was born in 1964 and received his B.S. degree in mechanical engineering from Tokyo University in 1987. He joined Sumitomo Electric the same year and has been engaged in research and development of fusion splice technology. He is a member of Japan Society of Mechanical Engineers and the Institute of Electronics, Information and Communication Engineers of Japan.

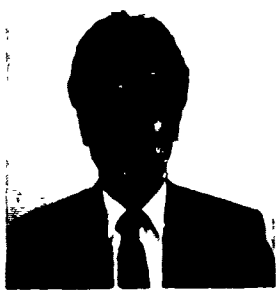

Masumi Fukuma

Sumitomo Electric
Industries, Ltd.

1, Taya-cho, Sakae-ku
Yokohama, Japan

Masumi Fukuma received a M.S. degree in Electrical and Electronic Engineering from Toyohashi University of Technology in 1985. He Joined Sumitomo Electric Industries, Ltd. in 1985, and has been engaged in research and development of optical fiber and cables. Mr. Fukuma is a member of Communication R & D Department in Yokohama Research Laboratories.

FIELD TRIALS ON MASS SPLICING FOR SUBSCRIBER LOOP APPLICATION

W. Zell, J.A. Becker, P. Deußer, W. Eutin, J.M. Schneider

Philips Kommunikations Industrie AG
Telecommunication Cables and Systems
Schanzenstr. 30, D 5000 Köln 80
Federal Republic of Germany

Abstract

For subscriber loop networks new economical solutions for cables, cable accessories, connectors and splicing techniques are of fundamental importance. After laboratory investigations the practical applicability of recently developed components were successfully tested in a field trial. Most emphasis is put on the mass splicing technique by which all ten single mode fibers of the fiber ribbons can be simultaneously fusion spliced by a high frequency arc. Mean splice losses of 0.07 dB obtained during the installation proove that the concept provides the basis of future subscriber loop networks.

1. Introduction

The present optical telecommunication techniques have been developed for longhaul transmission lines. Despite of their high performance they are, for economical reasons, not an appropriate solution for future subscriber loop networks. A completely new low cost design of all components is indispensable to meet the requirements of a high quality large scale production and installation. Because of the much shorter distances between interconnection points the interconnection techniques including cable accessories represent a much larger factor of cost than in trunk lines. The cable therefore has to be optimized in respect to an economical splicing procedure and an easy assembling of cable accessories. The ribbon cable[1] was developed to meet these requirements and the demand for a high fiber density.

Adequate splice organizers and closures as well as cross connecting cabinets and main distribution frames for ribbon cables were also presented[2]. A new low cost high performance connector design based on plastic parts has been developed[3] to provide detachable low cost connections in the switching units. The mass splicing technique presented in this paper completes the system of components for subscriber loop networks.

The structure of future subscriber loop networks may be a star net similar to the present copper networks. The components of such a subscriber network were tested by building-up a small scale model.

2. Cable

2.1 Ribbon Cable Design

According to our ribbon cable concept[1] ribbon cables with different fiber numbers can be produced without changing the manufacturing process. In order to prove the most critical design, we have chosen a 100-fiber cable for installation in our test line. The cable contains 10 ribbons with 10 fibers each. Eight ribbons contain single mode fibers, six of them depressed-cladding and two matched-cladding. Two ribbons with 50 µm-core graded index fibers are involved for future tests of the concept for LAN-applications.

The ribbons are placed in a central plastic tube one on top of the other. The ribbon stack is twisted in order to optimize the bending behaviour and to achieve a well defined mechanical operation range. To guarantee longitudinal water tightness, the plastic tube is jelly-filled and wrapped with a swelling tape.

Up to now we have designed different types of the outer sheath suited to different applications e.g. pulling into ducts or burying into the ground. For special environments we have developed an all dielectric cable sheath. Since the test-cable must be pulled into a duct, we have chosen metall free tensile elements and a LAP-sheath. The cable design is shown in Fig.1.

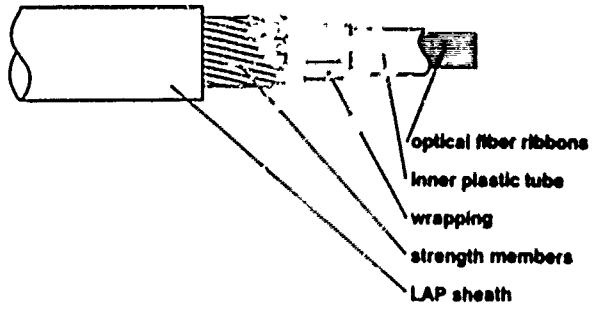

Fig. 1: Cable design

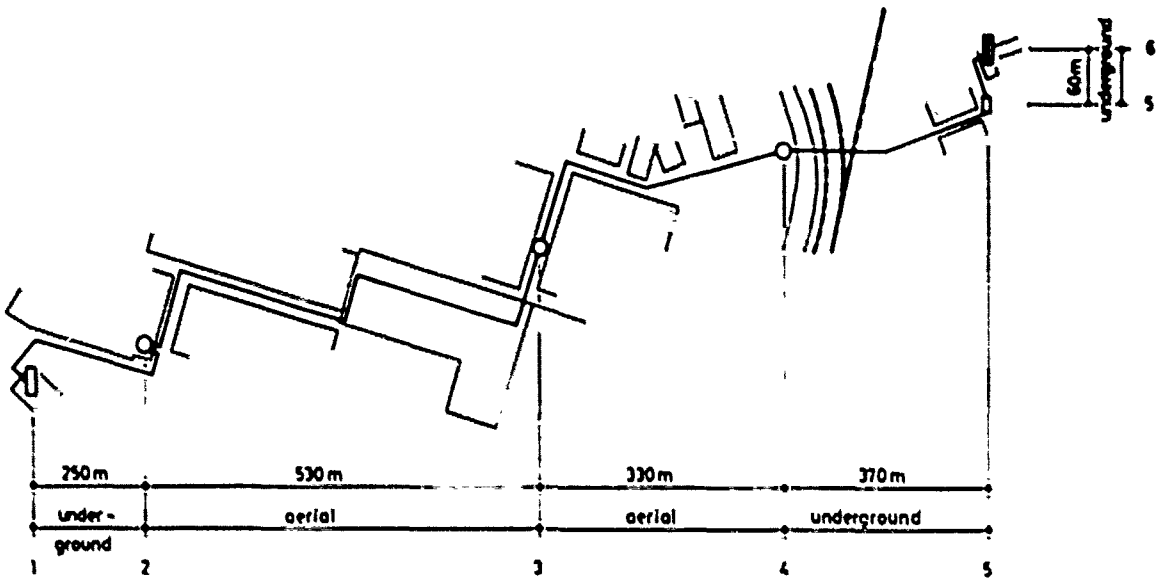

Fig. 2: Schematic plan of the test line
1,6 Cable terminals
2,3,4 Closures
5 Cross connecting cabinet

2.2 Cable Laying

The length of the test line (Fig. 2) is 1.54 km connecting two buildings of our factory. A PE-tube with an inner diameter of 45 mm serves as a duct. The cable is divided in 5 separate lengths including seven turn-arounds of 90°. Between the cross connecting cabinet (no. 5 in Fig. 2) and the cable terminal (no. 6) two parallel cables are laid. A length of 680 m of the duct is located under the ground and about 200 m inside buildings. The remaining length of 660 m leads over bridges and along the outside of buildings and is therefore exposed to all temperature changes over the year. Thus a very exacting long term test condition is created.

During the pulling procedure, a maximal pulling force of 2.5 kN was measured. The attenuation of the fibers was measured by OTDR after cable manufacturing (Fig. 3 a). After the pulling and splicing procedure the attenuation of one of the cable length was remeasured (Fig. 3 b). The mean value is nearly the same in both cases indicating that the pulling and installation procedure did not influence the fiber properties. In addition to the various tensile-,bending- and flexing-tests in the predevelopment phase, these results show the suitability of our ribbon cable design to practical use.

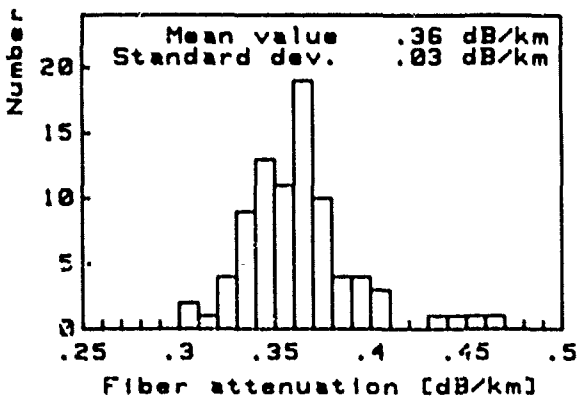

Fig. 3 a: Histogram of fiber attenuation at 1300 nm after cabling before installation

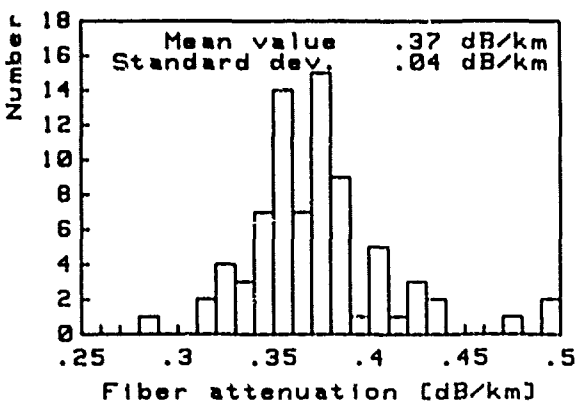

Fig. 3 b: Histogram of fiber attenuation at 1300 nm after installation

3. Cable Accessories

3.1 Splice Closures

To connect the cable lengths of this experimental network three cable closures were assembled. One of the closures (no. 2 in Fig. 2) was placed in a building, one (no. 4) in a culvert and one (no. 3) in the aerial section of the cable line thus exposing the latter to severe environmental test conditions.

The closure types chosen are field proved both in copper and fiber optic networks. To store the ribbon-to-ribbon connections and the appropriate splicing and repair lenghts the closures were provided with one- and two-chamber splice organizers[2]. The two chamber splice organizer can be taken out of the splice closure to place it closer to the mass splicer. The required manipulation length is stored in the inner part of the subdivided storage chambers.

After the preparation of the cable ends and the closures the fiber ribbons are inserted into the splice organizers prior to the splicing procedure. Before starting the splicing procedure the ends of the fiber ribbons are to be pulled out of the splice organizer. Thus length is gained to lead the ribbons to the splicing equipment. When the splicing procedure is finished the ribbons and the protected splice are pushed back into the organizer.

3.2 Cross Connecting Cabinet

The cross connecting cabinet (no. 5 in Fig. 2) is equipped with cable terminals, each of them consisting of plug-in units in a modular design. In each of the plug-in units one ribbon is spliced to ten individual pigtails. Each pigtail is terminated by a high performance plastic connector plug.

The splicing of a fiber ribbon to a multitude of single pigtails is carried out employing a fiber planarizer to get the pigtails into a ribbon like structure. The principle of the planarizer is shown in Fig. 4. The fibers are fed into the slit 1 one after the other, pushed into close contact by the blades 3 while lowering the slide 2 and fixed by the holder 4. The holders can be taken out of the planarizer and remain on the fibers until the splice is protected. The same holders are used for handling the ribbons.

Both splicing lenghts of the fiber ribbon and the fiber pigtails are stored in separate chambers of an integrated splice organizer. The terminated fibers can be connected by pre-connectorized jumper fibers. Their overlengths are stored in storage disks kept within the plug-in units.

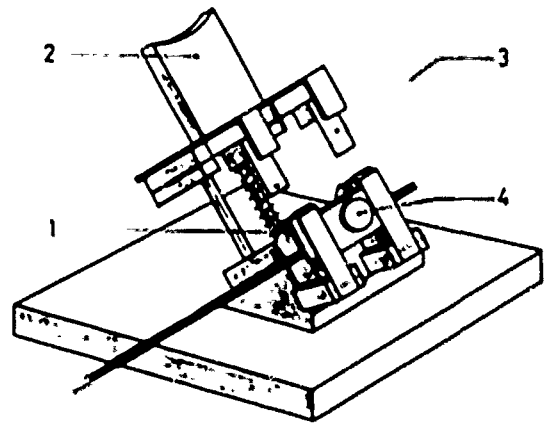

Fig. 4: Planarizer

3.3 Cable Termination Racks

At the ends of the trial network cable two termination racks were installed. One of them (no. 6 in Fig. 2) is of standard design as used by different telephone companies. The bracket mounted splicing field contains ten splice organizers which are each mounted on a distribution plate. The fibers of the fiber ribbon are spliced to single fiber pigtails provided with connector plugs as described above. The splicing and repair lenghts are stored in the splice organizer and the single fiber pigtails are fixed separately (one by one) to the distribution plate. To facilitate assembling the splice field can be turned out of the rack.

The pigtails of the outside plant cables are led to the rear side of the connector port which is mounted on a drawer. To insert the plugs into the adaptors from the rear side the drawer is pulled out. Devices are connected from the front side.
The other cable termination (no. 1) is set up by a 19 inch rack to demonstrate industrial applications as used in local area networks (LAN). The fiber ribbons of the outside plant cable are terminated in patch panel units. The frontside of these units consists of moduls carrying up to six connector adaptors. The fibers of the fiber ribbons are spliced to single fiber pigtails provided with connector plugs to be inserted in above mentioned adaptors. Splices including appropriate splicing and repair lengths of the fiber ribbon and the single fiber pigtails are stored in splice organizers as used in splice closures.
At the front of the patch panel the fibers of different outside cables can be connected via pre-connectorized jumper fibers.

4. Connectors

The connector[3] developed for subscriber loop applications meets the requirements of a low cost device with single mode precision by employing the V-groove fiber alignment principle. In the laboratory the connector has proven its supreme transmission characteristics with a mean loss of 0.05 dB, a loss repeatability of 0.01 dB and a mean return loss of more than 40 dB for single mode fibers.
After assembling the connector pigtails in the lab the plug-in units of the cable terminal are completed in the field by mass-splicing the fiber ribbons to the pigtails as described above.

5. Mass Splicing

5.1 Fiber Preparation

The splicing procedure starts by pulling the ribbons out of the organizers. The already mentioned holders of the planarizer are attached to the ribbons. The coating of the ribbon is then removed employing a thermo-mechanical method.
The most important precondition for low loss splicing is an endface preparation resulting in mirrorlike endfaces and low endface angles in respect to the fiber axis. Multiple endface preparation furthermore requires a small difference in lenght between the fibers.

In the field trial we used a fiber cleaver[4] based on the well known principle of scoring the bent and stressed fibers. It delivers endface angles of 0.5 degree in average (Fig. 5) and differences in fiber length of approx. 5 µm. Since the reliability of the unit is very high the endface angles were not measured during the field trial.

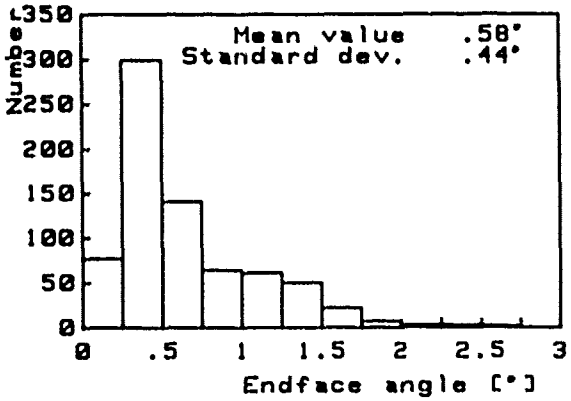

Fig. 5: Histogram of endface angles for multiple endface preparation

5.2 Fusion Splicing

The fusion splicer used in the field trial is based on the same theoretical and practical investigations about the fiber geometric tolerances[4] which led to the design of the plastic connector. For both applications the geometric tolerances like excentricity, non-circularity and diameter variations are low enough so that a core-core alignment is not necessary. In case of a passive alignment in V-grooves the resulting lateral offset of the cores is typically below 0.5 µm, resulting in a average contribution of less than 0.1 dB to the loss of the splice or connector.

The fusion splicer therefore does neither imply a XY-alignment system nor a system for getting information about the position of the fiber cores like core monitoring or local injection and detection. The central part of the splicer (Fig. 6) is a block 1 with high precision V-grooves and a sparing for the electrodes 2,2'. On both sides of the central V-groove block the ribbon holders 3,3' are inserted into translation tables 4,4' which can be moved by stepping motors. Thus an initial gap between the fiber ends can be set prior to fusion during which the fibers can then be stuffed as defined.

The electrodes are arranged in a horizontal plane with a small offset in respect to the ribbon plane providing an isothermal heat distribution to the fibers. The fibers are heated simultaneously by a high frequency discharge. After the setting of the initial gap the fibers are prefused and stuffed during the fusion. The stuffing length is 40 µm with a deviation of about 10 µm due to the individual differences in fiber lengths after the endface preparation. All ten fibers can be observed simultaneously unidirectional on an external TV-screen via a CCD-camera. During and after the fusion process a visual inspection of the splices is possible which in our experience is sufficient to detect bad splices.

The matched cladding and the depressed cladding fibers were spliced with the same set of splicing parameters without any significant difference in splicing results. A histogram of the splice

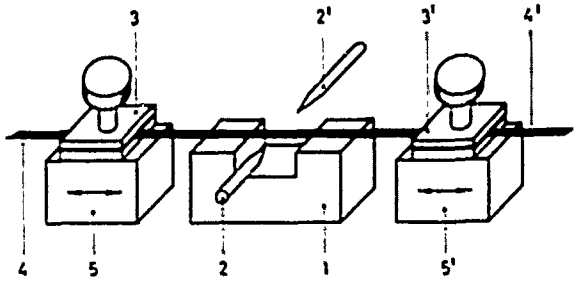

Fig. 6: Central part of mass splicer

losses of the single mode ribbons within the test line closures is shown in Fig. 7. The mean loss of 0.07 dB is slightly higher than the laboratory result of 0.05 dB obtained for repair splices before the field trial. In repair splices of ribbons the geometric tolerances of the fibers do theoretically not influence the splice loss because in a ribbon the fibers can not be turned around their axis. In the field trial the spliced cable sections originated from the same cable but were drawn in different directions. This way, different parts of the fibers were spliced. Since the geometry of the fibers varies slightly along the fiber length the situation in the field trial was comparable to the splicing of non-identical ribbons.
Laboratory tests with non-identical ribbons included fibers of different manufactures and resulted therefore in an even higher average splice loss of 0.11 dB.
The splice loss histogram for GI-ribbons is shown in Fig. 8.

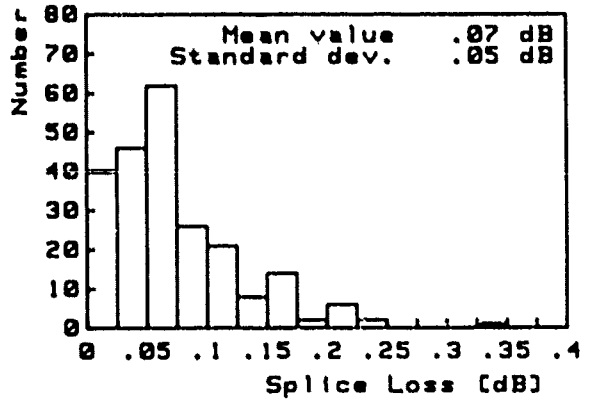

Fig. 7: Histogram of splice losses at 1300 nm for single mode ribbons.

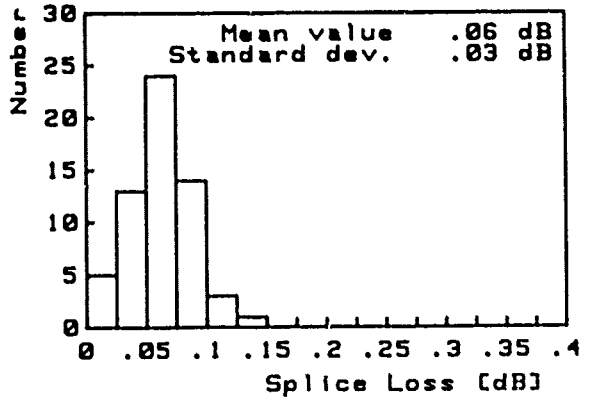

Fig. 8: Histogram of splice losses at 1300 nm for GI-ribbons

5.3 Splice Protection

As splice protection a sandwich structure was used. Two sheets of a ductile and adhesive material are attached between two rigid plates. The protection is accomplished by pressing the parts from both sides to the splice. Heating is not necessary.

There is no additional loss due to the splice protection. Temperature cycling between - 40°C and 60° C and high humidity up to 95 % on test samples before the field trial did not lead to any significant change of the splice losses. The tensile strength of the protected splices is about 40 N.

The last step of the splicing procedure is to push the ribbons back into the storage chambers of the splice organizer and insert the splice into the organizer.

6. Conclusions

The mass splicing technique leads to a significant reduction of installation time providing splice losses close to those obtained in present single fiber techniques. The results of the field trial indicate that all components for a star shaped subscriber loop network can soon be tested in a public network.

Acknowledgement

This work was supported by the Bundesminister für Forschung und Technologie of the Federal Republic of Germany. The authors alone are responsible for the content.

References

[1] W. Lackas, J.M. Schneider, "New Fiber Optic Ribbon Cable Design", IWCS Proceedings 1986, pp. 4 - 9
[2] P. Deußer, J.A. Becker, "Cable Accessories for Fibre Ribbon Cables in Subscriber Loop Networks", IWCS Proceedings 1988, pp. 292 - 296
[3] W. Eutin, U. Grzesik, E. Schürmann, "New Plastic Single Mode Fiber Connector for Subscriber Networks", IWCS Proceedings 1988, pp. 665 - 669
[4] J.A. Becker, W. Eutin, W. Zell, " Trends in Fibers, Fiber Cabling, Mass Splicing and Connectors for the Subscriber Area", ECOC 1989, Gothenburg, Sweden

Werner Zell was born in Cologne, West Germany, in 1953. In 1977 he received the diploma degree in physics and in 1981 the Dr. rer. nat. degree from the University of Cologne, where he worked on low temperature physics. In 1981 he joined the Philips Kommunikations Industrie where he was first engaged in the development of fiber-optic cables. Since 1983 he is responsible for the development of splicing technology.

Johann A. Becker was born in Rheinberg, West Germany, in 1944. He received the degree of Dipl.-Ing. in electrical engineering in 1969, and the degree of Dr.-Ing. in 1973, from the Rheinisch-Westfalische Technische Hochschule Aachen, W. Germany. In 1974 he joined the Philips Kommunikations Industrie AG where he is now head of the department for the development of interconnection technology.

Peter Deußer was born in Ellwurden, West Germany, in 1946. He received the degree Dipl.-Ing. in electrical engineering in 1971 from the Fachhuchschule Wilhelmshaven, W. Germany. In 1974 he joined the Philips Kommunikations Industrie AG where he is now responsible for the development and design of cable accessories.

Wolfgang Eutin was born in Recklinghausen, West Germany, in 1952. He received the Dipl.-Phys. degree from the Universität Dusseldorf, Düsseldorf, Germany, in 1981, where he worked on stabilized sealed CO_2 lasers. In 1981 he joined the Heinrich-Hertz-Institut, Berlin, Germany, where he was engaged in coherent fiber communication systems. Since 1985 he is with Philips Kommunikations Industrie AG, Cologne, Germany, where he is responsible for fiber optic connectors.

J. Michael Schneider studied at the Universities of Clausthal-Zellerfeld and Hannover and received the Diploma degree in 1980 and the Dr. rer. nat. degree in 1984, both in Physics. From 1980 to 1984 he was a research and teaching assistant at the Institut für Plasmaphysik in Hannover where he worked on lasers and optical diagnostic methods in plasma physics. He joined Philips Kommunikations Industrie AG in 1984. Since 1987 he is head of the department for telecommunication cable development.

PRE-CONNECTORIZED 1000-FIBER CABLE

H. YOKOSUKA S. TOGO H. HOSOYA H. HIRAO

OPTO-ELECTRONICS LABORATORY FUJIKURA LTD.

1440 MUTSUZAKI SAKURA-SHI CHIBA-KEN 285 JAPAN

ABSTRACT

A new pre-connectorized single mode 1000-fiber cable has been developed and introduced into fiber optic cable subscriber networks. The features of this cable are described as follow:

1. It employs the structure that can control the length of the fiber ribbon by turning the fiber once and changing the length of the loop whether into longer or shorter and store the 1000 fibers with 5 banks, 200 fibers in each bank.
2. The pulling hardware which contains 1000 fiber plugs inside has bending flexibility and tensile strength good enough to endure the force of cable installations.

Various tests to evaluate the 1000-fiber cable have been carried out and the results have proved that the pre-connectorized cable has excellent characteristics.

1. INTRODUCTION

The number of optical fibers in the cable used for the subscriber networks has been increased year after year. A few years ago, a maximum 200 fiber cable was introduced, then a maximum 600 fiber cable soon after; last year, it increased to maximum 1000 fiber cable. It became necessary to have a pre-connectorized cable which pre-connectorized in the factory so that it could shorten the time at the installation fields and respond promptly to the needs of the increased number of subscribers.

One of the biggest characteristics of the newly developed pre-connectorized cable which can store up to 1000 fibers of SM-8 fiber ribbons is that for this storing capacity, it is small and flexible so that it is readily installed. The pulling hardware can store two kinds of pre-connectorized 1000 fiber cables: one is to store 125 plugs of 8 fiber ribbon, and the other is to store 250 plugs of 4 fiber ribbon. The paper describes the structure and characteristics of the new pre-connectorized cable.

2. STRUCTURE

2-1. CABLE

As seen in figure 1, the cable has a tensile strength member in the center with five slotted-rods around it and a sheath covering them. A slotted-rod has five square-shaped spiral grooves in which five SM 8-fiber ribbons, 40 fibers, can be stored in each groove. Therefore, one slotted-rod can store 25 8-fiber ribbons, 200 fibers, and a total 125 8-fiber ribbons, 1000 fibers, in a cable.

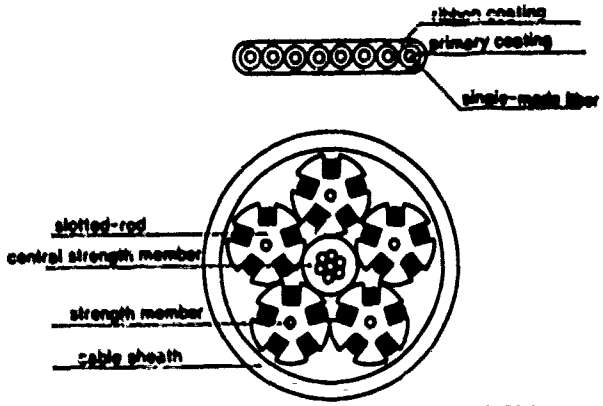

Figure.1.STRUCTURE OF A 1000-FIBER CABLE WITH 8-FIBER RIBBONS

2-2. FIBER RIBBON

The SM 8-fiber ribbon which is used for the 1000 fiber cable can be divided into two 4-fiber ribbons by the hand or with a ribbon separating tool. When all the 8-fiber ribbons of the 1000 cable are divided into two 4-fiber ribbons each, a total number of the 4-fiber ribbon becomes 250 ribbons that require 250 connector plugs for a pre-connectorized cable. Also, it becomes possible to have a SM 8-fiber ribbon on one end of the cable and SM 4-fiber ribbon on the other end.

2-3. CONNECTOR

The structure of the connector is shown in figures 2 and 3. When the connector is used in the fiber optic networks, the fiber ribbon can be mechanically transferred from one ribbon to another at high speed by using the cable transferring system. Thus, it is called "mechanically transferable connector, MT connector. Depending on the number of fibers in a fiber ribbon, the two kinds of ferrules, one for 4-fiber and the other for 8-fiber ribbons, are provided. The difference between these two ferrules is only the number of the fiber receiving holes in which optical fibers are inserted one has 4 holes and the other 8 holes. The structure and the size of both ferrules are the same. The two big holes on both sides of the ferrule mating face are for the alignment pins that are made of stainless steel of 0.7 mm diameter. The fibers of the ribbon are inserted into the receiving holes between the pin holes and fixed with an adhesive agent. The installation procedure of the ferrule onto the fiber ribbon starts with an attachment of a rubber boot to the back of the ferrule then a fiber ribbon insertion into the holes. Then applying the adhesive agent and hardening it, the ferrule mating face is polished to complete the job.

At the installation field, the alignment pins are attached to one of the ferrule of the pair and the refractive index matching gel is applied between the ferrules. Then both ferrules are pushed against by the plate spring with a pressure of 1 Kgf to get a stable optical coupling. The ferrule is made of thermoset epoxy resin and molded using a precision transfer molding method.

The dimensional precision of the center of the fiber receiving holes are less than 1 um and of the alignment pin pitch is less than 2 um.

The coupling loss of the connector is shown in figure 4. The average connecting loss of the SM 8-fiber ribbon is 0.27 dB and of 4-fiber ribbon is 0.25 dB with measuring wave length 1.3 um. The results of other evaluation tests on the connector are shown in the table 1.

The pre-connectorized fiber optic cable has been widely used in the subscriber cable networks. Compared to the fusion splicing method, the pre-connectorized cable can greatly shorten the time for joining work at the field and make a cable branching promptly for new customers. Although the connection loss may be greater than that of the fusion splicing, the increased loss would be still low enough to meet an acceptable level. Especially, in case of a very high fiber count cable like the 1000-fiber cable, which has many ribbons as 125 of 8-fiber ribbon, the pre-connectorized cable can finish the job much faster than the fusion splicing. What is more, in case 8-fiber ribbon is divided into two 4-fiber ribbons, the maximum number of the ribbon will be 250 which would make the balance of the connecting time between the fusion splicing and pre-connectorized cable joining much greater.

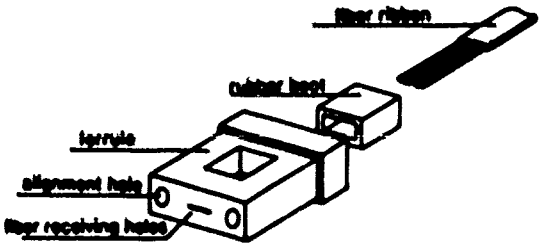

Figure.2 PLUG STRUCTURE FOR FIBER RIBBON

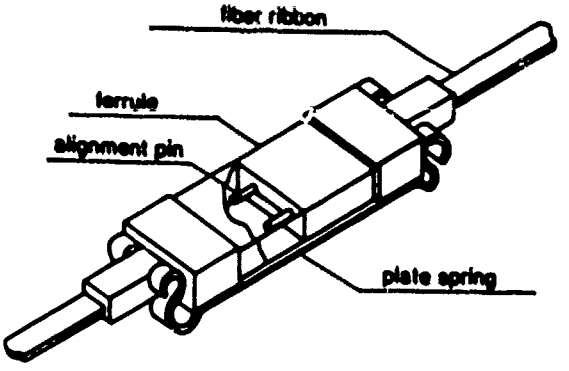

Figure.3 MT-CONNECTOR

TABLE.1 RESULTS OF EVALUATION TESTS ON THE CONNECTOR

TESTING ITEM	CONDITION	RESULT
TEMPERATURE CYCLING	-30 TO 60°C 4 cycles/day	LESS THAN 0.2dB
HIGH TEMPERATURE	60°C 100H	LESS THAN 0.1dB
LOW TEMPERATURE	-30°C 100H	LESS THAN 0.15dB
HUMIDITY	60°C 90%RH 100H	LESS THAN 0.1dB
REPEARABILITY	500 TIMES	LESS THAN 0.2dB
VIBRATION	10HZ AMPLITUDE 10mm 2 DIRECTIONS	LESS THAN 0.1dB

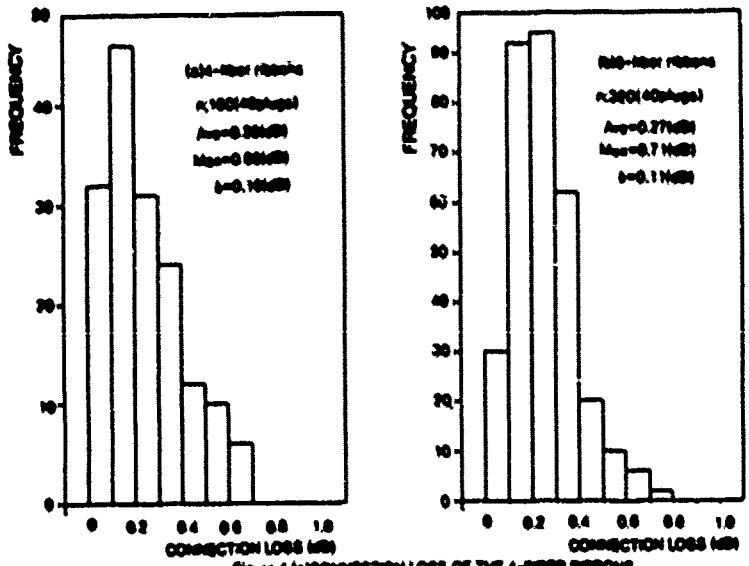

Figure.4 (a)CONNECTION LOSS OF THE 4-FIBER RIBBONS
(b)CONNECTION LOSS OF THE 8-FIBER RIBBONS

2-4. JOINT CLOSURE

The pre-connectorized cable is stored in the joint closure in the manhole of the field. As shown in figure 5, it is stored after removing the flexible hose and pulling wire.

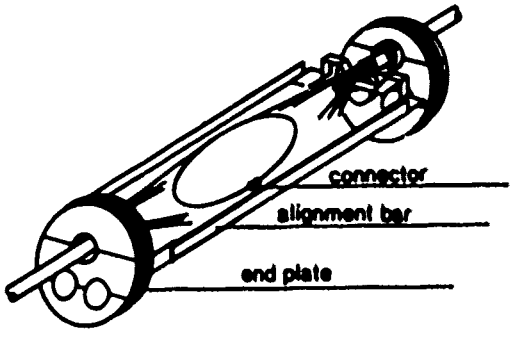

Figure.5.JOINT CLOSURE

2-5. PULLING HARDWARE

The structure of the pulling hardware of the 1000-fiber pre-connectorized cable with 8-fiber ribbon is shown in figure 6. The pulling hardware stores the connector plugs and protects them from external force, and the cable is installed by pulling the hardware at the field. The requirements of the hardware for the 1000 fiber cable are as follows:

1) It must be airtight so that there will be no humidity inside of the cable.
2) It must have a bending flexibility to make the cable installation easier.
3) The sheath and tensile strength member of the cable must be fixed to the pulling hardware so that there will be no discrepancy between them during the cable installation.
4) The maximum outer diameter must be less than 71mm .
5) Considering the workability of at the installation, the total length must be less than 1200 mm.
6) The length of the pre-connectorized fiber ribbon must be in the range of 580 - 900 mm.
7) Considering the installation condition, there should be no effect on the optical fiber ribbon and on the connector plug even if pulled with maximum 150 kgf, angle 90 degree, maximum bending radius 600 mm as well as there should be no leakage of air.

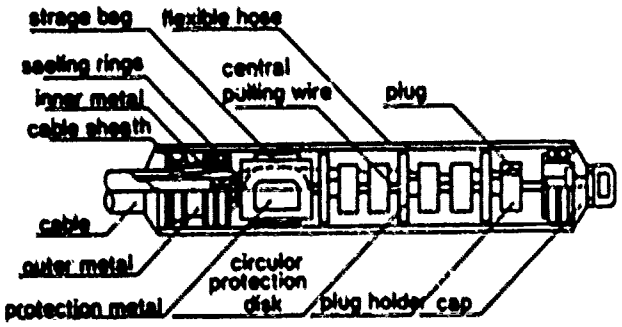

Figure.6.PULLING HARDWARE OF 1000-FIBER CABLE WITH 8-FIBER RIBBONS

In order to obtain airtightness in the pulling hardware, it is equipped with sealing rings on the joints of the spacer parts and the flexible hose, of the cap and flexible hose, and of the cap and pulling wire. Also, it holds a shrinkable tube and a sealing tape between the outer metal and the cable sheath, and then they are compressed by squeezing and deforming the outer metal to obtain the airtightness. the bending flexibility of the pulling hardware is kept by using the flexible pulling wire and a flexible hose which is made of two kinds of plastics, soft and hard. To unite the cable sheath and the tensile strength member, the cable sheath is held between the inner metal and outer metal, then it is fastened by squeezing and deforming the outer metal. The inner metal is attached to the connecting rod which is joined to the tensile strength member of the cable. The circular protection disks and fiber ribbon protection metals are attached to the central pulling wire. The circular protection disks prevent the flexible hose from deforming by an external force. The ribbon protection metal protects the extra length of the plug mounted fiber ribbon. The organization of the plug mounted fiber ribbon in the pulling hardware is explained below.

It would be ideal if the length of all the fiber ribbons with plugs for the pre-connectorized cable is the same, and if the plugs can be stored all in one place. However, in this case, it would make the outer diameter of the connector too large. Since the regulated outer diameter of the pulling hardware of the pre-connectorized cable is less than 71 mm diameter, the plugs have to be stored in several banks in the direction of length to keep the outer diameter small. Considering the size of ferrule and a way to store the plugs without any damage to them, 5 banks with 25 plugs each is appropriate in case of SM 8-fiber ribbon plug. If the fiber ribbon is divided into 5 different lengths and stored separately, the length of the pulling hardware of the pre-connectorized cable becomes longer, and it causes a trouble with the extra 100 mm of ribbon length which is provided for a possible failure at the plug mounting in the factory. Therefore, the length of the fiber ribbons is unified, and the plugs are divided into 5 banks. Then the extra length, which may be brought up when the plugs are stored, and the other extra Sincerely,length as a provision for plug mounting failure, are treated as follows:

making fiber ribbons a turn on the way to the plugs, a bank at a time,it protects the part which has made a turn with a plastic storage bag. The change of the fiber length occurring during the storage of the plug is absorbed by controlling the length of the turn. The fiber ribbon protection metal is responsible for the maintenance and protection of the fiber ribbon in the storage bags.

The method of calculation of the fiber ribbon length in the pulling hardware is explained next. (see figure 7) Assume the constants as follows:

The distance between the end of the spacer and the first plug holder .....A

the distance between the end of the spacer and the second plug holder.....B

the distance between the end of the spacer and the third plug holder.....C

the distance between the end of the spacer and the fourth plug holder.....D

the distance between the end of the spacer and the fifth plug holder .....E

the minimum bending radius in the storage bag.....R

the length of the fiber ribbon with plugs from the end of the spacer.....L

the length of the extra fiber ribbon as provision for failure in plug mounting ... .F

the length of the storage bag.....h

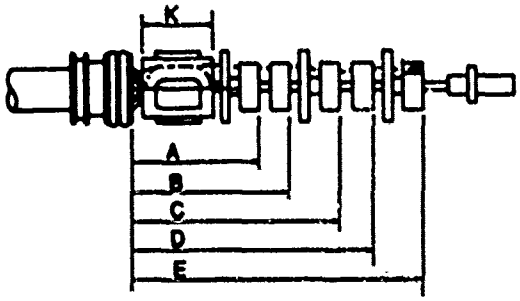

Figure.7 ARRANGEMENT OF THE FIBER RIBBON LENGTH IN THE PULLING HARDWARE

Figure 8 PULLING HARDWARE OF 1000-FIBER CABLE WITH 4-FIBER RIBBONS

The minimum length to store in the storage bag is K+2×R, but it is appropriate to make it K+2×R+F in consideration of the extra length in case of a plug mounting failure. The distance A - E is described as follows:

$$A \leq \{L - (2 \times R + F + E - A)\} \quad \cdots (1)$$

$$B \leq \{L - (2 \times R + F + E - B)\} \quad \cdots (2)$$

$$C \leq \{L - (2 \times R + F + E - C)\} \quad \cdots (3)$$

$$D \leq \{L - (2 \times R + F + E - D)\} \quad \cdots (4)$$

$$E \leq (L - 2 \times R + F) \quad \cdots (5)$$

$$K > 2R + (F + E - A)/2 \quad \cdots (6)$$

the length of extra fiber ribbon can be obtained by inserting a conditional value in (1) - (6).

However, when SM 8-fiber ribbon of the 1000 fiber cable is divided into two 4 fiber ribbons, the number of the plug becomes 250, and it would require 10 plug holders, if it is considered as the 8-fiber, which would make the storage difficult by merely turning once. Therefore, in this case, 800 fibers, 200 plugs, should be stored first after making a turn, and the rest of 200 fibers, 50 plugs should be straighten out, then the extra length for failure protection can be rolled around the cylindrical sponge which has the same length as the length for the failure protection.

In addition to it, a flat sponge can be rolled over to protect them as shown in figure 8.

3. PROPERTY

The result of the evaluation tests is shown in the table 2. The temperature cycling test was conducted for three cycles a day with a range of -20 C to 60 C degrees, total 10 cycles, and it confirmed that there was no leakage of air. The squeeze test was conducted with a testing system shown in figure 9. The test was given for 15 times under the condition of 150 kgf tension with 600 mm of radius and 90 degree angle to see if there was any leakage of air, physical loss or damage, and to measure residual loss of fiber. The residual loss was checked by measuring the loss before storing the fiber ribbon with plugs in the pulling hardware of the pre-connectorized cable and after taking it out of the pulling hardware and by measuring the changes in the loss. The bending test is given by using a bending test machine in 600 mm of radius and examined air leakage, physical loss or damage, and residual loss. The pulling test was conducted under the condition that the cable sheath was squeezed and fastened with the outer metal and inner metal but measured that the seizing power is more than 70 percent greater than the strength of the cable sheath. The result were all favorable.

TABLE 2 RESULTS OF EVALUATION TESTS ON THE CONNECTOR

TESTING ITEM	CONDITION	RESULT
TEMPERATURE CYCLING	-20 TO 60°C 3 cycles/day	NO LEAKAGE OF AIR
SQUEEZE TEST	150kg TENSILE 90°DEGREE 600mm RADIUS 15 TIMES	NO LEAKAGE OF AIR NO PHYSICAL DAMAGE NO RESIDUAL LOSS
BENDING TEST	600mm RADIUS 15 TIMES	NO LEAKAGE OF AIR NO RESIDUAL LOSS
PULLING TEST	MORE THAN 70% GREATER STRENGTH OF THE SHEATH	NO PROBLEM

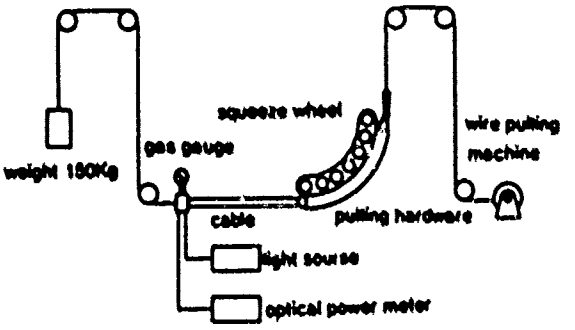

Figure.8.SQUEEZE TEST SYSTEM

4. CONCLUSION

The development of the SM 1000 pre-connectorized cable has brought a significant effect on the shortening the installation time and simplification of the joining work. It is a far better progress even though the manufacturing process in the factory has been more complicated because of this pre-connectorized cable which was accompanied with a high density and high count of fibers. The pre-connectorized cable has been introduced in actual circuits, but by this time, there has been no trouble arisen.

The use of the pre-connectorized cable with high density and high count of fibers will be increased rapidly.

Hiroshi Yokosuka

Opt-Electronics
Laboratory
FUJIKURA LTD.

1440,Mutsuzaki,
Sakura-shi,Chiba,285,
Japan

Hiroshi Yokosuka graduated in mechanical engineering from Tokyo metropolitan Technical Junior college in 1967.

Hiroshi Yokosuka joined Fujikura Ltd. in 1967 and has been engaged in research and development of automatic telephone cable splicing machines, joint closures and optical Connectors is now a chief of the fiber and cable accessory section in Opt-Electronics Laboratory. He is a member of the Institute of Electronics, Information and Communication Engineers of Japan.

Hideyuki Hosoya

Opt-Electronics
Laboratory
FUJIKURA LTD.

1440,Mutsuzaki,
Sakura-shi,Chiba,285,
Japan

Hideyuki Hosoya was born in 1959. He received the M.Sc. degree in physics from Yamagata University in 1983. He joined Fujikura Ltd. in 1983 and has been engaged in research and development of telecommunication cables and accessories. He is a member of the Institute of Electronics, Information and communication Engineers of Japan.

Syuichi Togo

Opt-Electronics
Laboratory
FUJIKURA LTD.

1440,Mutsuzaki,
Sakura-shi,Chiba,285,
Japan

Syuichi Togo was born in 1964. He received the M.E. degree in electronics engineering from Ohita University in 1985. He joined Fujikura Ltd. in 1985 and has been engaged in research and development of telecommunication cables and accessories. He is a member of the Institute of Electronics,Information and communication Engineers of Japan.

Hideo Hirao

Opt-Electronics
Laboratory
FUJIKURA LTD.

1440,Mutsuzaki,
Sakura-shi,Chiba,285,

Hideo Hirao was born in 1951. He received the B.E.M. degree agricultural mechanical engineering in 1974 from Mie University. He joined Fujikura Ltd. in 1974 and has been engaged in research and development of telecommunication cables and accessories.
He is now an Assistant Chief of the Cable Accessory section .

FULLY AUTOMATIC MASS-FUSION SPLICER FOR SINGLE-MODE OPTICAL FIBER RIBBON

Michito MATSUMOTO, Tadashi HAIBARA and Masaaki KAWASE*

NTT Network Systems Development Center * NTT Transmission Systems Laboratories
Tokai, Ibaraki, 319-11, Japan

ABSTRACT

A high speed and fully automatic mass-fusion splicer for single-mode optical fiber ribbon has been developed. All splicing processes , from fiber end preparation to reinforcement, are carried out automatically. Its performance has been evaluated for high-count optical subscriber cables in the field. An average splice loss of 0.09 dB and an average splicing time of about 5 min. have been obtained.

1. INTRODUCTION

In the construction of optical subscriber lines, a large number of fiber splices are required for high-density, high-count optical fiber cables[1]. Since splicing requires much labor, highly-efficient fiber splice techniques are indispensable for cost saving for and shortening the construction period. To date, several semi-automatic fusion splicers[2],[3],[4] have been developed. However, these still require some manual operations such as fiber cutting, fiber coat removing and fiber setting, which are dependent on the skill of the operator. Lack of skill can cause splicing delays and errors. Accordingly, it is necessary to develop a fully automatic splicer in which all splicing processes are carried out automatically.

In this paper, the design and performance of a high speed and fully automatic mass-fusion splicer for single-mode optical fiber ribbon are described. The results of field tests are also presented.

2. OUTLINE OF FULLY AUTOMATIC FUSION SPLICER

Fusion splicing procedures consist of three stages; fiber end preparation, fusion splicing and reinforcement. In an automatic machine, a fiber transport mechanism and functions for evaluating each process are also required. In the fully automatic mass-fusion splicer described here, the following basic principles are adopted to reduce splicing time and to attain low splice loss.

(1) Fiber transportation between the processes is assigned to two pairs of arms with different designs which enable parallel operation.

(2) Fiber axes are aligned by fixed V-grooves to simplify the mechanism.

(3) Mass-fusion splice is accomplished without the necessity of correcting the fiber end face position variance.

A flow chart and a diagram outlining the splicing procedures in the present machine are

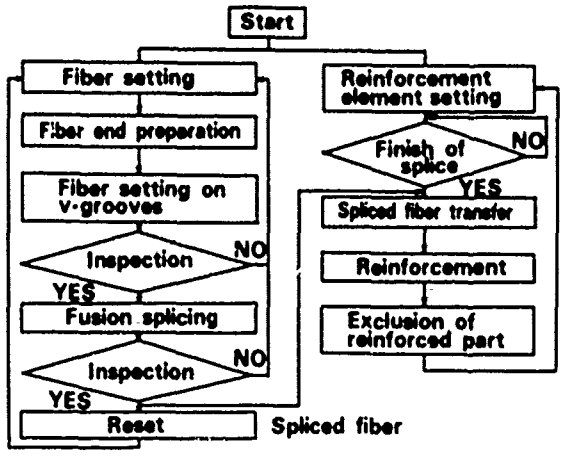

Figure 1. Flow chart of splicing procedures.

shown in Fig.1 and Fig.2, respectively. All splicing procedures are carried out automatically once the fiber ribbons have been set in the ribbon supply units. When the fiber end preparation is finished, the fiber end preparation parts evacuate, and the splicing part is inserted between a pair of fiber ribbons. The splicing part cleans the surface of the fibers and then sets them into V-grooves. The ribbons are gripped by a pair of arms until the fibers are spliced. Then, a second pair of arms receives the spliced fiber and transfers it to the reinforcement part. Subsequently, the first pair of arms can return to the first process position and be ready for the next fibers. The movements of the fibers and the implements, for which high-precision is required, are basically driven by a servo control mechanism.

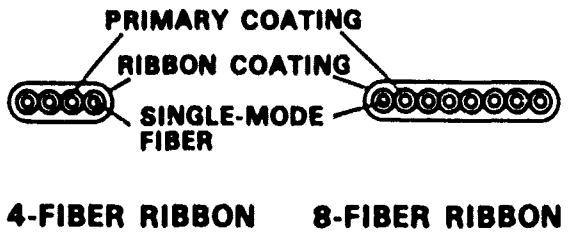

Figure 3. Structure of optical fiber ribbon.

3. STRUCTURE OF MAIN PARTS

3.1 Fiber end preparation

The fully automatic fusion splicer is designed for the two types of optical fiber ribbon shown in Fig.3. It is important to suppress fiber end-face position variance in mass-fusion splicing. A strongly bonded coat is adopted to reduce the variance, however this makes coat stripping very difficult using the conventional method. Therefore, a new method using a heater is adopted for stripping the strongly bonded coat. The mechanism is composed of a pair of blades and a ceramic heater. In addition to effective stripping, it also has the advantage of lessening the abrasion of the stripping blades. No abrasion was observed in more than 500 stripping operation.

Residual coating on the fiber surface affects the accuracy of fiber axis alignment. A misalignment of the fiber axis of more than 10 μm can easily occur due to residual coating on the V-grooves if the fiber surface is not cleaned.

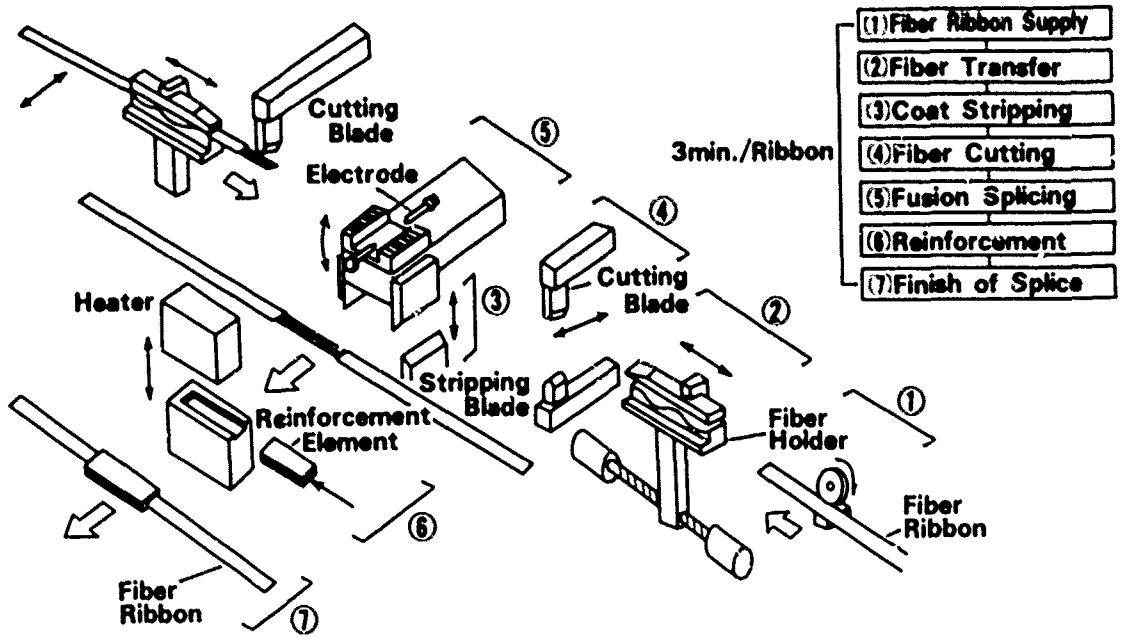

Figure 2. Outline of splicing procedures.

Accordingly, a cleaning mechanism is indispensable if single-mode fiber is to be spliced with low loss. Thus, a cleaning mechanism using an electric discharge has been adopted for burning off the residual coating on the fiber surface. Figure 4 shows the appearance of the fiber surfaces before and after cleaning with an electric discharge and clearly illustrates its effectiveness. Figure 5 shows the relation between butt joint loss and number of fiber setting trials using this mechanism. The measurement wavelength is 1.3 μm. As a result, it was confirmed that about 100 successful trials can be undertaken without cleaning the V-grooves. These resuts confirm the necessary requirement that the automatic fusion splicer be maintenance-free.

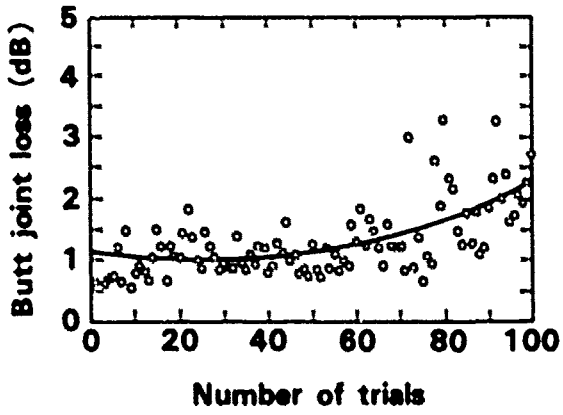

Figure 5. Relation between butt joint loss and number of fiber setting trials.

3.2 Fiber offset measurement and fusion splicing

Fusion splice loss is strongly influenced by fiber axis offset before fusion splicing. However, low splice loss can be obtained by making use of the effect of surface tension in the fusing fiber. Figure 6 shows the relation between the splice loss and the initial fiber axis offset before fusion splicing. From this result, a measurement accuracy of about 7 μm will be required for fiber axis offset before fusion splice, in order to attain a splice loss of below 0.3 dB.

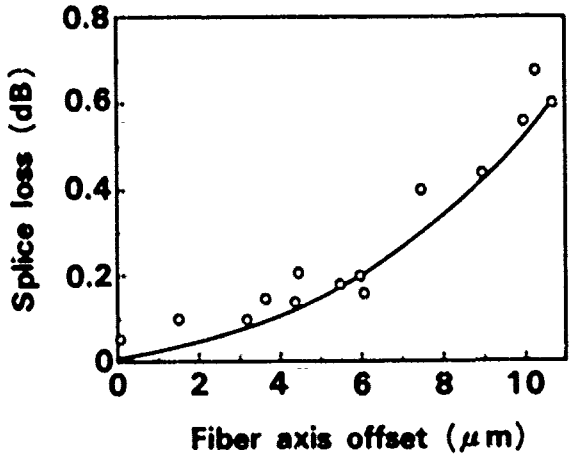

Figure 6. Relation between splice loss and fiber axis offset before fusion splice.

(a) before cleaning (b) after cleaning

Figure 4. Appearance of the fiber surfaces before and after cleanig with an electric discharge.

On the other hand, from the view point of simplification and miniaturization of the machine, a method for measuring the fiber offset in two directions by observing the fiber from only one direction as shown in Fig.7 has been adopted. In this method, an image of a fiber ribbon made by illumination is observed by a CCD camera, and the width of light line on the fiber surface occurring due to the lens effect of the fiber is measured by video processing. When a pair of fiber to be spliced is offset in the observation direction, the difference of the width corresponding to the offset arises, and the offset value is estimated by measuring the difference. The measurement accuracy of this method is about 3 μm and worse than the measurement method using two orthogonal directions. However, it is expected that the accuracy of the offset measurement satisfies the requirement for assuring the low splice loss mentioned above.

3.3 Reinforcement

It is necessary to reinforce the fusion spliced portion for protection from mechanical damage. A heat shrinkable tube method is one of the approved methods for reinforcement. However, if this method is used, the mechanism for setting and transferring the reinforcement elements becomes very difficult to automate. Therefore, a sandwich-type reinforcement composed of a plate made of magnetic material and a glass ceramic plate both coated with hot-melt film is adopted. The structure is shown in Fig.8. The size of the element is 30 mm x 5 mm x 2 mm. After splicing, the spliced portion is sandwiched between the elements, and the fiber and plate assembly is heated by an eddy current induced in the magnetic plate. The reinforcement process takes about 70 sec, which is about 1/3 the time taken by the conventional method. After reinforcement, the spliced fiber is ejected from the machine.

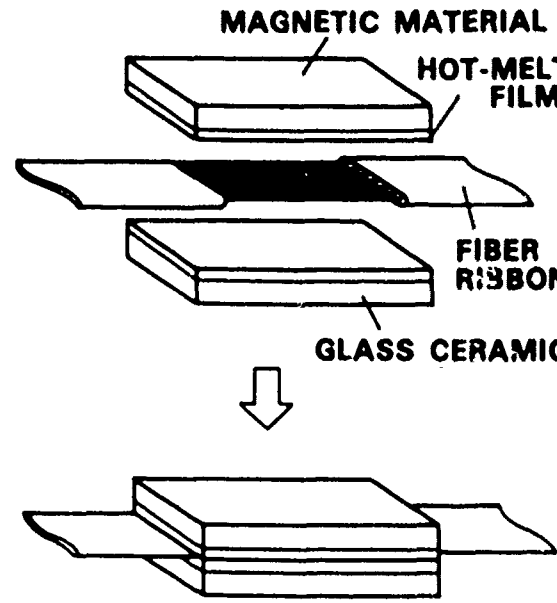

Figure 8. Structure of reinforcement element and reinforced part.

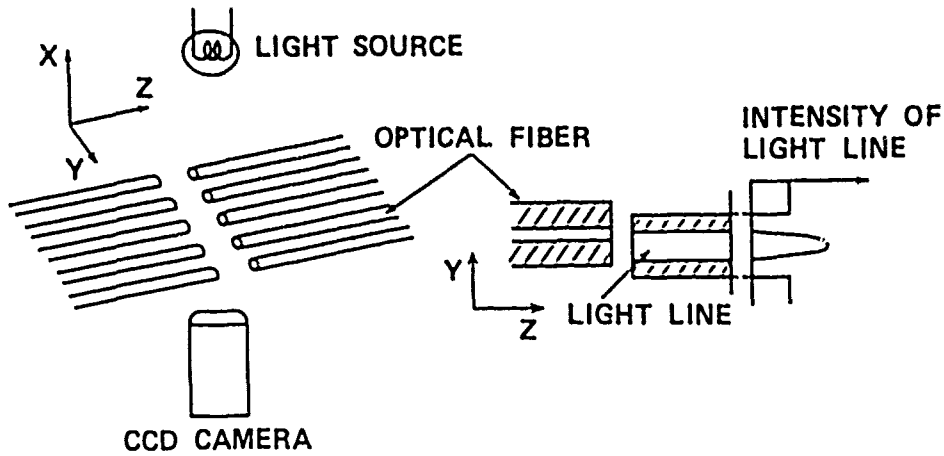

Figure 7. Fiber offset measurement.

4. PERFORMANCE OF THE MACHINE

A fully automatic fusion splicer is divided into a splicing unit and a control unit. The splicing unit is shown in Fig.9. It is about 20 cm long, 30 cm wide, and 40 cm high, with a weight of about 15 kg. Figure 10 show a splice loss histogram for a single-mode 4-fiber ribbon and an 8-fiber ribbon. Their average splice losses were 0.07 dB and 0.03 dB, respectively. The core eccentricity and mode field diameter of the fiber used in this experiment are about 1 % and 9.5 μm, respectively. These splice losses are almost same as those of a conventional splicer.

The tensile strengths of the reinforced parts for a 4-fiber and an 8-fiber ribbon are shown in Fig.11. An average strength of about 5 kg for the 4-fiber ribbon and 9 kg for the 8-fiber ribbon were obtained. No loss change was observed in the reinforced part during 80 heat cycles (-3° to 60°C). These results satisfactorily demon the reliability of the spliced part.

The operation times of all processes performed by this machine are shown in Fig.12. The time required for fiber end preparation, alignment and splicing, reinforcement, and transfer are 40 sec, 40 sec, 70 sec, and 30 sec, respectively. The total time for the first cycle from fiber setting to removing the completed splice after reinforcement is about 3 minutes. The time for the second and subsequent cycles is about 2

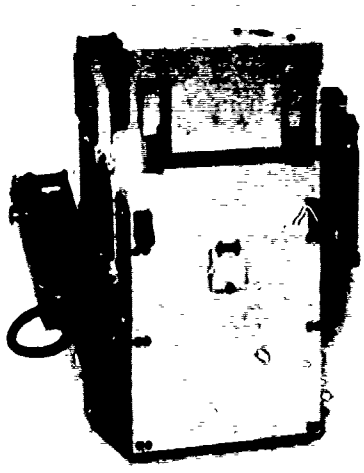

Figure 9. Splicing unit of fully automatic splicer.

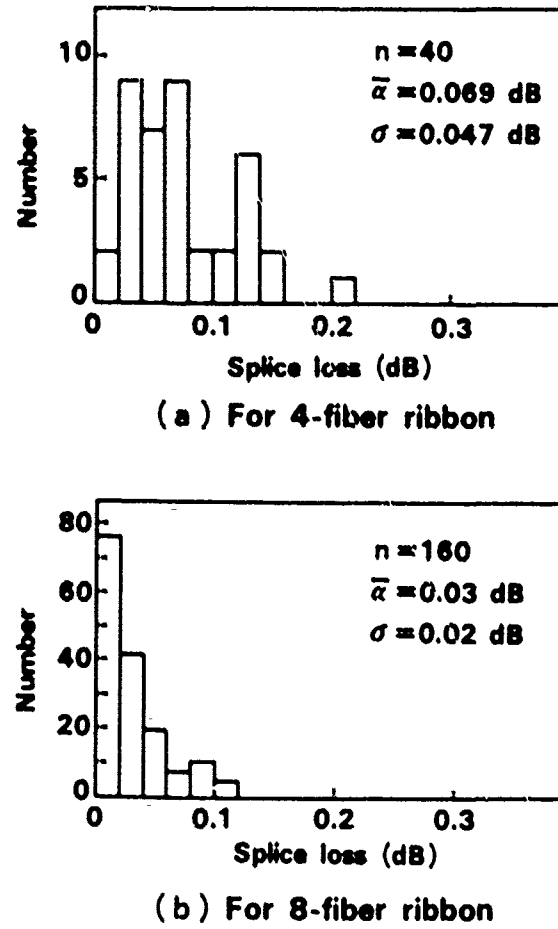

Figure 10. Splice loss histogram for a 4-fiber ribbon and an 8-fiber ribbon.

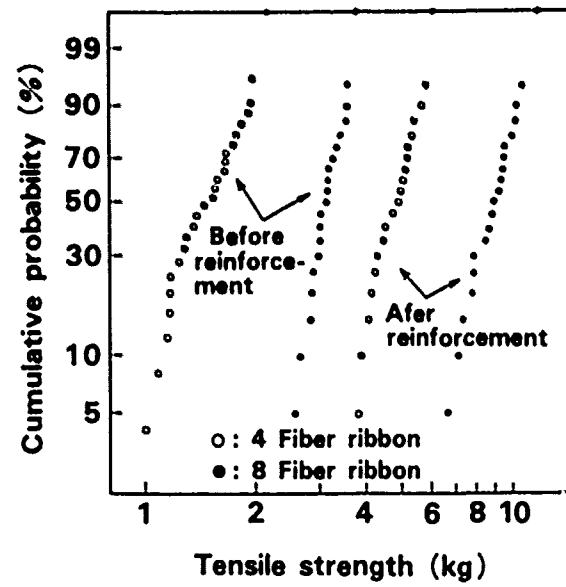

Figure 11. Tensile strength of reinforced parts.

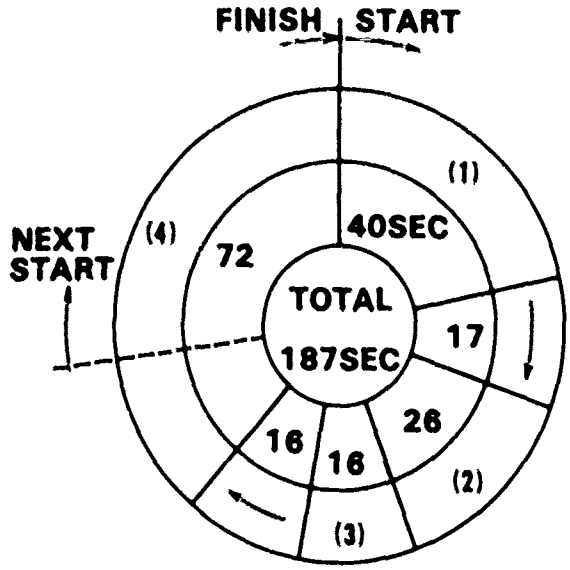

(1) FIBER END PREPARATION
(2) ALIGNMENT AND INSPECTION
(3) SPLICING AND INSPECTION
(4) REINFORCEMENT

Figure 12. Processing time.

minutes because of the parallel operation of the splicing process and the reinforcement process. This is about 3 times faster than the speed attained by a conventional splicer.

5. FIELD TEST RESULTS

A high speed and fully automatic fusion splicer has been evaluated in comparison with a conventional splicer in the field. The field lines were constructed of 800 fiber cables composed of 8-fiber ribbons.

Figure 13 shows the splice loss distribution. The loss was measured by OTDR from two directions. The average loss was 0.09 dB. This value is almost the same as that of the conventional splicer and is found to be highly practical for use in the construction of subscriber lines. Figure 14 shows the splicing time distribution per ribbon. About 85 % of the ribbons were spliced within 5 minutes, and the average splicing time was about 5 minutes per ribbon. This includes the time needed to accomodate the spare length of fiber in the closure. This is twice as fast

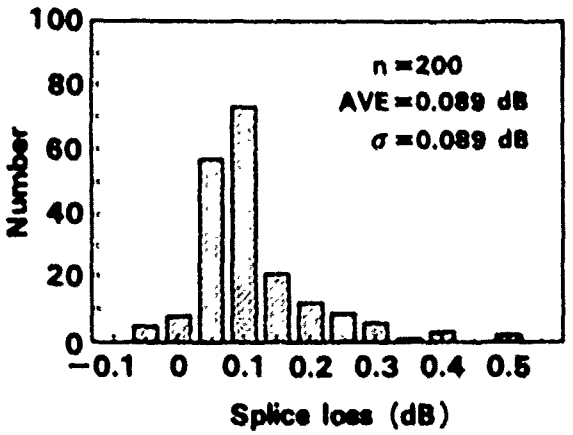

Figure 13. Splice loss histogram.

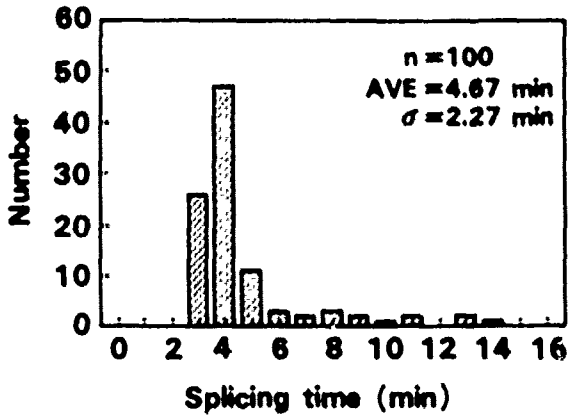

Figure 14. Splicing time histogram in the field.

as with a conventional splicer. About 85 % of the ribbons were spliced successfully with one trial and 99 % were spliced within three trials. These results are satisfactory for practical use in the field.

6. CONCLUSION

We have developed a high speed and fully automatic mass-fusion splicer for single-mode optical fiber ribbon. The following results have been obtained with this new splicer.

(1) In our laboratory, the average splice losses were 0.07 dB and 0.03 dB for 4-fiber ribbon and 8-fiber ribbon, respectively. These results are the same as those using a conventional fusion splicer.

(2) In the field, an average splice loss of 0.09 dB was obtained for 8-fiber ribbon.

(3) A total operation time of about 3 min. and 5 min. were obtained in our laboratory and in the field, respectively.

From these results, the fully automatic fusion splicer is found to be highly satisfactory for practcal use.

ACKNOWLEDGMENT

The authors express their sincere appreciation to S. Takashima and T. Uenoya for their helpful discussions and suggestions. Thanks are also due to N. Hirano and N. kanda for their valuable discussion and assistances.

REFERENCES

(1) M.Kawase, T.Fuchigami, T.Haibara, S.Nagasawa and S.Takashima: "Loop-network configuration for subscriber loops and single-mode optical fiber ribbon cable technologies suitable for mid-span access", Proceedings of 37th I.W.C.S.,pp141-149,(1988).

(2) Y.Kato, A.Ishikura, T.Sano and S.Takashima: "Single-mode optical fiber ribbon splicer", Proceedings of 36th I.W.C.S.,pp.386-391,(1987).

(3) T.Onoda, H.Taya, T.Yamada and M.Yoshinuma: "Development of single-mode 4 fibers ribbon splicer with the accurate splice loss estimation function" Technical digest of IOOC'89, 21C2-4,(1989).

(4) T.Haibara, S.Nagasawa, M.Matsumoto and M.Kawase: "Single-mode multifiber technique for high-density high-count subscriber cables", Proceedings of I.W.C.S.,pp576-584,(1988).

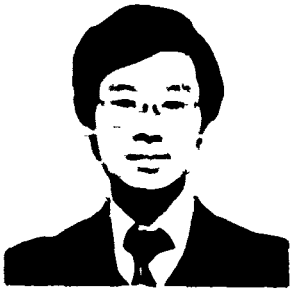

Michito Matsumoto

Network Systems
Development Center,
NTT
Tokai, Ibaraki-ken,
319-11,JAPAN

Michito Matsumoto is an Executive Engineer, Telecommunications cable Systems & Outside Plant Project Group, in the Network Syatems Development Center of NTT. He recieved his B.E. degree in electrical engineering from Kyushu Institute of Technology. He recieved M.E. and Ph.D. degrees in electrical engineering from Kyushu University in 1977 and 1987,respectively.

He joined NTT in 1977 and has been engaged in development of optical fiber splice technologies. Dr. Matsumoto is a member of IEICE of Japan.

Tadashi HAIBARA

Neteork Systems
Development Center,
NTT
Tokai,Ibaraki,
319-11, JAPAN

Tadashi Haibara is a senior Engineer, in the Network Systems Development Center of NTT. He recieved his B.E. and M.E. degrees in precision engineering from Hokkaido University in 1979 and 1981, respectively.

He joined NTT in 1981 and has been engaged in the development of optical fiber splicing equipment. He is a member of IEICE of Japan, and received the 1987 Young Engineer Award from IEICE of Japan.

Masaaki KAWASE

Transmission Systems
Laboratories,
NTT
Tokai, Ibaraki,
319-11, JAPAN

Masaaki Kawase is a Senior Research Engineer, Supervisor, Transmission Systems Laboratories of NTT. He recieved his B.E. and M.E. degrees in electrical engineering from Hokkaido University in 1970 and 1972, respectively.

He joined NTT in 1972. He has been engaged in research and development of optical transmission lines. He is a member of IEICE of Japan.

HIGH FIBER COUNT CABLE FOR SUBSCRIBER LOOP APPLICATIONS

Susan C. Grant
Werner Bernard

Siecor Corporation
489 Siecor Park
Hickory NC 28603

ABSTRACT

A family of high fiber count cables has been developed for use in the subscriber loop network. High fiber count cables are needed in single and double star topologies from the remote terminal to the service area interface. At the service area interface the high fiber count cable is branched to lower fiber count cables.

These high fiber count cables are unitized Mini-Bundle® cable designs with easy fiber identification for the large number of fibers involved. Loose tubes are stranded into sixty fiber cable cores with the cores then stranded together to make a unitized Mini-Bundle cable. The separate cable cores are distinguished by colored binders.

The buffer tubes in these doubly-stranded cores are in a double helix configuration. Upon examining the geometry of the double helix it was found that the bend radius changes along the path of the double helix. The laylengths of the buffer tubes in the core and the laylength of the cores in the cable must be chosen carefully such that the fibers have an acceptable bend radius over the length of the cable. The fiber bend radius is important for attenuation concerns as well as fiber fatigue considerations. This paper will discuss the equations derived for the double helix solution and important parameters to consider when designing a cable of this type.

For non-armored, all dielectric cables of 300 to 420 fibers, the cable diameters range from 28 mm to 31 mm.

These cables have excellent temperature performance with less than 0.2 dB/km attenuation change through the temperature range -40 to +70°C. The cables also exhibit excellent mechanical performance.

INTRODUCTION

Data rates continue to increase in order to meet the growing information needs of the subscriber. Bringing fiber optic technology to the subscriber will accommodate this increasing need for higher data capacity. Several field trials to bring fiber to the subscriber are already underway.

A family of high fiber count cables has been developed for use in the subscriber loop network. High fiber count cables will be needed in both single and double star topologies. The single star topology will require cables up to 400 fibers while the double star topology will require cables containing as many as 600 fibers. In the star topologies high fiber count cables are branched to lower fiber count cables as the network approaches the subscriber premise.

The loose tube approach was taken for the high fiber count cable designs since loose tube designs are proven performers in outside plant constructions.

CABLE DESIGN

The basic unit of the cable consists of five tubes containing twelve fibers each stranded around a dielectric central member. These stranded cores are used as building blocks for the overall cable structure. The sixty fiber units are distinguished from each other by different binder colors. Figure 1 shows a cross-section of the sixty fiber unit.

These sixty fiber units are combined into high fiber count cable cores. The units can be stranded around an overcoated central member or another sixty fiber unit to complete the core assembly.

The core is flooded with a water blocking compound in order to meet water penetration requirements which are usually specified for outdoor cables. High strength aramid yarns are applied over the cable core for tensile strength in the cable. The cable is completed with an outer jacket of polyethylene. Figure 2 shows cross-sections of two high fiber count cables.

These designs can be expanded for applications requiring more than 420 fibers by combining more sixty fiber units in a similar manner as described here.

There are two stranding passes, first stranding the buffer tubes into sixty fiber units then stranding sixty fiber units into the high fiber count cable core. The two stranding passes cause the buffer tube (and therefore the fibers in the buffer tube) to assume the configuration of a double helix. The double helix configuration of the fibers led to an investigation of the bend radius of the double helix. This investigation was based on work by Stein [1] who developed similar studies for wire ropes. The equations describing the double helix are:

$\vec{r}(0)$ is the vector describing the path of the double helix:

$$\vec{r}(0) = x(0)\,\vec{i} + y(0)\,\vec{j} + z(0)\,\vec{k} \qquad (1)$$

$$x(0) = (R_s + R_v \cos(\phi))\cos(0) + R_v \sin(\phi)\cos(\beta)\sin(0) \qquad (1a)$$

$$y(0) = (R_s + R_v \cos(\phi))\sin(0) - R_v \sin(\phi)\cos(\beta)\cos(0) \qquad (1b)$$

$$z(0) = R_s\, 0 \cot(\beta) + R_v \sin(\beta)\sin(\phi) \qquad (1c)$$

Where: R_s = radius of subunit center line measured from axis of cable

R_v = radius of buffer tube center line measured from subunit center line

$\phi = a0 + \phi_0$

$$a = -\frac{R_s \tan(\delta)}{R_v \sin(\beta)}$$

δ = layangle of the buffer tubes = $\tan^{-1}\left(\frac{2\pi R_v}{L_v}\right)$

β = layangle of the subunits in the cable = $\tan^{-1}\left(\frac{2\pi R_s}{L_s}\right)$

L_v = laylength of buffer tubes in subunit

L_s = Laylength of subunits in cable

ϕ_0 = dummy variable

0 = cylindrical coordinate

As mentioned before these equations were reduced by the method described by Stein [1] to determine the radius of curvature (ie the bend radius) along the path described by the double helix equations. The parameters which affect the radius of curvature (R) are: The pitch radius of the sixty fiber units (Rs), the pitch radius of the tubes (Rw), the laylength of the tubes in the sixty fiber unit (Lw), and the laylength of the sixty fiber units in the core (Ls). (See figure 3.) The pitch radii (Rs, Rw) are predetermined by the cable cross-section. An acceptable minimum fiber bend radius was designed into the cable by carefully choosing the laylength of the tubes and the laylength of the sixty fiber units

The radius of curvature along the double helix varies in a sinusoidal pattern. As can be seen in figure 4 these variations are very large. Figure 4 also demonstrates how dramatically one can affect the radius of curvature by changing the laylength of the sixty fiber units (Rs).

The relative direction of the two stranding lays also affects the radius of curvature. When two lays are in the same direction the radius of curvature tends to be lower than when the lays are in opposite directions. If either stranding pass is reverse stranded the lays will be in the same direction in some sections of the cable and in opposite directions in the rest of the cable. Figure 5 shows the difference in radius of curvature for equal and opposite lays in the same cable. Note that the curves in figure 4 represent a case where the tubes and sixty fiber units are stranded in opposite directions.

In most cases the laylength of the sixty fiber units will be larger than the laylength of the buffer tubes and the minimum fiber bend radius can be found at $\theta = 0$ deg. The curves in figures 4 and 5 show that the minimum R occurs at $\theta = 0$ deg for these two cases. The design equations can be reduced to the following at $\theta = 0$ so the cables can be designed around the minimum fiber bend radius present in the cable. This simplification assumes the worst case of the stranding lays being in the same direction.

$$R(0) = \frac{\left[R_v + R_s\left(1 + \frac{\tan(\delta)}{\tan(\beta)}\right)\right]^2 + [R_s(\cot(\beta) - \tan(\delta))]^2}{\left[R_v + \frac{\tan^2(\delta) R_s^2}{\sin^2(\beta) R_v} + R_s\left(2\frac{\tan(\delta)}{\tan(\beta)} + 1\right)\right]}$$

The cables were designed with the above equation to insure the minimum bend radius of the fibers remained above a value to insure good cable attenuation and acceptable long term fiber stress.

CABLE TESING

Since specifications do not exist at this time for fiber optic distribution cable the cables were tested per Bellcore TR-TSY-20, Generic Requirements for Optical Fibers and Optical Fiber Cable.[2] The cables tested contained single mode fiber Mechanical and environmental performance were quantified for this type of cable design.

Mechanical requirements and test results are summarized in Table 1. Because of the large diameters of the cables some of the mass tables had to be extrapolated to arrive at the correct test mass for the cable diameter. Each mechanical test was performed several times on different cable samples while several fibers were monitored for attenuation change. All samples passed the mechanical requirements in Bellcore TR-20. The results summarized in the tables are averages for each test The cables were temperature cycled and heat aged per Bellcore TR-20. Typical temperature cycling results are shown in figure 6. Each cable tested had 60 fibers monitored for attenuation change through the temperature cycle and heat age test. The maximum attenuation increase was less than 0.2 dB/km at 1300 nm and at 1550 nm which meets the requirements in Bellcore TR-20. There were no irreversible attenuation changes during the environmental tests.

CONCLUSION

A high fiber count cable for subscriber loop applications was developed successfully. The cables are unitized Mini-Bundle design with easy fiber identification. Sixty fiber units are stranded together to make a unitized Mini-Bundle cable.

Because of the cable design the fibers are placed into a double helix configuration. The bend radius along the path of the double helix changes and the minimum bend radius of the fiber must be considered for attenuation and fiber fatigue concerns

The cables easily met the requirements for mechanical and temperature performance specified in Bellcore TR-20.

ACKNOWLEGMENTS

We would like to thank Bernd Zimmermann and Marty Light for their work with the mathematical derivations of the radius of curvature of the double helix

REFERENCES

1. R. A. Stein, C. W. Bert, "Radius of Curvature of a Double Helix", Journal of Engineering for Industry, August, 1962, pp. 394-395.
2. Bell Communications Research Inc., "Generic Requirements for Optical Fibers and Optical Fiber Cable", Technical Reference, TR-TSY-000020, August 1988.

TABLE 1

MECHANICAL TEST RESULTS

TEST	REQUIREMENT[1]	RESULTS
Impact	25impacts avg increase < 0 10 dB	25 impacts avg < 0.01 dB
Flex	25 cycles avg increase < 0 10 dB	25 cycles avg < 0.01 dB
Compression	220 N/cm avg increase < 0 10 dB	220 N/cm max 0.03 dB
Tensile	rated load avg increase < 0 10 dB	avg < 0.04 dB
Cold Bend	-30°C avg increase < 0.20 dB	avg < 0.01 dB
Hot Bend	+60°C avg increase < 0.20 dB	avg < 0.01 dB
Water Penetration	1 hour 1 m cable	pass no water pen

[1] Test requirements per Bellcore TR-20

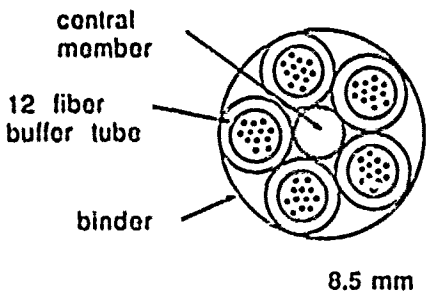

8.5 mm OD

Figure 1: Cross-Section of a Sixty Fiber Unit

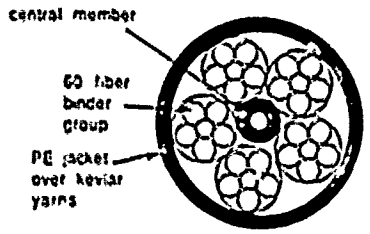

300 fiber design - 28 mm OD

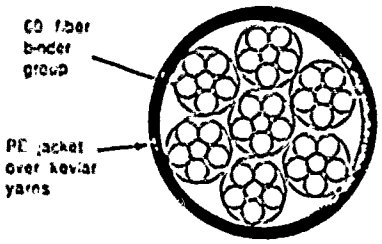

420 fiber design - 31 mm OD

Figure 2: Cross-Sections of the High Fiber Count Cables

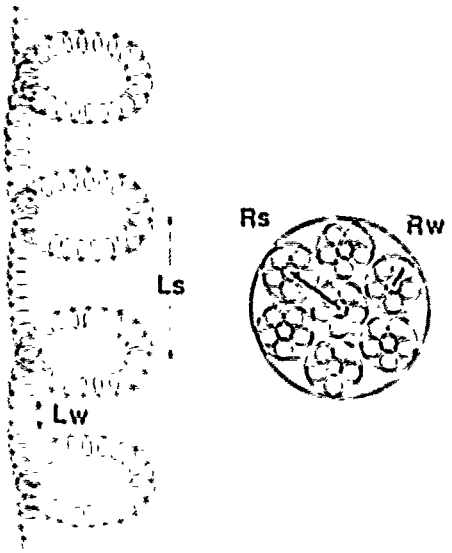

Figure 3: Cable Parameters

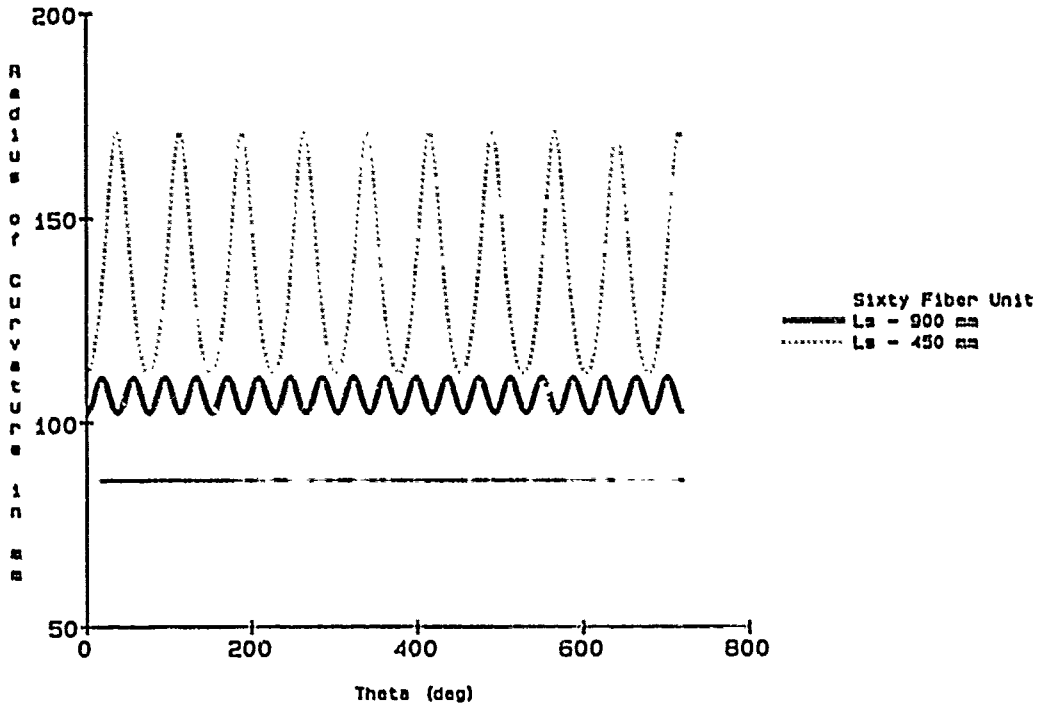

Figure 4: Change in Radius of Curvature with Change in Laylength of a Sixty Fiber Unit (The tubes and subunits are stranded in opposite directions.)

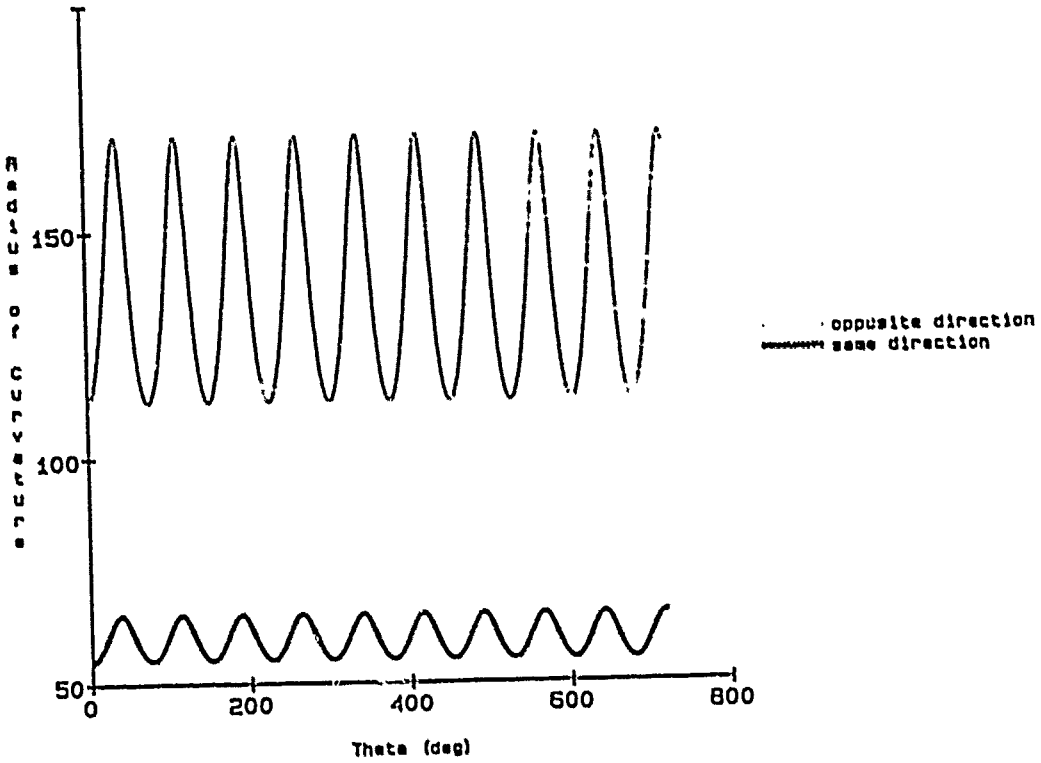

Figure 5: Difference in Radius of Curvature for Equal and Opposite Lays in the Same Cable

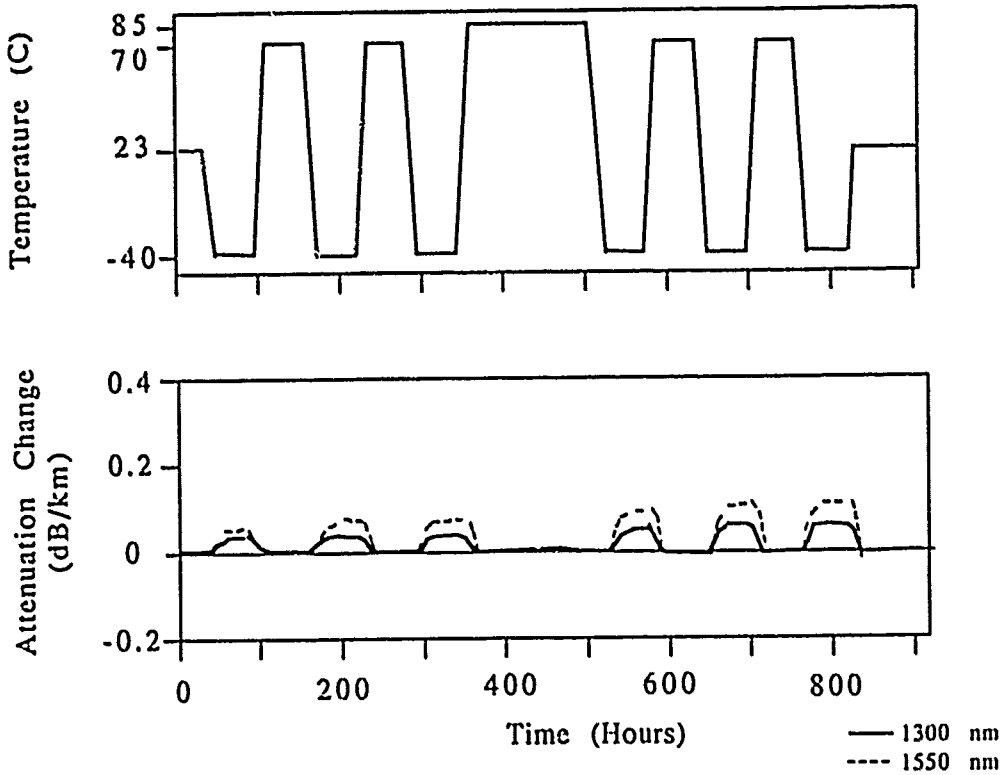

Figure 6: Temperature Cycling Results

Susan C. Grant

Siecor Corporation
489 Siecor Park
Hickory, NC 28603

Susan C. Grant graduated from Virginia Polytechnic Institute and State University in December of 1984 with a B.S. in Electrical Engineering. She then joined Siecor Corporation as a Product Development Engineer in R,D&E. Ms. Grant is currently employed as the Product Evaluation Supervisor in the Siecor Specialty Cable Plant.

Werner Bernard

Siecor Corporation
489 Siecor Park
Hickory, NC 28603

Werner Bernard was born in Solingen/West Germany in 1955. He received his Master's Degree in Mechanical Engineering from the University of Aachen in 1983. After graduation he was employed at Siemens AG in the Research, Development and Engineering department for copper cables. In 1988 he joined Siecor Corporation where he works as a process engineer in the Research, Development and Engineering department for fiber-optic cables.

ONE-THOUSAND-FIBER OPTICAL CABLE COMPOSED OF EIGHT FIBER RIBBONS

H.Sawano Y.Kikuchi K.Kobayashi N.Okada N.Misono H.Suzuki N.Sato

Fujikura Ltd.

Abstract

A high fiber count and high densely packaged single-mode optical fiber cable with rapid fiber splicing and mid-span access capability is required to construct economical subscriber network.

To meet this requirement,a 1000-fiber cable has been developed.1) The cable is composed of 8-fiber ribbons and slotted rods.

The cable was subjected to several evaluation tests. It was verified that the cable has enough performance to be applied to commercial use.

1. Introduction

An optical fiber cable is going to spread very quickly to subscriber networks.2) And it is expected that subscribers are going to demand high speed and broadband services such as video service. A single-mode fiber cable can address this demand flexibly and economically because of its intrinsic broadbaed transmission characteristics.

Moreover,designing subscriber cable configuration for metropolitan area, the following consideration have to be taken into account to construct economical subscriber networks.

1) High fiber count
A thousand fiber count cable is necessary to service growing number of subscribers in near future.

2) Compact cable diameter
A lot of cables get into end office so that there is no enough room to get big sized cable into the office.
So cable diameter must be as small as possible to escape cable jam in the office.

3) Rapid fiber splicing capability
An optical fiber is required to have a rapid splicing capability to make cable installation time short, in another word,to make installation cost less expensive.

4) Mid-span access capability
A mid-span access capability is necessary for a subscriber cable to make an investment for subscriber networks low.

5) Compatible configuration with a conventional cable

Based upon above criteria,a single-mode fiber cable which can accommodate a 1000-fiber was developed.

The cable is composed of specially designed 8-fiber ribbons. The ribbon is easily divided into two 4-fiber ribbons by a newly designed dividing tool without interrupting the signal transmission of the other fibers in commercial service.

This ribbon configuration make it possible 8-fiber ribbon to be spliced with a conventional 4-fiber ribbon.

Five 8-fiber ribbons are tightly stacked in each of five slots grooved on a polyethylene rod to make a two hundred fibers unit. And five units are cabled to make a 1000-fiber cable with only 40mm cable diameter.

This paper describes the results of several evaluation tests on a 1000-fiber cable such as ribbon dividing test,mechanical tests,temperature cyclic test and field test.

Table 1. Requirements and approaches to subscriber network.

Requirement	Approach
1. High transmission performance.	Single-mode fiber
2. High fiber count and compact cable.	Fiber ribbon Slotted core cable
3. Rapid splicing capability.	Fiber ribbon Multi fiber connector Mass fusion splice
4. Mid-span access capability.	
5. Compatibility to conventional cable.	Dividable fiber ribbon

2. Cable structure

Fig.1(a) shows the structure of developed 1000-fiber cable. This cable is 40mm in diameter, 1.2kgf in weight and contains five 200-fiber units stranded on a central strength member. Every unit has five rectangular slots shaped helically on a polyethylene rod and five 8-fiber ribbons are tightly stacked in each slot.

Slot structure has two advantages. One is easiness to take out 8-fiber ribbon from the slot and the other is to suppress fiber jam during mid-span access.

The sketch of 8-fiber ribbon is illustrated in Fig.1(b). Used single-mode fiber is 9.5um in mode field diameter, 125um in fiber diameter and 250um in diameter of UV curable resin coating. All the fibers are colored for fiber identification. 8 fibers are aligned in parallel and covered with UV curable resin in 2.2mm in width and 0.4mm in thickness.

From the view point of fiber jointing, multi fiber ribbon is most profitable because this structure can be applied to both multi fiber connector and mass fiber fusion splicing.3),4)

Fiber count in a ribbon is important factor because it affects the cable jointing speed and cable diameter. With regards to jointing speed, a calculation have taught us that the efficient fiber count in a ribbon is from six to ten fibers.5) So, taking into account of the compatibility with a conventional 4-fiber in terms of fiber splicing, 8-fiber ribbon is dividable into two 4-fiber ribbons.

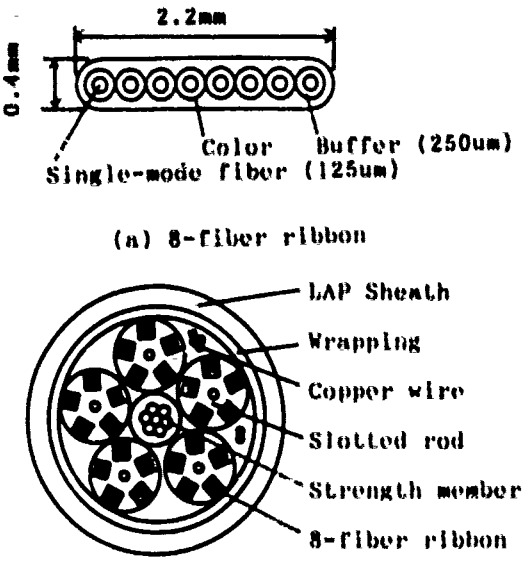

Fig.1 Structure of 1000-fiber cable.

Fig.2 Ribbon dividing tool.

Fig.3 Illustration of access form 8-fiber ribbon to 4-fiber ribbons.

3. Cable properties

3-1. 8-fiber ribbon

(1) Access performance

The main advantage of developed 8-fiber ribbon is to be divided into 4-fiber ribbons and mono fibers by means of simple tool to branch high fiber count cable to distribution lines in subscriber network. Fig.2 shows the dividing tool. An 8-fiber ribbon is set in and torn away into two 4-fiber ribbons at the center.

Fig.3 shows the connectorized 8-fiber ribbon and 4-fiber ribbons divided from a 8-fiber ribbon. Mass fusion splicing is also applied to newly produced 4-fiber ribbon.

To investigate the loss change of a live line during mid-span access, 8-fiber ribbons were subjected to the ribbon dividing test over hundred times. Added loss was so small as less than 0.5dB, this added loss does not disturb the signal transmission.

(2) Mechanical properties

To investigate the mechanical properties, 8-fiber ribbon was subjected to against lateral force test, twisting test and scrubbing test. Table 2 shows the results.

Neither added loss nor break was observed up to 25kgf/50mm of lateral force. Ten times per 100mm of twist with 300gf of tension caused no break in ribbon. Scrubbing with the radius of 5mm also gave no damage to ribbon.

Table 2. Mechanical properties of 8-fiber ribbon

Item	Result	Condition
Lateral force	No added loss	Up to 25kgf 50mm Ribbon
Twisting	No break	10 times Rotate 100mm 300gf Ribbon
Scrubbing	No break	R=5mm 300gf

Added loss due to temperature change also was measured. From -40C to 60C, no added loss was observed.

3-2. 1000-fiber cable

(1)Loss stability in manufacturing

Fig.4 shows the optical loss through manufacturing process. The average loss change and standard deviation change were 0.01dB/km and less than 0.01dB/km, respectively. Fig.5 shows the loss histogram of manufactured cables. Five cables were investigated and total measured fiber number and fiber length were five thousands and 3250km. The average loss and standard deviation were 0.35dB/km and 0.01dB/km, respectively. These results insure that this cable can be manufactured with excellent loss stability.

(2) Mechanical properties

This cable is designed as follows. An allowable tensile load and minimum bending radius of bending are 800kgf and 250mm under installation, and minimum radius of fixed bending is 240mm.

To investigate the mechanical properties under above conditions, crush, bending, tensile, squeezing, impact and torsion tests were performed. Results are shown in table 3. In every test, no added loss was observed.

(3) Temperature characteristics

Two types of temperature test were performed. One was cyclic test, the other was long term test.

To investigate the loss stability in short term temperature change, added loss due to temperature cycle from -40C to 60C per day was measured. Fig.6 shows the result. Added loss was so small as 0.02dB/km at-40C and 0.04dB/km at 60C.

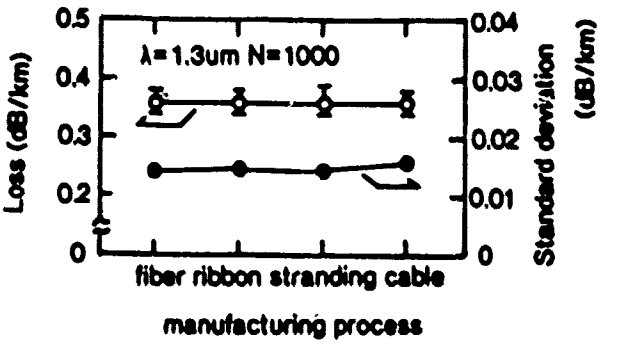

Fig.4 Loss stability of 1000-fiber cable in manufacturing process.

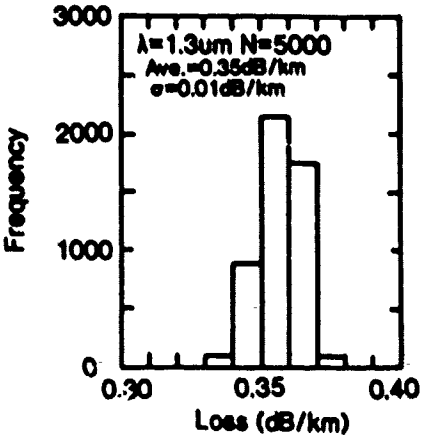

Fig.5 Loss histogram of manufactured 1000-fiber cable.

Table 3. Mechanical properties of developed 1000-fiber cable.

Item	Condition	Result
Crush	Up to 250kgf/50mm of lateral force	<0.01dB
Bending	R=400mm,180deg. 10 times	<0.01dB
Tensile	Up to 800kgf,l=100m	<0.01dB
Squeezing	R=600mm,T=800kgf l=100m	<0.01dB
Impact	1kgf,1m height	<0.01dB
Torsion	360deg./m	<0.01dB

A 1000-fiber cable had been exposed to 60C and -20C and loss was monitored for a month as long term loss stability test. Fig.7 shows the results. The optical loss degradation was scarcely observed.

These results shows that developed 1000-fiber cable has sufficient loss stability against actual temperature condition.

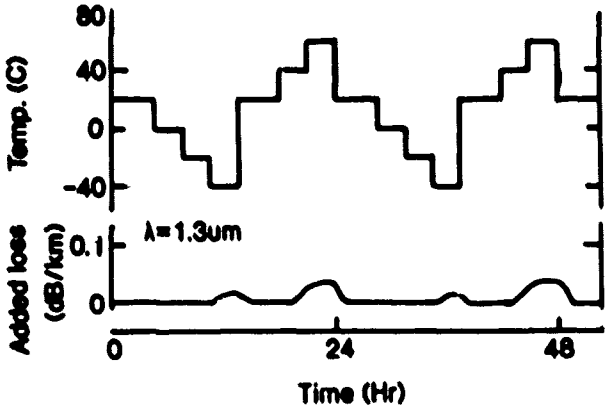

Fig.6 Added loss of 1000-fiber cable due to temperature change.

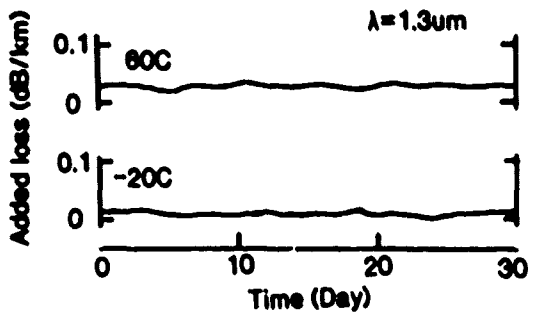

Fig.7 Loss stability 1000-fiber cable at high and low temperature.

4. Field test

(1) Installation

A preconnectorized 1000-fiber cable was installed in 300m long duct as shown in Fig.8. Test cable was placed by ordinary winch with 400kgf of maximum pulling load. Soon after the installation, damage on cable and loss of fibers were investigated. No harmful injury or deformation on cable was observed and average and maximum loss of

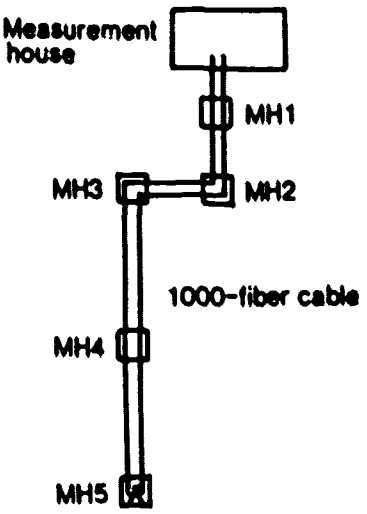

Fig.8 Aspect of field test.

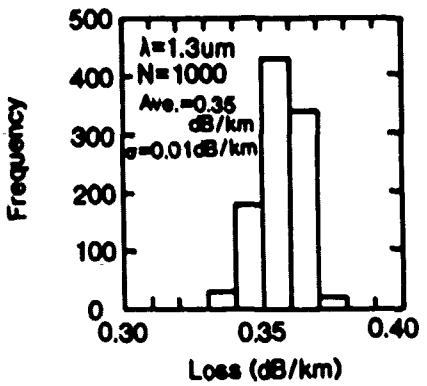

Fig.9 Loss histogram of installed 1000-fiber cable.

fibers were 0.35dB/km and 0.38dB/km as shown in Fig.9. This result is almost equal to factory data, so it can be concluded that developed 1000-fiber cable has sufficient strength to protect fibers from the force caused in installation.

(2) Long term reliability

Fig.10 shows the loss change for ten months. Monitored line was 7.2km long composed of 24 fibers. The loss change including the power change of measuring apparatus was within 0.2dB, this loss change is acceptable for practical transmission system.

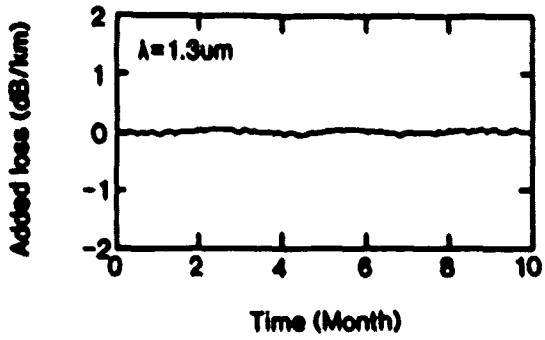

Fig.10 Loss stability of 10 months installed cable.

On the basis of above results, it can be concluded that the developed 1000-fiber cable has excellent reliability.

5. Conclusion

With the rapid spread of fiber optic technology to subscriber network, it has become necessary to take into account economical performance as well as transmission characteristics of the network.

To satisfy this requirement, a compact 1000-fiber cable using 8-fiber ribbons has been developed.

The results of ribbon dividing test, mechanical test, temperature test and a field test verified that the developed 1000-fiber cable for subscriber network has excellent performance to be used in actual field.

Acknowledgment

Authors express their sincere appreciation to Dr. Inada for his helpful discussions and suggestions.

References

1) M.Kawase, T.Fuchigami, T.Haibara, S.Nagasawa and S.Takashima, "Loop-network configuration for subscriber loops and single-mode optical fiber cable technologies suitable for mid-span Access", 37th IWCS (Reno, USA), 1988.
2) S.Hatano, Y.Katsuyama, T.Kokubun and K.Hogari, "Multi-hundred-fiber cable composed of optical fiber ribbons inserted tightly into slots", 35th IWCS (Reno, USA),1986.
3) Y.Kato, A.Ishikura, T.Sano and S.Takashima, "Single-mode optical fiber ribbon splicer", 36th IWCS (Washington, USA), 1987.
4) T.Haibara, S.Nagasawa, M.Matsumoto and M.Kawase, "Single-mode multifiber jointing techniques for high-density high-count subscriber cables", 37th IWCS (Reno, USA), 1988.
5) N.Kawasaki, T.Haibara, M.Shirai and M.Miyauchi, "Optimum number of single-mode fibers in ribbon", Trans. IEICE, J71-B, pp.77-80, 1988.

Hiroyuki Sawano

Fujikura Ltd.

1440 Mutsuzaki, Sakura, Chiba, 285, Japan

Mr. Sawano was born in 1955. He joined Fujikura Ltd. after his graduation from Hokkaido University with the M.S. degree in 1983 and has been engaged in research and development of optical cables. He is now an engineer of optical cable section and a member of IEICE of Japan.

Yoshio Kikuchi

Fujikura Ltd.

1440 Mutsuzaki, Sakura, Chiba, 285, Japan

Mr. Kikuchi was born in 1955. He joined Fujikura Ltd. after his graduation from Tohoku University with the M.E. degree in 1980 and has been engaged in research and development of optical fibers and cables. He is now a member of technical staffs of optical cable section and a member of IEICE of Japan.

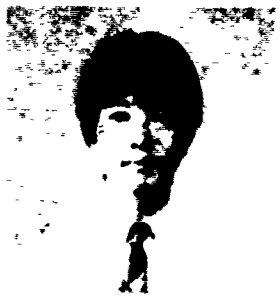

Kazunaga Kobayashi

Fujikura Ltd.

1440 Mutsuzaki,
Sakura, Chiba, 285,
Japan

Mr. Kobayashi was born in 1961. He joined Fujikura Ltd. after his graduation from Gunma University with the M.E. degree in 1985 and has been engaged in research and development of optical cables. He is now an engineer of optical cable section and a member of IEICE of Japan.

Hideo Suzuki

Fujikura Ltd.

1440 Mutsuzaki,
Sakura, Chiba, 285,
Japan

Mr. Suzuki was born in 1948. He joined Fujikura Ltd. after his graduation from Gunma University with the B.E. degree in 1971 and has been engaged in materials, polymer processing and development of optical cables. He is now the chief of optical cable section and a member of IEICE of Japan.

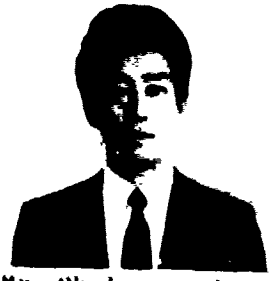

Naoki Okada

Fujikura Ltd.

1440 Mutsuzaki,
Sakura, Chiba, 285,
Japan

Mr. Okada was born in 1964. He joined Fujikura Ltd. after his graduation from Chiba University with the B.E. degree in 1986 and has been engaged in research and development of optical cables. He is now an engineer of optical cable section and a member of IEICE of Japan.

Nobuyasu Sato

Fujikura Ltd.

1440 Mutsuzaki,
Sakura, Chiba, 285,
Japan

Mr. Sato was born in 1943. He joined Fujikura Ltd. after his graduation from Tohoku University with the B.E. degree in 1966 and has engaged in research and development of transmission cable. He is now the general manager of transmission cable research division and a member of IEICE of Japan.

Nobuyuki Misono

Fujikura Ltd.

1440 Mutsuzaki,
Sakura, Chiba, 285,
Japan

Mr. Misono was born in 1949. He joined Fujikura Ltd. after his graduation from Chiba University with the B.E. degree in 1973 and has been engaged in research and development of transmission cables and optical cables. He is now the assistant chief of optical cable section and a member of IEICE of Japan.

A COMPOSITE OPTICAL AND METALLIC SUBSCRIBER CONNECTION CABLE FOR OVERHEAD INSTALLATION

S. T. Spedding, C. S. Pegge, W. W. Thomas, D. J. Walker, G. Thambythurai

BICC Cables Limited, Helsby, England

SUMMARY:

A subscriber connection cable was developed to address the emerging requirement for low cost optical cable to replace existing overhead subscriber connections. The new cable combines the ability to carry narrow band on copper, from existing telephony services or from street sited demultiplexers, with an upgrade path to all-optical broadband services.

The cable described offers a solution which negates the cost of returning to site to upgrade the network to adapt an installation to carry broadband services. Cable strain is minimized by providing strength in as much of the cable cross-section as possible, but this leads to some interesting side effects. Theoretical cable performance is predicted from models of aerial cable and its environment.

INTRODUCTION:

The telecommunications industry in the UK is building towards all optical broadband services. The advancement of digital communications technology means that technically these can now be supplied on the same transmission path as telephony.

To trial the supply of broadband services, customers in a selected pilot scheme in the United Kingdom will be connected to an optical local loop distribution network. The final connection to the customer premises in this scheme (the last mile drop) will be predominantly of the overhead type. Consideration was given to installing an additional cable to the premises because the existing metallic network must be maintained intact. However there are two objections to this plan; aesthetically it is unacceptable to connect two cables to every household and there is a limit to the number of cable drops existing poles can support.

Thus a need arises for a composite overhead drop cable which can maintain the final connection in the existing metallic network and support the future optical network.

ENVIRONMENTAL CONSIDERATIONS:

The environmental conditions which have to be considered in the design of this product are a temperature range for the optical performance of -20°C to +80°C, wind speeds of up to 128 km/hr, single unsupported span lengths of 68m and a radial thickness of ice of 5mm. A small diameter is desirable such that the cable can offer a minimum environmental impact.

These environmental considerations had to be catered for within the following boundary conditions:

-A maximum diameter for the cable of 10mm
-2 fibres and 2 copper pairs are to be provided
-All elements to be easily separated both from the structure and from each other
-A sag at installation of 1% of span length must be achieved.

The design of the cable has to satisfy a number of conflicting requirements. Fibre strain at maximum operational load must be limited in order to maximize the service life of the product. Installation tensions must be achievable by single man operation. The cable construction/geometry should allow easy break-out of the copper and fibre elements. Consideration must be given to enable the use of standard metallic overhead drop cable terminating devices and cable dispensers.

If fibre strain must be limited to a certain level, and the small diameter criterion rules out all but the smallest cables, cable strain must also be limited to a similar level to that allowable for the fibre. Necessarily this results in a high ultimate breaking strain for the cable, and if the cable then becomes tangled with, for example, a truck, then at all costs the supporting pole must survive!

Our solution to this dilemma was to part the strength member, though not the optical lobe at the point of suspension, and suspend the cable through a mechanical fuse as shown in figure 1.

CABLE DESIGN:

To meet the criteria set out above, several potential designs, including multiple lobe cables, were considered and ranked according to effective cable diameter, cable weight, cable strain at maximum operating tension, and required installation tension for a sag of 1% of span.

We chose a two lobe cable incorporating a composite steel/copper catenary lobe as figure 2. This design offered the prospect of employing standard installation practices and grips. Separate joint boxes are required for the copper and optical elements of the cable, the metallic distribution point (DP) will be situated at the top of the pole and the optical DP will be housed in a footway box at ground level, thus the copper wires in the form of the catenary lobe can be connected to the metallic DP without any need to break them out from the protection of their sheath.

To align with the future development of test devices using local light injection or detection, we chose loose tube protection for 250 µm primary coated fibres.

The resulting design parameters were:

-A major axis of 9.75mm
-A minor axis of 6mm
-Cable weight 63kg/km
-Installation tension 500N
-Maximum operational tension 2000N
-Maximum cable strain of 0.4%.

The cable geometry selected was then optimized to satisfy the environmental and mechanical requirements put on it. It became clear that with the boundary conditions as they were, we could not limit the fibre strain to the very low levels in current practice at any level of cost remotely commensurate with the eventual market. Convention suggests that the fibres must be proof tested to at least three times the maximum service strain, which we had set at 0.4%. BICC offers two versions of the cable, one with fatigue resistant fibres and the other with standard fibres proof tested to at least 1.25%.

THEORETICAL ANALYSIS:

We used a computer simulation for aerial cables on the environmental conditions that the cable will have to meet and obtained an output of tensions, vertical sags, horizontal blow-off and cable strain, shown in figures 3 and 4.

The equations relating cable tension, sag and strain have been formulated into a computer programme[1]. The programme solves a cubic equation relating cable stress, total cable loading and environmental parameters in order to give values of tension and sag and thus cable strain under a given set of conditions. The curve which represents the profile taken up by an aerial cable of constant mass per unit length is a hyperbola. However the calculations involved by using this profile are prohibitively complex. A good approximation for these sizes of cable and lengths of span is a parabolic profile. The following change of state equation applies;

$$f_2^3 + \left[\frac{w_1^2 L^2 E}{24 f_1^2 A^2} - f_1 - (t_1 - t_2)C_T E\right] f_2^2 - \frac{w_2^2 L^2 E}{24A^2} = 0$$

Where;

w_1	Total cable loading state 1
w_2	Total cable loading state 2
f_1	Tensile stress state 1
f_2	Tensile stress state 2
t_1	Temperature state 1
t_2	Temperature state 2
L	Cable length
A	Cross-sectional area of steel
C_T	Co-efficient of thermal expansion of steel
E	Young's modulus of steel

Solving for the stress on the cable at state two (f_2) leads to a predicted tension, sag and strain for the cable under the new environmental conditions.

We catered for non-circular cross-section cables by using a second computer model to calculate effective cable diameters and ice thicknesses. It is essential that the value of effective ice thickness calculated when applied over the effective cable diameter represents the same mass of ice as over the actual cable form.

MANUFACTURING CONSIDERATIONS:

The manufacture of this cable entailed addressing two problems, the shrink-back of the polyethylene over the optical fibre tube and adhesion of the insulation to the catenary. Tooling was considered which would generate a pressure set up over the catenary lobe and a tubing set up over the optical fibre unit. During early manufacturing trials this hybrid tooling set up proved unnecessary and a conventional figure '8' style set up with gradual cooling in water proved acceptable.

EXPERIMENTAL RESULTS:

Type approval of this product will consist of qualification of the cable against the design requirements. Some tests on prototype versions of the cable have been carried out at the time of writing.

Tensile testing of the cable in March 1989 resulted in a cable strain measurement of 0.36% at a load of 1500 Newtons (the design load at that phase of the project). The corresponding fibre strain at that load was 0.19% (see figure 5), the difference between the two strain measurements is attributed partly to the slack fibre installed in the tube during manufacture but mainly to the action of extra fibre being pulled into the tube during the test on the necessarily short sample. At the same time the break load of the cable was measured at 5,750 Newtons.

Having recognised the consequence of fibre uptake by the cable under the effect of strain, further testing was carried out to compare suitable methods of fibre locking, thus ensuring that fibre strain and cable strain are essentially equal.

Further cable strain measurements were performed on a version of the cable designed for higher loads. A predicted cable strain of 0.28% at 1600 Newtons correlates well to a measured value of 0.23%.

CONCLUSIONS:

For some time, the world has expected optical fibre technology to advance forward into the home. With this, most analysts agree, will come a step volume change and a quickening of the pace of development of both infra structure and services. We offer the upgrade path; by providing a cable capable of supporting existing services, whilst containing the optical fibre ready for future deployment without double installation costs, the scene can be set for the final push forward of the all optical telecommunications path.

A product now exists with which BICC can supply those who wish to take advantage of the emerging technology of broadband optical communication but do not wish to take the full step of changing directly to an all optical link to the subscriber premises. This cable represents a solution in that transition stage.

An additional piece of work has been carried out on an all optical aerial subscriber feed cable which will be the ultimate version of this category of cable.

REFERENCES:

1.) Bond R. W., "O.C.S. Design Manual", Balfour Beatty PLC.

2.) Oestreich U., Zeidler G., Bark P. R.,Lawrence D. O., "Fibre Optic Cable For Aerial Application", IWCS Proc. 1980.

3.) Armitt J., Cojan M., Manuzio C., Nicolini P., "Calculation Of Wind Loading In Components Of Overhead Lines", Proc. IEE, 122(11), Nov. 1975.

4.) Bradbury J., Kuska G. F., Tarr D. J., "Sag And Tension Calculations In Mountainous Terrain", IEE Conf. "Progress In Cables And Overhead Lines For 220 kV And Above", Sept. 1979.

ACKNOWLEDGEMENTS:

1.) British Telecom Research Laboratories, Martlesham Heath, IPSWICH.

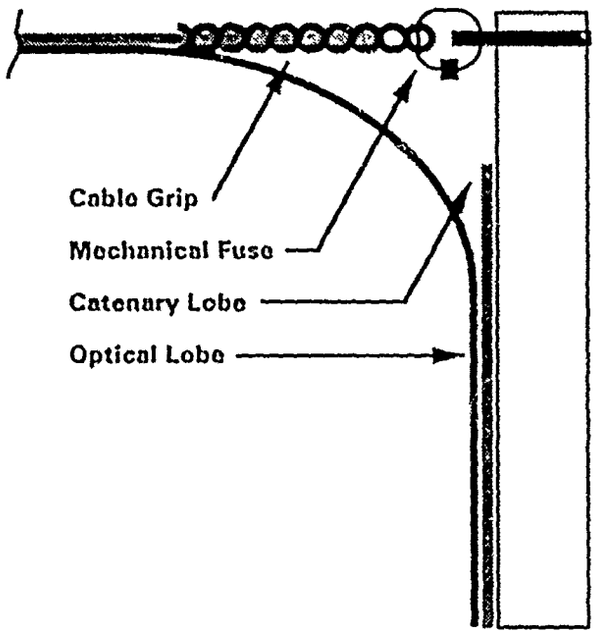

Figure 1: Cable Termination Scheme

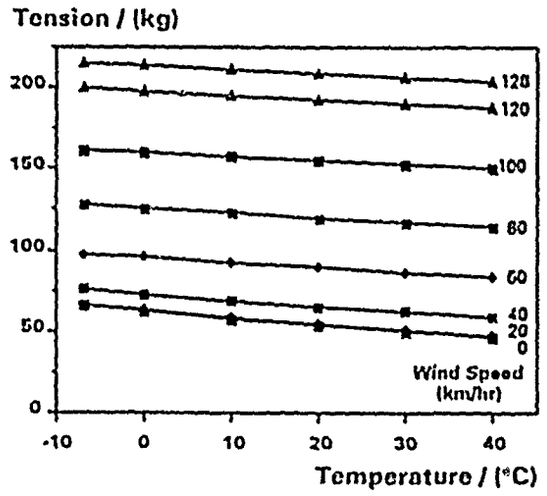

Figure 3: Predicted Tension Vs. Temperature & Wind Speed

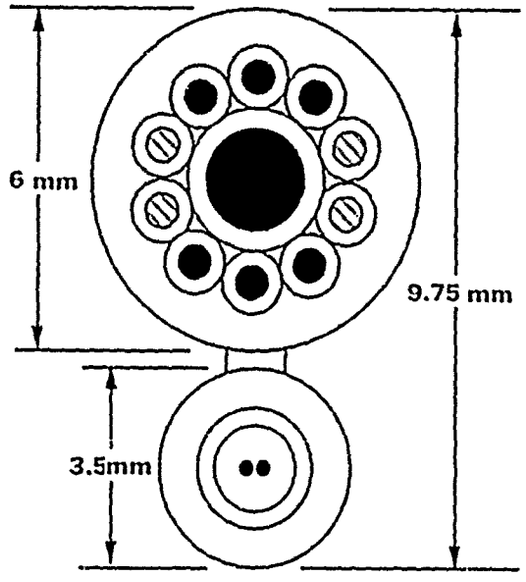

Figure 2: 2 Lobe Cable Design

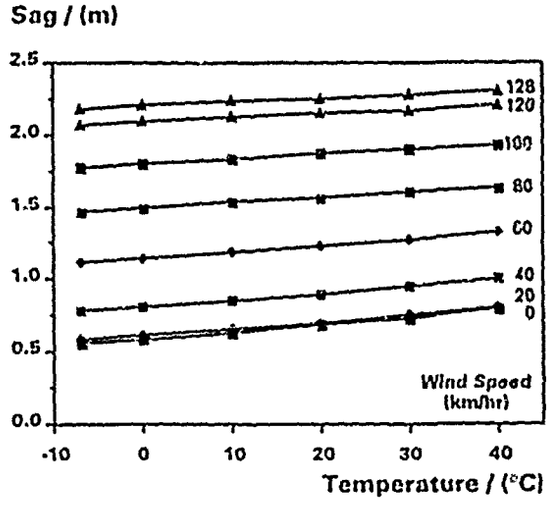

Figure 4: Predicted Sag Vs. Temperature & Wind Speed

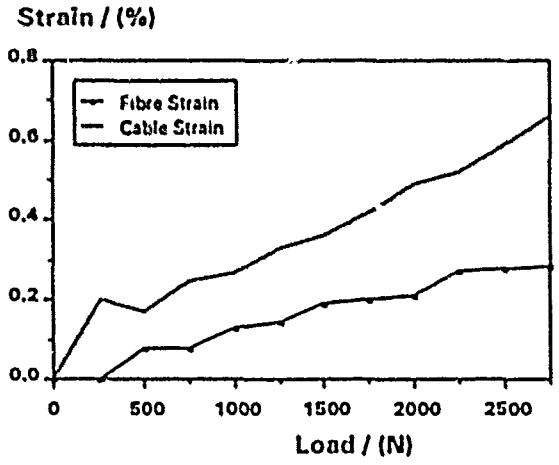

Figure 5: Results Of Cable Tensile Testing

DEVELOPMENT OF OPTICAL AND POWER FEEDER COMPOSITE CABLES AND THEIR CONNECTORS FOR HOME AUTOMATIONS

K. Ishikawa*, S. Ohira*, K. Nilkura**, H. Igarashi**, H. Horima**,
K. Ogata*** and A. Kurosawa***

*Tohoku Electric Power Co., Inc. 7-2-1, Nakayama, Aoba-ku, Sendai 981 Japan
**Sumitomo Electric Industries, Ltd. 1, Taya-cho, Sakae-ku, Yokohama 244, Japan
***Kitanihon Electric Cable Co., Ltd. 1-2-1, Koriyama, Wakabayashi-ku, Sendai 982, Japan

Abstract

With the evolution of an information-oriented society, study and evaluation of an optical transmission system which can be introduced to general households has been undertaken. Under such circumstances, the authors have designed optical/electric power feeder cable for outdoor and indoor use, integrating optical line for information transmission with power feeder cable in order to attain the goal of home automation (HA), keeping in mind the need for aesthetics, efficient utilization of space, and economy. A method of indoor installation has also been studied.

We have also developed an optical/electric power feeder composite socket, which permits the use of existing commercial power outlets as outlets for optical/electric power feeder cable in each room. An optical cord reel has also been developed to facilitate flexible connection of equipment with the socket.

This composite optical/electric power feeder cable, socket and optical cord reel have been installed in the "totally electrified model house" constructed in the compound of the Applied Technology Research and Development Center of Tohoku Electric Power Co., Inc., and the excellent workability, adaptability, technical characteristics, maneuverability and aesthetic features of the system and its components have been firmed.

1. Introduction

With the evolution of an information-oriented society, attempts are being made to introduce an optical transmission system to general households in order to cope with the strong demands for intelligent housing and home automation (HA). Various optical cable lines for subscribers have been developed to meet the diversified and high-grade demands being made on communication systems. Thus far, however, design of power distribution systems for operation of terminal equipment and devices has been limited to individual purposes.

Under such circumstances, problems may arise with the introduction of optical transmission to general households because of limited space and the need to consider demands for aesthetics and economy. The authors have designed a composite system for optical/electric power transmission which integrates optical lines with electric power feeder cable in order to meet the requirements for HA equipment in intelligent houses. The methods of installation and wiring of this system have also been studied. Also, a composite optical/electric power feeder socket has been developed, incorporating the push-pull optical connecter.

The socket can be used with the commercial power feeder outlet in individual rooms as the outlet for the composite optical/electric power feeder cable.

In a private house, HA equipment and devices are often moved from one place to another. If the conventional optical cord is used for the connection between the socket and the HA equipment, the range of mobility of the equipment is limited by the length of such cord. If a longer cord is used, problems may arise due to the excess length of cord when the equipment is moved. To solve this problem, an optical cord reel has been developed, in which optical cord with a connector at each end is wound on a reel, thus meeting the need for mobility as well as aesthetics.

The new system and product have been adopted in the "totally electrified model house" built in the compound of the Applied Technology Research and Development Center of Tohoku Electric Power Co., Inc. As a result, the practical features and the usefulness of the system and the product have been demonstrated.

In this paper, we will describe the unique features of this system and its components.

2. Evaluation of the composite optical/electric power feeder cable

This cable combining optical fiber with electric power feeder cable has excellent labor-saving features. Above all, when optical cable is introduced to the houses of subscribers, the combination of electric power feeder cable (for operation of optical transmission equipment) and optical fiber will result in an aesthetic appearance and efficient utilization of space.

We evaluated the features of the composite cable system, which combines optical fiber with power

feeder cable leading inside (cable for outdoor use).

2.1 Evaluation of the composite optical/electric power feeder cable for outdoor use

For the development of the compositeoptical/electric power feeder cable for outdoor use, evaluation was made according to the following design criteria:

(1) In order to reduce the number of connection points 600 V CE is adopted for the application regardless of whether it is outdoor weather proof polyvinyl chloride insulated wires or polyvinyl chloride insulated drop service wires lead-in line.

(2) For efficiency and general-purpose application, conventional anchoring and connecting procedures must be applicable and optical cable and power feeder cable must be easily separable.

(3) The number of optical fibers and the size of power feeder cable must be freely selectable.

With full consideration given to the above conditions, a pre-hanger (polyethylene connection piece) was adopted, which had exhibited a good record in the past in use with optical cable in power distribution systems and with regard to separability, and resistance to factors of weather such as wind and snow. As shown in Fig. 1, suspension wire, power feeder cable and optical cable are arranged in paralled and integrated by this polyethylene connection piecc with fixed spacing.

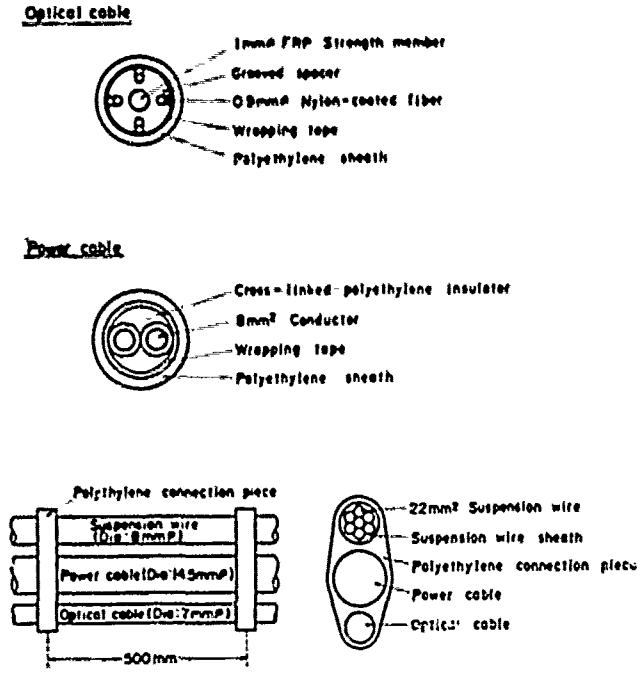

Fig. 1 Composite optical/electric power feeder cable for outdoor use

2.2 Evaluation of the composite optical/electric power feeder cable for indoor use

For the development of the composite optical/electric power feeder cable for indoor use, evaluation was made according to the following design criteria:

(1) To facilitate the installation of the cable in conjunction with existing indoor distribution channels, the outer diameter of the cable must be equal to that of conventional power feeder cable (about 11 mm).

(2) Optical fiber and power feeder cables must be easily separable for convenient workability.

With full consideration given to the above conditions, the structure of the indoor composite cable was evaluated, and the size of power feeder was set at 3.5 mm^2 (stranded annealed copper wire), assuming the maximum allowable current value to be 19 A and paying special attention to flexibility.

Two types of structures for the cable have thus been developed: a spacer type and a cord type. (Fig. 2)

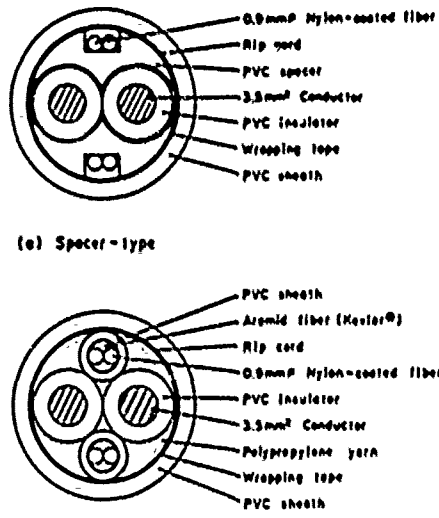

Fig. 2 Composite optical/electric power feeder cable for indoor use

The spacer type is a kind of slot type cable in which optical fiber is accommodated in a special grooved fan-shaped spacer and stranded around the power feeder in order to prevent the application of direct lateral pressure on optical fiber. This structure is not only excellent in mechanical properties but also 4-fiber ribbon tape can be accommodated in the fan-shaped spacer. Using ribbon fiber up to 24 optical fibers can be accommodated.

On the other hand, the cord type cable has a cord incorporating 4-nylon-coated optical fiber of 0.9 mmφ, which is stranded around the electric power [illegible] The 2 optical cords and the electric

power feeder cable can be easily separated, and independently used for indoor wiring.

2.3 Characteristics of the composite optical/electric power feeder cable

Table 1 summarizes the results of the evaluation of the characteristics of the composite optical/electric power feeder cable we have developed for outdoor and indoor use.

Both electrical and optical characteristics have been found to be satisfactory and suitable for practical application, and there is no indication of degradation in characteristics due to the combination of optical fiber and electric power feeder cable.

3. Composite optical/electric power feeder socket

A composite optical/electric power feeder socket has been developed according to the following design criteria:

Table 1 Characteristics of composite optical/electric power feeder cable

Item		Testing conditions	Cable for outdoor use	Cable for indoor use	
				Spacer-type	Cord-type
Electrical characteristics	Withstand voltage	JIS C 3005 8(1) AC 2000V for 1min	No short circuit	No short circuit	No short circuit
	Insulation resistance	JIS C 3005 9.1	280 GΩ · km	1100 MΩ · km	1000 MΩ · km
Optical characteristics	Temperature	−20 ~ +60°C	No loss change	No loss change	No loss change
	Tension	F ⊂ 1m ⊃ F	No loss change (F ≦ 3800kg)	No loss change (F ≦ 200kg)	No loss change (F ≦ 200kg)
	Compression	F	No loss change (F≦100kg/50mm)	No loss change (F≦100kg/50mm)	No loss change (F≦100kg/50mm)
	Bending	D = 200, 120, 100, 80 60mmφ	No loss change	No loss change	No loss change
	Impact	Impact load : 1kg Height(drop) : 1m Impact body : metal body of 25mmφ	No loss change	No loss change	No loss change
	Torsion	1m ±360° W=25kg	No loss change	No loss change	No loss change
	Vibration	Amplitude : ±5mm Frequency : 10Hz Vibration time : 10^6	No loss change	No loss change	No loss change

(1) Full consideration must be given to the use of general-purpose power outlet for the purposes of efficient use of space, aesthetics and low cost.

(2) To facilitate free movement, optical sockets and power sockets must be independent and usable separately.

(3) Existing optical connectors must be used for low cost and general-purpose applications.

Figure 3 shows the structure of the composite optical/electric power feeder sockets developed to meet the above conditions and Fig. 4 shows the external appearance of the socket.

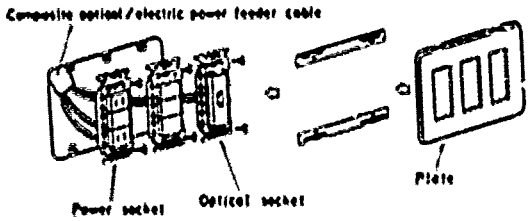

Fig. 3 Composite optical/electric power feeder socket

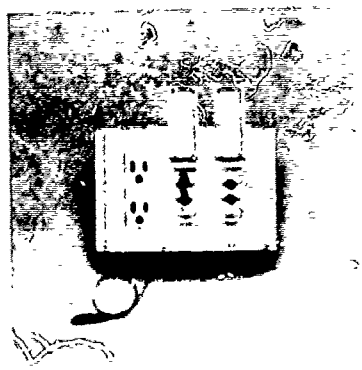

Fig. 4 Composite optical/electric power feeder socket

For the optical socket unit, the push-pull type connector[1] for single fiber as used in the NTT subscriber system was used. Unlike the conventional screw engagement type, this connector is detachable only in the longitudinal direction, providing extremely high maneuverability. This optical socket also has a dustproof and waterproof cover.

By incorporating this optical socket with the general-purpose power feeder outlet, optical fiber can be introduced into existing house without the need to install new optical socket units. It's possible to use the existing distribution conduit and power outlets, thus abling better external appearance and reduction of material and installation costs.

4. Optical cord reel

4.1 Structure of optical cord reel

An optical cord reel has been developed according to the following design criteria:

(1) The structure of the cord reel must allow for flexible movement of HA equipment and devices.

(2) When not in use, the optical cord must be accommodated in compact form.

(3) The reel should be able to withstand the impact of falling objects.

Figure 5 shows the external appearance of the

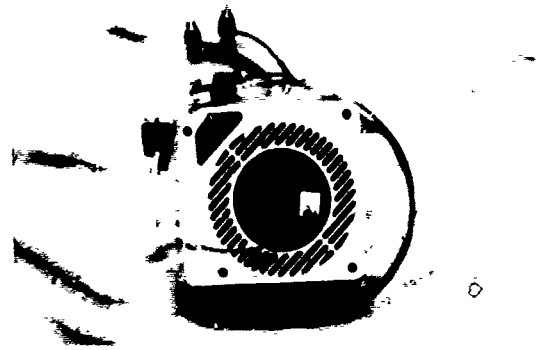

Fig. 5 Optical cord reel

optical cord reel thus developed. The optical cord incorporates 2-nylon-coated fiber in 2-fiber cord form, and has a connector at each end to facilitate easy handling, flexibility and protection from external force. The length of the cord was set at 10 m, a suitable length for the living room of an average Japanese house. When not in use, the optical cord is wound on an encased reel, and it can be conveniently unwound to various lengths thus providing for flexible movement of HA equipment.

4.2 Characteristics of the optical cord reel

This cord reel is primarily designed for use in general households. Therefore, it must have sufficient mechanical strength to withstand the impact or of being stepped on of falling objects.

The results of evaluation tests on the optical cord reel in an operating enviroment are summarized in Table 2. As evident from this table, satisfactory results were obtained in the tests of repeated pulling, impact and falling, thus, the practical usefulness of the product was demonstrated.

5. Cable installation

5.1 Evaluation of wiring procedure

The composite optical/electric power feeder socket is designed to facilitate the use of the general-

purpose electric power outlets.

Table 2 Characteristics of optical cord reel

Item	Testing conditions	Test result
Repeated pulling	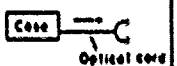	Loss variation is less than 0.05dB at 500 times
Impact	Impact body: Metal body of 25mm$^{\phi}$	No change in external appearance No loss change
Falling	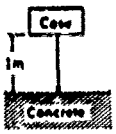	No change in external appearance

However it is not easy to perform fusion splicing and to handle excess length of cable in the composite socket unit due to the small internal space. In order to promote the workability of the composite socket unit, connector splicing was adopted for the connection with the optical socket.

The distribution conduit installed inside the wall in an ordinary house in small in diameter and it is not very practical for passage of a terminal with an optical connector.

For this reason, a joint box is installed in the upper part of the duct for installation of indoor composite cable, the cable with an optical connector at one end being run through the conduit from the composite socket toward the joint box.

5.2 Evaluation of wiring possibilities

Tohoku Electric Power Co., Inc. has built a "totally electrified model house" in the compound of the Applied Technology Research and Development Center for the study of intelligent houses and home automation of the future.

The newly developed optical/electric power feeder composite cable for indoor and outdoor use and the composite optical/electric power feeder socket were installed in this model house, in order to practically assess the workability and optical and electrical characteristics of this new system.

The outdoor cable was installed on a drum and on the inlet of the underground line, only the suspension wire was separated. After installing 110 m of underground line, 10 m of duct and 15 m of inlet pipe to the IDF of the main building. Figure 8-shaped wiring was performed, and 165 m of aerial line was installed up to the laboratory. Conventional tools and processing could be applied for installation and anchoring. Power feeder cable and optical cable could be easily separated, and satisfactory maneuverability was verified. Further more, there was no sign of degradation of either optical or electrical characteristics before or after installation, and the high degree of usefulness of the cable was verified.

For indoor cable, 150 m of spacer type cable was installed in the model house, and 100 m of cord type cable was installed in another main building in the compound. Figure 6 is a diagram of the cable installation, the composite cable with a connector at one end was installed from socket to joint box and from optical terminal station to joint box. Excess length of cable could be easily accommodated in the joint box, and optical connector splicing was used for the connection in the composite socket. It was confirmed that splicing was achievable within the socket without problem.

6. Conclusion

With the evolution of an information-oriented society, study and evaluation of the introduction of an optical transmission system to general households has been undertaken. The authors have developed and evaluated a new composite optical/electric power feeder cable for indoor and outdoor use and assessed the required installation procedures.

These cable incorporate the optical line for information transmission necessary for HA equipment with the power feeder cable. Further more, we have developed a composite optical/electric power feeder socket as an outlet for the composite cable in each room, facilitating the use of commercial power outlets. Also, an optical cord reel facilitating flexible movement of HA equipment and devices has been developed for the connection between socket and equipment.

The results of the evaluation revealed the practical usefulness and effectiveness of the optical/electric power feeder cable socket and optical cord reel through their application in the "totally electrified model house" built in the compound of the Applied Technology Research and Development Center of Tohoku Electric Power Co., Inc..

With the gradual introduction of subscriber optical systems to individual households, an increasing demand for composite cable sockets and cable to connect the socket and the equipment is expected. The application of our newly developed system will contribute greatly to more efficient wiring and power distribution in private houses.

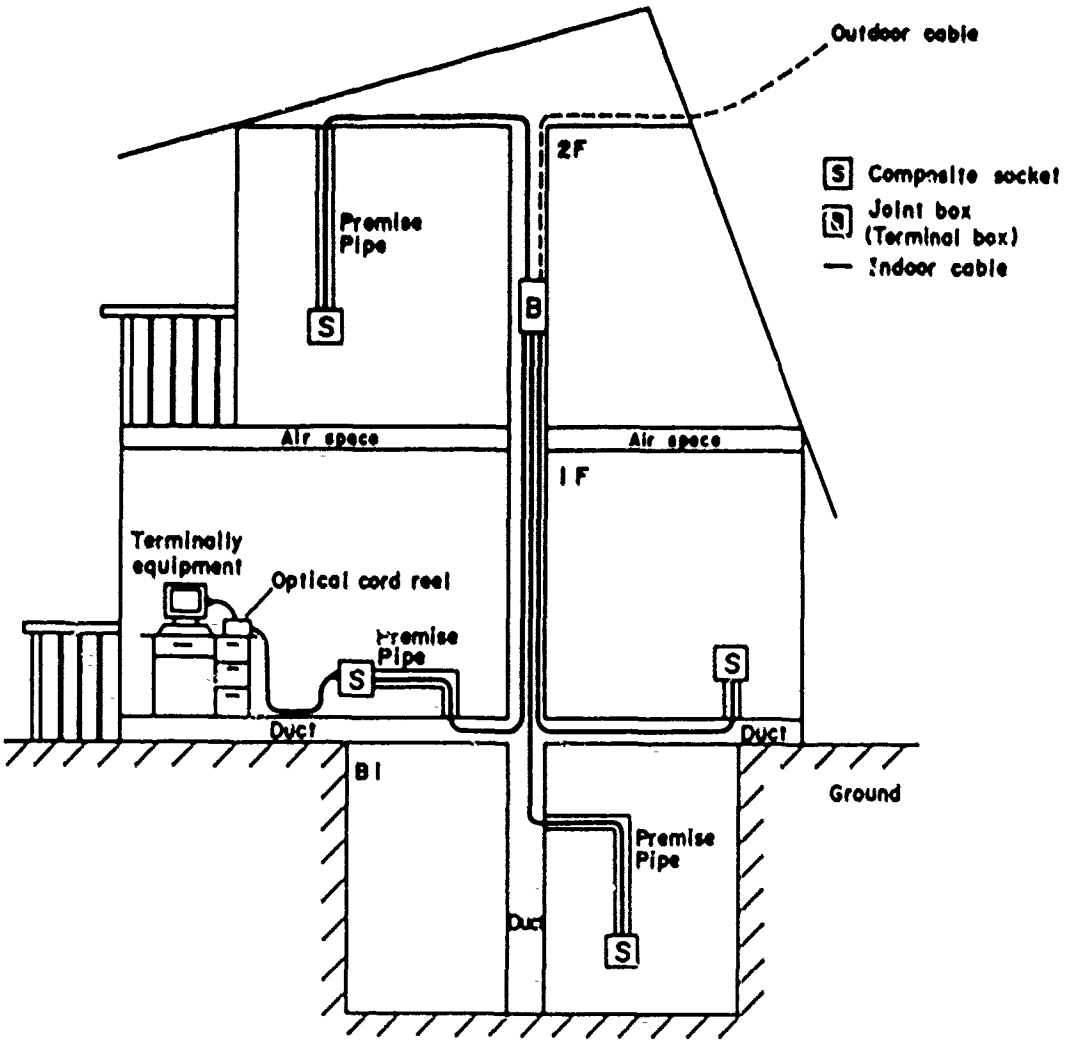

Fig. 6 Wiring diagram of composite optical/electric power feeder system

Refereces

(1) T. Kakii, K. Kashihara, T. Komiya, S. Suzuki, Y. Iwamoto and Y. Sakata: "Development of Optical Connectors for GI-Type Subscriber Fiber Optical Cablees", Sumitomo Electric Technical Review. Number 27, January 1988.

Koichi Ishikawa
Tohoku Electric
Power Co., Inc.
2-1, 7-Chome,
Nakayama, Aoba-ku,
Sendai 981, Japan

Koichi Ishikawa received the B.E. degree in engineering from Nihon University in 1982.
He then joined Tohoku Electric Power Co., Inc., where he has been engaged in telecommunication and electronics engineering. He is now an engineer for Applied Technology Research and Development Center and a member of the Institute of Electronics, Information and Communication Enginners of Japan.

Koji Niikura
Sumitomo Electric
Industries, Ltd.
1, Taya-cho,
Sakae-ku,
Yokohama 244, Japan

Koji Niikura received the B.E. degree in engineering from Waseda University in 1984 and joined Sumitomo Electric Industries, Ltd.
He has been engaged in the development and design of optical fiber cables in the Fiber Optics Division.

Sakari Ohira
Tohoku Electric
Power Co., Inc.
2-1, 7-Chome,
Nakayama, Aoba-ku,
Sendai 981, Japan

Sakari Ohira graduated from Frukawa Technical School in 1959. He then joined Tohoku Electric Power Co., Inc., where he has been engaged in telecommunication and electronics engineering.
He is now an assistant research manager for Applied Technology Research and Development Center and a member of the Institute of Electronics, Information and Communication Engineers of Japan.

Hajime Igarashi
Sumitomo Electric
Industries, Ltd.
1, Taya-cho,
Sakae-ku,
Yokohama 244, Japan

Hajime Igarashi received the B.E. degree in engineering from Waseda University in 1988 and joined Sumitomo Electric Industries, Ltd. He has been engaged in the development and design of optical fiber cable in the Fiber Optics Division.

Hiroaki Horima
Sumitomo Electric
Industries, Ltd.
1, Taya-cho,
Sakae-ku,
Yokohama 244, Japan

Hiroaki Horima received the M.S. degree in engineering from Osaka University in 1972. He then joined Sumitomo Electric Industries, Ltd. and worked on the development of CATV coaxial cables, multipair PEF-insulated junction cables and low loss unbalanced type cables. Thereafter, he concentrated on the development of optical fiber cables. He is now Section Manager of the Fiber Optics Division at Sumitomo Electric Industries, Ltd. He is a member of the Institute of Electronics and Communication Engineers of Japan.

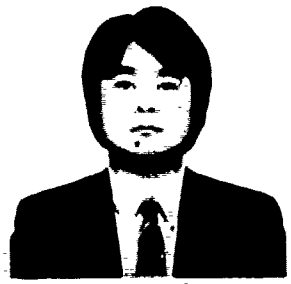

Koji Ogata
Kitanihon Electric
Cable Co., Ltd.
1-2-1, Koriyama,
Wakabayashi-ku,
Sendai 982, Japan

Koji Ogata received the B.E. degree from Tohoku Gakuin University in 1986. At Kitanihon Electric Cable Co., Ltd., he has been engaged in the development and design of optical fiber cables in the Engineering Division.
He is a member of the Institute of Electronics and Communication Engineers of Japan.

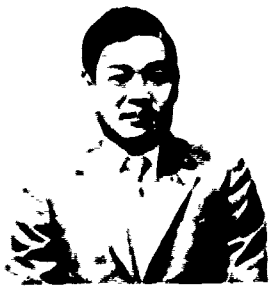

Akira Kurosawa
Kitanihon Electric
Cable Co., Ltd.
1-2-1, Koriyama,
Wakabayashi-ku,
Sendai 982, Japan

Akira Kurosawa received the B.E. degree from Tohoku University in 1970.
At Kitanihon Electric Cable Co., Ltd., he has been engaged in the design and development of communication cables.
He is now a section manager of the Engineering Division.
He is a member of the Institute of Electronics and Communication Engineers of Japan.

ELECTRICAL CHARACTERISTICS OF A METALLIC DIGITAL SUBSCRIBER LINE (DSL) FOR THE INTEGRATED SERVICES DIGITAL NETWORK (ISDN) BASIC RATE INTERFACE (BRI)

Russell C. Pepe and Jeffrey Poulsen

General Cable Company
South Plainfield, New Jersey

I. ABSTRACT

The objective of this paper is to explore outside plant metallic cables as the Digital Subscriber Line (DSL) intended to support the Integrated Services Digital Network (ISDN) Basic Rate Interface (BRI), using as a foundational substructure, the American National Standards Institute (ANSI) standard, ANSI T1.601-1988[1]. An overview of the ISDN is initially delineated to clarify the topic, which includes applications, the channel structure, the Basic Rate Interface (BRI), the Primary Rate Interface (PRI), the major configurations, the subscriber loop and the standards activity. Test data are studied in association with theoretical predictions to support a thorough discussion of the potential impact of the transmission media on the ISDN. The details of the theoretical analysis include primary electrical parameters, insertion loss and complex impedance. A model is presented which demonstrates the effects of a bridge tap on cable insertion loss and complex impedance. The test data encompass primary electrical parameters, insertion loss, complex impedance, crosstalk and pulse response. These parameters are explored as a function of various loop configurations accounting for mixed gauges, bridge taps and loop lengths.

II. BACKGROUND

Technological advances in association with an increased demand for the efficient collection, processing and dissemination of information are leading to the development of integrated systems that manipulate voice, data and video in the form of digital signals. The Integrated Services Digital Network (ISDN) is the next phase of telecommunications intended to support enhanced services to residential and commercial subscribers, over a digital transport system through a series of standard interfaces and digital switches. A uniformly accessible international network is under development implementing multiple, compatible ISDNs. Currently, trial ISDNs are under investigation in various parts of the world, including Europe, Japan and the United States. Large scale implementation of the ISDN in the United States is targeted for the early part of the next decade. Careful product development and network integration is, therefore, warranted to successfully achieve this extensive enterprise.

Unlimited services can be made available to the residential and commercial subscriber through the ISDN. With the increasing use of computers, especially personal computers (PCs), and the proliferation of user terminals and Local Area Networks (LANs), a huge and growing demand for data services has emerged.

The residential telephone subscriber, in addition to a standard voice capability, requires access to a multitude of data services. Such services, which could address the ISDN through a PC or terminal, include information retrieval systems, banking, shopping and other consumer transaction oriented services. Furthermore, the office could be extended to the home for file transfer, electronic mail and other office automation capabilities. The ISDN could eventually furnish the home with services, such as cable television, currently provided through other media. Other value added services could encompass interactive information retrieval systems such as videotex. Moreover, enhanced capabilities for standard telephone service can be readily accommodated, such as automatic dialing, answering and paging.

Initially, for the commercial subscriber, basic requirements concerning data rate, reliability, privacy and security can be addressed to provide a cost effective digital transport system. Offices can be interconnected for distributed processing and file transfer. Furthermore, video teleconferencing can be initiated without reconfiguration obstacles. Generally, the ISDN will need to provide a variety of data transmission services according to the application and class of service required. These basic data provisions can be further supplemented by more esoteric, miscellaneous services.

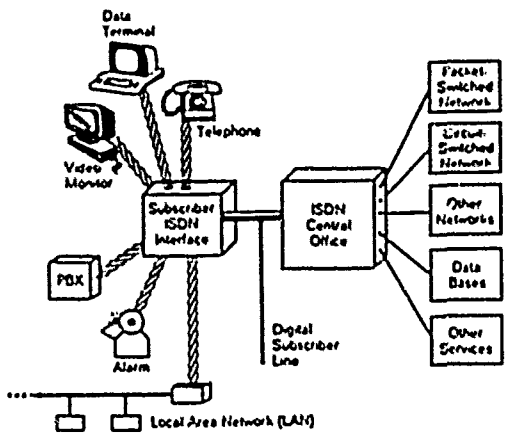

FIGURE 1

ISDN APPLICATION BLOCK DIAGRAM

(1) Integrated Services Digital Network (ISDN) - Basic Access Interface for Use on Metallic Loops for Application on the Network Side of the NT (Layer 1 Specification), ANSI T1.601-1988, September 16, 1988.

The data capacity required by each ISDN user may vary; therefore, the ISDN digital structure must be flexible. However, a totally flexible digital structure would be unmanageable for the network. Consequently, an expandable ISDN channel structure has been established, to provide versatility for the user yet exhibit maintainability for the network.

The major foundation for the ISDN channel structure is based on the B and D designated channels. The B channel is the fundamental user channel offering a 64 Kbps data capability. The D channel provides a 16 Kbps or 64 Kbps data capacity, for the exchange of control information between the user and the network and to support low speed data requirements.

Other recommended channel arrangements include a 384 Kbps H0 channel, a 1.472 Mbps H10 channel and a 1.536 Mbps H11 channel. The H0, H10 and H11 channels will provide a vehicle for high data capacity requirements.

TABLE 1

ISDN CHANNEL STRUCTURE

Channel Designation	Data Rate	Applications
B	64 Kbps	Digital Voice Circuit Switched Data Packet Switched Data Facsimile Slow-Scan Video
D	16 or 64 Kbps	Signaling Low Speed Data Videotex Alarms Energy Management
H0	384 Kbps	High Speed Data
H10	1.472 Mbps	High Speed Data Video
H11	1.536 Mbps	T1 Facility* Video

* 1.544 Mbps with overhead.

A two wire interface providing a 144 Kbps data capability to the ISDN user has been defined as the Basic Rate Interface (BRI). The BRI is mainly configured for the residential subscriber. The channel structure of the BRI is typically designated 2B + D (2 x 64 Kbps + 16 Kbps = 144 Kbps); however, alternate configurations are also possible. Due to overhead digital information such as framing and synchronization, the actual transmission rate for the BRI could be 192 Kbps, with 48 Kbps necessary to support the 144 Kbps capacity available to the ISDN user. However, with the advent of the CCITT Common Channel Signaling System Number 7 (SS7) Central Office (CO), the overhead is reduced to 16 Kbps for an actual transmission rate of 160 Kbps.

The ISDN Primary Rate Interface (PRI) is defined as a four wire interface providing a data capacity of 1.536 Mbps to the user. The channel structure of the PRI is typically designated as 23 B + D (23 x 64 Kbps + 64 Kbps = 1.536 Mbps); however, a multitude of configurations are possible using the H0, H10 and H11 channels, for example. With 8 Kbps for overhead digital information, the transmission rate for the PRI is 1.544 Mbps which coincides with the North American DS1 transmission rate. Based on the Conference of the European Post and Telecommunications (CEPT) digital hierarchy, a 2.048 Mbps, four wire interface is also under consideration. This interface, which is the European counterpart of DS1, offers additional capacity. A possible channel structure may be 30 B+ D (30 x 64 Kbps + 64 Kbps = 1.984 Mbps) with 64 Kbps for overhead to yield 2.048 Mbps.

Access to the ISDN for the Basic Rate Interface (BRI) and the Primary Rate Interface (PRI) is defined by Functional Groups and Reference Points.

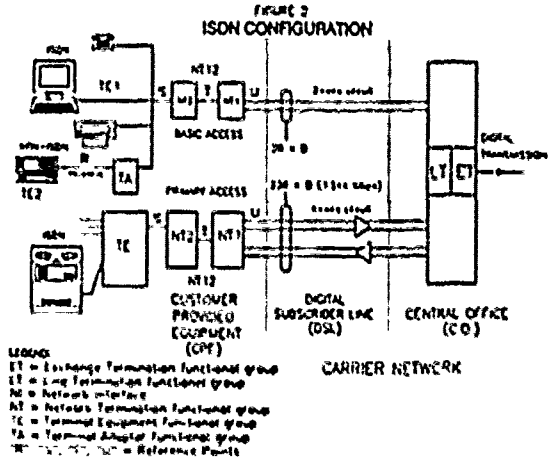

The Functional Groups are designated the Exchange Termination (ET), Line Termination (LT), Digital Subscriber Line (DSL), Network Termination (NT), Terminal Equipment (TE) and Terminal Adapter (TA). The major functions of the ET include channel separation, signal information processing, information control flow, network access and DSL termination. The LT terminates the DSL in the Central Office (CO), and the ET and LT jointly comprise the ISDN CO. The DSL provides the transmission path between the CO and the subscribers. The DSL and CO are collectively referred to as the Carrier Network. The NT is available as the NT1, NT2 or NT12. The NT1 includes functions associated with the physical and electrical termination of the ISDN on the user's premises. The NT1 may be controlled by the ISDN provider, and forms a boundary to the network to isolate the user from the transmission technology of the DSL and perform line maintenance functions. The NT2 is an intelligent device such as a digital PBX or LAN. NT12 is a single device which provides the combined functions of NT1 and NT2. Due to regulatory considerations, the NT12 will probably not be permitted in the United States. The TE refers to user equipment. TE1 designates ISDN compatible equipment where TE2 denotes non-ISDN equipment. TE2 requires a TA which assures ISDN compatibility. NT1, NT2, and TE1 or TA and TE2 comprise the Customer Provided Equipment (CPE).

The Reference Points are designated R, S, T and U. R is the point between the TE2 and TA, and is, therefore, omitted with the use of the TE1. S is the point between the TE1 and NT2 or the TA and NT2. T is the point between the NT1 and NT2. U is the Network Interface (NI), the point between the NT1 and DSL. It defines the access point to the CPE from the Carrier Network.

Since the PRI is a four wire interface at 1.544 Mbps, full duplex operation can be accommodated to standard T1 facilities incorporated into the ISDN structure. The BRI, however, poses a dilemma, as the installed physical plant employing a two wire interface cannot currently support high performance, full duplex operation at 160 Kbps.

A device called the echo canceler transceiver has been proposed as an adjunct to the existing subscriber loop. The transmission system uses the echo canceler with hybrid principle to provide full duplex operation at 160 Kbps with the level of performance required for the ISDN BRI. Since the BRI must provide full duplex operation at 160 Kbps over a two wire interface, rather than a four wire interface, the echo canceler transceiver must perform an intervening function. Using a coding technique designated 2B1Q for two binary 1 quaternary, the two 160 Kbps binary (two level) signals can each be expressed as quaternary (four level) signals at a signaling rate of 80 Kbps, for an overall bi-directional data rate of 160 Kbps. The echo canceler transceiver, therefore, provides full duplex operation over a two wire interface while maintaining the data rate of 160 Kbps.

The ISDN concept was officially initiated in 1968 through Special Study Group D of the CCITT. CCITT is the acronym for Consultative Committee of International Telegraph and Telephone, a United Nations treaty organization primarily composed of the postal, telegraph and telephone (PTT) authorities of the member nations. Governing the CCITT is the International Telecommunication Union (ITU), an organization dedicated to promoting and ensuring the operation of international telecommunication systems. The CCITT remains the major thrust for the ISDN. In Europe, the CCITT is working closely with the Conference of the European Post and Telecommunications (CEPT) to standardize the ISDN.

TABLE 2

STANDARDS GROUPS

ANSI	American National Standards Institute
Bellcore	Bell Communications Research
CCITT	Consultative Committee of International Telegraph and Telephone
CEPT	Conference of the European Post and Telegraph
COS	Corporation for Open Systems
ECSA	Exchange Carriers Standards Association
EIA	Electronic Industries Association
ICST	Institute for Computer Sciences and Technology
IEC	International Electrontechnical Commission
IEEE	Institute for Electrical and Electronics Engineers
ISO	International Standards Organization
ITU	International Telecommunications Union
NIST*	National Institute of Standards and Technology
OSI	Open Systems Interconnection
PTT	Postal, Telegraph and Telephone

* Formerly NBS (National Bureau of Standards)

In the United States, the T1 Committee of the Telephone Committee of the Exchange Carriers Standards Association (ECSA) is accredited by the American National Standards Institute (ANSI) and charged with producing standards for service providers and manufacturers. Much of the activity of the ECSA T1 Committee is directed towards the drafting of ISDN standards. Responsibilities are basically segmented into subcommittees and working groups. Other groups concerned with ISDN standards are listed in Table 2.

Overall, the ISDN is intended as a unified, integrated provider of transmission related services, whereby, the user can obtain a variety of voice, data and video services through a common access point, with the rate structure based on the type and volume of service required. The applications and subsequent services available will primarily be determined by the imagination of the provider and the demands of the subscriber. Technology will be driven by an escalation in advanced applications for the ISDN.

III. EVALUATION

As previously stated, the basis for this paper is the ANSI standard T1.601-1988. The ANSI document was drafted to provide the minimal set of requirements to enable satisfactory transmission between the network and the NT, while conforming to the international CCITT recommendations governing the ISDN. Furthermore, in an effort to facilitate an economical, uninterrupted transition to a high quality ISDN BRI, ANSI T1.601-1988 recognizes that the existing subscriber loop will be utilized as the DSL with minimal modification. The standard presents the electrical characteristics of the ISDN BRI, at the network side of the NT. As a Layer 1 or Physical Layer (Open Systems Interconnection (OSI) model) specification, the standard describes the physical interface between the network and the NT. The requirements of ANSI T1.601-1988 apply to a single DSL consisting of an LT, a two wire twisted metallic cable pair and an NT, designed to operate in a full duplex mode.

ANSI T1.601-1988 addresses non-loaded loops, composed of mixed gauges and bridge taps, possessing a maximum length of 18 kft. The resistance of the loops is specified as a maximum of 1300 ohms (or 42 dB attenuation at 40 kHz). Note that the effective BRI baud rate of 160 Kbps is compressed to 80 Kbps through the 2B1Q encoding with a power spectrum centered at 40 kHz. Generally, the standard addresses the electrical characteristics of the equipment rather than the cable which terminates at the NT. The electrical characteristics for the metallic DSL are tabulated in the form of the primary electrical parameters: resistance, inductance, conductance and capacitance, for Pulp and PIC (Air Core) cables. Fifteen loop configurations are listed, in the standard, ranging from a simple 12 kft. loop exclusively composed of 26 AWG wire without bridge taps, to complex loops with multiple bridge taps and gauge combinations.

For our study, three configurations were selected. Loop #4 from the standard was selected for its simplicity; Loop #3, for its complexity; and Loop #2, as an intermediate loop. Refer to Figure 3 for the configurations for Loops #4, #3 and #2. As shown in the diagrams, all three loops selected for our study are no greater than 18 kft in length and incorporate various gauges. Additionally, Loop #4 is a straight loop, Loop #2 possesses one bridge tap, and Loop #3 is composed of a network of interconnected bridge taps. Although the NT and LT were terminated into 135 ohms, the bridge taps were left unterminated, or open, as is the practice in the field. The specific cables selected for the evaluation were random samples of 25 pair air core PIC cables with an aluminum shield (Air Core Alpeth Sheath PIC Cable). The cables were interconnected using modular splices (3M, 400S, MS2, Super Mate Plugable Modular Splice). Refer to Appendix A for a list of the test equipment employed for the testing.

Although ANSI T1.601-1988 addresses many parameters of consequence to the ISDN, the standard is not ubiquitous. Several published studies have uncovered additional parameters which could impact the ISDN. A comprehensive study issued by Bellcore[2] comments on additional issues which could impact the ISDN. Another Bellcore Technical Reference[3] parallels ANSI T1.601-1988 in many respects, but provides further insight concerning the electrical performance of the DSL.

FIGURE 3

LOOP CONFIGURATION

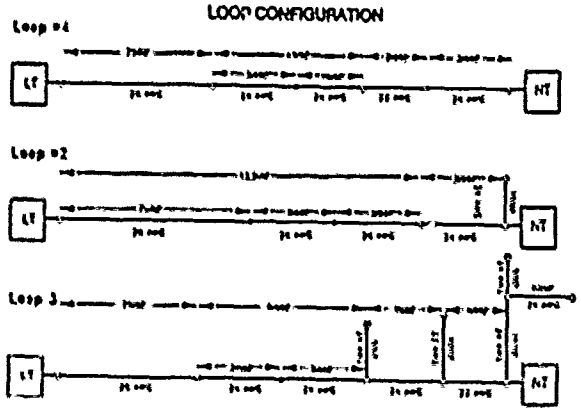

Subsequently, this paper will primarily follow ANSI T1.601-1988 with mutual consideration of the referenced Bellcore documents to deal with the multitude of transmission parameters of significance to the quality of a metallic DSL for the ISDN BRI. In some instances, the liberty has been taken to address the testing of metallic cables in accordance with test recommendations specifically intended for transmission equipment. Subsequently, this paper will investigate primary electrical parameters, attenuation, complex impedance, crosstalk and pulse response as a function of various loop configurations accounting for mixed gauges, bridge taps and loop lengths. Impulse noise, an important parameter which is discussed in the 1983 Bellcore Subscriber Loop Survey, has been omitted from this paper as it is a phenomenon which is best tested in field trials rather than in the laboratory. Bit error rate testing is also not considered as it is a system test rather than a cable performance parameter, which is also best addressed in the field.

(2) Characterization of Subscriber Loops for Voice and ISDN Services (1983 Subscriber Loop Survey), ST-TSY-000041, June 1987

(3) ISDN Basic Access Digital Subscriber Lines, TR-TSY-000391, Issue 1, May 1988.

IV. RESULTS

A. Primary Parameters

Primary electrical parameters for 26, 24 and 22 AWG Pulp and PIC (Air Core) cables are tabulated in ANSI T1.601-1988 at 0, 70 and 120°F. These tabulated data were used as a basis for the theoretical analysis and network modeling in this paper. Two of the tabulated primary parameters, dc resistance and mutual capacitance were measured for Loops #4, #2 and #3 to provide a basis for the subsequent characteristics studied in this paper. Furthermore, values for dc resistance and mutual capacitance were calculated for Loop #4 using the tabulated primary electrical parameters to portray correlation between calculated and measured data. The measured and calculated data are summarized in Table 3.

TABLE 3

PRIMARY PARAMETERS

Loop #	Loop Length (ft.)	Comments	Resistance dc (ohms)		Capacitance @ 100 Hz (nF)	
			Table	Meas.	Table	Meas.
4	17,000	LT-NT	1180	1170	267	270
2	16,500	LT-NT	--	1270	--	284
	18,000	LT-Bridge Tap	--	1350	--	284
3	16,000	LT-NT	--	1050	--	312

Although capacitance is typically measured at a frequency of 1 kHz, for our evaluation, the measurement frequency was selected as 100 Hz. Generally, to avoid corrections associated with propagation velocity, capacitance is measured on relatively short cable samples such that the cable sample length corresponds to a length which is less than 1/40 of the measurement frequency (1 kHz) wavelength. Due to the excessive length of the tested loops, a lower frequency (100 Hz) was selected. Since capacitance for PIC cable is constant with frequency between 100 and 1000 Hz, this technique is valid. Also, note that all primary parameter data are referenced from the LT.

The data for Loop #4 show excellent agreement between calculated and measured values. Such correlation reveals the usefulness of the tabulated primary parameters as an aid to predicting the electrical characteristics of a metallic DSL. However, tabulated data do not preclude the need for laboratory and field testing. Loop testing is necessary since several factors must be considered when making conclusions about the expected performance of a loop. Furthermore, the resistance values for each loop conform closely to maximum value of 1300 ohms specified in ANSI T1.601-1988.

B. Insertion Loss

For our discussion, attenuation will be considered equivalent to insertion loss when the termination impedance is perfectly matched to the loop impedance at both ends of the loop. Since impedance varies with frequency, insertion loss rather than attenuation is applicable for our discussion.

Using the primary parameters in ANSI T1.601-1988, the attenuation was calculated for the cables in Loops #4 and #2. The insertion loss was next calculated as follows:

$$L_I = L_R + A \qquad (1)$$

L_I = Insertion Loss
L_R = Reflection Loss
A = Attenuation

where

$$L_R = 20 \text{ Log } \frac{Z_o + Z_t}{2\sqrt{Z_o + Z_t}} + 20 \log \sqrt{\frac{\text{Cos } \theta_o}{\text{Cos } \theta_t}} \qquad (2)$$

$Z_o \angle \theta_o$ = Characteristic complex impedance of transmission line

$Z_t \angle \theta_t$ = Characteristic complex impedance of termination (or terminating transmission line).

Table 4 presents the calculated insertion loss for Loops #4 and #2 along with the measured data for all three loop configurations. Calculations are provided at 40 kHz only. For comparison with existing industry data, measured insertion loss is provided at 40, 80, 160 and 772 kHz. For Loop #2, measurements and calculations from the NT and the LT are offered to display the negligible variance in insertion loss when referenced from either end of the loop. Although not shown, such minor differences also apply for Loops #4 and #3. The measured data are also presented graphically in Figures 4, 5, and 6 for Loops #4, #2 and #3, respectively. Note that the insertion loss at voice and low carrier frequencies diverges greatly from the attenuation due to the mismatch between the high cable impedance and the 135 ohm test terminations at the NT and LT. As noted in Figures 5 and 6, the bridge taps possess a resonant region affect d by bridge tap location and length, which creates a frequency selective high insertion loss region.

The insertion loss values obtained at 40 kHz for each loop conform closely to the maximum value of 42 dB specified in ANSI T1.601-1988. In general, excellent correlation is exhibited between the measured and calculated data. Calculations and measurements were performed for Loop #2 without and with the bridge tap. As demonstrated by the excellent correlation between the calculated and measured data, equations (1) and (2) comprise a suitable model for determining the effect of a bridge tap on insertion loss. With the aid of a computer, the insertion loss of complex networks with multiple gauge changes and bridge taps can be calculated using this model.

TABLE 4

INSERTION LOSS

Loop No.	Loop Length (Ft.)	Comments	Calcu. (dB) @ 40 kHz	MEASURED (dB) @ 40 kHz	@ 80 kHz	@ 160 kHz	@ 772 kHz
4	17,000	NT-LT	39.7	39.7	46.8	55.0	105
2	16,500	LT-NT w/o BT	41.6	42.4	50.1	58.3	109
		LT-NT	43.8	44.6	57.0	61.9	115
		NT-LT	43.8	44.3	56.5	61.2	115
3	16,000	NT-LT	---	42.3	49.3	66.6	107

BT: Bridge Tap

FIGURE 4

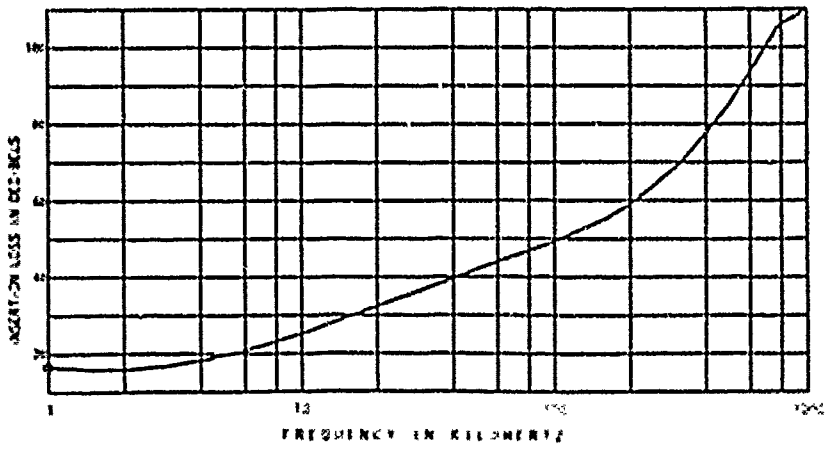

LOOP 4

FIGURE 5

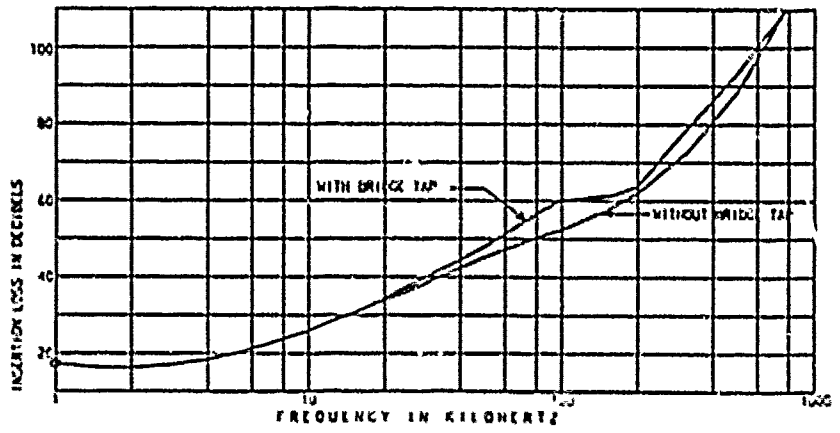

LOOP 2

FIGURE 6

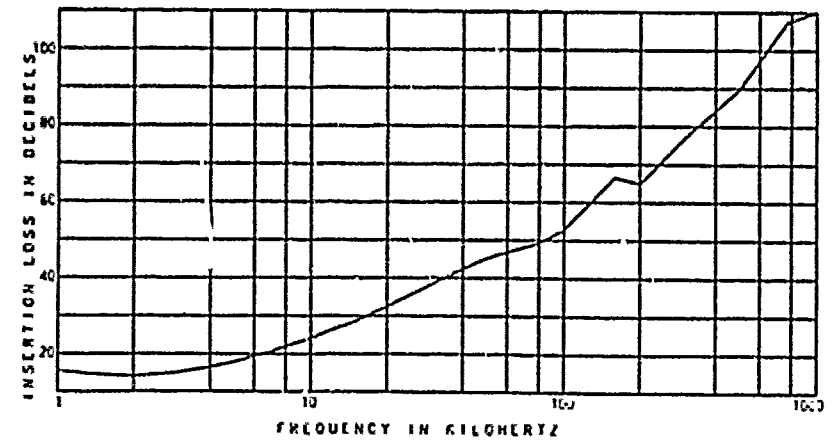

LOOP 3

C. Impedance

The nominal impedance at the U interface looking toward the NT is specified in ANSI T1.601-1988 as 135 ohms. In the standard, this value corresponds specifically to the impedance of the interface; however, for our discussion, the referenced impedance will be applied directly to the metallic DSL. Return loss is also specified in the ANSI standard; however, since re' as is directly related to impedance, complex impedance is solely discussed herein.

Using the tables of primary parameters in ANSI T1.601-1988, the complex impedance of each cable was calculated. The impedances referenced from the NT for Loops #4 and #2 were, subsequently, calculated using the following equation:

$$Z_i \angle \theta_i = Z_o \angle \theta_o \left[\frac{Z_o \angle \theta_o \sinh \gamma L + Z_t \angle \theta_t \cosh \gamma L}{Z_o \angle \theta_o \cosh \gamma L + Z_t \angle \theta_t \sinh \gamma L} \right] \quad (3)$$

$Z_i \angle \theta_i$ = Complex input impedance

$Z_o \angle \theta_o$ = Complex characteristic impedance of transmission line

$Z_t \angle \theta_t$ = Complex impedance of termination or terminating transmission line

L = Length of transmission line (miles) corresponding to $Z_o \angle \theta_o$

where

$$\gamma = \alpha + j\beta \quad (4a)$$

$$= \sqrt{(R + j\omega l)(G + j\omega c)} \quad (4b)$$

α = Attenuation (nepers per mile = dB per mile ÷ 8.686)

β = Phase shift (radians per mile)

and

$$\sinh(\alpha + j\beta) = \sinh\alpha \cos\beta + j \cosh\alpha \sin\beta \quad (5)$$

$$\cosh(\alpha + j\beta) = \cosh\alpha \cos\beta + j \sinh\alpha \sin\beta \quad (6)$$

Table 5 lists the calculated values for Loops #4 and #2. In addition, measured values of impedance for all three loops are provided. The complex impedances were measured using the 4 terminal method with an auto-balancing bridge and the pair terminated at the far end. The magnitude and phase of the impedance for Loops #4, #2 and #3 are graphically portrayed in Figures 7, 8 and 9, respectively. All impedances are referenced to the NT; however, for Loop #4, the impedances referenced to the NT and LT were similar.

The impedances were measured in complex form in terms of a magnitude and angle. The resistive (real) and reactive (imaginary) parts of the impedances were calculated for 40 kHz and included in Table 5 using the following relationship:

$$Z \angle \theta = Z \cos\theta + j\, Z \sin\theta \quad (7)$$

Real = $Z \cos\theta$

Imaginary = $Z \sin\theta$

This relationship is noted because of a reference in ANSI T.601-1988 regarding the NT possessing a terminating impedance of 135 ohms resistive.

Equation (3) provides a model for determining the effects of a bridged tap upon the loop impedance. Theoretically, gauge variations should effect the impedance; however, in practice, the effect is negligible when long lengths of cables are concatenated. Conversely, concatenated short lengths of cable of various gauges will have a noted effect on impedance. This relationship can be observed through equation (3). As the length of the cable (L) increases, the hyperbolic portion of the equation tends toward unity; therefore, the input impedance (Z_i) approaches the cable impedance (Z_o). Due to the presence of bridge taps in Loops #2 and #3, the impedance at the NT is affected significantly. For example, the single bridge tap in Loop #2 created a parallel circuit of relatively equal impedance which effectively cuts the input impedance at the NT in half. The intricate combination of parallel bridge taps in Loop #3 further reduces the input impedance at the NT. Although not shown, the impedances of Loops #2 and #3 were measured from the LT. Because the bridge taps are located a significant distance from the LT, the effect of the bridge taps on the input impedance at the LT is negligible, as previously explained for concatenated cables. Consequently, the impedances of Loops #2 and #3 referenced from the LT resemble the impedance of Loop #4 which does not possess bridge taps. Loops #2 and #3 exhibit a region above approximately 100 kHz, whereby the magnitude of the impedance assumes an oscillatory pattern.

This phenomenon is the result of cable resonance and is a function of the location and length of interconnected bridge taps. In effect, the bridge taps perform like tuned stubs. The excellent correlation between measured and calculated values of complex impedance verify the validity of equation (3) when applied to ISDN loops to determine the effect a bridge tap has on impedance. Using equation (3), complex loops can also be modeled with the aid of a computer. As evidenced by the data, impedance is significantly affected by the loop configuration. Since impedance is a parameter of concern to digital networks, the ISDN will require appropriate compensation at various termination points to insure compatibility.

FIGURE 7

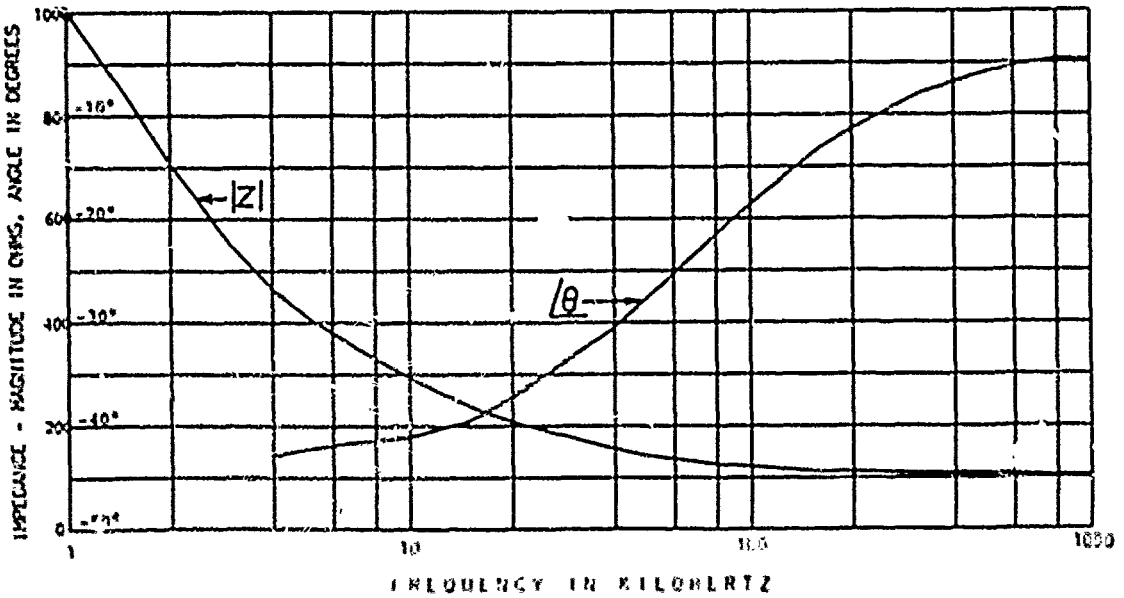

FIGURE 8

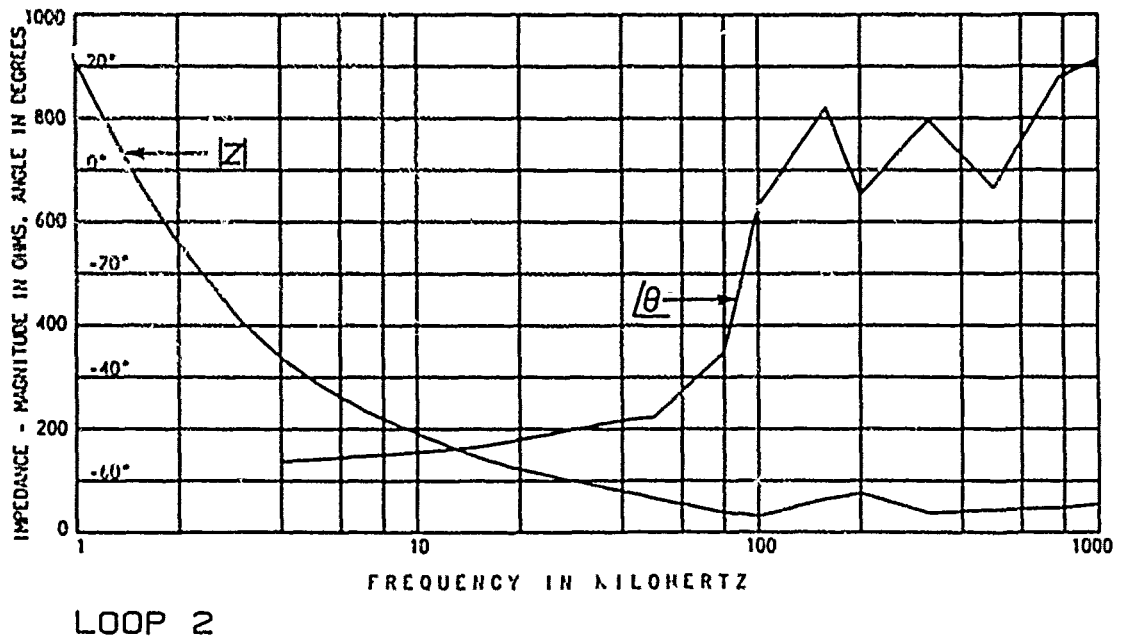

FIGURE 9

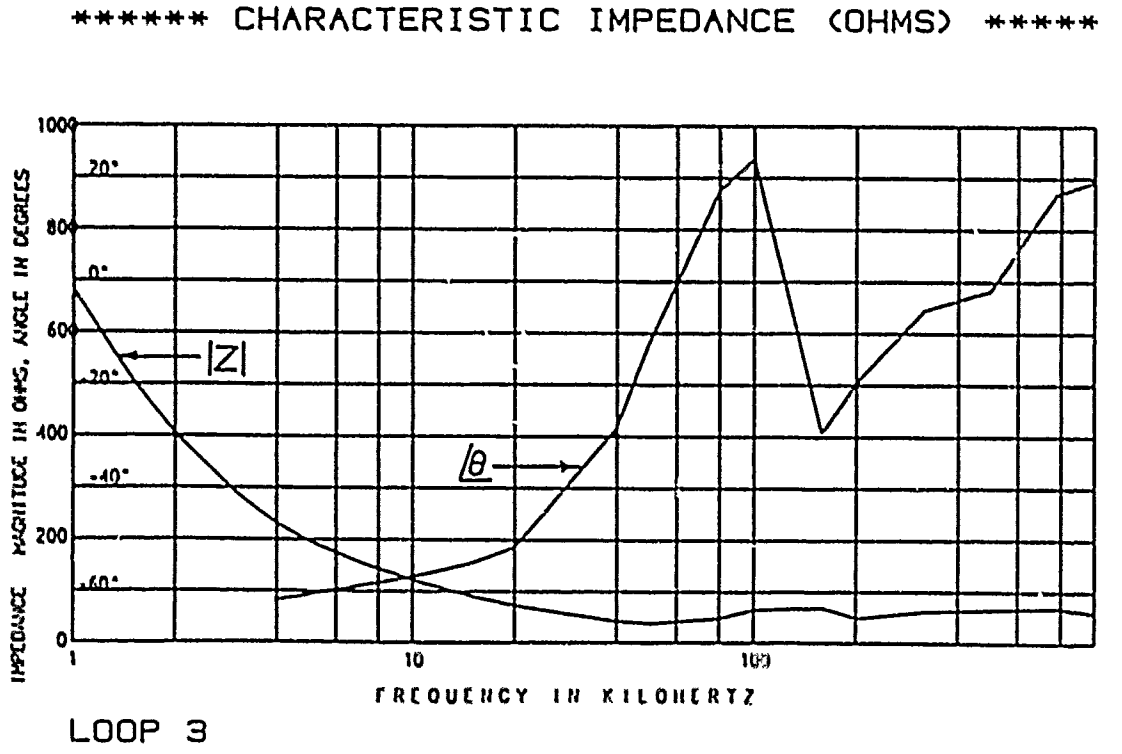

TABLE 5

COMPLEX IMPEDANCE

Loop No.	Loop Length (Ft.)	Comments	Impedance Magnitude | Phase (ohms | degrees)				
			Calculated	Measured			
			@ 40 kHz	@ 40 kHz	@ 80 kHz	@ 160 kHz	@ 772 kHz
4	17,000	NT	161 | -30.8 (Re = 138)	154 | -30.5 (Re = 133)	125 | -21.6	112 | -18.6	103 | -4.55
2	16,500	NT w/o BT	159 | -30.8 (Re = 136)	155 | -30.6 (Re = 133)	125 | -21.7	112 | -13.2	103 | -4.64
		NT	74.8 | -50.4 (Re = 47.7)	78.0 | -48.2 (Re = 52.0)	37.3 | -35.0	66.3 | 12.1	49.8 | 18.1
3	16,000	NT	—	39.8 | -28.4 (Re = 35.0)	47.9 | 17.6	68.2 | -29.1	65.6 | 16 9

BT: Bridge Tap

D. Crosstalk

The crosstalk was measured as power sum near end crosstalk (PS-NEXT). Figures 9, 10 and 11 exhibit the measured values of PS-NEXT for Loops #4, #3 and #2, respectively measured from both the NT and LT. Note that the values are based on the power sum for 25 pair cable. A measured and a corrected curve for crosstalk at the NT is provided for Loops #2 and #3. This correction is required due to an impedance mismatch between the cable and the test equipment. If the cable impedance is approximately equivalent to the test equipment terminating impedance, the correction is not necessary, as is the case for Loop #4 and all loops measured from the LT. However, the presence of bridge taps results in a significant decrease in the impedance at the NT. Consequently, an error is created due to the associated mismatch between the cable, and the generator and detector. Hence, a corrected curve is provided for the NT PS-FEXT measurements for Loops #2 and #3.

In Bellcore TR-TSY-000393, a graph is provided as Figure 4-1 which models the 1% NEXT for 18 kft of 22 AWG PIC cable. The model is a worst case scenario which is valid under several conservative conditions. The 1% point on the distribution of NEXT from 49 common binder group disturbers is plotted from 100 Hz to 1 MHz. By interpolating the 1% NEXT for 24 common binder group disturbers from the Bellcore graph, we were able to compare our measured NEXT values for 25 pair cables to the Bellcore values for 50 pair cables. The data is presented in Table 6. Note that the tested loops did not conform with the conservative conditions addressed in the Bellcore Technical Reference; however, the information is a useful relative indicator.

Our evaluation shows that the PS-NEXT is relatively linear and predictable at a loop interface which is not complicated by bridge taps. This relationship is exhibited by the agreement between the curves for Loop #4, and Loops #2 and #3 from the LT. The presence of bridge taps causes variations in the PS-NEXT characteristics, as portrayed by the curves for Loops #2 and #3 from the NT. Nonetheless, Table 6 shows that, although the loops tested do not conform with the conservative conditions stipulated in Bellcore TR-TSY-000393, the 1% NEXT values are within the specified values.

FIGURE 10

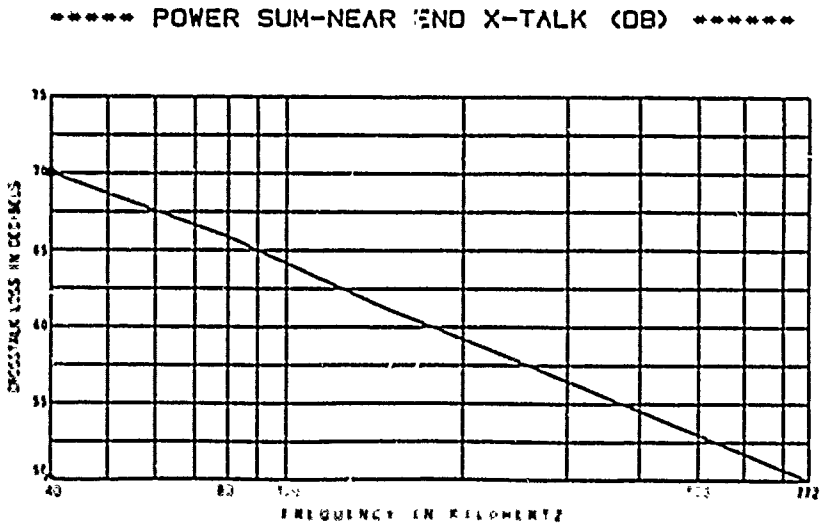

LOOP 4

FIGURE 11

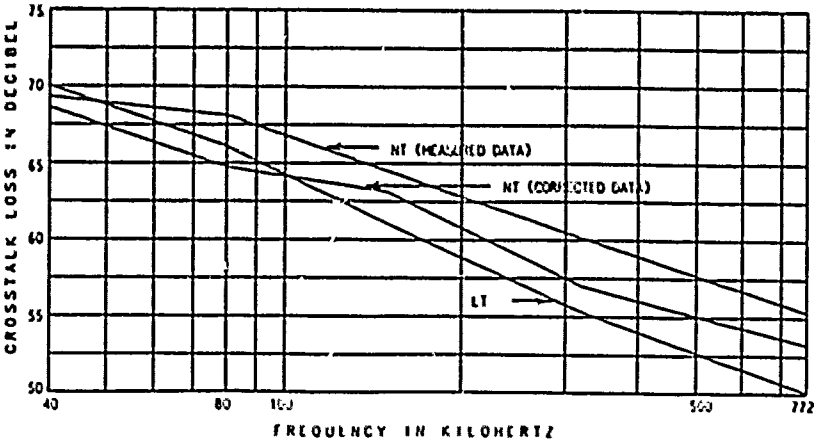

LOOP 2

FIGURE 12

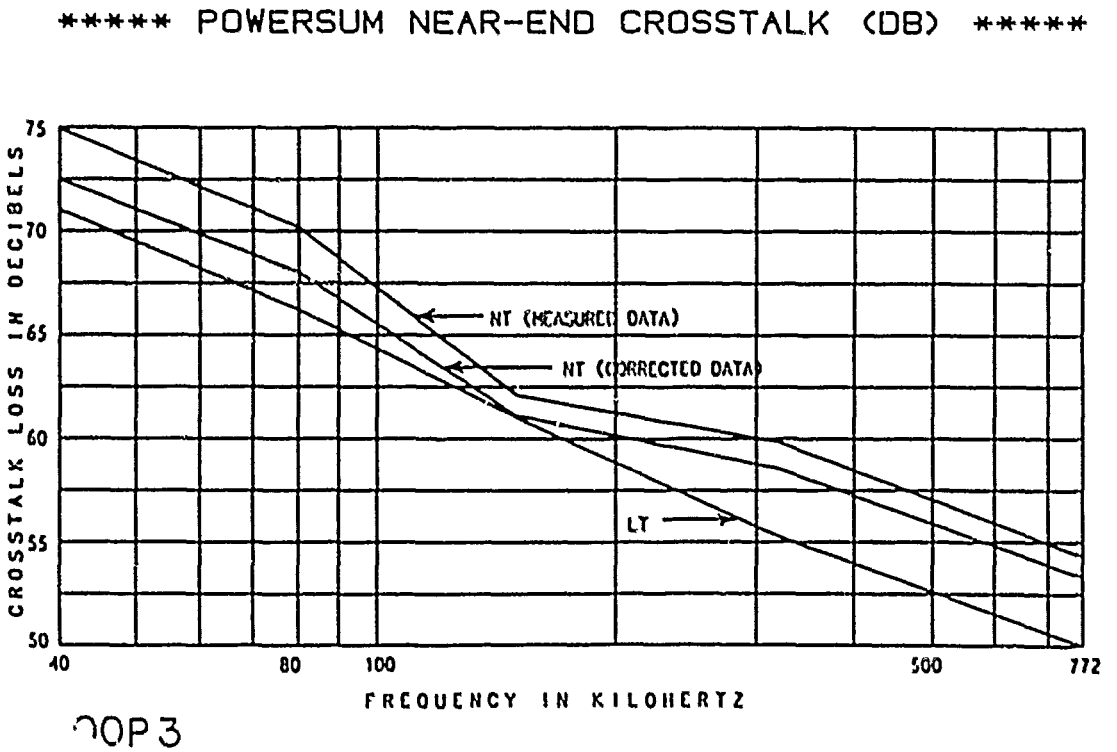

TABLE 6

1% NEXT

Loop No.	Loop Length (Ft.)	Comments	Bellcore Specified (dB)		Measured (dB)	
			@ 40 kHz	@ 80 kHz	@ 40 kHz	@ 80 kHz
4	17,000	NT	63	58	63	58
2	16,500	NT	63	58	66	60
		LT			65	59
3	16,000	NT	63	58	69	62
		LT			64	59

E. Pulse Response

ANSI T1.601-1988 specifies a mask for the shape of the 2B1Q pulses originating at the NT. For standard metallic cables intended for PCM telecommunications, a pulse template is often specified at a pertinent transmission rate, typically T1 (1.544 Mbps). The pulse template is a mask which defines the pulse shape and tolerances in terms of amplitude, duration, rise and fall times, over and under shoot and other related parameters.

We, therefore, characterized the pulse template in accordance with the mask supplied in the ANSI standard. However, since ISDN is a neoteric technology, a pulse simulator was not commercially available. We, consequently, generated a similar pulse using equipment currently available. Corresponding to the 2B1Q line rate of 80 Kbps, the pulse duration (10-90%) was selected as 12.5 μ sec.

Figure 13 portrays the generated pulse. The resultant received pulses are shown for Loops #4, #2, and #3 in Figures 14, 15 and 16, respectively. Note that all amplitudes are normalized to unity. For Loop #4, the received pulse at the NT is shown for the minimum and maximum insertion loss (IL). The received pulses at the NT and the LT are portrayed for Loops #2 and #3.

Corresponding to loop insertion loss, the received pulses are significantly attenuated. Due to the phase characteristics of the three loops tested, the received pulses exhibit dispersion. For Loops #4 and #2, the dispersion results in a pulse broadened to between 85 and 90 μ sec. from the initial 12.5 μ sec. pulse. Loop #3 displays a disparity between the pulses received at the NT and the LT. The pulse duration at the LT is approximately 65 μ sec., compared to 90 μ sec. at the NT. The Loop #3 NT results conform with Loops #4 and #2; however, the LT results are evidently a consequence of the multitude of bridge taps in the loop.

FIGURE 13

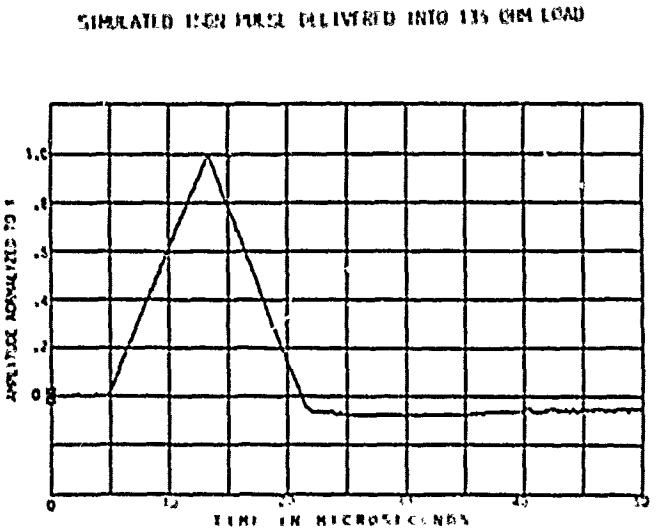

FIGURE 14

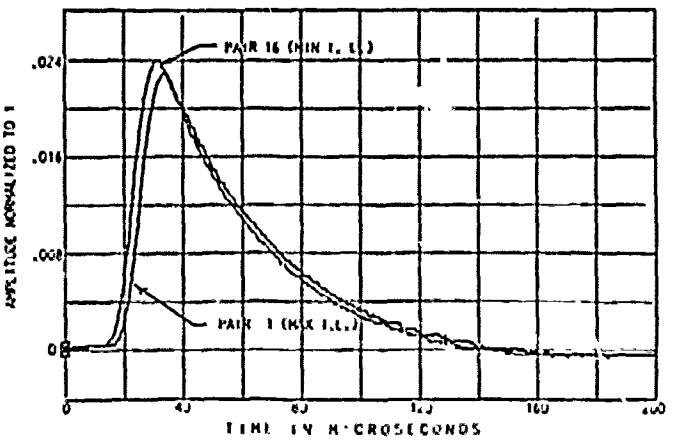

FIGURE 15

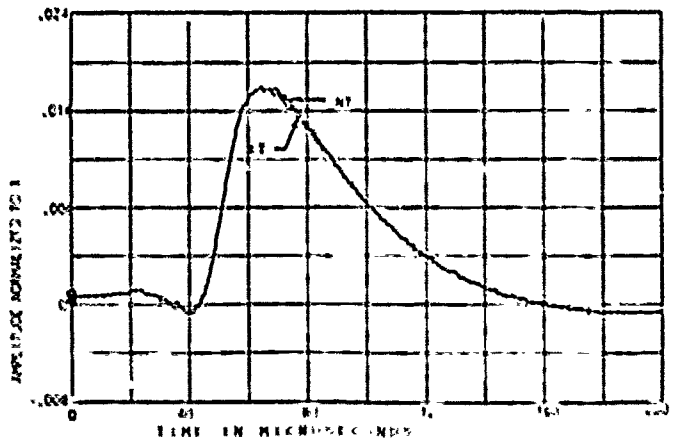

FIGURE 16

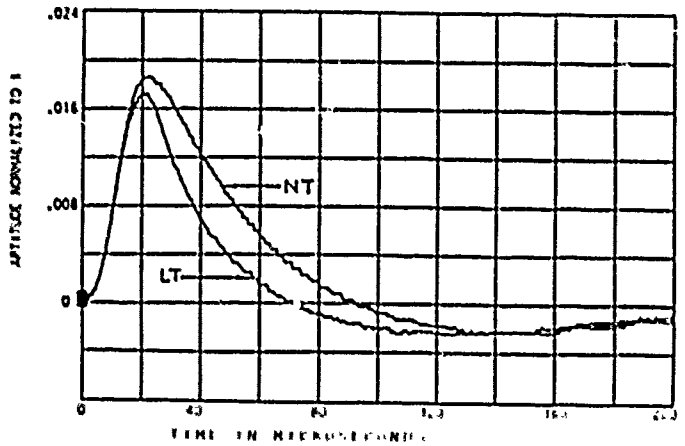

V. CONCLUSION

The premise of this paper was to investigate outside plant metallic cables as the DSL in the ISDN BRI. The ANSI standard, T1.601-1988 served as the infrastructure for our study. Three loops were explored embracing simple, intermediate and complex configurations comprised of various loop lengths, mixed gauges and bridge taps. Using primary parameters tabulated in the ANSI standard, a theoretical analysis paralleled test data.

The testing included primary parameters, insertion loss, complex impedance, crosstalk (PS-NEXT) and pulse response. Calculated values for dc resistance, capacitance, insertion loss and impedance exhibited excellent correlation to the measured data. In addition, models were developed, whereby the effects of bridge taps could be determined for insertion loss and impedance.

This paper is an initial step toward defining the metallic DSL for the ISDN BRI. A subsequent evaluation concerning the ISDN PRI may also be warranted. As three representative loops were investigated, a study of all fifteen loops designated in ANSI T1.601-1988 may provide additional insight. Moreover, field evaluations may uncover further valuable information not discovered in our laboratory study. The attenuation and complex impedance models can serve as beneficial tools for equipment and network designers developing the ISDN. Furthermore, the data supply a body of knowledge which can be consulted for the implementation of the ISDN. Overall the calculations and data provide insight into a metallic DSL for the ISDN BRI. However, further analysis is required, especially concerning impulse noise and possibly bit error rate which were not included in this paper. Moreover, the data reveals that complex impedance and pulse response necessitate further review as they are significantly affected by the loop configuration and will, therefore, impact the ISDN.

VI. ACKNOWLEDGEMENTS

The authors wish to thank A. Oprotkowitz and J. A. Olszewski of the General Cable Research and Development Laboratory for their support concerning various aspects of this work.

REFERENCES

1. Ahamed, Syed V., Peter P. Bohn and N. L. Gottfried. "A Tutorial on Two-Wire Digital Transmission in the Loop Plant". IEEE Transactions on Communications. Vol. COM-29, No. 11, Nov. 1981, pp. 1554-1564.

2. Bass, Charlie and Paul Berkowitz. "What Does ISDN Compatibility Really Mean". TPT/Networking Manager. Dec. 1988, pp. 29-35.

3. Braue, Joseph. "Will the Local Loop Choke ISDN" Data Communications. October 1988, pp. 73-78.

4. Characterization of Subscriber Loops for Voice and ISDN Service (1983 Subscriber Loop Survey Results). ST-TSY-000041, Bellcore, June 1987.

5. Deming, Robert, et. al., "ISDN - Bellcore's View", Bellcore 1987.

6. Eager, G. S., et. al., "Transmission Properties of Polyethylene Insulated Cables at Voice and Carrier Frequencies", Communications and Electronics, November 1959.

7. Gantz, John, "Standards: What They Are, What They Aren't," Networking Management. May 1989, pp. 23-34.

8. Generic Requirements for Metallic Telecommunication Cables, TR-TSY-000421, Bellcore, Issue 2, June 1988.

9. Integrated Services Digital Network (ISDN) - Basic Access Interface for Use on Metallic Loops for Application On the Network Side of the NT (Layer 1 Specification), ANSI T1.601-1988, September 16, 1988.

10. Interface Between Carriers and Customer Installations - Analog Voicegrade Switched Access Lines Using Loop - Start and Ground - Start Signalling, ANSI T1.401-1988, January 17, 1988.

11. ISDN Basic Access Digital Subscriber Lines, TR-TSY-000393, Bellcore, Issue 1, May 1988.

12. ISDN Basic Access Line Testing Requirements, TA-TSY-000783, Bellcore, Issue 1, August 1988.

13. ISDN Primary Rate - Customer Installation Interfaces (Layer 1 Specification), Draft ANSI Standard, ECSA TIE/89-046, May 1989.

14. King, Ronald W.P., Transmission Line Theory, New York: McGraw-Hill, 1955.

15. Morocco, Thomas D., "ISDN Implementation Over Copper Cables", Telephone Engineer and Management, December 1, 1986, pp. 56-57.

16. Proceedings from the International Symposium on Subscriber Loops and Services, Boston, September 11-16, 1988.

17. Seshadri, S. R., "Fundamentals of Transmission Lines and Electromagnetic Fields", Philippines: Addison-Wesley, 1971.

18. Singh, Ram R. P., "The Last Bell System Subscriber Loop Survey", Telephony, October 5, 1987, pp. 32-37.

19. Specifications for a Metallic Test Access Link, TA-TSY-000096, Bellcore, March 1986.

20. Stallings, William, Data and Computer Communications, New York: Macmillan, 1985.

21. Stallings, William, Integrated Services Digital Network (ISDN), Washington, D.C.: IEEE Computer Society Press, 1985.

22. Stewart, Alan, "A User's Guide to ISDN Standards", Telecommunications, May 1988, pp. 34-44.

23. Stine, Larry L., "Why Are ISDN Standards Important", IEEE Communications, Vol. 26, No. 8, August 1988, pp. 13-14.

24. Walker, Hugh, "Testing Future Telecom Networks", TE&M, November 1, 1988, pp. 72-76H.

APPENDIX A

Controller: HP Series 310

Digital Multimeter: Keithly 197

Digitizing Oscilloscope: HP 54201A

Impedance/Gain - Phase Analyzer: HP 4194A

Pulse Generator: Data Dynamics 5109

Pulse/Function Generator: HP 8116A

Russell C. Pepe, RCDD, received a BSEE from New Jersey Institute of Technology (NJIT) in 1977, and is currently completing a MSEE from NJIT. He is a member of the Building Industry Consulting Service International (BICSI); Iota Beta Sigma, a broadcasting honor society; the Institute of Electrical and Electronics Engineers (IEEE); the Order of the Engineering and the Optical Society of America (OSA). Russell has lectured at universities and technical conferences, provided seminars and published articles on various subjects related to communications. He is active in ISDN and cable standards activity through the ECSA T1 Committee, the EIA/TIA TR-41 Subcommittee and the NIST NIU-Forum. As a Senior Application Engineer for General Cable Company in New Jersey, Russell is responsible for copper and fiber optical cable technical support.

Jeff Poulsen is a Senior Research Engineer at the General Cable Research and Development Laboratory in Edison, New Jersey. He received his Bachelor's Degree in Electrical Engineering from New Jersey Institute of Technology (NJIT) in 1981. Jeff has helped in the development of products for General Cable Company and has been coauthor to several related patents. Currently, his responsibilities include the development of automated measurement techniques for the characterization of the electrical properties of cables, and the processing and analysis of cable related data.

Loop Survey in Taiwan and Some Follow-Up Proposals for ISDN Basic Rate Access

Wu-Jhy Chiu, Ming-Jung Wu
Wen-King Huang, Guy-Fen Luh

Telecommunication Laboratories
Directorate General of Telecommunications
P.O. Box 71 Chung-Li, Taiwan, ROC

ABSTRACT

About 2,800 lines out of a total of 8,500,000 ones in the whole Taiwan area have been sampled and characterized. Various kinds of physical compositions and transmission characteristics are investigated and measured respectively. Based on these statistics, the loop transmission capability on ECM and TCM schemes is evaluated. After studying the loop characteristics, some follow-up actions that may make the 2B+D transmission environment better are proposed. In this paper, we also present several important loop characteristics and give some general comments at the end.

1. INTRODUCTION

DGT (Directorate General of Telecommunications, ROC) has set ISDN as the ultimate goal for the instruction of telecommunication network at the end of 20th century. As a 2B+D transmission medium, the subscriber loop plant imposes severe noise constraints. Bridged taps (BTs), capacitance unbalance, mixture of underground, aerial and customer premises cables and multiplicity of gauge pairs and counts also contribute to inevitable transmission impairments.

To evaluate whether the existing subscriber lines have 2B+D bi-directional transmission capability over a satisfactory range. A loop survey odel was first established in Chung-Li in 1986 by TL (Telecommunication Laboratories), an R&D organization of DGT. Then the model was applied to the whole Taiwan in 1986-1988 by DGT's three district operating companies, i.e., NTTA (Northern Taiwan Telecommunication Administration), CTTA (Central Taiwan Telecommunication Administration), and STTA (Southern Taiwan Telecommunication Administration).

There are around 8,500,000 subscriber lines in the whole Taiwan. By using a double-stratified, two-stage random sampling method, 2,805 lines were sampled. Then the physical compositions were investigated and the transmission characteristics were measured.

We built a database with about 800,000 records of source data from these 2,805 lines and developed an interactive, user-friendly software package to perform the loop statistics. The loop statistics contains two parts: (1) physical compositions, including percentage of loading cable, working length, bridged tap configurations, etc., and (2) transmission characteristics, including loop resistance, insulation resistance, line loss, return loss, line unbalance, induced noise, NEXT (Near-End Crosstalk), FEXT (Far-End Crosstalk), impulse noise, etc. All these statistics can be illustrated in graphical and tabular forms, and some of them will be presented later in this paper.

Based on these statistics, the loop transmission capability in terms of various parameters such as line loss, loop resistance, crosstalk, etc., are calculated. The calculation results for ECM and TCM transmission schemes are compared. After loop survey, a loop test laboratory is built, and some follow-up actions are proposed.

The sampling plan is briefly described in section II, and the physical characteristics of the loop are presented in section III. Section IV shows the transmission characteristics of this survey. 2B+D transmission capability evaluation is reported in section V. Some follow-up proposals for better 2B+D transmission environment are given in section VI and finally some concluding comments will be given.

2. SAMPLING PLAN

Considering :
- Timesaving, economic and accurate.
- Geographical characteristics, i.e.,

metropolitan, suburban and rural areas.
- Administration territories, i.e., three district operating companies in Taiwan.

Several sampling methods had been carefully studied [1], and a double-stratified two-stage random sampling scheme was finally chosen. By using the data from Chung-Li loop survey [2] and from reference [1], we obtained the total number of sample lines for loop survey in the whole Taiwan. The number was 2,805.

Under DGT, there are three district operating companies in Taiwan. From the viewpoint of administration, we need three separate loop statistics for each of three administrations, this is the first stratum

Metropolitan, suburban and rural areas may differ from one another very much in loop distribution and hence their characteristics may be different greatly too. From the deployment strategy point of view, we decided to have the loop statistics for these three different categories of geography, this is the second stratum.

There are 35 central offices (COs) and 2,594,900 subscriber lines in metropolitan Taipei area, 43 COs and 991,200 lines in suburban areas, 70 COs and 286,200 lines in rural areas, as shown in Table 1.

In the 1st stage of random sampling, we sampled the central offices from all COs in each geographical category with the probability proportional to the line population of each central office. For example, there are 35 COs in metropolitan Taipei area, 20 ones out of 35 were sampled [1].

The total number of sample lines in each geographical area are proportional to its population size, for example, from Table 1, we got 860 sample lines out of 2,805 for metropolitan Taipei area as shown in Table 2.

In the 2nd stage, the same number of subscriber lines are randomly sampled from each selected COs, thus, in metropolitan Taipei area, 43 lines were randomly selected from each of 20 COs, as shown in Table 2.

Similarly, we obtained the sample COs and lines in CTTA and STTA. The total sample central offices in whole Taiwan are 198. All the sample lines were picked up from all the existing line population.

One of the most important features of double-stratified two-stage random sampling method is that we can straightforwardly obtain various kinds of loop statistics, such as statistics for overall Taiwan, for NTTA only, for overall rural areas, even for metropolitan Taipei area only. In this paper, due to the space limitation, only some statistics are presented.

3. PHYSICAL CHARACTERISTICS

Physical characteristics investigated in this survey include number, length and position of bridged taps (BTs), percentage of loading and out-of-service, working length, wire gauge, type of splicing, etc. Some of them will be reported in this section.

3.1 Loading

Only 121 sample pairs out of 2,805 were found loaded, this is equivalent to 4.3%.

3.2 Working Length

Fig.1 shows the cumulative distribution function (CDF) for working length of 2,503 sample lines in different geographical areas. The estimated overall mean working length from the central office to the subscriber end is 1,865m with 90% probability that the true mean value lie within 1,865m+/-90m, the figure also shows that about 97% loops of overall Taiwan have the length less than or equal to 4.5Km.

3.3 Bridged Tap (BT)

In this survey, we found that about 65% of all sample subscriber lines were with BTs. The other statistics include the number, the length and the position of BTs. The statistics of tap number of 2,805 sample lines are shown in Table 3.

It is noted [3] that the BT with length shorter than 350m causes little forward echo for ECM (Echo Cancellation Method) system with 2B1Q code. Statistics indicate that in the whole Taiwan only 69% of BTs are with lengths less than 350m. Reference [4] shows that BTs will cause very little backward echoes when their positions are away from the signal source more than 250m. Most BTs are far away (>250m) from the COs or subscriber ends as shown in Fig.2. It shows the BTs tend to be more concentrated near the subscriber ends, that means, much severe backward echoes will appear in the subscriber ends.

4. TRANSMISSION CHARACTERISTICS

Transmission characteristics measured

in this survey include DC/AC voltage, loop resistance, line loss, return loss, induced noise, NEXT, FEXT, line unbalance, insulation resistance, impulse noise, etc. Most of them will be presented in this section.

4.1 Loop Resistance

The statistics of loop resistance are shown in Fig.3. The overall mean loop resistance is 489ohms with standard deviation of 290ohms.

4.2 Line Loss

Line losses at various frequencies were measured and shown in Fig.4. Line losses at 40KHz, 60KHz, 80KHz and 160KHz are most interesting. Fig.5 shows the statistics in terms of different geographical areas at 80KHz and Fig.6 gives the overall statistics at the four different frequencies.

4.3 Induced Noise

As far as induced noise is concerned, the interference from AC power is most important, this is because 2B1Q code consists of DC and low frequency components. Table 5 illustrates the percentage that our loop statistics meet the ANSI (American National Standards Institute) requirements [5].

4.4 Near-End Crosstalk

The crosstalk coupling losses are measured by pair to pair method, about 70% pair combination of induced and inducing lines are within the same quad or between the adjacent quads. Frequency characteristics of overall NEXT loss are shown in Fig.7. The distribution characteristics at 80KHz are illustrated in Fig.8. Fig.9 gives the overall statistics at four different frequencies.

4.5 Far-End Crosstalk

Similar to NEXT loss characteristics, Fig.10 shows the frequency characteristics of FEXT loss, Fig.11 illustrates the overall statistics at four different frequencies. Fig.12 gives the statistics at 80 KHz. Fig.7 and Fig.10 reveal that the standard deviations of NEXT and FEXT losses of our loops are rather too high. It is noted that 100-pair unit structure star quad cable is used in Taiwan.

4.6 Line Unbalance

Line unbalance and insulation resistance are important parameters, since they account for the origins of noise. Fig.13 shows the cumulative distribution of overall statistics for line unbalance at four different frequencies.

4.7 Insulation Resistance

Table 4 shows the statistics of insulation resistance between the line and earth (L1-E, L2-E) as well as line 1 and line 2 (L1-L2).

5. PERFORMANCE EVALUATION

ECM with 2B1Q code, ECM with MMS43 code and TCM with AMI code are the most promising techniques to be implemented in 2B+D NT1 [5] [6] [7]. In this section, the performance of these three schemes on our loops will be evaluated.

Any pair in a cable may equally likely be chosen as a 2B+D circuit and will be subject to crosstalk interference from its neighbors. The performance evaluation models used in this paper are shown in Fig.14.

It has been shown that bit error ratio (BER) of 2.4×10^{-7} on digital subscriber loop can meet the error performance recommended by CCITT G.821. Therefore it is reasonable to set BEP at 10^{-7} for 2B+D loop transmission. Table 6 illustrates the parameters required for each of ECM (2B1Q), ECM (MM43) and TCM (AMI) transmission methods, including the required signal to noise ratio (S/N) at BER=10^{-7}.

In addition to the parameters shown in Table 6, the following assumptions are made to evaluate the transmission capability :

(1) Equal probability of "1" and "0" before line coder, thus equal probability of every voltage level in 2B1Q and MMS43 system will be achieved.

(2) By using the pair-to-pair crosstalk loss statistics in section 4.4 and 4.5, total crosstalk loss from nearby multiple interfering sources into the interfered pair, so called multiple crosstalk, is approximated by Gamma distribution model [8].

(3) 99% of the active 2B+D lines will be with the performance equal or better than BER=10^{-7}.

(4) Raised-cosine channel shaping with roll-off factor of 1 is assumed.

(5) Local power for ECM (2B1Q) transceiver is understood.

(6) System margin of 9 dB for all methods is assumed. It is supposed

that this margin is for all the uncertainty such as impulse noise, drop-out, imperfect circuit design, intersymbol interference, aging, etc.

Taking into account the parameters shown in Table 6 and based on the above assumptions and referred to the model shown in Fig.14, the limitation of transmission distance or the line loss required can be calculated by the following equations :

$$(S/N)_{fxt} = X_{fxt} + 10\log(1/\int_0^\infty P(f)(f/f_0)^2 \cdot 10^{-L(f)d/10} |S(f)\cdot E(f)|^2 df) - 10\log(d/d_0) \quad \ldots\ldots (1)$$

$$(S/N)_{nxt} = X_{nxt} + 10\log(1/\int_0^\infty P(f)(f/f_0)^{1.5} |S(f)\cdot E(f)|^2 df) \quad \ldots\ldots (2)$$

X_{fxt} : Multiple FEXT loss (dB) at 1% worst point by Gamma model
X_{nxt} : Multiple NEXT loss (dB) at 1% worst point by Gamma model
$P(f)$: Power spectrum of disturbing source
$S(f)$: Fourier transform of a single sending pulse, depending on the duty cycle of line code
$L(f)$: Cable frequency response, dB/Km, proportional to $f^{0.5}$
d : Working length, Km
f_0 : Reference frequency (Nyquist rate of line signal) for crosstalk loss measurement
d_0 : Reference line length (1Km) for crosstalk loss measurement

From Eq(1), we can calculate the maximum permissible working length for TCM method in terms of the number of interfering sources, and from the statistics of working length in Fig.1, we can find the coverage percentage of 2B+D service in various geographical areas for TCM (AMI) system.

From Eq(2), we can obtain the maximum allowable line loss for ECM method in terms of the number of working systems, and from Fig.5 and Fig.6, we can get the coverage statistics for different geographical areas on ECM (2B1Q) and ECM (MMS43) systems.

Table 7 gives some of the evaluation results. It can be expected that the performance in metropolitan areas would be better.

Fig.15 shows the overall transmission capability in terms of working distance and the number of working systems. It is noted that in the beginning stage of ISDN deployment, the limitation of TCM system is loop resistance.

6. FOLLOW-UP PROPOSALS FOR BETTER TRANSMISSION ENVIRONMENT

The results of loop survey and transmission capability evaluation disclose that satisfactory 2B+D transmission is a severe challenge to our existing loops. To make the transmission environment better for 2B+D signal in Taiwan, some measures are proposed in this section.

6.1 Pair Selection

On the premise that only some pairs of the 100-pair unit in a cable will be used to provide the 2B+D circuits, then the pair selection is proposed. The pair selection is a first-aid approach.

From section 4.4 and section 4.5, it is clear that the crosstalk loss characteristics are rather too low, when compared to NTT'S subscriber loops [7]. Crosstalk between the same quad pairs and between the adjacent quad pairs always tends to demonstrate the severest NEXT and FEXT characteristics. We propose two methods of pair selection :

(1) Prearrangement
Only pairs which are one adjacent quads apart will be selected, accordingly, only a total of 23 pairs in a 100-pair unit can be preassigned.

(2) Selection by measurement
Prearrangement method is attractive and good for the case of low pair utilization ratio. Selection by measurement means to select the qualified pair by measuring the crosstalk from the pairs of adjacent quads and the same quad.
The basic idea is that for crosstalk loss statistics, there always exists an abrupt descent near the 1 2% tail region, as shown in Fig.9 and Fig.11, the CDF of this tail region is about 1 2%.
By this method, the worst fraction of cable pairs can be identified, thus worst 1% or 2% of pairs can be discarded.

6.2 Bridged Tap Removal

Bridged Taps cause Forward and Backward echoes as stated in section 3.3. Since it is quite difficult to remove the BTs in the field, therefore, we propose that only after the pair selection approch is processed, and only the BTs that contribute the noticeable echoes be

removed.

6.3 New Cable Specification

DGT began to install FS (Foam-Skin) plastic quad cable instead of paper cable in 1985 for subscriber loops, and no more new paper cable has been installed since then. The crosstalk performance of FS and paper cables has been studied all the time [9] [10]. Recent study [11] shows that the crosstalk performance of our new FS cable cannot meet the loops specified by DGT in the "Basic design practice for local loop" [12], when serving 2B+D service.

From the DGT's design practice, we calculate the possible maximum line loss and DC resistance, and we find that only ECM (2B1Q) can serve all the FS cable loops in the condition that 99-pair NEXT loss at 1% worst point be less than 62 dB at 40 KHz.

Local cable manufacturers were asked to improve their fabrication process, and two of them have successfully fabricated the qualified cable. Fig.16 shows the before and after improvement.

6.4 New Installation Practice

(1) "OK/NG" for pair selection
Once a line is assigned to be a 2B+D circuit, we had better to check if its crosstalk performance is good enough before an NT1 is installed. Since crosstalk characteristics are very difficult to measure in the field. therefore, an "OK/NG" method is proposed by using much easier capacitance unbalance measurement to qualify the selected line in the field.
The correlation between crosstalk loss and capacitance unbalance were studied, Fig.17 shows how NEXT loss can be closely estimated by the capacitance unbalance. If the NEXT loss criterion of an assigned line is 55 dB at 40 KHz for the adjacent quads and same quad, then the line will be "OK", if all values of capacitance unbalance between (a) the assigned pair and the same quad pair, and (b) the assigned pair and the adjacent pairs are smaller than 120pF/500m. Here, 120pF is chosen for safe reason. It takes no more than 15 minutes to finish the measurement and only one technician with a compact portable measurement set is required.

(2) Sealing current
The twist splice is a unique feature of our subscriber lines. Drop-out due to twist splicing can be improved by sending a sealing current continuously.

(3) Splicing by connector or welding
By connector or welding, the cable can be permanently spliced with very small splicing resistance, and this prevents the drop-out.

(4) No BTs for newly installed cable
By introducing distribution box, the BTs can be eliminated without sacrificing the pair utilization and hence no more echoes will happen.

(5) Digital loop carrier
Digital loop carrier is the most promising technology to serve the out-of-range customers, with fiber as feeder, the Narrow-band ISDN (N-ISDN) can be smoothly evolved to Broad-band ISDN (B-ISDN).

6.5 Loop Test Laboratory

After loop survey, a loop test laboratory was established in TL. Every kind of loop configurations in the field can be emulated in the laboratory, no matter how it is composed. Similar to Bellcore's standard test lines [13], a set of 15 lines representing the unique loop environment of Taiwan are also established in the laboratory, so that the 2B+D transceivers can be really qualified.

7. CONCLUSION

The loop survey in the whole Taiwan for ISDN 2B+D transmission is reported in this paper. The performance of ECM (2B1Q), ECM (MMS43) and TCM (AMI) has been evaluated. The evaluation result shows ECM with 2B1Q code is most attractive. From the viewpoint of DGT's loop design rule, ECM (2B1Q) gives another merit. In this paper, we also show that the metropolitan areas are much easier to provide the 2B+D service. Some follow-up proposals have been discussed, and we believe all of these measures may make our transmission environment better for 2B+D signal.

8. ACKNOWLEDGMENTS

We would like to express our sincere appreciation to Mr. P.Y. Lee, Dr. S.C. Lu, and DGT's engineers who have given us numerous advice throughout this work. Thanks are also extended to the engineers of NTTA, CTTA, STTA and our fellow colleagues for their valuable advice and assistance.

9. REFERENCE

[1] G.J. Jaw, W.J. Chiu and M.J. Wu, "A Random Sampling Model for Subscriber Loops in Taiwan", Proceedings of 1986 Telecommunication Symposium, Dec. 1986, ROC, pp.267-271.

[2] W.J. Chiu, M.J. Wu and R.Y. Chen, "A subscriber Loop Survey for ISDN Basic Access" ICCS Nov. 1988 pp.7.7.1-7.

[3] Bell-Northern Research, "Digital Transmission Systems for ISDN Basic Access", CCITT Study Group XVIII Contribution, D.239/XVIII.

[4] R.Y. Chen, "A Computer Simulation Study of Transmission Characteristics of Subscriber Loop with Bridged Taps", Telecommunication Laboratories internal report, June 1986.

[5] "ISDN Basic Access Interface for Use on Metallic Loops for Application on the Network Side of the Layer 1 Specification", American National Standard for Telecommunication ANSI T1, XXX-1988.

[6] K. Szechenyi, F. Zapf, D. Sallaerts, "Integrated Full-Digital U-interface Circuit for ISDN Subscriber Loops", IEEE SAC-4, No.8, Nov. 1986 pp.1337-1349.

[7] R. Komiya, K. Yoshida, and N. Tamake, "The Loop Coverage Comparison Between TCM and Echo Canceller Under Various Noise Considerations", IEEE Trans. Commun., Vol. COM-34, No.11, Nov. 1986, pp.1058-1067.

[8] Nobuo Tomita "Study on Estimation Method of Multiple crosstalk loss for balanced cable", IEICE Technical Report 85/9, Vol. J68-B No.9 pp.1079-1080.

[9] Sammy Siu, W.J. Chiu, "Crosstalk consideration for metallic digital subscriber lines", Telecoms. Technical quarterly, Vol.4, No.3,4, May 1985, pp.313-327.

[10] W.J. Chiu, Sammy Siu, B.Y. Jaw, "Crosstalk performance of MS43 and bipolar (AMI) codes for ISDN basic access", ICC 1987, pp.308-313.

[11] C.L. Yang, W.K. Huang, "Crosstalk requirement for FS cable", Telecommunication Laboratories internal report, April 1988.

[12] DGT, "Basic design practice for local loop", 75-20-401(1), Jan. 1986.

[13] R.A. MC Donald, "Suggested Testing Plan to Determine Line Code Performance" T1D1. 3/86-095.

APPENDIX 'A

Fifteen Standard Test Lines for DGT's Loop Plants

After loop survey, we found that 2503 lines out of 2,805 samples were good for configuration study. We define the loop power loss (LPL) as follows :

$$LPL\ (dB) = [\int_0^{\infty}(1/4)P(w)dw] \ / \ [\int_0^{\infty}P(w)H^2(w)dw]$$

where

P(w) : Power spectrum of transmitted signal
H(w) : Transfer function of loop

H(w) is a function of wire gauge, wire length, the length of BT, location of BT, number of BT, and etc. We derive the H(w) of each 2,503 lines, and then calculate the LPL for 2B1Q signal.

After sorting the 2,503 lines by the magnitude of the LPL, we choose 15 lines from the worst 15% of them, in other words, among 2,503 lines, we first pick up the worst 375 lines, then 15 lines from 375 ones are selected according to the following rules:

(1) Representative of various configurations.

(2) One pair in 1% of 2,503 lines.

Thus, 15 pairs are selected and shown in Fig. A.

Table 1 Population distribution in NTTA

TOTAL	NTTA	AREA	CO	REMARK
8,466,800 (Note)	3,872,300	2,594,900	35	Metropolis
		991,200	43	Suburb
		286,200	70	Rural
Note : Including NTTA, CTTA, STTA				

Table 2 Sample Distribution in NTTA

TOTAL	NTTA	AREA	CO	SAMPLES	Remark
2805	1278	860	20	43	Metropolis
		322	23	14	Suburb
		96	32	3	Rural

Table 3 Statistics for the number of BTs

Tap number	0	1	2	3	≥4
Percentage	35%	41%	17%	4%	3%

Table 4 Overall Statistics of the Insulation Resistance

Sample	2503		
MΩ / % / Item	<5Ω	5Ω | 55Ω	>55Ω
L1 - L2	2.28	11.19	86.53
L1 - E	2.68	8.51	88.81
L2 - E	2.72	8.99	88.29

Table 5 Overall Induced Noise Statistics

Sample	2396		
Frequency	60Hz	180Hz	300Hz
ANSI RQMT	-47dBm	-49dBm	-59dBm
Percentage	99.88%	99.84%	99.72%

Table 6 Design parameters of different 2B+D transceivers

Method	Line code	Line rate	Line loss	S/N	Loop Resistance
ECM	2B1Q	80 KBauds	42dB(40KHz)	23.99dB	NA
ECM	MMS43	120 KBauds	40dB(80KHz)	20.43dB	900Ω
TCM	AMI	320Kb/s	50dB(160KHz)	20.46dB	812Ω

Table 7 Percentage statistics of 2B+D service coverage

GEOGRAPHY / PERCENT(%) / NO. OF SYS	METROPOLIS			SUBURB			RURAL			OVERALL		
	ECM 2B1Q	ECM MMS43	TCM AMI	ECM 2B1Q	ECM MMS43	TCM AMI	ECM 2B1Q	ECM MMS43	TCM AMI	ECM 2B1Q	ECM MMS43	TCM AMI
10	90	87	89	80	75	80	80	75	85	86	82	84
50	80	72	74	66	57	59	66	60	62	71	67	69
100	66	63	66	53	49	57	55	52	42	60	55	64

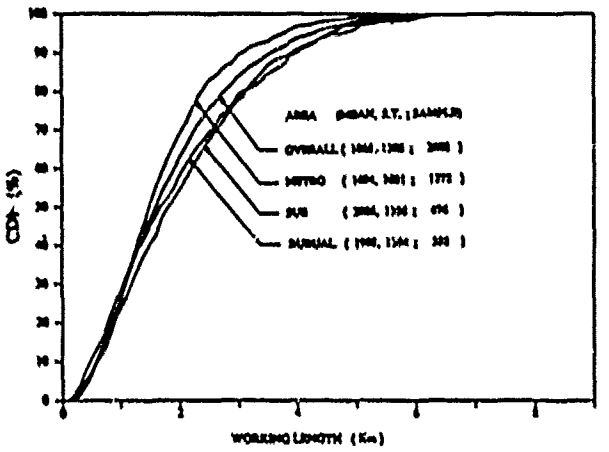

Fig.1 Distribution characteristics of the working length

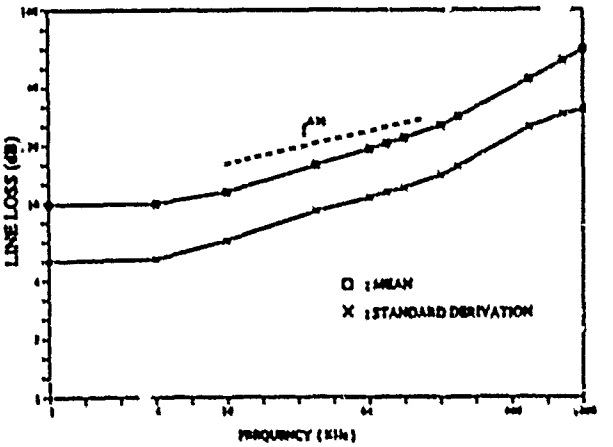

Fig.4 Frequency characteristics of the overall line loss

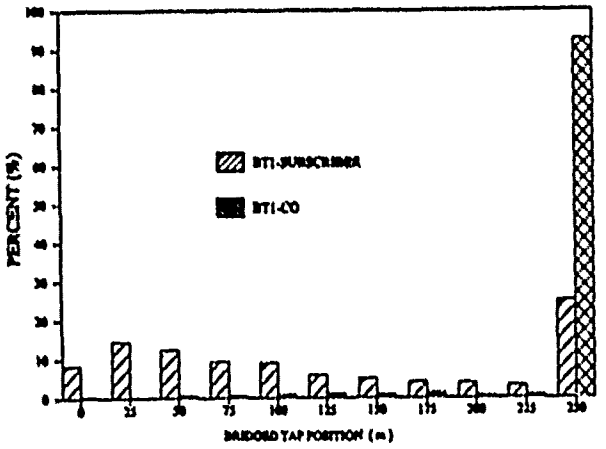

Fig.2 Distribution characteristics of the 1st bridged tap location

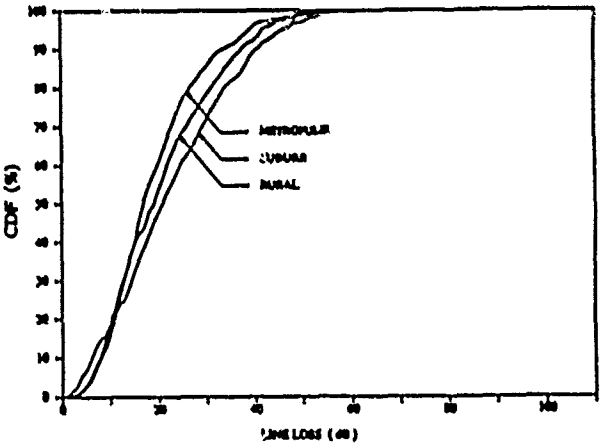

Fig.5 Distribution plots of the line loss at 80KHz

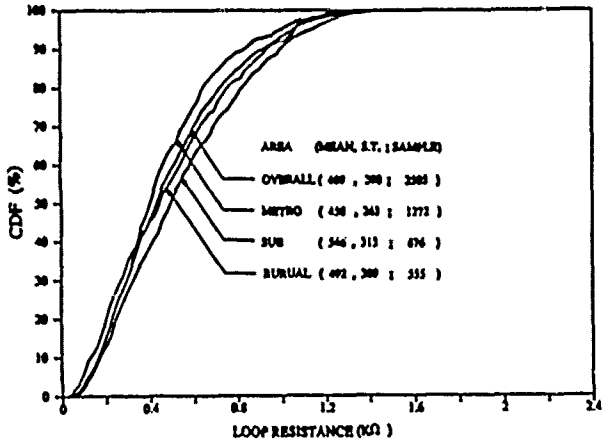

Fig.3 Statistics of the loop resistance

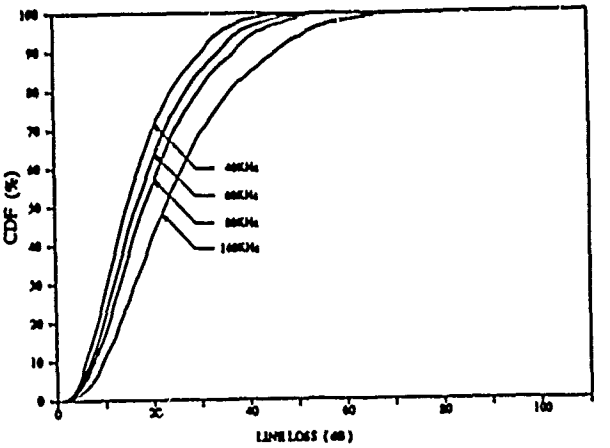

Fig.6 Distribution plots of the overall line loss

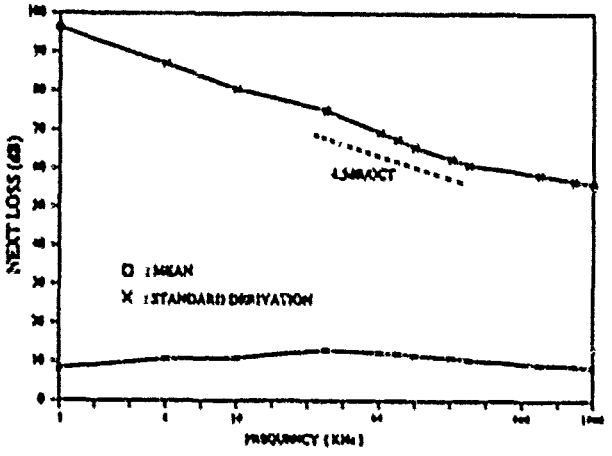

Fig.7 Frequency characteristics of pair-to-pair NEXT loss

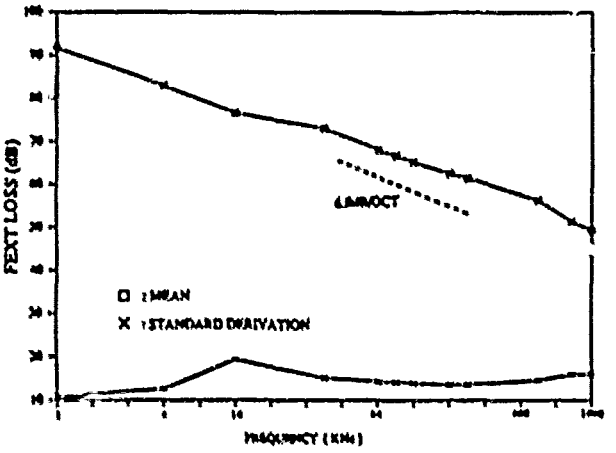

Fig.10 Frequency characteristics of pair-to-pair FEXT loss

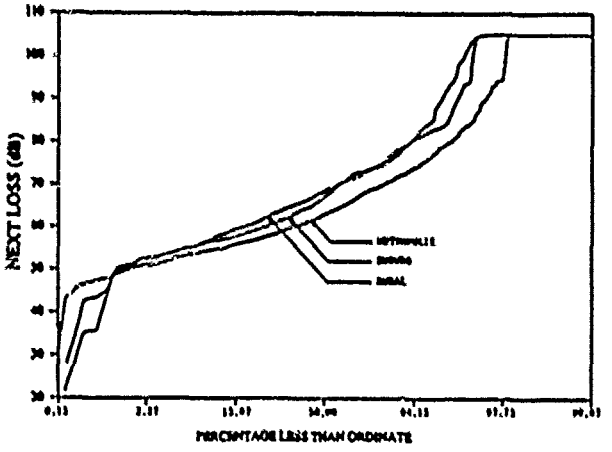

Fig.8 Distribution plots of pair-to-pair NEXT loss at 80KHz

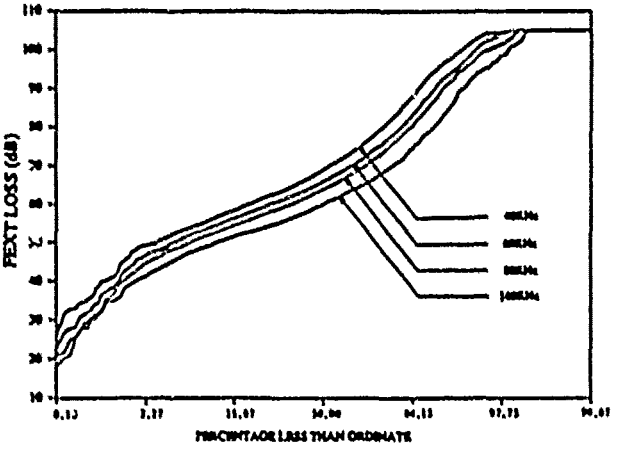

Fig.11 Statistics of the overall pair-to-pair FEXT loss

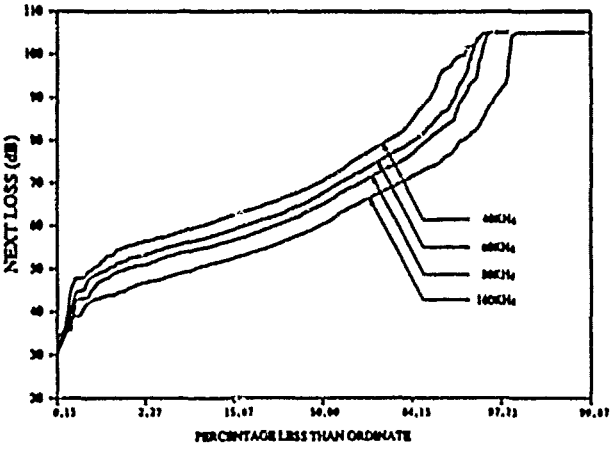

Fig.9 Statistics of the overall pair-to-pair NEXT loss

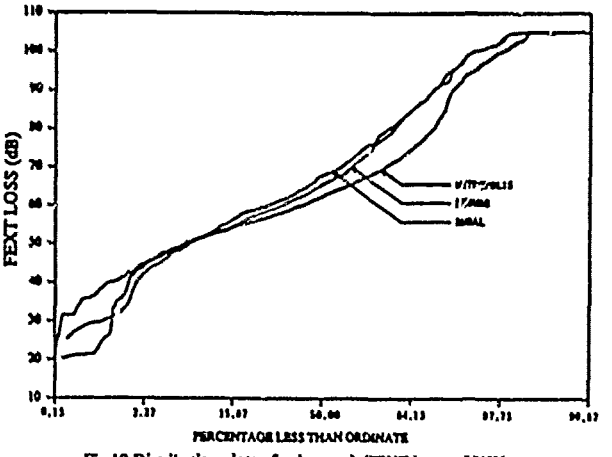

Fig.12 Distribution plots of pair-to-pair FEXT loss at 80KHz

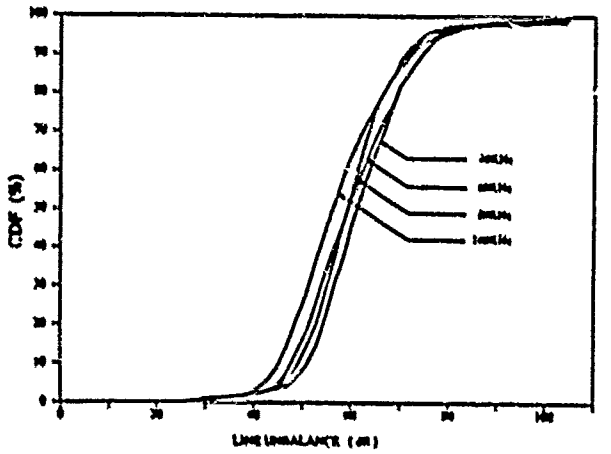

Fig.13 Characteristics of the overall line unbalance

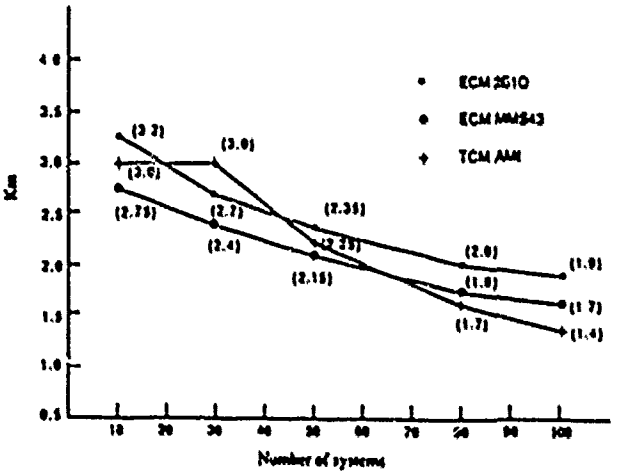

Fig. 15 Estimated performance capability of overall Taiwan

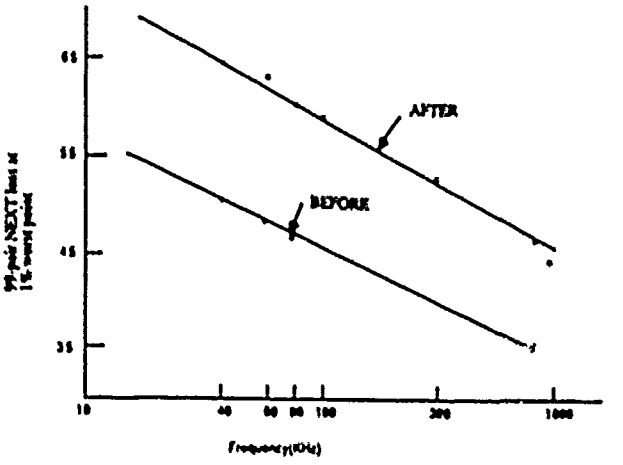

Fig. 16 NEXT characteristics of FS cable before and after improvement

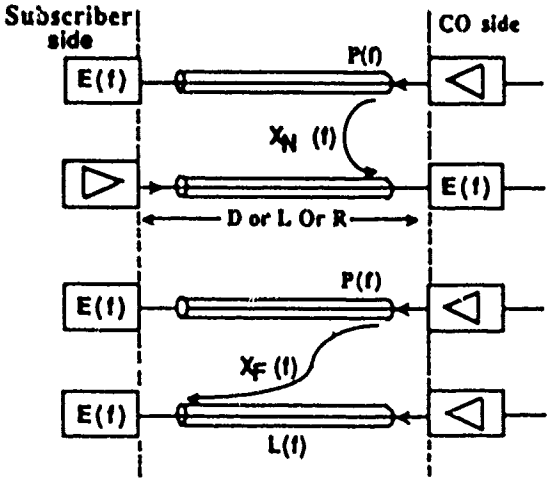

P(f) = Power spectral density of transmitted signal
L(f) = Cable frequency response
E(f) = Equalizer transfer function
$X_N(f)$, $X_F(f)$ = NEXT, FEXT transfer function
D = Working distance, Km
L = Total line loss, dB
R = Loop resistance, Ω

Fig. 14 Performance evaluation models for ECM(top) and TCM(bottom) systems

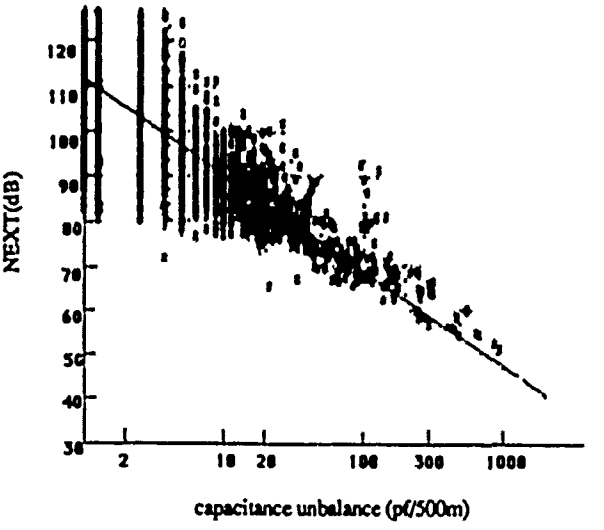

Fig. 17 Relationship between NEXT loss and capacitance unbalance

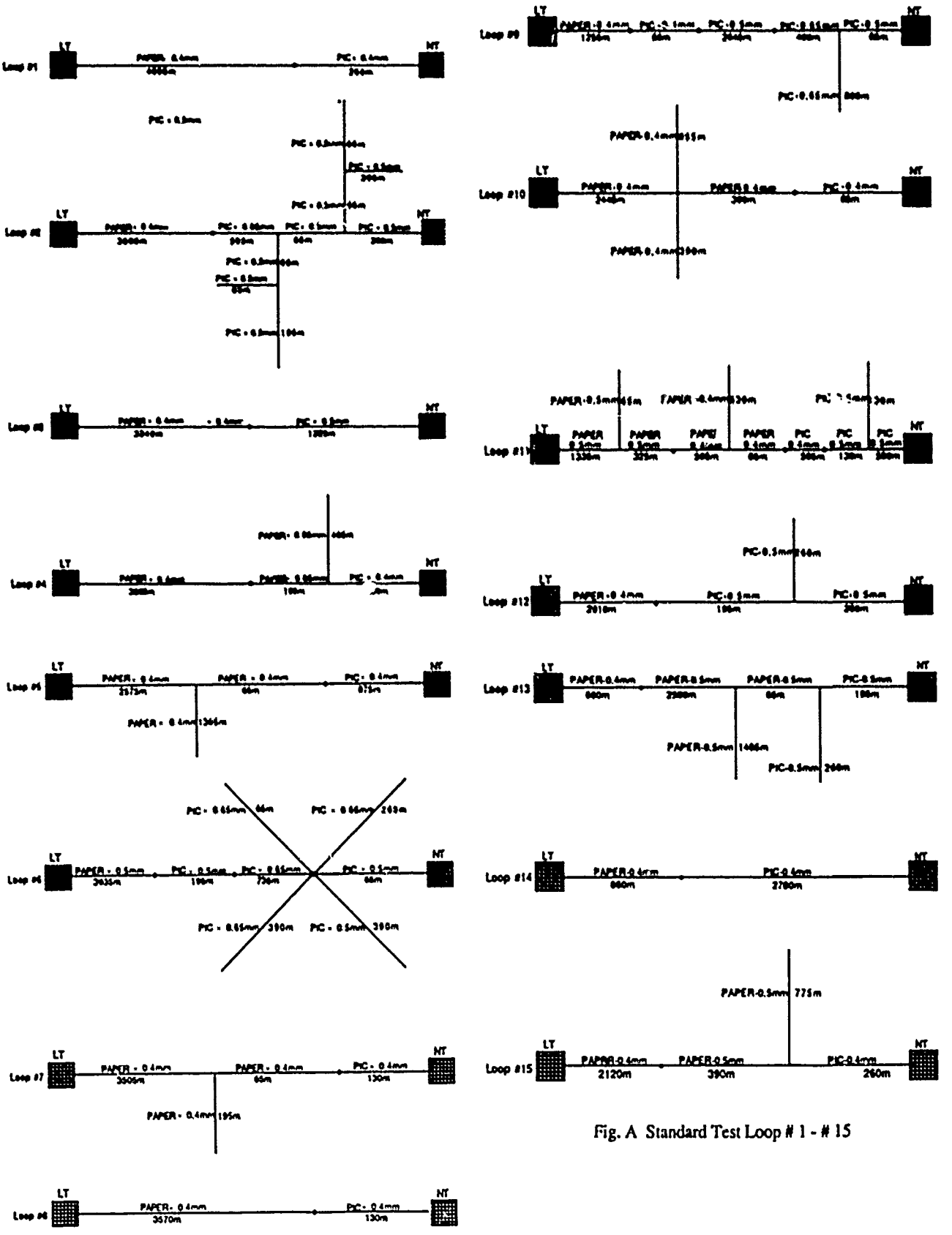

Fig. A Standard Test Loop # 1 - # 15

Wu-Jhy Chiu
System Technology Lab.
Telecommunication Labs.
P.O. Box 71
Chung-Li
Taiwan
R.O.C.

Wu-Jhy Chiu received his M.S. degree in Electrical Engineering from University of COLORADO in 1973 . He joined Telecommunication Lab. in 1969 and has been engaged in research and development of data transmission and digital transmission system . Mr. Chiu is now the director of System Technology Laboratory .

Wen-King Hwang
System Technology Lab.
Telecommunication Labs.
P.O. Box 71
Chung-Li
Taiwan
R.O.C.

Wen-King Hwang received his M.S. degree in Physics from CENTRAL UNIVERSITY in 1979 . He joined Telecommunication Lab. in 1981 and has been engaged in research and development of data and digital transmission system . Mr.Hwang is now a research scientist of System Technology Lab.

Ming-Jung Wu
System Technology Lab.
Telecommunication Labs.
P.O. Box 71
Chung-Li
Taiwan
R.O.C.

Ming-Jung Wu received his B.S. degree in Electrical Engineering from CHUNG YUN UNIVERSITY in 1978 . He joined Telecommunication Lab. in 1972 and has been engaged in research and development of data and digital transmission system . Mr.WU is now a project manager of System Technology Lab .

Guy-Fen Luh
System Technology Lab.
Telecommunication Labs.
P.O. Box 71
Chung-Li
Taiwan
R.O.C.

Guy-Fen Luh received her M.S. degree in Experimental Statistics of Agronomy from TAIWAN UNIVERSITY in 1987 .
She joined Telecommunication Lab. in 1988 and has been engaged in research and development of data and digital transmission system. Miss Luh is now a research scientist of System Technology Lab.

Leaky Coaxial Cables for Mobile Communication

by Helmut G. Haag, Günter Thönneßen and Karl Schulze-Buxloh

AEG KABEL Aktiengesellschaft
Mönchengladbach, Federal Republic of Germany

0. Abstract

This contribution describes a ... cable for mobile radio communication in ... tunnels and buildings. Out of a basic theo... consideration for those radiating cables the ... ciple of a new developed broadband leaky coaxial cable with a variety of small slots is described. The results in the frequency range from 50 to 900 MHz from a special measuring route are outlined. This leaky coaxial cable is based on a air-spaced dielectric, named bamboo-construction, which leads to low attenuation even at high frequencies. The contribution is finalised by considerations regarding the planning and erection of leaky coaxial cable routes.

1. Introduction

For communications between fixed and mobile subscribers normally radio links are used. The ongoing development of communications increases the demand for those communications between fixed and mobile subscribers at any point, even in tunnels. In tunnels especially in railway tunnels the propagation properties of radio waves at frequencies used for mobile communication are very unsatisfying. For longer tunnels therefore it is necessary to equip them with a separate radio link to enable an uninterrupted radio communication (Fig. 1). The critical tunnel length depends on the surroundings and the distance to the next radio link antenna but normally lays in the range of 400 to 500 m. The special support of tunnels by radio signals can be done by directive antenna before and inside the tunnel. But this is often not possible especially inside the tunnel. Therefore normally radiating cables are used [1].

For this, in the sixties acceptable results were reached with slotted coaxial cables. These slotted coaxial cables are open coaxial cables where a continuous longitudinal slot or separated holes are in no relation with the wavelength. Later in the development leaky coaxial cables with periodically ...paced radiation slots were investigated [2]. In ...his contribution we will report on newest results ...n new developed leaky coaxial cables.

2. Cable Design

Radiating cables have a coaxial design. They consist of a central conductor, a concentric insulating dielectric, an outer conductor which covers the insulation, and a final thermoplastic

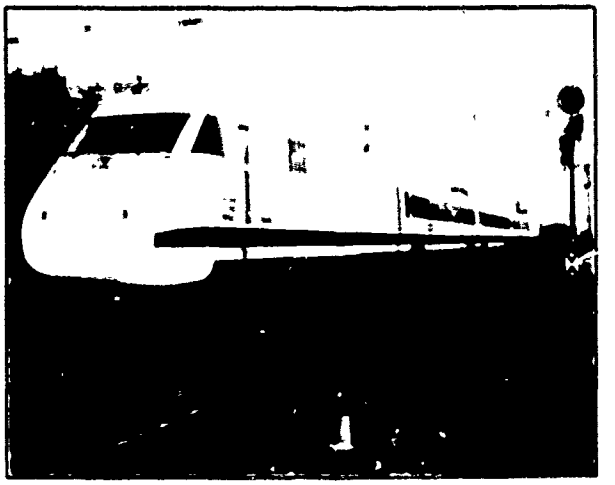

Fig. 1: High Speed train ICE

sheath. The characteristic impedance of the cable is normally 50 Ω.

The inner conductor is made of massive copper or for cables with larger dimensions made of copper-clad, which is a copper cladded aluminium wire, or a copper tube, to reduce weight and increase economy.

For the insulating dielectric a low dielectric constant is prefered to get low attenuation and also a broadband radiation characteristic. This can be realised by foamed polyethylene or by an airspaced dielectric in bamboo construction. With foamed polyethylene the polyethylene basic material is blown up with a large number of small airbubbles which are separated by thin cellular walls. By this it is possible, to reach a dielectric constant

between 1.3 and 1.5 depending on the degree of foaming.

In case of bamboo construction on the inner conductor in distances of a few centimetres polyethylene discs are placed. Over these discs a polyethylene tube of about 1 mm thickness is extruded. By this a system of air chambers is formed. The similarity of this chamber system over the inner conductor with bamboo led to the name "bamboo construction" for this type of insulation (Fig. 2). By the high portion of air in this dielectric the dielectric constant is in the range of 1.2 to 1.3.

To reach low attenuation at frequencies up to 900 MHz radiating cables must have large dimensions. The inner conductor has a diameter between 5 and 10 mm and to reach a characteristic impedance of 50 Ω the diameter over dielectric reaches 20 to 30 mm. Therefore the bending characteristic of the dielectric is of large importance. For both - foamed polyethylene and bamboo - this is realised.

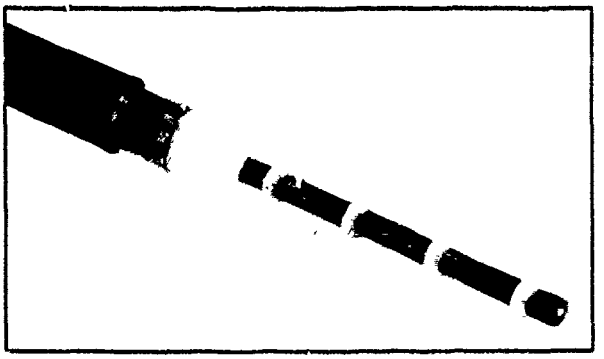

Fig. 2: Bamboo Dielectric

But the foamed polyethylene has only limited lateral stability. Lateral loading therefore can lead to permanent deformation. Moreover the foamed polyethylene is sensitive to humidity. For radiating cables, where the outer conductor is not totally closed the humidity can penetrate through the thin cellular walls into the dielectric. In long-term behaviour this results in an increase of the dielectric constant and therefore the attenuation increases.

The bamboo construction reaches a bending characteristic comparable to foamed polyethylene but has a much higher lateral stability. The air chamber system moreover is longitudinally and transverse watertight. The penetration of humidity through the tube of polyethylene is several decades lower than that through the thin walls of the foamed polyethylene.

For the outer conductor of radiating cables copper tapes are used. The copper tape is longitudinally formed around the dielectric as a tube.

For slotted coaxial cables the copper tape has a smaller width than the circumference of the dielectric. By this a longitudinal slot in the outer conductor results (Fig. 3 top). Also other constructions for slotted coaxial cables are known, where the outer conductor is a corrugated copper tube. By abrasing the peaks of corrugation along the cable axis short equidistantly spaced holes are formed in the outer conductor. The remaining copper sticks are very small and the hole distances are short compared to the wavelength. Such a row of holes behaves electrically like a homogeneous longitudinally slot in the outer conductor.

In leaky coaxial cables also copper tapes are longitudinally formed around the dielectric to a tube. In this outer conductor holes or groups of holes are punched which repeat periodically in longitudinal direction. The configuration of the holes with respect to shape, width and position within one period determines the radiating characteristic of the leaky coaxial cable.

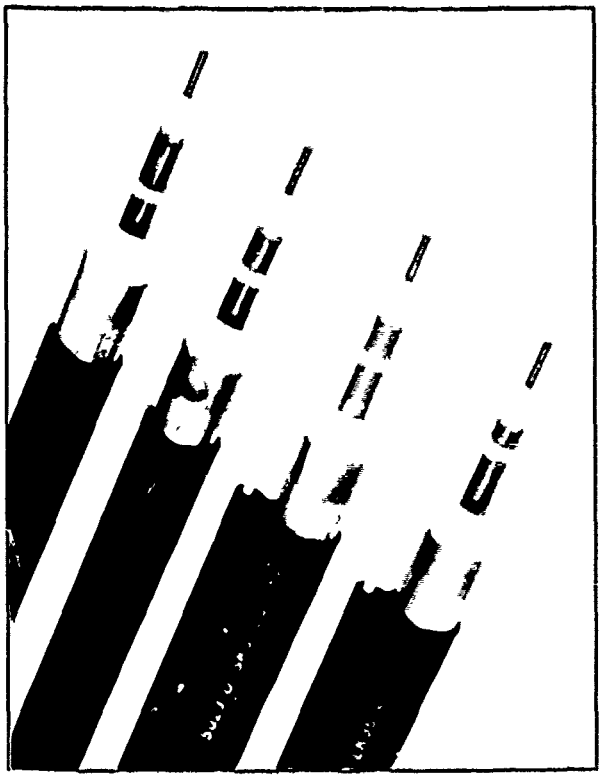

Fig. 3: Variety of radiating cables

The variety of possible slot configurations in the outer conductor is large. In one type of cable some few short slots in axial direction in a distance of some metres are applied. In another cable slot arrangements of some circular holes or small slots with repetition rates between 10 and 100 cm are typical. Or up to 100 small slots perpendicular to the cable axis over a periodic length of 2 m are arranged in well-designed distance between each other (Fig. 3 middle). The arrangement mentioned at the latest will be described here. Such an arrangement gives an intensive radiation, which means a low coupling loss over a broad frequency range between 70 and 1000 MHz.

Over the copper outer conductor a thermoplastic

sheath is extruded. Standard material for this sheath is polyethylene which is black coloured for UV-stability. For installation in rough tunnels or as aerial cables along radiation shadowed valleys these cables are also available with a dielectric supporting rope constructed as a Figure-8-Cable (Fig. 3 below).

3. Theory of Radiation

The basis for the radiating cables are coaxial cables. In such a cable with closed outer conductor a TEM-wave travels from the transmitter to the cable end and can be received there and will be more or less reflected depending on the impedance matching. By the totally closed outer conductor the wave inside the cable is totally screened from the surrounding. Alongside a coaxial cable no coupling of an electromagnetic field can be measured. In the same case no electromagnetic field outside the cable has any influence on the inside wave.

Openings in the outer conductor cause electromagnetic coupling between the field of the inner wave and the outside in the same way like single antennas work. The arrangement of the openings determines the mechanism of the coupling. With this respect two kinds of cables are distinguished, the surface waveguide and the leaky coaxial cable. In the first group of cables, the holes in the outer conductor are equidistantly spaced over the cable length with a small spacing compared to the operating wavelength. To this group also slotted coaxial cables belong where the outer conductor over the full length of the cable is opened to a distinct degree as well as cables with an open braid as outer conductor.

The mechanism of those cables can be explained with the following model: the largest part of the energy travels as an inside wave through the cable (Fig. 4) At any points of inhomogeneity of the outer conductor surface waves will be induced which spread in forward and backward direction along the outside of the cable and interfere with each other (Fig. 5). The field strength at a mobile antenna varies between doubling and extinguishing. The quality of the radio communication varies very much. Also the kind of installation and the surrounding near the cable affects the radiation field along the cable.

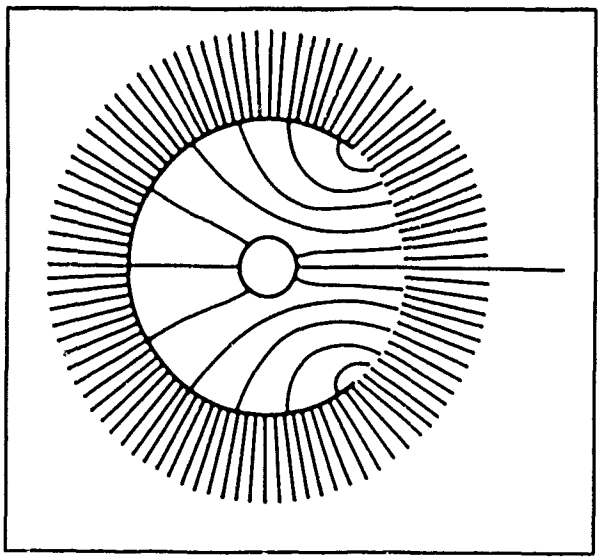

Fig. 4: Inner wave of an open coaxial cable (longitudinal slot)

The most important characteristic for energy transport along the cable by the inner wave is the longitudinal loss. This loss is mainly determined by the dimensions and the dielectric material of the cable. The maximum thickness of the cable is limited by mechanical and installation reasons to approximately 35 mm. But for radiating cables also the surrounding of the cable is important for the longitudinal loss because the inner wave also travels to a small portion on the outside of the outer conductor (Fig. 4).

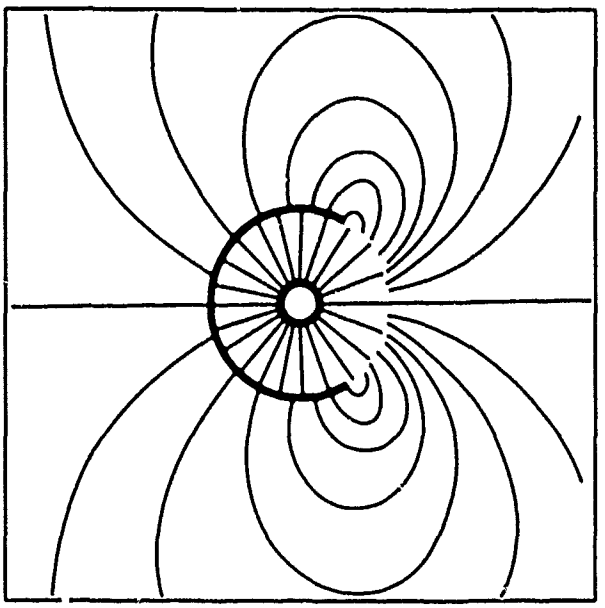

Fig. 5: Outer wave of an open coaxial cable (longitudinal slot)

The coupling from energy out of the cable through the outer space to the antenna is described by the coupling loss. This coupling loss is defined as the ratio of the received power at an antenna to the power in the cable nearest to the antenna. Because of the reciprocity analogue considerations are valid for the transmission from an antenna to the cable. The coupling loss for slotted coaxial cables depends on the width of the slot and is also affected by the interference and reflection in the surrounding.

The reached results were unsatisfying and considerations were undertaken to develop a cable with lower longitudinal loss, lower coupling loss and uniform radiation over a broad frequency band. This leads to a second group of radiating cables, the leaky coaxial cables. The idea was that a portion of the energy from the inner part of the cable will be radiated as leaky waves to the outside. This

radiation is caused by regular stimulation, this means by a periodic slot arrangement. In the simplest case small single slots spaced with half the operating wavelength - for example 1.5 m for 100 MHz - are arranged in the outer conductor (Fig. 6 a). The coupling loss is very low in a small frequency range but above and below this frequency it is increased by interference. For low coupling loss over the total frequency range between 50 and 1000 MHz the single slots must be arranged in a periodical slot pattern. This has two reasons:

1. Besides the fundamental mode at the lower cut-off frequency all higher order waves are stimulated so that at higher frequencies several leaky waves interfere and the receiving signal is highly disturbed. The higher order waves must be suppressed or at least damped very much.

2. By the fact that the single slots can be taken as small antennas or sources of radiation the possibility arises to double the radiation by doubling the number of holes per period, this means to reduce the coupling loss by a factor of 2 (6 dB). But the arrangement of slots must follow a complicated mathematical rule to suppress higher order modes.

In contrary to the up to now known slot arrangements the distances of the different slots in one period do not follow a simple law for the new leaky coaxial cables. The essential of this new cable is that the slots are as small as possible because the strength of the radiation is affected mainly by the width of the slots and only unessentially by the slot length. Moreover the special arrangement of slots results in the fact, that in the interesting frequency range disturbing poles are distinguished

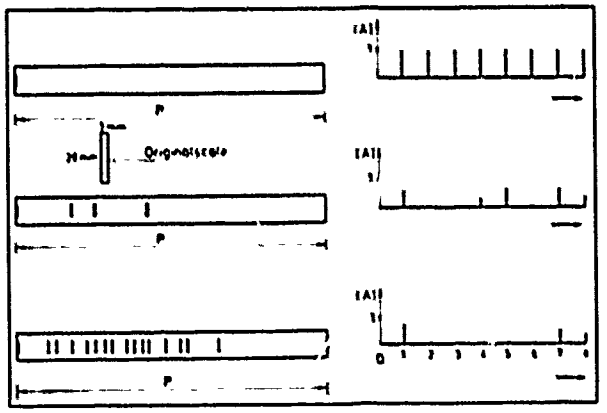

Fig. 6: Evaluation fo slot configuration for a leaky coaxial cable

or at least severely damped. Those small slots are on one hand easy to produce. On the other hand it is possible to punch in a given length of periodicity a larger number of slots than of all other hole configuration known up to now.

The calculation of the slot distance for the suppression of poles is mainly done by multiplying cosinus functions with following Fourier transform. With the Fourier transform a function in the frequency range is transformed to a function in the local range. The resulting function is realised by small slots perpendicular to the cable axis. The principle will be explained in the following.

By the arrangement of slots which are arranged pairwise a fundamental frequency f_0 is given. Also at each entire multiple of f_0 poles in the frequency range are given. For a uniform radiation the poles of 2nd, 3rd, 4th, n'th order should be suppressed as much as possible. This is achieved by successive multiplication of the basic spectrum with cosinus functions F_1, F_2, F_3, ..., this means a total function

$$F = F_1 * F_2 * F_3 * \ldots$$

These functions have their maximum at the frequency f_0, this means amplitude = 1. The function F_1 must have its 0-value at $2f_0$ to suppress the pole of second order. At $4f_0$ this function has the amplitude = -1. The periodicity is therefore $8f_0$. The Fourier transform of the product on the basic spectrum with this cosinus function gives a pair of slots with a distance of 2/8 of the periodicity length. This means one slot generates two slots per period. By this first doubling of the number of slots per period the poles of 2nd, 6th, 10th, 14th, ... order are suppressed. At the remaining poles the following amplitudes are expected:

Order of pole	1	3	4	5	7	8	...
rel. amplitude	0.707	-0.707	-1	-0.707	-0.707	1.0	...

In a next step the remaining spectrum in the frequency range will be multiplied by F_2 the cosinus with the periodicity $12f_0$. By this the poles of 3rd, 9th, 15th, ... order are suppressed. In the local range each of the two slots per period are replaced by double slots which are dislocated by 1/12 of the periodicity length to the right and to the left in the original location. The remaining amplitudes are now

Order of pole	1	4	5	7	8	...
rel. amplitude	0.612	0.50	0.612	-0.612	-0.5	...

In multiplying the remaining spectrum with F_3 a cosinus function with the periodicity $16f_0$ the 4th, 12th, ... pole are suppressed. The 4 slots are transformed to 8 slots per period. This principle must be executed until all higher order poles in the interesting frequency range are eliminated. For leaky coaxial cables with a low basic frequency f_0 and a broad transmission range this led to a large number of slots within one length of periodicity and therefore to sometimes very small slot distances (Fig. 6 b, c).

To avoid this and to get a larger number of suppressed poles for the same number of slots the zeros of the cosinus function are chosen that with one cosinus function several poles are not totally suppressed but weakened. For this the zeros are chosen not exactly at the pole frequencies but in such a way that the product of all cosinus functions gives values less than $5*10^{-2}$. By this the

number of cosinus functions for smoothening the frequency slope are reduced. By this the number of slots and the minimum distance between two slots are technically realisable in the chosen periodicity length. For a fundamental frequency of 65 MHz it is possible to suppress with 64 holes over a length of approximately 2 metre poles up to the order of 15 sharply and to stay with a minimum slot distance of approximately 7 mm. The first three optimised cosinus functions are

$$F_1 = \cos(n\pi/2 \cdot 2.02)$$
$$F_2 = \cos(n\pi/2 \cdot 3.06)$$
$$F_3 = \cos(n\pi/2 \cdot 4.41)$$

Fig. 7 shows such a leaky coaxial cable.

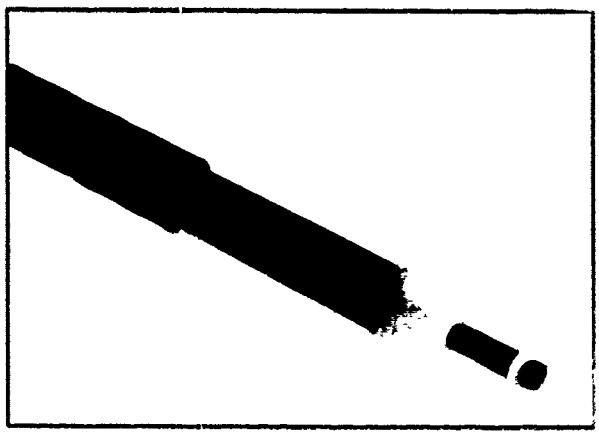

Fig. 7: Leaky coaxial cable with numerous periodically arranged slots

4. Measuring Technique

For the testing of radiating cables a test route has been built. On this approximately 100 m long route it is possible to measure the radiation characteristics of slotted coaxial cables and leaky coaxial cables and do comparisons between different cable constructions. The place for the test route was chosen in such a way that reflecting buildings or other elements are at least 20 m apart from the test route and the cable.

To get the bare cable characteristics the radiating cables are mounted on wooden poles in a height of approximately 2 m over a non-armoured concrete plate. This concrete plate is also the running path for an electrical vehicle with transmitter and antenna (Fig. 8). The vehicle is equipped with an independent power supply and allows measuring runs with mobile transmitter and also mobile receiver with variable distances to the cable.

As antennas normally /2-dipoles with vertical polarisation matched to the measuring frequency are chosen. But also other antennas like special vehicle antennas or biconic broadband dipole antennas can be mounted.

The measuring runs can be done with distances of 2 to 6 m parallel to the cable. Field deformations at

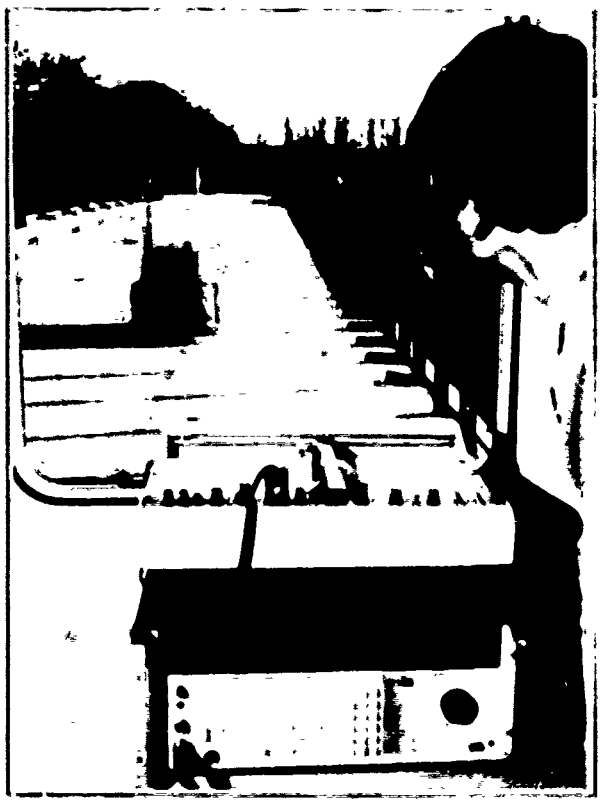

Fig. 8: Measuring route for testing of radiating cables

the ends of the route are eliminated by choosing for examination only 60 m in the middle of the route. At each measuring run with a constant frequency the receiving level is registered at some 1000 points along the route. In an ongoing calculation process correction is done for each point by the cable loss between the cable end and each measuring point. By this a plot of the field strength along the radiating cable is obtained. The local coupling loss is then calculated as the difference between the transmitter level and the measured receiving level.

This first measuring programme is followed by a statistical evaluation programme. By this the probability distribution of the local coupling loss is calculated. The mean value is the coupling loss with 50 % probability. Moreover the 95 % probability of the coupling loss is calculated because this value is relevant for radio link planning. For each test frequency one test run is required. Only 5 minutes are needed for this, including all calculations. As standard frequencies 70, 87, 110, 160, 460 and 960 MHz were chosen.

5. Results

In the course of development of leaky coaxial cables a large number of different measurements on test cables and standard cables taken from the current production were carried out on this test route. Moreover every possibility for measuring the

coupling loss and longitudinal loss in tunnels were taken to examine the correction factor for the values received from the free space propagation to the values in tunnels. For every cable longitudinal loss and structural return loss are measured. Examples for longitudinal loss are shown in Figure 9 and for structural return loss in Figure 10.

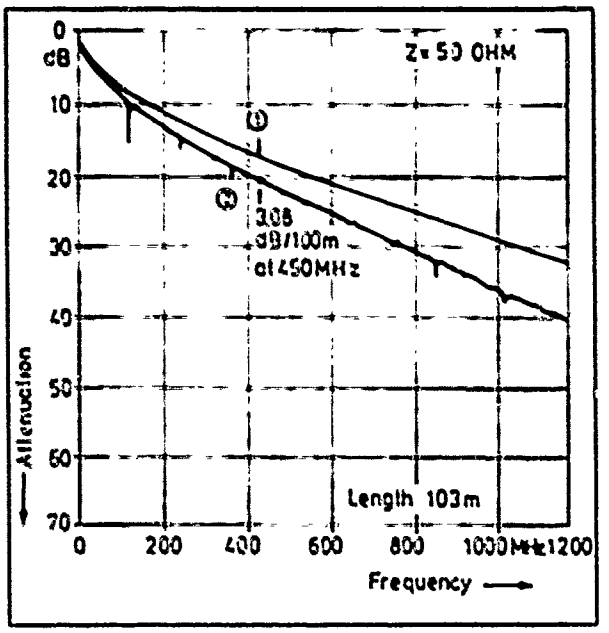

Fig. 9: Attenuation of leaky coaxial cable with auxiliary cable (2) and of auxiliary cable alone (1)

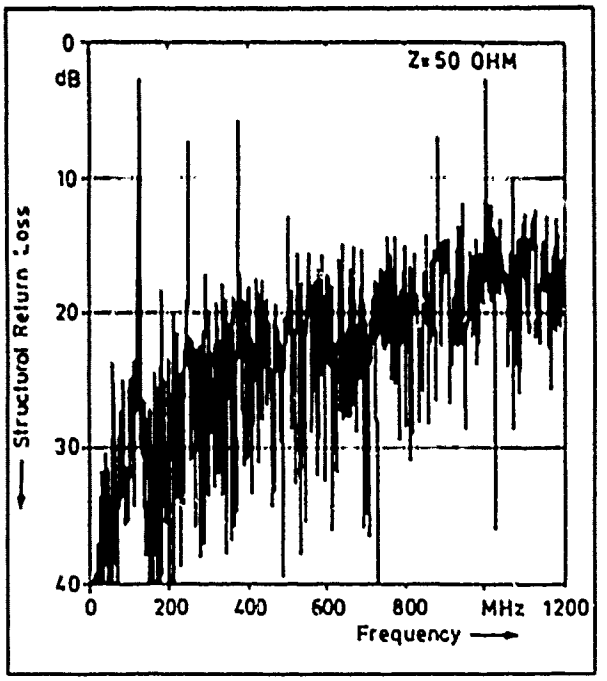

Fig. 10: Structural return loss of a leaky coaxial cable

These measurements are done more or less for quality control because the results are predictable with great accuracy. The peaks in the longitudinal loss and the structural return loss are related to the slot configuration.

But for the coupling loss this is quite different. At many frequencies in different distances between antenna and cable and under several mounting conditions test runs have been conducted. Especially the influences of the surrounding must be recognised and correlated to the results and then by changing the construction of the slot configuration and the mounting conditions they were

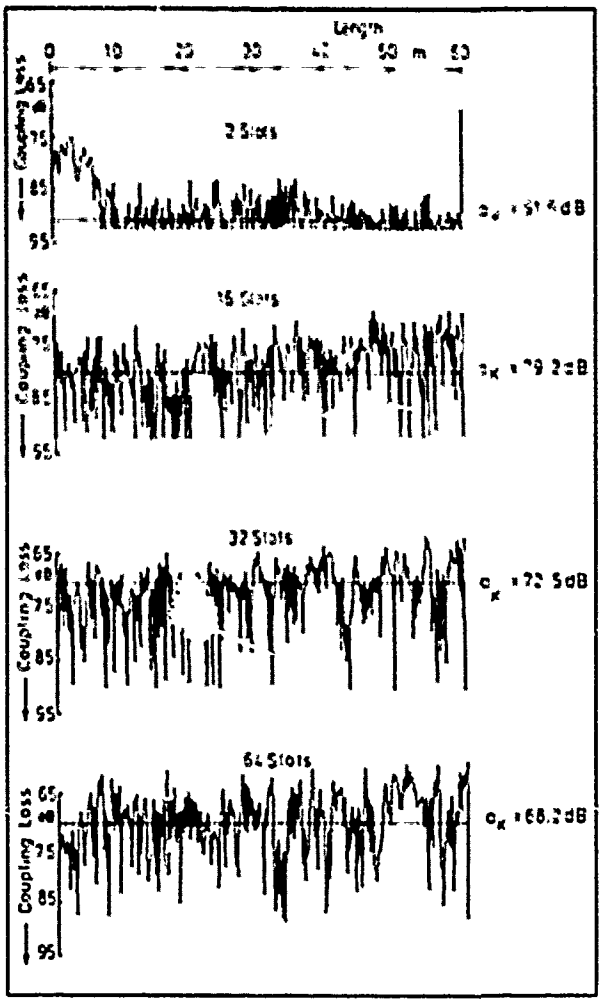

Fig. 11: Evaluation of coupling loss for a leaky coaxial cable depending on the slots per period

compensated. Figure 11 shows the development of the coupling loss at 460 MHz for leaky coaxial cables with the same periodicity but with increasing number of slots arranged systematically to suppress higher order modes. Here the decrease in coupling loss with increasing number of slots can be seen clearly. Figure 12 shows a measured curve of the coupling loss over a frequency range between 30 and 330 MHz using a biconical broadband dipole antenna.

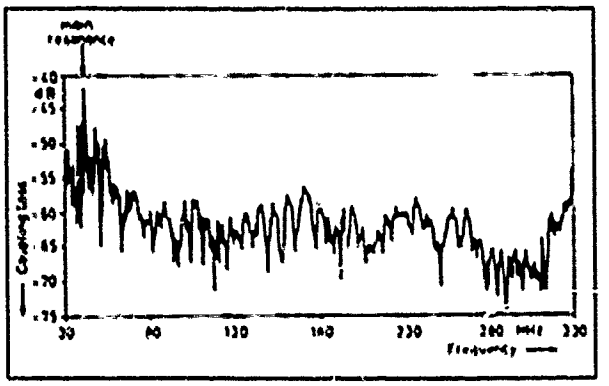

Fig. 12: Coupling loss of a broadband leaky coaxial cable versus frequency

Also another very important effect on the longitudinal loss was investigated. The so-called "Salt Effect" which describes the increase of longitudinal loss with increasing frequency by pollution on the cable by wet salt which happens in car traffic tunnels in winter time. The radio link communication collapses because of energy absorption of the polar molecules of the wet salt to the inner longitudinal transporting wave. By drying the salt and cleaning the cable this effect vanishes completely. A qualitative indication for this effect is the relative open space of the outer conductor.

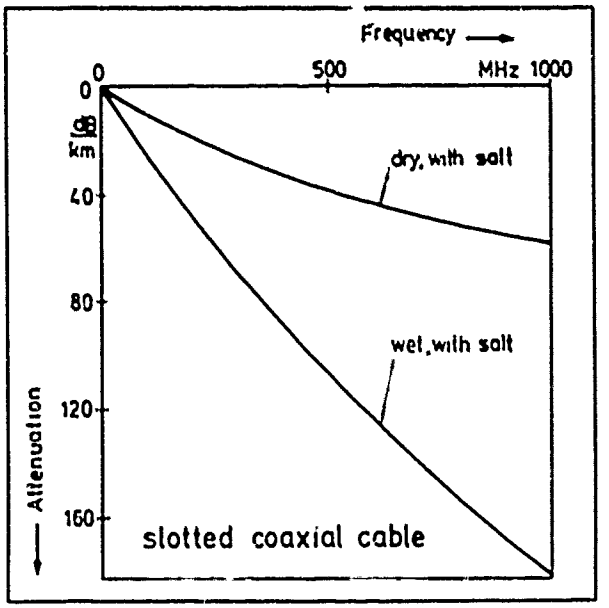

Fig. 13: Salt effect of a slotted coaxial cable

This is larger for slotted coaxial cables than for leaky coaxial cables of the newer type. Therefore for these leaky coaxial cables this "salt effect" is more or less negligible because here the apertures are very small. Figure 13 and 14 show this salt effect for slotted coaxial cables and leaky coaxial cables respectively.

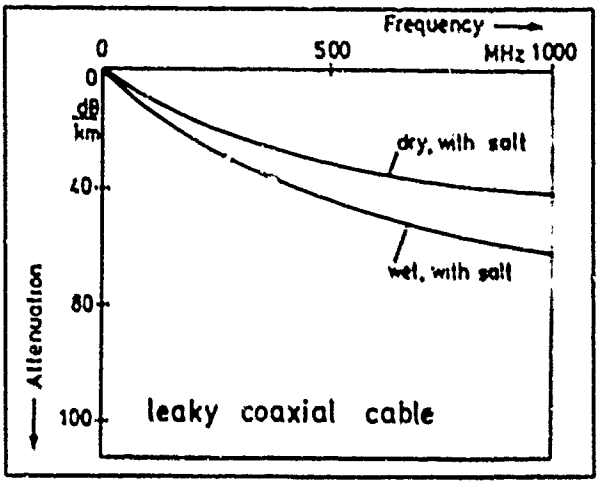

Fig. 14: Salt effect of a leaky coaxial cable

6. Planning and Erection of Cable Routes

For the planning of leaky coaxial cable routes the same rules are applied as for antennas. The radiating field strength at a mobile receiver coming from a local station must not come under a minimum receiver sensitivity level. The same rules are valid for the reverse direction this means from the antenna over the cable to the local station. The attenuation between the transmitter and the receiver is the sum of the longitudinal cable loss to the nearest point between cable and antenna and the coupling loss from the cable to the antenna. Table 1 shows the characteristic parameters of radiating cables. Whereas the longitudinal loss increases over the length and with increasing frequency the coupling loss for leaky coaxial cables is over a frequency range from 60 to 900 MHz more or less constant and fluctuates only locally. For frequencies 150 and 450 MHz Figure 15 shows the curves for the sum of longitudinal loss, coupling loss and its variation over the length. For both frequencies total losses of approximately 120 dB are bridgeable. For this a maximum non-repeatered section of 2700 m at 150 MHz and respectively

	Slotted Coaxial Cable		Leaky Coaxial Cable		
Type / Parameter					
Construction					
Inner conductor ø (mm)	6.3	9.5	7.8	9.5	11.9
Insulation material	Solid PE	Bandum	Bandum	Bandum	Bandum
Insulation ø (mm)	19.0	22.6	19.3	22.0	28.9
Outer conductor	Longitudinal slot	Longitudinal slot	Slot configuration	Slot configuration	Slot configuration
Outer sheath ø (mm)	23.0	27.2	23.7	27.2	33.0
Characteristic impedance (Ω)	50	50	50	50	50
Attenuation (dB/100 m) at 80 MHz		2.1			
150 MHz	2.0	1.6	1.5	1.2	1.0
450 MHz	4.1	2.1	2.8	1.7	1.4
900 MHz	--	3.0	4.5	3.3	2.6
		--	6.3	5.2	4.1
Coupling loss (dB) at 80 MHz	75 ± 10	70 ± 10	60 ± 5	60 ± 5	60 ± 5
150 MHz	80 ± 10	75 ± 10	65 ± 5	65 ± 5	65 ± 5
450 MHz	80 ± 10	75 ± 10	65 ± 5	65 ± 5	65 ± 5
900 MHz	-	-	65 ± 5	65 ± 5	65 ± 5

Table 1: Characteristics of different radiating coaxial cables

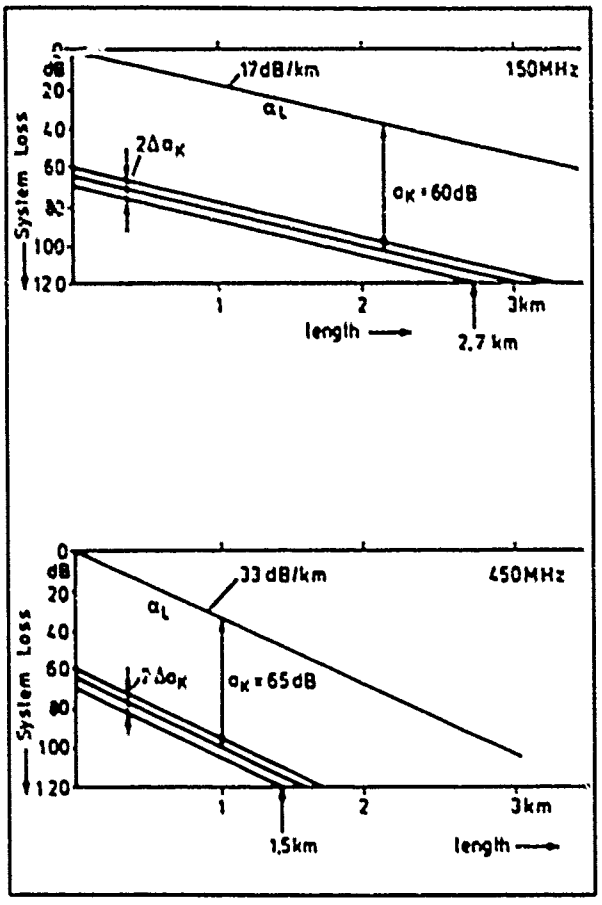

Fig. 15: System loss of leaky coaxial cable LK37 at 150 and 450 MHz

1500 m at 450 MHz can be calculated. Over this length a tunnel can be equipped with transmitter and receiver on one side (Fig. 16 a). If the feed-in to the cable is done at the middle of the cable route and therefore coupling respectively decoupling of energy is served via a T-coupler operating lengths of 5.5 respectively 2.8 km can be achieved for 150 respectively 450 MHz.

For longer operating lengths the older possibility of arranging multiple sections with central supply and connecting the in/outs with a modulation cable are chosen (Fig. 16 c). But more adequate is the usage of broadband repeaters which compensate the longitudinal loss (Fig. 16 d). The transmitter and receiver are on both sides of the tunnel and they are connected via a low frequency cable. It is possible to power-supply the intermediate repeaters via the leaky coaxial cable.

Normally one cable link is sufficient for the supply also for a double track tunnel. The cables are installed in the middle of the tunnel at the top, or on one side of the tunnel in a height which is a little bit higher than the largest vehicle in the tunnel to avoid shadow effects in two-way-traffic.

In tunnels with flat walls the cable is normally fixed to the wall with plastic clamps (Fig. 17) which are fixing the cable in a distance of approximately 8 cm from the wall. Every one metre such a clamp is installed. For the mounting of the cable in rough tunnels it is advantageous to use a cable with a non-metallic supporting wire which s

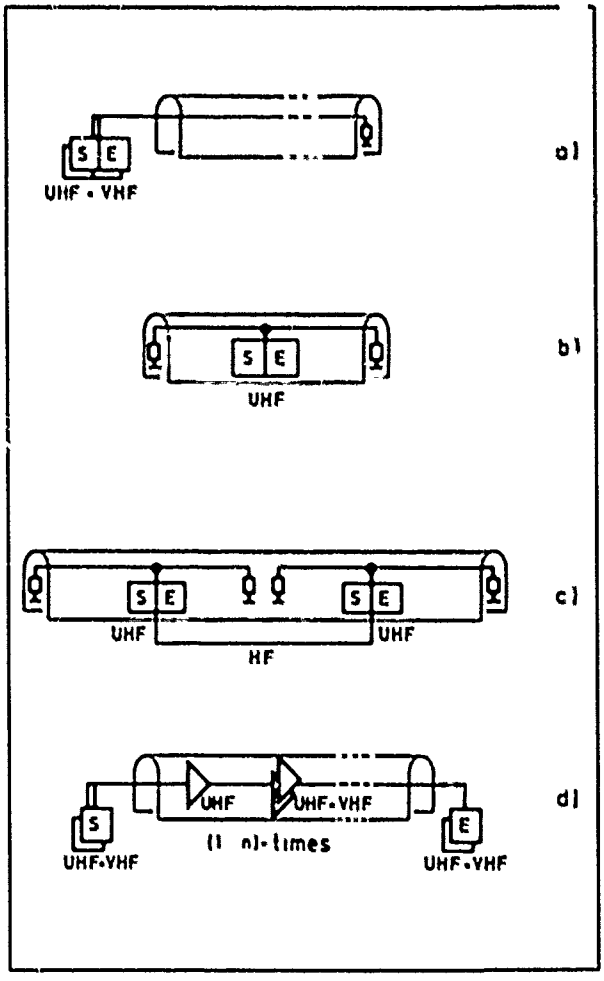

Fig. 16: Radiation systems for tunnels of different lengths

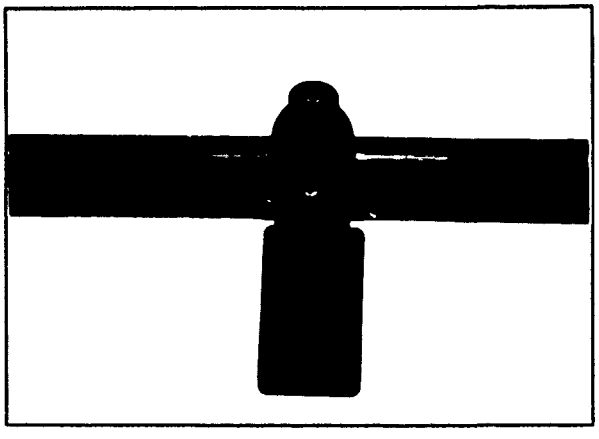

Fig. 17: Clamp for fixing radiating cables to the wall

fixed approximately every 10 metres to the tunnel wall. In railway tunnels it must be considered that the cable should be earthened every 500 m to limit the induced voltage. This is normally done at the connectors.

The repeaters in tunnels are mounted in niches which are normally already existing. By this the mounting place of the repeaters may be sometimes not at the optimised location.

7. Outlook

The leaky coaxial cables described here are well suited for the supply of radio energy in tunnels for railway and car traffic. By the fact that the cable has a low attenuation up to 900 MHz and also an excellent coupling loss with low fluctuation, links with these cables will be able not only to transmit the mobile traffic communication services of today but also those of the future especially the digital mobile communication system at 900 MHz.

8. Literature

[1] Grüssi O., P. König, Radio Links for Highway Tunnels, Techn. Mitt. PTT, CH, 7(1978), pp. 285

[2] Petri U., Zur Berechnung von geschlitzten Koaxialkabeln für den UKW-Funk, Wiss. Ber. AEG-TELEFUNKEN 51(1978)2/3, pp. 145

Helmut G. Haag (Speaker)
AEG KABEL AG
Manager Communication System Techniques
Mönchengladbach, West Germany

Helmut G. Haag (41) is head of the Technical Sales Division for Telecommunications. After reaching his Dipl.-Physiker-degree from the University of Stuttgart he joined AEG KABEL in 1975 for the development of coaxial cables. Later he has been also responsible for the development of optical fibre cables. From 1980 to 1983 he built up the production plant for these cables. In autumn 1983 he took his present position.

Günter Thönneßen
AEG KABEL AG
Telecommunications Development
Mönchengladbach, West Germany

Günter Thönneßen (51) is head of the Development Department for Telecommunication Cables. He finished his studies at Technische Hochschule Aachen in 1964. After a 3 years employment as a development engineer for CF measuring instruments he returned to Technische Hochschule Aachen, where he graduated as a Dr.-Ing. In 1971 he joined AEG KABEL.

Karl Schulze-Buxloh
AEG KABEL AG
Telecommunication Development
Mönchengladbach, West Germany

Karl Schulze-Buxloh (33) is Engineer in the Development Department for Telecommunication Cables. He finished his studies at Ruhr-Universität Bochum in 1986 as Dipl.-Ing. In 1986 he joined AEG KABEL. Since this time he is engaged in the development of leaky coaxial cables.

DEVELOPMENT OF FLAME RETARDANT HALOGEN-FREE JELLY-FILLED NON-METALLIC OPTICAL CABLE

H. Horima, K. Niikura, N. Akasaka, T. Yamanishi

1, Taya, Sakae-ku, Yokohama 244, Japan

Abstract

Non-metallic jelly-filled optical cables are widely used because they can make maximum use of the non-inductive characteristics of optical fiber and they are superior waterproof characteristics. Largely due to its recently expanding range of application, there is an intensifying demand for flame resistance.

However, jelly used as a component material generally accelerates cable firing. Jelly is a major obstacle to improve the flame retardancy of non-metallic optical cables.

By using a newly developed flame retardant jelly, we designed optical cables and succeeded in developing a flame retardant halogen-free jelly-filled non-metallic optical cable which satisfies the IEEE std. 383.

1. Introduction

The optical communication system using optical cables has been constructed for practical use not only in the public communication field, but also in the LAN and industrial fields.

Since optical fiber is composed of glass, that is, non-metallic material, it has non-inductive characteristics. Non-metallic optical cables aim to make maximum use of this non-inductivity. In such a cable, however jelly is generally filled into the cable to improve the waterproof characteristics while there is an intensifying demand for higher flame retardancy mainly due to the expanding range of application.

Such a non-metallic jelly-filled optical cable employs polyethylene sheath and has no flame resistant metal layer. In addition, the jelly material generally accelerates cable firing. Jelly has been a major obstacle to improve the flame retardancy of non-metallic optical cables.

For this reason, we have developed a flame retardant halogen-free having improved oxygen index compared with conventional jelly while it retains the same level softness.

By combining this flame retardant jelly with flame retardant slotted core and a sheath material, composed of polyethylene we designed and fabricated a non-metallic optical cable, and it was proved that not only its flame retardancy satisfies the IEEE std. 383, but also its transmission, physical, temperature and waterproof characteristics are satisfactory for practical use.

2. Characteristics of flame retardant jelly compound

Table 1 lists the characteristics of the newly developed flame retardant jelly compound. And Fig. 1 shows the temperature dependency of jelly cone penetration which has a close relationship with that of transmission characteristics of optical fiber, together with the conventional jelly compound usually employed for optical fiber or for ribbon fiber. As is obvious from the Table 1 and Fig. 1, this flame retardant jelly compound succeeds all the characteristics of the conventional jelly compound with only enhancement made in its flame retardation, namely oxygen index.

Therefore, it can be thought that the enhanced flame retardation of jelly compound hardly affects the characteristics of optical fiber cable.

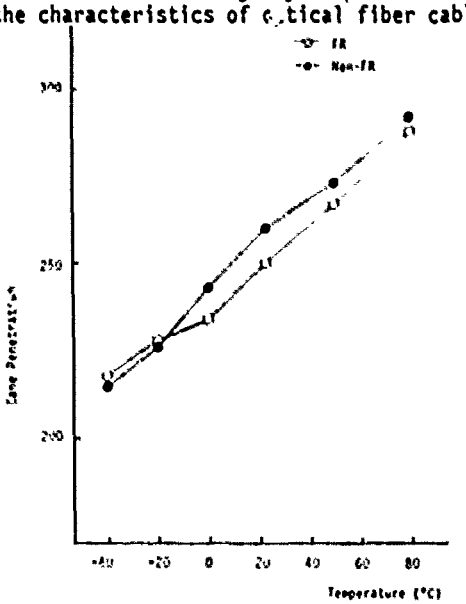

Fig. 1 Relationship between cone penetration and temperature of both jelly

Table 1 Characteristics of jelly compounds

Item		FR* Jelly Compound	Non-FR Jelly Compound
Specific Gravity		1.04	0.85
Cone Penetration	-40°C	218	214
	23°C	250	260
	60°C	748	292
Oil Separation (%)		0.5	0
Oxygen Index		30	17

*FR : Flame Retardant

3. Compatibility of the flame retardant jelly compound with coating materials of optical fiber

Compatibility was evaluated between this flame retardant jelly compound and UV (Ultra-Violet) curable resins as fiber coating materials. Optical fiber coating materials were dipped in the flame retardant jelly compound kept at a high temperature to test change in weight, tensile strength and elongation with time. Each result of these tests is shown in Figs. 2, 3 and 4. In each test, a significant change due to this flame retardant jelly compound was not found. Hence, it has been confirmed that this jelly compound does not adversely affect the optical fiber coating materials.

4. Flame-retardant characteristics for various optical cable constructions

In order to verify the effectiveness of the newly developed flame retardant jelly compound, the flame retardant characteristics were evaluated using various cable materials with different oxygen indexes.

The cable construction used for evaluation came in two kinds with a difference in outside diameter as shown in Figs. 5 and 6. Each cable is constructed by accommodating 2-fiber ribbon in the SZ slot, and has 48 and 128 optical fibers at maximum, respectively. Of the structure shown in Fig. 5, 3 kinds of cables were manufactured by using materials having different oxygen indexes, and of the structure shown in Fig. 6, only one kind of cable, which consists primarily of flame retardant materials, was manufactured, as listed in Table 2. These 4 kinds of cables underwent a vertical tray flame test stipulated in IEEE standard 383. Fig. 7(a) through(d) show the state of combustion of each sample at 0 to 20 minutes after start of vertical tray flame test. In consequence, the sample 2, which used a non-flame retardant jelly compound with other constituents given flame retarding property, burned over a length of 140 to 150 cm. Although this satisfied the test standard, flame rose up to 180 cm or more near the end of the test. So we conclude that the application of flame retardant jelly compound is essential for design of such cables in

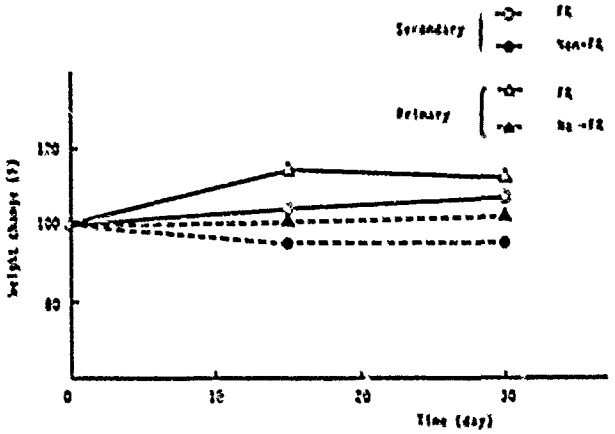

Fig. 2 Weight change of UV curable resins immersed in both jelly

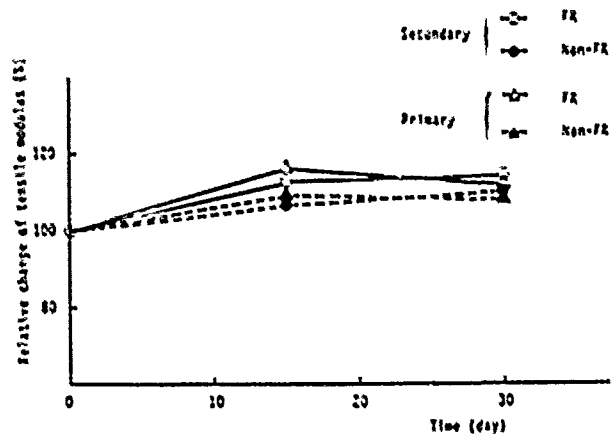

Fig. 3 Tensile modulus change of UV curable resins immersed in both jelly

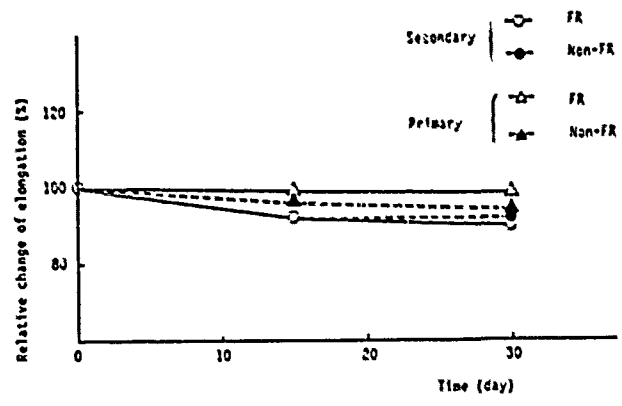

Fig. 4 Elongation change of UV curable resins immersed in both jelly

consideration of safety factor.

On the other hand, it was confirmed that the optical cable samples 1 and 4, whose slot, jelly and polyethylene (PE) sheath were all composed of flame retardant materials, burned within only about 70 cm and 75 cm, respectively, both proving an excellent flame retardant characteristics.

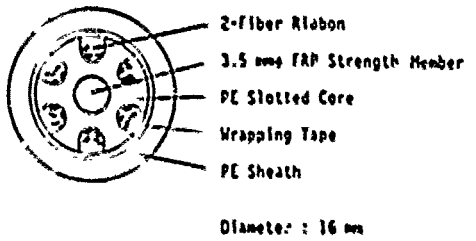

Fig. 5 Structure of 48-fiber non-metallic optical cable

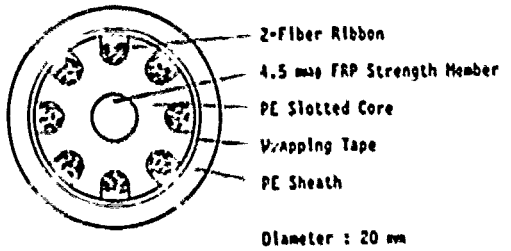

Fig. 6 Structure of 128-fiber non-metallic optical cable

Table 2 Oxygen index values

Items	Cable in Fig. 5			Cable in Fig. 6
Sample No.	1	2	3	4
FRP Strength Member	25 (Non-FR)	25 (Non-FR)	25 (Non-FR)	25 (Non-FR)
Polyethylene Slotted Core	29 (FR)	29 (FR)	19 (Non-FR)	29 (FR)
Jelly Compound	30 (FR)	17 (Non-FR)	17 (Non-FR)	30 (FR)
Polyethylene Sheath	33 (FR)	33 (FR)	33 (FR)	33 (FR)
Vertical Tray Flame Test Result	Pass	Pass	Fail	Pass

5. Characteristics of flame retardant non metallic optical cable

Cable characteristics were evaluated on the optical cable whose slot and PE sheath as well as the jelly compound were made of flame retardant materials and has a sectional construction as shown in Fig. 5.

5.1 Temperature Characteristics

Temperature dependence of optical loss characteristics was evaluated within a temperature range of -40 to 70°C. As a result, loss variation was 0.05 dB/km or less at 1.55 μm. That is, characteristic deterioration was not detected at all due to the use of flame retardant jelly compound.

5.2 Physical properties

Assuming a variety of external factors to be applied at the time of cabling and after it, tension, compression, bending and impact tests were carried out for the purpose of evaluating the optical loss variation at 1.55 μm. In addition, a waterproof test in conformity with IEC794-1-F5 and a compound flow test according to REA-PE90 were performed. The result of these tests is summarized in Table 3.

There was no problem on mechanical nor waterproof property. It was proven that jelly won't flow out during cable handling at a high temperature.

Table 3 Result of temperature characteristics and physical properties

Items		Characteristics
Temperature Characteristics -40°C ~ +60°C		Loss Variation <0.05 dB/km at 1.55 μm
Water Proofness (IEC 794-1-F5)		No penetration
Compound Flow (REA PE-90)		No drip after 24 hours at 70°C
Mechanical	Bending (Mandrel : 300 mmφ)	No loss increase at 1.55 μm
	Tension (200 kgf, 0.4 % elongation)	
	Crush (400 kgf/100 mm)	
	Torsion (1 m, ± 360°/m, 5 cycles)	

6. Conclusion

It was proved that the non-metallic jelly-filled optical cable, designed as a combination of the newly developed flame retardant jelly and flame retardant slotted core and a sheaths material can satisfy the vertical tray flame test in accordance with the IEEE std. 383. It was also proved that its transmission characteristics, physical characteristics, temperature characteristics and waterproof characteristics are satisfactory for practical use.

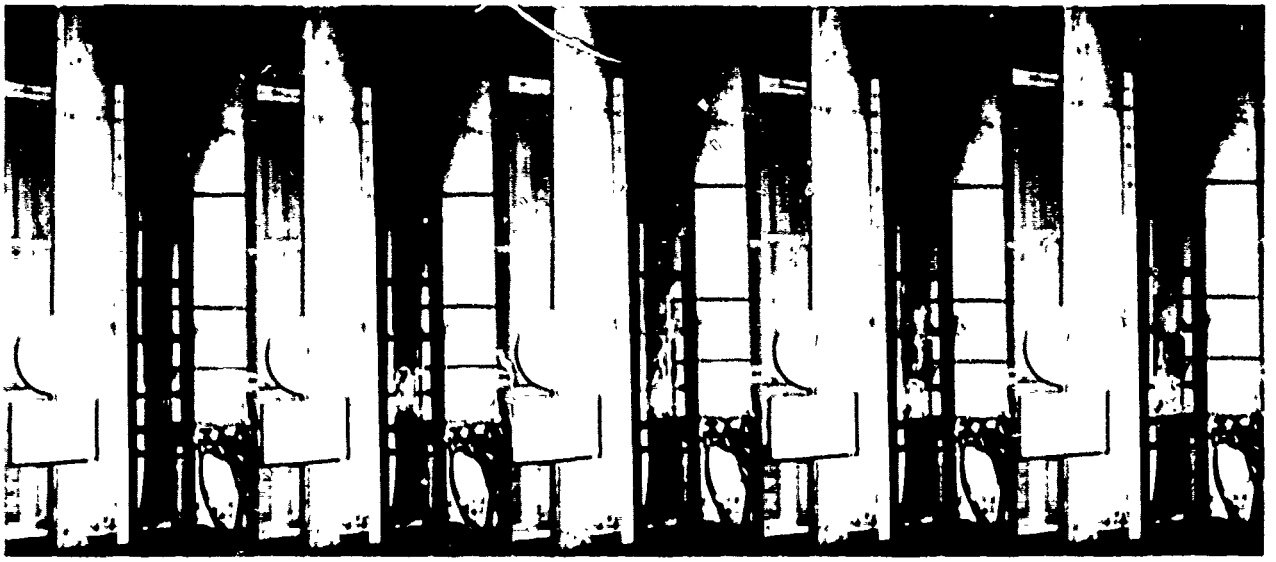

(a) Sample 1

(b) Sample 2

Fig. 7-1 Results of Vertical Tray Flame Test

(c) Sample 3

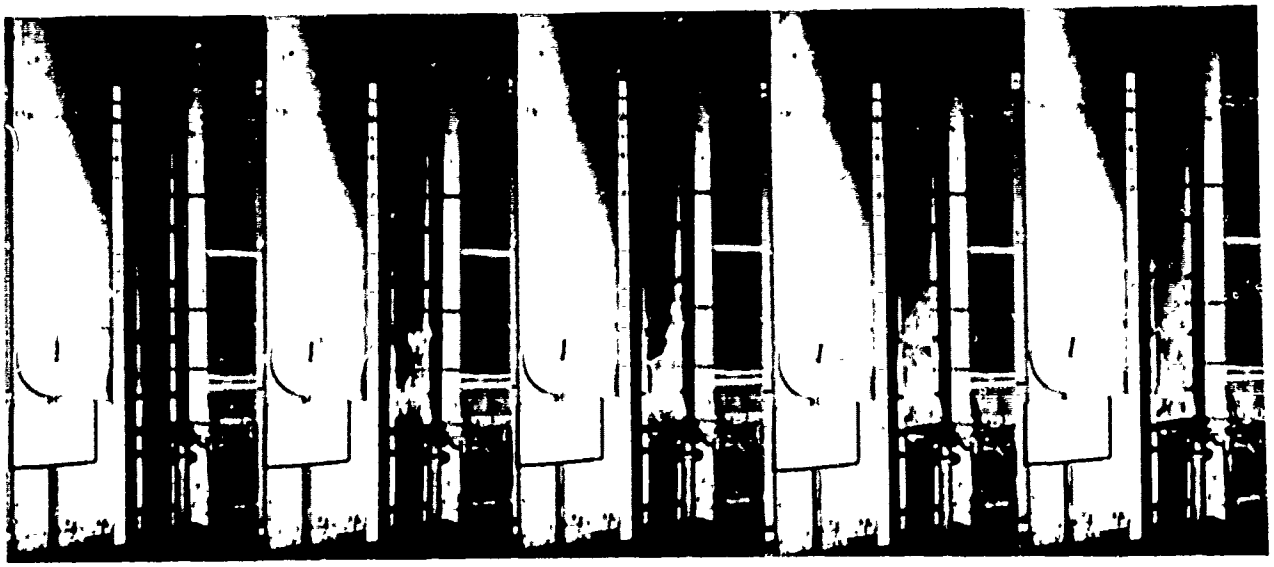

(d) Sample 4

Fig. 7-2 Results of Vertical Tray Flame Test

Hiroaki Horima
Sumitomo Electric
Industries, Ltd.
1, Taya-cho
Sakae-ku
Yokohama 244, Japan

Hiroaki Horima received the M.S. degree in engineering from Osaka University in 1972. He then joined Sumitomo electric Industries, Ltd. and worked on the development of CATV coaxial cable, multipair PEF-insulated junction cables and low loss unbalanced type cables. Thereafter, he concentrated on the development of optical fiber cables. He is now Section Manager of the Fiber Optics Division at Sumitomo Electric Industries, Ltd. He is a member of the Institute of Electronics and Communication Engineers of Japan.

Koji Niikura
Sumitomo Electric
Industries, Ltd.
1, Taya-cho
Sakae-ku
Yokohama 244, Japan

Koji Niikura received the B.E. degree in engineering from Waseda University in 1984 and joined Sumitomo Electric Industries, Ltd. He has been engaged in the development and design of opticcl fiber cables in the Fiber Optics Division.

Nobuhiro Akasaka
Sumitomo Electric
Industries, Ltd.
1, Taya-cho
Sakae-ku
Yokohama 244, Japan

Nobuhiro Akasaka received a M.S. degree in Chemical Engineering from Tokyo University in 1983. He joined Sumitomo Electric Industries, Ltd. in development of optical fiber and cables. Mr. Akasaka is a member of Transmission Media R & D Department, Yokohama Research Laboratories.

Toru Yamanishi
Sumitomo Electric
Industries, Ltd.
1, Taya-cho
Sakae-ku
Yokohama 244, Japan

Toru Yamanishi received a B.S. degree of Chemical Engineering from Hokkaido University in 1972. He joined Sumitomo Electric Industries, Ltd. and worked on the research and development of optical fiber fabrication, especially fiber drawing and coating. Mr. Yamanishi is now a chief research associate of Transmission Media R & D Department.

The 1990 National Electrical Code - Its Impact on the Communications Industry

By

Stanley Kaufman
AT&T Bell Laboratories
Norcross, Georgia 30071

ABSTRACT

The 1990 National Electrical Code has several new provisions which will impact the communications industry. The most important change is the requirement that all communications equipment in a building be listed as being safe to use. This requirement applies to all equipment electrically connected to a telecommunications network including telephones, connectors, PBX's, switches, modems and computers. The most important change impacting the wire and cable industry is the establishment of a new category of cables, multipurpose cables. These cables will be available in plenum (Type MPP), riser (Type MPR) and general purpose versions (Type MP) and will be suitable for communications, data (Class 2), remote control (Class 3) and fire alarm use.

INTRODUCTION

The National Electrical Code® is issued by the National Fire Protection Association (NFPA) and is revised every three years. Work on the 1990 edition of the Code has been completed. Substantial changes have been made that will affect the communications industry.

This paper deals with the changes in the Code relating to communications, data, signaling, fire alarm and cable TV circuits and cables, as well as optical fiber cables. A list of the articles that deal with these topics is given in Table I. Panel 16 of the National Electrical Code Committee is responsible for these articles.

TABLE I

NATIONAL ELECTRICAL CODE
LIMITED ENERGY ARTICLES

Article	Title	Typical Applications
725	Class 1, Class 2, Class 3 Remote Control, Signaling and Power Limited Circuits	Data Transmission Industrial Controls Door Bells
760	Fire-Protective Signaling Systems	Fire Alarm
770	Optical Fiber Cables	Local Area Networks
800	Communications Circuits	Telephone
820	Community Antenna Television and Radio Distribution Systems	Cable TV

Two trends, begun in earlier Code revisions continue. One is the increased regulation of telephone equipment in recognition of the revised status of the industry as a more competitive, less monolithic industry. The most important change is that all equipment used in a telephone system must be listed. The other trend is the establishment and refinement of the hierarchy of permitted cable substitutions and the creation of a new class of cable - multipurpose cable.

LISTING OF EQUIPMENT

The requirement in the 1990 NEC which most greatly impacts the communications industry is that all telephone equipment must be listed. This requirement applies to telephones, key telephone systems, PBX's, switches, transmission equipment such as subscriber loop carrier terminals, splice connectors, cross connect terminals, modems, computers, and any other equipment electrically connected to a telephone network except for telephone company equipment in a central office.

The exact wording of the new requirement is as follows:

800-51(1). Equipment. Equipment intended to be electrically connected to a telecommunications network shall be listed for the purpose.

(FPN):† One way of determining applicable requirements is to refer to "Standard for Telephone Equipment," UL 1459, December 18, 1987.

Exception. "This listing requirement shall not apply to reinstalled telephone equipment manufactured before January 1, 1990."

In order to appreciate the wide impact of this requirement, consider the definition of the word equipment:

Equipment: A general term including material, fittings, devices, appliances, fixtures, apparatus, and the like used as a part of, or in connection with, an electrical installation.

Under the 1987 Code, only cable and protectors had to be listed. Considering the definition of equipment, it is clear that everything else in the circuit path has to be listed. Splice cases do not need to be listed because they are not electrically connected to a communications circuit.

The words "listed for the purpose" are a very important part of the requirement. Panel 16 considered a public comment to reduce these words to just "listed". The panel rejected this suggestion because it

† "FPN" is an abbreviation for "Fine Print Note." These notes are informative, but they are not a part of the Code that is legally enforceable.

is necessary for the equipment to be suitable for communications and not some other use. The impact of this requirement on equipment listed for purposes other than communications, such as computers, is that the listing requirements that deal with connections to a telephone system will have to be harmonized with the listing requirements for telephone equipment.

Since any listing requirement for equipment obviously cannot be retroactive, an exception was added for telephone equipment manufactured before January 1, 1990. This exception was adopted to accommodate the tens of millions of leased telephones in use. These telephones can be installed and reinstalled many times during their lifetime. Note that the exception applies only to telephone equipment and not to other equipment such as computers. A tentative interim amendment has been submitted to NFPA to have this exception broadened to include all equipment connected to a telecommunications network. Action on this amendment should be completed by October 1989.

To complete our discussion of the listing of equipment let us review the scope of the NEC. It states:

90-2. Scope.
(a) Covered. This Code covers:
(1) Installations of electric conductors and equipment within or on public and private buildings or other structures, including mobile homes, recreational vehicles, and floating buildings; and other premises such as yards, carnival, parking and other lots, and industrial substations.

It also states:

(b) Not Covered. This Code does not cover:
(4) Installations of communication equipment under the exclusive control of communication utilities, located outdoors or in building spaces used exclusively for such installations.

Central office equipment installed in a telephone company central office does not have to be listed but the same equipment installed as part of a private network must be listed. Hence, manufacturers of switching and transmission equipment that is sold into the private network market will have to list their equipment. Likewise outside plant equipment such as subscriber loop carrier terminals, which are sometimes installed in buildings, will have to be listed.

CABLE SUBSTITUTIONS

There is a great deal of similarity between the cables used for communications, data (Class 2), controls (Class 3), cable TV, and fire alarm circuits. Under the provisions of the 1984 and earlier Codes, cables listed for Class 3 circuits (150V maximum) could substitute for cables used for Class 2 circuits (30V maximum, most applications). Power-limited fire-protective signaling (fire alarm) cables were listed for use with 300V power-limited fire alarm circuits but these cables were not allowed to substitute for Class 3 cables. In order to accommodate substitution, a manufacturer had to get a dual listing, both Class 3 and power-limited fire-protective signaling. Likewise, if a manufacturer had a coaxial cable used for data transmission and cable TV it would have to be listed for Class 2 (or Class 3) and CATV use.

The 1987 Code introduced some very substantial changes. It required, for the first time, that communications cables be listed, and it also established a fire resistance hierarchy. The 1987 Code also permitted limited substitutions of cable. The listing requirements for Class 3 cables are:

725-40(b) (2) Cables shall be listed as being suitable for Class 3, power-limited fire-protective signaling or communication circuits.

This established that communications cables and power-limited fire-protective signaling cables of equal or greater fire rating could substitute for Class 3 and Class 2 cables.

The substitution of communications cables and Class 3 cables for power-limited fire-protective signaling cables is more complicated. Cables used for fire alarm circuits must meet the requirements shown in Table II below:

TABLE II

AWG	Minimum Number of Conductors
16	1
19	2
22	4
24	6

Wires finer than 24 AWG are not currently permitted and the conductors have to be solid copper or bunch-tinned stranded copper. If stranded conductors are used, a maximum of 7 strands is permitted for 16 or 18 AWG, finer gauges must be solid.

Communications and Class 3 cables that meet the above gauge and stranding requirements are permitted to substitute for power-limited fire-protective signaling cable of equal or lower fire rating. Section 760-30(c) states:

Insulation. Cables shall be listed as being suitable for Class 3, power-limited fire-protective signaling, or communication circuits.

Even though Class 3 circuits are 150V maximum, substitution of these cables for power-limited fire-protective signaling cables was permitted because Underwriters Laboratories requires Class 3 cables to have a 300V rating.

Some controversy exists over the substitution of communications and Class 3 cables for power-limited fire-protective signaling cables because Section 760-30 requires that cables for this use "shall be listed for this use" and an exception had not been provided for substitute cables. This ambiguity has been corrected in the 1990 Code.

The status of cable substitutions under the 1987 Code is shown in Figure 1, where a dashed line indicates conditional substitutions, i.e., gauge and stranding requirements must be met in order for substitutes to be permitted.

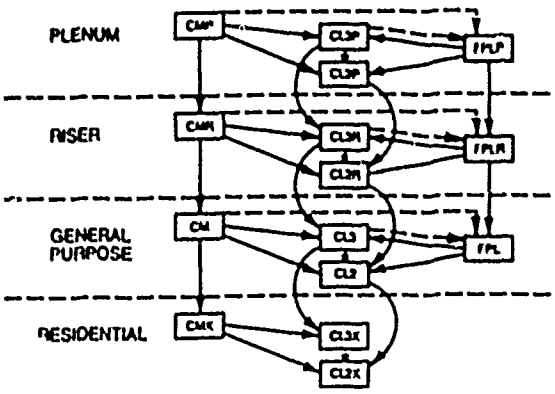

Figure 1. Cable substitutions permitted by the 1987 Code: CM = communications, CL2 = class 2, CL3 = class 3, FPL = power-limited fire-protective signaling.

This conditional substitution created problems for electrical inspectors because an inspector would have to check the gauge and number of conductors, and whether a cable had solid or stranded conductors before permitting communications or Class 3 cables to be used in a fire alarm application. The 1990 Code has addressed this problem with the establishment of multipurpose cables.

The requirements for multipurpose cables are in Article 800 Communications Circuits. Section 800-51(f) states:

Multipurpose (MP) Cables. Cables that meet the requirements for Types CMP, CMR and CM and also satisfy the requirements of Sections 760-51(a) and (b) shall be permitted to be listed and marked as Types MPP, MPR and MP, respectively.

Sections 760-51(a) and (b) contain the gauge and stranding requirements for fire alarm use. Most solid copper communications cables qualify for listing as multipurpose cables. The permitted gauges for power-limited fire-protective signaling circuit applications has been extended in the 1990 Code to permit 26 AWG conductors with a minimum of 10 conductors in the cable.

In order to clarify the permitted cable substitutions, a substitution section is included in each Article dealing with limited energy circuits (see Table I), and a substitution diagram (Figure 2) is also included. In addition to adding multipurpose cable, power-limited tray cable (PLTC), a type of Class 3 cable, is also included.

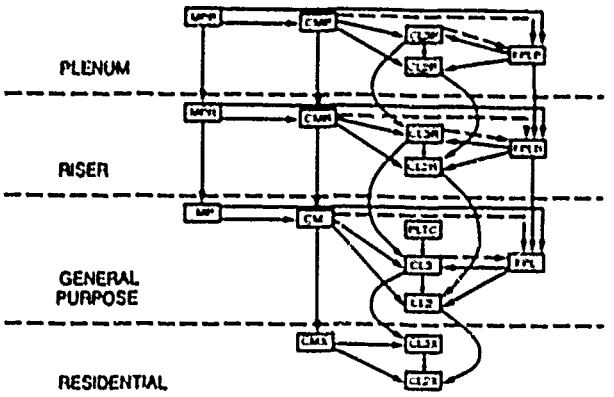

Figure 2. Cable substitutions permitted by the 1990 Code.

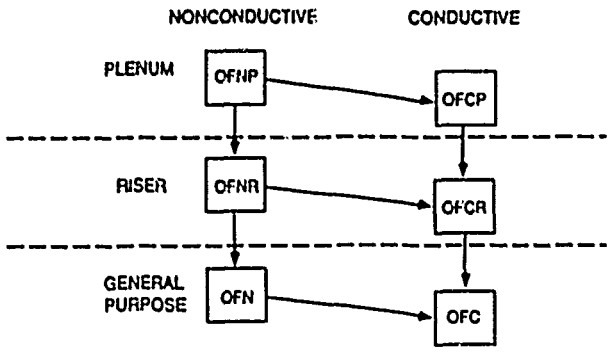

Figure 3. Permitted substitutions of optical fiber cables.

The substitution diagram for optical fiber cables is shown in Figure 3. It shows that nonconductive optical fiber cables may substitute for conductive optical fiber cables of equal or lower fire rating. No proposals were submitted to allow any other cable to substitute for cable TV cables, hence, cables used for cable TV as well as other applications will require dual listing.

The 1990 Code established voltage ratings of 300V minimum for Class 3, communications and multipurpose cables. The rationale for a 300V rating on Class 3 cables was use with 300V fire alarm circuits; this same rationale also applied to communications and multipurpose cables with the additional need to have the cable safely handle AC ringing voltages superimposed on 48V DC.

UNDERCARPET CABLE

The 1987 Code required the listing of undercarpet cable [800-3(e)]. It did not establish a cable type such as CM or CMX and did not suggest what the fire-resistance rating should be. The 1990 Code has established Type CMUC undercarpet wire and cable (Section 800-51(e)) and suggested (in a fine print note) that it should have the same fire rating as CMX (VW-1).

COMMUNICATIONS WIRES

The 1990 Code distinguishes between wires and cables, defining cables:

Cable: A cable is a factory assembly of two or more conductors having an overall covering.

And defining wires as:

Wire: A wire is a factory assembly of one or more insulated conductors without an overall covering.

These definitions recognize that a jacket differentiates a cable from a wire and that the jacket protects the cable core. The listing requirements for communications wire are:

800-51 (g) Communications Wires. Communications wires, such as distributing frame wire and jumper wire, shall be listed as being resistant to the spread of fire.

(FPN): One method of defining resistant to the spread of fire is that the cables do not spread fire to the top of the tray in the "Vertical-Tray Flame Test" in the "Reference Standard for Electrical Wires, Cables and Flexible Cords," ANSI/UL 1581 - 1985 (Rev. March 6, 1987).

Another method of defining resistant to the spread of fire is for the damage (char length) not to exceed 1.5m when performing the CSA "Vertical Flame Test - Cables in Cable Trays," as described in "Test Methods for Electrical Wires and Cables," CSA Standard C22.2 No. 0-3-M, 1985.

HYBRID POWER AND COMMUNICATIONS CABLES

The 1990 Code will allow the construction of a hybrid power and communications cable which includes a listed Type NM (nonmetallic sheathed power cable) and a listed Type CM (communications cable). The composite cable must pass the fire test for CM cable (vertical tray test). This cable will be permitted to be installed in one- and two-family dwellings.

FIRE TESTS

The 1987 Code suggests (in a fine print note) that the UL Vertical Tray Fire Test (IEEE 383) be used for listing general purpose cables Types CM, CL2, CL3, FPL, CATV, OFN and OFC. The 1990 Code added a reference to the Canadian FT4 test as an alternate test. The Canadian FT4 test is a more stringent test than the U. S. test. With the FT4 test accepted on both sides of the border, a manufacturer can use it to simultaneously satisfy U. S. and Canadian requirements.

The 1987 Code did not refer to the UL 1666 riser cable fire test for Type CMR and other riser cables because the test standard was not published when the 1987 Code was written. UL 1666 will be referenced in the 1990 Code.

THE 50 FOOT RULE AND OPTICAL FIBER CABLE

The 1987 Code requires that all communications cables in a building be listed but it exempted 50 feet of outside plant cable entering from outside the building. This exemption has its roots in Bell System Practices. This 50 foot rule has been extended to optical fiber cable.

RISER APPLICATIONS

The 1987 Code requires riser (or plenum) cable to be used where cables are "in a vertical run in a shaft." In modern construction, open shafts are not used. Typically, riser cables go from floor to floor through a series of floor penetrations. The intent of the Code is to treat these installations as shafts. The 1990 Code clarifies this intent with the following requirement:

Riser. Cables installed in vertical runs and penetrating more than one floor, or cables installed in vertical runs in a shaft shall be Type CMR. Floor penetrations requiring Type CMR shall contain only cables suitable for riser or plenum use.

This new requirement clarifies the intent of requiring riser or better cable when taking a cable through multiple floors but it does permit a general purpose cable (CM, OFN) to go through one floor only. The permitted uses of general purpose (MP, CM), riser (MPR, CMR) and plenum cables (MPP, CMP) are illustrated in Figure 4.

LIMITATIONS ON CMX

The 1987 Code permitted CMX cable such as D Station Wire, (tested to VW-1, the lowest level of fire resistance) to be used in any residence including high rise apartments except in a plenum or riser. In the 1990 Code, Type CMX cable will be permitted in one- and two-family dwellings anywhere except a riser or a plenum, but it will not be permitted in multifamily dwellings except in exposed applications such as stapled to the baseboard.

COMBINED DATA AND TELEPHONE CABLES

The 1987 Code permits Class 2 circuits such as data circuits and Class 3 circuits (signaling, control) to be run in a cable with communications circuits. In such a case the cable must be listed as a communications cable. Sometimes this requirement causes problems for cable designers who want to use foamed insulation for the data circuits because the foamed insulation will not pass the insulation crush resistance requirement in the UL standard for telephone cable. The 1990 Code offers relief by permitting a listed Class 2 or Class 3 cable to be combined with a listed communications cable with a common jacket joining the two cables into a composite cable. For example, a Type CL2 and a Type CM cable could be used in a composite cable. The fire resistance rating of the composite cable is determined by testing the composite.

CABLE TRAYS

Article 725, which covers Class 2 and Class 3 circuits, including data cables, requires that power limited tray cable Type PLTC be used where cable trays are used (Section 725-40(b) exception). Type PLTC is a heavy-walled cable designed for cable tray use in outdoor applications such as chemical plants. Ordinary data cable (Type CL2) may not be installed in a cable tray. The 1990 Code will contain two new sections pertaining to cable trays for optical fiber, communications and multipurpose cables.

770-52 (d) Cable Trays. Optical fiber cables shall be permitted to be installed in cable trays.

800-52(d) Cable Trays. Communications cables and multipurpose cables shall be permitted to be installed in cable trays.

MULTICONDUCTOR NON-POWER-LIMITED FIRE-PROTECTIVE SIGNALING CABLE

The Code recognizes two types of fire alarm circuits, non-power-limited fire-protective signaling circuits, and power-limited fire-protective signaling circuits. The power-limited types FPLP, FPLR and FPL are the most familiar because they are in the substitution chart discussed earlier. Power wires and power wiring methods (conduit, cable trays, etc.) are generally used for non-power-limited fire alarm circuits, but the 1987 Code does provide for (Section 760-17) a multiconductor, 16 or 18 AWG, cable for this application. The 1990 Code will provide for a plenum, riser and general purpose version of this cable with the following cable markings:

Cable Marking	Type
NPLFP	Non-Power-Limited Fire-Protective Signaling Circuit Plenum Cable
NPLFR	Non-Power-Limited Fire-Protective Signaling Circuit Riser Cable
NPLF	Non-Power-Limited Fire-Protective Signaling Circuit Cable

The cables will be permitted to be used with 150V non-power-limited fire-protective signaling circuits. The insulation voltage rating is 300V so these cables can substitute for 300V power-limited fire-protective signaling cables and the voltage rating on the insulation plus jacket combination is 600V so these cables can be run in a conduit with Class 1 circuits (600 V). The design of these cables may be similar to 16 or 18 AWG cables listed for communications Class 3 or power-limited fire-protective signaling use. The establishment of a non-power-limited plenum cable is a significant change since one has to be concerned with shock hazard when dealing with non-power-limited circuits. The expected use of these cables is to connect a series of annunciators (loud speakers). They will not be energized except when an alarm is sounded, so these cables are significantly different in application than other non-power-limited cables such as Type NM (Romex).

EDITORIAL REVISIONS

In addition to the foregoing changes in the five articles in Table I, they have been revised editorially. The objective of the editorial revisions was to make these articles easier to use and understand.

Stanley Kaufman is Supervisor of the Chemistry, Metallurgy and Product Safety Group at AT&T Bell Laboratories in Norcross, GA. He received a BS in Physics from the City College of the City University of the City of New York, and a PhD in Chemistry from Brown University. He is a member of the National Electrical Code Committee, serving on Panel 16 which is responsible for telephone, optical fiber, and data cable safety.

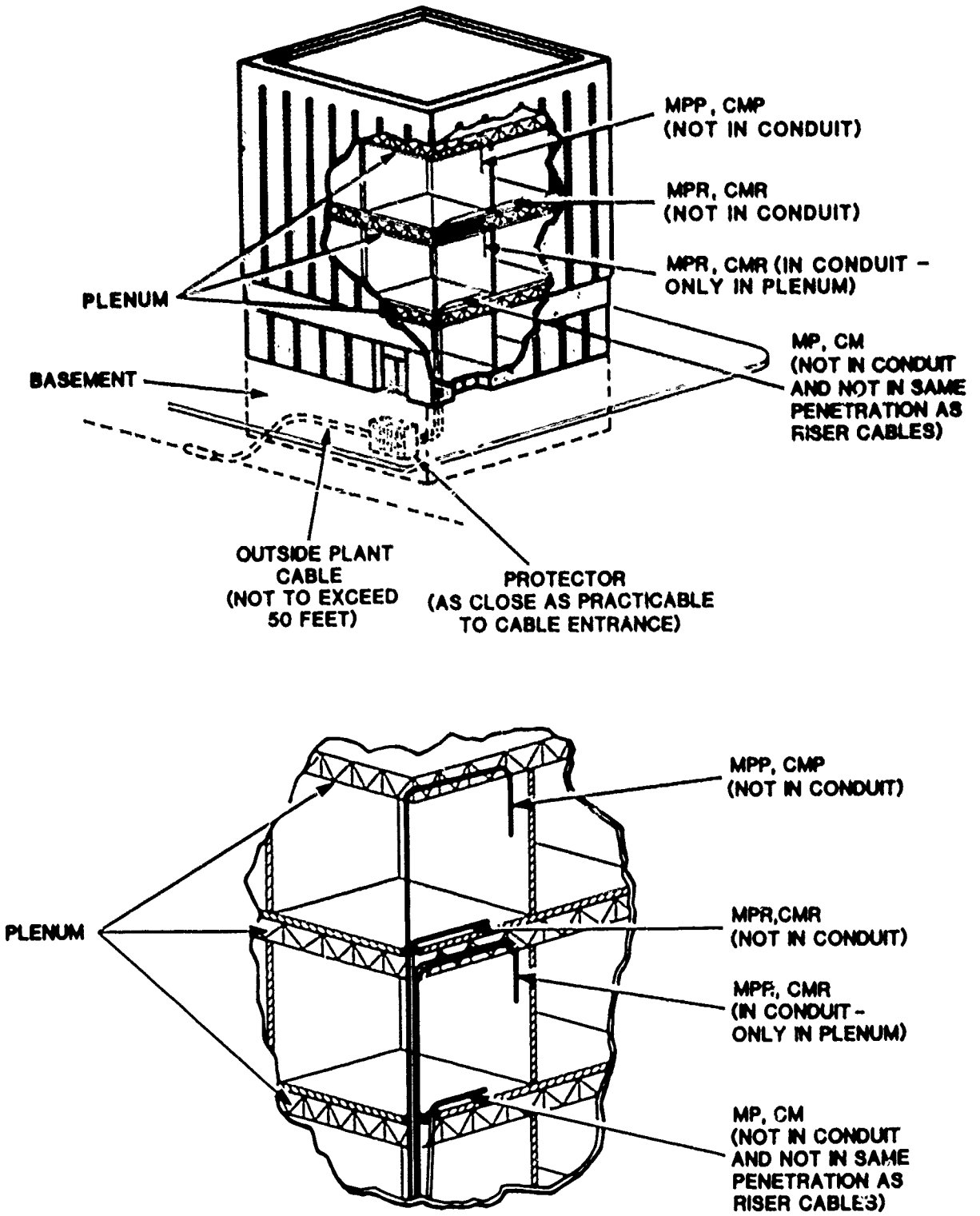

Figure 4. The limitation on the use of unlisted outside plant cable is shown in the top drawing. The uses of general purpose (MP, CM), riser (MPR, CMR) and plenum (MPP, CMP) cables are also shown. The bottom drawing shows that general purpose cables may not be run in the same floor penetration as riser and plenum cable.

DEVELOPMENT OF LOW HALOGEN AND NON HALOGEN FIRE RESISTANT LOW SMOKE CABLE SHEATHING COMPOUNDS BASED ON FUNCTIONALIZED POLYOLEFINS PVC BLENDS

L. K. Sanghi *, A.S. Bhattacharyya*, B. Mukherjee *, A.K. Sen *, P.P. De + and Anil K. Bhowmick+

*Fort Gloster Industries Ltd., (Cable Division), P.O. Fort-Gloster, Howrah - 711 310, India.
+Rubber Technology Centre, I.I.T., Kharagpur, India

Abstract

An attempt is made to develop a novel series of cable sheathing compounds with variation in chlorine content and sufficient fire retardance and unique low smoke characteristics. These have been prepared by blending PVC and functionalized polyolefins in different compositions. PE and EPDM have been functionalized by grafting dibutyl maleate (DBM) using DCP as initiator. FRLS compounds made from PVC functionalized polyolefin blends possess the special characteristics of low smoke, low acid gas generation, increased fire retardance and improved volume resistivity, which are much better in comparison with a typical PVC sheathing compound. Report has been made also on Thermoplastic Elastomer(TPE) based non-halogen FRLS compound. The mechanisms for grafting, polymer-polymer and polymer-filler interactions have been presented.

Introduction

The wide spread use of electric cables in a large number of areas often cause out breaks of fire either by accidental short circuit condition or the burning of some extraneous matter which subsequently ignites the cables. So, it is highly desirable to have a sheathing (protective or jacketing) compound which will be fire resistant on one hand and will have reduced or no hazards from generation of smoke, toxic and corrosive fumes.

For many years, many halogen containing polymers have been used as the base material for fire resistant sheathing compounds in the manufacture of electric cables. Poly (Vinyl Chloride) (PVC) having good flame resistanceproperties coupled with other desirable properties such as good mechanical properties and easy processing was obvious choice for cables of such applications for long time. However, recently it has been recognised that conventional cable sheathing compounds based on PVC can present serious problems in the event of fire due to the formation of large amount of dense black smoke together with acidic and toxic fumes. This becomes a serious concern particularly when a large number of people gather in a confined area like underground railways, hotels, exhibition halls, ships, factories etc. Moreover, the formation of highly acidic and corrosive fumes can damage the costly equipment such as computers, electronic systems, telephone exchages etc.

Well set of properties such as electrical, mechanical, weather resistance and very low smoke generation on burning possessed by polyolefins combined with fire retardance properties of PVC are expected to provide better combination of properties as cable sheathing compounds having significant technological importance. But as such polyolefins are not compatible with PVC and blending of these polymers result in poor mechanical properties.

In the present investigation, efforts are made to develop a set of compounds for sheathing applications based on functionalized polyolefins - PVC blends having sufficient fire retardance and low smoke properties retaining all other properties same. Attempts have also been made to develop non-halogen FRLS Thermoplastic Elastomer compounds based on functionalized polyolefins.

Experimental

Materials: Low density polyethylene(LDPE) (NESTE Polyethylene DFDS - 4445 of Neste Polyeten AB, Sweden) of density 0.915 g/cc and MFI 2.0 g/10 min (ASTM-D 1238), Ethylene propylene 1,4 hexadiene terpolymer (EPDM) (Nordel 2760 of Du Pont USA), Poly (Vinyl Chloride) (PVC) (Indovin of IPCL, India) of K-value 65, Acrylonitrile butadiene copolymer (NBR) (Krynac 3450 of Polysar, Canada) were used. Dibutyl maleate (DBM), dicumyl peroxide (DCP) and other ingredients were of standard laboratory grade.

Graft modifications and blending : Grafting of dibutyl maleate (DBM) on PE and

EPDM were carried out in Brabender Plasticorder (PLE 330) using a cam type mixing head N 50H. Different blend compositions were made in the same mixer. All the modified blends were characterized. PVC used always in stabilised and plasticised form with the formulation as PVC-100, Tribasic lead sulphate (TBLS)-6, Calcium Stearate (C.S.)-1, Trioctyl Trimellitate (TOTM)-50.

Infrared Spectroscopy : Infrared spectroscopy was carried out in Shimadzu IR-420 using thin film of polymer. Free DBM was removed by acetone extraction of the film.

Differential Scanning Calorimetry : A Mettler DSC-20 of TA-3000 system was used. Heating rate was 10°C/min.

Tensile properties : Tensile properties were studied by Zwick UTM (Model 1445) using dumbbell specimen (ASTM D 412-80).

Limiting Oxygen Index (LOI) : LOI of the samples were determined according to ASTM-D 2863-81 specification.

Smoke Density Test : The specification D-2843-81 and NBS Specification ASTM-E-662-83 were followed for smoke density measurement.

Hcl gas generation test : This test was performed according to the specification IEC 754-1.

Scanning Electron Microscopy (SEM) : SEM was carried out in Hitachi SEM Model S145A. Samples were prepared by extraction with cyclohexanone.

Volume Resistivity : Volume Resistivity was measured by a Hewlett Packard 4329A High resistance meter.

Results and Discussion

Functionalization of Polyolefins and its characterization

Both polyethylene (PE) and ethylene propylene diene terpolymer (EPDM) were functionalized by grafting dibutyl maleate (DBM) using dicumyl peroxide (DCP) as initiator at the temperature range of 140° to 220°C. Optimisation of the reaction conditions and reactant concentrations were also done. The optimum concentration of DBM is 10% for both the polymers. This result is in good agreement with that obtained by Greco et al, for ethylene propylene copolymer (EPR)[1]. The optimised concentration of DCP is 0.2% for EPDM and 0.5% for PE. Beyond this concentration of DCP crosslinking of the respective polymers take place. However, the time and temperature for graft modification reactions are same (20 minutes at 160°C).

IR spectra of starting and functionalized PE and EPDM are reported in Fig. 1. Both functionalized polymers show a typically strong absorption band at 1740 cm^{-1} associated with stretching absorption of C = O in the ester groups of the attached maleate units. In general, the resulting degree of functionalization is high for both the polymers. However, a higher degree of graft modification for PE is obtained due to the absence of unsaturation, high chain mobility and less steric hindrance of the more reactive tertiary C-H bonds. This result is also in line with that obtained by Benedetti et.al. for diethyl maleate grafting[2]. The graft modification reactions of PE and EPDM in presence of DCP may be visualised in Scheme 1 and 2 (Fig.2).

Blending of PVC with functionalized PE and EPDM.

The properties of the blends of PVC with PE and EPDM are given in Table 1. PVC shows a tensile strength of 20 MPa. But by the introduction of PE, the tensile strength drops gradually. Similar results are obtained for EPDM system. The elongation at break also shows similar trend in both the cases. The decrease in strength and elongation may be ascribed to the incompatibility of these polymeric systems. Mc. Grath et.al. reported the incompatibility of these two systems[3]. The SEM photographs of the pure polyolefins and PVC blends after cyclohexanone extraction are shown in Fig.3. The phase (layer)separation and non-uniform dispersion of the blends are apparent from the micrographs.

As expected the results also show the gradual improvement of volume resistivity and Hcl gas generation for the blends over PVC. However, decrease in LOI values were observed with the decrease in the PVC content. Smoke density test could not be precisely done due to the excessive smoke generation. However, both LOI and Smoke generation can be improved by the addition of flame retardants and smoke suppressants. But, the major constrain of these blend systems for its application in the cable manufacture is the very poor mechanical properties. The mechanical properties of the blends could be enhanced by improving the physical or chemical compatibility. These are reported for various polymer blends[4,5,6]. In order to compatibilize PVC with PE or EPDM we have functionalized PE and EPDM by graft modifications with DBM. Various properties of the PVC-functionalized polyolefin blends are reported in the Table 2. It may be observed from the table that the blends containing

functionalized PE and EPDM result in considerable improvement in tensile properties over pure blends. Other properties remain more or less same. This improvement in tensile properties is due to the inter penetration and uniform dispersion of the modified blends as shown in Fig.4. Better compatibility is also evident from the lower melting temperature and melting endotherm of functionalized PE in its blends with PVC (similar to the PE-EPDM blends[7]) as indicated in DSC traces(Fig.5).

However, the mechanical properties reported in the Table 2 are far below the industry norms. As such for further improvement the blend systems were modified with the help of the dynamic crosslinking. In a few cases a small portion of Acrylonitrile butadiene rubber (NBR) was also added for better compatibility. NBR was selected as it forms compatible blends with PVC[8].

The tensile properties of a few optimised systems are given in Table 3. These systems are well set to meet the industry norms.

It is observed from the Table 3 that significant improvement in tensile properties has been achieved. DBM being grafted on PE and EPDM gives rise to interaction mainly through a hydrogen bond between the carbonyl group of DBM and methine H of PVC. Besides, dipole dipole interactions of the type C = O .... Cl-C may also exist. This kind of interaction has been evidenced on the basis of progressive shift towards lower frequencies and broadening of the carbonyl band as a function of PVC concentration[2]. The NBR act as co-compatibilizer and increases the adhesion between functionalized polyolefins-PVC interface during mixing enabling further improvement in dispersion. Finally the morphology developed during mixing by chemical and mechanical compatibilization becomes permanent by dynamic crosslinking resulting such significant improvement in tensile properties. The compatibilization between the polymers may be visualised as shown in Fig. 6.

Preparation of fire resistant low smoke (FRLS) compounds based on PVC-functionalized polyolefis blends:

As pointed out that the blends which are optimised for tensile properties do not meet the fire resistance properties. Thus FRLS compounds were made by mixing with some common fire retarding additives such as Aluminium Trihydrate (ATH), Molybdenum trioxide (Mo_2O_3), Antimony trioxide (Sb_2O_3). As a smoke suppressing ingredient Zinc Magnesium sulfate complex was also used[9]. A typical formulation is given in Table 4.

Base polymer/polymer blends studied for FRLS compound are given in Table 5.

Properties of the FRLS Compounds

Mechanical properties :

The mechanical properties of FRLS compounds and its percentage change after heat air ageing at 100°C for 7 days are given in Table 6.

It is observed from the results tabulated in Table 6 that mechanical properties of the PVC drops significantly (21% for T.S. and 28% for E.B.%) on addition of ATH and other additives. But in the case of blends containing functionalized polyolefins there are rather a little improvement in tensile properties. This improvement may result from the compatibilization of ATH with polymer systems. The compatibilization presumably involves the reaction of the pendent ester groups with the hydroxyl groups of the ATH. The interaction between the maleate moieties and ATH - hydroxyl groups takes the form of H-bonding as shown in Fig. 7.

It is also to be noted that the tensile strength and elongation at break meet the industry norms even after the addition of flame retardants. The ageing resistance properties are also satisfactory and almost same for all the compounds.

Fire resistance, Smoke density and acid gas generation properties :

The Limiting Oxygen Index (LOI) values, Smoke denisty and HCl gas generation for the different compounds are given in Table 7.

The results of Table 7 show that LOI values of all the PVC PEgDBM and EPDMgDBM blends are higher than PVC FRLS compound. The most remarkable improvement is observed for the compound [illegible] i.e., for PVC-EPDMgDBM blends. [illegible], LOI decreases with decrease in [illegible] but here this improvement in flame retardancy occurs probably through the enhanced interaction of the maleate groups with the flame retardant additives ATH, Sb_2O_3 and Mo_2O_3. The rapid propagation of a fire occurs through the formation of very high energy H' and OH' radicals[10]. The maleate groups may also act as the scavenger of these radicals and suppress the propagation of the flame. In PVC PEgDBM blends though PE is crosslinked, crystallites may be melted in presence of high heat and flame.

Thus may generate fresh surface by dripping for flame propagation. But for PVC-EPDMgDBM blends there is no such possibility of dripping. Probably due to this reason PVC-EPDMgDBM blends result such improvement in flame retardancy.

It is also observed from the Table 7 that minimum % light transmission significantly increases i.e, smoke generation on burning decreases by the replacement of PVC with functionalized polyolefins. These compounds were also tested in the NBS-Smoke Chamber. The data obtained also support the above result.

It is very interesting to note from the results given in Table 7 that acid gas generation significantly decreases with the partial replacement of PVC, the potential source on liberated HCl. The decrease is above 50%.

Electrical Properties :

Initial volume resistivity of the compounds and its change after water immersion are plotted in Fig. 8. It is observed that initial volume resistivity increases with the increase in proportion of functionalized PE and EPDM in PVC blends. This is due to the non-polar nature of the PE and EPDM. The volume resistivity measured after immersion of the compounds in water decreases with time of immersion due to the diffusion of water into the systems. The decreasing trend is almost similar for all the blends.

Thermoplastic Elastomer based non-halogen FRLS Compound

One Thermoplastic Elastomer (TPE) based non-halogen FRLS compound has also been made. TPE has been prepared by dynamic vulcanization of PEgDBM and EPDMgDBM blends. FRLS compound has been made by mixing special fire retardant additives. The properties of the compounds are given in Table 8.

It is observed from the Table 8 that a good combination of mechanical properties, electrical properties and fire retardance with very low smoke characteristics have been achieved by this TPE based non halogen FRLS compound.

Conclusion

1. A series of low halogen cable sheathing compounds have been developed by blending PVC and functionalized polyolefins.
2. Precise comparisons among all the systems with respect to the electrical, mechanical, ageing and above all fire retardance, smoke generation and acid gas generation properties indicate superiority of the compounds made from PVC functionalized polyolefins blends.
3. [illegible]-halogen FRLS compound made from Thermoplastic Elastomer (TPE) also possess good electrical, mechanical, very low smoke generation and sufficient fire retardance properties.

References

1. R. Greco, G. Maglio and PV. Musto, J. Appl. Polym. Sci. 33, 2513 (1987)
2. E. Benedetti, A.D'Allessio, M.Aglietto, G. Ruggeri, P. Vergamini and F. Ciardelli, Polym. Eng. Sci, 26, 9 (1986)
3. J.E. Mc Grath and M. Matzner, U.S. Patent 3,798,289 (March 19, 1974)
4. M. Xanthos, Polym.Eng. Sci, 28, 1392 (1988)
5. A.Y. Coran in Handbook of Elastomers - New Developments and Technology - Ed. by Anil K. Bhowmickand H.L. Stephens, Marcel Dekker Inc, N.Y. 1988, Ch. 8.
6. N. Roychowdhury and A.K. Bhowmick, J. Appl. Polym. Sci, 37, XXX (1989).
7. A.K. Sen, B. Mukherjee, A.S.Bhattacharyya, L.K. Sanghi, P.P. De and Anil K. Bhowmick, Thermochimica Acta (in press)
8. M. Matsuo, C. Nozaki and Y. Jyo, Polym. Eng. Sci., 9, 197 (1969)
9. E.I. White, W.E. Robertson and J.Schwarez, U.S. Patent, 3, 996, 142, Dec. 7, 1976.
10. Encyclopaedia of Polym. Sci. Eng. Vol. 7, P. 181, John Wiley & Sons, N.Y. (1987).

TABLE 1

Comparison of properties between PVC and PVC-polyolefins blends

Blend system	T.S. (MPa)	E.B. (%)	Volume Resistivity (Ohm-cm)	L O I	Hcl gas generation(%)
PVC - 100	20	250	3×10^{13}	25.5	32.0
PVC-85+PE-15	5.5	62	7×10^{13}	24.8	27.5
PVC-75+PE-25	4	48	2×10^{14}	24.5	26.0
PVC-85+EPDM-15	5.9	68	7.5×10^{13}	24.8	27.6
PVC-75+EPDM-25	5.1	60	2.4×10^{14}	24.5	26.2

TABLE 2

Various properties of the PVC - functionalized poly-olefins blends

Blend system	T.S. (MPa)	E.B. (%)	Volume Resistivity (Ohm-cm)	L O I	Hcl gas generation(%)
PVC-85+PEgDBM-15	8.4	93	6.8×10^{13}	24.7	24.2
PVC-75+PEgDBM-25	7.5	88	1.5×10^{14}	24.5	22.9
PVC-85+EPDMgDBM-15	9.8	105	7.6×10^{13}	24.8	23.6
PVC-75+EPDMgDBM-25	9.1	98	2.6×10^{14}	24.4	22.0

TABLE 3

Comparison of Tensile Properties for different blend systems prepared by dynamic vulcanization techniques

	T.S.(MPa)	E.B.(%)
PVC-85+XLPE-10+PEgDBM-5	10.5	107
PVC-75+XLPE-20+PEgDBM-5	9.8	100
PVC-85+XLPE-10+PEgDBM-5+NBR-2	13.5	135
PVC-75+XLPE-20+PEgDBM-5+NBR-4	12.2	120
PVC-85+XLEPDM-10+EPDMgDBM-5	11.6	125
PVC-75+XLEPDM-20+EPDMgDBM-5	11.0	115
PVC-85+XLEPDM-10+EPDMgDBM-5+NBR-2	14.5	150
PVC-75+XLEPDM-20+EPDMgDBM-5+NBR-4	13.8	140

XLPE and XLEPDM are crosslinkable PE and EPDM containing peroxide.

TABLE - 4

Formulation of FRLS Compound

Base Polymer/Polymer blends	100
Molybdenum Trioxide(Mo_2O_3)	8
Antimony Trioxide(Sb_2O_3)	6
Aluminium Trihydrate(ATH)	45
Zinc Magnesium sulfate complex	2

TABLE - 5

A_F	PVC - 100
B_F	PVC-85+XLPE-10+PEgDBM-5+NBR-2
C_F	PVC-75+XLPE-20+PEgDBM-5+NBR-4
D_F	PVC-85+XLEPDM-10+EPDMgDBM-5+NBR-2
E_F	PVC-75+XLEPDM-20+EPDMgDBM-5+NBR-4

Suffix F denotes FRLS compound made according to the formulation given in Table 4.

TABLE - 6

Mechanical properties of different FRLS compounds

FRLS Compounds	T.S.(MPa)	E.B.(%)	Percentage change on ageing	
			T.S.	E.B.%
A_F	15.8	180	+ 2.0	- 3.5
B_F	14.0	150	+ 1.5	- 3.0
C_F	13.1	143	+ 2.5	- 4.0
D_F	15.1	160	+ 2.0	- 3.0
E_F	14.3	153	+ 3.0	- 4.5

TABLE - 7

The Limiting Oxygen Index (LOI), Smoke Density and HCl gas generation of the different FRLS Compounds

Compound	LOI	Minimum % light transmission	Smoke Density (Dm)	% HCl generated
A_F	33.0	41.0	388	15.3
B_F	34.0	50.5	350	7.5
C_F	34.0	58.4	327	6.8
D_F	35.0	51.7	348	7.3
E_F	36.5	60.6	317	6.6

TABLE - 8

Properties of TPE based non-halogen FRLS compound

T.S.(MPa)	E.B. %	Volume Resistivity (Ohm-cm)	LOI	Smoke Density (Dm)	Minimum % light transmission
8.4	270	8.2×10^{15}	30.3	108	81

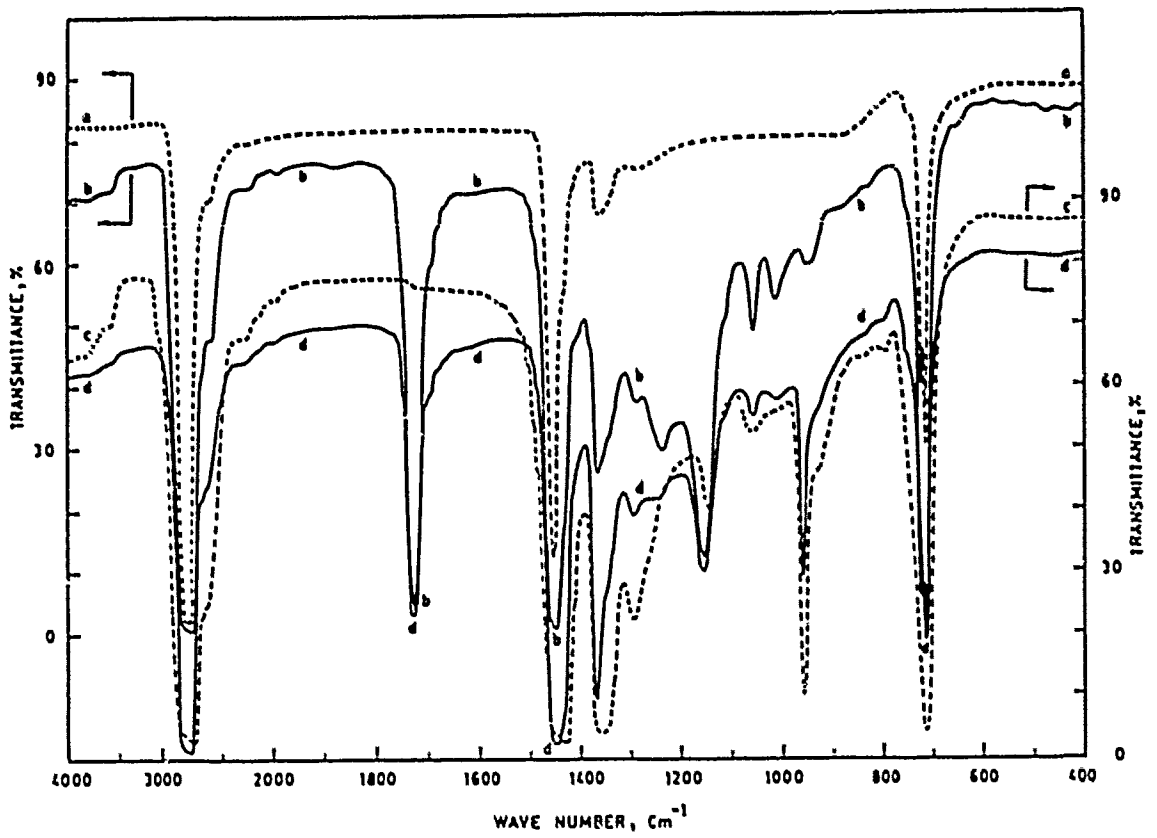

Fig. 1 Infrared spectra of (a) PE, (b) PE-g-DBM, (c) EPDM, (d) EPDM-g-DBM.

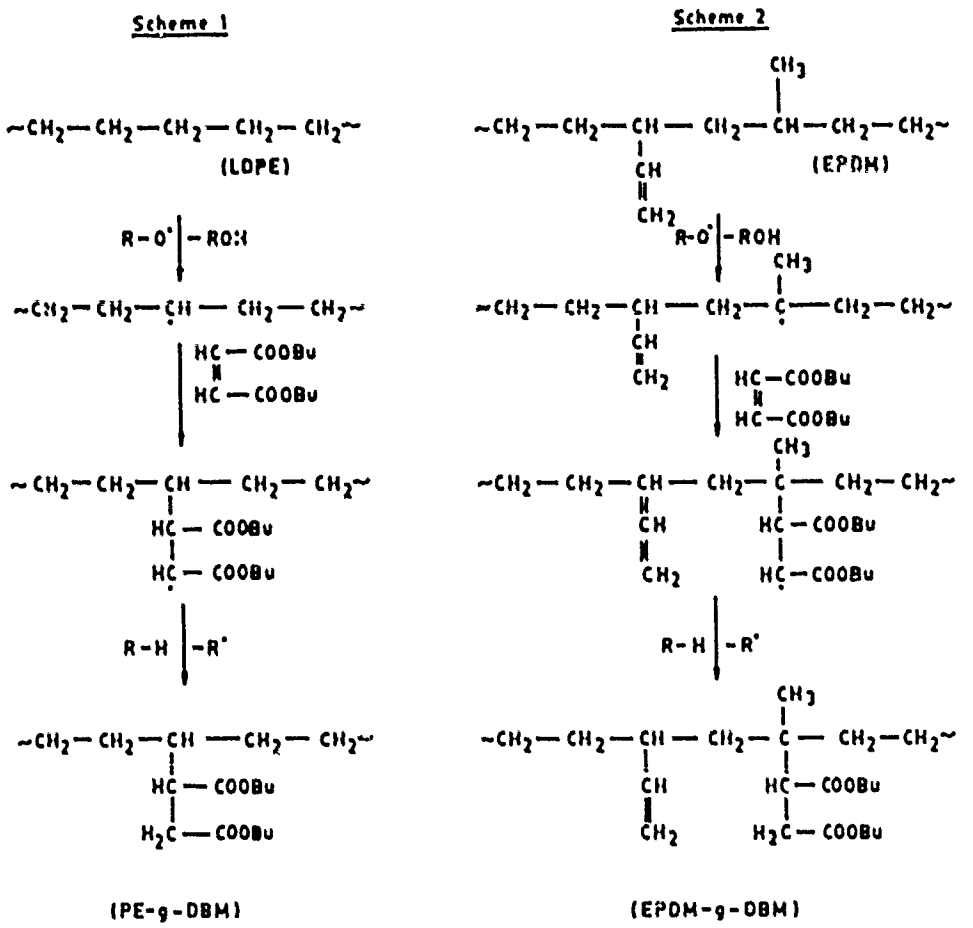

Fig.2 Schematic representation of the graft modification reactions. Scheme 1 for PE and Scheme 2 for EPDM.

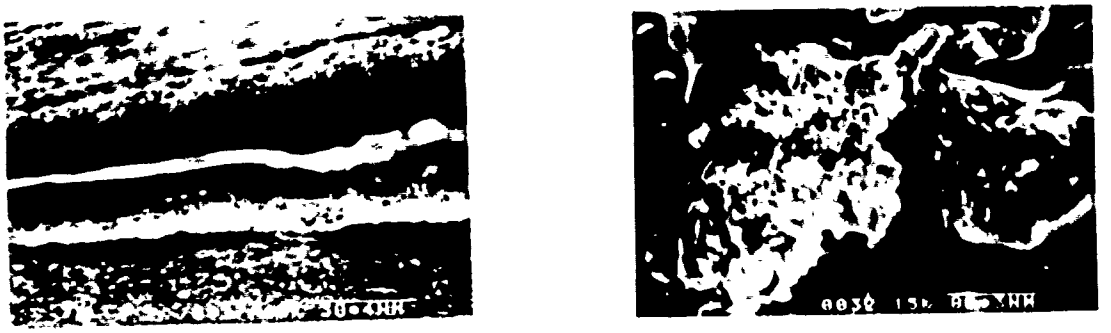

(a) (b)

Fig. 3 SEM Photograph of PVC-PE (75:25) blends (a) phase(layer) separation (b) non-uniform dispersion.

(a) (b)

Fig. 4 SEM Photographs shwoing interpenetration and uniform disperson of (a) PEg DBM and (b) EPDMgDBM in PVC blends.

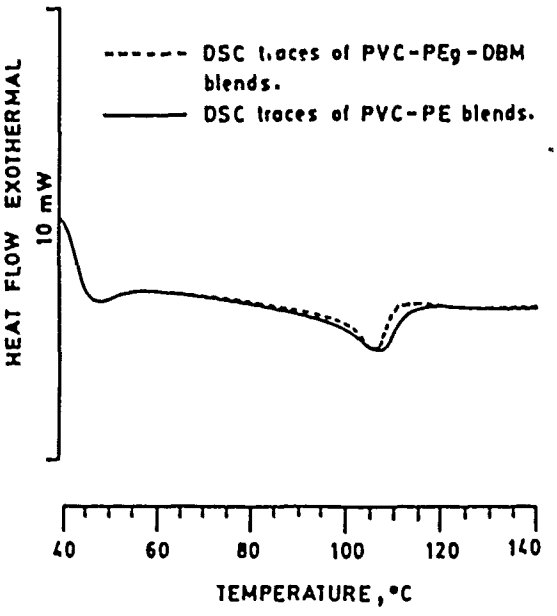

Fig. 5 DSC traces of PVC-PE and PVC-PEg-DBM blends.

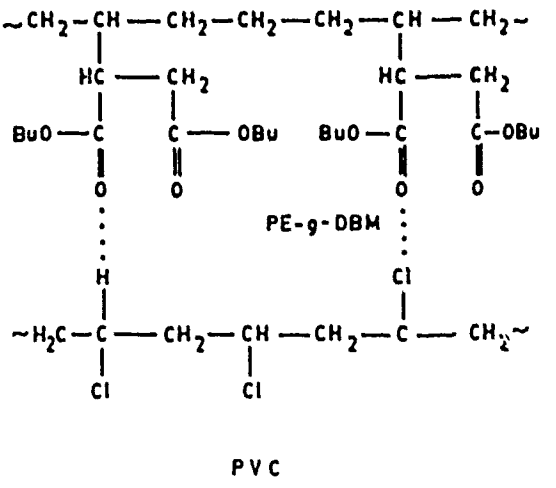

Fig. 6 Mechanism of compatibilization between PE-g-DBM and PVC through H-bonding and dipole-dipole interactions.

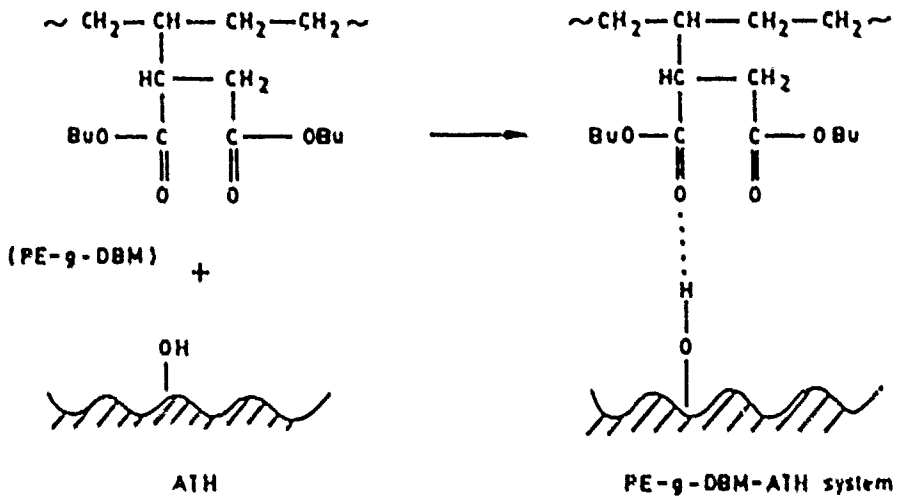

Fig. 7 Schematic representation of H-bond formation between the hydroxyl group of ATH and maleate group of PE-g-DBM.

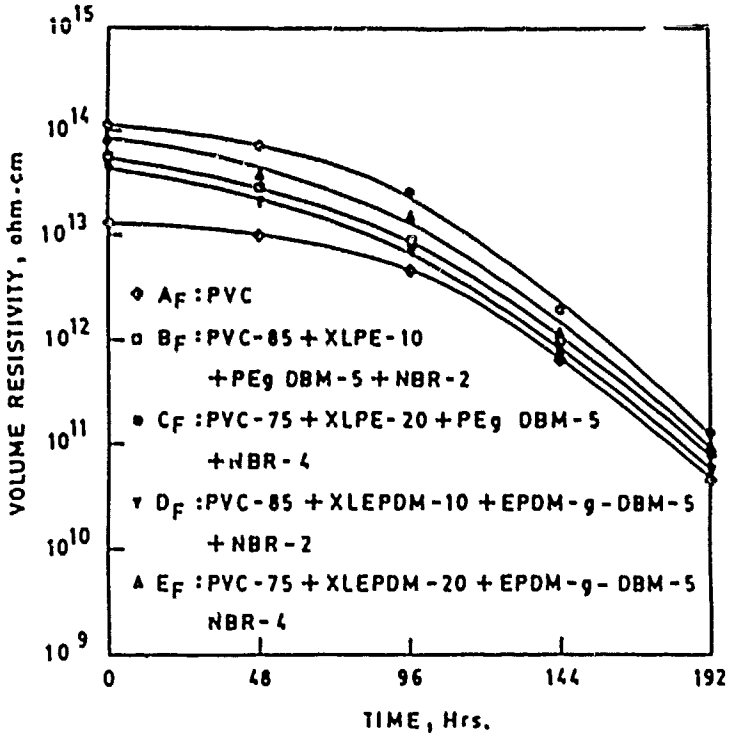

Fig. 8 Variation of volume resistivity with time of immersion in water of different FRLS compounds.

L.K.Sanghi
Fort Gloster Industries Ltd.,
(Cable Division)
P.O. Fort Gloster
Dist: Howrah
Pin: 711 310
INDIA

Lalit Kumar Sanghi was born on 2nd September 1926 at Narnaul, now in Haryana, India. He is a graduate of Science from Rajputana University. From 1951 to 1958, he worked for M/s. Digvijay Cement Co.Ltd, Jamnagar, Saurashtra, India, as a Senior Chemist and later on with M/s. Kettlewell Bullen & Co. Ltd, Calcutta, India, as Industries Development Officer. He joined Fort Gloster Industries Ltd, Calcutta, in 1958 as a Chief Chemist. M/s. Fort Gloster Industries Ltd, is one of the Companies managed by M/s. Kettlewell Bullen & Company Ltd.

He is associated with M/s. Fort Gloster Industries Ltd, right from its inception and has held the position of Administrative Secretary and later on as Chief - Chemist, Assistant Technical Manager from 1960 to 1965, Technical Manager from 1965 to 1971 and then Works Manager from 1972 to 1977. He was elevated to the post of General Manager of the Company which he is still holding.

During his assignments in the Industries he received the fellowship of Geological Mining and Metallurgical Society of India, Fellow Member of Institution of Instrumentation Scientists & Technologists (India), Life Associate of Institution of Chemists (India), Member ERA Technology (London), Convenor Bureau of Indian Standards - ETDC 59/P4, CIGRE (France), Corporate Member Indian Institute of Personnel Manager, Calcutta, and many other professional associations and academic Institutions in the Country.

Presently he is involved both in Technical and Administrative work. His interests include development of new cables and wires and manufacturing/process technology and side by side cable design, improvement in materials etc.

He has in his credit 17 Papers which have been published in various journals.

Dr.A.S.Bhattacharyya
Fort Gloster Industries Ltd., (Cable Division)
P.O. Fort Gloster
Dist: Howrah
Pin: 711 310
INDIA

Arabinda Shekhar Bhattacharyya was born in West Bengal, India on 2nd February 1937. He received M.Sc.(Chemistry) and Ph.D. (in Technology) degree from University of Calcutta, India. He Joined to Fort Gloster Industries Ltd (Cable Division)in 1965 as Technical Officer. At present he is working as Technical Manager. His research interests include, Cable Design, process development, new test method development, crosslinking, modifications, characterizations of polymer s, its blends and composites. He is the member of B.I.S. & PRI (London). He also holds the position of Invited Lecturer in the University of Calcutta and Indian Institute of Technology, Kharagpur.

Ms. B. Mukherjee
Fort Gloster Industries Ltd.,(Cable Division)
P.O. Fort Gloster
Dist:Howrah
Pin: 711 310
INDIA

Ms. Bibha Mukherjee received the M.Sc. (Chemistry) in 1982 and M.Tech.(Polymer) degree in 1984 from Indian Institute of Technology, Kharagpur. She joined to the R & D Centre of Fort Gloster Industries Ltd, (Cable Division) in 1984. As Asst. Research Officer she is now working in the field of Compound Design, Development of fire retardants and smoke suppressants, polymer modifications and thermal analysis.

A.K. Sen
Fort Gloster Industries Ltd,
(Cable Division)
P.O. Fort Gloster
Dist: Howrah
Pin: 711 310
India

Achintya Kumar Sen received B.Tech. in 1984 and M.Tech.(Plastics and Rubber Technology) in 1987 from University of Calcutta, India. Formerly, he was Technical Officer of Himalaya Rubber Products Ltd, West Bengal (1984-85). He has joined to Fort Gloster Industries Ltd,(Cable Division) as Polymer Technologist in 1987. His research areas include functionalization and crosslinking technology of polymers, polymer blends, polymer characterization and process development. He is associate member of Institution of Engineers (India).

Dr.(Mrs.)P.P.De
Rubber Technology-Centre,
Indian Institute - of Technology,
Kharagpur-721302
India

Dr.(Mrs.) Prajna Paramita De did her M.Sc. in Chemistry in 1966 and received Doctorate degree in Analytical Chemistry from Indian Institute of Technology in the year 1973. She also worked in Instrumentation in Biomaterial Sections of University of Tennessee, Memphis, U.S.A. for one year (1972-1973). At present she is working as Lecturer in Rubber Technology Centre and her field of research is Thermoplastic Elastomers, Blends and composites.

Anil K. Bhowmick
Rubber Technology - Centre,
Indian Institute of Technology,
Kharagpur -721302
India

Anil K. Bhowmick is Professor at the Rubber Technology Centre, Indian Institute of Technology, Kharagpur, India. Formerly, he was associated with the London School of Polymer Technology, U.K. (1987) and the Institute of Polymer Science, University of Akron, Akron, Ohio (1981-84). He is co-editor of the Handbook of Elastomers - New Developments and Technology (Marcel Dekker Inc. N.Y. 1988) and a special issue of the Journal if Macromolecular Science - Chemistry. He is a member of the American Chemical Society's Rubber Division and PRI. Prof. Bhowmick received the M.Sc.(1976) and Ph.D.(1980) degree from IIT, Kharagpur. His research interests include, Adhesion Science and Technology, Thermoplastic Elastomers, Polymer Blends and composites, Polymer modifications and characterization.

FLASH AND IGNITION CHARACTERISTICS OF FLAME RETARDANT MATERIALS

Shin Yoshida, Kazumi Ito, Yuko Tamamoto,
Fumio Aida, Etsuo Hosokawa

Showa Electric Wire & Cable Co., Ltd. Kawasaki, Japan

ABSTRACT

In this study, we measured flash and ignition points of various electric wire and cable materials based on ASTM D 1929.[1] Through such measurement, it came to be known that the temperature of material itself at flashing or ignition is affected much by its polymer structure and exothermic and endothermic reactions ascribable to various additives and does not necessarily reflect the flame retardancy of the material. At the early stage of a fire, on the other hand, the ambient temperature plays an important role because whether a material catches fire or not depends on the thermal energy supplied to it from its environs. A method which we devised allows to easily determine the ambient temperature necessary for ignition of materials using the same apparatus as that for the ASTM method with a slight modification.

INTRODUCTION

While many polymer materials such as rubbers and plastics are being used recently in almost everything we come across in our daily life including building materials and home electric appliances, the importance of nonflammability of such materials is getting recognized again with serious reflections on disastrous fires. Materials for electric wires and cables are no exception on this point, and many flame retardant cables have been developed.

It goes without saying that what is important at discussing the problem of making materials nonflammable is to understand the manners and underlying mechanisms of combustion of rubbers, plastics and other organic materials. Data on combustion characteristics, flash points and ignition points of such materials, especially, are rather insufficient.[2] In addition, combustion characteristics of materials such as flash point and ignition point depend much on environmental conditions, and test methods for determining such characteristics constitute a very important factor for assessing the problem.[3]

In this paper, we investigate flash and ignition characteristics of several materials for electric wires and cables, using an apparatus with some own features, conforming to ASTM D 1929 which is generally known as a method for measuring flash and ignition points of plastics. Findings of some interest obtained in the investigation are reported.

Test Method

Specimens

Samples were made into pellets of 3-mm cube, and 3 g of such pellets were used as a specimen for each test.

Apparatus

The overall configuration of the test apparatus is shown in Fig. 1. The heating furnace of the apparatus has a heating capacity greater than 600°C/h. The sample dish is furnished with a load cell of 5 g in weighing capacity and 0.01 g in sensitivity allowing to measure changes in sample weight. The furnace temperature (near the sample dish), sample dish temperature and sample temperature are measurable with thermocouples.

Details of the furnace is shown in Fig. 2. The specimen can be flashed either with sparks by the platinum electrode near the sample dish (Fig. 2A) or with the pilot burner on top of the furnace conforming to ASTM (Fig. 2B).

Measurement Procedure

Heating Test The approximate furnace temperature at which the specimen flashes or ignites is determined by raising the furnace temperature at the rate of 300 or 600°C/h while the air flows in the furnace at a flow rate of 5 or 10 ft/min. The air flow rate which gives lower furnace temperature for ignition in the heating test is used in the constant temperature test which follows.

Constant Temperature Test The constant temperature test is carried out as follows:

(1) The furnace is heated to a temperature 10°C below the temperature obtained in the heating test, while the furnace is fed with the air (at the flow rate determined in the heating test) from the bottom of the furnace.

(2) Setting the sample in the furnace, the sample is observed whether the combustible gas from the sample catches fire or not under the action of the pilot burner (ASTM) or sparks.

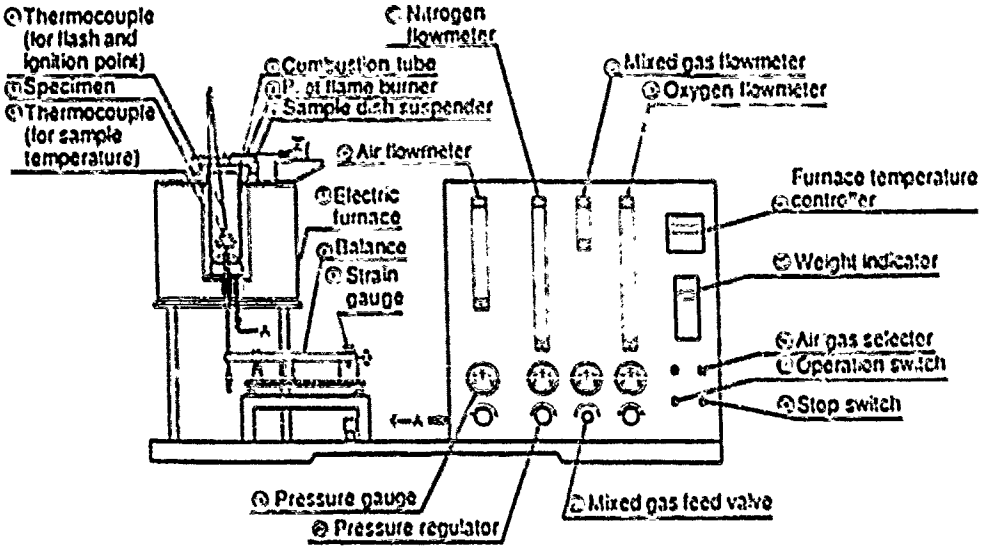

Fig.1 Apparatus for flash and ignition point measurement

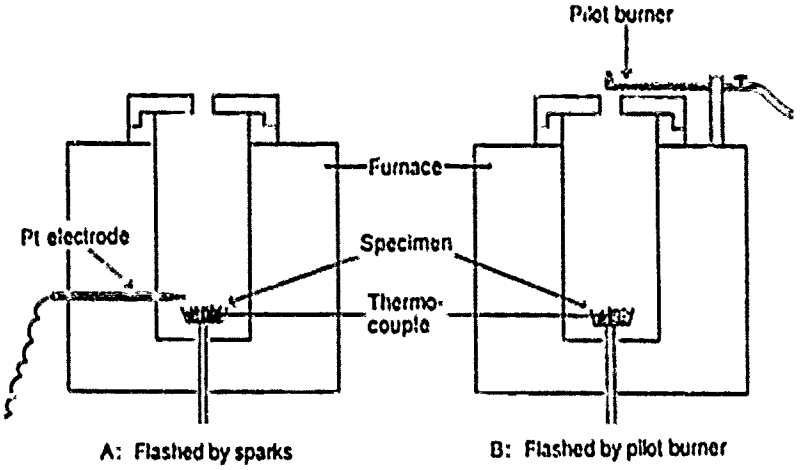

Fig. 2 Details of the furnace

(3) If flashed, the test is repeated after lowering the furnace temperature by 10°C. If not flashed, the test is repeated after raising the furnace temperature by 10°C.

(4) The flash point is obtained as the sample temperature at which flashing occurs under the lowest flashable furnace temperature.

(5) The ignition point is obtained as the sample temperature at which ignition occurs without pilot burner or sparks.

FLASH AND IGNITION POINTS OF WIRE AND CABLE MATERIALS

Samples

Polyethylene (PE), polyvinylchloride (PVC) and rubber which are being used generally as electric wire and cable materials were used as samples. Such samples are listed in Table 1.

Table 1 Samples for flash and ignition point measurement

Category	Sample	Symbol
PE	Cross-linked PE	XLPE
	Flame-retardant cross-linked PE	FR-XLPE
	Non-halogen PE	NH-PE
PVC	Soft PVC (DOP 50PHR)	PVC-1
	Semi-rigid PVC (DOP 40PHR)	PVC-2
Rubber	Ethylene-propylene rubber	EPR
	Chloroprene rubber	CR-1
	Flame-retardant chloroprene rubber	CR-2
	Flame-retardant Hyparon rubber	CSM

RESULTS

Flash and Ignition Points by ASTM Method Heating Test (Preliminary Test)

Effects of Air Flow and Heating Rate Heating tests were carried out at different air flow rates (5 and 10 ft/min) and heating rates (300 and 600°C/h) to determine the approximate furnace temperature at which flashing or ignition occurs on each sample.

The results of the heating test (5 ft/min, 600°C/h) obtained on XLPE are shown in Fig. 3 as an example. In addition, results on representative materials (XLPE, PVC-1 and EPR) are summarized in Table 2. Note that the flash point and ignition point of each sample in Table 2 are the furnace temperatures at which flashing and ignition, respectively, occurred on the sample.

The results given in Table 2 indicate that the furnace temperature at which flashing or ignition occurs is lower when the air flow rate is lower. In addition, it was found that neither flashing nor ignition occurs on PVC-1 in the heating test. It is estimated that the nonflammability of PVC-1 found in the test comes from the following sequence of events: The plasticizer, a combustible additive in PVC, evaporates at relatively low temperature and carbonization of the polymer progresses as the generation of hydrogen chloride gas follows,[4] reducing, in this way, the release of combustible gas near its intrinsic ignition point.

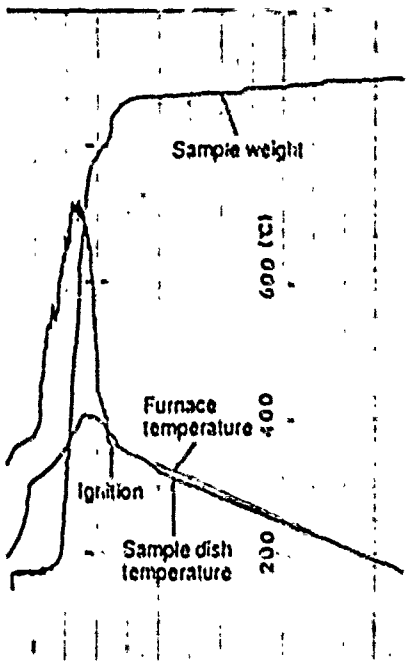

Fig. 3 Heating chart of XLPE

Table 2 Furnace temperatures at which flashing and ignition occurred on some representative samples in the heating test

Heating rate (°C/h)	Flow rate (ft/min)	XLPE		PVC-1		EPR	
		Flash pt.	Ignition pt.	Flash pt.	Ignition pt.	Flash pt.	Ignition pt.
600	5	360	360	No flashing	No ignition	385	385
	10	380	380	No flashing	No ignition	400	403
300	5	375	370	No flashing	No ignition	370	383

Constant Temperature Test (Main Test)

Following the heating test which determined approximate furnace temperature at which flashing and ignition occurs on each sample, the constant temperature test was carried out to determine accurate flash and ignition points of each sample. An example of temperature chart obtained in the constant temperature test is shown in Fig. 4, and flash points and ignition points of each sample determined from such temperature charts are given in Table 3.

Polyethylene Flash points and ignition points of three kinds of polyethylene are different among them reflecting differences in their composition. For XLPE, having no additive, its flash point and ignition point are fairly higher than the furnace temperature, while, for FR-XLPE, the furnace temperature is a little higher than its flash and ignition points. The difference between XLPE and FR-XLPE may come from the endothermic reaction of halogenic flame retardant contained in FR-XLPE and a rapid exothermic oxidation which occurs near the ignition point in XLPE containing no additive. NH-PE is showing characteristics just between those of FR-XLPE and XLPE possibly because the dehydration temperature of metal hydroxides added in NH-PE is lower than the acting temperature of the halogenic flame retardant added in FR-XLPE.

Polyvinylchloride The flash and ignition points of both PVC-1 and PVC-2 are relatively low compared with those of other materials. This may come from the plasticizer which evaporates at temperatures relatively lower than the temperature at which combustible gas is generated by pyrolysis in these polymers. The plasticizer, which evaporated gradually in the heating test at temperatures below the intrinsic ignition point of the material due to the slow rate of temperature rise, is released rapidly in the constant temperature test where the furnace temperature is high from the beginning, possibly affecting the ignition. Both samples have flash points which are comparable with the furnace temperature and ignition points which are lower than the furnace temperature. It is estimated that the endothermic effects associated with dehydrochlorination in these polymers contribute much to this phenomenon in addition to the temperature and rate at which the plasticizer is released from these polymers.

It can be said that PVC is a material of which flash and ignition points depend much not only on test conditions but also on the composition of three gaseous constituents, i.e., evaporation of plasticizer, release of hydrogen chloride gas and generation of combustible gas by pyrolysis of the polymers.

Rubber It is rather difficult to generally evaluate rubber because of its polymer structure which depends much on the kind. EPR, which, as XLPE, does not contain halogens in the polymer, has flash and ignition points close to those of XLPE, but its furnace temperature is fairly high compared with that of XLPE. It can be estimated that the high furnace temperature of EPR comes from the large amount of inorganic fillers added in EPR, which makes the ratio of combustibles small in EPR. CR and CSH have polymer structures similar to that of PVC, but their flash and ignition points are higher than those of PVC because of the smaller amount of plasticizers in them.

What peculiar to rubbers in their combustion characteristics is that there is a temperature gap of about 100°C between the furnace temperature at which flashing and ignition occur and that at which neither flashing nor ignition occurs. Flashing causing a fire ball occurred between these furnace temperatures. These combustion characteristics come from the effects of plasticizers, like those in PVC but small in amount.

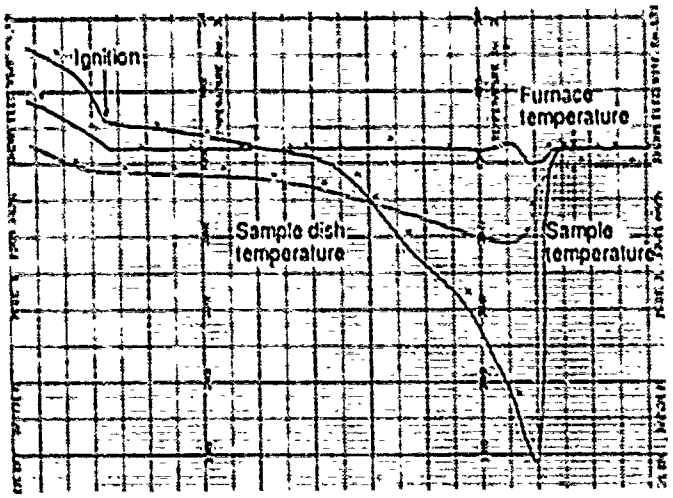

Fig. 4 Temperature chart of constant temperature test on NH-PE

Table 3 Ignition and flash points of materials

		Ignition point		Flash point	
		Ignition pt. (°C)	Furnace temp. (°C)	Flash pt. (°C)	Furnace temp. (°C)
PE	XLPE	427	360	425	360
	FR-XLPE	383	390	375	380
	NH-PE	457	430	454	430
PVC	PVC-1	311	350	308	300
	PVC-2	294	370	342	330
Rubber	EPR	413	41	430	400
	CR-1	390	46.	325	290
	CR-2	424	440	413	370
	CSH	384	460	364	4[illegible]0

Flash Points by Spark Method

The ASTM method using a pilot burner as the flashing source resulted, for some materials (PVC-2 and EPR), a flash point which was higher than the ignition point. Flash points of materials therefore were measured using a flashing source of electric sparks near the sample dish to examine the effects of the flashing source position on flashability of materials. Results are shown in Table 4 along with those obtained by the ASTM method.

As seen in Table 4, flash points of materials measured with a flashing source inside the furnace are clearly different from those measured with a flashing source outside the furnace.

With the use of the internal flashing source, the furnace temperatures of PE lowered by 10 to 30°C and their flash points lowered by about 20 to 50°C comparing with those measured with the external flashing source.

For PVC, the furnace temperature of PVC-2 did not change much but its flash point lowered by as much as 100°C, while those of PVC-1 lowered by about 30°C for both.

For rubber, both the furnace temperature and the flash point of EPR decreased. For CR-1 and CR-2, their furnace temperatures did not change, but their flash points lowered. For CSM, the furnace temperature lowered by 40°C but its flash point went up by about 20°C.

The phenomenon of the flashing point higher than the ignition point observed on PVC-2 and EPR in the ASTM method was not observed in the spark method where the flash point was lower than the ignition point for all materials. The flash point by the spark method was generally lower than that by the ASTM method except for the case of CSM for which the flash point by the spark method was a little higher than that by the ASTM method. It should be noted, however, that the furnace temperature at flashing tended to be lower by the spark method.

DISCUSSION

Flash and ignition points measured by the ASTM method having a flashing source outside the furnace and flash points measured by the spark method having a flashing source near the sample dish inside the furnace were presented in the previous section. This section discusses such results including some factors such as test conditions which affect the combustion characteristics of materials.

Effects of Furnace Temperature

Figure 5 shows temperature charts obtained in measuring the ignition point of PVC-2. The chart on the left is the one which allowed to determine the ignition point and the chart on the right is the one which was obtained at the furnace temperature lower than that of the left chart by 10°C resulting no ignition.

In the furnace of 360°C, the sample temperature rose as a function of the time without causing an ignition, and reached about 420°C in 7 minutes. Ignition occurred finally when the furnace temperature was raised by 10°C to 370°C, and the sample temperature (i.e., the ignition point) at ignition was 294°C.

This sequence of events indicate that it is very important, in discussing the combustion characteristics of a material, to consider not only the characteristic temperatures of the material such as flash and ignition points but also the ambient temperature (which is the furnace temperature in the test) at which the material is ignited.

Table 4 Ignition and flash points of materials

		Ignition point		Flash point			
				Spark method		ASTM method	
		Ignition pt. (°C)	Furnace temp. (°C)	Flash pt. (°C)	Furnace temp. (°C)	Flash pt. (°C)	Furnace temp. (°C)
PE	XLPE	427	360		330	425	360
	FR-XLPE	383	390		370	375	380
	NH-PE	457	430		420	454	430
PVC	PVC-1	311	350	277	270	308	300
	PVC-2	294	370	240	330	342	330
Rubber	EPR	413	410	378	390	430	400
	CR-1	390	400	307	290	325	290
	CR-2	424	440	321	370	413	370
	CSM	384	460	380	390	364	430

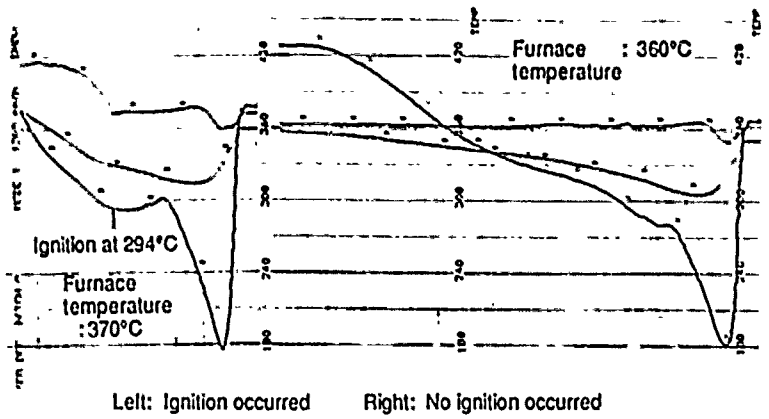

Fig. 5 Temperature charts obtained in measuring the ignition point of PVC-2

Effects of the Position of Flashing Source

The flash point obtained by the spark method was generally lower than that obtained by the ASTM method. This tendency can be explained as described below.

The sample in the furnace is covered near its surface with a layer of a mixture of saturated combustible gas generated by pyrolysis in the sample and the air. The combustible gas in the saturation layer diffuses upward from its top portion carried by the air flowing in the furnace while it is kept replenished through pyrolysis in the sample. That is, a diffusion layer is existing on top of the saturation layer, and the concentration of combustible gas in the diffusion layer can be getting smaller upward.

As shown in Fig. 6 therefore, the mixture of combustible gas generated by pyrolysis and the air is existing forming layers above the sample surface. The concentration of combustible gas in such layers can be the greatest in the layer closest to the sample surface and getting lower and lower in higher layers.

Assuming that the combustible range of the mixture of combustible gas and the air is defined by C1 and C2, the pilot burner or a spark would cause flashing if the mixture around the flashing source has a combustible gas concentration falling within its combustible range, and the surrounding layers of combustible gas will burn by the heat of this flashing. The combustion of the sample after flashing will continue if the pyrolytic combustible gas generated at sample surface by the heat associated with the burning balances with the rate of burning of the combustible gas.

If the furnace temperature is lower and the heat supplied to the sample is inadequate, the rate of generation of combustible gas by pyrolysis gets smaller, and the position of the layer of mixture which falls within the combustible range mentioned above will get closer to the sample surface. If the furnace temperature is much lower, the concentration of combustible gas would be lower than the lower combustible limit in any layer, and no flashing would occur.

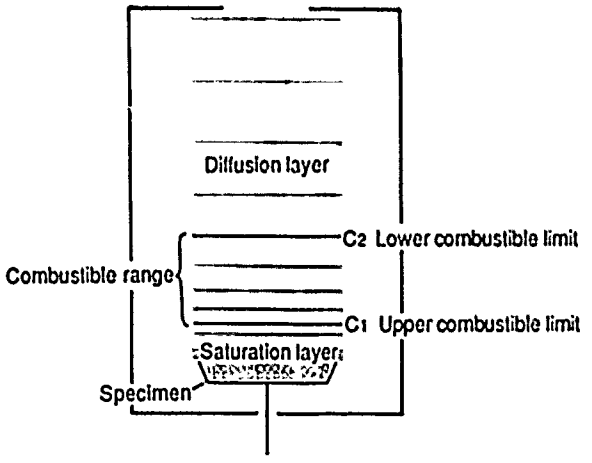

Fig. 6 A model of concentration of combustible gas in furnace

It can be conjectured that the flashing by the pilot burner requires the furnace and sample temperatures higher than those required for flashing by sparks because the combustible gas must be generated at a rate which is high enough to cope with the dilution which occurs in the course reaching the pilot burner for the layer of mixture to be within the combustible range near the pilot burner above the furnace.

Relations between the Furnace Temperature and the Time Required for Ignition

A very important problem in considering the early stage of fires is the ambient temperature at which materials would be ignited. The temperature of a material itself at the time of ignition may not necessarily reflect the flame retardancy of the material accurately because it depends much on the molecular structure of the polymer and exothermic and endothermic reactions ascribable to various additives contained in the material.[4, 5]

In order to evaluate the flame retardancy of materials with the eye only to the ambient temperature, we measured the time required before a material was ignited at different furnace temperatures for all the materials. The measurement indicated for all materials that the time required for ignition tends to get shorter when the furnace temperature is higher. In addition, plotting the furnace temperature (°C) on the abscissa and the inverse of the time required for ignition, t (sec) revealed that the relation between them is linear for all materials at a very high correlation. Such relations are shown in Fig. 7, as an example, for the case of polyethylene. The furnace temperature at point obtained by extending such a relation to zero on the ordinate indicates the highest furnace temperature at which the material would not be ignited, and such temperature coincide relatively well with the result obtained by the ASTM method.

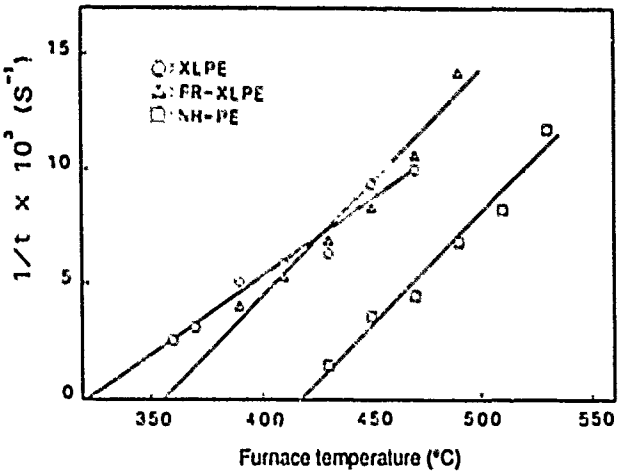

Fig. 7 Relations between furnace temperature and time required for ignition (PE)

To find the lowest furnace temperature at which a material is ignited by the ASTM method, it is necessary to repeat the test at different furnace temperatures in steps of 10°C. The method described above allows to determine the ambient temperature necessary for ignition of a material only by making measurements at three or more furnace temperatures in steps of a few tens of degrees centigrade and extending the line thus obtained. In addition, the temperatures thus obtained are thought to be reflecting well the flame retardancy of materials at the early stage of fires.

CONCLUSION

Flash and ignition points of various electric wire and cable materials were measured in accordance with the method specified in ASTM. It was found that sample temperatures vary with each sample because they are affected much by the molecular structure of polymers and exothermic and endothermic reactions ascribable to various additives. It was found in addition, that the value of flash point is susceptible to change affected much by the position of the flashing source and differences in experimental conditions. For evaluation of flame retardancy of materials in the early stage of fires, on the other hand, the ambient temperature becomes a very important factor, and it is desirable to use a test method which is not affected by other factors to the extent possible. For the purpose of evaluating the ambient temperature at which a material would be ignited, a basic flame retardancy factor of materials, we devised a method which allows to easily obtain the ambient temperature necessary for ignition of materials by using the same apparatus as that used for the ASTM method with a small modification.

It is desirable that such method be developed to a systematic test method for evaluation of flame retardancy of materials through further examinations. It is hoped also that the method can be a help for understanding ignition of materials at fire and for developing flame retardant materials for various applications.

REFERENCES

(1) ASTM D 1929-77, Standard Test Method for IGNITION PROPERTIES OF PLASTICS.

(2) Hilado: Flammability Hand Book, 3rd edition (1982)

(3) Lewins, Atlas, Pearce: Flame Retardant Polymeric Materials, Vol. 2 (1978)

(4) SFPE Handbook of Fire Protection Engineering, 1st edition (1988)

(5) Kuryla, Papa: Flame Retardancy of Polymeric Materials, Vol. 4 (1978)

Shin Yoshida
Showa Electric Wire & Cable Co., Ltd.
2-1-1 Odasakae, Kawasaki, Japan

Shin Yoshida was born in 1960. He graduated from Nagoya University with a B.E. degree in Synthetic Chemistry in 1987.

In the same year, he joined Showa Electric Wire & Cable Co., Ltd. and has been engaged in research and development of flame retardant cable and nuclear power plant cable.

Kazumi Ito
Showa Electric Wire & Cable Co., Ltd.
2-1-1 Odasakae, Kawasaki, Japan

Mr. Ito graduated from Suzuka College of Technology in 1975, where he majored in Industrial Chemistry

Then he joined Showa Electric Wire & Cable Co., Ltd. and has been engaged in research and development of rubber and plastic materials for nuclear power cable.

Mr. Ito is now a member of the Research and Development Division of Showa Electric Wire & Cable Co., Ltd.

Yuko Tamamoto
Showa Electric Wire & Cable Co., Ltd.
2-1-1 Odasakae, Kawasaki, Japan

Yuko Tamamoto was born in Hiroshima, Japan, in 1965. In 1988, she graduated from Science University of Tokyo with a B.E. degree in Industrial Chemistry.

Then she joined Showa Electric Wire & Cable Co., Ltd. and has been engaged in research and development of plastic materials for flame retardant cable.

Etsuo Hosokawa
Showa Electric Wire & Cable Co., Ltd.
2-1-1 Odasakae, Kawasaki, Japan

Etsuo Hosokawa was born in Tokyo in 1935. He received the B.E. degree in Chemical Engineering from Yokohama National University in 1959.

Then he joined Showa Electric Wire & Cable Co., Ltd. His work has been in research and development of insulation for magnetic wires.

Currently he is a general manager of Chemicals Research Department.

Fumio Aida
Showa Electric Wire & Cable Co., Ltd.
2-1-1 Odasakae, Kawasaki, Japan

Fumio Aida was born in Tokyo in 1948. He received the B.S. degree in Organic Chemistry from Tokyo Metropolitan University in 1971.

Then he joined Showa Electric Wire & Cable Co., Ltd. His work has been in research and development of electrical insulating materials.

Mr. Aida is a member of the Institute of Electrical Engineers of Japan.

REPARATION OF A FIBER OPTIC GROUND WIRE ON AN UHV OVERHEAD POWER LINE

JP. BONICEL* - G. COUVRIE* - P. KOUTEYNIKOFF** - O. TATAT* - M. DE VECCHIS***

* LES CABLES DE LYON - 170 Av Jean Jaurès - 69344 LYON - FRANCE
** E D F - Etudes & Recherche - 1 Av G. de Gaulle - 92141 CLAMART - FRANCE
*** LES CABLES DE LYON - 30 Rue des Chasses - 92111 CLICHY - FRANCE

ABSTRACT

Fiber Optic Ground wires (F.O.G.W.) have been selected by Electricité de France (EDF) to install telecommunication links on ultra high voltage overhead power lines (225 and 400 kV).
As several FOGW links has been and will be in the next future put into operation in the French power network, the possibility of FOGW damage had to be considered. Therefore, a specific reparation process was established, based on the development of a reliable mid-span joint (MSJ).
The MSJ can be used at any point between adjacent towers.It has the same mechanical strength as the FOGW most commonly used in the French power network (UTS : 118 kN). The present design of MSJ can accommodate 4 or 6 fibers jointed by low-loss fusion splices.
Prototype mid-span joints have undergone extensive laboratory and field tests. The MSJ has been used on an operating 400 kV line to repair the FOGW damaged in October 1988 by an helicopter. The reparation was successfull from both mechanical and optical point of view : the low optical splice losses made it possible to keep loss budget practically unchanged.

1 - INTRODUCTION

By the mid-80's, the French national power utility Electricité de France (EDF) decided to install Fiber Optic Ground Wires (FOGW) on all new 400 kV overhead transmission lines (the highest voltage on EDF transmission network). In addition, FOGW would also be installed on selected new 225 kV lines and 400 kV or 225 kV existing lines. A comprehensive research and development program resulted in a family of FOGW suited for the different climatic conditions in different areas of France, called THYM cables (1). With such a major FOGW installation program, possible failure of the FOGW had to be considered, even if extensive laboratory and field tests had demonstrated the high reliability of the THYM FOGW design (2).

The development of a Mid-Span Joint (MSJ) has been seen as an adequate answer to this requirement, both from the points of view of technical performance and of reparation cost and duration.

This paper is aimed at presenting the design and performances of a new MSJ ; it also gives results of extensive laboratory and field tests which have been carried on by EDF and Câbles de Lyon, and it shows how the MSJ has been used to repair an operating 400 kV overhead Transmission line whose FOGW has been damaged by an helicopter.

2 - TYPES OF FOGW USED IN THE FRENCH NETWORK

The THYM series of FOGW has been designed with a reinforced structure in order to be installed on UHV overhead lines in the same conditions as conventional AASCR ground wires. Compared to well know 1/2" FOGW, the THYM cables offer higher mechanical performance and reduced electrical resistance (for higher short circuit currents). They have one layer of aluminium alloy wires and up to three layers of steel wires. TABLE 1 gives the main parameters and Figure 1 shows a cross section of the THYM 157.

CABLE TYPE	THYM 157	THYM 268	THYM 368
Nominal section (wires) mm2	157.4	268	368
Cable diameter (mm)	19.2	23.6	27.0
Nominal Ultimate Tensile Stress (UTS) (kN)	118	242	382
Nominal electrical resistance Ω /km	0.22	0.17	0.15
Weight (kg/km)	0.88	1.6	2.4

Table 1

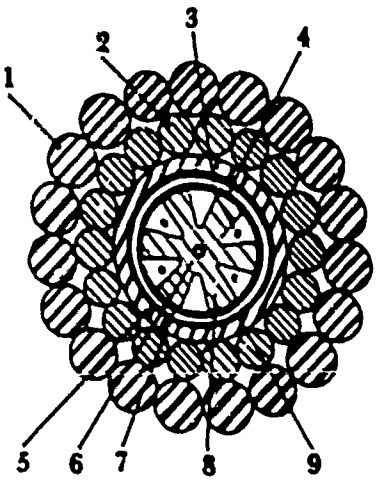

1. ALUMINIUM ALLOY WIRES
2. GALVANIZED STEEL WIRES
3. FIBER
4. POLYESTER RIBBONS
5. ALUMINIUM ALLOY TUBE
6. NON METALLIC STRENGTH MEMBER
7. SHEATH
8. SLOTTED CORE
9. BEDDING

Figure 1
Cross section of THYM 157

2.1. Mechanical Parameters

Because of its high mechanical strength, the THYM FOGW does not require a reduced tension (or increased sag) when installed on long length spans. Similarly, safe clearance with phase conductors is obtained without any increase of suspension height, even under extreme conditions (i.e. 20 mm thick ice sleeve combined with an average wind speed of 60 km/h).

2.2. Short circuit current parameters

For a maximum temperature increase of 170°C and a time of application of 0.75 second the maximum short circuit current is 21 kA for a THYM 268. 18.5 kA for a THYM 157 compared with 11 kA for 1/2 inch cable using a single layer of composite Aluminium clad steel wires (40 % IACS).

To insure a good reliability of fibers the maximum admissible temperature in a part of the cable during short circuits has been limited to the conservative value of 170°C well below the point where fiber attenuation starts increasing.

2.3. Types of fibers

Following the user's needs multimode fibers at 1300 nm and single mode fibers at 1300 or 1550 nm (dispersion - shifted fibers) can be used.

For export, cables with a similar optical core but using composite ACS wires instead of the two layers steel and aluminium alloy wires have been produced.
These cables have been tested for qualification and acceptance. The main tests are : temperature variations, breaking strength, alternate flexing, elongation, short time temperature increase (short circuit) and corrosion.

3 - REQUIREMENTS FOR AND DESIGN OF THE MSJ

3.1. Requirements for the MSJ

The main functional requirements are the following :
a) to be fully compatible with the existing THYM series of FOGW installed on the EDF network.
b) to be usable at any point between adjacent towers.
c) to keep unchanged the mechanical strength of the FOGW link.
d) to introduce an optical attenuation as low as possible.
e) to be easily installed by normally trained people.
f) to have a limited diameter so as to allow line maintenance vehicules to pass over the MSJ : 30 mm has been choosen.

3.2. Design of the MSJ

To fullfill requirement a), the MSJ had to have the same UTS as the THYM FOGW (118 kN for THYM 157, which is the most commonly used FOGW).
MSJ protection has been made by using a reduced size splice housing associated with two compression clamps of known design (used since many years for clamping ground wires with coaxial, quads or optical fibres).
Figure 2 shows the MSJ design with on both sides the compression clamps fixed to the two ends of FOGW.

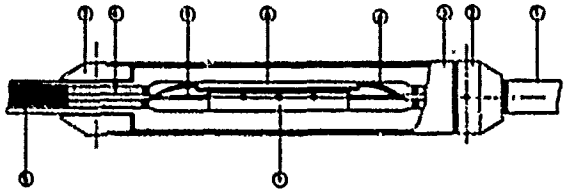

1. Clamping sleeve
2. Nut
3. Protective tube
4. Optical unit
5. Sleeve
6. Splice organizer
7. Clamping device for strength member
8. Fibers
9. Slotted core

Figure 2
M.S.J.

Fiber splicing inside the MSJ is done by using an automatic arc fusion splicer, for any type of fiber (1300 or 1550 nm).

4. TESTS RESULTS

Characterization is done by mounting a MSJ between two lengths of FOGW. The assembly is then submitted to test series with a monitoring of attenuation characteristics at 1300 and 1500 nm.

A prototype MSJ has been installed on a section of THYM 157 FOGW enclosing both 1300 nm and 1550 nm (dispersion-shifted fibers (3)) singlemode fibers and then subjected to a series of laboratory tests.

4.1. Tensile test

The aim was :

- no change in attenuation up to 70 % of the Nominal Breaking Load (N.B.L.) of the cable.

- no breaking up to 90 % of the N.B.L.

The following table shows the obtained results.

Tensile stress		Attenuation change	Remarks
% NBL	daN	(dB)	
0	0	0	
52	6711	0	
52	6711	0	After 1 hour
56	7228	0	
65	8260	0	
73	9292	0	
80	10325	0	
98	12600	0,03	
101	12950	∞	Breaking

4.2. Thermal test

The MSJ has been subjected to thermal cycling in a climatic chamber and the splice attenuation variations have been monitored. For both 1300 and 1550 nm fibers, the maximum variation between + 55°C and - 40°C has been 0.12 dB, which is satisfactory.

4.3. Vibration test

The assembly is submitted to the following test :
A tension equal to 20 % of NBL is applied and a vibration with a vertical amplitude between 1000 and 1500 µm and a frequency between 20 and 40 Hz is applied to one end. The sample is submitted to 10^7 cycles to simulate service fatigue.

No measurable attenuation variation has been recorded during and after the test.

4.4. Other tests : Other tests are :

- climatic ageing
- corrosion test
- short term temperature increase (short circuit or lightning current).

5 - EXPERIMENTATION

5.1. Experimentation at EDF test station

A 500 m FOGW span has been equipped with a MSJ at the "Le Minervois" EDF test station. This place is being used by EDF for many years to test new line equipment, fitting or conductors (4). High wind are experienced very frequently, resulting in accelerated ageing of the tested equipment.

After more than one year no change in transmission has been detected.

5.2. Installation on a 400 kV operating line

In October 1988 a FOGW installed on a 400 kV line between Tavel and Aramon has been damaged by an helicopter that hit the FOGW with its landing gear during a flight with very poor weather conditions.
In spite of the elongation of the FOGW created by the impact, transmission parameters were unaffected. These parameters were very well known as the link has been installed one year earlier, incorporating for experimental purpose two dispersion shifted fibres in excess of the four standard single mode fibres (3).

As the external wire layer was damaged it has been decided to repair the cable (see figure 3).

Figure 3
Damaged FOGW

Compression clamps are fixed at the ground level after the replacement of the length of damaged cable. Figure 4 shows the clamping on the FOGW.

Figure 4
Clamping on the FOGW

Due to external conditions in December 1988 (Temperature 0° C, wind : 100 to 120 km/h) splices have been done in a shelter (see figure 5).

Figure 5
Performing the splice

Figure 6 shows the terminated MSJ before tensionning the FOGW to adjust the sag.

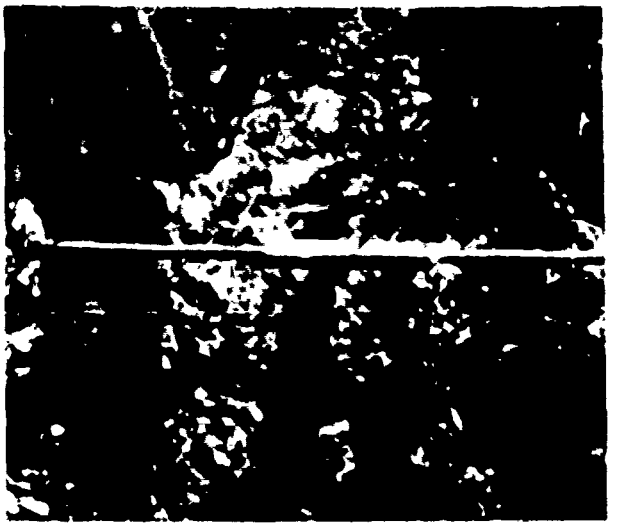

Figure 6
Terminated M.S.J

This reparation is installed between two towers, distant of 500 meters. The effect on the total attenuation of the link is undetectable both on standard 1300 nm single mode fibres and on dispersion shifted fibres.

6. CONCLUSION

A mid-span joint (MSJ) has been developed for efficient maintenance of FOGW links installed on the EDF Transmission network. The MSJ has been designed to have the same mechanical resistance as the FOGW themselves, to have a minimum diameter and to accept very severe mechanical stresses and temperature variations without significant change in its optical attenuation. Extensive laboratory and site testing, followed by the installation of a MSJ on a 400 kV line, has shown that :

- the MSJ has the same UTS as the THYM FOGW

- temperature variations, vibrations and tensile load have no significant effect on optical splice attenuation.

Provided that the access to the splicing point is adequate, such a MSJ can be feasible in one day with the optical test done before the watertight closure of the central part.

BIBLIOGRAPHY

(1) A. VICAUD, P. KOUTEYNIKOFF, P. TROMBERT, P. CHERON "Optical ground wire communications on high voltage transmission lines" (in French). OPTO 85, PARIS, 21-23 May 1985.

(2) F. DUCHATEAU, T. HAMET, P. KOUTEYNIKOFF, N. RECROSIO "Silica optical fiber links at EDF" (in French), Revue Générale d'Electricité, 1989, n° 5, pp 13-25.

(3) P. KOUTEYNIKOFF, M. de VECCHIS, JP. BONICEL "Single mode FOGW using dispersion shifted fibers", EFOC/LAN 88 AMSTERDAM, 27 July to 1 Aug 1988.

(4) "Natural site mechanical tests" LAB'ECHO Vol 1, n° 3, April 1983.

JP. BONICEL - LES CABLES DE LYON
170 Av Jean Jaurès - 69344 LYON - FRANCE

Jean Pierre BONICEL was born in 1952. He received his engineer degree from the Institut des Sciences de l'Ingénieur de Montpellier (ISIM) in 1976. He joined Les Câbles de Lyon in 1977 where he was in charge of material and mechanical problems for telecommunication cables. Now he is the head of telecommunication cables laboratory.

G. COUVRIE - LES CABLES DE LYON
170 Av Jean Jaurès - 69344 LYON - FRANCE

G. COUVRIE was born in 1949. He received his general certificate of education in 1968. After two years in mathematics and physics (1968 / 1970) he joined Les Câbles de Lyon outside plant. Now he works on junction cable activities.

P. KOUTEYNIKOFF - EDF - Etudes et Recherches
1 Av du Gal de Gaulle - 92141 CLAMART FRANCE

P. KOUTEYNIKOFF is graduated from the Ecole Supérieure d'Electricité in 1972. He is with the Research and Development Division of Electricite de France (EDF) since 1974.

His past research areas include : low-frequency and high-frequency modeling of earth electrodes for power line towers and substations, interference resulting from proximity between power lines and telecommunication lines.

He has been in charge of the EDF R and D program which resulted in the development and practical application of the THYM cables and related line equipment. He is presently head of "Electrical Coordination" Group. P. KOUTEYNIKOFF is a member of IEEE, of SEE and is the French representative to CIGRE Study Committee 36 (Interference).

O. TATAT - LES CABLES DE LYON
170 Av Jean Jaurès - 69344 LYON - FRANCE

Olivier TATAT was born in 1959. He received his engineer degree from the Institut des Sciences de l'Ingénieur de Montpellier (ISIM) in 1982. He joined Les Câbles de Lyon in 1985 where he is in charge of material and mechanical problems for telecommunication cables.

M. de VECCHIS - LES CABLES DE LYON
30 Rue de Chasses - 92111 CLICHY - FRANCE

Michel de VECCHIS was born in 1946. He is graduated from Ecole Nationale Supérieure des Télécommunications (1969). He joined LTT in 1970 where he worked on microwave components. He started to work on fiber optics in 1974 and has been Technical Director of the cable Division until the merging of LTT cable activities with Les Cables de Lyon in 1986. He his now Director of Technical International Marketing at Les Cables de Lyon Telecommunications Branch.
He is involved in International Standardization of optical fibers and Cables (Chairman of CECC WG 28 and Secretary of IEC SC 86 A).

DEVELOPMENT OF THE STRANDED FRP AND ITS APPLICATION TO OPTICAL CABLE

S. Matsuno*, M. Okada*, K. Nijkura**, H. Horima**,
A. Saito*** and K. Ogata***

*UBE-NITTO KASEI Co.,Ltd. 579-1, Yabuta, Gifu 500, Japan
**Sumitomo Electric Industries,Ltd. 1,Taya,Sakae-ku,Yokohama 244, Japan
***Kitanihon Electric Cable Co.,Ltd. 1-2-1,Koriyama,Sendai 982, Japan

Abstract

Optical communication systems by optical fibers are today widely used for public communication networks, local area networks(LAN) and so on. To make full use of the non-inductive characteristics of the optical fibers, non-metallic optical cables which contain fiber reinfoced plastics (FRP) rod strength members have come into general use. However, their large rigidity often affected the flexibility of the optical cables. For the purpose of improving the flexibility of the non-metallic optical cables, we designed the stranded FRP strength member and developed the novel manufacturing process which enabled to reduce the manufacturing cost. The stranded FRP strength member developed this time has excellent shape-retentivity by closely tightening the FRP elements, the remarkably improved flexibility and the same tensile characteristics as the FRP rod. Furthermore, we have confirmed that it's a very effective strength member for the optical cables by putting it to use in slot core cable.

1.Introduction

Practical introduction of optical communication systems using optical cables is expanding not only in the field of the public communication but also in the fields of LAN and various industries.

Being composed of a glass material, that is, a non-metallic material, optical fibers are imparted with the outstanding feature of non-induction which is never seen in the conventional copper communication cables. As compared with the copper cables, however, the optical fibers are sensitive to external force, and hence, are used in the state of cables together with strength members. The strength members are indispensable for assuring the service life of the optical fibers, being employed as an antitensional member in the laying operation and also in realizing the stability of transmission loss against temperature variation. Therefore, the favorable strength members now in use are those with higher tensile modulus of elasticity and lower coefficient of linear thermal expansion. Aside from the above, in order to make the most of the feature of non-induction in optical fibers, the non-metallic type optical cables completely free from a metallic material are being widely designed and manufactured, and at the same time, reinforced plastic rods using a glass fiber, an aromatic polyamide fiber, etc. as a reinforcement are being used. While the tensile modulus of elasticity of FRP rods using a glass fiber as a reinforcement (GFRP rods) is comparatively higher among the general plastics, the value is much lower than and about 1/4 that of the steel wire which is being widely used as the strength members for metallic type optical cables. Consequently, in the case when GFRP rods are applied to strength members,it is inevitable that GFRP rods with larger outside diameters are adopted to assure the prescribed tension characteristics. The problem with the larger outside diameter is the likelihood of loss of flexibility which is one of the major features of optical cables and also of the problem with safety in handling due to high rigidity of GFRP rods with larger outside diameters. In order to cope with the above problem, the application of the FRP rods using an aromatic polyamide fiber such as Kevlar® as a reinforcement (KFRP rods) in place of the above GFRP rods with larger outside diameters may be considered, but it will cause increase in cost, and more than twice in cost. In view of the above, the non-metallic type strength member without causing the loss of flexibility of optical cables, with minimum impact on cost and enabling stable cable manufacture has long been desired. On the basis of the understanding of the forgoing background, we have developed the stranded FRP, and further the process for manufacturing the same with less impact on cost. In this paper, the novel process for manufacturing the stranded FRP which has been developed so far, its characteristics, and the characteristics of the optical cable using the stranded FRP will be reported.

2.The Processing of the Stranded FRP

The stranded FRP is the stranded product of FRP elements with fine diameters, and the manufacturing processes include the process of stranding cured FRP rods with fine diameters, wrapping with tapes followed by applying polyethylene(PE) sheath. The above process enables to maintain the tensile characteristics and assures flexibility. However, when such manufacturing processes are employed, it is liable to cause repulsion and scattering of FRP elements with fine diameters which constitute the stranded FRP, causing difficulty in obtaining stable

stranded condition. In addition, referring to the processing steps, they involve the steps of producing cured FRP rods with fine diameters, and stranding the same, resulting in such problems as increase in the number of steps, complicated steps and also higher manufacturing cost.

In general, the FRP rods are manufactured by impregnating the continuous fiber such as a glass fiber with a thermosetting resin such as an unsaturated polyester resin and adjusting into the prescribed form and shape, followed by curing through a heating die, etc. On the contrary, uncured rod-like FRP products with favorable shape-retentivity and flexibility are obtained by thinly coating the fiber bundle, impregnated with uncured thermosetting resin using a flexible thermoplastic resin such as polyethylene. The structure of an uncured rod-like FRP product is shown in Fig.1.

The manufacturing process we have developd so far consists of producing the FRP elements with fine diameters by utilizing the favorable shape-retentivity and flexibility of the uncured rod-like FRP products, followed by stranding and then curing to produce the stranded FRP. Further, the novel process thus developed has enabled a series of the continuous process including curing by directly introducing the uncured rod-like FRP products into the stranding step. The manufacturing process of the novel process is illustrated in Fig.2 in comparison with the conventional process. In the novel process, the reinforced fiber bundles such as glass rovings are taken out, impregnated with a thermosetting resin such as unsaturated polyester resin, and adjusted to form the prescribed shape, and thereafter coating with thermoplastic resin such as polyethylene, polyamide 12 (PA-12), etc. through a multi-hole die (7-hole die) is carried out to obtain uncured FRP rod-like products, followed by stranding and then curing to form the stranded FRP. Fig. 3 shows the structure of the stranded FRP which has been developed by us. The novel process

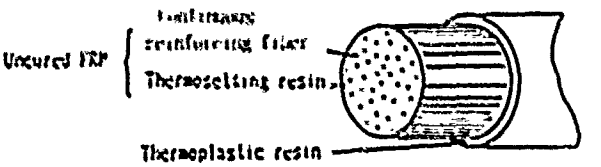

Fig.1 The structure of an uncured rod-like FRP product

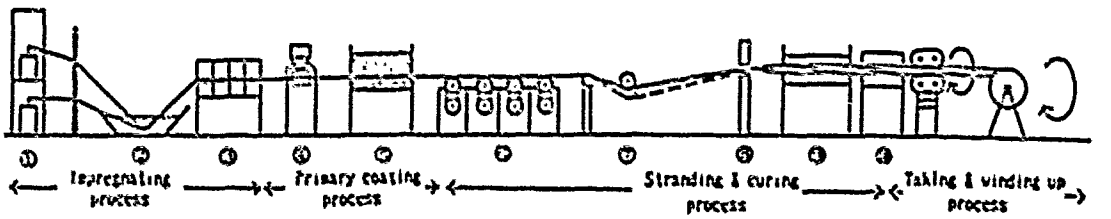

The novel process

① Glass rovings ② Thermosetting resin
③ Squeezing die ④ Extruder
⑤ Cooling chamber ⑥ Taking up machine
⑦ Dancer roller ⑧ Guides
⑨ Curing chamber ⑩ Dryer

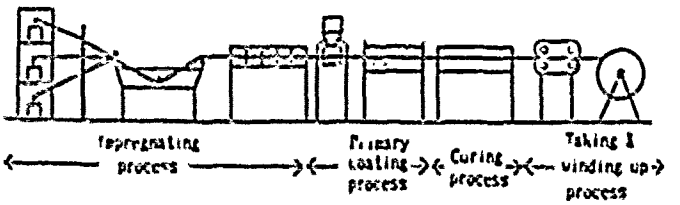

(1) The manufacturing process of cured FRP rod

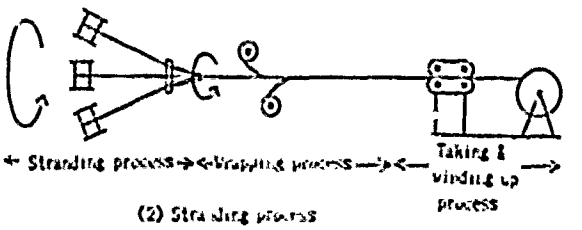

(2) Stranding process

Conventional process

Fig.2 The manufacturing processes of stranded FRP

has enabled reduction in manufacturing cost by virtue of curtailment of number of steps and simplification of the steps as well as improvement on the adhesion property of the elements themselves by curing under stranded condition, resulting in the improvement in handling and safety without causing scattering of elements in the cutting step which has frequently been seen in the conventional process.

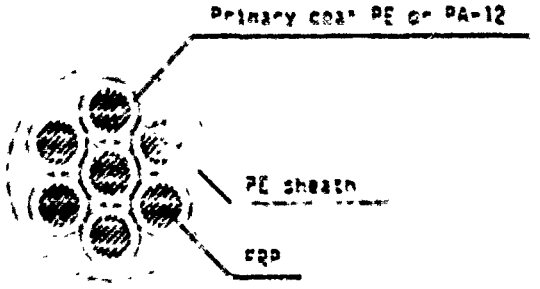

Fig.3 The structure of the stranded FRP

3.The Properties of the Stranded FRP

Table 1 shows the typical properties of the stranded FRP developed by us in comparison with GFRP rod and KFRP rod. As the criteria for the comparison, the same sectional area of FRP parts was adopted.

Table 1 Typical properties of non-metallic strength members

Item (unit)	Stranded FRP	GFRP rod	KFRP rod
FRP diameter (mmϕ ×n)	1.7×7	4.5×1	4.5×1
Polyethylene sheath diameter(mm)	7.5	8.0	8.0
Weight (g/m)	58	43	32
Cost ratio	150	100	200

3.1 Flexibility

In evaluation of flexibility, the load applied to bend the sample to a semicircle at a specified curvature (bending load) was measured as indicated in Fig.4. Fig. 5 shows the relationship between bending load and bend diameter. In addition, Fig.6 exhibits the relationship between the bending load at a bend diameter(400mmϕ) which is deemed usual in laying down underground cables, etc. and the load at 0.2% elongation of the sample. When compared at the load of 150 kg at 0.2% elongation from the present result, it is found that the stranded FRP is superior to GFRP rod and KFRP rod with respect to flexibility, since the bending load of the stranded FRP is about 20% of that of GFRP rod and about 50% of that of KFRP rod.

3.2 Tensile characteristics

The relationship between tensile load and strain is shown in Fig.7. Breaking strength and tensile modulus of elasticity are listed in Table 2. The stranded FRP has a tensile modulus of elasticity of about 4,570 kg/mm^2, retaining almost the same value as GFRP rod. In addition, the stranded FRP has proved to show tensile strength at break almost comparable to that of GFRP rod.

3.3 Minimum bending characteristics

By varying bend diameters at room temperature, the maximum bend diameter at which the sample or a part of the sample is broken (minimum bend diameter) was measured. The result is shown in Table 3. The stranded FRP possesses the excellent property in the minimum bend diameter, which is about half those of GFRP rod and KFRP rod, and is expected to enhance the reliability in laying down cables.

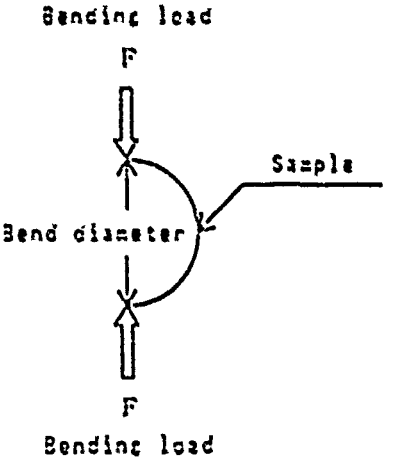

Fig.4 The measurement of bending load

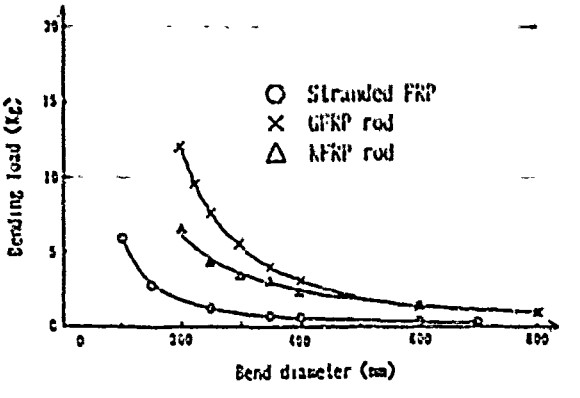

Fig.5 Bending load dependence of bend diameter for non-metallic strength members

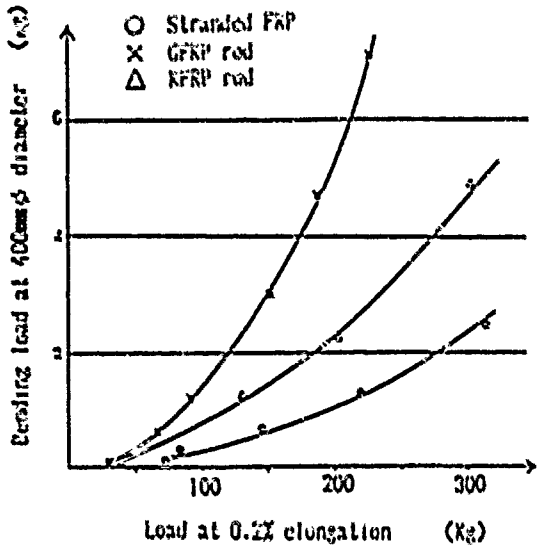

Fig.6 Bending load at 400mmφ diameter dependence of load at 0.2% elongation for non-metallic strength members

Table 2 Tensile characteristics of non-metallic strength members

Item (unit)		Stranded FRP	GFRP rod	KFRP rod
Tensile modulus (kg/mm²) n=5	Average	4,570	4,770	8,520
	Standard deviation	58	52	94
	Maximum	4,610	4,830	8,680
	Minimum	4,510	4,700	8,430
Breaking strength (kg) n=5	Average	2,130	2,100	2,300
	Standard deviation	92	122	85
	Maximum	2,240	2,250	2,500
	Minimum	1,990	2,050	2,290

Table 3 Minimum bend diameter of non-metallic strength members

Item (unit)		Stranded FRP	GFRP rod	KFRP rod
Minimum bend diameter (mmφ) n=5	Average	72	130	126
	Standard deviation	2.7	4.2	11.4
	Maximum	75	140	140
	Minimum	70	130	110

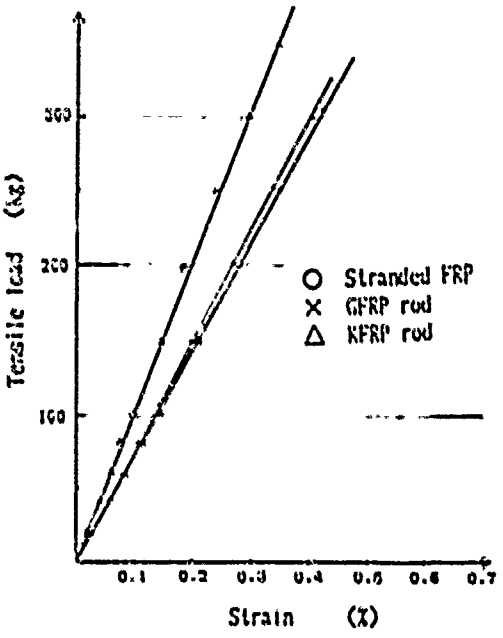

Fig.7 Tennsile load dependence of tensile strain for non-metallic strength members

3.4 Long-term reliabirity by heat-resistant bending test in hot water at 80℃

In order to compare the stranded FRP with GFRP rod in regard to long-term reliability, static bending-fatigue test was carried out in hot water at 80℃. Fifty(50) pieces of samples having several different bend diameters were measured for the period of time required to break the sample or a part of the sample in hot water at 80℃. The cumulative failure probabilities thus obtained were plotted on a Weibull probability paper. The log of time(ta) leading to a cumulative failure probability of 1.0% was plotted against the log of bending strain rate. The result is shown in Fig.8. The bending strain rate was based on FRP diameter for single GFRP rod, and on the rod diameter equivalent to the sectional area of FRP parts for the stranded FRP. As shown in the data, it is demonstrated that the stranded FRP has a superior service life of about 10^2 times to that of GFRP rod at every strain rate, and much higher long-term reliability.

3.5 Repeated bending fatigue characteristics

The dynamic fatigue characteristics by repeated bending were evaluated according to the method as shown in Fig. 9. Repeated bending strain of 10,000 times with a pair of rollers of 450mm in diameter was applied to the stranded FRP together with the load corresponding to about 0.1% elongation of GFRP rod (80 kg). As a result, it has been demonstrated that the bending load and tensile breaking strength of the stranded FRP after testing maintain the initial values without deterioration in its characteristics as shown in Table 4.

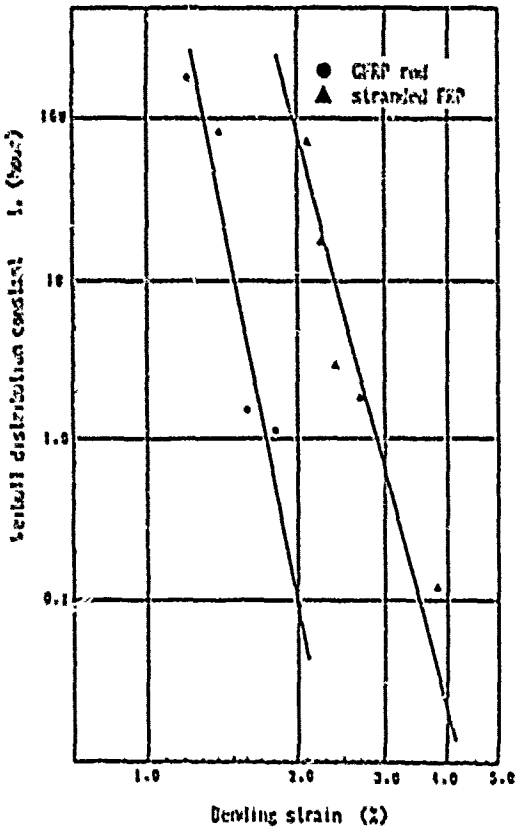

Fig.8 Weibull distribution constant(te) dependence of bending strain

Table 4 Repeated bending fatigue characteristics of non-metallic strength members

Item (unit)		Stranded FRP		GFRP rod	
		Pre-test sample	After test	Pre-test sample	After test
Bending load at 400mm φ diameter (g) n=5	Average	590	470	3,300	1,100
	Standard deviation	34	19	130	71
	Maximum	650	500	3,500	3,200
	Minimum	570	450	3,200	3,050
Breaking strength (kg) n=5	Average	2,130	2,080	2,100	1,820
	Standard deviation	92	37	122	68
	Maximum	2,240	2,120	2,250	1,890
	Minimum	1,990	2,030	2,050	1,750

The test conditions

Frequency	1/7 Hertz
Cycles	10^4
Load	W= 80 Kg (at 0.1% elongation)
Sample length	L=400 mm
Roller diameter	D=450 mm

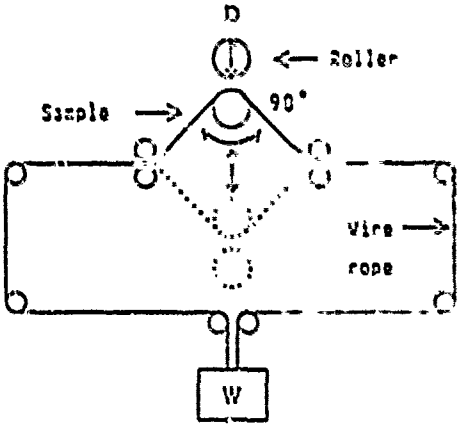

Fig.9 The method of dynamic bending fatigue test

4.The Characteristics of the Optical Cable using the Stranded FRP Strength Member

In order to confirm the effectiveness of the stranded FRP applied to the strength members of optical cables, slot core cable using the stranded FRP strength member

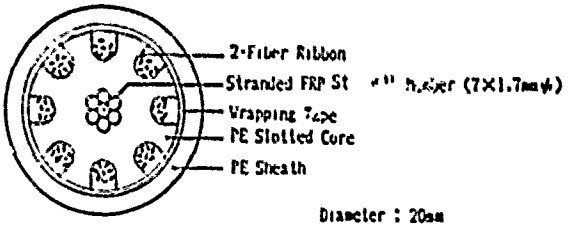

(a) Stranded FRP strength member type

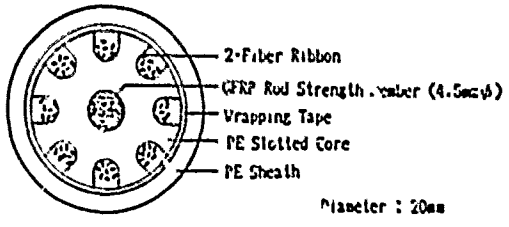

(b) GFRP rod strength member type

Fig.10 The structure of the cables used for evaluation

was designed and compared with the cable with the conventional single GFRP rod strength member for each characteristics. The structure of the cable used for evaluation is as illustrated in Fig.10, which is capable of accommodating 128 optical fibers at the maximum.

4.1 Tensile characteristics

The tensile load-elongation characteristics are exhibited in Fig.11. Both the cable using single GFRP rod and that using the stranded FRP display almost the same characteristics. It has been also proven that both single wire and stranded wire each in cable condition depend on sectional area of FRP.

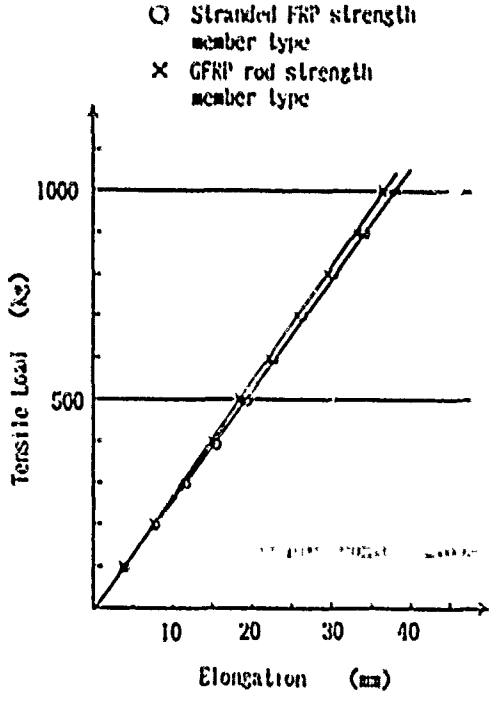

Fig.11 Tensile load-elongation characteristics of the cables

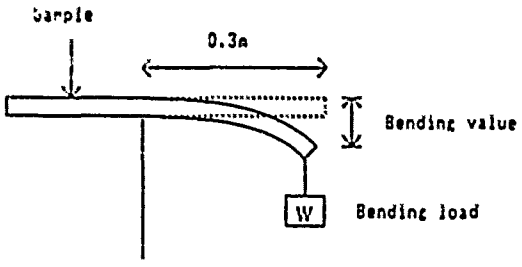

Fig.12 The measuring method of flexibility of the cables

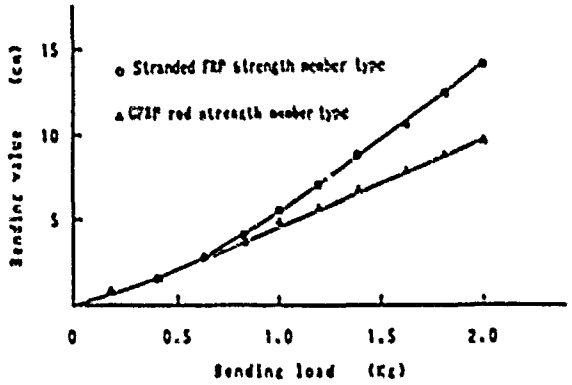

Fig.13 Measured flexibility of the cables

4.2 Flexibility

Flexibility evaluation was carried out in accordance with the measuring method as shown in Fig.12. The test results are as indicated in Fig.13 and demonstrate that the stranded FRP strength member has a notably improved flexibility in comparison with that of single GFRP rod strength member.

5. Conclusion

For the purpose of improving the flexibility of non-metallic type optical cables, the stranded FRP strength member was designed and produced using a novel process in which the step of curing FRP and the stranding step are integrated. As a result, the novel process has enabled us to produce the stranded FRP which is lower in cost and excellent in shape-retentivity. The design and evaluation of the stranded FRP thus developed and the optical fiber cable using the same have demonstrated the excellent flexibility as well as various properties comparable to those of the single GFRP rod and it has been confirmed to have excellent characteristics in practical application.

Shigehiro Matsuno
UBE-NITTO KASEI Co.,Ltd.
579-1 ,Yabuta
Gifu 500, Japan

Shigehiro Matsuno received the B.E. degree in engineering from Kyoto University in 1974 and joined UBE-NITTO KASEI Co.,Ltd. He has been engaged in research and development of fiber reinforced plastics in the optical fiver cables ,and so on.

Masao Okada
UBE-NITTO KASEI Co.,Ltd.
579-1 ,Yabuta
Gifu 500, Japan

Masao Okada received the B.E. degree in engineering from Kyoto University in 1963 and then joined Nitto Boseki Co.,Ltd.
Since 1968 he joined UBE-NITTO KASEI Co.,Ltd. and has worked on the development of fiver reinforced plastics of pultrusion, advanced composite materials and glasses by Sol-gel method and so on. He is now a Director of Gifu Research Laboratory. He is a member of the Society of Polymer Science of Japan.

Koji Niikura
Sumitomo Electric
Industries, Ltd.
1, Taya-cho
Sakae-ku
Yokohama 244,Japan

Koji Niikura received the B.E. degree in engineering from Waseda University in 1984 and joined Sumitomo Electric Industries, Ltd. He has been engaged in the development and design of optical fiber cables in the Fiber Optics Division.

Hiroaki Horima
Sumitomo Electric
Industries, Ltd.
1, Taya-cho
Sakae-ku
Yokohama 244,Japan

Hiroaki Horima received the M.S. degree in engineering from Osaka University in 1972. He then joined Sumitomo Electric Industries, Ltd. and worked on the development of CATV coaxial cables, multipair PEF-insulated junction cables and low loss unbalanced type cables. Thereafter, he concentrated on the development of optical fiber cables. He is now Section Manager of the Fiber Optics Division at Sumitomo Electric Industries, Ltd. He is a member of the Institute of Electronics, Information and Communication Engineers of Japan.

Arinobu Saito
Kitanihon Electric
Cable Co.,Ltd.
1-2-1, Koriyama
Wakabayasi-ku
Sendai 982, Japan

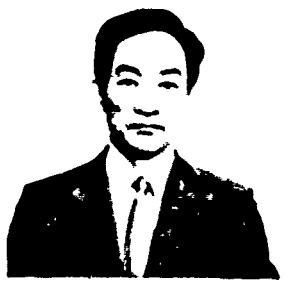

Arinobu Saito received the B.E. degree from Tohoku Gakuin University in 1968. At Kitanihon Electric Cable Co.,Ltd.,he has been engaged in the development and design of communication cables, power cables and accessories. He is now a deputy manager of the Manufacturing Department.

Koji Ogata
Kitanihon Electric
Cable Co.,Ltd.
1-2-1, Koriyama
Wakabayasi-ku
Sendai 982, Japan

Koji Ogata received the B.E. degree from Tohoku Gakuin University in 1986. At Kitanihon Electric Cable Co., Ltd.,he has been engaged in the development and design of optical fiber cables in the Engineer Division. He is a member of the Institute of Electronics, Information and Communication Engineers of Japan.

FEASIBLE OPTICAL CABLE DESIGNS WITH ADDITIONAL FUNCTIONS FOR LAN APPLICATIONS

Y. Kuwata*, H. Igarashi*, H. Horima*, K. Ogata**, A. Saito** and T. Shishido**

*Sumitomo Electric Industries, Ltd. 1, Taya-cho, Sakae-ku,
Yokohama, 244, Japan
**Kitanihon Electric Cable Co., Ltd. 1-2-1, Koriyama, Wakabayashi-ku,
Sendai 982, Japan

Abstract

Use of LAN systems using optical fiber is now increasing. The design of optical fiber transmission routes for LAN systems is very important from the standpoints of economic feasibility, reliability and maintenance of the entire system including branching.

In order to provide flexibility in the design of such transmission routes, we have developed two types of optical fiber cables with higher additional functions and assured the applicability of these cables to LAN systems.

1. Introduction

As often seen in intelligent buildings in recent years, LAN systems using optical fiber cable are increasingly used in various applications. In such optical fiber communication networks, economic feasibility of the entire system may be lost or problems of reliability and maintenance may arise if the cable distribution is not efficiently designed.

As an example of a cable distribution system in a building, there is a method of building up a star-like network with a cable center on one floor with cables being distributed from this center to other floors of the building. For this purpose, it is necessary to introduce multicore optical cable with a smaller diameter and with excellent branching characteristics for efficient utilization of the space within the cable ducts in a building. Furthermore, it is quite possible to expand the scale of the system on a specific floor to meet increasing demand.

To meet these requirements, we have designed and manufactured an optical cable using several hollow polyethylene slot core cables incorporating multi-core fibers. These multi-core fibers are stranded around the strength member in order to improve the availability and workability of the cable.

Also, for use as an outdoor cable between buildings or as a distribution cable within a building, a self-supporting optical cable[1] has been designed in which a round non-metallic optical cable is covered, with FRP and polyethylene in a hollow polyethylene pipe.

The hollow pipes of both cables can be utilized as the pathway for air blown fiber,[2] and provision is made for future increases in demand for optical transmission lines. Actual evaluation has demonstrated that 200 m or more of the optical fiber unit can be installed by air blowing.

In this paper, we will describe the characteristics of optical cable for LAN systems having two additional functions.

2. Optical Cable Design

First we present a description of the structural design of two types of optical cables with higher additional functions developed for LAN systems.

2.1 Multi-cable construction with tubular slot core

Figure 1 shows the structure of an optical cable developed primarily for improving the branching-off of optical fiber on each floor in order to efficiently utilize the space within the distribution ducts in a building.

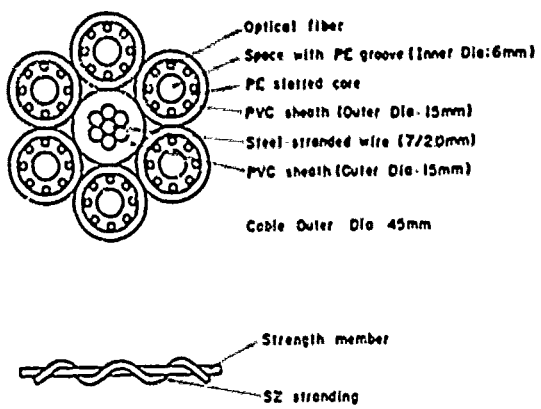

Fig. 1 Optical cable construction for building application

In this cable, 8-core fiber is inserted into a polyethylene slot core made of ordinary polyethylene having a tubular form with an inner diameter of 6 mm, where ABF (Air Blown Fiber) system is applied. To facilitate better branching characteristics, 6 non-metallic optical fiber cores with PVC sheath are stranded with a pitch of 1.5 m on SZ around the steel stranded tension member core with PVC sheath, and the cores are intermittently fixed with solvents.

To meet the demands on non-halogen type optical fiber cable, non-inflammable polyethylene is adopted for the outer sheath, and bind wires are used to fix optical fiber cable for better and easier intermittent bonding.

Such structure enables easy handling of the cable and is convenient for building up a star-like network. When loop construction is required, it is achieved without any difficulty by using jumper cable which connects floors.

2.2 Prehanger cable construction with tubular FRP suspension wire

We have also developed a new cable as shown in Fig. 2, which is suitable for outdoor installation between commercial buildings. In this cable, FRP (Fiber Reinforced Plastic) pipe is installed in PE pipe with an inner diameter of 6 mmφ to be used in an ABF system. Furthermore, it is covered with a PE jacket, the diameter of the whole being 12 mmφ.

The FRP core with PE pipe and the round non-metallic optical cable are fused together by molding intermittently using PE pieces.

This FRP pipe serves as a strength member during cable laying and may also fulfill the function of suspension wire when it is used as an aerial cable.

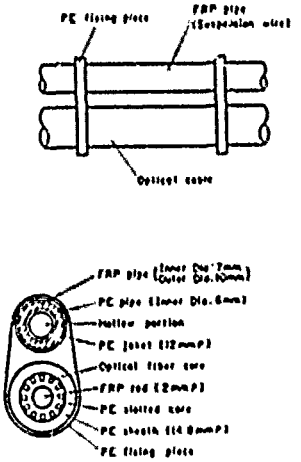

Fig. 2 Optical cable construction for aerial application

3. Cable characteristics

The two types of optical cable which have recently been developed are based on slot type construction, which assures excellent transmission properties and mechanical properties. During the manufacturing process of these cables, no degradation of the transmission characteristics was observed.

Here, a description is given mainly of the mechanical properties and the installation adaptability of the cable and of the air blowing characteristics of the air-blown fiber utilizing the hollow pipe portion.

3.1 Mechanical characteristics

(1) Flexibility

Cable flexibility of two types of recently developed optical cables and a multi-cable having a single cable core was evaluated. For comparison purposes, evaluation was also done for the prehanger type optical cable, in which the suspension wire is constituted of 7/2.0 mm steel stranded wire and FRP of 8 mm in diameter. The results are summarized in Fig. 3.

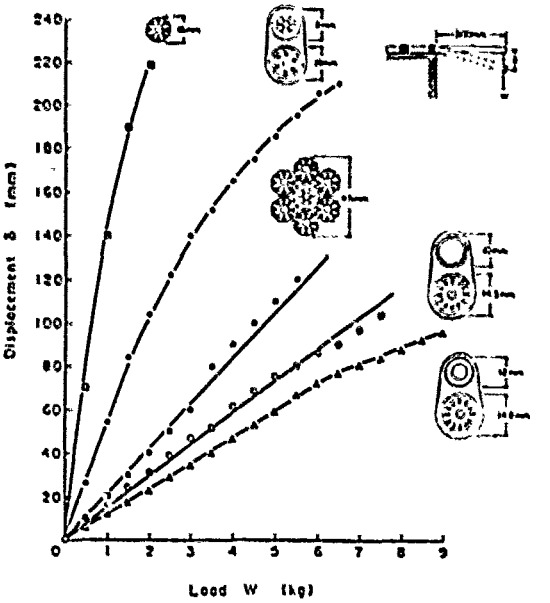

Fig. 3 Cable flexibility

The results of the test suggest that there is no substantial difference in flexibility between the prehanger type cable having hollow FRP suspension wire and the prehanger type cable having FRP rod suspension. Thus, it seems that no problem may arise even when suspension wire is replaced with FRP pipe.

(2) Tension tests

For comparison purposes, tension tests were performed on the prehanger type optical cable having FRP pipe as suspension wire as shown in Fig. 2 and on the prehanger type cable having FRP rod of 8 mm in diameter as suspension wire. Figure 4 shows the results of the evaluation of load elongation characteristics of the suspension wire. Both cables exhibited almost the same characteristics. In the cross-sectional area of FRP, FRP pipe has a cross-sectional area smaller by about 20%; however, a similar trend was observed because Young's modulus was raised by the same degree to improve the strength. Therefore, it appears that prehanger cable having FRP pipe as suspension wire has tension strong enough to meet the demands of the installation environment - not only for aerial installation on electric poles but also for hanging on pylons.

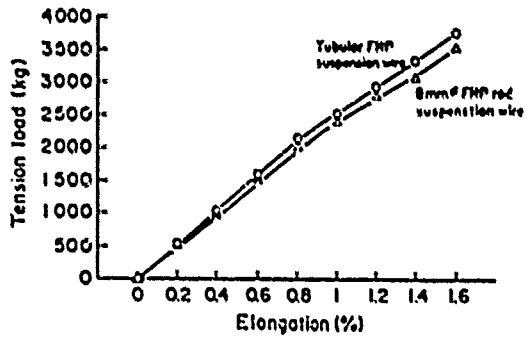

Fig. 4 Load elongation characteristics of the cable with FRP suspension wire

(3) Bending

Ten cycles of bending tests were performed using a mandrel of 600 mm in diameter on the two types of the cables shown in Fig. 1 and Fig. 2. The results of the tests revealed no increase of transmission loss of optical fiber in both cables at 1.3 μm; stablity characteristics against bending were also confirmed.

During the bending test, there was no sign of damage to FRP pipe, such as cracking, collapse, etc., on the prehanger cable with FRP pipe suspension wire of Fig. 2. It was thus confirmed that there is no problem from a physical standpoint.

(4) Impact

On the optical cable portion of the two types of cables recently developed, impact tests were performed using a cylinder with a diameter of 2.5 mm and a weight of 1-3 kg. Because the optical fiber of these cables is based on slot core construction to provide strong protection against external forces, there was no change of loss at 1.3 μm.

When a cylinder weighting 3 kg was dropped from a height of 1 m onto the FRP pipe, no damage to the FRP pipe was noted.

3.2 Branching operation for multi-cable

After the multi-cable shown in Fig. 1 was installed vertically in the distribution duct in a building, the workability of the cable for intermediate branching was assessed. As shown in Fig. 5(a) and (b), it is possible to pull the cables to each floor because the cable is stranded in SZ.

(a) Cutting of the cable

(b) Pulling the cable out

Fig. 5 Intermediate branching process of multi-cable

3.3 ABF system Application

An attempt was made to send a 6-fiber optical unit with an outer diameter of 2 mm by compressed air by means of the air blown fiber (ABF) system.

Table 1 summarizes the evaluation results of the cable shown in Fig. 1. It was demonstrated that

about 200 m of optical fiber unit can be easily sent by the ABF system and that additional functions of cable distribution within a building by the ABF system can be fulfilled with this cable structure. The pressure for air blowing is 5 kg/cm^2. Table 2(a) and (b) give the results of air blowing of the cable shown in Fig. 2 by the ABF system. The results reveal that an optical fiber unit of about 300 m can be easily installed in FRP pipe.

Figure 6(a) and (b) show the connection of the air-blowing pipe of the ABF system and the FRP pipe by means of the connector.

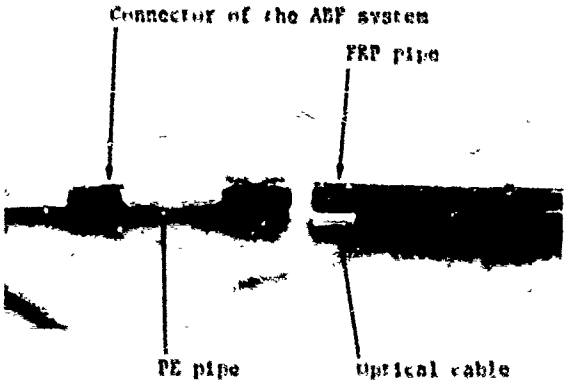

(a) Before connection of PE pipe with FRP pipe

(b) After connection of PE pipe with FRP pipe

Fig. 6 PE pipe connection with FRP pipe

Table 1 Air blowing performance for multi-cable in Fig. 1

Air blowing distance	Air blowing time	Blowing speed
0 m	0'	
		30 m/min.
50 m	1'40"	
		24 m/min.
100 m	3'40"	
		20 m/min.
150 m	6'00"	
		21 m/min.
200 m	8'30"	
		8 m/min.
250 m	12'30"	
		0 m/min.
277 m	15'40"	

Table 2 Air blowing performance for prehanger cable in Fig. 2

(a) Cable length: 300 m

Air blowing distance	Air blowing time	Blowing speed
0 m	0'	
		26.2 m/min.
45 m	1'43"	
		29.0 m/min.
90 m	3'16"	
		28.7 m/min.
135 m	4'50"	
		25.9 m/min.
180 m	6'34"	
		25.0 m/min.
225 m	8'22"	
		13.2 m/min.
270 m	11'45"	
		7.2 m/min.
300 m	16'00"	

(b) Cable length: 250 m

Air blowing distance	Air blowing time	Blowing speed
0 m	0'	
		29.2 m/min.
50 m	1'32"	
		29.2 m/min.
90 m	3'04"	
		29.9 m/min.
135 m	4'34"	
		29.5 m/min.
180 m	6'05"	
		29.2 m/min.
225 m	7'37"	
		29.4 m/min.
250 m	8'30"	

4. Conclusion

Two types of newly developed optical fiber cables provide for the sending of optical fiber unit by compressed air through the air blown fiber (ABF) system in order to flexibly cope with increased demands for installation of optical cable line and with changes of optical transmission routes in LAN systems. The results of the recent evaluation revealed that 200-300 m of optical fiber unit can be sent by compressed air without specific problems. In addition, it was clarified that these new

cables are also suitable for vertical cable laying within buildings or for the leading-in of optical cable on each floor. They were also found to be usable without problem as optical fiber cable for aerial transmission line.

References

(1) E. Hayasaka et al., "Non-Metallic Optical Cable with Optical Fiber Catenary for Long Span Aerial Application," Proceedings of International Wire & Cable Symposium, 1983.

(2) S. Hornung et al., "Manufacture and Performance of Fibre Units for Installation by the Viscous Drag of Air," Proceedings of International Wire & Cable Symposium, 1985, pp.342-345.

Yuji Kuwata
Sumitomo Electric
Industries, Ltd.
1, Taya-cho
Sakae-ku
Yokohama 244, Japan

Yuji Kuwata received the B.E. degree from Waseda University in 1984 and joined Sumitomo Electric Industries, Ltd. He has been engaged in design and development of optical fiber cables. He is now an engineer of fiber optics division.

Hajime Igarashi
Sumitomo Electric
Industries, Ltd.
1, Taya-cho
Sakae-ku
Yokohama 244, Japan

Hajime Igarashi received the B.E. degree in engineering from Waseda University in 1988 and joined Sumitomo Electric Industries, Ltd. He has been engaged in the development and design of optical fiber cables in the fiber optics division.

Hiroaki Horima
Sumitomo Electric
Industries, Ltd.
1, Taya-cho
Sakae-ku
Yokohama 244, Japa

Hiroaki Horima received the M.S. degree in engineering from Osaka University in 1972. He then joined Sumitomo Electric Industries, Ltd. and worked on the development of CATV coaxial cables, multipair PEF-insulated junction cables and low loss unbalanced type cables. Thereafter, he concentrated on the development of optical fiber cables. He is now Section Manager of the Fiber Optics Division at Sumitomo Electric Industries, Ltd. He is a member of the Institute of Electronics and Communication Engineers of Japan.

Koji Ogata
Kitanihon Electric
Cable Co., Ltd.
Wakabayashi-ku
Sendai 982, Japan

Koji Ogata received the B.E. degree from Tohoku Gakuin University in 1986. At Kitanihon Electric Cable Co., Ltd. He has been engaged in the development and design of optical fiber cables in the Engineering Division. He is a member of the Institute of Electronics and Communication Engineers of Japan.

Arinobu Saito
Kitanihon Electric
Cable Co., Ltd.
1-2-1, Koriyama
Wakabayashi-ku
Sendai 982, Japan

Arinobu Saito received the B.E. degree from Tohoku Gakuin University in 1966. At Kitanihon Electric Cable Co., Ltd. He has been engaged in the development and design of communication cables, power cables and accessories. He is now a deputy manager of the Manufacturing Department.

Takeo Shishido
Kitanihon Electric
Cable Co., Ltd.
1-2-1, Koriyama
Wakabayashi-ku
Sendai 982, Japan

Takeo Shishido was born in 1939, he joined Kitanihon Electric Cable Co., Ltd. He has been engaged in the design and development of communication cables, power cables and accessories. He is now a general manager of the Manufacturing Department.

NEW COMPOSITE CABLE APPLYING THE AIR BLOWN FIBER TECHNIQUE

S. Kondo.* K. Kikuchi.* A. Ono.** K. Yamashita.** G. Horikawa.** M. Kyuto**

* East Japan Railway Company. Tokyo. Japan
** Sumitomo Electric Industries. Ltd. Yokohama. Japan

Abstract

The demands for composite communication cables containing optical fibers and metallic conductors have been increasing. Based on the fundamental technique of air blown fiber (ABF), a new kind of composite communication cable has been developed that integrates a metallic conductors with ABF tubes. Compared to conventional optical fibers/metallic conductors composite cables, the new ABF metallic conductors composite cable has an advantageous feature that it is possible to draw optical fiber units into the cable after installation. This feature allows a smooth changeover from metallic conductors transmission system to optical fibers transmission system.

A prototype ABF/metallic conductors composite cable was fabricated which integrated 100 pairs of quad-type copper conductors with two ABF tubes, and its characteristics were evaluated. The evaluation revealed that the cable has good electrical and mechanical characterestics for practical use. It was also confirmed that the optical fiber unit as long as 1,000m can be inserted into the cable with air blown fiber technique.

1. Introduction

As fiber optic communication systems proliferate both in Japan and abroad, demands for optical fiber cables are growing. As a part of them, the demand for composite communication cables, which combine metallic conductors with optical fibers, has also been increasing for the purpose of the saving of duct spaces and the reduction of installation costs.

On the other hand, we have introduced the fundamental technique of air blown fiber (ABF) from British Telecommunications plc. in 1987. The ABF technique makes it possible to draw easily the optical fiber unit into a preinstalled empty tube (ABF tube) by using compressed air. This technique has been used for the optical fiber cable distributions which will require additional installation or replacement of optical fibers in the future.

Based on the above ABF technique, we have developed a new kind of composite cable which integrates metallic conductors with ABF tubes. It's possible to draw the optical fiber unit into the new composite cable after it has been installed. This ABF metallic conductors composite cable can be used as a conventional metallic conductors communication cable at the initial stage. When the optical fiber communication system is actually required, this new composite cable can be applied as a optical fibers-metallic conductors composite cable by drawing the optical fiber units into ABF tubes.
We manufactured the new composite cable which integrated 100 pairs of quad-type copper conductors with two ABF tubes, and evaluated its characteristics.

In this paper, the advantages, construction and characteristics of this ABF/metallic conductors composite cable are described.

2. ABF/Metallic Conductors Composite Communication Cable

2.1 Advantages of the new composite cable

Compared to conventional optical fibers/metallic conductors composite cables, the new ABF/metallic conductors composite cable has the following advantageous features. These features combine to allow a smooth changeover from metallic conductors transmission systems to optical fibers/metallic conductors composite transmission systems.

(1) The introduction of optical fibers to transmission system can be delayed until the actual demands of optical fiber transmission system occur, because it is possible to draw the optical fiber unit into the new composite cable after installation. In addition, it is easy to install more optical fibers or replace existing ones after the optical fibers unit has been drawn into the cable. This feature reduces the initial cost for transmission system.

(2) No special tension member is required in the cable structure, and the cable can be installed using traditional technique without special care, because the ABF technique reduces the optical fiber's elongation strain.

(3) It is possible to decrease the fusion spliced number of optical fibers. In the ABF system, it is possible to introduce the optical fiber unit of up to 1,000m length into the ABF tube even though the metallic conductors and the ABF tubes are connected at intervals of several hundred meters.

2.2 Cable Construction

Various constructions of the ABF/metallic conductors composite cable can be designed, and the combination of the number of ABF tubes and metallic conductors is decided according to the requirment of the system. We manufactured a prototype ABF/metallic composite cable which integrated 100 pairs of quad-type copper conductors (0.9 mm diameter each) with two ABF tubes.

In this paper, we introduce this 0.9mm × 100p + ABF ×2T size ABF/metallic conductors composite cable. The construction and the appearance of the new composite cable are shown in Fig.1 and Photo.1, respectively. Table 1 shows the make-up and the dimensions of the new composite cable, and those of standard 0.9mm ×100p size copper conductors cable for reference.

We designed the construction of this cable based on the existing metallic conductors cable so as to apply the same technique of installation and jointing. ABF tubes are made of colored polyethylene, and its outer/inner diameters are 8mm/6mm. Two ABF tubes and one copper conductor unit are placed in the center, and nine copper conductor units are stranded around the center layer. The cable core is covered with LAP (Laminated Aluminum Polyethylene) sheath.

Compared to the standard 0.9mm × 100p size copper conductors cable, the increase in the outer diameter of the composite cable is only 2mm, because no special tension member is required in the new composite cable structure.

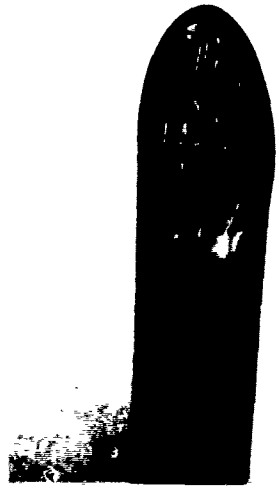

Photo. 1. Appearance of new composite cable.

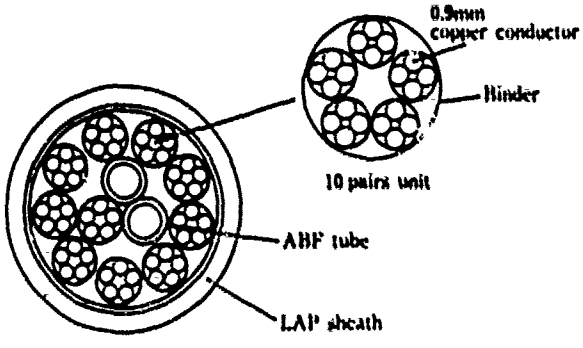

Fig.1. Construction of ABF/metallic conductors composite communication cable. (0.9mm * 100P+ABF * 2T size)

Table 1 Make-up and dimensions

Item \ Cable		ABF/metal conductors composite communication cable. (0.9mm * 100P + ABF * 2T)	Metal conductors communication cable. (0.9mm * 100P)
Conductor	Material	Annealed copper wire	
	Diameter	Nom. 0.9mm	
Insulation	Material	Polyethylene	
	Thickness	Nom. 0.27mm	
Twisting		Quad type	
ABF Tube	Inner Diameter	Nom. 6mm	
	Outer Diameter	Nom. 8mm	
Make-up	Center Layer	10pairs unit ×1 +ABF tube ×2	10pairs unit ×3
	First Layer	10pairs unit ×9	10pairs unit ×7
LAP sheath Thickness		Nom. 2.0mm	
Cable Diameter		Approx. 36mm	Approx. 36mm
Cable Weight		Approx. 1.7kg/m	Approx. 1.7kg/m
Standard Lenght		500m	

3. Electrical Characteristics

The fundamental design of the copper conductor part of the new composite cable is the same as that of 4mm dard quad type copper conductor cables.

Table II shows the electrical characteristics of this cable. It was confirmed that the ABF metallic conductors composite cable has good electrical characteristics equal to those of standard metallic conductors communication cable.

Table II Electrical characteristics

Item	Specified value	Measurement value		
		Ave.	Max.	Min.
Conductor Resistance (at 20°C)	Max. 29.0Ω/km	28.0	28.3	27.8
Mutual Capacitance (at 1kHz)	Max. ave. 46nF/km	44.0	45.4	41.8
Capacitance Unbalance (between pairs in quad)	Max. 330pF/300m Max. ave. 150pF/300m	37	156	2
Insulation Resistance	Min 5kMΩ・km	≧ 1000		
Dielectric Strength	DC 500V for 1min	good		

4. Mechanical Characteristics

The important mechanical characteristics of the ABF metallic conductors composite cable is the deformations of the ABF tubes by external mechanical forces applied to the cable at installation. The large deformation of ABF tube don't allow the insertion of the optical fiber unit.

Various severe mechanical conditions were applied to the cable taking into account the actual cable installation and the deformations of ABF tubes in the cable were investigated.

4.1 Bending Test

In order to investigate the deformation of the ABF tubes in the bent part of the cable, the steel ball (5.4mm in dia.) was inserted into the ABF tubes in the cable sample which was bent around the mandrel. This bending test was repeated for various bending diameter conditions. The test results are shown in Table III. It was confirmed that the steel ball passed through the ABF tubes down to the 170mm bending radius of the cable sample. That is 4.5 times as large as the outer diameter of the cable.

Generally the allowable cable bending radius is 6 times of the outer diamter of the cable. Therefore, this result indicates that there is no significant deformation of the ABF tubes due to the bending conditions during the standard installation of the cable.

Table III Bending test results

ABF tube No. \ Bending radius	6D (228mm)	4.5D (170mm)	3.2D (125mm)
1	○	○	×
2	○	○	×

D : Cable diameter (38mm)
○ : Steel ball passed through ABF tube
× : Steel ball didn't pass through ABF tube
The diameter of the steel ball : 5.4mm

4.2 Compression Test

A lateral compression force over the 50mm width plate was applied repeatedly to the 50mm length cable sample. Fig.2 shows the changes of the short outer diameter of the cable and the short inner diameter of the ABF tubes in the cable against compression force. Photo. 2 shows the cross sectional view of the cable when compression force is applied and released. It was confirmed that the inner diameter of ABF tubes is almost restored to the initial diameter after compression force (100kg/50mm) is released.
This result indicates that this cable has good compression force resistance for practical installation in a trough or a duct.

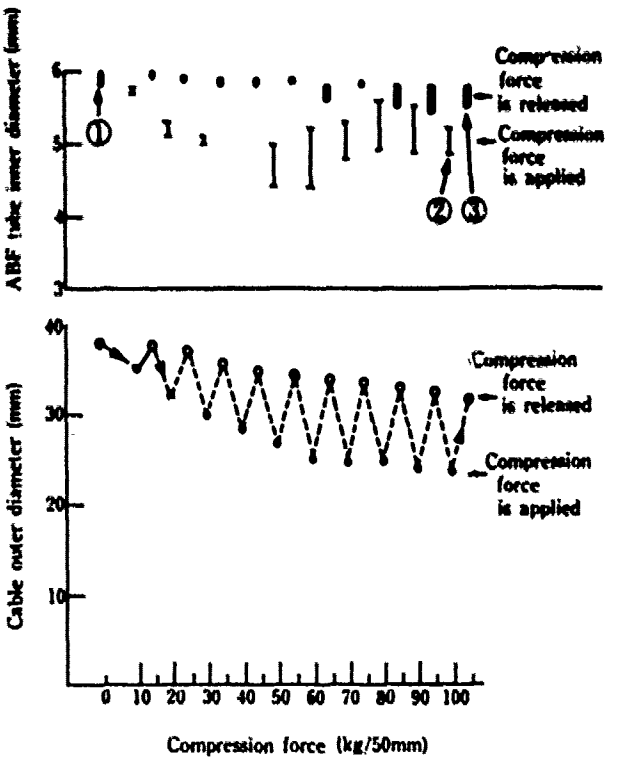

Fig.2. Compression test results.

① Initial.

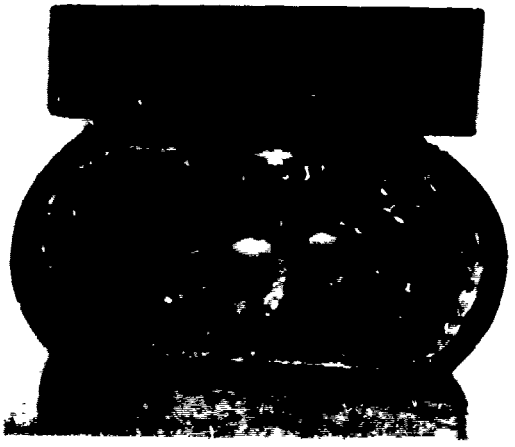

② Compression force (100Kg/50mm) is applied.

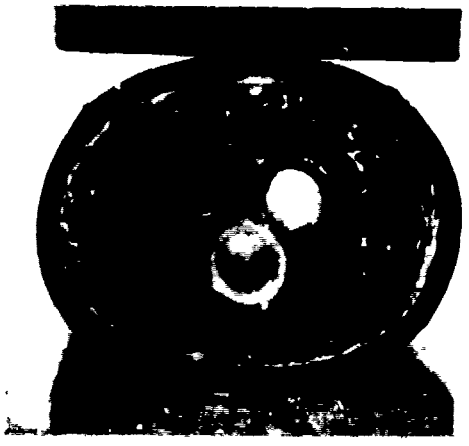

③ Compression force (100Kg/50mm) is released.

Photo.2. Cross sectional view of the cable under compression test.

4.3 Other Mechanical Test

Other various mechanical tests of the cable were carried out such as tensile test, repetitive bending test, torsion test and squeezing test. After these tests, the deformation of the ABF tubes in the cable samples were observed, and the inner diameters of them were measured.

Test methods and results are shown in Table IV. No visual deformation of the ABF tubes was observed, and the inner diameters of them were over 5.6mm in each test sample. It was confirmed that the new composite cable has good mechanical characteristics for practical use.

Table IV Mechanical test methods and results

Item	Test methods and conditions	Inner diameter of ABF tube
1 Tensile Test	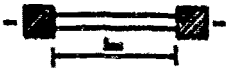 Tensile load , = [illegible]kg	≧ 5.7mm
2 Repetitive Bending Test	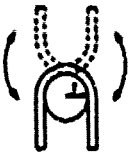 Bending radius (r) , 60 (220mm) ±180° repetitive bending ×3times	≧ 5.6mm
3 Torsion Test	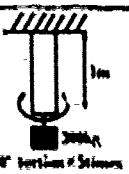 1m 3000g ±360° torsion ×5times	≧ 5.6mm
4 Squeezing Test	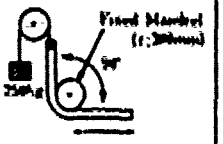 Fixed Mandrel (r;300mm) 90° 250Kg Squeezing length ; 2m Number of squeezing , 5times	≧ 5.6mm

5. Inserting Characteristics

The inserting characteristics of the new composite cable were examined using the standard optical fiber unit shown in Fig.6. This optical fiber unit consists of 6 optical fibers (3 single mode optical fibers and 3 graded index optical fibers) and its outer diameter is 2mm.

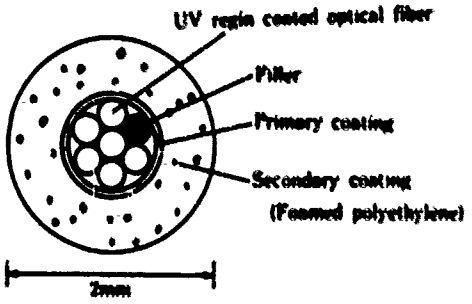

Fig.3. Construction of standard optical fiber unit for ABF system.

5.1 Heat Aging Test

The inserting characteristics were investigated before and after heat aging of the cable. The test was carried out by the 500m length cable which was wound on a reel of 1m diameter. The time it took to insert a 500m length optical fiber unit into the cable by compressed air was measured. The compressed air pressure was 5kg/cm².

Then the 500m length cable was placed in a temperature test chamber and kept under a high temperature condition of 80℃ for 72 hours. After it was returned to room temperture, the inserting time was measured again under the same conditions as before heat aging.

Fig.4 shows the test results. The inserting time of a 500m length optical fiber unit was about 20 minutes for the composite cable before and after heat aging. There was no deterioration of inserting characteristic after heat aging. It was confirmed that the new composite cable has good stable inserting characteristics.

5.2 After Cable Installation

Inserting characteristic of a 1,000m length optical fiber unit was investigated after the cable was installed. The 500m length cable was experimentally installed on the ground as shown in Fig.5. The cable was turned at the middle point of 250m, and the elevation (5m hight) was made at near the cable ends. The two ABF tubes in a 500m length cable were connected at one side of the cable end to form a 1km length test loop of ABF tube.

Fig.6 shows inserting characteristic. The 1km length optical fiber unit was successfully inserted into the test loop in about 50 minutes. The compressed air pressed air pressure was 7.0 kg/cm².

After the optical fiber unit was installed, the transmission characteristics was examined using OTDR. The transmission loss of SM fibers was measured at wave lengths of 1.3/m and 1.55/m, respectivily. That of GI fibers was measured at a wavelength of 1.3/m. No significant loss increase was observed for both SM and GI fibers compared with before inserting.

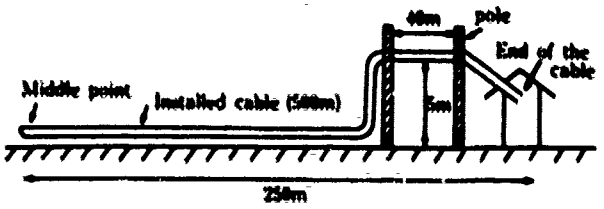

Fig.5. Scheme of experimental installation of the cable.

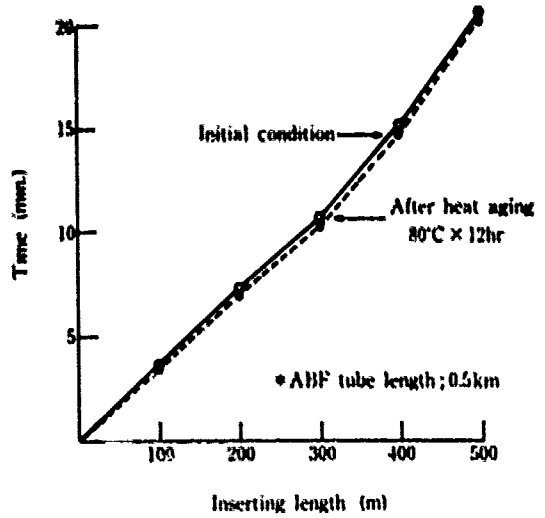

Fig.4. Inserting characteristics on rolled up cable before and after heat aging.

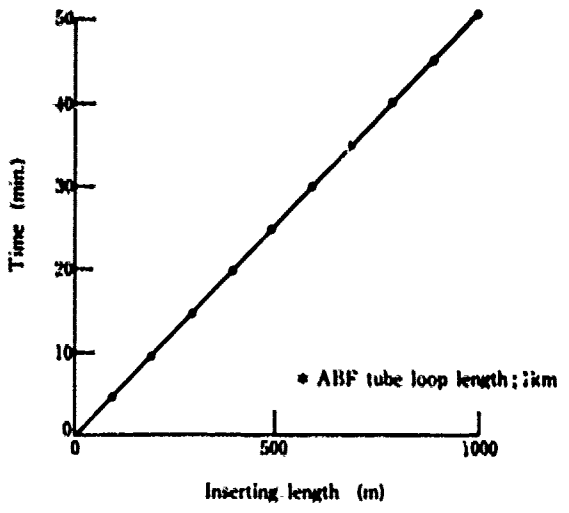

Fig.6. Inserting characteristic on experimentally installed cable.

6. Jointing of the Cable

The jointing of the new composite cable was examined. There are two cases of cable jointing.

Case 1. A optical fiber unit passes through the cable joint without fiber fusion splices.

Case 2. A cable joint contains fiber fusion splices.

It was experimentally confirmed that the conventional metallic conductors communication cable jointing method can be applied to the jointing of the new composite cable in the case 1. In the case 2, three components, which are metallic conductor joints, ABF tube connections and optical fiber fusion splices, are nessesary in a cable joint. In this case, the jointing method using a closure, which are widely applied to optical fiber cable, was examined. It was confirmed that the jointing in the case 2 is possible by using the clousure shown in Photo.3.

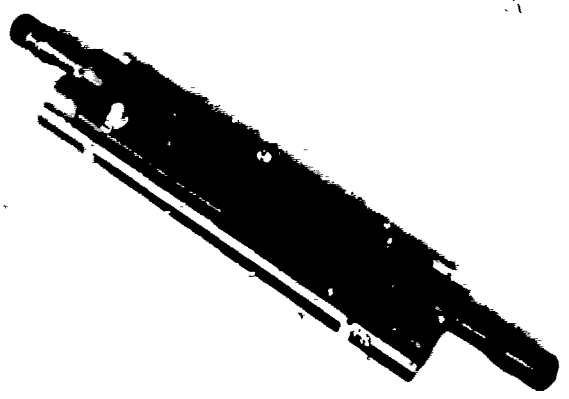

Photo.3. Jointing of the cable using a clousre.

7. Conclusion

We have developed a new kind of composite communication cable applying the ABF technique, which integrates metallic conductors with ABF tubes.
It was confirmed that the new composite cable has good electrical and mechanical characteristics, and that the optical fiber unit can be successfully inserted into the cable u, to 1,000m.

The new composite cable has various advantages compared with conventional optical fibers/metallic conductors composite cables. This cable is useful for metallic conductors transmission systems which will change to optical fibers transmission systems in the future.

Reference

(1) S.Hisano et al., "A STUDY ON DESIGN OF COMPOSITE CABLE CONTAINING OPTICAL FIBER AND MULTI PAIRS". Proc. of 36th IWCS, 1987.

(2) S.A.Cassidy et al., " A radically new-approach to installation of optical fibers using the viscous flow of air", Proc. of32 the IWCS, 1983.

Shinzo Konno

East Japan Railway Company.

1 6 5, Marunouchi, Chiyoda-ku, Tokyo, Japan

Shinzo Konno received his M.S. degree in Physical Engineering from Tokyo Univ. in 1977. He then joined Japan National Railway and has been engaged in plan of railway communication network. Mr. Konno is now a manager of signal and communication section in Tokyo area operation headquarters of East Japan Railway Company.

Kiyoshi Kikuchi

East Japan Railway Company.

1-6-5, Marunouchi, Chiyoda-ku, Tokyo, Japan

Kiyoshi Kikuchi graduated from Yamagata technical high school in Electrical Engineering in 1966. He then joined Japan National Railway and has been engaged in maintenance of railway communication network. Mr. Kikuchi is now a assistant manager of signal and communication section in Tokyo area operation headquarters of East Japan Railway Comany.

Atsuhiro Ona

Sumitomo Electric Industries, Ltd.

1, Taya-cho, Sakae-ku, Yokohama, Japan

Atsuhiro Ona received his M.S. degree in Electrical Engineering from Yokohama National Univ. in 1984. He then joined Sumitomo Electric Industries and has been engaged in development and design of optical fiber cable. Mr. Ona is now a member of communication cable engineering section.

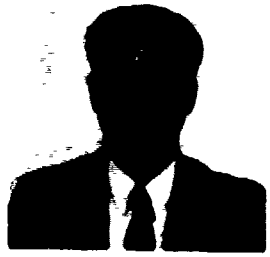

Katsumi Yamashita

Sumitomo Electric Industries, Ltd.

1, Taya-cho, Sakae-ku, Yokohama, Japan

Katsumi Yamashita received his B.S. degree in Electrical Engineering from Kanagawa Univ. He then joined Sumitomo Electric Industries in 1968 and has been engaged in development and design of accessories for communication cables. Mr. Yamashita is now a member of communication cable accessories engineering section.

Gen Morikawa

Sumitomo Electric Industries, Ltd.

1, Taya-cho, Sakae-ku, Yokohama, Japan

Gen Morikawa received his M.S. degree in Electrical Engineering from Kyoto Univ. in 1977. He then joined Sumitomo Electric Industries and has been engaged in development and design of optical fiber cable and communication cable. Mr. Morikawa is now a senior engineer of communication cable engineering section.

Masahiro Kyuto

Sumitomo Electric Industries, Ltd.

1, Taya-cho, Sakae-ku, Yokohama, Japan

Masahiro Kyuto received his B.S. degree in Electrical Engineering from Tokyo Institute of Technology in 1970. He then joined Sumitomo Electric Industries and has been engaged in development of metallic cables and optical fiber cables. Mr. Kyuto is now a manager of communication cable engineering section.

LOW SMOKE, FIRE RETARDANT CABLE JACKETS BASED ON ETHYLENEVINYLACETATE AND HYDROGENATED NITRILE RUBBER

Hermann Meisenheimer

Rubber Division, Bayer AG, D-5090 Leverkusen, FRG

Summary

Levapren, a copolymer of ethylen and vinylacetate (EVM) and Therban, a hydrogenated copolymer of butadiene and acrylonitrile (HNBR) help to meet the requirements for fire retardant, non corrosive cables. They posses high temperature resistance and high oil resistance. Compounds based on these polymers can pass fire tests and the combuction gases are within the toxicity index requirements of NES.

Introduction

In case of fire conventional cables form a large amount of smoke (obscure escape routes and fire service approach routes) and cause severe secondary damage by releasing corrosive gases (corrosion of equipment and buildings).

Hence materials are now demanded which have less serious effects in a fire. These fire retardant non-corrosive (FRNC) materials have

- fire retardance
- low smoke density in case of fire
- non corrosive smoke
- very low concentration of hazardous gases

EVM as base for FRNC cables

High fire retardance

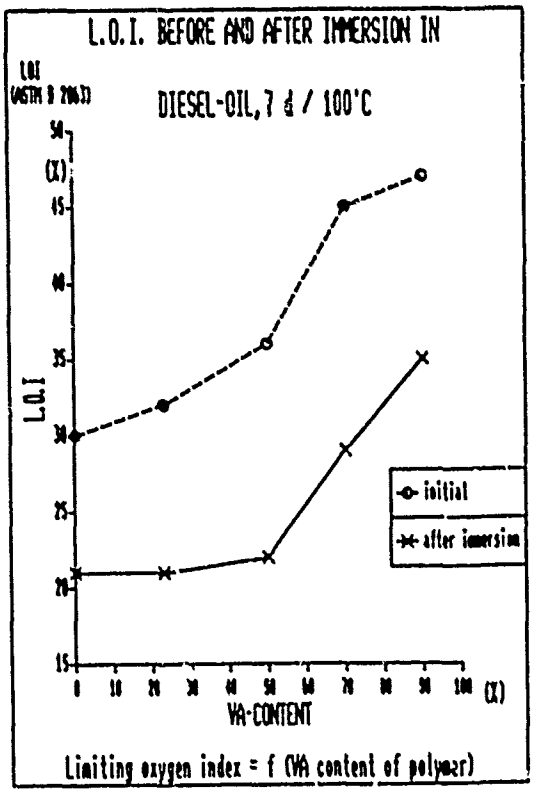

Limiting oxygen index = f (VA content of polymer)

Low smoke density

Polymer	Compound type	$D_{max.corr.}$
EVM	FRNC	120
SBR	with chlorinated paraffin	750
EPR	with chlorinated paraffin	400
PVC	with DOP	800
PVC	with phosphate	950
CR	with chlorinated paraffin	950
CR	low smoke	350
CSP	with chlorinated paraffin	750
CSP	low smoke	250
CPE	with chlorinated paraffin	750
CPE	low smoke	250

Smoke densities of various cable compounds. Smoke density $D_{max.corr.}$ according ASTM D 662 E (flaming mode)

Low concentration of hazardous gases

According to NES 713
(Naval Engineering Standard)

Toxicity index

EVM FRNC	Limit
1	< 5

According to RATP Specification K 20/ Annexe 19 (Régie Autonome des Transports Parisiens)

Toxicity index

EVM FRNC	Limit
39	< 100

Low corrosivness of combustion gases

According to DIN 57 472, (Part 813)	Spec. VDE 0207 Part 24	EVM-FRNC
pH value of the water	> 3,5	4,3
Conductivity of the water (µS/cm)	< 100	31

Good oil resistance

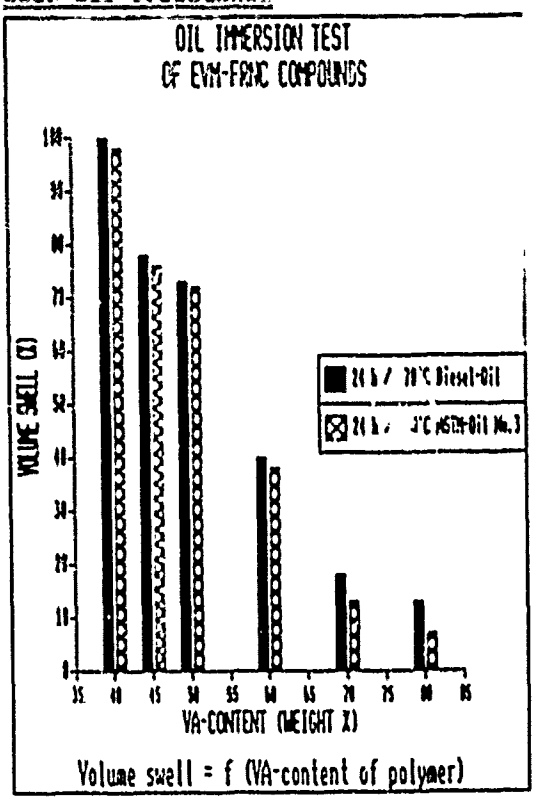

Good heat ageing properties

Tensile strength

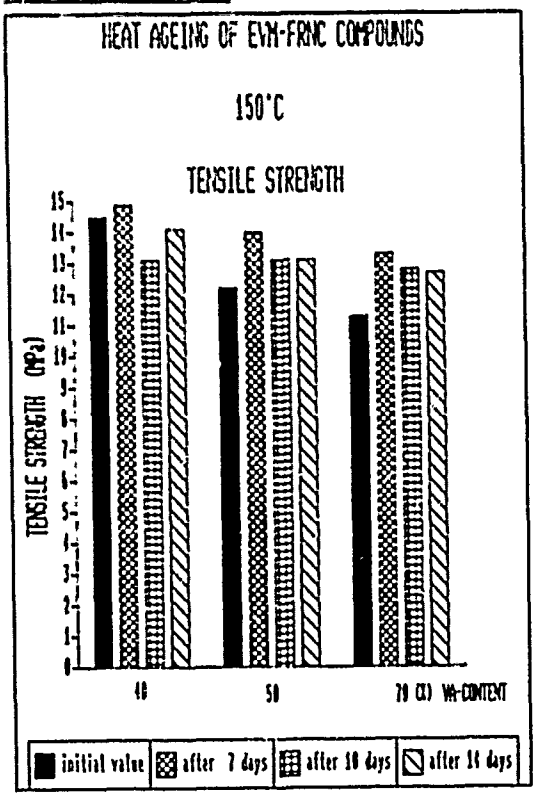

Elongation at break

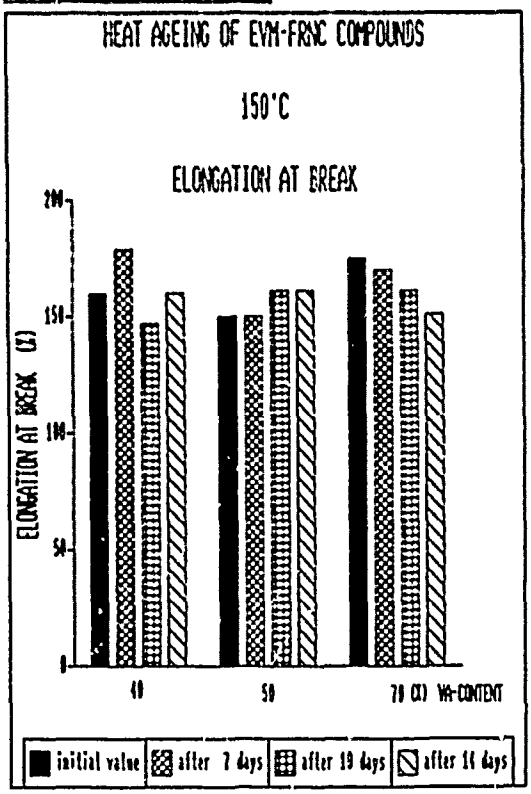

PROPERTIES OF FRNC CABLE JACKETS BASED ON EVM
BEHAVIOR UNDER FIRE CONDITIONS

Conventional thermoplastic cable
black smoke formation
flame app. 250 cm after 10 mins

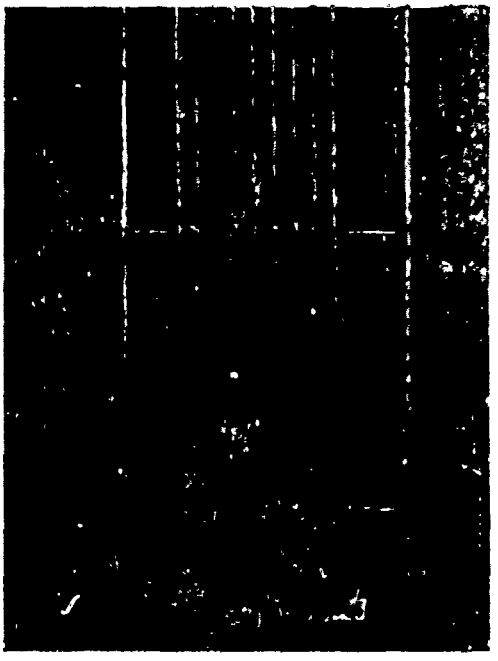

Cables w'th EVM thermoset jacket
nearly no smoke visible
flame app. 30 cm after 10 mins

Characteristics of EVM FRNC compounds

- Polymers with fire-retardant behavior in combination with ATH, which improves with their VA-content.
- Low smoke gas density.
- High limiting oxygen index (LOI) values.
- Low concentration of hazardous gases.
- Low corrosivness of combustion gases.
- Good oil resistance.
- Good heat ageing properties.

HNBR/EVM AS BASE POLYMERS FOR CABLE JACKETS ACC. NES 518

Navy cables need good flame retardation and high mechanical properties. To withstand enviromental attack good ozone resistance and resistance to various fluids are required.

Cable jackets for fire retardent cables

EVM (70 % VA) (1)	100.0	50.0	-	-
HNBR (34 % ACN) (2)	-	50.0	100.0	-
HNBR (43 % ACN) (3)	-	-	-	100.0
Stabilizer (4)	3.0	3.0	-	-
Silane (5)	2.0			
ATH (6)	190.0			
Zinc stearate	1.0			
Zinc borate	10.0			
Antioxidant SDPA (7)	1,9			
Dioctylsebacate	6.0			
TRIM	0.7			
Peroxide (8)	6.0			
Total parts	319.7	319.7	316.7	316.7

(1) Levapren 700 HV, Bayer AG/FRG
(2) Therban 1707, Bayer AG/FRG
(3) Therban 2207, Bayer AG/FRG
(4) Rhenogran P 50, Rhein-Chemie/FRG
(5) Ucarsil RC-1, UCC/CH
(6) Apyral B 120, Bayer AG/FRG
(7) Vulkanox DDA, Bayer AG/FRG
(8) Perkadox 14/40, AKZO/FRG

Mechanical properties of EVM and HNBR cable jackets

Cure conditions: 90 s/200°C steam

Polymer base	EVM (70% VA)	EVM (70% VA) HNBR (34%ACN)	HNBR (34% ACN)	HNBR (43% ACN)	Spec. NES 518
TS (MPa)	11.7	10.7	13.8	14.9	>8.0
ED (%)	220	230	270	240	>200
H (Sh.A)	75	78	76	78	
Tear (N/mm) ASTM D 470	2.1	3.9	5.8	5.1	>5.0

Ozone test

Ozone resistance of EVM and HNBR cable sheaths

Elongation: 40 %, Ozone concentration: 100 ppm, Duration of exposure: 5 days

No cracks for all samples, all samples pass the test.

Cold bend test

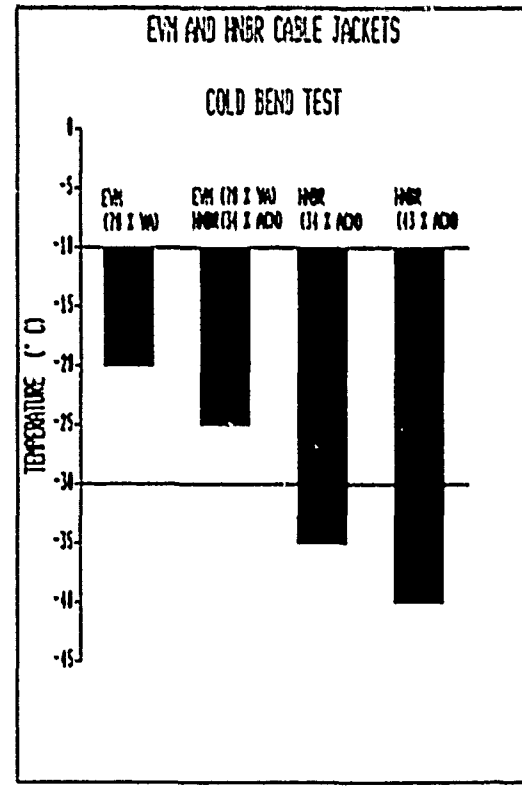

Immersion tests (Changes in %)

Polymer	EVM 70% VA	EVM (70% VA HNBR 34% ACN)	HNBR (34 % ACN)	HNBR (43 % ACN)	Spec. NES 518 (max.Change)
Diesel oil NATO F-76, 28d/23°C					
TS	9	20	27	16	-40
EB	-19	-25	-24	-29	-40
Δ V	19	25	11	6	25
Hydraulic Fluid, Petroleum based OX-30, 28d/50°C					
TS	15	21	27	28	-40
EB	-19	-25	-15	-15	-40
Δ V	6	8	2	0	15
Hydraulic Fluid, Silicone Based OX-50, 28d/50°C					
TS	21	34	37	38	-40
EB	-24	-21	-19	-19	-40
Δ V	- 2	- 2	- 2	- 2	15
Hydrauli Fluid, Silicone based OX-50, 28d/50°C					
TS	21	34	37	38	-40
EB	-24	-21	-19	-19	-40
Δ V	- 2	- 2	- 2	- 2	15
Lubricating Oil, detergent Mineral OMD-113, 28d/50°C					
TS	15	27	36	37	-40
EB	-24	-25	-19	-21	-40
Δ V	- 1	1	0	- 1	10
Lubricating Oil, Syntheticester base OX-38, 28d/50°C					
TS	-42	- 7	27	25	-40
EB	-48	-36	-19	-17	-40
Δ V	62	40	8	3	50
Deionized Water, 28d/50°C					
TS	-17	- 5	- 6	- 7	-20
EB	17	27	14	6	-20
Δ V	16	9	5	5	10
Deionized Water with 3,5 % NaCl, 28d/50°C					
TS	3	4	- 9	- 9	-20
EB	8	5	7	- 4	-20
Δ V	5	5	0	0	10

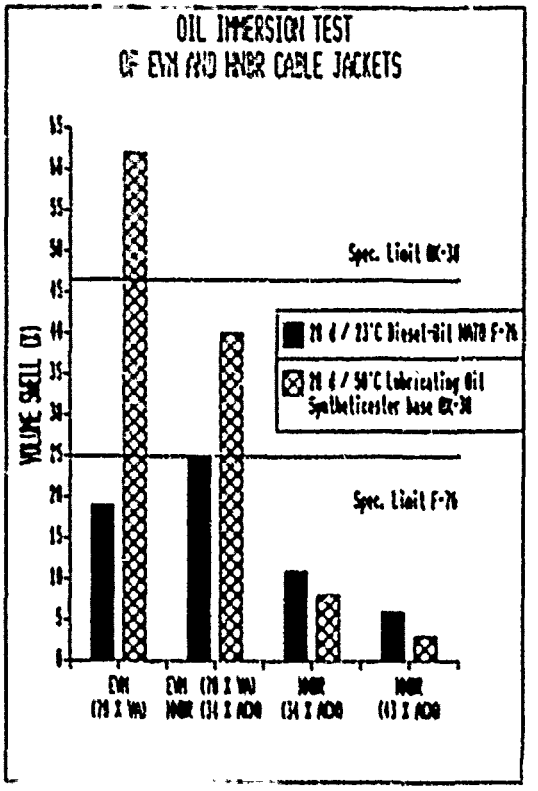

Results of flame test

Results formulated on the basis of small scale laboratory tests conducted at Bayer AG for purpose of relative comparison and are not intended to reflect hazards presented by this or any other material under actual fire conditions.

Polymer base	EVM (70 % VA)	EVM (70 % VA)/ HNBR (34 % ACN)	HNBR (34 % ACN)	HNBR (43 % ACN)	Spec. NES 518
LOI acc. ASTM D 2863 (%)	41	43	42	45	> 29
Temperature-Index acc. NES 715 (°C)	330	300	290	310	> 250
Toxicity-Index acc. NES 713	1.0	1.9	3.2	3.7	< 5.0
Smoke Density, NBS Chamber acc. ASTM E 662-83 non flaming ($D_{max.corr.}$)	200	180	170	120	
flaming ($D_{max.corr.}$)	170	110	250	150	
Corrosivity of smoke acc. VDE 0472 Part 813 pH-value	3.8	4.2	8.3	8.5	

Characteristics of HNBR FRNC Compounds

- Polymers with fire-retardant behavior in combination with ATH
- low smoke formation
- low smoke gas density
- high limiting oxygen index (LOI) values
- excellent oil resistance

The conditions of your use and application of the products and information (whether verbal, written, or by way of production evaluations), including any suggested formulations and recommendations, are beyond our control. Therefore, it is imperative that you test the products and information to determine to your own satisfaction whether they are suitable for your intended uses and applications. This application - specific analysis at least must include testing to determine suitability from a technical as well as health, safety and environmental standpoint. Such testing has not necessarily been done by Mobay or affiliates. All information is given without warranty or guarantee. Mobay Corporation and its affiliates disclaim any liability in negligence or otherwise, incurred in connection with the use of the products and information. Any statement or recommendation not contained herein is unauthorized and shall not bind Mobay Corporation or its affiliates. Nothing herein shall be construed as a recommendation to use any product in conflict with patents covering any materials or its use. No license is implied or in fact granted under the claims of any patent.

Dr. Hermann Meisenheimer is in the Rubber Business Group, Application Technology Section, Rubber/Rubber Chemicals, Bayer AG. He attended the University of Cologne/German and received a degree in Physical Chemistry. He is presently the Manager of Technical Services for Wire and Cable with Bayer AG.

DESIGN AND MEASUREMENT OF CONSTRUCTING TENSILE FORCE IN AERIAL CABLE SUSPENSION LINE

T. S. Lai, G. T. Tzeng, H. K. Peng, C. T. Chang, Y. J. Huang

TELECOMMUNICATION LABORATORIES, DIRECTORATE GENERAL OF TELECOMMUNICATIONS, MINISTRY OF COMMUNICATIONS, R. O. C.

Abstract

A personal computer program used for calculating the constructing tensile force of an aerial cable suspension line is presented in this paper. It is based on the theory of cable mechanics. Wind loading used for design is calculated according to ANSI provisions. The basic design wind speed map for Taiwan area with return period of 50 years is used to calculate velocity pressure.

A field-measuring instrument has been set up to improve the construction quality of the aerial cable structure system. A cable vibration counter has been designed and used to measure the tensile force of the suspension line.

1. Introduction

The aerial cable structure systems are constructed outdoors, so they are usually affected by the soil bearing capacity and the natural forces such as typhoon, earthquake etc. According to our investigation, 40,369 telecommunication poles were overturned and 15,644 telecommunication poles were broken during four typhoons from 1986 to 1987 in Taiwan area. The data are shown in Table 1.

Based on our research, there are three major reasons causing these damages. They are :

(1) The flexural strength of the poles is not strong enough. When wind blows, the bending moment in poles induced by wind pressure is larger than the flexural strength of the poles, then the poles break.

(2) The shearing strength of soil is not strong enough, or the buried depth of the poles is not deep enough, or reinforced members, e.g. buried log, guy, strut and guy anchor etc., are not properly designed. The poles will overturn when wind pressure act on poles and cables.

(3) The diameter of the suspension lines of cables are too small, or the sags of them are not adjusted to a proper value, then the suspension lines will break when tensile force induced by the wind pressure is larger than their tensile strength.

2. Constructing tensile force design for suspension line

There are two groups of aerial cable systems classified according to purpose of usage. One is called local aerial cable system which is constructed in city or suburban area. It is not impeded by topography and the span between two poles is generally from 20 to 50 meters. The other is called flying cable system (or long-span aerial cable system) which is constructed in mountain, forest or valley etc. Owing to characteristics of topography, the span between two poles is usually from 100 to 500 meters.

There is very large tensile force in cable systems due to gravity force and wind force. This tensile force must be taken by the suspension line. There are two types of cables used in aerial cable systems. One is self-supporting cable which is combined supporting line and cable together. The other is round-cable which is supported by a suspension line. The material of suspension line is galvanized steel wire strand. In local aerial cable system, the round-cable and suspension line are bound together by stainless or aluminum alloy lashingwire. But in the flying cable system, it is impossible to use this method to bind

cable and suspension line together. We design a figure-8 shaped suspension line clamp. One end is fixed at the supporting line of self-supporting cable. The other end is hooked at the suspension line (see Fig.1). The cable is moved along the suspension line from one end to the other end just like drawing the curtain.

3. Design theory

The tensile force of suspension line is calculated based on the theory of cable mechanics. The tensile force of the suspension line is highly related to the sag of cable, the strength of suspension line which is different according to its diameter and material, and the design wind speed which is different by area. To avoid the tensile force of the suspension line exceeding its safety limit, or the sag being too large such that the cable severely swings in the wind, we should make reasonable tension design of the suspension line.

There are two conditions considered in the design loads (including gravity load, wind pressure and temperature effect) of suspension line. The first condition is the worst condition which occurs at the time of typhoon attacking in the summer. The second condition is working condition which occurs at the time of suspension line being constructed. The fundamental principle of suspension line design is : under the maximum allowable tensile force which suspension line can sustain, the sag of it must be kept in minimum value. Based on this principle, we always let the design tensile force of suspension line at worst condition equal to its maximum allowable tensile strength, and then calculate the tensile force and sag of suspension line at working condition.

Let the worst condition be the first condition, and the horizontal component of allowable tensile force of suspension line is T1, uniform load is W1, and temperature is t1. Let the working condition be the second condition, and the horizontal component of tensile force of suspension line is T2, uniform load is W2, and temperature is t2. The horizontal component of tensile force of suspension line at working condition is obtained by solving the following equation:

$$T_2^3-(K-A\cdot E\cdot\alpha\cdot t)\cdot T_2^2-H=0 \qquad (1)$$

where

$t=t_2-t_1$

$H=A\cdot E\cdot W_1^2\cdot S^2/24$

$K=T_1-A\cdot E\cdot W_1^2\cdot S^2/24T_1^2$

A = crosss section area of suspension line (m^2)
E = Young's modulus of suspension line (kg/m^2)
S = horizontal span of two ends of suspension line (m)
α = coefficient of thermal expansion of suspension line

At the time of construction, the maximum sag (flat suspendsion line) or inclined sag (inclined suspension line) of suspension line is

$$h_2=W_2\cdot S^2/8T_2 \qquad (2)$$

the actual length of suspension line is

$$L_2=S+W_2^2\cdot S^2/24T_2^2+H^2/2S \qquad (3)$$

where

H = latitude difference of two ends of suspension line

T2, h2, L2 are the data which designer should calculate before suspension line was constructed. $T_1=T_u/f$, Tu is the tensile strength of the galvanized steel wire strand, f is the safety factor, f=2.0.

The uniform load(W) per unit length of the suspension line is the resultant vector of weight per unit length of cable(Wc), weight per unit length of suspension line (Ws) and wind pressure per unit length acting on cable and suspension line (Ww), then $W=\sqrt{(W_c+W_s)^2+W_w^2}$.

In the past, we used the following formula to calculate the wind pressure per unit length of cables.

$$W_w=0.0667V^2\cdot D \qquad (4)$$

where

V = design wind speed, 40m/sec is used in the suburban area, 28m/sec is used in city.
D = projective widths of cable and suspension line against the wind

According to the recent research, wind pressure is changed depending on the structure characteristics and wind speed which is different by area, type of exposure and height of the structure, so equation (4) is not resonable.

Based on codes in " American National Standard Minimum Design Loads for Buildings and Other Structures " published by ANSI in 1982, the wind pressure per unit length acting on cable and suspension line should be

$$W_w = q(z) \cdot G(z) \cdot C_f \cdot D \qquad (5)$$

where, q(z) is the wind velocity pressure of different structure and different type of exposure at z meters height.

G(z) is gust response factor which is considered the variation of wind pressure, area correlation of wind pressure and dynamic effect induced by wind acting on structure. Cf is wind pressure coefficient depending on the roughness of structure surface.

Wind velocity pressure q(z) is calculated by the following formula (unit : kgf/m²)

$$q(z) = 0.0625 \cdot K(z) \cdot [I \cdot V_{10}(c)]^2 \qquad (6)$$

where

$$K(z) = \begin{cases} 2.774 (Z/Z_g)^{2\alpha} & Z > 5m \\ 2.774 (5/Z_g)^{2\alpha} & Z \leq 5m \end{cases}$$

V10(c) = basic design wind speed of 50 years return period calculated by statistic method

I = importance factor which multiplied by V10(c) may get basic design wind speed of 25 years or 100 years return period, see Table 2. Generally, the life time of aerial cable system is about 20 years, so we use 25 years return period as standard, that is, I=0.91.

Type of exposure: based on the characteristics of ground exposure, exposure conditions are typically divided into four types, see Table 3.

z_g, α : depending on type of type of exposure, see Table 4.

Gust reponse factor G(z) is calculated by the following formula

$$G(z) = 0.80 + 5T(z) \qquad (7)$$

where

$T(z) = 2.25 C_d^{0.5} / (Z/10)^{\alpha}$

C_d: surface drag coefficient, depends on the type of exposure, see Table 4.

C_f: Wind force coefficient, depends on the roughness of structure surface, see Table 5.

4. Design example

Basing on the above theory, three examples are given in the following.

(1) Constructing local aerial cable system in HSINCHU area, where basic design wind speed of 50 years return period V10(c)=35.81m/sec and the type of exposure in using is type B. Cable suspended is CCP-LAP-0.5-100P self-supporting cable, whose supporting line is 22 m/m galvanized steel wire strand. Suspension height is 5.1 meters. Working temperature is 5 ℃ , 20 ℃ , and 35 ℃ respectively. Span is from 20 to 50 meters. And no other suspension line is suspended. The relation between span and sag at working condition is shown in Fig. 2. The relation between span and tensile force at working condition is shown in Fig. 3.

(2) Constructing local aerial cable system in CHIAYI area, where basic design wind speed of 50 years return period V10(c)=31.58m/sec and the type of exposure in using is type C. Cable suspended is CCP-LAP-0.5-50P round-cable. Suspension height is 5.1 meters. Working temperature is 5 ℃ , 20 ℃ , and 35 ℃ respectively. Span is from 50 to 100 meters. Suspension line is 35 m/m galvanized steel wire strand. The relation between span and sag at working condition is shown in Fig. 4. The relation between span and tensile force at working condition is shown in Fig. 5.

(3) Constructing flying cable system in ALI mountain area, where the basic design wind speed of 50 years return period V10(c)=22.97m/sec and the type of exposure in using is type C. Cable suspended is CCP-LAP-0.5-100P self-supporting cable, whose supporting line is 22 m/m galvanized steel wire strand. Suspension height is 5.1 meters. Working temperature

is 5 ℃ , 20 ℃ , and 35 ℃ respectively. Span is from 100 to 300 meters. And suspension line is 55 ㎟ galvanized steel wire strand. The relation between span and sag at working condition is shown in Fig. 6. The relation between span and tensile force at working condition is shown in Fig. 7.

5. Measuring instrument for construction ---cable vibration counter

If the suspension line is too loose , the sag will be too large and the cable will severely swing in the wind. It is very dangerous. If the suspension line is too tight, the tensile force of the suspension line will exceed its tensile strength. It will break when typhoon is attacking. Therefore, the tensile force of the suspension line at working condition must be calculated basing on Eq.(1) and measured with tension meter during construction. But, it is not convenient to use tension meter in situ, so we developed a photo-sensing cable vibration counter, according to the theory of cable vibration, to measure the tensile force of the suspension line.

According to the theory of cable vibration, the frequency f of each vibration mode is

$$\frac{1}{\lambda^2}\cdot\bar{T}^2=2\cdot\left(\frac{\bar{T}}{2}-\tan\frac{\bar{T}}{2}\right) \qquad (8)$$

where

$\bar{T}=2\cdot\pi\cdot f\cdot l/\sqrt{H/m}$

l = horizontal span of two ends of suspension line

m = mass per unit length of cable and suspension line (Kg/m)

H = tensile force of suspension line

$\lambda^2=(m\cdot g\cdot l/H)^2\cdot l/(H\cdot Le/E\cdot A)$

$Le=l\cdot[1+(m\cdot g\cdot l/H)^2/8]$

When we exert a transverse man-made force on suspension line to make it vibrate, the frequency of first vibration mode is the lowest and easier to be excited, and the magnitude is maximum at the middle of the line. Therefore, when the vibration of the suspension line is stable, the first vibration mode of the suspension line can be obtained. At this moment, we use the cable vibration counter to measure the vibration number per unit time (generally 15 seconds) at the middle of the span, and the tensile force is solved by using Eq.(8).

According to this principle, we designed and manufactured a cable vibration counter which is composed of timer, counter, 12V DC-battery, photo sensor, optical fiber and supporting frame. The prototype of the device is shown in Fig. 8.

We made a series tests in the following two conditions in our civil engineering laboratary to check this instrument. The device for exerting tensile force is a 10-ton tension machine shown in Fig. 9. The operation of tensile force control is shown in Fig. 10. The tensile force exerted on suspension line is 500kg, 600kg, ..., 1200kg respectively, and we made ten tests for each condition. The operation of vibration frequency measurement is shown in Fig. 11.

(1) A 45㎟ galvanized steel wire strand having a mass per unit length of 0.366kg/m is suspended with span of 21.6m. The cross section area of steel wire is 46.24㎟ . The Young's modulus is 17,500 kgf/㎟ . The test results are shown in Table 6.

(2) A 45㎟ galvanized steel wire strand having a mass per unit length of 0.366kg/m and a CCP-JF-LAP-SZ round-cable having a mass per unit length of 0.366kg/m are binded together by lashing wire is suspended with span of 21.6m. The test results are shown in Table 7.

From the above results, it is evident that the vibration number per 15 seconds measured by our instrument are very much coincided with the theoretical value of Eq.(8), and they are very stable. When measuring the tensile force with this instrument, the aerial cable system will not be damaged. It is an nondestrutive test. Since this instrument is light, portable and not expensive, it is worthy to be widely used in situ.

6. Acknowledgement

The authors would like to thank Mr. J. H. Lin, the manager of the Outside Plant Department of Telecommunication Laboratories, and Dr. J. P. Tang, the consultant of Telecommunication Laboratories for their many valuable suggestions and encouragement. We are also grateful to Miss Y. Y. Chen for her great help on electric circuit design and installation of the cable vibration counter.

References

1. American National Standards Institute, " American National Standard Minimum Design Loads for Buildings and Other Structures ", ANSI, A 58.1-1982, Mar., 1982.

2. Irvine, H. M., and Caughey, T. K., " The Linear Theory of Free Vibrations of a Suspended Cable, " Proceedings of the Royal Society, London, England, Series A, Vol. 341, 1974, PP. 299-315.

3. Irvine, H. M., and Griffin, J. H., " On the Dynamic Response of a Suspended Cable, "International Journal of Earthquake Engineering and Structural Dynamics, Mar., 1976.

4. Irvine, H. M., " Free Vibrations of Inclined Cables, " Journal of the Structural Division, ASCE, Vol. 104, No. ST2, Feb., 1978.

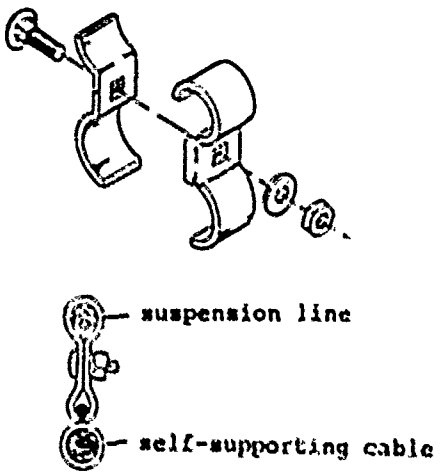

Fig. 1 Figue-8 shaped clamp

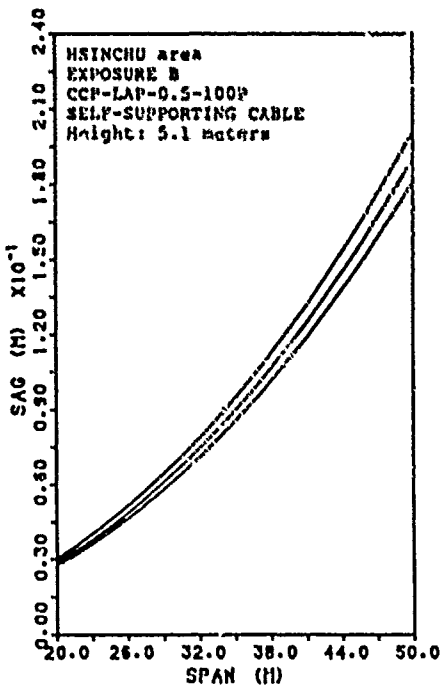

Fig. 2 Constructing sag of 22 mm² steel wire strand

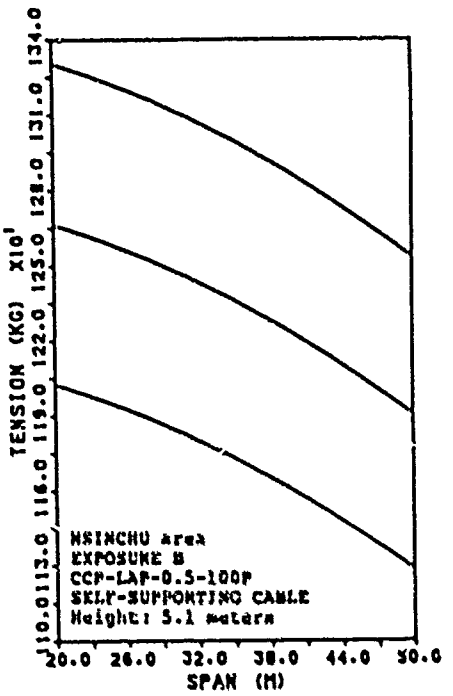

Fig. 3 Constructing tensile force of 22 mm² steel wire strand

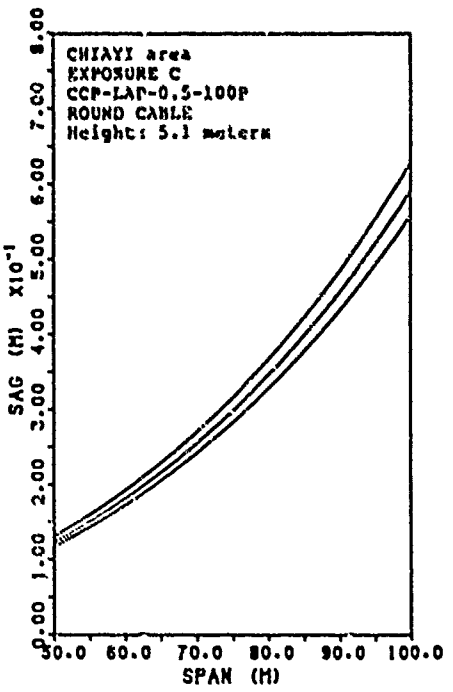

Fig. 4 Constructing sag of 35 mm² steel wire strand

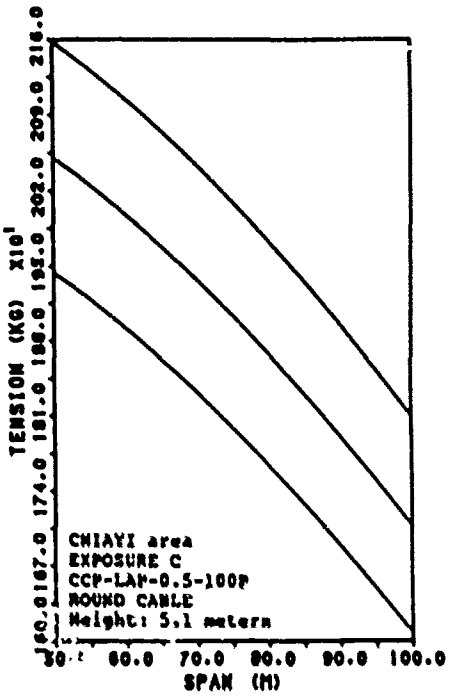

Fig. 5 Constructing tensile force of 35 ㎟ steel wire strand

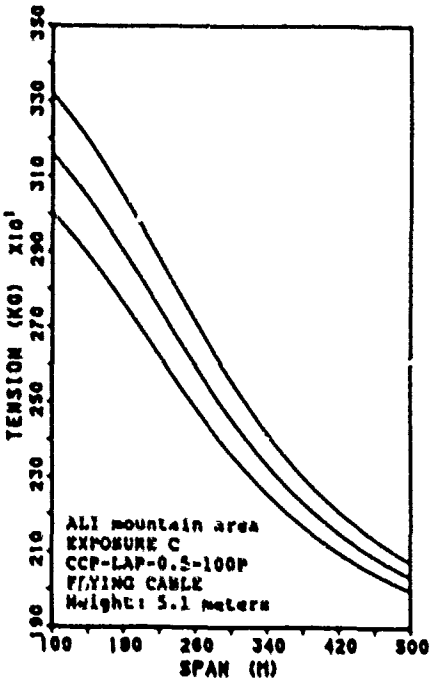

Fig. 7 Constructing tensile force of 55 ㎟ steel wire strand

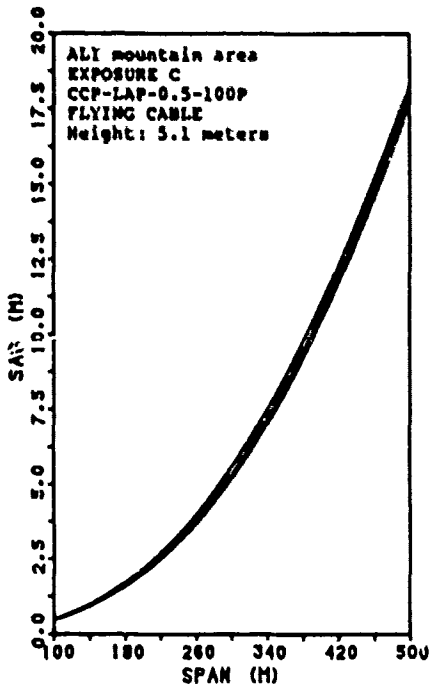

Fig. 6 Constructing sag of 55 ㎟ steel wire strand

Fig. 9 10-ton tension machine

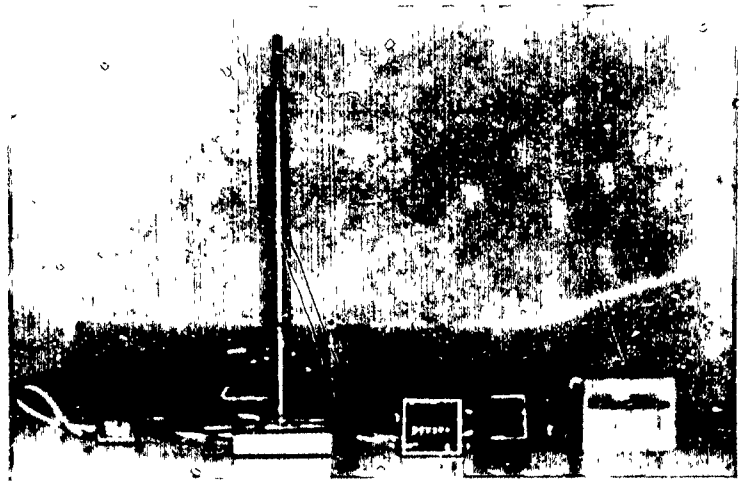

Fig. 8 Prototype of cable vibration counter

Fig. 11 Operation of cable vibration frequency measurement

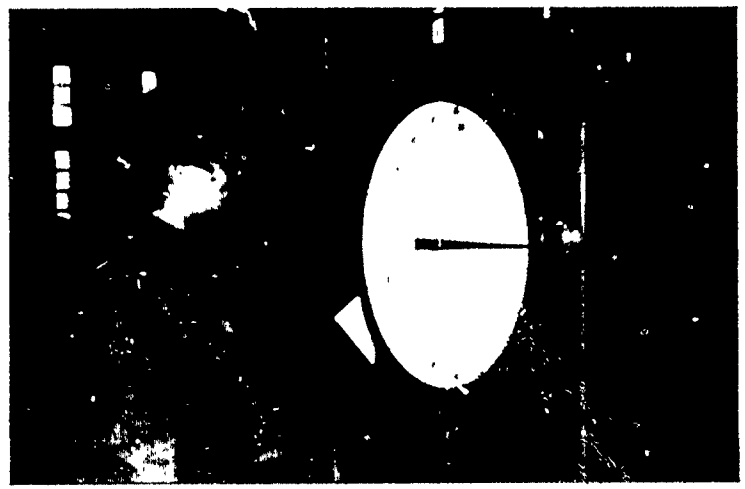

Fig. 10 Operation of tensile force control

TYPHOON / AREA	WAYNE (1986,8)		ABBY (1986,9)		GERALD (1987,9)		LYNN (1987,10)	
	OVERTURNED	BROKEN	OVERTURNED	BROKEN	OVERTURNED	BROKEN	OVERTURNED	BROKEN
NORTH TAIWAN	36	18	375	57	46	34	176	61
MIDDLE TAIWAN	11010	8925	6762	2072	165	43	15	3
SOUTH TAIWAN	5940	1504	6415	1451	9385	1479	39	0
SUM	16991	10447	13552	3580	9596	1556	230	64

Table 1 Data of damaged poles

RETURN PERIOD (years)	IMPORTANCE FACTOR I
25	0.91
50	1.00
1	1.10

Table . Importance Factor, I

EXPOSURE	CHARACTERISTICS OF GROUND SURFACE
A	Large city centers with at least 50% of the buildings having a height in excess of 20 meters.
B	Urban and suburban areas, woods area, or other terrain with numerous closely spaced obstructic having the size of single family dwellings or larger.
C	Open terrain with scattered obstructions having heights generally less than 10 meters.
D	Flat, unobstructed coastal areas directly exposed to wind flowing over large bodies of water.

Table 3 Type of Exposure

EXPOSURE	α	Zg(m)	Do
A	0.36	500	0.025
B	0.25	400	0.010
C	0.15	300	0.005
D	0.11	233	0.003

Table 4 α , Zg, and Do in different exposure type

Roughness of surface	Cf		NOTE
	D[illegible] ≤1.5	D[illegible] >1.5	
smooth rope, pole and pipe	1.2	0.5	D: DIAMETER (m) q(z): VELOCITY PRESSURE (kgf/m²)
moderately smooth rope, pole and pipe	1.2	0.7	
thin cable and wire	1.2	0.9	
thick cable and wire	1.3	1.1	

Table 5 Wind force coefficient, Cf

TENSILE FORCE (kgf)	THEORETICAL DATA (times)	TEST DATA (times)
500	40.86	40.5
600	44.45	44.5
700	47.85	47.5
800	51.05	51.0
900	54.08	53.5
1000	56.96	56.5
1100	59.71	59.5
1200	62.35	62.0

Table 6 Comparison of vibration number per 15 seconds of test data and theoretical data of steel wire strand

TENSILE FORCE (kgf)	THEORETICAL DATA (times)	TEST DATA (times)
500	28.96	30.0
600	31.72	32.5
700	34.27	34.5
800	36.63	37.0
900	38.85	39.0
1000	40.95	41.0
1100	42.95	42.5
1200	44.86	44.5

Table 7 Comparison of vibration number per 15 seconds of test data and theoretical data of steel wire strand bound with round cable

Tian-Sheng Lai

Telecommunication
Laboratories
P.O.BOX 71,
CHUNG-LI, TAIWAN,
R.O.C.

Tian-Sheng Lai was born in 1957 and received the M.S. and Ph.D. degrees from National Taiwan University in 1981 and 1988, respectively. He joined the Telecommunication Laboratories in 1988, and has been engaged in Outside Plant technology.

Gwo-Tay Tzeng

Telecommunication
Laboratories
P.O.BOX 71,
CHUNG-LI, TAIWAN,
R.O.C.

Gwo-Tay Tzeng was born in 1958 and received the M.S. degree from National Taiwan College of Marine and Oceanic technology. He joined the Telecommunication Laboratories in 1985, and has been engaged in Outside Plant technology.

Hai-Kuen Peng

Telecommunication
Laboratories
P.O.BOX 71,
CHUNG-LI, TAIWAN,
R.O.C.

Hai-Kuen Peng was born in 1959 and received the M.S. degree from National Taiwan University in 1985. He joined the Telecommunication Laboratories in 1985, and has been engaged in Outside Plant technology.

Cherng-Tzong Chang

Telecommunication
Laboratories
P.O.BOX 71,
CHUNG-LI, TAIWAN,
R.O.C.

Cherng-Tzong Chang was born in 1957 and received the M.S. degree from National Cherng-Kung University in 1985. He joined the Telecommunication Laboratories in 1985, and has been engaged in Outside Plant technology.

Yuan-Jenn Huang

Telecommunication
Laboratories
P.O.BOX 71,
CHUNG-LI, TAIWAN,
R.O.C.

Yuan-Jenn Huang was born in 1939, and graduated from National Taiwan Academy of Arts. He joined the Directorate General of Telecommunications in 1959 and joined the Telecommunication Laboratories in 1987, and has been engaged in Outside Plant technology. Now, He is a project leader in department of telecommunication Civil Engineering.

FIBER STRAIN DURING CABLE PULLING: AN IMPORTANT FACTOR IN CABLE DESIGN

W. Wenski, B. Menze, J. Schulte

Kabelmetal Electro GmbH, P.O. Box 260
3000 Hannover, Fed. Rep. of Germany

Summary.

The monitoring of attenuatic changes during cable pull tests is generally considered to be sufficient for the evaluation of the tensile strength of fiber optic cables. However, this measurement provides only indirect insight into the fiber strain conditions while the cable is subjected to tensile stress. The dependence of the fiber elongation on the cable design and the relation between the attenuation and the fiber elongation is investigated experimentally. It is shown that the measurement of fiber strain must be included in a cable pull test so as to ensure adequate fiber lifetime.

Introduction.

The design of fiber optic cables must be selected so as to meet the required pulling load. The expected lifetime of the optical fiber must not be reduced by the forces applied to the cable during installation and operation. The fiber strain resulting from cable bending and pulling should be limited to a certain fraction of the mechanical fiber proof test level. However, optical cable qualification testing generally does not include the direct measurement of fiber strain. Instead, according to IEC 794-1-E1, the change of fiber attenuation is measured and limited to a certain permitted value. This increase in attenuation is caused by macro- and microbending of the fiber and it is, at best, an indirect indicator of fiber strain. This paper suggests that the fiber elongation measurement be included in the fiber optic cable pulling test. Different fiber optic cable constructions have been evaluated, using a combination of attenuation and elongation measurements.

Fiber lifetime.

The long-term mechanical reliability of optical fibers is generally assured by means of a proof test. The prediction of the probable lifetime of a length of fiber after proof testing is the subject of various publications, e.g. Ref. [1] and [2]. The probable lifetime depends on the environmental conditions of the fiber and on the applied stress. Using assumptions which are applicable to telecommunications fibers, the failure probability of a 1,000 km length of fiber in 25 years is less than 10^{-2}, provided that the ratio between long-term residual stress and the proof test stress is about equal to or less than 0.3 to 0.4. By the same reasoning, for an 8-hour period (during installation) this ratio can be about equal to or less than 0.5 to 0.6 [1]. These considerations apply for uniaxial tension on the fiber. The lifetime of a fiber in bending is longer than that predicted from its strength in uniaxial tension[2]. The latter therefore results in a conservative value. For example, after a proof test using 5 N, which corresponds to an elongation of 0.57%, the maximum allowed residual stress is 1.5 N. This corresponds to an elongation of 0.17% or to a bending with a radius of 36 mm over the whole length of a 125 µm diameter quartz glass fiber. The cable design must ensure that these values will not be exceeded during installation or service.

Fiber excess length.

Sufficient excess length of fiber in the cable must be provided so that during cable elongation caused by forces on the cable or during temperature changes the fibers will not be strained. The cable pull test must prove that the required fiber excess length is available in the manufactured cable. The resulting fiber excess length depends on the cable design and fabrication tolerances. Three main designs have been tested: stranded[3,4] (loose tube, Fig.1, slotted-core, Fig. 2), central buffer (Fig. 3) and stacked fiber ribbons in a central tube (Fig. 4).

Assuming that the fibers in an unstressed cable are in the axes of the tubes, the approximate fiber excess length can be calculated by Eq.(1)[5]:

$$\varepsilon = \left[1+\left(\frac{2\pi R}{s}\right)^2 \cdot \left[\frac{2\delta R}{R} - \left(\frac{\delta R}{R}\right)^2\right]\right]^{1/2} - 1 \quad (1)$$

wherein $\delta R = R_i - R_f$,

R = the stranding radius

R_i = the tube inner radius

R_f = the radius of the coated fiber

s = the pitch

If more than one fiber is placed into a loose tube or slot, R_f becomes the radius of a virtual circle around the fibers.

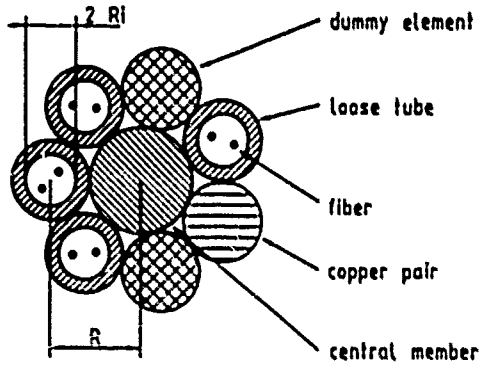

Fig. 1. Stranded loose tube cable core.

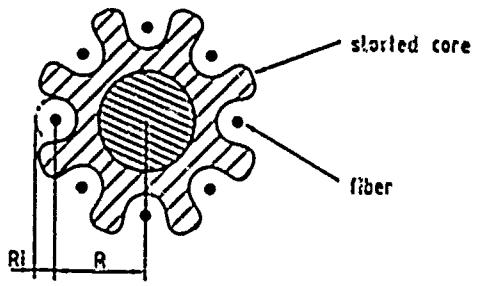

Fig. 2. Core of slotted-core cable.

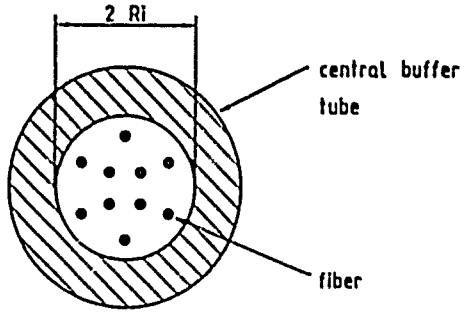

Fig. 3. Central buffer tube cable core.

In central buffer tubes the maximum tensile window is limited by the minimum allowed fiber bending radius r_{min} because of lifetime and bending loss considerations[6] :

$$\varepsilon_{max} = \left(\frac{r_{min}}{r_{min} - \delta R}\right)^{1/2} - 1 \quad (2)$$

This range of excess length is attributable to two situations: the excess length due to cable expansion under tension and temperature increase and the excess length resulting from cable shrinkage as a result of temperature decrease.

In a ribbon cable with a square (a = b) ribbon stack that follows a helical path in the core tube, as shown in Fig. 4, the stack excess length is given by:

$$\varepsilon_s = \left[2\,(r_s/s)^2 + 1\right]^{1/2} - 1 \quad (3)$$

wherein r_s = the helical path radius of the stack center

s = the pitch of the stack

The pitch must be chosen long enough to keep the bending radii of the outer fibers of the stack sufficiently large. The maximum achievable stack excess length corresponds to the situation where the stack comes into contact with the inner wall of the core tube. In this case the following approximate relationship can be used:

$$r_{smax} = \left(R_i^2 - s^2/4\right)^{1/2} - s/2 \quad (4)$$

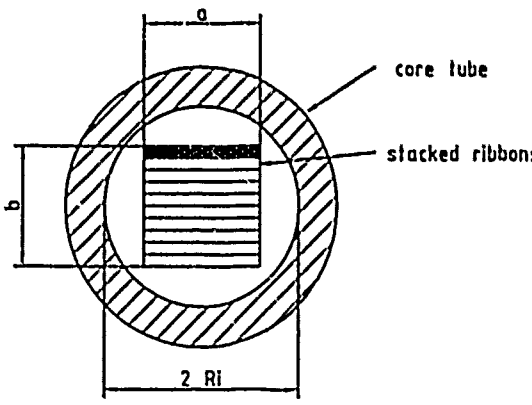

Fig. 4. Ribbon cable core.

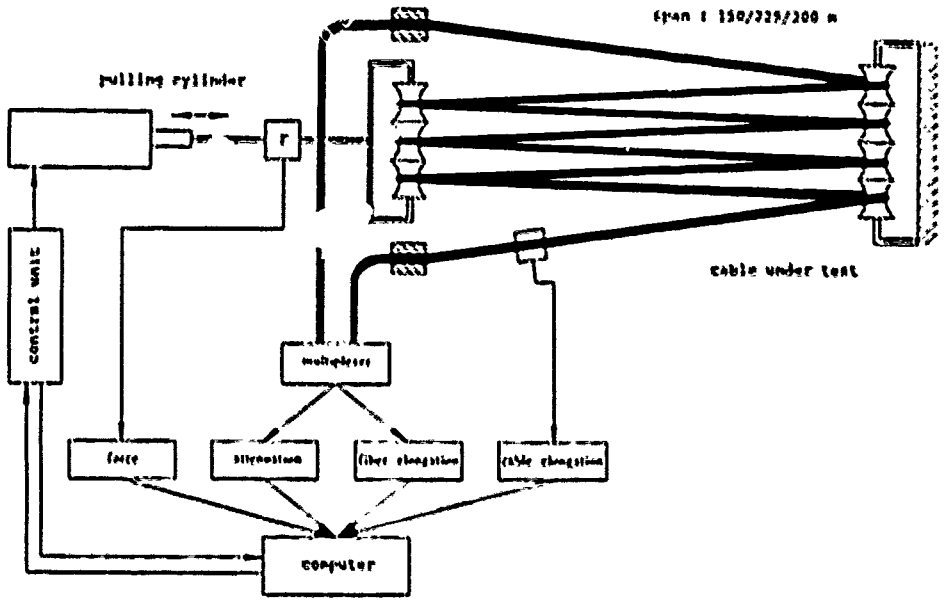

Fig. 5. Experimental set-up (computer-controlled pulling bench)

Experimental procedure.

The experiments were carried out on a computer-controlled pulling bench capable of holding a 300 m length of cable with a pulling force up to 15,000 N. The test equipment used allows measurement of the fiber elongation and change of fiber attenuation (Fig.5). The measurements were carried out on up to 16 fibers at a time, using two 1-to-16 fiber switches as multiplexers. In addition, cable elongation and pulling force were monitored. All measured values were stored and compared afterwards.

The change of fiber attenuation $A\alpha$ and fiber elongation were measured using an optical fiber strain measurement system, capable of measuring the phase shift of sinusoidally-modulated light. The phase shift $A\phi$ caused by fiber elongation is given by:

$$A\phi = \frac{2\pi \cdot f}{c} (n\Delta L + \Delta n L) \qquad (5)$$

wherein:

f = modulation frequency
c = velocity of light
n = fiber refractive index
L = length of fiber
ΔL = fiber elongation
Δn = change of refractive index due to fiber elongation

The first term results from changes in the physical length of the fiber. The second is due to changes in the refractive index caused by the tensile stress. The second term has a negative sign and can be written approximately as 0.2 times the first term[7]. We can therefore write:

$$A\phi = \frac{2\pi \cdot f}{c} \cdot n \cdot \Delta L \cdot \Lambda \qquad (6)$$

$\Lambda = 0.8$

In order to determine the precise value of Λ (which corrects for strain-induced changes of the refractive index), we stretched the fibers in a mechanical set-up to mechanically-defined elongation values. The elongation measured by means of the phase shift technique is depicted in Fig. 6 against the mechanically-defined true elongation. Both are in perfect agreement for $\Lambda = 0.806$, which holds for the fiber types under investigation.

The refractive index is also influenced by fiber bending. However, bending-induced changes of the group index are very small and can be neglected when compared to those induced by elongation[7]. The temperature was constant during the measurements and it can be shown that pressure-induced phase shifts can be neglected[8].

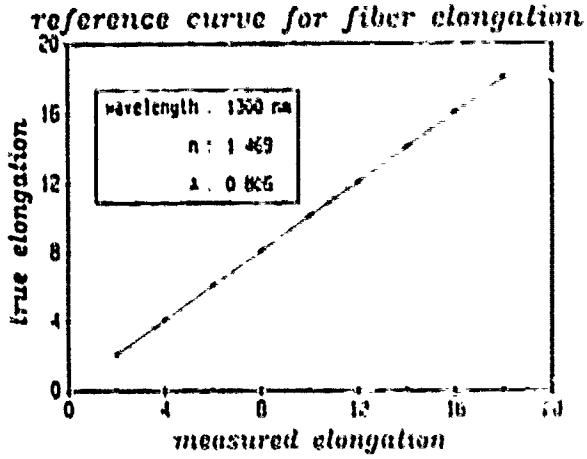

Fig. 6. Measured elongation vs. true elongation (phase shift technique).

Experimental results.

For the purpose of our measurements we used specially-designed cables with low fiber excess length in order to generate an early onset of fiber elongation at moderate pulling forces and cable elongation. The measurement results of attenuation change (normalized to 150 m of fiber) and fiber elongation as a function of cable elongation for the cable constructions taken into consideration are presented and compared hereafter. Figs. 7, 8, 9 and 10 are representative curves of the multiple fiber measurements.

Fig. 7 shows the traces for a stranded loose tube cable designed to have an excess length of 0.37%. The fiber elongation is accompanied by an increase in attenuation due to the fibers touching the tube walls which generates micro-bending loss. The results of a slotted-core cable with a designed excess length of 0.32% exhibits a similar increase in attenuation and fiber elongation (Fig. 8).

Fig. 9 depicts the results for the central buffer tube cable designed for 0.2% excess length. No attenuation change was observed throughout this test. The same was found to be true for the ribbon cable (Fig. 10) where the attenuation does not change, even under considerable fiber tension. The deviation of expected (dotted line) and measured (solid line) traces for the ribbon cable is due to slippage of the ribbon stack in the cable clamps of the pulling bench at elevated forces. This slippage occurs because of low friction between the square ribbon stack and the core tube of the 100 optical fibers in the stack in conjunction with high applied force. For the purpose of this paper no further attempt was made to overcome this experimental problem.

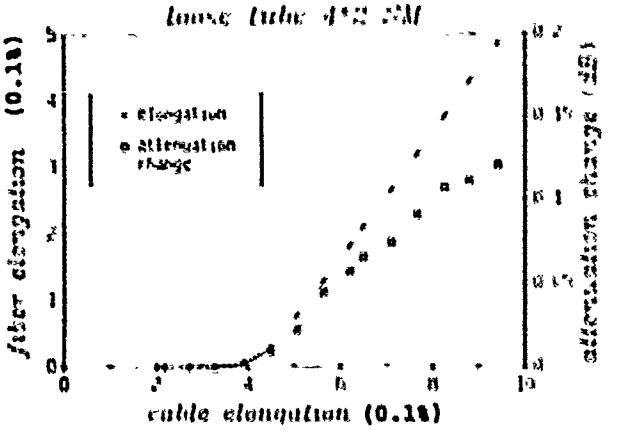

Fig. 7. Attenuation/elongation measurements (stranded loose tube cable).

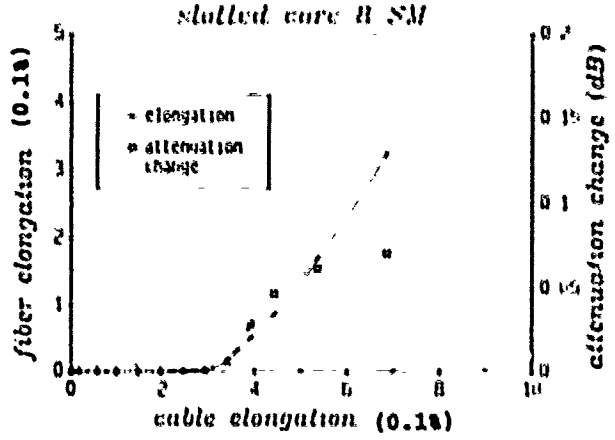

Fig. 8. Attenuation elongation measurements (slotted- core cable).

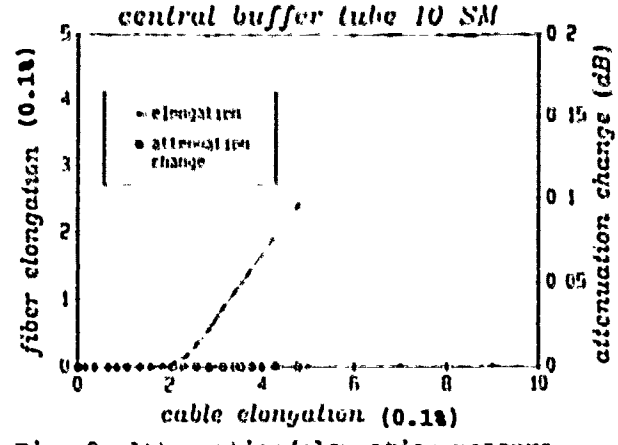

Fig. 9. Attenuation/elongation measurements (buffer tube cable).

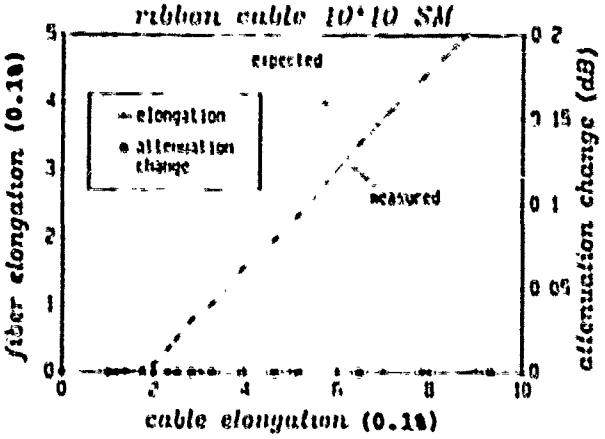

Fig. 10. Attenuation/elongation measurements (ribbon cable).

The measurements show that for the stranded loose tube and slotted-core designs the fiber elongation is accompanied by an increase in attenuation. On the other hand, for designs with a central tube (with fiber bundles or ribbons) the fiber elongation can have considerably high values without any change in fiber attenuation. The onset of fiber elongation during cable pulling can be calculated for a given cable design.

These values agree with the results of our measurements. It appears that direct fiber elongation measurement during the cable pull test is necessary, especially for unstranded cable designs.

Conclusion.

By measuring both the fiber elongation and attenuation the tensile behavior of the cable with regard to fiber strain can be more thoroughly understood. With this knowledge the appropriate cable and jacket design as well as the required fiber proof test level can be selected for a given application. The measurement of only the attenuation does, in several cases, not even give an indication of considerable fiber tension which can reduce the lifetime of the cable. Only the direct fiber elongation measurement, as shown in this paper, allows for a comparison of different cable designs with regard to fiber strain and lifetime.

Acknowledgments.

The authors wish to thank Mr. H. Hofheimer of Cable Consultants Corp., Larchmont NY for his valuable assistance in preparing this paper.

References.

1. Y. Mitsunaga, Y. Katsuyama, Y. Ishida, "Reliability Assurance for Long-Length Optical Fibre Based on Proof Testing", Electronics Letters, 1981, 17, p. 567
2. M.J. Mathewson, C.R. Kurkjian, S.T. Gulati, "Strength Measurements of Optical Fibers by Bending", J. Am. Ceramic Soc., 1986, 69, p. 815
3. P.R. Bark, U. Oestreich, G.H. Zeidler, "Fiber Optic Cable Design, Testing and Installation Experiences", Proc. 27th IWCS, 1978, pp. 379-384
4. U. Oestreich, G.H. Zeidler, P.R. Bark, H.M. Liertz, "High Fiber Count Cables of the Mini-Bundle Design", Proc. 30th IWCS, 1981, pp. 255-258
5. G. Mahlke, "Lichtwellenleiterkabel", Berlin, 1988, p.119
6. M.C. Light, J.A. Moses, M.A. Sigmon, C.A. Story, "Design and Performance of Telecommunication Cables Optimized for Low Fiber Counts", Proc. 37th IWCS, 1988, pp. 63-71
7. A. Bertholds, R. Dändliker, "Determination of the Individual Strain-Optic Coefficients in Single-Mode Optical Fibers", J. Lightwave Technology, 6, 1988, p.17
8. S. Tanaka, Y. Kameo, O. Ichikawa, M. Hoshikawa, N. Kurauchi, Y. Katsuyama, Y. Mitsunaga, "Lifetime Design of Optical Fiber Cable for Long Term Use", Sumitomo Electric Technical Review, 21, 1982, p.47

Wolfgang Wenski
Kabelmetal Electro GmbH
P.O. Box 260
3000 Hannover 1
Fed. Rep. of Germany

Wolfgang Wenski received his electrical engineering degree from the University of Braunschweig in 1984. After developing electronic circuits for laser and LED modules he joined Kabelmetal Electro GmbH in 1986 as a development engineer in the field of telecommunication cables. As a group leader he is responsible for development of telecommunication cables and, especially, for fiber optic cables.

Bernd Menze
Kabelmetal Electro
GmbH
P.O. Box 260
3000 Hannover 1
Fed. Rep. of Germany

Bernd Menze studied at the Fachhochschule in Lübeck, with the main focus on optical telecommunications. He joined Kabelmetal Electro GmbH in 1986. As a development engineer he is active in the field of cable design and measurement techniques for fiber optic cables.

Johann Schulte
Kabelmetal Electro
GmbH
P.O. Box 260
3000 Hannover 1
Fed. Rep. of Germany

Johann Schulte received his physics degree in quantum optics in 1981 and his Ph.D. in engineering in 1986 from the Technical University Hannover. After a research fellowship at IBM, Yorktown Heights NY, he joined Kabelmetal Electro in 1987, where he is presently engaged in the development of components for optical communications.

Automated Test System for Optical Fiber Cable Plants

Siegfried Heckmann, Volker Hecht

Philips Kommunikations Industrie AG
Nachrichtenkabel und -anlagen
Schanzenstraße 30, D-5000 Köln 80, West Germany

Abstract

Economical optical fiber cable production has become necessary in order to meet the increasing demand of optical fiber networks. One pre-condition for reducing cable costs is an optimized handling of quality assurance tests in optical fiber cable plants. As optical fiber cable testing has been more time-consuming than copper cable measuring procedures, reduction of test time is of vital interest. Accuracy and reliability of test results are important objectives as well.

Starting with measuring procedures which are commonly used today the requirements for automated optical fibre cable test systems are analysed. Configuration and operation of a computerized test system specially designed for quality assurance in cable plants are presented. Compared to manually operated test sets the automated system offers a number of specific advantages such as short testing times, multiple parallel fiber connection, automatic data evaluation and high accuracy irrespective of operator skill.

Introduction

During the last years the applications of optical fiber cables have shown an impressive rise. Precondition for a further increasement is a considerable reduction of cable costs, which in turn are essentially determined by the costs of a number of tests during production. Today most of these tests are carried out by measuring each fiber of a cable separately and manually. To decrease the testing time and the cable costs the fibers should be measured automatically and in parallel.

Additionally cable costs can be reduced by optimizing quality assurance during production. Due to this step the number of defective goods can be minimized.

Hence in the future manually operated equipment will have to be replaced by automatic measuring systems.

The requirements for such an automatic system will be discussed on the basis of the measuring methods currently used. Subsequently the structure and potential use of an automatic measuring system will be defined, particular attention being paid to the specific advantages.

Relevant test parameters in the cable factory

Quality assurance in a plant for optical fiber cables must be carried out in each step of the production process:

It starts with the checks on incoming goods, for example on the delivered fibers, accompanies the various manufacturing steps and ends in the acceptance tests on the produced cable. Because of the considerable testing times, especially in case of multifiber cables, economic considerations will require that quality assurance is restricted to the measurement of the relevant parameters.

These are the parameters which are influenced during the cabling process in contrast to those which are predetermined by the fibers and do not change during further processing. The latter group includes, for example, core and cladding diameter and refractive index profile. In single-mode fibers, the dispersion and, with certain restrictions, the cut-off wavelength are also independent of the cabling. These parameters are measured by the fiber manufacturer and their results are documented. During the check on incoming goods at the cable plant, the data are examined and are usually accepted as final data if they meet the specifications.

Thus, the most important parameters still to be measured are the loss and the local attenuation characteristics. On the one hand, they are important regarding the subsequent use of the cable in a transmission line. On the other hand, these parameters are influenced by the cabling process itself and can therefore be used for a direct monitoring of the manufacturing process. The attenuation parameters should be measured for all fibers during production, since only in this way crap can be minimized by early detection of defects. It can be assumed, that if attenuation values still coincide with the cable specifications and proper checks on incoming fibers were carried out, then all optical parameters will meet the requirements.

Current state of measuring technology

In the cable factory, the attenuation of fiber cables is advantageously measured by the backscattering method. This method enables not only the measuring of the desired attenuation coefficient, which, for example, is defined in all PTT-specifications. Also production-related anomalies in the cable like local attenuation peaks, irregularities and broken fibers, can be detected and localized.

The conventional measuring process is divided into the following parts:

- preparation of the cable
- preparation of the end face of each fiber to be measured
- coupling of each fiber to the measuring equipment
- measurement on the basis of manual instrument settings
- transfer of data to the relevant measurement record.

Consequently a characteristic feature of the current state of measuring technology is that each fiber is measured individually and manually. The accuracy of the measurements is determined by various factors:

After the preparation the fiber end face is assessed subjectively by the operator during the coupling process. Then depending on the coupling attenuation, the input amplification of the OTDR is modified to compensate the end face quality. Since this may result in the use of any dynamic range of the instrument, the linearity and accuracy of measurements are not guaranteed any longer, depending on the end face quality.

It is known that the accuracy is reduced at the beginning and the end of the backscatter curve, for example as a result of overloading the optical and electronic input stage of the instrument. During the manual instrument setting, the cursors are used to select the part of the curve, which is used for determining the attenuation. Considerable measuring errors can occur, depending on that choice.

Since the backscatter signals have very small amplitudes, the backscatter curve generally is superimposed by noise and has to be smoothed by averaging procedures. A suitable averaging time must be set manually and influences again the measurement accuracy.

Because of the twisting of the fibers in the cable, the fiber length is a few percent longer than the cable length. It is the attenuation per cable length which is specified and should be measured but in fact the attenuation per fiber length is measured. The operator usually takes this difference into account by a manual mis-setting. Since this mis-setting directly influences the measured attenuation or the location of a fault, this procedure is critical.

Possible incorrect settings and wrong data due to transfer errors give rise to many errors, i.e. the measurement accuracy depends on a decisive extent on the operator and his experience.

Requirements for an automatic measuring system

To avoid the disadvantages discussed before, a new measuring system has to have two main features:

On the one hand, it should be possible for a number of fibers to be processed simultaneously, as has been the usual practice since many years in copper cable technology. On the other hand, operating errors, and hence measuring errors, must be substantially avoided, i.e. an automatic, closed measuring system conforming to ISO 9000 /1/ is indispensable.

Easy operation of the system is of great importance to enable reliable measurements independent of the level of training and experience of the test personnel. For example, it would be expedient if the measuring system automatically sets all required parameters when a coded cable specification is input. An automatic plausibility test should make the operator aware of obvious operating errors. Since it is planned to use the automatic measuring system in a cable factory, its environmental conditions must be considered.

Structure of the automatic measuring system

On the basis of these requirements, the presented measuring system was designed for up to 12 fibers to be connected simultaneously. The actual measuring system is shown schematically in figure 1. It consists of the following components:

- Optical connection frame
- Measuring unit (OTDR)
- Control- and evaluation unit (computer)
- Operating unit
- Output unit

Additional components necessary to prepare multiple fiber end faces in parallel and to create a planar structure of the fibers to be measured complete the system. In such a measuring system, the accuracy and the operating characteristics are essentially determined by the properties of the optical connection frame. The coupling unit must on the one hand permit a reproducible and reliable coupling of all fibers, and on the other hand be robust in case of improper handling.

These requirements are met if the coupling unit, the interface to the operator, is spatially separated from the sensitive switching unit, and the signals are transferred via

a fiber ribbon cable. If an end face of this internal ribbon cable is destroyed, for example by incorrect coupling of the fibers to be measured, it can be pulled slightly out of the ribbon stock cassette (figure 1) and after new preparation inserted into the coupling unit again. The switching unit is not affected by this procedure.

Operating and measuring procedure

Figure 2 shows the automatic measuring system in the environment of a cable factory. The first step to test a cable is to prepare it in the conventional manner, except that up to 12 fibers can now be processed simultaneously.

Subsequently the fibers to be measured are coupled to the internal ribbon cable using a flat silicon plate with V grooves (figure 3). To enable this coupling technique the fibers have to be arranged in a ribbon structure. This requirement is automatically met, if optical cables with fiber ribbons are to be measured. In the case of bundle cables, however, the individual fibers must first be converted into a planar structure, i.e. a ribbon structure, using a multifiber planar organizer (figure 4).

The actual measuring procedure is controlled by a computer and a user-guiding menu. The upper part of this menu contains all data required for a clear assignment and characterization of each cable in accordance with ISO 9000. In addition, the menu contains data which define the measuring procedure and the parameters to be measured, as well as information on data output.

When the measuring program is started, an automatic coupling test is carried out first to ensure that the coupling attenuation is smaller than a predetermined limiting value and the measuring unit is therefore still operated within the approved dynamic range.

In the automatic measuring procedure, the system first determines the optimal instrument settings according to criteria exactly defined before, and selects these optimal settings. With the aid of the computer-controlled switching unit, each of the fibers to be measured is then sequentially connected to the measuring unit and the parameters defined in the menu are measured.

Only in this way it is possible to ensure that the measuring system always operates under optimal conditions and that reproducible measurements with a guaranteed accuracy can be obtained.

The data transferred from the measuring unit to the computer are evaluated there following the menu specifications. Among other parameters, attenuation, attenuation coefficient and length can be determined and compared with the specified values. In addition the backscatter curves are investigated automatically with respect to nonlinearity and inhomogenities.

The specification data, system parameters and results are recorded in a suitable form and can be stored for later statistical evaluations. Figure 5 shows a part of such a record, the list of measurement results.

Test results

As discussed before the presented automatic measuring system has two main features:

On the one hand, it enables the operator to process a number of fibers simultaneously with each measurement. For example, to check ten fibers of a cable at one wavelength will take about five minutes:

Four minutes are required to remove the coating, for the planar organizing, the preparation of the ten end faces and for the coupling of the fibers to the connection frame. Within the next five minutes the automatic coupling check is carried out by the system and the parameters are measured as specified in the menu. During this system operation time the operator is able to prepare the next fibers to be measured. Consequently up to 1,000 fibers per day can be checked with the presented measuring system and one operator.

The second feature is the improved reliability and accuracy. To demonstrate this a single-mode fiber ribbon cable of 2 km length was coupled 20 times to the connection frame. With each coupling the end faces were replaced. The maximum deviation of the measured attenuation coefficient for the individual fiber was 0.007 dB/km, the corresponding standard deviation 0.003 dB/km.

Summary and prospects

An automatic measuring system for optical fiber cables was developed to meet the requirements of a modern cable factory.

The presented system has substantial advantages in comparison to state-of-the-art measuring techniques:

- It represents a closed system within the meaning of ISO 9000. All adjustments of the equipment, each decision and the data transfer are carried out following clearly defined preconditions. Therefore all test results are independent of experience and qualification of the operator.
- The testing time for each cable will be substantial decreased with the presented system. This is mainly due to preparing and measuring a number of fibers instead of one in each measuring cycle. Due to the structure of ribbon cables, especially for this cable type a drastical decreasement in testing time was found.
- In the future the important requirement of a periodical test-system-recalibration will be induced by menu messages. During this recalibration the OTDR-wave length spectrum will be measured and its data are stored in the evaluation unit to correct the measuring results. Additionally a special recalibration fiber allows to check the OTDR-linearity. Deviations from ideal linearity will also be considered by the evaluation unit.
- For future applications it is of great importance that the test system itself is able to be controlled by a master computer. So it may become part of a quality assurance system with a hierarchical organization. For the different test systems in a plant individual specifications and measuring procedures can be determined by a central computer.

Thus, such automated testing is an essential contribution to improve efficiency and achieving the goal of economical production.

References

/1/ ISO 9000 "Quality management and quality assurance standards-Guidelines for selection and use"

Siegfried Heckmann studied at the University of Bochum and graduated in 1978 in electrical engineering. 1983 he obtained his doctorate at the University of Wuppertal. Since 1983 he has been active as group leader within Philips Kommunikations Industrie AG, where he is responsible for the development of optical measuring equipment.

Volker Riech studied at the Technical University of Aachen and received the doctor's degree in 1976. He joined Philips Kommunikations Industrie AG in 1980 as a group leader for computerized measuring systems for copper cables. Today he is the head of R&D for optical and copper cable measuring equipment within PKI.

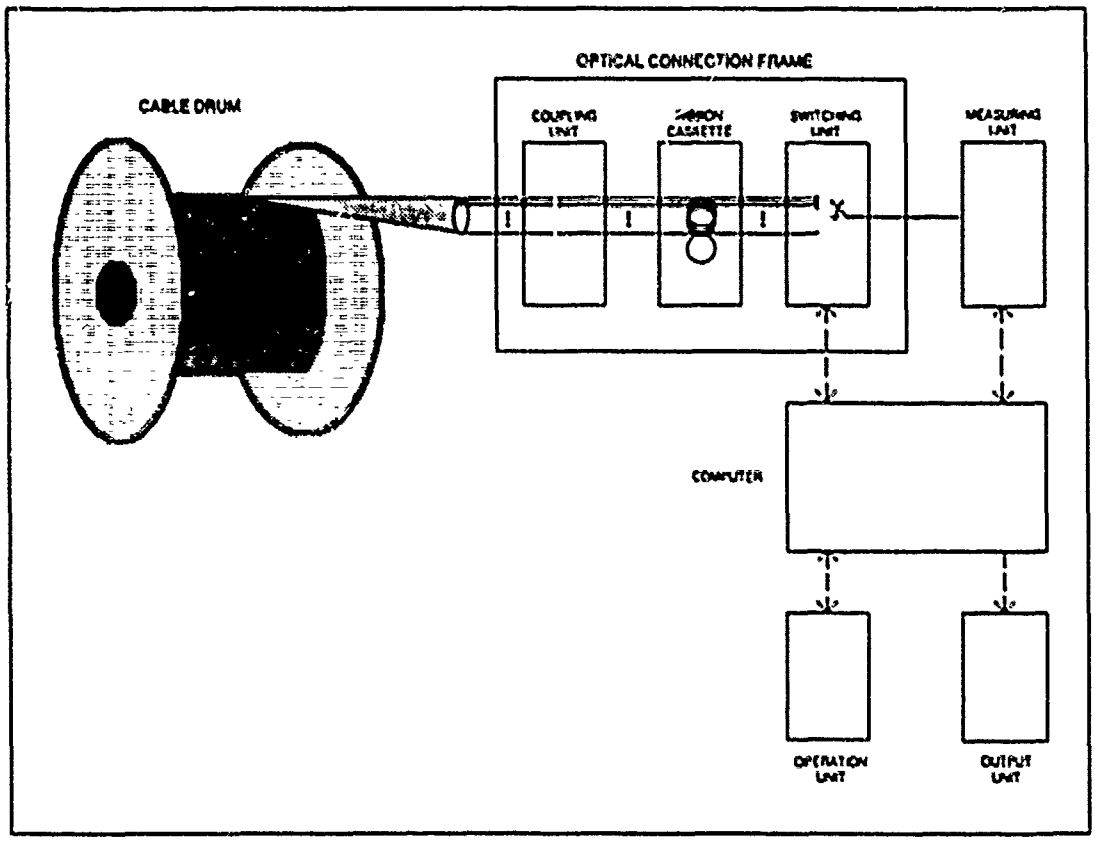

Figure 1: Schematic Structure of Automatic Measuring System

Figure 2: Computerized Optical Fiber Measuring System

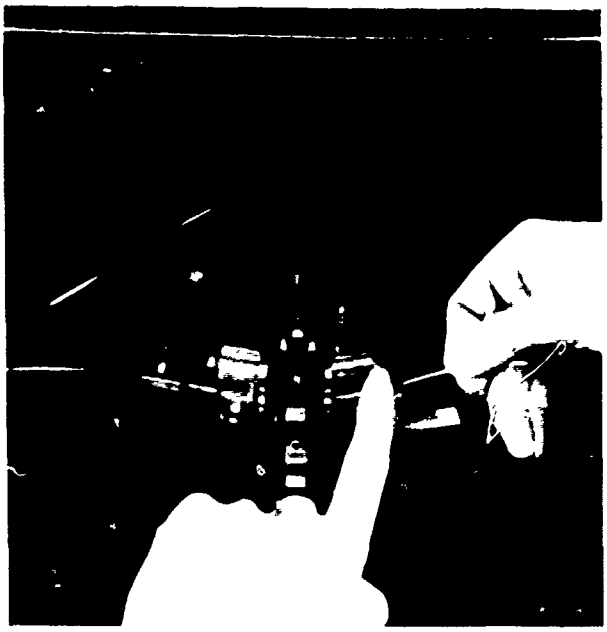

Figure 3: Optical Coupling Unit, Handling of Fibers

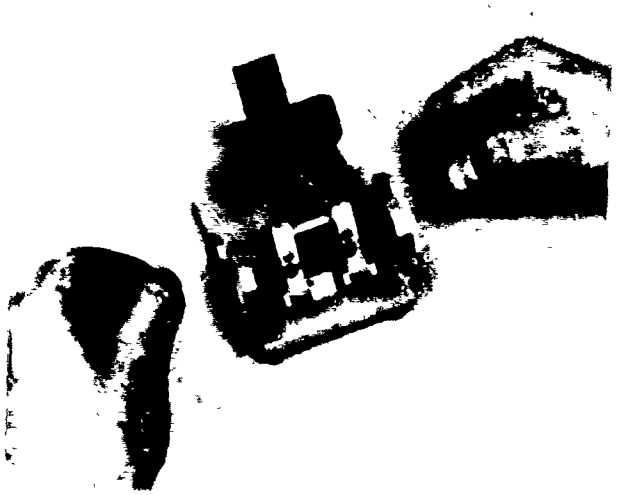

Figure 4: Planar Organizing of Optical Fibers

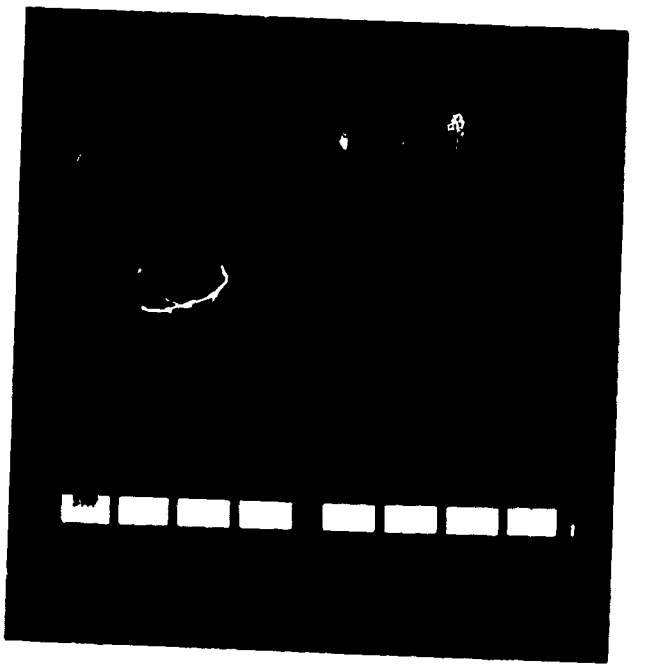

Figure 5: List of Measurement Results

Reliability and Environmental Performance of Cabled Single-Mode Optical Fibers

J. Kurki, L. Stormbom, L. Oksanen, T. Räsänen and E. Leino

Nokia Telecommunication Cables
P.O.Box 77, 01511 Vantaa, Finland

Abstract

The effect of the dual acrylate coating on the performance of single-mode optical fibers has been studied. Good optical and environmental performance was achieved with fibers coated with tandem and double coating process using optimized material combination having good adhesion to glass. FTIR technique is presented as a fast and accurate method for determining the degree of cure of the acrylate. The stripping force of the coating is shown to correlate well with the degree of cure. High stress screen testing technique at levels up to 4 GPa is used for rapid determination of the strength parameters of the fiber. Lifetime estimates made by this novel approach agree with the earlier estimates. The cabled fibers showed good performance in northern environment.

Introduction

Single-mode optical fiber has become a standard in optical communications. Most of the fiber delivered today has a 250 μm dual layer acrylate coating composed of an inner soft layer protecting the fiber from attenuation increase induced by temperature change or microbending, and an outer harder layer for protection and easy handling.

The structure, materials, and manufacturing process have been seen to be important to achieve a coating that will give the fiber good optical characteristics (attenuation, microbending behavior and temperature performance); and good reliability (strength, minimal aging effect in various environments) [1,2]. Initially we tested coating combinations having low adhesion to glass and good adhesion to glass for temperature behavior and strength. The results indicated that coatings with low adhesion to glass had good temperature characteristics but lowered strength whereas coatings with good adhesion to glass had good strength but it was more difficult to achieve good temperature characteristics. After this it was decided that various coating combinations should be tried to find a system that would give good reliability and at the same time good optical characteristics and good temperature behavior. This paper deals with the effect of acrylate coating on the performance of the fiber. The coating processes and results for various acrylate coating combinations are presented. Reliability and environmental characteristics are presented for the optimized coating combination.

Coating process and characterization

Coating application.

The application of the two layer primary coating can be made in two ways, either by the Tandem Coating process, where the primary coating is cured before the secondary is applied, or by the Double Coating process, where the two layers are applied wet on wet and cured simultaneously.

In the Tandem Coating process the diameter and concentricity of both layers can be recorded. In the Double Coating process the primary coating can't easily be monitored, but is well controlled by using optimum die shapes and pressures. The advantages of the Double Coating process are higher drawing speeds, because of more cooling space in the drawing tower, and easy operation. To obtain good attenuation behavior also the curing process for the coating material in question must be well understood, since the uncured layer is thicker in the Double Coating process and the curing degree showed to affect the adhesion.

The theory of the one-layer application is described in several references e.g. [3,4]. The method to obtain a smooth and well controlled coating is to keep the shear rate of the coating material flow equal to zero at the fiber surface during the process by a proper pressure. The resulting equation for the dependence between coating thickness and required die diameter can be used for the primary coating both in the Tandem and Double Coating process and with some substitutions for the secondary coating in Tandem Coating process. By using the optimum pressure, the desired die diameter is independent of viscosity and drawing speed V. The secondary coating in the Double Coating process can be determined using the same algorithm as before, now for two flows v_1 (inner wet layer with viscosity μ_1) and v_2 (second layer with viscosity μ_2) and with following boundary conditions (see Fig. 1)

$v_1=V$ at $r=f$
$v_2=0$ at $r=R(z)$
$v_1=v_2$ at $r=r_1$
$dv_1/dr=dv_2/dr$ at $r=r_1$

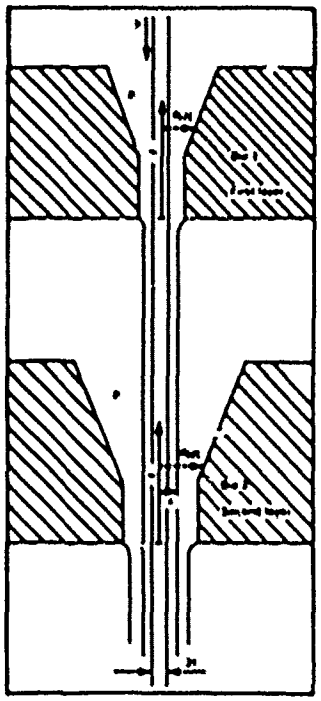

Fig. 1. Double Pressure Coater.

The dependence of the die versus coating diameter under the optimum pressure

$$\frac{dP}{dx} = 4V(2f^2(\ln(r_1/f)/\mu_1 - \ln(r_1/R)/\mu_2) + 2\ln(r_1/R)(r_1^2-f^2)(1/\mu_1 - 1/\mu_2) - (\frac{r_1^2-f^2}{\mu_1} - \frac{r_1^2-R^2}{\mu_2}))^{-1}$$

cannot be solved analytically, but is independent of the drawing speed and a function of the viscosity ratio μ_1/μ_2. In Fig. 2 the die diameter as a function of the viscosity ratio is shown for a 125 μm fiber with final coating diameters 205/250 μm.

The double coater used in our standard drawing process gives the predicted coating diameters in the first die. In the second die there is a difference of about 4% between the measured and theoretical diameter. Also the tandem coating process was examined giving diameters exactly according to the theory. When using the optimum pressures both processes were very stable and the coating diameter variations were less than +/- 1 μm.

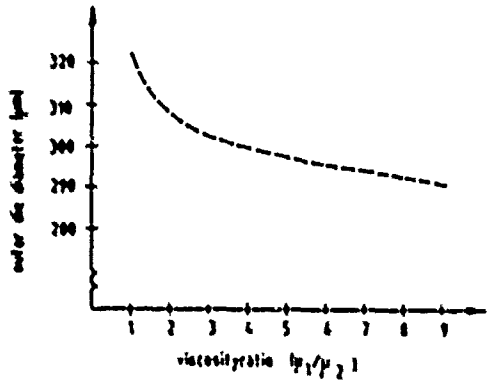

Fig. 2. The second die diameter for the double coater as a function of the materials viscosity ratio. The fiber diameter is 125 μm and the final inner/outer layers are 205/250 μm.

Curing of acrylates.

Acrylates as coating material for optical fiber: UV-acrylates have become standard for optical fiber coatings. They maintain the optical properties of fiber and offer good mechanical and chemical durability in many environments [5,6]. Acrylates are also easy to apply on the fiber in liquid form and they are rapidly cured by UV-light. Typical properties of primary and secondary coating materials for optical fibers are presented in Table 1. The viscosity of the resin is a strong function of temperature and therefore temperature control of the coating liquid can be exploited in the application process.

UV-curable acrylate resins contain three main components: photoinitiators, oligomers and monomers. Besides these additives are used to increase thermal stability, shelf time, and adhesion to glass. Photoinitiators are e.g. aromatic ketones. They affect physical properties of the polymer, such as hardness, elongation and tensile strength, although their concentration is only 2 - 4% of the resin [6].

Oligomers form the body of the actual polymer network [7]. The resin contains 50 - 70 wt% of oligomers.Oligomers are the reactive part of the polymer and they are multifunctional i.e. one molecule may contain 2 - 6 reactive acrylic functional groups -CH = CH2. When these acrylic groups react the polymer will get its 3-dimensional network. The length, nature and functionality of the oligomer molecules affects the mechanical, chemical and optical properties of the coating. The oligomers of the primary coating are urethane acrylates. They give the primary layer more soft and stiff properties than the additional epoxy acrylates used in the secondary layer. In the primary layer polymer chains are longer and cross-link density lower than in the harder jacket layer. This leads to lower glass transition temperature (T_g) and lower Young's modulus.

Table 1. Typical properties of UV-acrylates

Resin 25°C		Primary	Secondary
Viscosity	cps	7 000-10 000	7 000-9 000
Density	kg/dm³	1.00-1.11	1.11-1.16
Surface tension		41	25
Cured Polymer 25°C, 50% RH			
Hardness (Shore)		47-55 (A)	60-75 (D)
Refractive index		1.49-1.54	1.53-1.56
Tensile strength	MPa	1.6-4.1	19-38
Young's modulus (ε = 2,5%)	MPa	2.1-3.7	600-1128
Elongation	%	40-200	8-[illegible]
Tg	°C	-35 - +25	[illegible]
Water absorption (24 h)	%	1.4-3.6	
Temperature coefficient above Tg	cm/cm/°C	$30*10^{-5}$	
below Tg	cm/cm/°C	$5*10^{-5}$	
Shrinkage at cure	%	2.4-5.[illegible]	4.[illegible]
Hydrogen generation (80°C, 24 h)	µl/g	0.3	0.5

Rate of polymerization: The rate of polymerization of radiation curable resins depends on [7,8,9]: the capability of the photoinitiators to absorb radiation and produce active radicals, the reactivity of the initiator radicals and the polymer radicals to form double bonds, and functionality of monomers and oligomers [6].

Oxygen inhibits the curing of multifunctional acrylates. As a result, the surface of coating remains tacky and physical properties, such as impact strength and hardness, become lower. This is related to decrease of molar weight and decrease of crosslink density. For this reason the UV-lamps used to cure the acrylate are commonly purged by nitrogen.

Overcure was seen to decrease the Shore hardness and cause a yellowish color for acrylic films in our experiments in the case of primary coatings. In the case of secondary coating only the hardness decreased. We assume that this is related to the dissociation of the reacted photoinitiator.

Determination of the degree of cure: The degree of cure affects the physical properties and reliability parameters of the coating. We made experiments with coating having 80-85 % degree of cure. The adhesion to glass of these coatings was essentially more reduced after 24 h aging in 20°C water as compared with coatings having adequate cure of more than 95 %. Inadequate cure may also lead to reduction in strength of the fiber. If coating becomes loose e.g. due to chemical effects, the water diffused in the coating may form liquid water on the glass. This will enhance stress corrosion [10].

The degree of cure of the coating material can be measured by Soxhlet-extraction or FTIR spectroscopy. Soxhlet-extraction is an economical method to determine the average degree of cure of the whole acrylate layer. The method is based on the assumption that the uncured polymer can be dissolved e.g. by methyl-ethyl-ketone (MEK). The quantity that is actually measured is gel fraction (GF), given as

$$GF\ (\%) = (A-C)\,/\,(B-C)*100$$

where

A = mass of the sample after extraction
B = mass of the sample before extraction
C = mass of glass in the sample

In our experimental procedure approximately 50 m fiber is cut into small pieces. The mass of fibers is measured. The fibers are then erted into an extraction flask and extracted 12 hours. After this they are first dried in [illegible]r and then in vacuum for 12 hours and the weight is measured. The mass of glass was determined by peeling a fiber with same length and measuring the mass. The inaccuracy of weighing is +/- 0.005 g, which gives the error margin of +/- 2 %. Further uncertainty for determining the degree of cure is caused because there is not a certainty that MEK would not dissolve something else than uncured polymer from the material.

The FTIR-method is based on the visibility of acrylic double bonds in the infrared spectra. During polymerization the amount of acrylic groups decreases as they react to form the polymer network. Double bonds can be seen at wave numbers 810 1/cm (CH_2=CH twist) and 1408 1/cm (=CH_2 deformation). We determined the degree of cure from relative intensities of 1408 1/cm peaks. The peak indicating the carbonyl group =C=O at a wave number 1724 1/cm is used as reference.

Preparation of the sample begins with cleaning the fibers with propanol, in order to remove any contaminations caused by handling. After cleaning fibers were handled with gloves. After drawing the sample fibers were kept in black plastic bags before testing to avoid additional cure. The sample is prepared by cutting the fibers into about 50 mm pieces and fastening tightly with tape on both sides of the crystal of the FTIR spectrometer (Fig. 3). FTIR-spectra was taken with attenuated total reflectance (ATR) -method. The equipment used for the tests was Perkin Elmer FTIR model 1760. The tests were made with KRS5-crystal (thallium-bromide-iodide; refractive index 2.37), but germanium- and ZnSe-crystals were also tested. The beam is introduced to the crystal in such an angle, that it is reflected from the sample. The penetration depth, where the reflection occurs depends on the wavelength and refractive indexes according to

$$d_p = \frac{\lambda\ /\ n_{cr}}{2*\sqrt{\sin^2\theta - (n_s\ /n_{cr})^2}}$$

d_p = penetration depth
n_{cr} = refractive index of the crystal
n_s = refractive index of the sample
θ = angle of the incoming beam
λ = wavelength

Typical penetration depth is only a few um and therefore FTIR is only applicable to test the degree of cure at the surface of the material.

A measured spectrum for a partly cured polymer combination E is shown in Fig. 4. showing the peak at 1408 1/cm which indicates that the material is not fully crosslinked. The heights of the absorption peaks at 1408 and 1724 1/cm are measured and ratio between the heights of 1408 1/cm peak and 1724 1/cm peak is calculated.

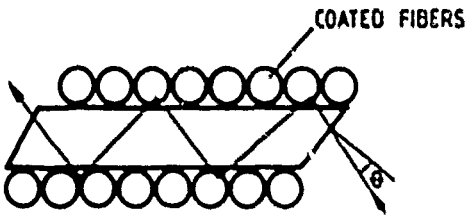

Fig. 3. Fibers fixed on both sides of the crystal of the FTIR-machine.

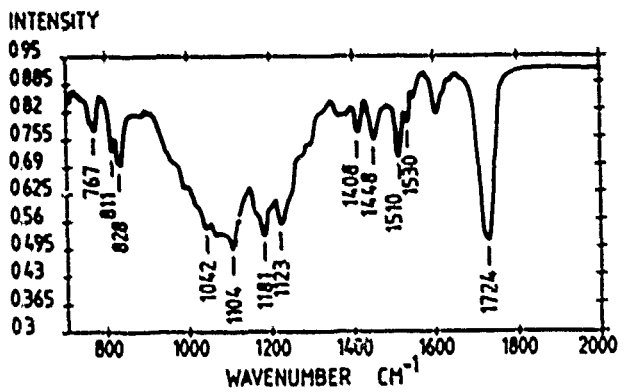

Fig. 4. FTIR-spectrum of a partly cured acrylate. The peak used to determine the degree of cure is at 1408 1/cm. The carbonyl peak at 1724 1/cm is used as reference.

The calibration is done in the following way. From a figure where 1408/1724 1/cm peak ratio is presented as a function of fiber drawing speed the peak ratio for totally cured material is achieved by extrapolating the curve to drawing speed = 0 m/s. This point represents 100 % degree of cure. This can be done because with very low drawing speeds (0.15 m/s) the coating is in practice fully cured. The peak ratio of uncured coating represents the degree of cure = 0 %. In our experiments the spectrum for the uncured material was taken as a transmission spectrum by inserting a drop of uncured material between two NaCl-tablets. The degree of cure for different UV-irradiation times (different drawing speeds) could the be calculated.

FTIR is a faster and more accurate method than Soxhlet-extraction when determining the degree of cure from the surface of the fiber. We found it difficult to achieve adequate repeatability with Soxhlet extraction. On the other hand gel fraction gives the average degree of cure over the cross section of the coating and would thus be a more interesting parameter since from the reliability point of view the degree of cure at the glass coating interface is most important. However, the curing is a fast process and it may be anticipated that the degree of cure beneath the surface is close to the degree of cure at the surface. Further on it is possible to make sure of adequate degree of cure at the glass - coating interface by measuring the stripping force of the coating.

The speed of the curing process was examined with an acrylate testing unit, where a film of acrylate is cured on a conveyor belt passing slowly over a UV-lamp. To up to 96-97% degree of cure the polymerization proceeds very quickly. After that curing speed becomes lower because the viscosity of the system increases. The reactive acrylic groups cannot polymerize with each other when they are blocked into the polymer network.

A series of tests were made to calibrate the fiber drawing tower for the degree of cure. The preforms that were used to draw fibers were MCVD depressed cladding preforms resulting in 9 µm mode field diameter in the fiber. The drawing tower was equipped with standard Fusion System lamps. The first lamp had a D-bulb and the latter a H-type bulb which is characterized by shorter wavelength radiation. This results in better cure at the surface since the penetration depth for shorter wavelengths is smaller. In tandem process there was one lamp after each coater (D + H bulb). The drawing speeds were varied between 10 and 200 m/min in the experiments. The results can be linearly scaled for higher drawing speeds for production equipment having more lamps.

By applying and curing one layer of coating it was noted that the primary coating material cures at least two times faster than the secondary coating material. This is expected because the crosslinking density in the soft primary layer is much smaller than in the hard secondary layer. Also one of the reactive groups in the primary layer is generally a monofunctional acrylate that lowers the viscosity of the material thus allowing for easier movement of the molecules. It could then be estimated that in tandem process the number of lamps for the secondary layer should be twice the number of lamps for the primary layer. In double coating process also a desired degree of cure can be achieved for the primary layer with a reasonable number of lamps although it is cured through the secondary layer.

Adhesion test: A series of fibers were drawn with varying speed between 10 and 200 m/min to test the effect of uncured coating on adhesion to glass.

The adhesion to glass was tested by measuring the stripping force of the coating. The tests were carried out with tensile testing machine equipped with the Miller fiber stripper. Tension was measured with a tensiometer having a 600 cN sensing head. Each fiber was tested 15 times to achieve an adequate statistical accuracy. The stripping length was 4 +/- 0.5 mm, and the speed was 70 mm/min. The curve received from the recorder has two peaks. The first one comes when the coating ruptures and the stripping begins. The other one is caused by coating lump under the stripping tool. Following results are obtained by examining the first peak.

The stripping force of the coating proved to be proportional to UV-irradiation time in the region where the coating is not fully cured (see Fig. 5). The stripping force is presented as a function of the degree of cure as measured by the FTIR technique in Fig. 6. Stripping force as a function of degree has a linear relationship. This indicates that with precaution the stripping force can be used to determine the degree of cure at least of coatings having similar structure, materials, and dimensions (both primary and secondary layers).

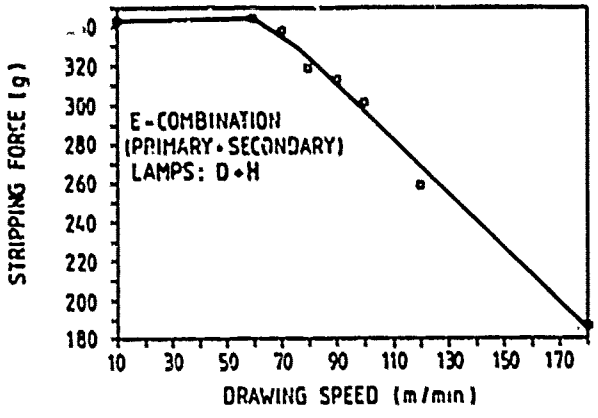

Fig. 5. Stripping force of the coating as a function of the drawing speed. First lamp had D-bulb and second a H-bulb. (Double coater)

Comparison of low and high adhesion coating combinations

A common requirement in the cable field work is easy (mechanical) strippability of the primary coating. Strippability depends on coating adhesion which affects both temperature behavior and reliability of the fiber. To find a coating with good overall characteristics several tests have been made for three different coating combinations.

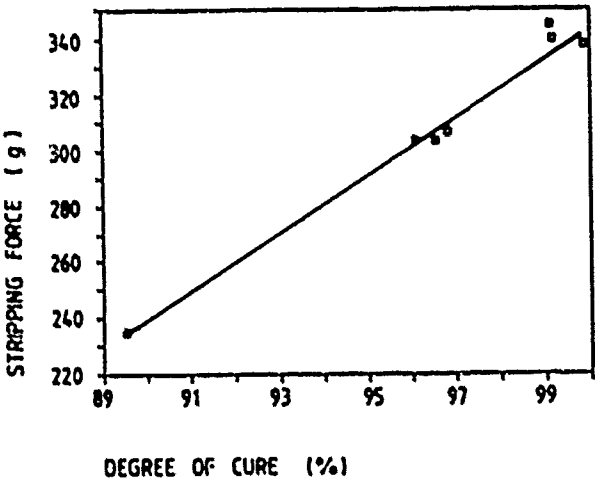

Fig. 6. Stripping force of the coating as a function of the degree of cure.

The adhesion was measured in normal room conditions (15%RH, 23°C) for coating combinations A, E, and D by stripping 4 mm of coating with a Miller-tool using 70 mm/min speed. 15 measurements of each combination were plotted on a Weibull scale and the 50% probability was taken as the result. The test was then repeated after treatment in 85°C water for 24 h. The measurement was done within 15 min after removing the samples from the treatment conditions. The results are shown in Fig. 7 for coating combination E and the rest in Table 2.

The dynamic strength was also measured for the same coating combinations in room conditions. The sample length was 45 cm and 25 measurements were made. The breaking strength was plotted on a Weibull scale. The 50%-probability results are shown in Table 2. More over, to get a picture of the long length strength of the fiber, a 3 GPa "proof test" of 1 s duration was performed for all three combinations and as results the mean survival lengths are given in Table 2. For comparison, mean survival lengths of three different commercial available fibers were measured giving values of 250-500 m.

Table 2. Strength and adhesion results for different coating combinations

COATING COMB.	STRIPPING FORCE 15%RH 25°C	STRIPPING FORCE 85°C water 24 h	DYNAMIC STRENGTH 50%PROB 22°C 25%RH	3 GPa MEAN SURVIVAL LENGTH
	g	g	GPa	m
A	725	19	5.62	1300
E	430	222	5.32	400
D	22	25	2.75	<10

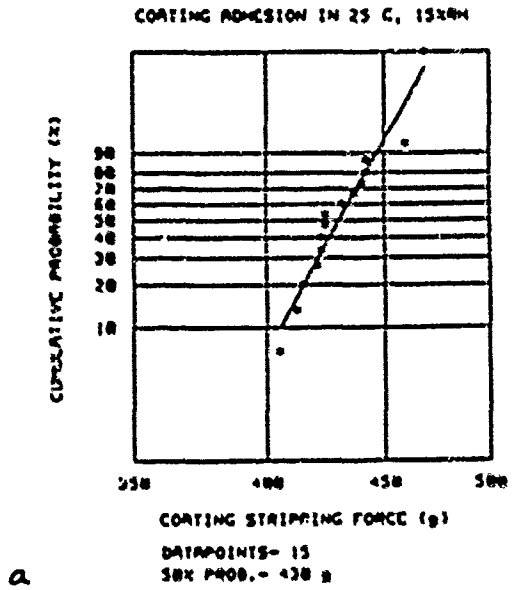

a

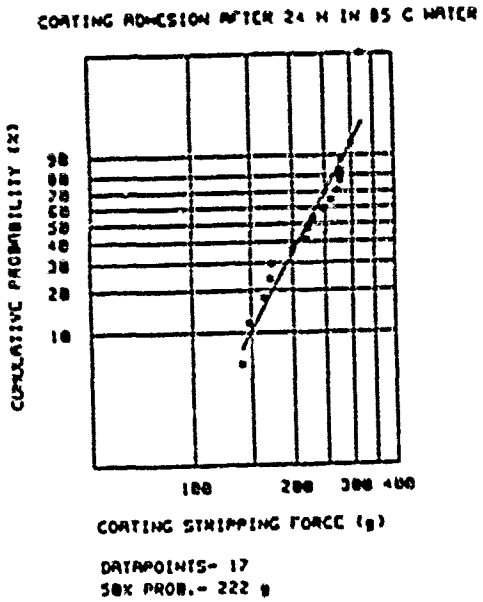

b

Fig. 7a. Coating stripping force at 15%RH and 25°C in a Weibull plot. b. The stripping force of the coating after treatment in 85°C water for 24 hours.

The most important external fiber loss mechanisms affected by the coating are temperature and microbend effects. Microbend loss susceptibility was evaluated for the different coating types with the sandpaper method. A 150 grit sandpaper was placed on top of 1 m of fiber and the loss increase was measured for various loads up to 5 kg. After every test series the fiber was measured under zero load to ensure that no fiber breakage had occurred. The results reported in Fig. 8 for a 5 kg load are calculated from several repeated measurements.

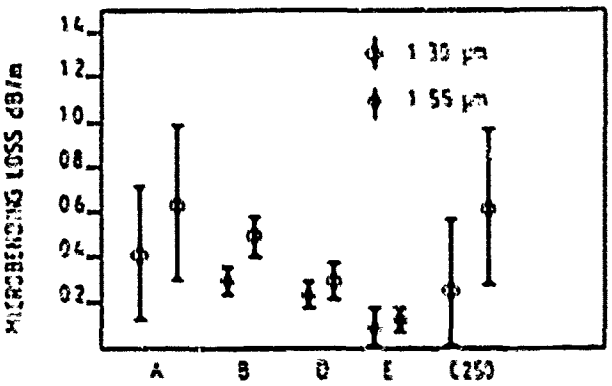

Fig. 8. Measured microbending loss of DC fibers with various coating combinations (A,B,D,E) and a MC fiber (C250) from another supplier. Load on sandpaper 5 kg.

C250 is a commercially available 250 µm coating, matched clad fiber used as a reference. It should be noted that it has a higher MFD (10 µm versus 9 µm) than the other fibers so it can be expected to have higher microbending loss. Coating type E shows the best microbending performance with the lowest average loss and low scatter of measured loss values.

Fibers with the same coating combinations were also subjected to temperature cycling in a temperature range of -60..+85°C. Coating combination D behaved best with excess attenuation below 0.03 dB/km at both 1.3 µm and 1.55 µm wavelengths. Combination A exhibited an increased attenuation up to 0.06 dB/km at 1.3 µm and 0.11 dB/km at 1.55 µm. E-combination (Fig. 9) fibers had maximum excess attenuation below 0.05 dB/km at both wavelengths.

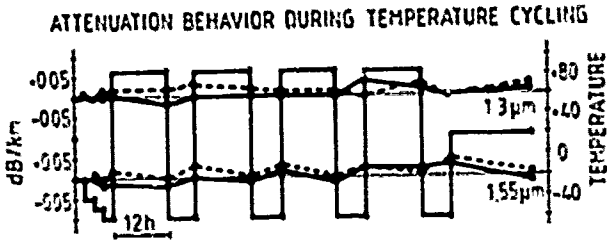

Fig. 9. Temperature cycling results for two fibers with coating E.

The strength results are consistent with reported behavior [9] and show that as the adhesion decreases the strength also decreases. Therefore combinations as D or A have poorer reliability characteristics because the adhesion is too low or can decrease enough to cause failure. The temperature behavior on the other hand would require low adhesion and therefore coating combination E was chosen as a good compromise, fulfilling both optical and reliability requirements. The E-coating combination can be stripped mechanically with proper tools or chemically with MEK.

Reliability tests and results

Strength.

Reliable operation of optical fibers requires knowledge of the strength distribution since the failure occurs at the weakest point. Usually fatigue parameters are determined from breaking strength measurements for gauge lengths in the range of 0.5-20 m. However the probability to find low stress flaws is very low in modern fibers and the conventional method will become very laborious and time consuming and is mainly suitable for lengths of 100-1000 m. In addition, high proof-test stress testing of several kilometer long fiber lengths detects large flaws that can be distributed several hundred meters or even kilometers apart, and can thus give reliable lifetime prediction [11].

Using a commercially available proof test equipment, "screen tests" were performed at 1 GPa, 1.4 GPa, 2 GPa, 3 GPa and 4 GPa stress levels. The time duration of the stress was normalized to 1 sec (using n=23) because in practice the proof-test speed was reduced in order to minimize fibre portions breaking during the start-up acceleration period of the proof-tester. The fiber samples were drawn from preforms made by the MCVD process using commercially available silica tubes and coated with a UV curable acrylate. The fiber samples were tested only once excluding the routine proof test during the fibre manufacturing. Counting the number of breaks (min 10 or 20 km tested fiber) the failure probabilities per m were calculated at every stress level. The results are shown in the Weibull plot in Fig 10.

The screen test results were fitted to the following conventional equation

$$\ln(1-F_f)^{-1} = m \ln \sigma_s + \ln C$$

which implies that the corresponding inert strength have a similar distribution. The obtained m= 1.69 and C=0.000418. The Weibull parameters in the equation are related to the inert strength distribution through the static fatigue equation b.cause of the test method. The well known expression for lifetime prediction [12]

$$\frac{\sigma_a}{\sigma_p} = \left(\frac{t_p}{t_a} \left(\left(1 - \frac{\ln(1-F_f)}{N_p L} \right)^{\frac{n-2}{m_i - 1}} \right) \right)^{1/n}$$

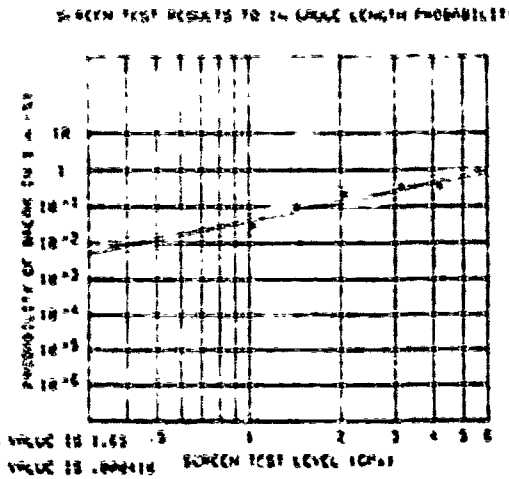

Fig. 10. The screen test result in a Weibull plot. The obtained m and C are used in the lifetime prediction.

can then with the next substitutions

$$m_i = \frac{n-2}{n} m$$

$$C_i = (B/t_p)^{m/n} C$$

$$N_p = \left(\frac{\sigma_p^n t_p}{B} \right)^{m_i/(n-2)} C_i$$

be written

$$\frac{\sigma_a}{\sigma_p} = \left(\frac{t_p}{t_a} \left(\left(1 - \frac{\ln(1-F_f)}{C_i (\sigma_p^n t_p)^{m/n}} \right)^{n/m} - 1 \right) \right)^{1/n}$$

In order to obtain the n value, two dynamic fatigue tests were performed and the results were n=25+/-1 in 35%RH and n=21+/-2 in 60%RH. Both tests were performed at 22°C. Assuming F_f=0.01, L=1000 and t_p=1 sec and using the obtained n, m and C values the lifetime estimate shown in Fig. 11 can be made. The results of this method are consistent with previous estimations [12].

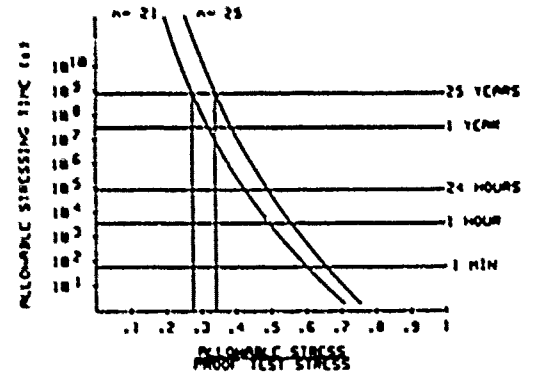

Fig. 11. Lifetime prediction based on the m and C values obtained from the screen test. The n=21 refers to 60%RH while the n=25 was measured in 35%RH in 22°C.

Chemical durability: Fibers coated with E-combination were studied for chemical durability for the compound used for cabling and also for some other chemicals. The testing was done by measuring the stripping force (4 mm stripping length) of the coating after ageing. Results are shown in Table 3 for E-coating prepared by tandem and double coating process.

Table 3. Adhesion after 24 h aging

Fiber	Original	60°C Jelly		100°C Water		Seawater 20°C	
	g	g	%	g	%	g	%
E-Tandem C.	412	406	98	252	61	318	77
E-Double C.	324	338	104	195	60	255	79
Com.Fiber I	228	191	84	123	54	124	54
Com.Fiber II	315	342	108	114	36	188	60

The jelly is of a type commonly used in loose tube buffering lines. The stripping force after ageing in various other types of jellies varied between 95 and 105 % of the original value. Aging results are the same for both coating methods within experimental accuracy. A noticeable feature of the E coating is good resistance to water: even after boiling in 100°C water for 24 hours the stripping force is still 60 % of the original value (see also Fig. 7a-b). Comparison was also made with two types of commercially available fibers - Fiber I having lower adhesion to glass and Fiber II having similar adhesion to glass as the E-coating. The lower adhesion fiber shows somewhat more reduction in stripping force in the tests as compared to the higher adhesion coatings.

Hydrogen can cause long term increase in attenuation. Therefore hydrogen generation of the coating and the cabling materials should be at the minimum.
The hydrogen generation of the coating was measured to be 0.5 µl/g (80°C, 24 hours). The fibers were also subjected to a hydrogen treatment (20°C, 14 days). The attenuation recovered fully after the treatment.
Shore-hardness was measured from 0.5 mm thick UV-acrylate films, cured by a conveyor belt radiator. Films were stacked and air bubbles were removed so the resulting sample was 6 mm thick. The measurement was done according to ASTM D2240. Primary coating was tested with A-type durometer giving the value 45-50 for the E-combination. Secondary coating was tested with D-type durometer giving the value 60-65.

Abrasion resistance was tested by pouring sand through a 1 m long 20 mm diameter tube onto the fiber under 0.4 GPa tension. After 20 kg of sand only the surface of the coating became dimmer, but no other effects were observed.

Fiber and cable results

With the E coating typical attenuation values for the manufactured fiber are below 0.38 and 0.35 dB/km at 1310 and 1550 nm respectively. The best achieved values are 0.34 and 0.18 dB/km for the respective wavelengths. This is very close to the theoretical limits of the fiber type so it is evident that the coating does not impair the attenuation performance of the fiber. The coating also acts as an efficient cladding mode stripper facilitating easy measurements, though on some rare occasions whispering gallery modes have been observed in cutoff wavelength measurements.

The E coated fibers have been used in the delivery of the figure-8 type of aerial cables (Fig. 12 a) and stranded loose tube buried cables to very severe conditions in the northernmost part of Finland (arctic latitude 68°C). The cables were installed and fusion spliced in sub zero temperature field conditions with no problems. An example of temperature cycling results for the aerial cable is shown in Fig. 13.

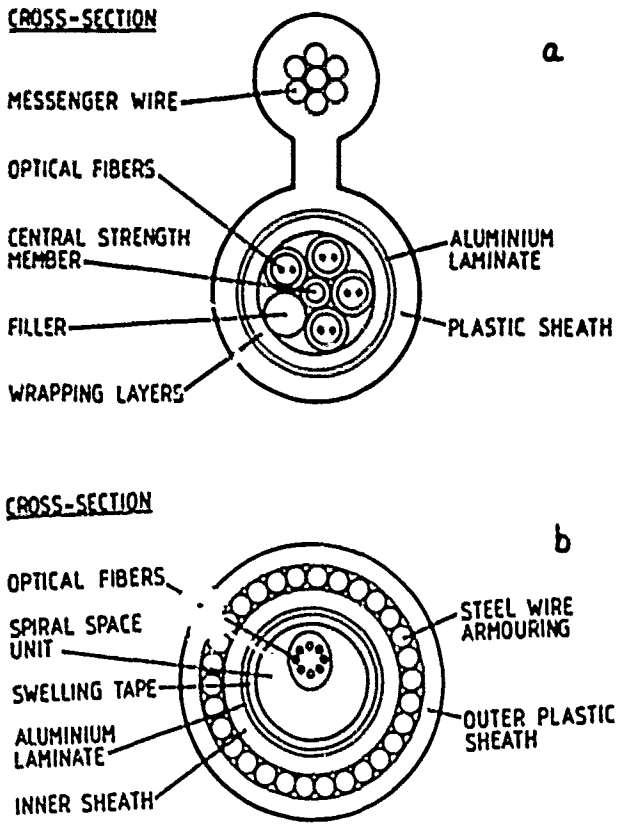

Fig. 12 a. Figure-8 type of aerial cable. b. Single loose tube cable design with spiralling channel for direct burial.

The E coated fibers have also been used in manufacturing the experimental single loose tube cable where fibers are arranged through a spiralling channel in the tube, see Fig. 12 b. In this new Spiral-Space™ design the cable core has largely the same strain and contraction margins as in stranded loose tube designs but typically smaller outer diameter. Temperature cycling results are comparable to the stranded loose tube aerial and buried cables but the crush strength is considerably improved, Fig. 14. Because of simple manufacturing this new design can offer a very attractive small size and potentially low cost alternative for direct burial by ploughing.

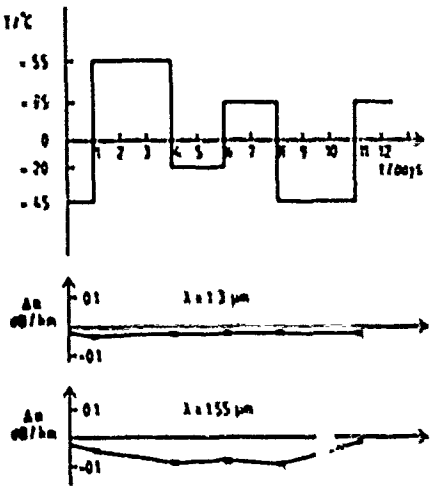

Fig. 13. Temperature cycling results of aerial cable.

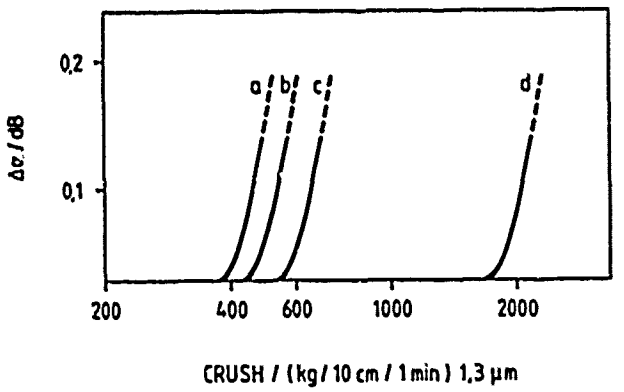

Fig. 14. Typical attenuation increase as function of crushing force for various cable designs. a) stranded tight, b) stranded loose tube, c) slotted core, d) single loose tube with spiralling channel. a, b, c with 1.4 mm diam. steel wire armoring, d with 0.8 mm wire armoring.

Summary

We have used both tandem and wet-on-wet double coating processes for application of the acrylate coating in production conditions. Double coating is a convenient method and provides faster drawing speed in short towers. A theoretical model developed for the coating application process agrees well with experimental results and can be used for optimizing coating dies and pressures. Performance of the fiber and the reliability parameters were equivalent with both methods.

The curing process has an important effect on the optical and environmental performance of the coated fiber. The FTIR-technique was used for investigation of the curing process and to make sure of an optimized degree of cure. The FTIR technique is a fast and accurate method for measurement of the degree of cure of the coating surface. In our process the degree of cure at the glass coating interface can be tested by measuring the stripping force. A linear relationship was found between the stripping force and the degree of cure as measured by the FTIR technique.

Lifetime estimates based on a novel high stress screen test technique agree well with results reported elsewhere.

Coatings with varying adhesion to glass were tested for optical and reliability performance. It was found that coatings with low adhesion to glass had lower strength, although the temperature and microbending properties were good. A coating combination (E) having good adhesion to glass in all conditions was chosen as the best one fulfilling both optical and reliability requirements. This combination has good temperature and microbending performance while attaining good predicted lifetime and reliability. The coated fiber has proven easy to handle in cabling and splicing.

Fibers coated with E-combination have been produced and used in buried and aerial fiber optic cables. These cables have shown good field performance in northern climatic conditions.

Acknowledgements

The authors wish to thank Dr. Koichi Abe for initiative for the strength test method and helpful discussions. The authors also wish to thank Mr. Mikko Tyni and his colleagues at the Finnish PTT for collaboration. The assistance of Ms Eva Kuula de Peréz in preparing the manuscript is gratefully acknowledgement.

References

1. S.K. Nagel: Reliability issues in Optical Fibers. SPIE Vol. 717, Reliability considerations in fiber optic applications, 1986, pp. 8 - 20
2. B.J. Skutnik, B.D. Munsey, C.T. Brucker: Coating adhesion effects on fiber strength and fatigue properties. Mat. Res. Soc. Symp. Proc., Vol. 88 (1987), pp. 27-34
3. S. Sakaguchi, T. Kimura: High-Speed Drawing of Optical Fibers with Pressurized Coating. J. Lightwave Techn. LT-3 (1985), No. 3, pp. 669-673
4. A. Panoliaskos, W.L.H. Hallett, I. Garis: Prediction of optical fiber coating thickness. Appl. Opt., Vol. 24 (1985), No. 15, pp. 2309-2312
5. G. Kar: Coatings for Optical fibers. SPIE Vol. 584 "Optical Fiber Characteristics and Standards" (1985), pp. 40-47
6. H.N. Vazurani, H. Schonhorn, T.T. Wang: U.V. Cured epoxy-acrylate Coatings on Optical Fibers I. Topical meeting on Optical Fiber Transmission II, Williamsburg, Virginia, 1977, paper TuB3
7. C. Decker, T. Bewndaikha: Photopolymerisation de macromers multifonctionels - 1. Eur. Polym. J., Vol. 20 (1984), No. 8, pp. 753 -758
8. V.D. McGinniss, D.M. Dusek: Comparative kinetics of ultraviolet curable coating systems. Vol. 46 (1974), No. 46, pp. 23-30
9. R. Phillips: The UV-curing of acrylate materials with high intensity flash. J. Oil Col. Chem. Assoc., Vol. 61 (1978), pp. 233-240
10. K. Walker: Mechanical reliability of optical fibers. Proc. OFC'89, Houston, Texas, 1989, paper WA1
11. K. Abe: Private communication.
12. Y. Mitsunaga, Y. Katsuyama, Y. Ishida: Reliability assurance for long-length optical fibre based on proof testing. Electr. Lett. Vol. 17 (1981), No. 16

Jouko Kurki was born in 1953. He has received the Dipl. Eng. and Dr. Techn. degrees in Electrical Engineering from the Helsinki University of Technology in 1977 and 1983, respectively.
His work has included development of optical fiber fabrication process and optical fiber measurements in the Technical Research Center of Finland in 1977-82, and development of optical fiber production equipment in Nokia Cable Machinery in 1982-1987. He is currently responsible for development and production of single-mode fiber at Nokia Cables. Dr. Kurki has several publications in the field of optical fiber measurements and fabrication.

Lena Stormbom was born in 1961. She received the Dipl. Eng. degree in physics in 1986 from the Helsinki University of Technology.
Before joining the product development group for optical fibers at Nokia Cables in 1987 to focus on strength and reliability she worked at Nokia Cable Machinery with the development of the fiber drawing tower.

Lauri Oksanen was born in 1957. He received the Dipl. Eng. degree, in 1984, and the Lic. Tech. degree, in 1986, in Electrical Engineering from the Helsinki University of Technology having worked on fiber communication systems, and fiber theory and measurements.
He worked as a research engineer in the university until 1988. He is currently working as Development Manager responsible for fiber measurements at Nokia Cables, Helsinki, Finland.

Timo Räsänen received the Dipl. Eng. degree in electronics in 1971 from the Helsinki University of Technology.
Before joining Nokia Cables he was engaged in R&D of digital transmission technology in the Telecommunications Laboratory of the university and in Nokia Electronics.
In Nokia Cables he has since 1979 been responsible for the development of optical fiber cable technology including transmission systems and for technical support of marketing of optical fiber cables and systems.

Eliisa Leino was born in 1963. She received her degree of Dipl. Eng. in Chemical Engineering from the Helsinki University of Technology in 1988.
Her work with Nokia Cables consisted of development of methods to determine the degree of cure of optical fiber coatings, and reliability studies ofoptical fiber. Ms. Leino is currently Project Manager in Teknolink Oy.

THE FINGER SPLICE - A TOOLLESS MECHANICAL SPLICE FOR OPTICAL FIBERS

Lothar Finzel
Manfred Meier

RXS Schrumpftechnik-Garnituren GmbH, Hagen, FRG

ABSTRACT

Low-loss jointing of optical fibers generally requires sophisticated devices. Worldwide, optical fibers are today joined by fusion splicers or rather complex mechanical splicers, as this method yields good results.
Now, a reusable mechanical splice has been developed which does not only yield excellent splice results, but can rapidly be assembled and dismantled. This splice is, therefore, the ideal jointing device for all jumpering and distribution points in fiber optic cable networks.
The fiber optic mechanical splice is quick and easy to assemble and requires no special tools or external power source. It works on a clamping principle so that adhesives become unnecessary. The fiber end faces need no polishing.

INTRODUCTION

In the immediate future, the extension of the fiber optic cables network will require a splicing method to achieve optimal values of attenuation at the least possible cost. In particular local area networks (LAN) with their large number of splices require a highly productive splicing method. As only short fiber routes need to be spliced, the insertion loss is not of such importance. Thanks to today's production methods, optical fibers are produced to such close tolerances that they can be aligned with each other very exactly in a high-precision V-groove. The reusable mechanical jointing technique here provides a high-quality and durable splicing technique for individual fibers or units. Since no bonding or polishing is necessary, the splices can be assembled in a very short time under field conditions without requiring special tools. The reusable mechanical splice can also be used for jumpering optical fibers. Field trials confirm their suitability for route installation in every respect. Being easy to handle, the splices very rapidly gained acceptance among the craftsmen.

The following paper describes this new mechanical splicing technique for single and ribbon optical fibers. The mechanical design, mode of operation and preferred installation locations are described. Results of extensive laboratory tests and field experience are discussed.

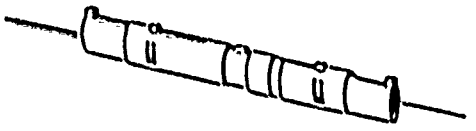

Fig. 1
Reusable Mechanical Splice

FEATURES OF THE REUSABLE SINGLE-FIBER CONNECTOR

With the reusable single-fiber splice (Fig. 1) single-mode and multimode optical fibers with a coating diameter of 250 µm can be quickly installed without special tools and external energy. For fibers with a larger coating diameter the clamping jaws are serially graded and appropriately color-coded. In contrast to the conventional mechanical splices, the fiber ends need no special preparation (Fig. 1, 2). Bonding and laborious grinding of the end faces with special tools are no longer necessary. Both fiber ends are simply cut to length with a fiber cutter and inserted into the single-fiber splice. By pushing specially shaped clamping rings into position the optical fibers are durably joined and held together.

The compact dimensions of the splice allow it to be accomodated in a confined space. Several splices can be stored under vibration-free conditions in a plastic splice holder. (Fig. 2). The securing combs permit easy insertion and removal of the splices by applying pressure on one side. This considerably simplifies later jumpering of the fibers. As a rule the fiber requires no new cutting for the jumpering process. In addition to the usual single-mode permanent connection for on route installation in closures, the reusable single-fiber splice can also be installed at jumpering points such as in exchanges and cable distribution cabinets.

Spare fibers can be capped with a splice and accomodated in the splice holder. If required, they can be lined up and allocated at any time. Thanks to its simple handlin the splice can also be used as a fast repair splice. Furthermore, given its compact design, it is suitable as a low-cost splice in building installations.

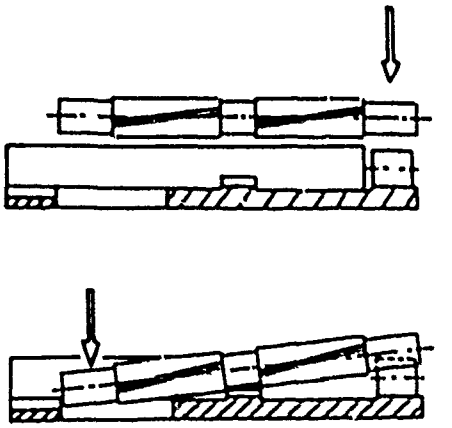

Fig. 2
Splice Holder

FUNCTIONAL PRINCIPLE OF THE SINGLE-FIBER SPLICE

The fiber manufacturing tolerances guarantee adequately exact centering of the fiber core via the cladding glass. Adjustment of the optical fibers to be connected is elegantly simple. In a high-precision V-groove, the heart of the splice, the two fiber ends are aligned via their outside diameters (Fig. 3).

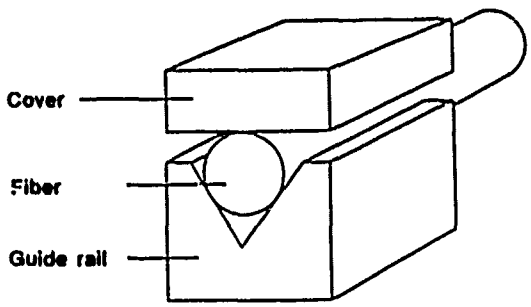

Fig. 3
Functional Principle

This part is made of monocrystalline silicon - a material that is known from semiconductor technology and has found an increasing number of applications in micromechanics over the past few years. By an anisotropic etching method the silicon is controlledly removed along the crystal orientation, thus producing a high-precision V-groove (Fig. 5, 6, 7). The fiber cores are aligned as on an "optical bar". A cover fixes the fiber ends and adjusts them in the V-groove. The fibers are thus well protected against mechanical stress.

DESIGN OF THE FIBER OPTIC MECHANICAL SPLICE

The reusable single-fiber splice is about 40 mm long and 4 mm in diameter (Fig. 4). It is cylindrical in shape and composed of the following parts:

- basic body (aluminium)
- three section guide rail (silicon)
- transparent cover (plastic)
- two clamping jaws (plastic)
- two clamping rings (metal)

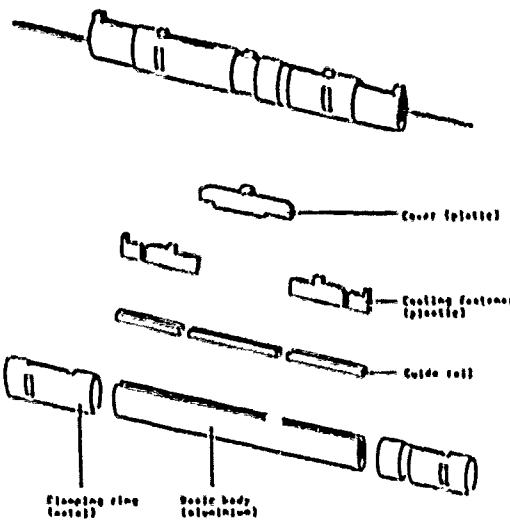

Fig. 4
Components of the Mechanical Splice

The three section guide rail is bonded into the basic body at the works. The central section of the guide rail has a high-precision V-groove etched into its top side. The optical fiber can be readily pushed forward into the splice plane under the radially movable cover. The cover is transparent to permit observation of the splicing process if required. The underside of the cover has a recess at either end to accept the coating. This step forms a longitudinal stop for the end of the coating. The coating is only allowed to enter within this recess. This ensures that the fiber is spliced in the middle, flat part of the cover. When assembled, the cover presses the fiber ends in the cladding area into the common V-groove. In the same operation, the optical fibers are also mechanically stress-relieved by two clamping jaws.

These press radially on the coating thus fixing the fibers. Together with the cover they close off the upper side of the basic body. The optical fibers are thus protected against environmental influences.

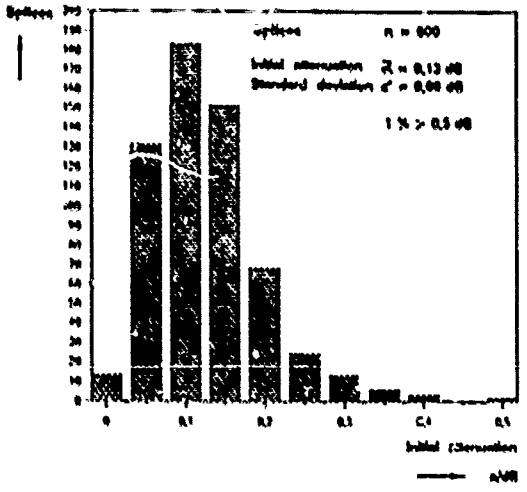

Fig. 5
Fiber Optic Mechanical Splice Attenuation
(250 µm/250 µm)

The splice is supplied at the works with index-matching fluid, guaranteeing good insertion loss with high return loss and good longitudinal stability (Fig. 5). The filling of index-matching fluid is sufficient for several splicing processes. Tests have shown that the insertion loss does not appreciably change if a splice is used several times (Fig. 6).

If necessary, the splice can be easily dismantled by pushing apart and turning the clamping rings. After refilling the splice with index-matching fluid, it is ready for further splicing.

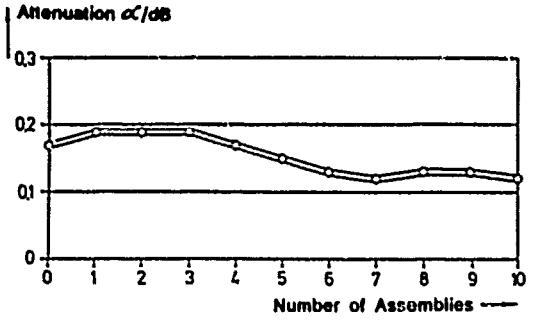

Fig. 6
Attenuation

SPLICING PROCEDURE

The splicing of optical fibers with the reusable splice is very simple. The coating is removed from the fiber using a stripper, the cladding area is cleaned of residues with an alcohol-soaked cloth and the fiber is cut with a fiber cutter. The cutting length can be easily adhered to accurately enough with a simple optical marker.

The insertion funnels at the end of the splice permit easy insertion of the fibers. While pushing the fibers into the funnels they can be observed through the transparent cover. The optical fiber is fixed with the clamping ring when it abuts against the length limit. The splicing procedure is completed by sliding the clamping rings as far as the prescribed stop. The fibers to be connected are thus optimally aligned and mechanically strain-relieved.

MULTI-FIBER SPLICING TECHNIQUE

Thanks to the modular design of the single-fiber splice, it can easily be converted into a multi-fiber splice. Only the silicon part needs replacing by a 2- or 4-groove part (Fig. 7). Constructional design, function, handling and outer dimensions are identical to those of a single-fiber splice. Also the installation time remains the same, even if 2- or 4-fiber ribbons are spliced. This considerably increases productivity.

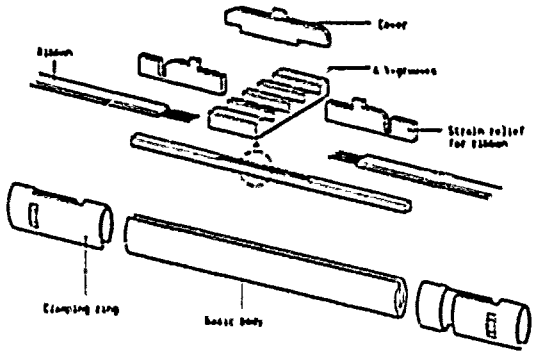

Fig. 7
Four Fiber Mechanical Splice

On conventional ribbon fibers the cladding can often only be removed by a thermal method. As the fibers still need to be cut without great length differences, they are cut in one operation. The individual installation steps are made easier by a simple installation unit. With this auxiliary unit, ribbons can be thermally stripped of coating and subsequently cut to length by a fiber cutter.

The cut fiber ends are inserted into the splice on a mounting rail. Installation is thus very simple and not craftsensitive.

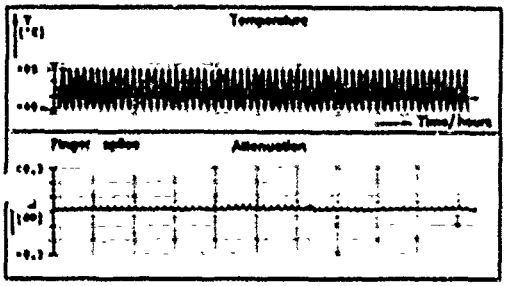

Fig. 8
Temperature Test

RESULTS OF THE FINISHED INSTALLATIONS

Comprehensive splicing tests were carried out in the laboratory and in the field (Fig. 5, 6, 8). It was shown that even with frequent reconnection, the loss values were subject to only very low scatter. High reproducibility of the splice quality is thus assured (Fig. 6). The insertion loss was measured in single-mode fibers at 1300 and 1500 nm (Fig. 5). No appreciable difference in loss behavior was ascertained. The return loss is greater than 40 dB. The splice meets Bellcore Technical Reference TR-TSY-000042. The 4-fiber splice (Fig. 9 and 10) showed a similar behavior.

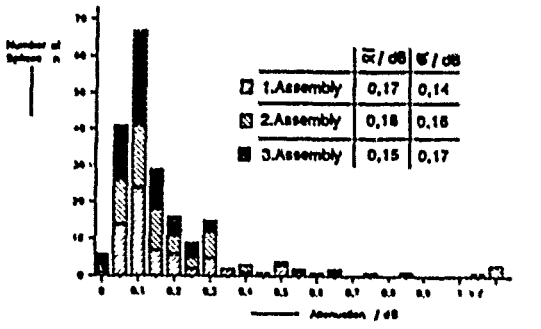

Fig. 9
Reusable Multifiber Splice for Ribbons

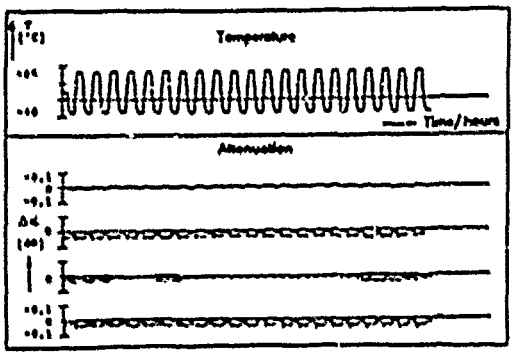

Fig. 10
Multifiber Splice - Temperature Test

APPLICATION RANGE OF THE MECHANICAL SPLICE

For a number of applications, such as repair splices, branching closures, terminal distribution boxes and subscriber lines, the mechanical splice provides a fast and durable splicing method without great technical complexity. The results obtained in the laboratory and field trials allow even more widespread applications of the reusable splice. With this splice all incoming and outgoing fibers can be joined safe, simple and cheaply.

SUMMARY

The design and functional principle of the mechanical splice were explained in this paper, starting with the single-fiber up to the 4-fiber splice. The single- and multi-fiber splices are made of a modular design so that all splices can be handled in a similar manner. They have the same dimensions and can thus be adopted into the universal technology without modifications. As the mechanical splices require no special preparation, they can also be used as repair splices in the field. Thanks to their mechanical design, adhesives and the grinding of end faces become unnecessary. Permanent cohesion is obtained by clamping on the cladding glass, whereby the optical fiber is strain-relieved.

AUTHORS

Lothar Finzel received his diploma degree in mechanical engineering from the Technical University of West Berlin in 1984. Since then he has been employed at Siemens AG, Munich, West Germany, where he at first worked on copper cables. Since 1987 he is responsible for the development of mechanical splicing equipment for fiber optic cables.

After studying electrical engineering and business administration, **Manfred Meier** joined Siemens AG, Munich, West Germany, in 1968. Since then he has been active in the field of telecommunication cables. From 1974 to 1976 Manfred Meier worked as a sales manager for Siemens in the Republic of South Africa. He then resumed his work for Siemens in Munich until 1985 when he joined RXS Schrumpftechnik-Garnituren GmbH, Hagen, West Germany, as Managing Director.

A NOVEL, EASY ENTRY, AERIAL SPLICE CLOSURE

KENNETH D. REBERS

3M

ABSTRACT

The design of aerial telephone cable systems typically incorporates free breathing cable and splice closures. Aerial splice closures, installed at any point of access to the cable core, provide physical protection and shielding from weather, sunlight and insects.

A new splice closure system has been developed which incorporates a novel, double wall blow molding technology to form a very lightweight, strong closure body. The system also includes a two-segment, rubber end-seal which provides easy installation and superior integrity. All components are preassembled for ease of installation. The new aerial closure system has been subjected to all industry performance, application-specification tests. The results of these tests, in addition to field tests will be reported.

INTRODUCTION/BACKGROUND

Aerial Splice Closures are used by the telephone industry to protect telephone cable splices, provide mid-span draining, and to cover areas that have been damaged by rodents and birds. Telephone companies, for years, have had to use closures that were difficult to install, had many loose parts, and did not do an effective job of keeping out bugs, birds, or rodents. Closures with a number of piece parts run the risk of being installed improperly because of missing parts or incorrect assembly. Many closures were also very heavy and required more than one person to install.

Sealing the cable entry to the closure is a major issue. Most closures use end caps which require cutting of material, which many times is a difficult process and may even require the use of a saw. A number of closures require the use of drip collars because of ineffective tape seals or fasteners such as cable ties and rails. A conical end cap design requires customers to stock single, double, or triple caps. Some closure end-seals use soft elastomers that have poor hydrocarbon resistance, and promote the growth of fungus.

Ventilation is necessary to dry out splices that become wet from water traveling inside the cable due to cracked sheath or from damage caused by rodents. There is also a need to dry out the splice from high humidity in certain areas. The hanging system for closures is accomplished in two different ways. Some closures are banded directly to the strand, while others are placed in position by hangers. The grounding system for closures that are banded to the strand needs a separate wire run through the end-seal, and requires a grounding clamp, (typically not provided) to attach to the strand. When using a hanger system, no extra parts are necessary. The ground path goes directly through the hanger, which is a conductive material, preferably aluminum.

Access to splice closures depends on the closure design. Some closures have bottom rails that secure the closure by sliding on parallel to the closure, and others use screws or hose clamps to secure the closure. All of the above are time-consuming ways to gain splice access. The trend of aerial closure design is to make it as easy as possible to gain splice access by using latches or similar devices that are an integral part of the closures.

Extending aerial closures for sheath pullout has always been very cumbersome, if not impossible. Some designs require additional kits for extension.

TARGET REQUIREMENTS

Target requirements were set in cooperation with a telephone operating company at the initiation of the closure design program. The closure was designed to meet all industry specifications for aerial splice closures. Also, it was decided that a minimum number of parts would be used for kit assembly and installation. The closure would be available in sizes ranging from 2.2 inches (55.9 mm) inside diameter to 7.6 inches (193.0 mm) inside diameter. The splice opening would range from 14" inches (355.6 mm) to 21 inches (533.4 mm).

The end-seals need to be easy to install, should not require the use of drip collars, and should accommodate cable diameters ranging from 0.2 to 3.8 inches (5mm to 97mm). The closure should provide adequate ventilation and still prevent insects from entering. Standard closures should have an integral hanger system with a floating bond.

Installation of the closure should be accomplished with the use of a standard terminal wrench, snips, and a sheath knife. Reentry of closure should be done without special tools, without disruption of end-seals, and would take no longer than one minute for the person to gain access. Extendibility of the closure must be craft friendly and require a minimum amount of time.

DEVELOPMENT PROGRAM

The new aerial closure was designed to meet the changing needs of customers. The requirements listed above could not be satisfied by any existing closure.

The method of manufacture was a deciding factor when it came to picking a material for the closure body. The closure needed to withstand high impact loads at -40°F to 140°F (-40°C to 60°C) and still remain flexible at these temperatures. Because of these requirements, a double-wall blow molding process using a polyethylene material was selected. The double-wall feature gives the closure superior strength with minimum weight. The strength is derived from the box structure obtained with the double-wall blow molding process. A similar injection molded part with the same strength characteristics would have to be much thicker and therefore heavier. Even then, warping problems may be encountered with injection molding.

The process of double wall blow molding permits more design freedom than standard blow molding or injection molding. Design features on the inside wall are independent of features on the outside wall. Also compression molding the two walls together gives similar strength characteristics of injection molded parts. The compression molding process was used to increase the strength of the hanger bracket and latch areas. It also was used to seal the two walls together at the center of the closure. This permits cutting a closure in half for extending, while still maintaining environmental and structural integrity. The double-wall feature permitted a unique design for extending the closure by allowing the design of the interlocking tongue and groove system. The end-seal retention area is designed on the inside of the closure while the extendibility features are on the outside. The interlocking tongue and groove design locates the extension half radially with respect to the main closure. In total, the double-wall blow molded closure could be in a one-piece design having superior strength, light weight, excellent hinge strength and flexibility characteristics, with design features on the inside and outside.

The end-seal material needs to be very stable in flexibility and be fungus resistant. The material chosen was a thermoplastic rubber. The thermoplastic rubber is made of two main components, a rubber component that gives cold temperature flexibility, and a plastic component that improves the rigidity at high temperatures. Also, the material can be injection molded at superior rates to rubber molding. The end-seal design had to be craft friendly for ease of installation while providing environmental protection. This has been accomplished by the accordion design of the end-seal which allows the material to conform to cable irregularities. For installation on existing cable each half of the two piece end-seal design is cut at a different radial angle so that there is no direct path for water. The offset cuts stop the flow of water into the closure. The installation time for these end-seals is approximately one minute for both seals.

The vents in the bottom of the closure are positioned in such a way as to provide ventilation in all situations. Since the screen is positioned at an angle and not even with the bottom of the closure, the use of filled cable that leaks into the inside of the closure will result in the filling material only covering a portion of the screen. It is made out of

stainless steel to prevent corrosion build up. Being woven wire, it drains better than molded in vents. The hardware features of the closure were designed to satisfy the remainder of the product requirements. The hanger system, the bond bar, and the hanger brackets are made of aluminum to provide good electrical conductivity. The bond bar is formed into a channel which provides superior strength for securing splice bundles.

The stainless steel closure latches are designed to be craft friendly and provide an environmentally sound way of securing the closure. Reentry of the closure is simplified with this latch design, and disruption of the end-seals is not necessary. Reentry takes approximately five seconds.

DEVELOPMENT TESTING

The new aerial closure passed all Bell and GTE test requirements. Testing of closure is reported in Appendix A.

FIELD TRIALS AND RESULTS

The first field trial was with Bell Canada. Bell Canada was helpful in communicating their requirements for an aerial closure. They were also helpful in providing information about the Bell Canada Standards. The first closures were installed in December 1987 and are still in service for Bell Canada. During the field trial, and while doing the Bell Testing, areas of concern were brought to our attention. One area of concern was end-seal installation. Bell Canada wanted to be able to install the end-seal with minimal cutting. That is one reason why the thermoplastic rubber was chosen. After minimal cuts are made in the end-seal the craftsperson can tear out the center of the end-seal. Another concern was the need to band the closure to the strand. This was accomplished with the design of a hanger bracket that accommodated stainless steel banding. Numerous field trials are currently underway in the United States and in other countries. The results to date are extremely positive.

CONCLUSIONS

The new aerial splice closure has met the customer requirements. From the tests performed and field trials now in process it shows that the domestic and international customers are very interested in a splice closure of this type. The new aerial closure is a one piece closure. The end-seals and the hanger system are integral parts of the closure. The overall simplicity, superior environmental protection and stability, ease of installation and reentry time without the use of special tools, and ease of extendibility are all features of this closure, which are unsurpassed by any other aerial splice closures on the market today.

APPENDIX A

CLOSURE TESTING

SEALING CAPABILITY

WATER INTRUSION: This test is designed to determine the capabilities of the splice closure to prevent water intrusion. The samples are prepared with cable ends extending 12.00 inches (.3 meters) beyond the entrance point of the splice closure. The cable ends are capped using an approved method. Water is sprayed at a 45° angle, with a flow rate of 14.5 gallons (55 liters) per minute and a water head pressure of 10 ft. (3 meters). The spray head is positioned 6.5 feet (2 meters) from the test samples. The water is sprayed for a period of five minutes. This test is intended to simulate a severe wind driven rain. Any amount of water permitted to penetrate to the splice bundle would constitute a failure. During the test, watesmo paper, which if exposed to water would turn blue, was wrapped around the cable splice and around the cable near the inside of the end-seal. During the test there were no failures where water contacted the watesmo paper and turned it blue.

WATER FLOW 14.5 GAL (55 liters) PER MIN
WATER PRESSURE 10FT (3.0 meters) HEAD

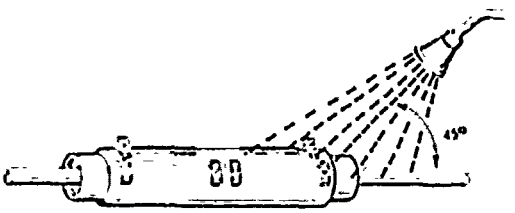

WEATHER TIGHTNESS: This test is designed to determine the capabilities of the splice closure to prevent dust intrusion. The samples are prepared with cable ends extending 12.00 inches (.3 meters) beyond the entrance point of the splice closure. Three black foam dust collectors are placed inside the closure in a horizontal plane. On closures with extensions, one more dust collector was added. Two pounds of 325 mesh white silicate dust is accelerated to a velocity of 60 mph (96.5 kph) aimed at the closure.

Any dust collector with a "whiting" rating greater than 4 results in failure. Of the all the closures tested, only one dust collector showed a rating of 1 and this collector was located near the vent screen. The screens were not covered for this test and air flow was permitted through the closure. The other collectors had a 0 rating. (See scale for "whiting" below).

SILICATE DUST

60 MPH (96.5 KPH)

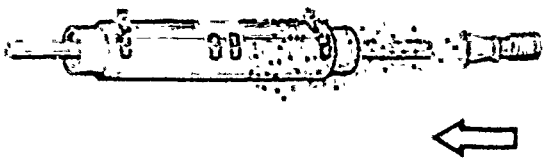

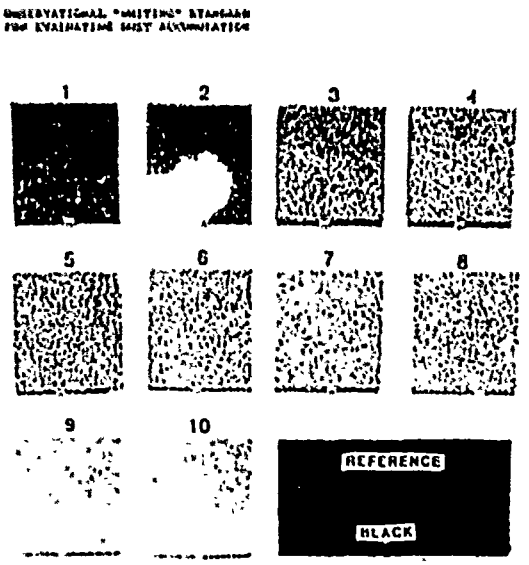

SALT SPRAY: The salt fog spray test is performed in accordance with ASTM B117 for 30 days. Both ends of a 200 pair cable shall exit the test chamber. The pairs at one end are energized with 48 VDC while the other end is cleared and/or capped. All tips are joined together and all rings are similarly treated as one ring conductor. Measurements are made between the tip group and ring group with an applied voltage of 100 VDC; a measurement is made every 24 hours. The 48 VDC is temporarily removed during the measurement process. The minimum insulation resistance shall not be less than 1 Megohm. Evidence of corrosion on any of the metal components constitutes a failure. The closures that were tested maintained resistance readings above 4500 megohms and showed no corrosion on any of the metal parts.

MECHANICAL INTEGRITY TESTS

VIBRATION: A two hour vibration test in two mutually perpendicular planes is required. During each test the samples are secured to a vibration table. The cables leading out of the closure are clamped to an independent fixture at a distance of 1.6 ft. (0.5 meters), from the splice closure ends. The cable ends are separated into tip and ring groups. Insulation resistance is measured before and after each two hour vibration period. The vibration rate should sweep from 10 Hz. to 100 Hz. to 10 Hz. in a period of fifteen minutes. Throughout the vibration sweep the samples should receive a constant 0.5 g acceleration. All of the vibration testing is conducted at room temperature. Any insulation resistance lower than 1.0 megohm or any sign of damage to the closure body or end-seals constitutes a failure of this test. The insulation resistance readings after the vibration tests ranged from 2-30 megohms. There was no physical damage to any of the closures tested.

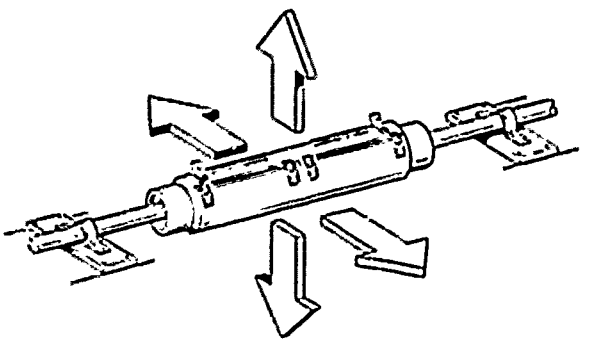

IMPACT TESTS: The closure must withstand an impact of 14.75 ft-lbs (20 Joules) at -40°F to 140°F (-40°C to 60°C). The impact is to be delivered by a 4.4 lb (2kg) weight dropped 3.3 ft (1 meter). The weight is a 2.0 inch (50.8mm) diameter cylinder with a 1.0 inch (25.4mm) spherical radius at the striking end. The impact test is repeated in three different areas on the closure. The impact tests showed no damage to the closure.

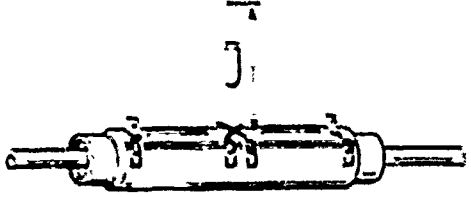

STATIC CRUSH TEST: The closure is to be subjected to a 10 minute "crush test" at room temperature. A static load of 225 lbs (1 KN), is applied over a 3.9 in^2 (25 cm^2) area. After this test the closure body must maintain its integrity without any damage. The samples that were tested showed deformation under the load applied, however each sample resumed its original shape after the load was removed.

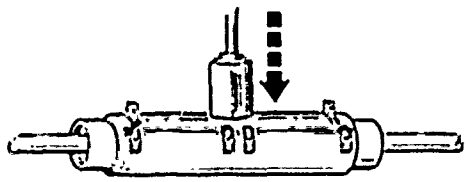

CABLE FLEXING TEST: This test requires a cable to be installed in a closure and flexed 30° above and below the neutral cable position. The cable is flexed five times at each temperature: -22°F (-30°C); 73°F (23°C); and 140°F (60°C). After this test the closure must maintain its integrity without any damage to end-seals or to the closure body. No damage resulted to the end-seals or to the closure body.

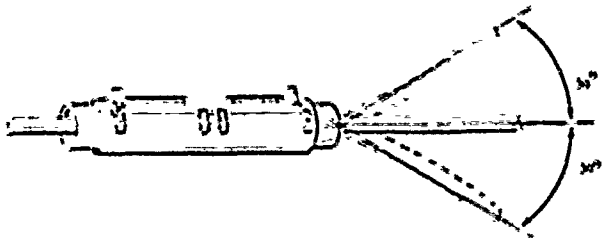

AXIAL TENSILE PULL TEST: The closure must withstand an axial pull without any loss of mechanical integrity at room temperature. The closure should provide a minimum sheath movement of 4 inches (101.6mm) on all cables. Minimum loading of a 0.75 inch diameter (19mm) cable must be 146 lbs (650N). Minimum loading of a 0.75 inch diameter - 1.93 inch diameter (19mm - 39mm) cable must be 292 lbs (1300N). Minimum loading of a 1.93 inch diameter (39mm) cable and larger must be 496 lbs (2200N). The closures tested did not have to meet these requirements due to the floating bond system. The limiting factor was the flexible bond system, in all tests the bond failed the tensile force required. The bond strap ruptured between 100 - 135 lbs (450 - 600 N). None of the end-seals were damaged as a result of the cable being pulled through them.

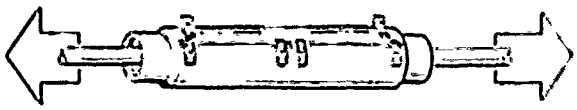

ELECTRICAL INTEGRITY TEST

HIGH CURRENT: All closure bonding must withstand 1000 amperes applied through the cable shield for a period of 20 seconds.Shield resistance is to be measured before and after the 1000 ampere surge. Any loss in electrical circuit continuity or resistance greater than 10

milliohms through the bonding system constitutes a failure. This surge test is to be repeated three times. Of all the closures tested, the highest reading reported was .75 milliohms.

MATERIAL INTEGRITY

PLASTIC PARTS: The plastic parts of the closure must be resistant to solvents, sprays and stress cracking. They must be compatible with metals and other materials used in connectors and in cables such as conductor insulation and filling compound. Plastic materials used must be non-corrosive to metals and resist deterioration when exposed to industrial chemicals, pollutants or ultraviolet light.

METAL PARTS: The metal parts must be resistant to or protected against general corrosion and various forms of localized corrosion, including stress corrosion cracking and pitting. They should not produce significant galvanic corrosion effects in wet or humid conditions on other metals likely to be present in the closure.

CHEMICAL RESISTANCE: The chemical resistance of the closure and its materials are subject to the following two tests. In the first test, sample plaques of the body and end-seal materials are exposed to chemicals commonly used in the telephone industry. In the second test complete closure assemblies are prepared and soaked in selected chemicals.

FLEXIBLE MATERIALS: Testing of flexible samples performed according to ASTM D1693 and exposed to the following commonly used chemicals:

2251 Oil - used in filling compounds
Isopar M - isoparaffinic solvent derived from petroleum
Black Flag - insect spray

The samples are soaked in the above chemicals for 14 days at a temperature of 120°F (49°C). The samples must maintain 80% of their original values. The end-seal samples tested showed 83.3% of initial hardness readings for the 2251 oil, 80.3% of the initial hardness readings for the isopar m, and 93.9% of the initial hardness readings for the black flag insect spray.

RIGID MATERIALS: Testing of rigid materials is done using test bars 2.5" x 0.5" x 0.125" (64mm x 13mm x 3.2mm). The samples are bent in a three point fixture to yield an outer fiber strain of .0075 inches/inch (.19mm/mm). Immediately after installation into fixture they are placed in the chemicals listed below for 30 days. Any sign of cracking or crazing constitutes a failure.

2251 oil - used in filling compounds
Isopar M - isoparaffinic solvent derived from petroleum
Black Flag - insect spray

None of the test closure samples showed any signs of stress cracking or crazing.

ASSEMBLED CLOSURE CHEMICAL EXPOSURE: A complete closure assembly is immersed in the following chemicals for 72 hours at room temperature.

3% Sulfuric Acid
100 pm trichloromethane in water
0.2 N sodium hydroxide

Swelling, deformation or softening of the closure as well as discoloration of the solution must be explained. A hardness test is performed prior to and after immersion. The closure assembly must retain 80% of the original hardness. The results of this test are 86.2% of the initial hardness readings with 3% sulfuric acid, 91.2% of the initial hardness readings with 100 ppm trichloroethane, and 84.1% of initial hardness readings with 0.2 N sodium hydroxide.

ULTRAVIOLET RESISTANCE: Ultra violet test bar samples of closure are exposed to photo degradation for 700 hours in accordance with ASTM G26 and ASTM D2565 procedure A, using a Xenon Arc-Type weatherometer. The test bars must maintain 80% of their original tensile strength and elongation. The closure body results of this test showed a retention of 102.3% of initial tensile strength and 86.6% of initial elongation. The closure end-seal results of this test showed a retention of 80% of initial tensile strength and 105% of initial elongation.

FUNGUS RESISTANCE: The closure and end-seal materials must not support fungus growth per ASTM G-21. This test requires samples to be incubated for 21 days at 82°F (28°C). A rating of 0 is required to pass. The results of these test were a rating of 0 for the end-seal and the closure body.

JM
PO Box 2963
Austin, Texas 78769-2963

Ken Rebers is a Senior Designer in the Network Accessories Group Laboratory at JM TelComm Products Division. He has been engaged with the design and development of outside aerial plant since 1981.

FIBER OPTIC DROP CABLES IN THE SUBSCRIBER LOOP

Werner Bernard
Susan C. Grant

Siecor Corporation
489 Siecor Park
Hickory, NC 28603

ABSTRACT

Optical fiber telecommunication networks require drop cables to close the gap between the last service access point and the subscriber premises. A dielectric drop cable was developed for use in fiber-to-the-home field trials. An armored version is being developed to meet Bellcore TR-TSY-000843 "Generic Requirements for Optical and Optical/Metallic Buried Service Cables" [1].

The performance of the dielectric cable meets or exceeds all requirements of Bellcore TR-TSY-000843. Outstanding values are achieved for the flex and impact test; after 1000 cycles or impacts the maximum attenuation increase is less than 0.05 dB/km. The maximum attenuation increase during the cold bend test is 0.11 dB/km. The combination of suitable materials has earned the cable UL approval for the flammability test VW-1 of UL 444, section 25. The maximum attenuation change during temperature cycling (-40 °C to +70 °C) is less than 0.3 dB/km.

The armored prototype showed similar test results as the dielectric version. The test results fulfill the requirements of Bellcore TR-TSY-000843.

The paper will discuss in detail the design, materials selection and performance of both the dielectric and armored cables.

1.0 INTRODUCTION

Optical fibers have been used for several years in a large part of the long distance telecommunication network in the U.S. Usually the optical fiber network ends at the central office, increasingly at the remote terminal. At the central office or the remote terminal the optical signal is then converted into an electrical signal and continues to the subscriber premises.

With the introduction of new services which require high data transmisson to the subscriber, optical fibers will be necessary for the data transport [2],[3]. Several field trials have recently started throughout the U.S. to bring the fiber to the home [4],[5]. Many different topologies of the network are being considered. Our effort focused on a Two Fiber Star Network [6]; see Figure 1. In this topology a 2-fiber drop cable will be necessary to close the gap between the pedestal and the subscriber premises.

2.0 CABLE DESIGN

2.1 Dielectric Drop Cable

During the design stage of the dielectric drop cable no specifications for optical drop cables had been published. Bellcore TA-843 was used as a guideline for the performance of the drop cable design. Similar requirements were given by customer specifications.

Two single mode fibers with a nominal modefield diameter of 9.5 µm and a coating diameter of 500 µm were used as optical waveguides. The fibers were buffered to 900 µm to make handling during connectorization as easy and safe as possible. The proven loose tube concept of Mini-Bundle® cables was used as a basis for the cable design. The VW 1 flame test and the cold bend test as required in Bellcore TA-843 made it impossible to use standard tube materials. After the evaluation of several tube materials, a flame retardent thermoplastic elastomer proved to be the best choice to achieve good results. The tube is filled with a highly viscous filling compound during processing to waterblock the cable. Fiberglass and impregnated glass yarns are spun around the tube as strength and antibuckling members. A thermoplastic elastomer was chosen as jacket material to achieve good results during cold bend and VW 1 flame tests. The outer diameter of the cable is 7.5 mm. A cross section of the cable is shown in Figure 2.

2.2 Armored Drop Cable

During the development of the armored drop cable Bellcore TR-TSY-000843 "Generic Requirements For Optical and Optical/Metallic Buried Service Cables" was issued. Subsequent development was performed using this document as a guide.

Two single mode fibers with a nominal modefield diameter of 9.5 µm and a coating diameter of 500 µm were also used as optical waveguides in this cable design. The fibers were buffered to 900 µm with nylon. These two buffered fibers were then put in a PE tube, which was filled with a high viscosity filling compound. Because this cable was armored with a steel tape, flame resistance of the tube material was not required. Fiberglass used as strength members was spun around the tube. A corrugated 5 mil stainless steel tape was applied over the core. A flame retardant PVC was

used as jacket material. The outer diameter of the cable is 8.5 mm (Figure 3).

3.0 CABLE PERFORMANCE

The cable performance of both the dielectric and armored version was determined after intensive temperature, mechanical and environmental testing. Tests were mainly done in accordance with Bellcore TR-TSY-000843 "Generic Requirements for Optical and Optical/Metallic Buried Service Cables". The following gives a summary of the most critical tests.

3.1 Temperature Cycling

The temperature cycle was performed in the following way: 3 cycles from -40 °C to +70 °C, heat age at 85 °C for 120 hours, 2 cycles from -40 °C to +70 °C.

During the test the fibers were continuously monitored at wavelengths of 1300 nm and 1550 nm.

Dielectric Drop Cable

Fig.4 shows the attenuation change during temperature cycling. The maximum increase for all cables occured at -40 °C. The maximum increase before heat aging is 0.02 dB/km for 1300 nm and 0.15 dB/km for 1550 nm. After heat aging the maximum increase is 0.10 dB/km for 1300 nm and 0.20 dB/km for 1550 nm. The greater attenuation increase after heat aging indicates some cable shrinkage during the 85 °C heat soak.

Armored Drop Cable

Fig.5 shows a typical graph of the attenuation change during temperature cycling. The changes for all monitored wavelengths were 0.01 dB/km before heat aging. After the heat soak the attenuation increased by 0.01 dB/km for 1300 nm and 0.04 dB/km for 1550 nm. The steel tape, as expected, stabilized the core structure and prevented the cable from shrinking.

3.2 Mechanical Testing

Longitudinal shield fatigue test

The armored cable was wrapped around a mandrel with 70 mm in diameter according to the test procedure required by Bellcore TR-TSY-000843. The middle five turns which were examined did not show any cracks in the shield.

Low and high temperature cable bend test

The dielectric drop cable was tested according to FOTP 37 with a mandrel of 50 mm and a test temperature of -30 °C for the cold bend and of +60 °C for the hot bend test. The cable passed this test with an average attenuation increase of less than 0.1 dB at both 1300 nm and 1550 nm.

The armored drop cable was also tested according to FOTP 37. The mandrel diameter was 50 mm. The test temperature was -20 °C for the cold bend test and +60 °C for the hot bend test.

The cable passed the bend tests without an attenuation increase or cracks in the jacket.

Impact resistance

Both the dielectric and armored cable were impact tested according to FOTP 25 with an impact energy of 4.5 J. The cables had no difficulty passing the required 20 impacts. The attenuation increase was 0 dB for all samples. Jacket cracking or splitting did not occur. The test was even extended to 500 impacts with a maximum increase of 0.07 dB.

Compressive strength

The cables were tested in accordance with FOTP 41 up to 700 N/cm load. At this load the maximum attenuation increase of the dielectric drop cable was only 0.02 dB, while the armored drop cable did not show any increase. The cables easily passed the required load of 175 N/cm for the nonarmored and 220 N/cm for the armored version. After maintaining the load for ten minutes (which did not result in an attenuation increase) the load was released and the attenuation change of the dielectric drop cable returned to 0 dB.

Tensile strength of cable

The cable shall withstand an installation strength of 668 N (150 lbs) and a long term tensile load of 178 N (40 lbs). Fig. 6 shows the cable strain over the tensile load for the Dielectric Drop Cable. At a load of 178 N the cable strain was 0.10 % and at 668 N the strain went up to 0.28 %. There is no attenuation increase resulting from the measured cable strain.

Fig. 7 shows the cable strain over the tensile load for the armored drop cable. At a load of 178 N the cable experienced a strain of 0.10 %. The cable strain at 668 N was 0.30%.

In further development work it is intended to spin more strength members around the cable core in order to reduce cable strain to approximately 0.20 %.

Cable cyclic flexing

Both cables were flex tested according to the Bellcore requirements for drop cables. All fibers were monitored at 1300 nm and 1550 nm. Bellcore requires 100 flex cycles with the fibers exhibiting an average increase of less than 0.2 dB/km. All samples passed this requirements and did not show any cracks in the jacket.

3.3 Environmental Testing

Flammability

Both cable versions meet the VW-1 Vertical Tray Flame Test of Underwriters Laboratories UL 444,Section 25. There were no difficulties for the armored version passing this test because the armor prevents the filling compound from burning. But the material selection for the dielectric drop cable was very critical. A flame-retardant thermoplastic elastomer was a suitable material for the tube and the jacket. The flames self-extinguish far before the allowed limit of 60 seconds.

Gopher Protection

To protect the cable against gopher attacks a 5 mil stainless steel tape is longitudinally applied over the core. The tests performed by the U.S. Fish and Wildlife Service in Denver, Colorado showed that cable samples with a good seal of the overlap gave a sufficient protection. In this case the gopher can not get his teeth under the tape and pull it up. The 5 mil tape is strong enough to withstand the attacks of the gopher. Sealing the overlap is also an important parameter for the quality of the bend performance of the cable [7],[8].

4.0 CONCLUSIONS/SUMMARY

A 2-fiber dielectric and armored drop cable have been developed to fit in the topology of an all fiber subscriber loop. The development was done to meet the requirements of Bellcore TR-TSY-000843 "Generic Requirements for Optical and Optical/Metallic Buried Service Cables".

For ease of handling and field connectorization, the optical elements in all cables are two single mode fibers, tight buffered to 0.9 mm.

In the dielectric cable the fibers are contained in a filled loose tube made of flame-retardant thermoplastic elastomer. Fiberglass and impregnated glass yarns are spun around the tube as strength and antibuckling members. The core is jacketed with flame-retardant thermoplastic elastomer.

The design of the armored cable is similar to the dielectric cable. Two tight buffered fibers are contained in a filled polyethylene tube. The tensile and antibuckling requirements are met with a steel tape and fiberglass yarns. The jacket material is polyvinyl chloride.

Both cables showed excellent performance during temperature cycling. The cables met or exceeded all mechanical requirements of the TR. Great efforts were put on the selection of the cable materials to pass the flammability tests. The result is that even the dielectric version meets the UL VW-1 flame test. The dielectric drop cable has an outer diameter of 7.5 mm and the armored one of 8.5 mm.

REFERENCES

[1] Bellcore TR-TSY-000843, "Generic Requirements for Optical and Optical/Metallic Buried Service Cable", Issue 1, January 1989

[2] P.W. Shumate "Fiber Optics in the Subscriber Loop" Symposium by Lightwave Journal, Cambridge, MA, June 1988

[3] G.Cagle "Fiber's Path in the Subscriber Loop", Rockwell International

[4] R.M. Huyler, D.E. McGowan, J.A. Stiles, F.J. Horsey "The Architecture and Technology for the All-Fiber Loop", International Wire and Cable Symposium Proceedings, Reno 1988

[5] P.Goessing, C.Story "Fiber-optic Cable Characteristics and Field Performance for Subscriber Loop Applications", Optical Fiber Communication Conference Proceedings, Houston 1989

[6] Siecor Report, "On Fiber to the Home", October 1,1989, Volume 1, No 23, Siecor Corp., Hickory, NC

[7] W.F. Busch, K.E. Bow "Armored Sheath Designs for Military Base Fiber Optical Cable", Dow Chemical, Grainville, OH

[8] W.F. Busch, K.E. Bow "Measuring the performance of Bonded Sheaths For Cable Applications", Antec 1986, pp. 243-245

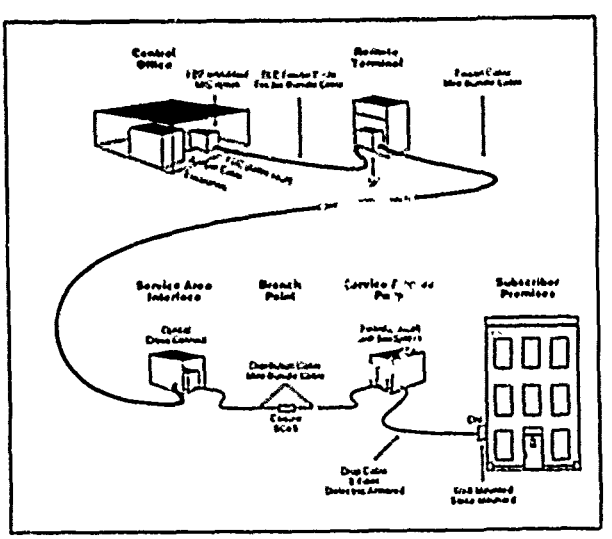

Figure 1: Two Fiber Star Network

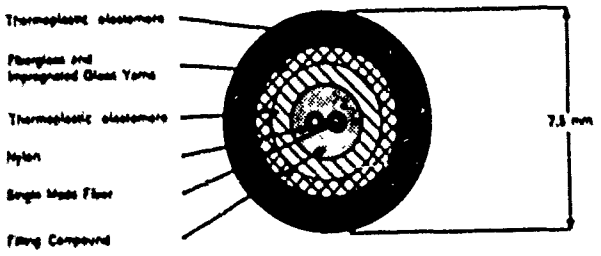

Figure 3: Cross-section of a 2-Fiber Dielectric Drop Cable.

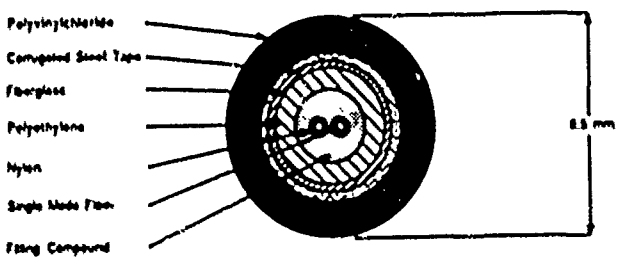

Figure 3: Cross-section of a 2 Fiber Armored Drop Cable.

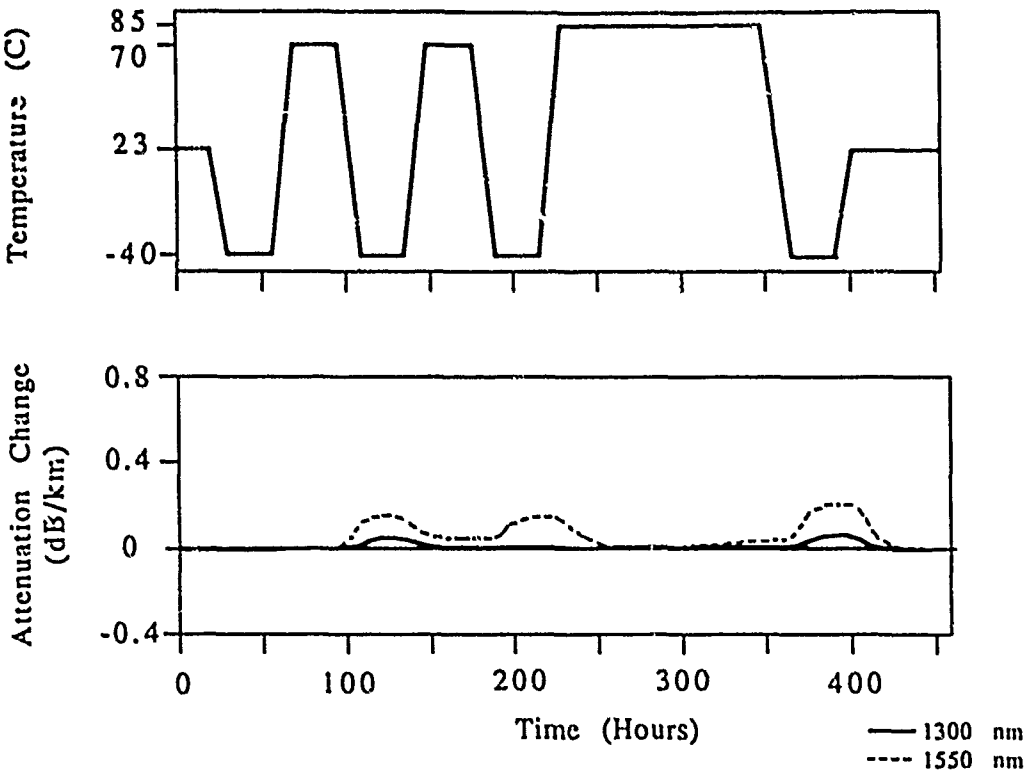

Figure 4: Temperature Cycling Behavior of the Dielectric Drop Cable

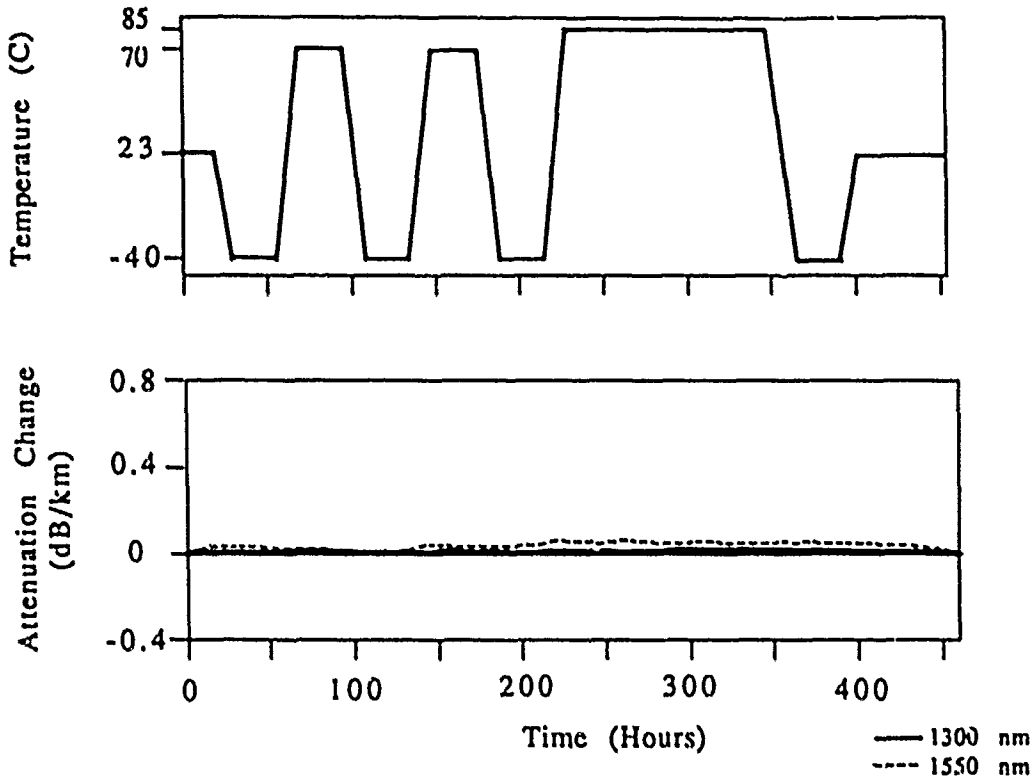

Figure 5: Temperature Cycling Behavior of the Armored Drop Cable

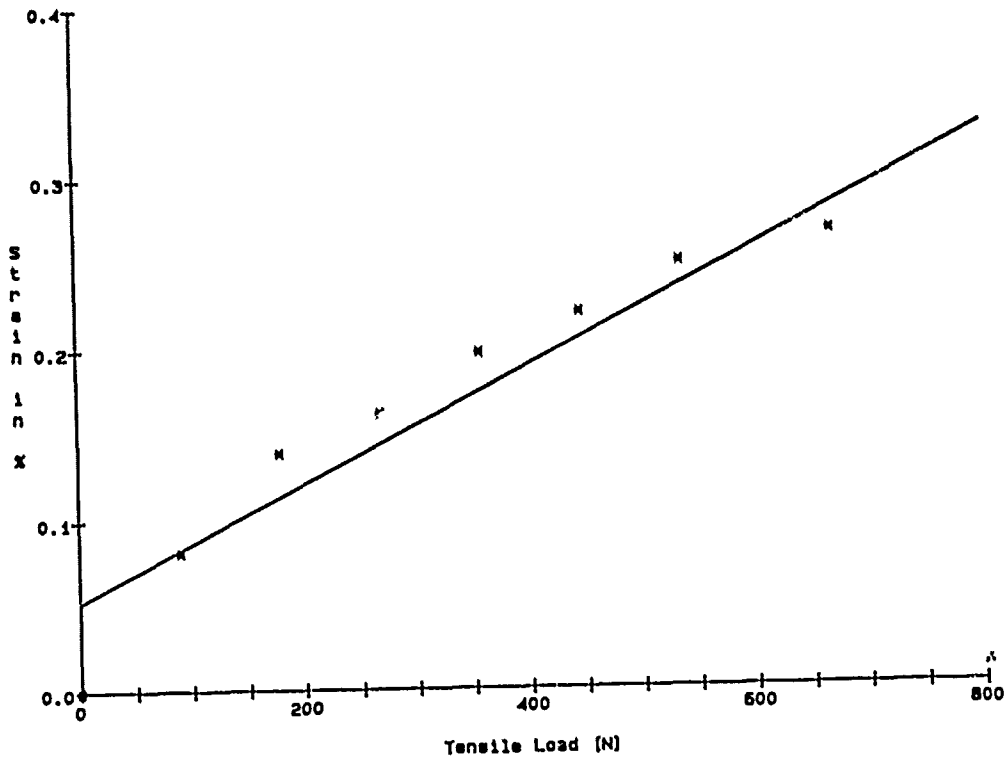

Figure 6: Tensile Load Behavior of the Dielectric Drop Cable

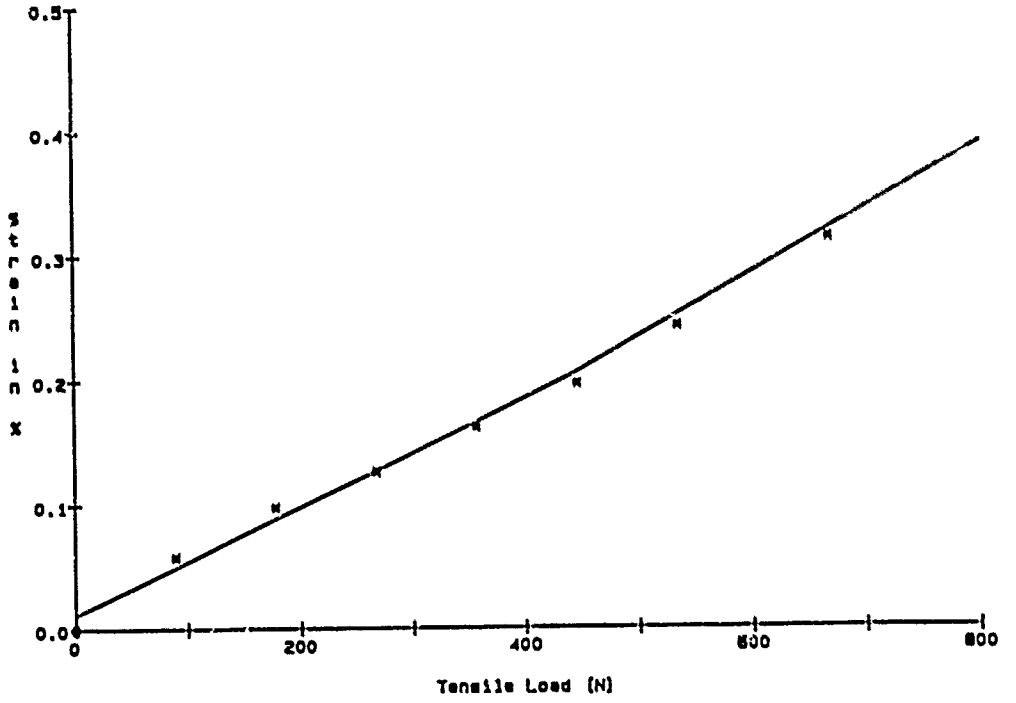

Figure 7: Tensile Load Behavior of the Armored Drop Cable

Werner Bernard

Siecor Corporation
489 Siecor Park
Hickory, NC 28603

Susan C. Grant

Siecor Corporation
489 Siecor Park
Hickory, NC 28603

Werner Bernard was born in Solingen/West Germany in 1955. He received his Master's Degree in Mechanical Engineering from the University of Aachen in 1983. After graduation he was employed at Siemens AG in the Research, Development and Engineering Department for copper cables. In 1988 he joined Siecor Corporation where he works as process engineer in the Research, Development and Engineering Department for fiber-optic cables.

Susan C. Grant graduated from Virginia Polytechnic Institute and State University in December of 1984 with a B.S. in Electrical Engineering. She then joined Siecor Corporation as a Product Development Engineer in Research, Development and Engineering. Ms. Grant is currently employed as Product Evaluation Supervisor in the Siecor Specialty Cable Plant.

NEW FIBER OPTIC PULLING GRIP INSTALLATION PROCEDURE

Mark E. Conner, Steven L. Hassett, Richard S. Wagman

Siecor Corporation, 489 Siecor Park
Hickory, NC 28603-0489

ABSTRACT

An improved pulling grip installation procedure was developed for fiber optic cables that utilize high strength yarns as primary strength members. In the procedure, coupling strength between yarns and the pulling grip is obtained by using the compressive force of the grip. Increased reliability is obtained using Chinese fingers type pulling grips and a procedure that is suitable for both factory and field installation.

Covered are the key areas of the development program and a discussion of the procedure and the concepts behind it. The development program included a tensile cycling test designed specifically for the procedure, testing under varying environmental conditions, and evaluation of the affects of poor installation practices and field trails. The result of the program was the development of a superior pulling grip installation procedure that utilizes at least 50% more of the strength of the high strength yarns.

INTRODUCTION

For a number of years, the use of a wire mesh (Chinese fingers) type pulling grip was recommended for duct cable installation. This pulling grip also contains a tie-off loop for anchoring the yarn strength member in the optical cable. This procedure or some variation of it was widely used.

Recent field experience has shown that in long pulls, where the cable's maximum tensile load is approached (typically 600 pounds), the grip installed as above may fail. This may be described as a difficulty in reaching the maximum load, as well as a large variability in the load achieved before failure.

The main contributor to failure in the procedure is the knot in the yarn at the tie-off loop. Any time a material is tied, it creates a weak spot by concentrating great pressure in a small region containing a sharp bend in the material. In this case, the knot is tied to a loop of stranded steel cable, which contains many sharp edges. Other variations exhibited failure due to slippage -- an inability to grasp cable components tight enough to withstand the tension being placed upon them.

The need for an improved pulling grip installation procedure was then apparent for customers to be able to pull a cable reliably to its rated maximum tension. The following are the objectives for a new procedure:

Improved Reliability

Craft-friendly

Average load at failure of 1,000 lb (400 lb safety margin)

Inexpensive

Lack of a formal grip testing method required that there be an objective way to compare various gripping procedures. A second objective then became to develop a test procedure simulating actual field conditions and quantifying them for comparison purposes.

This document describes the research done to successfully confront these issues and revise the thinking on pulling grips resulting in a better grip. It starts with current methods, describing their strengths and weaknesses. Better simulation of field conditions in the test lab is addressed. A prototype method is decided upon and taken to the field. Test and customer feedback show the new method meets the stated objectives.

PULLING GRIPS

The purpose of a pulling grip is to provide an attachment point that is used to pull the cable through a duct. A good pulling grip couples to a maximum amount of a cable's tensile strength. A number of commercially available types of pulling grips and techniques are used successfully with fiber optic cable. Each type has its own advantages and

disadvantages. Among pulling grips there are varying reliability, installation ease, reusability, complexity and degrees of cost.

Crimp Style Grips

One general type of pulling grip is the crimp type pulling grip (see Figure A). Its main feature is a closely fitting metal tube that is placed over the cable. During grip installation the tube is radially crimped into the cable at several locations. A crimped tube provides some coupling to the cable's tensile strength. Additional gripping elements are typically used in conjunction with the crimped tube. The tube keeps the cable from flexing at these gripping elements.

The type of gripping element used with a crimped tube depends on the cable design. When a cable's primary strength element is a steel or a composite fiberglass rod, the gripping element attaches to the rod with compression. Set screws are typically used for this purpose. With set screws the fiberglass rod requires the protection of a brass sleeve. When a cable's primary strength element is a yarn wrapped over the cable core, the gripping element attaches to the yarns with a thermosetting compound, typically an epoxy. In a hollow section of the grip a plug is made with the yarns and the epoxy.

The many types of crimp pulling grips are relatively inexpensive, however they cannot be reused. They require special hydraulic crimping equipment and tooling. When installing a grip in the field, this equipment needs to be taken along. The grips that use epoxy can take longer to apply as the epoxy requires a cure time. Crimp type grips are not as widely used in field installations as Chinese fingers type pulling grips.

Chinese Fingers Type Grips

Chinese fingers type pulling grips are a woven sleeve that are typically placed over the cable jacket (see Figure A). They are woven so the sleeve compresses tighter onto the cable as the pulling force increases. A Chinese fingers grip can be woven from many materials, however stranded steel is typically used. They are generally more expensive than a crimp type grip. Advantages of the Chinese fingers grips include no special equipment is requirements, a simple installation procedure, and the ability to be reused many times. A Chinese fingers grip can be reused until an inspection of the grip finds broken or partially broken steel strands. In reusing a grip the woven sleeve should be smoothed down to recondition the weave.

In a Chinese fingers grip additional elements are sometimes added to grip to other cable components besides the cable jacket. A typical addition is a loop for attaching cable strength elements. In many of todays fiber optic cable designs the primary strength elements are high strength yarns wrapped around the cable core. These yarns are connected directly to the Chinese fingers pulling grip by knotting them on the loop. High strength aramid yarns are typically used to obtain high knot strengths. Their high strength, good cut through resistance and toughness make them good choices for knotting. Other high strength yarns are used in fiber optic cables. Fiberglass yarns are used; however, to achieve good knotting properties they need to be mixed with aramid yarns. Fiberglass yarns have less cut through resistance and abrasion resistance than aramid yarns.

Siecor recommends the use of a Chinese fingers type pulling grip with their loose tube cable designs. In the past the recommendation included knotting a cable's high strength yarns to the loop. A problem with knotting is that knot strengths depend on the skill of the person making the knot. Even when an experienced person ties the knot strength, variability still exists. To address this issue the authors tested various techniques and types of knots.

Knot Strength

There were several approaches investigated to increase the reliability of the knot strength. The normal way of knotting the high strength yarns was the use of multiple half hitches. The new knots tried included the noose, timber hitch, the clinch knot, the studdingsail halyard bend, the fish knot and some modified knots. Other attempts included splitting the yarns before knotting them and coating the knotting loop with plastic or a cotton tape. Some of these attempts yielded modest improvements, however significant gains in strength and repeatability were not obtained.

In some tests, the Chinese fingers were not used. This isolated the strength of the knot. Test results are summarized in Figure B. The average strength of the knot types was very close to 20% of the yarns average breaking strength. There was considerable variation in the range of knot strengths obtained. The data was generated by a simple ramping up of the tension until the pulling grip separated from the cable. The failure location of the knots was consistently the first bend in the knot. This is the highest stress area in the knot. A suggested explanation for the knot failures is that the high strength yarns are cutting themselves. At this bend the bundles of small diameter yarns cross over each other at very high tensions. Although the yarns

were saturated with grease, after testing the yarns at the failure location were grease free. This indicates extremely high pressures.

Testing with both the knots and the Chinese fingers was done on the same length of cable. The difference between the tests with and without the Chinese fingers was approximately 500 Newtons. Because the failure mechanism for the Chinese finger's gripping was the cable jacket sliding over the rest of the cable this indicates that the jacket contributed 500 Newtons to the pulling strength of the cable.

DEVELOPMENT

A desire was to stay with a Chinese fingers type grip because of its simplicity, lack of special tooling required and user friendliness in the field. However, reliability in knotting was a problem. There were many ideas on how to improve the coupling between the yarns and the pulling grip. These did not incorporate a knot; however, they added to the complexity of the grip and the procedure.

One of the key problems was the hardness of the cable jacket combined with the thick jacket walls and small size of fiber optic cables. The compressive gripping force of the Chinese fingers is not transferred through the relatively hard Medium Density Polyethylene (MDPE) jacket. MDPE is used for its hardness to protect the cable core and its low coefficient of friction to provide easier cable installations. Bonding the high strength yarns tightly to the cable would be a solution; however, this would make a very stiff, inflexible cable. It would also be more difficult to access the cable core through these tightly bonded layers.

Developmental Details

To solve the problem of the hard jacket interfering with the gripping force, part of the jacket was removed, and the Chinese fingers were placed directly over the high strength yarns. This does not require special tooling or modifications to the pulling grip. The concept was proven by excellent initial test results on standard cable and by good results on a cable with a soft jacket. On the cable with the soft jacket the jacket was not removed, and the high strength yarns were not knotted. There was sufficient coupling of the yarns through this soft jacket to obtain good test results.

Work began on identifying the proper length of yarns to expose and other details to optimize the new pulling grip installation procedure. The concept of placing the Chinese fingers pulling grip over the high strength yarns was expanded to include placing the grip over all of the cable materials outside the cable core that provide significant strength. These materials could include cable jackets, steel armors and the high strength yarns. The length of a material exposed to the Chinese fingers was made proportional to the strength that the material provides; however, a minimum exposure length was maintained. This length is the minimum amount required to couple to the Chinese fingers.

To optimize the new pulling grip installation procedure, tape was wrapped around a portion of the exposed high strength yarns. This tape is a sticky rubber coated cotton fabric tape known as friction tape. The original purpose of the tape was to reduce the cutting of the yarns by the steel wires of the Chinese fingers grip. The tape spreads the compressive force of the steel wires where the yarns are under the highest tension. This area is furthest away from the end of the cable. Further testing showed that the friction tape improved the gripping action of the Chinese fingers.

Additional enhancements were made to the procedure to increase reliability without sacrificing user friendliness. To avoid damaging or disrupting the high strength yarns a new method of preparing the cable was developed. To remove the jacket over the high strength yarns the jacket is first radially notched, then bent to complete the break and pulled off. By not cutting the whole way through the jacket yarns are not accidentally cut. By pulling off the jacket the yarns are not disturbed from their uniform positioning obtained during manufacturing. The jacket over a steel armor is removed by shaving the jacket off on two sides with a common cable knife, and then simply peeling and cutting off the remaining two sections of jacket. This procedure avoids damaging the armor.

Description of the Procedure

A pulling grip is installed by first sliding the Chinese fingers grip over the cable and past the working area. The cable is prepared by removing the required amounts of material to expose the strength elements (See Figure C). The length of materials exposed is determined by a simple chart. A particular size of Chinese fingers pulling grip will work well within a certain diameter range of cable. Grips for larger cables are generally longer. To optimize the gripping strength for the longer pulling grips, all of the exposure lengths are increased. For ease of use this information is summarized in the form of a chart. For an example see Figure D.

After exposing the cable components, the friction tape is wrapped in a single layer around the high strength yarns. It is applied along one third of the length of the yarns (See Figure C). The pulling grip is then pulled

back over the prepared cable end, and tightly taped down with a Polyvinyl Chloride (PVC) tape. The cable is now ready to be installed.

TEST METHODS

Once a procedure was found for installing the pulling grip, a test procedure was needed which simulated field conditions. The procedure must test the grips under what is assumed as the worst conditions, yet must be consistent from test to test. The most stringent condition would be to put the grip under tension beyond the specified rating.

Typically, most tensile tests performed on cables are static loading over a period of time. The test procedures must simulate in the lab the various conditions a grip experiences in the field. The most stringent of the field pulls for tension would be a long haul pull through a duct with bends and/or pulleys. The optical cable would be pulled into existing ducts or plastic subducts. A pulling grip captures the strength members of the cable and is used to pull the cable into the duct via a preexisting pull rope. During the pull-in, the tension on the cable can be monitored and should not be allowed to exceed the specified tensile rating of that specific cable. However, during the pull, as more cable enters the duct, the force required to pull it increases. This force can be decreased by using lubricant to reduce friction, or by center pulls to reduce the cable mass being pulled over a specific route. The cable also experiences surges and jerks as it goes around bends and pulleys.

One can see then that the two most important variables to duplicate in the lab would be a gradual increase in tension over time, combined with surges or sudden increases and decreases in tension. We had an opportunity to monitor the tension on duct installations in Hudson, North Carolina. The graphs of tension versus time seen in Figure E were used as the model for the laboratory test procedures. From the model, a tensile loading cycle was implemented in which a stair step tension was introduced (See Figure F). The tension started at zero, increased to 100 pounds in 20 seconds, held at load for 1 minute, and then proceeded to 200, 300, ... , 1000 & 1050 pounds in the same manner. After three such cycles, the tension is reduced to 600 pounds and a wheel is pulled across the grip, simulating surging and banding (See Figure G). The reason behind three cycles is to see if fatigue is a factor in grip testing. The wheel pull is done at a reduced load so that the tension peaks during surging would not significantly exceed the safety factored loading. The entire procedure takes just over an hour. Alternate test procedures have been developed that contain the same key features (See Figure H).

A long-length tensile test machine was used for the testing. The scheme involves a movable capstan, anchored steel cable, steel wheel, motorized tensioning device and a load cell with digital tension readout. The pulling grip and a swivel are attached to the anchored steel cable and 15 meters from the grip, the optical cable is anchored by wrapping it around the capstan five times (Refer back to Figure G).

TEST RESULTS

The new method of installing pulling grips was tested with the developed test procedure. Initially the cable tested was the same cable design used for knot testing. This gives very good comparative data, and the cable design is a worst case. Significantly better results were obtained with the new procedure. In most cases the pulling grip did not fail; it remained firmly attached to the cable during the entire cycling test. These results are contained in Figure I. The percentages listed are derived from the maximum tensile load minus an assumed tensile contribution of the cable jacket (500 Newtons). This allows an easier comparison with the knot strength results in Figure B. The new method shows over a 50% improvement. In the new procedure there is a 33% contribution of the high strength yarns compared to the 20% for knotting. The 33% is conservative because most of the cables using the new procedure did not fail. All of the knot results were failures. In an additional test all of the aramid yarns were removed and just the fiberglass yarn reinforced cable was tested. In this test the contribution of the fiberglass was over 60%.

The testing was expanded to include steel tape armored cables and a range of cable designs and cable sizes. In all there were 10 unique cables tested with a total of 60 tests performed. In the expanded testing there were no pulling grip failures. In all cases the pulling grips exceeded 167% of the rated cable strength. The grips were not taken to failure because of tensile load limitations. The limitations were due to problems caused by greatly exceeding the rated cable strength. At the fixed attachment point for the cable there were cable abnormalities when extremely high tensile loads were attempted. At the fixed attachment point the cable goes from low tensile loading to high tensile loading in a short distance. Safety was another significant concern. The loading was kept below the tensile rating of steel cable and the swivel used in the test apparatus.

Field Conditions

Once it was determined that the new grip procedure works better than the knotting procedure, we needed to ensure that it was better under extreme field conditions. The four variables examined were 1)

method of stripping the cable 2) with/without friction tape 3) with/without a swivel 4) temperature extremes.

The first objective was to determine the effect of removing the optical cable's jacket using two different techniques. One technique employed using the ripcord to strip the jacket thus reducing the chance of cutting any high strength yarns. The second technique was to ring cut the jacket and pull it off the core. If the two methods were within 10% of each other, then the two methods were believed to be similar. Six tests conducted for each method showed there was no difference between the results. The maximum load was 1000 pounds and there were no other modes of failure (ie. slippage, movements between the grip and cable) noted during the test.

The second objective was to determine the importance of the friction tape. Again six pulls were conducted with tape, and six pulls were conducted without tape. Although the static pulls (ie. cycle 1 and cycle 2) showed that the two methods performed similarly, it was not until the surging in cycle 3 that the two methods were differentiated. The method of using friction tape saw less slippage and no failures when pulled around the wheel. The no tape method saw failures at the peak surges.

The next objective was to determine how twisting of the cable during installation would effect grip strength. It was found that not using a swivel to eliminate twisting did not skew the test results in any way. However, it is still recommended that a swivel be used during any cable duct installation.

The fourth objective was to quantify the effects of temperature on the performance of the pulling grip. Six grips were installed on cable sections and placed in a temperature chamber at -20°C for four hours. They were removed one at a time and tested to the tensile cycle. Another group of six grips were exposed to +40°C for four hours and tested in the same manner. The results showed no difference in grip performance at the two temperature extremes.

Craft Snsitivity

As an additional precaution tests were conducted to determine the sensitivity to the precision of installation. A standard pulling grip one size larger than optimum was installed on cables. There was no difference in the test results. Friction tape was applied over twice the length of the yarns than recommended. Here there was a loss of 100 pounds of tensile load capability, but still well over the cable rating. To model the field environment the installed pulling grip was soaked in pulling lubricant for 16 hours and then tested. The presence of the lubricant did not effect the test results.

Good test results were obtained from a number of different manufacturers' Chinese fingers pulling grips. There was differentiation between the different styles of pulling grips using slippage and broken yarn filaments as a criteria. (1) Very flexible grips worked better. (2) Grips with Chinese fingers that compressed with a wider, flatter surface worked better. A non-standard grip that was the least flexible would not work when it was one size too small for the cable. Even unusual modification worked well. A grip was made by weaving an aramid yarn pull tape (used like a rope to pull cables in a duct) around the cable to form a psuedo-Chinese fingers grip. This worked as well as any of the manufactured pulling grips in laboratory testing. Friction tape was not used with this aramid grip, however it had the widest, smoothest application of compression on the high strength yarns.

Field Results

Field results take three forms: Field trial, reports, craft reaction during training.

An initial field trial was performed at an actual customer site to determine two things: accuracy of the lab/field simulations and viability of the method in real-life conditions. Once underway, the cable was pulled with no grip failure or slippage. The span length was approximately 5,000 feet through one-inch subduct with lubrication. Tensions up to 400 lb were witnessed with surges of 50 to 120 lb. A capstan winch was used to pull the cable with its brake set to 600 lb. Figure J is a graph of tension versus time for this pull.

Favorable craft reaction during the field trial showed the procedure to be easily learned and installed. It was perceived as quicker than current methods. It has been used in regular training classes since its introduction, and the procedure has been well received for its simplicity.

CONCLUSION

From the work done on the pulling grips, two major objectives were achieved. On was a new qualification program for pulling grips which included a new tensile simulation. The simulation more accurately models actual field loading of the pulling grip. The program looks at normal variations in the field environment as well as variations in the grip installation practices.

The second achievement was the new procedure met the following requirements:

Improved Reliability

Craft-friendly

Average load at failure of 1,000 lb (400 lb safety margin)

Inexpensive

By eliminating knots from the installation procedure high strength yarns with low knot strength can be considered in new cable designs. Additionally, testing proved that the grip installation procedure was relatively craft insensitive. This was also proven over a range of cable sizes and designs. These facts make for a grip installation procedure which is quick to learn as well as reliable.

The key to the success of this program was the integration of customer requirements directly with development and testing. There was interaction with various customers throughout the program. This allowed for the development of a new procedure which met all the customers' requirements, and a trouble-free field introduction.

ACKNOWLEDGEMENTS

The authors would like to acknowledge the Telephony Cable Plant Product Evaluation Group and the Engineering Services Group for their support work and testing.

Figure A: Pulling Grip Types

Representation of a Crimp Type Pulling Grip

Representation of a Chinese Fingers Type Pulling Grip

Figure B:
Knot Strength Test Results
Data From Tests on a Length of Cable

Type of Knot	Number of Tests	Yarns Used	Strength of the Knot as a Percentage of the Average Breaking Strength of the Yarns		
			Minimum	Average	Maximum
Half Hitches	1	Aramid Only		29.3 %	
Half Hitches	1	Fiberglass Only		21.5 %	
Half Hitches	10	Aramid & FG	15.2 %	20.3 %	30.8 %
Two Half Hitches	11	Aramid & FG	16.8 %	21.9 %	26.3 %
Timber Hitch	3	Aramid & FG	20.3 %	22.1 %	24.5 %
Noose	1	Aramid & FG		18.4 %	
Clinch Knot	2	Aramid & FG	19.1 %	19.7 %	20.3 %
Studding Sail	6	Aramid & FG	13.3 %	20.0 %	24.3 %
All Knot Types	33	Aramid & FG	13.3 %	20.8 %	30.8 %

Two Half Hitches indicates the yarns were split into two groups and knotted seperately.
Studding Sail is short for Studdingsail Halyard Bend Knot.
Fiberglass has been abreviated as FG.

Figure C: Steps in Installing a Pulling Grip

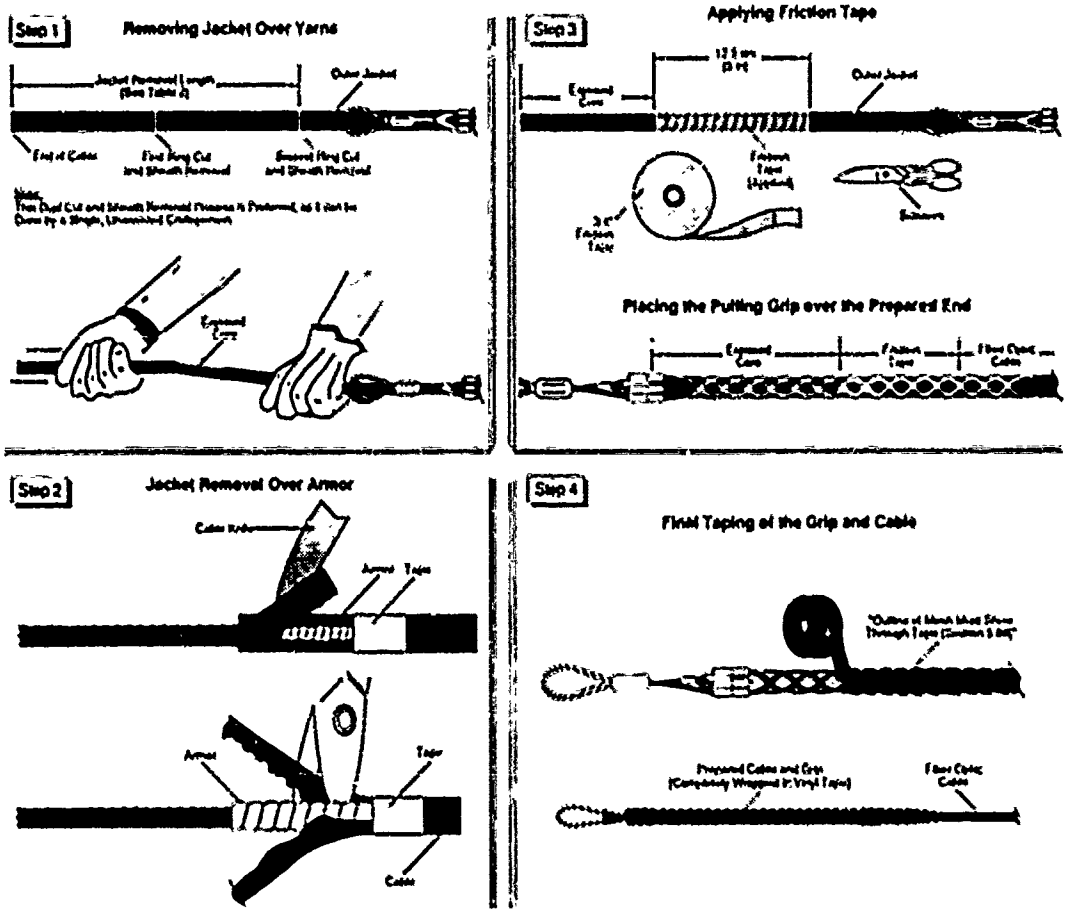

Figure D: Chart and Diagram for Preparing Cable

Pulling Grip		Dimensions of Cable	
Seccor Part Number	Mesh Length	C	A
GRP-012	18 in (45 cm)	14 in (36 cm)	6 in (15 cm)
GRP-013	21 in (40 cm)	16 in (40 cm)	7 in (18 cm)
GRP-014	24 in (45 cm)	18 in (45 cm)	8 in (20 cm)
GRP-015	27 in (50 cm)	20 in (50 cm)	10 in (25 cm)
GRP-016	30 in (53 cm)	21 in (53 cm)	12 in (30 cm)

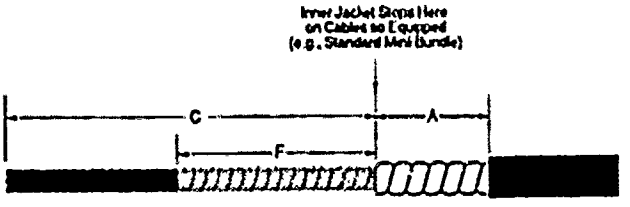

C — Length of Cable Core to Expose

F — Length of Friction Tape (5 in) to Apply

A — Length of Outer Jacket to Expose

Figure E: Pulling Force Diagrams for Cable Pulls in Hudson, North Carolina

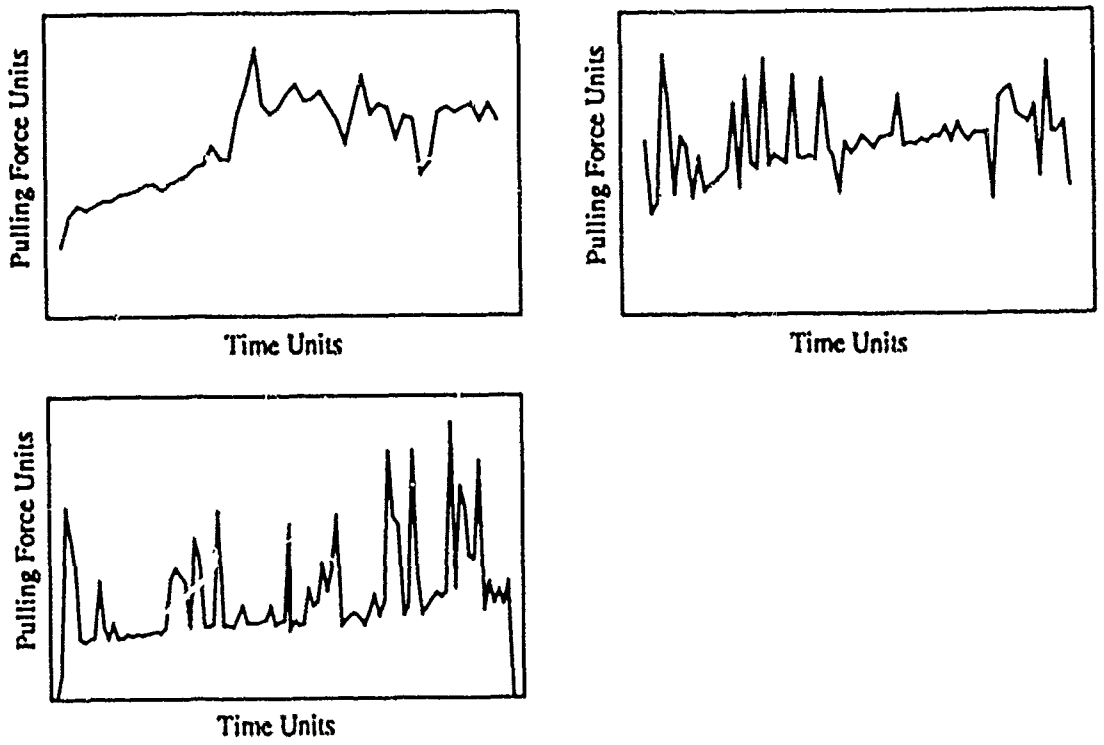

Figure F: Tensile Loading Process for Typical Pulling Grip Test

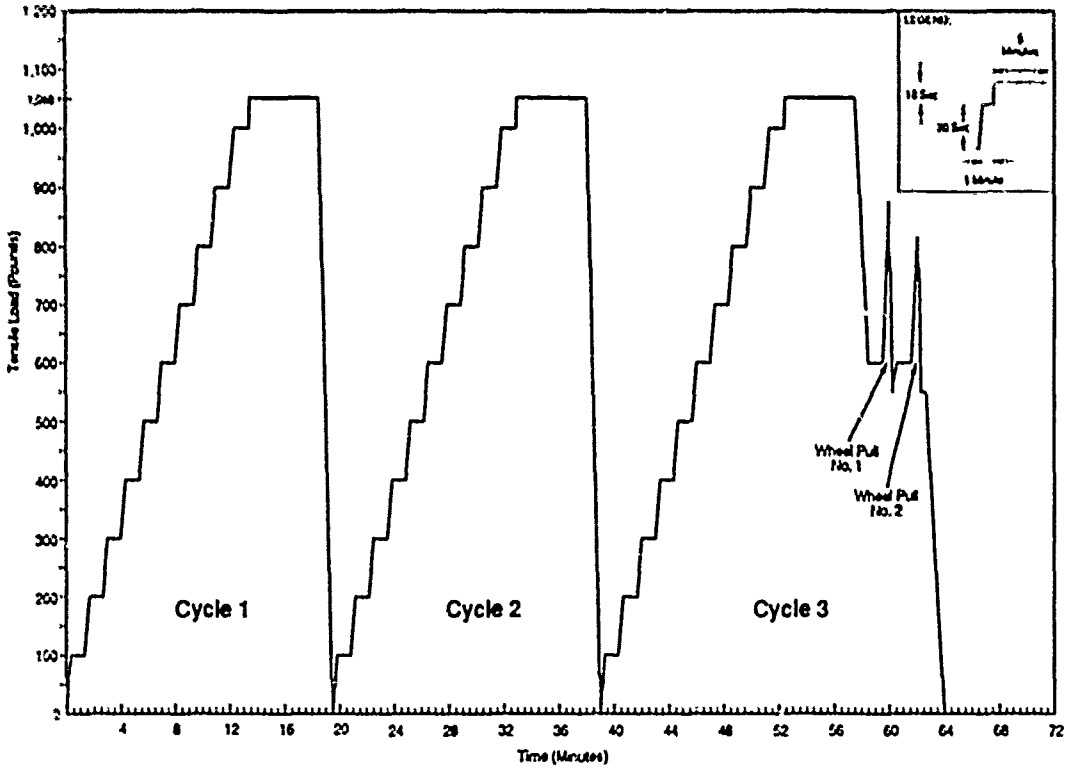

Figure G: Diagram of Test Equipment

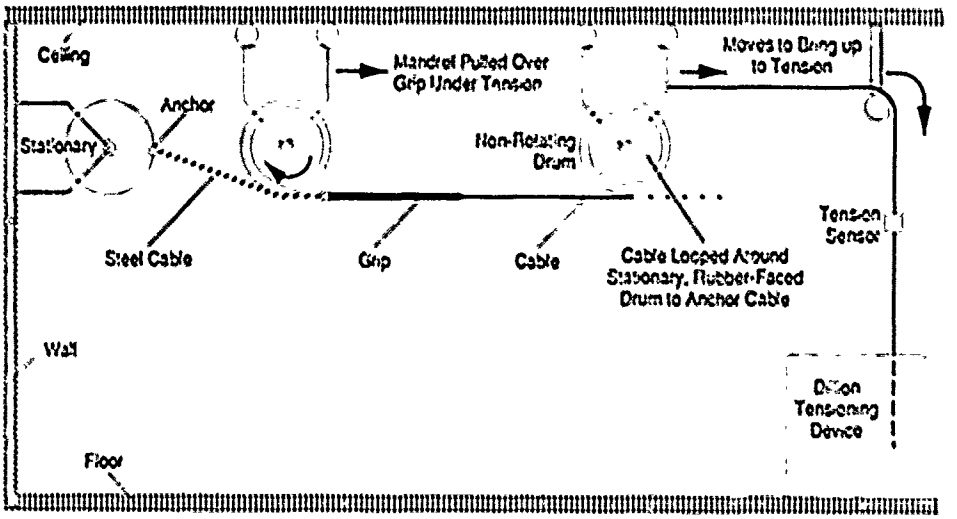

Note: This Illustration is Not to Scale

Figure H: Alternate Tensile Loading Process for Pulling Grip Test

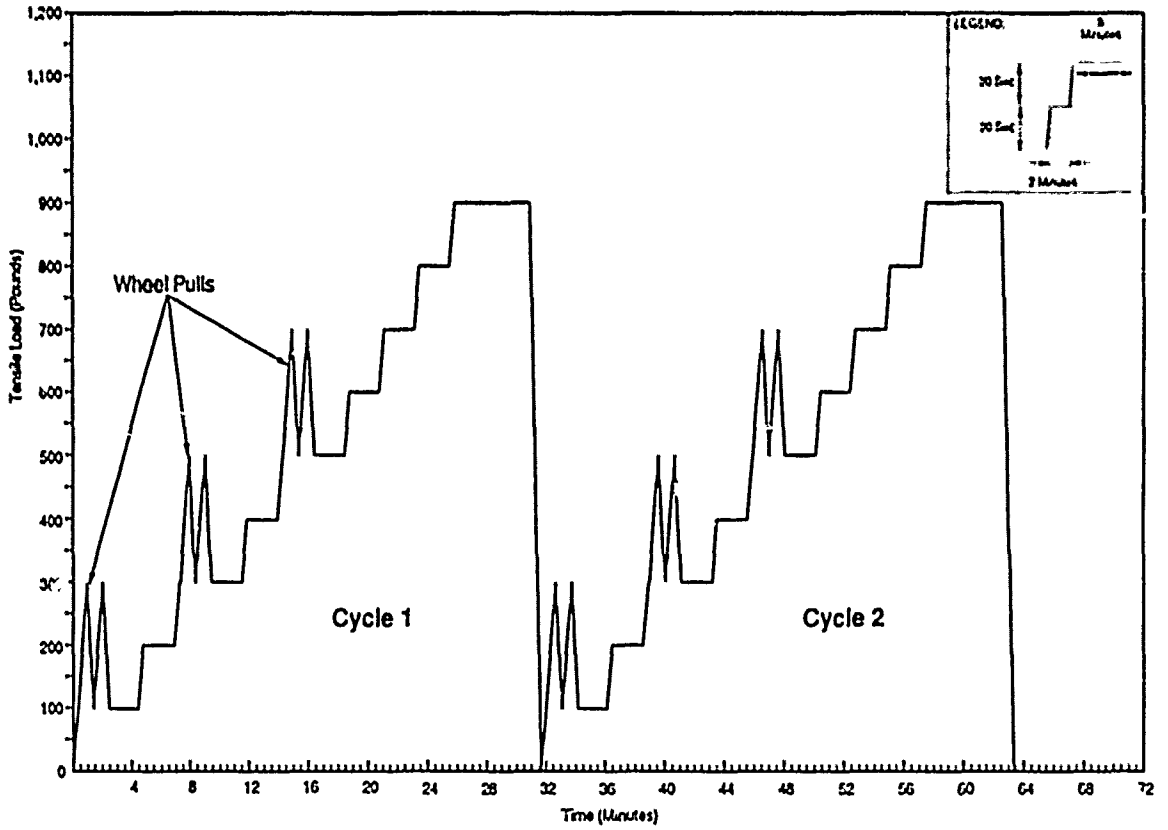

Note This Illustration is Approximately to Scale

Figure I:
Coupling Strength Between the High Strength Yarns and the Pulling Grip Using the New Pulling Grip Installation Procedure

Number of Tests	Yarns Used	Coupling Strength as a Percentage of the Average Breaking Strength of the Yarns		
		Minimum	Average	Maximum
25	Aramid & FG	28.0 %	33.0 % *	34.2 % *
3	Fiberglass Only	47.0 %	53.6 %	62.1 %

The average and maximum are conservative. They include non-failing tests.
Fiberglass has been abreviated as FG.

Figure J: Pulling Force Diagram for Initial Field Trial of the New Procedure

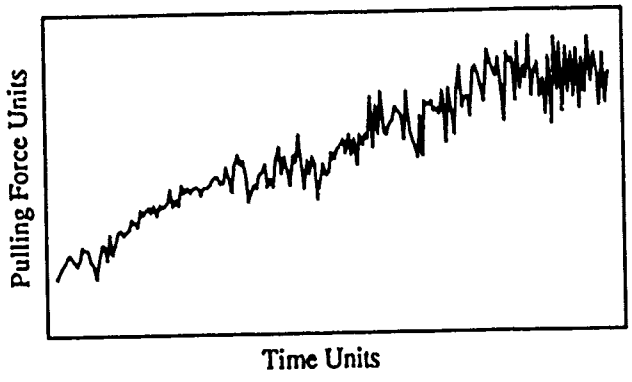

Mark E. Conner

Siecor Corporation
489 Siecor Park
Hickory, NC 28603

Mark E. Conner, originally from Winchester, Virginia, received his Bachelor of Science Degree in Engineering Physics from West Virginia Wesleyan College, Buckhannon, West Virginia in 1984. In 1987, he completed his Masters in Business Administration from Virginia Tech in Blacksburg, Virginia, after which he joined Siecor Corporation. He is currently a Project Engineer in Engineering Services, Siecor's Sales Support Group.

Steven L. Hassett

Siecor Corporation
489 Siecor Park
Hickory, NC 28603

Steven Hassett received a Bachelor of Science Degree in Engineering Science & Mechanics in 1981, a Bachelor of Science in Mechanical Engineering in 1982 and a Masters of Science in Mechanical Engineering in 1984 all from The Georgia Institute of Technology in Atlanta, Georgia. In 1984, he joined Siecor Corporation as a Process Engineer. He was the key member in the development and manufacture of Siecor's Pre-Connectorized Multi-Fiber Mechanical Splice. His current position is the Product Evaluation Supervisor for the Telephony Cable Plant in Hickory, North Carolina.

Richard S. Wagman

Siecor Corporation
489 Siecor Park
Hickory, NC 28603

S. Wagman was born in Dallastown, ania in 1956. He received his Bachelor of ence Degree in Engineering Science from The Pennsylvania State University in 1978, and his Bachelor of Science Degree in Electrical Engineering from The John Hopkins University in 1984. He worked for 7 years as a Product Engineer at Continental Wire & Cable before joining Siecor Corporation in 1985. At Siecor, he has worked in the product development area. He is currently employed as a Senior Product Development Engineer in the Research, Development and Engineering department.

"INTEGRATED FAMILY OF JOINING PRODUCTS FOR HIGH DENSITY FIBER OPTIC NETWORKS"

John C. Huber

3M TelComm Products

Abstract

The use of fiber optic networks for residential services, also called Fiber-to-the-Home (FTTH), Local Area Networks (LANs), and Multiplexed Backbones (MBs) has resulted in a need for cable jointing products that accommodate high fiber count cables (144+) and yet are easy to use by the ordinary craft person. An integrated family of jointing products for high density fiber networks is described. Each one has been specifically designed for large fiber count cables. Each one features both compact size and fast installation. Included in the family are -- splice (fiber joint), splice closure (sheath joint), patch panel (fiber distribution unit), connector/splice module, and fiber termination unit.

Description

The splice was described in a paper, "Mechanical Optical Fiber Splice Containing an Articulated Conformable Metallic Element" by Richard A. Patterson, at the 1988 International Wire and Cable Symposium and will not be described in detail. Its uniqueness is its speed of installation (90% less than 30 seconds), low loss (90% less than .2 dB), low reflection (90% better than -35 dB), important advantages in FTTH, LAN and MB applications. It is faster to install because it only requires insertion of the fiber ends and pushing a button, contrasted to other splices which require assembling several pieces together.

The connector/splice module will be described in a companion paper "Fiber Optic Terminating Units with Low-Loss Mechanical Splicing" by Roger H. Keith. Its uniqueness is its speed of installation (90% less than 30 seconds), low loss (90% less than .6 dB), low reflection (90% less than -40 dB), important advantages in FTTH applications. Its modularity and ease of use are important advantages in LAN and MB applications. It is faster to install because it uses the splice discussed above to attach a fiber to a connector.

The fiber termination unit is also described in the above companion paper. It uniqueness is its small size (8 ST or FC connectors in 14x5x1 inch (35.5x12.7x2.5 cm) and yet easy access, important advantages in FTTH, LAN and MB applications. It is faster to install because it uses the connector/splice module described above to put fibers into service.

The splice closure is unique in providing a separate storage volume for uncut (express) fibers and split cable ports, important advantages in tapered cable FTTH installations. It is also unique in the ease of adding additional cable ports, an important advantage in expanding the number of branch cables in FTTH, LAN and MB installations. The fiber termination unit described above fits inside the closure, so it provides an environmentally secure connection field, an important advantage in FTTH applications. It is also unique in being appropriate for buried, underground, aerial and indoor applications, an important advantage in craft training. Being unfilled, it can be installed in buried or underground applications faster than others.

The patch panel is uniq in

providing high density of interconnections (624 in a 7 ft (2.1 m) rack), yet easy access by sliding the connector forward from its neighbors.

The family of products is integrated by using the splice in the connector/splice module, by inserting the connector/splice module in the fiber termination unit, providing an easy to use method of incrementally adding connectors, this is important for Fiber-to-the-Home, Multiplexed Backbone and Local Area Networks. For Fiber-to-the-Home applications, integration is further accomplished by inserting the above modular system inside the splice closure, providing an easy to use method of attaching subscriber drops to the distribution cable.

Conclusion

An integrated family of products provides improved ease of use and speed of installation. Craft training is simplified and a consistent "look and feel" throughout installations results in fewer errors. Integration is achieved by designing each component for ease of use in its individual application and also designing each component for intermateability with companion components in more complex applications.

John C. Huber
TelComm Products/3M
Bldg A147-2N-01
PO Box 2963
Aust TX 78769-2963

John C. Huber received his PhD in Electrical Engineering from the University of Missouri - Columbia in 1965. Previous to joining 3M Company that year, he worked for Texas Instruments, Emerson Electric, Oak Ridge National Lab and Argonne National Lab. At 3M he has spent 13 years in product development and 11 years in sales and marketing. Most of this work has been with telecommunications related products. Presently he is manager of Fiber Optic Component Development in the TelComm Products Div.

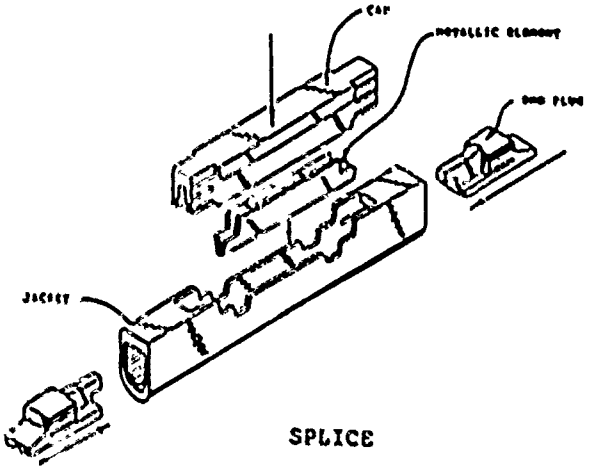

SPLICE

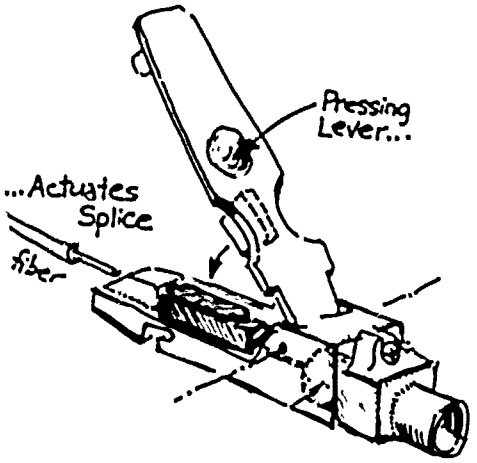

SPLICE/CONNECTOR MODULE

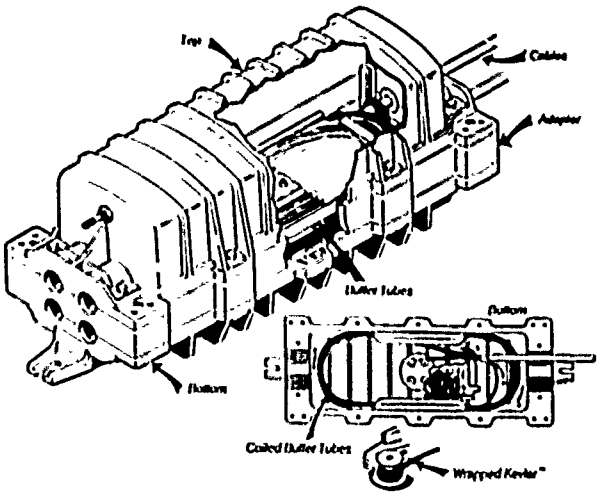

SPLICE CLOSURE WITH FIBER TERMINATION UNITS

FIBER OPTIC TERMINATING UNITS WITH LOW-LOSS MECHANICAL SPLICING

Roger H. Keith, P.E.

3M TelComm Products Laboratory

Summary

A new, versatile system of plug-in units accomodates a wide variety of fiber optic and electrical connectors in a single family of housings. Reliable fiber mechanical splices are combined with connector pigtails in the plug-ins, which include a splice actuator tool and thus eliminate long fiber slack formerly needed for splicing at a separate workstation. A unique tip-up feature gives full finger access to connector plugs along with high plug density.

A number of different housings accomodate the plug-ins, and are tailored for building entrances, riser and distribution closets, work stations, trunk cable splice points, and home/apartment drop terminals.

Introduction. The rapid growth of optical fiber use and the parallel improvments in fiber technology make the choice of fiber terminations a crucial concern to allow emerging connector improvements and standards in a system specified and installed today. The flexibility to handle electrical along with optical media is a requirement for fiber systems which augment existing copper networks, but may be a key feature of future systems as well. A complementary design for network housings incorporates interchangeable plug-in modules which can be added or exchanged to give unique optical fiber splice and connection abilities. Modules can also provide electrical connections for order talk pairs, coaxial cabling, or auxiliary signalling power.

Compactness. Fiber optic connectors have been packed densely, but in the process, it has been difficult to get finger access to add or remove connectors. Staggering or wide spacing of rows have addressed this problem, but the resulting connector arrays either compromise accessibility or compactness.

Figure 1 shows the new arrangement. Connectors are tightly packed in a row, but are hinged so each can be individually

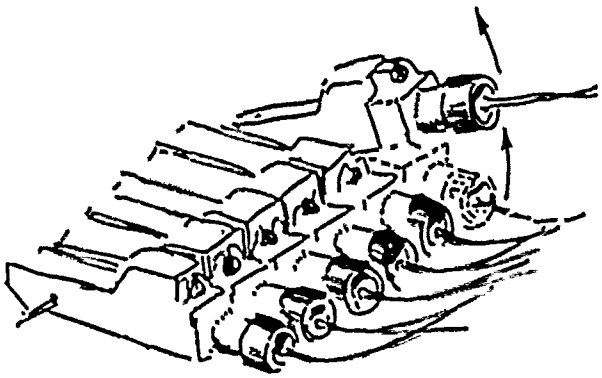

Figure 1. Row of Tip-up Connectors

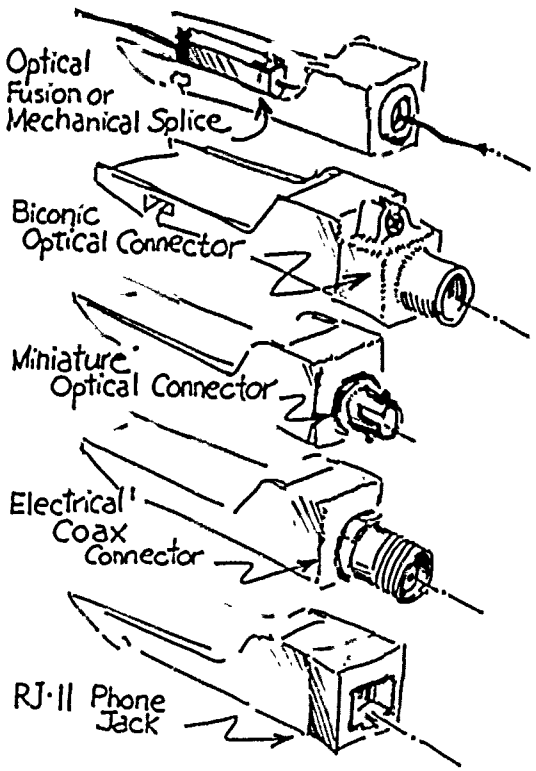

Figure 2. Plug-in Functions

tipped up for finger access at will. It can be seen that this arrangement is particularly appropriate for fiber optic connectors. A tip-up action places a negligible bend on the fiber and has little tendency to disturb adjacent lines. A resulting array of 6 biconic connectors can be as little as 4.6 inches (11.6 cm) wide, and on the order of 1 inch (25 mm) high.

Versatility. The plug-in cartridges can be made to accomodate practically any type of optical fiber connector: biconic, FC, ST, SMA, and other miniature connectors are easily incorporated into the cartridge, and electrical connections for talk pairs (RJ-11,) RCA type phono, Motorola type antenna, and a host of commercial coax or military-type multipin bulkhead connectors can be accomodated. If a single housing is needed for a small number of splices, alongside a few connectors, some of the plug-in units may be dedicated to splices. Examples of these plug-ins are shown in Figure 2.

Optical Splice + Connector. A particularly useful type of plug-in incorporates a splice and a short connector pigtail plug, installed in a mating connector. This arrangement allows rapid field attachment of a plug, using a factory made plug pigtail. This scheme has special merit if the splice is a reliable mechanical splice which can be crimped onto the fiber using a simple tool. The requirements for expensive fusion apparatus, or field fiber polishing and plug epoxying are eliminated with mechanical splices. A splice actuated with a simple crimping tool is particularly appropriate. With the provision of a crimping tool action within each of the plug-in units, the need for fiber slack to reach a fusion splicer or tool, and the problems with subsequent fiber storage are also eliminated. This arrangement in its simplest form is shown in Figure 3.

Plug-in Unit Housing. By building the splice actuator in each plug-in unit, and thus eliminating the need for excess fiber slack to reach an external splicing station, a housing can be designed and built which needs only accomodate the slack necessary for managing radius and direction changes. An extremely compact arrangement can result, holding six connectors and their splices, yet meeting all requirements for a 4" (100mm) fiber diameter for the most exacting single mode fiber bend optical and strength requirements. The resulting design is barely over 1" (25 mm) high, about 5.6 inches (14.2 cm) wide, and its 13.3 inch (33.8 cm)length easily fits between standard 2 x 4 stud centers or within utility cabinets sized to fit that opening. The housing can be applied to the backplane of a communications closet, or used as a surface mount box. Figure 4 shows one such design.

Figure 5 shows how a transparent divider fits over the fiber loop to retain and protect it, and also holds the plug-in operating levers to retain a plug-in the the uptilted position for connector access.

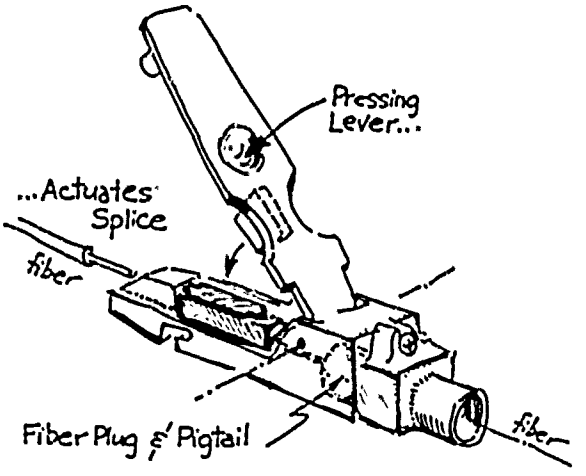

Figure 3. Plug-in With Integral Mechanical Splice Crimp Tool

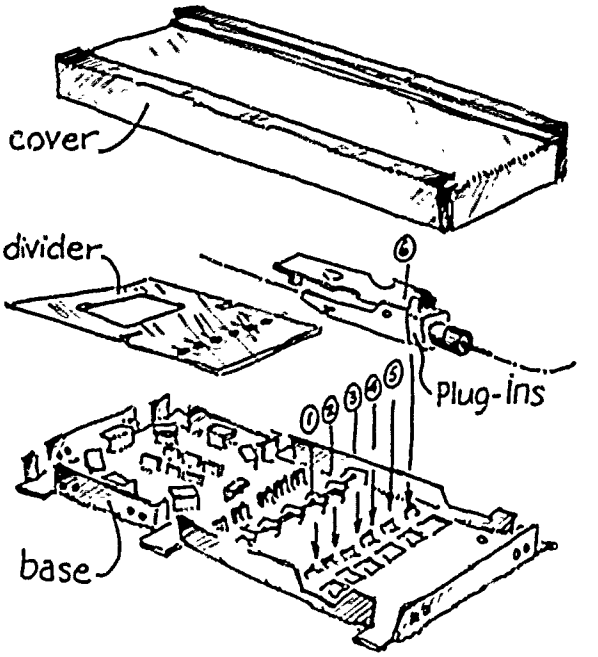

Figure 4. Housing for Plug-ins

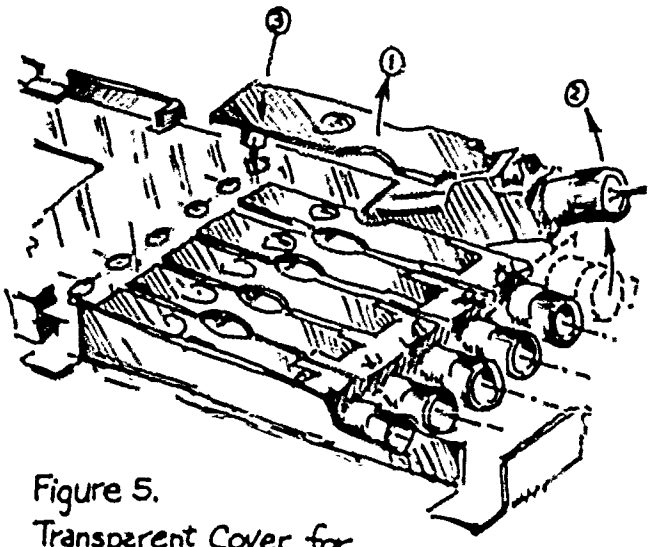

Figure 5.
Transparent Cover for Fiber Slack Holds Plug-in Up for Connector Access

In installation, the fiber splicer would dress each fiber in the housing, cleave it to the proper length, and insert it into the mechanical splice of the appropriate plug-in. Pressing the actuator lever crimps the splice. When all splices have been made, the splicer inserts the transparent divider to retain the looped fiber. The fibers, the splices, and the divider are not touched again.

To make or change fiber connections, the actuator lever is used to tilt each plug-in upwards to attach a fiber plug to each connector in turn. A series of holes in the divider receive pins in the levers to hold each plug-in in the "up" position while the connection is being made.

The plug-in is tipped back to the lower position, in line with the other connectors, until access may be needed for jumper or other plug changeout.

Copper cable compatibility. The box can be mounted on 1.2 inch (32 mm) standoffs on a backplane to give room for cabling in the same location, either terminating or passing through as part of a new or existing installation: This arrangement runs fiber or copper cables in a full width "subway" beneath the box, so space between studs or on the backplane is conserved, yet the fiber installation is fully accessible.

In still another way, the new housings are "compatible with copper," and are logically laid out in accord with experience in the way a telephone protected entrance terminal is arranged, with the incoming "field" cabling at one side, and the separate "house" lines exiting at the other. The fiber plug-ins of the new design are analogous to the protector options for many duties they can perform in the common PET. Figure 6 illustrates this design parallel.

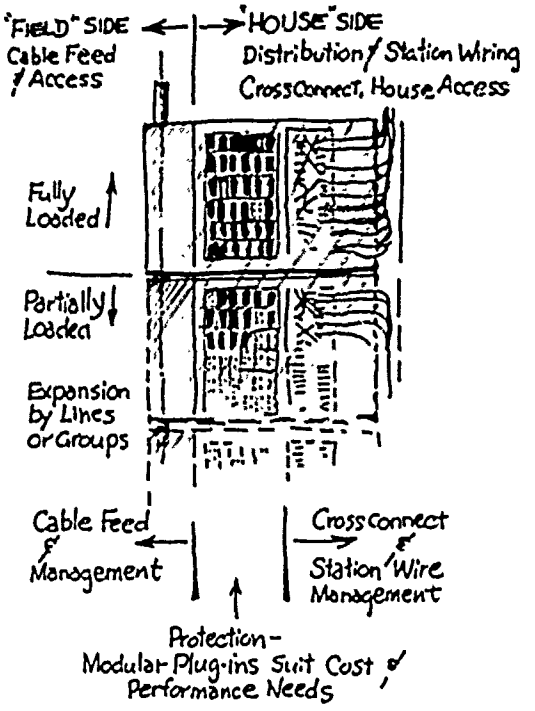

Figure 6A. Protected Entrance Terminal - Traditional Flow of Wiring & Allocation of Functions.

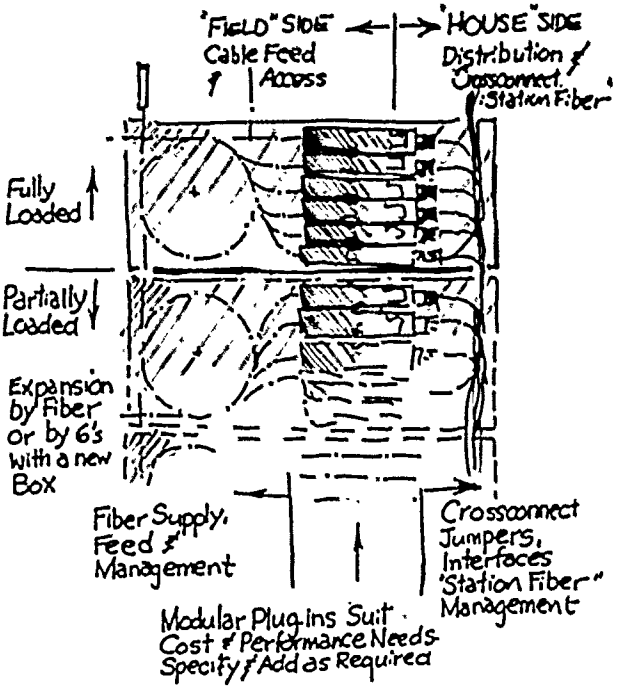

Figure 6B. Fiber Housing - Analogous Flow of Fiber & Allocation of Functions

The Interchangeablility Principle. Just as a camera system which has interchangeable lenses provide versatility and accomodate drastic future changes in mission, scope and skill, this new system for fiber optic connectors and splices gives future flexibility which optical systems designers need:

The plug-in units have a common footprint interface, so practically any present or future fiber optic plug standard can be accomodated in the same family of housings. --And housings can be designed to suit a given location or service universally, without special regard for the connectors they contain, since the same housing can hold any of a number of connector options.

The resulting system is tailored much like the lenses and bodies of a camera system: the connector/splice plug-in suits the communications line employed, and depends upon the medium, the service and standards involved, much like the lens of a camera suits the picture-taking task. The connector housings, on the other hand, are like camera bodies which are designed for the location and assignment mission.

Figure 7 illustrates several designs for housings to meet the needs of closet backplanes and utility boxes, miniature housings mounted over electrical outlet boxes at workstations, fiber home distribution garden terminals, and trunk cable splice case crossconnecting, all using the same plug-in design interface. Other applications and designs come readily to mind and are being added.

A broad view of the way in which these housings are a part of a comprehensive equipment plan for optical fiber systems is given in a related paper "Integrated Family of Joining Products for High Density Fiber Optic Networks" being presented by John C. Huber at this Symposium.

System Components. Housings can be combined to accomodate larger numbers of fiber or copper lines: Lines can be added one at a time to an existing housing, or 6 at a time in new housings. Connectors and media can be changed out at any time by substituting the appropriate plug-in.

A related enclosure houses loose fiber or buffer tube slack, and another can be used solely as a case to contain either fusion or mechanical splices. These related housings have a footprint, cover, and similar cable entries and exits in common so they work with the splice/connector housing described earlier.

A novel expandable hook set accumulates excess cable or buffered fiber. The hooks

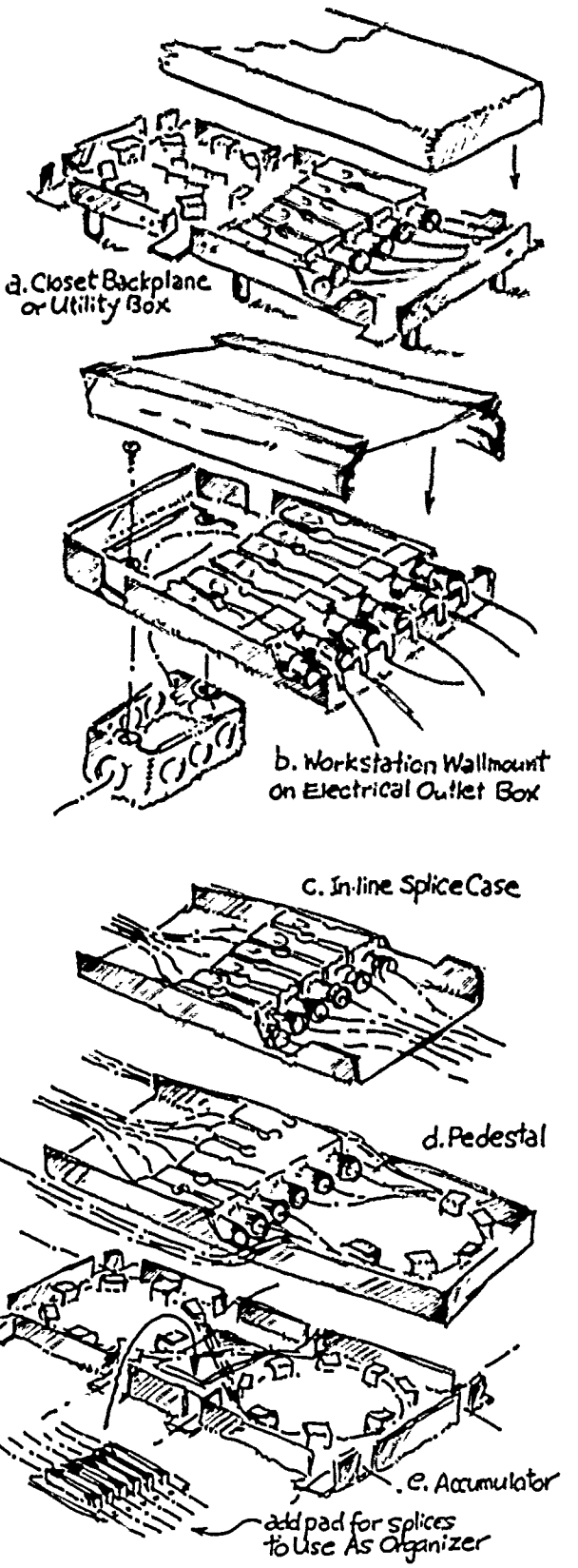

Figure 7. Housing Designs for Various Locations

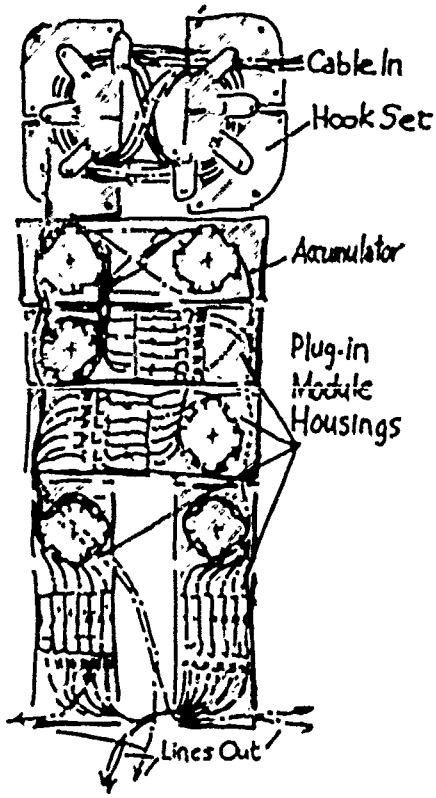

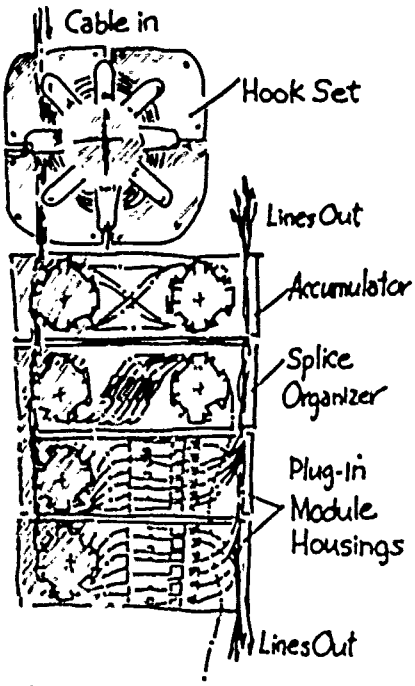

Figure 8. System Components Combined - Plan Views

can be spaced closely to give a cable reel with a diameter of about 8 inches (20 cm), or installed so each quarter circle of hooks is spaced out from its neighbors to give larger radii or capacity. A pair of hook sets allows figure-8 cable accumulation, and half-sets can be used to hang jumpers and spare cable. Figure 8 shows how these components can be related and combined.

Acknowledgements.

Ron Bossard of 3M conceived and developed the splice and connector unit, and the features which incorporate a mechanical splice crimp actuator in it. Ray Kastens of 3M is co-designer of the expandible slack storage hook system, and performed the computer drafting for the system.

References.

Huber, J.C, "Integrated Family of Joining Products for High Density Fiber Optic Networks" Proc. Intl Wire & Cable Symp. Nov. 1989

Lin, T. & Justice, B. "Return Loss of Fibrlok[tm] Optical Splice" private communication, 3M Co. June, 1989

Patterson, R.A. "Mechanical Optical Fiber Splice Containing an Articulated Conformable Metallic Element" Proc. 37th Intl. Wire & Cable Symp. Nov. 1988

Suhir, E. "Bending Performance of Clamped Optical Fibers: Stresses Due to the End Off-set" Applied Optics V.28, 3. pp 573-6, Feb 1989.

Roger H. Keith is a Senior Product Development Specialist with 3M TelComm Products Division Austin Laboratory, Bldg A147-2N, P.O. Box 2963, Austin, TX 78769, where he is responsible for fiber optic system component designs. Roger is a senior member of the Instrument Society of America and Director of their Telecom Division, and chairman of the Balcones Fault (Austin) Section of the American Institute of Chemical Engineers.

EFFECT OF SHEATH PROCESSING PARAMETERS ON CABLE PERFORMANCE

William F. Busch, Kenneth E. Bow, Daniel G. Pikula

Dow Chemical, USA

ABSTRACT

The improved mechanical properties of a cable sheath using coated metal tape is the result of the synergistic effect of bonding the metal tape to the jacket. Mechanical properties of the cable showing improvement due to this "bonded sheath" include bend performance and resistance to buckling or crushing during installation.

This paper will show that a fundamental relationship exists between the jacket bond strength and cable bend performance. The relationship between corrugation depth and the Young's Modulus of the cable sheath will also be shown. The effect of corrugation fill and profile also play roles in cable performance. Seam sealing techniques will also be discussed.

INTRODUCTION

The performance of a cable during installation and use is a function of the total cable design, including both the core materials and construction, and the sheath materials and construction.[1] This paper will address performance of cables using polyethylene copolymer coated steel armoring tapes in the cable sheath construction. Also addressed, as a benchmark, will be the performance of similar cables which utilize bare steel armoring tapes. The analysis of measuring the mechanical performance of a cable using a bonded sheath design is complex. For purposes of this paper, an attempt has been made to minimize the core material variations such that the data presented within this paper will show what effect the sheath has on the properties of the finished cable.

The performance of a cable with a bonded sheath is the result of the synergistic effect of bonding a metal tape to the jacket. The factors which affect this synergy include:

- The properties of the jacketing material;
- The properties of the metal armoring tape;
- The properties of the adhesive coating on the metal armoring tape; and
- The manufacturing process used to produce the cable sheath.

All of these individual factors, and their inter-relationship in the cable sheath, result in a cable which will meet the desired end use requirements.

THE BONDED SHEATH

Shielding and armoring tapes can be longitudinally applied to the cable core. If these tapes are plastic coated, they can be adhesively bonded to the cable jacket thereby forming a bonded sheath. The numerous advantages of utilizing the bonded sheath in cable construction compared to the same metal tape if bare are well known.[2,3] These advantages include improved mechanical properties, ability to provide a radial moisture barrier if the overlap seam is sealed, and corrosion protection for the metal tape. These advantages of the bonded sheath are contingent upon proper processing technique during the cable manufacturing process. Improper processing of the cable sheath materials may result in decreased or even unacceptable mechanical performance. One example, discussed at the 37th International Wire and Cable Symposium, is that improper forming of the coated steel armoring tape can result in a phenomenon known as 'zippering'.[4] This paper will discuss the processing parameters associated with the manufacture of a bonded sheath using coated steel armoring tape. It will be shown that by control of these parameters a sheath can be manufactured which does not possess any inherent weakness, such as 'zippering.' Instead, a superior cable sheath will result which will meet or exceed all of the industry cable performance requirements.

SAMPLE PREPARATION

All of the cable samples for this investigation were produced on an experimental cable line using commercially available equipment. The coated steel tapes were formed using a commercially available cone former and sizing dies. Typical line speeds were 32 fpm (10 m/mn). Standard conditions were used to extrude a commercially available linear low density polyethylene jacketing resin. All the plastic coated steel tapes used for the armoring of the cable specimens utilized ethylene acrylic acid copolymer coatings. The coatings were 0.002 inch (0.05 mm) thick. The steel was 0.006 inch (0.15 mm) thick, and electrolytically chrome coated (ECCS). This product meets the requirements of various industry specifications including Bellcore TA-TSY-000421 and REA Specifications PE-39 and PE-90.

For laboratory studies, the method of producing the specimens for evaluation involve preparing a plaque of the jacketing resin using platen presses, and then bonding the coated metal to the jacketing resin plaque. For polyethylene jacketing resins, the temperature of the platen press is set to 320°F (182°C). Sixty grams of resin are poured into a mold which will produce a plaque 0.075 inch (1.9 mm) thick. A non-

adhesive plastic is used to prevent the jacketing resin from adhering to the metal molding frame. The composite structure is then placed into the platen press and activated to a pressure of 25 ton (222.4 kN) force for 2.5 minutes. The assembly is then removed from the hot side of the platen press and placed in the cold side at 60°F (16°C), where the assembly is again activated to a pressure of 25 ton (222.4 kN) force for 2.5 minutes, after which the assembly is removed and dismantled, with the plaque of jacketing resin available for testing.

The formation of the composite coated metal/polyethylene jacketing resin structure follows a similar procedure. The platen press is again set at 320°F (182°C). The plastic coated steel tape and the jacketing resin plaque are placed between sheets of non-adhesive plastic and the molding frame used earlier to produce the plaque. The press is activated to a pressure of 5 ton (44.5 kN) force for 2.5 minutes, after which the assembly is placed on the cold side of the platen press at 60°F (16°C), at 5 ton (44.5 kN) of force, for another 2.5 minutes, after which the assembly is removed from the press and disassembled. The conditions for the plaque preparation have been closely studied, and the above conditions simulate to a certain degree both the temperatures and time involved in the actual cable line during the jacket extrusion process.

RESULTS AND DISCUSSION

Five different material and processing parameters for the cable sheath will be addressed in this paper. They are:

1. Jacket Bond Strength
2. Jacket Resin Thickness
3. Corrugation Depth
4. Corrugation Fill
5. Overlap Forming

A discussion of each parameter will be presented.

1. JACKET BOND STRENGTH:

One of the first studies undertaken with the introduction of the bonded sheath was to determine what effect the adhesion of the coated steel to the jacketing resin had on the mechanical performance of the cable. Procedures based on ASTM 4565 were used to measure the jacket bond strength. Figure 1 shows the effect of the jacket bond strength of the coated metal and jacketing resin on the resulting cable bend performance. By modifying the polyethylene copolymer and cable line processing conditions, we were able to generate a family of cable samples with varying degrees of bond strength. As shown by the data, a fundamental relationship exists between the jacket bond strength between the coated steel tape and jacketing resin and the cable bend performance, the higher the jacket bond strength the greater the cable bend performance. This fundamental relationship holds true for all types of substrate metals, including steel, aluminum, copper, and stainless steel.

2. JACKET RESIN THICKNESS:

For a given set of processing parameters, it has also been shown that a fundamental relationship exists between jacket resin thickness and cable bend performance. As the thickness of the jacketing resin increases, the measured jacket bond strength increases, as does the cable bend performance. There are two possible causes for this increase in jacket bond strength. The first is that the thicker jacket imparts a greater amount of thermal energy to the coated metal tape during the manufacture of the cable sheath. This increased thermal energy imparted to the system results in a stronger bond between the coated metal and the jacketing resin. A second explanation is related to the parameters of the standard jacket bond strength test. If the tail of the composite structure is allowed to float during the adhesion test, then the angle of separation is altered continuously between the jacket and the coated steel tape, resulting in different adhesive bond strength numbers depending on the angle of separation. A thicker jacket can alter the angle of separation differently than a thinner jacket.

The relationship between the angle of separation and the measured adhesive strength between two different materials has been explored. As the angle of separation changes from 90 degrees to 180 degrees, the measured adhesive strength between the two materials will increase.[5] Using a backing plate to fix the angle of separation at 180 degrees eliminates the possibility of the test geometry affecting the measured adhesive strength between the two materials.

Determination of the effect of thicker jackets on the jacket bond strength involved running the jacket bond strength test using a platen press to produce jacketing resin plaques and composite samples. In this case, the same amount of total energy is put into the system with the differences being jacketing resin thickness. Running this test with a backing plate to fix the angle of separation at 180 degrees shows no difference in measured adhesive strength. When the the tail was allowed to float, the thicker the jacketing resin plaque the higher the measured adhesive strength. The use of a backing plate with samples produced on the cable line under the same processing conditions, except for the jacketing resin extruder output, indicates that the thicker the jacket the higher the jacket bond strength. Thus the measured increase in adhesion is due to the increased thermal energy imparted to the system, and is not a function of the jacket thickness.

The current jacket resin thickness requirements are significantly different between those specified by the Rural Electrification Administration (REA) and Bell Communications Research (Bellcore) for copper pair cable. Column 1 in Table 1 is a listing of different cable over the core diameters. Column 2 in Table 1 is developed from REA PE-22 and shows the minimum average thickness permitted for Air Core Aerial and Underground Telephone Cable using the End Sampling Measurement Technique for the given over the core diameter. Column 3 in Table 1 is developed from REA PE-39 and shows the minimum average thickness permitted for Filled Telephone Cable using the End Sampling Measurement Technique for the given over the core diameter. Column 4 in Table 1 is developed using Bellcore TR-TSY-000421, Issue 2, June 1988, and shows the minimum average thickness requirements for the same over the core diameter for Metallic Telecommunication Cables using the End Sampling Measurement Technique. As one can see, the minimum jacket resin thickness requirement is much greater for cable produced against the PE-22 and PE-39 specifications than the TR-TSY-000421 at the larger over the core diameters.

Also worthy of mention here is that the choice of jacketing resin is also a factor in determination of the functionality of the cable sheath. As developed by Maguire and Rossi, it appears that flexular modulus should be used to determine the choice of jacketing resin, with a upper limit of about 80,000 psi (55.2 MPa).[6]

3&4. CORRUGATION DEPTH AND FILL:

Theoretical (Laboratory) Relationships of Corrugation Parameters

To achieve cable flexibility, corrugated coated steel tapes are most frequently used. The corrugated coated steel tape acts as a bellows, imparting much greater flexibility to the cable than if the coated steel tape is used smooth. Important parameters in the functionality of a cable

sheath are the number, depth, profile, and amount of fill of the corrugations in the coated steel armoring tape. The industry appears to follow the practice of increasing corrugation depth with increasing cable diameter. For smaller cable diameters, the number of corrugations per inch are increased, but with shallower corrugation depth. But the question which remains is which corrugation parameters impart the greatest flexibility to the cable using coated steel tape?

When the use of coated steel armoring tapes was introduced to the industry, one study which was initiated was to evaluate the effect of the coated steel armoring tape on the tensile strength of the cable sheath. Figure 2 shows the relationship between the depth of corrugation of the coated steel armoring tape and the Young's Modulus of the composite coated steel/jacketing resin structure. This structure was made by corrugating coated steel tapes to various depths, and then forming a coated steel/jacketing resin composite plaque as described earlier to evaluate the jacket bond strength of the coated steel. For this study 10 corrugations per inch (25.4 mm) were used. The cross-sectional area used in the calculation of the Young's Modulus is based only on the coated steel tape, not the composite structure. Instead of measuring the jacket bond strength of the composite plaque, a one inch wide strip of material was cut out of the plaque, pulled in a tensile test, and the Young's Modulus was measured.

With no corrugations, the Young's Modulus of the cable sheath is equal to that of the substrate steel used in the coated steel armoring tape, about 30 MM psi (20,000 kN/cm²). The strength of the cable sheath is equal to that of the steel substrate component. As the depth of corrugation increases, the Young's Modulus of the cable sheath (based on the thickness of the substrate steel) becomes less; at a corrugation depth of about 0.022 to 0.024 inch (0.56 to 0.61 mm) the Young's Modulus equals that of the cable sheath jacketing resin, about 200,000 psi (133.3 kN/cm²).

This same type of information is shown in Figure 3, where the relationship between smooth and corrugated coated steel tape versus sheath tensile strength at very low elongations is presented. The same laboratory procedure to produce the above samples was followed to produce these samples as well. The corrugation depth of the steel was set at a standard depth of about 0.032" (0.81 mm), with 10 corrugations per inch (25.4 mm).

A tensile force on the specimen tends to pull the corrugations out, resulting in very low load values to achieve a given sheath elongation. For example, at 0.1% elongation, the total load on the plaque with smooth coated steel is about 40 lb (18.1 kg), while at the same elongation for the plaque with corrugated coated steel the load is only about 5 lb (2.3 kg).

This work gives significant insight into the functionality of the cable sheath. There exists a fundamental relationship between the corrugation depth and the cable mechanical performance; a critical depth is required before the bellows effect is present and the cable has sufficient flexibility. Next we will show that this flexibility can be related directly to the cable bend performance. As the depth of corrugation increases, the cable bend performance increases.

Cable Performance Relationships To Corrugation Parameters

Extensive testing of finished cable by a number of different manufacturers indicates that there is a 'critical depth' of corrugation, below which the cable bend performance is marginal. Measurements indicate that this depth is around 0.020 inch (0.51 mm) to 0.024 inch (0.61 mm), the same depth where the Young's Modulus of the corrugated coated steel tape equals that of the jacketing resin compound. Figure 4 shows the cable bend performance as a function of the actual coated steel tape corrugation depth.

The cable bend performance around any given mandrel, in general, improves as a function of corrugation depth once the parameters are understood. As the data indicates, the bend performance is not a linear function with corrugation depth, i.e., it varies depending upon the depth of corrugation. Below about 0.022 inch (0.063 mm), the cable bend performance is marginal. We found it difficult to produce cable specimens with such shallow depth of corrugation, as the forming of the coated steel tape was difficult with a cone former due to springback. As the depth of corrugation increased beyond this minimum, the relationship appeared to enter a second 'zone' of linear functionality, where the cable performance improved with corrugation depth.

In order to assess the relationship between corrugation depth and bend performance it is necessary to use the corrugation depth of the finished cable as the measured parameter. If one chooses the set corrugation depth as the corrugation parameter, there are possibilities that the actual corrugation depth may be reduced during forming. The sizing dies may squeeze the corrugations out, resulting in a decrease in the corrugation depth. Further efforts in this area have shown that if this squeezing of the corrugations is excessive, actual weakening of the coated steel tape and a resulting drop in cable bend performance can occur.

In addition to the depth of corrugation, the profile of the corrugation is critical to the functionality of the cable sheath. A study undertaken by Dow and a cable manufacturer to determine why some cable failures were experienced resulted in the conclusion that all of the cable failures which were occurring were produced on one specific cable line. Examination of this line showed that one significant difference between it and the others was that the corrugating rolls were produced by different manufacturers, and resulted in significantly different profiles on the coated steel tape. The corrugating rolls which produced good cable resulted in a smooth, sinusoidal profile, while the corrugating rolls which produced the poorer cable had sharp peaks and valleys, a triangular profile.

The amount of jacketing resin which penetrates into the corrugation valleys, or corrugation fill, is also critical to the functionality of the cable sheath. Figure 5 shows the relationship between corrugation fill and cable bend performance. As the amount of corrugation fill increases, the cable bend performance increases. Three methods are currently used in the extrusion of the cable jacketing resin over the corrugated coated steel tape: tube, vacuum, and pressure. Pressure extrusion is recommended, as it provides good filling of the corrugations with the resin. Vacuum extrusion is an improvement over tube extrusion, but the amount of corrugation fill is dependent upon the efficiency of vacuum pulled. Tube extrusion is not recommended due to the inability to squeeze the resin down into the corrugations. The lack of corrugation fill will reduce the measured jacket bond strength and the cable bend performance.

5. OVERLAP FORMING:

Another critical factor in the performance of the cable sheath is the coated steel tape overlap area. A well formed overlap with the coated steel tape bonded to itself as well as bonded to the jacketing resin will result in a cable sheath construction which will behave as a "seamless" thin walled tube. This area in cable manufacture is probably the most difficult as far as the development of a functional bonded cable sheath is concerned. Much effort has been spent on understanding the problems associated with the coated steel tape overlap.

Parameters which affect the ability to achieve a sealed seam and bonded sheath at the coated steel tape overlap include.

- steel tape forming,

- extrusion conditions, and
- processing aids.

Difficulty in forming of the coated steel tape is due to the mechanical properties of the substrate steel as specified in various specifications. These mechanical properties are required so the steel can perform many of its functions, such as to provide rodent protection, impart mechanical strength to the cable sheath, and to otherwise protect the cable core. Important parameters in the forming of the coated steel tape include the ability to form the steel tape longitudinally without excessive springback, which can cause the overlap to open, and registration of the corrugations at the overlap to provide a snug fit.

Preforming or extra forming of the coated steel tape edges has been utilized to reduce the tendency of the top edge of the tape to cut into the cable jacket.[3] When forming the top edge of the coated steel tape downward at the overlap to reduce the tendency of the edge to cut into the jacketing resin, one will prevent the snug fit of the top and bottom edges of the overlap. This in turn will reduce the ability to achieve a sealed seam.

Another area of concern for the overlap area occurs when running flooded cable core designs. Due to the need for complete water blocking of the core, the floodant is typically pumped into the core in copious amounts. Contamination of the overlap area can occur if the floodant is squeezed out of the cable core during the coated steel tape forming process. This will prevent the ability to achieve a sealed seam. If floodant seeps out of the overlap onto the surface of the coated steel tape, it can also prevent a jacket bond in the overlap area. Use of water swellable tapes in the core to prevent longitudinal water flow would eliminate the presence of floodants which can interfere with the adhesion of the coated steel tape to itself or the jacketing resin.

The extrusion of the jacketing resin onto the coated steel tape is also critical, for the more intimate the contact between the jacketing resin and the plastic coating on the coated steel tape, the stronger the resulting bond will be between the two materials. Pressure extrusion, discussed earlier in conjunction with filling the corrugations, is recommended to achieve the strongest possible bond between the coating at the overlap area and the jacketing resin. This intimate contact will provide the best heat transfer into the coated steel tape from the jacket melt and provide the best sealed seam between the top and bottom coatings on the steel tape at the overlap.

It is possible to achieve exceptional cable sheath performance with the use of processing aids to insure a good sealed seam and jacket bond at the coated steel tape overlap. One method is to increase the amount of heat energy available to allow the coatings on the coated steel tape to melt and fuse together at the overlap. Methods of imparting additional heat include using infrared preheat ovens or induction preheating. Induction preheating has been successful, and units for cable lines are commercially available.

A second method of achieving a sealed seam is to inject adhesive hot melts into the coated steel tape overlap. Data was generated showing the use of a hot melt in the overlap of a moisture barrier power cable, where the longitudinally formed tape is one side coated 5 mil copper. Table 2 shows the effect of mechanical stress on the overlap sealed with an ethylene vinyl acetate (EVA) hot melt. The cable was pulled through a duct bank at the two levels of side wall bearing pressure shown. The adhesion of the hot melt forming the seal was unchanged after the test indicating that the integrity of the sealed overlap was maintained.

The use of hot melts in the overlap provides a good sealed seam and exceptional cable performance. Several cable grade hot melts are available, some specifically designed for high temperature environments as would be present in power cable applications. While the use of these hot melts should improve the seam strength between the coated metal surfaces in the overlap, they should not affect the adhesion between the coated metal tape and the jacketing resin.

One method of achieving a functional bonded cable sheath by using an aid to seal the overlap has been reported.[4] In this case an adhesive tape is applied over the coated steel tape overlap seam. Use of this bridging tape has virtually eliminated jacket notching and slippage of tape from the overlap area even with poorly formed armoring tape. During a study of the failure mechanism of copper pair cable with a bonded sheath, the ratio of the cable unbonded zone width (at the longitudinally formed corrugated steel tape overlap) to the jacketing thickness, b/t_j, was found to be an important criterion for determining the failure mode of cable.[5] With the proper forming and seam sealing of the coated steel tape overlap, no unbonded area will be present and the ratio b/t_j will be zero, resulting in the cable sheath always acting like a thin walled tube with no zippering of the cable jacket.

Figure 6 shows the bend performance data for cable produced by controlling the cable parameters as described in this paper. This figure shows the relationship of corrugation depth to bend performance versus mandrel to cable diameter ratio. The industry requirement of 25 bends around a 20 times mandrel is easily exceeded at a depth of 0.024 inch (0.6 mm). Increasing the depth of corrugation to 0.035 inch (0.9 mm) results in a cable having superior bend performance. The overlap was positively sealed using induction preheat. As a result, both of these cables have withstood 10 full revolutions on the twist test equipment with no damage or opening of the coated steel tape overlap.

CONCLUSIONS

1. A critical corrugation depth is present for cables using longitudinally formed corrugated coated steel tape below which the cable sheath will not function well. For tapes having 10 corrugations per inch, this depth is 0.020 to 0.024 inch (0.51 to 0.61 mm).

2. Critical processing parameters include corrugation depth, corrugation profile, corrugation fill, and overlap forming and sealing.

3. Resin choice and jacket thickness also play an important role in the functionality of the cable sheath.

4. Industry requirements for flexibility and sheath performance can be easily exceeded with proper attention to these various parameters.

ACKNOWLEDGMENTS

The authors would like to thank Don Gromacki of the Engineered Laminates TS&D group for generation of much of the data presented herein. We would also like to thank the many customers who have utilized coated metal armoring tape in their cable's sheaths, and who have worked with us in the understanding and application of the various process parameters which effect the functionality of the bonded sheath.

REFERENCES

1. Neveux, Paul Jr. and Hatton, William, *"Designing Compression Resistance In Loose Tube Cables,"* Proceedings of the 36th Annual International Wire and Cable Symposium, November, 1987.

2. Yanizeski, Johnson, and Schneider, *"Cable Sheath Buckling Studies and the Development of a Bonded Stalpeth Sheath,"* Proceedings of the 29th Annual International Wire and Cable Symposium, November, 1980.

3. Mitchell, Collins, West, and Kinard, *"Bonded ASP: A Superior Sheath for Buried and Underground Filled Cables,"* Proceedings of the 29th Annual International Wire and Cable Symposium, November 1980.

4. Gebizlioglu, Grimado, Avant, and Biron, *"Zippering Failures in Telecommunications Cable Jackets,"* Proceedings of the 37th Annual International Wire and Cable Symposium, November, 1988.

5. Johnson, John, *"Peel Adhesion Testing of Pressure-Sensitive Adhesive Tapes,"* Adhesives Age, Volume 11, Number 4, April, 1968.

6. Maguire, C. V. and Rossi, R., *"Cable Sheath Design and Performance Criteria,"* Proceedings of the 36th Annual International Wire and Cable Symposium, November, 1987.

7. Bell Communications Research Technical Reference TR-TSY-000421, *"Generic Requirements for Metallic Telecommunication Cables,"* Issue 2, June 1988.

TABLE 1

Minimum Average Jacket Resin Thickness (End Sample Measurement Technique)

Cable Over Core Diameter in. (mm)	REA PE-22[1] in. (mm)	REA PE-39[2] in. (mm)	TR-TSY-000421[3] in. (mm)
0.75 (19.05)	0.054 (1.35)	0.054 (1.35)	0.057 (1.45)
0.90 (22.86)	0.063 (1.62)	0.063 (1.62)	0.057 (1.45)
1.05 (26.67)	0.063 (1.62)	0.063 (1.62)	0.057 (1.45)
1.20 (30.48)	0.072 (1.80)	0.0675 (1.71)	0.057 (1.45)
1.35 (34.29)	0.072 (1.80)	0.0675 (1.71)	0.058 (1.47)
1.50 (38.10)	0.081 (2.07)	0.072 (1.80)	0.060 (1.54)
1.75 (44.45)	0.081 (2.07)	0.072 (1.80)	0.065 (1.65)
1.90 (48.26)	0.090 (2.25)	0.081 (2.07)	0.067 (1.71)
2.05 (52.07)	0.090 (2.25)	0.081 (2.07)	0.070 (1.77)
2.20 (55.88)	0.099 (2.52)	0.090 (2.25)	0.072 (1.84)

1. Aerial Cable With Air Core
2. Filled Telephone Cable
3. Metallic Communication Cables

TABLE 2

Overlap Seam Seal Adhesion Side Wall Bearing Pressure Test

DESCRIPTION	BEFORE TEST LB/IN	BEFORE TEST N/MM	AFTER TEST LB/IN	AFTER TEST N/MM
1,600 lb/ft (23.4 kN/m)	56.3	9.86	59.8	10.47
2,000 lb/ft (29.2 kN/m)	56.3	9.86	51.0	8.98

FIGURE 1

Cable Bend Performance versus Jacket Bond Strength Coated Steel with LLDPE Jacket Resin, 12x Mandrel

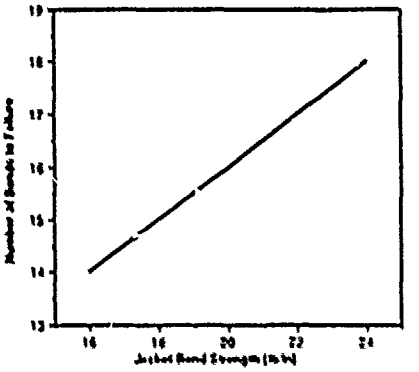

FIGURE 2

Sheath Young's Modulus versus Corrugation Depth

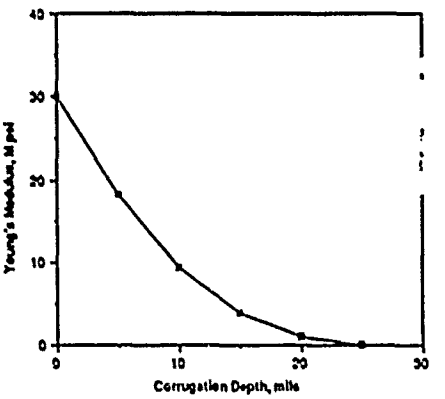

FIGURE 3

Sheath Tensile Strength versus Sheath Elongation

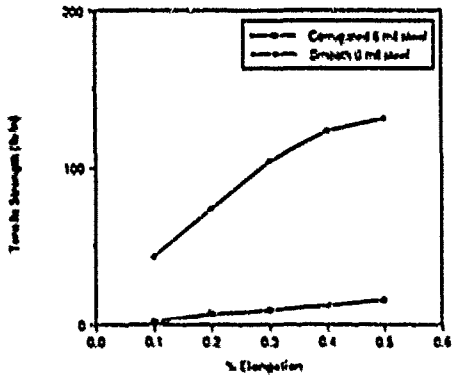

FIGURE 4

Cable Bend Performance versus Actual Corrugation Depth Coated Steel with LLDPE Jacketing Resin, 7X Mandrel

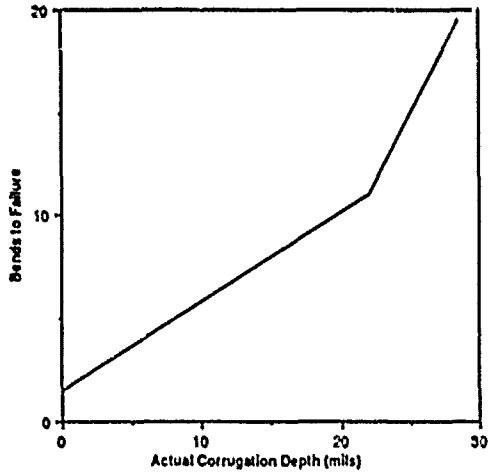

FIGURE 5

Cable Bend Performance Versus Corrugation Fill Coated Steel with LLDPE Jacketing Resin, 12x Mandrel, 35 mil Corrugation Depth

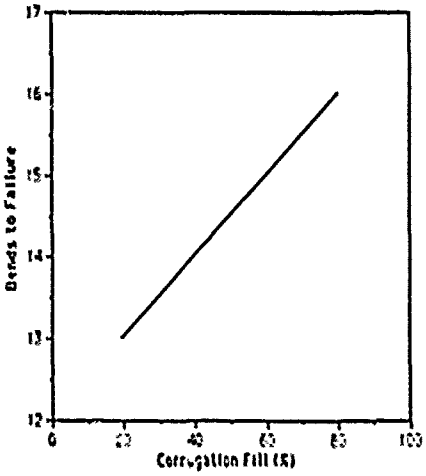

FIGURE 6

Cable Bend Performance versus Mandrel to Cable Diameter Ratios for Different Tape Corrugation Depths Coated Steel with LLDPE Jacketing Resin

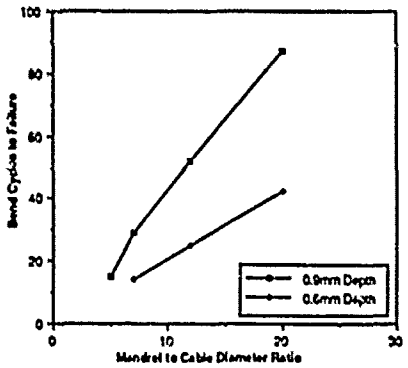

BIOGRAPHIES

Kenneth E. Bow is a Senior Associate Development Scientist with Dow Chemical USA, Granville, Ohio. He has been involved in the research and development of materials for the wire and cable industry for over 20 years. He is currently the Chief Scientist for the Coated Metals business and the Technical Manager of the Coated Metals Technology Center. He is responsible for the global development of coated metal shielding and armoring tapes for applications in cables. Mr. Bow graduated with a B.S. E.E. degree from Michigan State University in 1962. He is a member of IEEE, the Wire Association International, the Society of Plastics Engineers, the National Association of Corrosion Engineers, and ASM.

William F. Busch is a Project Leader with Dow Chemical USA, Granville, Ohio. He is currently the Team Leader for the wire and cable business, and is responsible for the coordination of efforts to both support the existing business and to develop new opportunities for coated metal tape in cable. Mr. Busch received his B.S. degree in Chemical Engineering from the State University of New York at Buffalo in 1977, and his M.S. degree in Chemical Engineering from the University of Virginia in 1979. He is a member of the Telecommunications Industry Association and the Wire Association International.

Daniel G. Pikula is a Product Development Representative with Dow Chemical USA, Granville, Ohio. He has been involved in technical service and development of materials for the wire and cable industry for over seven years. He is currently responsible for development of coated metal shielding and armoring tapes for applications in power, control and instrument cables. Mr. Pikula graduated with a B.S. degree in Chemistry from Otterbein College in 1988. He is a member of TAPPI and The American Chemical Society.

SOME RECENT DEVELOPMENTS IN HIGH TEMPERATURE COMPOSITE MATERIALS FOR TAPE WRAPPED WIRE AND CABLE CONSTRUCTIONS

E.C.Lupton Jr., H.N. LaTorra, J.A. Effenberger, K.G. Koerber and J.V. Petriello

Chemical Fabrics Corporation (CHEMFAB)
701 Daniel Webster Highway, Merrimack, NH 03054

I. ABSTRACT

Technology has recently been refined to manufacture high performance thin films with multiple thin layers. Films with up to eight layers have been manufactured using polyimide, various fluoropolymers and heterogeneous components such as pigments. Adhesion between layers of the film is excellent. With proper selection of film construction, fusing a tape to itself or to another tape is easily achieved at reasonable temperatures.

Methods are described to use these tapes to address surface smoothness, arc track resistance, laser markability, color and conductivity.

II. INTRODUCTION

The design and selection of materials for high temperature wire and cable insulation is a difficult task. One must balance and optimize requirements for space, weight, electrical properties, cut through and abrasion resistance, chemical resistance, high and low temperature resistance and freedom from unusual occurrences, such as arc tracking.

Over the years, several polymeric systems have been evaluated for this application. Over time, polyimides and fluoropolymers have proven to offer the most promising balance of properties. A comparison of the properties of these materials is illustrated in Table I.

II. WHY COMPOSITE MATERIALS

As can be seen from Table I, neither fluoropolymers or polyimides taken alone exhibit all of the properties desirable for service as a high temperature wire and cable insulation. Also, it has not been possible to synthesize a single polymeric material able to meet all performance requirements. There is also some resistance to consideration of new materials without very extensive testing because of experience with at least two

TABLE I
Comparison of Polyimide (PI) and Fluoropolymer (FP) Properties

	PI	FP
Temperature Resistance	+	+
Chemical Resistance	-	+
Cut through & Abrasion Resistance	+	-
Space & Weight Saving	+	-
Arc Track Resistance (AC Power)	-	+
Electrical Properties	+	+

Code: + Area of strength
- Area of relative deficiency

candidate materials developed in the last 30 years which exhibited severe deficiencies which were discovered only after the materials were in service.[1]

However, composite multilayered structures have shown great promise for exploiting the advantages of each material while minimizing or even eliminating the flaws of each. This approach is used in creating modern rigid advanced polymer composites from high performance thermoplastics and thermosets and from glass, carbon fiber, aramids and other reinforcements. A similar technology has proven very powerful in the packaging industry where flexible films, sheets, thermoformed tubs and bottles are made with multiple thin layers of different plastics. Such flexible packaging composites are principally produced by melt coextrusion or by extrusion coating.

While melt process fluoropolymers and polyimides have been made and offered commercially for many years, the high melt temperatures, high melt viscosities, tight crystal line structures and/or three dimensional molecular networks of the best performing fluoropolymers and polyimides make them impossible to process by conventional melt extrusion. This has dictated that tape

wrapping be used to process these materials into wire insulation. A few high performance composite tapes have been available to wire manufacturers for some time[1]. We have recently made many advances in the technology of manufacture and use of flexible composite materials and we would like to make this preliminary report on films which are now available and which may offer unique opportunities for upgrading the performance of wire and cable constructions. Individual layers in these composite films range in thickness from .05 to .6 mils (1.2 to 13 microns).

Our efforts are continuing and we expect soon to define other attractive complex films and tapes as well as to offer specific data regarding the performance of these novel insulating materials in service.

III. FILM CONSTRUCTIONS NOW AVAILABLE

A. Easy to Use PTFE Based Films

The fluoropolymer with the highest continuous service temperature capability is polytetrafluoroethylene (PTFE). We have refined the technology for processing this material into extremely thin films, for manufacturing films with multiple PTFE layers with different properties, and for producing multilayer films where some layers are pure PTFE for the highest temperature capability and other layers are thermally bondable due to the presence of fluorinated copolymers such as FEP or PFA or of fluoropolymer alloys which can achieve tenacious bonding to themselves or other films at moderate processing temperatures but will retain bond strength at the 260°C use temperature of PTFE.

These films are highly consolidated and have a high tensile strength. They are easy to work with and can be set up and used on conventional tape wrapping equipment. We believe that the high consolidation of these films provides an improvement in cut through relative to paste extruded PTFE films.

A reported problem with highly consolidated PTFE films in the past has been that the lip which is formed during the tape winding would tend to catch and tear during the pulling of the construction over a corner or sharp surface. To address this concern, we have developed a film material in which a sizeable portion of the thickness can flow to form a uniform smooth outer surface. This material is now in use in these applications where ease of installation is a serious concern.

An illustration of the properties of bondable PTFE films is given in Table II.

TABLE II

Properties of PTFE melt bondable films[1]

Property	Value	ASTM Method
Tensile Strength		
Machine Direction psi	4200	D882-54B
Transverse Direction psi	4200	D882-54B
Elongation		
Machine Direction	400%	D882-54B
Transverse Direction	400%	D882-54B
Specific Gravity	2.1-2.2	D792-50
Tear Strength, psi	400-800	D624
Stiffness, 77°F,psi	50,000	D747
Water Absorption	0.00	D570-42
Moisture Permeability @.001" g/100 sq in/24 hrs	0.2	
Specific Heat BTU/lb/oF@100-260°F	.25	
Coefficient of Thermal Expansion /oF@77-144°	5.5×10^{-5}	D698-44B
Embrittlement Temperature	<-100°F	
Maximum Continuous Service Temperature	260°C 500°F	
Flammability, in/min	non-flammable	D835-44
Resistance to Weathering	excellent	
Static or Kinetic Coefficient of friction against Polished Steel	0.04	
Solvent Resistance	chemically	

Electrical Properties

Dielectric Constant 60-10^6 hz	2.0	D150-54
Dissipation Factor 60-10^6 hz	<0.0003	D150-54
Volume Resistivity	>10^{15}	D257-52
Surface Resistivity, 100%RH megohms	3.6x10^6	D257-52
Dielectric Strength, Short Time .001" V/Mil	4200	D149-55
Surface Arc Resistance, Sec	Does Not Track	D495-48

B. Elimination of Arc Tracking

Although polyimide films may exhibit arc tracking under both wet and dry conditions at relatively low voltages, fluoropolymer materials show particularly excellent arc track resistance in tests designed to simulate current aircraft power systems. An exhaustive analysis of arc tracking is beyond the scope of this report. However, a number of organizations have reported to us that PTFE films and/or polyimides layered with PTFE can reduce or eliminate any tendency of the polyimide to arc track under realistic use conditions. It is suggested that maximizing the ratio of PTFE to polyimide in an appropriate geometry will minimize the tendency to arc track.

Developing a usable polyimide layered with PTFE is very difficult because of the poor adhesion between polyimide and PTFE which causes the layers to separate easily and can cause the composite to have poor insulation integrity and relatively poor cut through resistance. We have developed technology for producing excellent adhesion between polyimide and PTFE. Tapes using this technology will retain a strong bond at temperatures up to and beyond 260°C.

Two different approaches to arc track reduction have been used involving polyimide/PTFE laminated films. One approach uses a relatively thick layer of PTFE, such as a .5 mil/1 mil/.5 mil film to build the concentration of PTFE in the finished product[3]. The other uses a thin layer of PTFE, such as a .125 mil PTFE/1 mil polyimide/.125 mil PTFE and bonds the PTFE layers to pure fluoropolymer layers, such as are described in A above.

Arc tracking appears to be self perpetuating once the phenomenon starts. To eliminate arc tracking, it is important that the fluoropolymer be present at the exact point in the construction where the arc tracking is occurring. The two approaches listed above allow the wire designer to position the PTFE precisely where it is desired in the construction.

C. Laser Markability

Wire constructions are being developed which will use lasers to mark the wire. Infrared lasers (both conventional and excimer) and ultraviolet lasers are now being used. We have been able to design tapes using our multilayer technology where a layer of one color will ablate under the laser light to reveal a layer of another color. These tapes give excellent permanent laser markability with no compromise of high temperature properties.

D. Uniquely Colored Tapes

On occasion, requirements appear for unique coloration such as transparent coloration or special colors. Our ability to produce thin layers with discrete colors, such as is mentioned in C above, allows us to address these requirements also.

E. Conductive Tapes

Our multilayer film technology allows us to manufacture filled conductive tapes[4]. These materials have resistivity in the range of 3000 ohms/square. They will readily heat seal and the conductivity is totally maintained across the heat seal.

REFERENCES

1) An early fluoropolymer, polychlorotrifluoroethylene (PCTFE) had a thermal embrittlement problem which only appeared after the material had been in service as a wire insulation for a period of time. An aromatic polyketone insulation, which was promoted in the mid 1970, was attacked by certain solvents and this problem was not realized until the material was in service.
2) The Kapton® F polyimide/fluoropolymer films offered by the DuPont Company and the

fluoropolymer and polyimide/fluoropolymers films offered by the Diletrix Corp. and by the Toralon Corp and now offered by the Toralon Division of the Chemical Fabrics Corporation under the tradename CHEMFILM are notable examples of composite constructions.

3) This material is designated CHEMFILM DF 2919XR.

4) This material is designated CHEMFILM DF 1471.

5) These materials are designated CHEMFILM DF 1700 when one side is melt bondable and CHEMFILM DF 1700DB when both sides are melt bondable.

PLASTIC CLADDING FIBER CABLE AND ITS FUSION SPLICING FOR INDOOR AND OUTDOOR INSTALLATION

Shigeo Shimizu, Kenichi Kuwura, Tsuguo Sato and Yoshikazu Matsuda

The Furukawa Electric Co., Ltd.
Ichihara, Chiba, 290 Japan

Summary

PCF(plastic cladding fiber) with a large core diameter and high N.A. is advantageous for short distance application such as LAN(local area networks). Indoor and outdoor cables, and reliable jointing techniques were required.

PCFs with pure silica core and fluoroacrylate resin cladding was developed, and its N.A. was 0.4.

Three types of cables were designed, fabricated and studied on transmission, mechanical and environmental properties.

Up to now, only connectors with loss of 1 to 3 dB have been available for jointing the PCF. Fusion splicing is expected to be desirable for a system with long length outdoor PCF cables. A practical fusion splicing technique was developed for the first time. Splicing loss was not larger than 0.4 dB at the temperature from -40℃ to +80℃.

From these results, it is concluded that applicability of the PCF cables can be expanded to both indoors and outdoors.

1 Introduction

LAN is one of the important applications of fiber optic transmissions. Because of the large core and high N.A., it is easy to couple the PCF to LED light source, and then cost for fabricating transmission module is reduced. Therefore, in view of realizing a economical system, the PCF cables are advantageous for the short distance system. Fig.1 shows an outline of the system.

When practically using the PCF in various LANs, following are required.

(1) PCF cables can be available for indoor and outdoor applications.

(2) Field splicing can be easily done in short time.

This report presents the developments of new PCF cables and splicing technique for the PCF, which meet the above requirements.

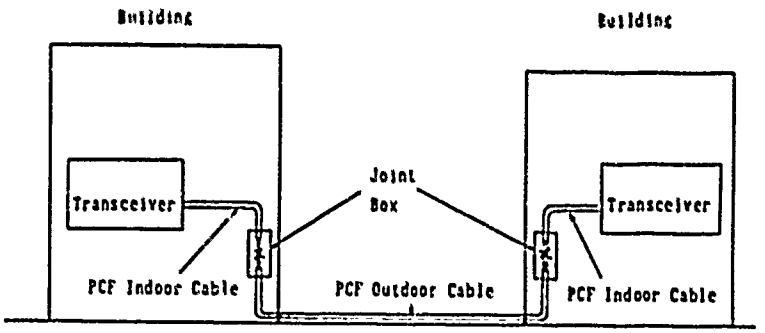

Fig.1 Inter-building Wiring System

2 Cable Descriptions

2.1 Jacketed Fiber

PCFs with pure silica core and fluoroacrylate resin cladding were jacketed by PTFE (Ethylene tetrafluoroethylene co-polymer). Diameters of core, cladding and jacket were 200 μm, 230 μm and 500 μm respectively. N.A. was 0.4.

2.2 Indoor Cables

Two types of PCF cables were fabricated and examined by environmental tests. One was a 2-core flat cable and the other was a 2-core stranded cable, as shown in fig. 2(a) and 2(b), respectively. The flat cable has good flexibility and then is suitable for wiring the PCF in small bend. The stranded cable has high mechanical strength and is advantageous for trunk line in the buildings.

2.3 Outdoor Cable

It is required for the cable to be constructed by n metallic materials for preventing transmission modules from damages by lightning, electromagnetic induction and so on. And in view of economical design and high resistivity to environment, the PCF cable with a slotted core and PE(poly ethylene) sheath was fabricated for outdoors.

The thermal expanding coefficient of the cable is larger than that of the jacketed PCF placed in the slot. At elevated temperature, the PCF can not elongate with the slotted core, and then the jacketed PCF may be pressed to the wall of the slot by the reduction of wound radius of the PCF.

By proper design of the shape and size of slot, the jacketed PCF in the slot may freely move in the slot and loss degradation at elevated temperature could be remarkably improved.

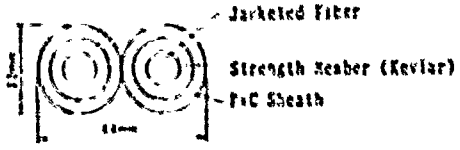

(a) 2-Core Flat Cable

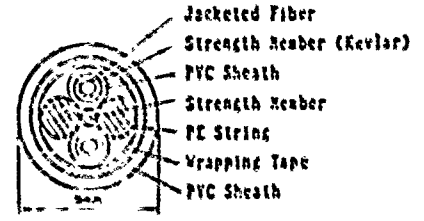

(b) 2-core Stranded Cable

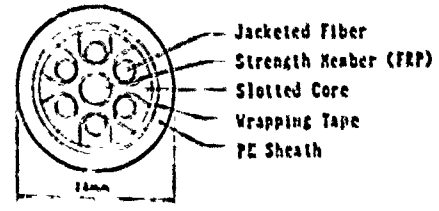

(c) Slotted Cable

Fig. 2 Cross-sectional Structure of PCF Cables

Items	Test Condition	2-core Flat Cable	2-core Stranded Cable	Slotted Cable
Tensile Strength (kg)	Gauge Length 10m	10 (0 dB)	160 (0.04 dB)	250 (0.06 dB)
Bending (mm^{ϕ})	180° Bending	20 (0 dB)	25 (0.01 dB)	100 (0 dB)
Twisting	5 Turns/1 m	(0 dB)	(0 dB)	(0 dB)
Impact (pound·feet)	25 mm$^{\phi}$Weight 1 Time	3 (0 dB)	9 (0.02 dB)	9 (0 dB)
Compression (kg)	50 mm Width Plate	60 (0.10 dB)	100 (0.13 dB)	250 (0 dB)

λ=0.82 μm

Table 1 Results of Mechanical Tests

3 Cable Performance

Attenuations of these cables were less than dB/km at 0.82 μm.

Table 1 shows results of mechanical tests. From these results, it was found that these cables have excellent mechanical properties sufficient for practically handling.

Results of temperature cycle test for the flat cable, the stranded cable and the slotted cable are showed in figs. 3 ~5, respectively. Light source was kept at a constant temperature during the tests and optical output power of the cables were measured at various temperatures. Averaged value of loss variation of the PCF in the cables were plotted in the figures.

Loss increase of the indoor cables were less than 2 dB/km at temperature from -20℃ to +60℃ and that of the outdoor cable was less than 2 dB/km at temperature from -40℃ to +50℃.

The variation of N.A. of the PCF with temperature is essentially due to the variation of refractive index of the plastic cladding resin. The loss variation is resulted from the variation of N.A. and the microbending. The loss variation of the coated fiber is mainly due to the variation of N.A..

Loss increase of the jacketed fiber was almost same as that of the coated fiber at low temperature. Therefore contribution of the microbending to loss variation was considered to be small. At low temperature in the test, loss increase of the 2 core flat cable was same as that of the jaketed PCF, while that of the stranded cable was slightly larger than that of the jaketed PCF, because of compression of PVC sheath.

Loss increase of the slotted cable was same as the jaketed PCF. This was resulted from the proper design of slotted core, and then it was found that the large elongation of the cable did not influence on the transmission properties of the PCF.

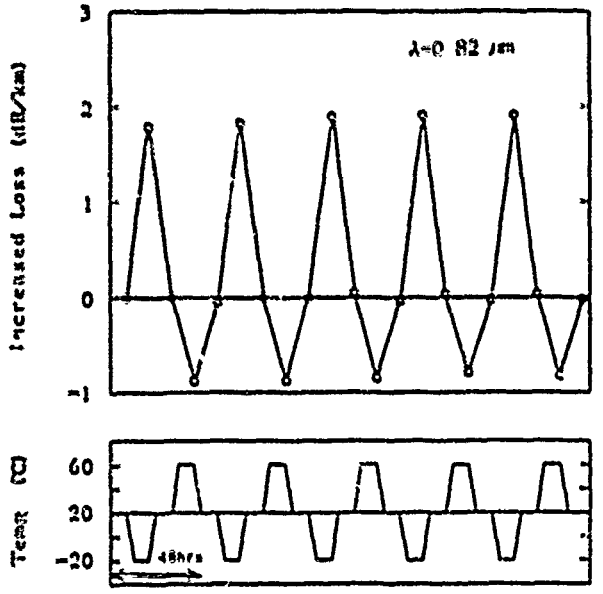

Fig. 4 Temperature Cycling Result of Stranded Cable

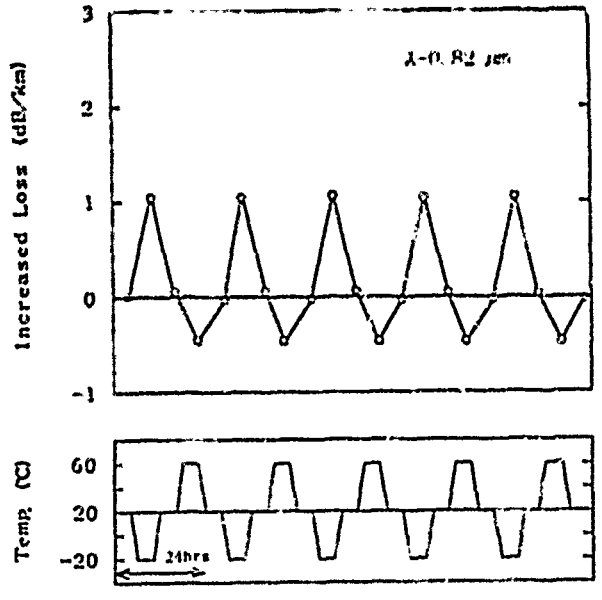

Fig. 3 Temperature Cycling Result of Flat Cable

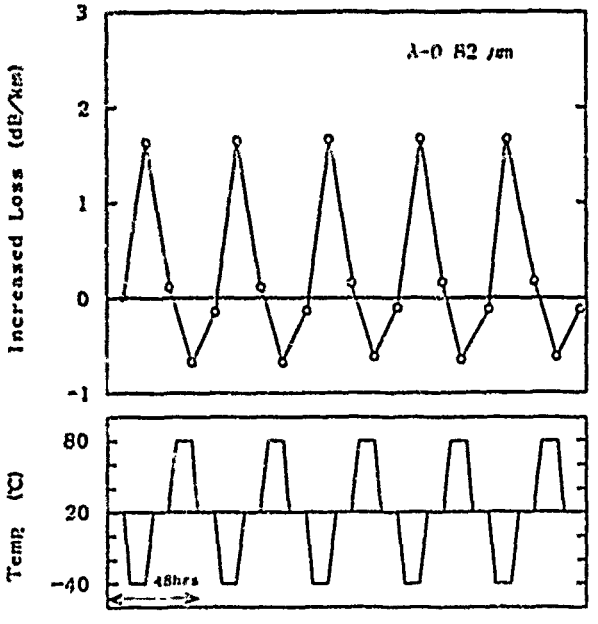

Fig. 5 Temperature Cycling Result of Slotted Cable

4. Fusion Splicing Technique

It is well known that fusion splicing method for optical silica fibers has low jointing loss and high reliabilities. However, up to now, it was difficult for the fusion splicing technique to be used for the PCFs. The reasons were as follows :

1) It was needed to strip the cladding resin before the fusion splicing procedure. However, it was difficult to do so, because of tight adhesion of the cladding resin to silica core for realizing good transmission and mechanical properties.
2) It took a long time to repair the cladding layer after the fusion splicing procedure.

Fig.6 shows a procedure of the newly developed fusion splicing method for the PCFs.

Firstly, ETFE jacket is stripped, while resin cladding is not stripped.

Secondly, fibers are cleaved and spliced by fusion. Here, a conventional splicing machine for silica glass graded index fiber was used, but the splice condition was optimized for the PCF.

Thirdly, as the cladding resin of the PCF is thermally decomposed by fusion, another thin resin is recoated on the spliced fiber as a newly recovered cladding.

Finally, the spliced fiber is covered with a thermoplastic resin sleeve for additional cladding and a heat shrinkable plastic tube with reinforcement as shown in fig.7.

Features of this new method are as follows .

1) The splice can be made without stripping the cladding resin. For this purpose, new plastic resin for cladding was developed, and thickness was reduced for easily decomposed.
2) Fresh cladding on the spliced fiber can be recoated in short time. Newly developed solution for cladding resin is quickly cured and has a function for smoothing the boundary between core and additional cladding.
3) The spliced fiber is protected by the thermoplastic sleeve for additional cladding and the shrinkable tube for reinforcement.

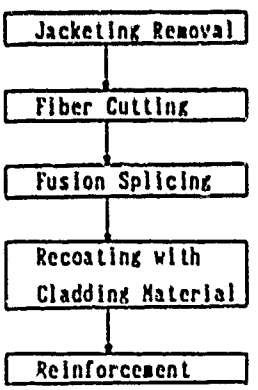

Fig. 6 Fusion Splicing Procedure

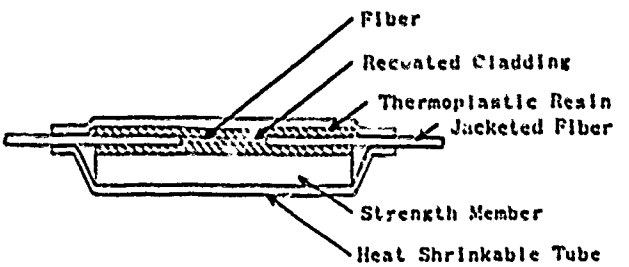

Fig. 7 Spliced Fiber with Reinforcement

5. Fusion Spliced Fiber Properties

Fig.8 shows fusion splicing loss. It was clarified that averaged jointing loss was 0.22 dB and one fifth to one fifteenth of connectors. Fig.9 shows a temperature dependence of splicing loss. Averaged total jointing loss including loss increase due to temperature change was not larger than 0.4 dB at the temperature from -40 ℃ to +80 ℃.

Fig.10 shows the tensile strengths of the fusion splicing. The strength at the probability of 50% was 4 kgf and equivalent to that of silica fiber at 1 % elongation.

6. Conclusion

Three types of cables using the PCF with pure silica core, fluoroacrylate cladding and ETFE jacket were developed. Two were indoor cables and one was a nonmetallic outdoor cable. Transmission and mechanical properties of these cables were revealed quite satisfactory.

A practical fusion splicing technique for the PCFs was developed. Averaged splicing loss was not larger than 0.4 dB at the temperature from -40℃ to +80℃. It was clearly less than connector loss.

From these results, it is concluded that applicability of PCF cables can be expanded to both indoors and outdoors.

Acknowledgements

The authors wish to thank Dr. K. Okubo for his helpful discussions, and to Mr. M. Nitjima for his valuable assistance.

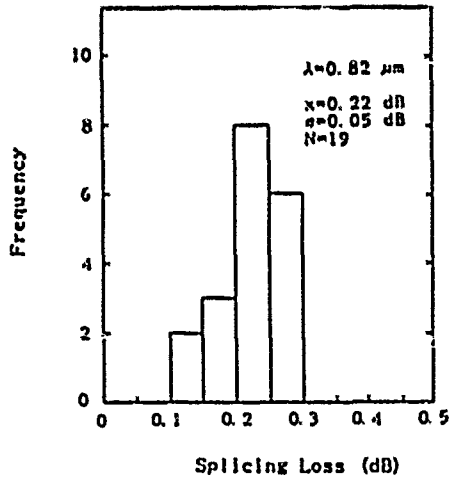

Fig. 8 Histgram of Fusion Splicing Loss

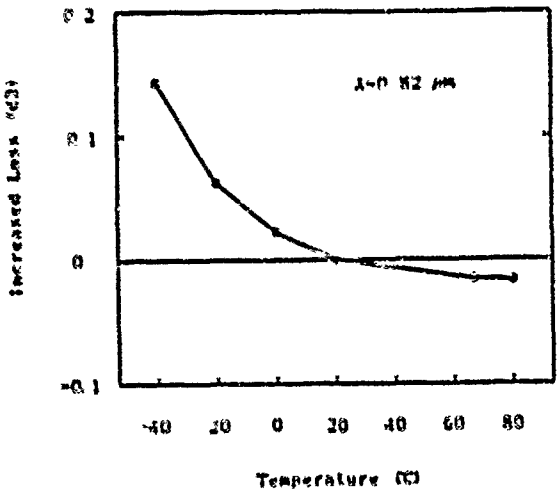

Fig. 9 Temperature Dependence of Fusion Splicing Loss

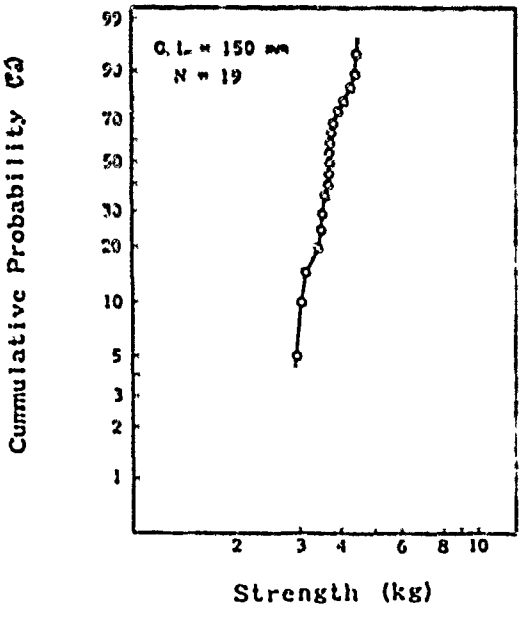

Fig. 10 Weibull Plots of Breakage Strength of Spliced Fiber

Shigeo Shimizu

The Furukawa Electric
Co., Ltd.
6 Yawatakaigan Dori,
Ichihara-shi, Chiba-ken,
290, JAPAN

Shigeo Shimizu was born in 1957. He received B.S. from Nagoya University, Japan, in 1980. He jointed The Furukawa Electric Co., Ltd. in 1981, and has been engaged in development of optical fibers since 1981.

He is now a staff research engineer of Optical Fiber Transmission section in Opto-Technology Laboratory.

Kenichi Kawura

The Furukawa Electric
Co., Ltd.
6 Yawatakaigan Dori,
Ichihara-shi, Chiba-ken,
290, JAPAN

Kenichi Kawura was born in 1951. He jointed The Furukawa Electric Co., Ltd. in 1970, and was engaged in development of plastic materials, optical fibers and its fusion splicing.

He is now a staff research engineer of Functional Material section in Opto-Technology Laboratory.

Tsuguo Sato

The Furukawa Electric
Co., Ltd.
6 Yawatakaigan Dori,
Ichihara-shi, Chiba ken,
290, JAPAN

Tsuguo Sato graduated from Science University of Tokyo, Japan, in 1963. He jointed The Furukawa Electric Co., Ltd. in 1957, and was engaged in chemical analysis and has been engaged in development of optical fibers.

He is now a senior research engineer of Functional Material section in Opto-Technology Laboratory.

Yoshikazu Matsuda

The Furukawa Electric
Co., Ltd.
6 Yawatakaigan Dori,
Ichihara-shi, Chiba-ken,
290, JAPAN

His photograph and biography are not available at time of submission.

He is now a manager of Functional Material section in Opto-Technology Laboratory.

DEVELOPMENT OF NOVEL MULTIPLE SINGLE-MODE FIBER CONNECTOR COMPOSED OF V-GROOVED SILICON CHIP AND GUIDE-PINS

KAZUHITO SAITO TOSHIAKI KAKII HIDETOSHI ISHIDA SHUZO SUZUKI

Sumitomo Electric Industries, Ltd.
Yokohama, Japan

ABSTRACT

A multiple single-mode fiber connector has been developed for use in optical communications systems, especially for connection of high-fiber count subscriber cables. In order to achieve a low loss connection, the connector design mainly comprises a high precision grinding technique for a silicon bonded chip. This technique is used to produce many triangular fiber holes between two guide-pin V-grooves which provide precise connector alignment. The connector has a simple structure, therefore it is possible to reconnect it easily and quickly. It has been found that the mean connecting loss for non-identical single-mode 12-fiber is approximately 0.3dB, the loss variation is less than 0.2dB for 50 reconnections.

1. INTRODUCTION

In fiber optic communications systems, single-mode fibers are used to provide high quality services to meet the various demands of subscribers. Because high fiber count cables are demanded for subscriber transmission lines, multiple fiber connectors will be required [1][2]. In this system, it is necessary to accommodate a large number of connectors in a closure or pulling eye of a pre-connectorized cable, therefore the connector is required to be small in size and easy to connect. Furthermore, lower cost and lower loss are important factors because of the higher number of connectors between a telephone office and subscribers, and the introduction of lower cost emitting and receiving devices into the system.

For this purpose, we have developed a novel multiple single-mode fiber connector which we call the SV connector. The connector has a Silicon V-grooved capillary chip which is a high precision connector ferrule using an advanced grinding technique, and is suitable for mass production [3]. This paper describes the design and characteristics of the new connector for 12-fiber ribbon.

2. SV CONNECTOR DESIGN

The connecting method, with guide-pins, has the advantage of reducing the size of the connector. Figure 1 shows the basic structure of the SV-12 (for 12-fiber ribbon) connector. Two connector plugs with 12-fiber ribbon and precisely aligned by two guide-pins and four spring clamps. Thus, the connector has a simple structure and the connecting operation is easy. Generally connectors using guide-pin for alignment are affected seriously by two factors: First, there are the eccentricity of the fiber position against the guide-pin position, second, the destribution of the guide-pin diameter. However, our newly developed SV connector can avoid these problems for its superior constructions. We explain about it in the following.

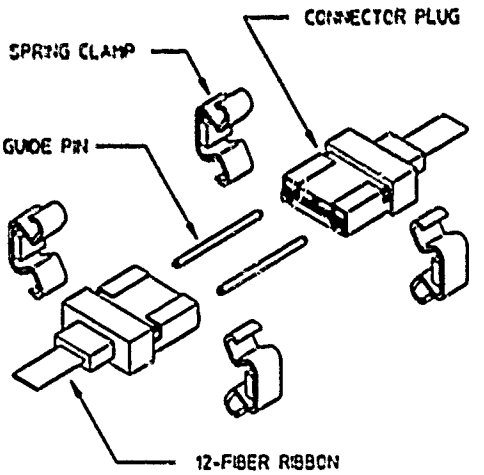

Figure 1 Structure of SV-12 connector (for 12-fiber ribbon)

2.1 PRINCIPLE OF ALIGNMENT MECHANISM

In order to achieve low loss for multiple fibers, we adopted the aligning mechanism of compressing and fixing the guide-pins on the guide-pin grooves which are parts of the silicon chip. Figure 2 illustrates the contact surface of the silicon chip. The silicon chip has many triangular fiber holes between two V-grooves for guide-pins. The V-grooves are manufactured without a precise etched process, which is generally utilized in the field of semiconductor technology, thus the only process needed is the advanced grinding technique. It is difficult to produce the two kinds of V-groove which differ in depth, for fiber and guide-pin, if the V-grooves are manufactured by the use of an etched process. However, the grinding technique will successfully produce the dirferent V-grooves together using only one process. Moreover, the grinding technique has few processes than the etched one, so it is suitable for mass production attribute to lower cost. The deviation of relative position between each fiber holes and guide-pin grooves are within ±0.5μm in the direction of both the pitch and depth of the V-groove, and that of the othar surrounding chip size do not influence the connecting loss.

To align connectors by two guide-pins, the guide-pin position must be precisely fixed on the silicon chip against fiber position. For this purpose, the guide-pin is pressed against the wall of the V-groove of the silicon chip. If the V-groove for guide-pin is covered by the wall and forms a triangular hole like those for fibers, a serious problem for a clearance between the triangular hole and the guide-pin will occur, and we can't expect a stable connecting loss. Therefore this exposed V-groove structure is necessary for low loss and stable connections.

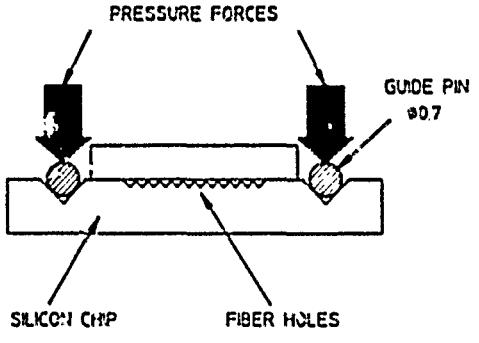

Figure 2 Contact surface of silicon ship

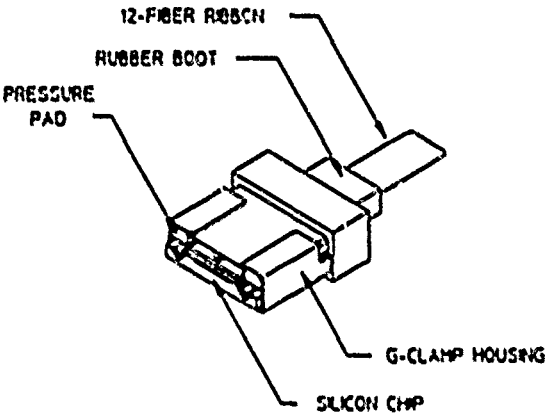

Figure 3 SV-12 connector plug

2.2 DETAIL OF DESIGN

Figure 3 shows a SV-12 connector plug. The plug consists of a G-clamp housing, the silicon chip and a rubber boot. The G-clamp housing fixes the guide-pins to V-grooves realizing low loss and a stable connection. When the guide-pin is inserted into the guide-pin groove, the pressure pad, which is a part of the G-clamp housing, elastically deforms upward and the reaction force compresses the guide-pin on the V-groove. The pressure force is not strong, and the inserting friction for the guide-pin is less than 100gf, which is the desirable value for the operation of guide-pin inserting. This first connecting step is sufficient to provide the pre-alignment of the guide-pin, however, the situation of the connecting plugs are unstable, by external forces such as tension, flex, twist etc. Therefore, in the second step of the connecting procedure, the spring clamp is attached to the plug as shown in Figure 1. As a result, the total pressure forces for guide-pin increases up to 3kgf, and the stable connection is realized.

The size of the SV-12 connector plug is 8.4(W) x 3.4(H) x 12.0(L) mm^3, and the cross-sectional area is only 2.4mm^2/fiber. The diameter of the guide-pin is 0.7mm, the length is 14mm. The dimension of two plugs joined and four spring clamps is 11.2(W) x 6.5(H) x 26.0(L) mm^3 as shown in Figure 4. These sizes are suitable for easy handling and accommodating in a narrow space, such as a closure. The spring clamp is slightly larger than the plug, because the clamp is attached using a clamping tool and it has a catching portion against the tool.

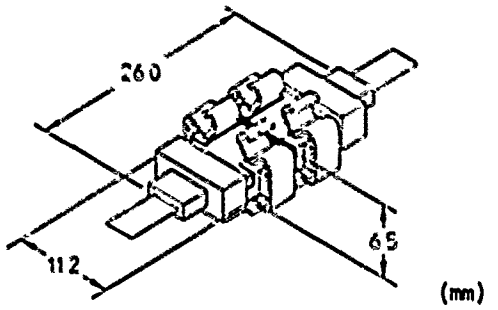

Figure 4 Dimensions of two connectors joined

2.3 ASSEMBLY PROCESS

Assembly of the silicon chip and the G-clamp housing is done before the insertion of fibers into the chip. The assembled chip which we call the SV ferrule is small enough to carry. Therefore the SV connector can be assembled in both the factory and the field.

Figure 5 indicates the assembly process of fiber. The fibers are inserted into the ferrule from the end surface of the chip with adhesive through the rubber boot. This procedure is basically the same as one for a general single fiber connector, and is possible to assemble without being skilled and without special tools. After fibers are fixed by the adhesive, the front surface of the ferrule is polished, and last, the rubber boot is attached.

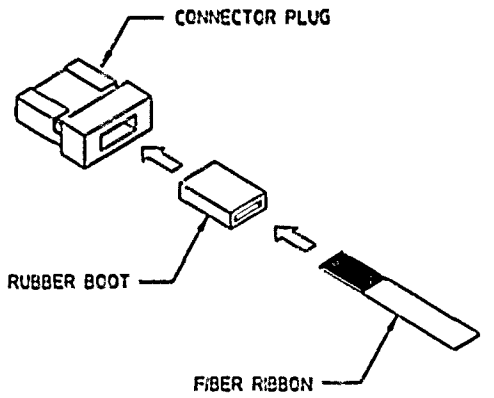

Figure 5 Assembly process of fibers

3. CONNECTOR TESTS

The SV connector design objectives of small size, low loss and low cost were evaluated by testing samples to standard mechanical and environmental tests. The samples were assembled with 12-fiber ribbon made from standard Sumitomo single-mode fibers. The loss measurements were made with 1.3μm LED sources, and the loss measured with index matching material.

3.1 CONNECTING LOSS

Sixteen 12-fiber SV connector (SV-12 type) were assembled for insertion loss measurements, all combinations of the two SV connectors were connected. Figure 6 shows the histogram of the connecting loss for 760 non-identical fiber connections. The averaged loss was 0.33dB. This value includes some large losses such as the maximum loss 1.77dB. It is considered that the larger loss is caused by the distribution of the fiber diameter and core eccentricity in addition to processing errors of the silicon chip. Consequently the large value is reasonable in the random fiber connections.

The relationship between the connecting loss and each fiber position is shown in Figure 7. The result indicates that the fiber position does not exert an influence on the loss, and that the processing precision of V-groove position and quantities. Therefore the number of fibers to be connected can be chosen without loosing connector quality. Actually we prepared a variety of SV connectors that included up to 18 fibers, upon the user's request.

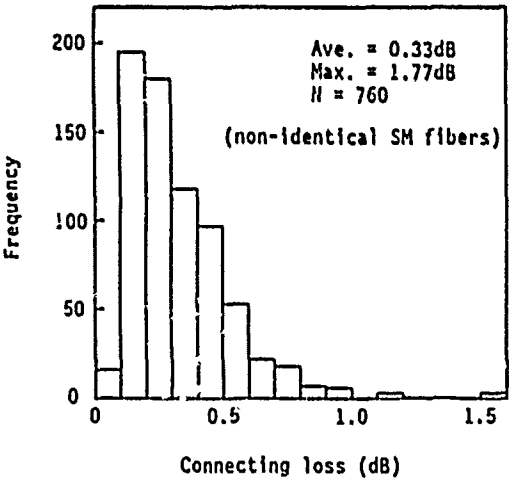

Figure 6 Connecting loss histogram of all fibers

3.2 REPETITION

Figure 8 shows the loss changes of the two fiber positions (No.6 and No.12) in same connector for 50 connections and reconnections. The behaviors of the loss change closely resemble each other in spite of the difference of the initial connecting losses. This tendency can be explained in terms of the miss-alignment of the guide-pin. The standard deviations were 0.06dB and 0.11dB respectively, and these values have no problem for practical use.

3.3 TEMPERATURE CYCLING

The temperature cycling performance was measured over the range of -30°C to 60°C. The loss change of two fiber positions (No.1 and No.6) and the schedule of the thermal cycle are shown in Figure 9. Loss changes of less than 0.2dB occured over the given temperature range.

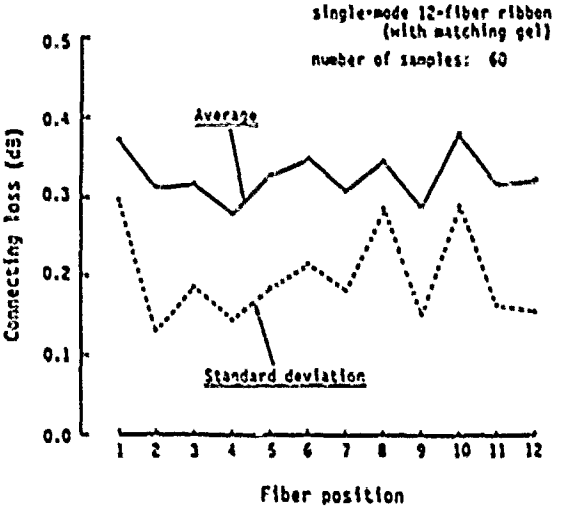

Figure 7 Relationship between connecting loss and fiber position

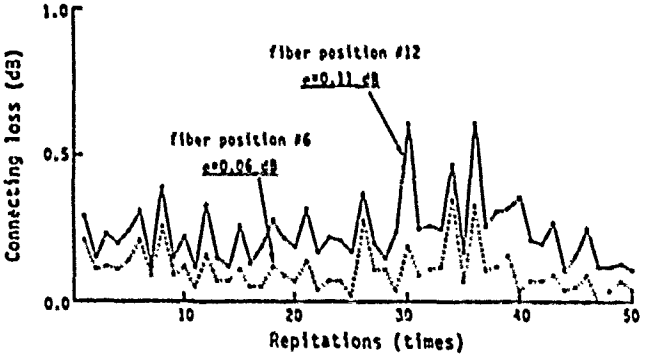

Figure 8 Repetition test

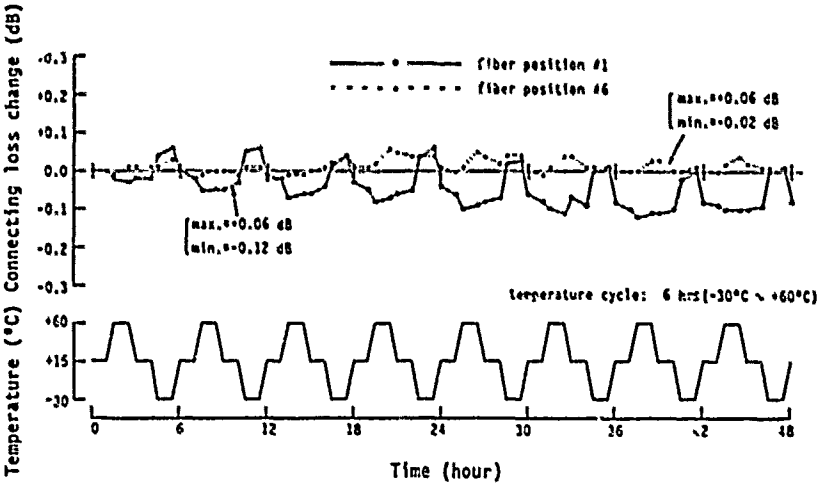

Figure 9 Temperature cycling test

3.4 SUMMARY OF PERFORMANCE

In addition to above tests, testing samples were measured to vibration, humidity resistance, and retention. These test results are also summarized in Table 1. The results were found to be satisfactory.

4. CONCLUSION

A novel multiple single-mode fiber connector has been designed for use in optical communications systems and is composed of a precisely V-grooved silicon chip, G-clamp housing and two guide-pins. The silicon chip is manufactured by using an advanced grinding technique which is suitable for mass production. The processing precision of the silicon V-groove is within ±0.5μm.

To reduce the ferrule size and to realize low loss with simple structure, we adopted the aligning method to use two guide-pins and V-grooves. The dimension of two joined 12-fiber SV connectors with spring clamps is 11.2(W) x 6.5(H) x 26.0(L) mm^3. The average connecting loss for single-mode 12-fiber ribbon was 0.33dB (with matching oil) which is a satisfactory value for a multiple single-mode fiber connector.

REFERENCE

[1] T. Satake, N. Kashima and M. Oki, "Very small single-mode ten-fiber connector", IEEE, J. Lightwave Tech., Vol.6, No.2, 1988.

[2] T. Haibara, S. Nagasawa, M. Matsumoto and M. Kawase, "Single-mode multifiber technique for high-density high-count subscriber cables", in Proc. 37th IWCS, 1988.

[3] T. Kakii, K. Saito and S. Suzuki, "Development of a silicon V-groove guide hole type SM multi-fiber connector", 1987 Natl. Conv. Rec., IEICE, 2004.

Table 1 Optical characteristics and reliability test

Test	Condition	Loss
Connecting loss	λ=1.30μm, LED Single-mode 12-fiber ribbon (with matching gel)	Average < 0.5dB
Papetition	50 times Connector cleaning on every 5 times	Standard deviation < 0.15dB
Vibration	In direction of X, Y and Z Amplitude: ±1mm, 50Hz	Loss change < 0.1dB
Temperature cycling	-30°C to +60°C 6 hrs/cycle x 8 cycles (total 48hrs)	Loss change < 0.2dB
Humidity resistance	80°C, 95%RH, for 72hrs	Loss change < 0.2dB
Retention	Tension: 1.0kgf, 0.5mm/sec	Loss change < 0.1dB
Return loss	λ=1.31μm (measure back reflection)	< -45dB

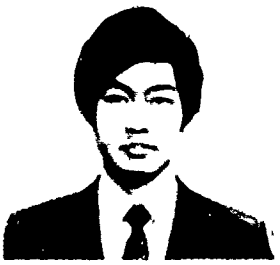

Kazuhito Saito

Sumitomo Electric
Industries, Ltd.

1, Taya-cho, Sakae-ku
Yokohama, Japan

Kazuhito Saito received a M.E. degree from Tokyo institute of technology in 1986. He joined Sumitomo Electric Industries, Ltd. in 1986, and has been engaged in research and development of optical connectors. He is an engineer of Communication R&D Department in Yokohama Research Laboratories.

Toshiaki Kakii

Sumitomo Electric
Industries, Ltd.

1, Taya-cho, Sakae-ku
Yokohama, Japan

Toshiaki Kakii was born in 1955 and received a M.E. degree from Keio University in 1980. He joined Sumitomo Electric Industries, Ltd. in 1980 and has been engaged in research and development of optical fiber jointing technologies. He is a senior engineer of Communication R&D Department in Yokohama Research Laboratories.

Hidetoshi Ishida

Sumitomo Electric
Industries, Ltd.

1, Taya-cho, Sakae-ku
Yokohama, Japan

Hidetoshi Ishida received a M.E. degree from Tohoku University in 1987. He joined Sumitomo Electric Industries, Ltd. in 1987, and has been engaged in research and development of optical connectors. He is an engineer of Communication R&D Department in Yokohama Research Laboratories.

Shuzo Suzuki

Sumitomo Electric
Industries, Ltd.

1, Taya-cho, Sakae-ku
Yokohama, Japan

Shuzo Suzuki received a M.S. in 1972 from Tokyo University. He joined Sumitomo Electric Industries, Ltd. in 1972, and has been engaged in research and development of optical fiber, cable and jointing technologies. He is a chief research associate of Communication R&D Department in Yokohama Research Laboratories.

DEVELOPMENT OF A NON-DESTRUCTIVE TEST FOR MICROBEND LOSS MECHANISMS IN CABLED FIBRE.

P.A.Sutton, J.L.L.Roberts, A.T.Summers - STC *
A.Phoenix, D.Rees - Polytechnic of Wales **

* Cable Products Division, Newport, Gwent, UK.
** Treforest, Mid Glamorgan, UK.

ABSTRACT.

Microbending within optical fibres is a loss mechanism which is accentuated during cable manufacture. Whilst the fibres' transmission characteristics are invariably within the required specification, some deteriorate due to the cabling process. No method currently exists for identifying fibres most likely to exhibit this behaviour. This paper describes attempts to address this issue and to identify the parameters dictating microbend performance. A new microbend test is developed which is repeatable and representative, and a model is presented which enables fibre performance to be predicted.

INTRODUCTION.

Optical fibre cables have many advantages over their co-axial and copper equivalents which include light weight, small diameter and excellent transmission characteristics. However, optical waveguides are sensitive to mechanical and environmental influences and the preservation of the fibre's properties is a major challenge in cable manufacture.

Two major mechanisms of signal loss in cabled fibres have been classified as macro and microbending. While the mechanisms of macrobending are well documented and understood [1,2], those of microbending are not. Broadly, microbending is a mechanism of loss caused by perturbations along the fibre axis. The magnitude of the microbending effect in a cabled fibre is a function of both the fibre's parameters, and the way the fibre rests in the cable.

When a bobbin of fibre is tested before cabling to establish its inherent loss, the observed attenuation will not only be a function of the fibre itself, but also of the way it is wound onto the drum. A fibre within specification can appear to have an excessively high loss simply because of poor drum winding. It was for this reason that tests which deduced fibre performance from a short sample taken from a drum were developed.

The causes of microbending are diverse, with the phenomenon being unpredictable and difficult to quantify. This is reflected in the industrial tests which are currently used to measure the effects of microbending and in the general approach to the problem. Two tests for microbending currently in existence are the basket weave and the graphite paper tests [3,4]. They are examples of the traditional approach to microbending and use fibre cross overs and irregular perturbations to promote losses. These methods in general produce unrepeatable results and in the case of the graphite test, can prove destructive to the fibre sample.

Any test should not only classify the loss of a fibre compared to others, but also allow an actual prediction of cabled fibre performance. For this reason, the emphasis of this investigation compared with previous papers [5,6] (which have provided indices of relative performance for various fibre designs), has been the prediction of actual cabled fibre attenuations rather than the comparison of test performances

A feature of the conventional approach to microbending is to assess the susceptibility of fibres to the phenomenon, without explaining the causes of that susceptibility. An aim of this investigation has therefore been to relate microbend sensitivity to fibre parameters.

From the above considerations, the requirements in analysing the microbending phenomenon were taken to be as follows:-

(i) A repeatable, representative microbend test was required which would be non destructive to the fibre samples;

(ii) The results of the microbending tests should be linked to a fibre's physical characteristics in an attempt to develop loss prediction algorithms relevant to all fibres.

These considerations were predominant in progressing the work.

TEST DEVELOPMENT AND OBJECTIVES.

In the previous section, the objectives of the work were outlined. A microbending test was required which was both repeatable and representative. Repeatability implied not only the need for consistent results across several samples of the same fibre, but also embodied the notion of total test non-destructiveness.

The test was intended to be representative in as far as the results measured could be extrapolated to predict microbend attenuations within cables. The ultimate aim was to quantify the relationship between measured test attenuations and individual fibre parameters. This would allow the test to be superseded by a performance prediction algorithm utilising fibre parameters.

In designing a new microbend test, the shortcomings of existing tests were considered and the design modified to eliminate them. Inconsistencies in results commonly arise due to problems such as:-

(i) The method of perturbation inducement is a random pattern;

(ii) The fibre is placed on the inducement differently each time the test is performed;

(iii) Inconsistent placing of the fibre causes a different length to be compressed during each test.

These shortcomings lead to inaccurate results, producing tests with limited integrity.

The rig designed for this test is shown in Figure 1. It incorporated features to specifically overcome the problems listed above. Mesh was used so that a regular rather than random perturbation pattern was imposed on the fibre; two locating pins prevented all movement between surfaces; and the fibre was laid in a loop so that the sample would experience all directions of mesh to minimise directional inconsistencies. Dimensional accuracy was ensured by marking a circle on the holding material. A slot cut at the fibre crossover prevented spurious

losses due to unwanted compression at this point. The fibre sample was arranged (in a circle of known diameter in a fixed position) on the holding material, which was attached to the top block. This ensured that every sample had an identical position on the mesh. Both the mesh and the top block were located on the pins to ensure consistency of placement.

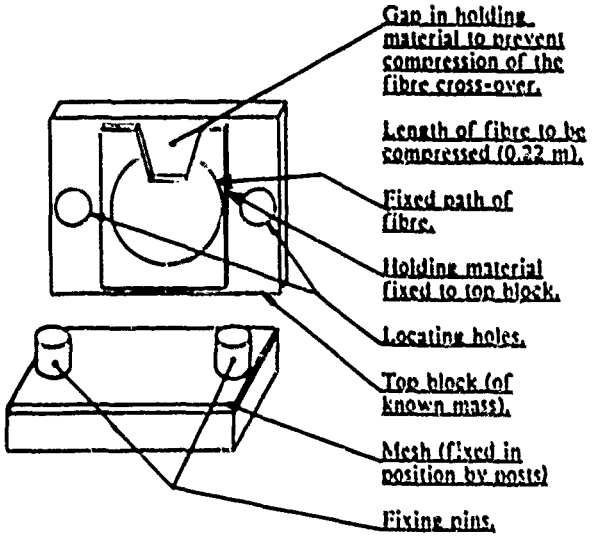

Figure 1. Microbending Test Design.

Two types of gauze, 50 (fine) mesh, and 20 (rough) mesh were used as perturbation inducements in conjunction with two kinds of holding material, neoprene rubber and card. Combinations of these materials produced four variations of the test. On all of these tests, 0.22 m of fibre was compressed by forces of 30, 40, 50, 60 and 70 N. The resulting attenuations were analysed and related to their respective fibre parameters.

The fibre samples were selected at random without regard for their parameters. For this reason, no performance related conclusions should be drawn from the parametric distributions.

CHARACTERISTICS OF CVD AND OVD FIBRE.

Three fibre types were chosen in order to evaluate the validity of the test. The designs were:-

(i) Modified Chemical Vapour Deposition (MCVD) matched cladding single coat fibre;

(ii) Modified Chemical Vapour Deposition (MCVD) depressed cladding double coat fibre;

(iii) Outside Vapour Deposition (OVD) double coated fibre.

For brevity, throughout the remainder of this paper, the aforementioned fibres will be referred to as types A, B and C respectively. The refractive index profiles of these fibres are shown in Figures 2,3,4.

For all fibres, certain parameters were measured in order to relate them to test performance. The refractive index parameters measured are shown in Table 1, along with additional derived values. Figure 2 shows the points on the profiles from which the refractive index parameters were taken.

In addition, the fibre transmission parameters shown in Table 2 were measured for each of the fibres.

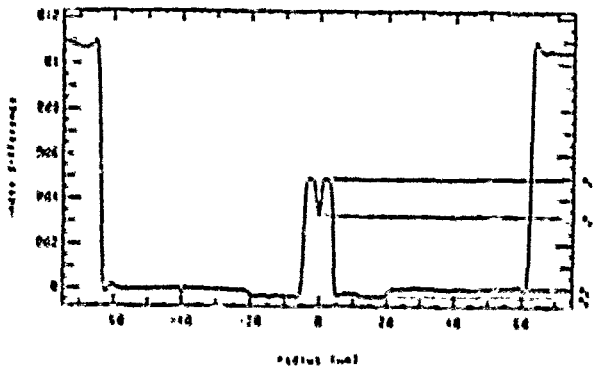

Figure 2. Refractive Index Profile of Type A Fibre.

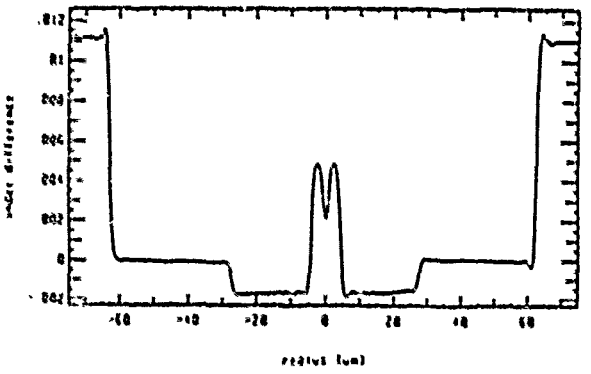

Figure 3. Refractive Index Profile of Type B Fibre.

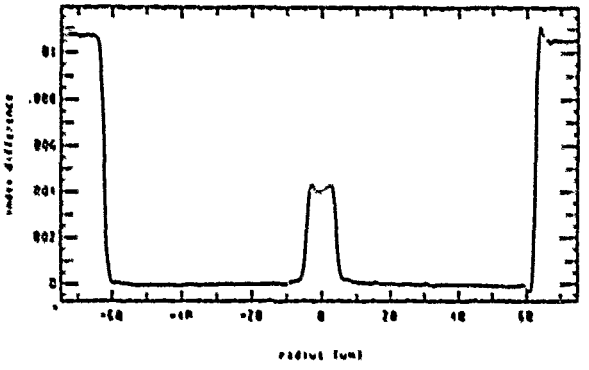

Figure 4. Refractive Index Profile of Type C Fibre.

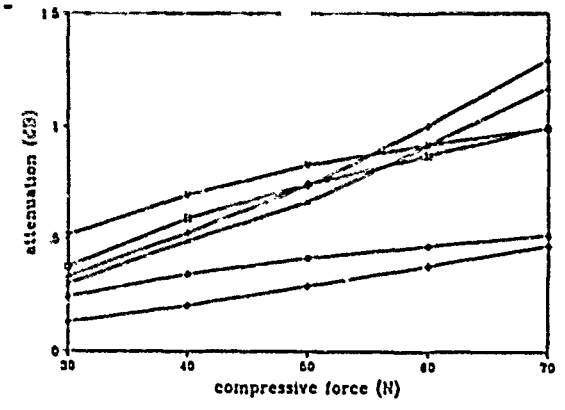

Figure 5. Absolute Attenuations from Type A Fibres on the Smooth Mesh and Rubber Test at 1550 nm.

Parameter	Symbol
dip index	n_d
peak index	n_1
cladding index	n_2
cladding depressed index	n_3
dn* $(n_1 - n_2)$	Δ_n
dip size* $(n_1 - n_d)$	Δ_p
cladding depression* $(n_2 - n_3)$	Δ_c

* derived values.

Table 1. Measured and Derived Refractive Index Parameters with Symbols.

Parameter	Symbol	Dimension
cut off wavelength	λ_c	nm
1300nm Petermann mode field diameter	ω_{p13}	μm
1300nm Gaussian mode field diameter	ω_{g13}	μm
1550nm Petermann mode field diameter	ω_{p15}	μm
1550nm Gaussian mode field diameter	ω_{g15}	μm

Table 2. Measured Fibre Transmission Characteristics, Symbols and Units.

RESULTS.

Figure 5 is an example of a plot of attenuation against applied force for the smooth mesh and rubber test. The graphs demonstrate the individual loss characteristics resulting from each of the tests. Each variant of the test induced differing levels of attenuation in the fibre sample. The rough mesh tests tended to be more severe than the smooth mesh ones, while the rubber caused higher losses than the card.

The tests were designed to induce only the microbending mode of loss. However, it was recognised that other modes of loss might exist, affecting to varying degrees the accuracy of results from the different tests. For this reason, the tests were critically assessed to identify those most likely to produce pure microbending induced attenuations.

The card tests were likely to lead to the fibre undergoing periodic constriction rather than the axial perturbations required for microbending. Therefore whilst producing consistent results, there was evidence that the test promoted modes of loss other than microbending.

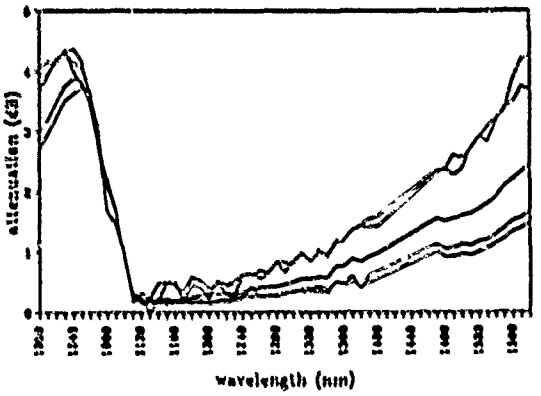

Figure 6. Absolute Spectral Attenuations for Type A Fibres on the Rough Mesh and Rubber Test for Various applied forces.

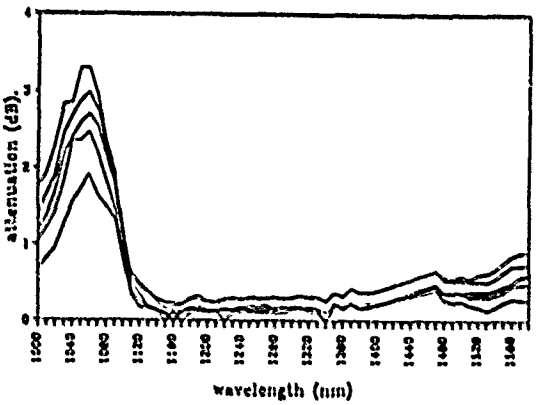

Figure 7. Absolute Spectral Attenuations for Type A Fibres on the Smooth Mesh and Rubber Test for Various applied forces.

The rubber based tests were more likely to cause pure microbending. It was however necessary to ensure that the degree of macrobending was insignificant. This was proved by examination of the information in Figures 6,7, showing spectral attenuations for the rubber tests. For both graphs, each line is a different applied force increasing at intervals of 10 N from 30 to 70 N. Macrobending is evidenced by the attenuation at 1550nm being greater than twice the attenuation at 1300nm [7]. In Figure 6 for some compressive forces, the attenuation at 1550nm met this criterion, suggesting slight macrobending had been induced. On the smooth mesh and rubber test in Figure 7 however, the 1550nm attenuation was always less than twice the 1300 nm result proving the absence of macrobending. The smooth mesh and rubber tests therefore did not produce macrobending as a major mode of loss.

The smooth mesh and rubber test could promote other undesirable modes of loss. If the mesh were too fine, the fibre

would be unable to follow its form and the test would cause mainly compression. The possibility of this effect having any significance, was eliminated by carrying out compression tests between two flat plates. The forces required to produce attenuations of the magnitude observed in the smooth mesh and rubber test, were many times greater than those used in the test itself. Another mode of loss other than compression was therefore in operation, which indicated that microbends had been induced. It was concluded that the smooth mesh and rubber test provided the desired microbending effects.

The observed increase in signal attenuation with applied force, while not being a linear relationship was characteristic for each individual fibre. This suggested that the fibre parameters dictated not only the absolute attenuation, but also the nature of the loss/force relationship.

The signal attenuations for all fibres within a test variation were of comparable magnitude. It could therefore be concluded that the combined effect of each fibre's characteristics, ie. refractive index profile, process method and coating type, lead to microbend resistance levels of a similar order.

The precautions already described for the design and construction of the smooth mesh and rubber test, contributed positively to the repeatability of the measured attenuations. The performance of a fibre was measured by taking five readings on a test and then calculating their average. The repeatability of the test is demonstrated by Figure 8 where for various forces, the distributions of a typical fibre's measured attenuations about their averages are shown. It can be seen that the measured attenuations never exceeded ± 10% of the average attenuation, giving a very high degree of repeatability.

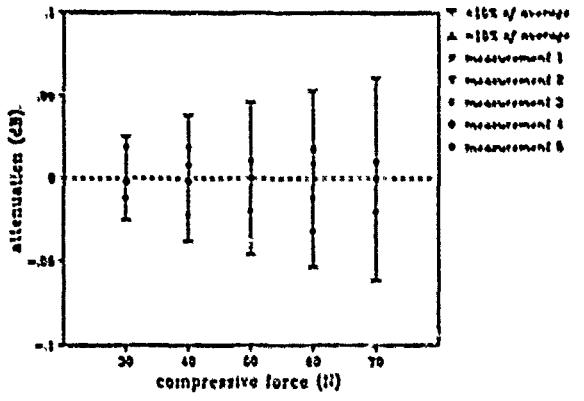

Figure 8. Error in Measured Values at Particular Applied Forces at 1550nm about their Averages.

ANALYSIS.

The consistency of the results verified that a mathematical model could be used to predict the fibre performance, obviating the need to perform the test. The first attempt to quantify the link between parameter and performance involved plotting a fibre's parameters one at a time against its attenuations at each value of applied force for each test. This method was abandoned since it was realised that not only was performance a function of multiple parameters, but the parameters themselves were interrelated. Clearly, no attenuation could be linked to a parameter in isolation, since the mechanism of loss was a function of many variables.

It was for this reason that the method of stepwise multiple regression [8,9], was used to develop the mathematical models. Stepwise multiple regression investigated each of the parameters in turn, its relationship with the fibre performance and its interrelation with other parameters. In this way, it was possible to eliminate parameters detrimental to the model, or so closely linked to other parameters that they contributed nothing to its accuracy.

It was found that the sample of type A fibres had a sufficient spread of parameters to allow the multiple regression programme to run successfully resulting in models with a high confidence limit. This unfortunately was not the case with the type B or C fibres, which had a narrower base of parameters. In these cases, the multiple regression package failed to uncover any attenuation-related parameter trends.

Having selected smooth mesh and rubber as the optimal test, the analysis enabled a mathematical relationship to be developed for the prediction of type A fibre performance. Table 3 displays some of the statistical data which shows the high degree of accuracy to which the model predicted the measured performance. The coefficient of determination, R^2 is a measure of the accuracy of the predicted figures compared with the measured ones. The significant T value is the probability that T, the ratio of each coefficient to its error, occurred as a result of random effects. F is the ability of the equation to explain the variability of the measured values. Significant F is the probability that the relationship stated in the model could have come about by chance. Therefore the combination of high values of R^2,T and F, and negligible 'significant' T and F values, demonstrated the validity of the model.

Table 4 shows the parameters used in the model and the individual coefficients of determination of each when regressed with the microbend attenuation values.

Parameter	Model value
R^2	87%
Signif T (ω_{p15}) (Δ_p) (Δ_n) (constant)	 0.0000 0.0001 0.0117 0.0000
Signif F (all variables)	 0.0000

Table 3. Statistical Parameters Showing Accuracy of Model Relating to the Smooth Mesh and Rubber Test.

Variable	Coeff. of Determination
(ω_{p15})	75%
(Δ_p)	1%
(Δ_n)	21%

Table 4. Coefficients of determination of the individual model variables.

The parameter with the greatest influence on the model's predictions was the 1550nm Petermann mode field diameter (ω_{p15}). The reason for this being that the mode field diameter (mfd) is indicative of the amount of light being carried outside the fibre core. The larger the proportion of light outside the core, the greater the possibility of light leaking out of the fibre when it encountered perturbations. The various mathematical descriptions of mfd are strongly interrelated; thus the multiple

regression programme required only one in the model. The choice of the 1550 nm Petermann representation suggested that for this test, it was the best description of the power distribution within the fibre.

Equation (1) models the 1550 nm performance of type A fibres for the smooth mesh and rubber test using an applied force of 60 N.

$$\text{predicted test attenuation (dB)} = 0.99(\omega_{p15}) + 245(\Delta_p) - 196(\Delta_n) - 9.517 \qquad (1)$$

where ω_{p15}, Δ_p and Δ_n have been defined in Tables 1,2.

Figure 9 shows a plot of predicted against actual attenuation on the smooth mesh and rubber test at 1550 nm using the above equation.

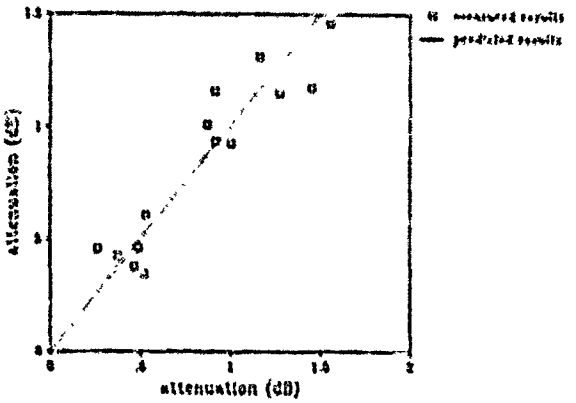

Figure 9. Absolute Attenuations Predicted by the Model for Type A Fibre on the Smooth Mesh and Rubber Test at 1550nm for an Applied Force of 60 N.

CONCLUSIONS.

A repeatable, non destructive optical fibre test was developed which induced microbending as the dominant loss mechanism.

Results using the above test on CVD matched cladding single coat fibre, have been analysed using a stepwise regression technique. This has produced a mathematical model which gives high statistical correlation with measured values, and in which the 1550nm Petermann spot size was the most significant parameter.

ACKNOWLEDGEMENTS.

The authors would like to thank the DTI/SERC, Teaching Company Directorate for their part funding of this programme of work, and STC's directors for their permission to publish this paper.

REFERENCES.

[1] Gambling W.A., Matsumura H., Ragdale M.,'Curvature and Microbending Losses in Single-Mode Optical Fibres.',Optical and Quantum Electronics 11, 1979.
[2] Roberts J.L.L., Summers A.T., Harner S.R.,'Bend Characteristics of Fibres Manufactured by CVD, OVD, and VAD Techniques.', Proc. EFOC/LAN '88, Amsterdam, June 1988.
[3] Grasso G., Meli F., SOCIETA' CAVI PIRELLI S.p.A.-Italy. ECOC '88 Conference publication number 352 Part 1
[4] Brambley R.J., Ashworth D.M., STL Report,'Microbending Performance of Fibre Packages.', Private Communication, June 1988.
[5] Arjalia M. et al,'Bending Loss Characterization in Single-Mode Fibres.', Proc 13TH ECOC '87, Helsinki, September 1987
[6] Francois, Bayen, Alard. 'Characterisation Procedure of Fibre Packaging Relative to Microbends.', Electron. Lett. (G.B.), Vol 21 N°.11, pp 471-2, 23 May '85.
[7] Oswald T., STC Report, Private Communication, December 1988.
[8] Bond K.M., Scott J.F., 'Essential Business Statistics: a Minitab Framework.', PWS Kent, 1988.
[9] Ryan, Joiner, Ryan, 'Minitab Handbook.', Second Edition, Duxbury Press, 1985.

AUTHORS.

Paul Sutton was born in Birmingham, England in 1966. He attained a B.Eng (Tech) Honours Degree in Mechanical Engineering from the University of Wales Institute of Science and Technology in 1988. In September of the same year, he began a two year Teaching Company Programme with STC and the Polytechnic of Wales for an M. Phil in optical fibre technology. This paper is the result of his work to date. Paul is an associate member of the I. Mech. E.

Llyr Roberts was born in Barry, S. Wales in 1964. He graduated from the Polytechnic of Wales in 1986 with a B.Sc. in Electrical and Electronic Engineering, and then in 1989 with an M. Phil in Optical Fibre Cable Technology gained via a Teaching Company programme with STC. He is currently a senior engineer with STC, where he is the industrial supervisor for this project. In addition, he is studying for a part-time MBA which he hopes to complete in 1990.

Andy Summers was born in Haverfordwest, Wales in 1961. He graduated from Aston University in 1984 with a B.Sc in Electrical and Electronic Engineering. After this he joined STC as Measurements Engineer, to develop production and reference test methods for optical cable manufacture. In 1986, he became Quality Manager for the Optical Fibre and Cable Manufacturing Units. He transferred to the Technical Department in 1987 with responsibility for optical cable development. He is now the technical manager of STC's cable products division in Newport

Allan Phoenix graduated in 1972 from Liverpool University with a degree in Electrical Engineering. He was appointed to British Telecom where he had responsibility for Exchange modernisation in Liverpool and later became head of Technical support in the South Wales District. In 1985 he moved to London where he had responsibility for the computerisation of B.T's network information. In 1987 he took a Senior lectureship in the Polytechnic of Wales where he lectures in Information Technology and related subjects.

David Rees is the Deputy head of Department of Electrical and Electronic Engineering at the Polytechnic of Wales. He gained the degree of B.Sc. in Electrical Engineering from University College Swansea in 1977, and a Ph.D in Signal Processing applied to composite frequency testing in 1976. His industrial experience includes five years with British Steel and two years with Imperial Chemical Industries. Over the past ten years he has managed a SERC/DTI teaching company between the Polytechnic of Wales and STC He is a fellow of the IEE

LOW LOSS SINGLE-MODE MULTI-FIBER PLASTIC CONNECTOR

T. Ohta T. Sigematsu Y. Kihara H. Kawazoe

THE FURUKAWA ELECTRIC CO., LTD

Summary

High-count single-mode (SM) fiber ribbon cables have been used in optical subscriber network to provide high quality services.

Low loss and high speed multi-fiber connection techniques are strongly required for construction of economical SM subscriber network systems.

The precisely molded plastic multi-fiber connector has been developed for a SM multi-fiber ribbon.

After study of molding condition using high-precision molds and plastic material of low mold shrinkage, the average insertion loss of 0.190dB was obtained for SM 4-fiber ribbon, and the loss variation was less than 0.2dB in various reliability tests.

1. Introduction

Recently, high-count SM fiber cables have been used in optical subscriber network to provide high quality service. And the high-density SM fiber ribbons have been used in cables. The structure of SM fiber cable and ribbon is shown in Fig.1.

Thus, the SM multi-fiber plastic connector has been developed for the SM fiber ribbon with low insertion loss, long term reliability, very small size and light weight.

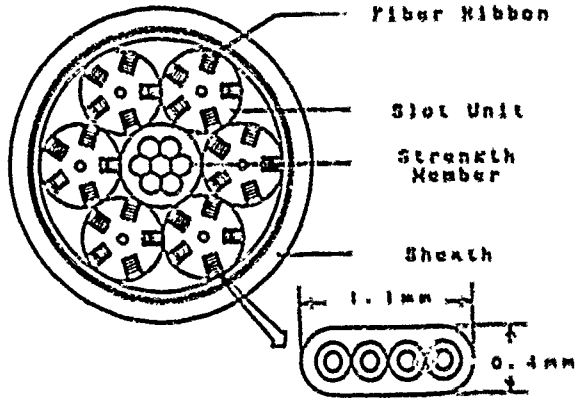

Fig.1 Structure of Cable and Ribbon

2. Structure

The ferrule structure of SM multi-fiber plastic connector is shown in Fig.2. The multi-fiber ferrule has two guide holes for alignment and multi-fiber holes that the optical fibers are inserted through.

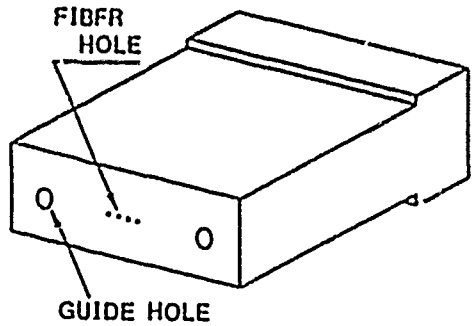

Fig.2 Ferrule Structure

The structure of the SM multi-fiber plastic connector is shown in Fig.3. A pair of connectors is aligned by two guide pins and held by the clamp spring.

To obtain a low insertion loss, the mating face dimensions of the multi-fiber ferrule should be highly precise.

The multi-fiber ferrule is required that reproducibility of the fiber hole diameter, the guide hole diameter and the fiber holes eccentricity error against guide hole is less than 1.5μm.

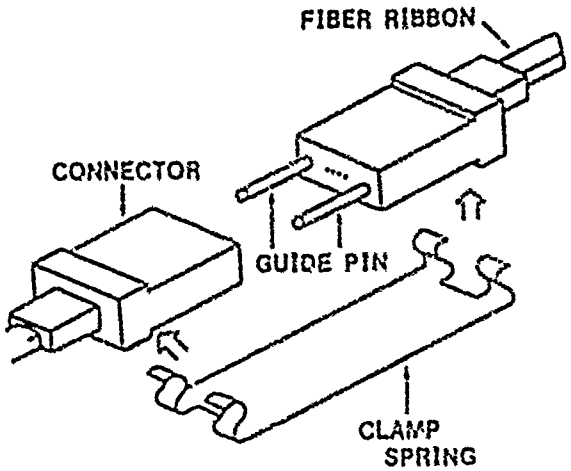

Fig.3 Connector Structure

3. Mounting Procedure of SM multi-fiber connector.

The SM multi-fiber plastic connector is produced through the steps as follows.

(1) The ferrule is formed by transfer molding thermosetting epoxy resin. In this molding, a high-precision mold and epoxy resin of low mold shrinkage are used.
(2) The mating face dimension of the ferrule is measured with the precision measuring instrument of non-contact type.
(3) Optical fibers are inserted into fiber holes and fixed with epoxy adhesive.
(4) The mating face of the ferrules is polished.

4. Relationship between dimension and insertion loss

In this connector, following two factors are considered having influence on the insertion loss.

(1) Eccentricity error of the fiber holes
(2) Clearance between the fiber hole diameter and the optical fiber outer diameter.

Here, the influence of these factors on insertion loss is made clear.

(1) Relationship between eccentricity error of the fiber holes and the insertion loss

The test was put through the steps as follows:

Eccentricity error of the fiber holes for the 4-fiber ferrule mating face was measured with the precision measuring instrument. The optical fiber ribbon was inserted into fiber holes. Clearance between the fiber holes and the outer diameter of the fibers is less than 1μm. Insertion loss of the SM 4-fiber connector against master connector with an index matching material was examined.

Relationship between eccentricity error of the fiber holes and the insertion losses of SM 4-fiber connector against master connector is shown in Fig.4.

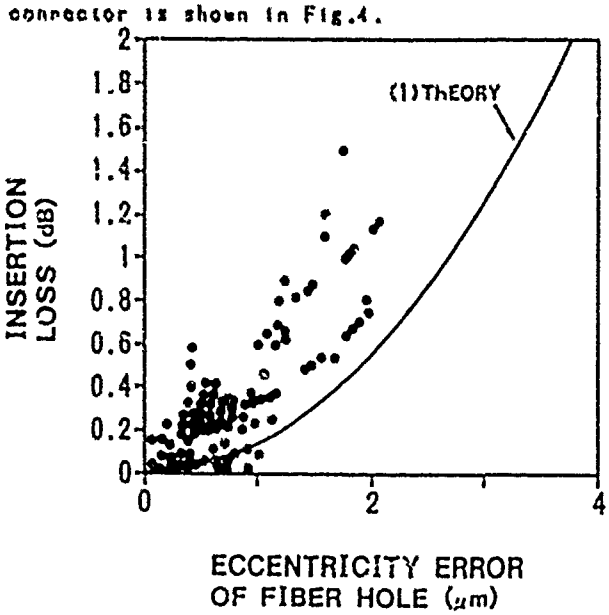

Fig.4 Relationship between Eccentricity Error of the Fiber Holes and Insertion Losses

It is known that jointing loss of the SM optical fiber is expressed as below against eccentricity error of SM fiber mode field diameter.

$L = 4.34 (r_e / w)^2$ L : Insertion Loss
r_e : Eccentricity error
w : Mode Field Diameter

However, the insertion loss of the SM connector is different from the theoretical curve (1). This is considered to be caused by eccentricity error of SM optical fiber mode field diameter, clearnce between the fiber hole diameter and optical fiber outer diameter, and surface angle of connector.

In actual use of the connector, eccentricity error of fiber holes of the SM multi-fiber plastic ferrule should be less than 1.5μm to obtain insertion loss below 1dB.

(2) Effect of clearance between the fiber hole and the fiber outer diameter

The clearance between the fiber hole and the fiber outer diameter was set to be 1, 2, and 3μm. Insertion losses were measured against master connector and the random connection of each connector. The 4-fiber ferrule used in the test was less than 1μm in eccentricity error of fiber holes.

Relationship between clearance of the fiber holes to the optical fiber outer diameter and insertion loss is shown in Table 1 and Fig.5.

It has been clear that smaller clearance brings about lower insertion loss both in random and master connections. In the random connection, this trend was more clear.

Table 1. Clearance and Insertion Loss

CLEARANCE (μm)		1	2	3
Insertion Loss Against Master	Av.	0.109	0.145	0.193
	S.D.	0.063	0.067	0.136
Insertion Loss Random	Av.	0.161	0.256	0.341
	S.D.	0.104	0.166	0.283

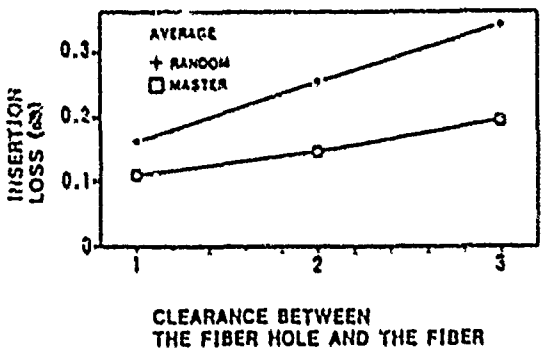

Fig.5 Relationship Between Clearance and Insertion Loss

5.Dimension of multi-fiber plastic ferrule

As described above, dimensional accuracy of the multi-fiber plastic ferrule for the SM multi-fiber connector has a large influence.

In this section, the precise dimension of the SM 4-fiber plastic ferrule is described.

A histogram of eccentricity error of the fiber hole of the SM 4-Fiber plastic ferrule is shown in Fig.6 and eccentricity error of each hole is shown in Table 2.

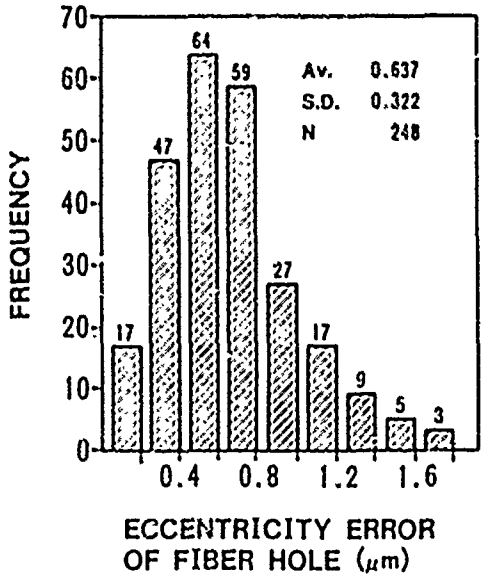

Fig.6. Histogram of Eccentricity Error of Fiber Hole

Table 2 Eccentricity error of Fiber Hole

	HOLE NUMBER (μm)			
	1	2	3	4
Av.	0.641	0.68	0.634	0.594
S.D.	0.313	0.345	0.295	0.364
MAX	1.56	1.2	1.78	1.68

The average eccentricity error of the fiber hole was 0.637μm and its standard deviation was 0.322μm for 4-fiber plastic ferrule.

6.Insertion Loss of SM Multi-fiber Connector

SM 4-fiber ribbon whose outer diameter was 125±1μm and mode field eccentricity error was below 1μm,was fixed by epoxy resin. 1200 connecting losses against master connector were measured with an index matching material. A histogram of insertion loss of the SM 4-fiber plastic connector is shown in Fig.7 and insertion loss of each fiber is shown in Table 3.

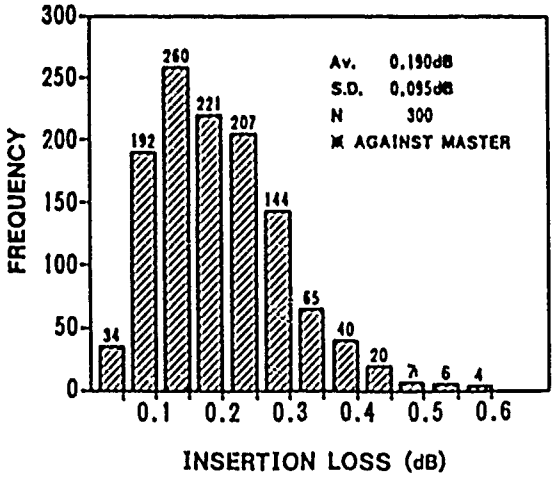

Fig.7 Histogram of Insertion Loss of SM 4-fiber Connector

Table 3 Insertion Loss of Each Fiber

	FIBER NUMBER (dB)			
	1	2	3	4
Av.	0.202	0.23	0.164	0.164
S.D.	0.09	0.109	0.075	0.087
MAX	0.56	0.55	0.49	0.52

The average insertion loss was 0.190 dB and the standard deviation was 0.095 dB.The average insertion loss was obtained 0.164~0.230dB. This result indicates that a SM multi-fiber plastic connector has very low loss and small deviation.

In actual use in the field,the SM multi-fiber connector is used as random connection. A histogram of insertion loss in random connection is shown in Fig.8 and insertion loss of each fiber is shown in Table 4.

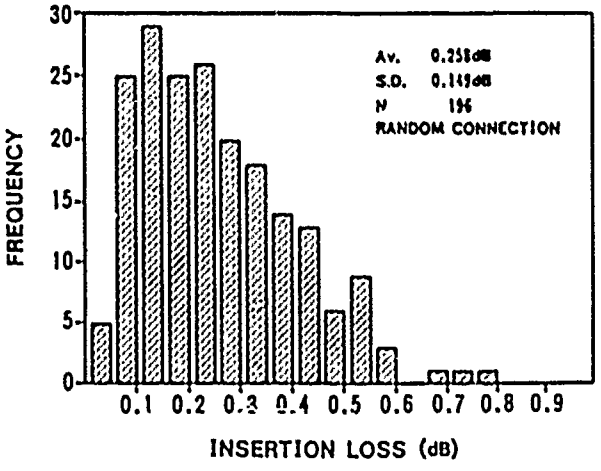

Fig. 8 Histogram of Insertion Loss of SM 4-fiber Cnnector (Random Connection)

Table 4 Insertion Loss of Each Fiber(Random Connection)

	FIBER NUMBER (dB)			
	1	2	3	4
Av.	0.204	0.266	0.269	0.292
S.D.	0.157	0.142	0.123	0.156
MAX	0.8	0.75	0.69	0.6

The average insertion loss was 0.258dB and standard deviation was 0.149 dB. Insertion loss increase of 0.062 dB was revealed for the average value and also deviation increase of 0.063 dB was revealed as compared with the insersion loss againt master connector. But,these connectors have sufficient property of connection loss for practical use.

Insertion loss of 2-,8- and 10-fiber connectors were measured by the same method as the SM 4-fiber connector. The results are shown in Fig.9,10 and 11. As the results, the average of insertion loss of SM 2-,8- and 10-fiber connectors were 0.226 dB,0.172 dB and 0.210 dB.

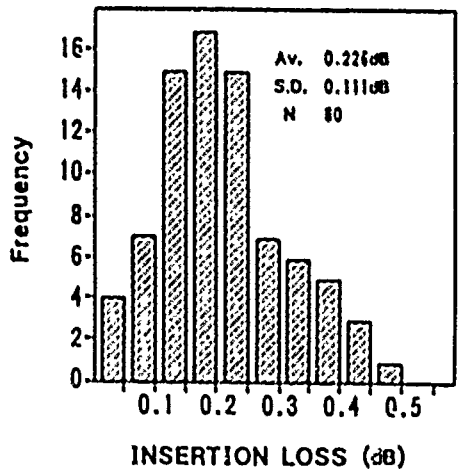

Fig.9 Histogram of Insertion Loss of SM 2-fiber Connector

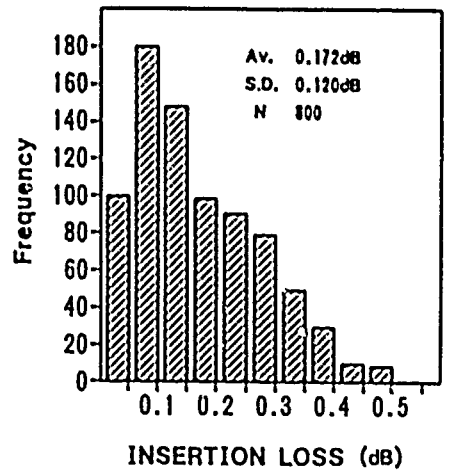

Fig.10 Histogram of Insertion Loss of SM 8-fiber Connector

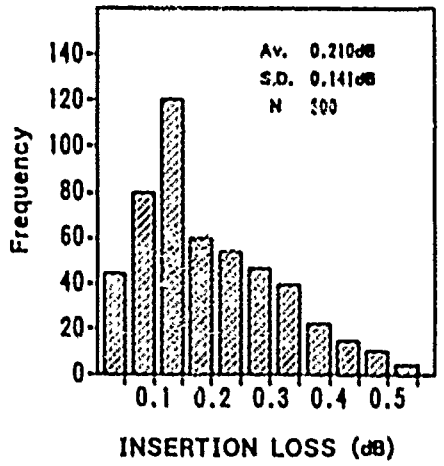

Fig.11 Histogram of Insertion Loss of SM 10-fiber Connector

7.Reliability Test

Various kinds of reliability tests were conducted to confirm the long term stabilities of the SM multi-fiber plastic connectors.

(1) Environmental Tests

As environmental tests,the SM 4 fiber connector was placed under high temperature and high humidity(+60℃×95%RH×500hrs),high temperature(+80℃×100hrs),low temperature (-40℃×100hrs)and heat cycle (-40℃~+60×100 cycles) conditions respectively. Environmental test conditions and results are shown in Table 5. Variation of connection loss under heat cycle condition is shown in Fig.12.

Table 5. Reliability Test Condition and Result

	HUMIDITY	HIGH TEMPERATURE	LOW TEMPERATURE	Heat Cycle
CONDITION	60°C 95%RH 500H	80°C 100H	−40°C 100H	−40~+60°C 100cycles
LOSS INCREASE	<0.2dB	<0.2dB	<0.2dB	<0.2dB

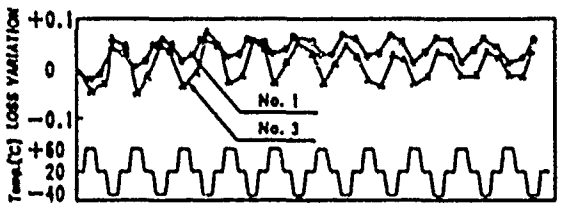

Fig.12 Heat Cycle Test

In all these tests, loss variation during and after test was less than 0.2 dB, and these results show that a SM multi-fiber plastic connector has stable connection for long term.

(2)Mechanical test

To check the mechanical characteristics of the SM 4-fiber connector, impact test (500G) and vibration test(10~55Hz×1.5mmpp×2hrs)were carried out.
No variation was observed in both tests.

Conclusion

A multi-fiber plastic connector has been developed for SM optical fiber ribbon.

(1) To obtain low insertion loss of the SM multi-fiber plastic connector, precisely molded SM multi-fiber plastic ferrule has been developed, and the repoducibility of the eccentricity error of fiber hole is less than 1.5μm.
(2) The average insertion loss of the SM 4-fiber plastic connector against the master connector was 0.190 dB and the average of random connection loss was 0.258 dB.
(3) The loss variation was less than 0.2 dB in various reliability tests.

References

(1) T.Satake,S.Nagasawa and Arioka: "A new type of demountable plastic-molded single-mode multifiber connector" ,IEEE/OSA,J.Lightwave Technol.,LT-4, pp.1232-1236,(1986).
(2) T.Satake,N.Kashima and M.Oki: "Very small single-mode ten-fiber connector" ,IEEE/OSA,J.Lightwave Technol.,LT-6, pp.269-272,(1988)
(3) N.Kashima and T.Satake: "Relation between connection loss and single-mode optical fiber diameter in a multifiber connector" , Trans.IEICE,E-70,pp.1120-1124,(1987)
(4) T.Haibara,S.Nagasawa,M.Matsumoto and M.Kawase: "Single-Mode Multifiber Technique for High-Density High-Count Subscriber Cables." ,37th IWCS pp.576-585 (1988)

Toshihiko Ohta

The Furukawa Electric Co.,Ltd.
6,Yawata-Kaigandori, Ichihara,Chiba,Japan

Mr.Ohta graduated from Shinshu Univ.with a B.Sc.in physics in 1985. Then he joined The Furukawa Electric Co.,Ltd. and has been engaged in research and development of the optical fiber.

Mr.Ohta is now a engineer of optical component,Development and Engineering Department ,Opto-technology Laboratory.He is a member of the Institute of Electronics and Communication Engineers of Japan.

Yasushi Kihara

The Furukawa Electric Co.,Ltd.
6,Yawata-Kaigandori, Ichihara,Chiba,Japan

Mr.Kihara graduated from Shibaura Institute of Technology with a B.Sc.in cominications engineering in 1986. Then He joined The Furukawa Electric Co.,Ltd. and has been engaged in development of optical component.

Mr.Kihara is now a engineer of Production Engineering Section of Optical Component.

Takashi Shigematsu

The Furukawa Electric Co.,Ltd.
6,Yawata-Kaigandori, Ichihara,Chiba,Japan

Mr.Shigematsu graduated from Yamagata Univ.with a B.Sc.in mechanical engineering in 1986. Then he joined The Furukawa Electric Co.,Ltd.and has been engaged in development of the precision mold.

Mr.Shigematsu is now a engineer of R&D Department Plant &Facilities Division.

Hideyo Kawazoe

The Furukawa Electric Co.,Ltd.
6,Yawata-Kaigandori, Ichihara,Chiba,Japan

Mr.Kawazoe graduated from Tokyo Univ.with a B.Sc.in mechanical engineering. Then he joined The Furukawa Electric Co.,Ltd.and has been engaged in research and development of high strength cable,VAD method,accessories of optical fiber cables, and now a cable system.

Mr.Kawazoe is now a senior research engineer of cable system,Development and Engineering Department,Opto-technology Laboratory. He is a member of the Institute of Electronics and Communication Engineers of Japan.

Development of Dry-Type Water-Blocking Optical Fiber Cable Using Swelling Material

H. Hiramatsu, N. Ishii, and K. Nagai

The Furukawa Electric Co., ltd.

Abstract

Development of Non-metallic water-blocking cable is achieved by using absorbing polymer that is available for seawater. This new cable took away the environmental limitation for installation which was a problem of conventional cable. And at the same time, the long-term reliability of the cable itself was improved.

1. Introduction

The Non-Metallic cable is a cable structure that utilizes the non-inductivity, which is one of the characteristics of the optical fiber cable. This structure is known to be very effective in installation in inductive areas.

In these cables, water-blocking function have been given to enhance optical fiber reliability. Generally, the method to provide this function is to fill a grease compound or use a water-absorbing polymer. When water-absorbing polymer is used, the water-blocking performance has not been sufficient against high ionic solution like seawater in the case of conventional cables.

We have developed non-metallic water-blocking cable that can be used without choosing an installation environment by improving these shortcomings. In this cable, water-absorbing polymer is used only as wrapping to hold cable composite materials, enabling the cable to guarantee the water-blocking performance against seawater and to achieve the easiness of handling equal to that of ordinary optical fiber cables.

2. Cable Design

2-1 Comparison of Cable Constructions

Table 1 compares cables that are generally used at present as optical fiber cables. The gas maintaining type cable is frequently used in Japan and shows excellent characteristics in reliability. On the other hand, a gas facility is needed for its construction and it is costly in maintenance and management. These are the reasons that seem to prevent these cables from prevailing throughout the world.

Cables filled with jerry are normally used in countries other than Japan and are seen to excel in reliability for a non-gas maintaining cable. Nevertheless, it presents a problem when removing jerry during optical fiber splicing work, therefore jerry cable does not always have good reputation.

As mentioned above, cables using a water absorbing material have various advantages such as maintenance cost and ease of handling. Therefore they are considered to be promising as structures of future low-cost cables. However, at present, the water-blocking performance of them is not sufficient with aqueous solutions of high ionic density such as seawater. For this reason, in the past, these dry cables have been used only in limited areas. If seawater can be blocked, they can be installed in all areas in Japan without considering installation environments.

2-2 Performance Requirement

The characteristics required for water-blocking cables to expand as the maincurrent of optical fiber cables are listed below.

TABLE 1 Comparison of Cable Structure

	Gas-Maintenance	Jerry-Filled	Water-Absorbing
Jointing Workability	○	×	○
Maintenance Cost	×	○	○
Long-term Reliability	○	○	△
Manufacturability	○	△	○
Cable Characteristics	○	△	△

1 Development of seawater-blocking structure

As mentioned above, the cables that are available at present do not have sufficient water-blocking performance with solutions which have a high ionic density. Guarantee is given by restricting water quality. Among aqueous solutions which exist in the nature, seawater has the highest ionic density. It is quite possible that seawater enters manholes in the coastal areas of Japan. For this reason, reliability on waterblocking greatly improves by blocking seawater.

2 Development of 100-fiber cable

To increase the maximum number of fibers from 40 (at present) to 100.

3 Elimination of water-absorbing material between optical fiber ribbons.

To eliminate water-absorbing narrow tape between fiber ribbons that has been used with conventional cables. Lowering of the friction resistance between ribbons reduces strain applied to the optical fibers and improves reliability in cables of this type which contains optical fiber ribbons in a slot.

2-3 Cable Construction

Figure 1 compares the constructions of the newly developed and conventional cables. For the diffusion of this cable in the future, the cable is composed of ribbon/slot structure which is popularly used in Japan at present.

The cables are made entirely of non-metallic materials and are non-inductive. The cable outer diameter is approximately 18 mm, and the weight is approximately 200 kg/km.

By choosing certain kinds of sheath material, the cable can be made to be flame-retardant.

The optical fibers are 250um UV-coated Dispersion Shifted Fibers (DSF) and 4-fiber ribbons are formed. Compared with the conventional structure, the following principal changes and improvements have been made.

1 Strength Member

In the past, FRP reinforced by glass fiber (G-FRP) has been used as non-metallic strength members. However, G-FRP has been strong against the bending rigidity and has presented a problem in handling during installation. By using aramide fibers (K-FRP) as strength member replacing glass, an excel flexibility is achieved even though the outer diameter of the strength members have increased from 3.6 to 4.5 mm.

2 Maximum number of fibers

To realize a 100-fiber cable as the maximum number of fibers in cable, five 4-fiber ribbons are inserted in one groove. This achieves an compatibility with the present feeder and subscriber cable structures.

3 Water-Absorbing Construction

To improve the cable characteristics, reliability and manufacturability, the water-absorbing tape which has been used between optical fiber ribbons has been removed, and water penetration inside the cable can be blocked only by water-absorbing wrappings around the core. The number of ribbons inside the grooves has increased to five and the holding tape assures the water-absorbing material to drop from the tapes and spreads inside the grooves if water enters.

PE outer Jacket
Water-absorbing tape
Optical fiber ribbon
Strength member (FRP)
Water-absorbing wrapping

a) Conventional design (40 fibers)

PE outer Jacket
Optical fiber ribbon
Strength member (FRP)
Water-absorbing wrapping

b) New structure (100 fibers)

FIG.1 Cross Section of Cable Structure

3. Waterproof Design

The key technology for the development of this cable was to endow a cable with a water-blocking characteristic against seawater.

3-1 Water-Absorbing Material and its Mechanism

The requirements on the water-absorbing material used in optical fiber cables are as follows:

1 Waterblocking structure against seawater.

2 Rapid expansion by absorbing water to prevent water penetration when water enters.

3 No corrosion by bacteria (no generation of hydrogen)

A polyacrylic water-absorbing material has been used for the structure to meet these requirements. Figure 2 shows a model of the water-absorbing mechanism of the polyacrylic water-absorbing material. The polyacrylic water-absorbing material is a copolymer of a polymer which has a carboxyl radical. In water, sodium ions of -COONa dissociate to increase the ionic density in fibers, thus enabling absorption of water around it. The water absorption magnification of a polymer varies in proportion to the osmotic pressure by ionic density difference and to affinity of the polymer itself with water and is a constant that is determined in inverse proportion to the molecular crosslinking degree in the polymer. Because an osmotic pressure is used as a water-absorption mechanism, the water-absorbing magnification of it is forecasted to be affected by the ionic density of the aqueous solution which entered. The water-absorption performance is expected to deteriorate substantially with an aqueous solution whose ionic density is very high such as seawater.

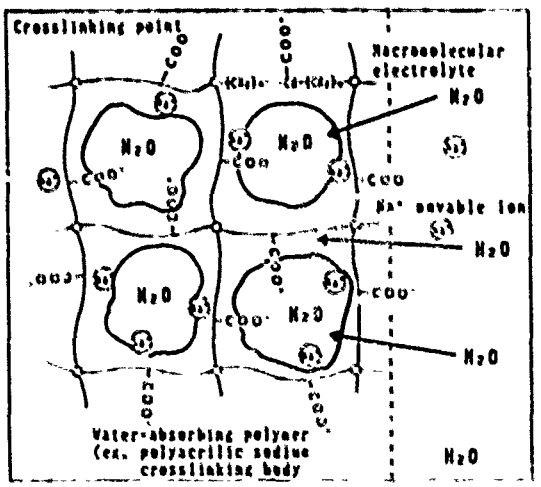

FIG.2 Water-absorbing principle of polymer

TABLE 2 Electrolyte Density of Limited Water and Seawater

Water Quality	Electrolyte Density (g/litter)					Total Density (Wt%)
	NaCl	KCl	$CaCl_2$	$MgCl_2$	Other	
Limited Water	0.75	0	0.5	0	0	0.13
Seawater	24.53	0.69	1.16	5.20	4.47	3.65

Limited Water: Average quality of water in manholes throughout Japan
Seawater : Prescribed by ASTM D1141

3-2 Comparison of Water Quality

Table 2 compares composite components of limited water (aqueous solution which have been guaranteed in the past) and seawater. The limited water has been determined based on the results of the survey of water accumulated in manholes throughout Japan. This allows covering of approximately 99% of the whole areas. Compared with conventional limited water, seawater contains salts which are several ten times more in density.

3-3 Water-Blocking Characteristics with Bivalent Ions

During the process of studying the water-blocking characteristic against seawater, it became clear that the water immersion length gradually advanced if a conventional water-absorbing material was used. To study the causes for this phenomenon, effects by the kinds of the electrolyte were studied.

Figure 3 plots fluctuations of the gel viscosity of the material when NaCl and $CaCl_2$ aqueous solutions were absorbed by the water-absorbing material. The gel viscosity very well matches the water-blocking ability of the water-absorbing material. As the diagram shows, the polymer gel viscosity has a saturation value, that is, water-blocking performance to some extent exist with univalent ions such as NaCl, even if the electrolyte density increases. The saturation value is not recognized with bivalent ions such as $CaCl_2$, and the gel viscosity monotonously lowers as the electrolyte density increases. A waterblocking test using an aqueous solution of 1 wt% $CaCl_2$ shows that the water penetration length increases in proportion to time.

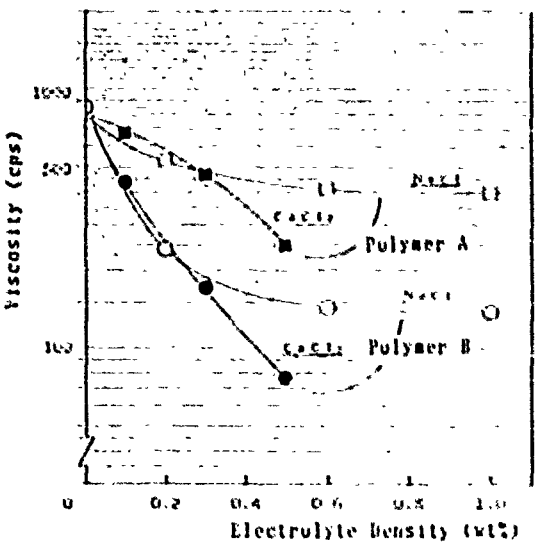

FIG.3 Effects of electrolyte of polymer on water absorbing characteristic

Against aqueous solutions containing bivalent ions, the water-absorbing polymer, in the first stage, dissociates Na^+ ions from -COONa when water attacks and generates osmotic pressure as against deionized water, to absorb water inside the polymer. However, Na^+ ions enter inside the polymer as time passes and couple with two -COO- to form a stable state. This shrinks the network construction of the water-absorbing polymer and is estimated to discharge the water it absorbed once. To solve this problem, a material with a low metal ion dissociation degree and with a large affinity between the polymer and water, has been used to enhance the water blocking performance against bivalent ions.

3. Cable Characteristics

The characteristics of this water-blocking cable are described below.

3-1 Transmission Loss

Figure 4 shows loss fluctuations between cabling processes of test manufactured cable using dispersion shifted fibers. The average loss values between processes fluctuated less than 0.02 dB/km, showing stable characteristics.

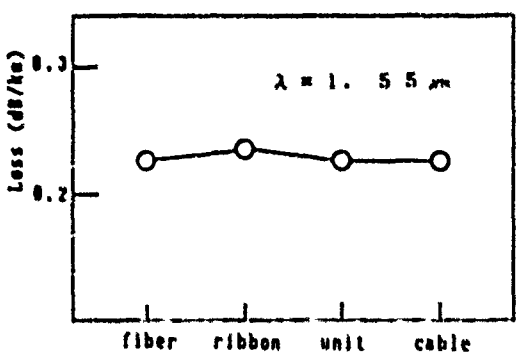

FIG.4 Loss fluctuations in cabling-process

3-2 Waterblocking Characteristics

The waterblocking characteristics of the test-manufactured cable were measured by the two methods shown in Figure 5. 1 m water head pressure was imposed upon the cable in each test. In both cases, the aqueous solution used had the same composition as that of seawater.

In the evaluation of 5-A, no water leak after 24 hours was observed at the end of 1.5 m cable end. Long term tendency of the penetration length was evaluated by the method shown in figure 5-B. Figure 6 shows the test results of B. In B, cable of the same structure was test manufactured using the conventional swelling material to compare the water-blocking characteristics, and they were tested. In both cases, the initial water penetration length did not make a large difference. But as time passes the penetration length of the non-seawater cable did not show a saturation trend and the immersion length increased on a near semi-log straight line relative to time. On the other hand, the penetration length did not increase nearly at all with the cable protected against seawater, and the immersion length is estimated to be less than 10 m even after 20 years, which is the guaranteed period of the cable.

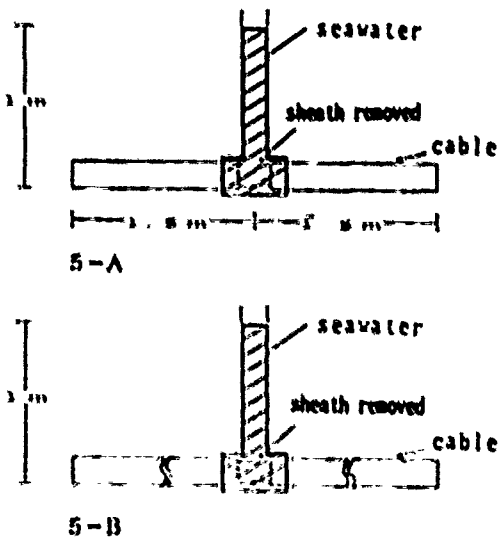

FIG.5 Evaluation method of water-blocking performance

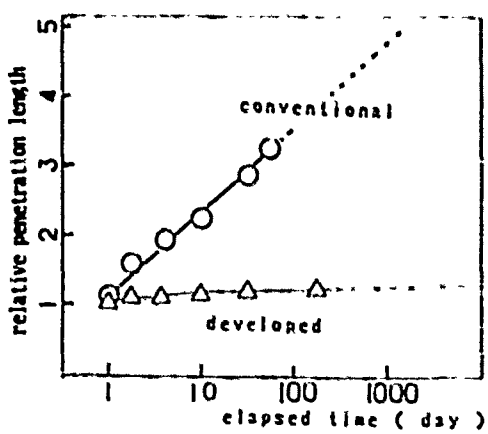

FIG.6 Penetration length V.S. elapsed time

4-3 Temperature Characteristics

Figure 7 shows the evaluation results of the temperature characteristics of the cables. The measurement wavelength is 1.55 um as DSF fiber is used. The maximum loss fluctuations was +0.02 dB/km at a temperature range of -30 to +60 ℃.

4-4 Mechanical Characteristics

Table 3 lists the results of the cable mechanical tests. In all evaluation, results that indicated trouble during cable use could not be obtained, and the same satisfactory results as those of gas-maintained cable could be achieved.

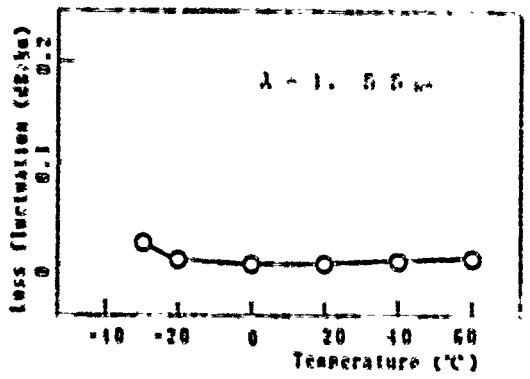

Fig.7 Temperature dependence

TABLE 3 Cable Mechanical Characteristics

Item	Conditions and Results
Lateral pressure	200kg/50mm × 1min No loss fluctuations
Bending	R=100×10cycles, 60×1cycle D: Cable outer diameter No loss fluctuations, No sheath trouble
Impact	1kg×1m (25mm column) No loss fluctuations
Torsion	±180° /m , Tension 50kg No loss fluctuations
Squeeze	R=600mm (tools for installation) Tension 200kg Number of operations 4times No loss fluctuation Optical fiber strain 0.2% or less

5. Conclusion

A cable with water-blocking performance against seawater was developed by improving the water-absorbing material, and is considered to be a promising structure as non-metallic non-gas maintenance cable.

Until now, although the dry-type water-blocking cable is easy to handle, it can be installed only after studying installation environments. The recent development enables a dry cable that blocks seawater and that does not have to select installation environments.

The latest development of the dry non-gas cable allows to enjoy an advantage over jerry-filled cable in terms of handling and over gas-maintenance cable in terms of maintenance cost. The water-blocking performance for seawater also, which has been trouble in commercializing this cable, has been guaranteed.

6. References

(1) S.Kukita, et al. "A New Nonmetallic and Water Proof Optical Fiber Cable with Absorbent Polymer Ribbon" 1987 36th IWCS

(2) N.Koga, et al. "Hydrogen Generation due to decomposition of Carboxymethyl-Cellulose in Muddy Water" 1985 Electron. Lett., .91.26

Hideyo Hiramatsu

Mr. Hiramatsu graduated from Kyoto Univ. in 1984 with a B.Sc. in electric engineering, then joined The Furukawa Electric Co., Ltd. and has been engaged in the development of the optical fiber cable.

He is now a staff engineer of the Optical Fiber Transmission Section, Opto-Technology Laboratory.

Kiyotoshi Nagai

Mr. Kiyotoshi Nagai graduated from Kyoto Univ. in 1987 with a B. Sc. in Electric engineering, then joined The Furukawa Electric Co., Ltd. and has been engaged in the development of the optical fiber cable.

He is now a staff engineer of the production Engineering Section of Optical Fiber Telecommunication Division, in Chiba Works.

Nobuhisa Ishi

Mr. Ishii graduated from Waseda Univ. in 1987 with a M. Sc. in Applied Chemistry, then joined The Furukawa Electric Co., Ltd. and has been engaged in the development of the materials for optical fiber cable.

He is working as a staff member of Cable Material Research Section, Chiba Research Laboratory.

Low Temperature Loss Stabilized Cables with Optical Fibers Coated by UV Curable Resins

K. Maeda, S. Okagawa, M. Mikami and S. Sentsui

THE FURUKAWA ELECTRIC CO., LTD.

ABSTRACT

The thermal expansion behaviors of Ultraviolet(UV) curable resins for optical fibers were investigated for the low temperature use. It was found that some UV resins showed anisotropy in the thermal expansion behaviors to axial and radial direction after coating in drawing process. To prevent transmission loss increase at low temperature, it was most important to keep a certain level of the gripping force of coatings in the radial direction. From the view point, suitable requirements for the coatings in optical fibers were elucided theoretically and experimentally, which suppressed loss variation in cables to be less than 0.05dB/km at 1.55μm in temperature range of -40 to +80°C.

INTRODUCTION

High count subscriber cables have been extensively applied to telecommunication network in Japan. In the optical cables various kinds of UV resins were used for maintaining the reliability. Particularly the coating materials in optical fibers could play an important role with respect to the fiber properties as summarized in Table 1. Since the coating materials had linear thermal expansion coefficient which were much larger than that in silica glass, the transmission loss increase at low temperature was found in optical fiber coated even with thin layer to outside diameter of 250μm. In the previous papers[1-3], the loss increase at low temperature had been explained to result from buckling of glass parts in the primary layers which was caused by the shrinking force of the secondary layer. By our calculation results of the shrinking force in the optical fibers of 250μm outside diameter, however, it was found to be too small to cause buckling of glass parts in the primary layers. Therefore, thermal expansion characteristics which could affected to the loss increase at low temperature were also noted in the present study. The novel results obtaind were available for manufacturing loss stabilized cables within a temperature range of -40 to +80°C.

Table 1 requirements for Coatings of Optical Fiber

Material property	Requirements	Related fiber property
Young's modulus	Primary 1~5MPa Secondary 0.2~1GPa	• Lateral property
Glass adhesion	Mechanical strippable	• Strippability • Reliability
Curing speed	UV exposure<0.1J/cm²	• Productivity
H_2 generation	<10μl/g	• Infrared loss increase
Water absorption	<3%	• Reliability
Heat resistance	Mechanical property change <30% (80°C×30days)	• Reliability

EXPERIMENTS

(1) UV Resins

Three soft UV resins for primary coating, called soft-A, B and C, and a hard UV resin for secondary coating, called hard-a were investigated. Those resin fully satisfied the requirements specified in Table 1. All the resins were UV curable urethane acrylates widely applied to optical fibers. Young's moduli and thermal expansion coefficients of the UV resins in film form were shown in Table 2.

Table 2 Properties of UV Resins

Resin	Young's Modulus (MPa)		Thermal expansion coef. -60 to +80°C
	23°C	-60°C	(1/°C)
soft-A	1.2	10	1.4×10^{-4}
soft-B	1.5	136	1.4×10^{-4}
soft-C	1.3	95	1.4×10^{-4}
hard-a	780	2800	$1.0\times$ [illegible]

(2) Loss increase dependency on temperature

The single-mode fibers with cladding diameter of 125μm and mode field diameter of 9μm were used for the study, which were dual-coated with soft and hard UV resins. The outside diameter of primary and secondary layer were 200μm and 250μm, respectively. The measurements for loss increase in coated fibers and cables were carried out at a wavelength of 1.55μm in temperature range of -60 to +80°C and -10 to +80°C, respectively.

(3) Thermal expansion behaviors in UV resins

A single layer of UV resins were coated over optical fibers to an outside diameter of 400μm as shown in Fig.1, and removed from the fibers to study the influence of drawing on thermal expansion behavior.

The thermal expansion was characterized with the measurement of change of the sample size in both axial and radial directions within temperature range of -60 to +80°C. During the tests tensile or compression force of 1 gf was always applied for axial or radial direction in the samples, respectively.

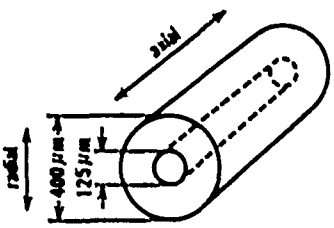

Fig.1 Tube sample

RESULTS

(1) Loss increase dependency on temperature

Fig.2 shows loss increase dependency on temperature in optical fibers dual coated with soft-A, B, or C resin as primary and hard-a resin as secondary. The optical fiber dual coated with soft-C resin as primary and hard-a resin as secondary showed no loss increase in the range of -60 to +80°C. In the contrast the significant loss increases were found in the optical fibers dual coated with soft-A or B resin as primary and hard-a resin as secondary.

The minimum force which generated the buckling in glass parts was given by the following equation .

$$F_{min} = \sqrt{E \cdot I \cdot Ep} \qquad \cdots\cdots(1)$$

Where

E Young's modulus of silica glass (= 71.6 GPa),
I geometrical moment of inertia for the fiber ($=D^4 \cdot \pi/64$, $D=125\mu m$),
Ep Young's modulus of primary coating.

The shrinking force in secondary coating at temperature range of +20 to -60°C was expressed as follows.

$$F = Es \cdot Ss \cdot \left(\int_{20}^{60} \alpha s(T)dT - \int_{20}^{60} \alpha(T)dT \right) \qquad \cdots\cdots(2)$$

where

Es Young's modulus of secondary coating,
Ss cross section area of secondary coating,
$\alpha s(T)$ linear expansion coef. of secondary coating,
$\alpha(T)$ linear expansion coef. of silica glass.

The calculation results are shown in Table 3. Since the shrinking force in hard UV resin was much smaller than the minimum force generating the buckling in glass parts at -60°C, loss increases at the low temperature were estimated not to occur by the model. As shown in Fig.2, however, loss increases at low temperature were observed in the optical fibers dual coated with soft-A or B resin as primary and hard-a resin as secondary. Therefore, the following studies were carried out to clarify the mechanism of loss increase dependency on temperature.

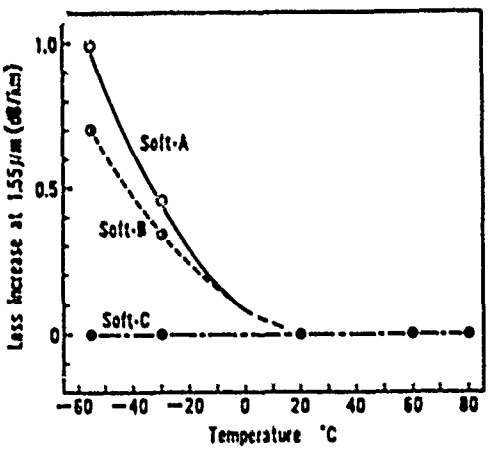

Fig.2 Temperature dependence of 250μm fibers

Table 3 Calculated values of Fmin and shrinking force at -60°C

Soft UV resin	Critical axial force for buckling (Fmin)	Shrinking force of hard UV resin
A	5.7 N	0.5 N
B	21.6 N	0.5 N
C	18.1 N	0.5 N

(2) Microscopic observations

The photograph taken at -40°C "in situ" in the dual coated fibers is shown in Fig.3. The gap between the glass parts and primary layers was found to be present in the optical fibers dual coated with soft-A or B resin as primary and hard-a resin as secondary which showed remarkable loss increases at low temperature. While there was no gap in the optical fiber with soft-C resin as primary which showed no loss increase at the low temperature.

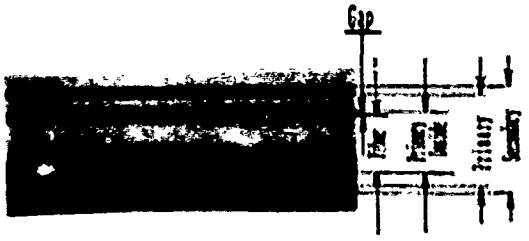

Fig.3 Photograph of the fiber coated with soft-A and hard-B at -40°C

(3) Thermal expansion behaviors in UV resins

Figs.4, 5 and 6 show the thermal expansion bihaviors of soft-A, B and C resin, respectively. The remarkable difference in thermal expansion behavior was found among three soft UV resins. Soft-A resin kept axially the same size from -60 to +80°C, but in the radial direction the significant change of diameter occured in the temperature range as shown in Fig.4. The difference of size change percent between axil and radial direction in the tube samples made from soft-B resin was smaller than that in the soft-A tube samples as shown in Fig.5. Additionally the size change percent in both direction in the temperature range was almost same in the tube samples made from soft-C resin as shown in Fig.6. Also the size change in tube samples made from hard-a was investigated. As shown in Fig.7, the thermal expansion behavior in both direction were almost same.

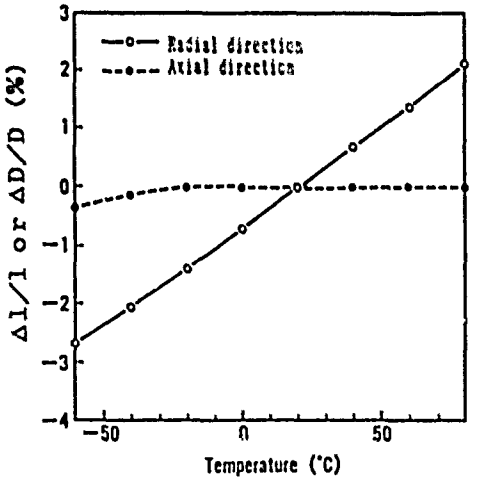

Fig.4 Thermal expansion behavior of soft-A

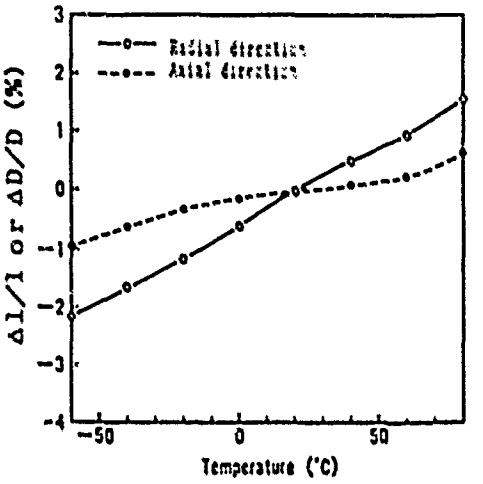

Fig.5 Thermal expansion behavior of soft-B

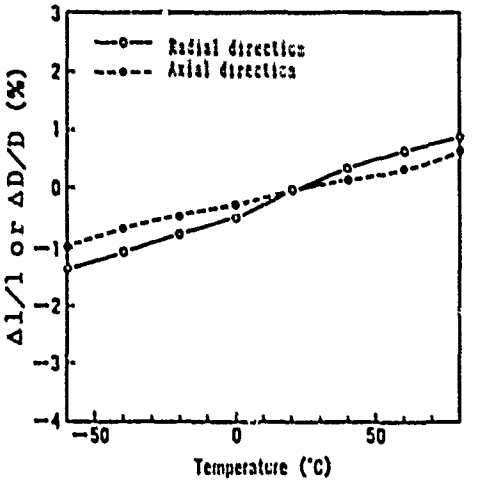

Fig.6 Thermal expansion behavior of soft-C

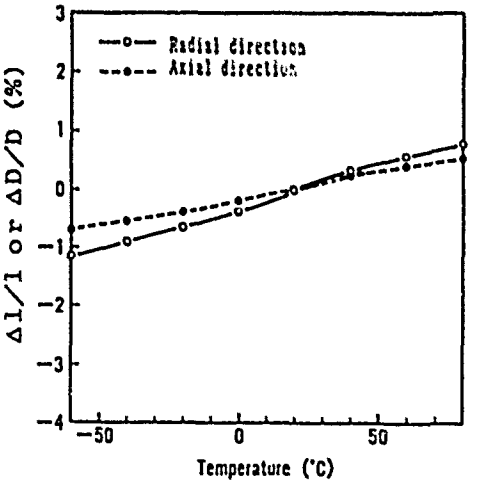

Fig.7 Thermal expansion behavior of hard-a

DISCUSSIONS

It was made clear that some soft UV resins showed different thermal expansion characteristics in axial and radial direction after the drawing. This suggested that the molecule orientation which caused the anisotropy was produced in the UV resins after the drawing.

Based on these results, we calculated the change of primary inside diameter with temperature in dual-coated fibers to clarify the mechanism of loss increase at low temperature[11]. The cross section of dual-coated layers in the optical fiber is shown in Fig.8. The primary inside diameter would be increased at low temperature for the shrinkage in radial direction, which could cause the gap between the glass part and the primary layer.

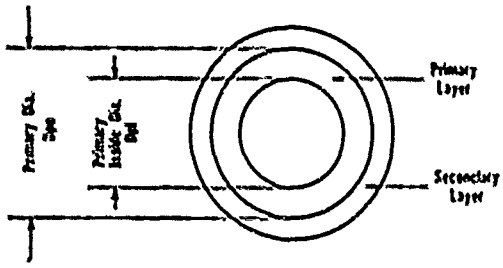

Fig.8 Cross section of 250μm fiber

The volume of primary layer $V_1(T)$ is given by Eq.(3), in which the thermal expansion characteristics to radial direction in the primary layer was assumed to be identical with those to radial direction in the secondary layer because the secondary layer could play a role as "wall" against the size change.

$$V_1(T) = \frac{\pi}{4}\{D_{2r}^2(1+\beta_{2r})^2 - D_{1i}(T)^2\}L(1+\beta_f) \quad \cdots\cdots(3)$$

where

D_1 primary coating outside diameter at 20°C,
D_{1i} primary coating inside diameter at 20°C (= 125μm),
$D_{1i}(T)$ primary coating inside diameter at T°C,
β_{2r} size change ratio in radial direction of secondary coating (= $\int_{20}^{T}\alpha_{2r}(T)\,dT$),
$\alpha_{2r}(T)$ linear expansion coef. in radial direction of secondary coating,
$D_2(T)$ primary coating inside diameter at T°C,
β_f size change ratio in axial direction of silica fiber (= $\int_{20}^{T}\alpha_f(T)\,dT$),
$\alpha_f(T)$ linear expansion coef. in axial direction of silica fiber.

On the other hand, the volume $V_2(T)$ in tube sample as shown in Fig.1 is given by Eq.(4)

$$V_2(T) = \frac{\pi}{4}(D_{2r}^2 - D_{1i}^2)(1+\beta_{1r})(L+\beta_{1z}) \quad \cdots\cdots(4)$$

where

β_{1r} size change ratio in radial direction of primary coating(= $\int_{20}^{T}\alpha_{1r}(T)\,dT$),
$\alpha_{1r}(T)$ linear expansion coef. in radial direction of primary coating at T°C,
β_{1z} size change ratio in axial direction of secondary coating(= $\int_{20}^{T}\alpha_{1z}(T)\,dT$),
$\alpha_{1z}(T)$ linear expansion coef. in axial direction of primary coating at T°C,
L length.

By combining Eq.(3) and (4), the primary coating inside diameter $D_{1i}(T)$ is given by Eq.(5), in which too small β_f was neglected.

$$D_{1i}(T) = \sqrt{D_{2r}^2(1+\beta_{2r})^2 - (D_{2r}^2 - D_{1i}^2)(1+\beta_{1r})^2(1+\beta_{1z})} \quad \cdots(5)$$

Fig.9 shows the calculated results for the fibers dual-coated with the primary coating of soft-A, B or C resin and the secondary coating of hard-a resin. In the figure the inside diameters for the fibers with soft-A or B were increased at low temperature. This means that the force to grip the fibers was weakened between the glass part and primary layer. On the other hand, the inside diameter for soft-C resin shows no change with decreasing temperature. The calculation results could acount for the gap between the glass part and primary layer as shown in Fig.3. Since the microbending loss at the low temperature range probably result from the gap or weakened gripping force in the interface, it was most important to keep a certain level of the gripping force of primary coating in the radial direction for loss stabilization at the low temperature. By converting Eq.(5) under a condition of $D_{1i}(T) \leq D_{1i}$, we can obtain the following Eq.(6), that shows the requirement not to cause the gap between glass part and primary layer for the coating materials in drawing process.

$$\frac{2\beta_{2r} + \beta_{2r}^2 - 2\beta_{1r}}{2\beta_{1r} + \beta_{1r}^2} \leq \frac{D_{2r}^2}{D_{1i}^2} \quad \cdots\cdots(6)$$

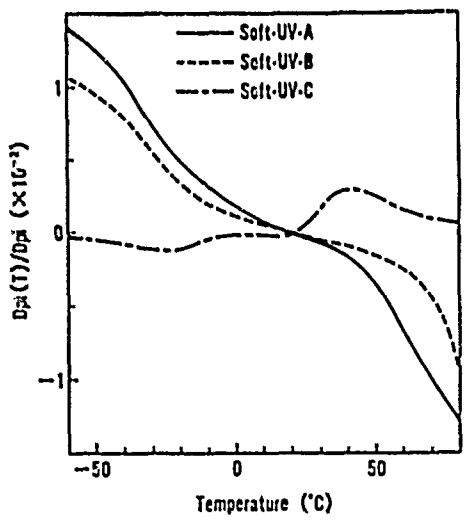

Fig.9 Calculated inside diameter changes of primary coatings.

APPLICATION TO A CABLE

A 100-fiber cable as shown in Fig.10 was manufacctured, in which soft-C as a primary layer and hard-a as a secondary layer were employed for the optical fibers. Fig.11 shows the loss increase dependency on temperature in the cable. Loss increases of the cable at the wavelength of 1.55μm were less than 0.05dB/km in range of -40 to +80°C.

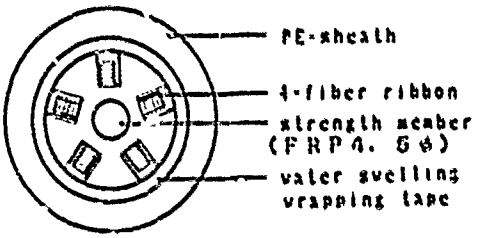

Fig.10 Cross section of 100-fiber cable

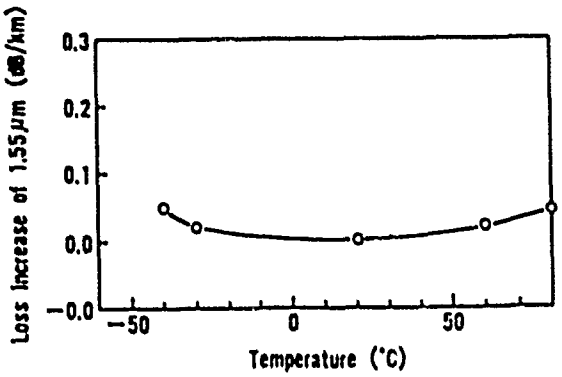

Fig.11 Temperature dependence of the 100-fiber cable

CONCLUSIONS

Thermal expansion behaviors of UV resins for optical fibers were studied theoretically and experimentally to stabilize the transmission loss at low temperature. It was found that some UV resins showed anisotropy after coating in drawing process. The anisotropy was pointed to cause loss increase at low temperature by lowering the gripping force of coatings in radial direction. Based on the results, suitable requirements for the coatings were derived theoretically. With the selected UV resins loss variation in cables was achieved less than 0.05dB/km at 1.55μm in temperature range of -40 to +80°C.

References

[1] Y.Katsuyama, Y.Mitsunaga, Y.Ishida and K.Ishi[illegible]a, Appl.Opt.,vol.19, pp.4200-4205, 1980.
[2] T.Yabuta, N.Yoshizawa,and K.Ishihara,Appl.Opt.,vol.22, pp.2356-2362, 1983.
[3] P.C.P.Bouten, D.J.Broer, C.M.G.Jochem, T.P.M.Meeuwsen and H.J.M.Timmermans,J.Lightwave Technol.,vol.7,No.4,April 1989.

Keigo MAEDA

The Furukawa Electric Co.,Ltd.
6 Yawata-Kaigandori,
Ichihara, Chiba, 290
Japan

Mr. Maeda graduated from Kyoto University in 1981 with a B.Sc. in industrial chemistry. Then he joined The Furukawa Electric Co.,Ltd., Chiba, Japan, and has been engaged in research and development of plastic materials and manufacturing methods for optical cable.

He is now a staff engineer of Optical Fiber Transmission Section, Opto-Technology Laboratory, The Furukawa Electric Co., Ltd. and a member of Institute of Electronics, Information, and Communication Engineers of Japan.

Masatoshi MIKAMI

The Furukawa Electric Co.,Ltd.
6 Yawata-Kaigandori,
Ichihara, Chiba, 290
Japan

Mr. Mikami graduated from Utsunomiya University in 19[illegible] with a B.S. and M.S degree in mechanical engineering. Then he joined The Furukawa Electric Co.,Ltd., Chiba, Japan, and has been engaged in development of optic fibers.

He is now a production engineer of Optical Fiber, Fiber Telecommunication Division at The Furukawa Electric Co., Ltd.

Shoji OKAGAWA

The Furukawa Electric Co.,Ltd.
6 Yawata-Kaigandori,
Ichihara, Chiba, 290
Japan

Mr. Okagawa graduated from Osaka University in 1981 with a M.Sc. in chemistry. Then he joined The Furukawa Electric Co.,Ltd., Chiba, Japan, and has been engaged in research and development of plastic materials and manufacturing methods for optical cable.

He is now a senior research engineer of Optical Fiber Transmission Section, Opto-Technology Laboratory, The Furukawa Electric Co., Ltd.

Shintaro SENTSUI

The Furukawa Electric Co.,Ltd.
6 Yawata-Kaigandori,
Ichihara, Chiba, 290
Japan

Mr. Sentsui graduated from Tokyo University in 1970 with a B.S degree in physical engineering. Then he joined The Furukawa Electric Co.,Ltd., Chiba, Japan, and has been engaged in research and development of superconduction co-axial line, characterization and measurement of optical fiber.

He is now a manager of Optical Fiber Transmission Section, Opto-Technology Laboratory, The Furukawa Electric Co., Ltd. and a member of Institute of Electronics, Information, and Communication Engineers of Japan.

A NEW ANALYTICAL METHOD FOR HYDROGEN EVOLUTION FROM OPTICAL FIBER CABLE

Ting-Chung Chang , Jin-Chung Lin , Yiang Liu

Telecommunication Laboratories , Chung-Li , Taiwan , R.O.C.

ABSTRACT

Hydrogen contamination of optical fiber causes increased transmission loss due to enhanced H_2 and/or -OH absorption. Hydrogen evolution from degradation of cable materials has been intensively studied to evaluated optical fiber reliability in the recent years. In most studies cable testing samples were thermally aged in sealed glass tubes or headspace vials at different temperatures. The hydrogen concentrations generated were sampled from those sealed glass containers with syringe and analyzed by GC. The escape of hydrogen during aging and sampling were observed.

In this paper a new procedure is established to evaluate hydrogen evolution from thermal degradation of optical cable materials. A supported Pd/Al_2O_3 catalyst is selected as hydrogen absorbent for its high efficiency of adsorbing and absorbing H_2 to Pd atom surface and bulk.The uptake hydrogen can be desorbed completely at about 400° C and detected by GC with TCD directly.

Different optical cable samples and cable components such as fiber coating materials,water-proof filling compounds, jacket, sheath, central member, etc. are evaluated with this new procedure and headspace vials method for comparison. By the new procedure, the collected hydrogen contents for same samples are about 1.6 times compared with those from the latter method. It is also found that the major sources of hydrogen evolution of optical fiber cables used in Taiwan are water-proof filling compounds and fiber coating materials.

INTRODUCTION

Hydrogen related loss increase of optical fiber cables has been found and studied for quiet a few years[1,2,3,4,5,,6]. The hydrogen concentration in the cable can be determined by the evolution from organic cable materials and the permeation through the cable sheath. It is important to measure the hydrogen evolution for cable materials selection.

There are many studies about hydrogen analytical methods [3,4,5,7,]. Generally speaking, test samples were put in either sealed glass tubes or headspace vials and aged at different temperatures; the hydrogen concentration generated was analyzed by gas chromatography. But the above analytical methods have some drawbacks, such as the escape of hydrogen from the septum-sealed headspace vials during aging process and the difficulty of withdrawing sample volume via syring from the sealed glass tube.

In this paper, a new procedure using Pd/Al_2O_3 catalyst as hydrogen absorbent to measure hydrogen evolution from optical cable samples during thermal aging process is established.

EXPERIMENTAL

Catalyst Preparation

The catalyst was prepared by the anion exchange method[8],$PdCl_4^{-2}$ anions from $PdCl_2$-HCl were exchanged with OH^- groups on alumina in acidic aqueous solution (pH = 2 $\pm$ 0.2). The sample was subsequently dried at 110°C and calcined at 400°C.

Test Equipment

Figure 1 is a schematic diagram of the apparatus used for the hydrogen evolution measurement of optical fiber cable materials. A pure argon flow was passed through the quartz reactors. Hydrogen evolved by optical fiber samples was sorbed by the precalcined Pd/Al_2O_3 catalyst and the subsequently desorbed hydrogen was monitored by a thermal conductivity detector. The temperature of the reactor was controlled by a Eurotherm 127 temperature programmer.

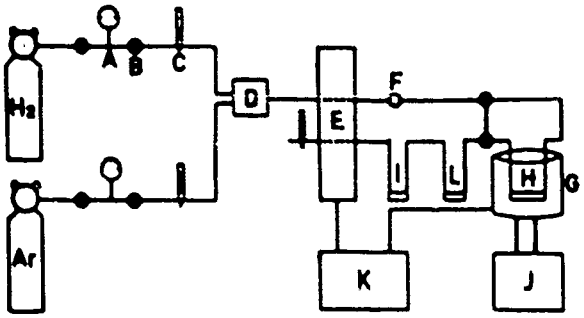

A: Pressure Gauge
B: Needle Valve
C: Flow Meter
D: Mixing Chamber
E: T.C.D.
F: Injector
G: Furance
H: Quartz Reactor(Contain Sample)
I: Quartz Reactor(Contain SiO_2)
J: Temperature Controller
K: Recorder
L: Quartz Reactor(Contain Pd/Al_2O_3)

Figure 1 : Schematic diagram of the hydrogen adsorption system.

Test Procedure

The precalcined Pd/Al_2O_3 catalyst and optical cable sample were inserted into the two quartz tube reactors respectively. A stream of 10% H_2/Ar gas mixture at 1 atm was regulated by a needle valve . The temperature of the reactor was raised to 120°C by a temperature controller and kept for 1 hour to reduce the Pd/Al_2O_3 catalyst. After the reduction process,the temperature was raised to 400°C and kept for 1 hour to desorb the hydrogen in the catalyst surface and bulk. By means of the above process,we could get a metal state of Pd/Al_2O_3 catalyst. After catalyst pretreatment the catalyst reactor was cooled down to room temperature,the stream of gas was convert into pure argon and passed through both optical cable fiber reactor and catalyst reactor,then optical fiber cable aging process was performed. The hydrogen evolved in aging process were absorbed by the Pd/Al_2O_3 catalyst. When the degradation test came to an end, we raised the catalyst reactor temperature to 400°C at a rate of 10°C/min. The time profiles of the H_2 desorptions from the Pd/Al_2O_3 catalyst and the temperature of the reactor were measured simultaneously by a TCD-GC and a thermocouple, respectively.

Sample

Different optical cable samples and cable components such as fiber coating materials,water-proof filling components, jacket, sheath,central member, ect. are evaluated with above method. All the cable components tested are listed in table 1.

Table 1 : Cable Components Analyzed for H_2 Generation

Sample	Discription
Cable A	Jelly-Filled Cable
Cable B	Pressurized-Cable
Cable C	Jelly-Filled Cable
Silicone	Coating Material
Desolite	Coating Material
Acrylate	Coating Material
Mylar	Wrapper Material
Kevlar	Wrapper Material
Polyisobutene	Filling Compound
Thixotropic A★	Filling Compound
Thixotropic B○	Filling Compound
Thixotropic C▲	Filling Compound
HDPE	Tube and Sheath Material
LDPE	Tube and Sheath Material
Nylon	Tube and Sheath Material
Fiber A	S.M. Fiber
Fiber B	M.M. Fiber
Fiber C	S.M. Fiber

★:major composition: mineral oil,SiO_2 polyisobutene
○:major composition: polymethyl siloxane SiO_2
▲:major composition: mineral oil,SiO_2

RESULTS AND DISCUSSION

Amoung the common catalytic metals,palladium is unique in its ability to dissolve hydrogen atom to form palladium hydrides. Yamabe et al.[9] had investigated the desorption of hydrogen sorbed by palladium supported on silica-alumina between 273°K and 308°K. They concluded that hydrogen is sorbed by palladium in three states' i.e weakly adsorbed H_2 absorbed H and strong adsorbed H. Their results show that the absorbed H and the weakly chemisorbed H can be removed by outgassing for 1 hour at 293°K,after which only the strongly chemisorbed H remained on the surface. Boudart et al.[10] had investigated the hydrogen sorbed by supported palladium catalyst. They pointed out that at 303°K and the hydrogen pressure below 17 torr,hydrogen atoms can be strongly chemisorbed on palladium surface not absorbed into palladium crystallites.

From the above discussion and the fact that the hydrogen pressure which evolved from optical fiber cable was far bellow 17 torr,we could recognize that in our case,the hydrogen atom was strongly chemisorbed in palladium atom surface and was not flushed away by argon gas stream. In all the experiment procedure,we had detected the gas composition of argon gas stream by TCD and recorder and did not find any hydrogen gas. This also confirmed our recognization.

Figure 2 is the variation of hydrogen desorption over a Pd/Al_2O_3 catalyst versus reactor temperature. The temperature was kept at room temperature for a period of time then raised to 400°C at a rate of 10°C/min. At room temperature,the hydrogen did not desorb and near 325°C,the adsorbed hydrogen could desorbed completely.

The following equation was assumed to happen at this stage.

$$Pd_{(s)}H \longrightarrow Pd_{(s)} + 1/2\ H_2$$

In this reaction (s) represents species on the surface.

The desorbed hydrogen volume was calibrated by injecting a known amount of hydrogen gas into TCD-GC with a Hamilton gastight syring and data were analyzed with multiple regression method. The relation between the hydrogen volume(ul) and the hydrogen desorption peak area integrated could be expressed with the following equation and the coefficient of determination was 0.985.

H_2 Volume (ul) = 8.89 + 8.88 * 10^{-3} area integrated

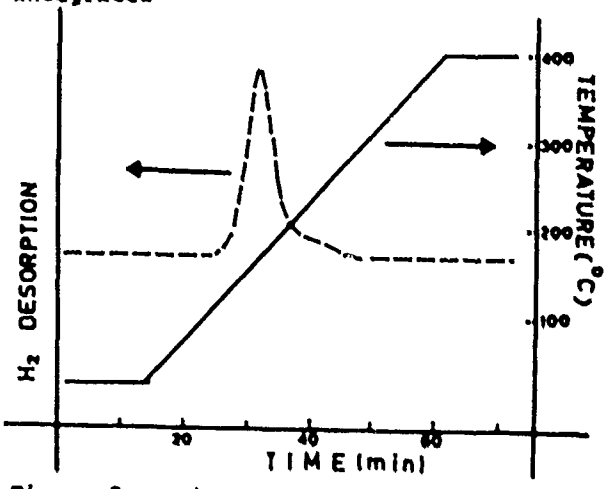

Figure 2 : The variation of hydrogen desorption over a Pd/Al_2O_3 catalyst versus reactor temperature.

Table 2 shows the comparison of the results of hydrogen evolution from fiber coating material by different methods. The evolved hydrogen slowly escaped from either septum-sealed headspace vial or glass tube containers,while palladium had a strong ability to uptake hydrogen.Consistently the experimental data showed that the collected hydrogen amount with palladium catalyst method are about 1.4 and 3.3 times compared with headspace vials and glass tube sets methods respectively.

Table 3 lists the amount(ul/g) of hydrogen evolved from organic cable materials after aging at 100°C for 360 hours. The major sources of hydrogen evolution from optical fiber cable used in Taiwan are water-proof filling compounds and fiber coating materials. After aging both the water-proof filling compounds and coating materials discolored from colorless to pale yellow or yellowish brown.The origin of the evolution of hydrogen was presumed to be through thermo-oxidative scission mechanism[7,11,12]. The evolution of hydrogen can be inhibited by addition of

some sulfur-containing or phenolic antioxidant[12].

Table 2: Comparison of H_2 Evolution from Coating Material by Different Methods

H_2 Collect Method	Headspace vials method	Glass Tube Sets	Catalyst Adsorption Method
H_2 Amount(ul/g)	243±8	104±10	348±6

Table 3 : Amount(ul/g) of hydrogen evolved by organic cable materials after heating 380 hours

Materials	Cable		Fiber Coating			Wrapper	
			Silicone	Desolite	Acrylate	Mylar	Kevlar
Hydrogen Evolution(ul/g)	93	74	340	8	38	15	34

Materials	Water-Proof filling Compounds			
	Polyisobutene	Thixotropic A	Thixotropic B	Thixotropic C
Hydrogen Evolution(ul/g)	120	420	318	21

Materials	Tube and Sheath Materials			Fiber		
	HDPE	LDPE	Nylon	Fiber A	Fiber B	Fiber C
Hydrogen Evolution(ul/g)	1.3	8.2	68	54	23	3.1

CONCLUSION

1. A new procedure using Pd/Al_2O_3 as hydrogen absorbent to measure the the hydrogen evolution from optical fiber cable is established.
2. Our results show that the collected hydrogen contents from the new procedure for same samples are about 1.4 and 3.3 times compared with headspace vials and glass tube sets methods respectively.
3. The phenomenon of hydrogen evolution from organic compounds which used in cables depend upon their chemical structure and had a great difference. With this procedure the polyisobutene, polymethyl siloxane, silicone and acrylate coating materials , nylon , kevlar wrapper,are found as major contributors to H_2 evolution.

REFERENCE

1. R.J.Stone,Opt.Letts.,p297(1982).
2. Y.Mitsunage et al.,Eletron.Lett.,p76 (1984).
3. K.Noguchi et al.,Electron.Lett.,p246 (1984).
4. S.R.Barnes et al.,Eletron.Lett.,p712 (1985).
5. Abe.K.,Lowe.R.,IWCS Proceeding,p424 (1984).
6. D.L.Philen,IWCS Proceeding,p415 (1984).
7. Irene Plitz, Paul C.Warren,IWCS Proceeding p616(1987).
8. Ting-Chung Chang, C.T.Yeh, J.Catal., p51(1985).
9. Yamabe,T.,et al.,Nippon Kagaku Kaishi p1264(1973).
10. M.Boudart.,J.Catal.,p164(1973).
11. D.Simoff et al.,SPE Proceeding p386 (1988).

12.Kazutoshi Ohashi et al.,Poly.Deg.and Stab.,p223(1988).

Ting-Chung Chang
Outside Plant Lab.
Telecommunication Lab.
P.O. Box 71
Chung-Li
Taiwan
R.O.C.

Mr. Ting-Chung Chang received his M.S. in Applied Chemistry in 1984 from Tsing Hua University and then directly joined Telecommunication Laboratories. He is now a research scientist and a member of out-side plant Laboratory in T.L..

Jin-Chung Lin
Outside Plant Lab.
Telecommunication Lab.
P.O. Box 71
Chung-Li
Taiwan
R.O.C.

Mr. Jin-Chung Lin received his M.S. in Polymer Science in 1983 from Tsing Hua University and then directly joined Telecommunication Laboratories. He is now a research scientist and a member of out-side plant Laboratory in T.L..

Yiang Liu
Outside Plant Lab.
Telecommunication Lab.
P.O. Box 71
Chung-Li
Taiwan
R.O.C.

Ms. Yiang Liu received her M.S. in Organic Chemistry in 1979 from Rutgers,the state of university. She jointed T.L. in 1984 and presently worked as a project manager in OSP Lab. of T.L.

HIGHLY ACCURATE BACKSCATTER MEASUREMENT IN THE QUALITY CONTROL OF THE CABLING OF SINGLE MODE FIBERS

Reinhard Girbig, Michael Hoffart

AEG KABEL AG Mönchengladbach
Federal Republic of Germany

ABSTRACT
Techniques are developed to measure fiber attenuation with an accuracy of better than 0.005 dB/km (2σ) using a standard OTDR. To get this high accuracy special characteristics of the OTDR such as variability of laser diodes, Fresnel reflections, dead zones, signal averaging and linearity have to be taken into account. Computerized techniques to avoid them negatively influencing accuracy are shown. To calculate attenuation coefficients with the highly accurate OTDR method a special regression analysis was developed. The accuracy of attenuation has been verified with measurements on a calibration cable of a loose tube construction. This cable was calibrated with cut-back measurement to an accuracy of 0.003 dB/km (2σ). Results from production OTDR measurements compared to those from reference cut back method show the high accuracy of the developed OTDR techniques.

1. INTRODUCTION

Today OTDR measurements are standardly used to determine the optical length, the position and the magnitude of point defects, and splice losses for optical fiber whether cabled or not cabled /1/. Precise attenuation measurements are performed with the cut back method. This method is not readily applicable to cabled fiber and by definition requires a cutting of the fiber. Neumann showed theoretically in 1980 that it was possible to measure the attenuation of single mode fibers with OTDR /2/. Nowadays OTDR's are in principle available to measure low loss single mode fibers with a high degree of accuracy. As many instrument effects must be taken into account, a manual implementation of the quality control of the cabling of single mode fibers with OTDR is difficult to perform. Thus the OTDR measurements must be computerized in order to optimize the conditions necessary for precise measurements. In this contribution the conditions for such an optimised operation are presented.

2. OTDR CHARACTERISTICS

The measuring equipment used in this study is a commercially available OTDR switchable between 1310nm and 1550nm. For best results with respect to signal-to-noise ratio, output pulse power and fiber length, a pulse width of 1μs is used. All measurements are done under computer control to get a high level of accuracy and repeatability.

In the following subsections the techniques necessary to make an accurate OTDR attenuation measurement are discussed. The discussion is organized about the typical characteristics of an OTDR measurement which must be well controlled.

2.1. DEAD ZONE

Due to the Fresnel reflections at the optical output port of the OTDR there is a region at the beginning of the backscatter trace which does not show the true backscatter level of the fiber. This region is called the dead zone and its length depends on the pulse width and pulse power of each laser diode and on the reflection at the connectors both within and without the OTDR. For a pulse width of 1μs the expected dead zone is 100m. In reality a dead zone length of about 500m to 600m is observed. The reason for this disagreement is disturbances within the optical receiver which lead to oscillation of the backscatter trace. Thus in order to minimize the length of the dead zone in the test fiber it is necessary to use a single mode fiber of about 1000m length as a launching fiber.

The test fiber is coupled to the launching fiber by using a single-mode fiber-to-fiber coupler. To suppress additional Fresnel reflections an index matching oil is used. The coupling procedure is controlled by hand and monitored on the OTDR screen. To simplify coupler manipulation and to obtain low coupling losses, the launching fiber should have a greater mode field diameter than the test fiber. That is, for example, with the coupling of a 10um mode field launching fiber to a 9um mode field test fiber one gains 0.4dB in capacity in principle /3/. Thus in practice coupling loss is reduced. Now with the use of a launching fiber, the dead zone of a test fiber is reduced greatly to only that which in a result of a small reflection at the coupler (non optimal index matching). For the

methodology reported here the typical reflection is 0.1dB.

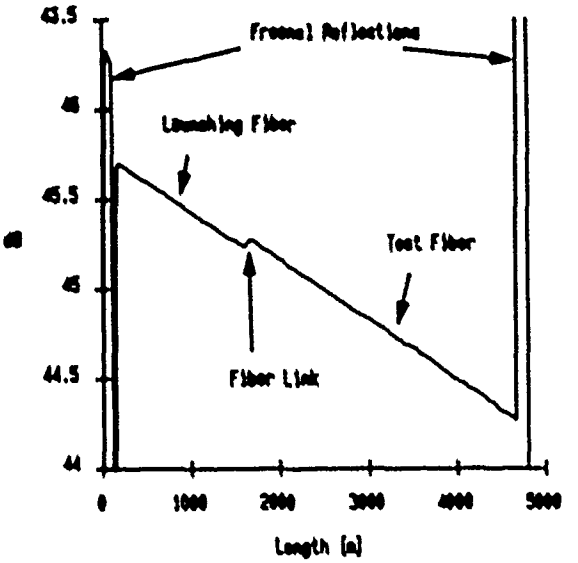

Figure 1: Dead zones

Careful examination of many backscatter traces shows that the difference between the falling edge of the reflection and the linear regression curve of the backscatter trace of a test fiber is 1.5 dB for a dead zone of 150m at 1310nm of 180m at 1550nm (Fig. 2).

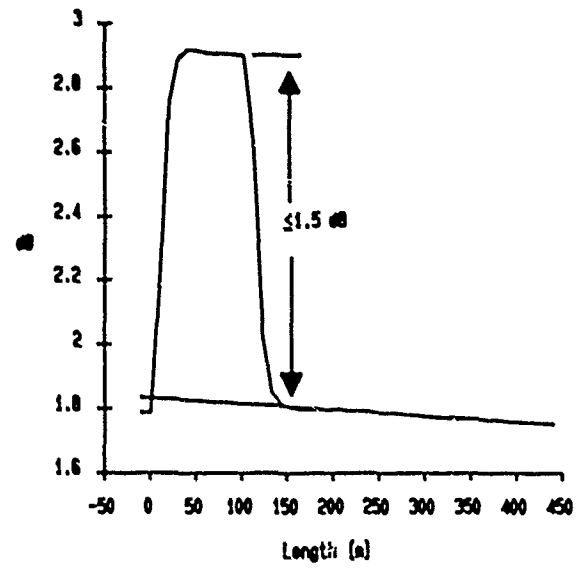

Figure 2: Dead zone and height of reflection at the fiber link

With the computerized methodology reported here if a 1.5dB value is observed the measurement is automatically stopped.

2.2. FRESNEL REFLECTION

High Fresnel reflections at all connections and at the fiber far end will cause disturbances within the optical receiver in the OTDR which lead to incorrect attenuation values. Fresnel reflections which saturate the receiver must be suppressed by means of a small fiber loop, index matching or an optical masking of the far end. In our study a small fiber loop is used with all measurements.

A comparison of measurements with and without Fresnel reflections at the fiber far end shows a typical attenuation value 0.01dB lower with reflection than that without reflection.

2.3. WAVELENGTH CHARACTERISTICS

The wavelength of the laser diodes inside the OTDR differ from the nominal values of 1310nm and 1550nm. To compare attenuation measurements between different OTDR's or to cut back measurements, the center wavelengths and bandwidths of the laser diodes have to be known. Therefore the spectra of the OTDR's laser diodes are recorded by means of an optical spectrum analyzer.

Knowing the center wavelength, the attenuation coefficients at 1310nm and 1550nm are calculated by using the Rayleigh scattering loss formula:

$$\alpha_s = (0.751 + 37.1 \cdot \Delta n^+)/\lambda^4 \qquad (1)$$

The values of the coefficients in equation (1) are correct for internally produced fibers. These values depend on fiber design and could be different for fiber from a different manufacturer.

Variations by power mode partition of the spectral distribution of the emitted light's power causes an additional error in the attenuation measurement. Although the variation of the spectral distribution in power is not known, it is possible to make a rough estimation of the influence in terms of the bandwidth of the laser diodes.
Using equation (1) the variation in attenuation is

$$\Delta\alpha_s = -4\,\frac{0.751 + 37.1 \cdot \Delta n^+}{\lambda^5}\,\Delta\lambda \qquad (2)$$

with $\Delta\alpha_s$ in dB/km and $\Delta\lambda$ in µm.

2.4. LENGTH ACCURACY

In order to accurately measure fiber length with an OTDR it is necessary to know the group index of refraction of the group of test fibers. As it is very difficult to measure the group index directly, a high precision mechanical length measurement of a single fiber is used to determine the group index of refraction for all the fibers by changing the index of refraction on the OTDR until the shown length corresponds with the measured mechanical length.
For internally produced fibers the group index at 1310nm is 1.4694 and at 1550nm is 1.4699.

The length accuracy of the OTDR used in this study at the highest possible resolution setting is ± 1m.

2.5. AVERAGING

For highly accurate attenuation measurements, the averaging time of the OTDR has to be optimized. The best way of optimization is to control the averaging time by checking the signal-to-noise-ratio of the backscatter trace at the fiber far end. The averaging process can be stopped when there is no significant change in the signal-to-noise-ratio.

With the type of OTDR used for this study, this procedure is not recommended as when data are read out, the averaging process is interrupted. Therefore a method in which the averaging times are scaled to the total attenuation at the far end of the test fiber is used.
The averaging process within the OTDR used in the study is a combination of arithmetical and exponential averaging. Because of the fact that exponential averaging will not converge, the averaging time should not be allowed to exceed 20s. Otherwise it is possible that incorrect attenuation values are observed. This is true for a dynamic range limitation of up to 5dB including the launching fiber.

In the optimised measuring computer program averaging times of 10s and 15s, respectively, for a total attenuation at the fiber far end of 3dB and 5dB are used.

The results to be discussed later in this paper show that these times are sufficient for highly accurate attenuation measurements.

2.6. LINEARITY

The backscattered light level varies with pulse width, pulse energy and fiber characteristics. In order to handle a large variation in backscattered light level, an electronic attenuator with a range of possible settings is included in commercially available OTDR's.
For accurate measurements it is important to choose the correct setting to be in the linear optical range.

The determination of the correct setting is done easily by observing the change in the total attenuation at the far end of the launching fiber as stepping through the electronic attenuator positions from low to high. A linear fit to the measured attenuation values will show the lowest possible setting to be within the linear optical range. The check of the linear region is done automatically by the computer in a special service routine which is called upon whenever the OTDR equipment or the launching fiber is changed.

An example is shown in figures 3 and 4.

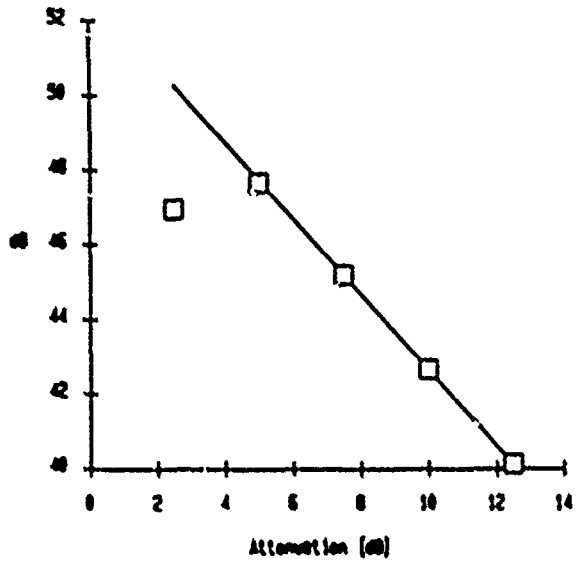

Figure 3: Optical attenuation vs. electrical attenuation at 1310nm

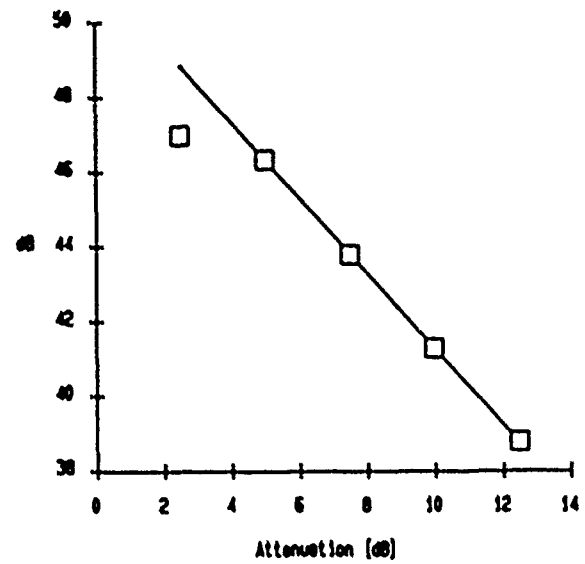

Figure 4: Optical attenuation vs. electrical attenuation at 1550nm

Boxes are measured values; the straight lines are the linear fits.
In this example settings which give optical attenuations of 7.5dB at 1310nm and 5dB at 1550nm are shown.

3. REGRESSION ANALYSIS

To obtain high accuracy in the attenuation coefficients a special regression analysis is

used.

The fiber is measured with the OTDR from both ends. A linear fit is done to all the measuring points of the backscatter trace. The deviations at the measuring points form a linear fit are then calculated. Figure 5 shows the results of the regression analysis for a 12km fiber with slightly inhomogeneous regions. An inhomogeneous fiber has been chosen in order to better show the principle of the analysis.

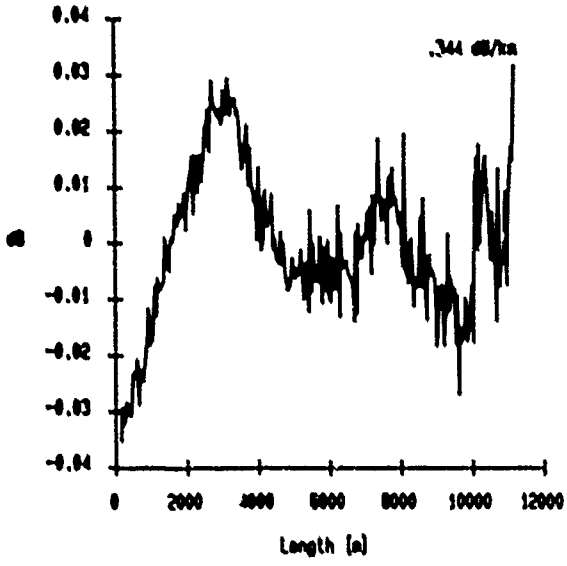

Figure 5: Deviation between measured values and linear fit

The coefficient of attenuation for this example for the entire fiber length is 0.344 dB/km and the maximum deviation is about + 0.03 dB. It can be seen that there are regions where the slope of the curve is linear; i. e. the first 2.5 km and the region between 2.5km and 5.5km.

The computer program looks for such linear regions and again does a linear fit to the measuring points for each region. The deviations between the measuring points and the linear fit for the regions cited above are shown respectively in figure 6 and figure 7.
The deviation within both regions is below 0.01 dB.

The computer program automatically searches out all linear regions of minimum deviation.

With this method it is first possible to determine homogeneous regions of a fiber, and secondly possible by summing over these linear regions to obtain a total fiber attenuation

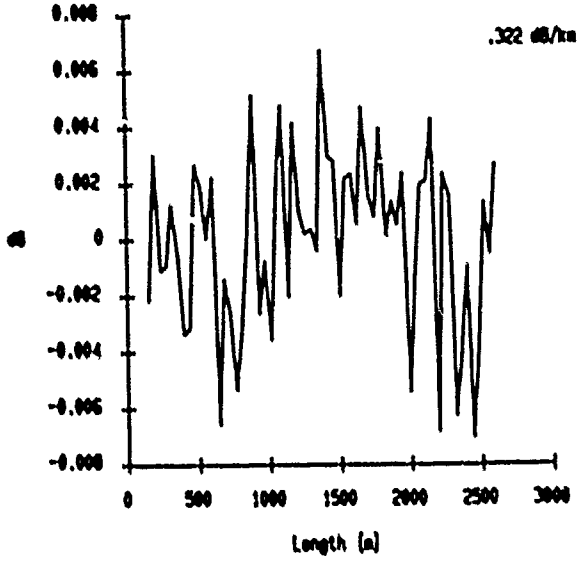

Figure 6: Deviation between measured values and linear fit for the first region

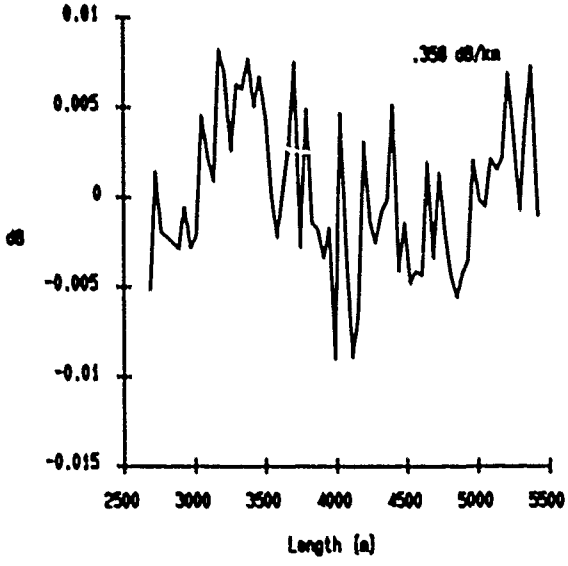

Figure 7: Deviation between measured values and linear fit for the second region

coefficient which is more accurate than that obtained by either a least square fit over the entire fiber or a two end point analysis.
The application of this regression analysis to a calibration cable that the measurement of is described in the next chapter is plotted in figure 8.

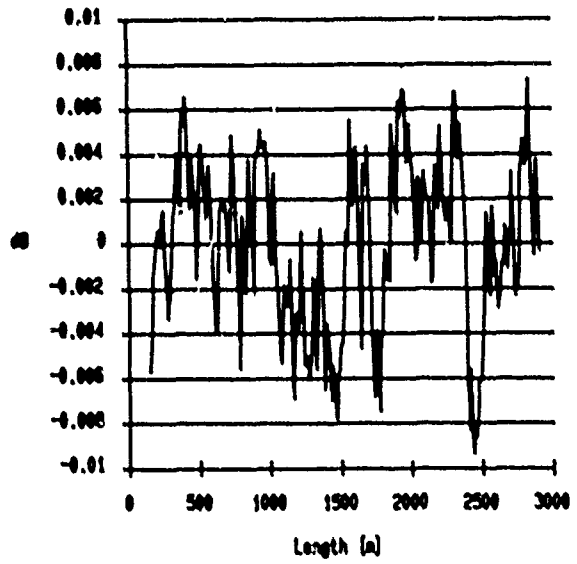

Figure 8: Deviation between fiber attenuation and linear fit for the calibration cable at 1310nm

4.MEASUREMENT RESULTS

Incorporating together all the techniques discussed above a computerized OTDR measurement of a calibration cable was performed.

The loose tube construction of this calibration cable is shown in figure 9.

1 – WY 1E9/125

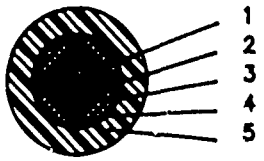

1: singlemode fiber

2: loose tube 2mm ø

3: strength members

4: wrapping

5: PVC outer sheath

Figure 9: Construction of the calibration cable

The cabled fiber has a mode field of 9um. The optical parameters of this fiber are such that it is very insensitive to environmental changes. One expects to see only attenuation changes on the order of thousandths of a dB/km over many years.

The attenuation of the calibration cable was measured with an accuracy of 0.003dB/km (fiber length: 3km) by a high precision cut-back measurement at the research center of the German PTT /4/. The result is shown in figure 10.

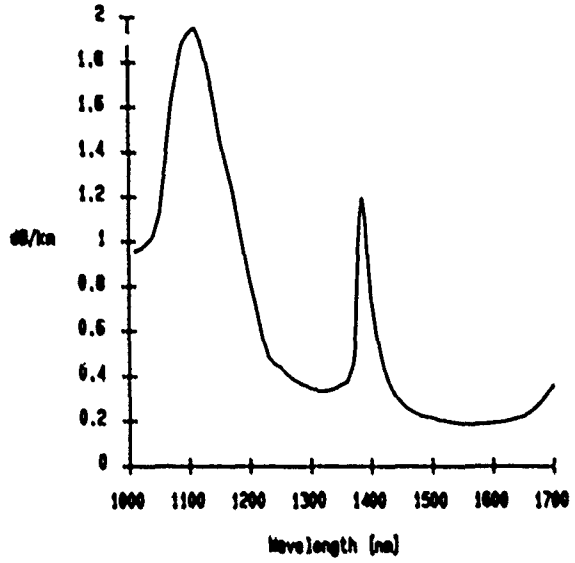

Figure 10: Spectral attenuation of the calibration cable

A comparison of the result of an OTDR measurement (Fig. 11) with the result of the cut back measurement shows exactly the same value of attenuation: 0.333dB/km @ 1318nm.
Correcting the OTDR attenuation to 1310nm gives a value of 0.339dB/km which deviates by 0.001dB/km from the cut back result (0.338dB/km). This is within the measuring

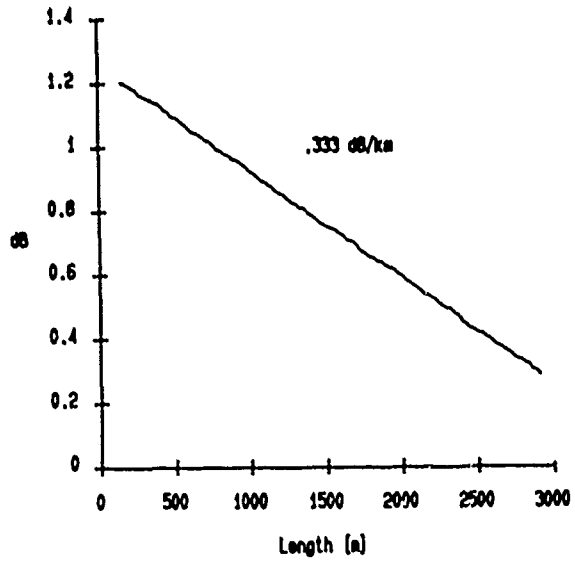

Figure 11: Attenuation of the calibration cable at 1318nm measured with OTDR

accuracy of this cut back system which is 0.003dB/km for a standard cabled fiber length of 2km.
To verify the accuracy of the OTDR technique reported here the attenuations of 58 fibers taken from internal production as measured with OTDR and cut back were compared (Fig. 12).

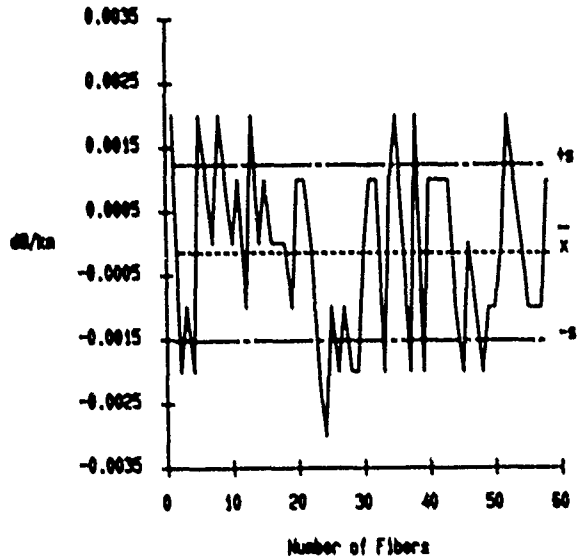

Figure 12: Deviation of attenuation values between OTDR and cut back measurements

The average value of the deviation between the two measuring methods is $\bar{x}$ = -.00014dB/km with a standard deviation s = ±0.00137dB/km.

This result shows that with the OTDR methodology reported here an accuracy of 0.005dB/km (2σ) in attenuation is possible.

5. CONCLUSION

The different causes of measurement errors in the measuring of attenuation with OTDR were studied. Optimized conditions were developed for a computerized OTDR measurement system. A special calibration cable was used to verify the accuracy of the OTDR attenuation method against the reference cut back method. A high accuracy of 0.005dB/km (2σ) with this computerized OTDR technique was obtained.

6. ACKNOWLEDGEMENTS

The authors wish to thank Dr.W. Heitmann of the German Research Center of the German PTT for the attenuation measurements of the calibration cable and Dr.R.G. Sommer, AEG KABEL for reading the manuscript.

References

/1/ BIRD,M. MILLER,W. SAIKKONEN, S.: 'OTDR automation - methodology and results', IWCS (1987) pp. 85-90
/2/ NEUMANN,E.G.: Analysis of the backscattering method for testing optical fiber cables', AEÜ 34 (1980) pp. 1 -160
/3/ KAPRON,F. et al: 'Mode field diameter effects on OTDR splice measurements', NBS Sympos. on Optical Fiber Measurements (1986) pp. 81-84
/4/ HEITMANN,W.: 'Precision single-mode fiber spectral attenuation measurement', J. Opt. Commun. 8 (1987) pp. 2-6

Reinhard Girbig AEG KABEL (Optical Cable Division) Mönchengladbach, West Germany.
Reinhard Girbig was born in 1954. He received his Dipl.-Ing. degree from the "Ruhr University, Bochum" in 1987. He joined AEG KABEL on graduation and has since worked as a development engineer in the fiber optics area with overall responsibility for the technical aspects of OTDR measurement.

Michael Hoffart AEG KABEL (Optical Cable Division) Mönchengladbach, West Germany.
Michael Hoffart was born in 1956. He received his Dipl.-Ing. degree from the "Bergische University Wuppertal" in 1983. He joined AEG KABEL on graduation and has been engaged in the field of optical measurement technique. He is now responsible for the development of telecommunication cables.

RIGID PVC AS THIN WALL INSULATION FOR INDOOR TELEPHONE EXCHANGE CABLES

Carl-Gustaf Ekroth, Sören Halvarsson, Elof Nilsson.

ERICSSON CABLES AB, TELECOM CABLES DIVISION,
BOX 457, S-824 01 HUDIKSVALL, SWEDEN

ABSTRACT

A rigid polyvinylchloride (PVC) compound has been extruded as thin wall insulation ø 0.4/0.6 mm for indoor telephone exchange cables. The insulation has been extruded with standard extrusion equipment. The compound does not contain any primary plasticizer and is based on a PVC-resin with a K-value = 58. Test results from measurements on rigid PVC compound insulation are compared with results of standard insulation grades of plasticized PVC, polyamide 12 and modified polyphenylene oxide. The cables are designed as flame retardant and to be installed using wire wrapping techniques. The cables can be manufactured with sheaths of plasticized PVC compound or halogen free compound.

INTRODUCTION

Development work has been done to find a flame retardant insulation material for thin wall insulation as replacement for polyamid 12 (PA 12). Several polymers and polymer blends have been investigated. Allergy problems (1) associated with the type of modified polyphenyloxide (PPO) used hitherto was also a reason for the development work.

A rigid PVC compound was found to give the properties required. It also showed to be suitable for processing on standard extrusion equipment at moderate costs. The compound is based on a PVC resin (2) with a K-value = 58 (3) instead of resins with K values 65-72 normally used for plasticized PVC compounds in the wire and cable industry.

Good mechanical properties are necessary due to the requirements (4) for a wall thickness of 0.1 mm and the use of wire wrapping technics when installing the cables. Practical wire wrapping tests on different types of insulated conductors indicate that the value for cut-through should be a minimum of 800 g, determined in accordance with MIL-W 81222/4.6 18 (5).

The cables are designed to meet the flammability requirements of the IEEE 383 (6) standard test. Cables meeting the flammability requirements can be designed with sheaths of PVC-compound as well as halogen free compound.
The halogen free compounds are used if reduced halogen content is required.

Examples of overall diameters for cables with insulations of rigid PVC compound are given in table 1.

Table 1 Overall diameter of cables

Number of pairs	Overall Diameter (mm)
4	3.8
8	5.0
12	5.6
16	6.0
24	7.0
32	8.0
48	9.5

COMPOUND CHARACTERISATION

Rigid polyvinylchloride (u-PVC) compound is essentially an intimate blend of PVC resin with impact modifiers, processing aids, stabilisers and lubricants. The significant difference from other PVC compounds normally used in the cable and wire industry is the absence of plasticizers and fillers. The rigid PVC-formulation is listed in table 2.

Tabel 2 Formulation of rigid PVC compound

Components
1 PVC-resin k-value 58
2 Stabilizer/Lubricant mixture, based on lead
3 Stabilizer, tribasic lead sulfate
4 Impact modifier, terpolymer
5 Processing aid, acrylic polymers
6 Release agent, based on calcium compounds

The formulation of the rigid PVC compound for use as a wire insulation has required the incorporation of two types of stabilizers to act as a HCL-acceptor and a stabilizer according to the Frye-Horst mechanism (7).
The components were mixed in a high speed mixer to a temperature of (110°C - 120°C). The dry blend was compounded in a Buzz ko-kneter type PT 200 with an output of 1000 kg/h.

EXRUSION OF RIGID PVC

Extrusion equipment

The insulation material can be processed on standard thermoplastic extrusion equipment as designed for wire coating. In this experiment rigid PVC has been satisfactory processed on a 30 mm extruder with a L/D ratio of 20: 1 and a compression ratio of 2,5:1.

Free extrusion (tubing) has been used in this process, which is normally chosen when insulation of small conductor is carried out. A drawn-down ratio of 10.2 and a line speed of 600 m/min was successfully employed for the thin wall insulation of 0,1 mm radial thickness.

Extrusion conditions

Typical extrusion conditions employed for the insulation of 0,4 mm tinned copper conductor with 0,1 mm radial thickness of rigid PVC are listed below, see table 3.

Table 3 Extrusion conditions

Die diameter (mm)		2.0
Guider tip diameter (mm)		1.4
DDR		10.2
DRB		0.96
Extruder set temperatures (°C)		
Zone	1	175
	2	185
	3	195
	4	205
Crosshead		215
Screw speed (rpm)		40
Conductor preheat (°C)		100
Line speed (m/min)		600

PROPERTIES OF RIGID PVC INSULATION MATERIAL

The most important properties of extruded rigid PVC have been investigated. The results have been compared with some other extruded insulation material. Abbreviations of the insulation material used in this study are listed in table 4.

Table 4 Plastic insulation material

Insulation Material	Abbreviation
Rigid Polyvinylchlorid	u-PVC
Standard plasticized polyvinylchlorid	p-PVC
Modified polyphenylene oxide	m-PPO
Polyamid 12	PA 12

Mechanical properties

Table 5 presents mechanical properties obtained from 0,1 mm radial thickness insulation. Tensile strength at break and elongation at break are determined according to IEC 189-1 (8) with a cross head speed of 50 mm/min. Stripping force was determined in a tensile testing machine. Cross head speed 50 mm/min, and sample preparation according to IEC 189-1. Insulation cut-through was measured according to Mil-W-81822.

Table 5 Mechanical properties of insulation materials as 0,4/0,6 mm wires.

Material	Tensile strength MPa	Elongation at break %	Stripping force N	Cut through g
u-PVC	52	215	3.0	1000
p-PVC	24	225	6.0	500
m-PPO	40	175	9.0	800
PA 12	50	300	5.0	900

Ageing and heat stability

The ageing performance of the u-PVC at the radial wall thickness of 0.1 mm is shown in figure 1. The samples were aged at 80°C, 100°C and 120°C and measured according to IEC 189-1 . The stability was measured at 200°C according to VDE 0472/09.71 (9) both before and after ageing. The results are presented in figure 2.

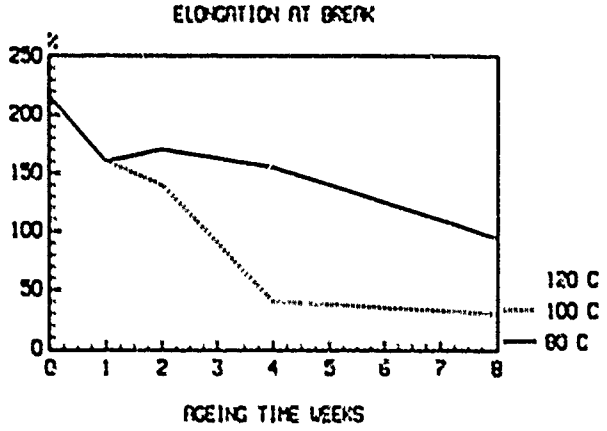

Fig.1 Ageing preformance of the insulation at 80°C 100°C and 120°C.

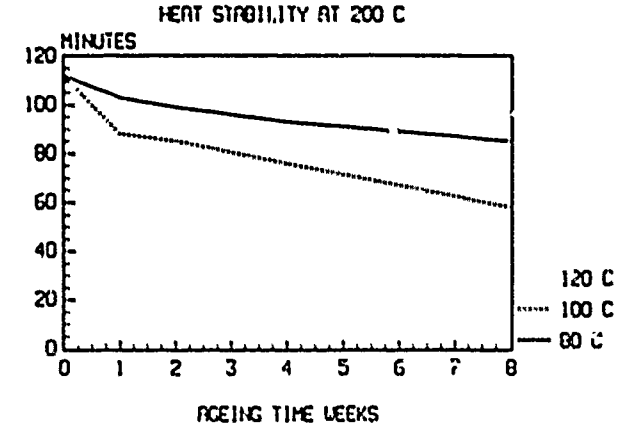

Fig.2 Stability of u-PVC at 80°C, 100°C, 120°C.

Compatibility

Determination of compatibility between polymers is necessary because of suspected migration of low molecular substances from the jacketing material into the u-PVC. Moulded specimens were put together to form a "sandwich" between two glass plates. The glassplates were placed in an air oven maintained at 70°C and a weight of 5 kg was placed on the test assembly. The investigation was performed on u-PVC in connection with molded sheets of jacketing material consisting of plasticized PVC and flame retardant halogen free material. The result are presented in figure 3 with a comparison of migration between m-PPO and PVC jacketing material.

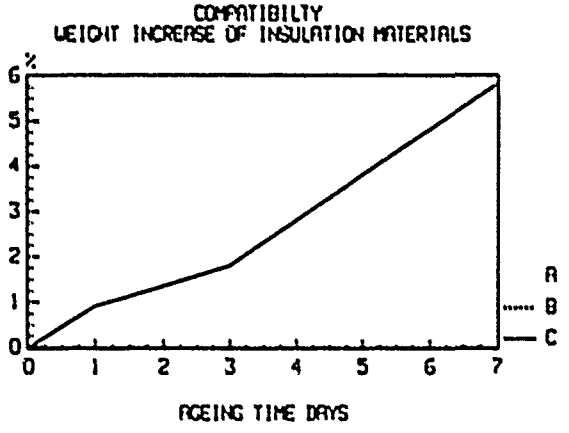

Fig.3 Compatibility (A) u-PVC/PVC sheath, (B) u-PVC/halogen free sheath, (C) m-PPO/PVC sheath.

Fire property

The experimental results (10) reported here of u-PVC have been subjected to standard test procedures, oxygen index, vertical flammability UL 94, flammability temperature Araphoe smoke and NBS smoke chamber. The results are presented in table 6.

The u-PVC has also been tested in a cone calorimeter (11) at three different heat flux levels 15, 20 and 25 kW/m^2. Samples were prepared from moulded sheets with dimensions (100x100x3)mm. The amount of chloride presented in combustion gases was analyzed, see table 7. Time to ignition and heat realease rate was measured, see table 8.

Table 6 Fire properties of some insulating material.

Property	u-PVC	p-PVC	m-PPO	PA-12
Oxygen Index (%)				
23°C	37	28	24	17
100°C	33.5	26	[illegible]	-
200°C	29.5	24	30	-
300°C	25.0	20	26	-
400°C	19.5	15	18	-
Flammability Temperature (°C)	370	270	360	<23
Vertical flammability		*		
UL 94 V-0 (mm)	0.5	1.0	3.2	-
Arapahoe, % smoke	11.4	12	23.6	Dripping
NBS Smoke chamber smouldering D_s(corr)	149	390	122	Dripping
Flaming D_s (corr)	361	530	347	-

* V-1

Table 7 Chloride in combustion gas

Incident flux kW/m^2	Amount chloride g	Amount chloride g/ of g PVC consumed, g/g
15	1.35	0.12
20	1.33	0.07
25	1,02	0.03

Table 8 Time to ignition and heat realease rate

Incident flux kW/m^2	Time to ignition min:s	Heat realese rate peak kW/m^2
15	*	-
20	**	71
25	4:00	178

* No ignition
** Ignition with a match 6:30 (min:s)

Electrical properties

Volume resistivity, dielectric constant (1 kHz, 1 MHz) dissipation factor (1 MHz) and dielectric strength < 1,5 kV was measured, see table 9.

Table 9 Electrical properties of some insulated material

Material	Volume Resistivity TΩm	Dielectric Constant 1 kHz	Dielectric Constant 1 MHz	Dissipation factor 1 MHz	Dielectric Strength <1,5 kV
u-PVC	<10	3	2.8	8.9 10^{-3}	Pass
p-PVC	<1	4.1	3.0	30.0 10^{-3}	Pass
m-PPO	<10	2.6	2.6	4.5 10^{-3}	Pass
PA-12	<0.1	3.8	3.0	18.0 10^{-3}	Pass

Permittivity and dissipation factor have been measured at several distinct frequences 1, 6, 10, 20, 40, 70 MHz, see figures 4 and 5. Comparison is made with PA-12.

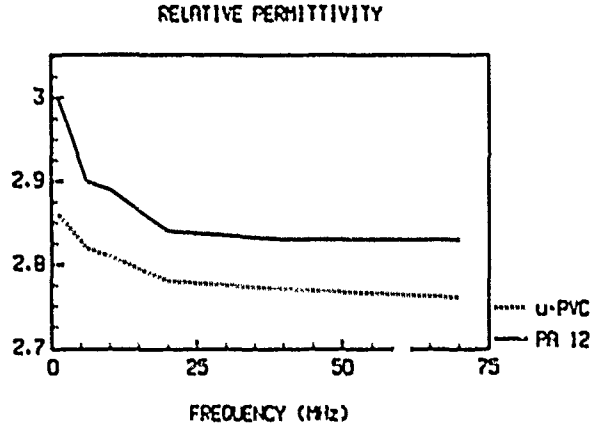

Fig.4 Frequency dependence of permittivity

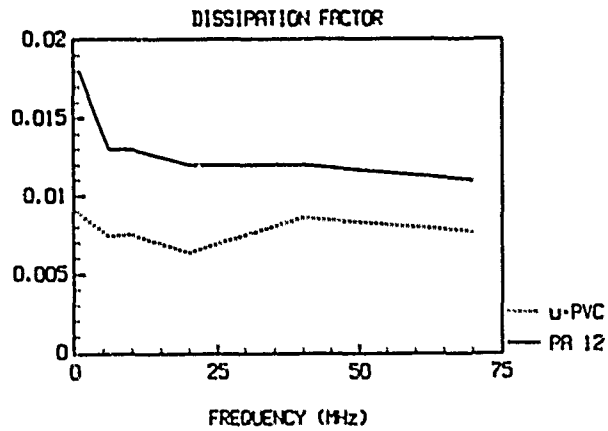

Fig.5 Frequency dependence of dissipation factor.

Cracking at low temperature

Registance to cracking at low temperature (-15°C) has been measured according to IEC 189-1 clause 4.4. No cracks were observed.

PROPERTIES OF COMPLETED CABLE

In the present work, trial lengths of 32-pair cables were produced using 0,4 mm tinned copper conducters and u-PVC as insulation material. Two types of materials were used for jacketing of u-PVC insulated conducter. The sheathing materials used were a flame retardent PVC compound and a flame retardent halogen free termoplastic having an oxygen index (OI) = 35.

Cold bend test

Bending test at low temperature (-15°C) for sheaths according to IEC 811-1-4, clause 8.2 (12) showed no cracks.

Electrical property

Mutual capacitance of cabel was measured to 62-68 nF/km according to IEC 189-1 clause 5.4.

Flame propagation

The cables were subjected to a vertical flame test (IEEE 383). Cables were vertically mounted on a ladder and burnt by a 70 0000 BTU/HR ribbon burner 250 mm wide placed in front of and 610 mm from the bottom of the cable ladder. The two types of cables fullfill all requirements of the IEEE 383 vertical flame test.

CONCLUSION

A flame retardant thin insulation of rigid PVC compound can be processed with standard extrusion equipment. The rigid PVC compound is based on PVC resin of a K value = 58. The PVC-material can be used for wire wrapping instead of insulation of polyamid 12, if moderate operating temperatures are required. Migration shows that PETP-foil is needed as a migration barrier when plasticized PVC compound are used as jacketing material. Rigid PVC insulation together with plasticized PVC or halogen free flame retardant sheaths have shown to be suitable for indoor telephone exchange cables.

ACKNOWLEDGMENT

The authors wish to thank the technical service and research staff at Norsk Hydro Petrochemical Division for their help during the development work. The authors also whish to acknowledge the colleagues involved at Ericsson cables for their contribution to this project.

REFERENCES

1. Arne Ulander " Utredning av flamskyddad kabel vid Ericsson, Katrineholm". 890215 Örebro läns landsting, yrkesmedicinska kliniken.
2. Norsk Hydro data sheet Norvinyl S4-58.
3. Bestimmung der Viskositätszahl und des K-Wertes von Vinylchlorid (VC) -Polymerisaten, DIN 53726.
4. Ericsson material specification, Switch board cable 105 49-YEN 2503.
5. Military Specification Wire, Electrical, Solderless Wrap, Insulated and Uninsulated. MIL-W-81222 (Navy) 4 april 1972.
6. IEEE standard for Type Test of Class IE Electric Cables, Field Splices, and connections for Nuclear Power Generating Stations, IEEE std 383-1974.
7. Tibor Kelen, Polymer Degradation, van Nostrand Reinhold company 1983.
8. International Electrotechnical Commission IEC-standard, Publication 189-1, Second edition 1986, Low-frequency cables and wires with PVC-insulation and PVC-sheat Part 1 General test and measuring methods.
9. Verbandes Deutscher Elektrotechniker VDE 0472./09.71
10. Tor Corneliussen, test report 21.06.1989 Norsk Hydro AS, Porsgrunn, Norway.
11. Per Thureson, Brandprovning i konkalorimeter inklusive kloridanalys av rökgaserna från styv PVC, ref 88 R 2028, Swedish National Testing Institute.
12. International Electrotechnical Commission, IEC standards, Publication 811-1-4, First Edition 1985, Common test methods for insulating and sheathing materials of electric cables. Part 1: Methods for general application, Section Four-Tests at low temperatur.

AUTHORS

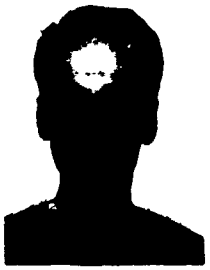

Mr Carl-Gustaf Ekroth received his B.Sc (Eng.) in chemical technology from the Swedish Institute of Technology, Helsinki Finland 1969. He joined Ericsson Cables, Telecom Cables Division, Sweden 1969. He has been working as a Development Engineer, Manufacturing Manager, Quality Control Manager. Since 1984 he is Manager of Material Technology.

Mr Elof Nilsson joined Ericsson Cable Telecom Cable Division 1963. Since 1969 he has been working with development and testing of polymeric materials. At present he is working as a extrusion process specialist.

Mr Sören Halvarsson joined Ericsson Cables AB in 1988 and is group manager and specialist of polymeric material. He received a M.S Degree in chemical engineering and a Tekn. Lic. Degree in polymer technology from Chalmers university of technology in Gothenborg, Sweden. Before his present position he worked for 2 years with polymeric coating of glass fiber at Gedevelop AB, Research Park, Ideón, Lund, Sweden.

Ericsson Cables AB
Telecom Cables Division
Box 457, S-824 01 Hudiksvall
Sweden

DESIGN AND PERFORMANCE OF SINGLE-MODE PLUG-IN TYPE OPTICAL FIBER CONNECTORS

Shin'ichi Iwano, Etsuji Sugita, Kazunori Kanayama, Ryo Nagase, and Ken'ichi Nakano *

NTT Opto-electronics Laboratories, Ibaraki, Japan
* NTT Applied Electronics Laboratories, Tokyo, Japan

Summary

A new system of compact single-mode plug-in type optical fiber connectors is developed for multiple optical connections between a printed board and a backpanel. This new system consists of two types of plug-in connector; two optical plugs /jacks with 64 electrical terminals and four optical plugs/jacks. This system utilizes a novel alignment mechanism for plugs and jacks and a novel fiber-core adjustment technology.

It is confirmed that the connectors have a low insertion loss of less than 0.4 dB and a high return loss of more than 28 dB, and are highly reliable.

1. Introduction

In advanced lightwave transmission systems, low loss and low reflection single-mode optical interconnections which take up little space are required for connecting printed boards to backpanels in equipment such as an optical transmitter/receiver for synchronous digital hierarchy (SDH). In such equipment, many electrical interconnections are also required for transmitting wideband digital signals and distributing clocks through a backpanel to a printed board.

Moreover, optical and electrical interconnections should be completed at the same time by plugging the printed board in to the backpanel as this facilitates both maintenance and testing.

To realize these requirements, we have developed two types of single-mode plug-in optical fiber connector: One type has two plugs and two jacks and includes 64 electrical terminals, and the other has four plugs and four jacks without the electrical terminals. Individual coupling for these plugs and jacks connected with single-mode fibers is carried out simultaneously by plugging in the printed board.

This paper describes the design and characteristics of the single-mode plug-in optical fiber connectors.

2. Design

2.1 Design Concept and Structural Features

The design concept of the plug-in connector system is as follows:

a) The connectors are mounted in an area 80 mm long and 10 mm high.

b) Each single-mode optical fiber is connected based on the ferrule-slitted-sleeve system [1].

c) Superior optical performance, an insertion loss of less than 0.5 dB and a return loss greater than 25 dB, are required.

In light of these requirements, a new single-mode plug-in connector system is proposed as shown in Fig. 1, in contrast to existing electrical connectors[2].

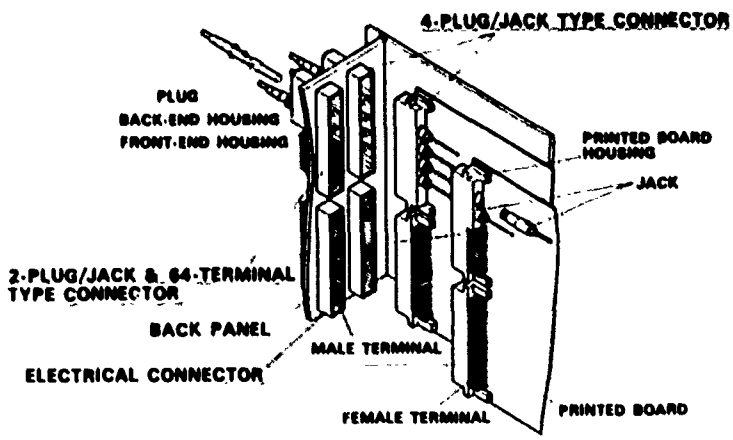

Figure 1 Single-mode plug-in optical fiber connector system

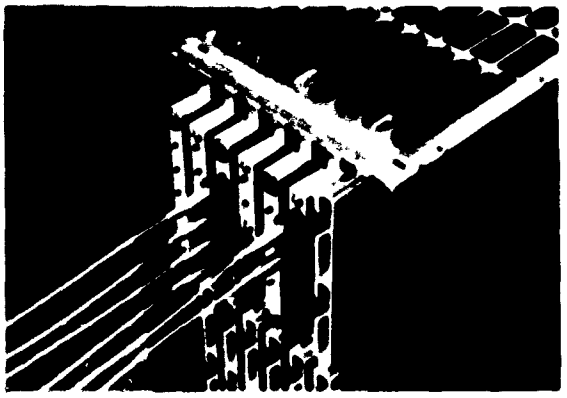

Figure 2 Rear view of back-end housings and plugs

Figure 3 Photograph of single-mode fiber plug and jack

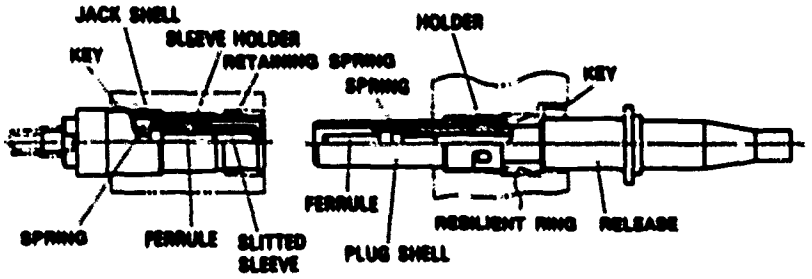

Figure 4 Structure of single-mode fiber plug and jack

The type with two optical plugs/jacks and 64-electrical terminals is mainly employed for long-haul transmission systems, and the type with four optical plugs/jacks[3] is employed for local loop networks.

The jacks are accommodated in the printed board housing, and the plugs in the front-end and back-end housings of the backpanel.

When the printed board is inserted into the backpanel, the printed board housing aligns the back-end housing which is float-mounted to the front-end housing by a guide-float pin(described later). Then, the printed board housing is coupled to the front-end housing which is fixed to the backpanel. The plugs are individually inserted and removed from the back-end housing from the rear of the unit as shown in Fig. 2.

The appearance and sectional view of the jack are shown together with the plug in Figs. 3 and 4. The jack consists of a slitted sleeve, a zirconia ceramic ferrule[4], a plastic-molded jack shell, a sleeve holder, and a spring. The sleeve holder including the ferrule and the sleeve is pressed in the axial direction by the spring. The shell has a positioning key which prevents the jack from rotating when it is mounted on the printed board housing.

The plug is composed of a zirconia ceramic ferrule, a plastic-molded plug shell, a holder, and a spring. The shell and the holder are fixed to each other by means of bayonet-like couplings. The holder also has a positioning key.

The ferrule ends are polished to a spherically convex shape with a 20 mm radius so as to realize stable physical contact.[4]

A sectional view and a photograph of the plug-in connector with two plugs/jacks and 64-electrical terminals are shown in Figs. 5 and 6, respectively.

The jacks are mechanically retained 12.7 mm apart by retaining springs on the upper half of the printed board housing, center-to-center. Two guide holes are provided on each side of the jack position 30.5 mm apart. 64 electrical female terminals are mounted on the lower half of the housing. The housing is fixed to the printed board.

The front-end housing of the backpanel with 64 press-fit male terminals is fixed

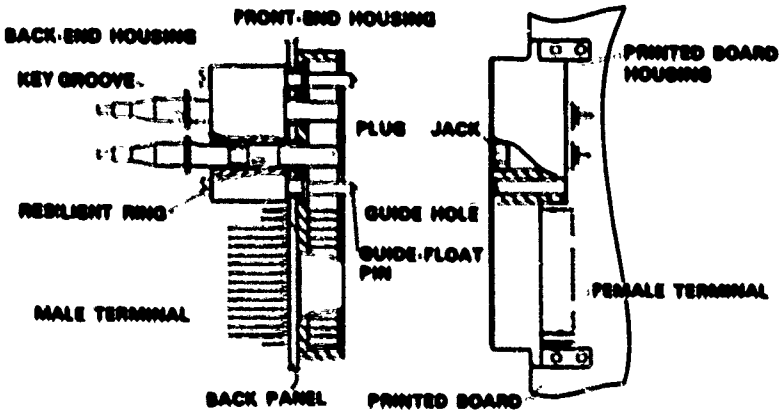

Figure 5 Structure of 2-plug/jack & 64-terminal type plug-in connector

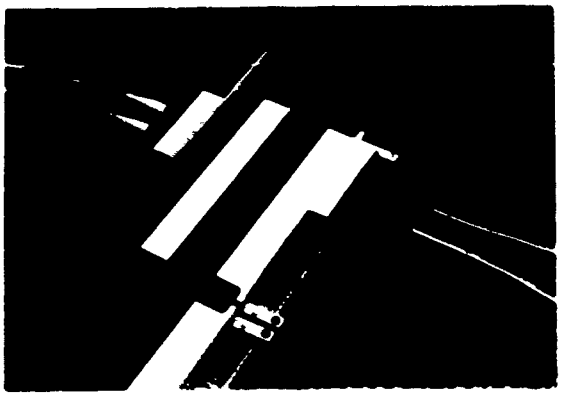

Figure 6 Photograph of 2-plug/jack 64-terminal type plug-in connector

to the back panel. The back-end housing of the backpanel with two resilient rings is float-mounted on the front-end housing by two guide-float pins. The plugs are retained in the housing by the resilient rings. Each p[illegible] can be removed individually from [illegible] using using a release of the plug b[illegible].

2.2 Alignment Mechanism

When single-mode fibers are butt-coupled, the misalignment between cores is reduced to less than 1.6 μm to achieve 0.5 dB insertion loss. However, a printed board mounting jacks have tolerances about of 1 mm in both the radial and axial direction in a plug-in unit.

The most important point for the realization of high performance single-mode plug-in optical fiber connectors is to achieve accurate alignments between plugs and jacks in which the tolerances and misalignment are automatically absorbed.[3] Therefore, the following alignment mechanisms are introduced.

As the the printed board is plugged in to the backpanel, the guide-float pins are inserted into guide holes in the printed board housing so as to align the back-end housing with plugs to the printed board housing with jacks. Next, the printed board housing is inserted into the front-end housing to align the electrical terminals.

This guide mechanism can absorb radial tolerance and facilitate the alignment of the plugs and jacks.

(1) Radial Movement

First, the printed board housing and the back-end housing are roughly aligned, then the plugs and jacks are aligned, and finally the two ferrules are aligned.

In order to align the two housings, the back-end housing is floated and guided by the guide-float pins and the guide holes. The floating range of the float is designed to be larger than the radial tolerance. The range of the guide is also designed to be more than 2 times as large as that of the float. Even if the printed board is inserted at the worst position, the top of the guide-float pins can be guided into the guide holes, thus making it possible to align these two housings.

Misalignment between a plug and a jack is caused by housing alignment error between the two housings and positioning error in each housing. Plugs and jacks have a guide portion on their shell top and are slightly floated from each housing. The range of these guides and the float are designed to be sufficiently larger than that of the above misalignment. Thus, a plug shell and a jack shell can be coupled effectively.

Two ferrules are aligned by a slitted sleeve. Both ferrules and the slitted sleeve are unattached to the shell of each

plug and jack, so they can absorb the misalignment.

(2) Axial movement

Axial tolerance is absorbed by a coil spring in the jack. The sleeve holder of the jack is unattached to the jack shell in the axial direction and is pressed in the axial direction by the spring. The ferrule and slitted sleeve float slightly.

When the plug is inserted into the jack, the sleeve holder is aligned by the inner surface of the plug shell. The ferrule in the plug is also floated from the plug shell and is guided by the aligned sleeve holder. Thus, smooth connection and fine alignment can be achieved.

2.3 Adjustment

(1) Adjusting operation

To achieve good repeatability of insertion loss during connect/disconnect cycles, positioning keys for the plug and the jack, and key grooves for the back-end housing and the printed board housing are provided.

In order to realize low insertion loss in single-mode fibers, it is necessary to adjust the direction of the optical fiber core center to the ferrule center to that of the positioning key.

The principle of the adjustment operation is shown in Fig. 7. The operation is as follows.

(a) The direction of the optical fiber core center to the ferrule center (shown by A and B in Fig. 7) is determined by measuring the insertion loss using a standard adjustment connector. The direction of the positioning key of the connector coincides with the direction of the fiber core to the ferrule center.

(b) Then, the shell of the plug or jack is rotated by a given angle so as to match the direction of its positioning key to the direction with the minimum insertion loss. Accordingly, the position of the optical fiber core center is adjusted to the direction of the positioning key (shown by A' and B' in Fig. 7). The distance between the two cores d, which causes the insertion loss, is reduced by means of this operation.

(2) Optimization

The relationship between the angle of the adjusting operation and insertion losses is investigated by computer simulations in order to optimize the angle.

Eccentricity of the core from the ferrule center r is assumed to be represented by two dimensional Gauss distribution f(r):

$$f(r) = \frac{1}{2\pi\sigma^2} \exp\left(-\frac{r^2}{2\sigma^2}\right) \quad (1),$$

where, σ is a characteristic length which denotes the average eccentricity of the core from the ferrule center. A value of 0.6 μm is selected based on field data. The ferrule is rotated by an adjusting operation angle θ so that the core center enters the adjusting area (see Fig.7.) Then, the insertion loss L(d) for butting two adjusted ferrules is calculated based on the following equation[5]:

$$L(d) = L_0 (d/w)^2 , \quad L_0 = 4.34 \quad (2)$$

where, d is the distance between two cores, and w is the mode field radius of the optical fiber and is chosen as 5.0 μm.

The simulated results for a set of randomly-concatenated single-mode fibers are shown in Fig. 8. The adjusting operation angle θ of 120 degrees and 60 degrees correspond to 3 and 6 adjusting operations, respectively. Measured values in each division calculated by dividing the number of measured data by the total number of data are plotted in the same figure. The simulated results agree well with the measured ones.

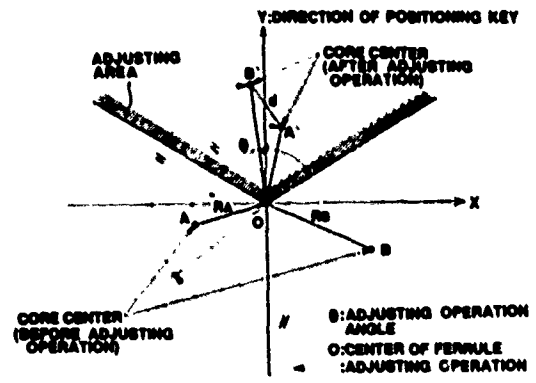

Figure 7 Schematic explanation of adjusting operation

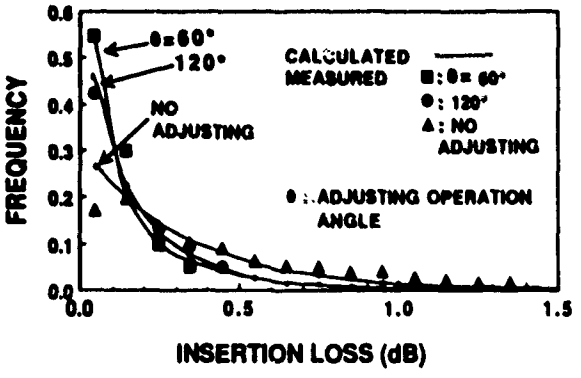

Figure 8 Calculated probability density of insertion loss

Figure 9 shows the cumulative probability of insertion losses calculated by computer simulation based on the above explanation.

It is confirmed from Fig. 9 that an adjusting operation angle of 120 degrees is sufficient for achieving an insertion loss of less than 0.5 dB with a cumulative probability of over 94 % in a set of randomly-concatenated single-mode fibers.

To simplify adjustment, a bayonet like coupling, whose projections and ramps are distributed through 120 degrees, is introduced in both plugs and jacks.

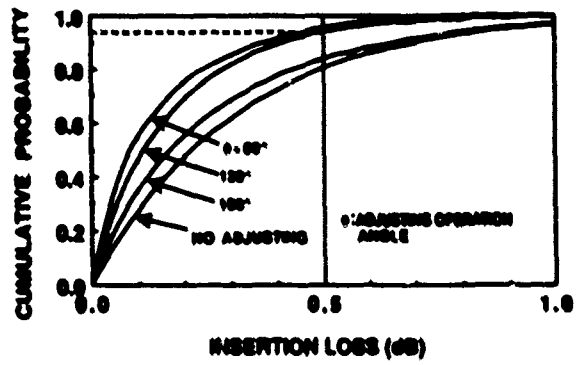

Figure 9 Cumulative probability of insertion loss

3. Characteristics

3.1 Insertion Loss and Return Loss

The insertion losses and return losses of single-mode plug-in connectors were measured using a 1.3 μm wavelength LD source. The results are shown in Table 1 and Fig. 10. An average insertion loss of 0.18dB was obtained for a set of randomly-concatenated single-mode fibers. The return losses were larger than 28 dB.

The insertion losses and return losses were also measured for the worst case in which the printed board housing was 1.2 mm from the front-end and back-end housings of the backpanel. No changes in average insertion loss and return loss were observed between the ordinary case and the worst case.

Table 1 Characteristics of single-mode plug-in optical fiber connectors

Items		Conditions	Results
Optical characteristics	Insertion loss	λ =1.3μm n=60	Ave. 0.18dB σ 0.11dB
	Return loss	λ =1.3μm n=54	Ave. 29.8dB σ 1.4dB
Mechanical tests	Mating	500 (plug element) 60 (printed board)	ΔL_i<0.2dB* L_r>25dB
	Vibration	10~55Hz,Amplitude 1.5mm 2hours×3directions	〃
	Shock	100G, 6ms duration 10shocks×3directions	〃
Environmental tests	Temperature cycling	−25~70℃, 4hours/cycle 100cycles	〃
	Thermal aging	85±2℃ 960hours	〃
	Temperature & humidity cycling	−10~25~65℃,93±3%R.H 1cycle/day, 20cycles	〃

*ΔL_i; Insertion loss increase

L_r; Return loss

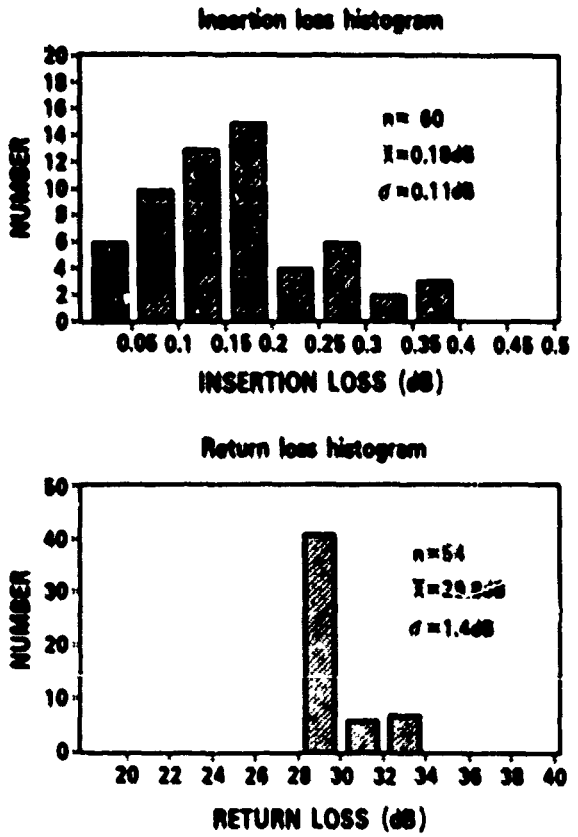

Figure 10 Insertion losses and return losses of randomly-concatenated single-mode fibers

3.2 Repeatability

Connection repeatability for 200 insertions of a printed board into a backpanel was measured. The results are shown in Table 1 and Fig. 11. The insertion loss increases were smaller than 0.2 dB and the return losses were larger than 25 dB during the tests.

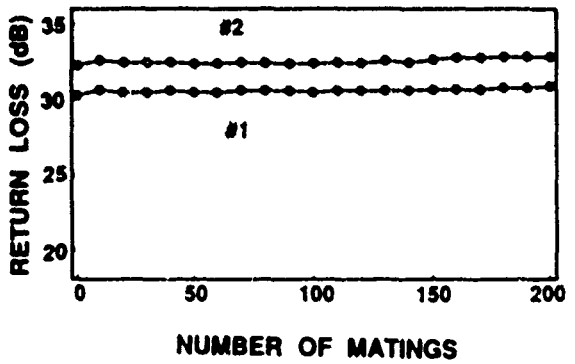

Figure 11 Repeatability of return loss for 200 insertions of printed board into backpanel

3.3 Mechanical and Environment Test

The results of temperature cycling tests and high humidity with temperature cycling tests are also shown in Figs. 12 and 13. Table 1 summarizes the test results for mechanical tests such as vibration, shock, and plug mating, and environment tests such as temperature cycling, high and low temperature endurance, and high humidity with temperature cycling. These results reveal extremely stable characteristics.

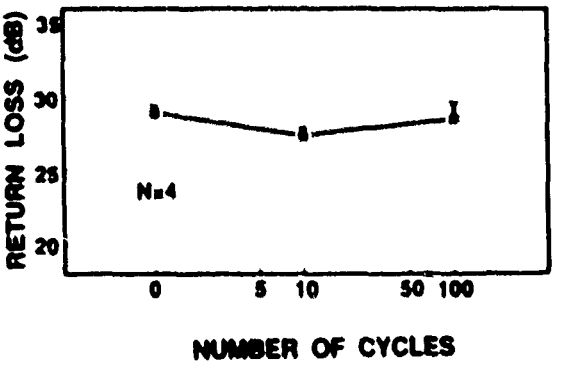

Figure 12 Temperature cycling test results

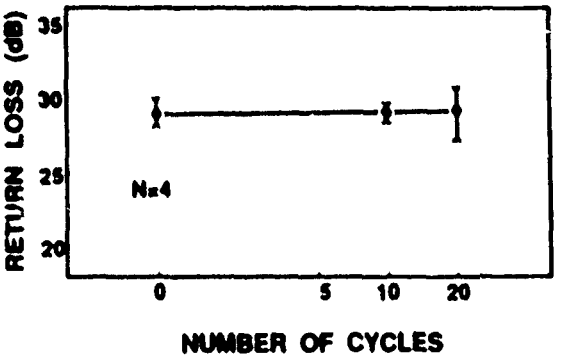

Figure 13 High-humidity with temperature cycling test results

3.4 Transmission Test

Bit error rate measurements have been made under the various conditions shown in Table 2. The measurement set-up is shown in Fig. 14. Six pairs of plugs and jacks were connected in series. The transmission signal was a 1.8 Gbit/s return-to-zero(RZ) format pseudorandom bit sequence ($2^{11}-1$). A power margin of 3 dB was set from the minimum optical power level of the system.

The results are also summarized in Table 2, indicating low error rates of less than 10^{-11}.

Table 2 Transmission tests conditions and results

Items	Conditions	Results
Temperature cycling	-25-70°C, 4hours/cycle 100cycles	no error (error rate less than 10^{-11})
Temperature& humidity cycling	-10-25-65°C, 93±3%R.H. 1cycle/day, 20cycles	
Thermal aging	85±2°C 96hours	
	-25±2°C 96hours	
Vibration	10-55Hz, amplitude 1.5mm 2hours×3directions	
Shock	100G, 6ms duration 10shocks×3directions	

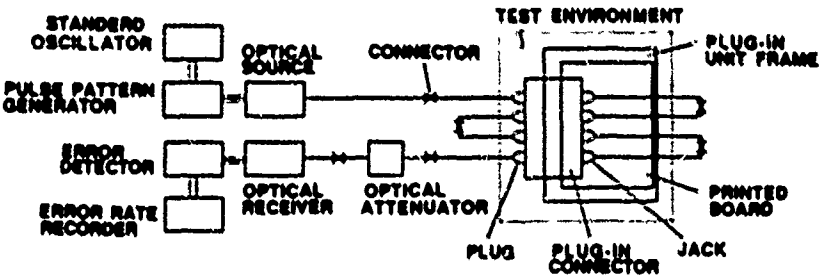

Figure 14 Measurements set up for transmission tests

4. Conclusion

A new system of compact single-mode plug-in type optical fiber connectors is developed for multiple optical connections between a printed board and a backpanel.

This new system consists of two types of plug-in connector; two optical plugs /jacks with 64 electrical terminals and four optical plugs/jacks.

A novel alignment mechanism for plugs and jacks and a novel fiber-core adjustment technology are utilized.

The alignment guide mechanism adopted for this system can absorb about 1 mm radial tolerance of a printed board to a plug-in unit. Axial tolerance is absorbed by the coil spring in the jack.

It is confirmed that an angle of adjusting operation of 120 degrees is sufficient to realize an insertion loss of less than 0.5 dB with 94 % cumulative probability. To simplify adjustment, a bayonet-like coupling is introduced in both the plugs and the jacks. To prevent free rotation of plugs and jacks in the housings, positioning keys are arranged.

Performances of assembled plug-in optical fiber connectors with 10/125 micron single-mode fiber were measured, and were confirmed to have the following satisfactory characteristics. a) Insertion losses were less than 0.4 dB and return losses were larger than 28 dB. b) Mechanical tests such as vibration, shock, and connect-disconnect cycles, and environment tests such as temperature cycling, high and low temperature endurance, and high humidity with temperature cycling, revealed extremely stable characteristics. c) Transmission tests using 1.8 Gbit/s pseudorandom pulse patterns showed low error rates of less than 10^{-11}.

Acknowledgment

The authors would like to thank N. Uchida, Y. Ando, and K. Sasakura for their helpful guidance and encouragement during the course of this development. They are also grateful to H. Tsuji and M. Amamiya for their helpful advice.

References

1. N. Suzuki, Y. Iwahara, M. Saruwatari and K. Nawata: Ceramic Capillary Connector for 1.3 μm Single-Mode Fibers, Electron. Lett. 15, 25, p.809, 1978.
2. Y. Ando, T.Kanai, S. Inagaki and S. Furukawa: Connectors for Equipment Practice Suited to Digital Communications Systems(In Japanese), ECL Tech. Jour. NTT, Jpn, 33, 10. P.2391, 1984.
3. E. Sugita, T. Shintaku and K.Sasakura: High Performance Push-Pull Coupling Single Fiber Connectors and Plug-In Fiber-Optic Connectors, Review of the ECL, NTT, Jpn, 35, 5, pp.529-534,1987.
4. T. Shintaku, E. Sugita, R. Nagase and J. Watanabe; Highly Stable Low-Insertion- and High-Return-Loss PC Optical Fiber Connectors, ECOC 88, pp.599-602, 1988.
5. D. Marcuse:Loss Analysis of Single-Mode Fiber Splices, BSTJ,56,5, pp.703-718,1977.

The Authors

Shin'ichi Iwano

NTT Opto-electronics Laboratories
Tokai,Nakagun,Ibaraki
319-11 Japan

Research Engineer in the NTT Opto-electronics Laboratories. Since joining the ECL system in 1983 he has been engaged in research on optical fiber connections and the development of optical fiber connectors. Mr. Iwano received his B.E. and M.E. degrees from Kyushu University in 1981 and 1983. He is a member of the Institute of Electronics, Information and Communication Engineers of Japan.

Etsuji Sugita

NTT Opto-electronics Laboratories
Tokai,Nakagun,Ibaraki
319-11 Japan

Research Group Leader in the Opto-electronics Laboratories. He is in charge of supervising work on fiber-optic components. Since joining the ECL system in 1970 he has carried out the research and development of circuit components for transmission systems and the physical design technology of electronic equipment. Mr. Sugita received his B.E. and M.E. degrees from Shinshu University in 1968 and 1970. He is a member of the Institute of Electronics, Information and Communication Engineers of Japan.

Kazunori Kanayama

NTT Opto-electronics Laboratories
Tokai,Nakagun,Ibaraki
319-11 Japan

Research Engineer in the NTT Opto-electronics Laboratories. Since joining the ECL system in 1986 he has been engaged in research on optical fiber connectors. Mr. Kanayama received his B.E. and M.E. degrees from Waseda University in 1984 and 1986. He is a member of the Institute of Electronics, Information and Communication Engineers of Japan and the Japan Society of Precision Engineering.

Ryo Nagase

NTT Opto-electronics Laboratories
Tokai,Nakagun,Ibaraki
319-11 Japan

Research Engineer in the NTT Opto-electronics Laboratories. Since joining the ECL system in 1985 he has been engaged in the development of optical fiber connectors. Mr. Nagase received his B.E. and M.E. degrees from Tohoku University in 1983 and 1985. He is a member of the Institute of Electronics, Information and Communication Engineers of Japan and the Japan Society of Mechanical Engineers.

Kenichi Nakano

NTT Applied Electronics Laboratories
Midoricho,Musashinoshi,Tokyo, 180 Japan

Senior Research Engineer, Supervisor, in the NTT Applied Electronics Laboratories. There he is in charge of supervising work on equipment practice suited to advanced digital communication systems. Mr. Nakano received his B.E. degrees from Hokkaido University in 1971. He is a member of the Institute of Electronics, Information and Communication Engineers of Japan.

A SMALL DIAMETER HIGH FIBER COUNT OVERHEAD OPTICAL GROUNDWIRE

George B. Anderson

Alcoa Fujikura Ltd.

Abstract

A novel optical overhead groundwire cable has been developed which significantly reduces the required installation and service tensions for this class of cable. The conventional multi-unit approach to OPT-GW designs requires exotic materials in order to miniaturize the individual units. The proposed design utilizes a single fiber unit containing up to 48 fibers, thus saving as much as 0.75mm in outside diameter. Data are presented relating typical cable diameters to the sag and tension for various spans under heavy loading conditions. The individual fibers are fully color coded in accordance with industry standards. The cable has been subjected to the temperature performance tests prescribed in BELLCORE specification TR-TSY 000020 as well as the more stringent mechanical tests required by the utility industry such as the sheave test, aeolian vibration and fault current. In all cases the cable experienced no significant degradation of optical power. Additionally, data are presented comparing the sag/tension characteristics of the new design vs. existing designs including an all dielectric design.

Nomenclature

The following terms and abbreviations are used throughout the text of this paper:

- OPT-GW - OPTical Ground Wire, a cable containing optical fibers and capable of protecting electrical phase conductors from lightning and fault current damage.
- AW wire - AlumoWeld wire, an aluminum clad steel wire.
- Fault Current - Short circuit current
- RBS - Rated Breaking Strength

Discussion

Background

One of the primary design considerations for OPT-GW is to minimize the overall diameter of the cable structure. Under heavy wind and ice conditions cable diameter is a major factor in determining the forces imparted to the support tower. Since many OPT-GW installations are retrofits, this becomes an important consideration. The OPT-GW installation cannot exceed the design limits of existing towers which were designed for ordinary groundwire. Differences of 10ths of a millimeter can make a difference between whether an existing structure can withstand such forces under heavy loading conditions. The combination of an optical cable within a grounding cable tends to result in a larger overall cable structure. The OPT-GW thus performs two functions. First, the cable must be capable of withstanding lightning strokes and/or fault current loads. This capability requires that the wires on the outside of the cable be of sufficient size to carry high current levels without sustaining mechanical damage. This requirement is in conflict with minimizing diameter. Second, the cable must carry optical signal traffic without interruption. In addition there is a need for higher fiber counts (24-48) which exaggerates the diameter constraint.

Design The conventional approach to making OPTGW involves the manufacture of fiber units containing up to 16 fibers each. These units are then cabled around a central support member and wrapped with a thermal ablative layer. An aluminum pipe drawn around the cabled core and AW wires stranded over the pipe complete the construction. The proposed design consists of a single optical unit containing up to 48 fibers. No cabling is required before piping and AW stranding (see Figure 1). The resulting cable is smaller in diameter allowing significant reductions in installation and service tensions.

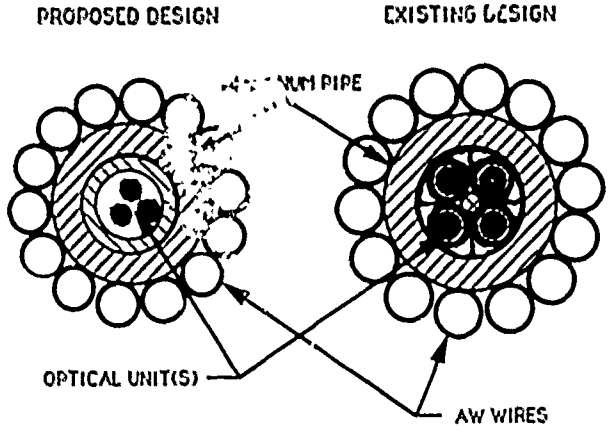

Figure 1 Cable Cross Sections

Mechanical Testing.

Tensile Cycling. One of the development tasks was to determine the effect of strain on the positioning of the optical unit within the optical ground wire. The primary concern was the possibility of the optical unit migrating axially during successive expansions and contractions of the cable structure due to temperature changes.

Bolted deadends were then attached to a 15 meter sample of the OPT-GW cable with approximately 3 meters of OPT-GW extending beyond each deadend. The cable was then stripped back in layers to expose the optical unit and optical fibers. The lengths of the wire, pipe, optical unit, and the fibers thus exposed were recorded as reference points for the data taken during the test. (See Figure 2).

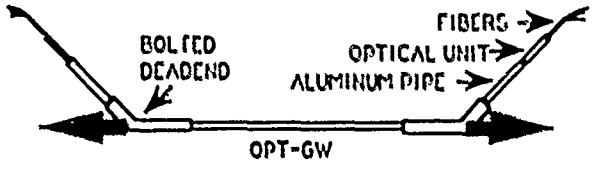

Figure 2 Tension Cycling Setup

The test was set to cycle from 15% RBS to 40% RBS for a specific number of cycles after which measurements of the wire, pipe, optical unit, and fibers were taken to monitor any change from initial conditions. A total of 220 cycles were run, simulating 30-40 years of service. There was no change in the wire or pipe measurements indicating no slippage in the deadends. There was no change and therefore no migration in the optical unit either. The only change noted in the fiber measurements was a decrease in the fiber length equal to the elongation of the cable. Thus the fiber was free to move in relation to the cable structure and relieve any induced stresses.

Tensile vs. Strain. A fiber strain versus cable strain test was performed to characterize the tensile behavior of the design. The cable was elongated a known amount while the fiber length and attenuation were being monitored. The difference between fiber and cable length was taken to be the fiber excess length. The test equipment consisted of a tensile/bend machine and a Photon Kinetics Model 2300 dispersion/strain measurement system.

The pipe was removed approximately 1 1/2 meters from each end to expose the optical unit and fibers. Fittings were used to secure the optical unit to the aluminum pipe. The fibers were also secured by epoxying them to the inside of a cleaned section of optical unit and splinting this section to the end of the specimen's optical unit with a section of the aluminum pipe. One fiber was selected as an optical path for the fiber strain measurement. With a gauge length of 50 meters divided between two spans a 0.5% strain value would be reached at a ram displacement of 127.5 mm.

The sample was strained to 0.25% and 0.5%, 0.7%, 0.83, 0.9% and 1.1% over the course of 20 minutes. After the test the pipe was measured dimensionally and for tensile elongation to determine the degree of excess/strain imparted to the sample. The final cycle took the specimen to failure at approximately 1.13% elongation. Several data points were taken to establish the linearity of the fiber strain as compared to pipe elongation. Figure 3 shows the stairstep plot of the various strain levels. The fiber strain measurements taken at the lower pipe elongation values may be biased to the low side due to the slight bend in the pipe which were straightened out at the higher tension levels. The data would indicate that excess length increases with higher cable strain. This is probably due to an increase in the effective refractive index of the fiber due to stress. The average of all measurements agrees with the physical measurement to within 0.1%. There was no change in optical power up to the point of pipe failure.

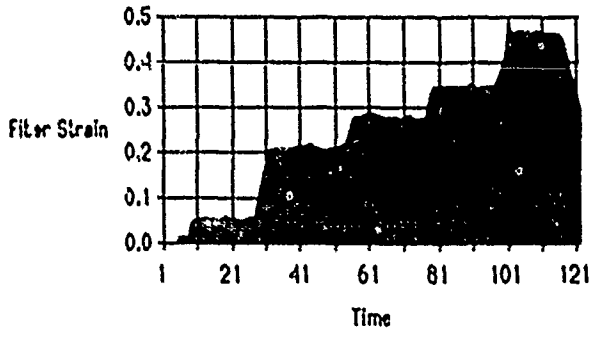

Figure 3 Fiber Strain vs Time

Physical measurement of the pipe after the test showed a reduction in diameter of approximately 0.05 mm and a tensile elongation at break of 0.3%. Hard drawn aluminum normally experiences tensile failure at approximately 1%. The sample had already been elongated to over 1%, therefore this result is not surprising.

Sheave Test. The sheave test is performed to evaluate how a design will withstand the bending and lateral forces encountered during installation. For this test the cable was pulled through a 610 mm diameter sheave a total of seventy times at an angle of 30° at 25% RBS (see Figure 4). Optical power was monitored during the test and dimensions of the aluminum pipe were measured afterwards to determine if any deformation had occurred. An ovality of 0.05 mm was induced by the compressive forces exerted on the cable. This value is well within the design limits. Optical power increased 0.05 dB during the test.

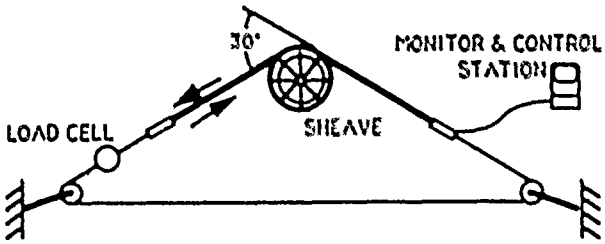

Figure 4 Sheave Test

Splice Box Evaluation. Another installation consideration is how the optical unit will perform when coiled inside a splice enclosure. A splice box was therefore evaluated for its effect on the optical power of the coiled and spliced optical unit.

A section of cable was prepared in accordance with installation instructions for the Alcoa Fujikura splice box. Approximately 1.5 meters of the optical unit was left protruding from the end of the OPT-GW section outside the splice box. The remainder of the 10 meter sample stretched from the entry port on the inside of the splice box, around a cylindrical mandril and back to the work surface (this was done to remove any coiling memory inherent to the sample). Fittings were used to prevent movement of the optical unit through the splice box. A profile alignment fusion splicer was used to concatenate four fibers randomly selected from each of the three subunits within the optical unit. One end of the concatenated fiber path was connected to a 1550nm LED and the other end was connected to an optical power meter.

The procedure for coiling the optical unit consisted of moving the cylindrical mandril closer to the work bench and then coiling the optical unit into the splice box (re: Cable "A", Figure 5). The use of the cylindrical mandril prevented sudden coiling of the whole unit. A reading was taken after each coil was placed in the splice box.

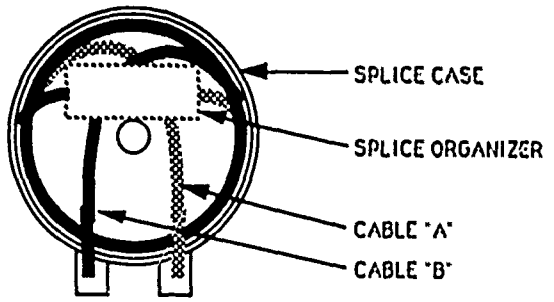

Figure 5 Splice Box

Optical power increased during the initial movement of each coil but settled down to negligible change once movement stopped. Therefore coiling the optical unit into the splice box will not have a derogatory effect on optical power.

If it is necessary to secure the optical unit against axial movement in the splice box, then processing as well as environmental effects must be taken into account. Table 1 shows the expected range of post extrusion shrinkage from an optimized process.

Sample	Time (hrs)	Temp (°C)	Shrinkage	Std Dev
1A	120	85	0.37	--
1B	120	85	0.37	0.009
1C	120	85	0.36	--
1D	120	85	0.36	0.015
2A	120	65	0.28	0.006
2B	120	65	0.28	--
2C	120	65	0.29	--
2D	120	65	0.28	0.007

Table 1 Optical Unit Shrinkage

Using the worst case of shrinkage plus the maximum expected short term cable elongation results in a force imparted to the optical unit at the strain relief device of approximately 17 kgs. A test was devised whereby 25 kg were hung from the optical unit which was being held in a stationary fixture for 30 days. The permanent deformation of the optical unit was negligible.

Environmental Testing.

Temperature Cycling/Aging Attenuation was measured by OTDR after each manufacturing stage and the cable was put into a walk in environmental chamber for temperature cycling and ageing in accordance with BELLCORE specification TR-TSY-000020. All except one fiber from each of the three units were fusion spliced to form an optical path approximately 33 km long. This path was monitored continuously for the duration of the test. The other three fibers were measured by OTDR at the end of each temperature soak.

The average baseline attenuation at 1550 nm was 0.21 dB/km with a maximum of 0.24 dB/km. The cable was exposed to temperatures from -40°C to +65°C plus a five day exposure to +85°C. The highest average attenuation throughout this exposure was 0.25 dB/km with a maximum of 0.34 dB/km.

Vibration A 20 meter sample cable was subjected to an aeolian vibration for 100,000,000 cycles at 50±5 Hz with a free loop amplitude of 3 mm and tension of 25% RBS. this combination of frequency and amplitude simulates lifetime field conditions of 13.5-16 km/hr winds.

During the first eight hours of the test the fibers experienced an increase in optical power of approximately 0.03 dB due to reorientation of the fibers to a more stable equilibrium position. For the remainder of the test (>720 hrs) the optical power fluctuated from this value less than ± 0.01 dB. This condition is attributed to the normal variation in the measurement system. (See Figure 7). Inspection of the cable after completion of the test revealed no

adverse effect due to fatigue.

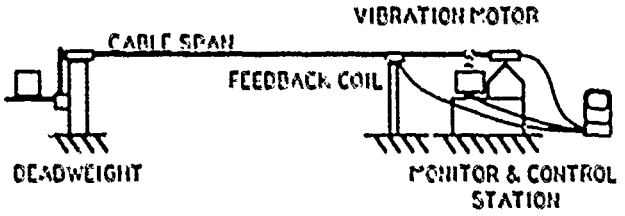

Figure 6 Vibration Span

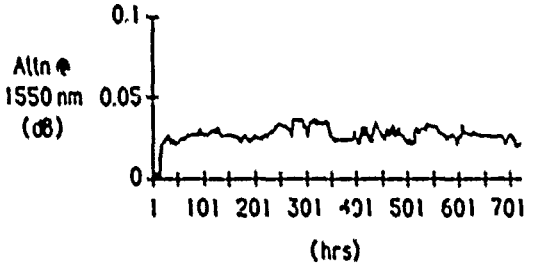

Figure 7 Optical Power vs Time; Aeolian Vibration

Vertical Rise There are two concerns associated with vertical rise. The first is whether the waterblocking gel will leak out at the termination points due to hydrostatic pressure. A 10 meter cable sample was hung vertically for more than 60 days with a flask under the open bottom end to catch any gel which might leak out. Measurements of protrusion-retraction were made periodically. Only a slight oil separation was observed.

Three samples were hung in a catenary loop and vibrated at low frequency and high amplitude to determine if or by how much the optical fibers would "bunch up" at the midpoint of a span. Measurements were made periodically to on the amount of fiber that either protruded from the optical unit or retracted into the optical unit. This test was not completed in time to include data in this report.

Electrical Testing.

Fault Current As mentioned in the abstract, one of the primary functions of an OPT-GW cable is to act as a grounding circuit. In order to test this capability a target short circuit value of 136kA^2 sec was applied to each of four three meter samples. The sample was allowed to cool down to ambient temperature after the short circuit was applied. The sample was then inspected visually for any physical damage. this procedure was repeated a total of ten times for each sample. After completion of he tests the optical units were removed and visually inspected for damage, charring, etc. No adverse effects were found on either the metallic or plastic portions of the cable. The summary I^2t values are shown in the table below.

Duration (cycles)	Current (A_{rms})	I^2t (MA^2sec)	AW Temp (°C)
37.9	14.8	138.2	118.4

Primary Result.

This project has resulted in a 3.5% reduction in diameter for 36 fiber cable and an 11.1% reduction for 48 fiber cable. The design has been subjected to and passed relevant industry performance requirements. The design change also resulted in the elimination of one manufacturing step. The elimination of this step removes a source of variation in the manufacturing process and therefore enhances the long term reliability of the product.

Acknowledgements.

The author would like to recognize Randy Ferrell, W. E. King, Andy Panuska, P. D. Patel, Bob Roman, Bob Russ, Dan Tatarka, .

References.

1. Alcoa SAG10 software
2. Transmission Line Reference Book. "Wind-Induced Conductor Motion", Electric Power Research Institute, Palo Alto, CA, 1960.
3. Various internal test reports, Alcoa Fujikura, Ltd, Spartanburg, SC.

Appendices.

Summary of test results.

Mechanical

Tensile Cycling	20-25 mm fiber contraction
Tensile vs Strain	no attenuation change
Sheave	0.05 dB gain, 70 passes
Splice box	0.01 dB gain, 8 coils

Environmental

Temperature Cycling	≤ 0.25 dB/km, -40° C to +85°C
Vibration	≤ 0.04 dB gain
Vertical Rise	slight oil separation
Fiber Migration	none found

Electrical

Fault Current	136 kA^2-sec, no damage

Diameter Comparisons

	Existing	Proposed	All Dielectric
Diameter (mm)	15.95	15.2	15.3

Sag and Tension Comparisons

150 m span

	Sag (m)			Tension (kgf)		
Loading	Exist	Prop	Diel	Exist	Prop	Diel
Light	0.9	0.8	4.1	3744	3391	557
Medium	1.2	1.2	4.8	3777	3415	675
Heavy	1.8	1.8	6.0	3966	3594	928

300 m span

	Sag (m)			Tension (kgf)		
Loading	Exist	Prop	Diel	Exist	Prop	Diel
Light	3.3	3.1	--	3881	3538	---
Medium	4.3	4.1	--	4120	3743	---
Heavy	5.8	5.6	--	4667	4271	---

450 m span

	Sag (m)			Tension (kgf)		
Loading	Exist	Prop	Diel	Exist	Prop	Diel
Light	6.9	6.4	--	4050	3728	---
Medium	8.6	8.2	--	4496	4114	---
Heavy	11.0	10.8	--	5376	5001	---

Author

George Anderson joined Alcoa Fujikura Ltd in March of 1987 and is the Design Engineering Manager of the Telecommunications Division. He received a BS in Mechanical Engineering from N. C. State University in 1977. Mr. Anderson has been in the wire and cable industry since his graduation and has experience in many areas of telecommunications cable and cable related products, including conventional twisted pair cable, military and commercial fiber optics, and overhead groundwire.

A Unique Approach to Air Pressurized Optical Cable Employing Standard Fiber Tubes

Randy J. Smith, P. Eng. & Neale E. Felske

Northern Telecom Canada Limited

BACKGROUND

Dynamically air pressurized cables have been used as a means of purging humidity from conventional copper communications cables and as a means of sheath fault detection for many years. Air pressure systems and equipment already in place and operating allow for the use of air pressurized optical cable. A need exists in the marketplace for pressurized optical cable which exhibits the fiber performance characteristics and rugged mechanical properties of filled cable using loose buffered fibers.

INTRODUCTION

The use of established cable pressurization systems for standard copper communications cables provides the need for a dynamically pressurized optical cable exhibiting the same optical and mechanical performance found in filled cables. A unique hybrid cable design was developed to meet the air flow requirements of standard telecommunications air pressure systems and to provide a product to meet the specifications required in today's modern outside plant optical cables. A core was developed which allows for a variety of loose buffered fiber tubes and twisted PIC pairs to be jacketed with standard single or multiple sheaths. Northern Telecom's Optical Cable Division is manufacturing an exclusive air pressurized version of its TUBESTAR outside plant design fully capable of meeting Bellcore specification TR-TSY-000020, issue 4. Due to the nature of pressurized cable, sections 5.1.7 Cable Freezing and 5.1.8 Resistance to Water Penetration do not apply to pressurized cable. As in the filled TUBESTAR cable design, superior mechanical performance is provided over conventional loose tube cables in terms of crush, impact, and twist requirements.

The unique feature of the air pressurized TUBESTAR design is the active purging of humidity throughout the core and the passive repelling of water provided by the gel filled buffer tubes. This paper will summarize the applied development work such that an acceptable pneumatic resistance was obtained for use in existing air pressure systems. The novel concept of fully filled tubes in a pressurized core raises the question of filling compound flow due to the static pressure on the cable cross section. This concern is addressed by presenting test data on aged and unaged tubes at elevated temperatures exposed to static air pressure.

CABLE DESIGN

The design incorporates conventional loose buffered fibers, single mode or multimode, in a nylon tube. Any number of fibers from two to 12 may be contained within the filled tube. The buffer tubes are then inserted into a slotted cable core. The star shaped core profile has been precisely designed to position the tubes around the central strength member. Enough air passages are available around the tubes to provide sufficient air flow to effectively purge humidity from the cable and utilize flow sensors as an alarm in the event of sheath damage. These air passages are all interconnected to ensure free air flow throughout the cable structure. Other aircore cables using tubed fiber are available. However, in these designs, unfilled tubes of fiber are bundled around a central strength member in conventional loose tube cabling fashion. The drawback to this design is the very high pneumatic resistance caused by the cable core. Much of the path for air flow is provided by the hollow tubes acting as air pipes. In a core which is highly resistive to air flow, humidity and condensation can build up around the tubes resulting in possible long term corrosion of metallic components. In the event of sheath damage, a change in flow rate or pressure drop would be difficult to detect. Clearly, damage would have to result to the fiber tubes themselves, which in most cases would result in broken fibers.

The concept of filled fiber tubes in an aircore cable provides extra protection to the fibers by way of the tube buffering gel, while still allowing dynamic pressurization and free air movement through the core and sheath. This provides a design which allows enough air flow without having to depend solely on the core slots to protect unbuffered fibers as in the open channel design.

AIR PRESSURIZED

TUBESTAR

OPTICAL CABLE

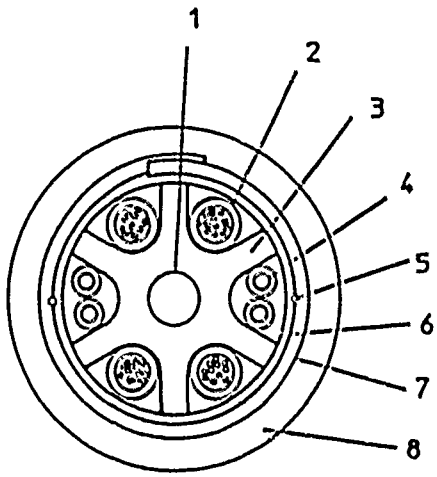

1. CENTRAL STRENGTH MEMBER
2. FILLED FIBER TUBE
3. HDPE CORE EXTRUSION
4. TWISTED COPPER PAIR
5. RIPCORD
6. COR WRAP TAPE
7. COR UGATED STEEL ARMOUR
8. HDPE OUTER JACKET

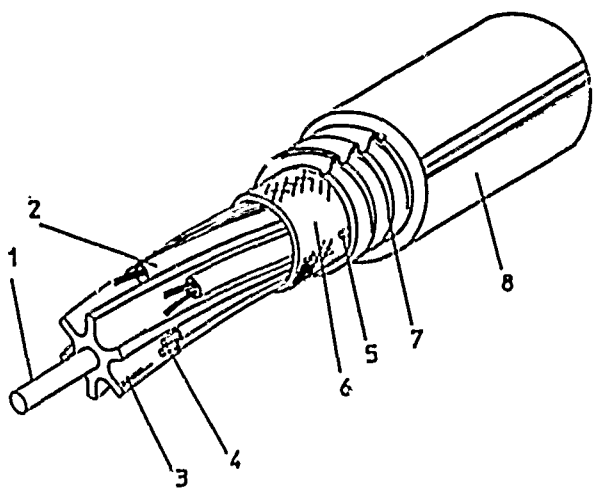

If sheath damage occurs in this case, flow and pressure alarms are easily activated while the fibers remain intact and buffered by a layer of gel inside the tube protecting the fibers from water.

PNEUMATIC RESISTANCE REQUIREMENTS

The objective of the cable design was to achieve the lowest pneumatic resistance possible while still maintaining fiber and copper pair counts commonly required by users. Much difficulty was encountered in trying to set an upper limit for pneumatic resistance. There appeared to be no common specification in the industry. Utility companies would accept a pneumatic resistance as high as 10. (Note that the unit of measure for pneumatic resistance is psi/kft/ft^3/hr) Telcos quoted only the Bell Canada requirement for pneumatic resistance. Upon further investigation, it appeared that a Bell Canada upper limit of 5 was derived only from the past performance of an open channel slotted core design where the fibers lay loosely in the V-grooves of the core. It was readily apparent that for the same empty core cross-sectional area, the addition of filled tubes would dramatically increase the pneumatic resistance over that found for fibers laying loosely in the slots of a open channel core.

JACKET EFFECTS

Jacket configuration appeared to have an effect on the total pneumatic resistance for the cable. As successive jackets were added to the core, additional air paths were created. A single polyethylene jacket extruded over the core would result in the highest pneumatic resistance for a given fiber/copper count. The type of construction of the second jacket could lower the original pneumatic resistance found with the plain poly first jacket by as much as 10 - 20%. Some factors affecting pneumatic resistance in the sheath include:

1. Corrugated versus smooth metallic sheaths.
2. Presence of aramid fibers and their location in the cable.
3. Use of core wrapping tapes.
4. Clearances provided by the sizing of forming tooling.

EXPERIMENTAL CABLE TRIALS

Early development began on the 10mm TUBESTAR core using 6-fiber tubes with 22 AWG copper pairs in order to establish the pneumatic resistance limits of the core. In addition, experiments were set up to try to predict the individual contribution to pneumatic resistance given by a single tube and single copper pair in the core slot.

With this information, it was thought that a pneumatic resistance model could be created to predict the total resistance of the cable using a combination of available flow area and a parallel resistor network approximation. After obtaining individual resistance values for the cable components, predicted pneumatic resistance and actual measured values correlated poorly. Factors that can affect the measurements are core lay length, core over wrap and sheath type, tube and copper pair fit in the slots, and cable end preparation. Because of these variables, attempts to make theoretical predictions for pneumatic resistance were abandoned and, wherever possible, a short sample cable was manufactured and pneumatic resistance was measured for the given fiber/copper count. Table 1 shows a summary of the experimental configurations tested and results obtained.

After initial trials and experiments using the standard 10mm core, much of the development thrust was placed on a 12mm/6 slot TUBESTAR core for Bell Canada requiring 12-fiber tubes and non-standard heavy wall copper pairs. This design can provide a cable with a maximum loading of 48 fibers and two copper pairs while still achieving a pneumatic resistance of less than 10. A lower resistance can be achieved by eliminating the requirement for copper pairs. Depending on the absolute upper limit of pneumatic resistance, a maximum loading of 72 fibers with no copper pairs can be achieved.

GEL CREEP UNDER PRESSURE

As mentioned previously, concern was expressed regarding the movement or creeping of the tube filling gel due to static pressure over an extended period of time, in a short length of cable. A number of tests were set up to discover whether the filling gel would creep into splice closures or other termination points. Initially, a two meter piece of tube was exposed to 20 psi at room temperature for 1 hour. A two meter length at 20 psi was thought to be an absolute worse case scenario and if no gel movement was found, the expressed concerns would be unfounded. Results showed that the filling gel had actually blown out of the tube and the fibers had moved. This test was found to be too severe and impractical. It was decided that a more realistic test was to expose each of three 500 meter lengths of 6-fiber tubes to 15 psi at room temperature. 15 psi was thought to be the maximum field operating pressure that might actually be used on a short length of cable. After 60 days at room temperature there was no gel movement from the end of the tube and the test was discontinued.

A larger tube containing 12 fibers was tested for gel creep under severe conditions. A 50 meter piece of gel filled tube with 12 fibers in it was aged for 5 days at +85°C. Following the aging condition cycle, it was then held at +70°C with a static pressure of 11 psi applied at one end of the tube. The other end was open to the atmosphere.

TABLE 1

PNEUMATIC RESISTANCE VALUES FOR SELECTED AIRCORE TUBESTAR CABLE DESIGN CONFIGURATIONS

CORE CONFIG. FIBER - COPPER[1]	AVAILABLE CORE AREA (mm^2)	PNEUMATIC RESISTANCE (PSI/FT/FT^3/MM)
10mm/6 SLOT 6F TUBES		
0 - 0	37.2	1.2
18 - 1	18.8	11.5
24 - 2	16.6	20.0
36 - 0	12.2	31.0
12mm/6 SLOT 12F TUBES		
30 - 2	32.6	7.2
36 - 2	40.9	3.0
48 - 2	36.7	5.5
[2] 45 - 2	34.5	7.4
[2] 48 - 2	34.5	8.3
[2] 72 - 0	33.4	13.0

NOTE:

[1] All copper pairs are 22 AWG

[2] .035" heavy wall pairs

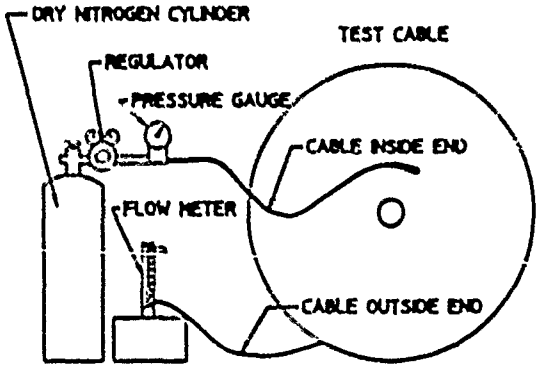

PNEUMATIC RESISTANCE TEST SET UP

TABLE 2

SUMMARY OF GEL CREEP TESTS FOR LOOSE BUFFER TUBES

TUBE SAMPLE	LENGTH	--TEST EXPOSURE CONDITIONS-- TEMP.	PRESS.	TIME	AGED	GEL FLOW
6F TUBE						
TUBE 1	2m	+25°C	20 psi	1 HOUR	NO	EXTREME
TUBE 2	500m	+25°C	15 psi	60 DAYS	NO	NONE
TUBE 3	500m	+25°C	15 psi	60 DAYS	NO	NONE
TUBE 4	500m	+25°C	15 psi	60 DAYS	NO	NONE
12F TUBE						
TUBE 5	50m	+70°C	11 psi	24 HOURS	YES	NONE
TUBE 5A	30m	+70°C	11 psi	24 HOURS	YES	YES
TUBE 5B	15m	+70°C	11 psi	24 HOURS	YES	YES
TUBE 5C	10m	+70°C	11 psi	24 HOURS	YES	YES
TUBE 5D	5m	+70°C	11 psi	24 HOURS	YES	YES
TUBE 6	15m	+40°C	11 psi	4 DAYS	NO	NONE
TUBE 7	15m	+40°C	11 psi	4 DAYS	NO	NONE

NOTE:

Aged conditioning is a 5 day exposure to +85°C.
Common operating pressure is between 8 and 15 psi.
A foreseeable field condition could be +40°C for 12 to 18 hrs.

After 24 hours no gel or fiber movement was observed. In order to determine a threshold limit, the same tube was then cut into four shorter pieces. Each of the 5, 10, 15 and 20 meter pieces failed within 24 hours at 11 psi. Gel pooling was observed. The test temperature was thought to be somewhat greater than what might be expected in actual field conditions so two new tubes were tested. Two pieces between 10 and 20 meters were exposed to 11 psi at +40°C for four days. No gel creep was observed. Table 2 shows a summary of the gel creep tests.

CABLE TEST RESULTS

All aircore TUBESTAR cables are designed to withstand the same mechanical loading conditions specified in TR-20 for filled cables with the exception, of course, of water penetration. Table 3 shows the results of mechanical testing performed on a 12mm/6 slot core with a single steel armor and polyethylene jacket. Individual loss measurements are not shown for the temperature cycling test however, the cable is capable of fully meeting the TR-20 requirements.

CONCLUSIONS

Much was learned from the experimental program. An understanding of the factors affecting pneumatic resistance was obtained as well as the contribution of various sheaths, fiber count, and copper count. Fear of static operating pressure causing gel and fibers to be pushed out of the tubes was removed. Only under very short lengths, less than 20 meters, at temperatures above +40°C will a small amount of gel be moved in the tube. Mechanical and optical performance of filled TUBESTAR cable is maintained in the aircore versions. The 10mm core with 6-fiber tubes and the 12mm core with 12-fiber tubes allows flexibility in system design by providing for a wide range of fiber and copper counts while still maintaining an operating pneumatic resistance ranging from 3 to 8 psi/kft/ft^3/hr.

TABLE 3

MECHANICAL TEST RESULTS
[illegible]

TEST	PARAMETERS	SPEC (TR-20 Sec 4)	TEST RESULT
CYCLIC FLEXING	Bending OD (m)	36	33
	# Cycles	25	25
	Steel Tape	Pass	Pass
	Splitting		
	1310 Residual (dB)	<0.1	0
	1550 Residual (dB)	"	0.1
CYCLIC TWIST	Length (m)	1	1
	Degrees of Twist	±180	±360
	Sheath Splitting	Pass	Pass
	1310 Residual (dB)	<0.1	0
	1550 Residual (dB)	"	0
COMPRESSIVE STRENGTH	Load (N/cm)	440	440
	1310 Peak (dB)	<0.1	0
	1310 Residual (dB)	"	0
	1550 Peak (dB)	"	.02
	1550 Residual (dB)	"	.02
IMPACT RESISTANCE	Impact Mass (kg)	5	5
	# Impacts	25	25
	1310 Residual (dB)	<0.1	.02
	1550 Residual (dB)	"	0
CENTERLINE FLOW	Temperature (C)	+40	+40
	Preconditioning Cycle (21 hrs)	Leakage Allowed	
	Conditioning Cycle (21 hrs)	No Leakage	Pass
COLOR PERMANENCE	Temperature (C)	+85-120 hrs	+85-120 hrs
	Pass/Fail Criteria	Discoloration	Pass
OUTER CABLE JACKET REQUIREMENTS	Yield Strength (min)	11.0 MPa	14.2 MPa
	Ultimate Elong (min)	400%	500%
	Jacket Shrinkage (%)	<5.0	2.5
	Jacket Adhesion (lb/in)	20 lb/in	Not Appl.

Randy Smith

Neale Felske

Randy Smith received his B.S. degree in Mechanical Engineering from the University of Saskatchewan in 1983. Since graduation, Randy has worked in Manufacturing Engineering at Northern Telecom Canada's Optical Cable Division in Saskatoon, Saskatchewan. Randy has twice been named to Northern Telecom's Order of Excellence for Technical Achievement for work in optical cable design and sheath water blocking. Randy is currently a senior member of the process engineering group involved with jacket process support and new product introduction.

Neale Felske is a Cable Process Engineer in the Manufacturing Engineering Department at Northern Telecom's Optical Cable Division located in Saskatoon, Saskatchewan. He joined Northern Telecom Canada in 1985 after receiving a Bachelor of Applied Science Degree in Industrial Systems Engineering from the University of Regina. Neale has been named to Northern Telecom's Order of Excellence for Technical Achievement for optical cable design. Neale is currently involved with cable design and customer service support.

FACTORS AFFECTING MECHANICAL STRIPPING OF POLYMER COATINGS FROM OPTICAL FIBERS

J. R. Toler & C. K. Chien

Corning Incorporated

Today's polymer coatings on optical fibers are stable over a broad range of environments, protect the glass fibers curing cabling and installation, and are easily removable in the field for making connections. Now that fiber is moving from its more traditional application in the telephony plant into more connector intensive applications, the ability to remove the coating easily has increased in importance.

The mechanical strippability of a fiber coating is evaluated by measuring the force required to completely remove the coating from the fiber with a commercially available stripping tool drawn at a constant rate along the fiber. This paper discusses the effects of a variety of factors on the stripping force for 250 micron diameter coated fibers. These factors include: stripping tool design, stripping speed, length of fiber stripped, stripping in hot and cold environments, and varying fiber storage conditions of relative humidity and temperature.

Introduction

In order to connect optical fibers to electronic equipment or to one another, it usually is necessary to remove the coating. The most common way of accomplishing this is to mechanically remove the coating using stripping tools available for this purpose. The work described here was undertaken to determine which factors affect the difficulty of this mechanical stripping process.

The factors investigated include:

- the length of fiber stripped
- the speed at which the fiber is stripped
- the temperature at which the fiber is stripped
- the humidity at which the fiber is stripped
- the design of the stripping tool

Three of these factors were investigated in a factorial design experiment as diagrammed in Figure 1. The remaining two factors, humidity and temperature, were investigated separately due to the increased difficulty of measuring the effects of these.

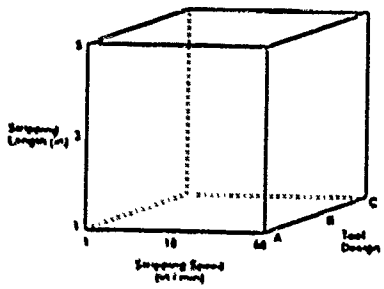

Figure 1

These effects were evaluated using testing equipment shown in Figure 2, which is very similar to that described earlier.[1] The apparatus consists of a fiber-optic stripping tool mounted on a motorized stage, the speed and travel length of which can be controlled. The fiber is mounted in the apparatus such that coating is removed from one end of the fiber by the stripping tool. The opposite end of the fiber is connected to a load cell which indicates the load applied to the fiber as the stripping tool is moved at a constant speed to remove the coating. In this study, the output of the load cell was fed into a computer to facilitate data manipulation.

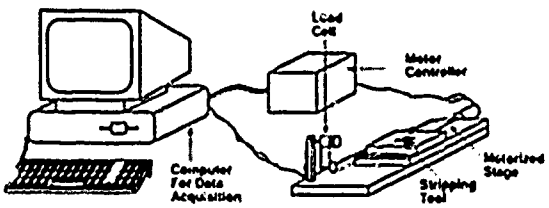

Figure 2

Fibers Evaluated

Type IVA fibers with dual layer UV-cured acrylate coatings were studied. The fiber coatings had an outside diameter of 250 um. The coated fibers were typical of those commercially available for use in loose-tube telecommunications cables.

Types Of Stripping Tools Investigated

Three stripping tool designs were investigated in this study.

The first of these, designated Type A, incorporates blades that come together like the blades of a pair of scissors. The blades each have a semicircular hole in the cutting edge. On closing the blades, these holes come together to form a hole slightly larger than the diameter of the glass part of the optical fiber (125 um). This type of tool has no guides to keep the fiber perpendicular to the blades and aligned with the blade holes.

The second type, designated Type B, contains blades that close around the fiber in the same plane (butting blades). This type also has a semicircular hole in each blade, which come together to form a circular hole slightly larger than the glass part of the optical fiber (125 um). The Type B tool incorporates metal supports with vee-shaped grooves close to the blades to hold the fiber in alignment with the blade hole during the stripping process.

The third type, designated Type C, is similar to Type B in that it also has butting blades that close around the fiber in the same plane. Instead of supports on either side of the blades as Type B has, Type C incorporates a metal tube to maintain fiber alignment with the blades during stripping.

All three types of stripping tools are available in a variety of sizes for stripping fibers with different glass diameters or different coating diameters.

Effect Of The Length Of Fiber Stripped

The length of coating stripped in one pass of the stripping tool varies with the person doing the stripping or the test method specified.[2] The effect on peak strip force of different strip lengths between 1 and 5 inches (25.4 to 127 mm) was evaluated using three commonly available stripping tools. The results are shown in Figure 3. Comparing the three types of tools, the scissors blade, Type A, showed the highest peak strip forces and the highest variation. The stripping tool of butting blade Type B showed results that overlapped with those of the scissors-type tool. The butting blade Type C showed the lowest peak strip forces at all lengths investigated and the lowest overall variation.

These results clearly indicate that, for the tools tested, the length of coating removed in one pass does not strongly affect the peak strip force for 250 um diameter fiber coatings.

Effect Of Stripping Length And Tool On Peak Strip Force

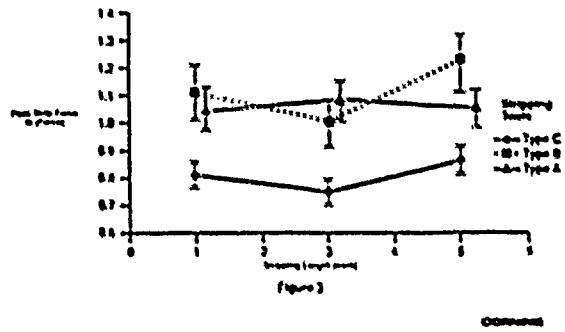

Effect Of Stripping Speed

Stripping speed was evaluated since this normally is uncontrolled in field installation, and repair of optical fibers and potentially is a factor in the force required to remove the coating from a fiber. Typically, field personnel strip coatings from fiber at speeds estimated to be between 15 and 60 inches per minute.

Figure 4 shows the peak strip force developed during the stripping of a 3 inch length of coating at speeds between 1 and 60 inches per minute. Tool types A and B give significantly higher forces at all speeds than does tool type C. Each of the tools appears to give a slightly higher force at 20 inches per minute than at higher or lower speeds. For all three tools, variability, represented by the one sigma limits shown, decreases as speed increases.

Effect Of Stripping Speed And Tool On Peak Strip Force

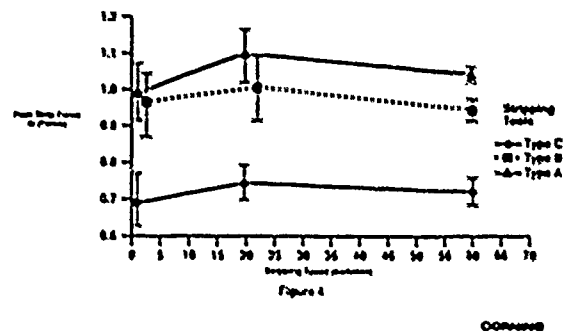

Results from this study show that the peak strip force depends more on the tool selected than on the speed of stripping. Peak strip force was not found to vary widely over the range evaluated.

Effect Of The Temperature At Which The Fiber Is Stripped

The effect of temperature on the force required to remove the coating was evaluated since fibers are stripped in the field under a wide range of temperatures. The fibers were conditioned and tested at temperatures from -30° to +60° C. Figure 5 shows the results for 250 um diameter coated fiber using a Type B stripping tool. The line at each temperature shows the one standard deviation limits. There appears to be no significant difference between the force required at room temperature (23°C) and at -30°C. The force required at 60°C is significantly lower than either of these. One explanation of the decrease at higher temperatures is the relaxation of the secondary coating. One of the factors believed to control strip force is the mechanical adhesion of the primary coating to the glass surface of the fiber. The secondary coating shrinks as it cures and compressively loads the primary coating underneath increasing the mechanical adhesion of the primary coating to the glass. When the secondary coating is heated, it relaxes and reduces its compressive loading of the primary coating. This results in a lowered strip force.

Peak Force As Function Of Temperature

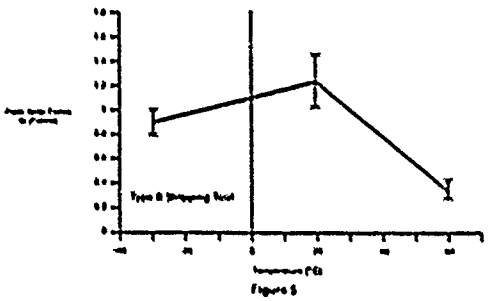

These results lead to the conclusion that temperature has little or no effect on peak strip force for temperatures below room temperature. At higher temperatures, peak strip force declines and the reason is postulated to be a change in coating properties.

Effect Of Humidity

Since humidity in the atmosphere surrounding optical fiber ends being installed or repaired is another factor that potentially might affect the difficulty with which the coating can be removed, it was evaluated to see how strong its affect would be. The peak strip force of a 250 u fiber as a function of relative humidity was determined The fibers were conditioned in chambers with various relative humidities, all at room temperature, for 24 hours prior to testing. The fiber coatings were then stripped from the test fibers immediately on their removal from the chamber (at a rate of 1 inch/minute with a strip length of one inch). As can be seen in Figure 6, the peak strip force value declines as the humidity increases. The drop off in peak strip force becomes more pronounced as the relative humidity increases over the 50% to 60% level.

Dependence Of Strip Force On Humidity

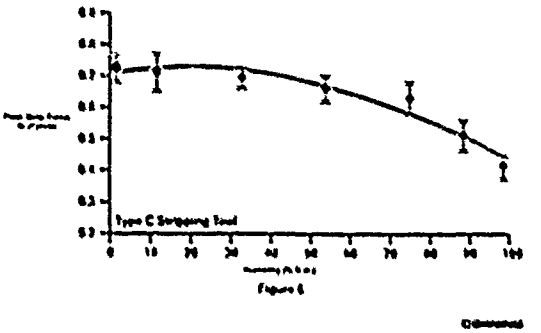

The strip force of optical fibers coated with UV-curable acrylates changes as the relative humidity of storage conditions and of the test environment changes for at least two reasons. The first of these is that the water content of the coating is a function of the relative humidity. As the water content increases, mechanical properties such as modulus decrease. Water molecules in the polymer matrix function as "ball bearings" to permit polymer molecules to move over one another more easily. Absorption of water causes the coatings to swell slightly. If no polymer bonds are broken as a result of the swelling, then a given number of crosslinks is spread over a larger volume of polymer which must result in a lower modulus. The second reason is that water in the coating can decrease the adhesion of the coating to the glass surface of the optical fiber. This decreases peak strip force by making the coating matrix easier to slide off the fiber.

Relative humidity exerts a smaller effect on peak strip force than several of the other factors investigated. Higher humidities cause a decrease in the force required. This is thought to be due to a change in coating properties as the coating absorbs water from the atmosphere.

Conclusion

A number of factors which could influence the force required to mechanically strip 250 um diameter coatings from optical fibers have been investigated. Of these factors, stripping tool design was found to have the greatest influence. One design was found to require a significantly lower force than the other two types. The temperature of the environment was found to have the second largest effect. Humidity in the environment had a smaller effect and stripping length and stripping speed had the smallest effects.

References

1. J. Moses and M. Sigmon, "A Test for Optical Fiber Coating Strippability", IWCS Symposium Proceedings, 1987, pp. 163 - 168.

2. Field personnel have been reported to strip anywhere from one-quarter inch to 3 inches or more with one pass of the tool. FOTP-178, currently being developed by the TIA, specifies a strip length of 30 mm for 250 um diameter fiber and 15 mm for 500 to 900 um diameter fiber.

J. Richard Toler
Corning, Incorporated
SP-DV-01-8
Corning, NY 14831

Dick Toler was born in Richmond, Virginia. He received his B.S. in Chemistry from Virginia Commonwealth University and his Ph. D. degree in Organic Chemistry from the University of Virginia in 1975. He worked with Owens-Corning Fiberglas Corp. until 1986 when he joined Corning, Incorporated where he is currently Supervisor of Optical Fiber Coating Development.

Ching-Kee Chien
Corning, Incorporated
SP-DV-01-8
Corning, NY 14831

Ching-Kee was born in China. He received his B.S. degree in Chemistry in Taiwan and his Ph. D. degree in Polymer Chemistry from the State University of New York. After working at the Carnegie Mellon Institute and City College of New York, he joined Corning, Incorporated in 1985 where he has worked on coating development for optical fibers.

AN ENVIRONMENTALLY SEALED TERMINAL BLOCK WITH ROTARY CONNECTION

Erwin DeBruycker James Pinyan Gerald Shimirak

RAYCHEM CORP. Fuquay-Varina, NC

RAYCHEM CORP. Menlo Park, CA

ABSTRACT

Design requirements for an environmentally sealed terminal block are established in order to meet the enhanced transmission requirements of outside plant telecommunications.

A novel electrical connection system, called rotary connection, while used in conjunction with a gel sealing material provides total environmental protection.

Comprehensive electrical and environmental tests are discussed to show the preservation of electrical integrity under severe environmental conditions.

INTRODUCTION

The advent of digital voice, data communications and other future enhanced services is making the transmission requirements more sophisticated. Many attempts have been made to stabilize the electrical characteristics and capabilities of current outside plant, with some notable successes. New technologies have been developed which effectively isolate exposed wirework from the ravages of moisture, pollutants, salt insects and flooding, but until recently these advances have stopped short of the terminal block.

In case of a terminal block, these environmental conditions can cause acute and/or chronic physical changes due to corrosion, loss of electrical integrity and connection deterioration. These changes can affect the characteristic impedance and the attenuation factor of the transmission line and result in power/data loss and noise/crosstalk.

. The characteristic impedance and the attentuation factor depend on the following five parameters:

A. Series inductance L
B. Series resistance R
C. Interconductor capacitance C
D. Interconductor conductance G, which is the reciprocal of the leakage resistance
E. Frequency f

Environmental conditions can vary only two of these parameters:

A. Series resistance
B. Interconductor leakage resistance

In case of a terminal block, these parameters can be defined as:

A. Contact resistance of every connection
B. Insulation resistance between conductors

Ideally, both parameters should be constant in time over the designed lifetime of the product with the contact resistance as low as possible and the insulation resistance as high as possible. If met, these requirements guarantee an electrically stable interconnection under all environmental conditions, which is desirable as well for analog as for digital transmission.

DESIGN CRITERIA

Based on the previously mentioned electrical requirements and other field requirements, following design criteria for an enhanced terminal block were established:

A. Weatherproof/corrosion resistant. This can be quantified by the following electrical requirements: a maximum of 2 milliohms increase in contact resistance of every connection and a minimum of 10^9 ohms insulation resistance between connections and/or ground over the total designed lifetime of the product. Also, no visual corrosion of any current carrying metal is allowed.

B. Resistant to temporary flooding, up to 14 days.

C. Availability of a built-in, environmentally sealed test capability.

D. Quiet front for data transmission (no exposed terminal connection).

E. Possibility of built-in electrical circuit protection.

F. Craft-friendliness which includes no stripping of the terminated wires, multi-gauge wire capacity and re-enterability without affecting the performance.

GEL AS A SEALING MATERIAL

A class of materials which are called GELS can provide total environmental protection when combined with a compatible design. A gel can be described as a highly swollen macromolecule structure. It is different from the solution state because it is cross-linked.

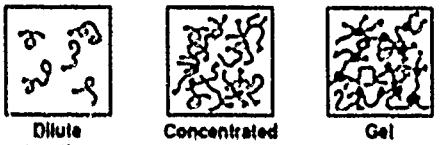

Dilute Solution | Concentrated Solution | Gel

Gels perform the way they do because they exhibit the properties of both a liquid and a solid. In fact, they are a combination of the two. Under compression gels flow and conform to intricate shapes like liquids but their cohesive force is greater than their adhesive strength so they can be handled as solids. Gels have elastic memory and removal of the compressive force will retract the gel. Table 1 compares the properties of a gel with those of a grease and a rubber.

TABLE 1
COMPARATIVE MATERIAL PROPERTIES

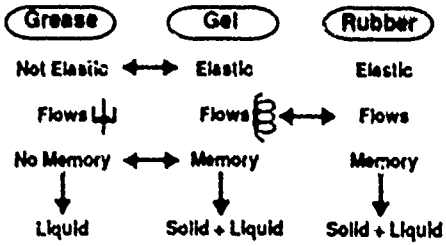

In a terminal block configuration, the gel must be temperature stable and highly elastic to allow repeated re-entry. It must also effectively provide an environmental seal without degrading the electrical contact. Some typical physical properties are listed in Table II.

TABLE 2

Terminal Block - Gel Properties

Tensile strength	Minimum	10^2 MPA
Ultimate elongation	Minimum	700%
Cone penetration	Minimum	240×10^{-1} mm
Hydrolytic stability (7 days, 100 °C)	No reversion	
Volume resistivity	Minimum	10^{12} ohm cm
Slump resistance (16 hrs, 100 °C)	No slump or flow	
Corrosive effect	No corrosion	

TERMINAL BLOCK WITH ROTARY CONNECTION

A novel connection system has been designed and is used in conjunction with gel sealing material to establish electrical contact. A connection, similar to a cap or nut with a contact edge on the bottom, makes electrical contact while cutting through the insulation of the dropwire. The center post is designed with a depth-limiting shoulder so the connection cannot be tightened far enough to damage a lighter (22 to 24 gauge) conductor.

The terminal block, gel and rotary connection function together. As a drop is inserted into the gel filled block the gel envelops and clings to the insulation of the conductor, displacing any moisture on the insulation. As the rotary connection tightens, cutting through the insulation and establishing contact, surplus gel is displaced into the block's internal reservoir. As the connection is backed off, for disconnect or drop removal, the gel is drawn back into the main cavity from the reservoir. As the drop is withdrawn, the self-healing gel refills the main block cavity. At all times when the conductor is within the block, it remains fully insulated from the environment.

Figure 1 shows for the 3 installation steps a single diagram of the concept and a similation of the gel functional behavior.

Figure 2 is doing the same for the breaking of the contact and the removal of the dropwire.

A built-in strain relief to protect the conductors from the effects of vibration and mechanical stress is provided by a gripping action on the insulated conductor. This gripping action occurs between the contact edge and the block cavity wall and is adjacent to the area of electrical contact.

FIGURE 1
TERMINATING A DROPWIRE

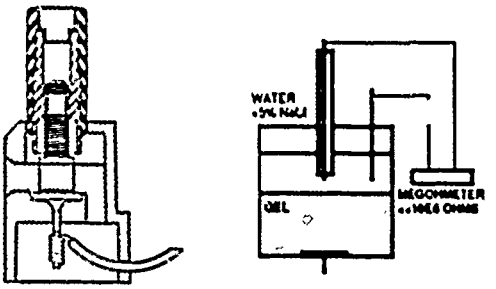

STEP 1:
ROTARY CAP IN FREE FLOAT POSITION
DROPWIRE OUTSIDE THE GEL

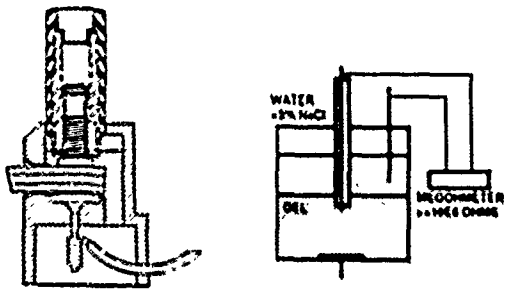

STEP 2:
DROPWIRE INSERTED
WATER DISPLACEMENT - WETTING -
SEALING ACTION OF THE GEL

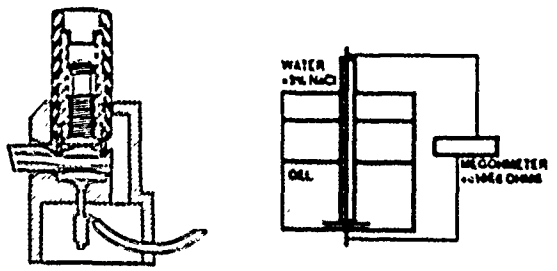

STEP 3:
CONNECTION MADE
ELECTRICAL CONTACT THROUGH THE GEL

FIGURE 2
REMOVING A DROPWIRE

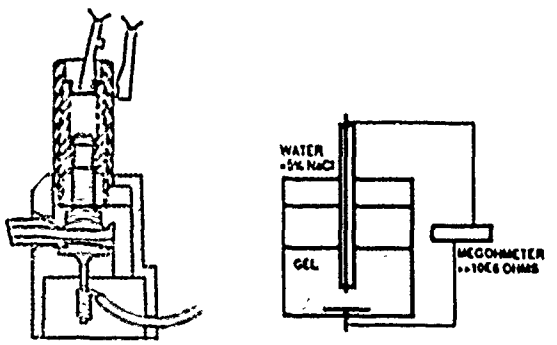

STEP 1:
BREAKING OF THE CONNECTION
AND CO LINE TESTING

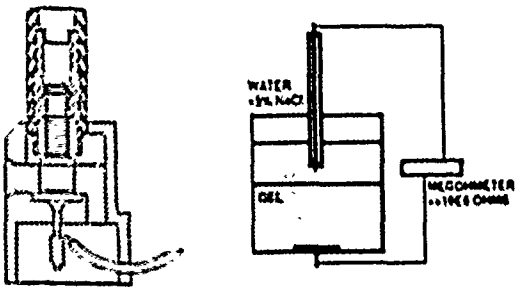

STEP 2:
DROPWIRE REMOVED
SELF-HEALING ACTION OF THE GEL

PERFORMANCE TESTS

Performance tests, designed to accelerate real life environmental conditions, were defined and requirements established.

The electrical and environmental tests to be performed on the installed product can be split up in two categories: The first category of tests deals with the insulation resistance between each pair of tip and ring conductors while in the second category the focus is on the change in contact resistance of every connection. A voltage of 48 Vdc, typical of on hook battery voltage, is supplied across tip and ring conductors during each test.

A. Environmental tests -
Insulation resistance requirements

A minimum of 10^9 ohms insulation resistance between tip and ring conductors is required over the total duration of every test. Insulation resistance measurements shall be made with an applied voltage of 100 Vdc. The 48 Vdc shall be temporarily removed during the measurement process.

1) Water immersion test: The installed terminal blocks shall be submerged in 70° F water/5% salt solution to a depth of two feet for a period of 14 days.

2) Salt fog test: The installed terminal blocks shall be exposed to a salt fog test of 5% salt solution, 95° F in accordance with ASTM B 117 for 30 days.

3) High humidity cycling: The installed terminal block shall be exposed to a temperature cycle from +40 to +140° F at 95% R. H. for 30 days as depicted in Figure 3.

FIGURE 3
HIGH HUMIDITY CYCLING

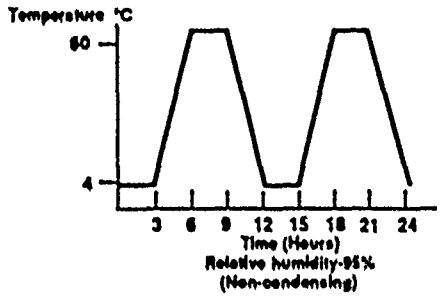

Prior to the tests, all samples are subjected to a conditioning of 50 temperature cycles, as depicted in Figure 4 and 5 re-entries, performed on every dropwire. This sequential test program is outlined in Figure 5.

FIGURE 4
TEMPERATURE CYCLING

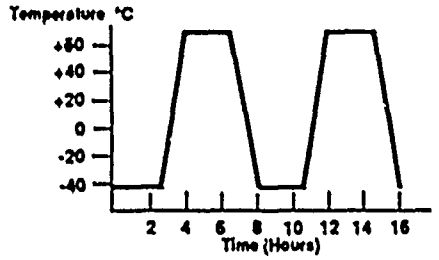

FIGURE 5
SEQUENTIAL TEST PROGRAM

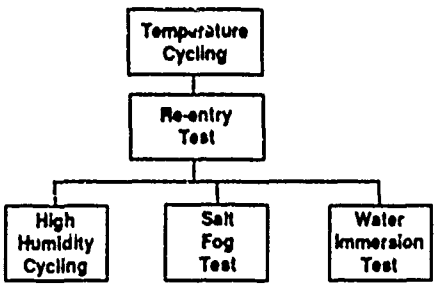

B. Environmental tests - Contact resistance requirements

The contact resistance of every connection shall not change by more than 2 milliohms over the duration of each test. Contact resistance measurements from dropwire to tail wire shall be made using the 4 wire test method per ASTM B539-80.

1) Temperature cycling test: The installed samples shall be placed in an environmental test chamber and subjected to 500 cycles as depicted in Figure 2.

2) High humidity cycling: The installed samples shall be exposed to a temperature cycle from +40 to 140° F at 95% R.H. for 300 cycles as depicted in Figure 1.

3) Heat aging test: The installed samples shall be subjected to 158° F for a period of 90 days.

4) Salt fog test: The installed samples shall be exposed to a salt fog in accordance with ASTM B 117 for 90 days.

5) Thermal shock test: The installed samples shall be subjected to 1000 cycles as depicted in Figure 5.

FIGURE 6
THERMAL SHOCK

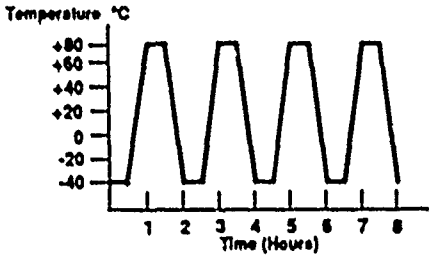

Additional electrical material and mechanical tests complement these environmental tests, but are not the subject of this paper.

CONCLUSION

As well for analog as digital transmission it is desirable to have an electrically "stable" interconnection at the terminal and this under all environmental conditions. Design criteria and performance tests were established for such and environmentally sealed terminal block. A novel rotary connection design which uses a gel as sealing material meets all these requirements and gives total environmental protection.

ACKNOWLEDGEMENT

The authors would like to thank Mrs. Theresa Elliott and Mr. Mark Toomey for the preparation of this manuscript.

REFERENCES

1. ABC TeleTraining, Inc. "ABC of the Telephone Training Workshop"

2. K. Dawes/C. Debbaut/A. Sutherland: "Gels and Their Sealing Application in the Outside Plant", proceedings of the 37th International Wire and Cable Synmposium, P. 5 (1986)

3. B. Schuetz/C. Debbaut: Personal communication

Erwin DeBruycker received his M.S. degrees in Metallurgical Engineering and Safety Engineering from the University of Leuven, Belgium in 1975 and 1978 respectively. He worked at BASF Antwerp and SAVEMI before joining Raychem Corporation in 1979. He started in Raychem's Belgian facilities as Safety Engineer and later on worked as Quality Assurance Engineer and Development Manager for the Telecom Division. Since 1987, he is working as a Development Manager in North Carolina and he is Technical Manager for the DTerminator™ project. He holds several patents in outside plant products.

Jam s A. Pinyan is a Development Engineer at Raychem Co poration's Telecommunications Division in Fuquay-Varina, N. C. He received B.S. and M. S. degrees in mechanical engineering at North Carolina State University and Stanford University respectively. Previously, he has worked for Bell Labs, Indianapolis and Cochlea Corp., San Jose, California. He holds patents in various fields including automated inspection and parts handling, acoustics, and control systems.

Gerald Shimirak is a Development Manager at Raychem Corporation's Telecommunications Division in Menlo Park, California. He spent 7 years in the Royal Canadian Signal Corps as an Associate Engineer dealing in all phases of outside plant communications. He worked for Bell Canada for 12 years in outside plant engineering, construction and maintenance. He joined Raychem in 1979 as a Development Engineer in Menlo Park, CA; he then worked as Regional Sales Manager in Canada and as a Development Manager in North Carolina before relocating to Menlo Park. He holds 7 US patents in outside plant products. In 1988 he was nominated for the Telephony's Ray Blain Outside Plant Achievement Award.

AGEING EFFECTS IN SUBMARINE OPTICAL CABLES

J. N. RUSSELL* P. WORTHINGTON* G. J. CANNELL**

* STC SUBMARINE SYSTEMS, SOUTHAMPTON U.K.
** STC TECHNOLOGY, HARLOW U.K.

1. SUMMARY

Long term loss stability in submarine optical fibre cables is increasing in importance as repeater section lengths are maximised and system margins are squeezed. The move to operation at 1550nm with cabled fibre losses of 0.2dB/km and below mean that even small changes in attenuation in service are unacceptable. STC has extensively studied ageing effects in submarine cable over the last ten years. In addition to long term dry trials, the optical performance of a number of submarine links have been monitored. These include the first link laid in Loch Fyne, Scotland in 1980, UK-Belgium 5 and UK-Channel Islands. Periodic spectral and discrete wavelength attenuation measurements have been made and data will be presented at the conference together with a discussion of loss mechanisms. Experimental work is continuing on long term assessment of material used in cables to assist in the continuous design evolution of cables with low and stable attenuation characteristics.

2. AGEING MECHANISMS

There are several potential mechanisms for loss increase in silica fibres which pose a potential threat to the long-term stability of submarine cables:-

- Hydrogen
- Radiation
- Bending and Temperature effects

2.1 Hydrogen

Hydrogen generation in submarine cables has been known for many years, and was observed during repairs on coaxial cables manufactured from the 1950s onwards. However, the potential problem with fibre was not identified until 1983 (Ref. 1). Since then cables have been designed to minimise contamination of the fibre environment by hydrogen and problems encountered on early systems and trials have been largely overcome.

However, the large effect that even a low level of hydrogen contamination can have on fibre attenuation means that this is still considered to be the most serious potential ageing mechanism for submarine cable systems.

Current STC cable designs incorporate a hermetic barrier to protect the fibres from hydrogen ingress. Alternative designs using hermetic fibre have been assessed but are not yet in use for commercial systems.

2.2 Radiation

Ionising radiation will increase the attenuation of fibres through the creation of defect centres, and while the dose rates at the sea bed are relatively low the combination of long section lengths and 25 year design life requires confirmation that optical power budgets will not be compromised. Potential sources of ionising sea bed radiation have been analysed by Schulte (2) who concluded that in only exceptional locations would the dose rate exceed 1.0 Rad/year.

Data from the UK Ministry of Agriculture, Fisheries and Food (3) gives typical background levels of 13 - 140 mrad/year.

Fibre for current STC submarine cable systems is specified to have a maximum radiation sensitivity of less than 0.01 dB/km at 1550nm at an exposure level of 1.6 Rad/year for 25 years.

Hence at 140 mrad/year exposure, the increase in attenuation will be less than 10^{-3} dB/km in 25 years or about 0.1 dB increase on a 120km cable section.

2.3 Bending and Temperature Effects

Fibre subjected to non-uniform stress, or subjected to thermally induced stresses in the cable can exhibit loss increases. These effects are minimised by protecting

the fibres from external stress by a thick walled metal tube in the cable. This has been a basic feature of the STC cable since the first trial cables were designed in 1979.

The fibre package uses parallel lay fibres in an elastomeric buffer material so that there is no intrinsic bending induced loss.

Qualification tests of the cables have shown no significant loss changes in the temperature range -20°C to + 50°C. In service, deep water cable is subjected to almost constant temperature (typically 2-3°C) so that the stability of the transmission characteristics can be confidently assured.

Bend loss in joints and repeaters is minimised by using a minimum coiling diameter of fibre of 50mm. Fibre parameters are specified so that there is no significant loss at the operating wavelength at this coiled diamter.

3. SYSTEM TESTS

3.1 Loch Fyne

The first experimental optical submarine cable was laid in Loch Fyne, Scotland, in 1980. The 10 km length of armoured cable contained 2 single mode fibres and 4 multimode fibres. There was a 140 Mbit/sec repeater midway in the cable operating on two of the multimode fibres.

The cable design used for this trial is shown in Figure 1a. The single mode fibres were 1.0 mm O/D Sylgard/Nylon packaged fibres. The multimode fibres used Sylgard/ Hytrel.

The fibre package was contained in a thick walled aluminium 'C'-tube with 14 x 2.1 mm HTS wires around this to provide the cable strength. A continuous seam welded copper tube was formed around the steel wires. There was no waterblocking in the fibre package or steel wires in this experimental cable.

Attenuation measurements were made by STC and British Telecom from 1980 onwards. The results of the STC measurements on the single mode fibres from 1980 to 1984 are shown in Figure 2.

By 1982 it had become apparent that the loss of the cable at both 1300nm and 1550nm was increasing, and at this stage frequency of measurement was increased.

The attenuation continued to rise until 1985, when the cable was damaged by an external agency which required a repair operation.

At the same time as the repair, the repeater was removed from the cable. This operation involved cutting the cable at three points, removing the repeater and damaged cable and re-jointing. Gas samples were taken at the cut cable ends and these showed that there was a considerable level of hydrogen of up to 20% by volume in the centre of the cable.

From May 1980 to June 1984 (4.1 years) the average increase in attenuation was:-

1300 nm: 0.012 dB/km/year
1550 nm: 0.033 dB/km/year

The ratio of the loss increase at 1550nm to the loss increase at 1300nm is about 2.8:1.

The increase that would be expected from hydrogen is given by (Ref. 4):-

$$\alpha_{H_2} = 1.4 \times 10^{-2} \; P(H_2) \cdot S_\lambda \exp\left(\frac{1550}{RT}\right) \text{dB/km}$$

Where: S_λ = 1.0 for λ = 1300
= 2.7 for λ = 1550

R = 1.987 cal/mol/°K
T = 283°K (10°C average Loch Fyne temperature)

Hence for 1 atm hydrogen pressure:-

$\alpha_{H_2}(1300)$ = 0.22 dB/km
$\alpha_{H_2}(1550)$ = 0.60 dB/km

In order to account for the observed losses on Loch Fyne a partial pressure of approximately 0.23 atm is required. This is somewhat higher than the maximum values measured by gas samples of the cut cable ends.

However, the samples may not be representative of the highest levels of hydrogen along the cable length. The close correlation of the measured and theoretical values of the ratio of loss increase at 1300 and 1550 suggest that all or nearly all of the loss increase on Loch Fyne was caused by hydrogen.

Since 1985, when the cable was repaired, the attenuation has continued to increase at a similar rate to before.

3.2 UK-Belgium No. 5

UK-Belgium, which was installed in 1986, was the first inter-continental commercial optical system to go into service. It is a 115 km armoured cable system with three fibre pairs and three 140 Mbit/sec repeaters operating at 1310 nm.

Since 1983 when the effect of hydrogen on fibre was first reported (Ref. 1) and subsequently proven to be the cause of the attenuation increase observed on Loch Fyne, modifications were made to the STC submarine cable design in order to protect fibres from contamination by hydrogen.

The basic cable design used for UK-Belgium incorporating these modifications is shown in Figure 1b.

The fibre package (using Sylgard/Nylon coated fibre) is contained within a welded hermetic copper tube which forms a barrier to prevent ingress of hydrogen. There is no mixture of metals in contact inside the hydrogen barrier and the spaces within the fibre package and inside the copper tube are filled with a high viscosity waterblocking compound. This compound greatly reduces the quantity of moisture that is enclosed in the cable structure during manufacture and provides an axial block to prevent penetration of water if the cable is cut on the sea bed.

At each end of the UK-Belgium system there is an additional pair of fibres which are looped back at submerged joint housings (see Fig. 3). These provide two long fibre paths (18 km at Broadstairs, 30 km at Ostende) for attenuation monitoring of the submerged cable. Fibre test tails spliced at the terminal stations increase the overall loop lengths to 20km and 32km.

Measurements have been made by both STC and British Telecom at approximately 6 monthly intervals since installation.

The STC results at 1310 and 1550 nm are summarised in Fig. 4 and Fig. 5.

(Note that the average attenuation level is high on these monitored fibres because of the many joints in the land part of the route. The attenuation of the main sea cable is less than 0.4 dB/km at 1310 nm.)

Initial results in the first two years suggested that there was significant increase in attenuation at both wavelengths. However, the most recent results show a reversal of this trend.

The highest apparent increase was on the Broadstairs loop at 1550 nm. However, the initial measurements on this loop, which has an attenuation at 1550 nm of over 18 dB, was done with spectral attenuation equipment of limited dynamic range. The effect of noise in the detector of a cut-back measurement is to give apparent attenuation results which are generally lower than the true fugure. From 1987, using improved equipment, the results are considered to be much more reliable.

From these results the average increase in attenuation in the 3.1 years from June 1986 to July 1989 has been:-

1300 nm - approx. equal to 0.003 dB/km/year

1550 nm - approx. equal to 0.006 dB/km/year

For a total loss increase in 3.1 years of 0.018 dB/km at 1550 a hydrogen partial pressure of about 0.03 atmospheres is required.

Long term outgassing tests on the optical package used in UK-Belgium have been in progress since 1986 (see Section 4.2).

These show that outgassing of about 20 - 30 cc/km may be expected over a three year period, which will produce partial pressure in the fibre environment of about 0.02 - 0,03 atmospheres.

Hence the observed loss increase on UK-Belgium is similar to that predicted by measurements of hydrogen outgassing from the fibre package.

3.3 Sea Trials Cable

In February 1986 STC manufactured the first lengths of NL lightweight cable using a newly developed acrylic fibre package. The fibres were embedded in an elastomeric buffer material (Hytrel) around a central copper plated kingwire (Fig. 1c).

All the materials used in this new design were selected for low hydrogen evolution characteristics.

Up to 12 fibres can be accommodated in the package which has an overall diameter of 3.1 mm. This package is then enclosed in the same composite copper tube with polybutene waterblocking as used in the earlier UK-Belgium cable design (Fig. 1b).

Two 12 km lengths of cable were manufactured which were used for deep water sea trials in 1986 and 1987. The cable was subsequently returned to the Southampton factory where it is used for long term monitoring of stability of the fibre attenuation.

Measurements made 2.5 years after cable manufacture have shown no change in attenuation.

Fig. 6 shows a recent spectral measurement (Nov. 988) made on a 22.6 km loop of fibre.

If any increase in attenuation had occurred due to hydrogen then this would be most apparent at a wavelength of about 1240 nm, where the attenuation increase due to interstitial hydrogen is about 9 dB/km at 1 atm hydrogen pressure.

However, there is also an attenuation peak due to water at the same wavelength region which is typically about 5% of the height of the primary peak at 1380 nm.

From Fig. 6 the peak at 1380 nm is approximately 0.56 dB/km so that the expected peak due to water at 1240 nm is about 0.028 dB/km.

The measured peak at 1240 nm is approximately 0.024 dB/km which, therefore, is all attributable to water. Hence there is no detectable loss increase at 1240 nm caused by hydrogen after 2.5 years from manufacture.

3.4 UK-Channel Islands No. 7

UK-Channel Islands is a 130 km 12 fibre unrepeatered cable which was installed in late 1988. Following completion of splicing and commissioning by British Telecom a base line set of attenuation measurements on two fibres looped back was carried out by STC in July 1989.

This measurement is on 260 km of fibre (60 dB approximately at 1550 nm) and will provide a test facility with very high resolution of any attenuation change (resolution of about 5×10^{-4} dB/km). It is proposed to monitor this system at approximately 6 monthly intervals.

4. MATERIALS AND SAMPLE TESTING

Since 1985 the STC NL submarine cable has incorporated a hermetic copper tube around the central fibre package. Long term tests have been carried out to demonstrate the effectiveness of this tube as a barrier to hydrogen, and to assess the materials within the tube to ensure negligible outgassing of hydrogen in the fibre environment.

4.1 Hydrogen Permeation through Copper Tube

The hermetic copper tube in the NL cable consists of a continuously seam welded tube of 0.4 mm thickness.

Using published figures for hydrogen permeation through copper (Ref. 5) the estimated permeation rate is only about 1.2 cc/year at an external pressure of hydrogen of 10 MPa (1500 psi).

(10 MPa represents the worst case pressure that could be generated at hydrostatic pressure in armoured cable at a depth of 1 km. For unarmoured cable in deeper water there is no exposed metal in contact with sea water to generate hydrogen by electrochemical action.)

In order to ensure that the welded tube in cable could meet this theoretical figure a series of tests were set up to measure the permeation rate through 2 metre lengths of copper tube removed from cable.

The results are shown in Fig. 7. This shows the measured ingress of hydrogen (cc/km at STP) for an applied external pressure of hydrogen of 10 MPa.

After 2.5 years the measured permeation rate is less than 0.5 cc/km/year, or less than 20% of the theoretical figure.

Extrapolated to 25 years, an external pressure of 10 MPa would produce a partial pressure in the fibre environment of less than 5×10^{-3} atm (less than 0.003 dB/km at 1550 nm).

4.2 Outgassing Tests

Several types of test have been used in order to investigate and quantify hydrogen outgassing of the fibre package inside the hermetic copper tube:-

- Accelerated tests on the individual components at elevated temperatures.
- Accelerated tests on representative samples of package in cable.
- Long term, ambient temperature tests on representative samples of package in cable.

Accelerated tests are useful in quickly identifying potential problems and in assessing new materials. However, for prediction of performance of cable in service the long term tests at ambient temperature provide the most reliable data.

Fig. 8 shows the results of these long term tests on both the UK-Belgium package (Nylon/Sylgard) and the more recent Acrylic/Hytrel fibre package. In each case the tests were carried out on samples of copper tube recovered from cable containing the fibre package and waterblocking compound..

The tests have shown that there is a small but significant amount of outgassing from the Nylon/Sylgard package (20 - 30 cc/km after 3 years).

(This is consistent with the small amount of attenuation increase that has been observed on the UK-Belgium system, see Section 3.2).

The current Acrylic Fibre/Hytrel Package with polybutene waterblocking has shown little or no outgassing (approx. 1 cc/km in 3 years). This again is consistent with measurements on cables using this package, which have shown no detectable attenuation increase due to hydrogen (see Section 3.3).

5.0 CONCLUSIONS

The ageing behaviour of several optical submarine cables systems have been studied, and these studies will continue on more recent systems operating over long fibre spans.

The principal ageing mechanisms observed to date have been attributable largely or wholly to hydrogen. No other significant cause of attenuation increase from radiation or temperature induced bending effects have been identified.

The UK-Belgium cable, which uses a Sylgard/Nylon fibre package, has shown a small increase in attenuation in the three years since installation. The most recent measurements indicate that the loss is no longer increasing and the transmission characteristics are now stable.

The current NL cable design using an acrylic fibre package and a hermetically sealed hydrogen barrier has shown no detectable ageing over a period of three years.

Materials tests have confirmed that there is no significant level of hydrogen outgassing for this cable design.

ACKNOWLEDGEMENTS

The authors would like to thank the directors of STC and British Telecom International for permission to publish the information in this paper.

REFERENCES

1. Mochizuki, K., Namihira, Y., Yamamoto, H.,

   "Transmission Loss Increase in Optical Fibres due to Hydrogen Permeation".

   Electronics Letters, 1983, 19, pp 743-745.

2. Shulte, H.J.,

   "Radiation Effects on Undersea Lightguide Cables".

   Technical Digest, Conference on Optical Fibre Communication, San Diego, Feb. 1985.

3. Woodhead, D.S. (UK Ministry of Agriculture, Fisheries and Food),

   Report to STC, July 1985.

4. Barnes, S.R., Pitt, N.J. Hornung, S.,

   "A model for predicting hydrogen degradation in optical cables".

   IOOC - ECOC 1985, pp 897 - 899

5. Perkins, W.E., Begeal, D.R.,

   "Permeation and Diffusion of Hydrogen in Ceramuar, Copper and Ceramuar-Copper Laminates".

   Sandia Labs, Albuquerque, New Mexico, 1972.

BIOGRAPHIES

John N. Russell was born in 1954 in Birmingham, England. He graduated in applied physics from University College, London, in 1975. In the same year he joined STC Transmission Products Division at Basildon. Later he moved to the new optical fibre unit which was being set up at Harlow, where he worked on measurements, installation and cable design for land line systems. In 1982 Mr. Russell moved to the STC Submarine Systems in Southampton where he is working on the design of submarine cable as head of the cable design section.

Peter Worthington is a development engineer with STC Submarine Systems which he joined in 1974.

He received a BSc. in Electronics and Electrical Engineering from the University of Birmingham in 1971. Since 1977 he has been involved in the development of optical cables for submarine systems.

George Cannell joined STC Technology Ltd. in 1973.

He has been responsible for the evaluation programmes of a number of large optical fibre and fibre cable contracts including long haul, land and submarire, and military applications from conception to acceptance testing in the field. In this time he has helped to develop a number of measurement techniques which have now been adopted as reference test methods.

More recent work has included research and development into wavelength selective distributed fibre sensors and non-intrusive optical fibre networks. He is currently working on wavelength demultiplexers and integrated optics. He has been the author of twenty papers.

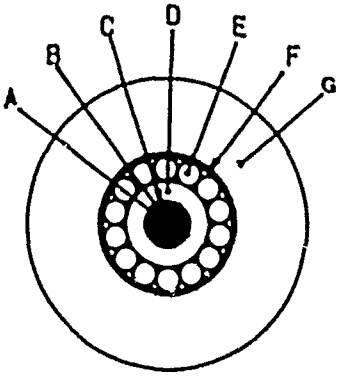

1a. LOCH FYNE

A - NYLON COATED KINGWIRE
B - SYLGARD/NYLON FIBRES
C - MYLAR TAPE
D - ALUMINIUM C-TUBE
E - UNILAY STEEL STRENGTH MEMBER
F - COPPER TUBE
G - POLYETHYLENE

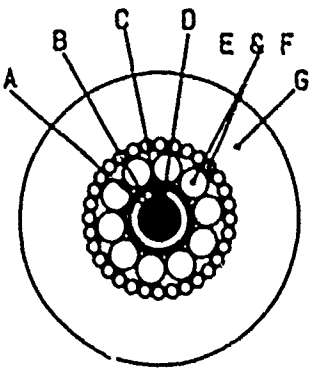

1b. UK-BELGIUM

A - NYLON COATED KINGWIRE
B - SYLGARD/NYLON FIBRES
C - KEVLAR WHIPPING
D - COMPOSITE COPPER TUBE
E - } TWO LAYER, TORSIONALLY BALANCED
F - } STRENGTH MEMBER
G - POLYETHYLENE

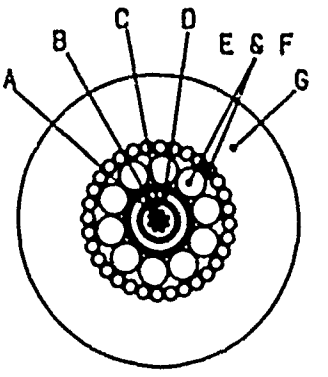

1c. CURRENT NL

A - HYTREL COATED KINGWIRE
B - ACRYLIC COATED FIBRES
C - HYTREL BUFFER ELASTOMER
D - COMPOSITE COPPER TUBE
E - } TWO LAYER, TORSIONALLY BALANCED
F - } STRENGTH MEMBER
G - POLYETHYLENE

FIG.1 EVOLUTION OF NL CABLE

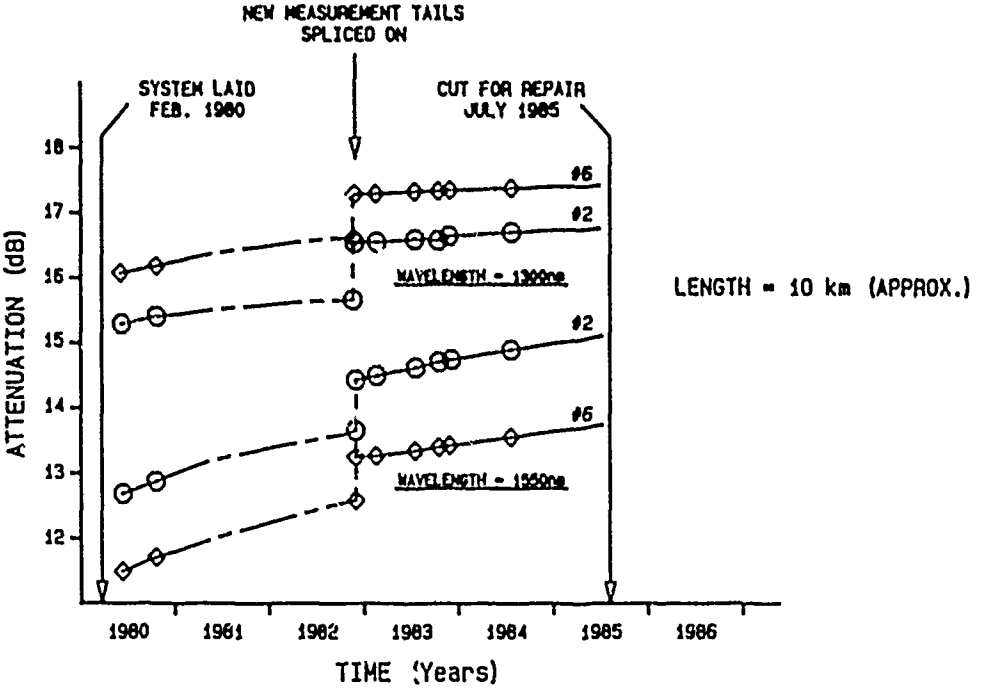

FIG.2 ATTENUATION OF LOCH FYNE SINGLE MODE FIBRES

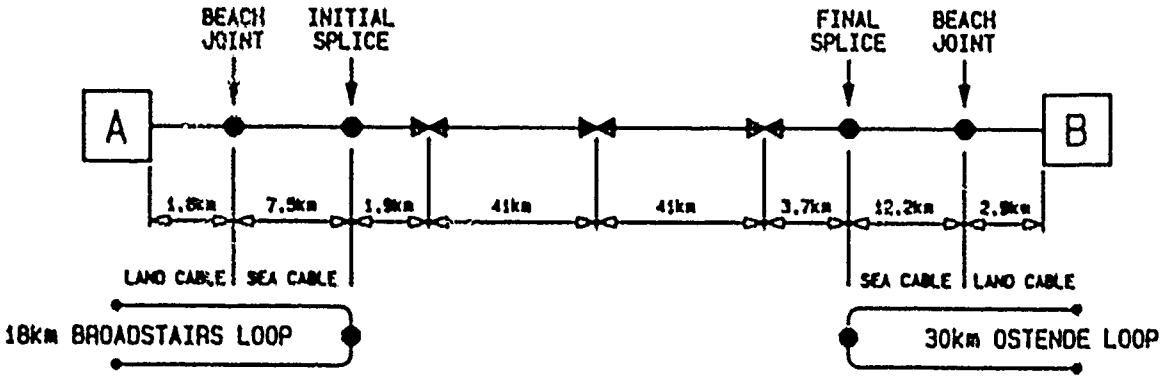

FIG.3 U.K. - BELGIUM MONITOR LOOPS

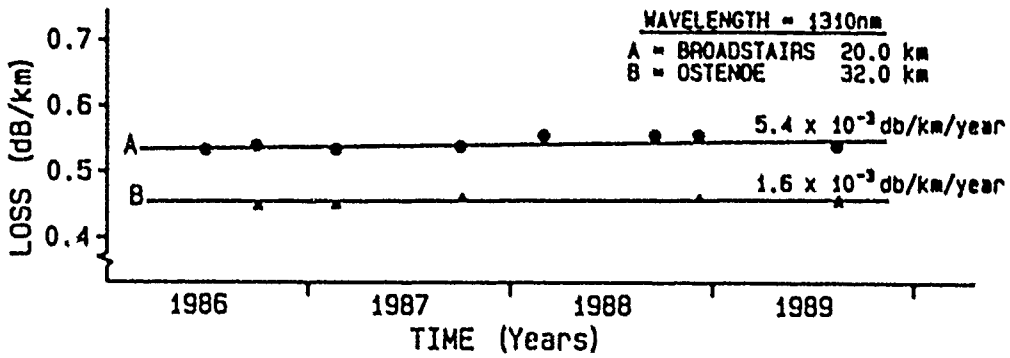

FIG.4 U.K. - BELGIUM MONITOR FIBRES AT 1310nm

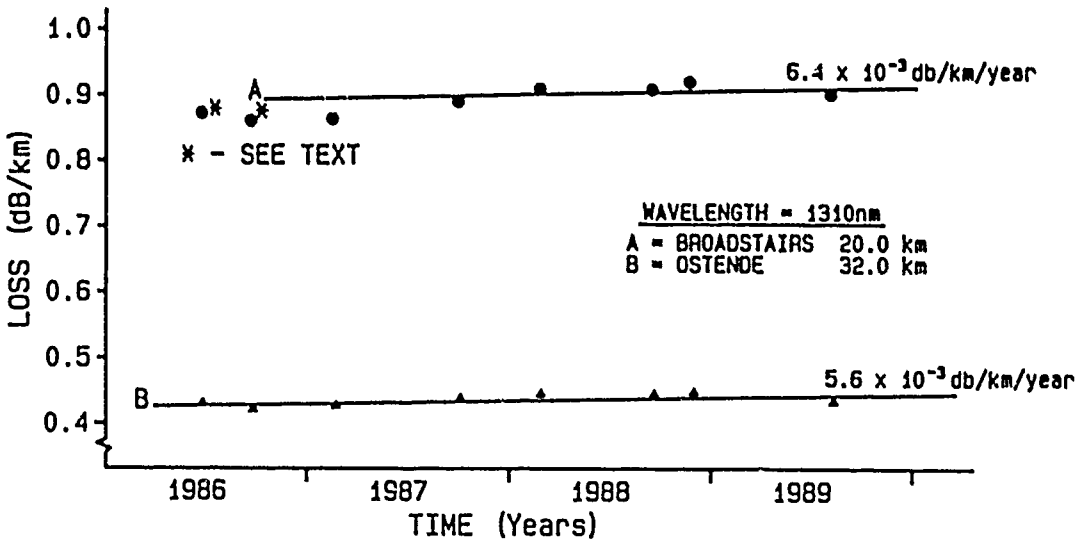

FIG.5 U.K. - BELGIUM MONITOR FIBRES AT 1550nm

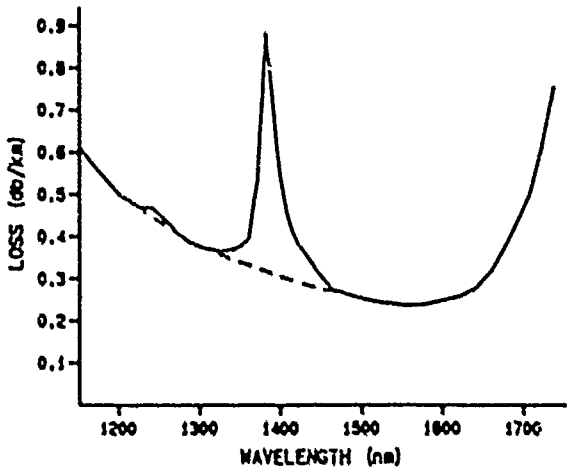

FIG.6 SPECTRAL ATTENUATION OF 22.6km LOOP OF SEA TRIALS CABLE

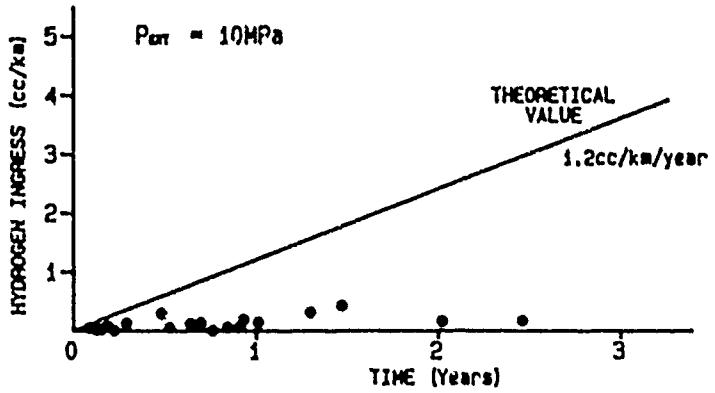

FIG.7 HYDROGEN PERMEATION THROUGH COPPER TUBE

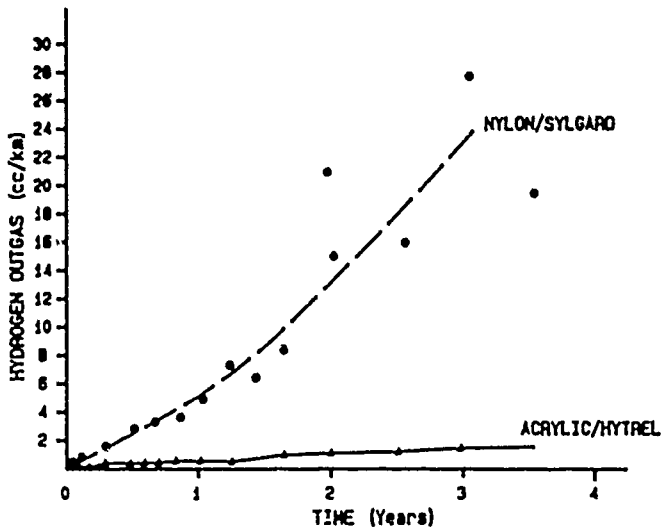

FIG.8 HYDROGEN OUTGASSING OF OPTICAL FIBRE PACKAGES

ON THE CHOICE OF SINGLE-MODE FIBERS IN LOOSE TUBE CABLES WITH RESPECT TO BENDING PERFORMANCE

S.Stueflotten L.Bjerkan E.Nesset S.Hopland*

EB Cables, Asker, Norway
* Norwegian Telecommunication Administration, Oslo, Norway

ABSTRACT

An experimental investigation of the bending resistance of single-mode fibers in loose tube cables has been carried out. Fibers with different mode field diameters and cut-off wavelengths were chosen from current matched clad and depressed clad designs. Samples of dispersion shifted and dispersion flattened fibers were also included. Various micro- and macrobending tests were carried out on primary coated fibers as a reference for the cable tests. Three loose tube cables were specially designed to emphasize bending losses in temperature cycling and tensile tests. Except for weak macrobendings at low temperature all tests gave the same ranking of fiber bending sensitivity. High MFD and low cut-off wavelength proved to be the most sensitive combination, while the opposite case always revealed the best performance. For depressed clad fibers weak macrobendings revealed a poorer performance than indicated by the other experiments.

INTRODUCTION

In the design of optical fiber cables it is very important to prevent excess losses originating from various bending phenomena when cables are subjected to environmental stresses in service. At 1.3 μm wavelength bending losses are normally negligible, but at 1.55 μm bending loss sensitivity of single-mode (SM) fibers may become a critical factor in cable design.

Macrobends, which are bending phenomena on a macroscopic scale, (i.e. centimeter scale), are usually understood as pure bends with constant curvature, and the associated losses are conveniently measured by various fiber winding arrangements.[1-3] In loose tube cables subjected to low temperatures, buckling of the fibers within the tubes may occur as a result of cable contraction. This phenomenon is also macroscopic in nature and may be defined as random macrobends, and it has not been extensively studied so far. Microbends occur when the fiber is pressed against a surface with microscopic irregularities of a random nature. Microbending losses may occur when cables are subjected to high tensions or temperatures. Microbending sensitivity of SM fibers is measured on relatively short lengths of fiber by tests such as the sandpaper test[3,4] and other lateral pressure tests.[5,6,7] Winding of longer lengths of fibers under tension in a split tube arrangement has also been published recently.[8] However, few experiments have been carried out to study bending loss mechanisms using actual cable materials and complete cables. Therefore a comprehensive experimental program which evaluates the performance of various commercially available SM fiber types in a loose tube cable structure is described in this paper. Based on the results of these experiments the performance of different SM fiber types are compared with respect to bending induced losses at 1.55 μm in loose tube cables.

BENDING LOSS THEORY

For SM fiber systems operating at 1.3 μm either the match clad (MC) or depressed clad (DC) designs are usually employed. At 1.55 μm additional fiber types such as the dispersion shifted (DS) and the dispersion flattened (DF) fibers have been introduced.[9] The two most important parameters which determine the bending loss properties of SM fibers are the mode field diameter (MFD) and cut-off wavelength (λ_c). The theoretical pure bending losses α of an ideal step-index fiber can be written in the form[1,2,10]:

$$\alpha = (A/\sqrt{R})\cdot\exp(-BR) \qquad (1)$$

where R is fiber bending radius, and A and B are functions of wavelength and fiber refractive index profile. By introducing the mode field diameter $w_- = 2a/W$, where a is the core radius and W is the usual wavenumber parameter ($W^2 = a^2(\beta^2 - k_2^2)$), α in Eq.(1) can be expressed as follows[11]:

$$\alpha = f(\lambda)\frac{w_-^{3/2}}{\sqrt{R}}\exp\left[-\frac{4\lambda^2 R}{3\pi^2 n^2 w_-^3}\right] \qquad (2)$$

The general formula expressing microbending losses is[12]:

$$\alpha = \frac{1}{4}(kn_1 w_0)^2 \phi(\Omega) \qquad (3)$$

where w_0 is the near field MFD and $\phi(\Omega)$ is the power spectrum of the fiber deformation giving rise to the microbending losses. The power spectrum is normally assumed to follow a simple inverse power relationship $\phi(\Omega)=K\Omega^{-3p}$. The spatial frequency Ω is in general given by:

$$\Omega = 1/kn_1 w(p)^2 \qquad (4)$$

where $w(p)$ is a MFD characterized by the microbending mechanism.

The measured MFD is usually the far field or Petermann II definition[13], which in general is different from the definitions appearing in Eqs.(2)-(4). However, for a step-index profile fiber the differences are relatively small and proper fitting parameters can easily be found. For more sophisticated profiles like that of DS and DF fibers this is more difficult because the differences may become considerable.[14]

EXPERIMENTS

Fiber characteristics

Different types of commercially available fibers were selected for the experiments. Fig.1 shows the refractive index profiles of the four classes investigated. For the MC and DC classes, fibers were chosen from regular production with parameter combinations (MFD and λ_c) as close as possible to the manufacturers specification limits. The DS and DF classes are only represented by single fibers selected at random. The MC fibers are divided into two subclasses, MC1 pertaining to standard fibers designed for 1.3 μm operation and MC2 which is a more bending resistant design having tighter MFD and higher λ_c specifications than the MC1 fibers. All fibers were supplied with a 250 μm diameter acrylate primary coating, which brand may be sligthly different for fibers from different suppliers.

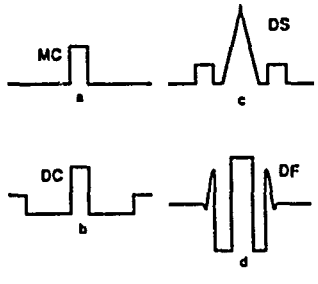

Fig.1: Refractive index profiles of: a) matched clad (MC), b) depressed clad (DC), c) dispersion shifted (DS),and d) dispersion flattened (DF) fibers.

Fiber class	MFD range [μm] (1.3 μm)	Cut-off wavelength [nm]
MC1	9.82-10.52	1153-1260
MC2	9.13-9.80	1219-1320
DC	8.20-9.20	1205-1275
DS	8.54 (1.55μm)	1254
DF	6.0±0.6 (1.31μm) 7.0±0.7 (1.55μm)	948

Table I: Summary of parameter variations for fibers used in this study.

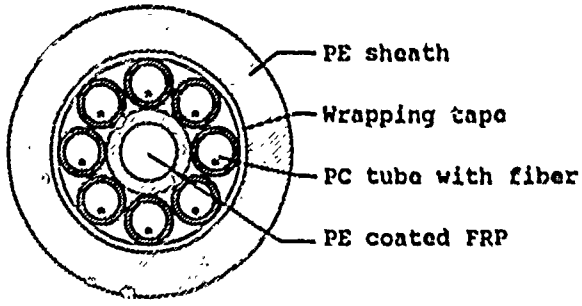

Fig.2: Cross section of loose tube cable.

Cable construction

The cables tested in this study are of the well-known loose tube construction shown in Fig.2. Each jelly-filled plastic tube can contain from 1 to 6 fibers. The tubes are helically stranded around a FRP central strength member. This ensures that the fibers are free from stresses as long as the cable is strained within certain limits by exposure to external forces. This stress-free buffer region can be tailored to given specifications by the correct choice of tube dimensions (d_0/d_1), stranding pitch (S), and tube helix radius (R) as follows:

$$-\varepsilon_r \approx -(2\pi/S)^2(R-r/2)r < \varepsilon_x < (2\pi/S)^2(R+r/2)r \approx \varepsilon_y \qquad (5)$$

where ε_r is the relative length difference between the fiber path following the center line and the inner path of the tube, ε_y the corresponding relative length difference with respect to the outer path, and $r = (d_1-d_f)/2$ the fiber clearance inside the tube.

Micro- and macrobending excess loss phenomena can be eliminated by proper choice of the above mentioned parameters when the fiber excess length ε_x, and hence the cable strain, is kept within the limits given by Eq.(5). ε_x is expressed by the cable tensile and thermal strains as follows:

$$c_M = c_o - F/EA + (\alpha_M - \alpha_f)(T_o - T) \qquad (6)$$

where c_o is the fiber excess length with respect to the tube center line at room temperature T_o, F/EA is the cable strain caused by an external tensile force F acting on the cable, α_M and α_f are the linear thermal expansion coefficients of the cable and fiber respectively. $EA = \Sigma E_i A_i$ is the effective elastic stiffness of the cable, and $\alpha_M = \Sigma \alpha_i E_i A_i / \Sigma E_i A_i$ the effective thermal expansion coefficient of the cable. The summations are taken over all elements of the cable structure.

Experimental results

Fiber experiments. The micro- and macrobending sensitivity of optical fibers are normally characterized by well-defined laboratory tests on short sample lengths of the fibers. The question we wanted to ask was if such tests fully reveal the bending loss behaviour of fibers in real optical cable structures. To serve as reference for the cable experiments we carried out the following tests on primary coated fibers: sandpaper test[5] and split tube winding test[6] to study microbending losses, and mandrel winding tests to study pure macrobending effects.

For the sandpaper tests we used 150 grit sandpaper and lateral loads from 1.4 to 5.6 g/mm. The fiber length under pressure was 1.6m and the microbending loss was recorded as a function of wavelength. The results obtained are in good agreement with those reported elsewhere for comparable experiments.[5,7] Attempts which were made to fit the measured data to the theoretical formulas of Eqs.(3) and (4) gave p = 1.7-2.1. The DS fiber was the least sensitive and MC1 the most sensitive type tested (about 3 times that of MC2 fibers and >10 times that of the DS fiber).

The split tube winding test[6] was developed to simulate a real microbending mechanism as experienced by fibers pressed against the inside wall of loose plastic tubes in cables under high tension. A standard loose tube is split in two along its entire length and wound in one layer onto a 340 mm diameter drum. A fiber is then wound with controlled tension into the jelly-filled groove formed by the split tube. Total length of fiber on such a drum was 140 m, and the maximum tension used was 2 N which corresponds to a lateral pressure of fiber against tube wall of 1.2 g/mm. Some typical spectral plots of measured induced loss are shown in Figs. 3 and 4. The attenuation increased almost linearly with the fiber tension. High MFD/low λ_c was the most sensitive and low MFD/high λ_c the least sensitive combination for both the MC and DC fiber classes. The microbending loss did, however, depend more strongly on the MFD than on the cut-off wavelength.

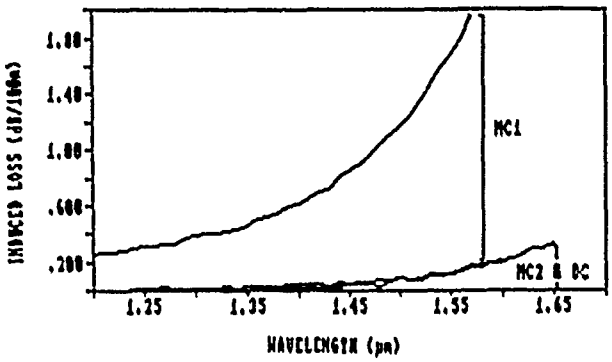

Fig.3: Induced losses (max and range) of MC1, MC2, and DC fibers measured by the split tube winding method with 0.22% fiber strain.

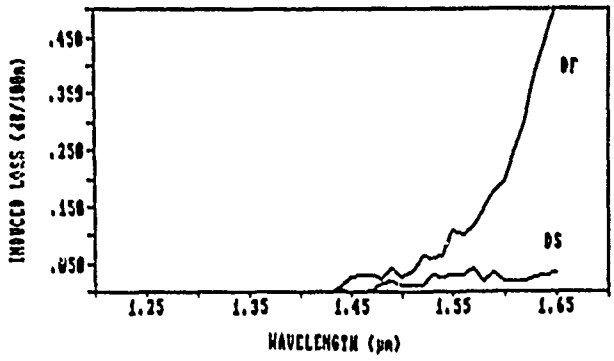

Fig.4: Induced losses of DF and DS fibers measured by the split tube winding method with 0.22% fiber strain.

Attempts which were made to fit the results to the microbending loss formulas Eqs.(3) and (4) assuming an Ω^{-2p} dependence for the power spectrum, yielded values of p in the range p = 3-5. This is higher than for the sandpaper tests, indicating different microbending power spectra for the two cases. As an example, a MC1 fiber with MFD/λ_c of 10.5 μm/1153 nm gave p = 1.9 in the sandpaper test and p = 3.7 in the split tube winding test. In spite of this difference the split tube winding experiments rank the microbending sensitivity of different fibers similar to the sandpaper test.

Two types of tube materials were investigated, polycarbonate (PC) and PBT. The PBT tubes gave slightly lower induced losses than the PC tubes. A microstructure analysis of the inside wall of the tubes revealed a smoother and finer structure of the PBT tube than the PC tube[6], and therefore less microbending can be expected for the same winding tension. The results do

also indicate that differences in the tube filling compounds may have some effect on the measured loss increase.

Finally, some simple macrobending loss measurements were made by winding fibers with zero tension five turns around smooth cylinders of varying diameters from 18 to 70 mm. The pure bending loss measured were in accordance with previously published results from pure bending experiments[1,2] as regards wavelength and bending diameter dependence. The macrobending loss sensitivity showed the same dependence on the MFD/ λ_c combinations as the microbending tests above. Among the different fiber classes, the DS fiber was found to be the least sensitive, while the MC2 and DC fibers showed comparable behaviour down to the loss limit of 10^{-2} dB/m. The MC1 and DF fibers were the two most sensitive classes.

Cable experiments. The fibers were also cabled in three different test cables specially designed to emphasize on bending loss effects in temperature cycling and tensile strength experiments.

In loose tube cables the fibers will not be strained before a certain cable tension has been reached (strain buffer effect). For the experimental cables this strain buffer was 0.1-0.3%. Above this value the microbending attenuation increased fairly linearly with fiber strain. Table II gives a summary of the excess attenuation from the cable tension tests measured at both 1.3 µm and 1.55 µm. Mean values refer to fibers with MFD and λ_c close to the mean values of Tab.I. Max values refer to fibers with extreme combinations of high MFD and low λ_c that for MC fibers apply to less than 1% of the total fiber production.

Fiber class	Microbend loss [dB/km]/% strain			
	1.3 µm		1.55 µm	
	mean	max	mean	max
DS	0.00	-	0.00	-
DC	<0.10	<0.20	<0.20	0.55
MC2	<0.20	0.35	0.40	1.00
DF	0.25	-	0.65	-
MC1	0.45	1.70	1.55	7.40

Table II: Summary of measured microbending loss per % fiber strain.

The cable tension experiments yielded microbending sensitivities with a qualitative ranking of the fibers similar to the sandpaper and split tube winding tests, with MC1 being the most sensitive and DS the least sensitive fiber. In the cable tension experiments DC fibers came out slightly better than MC2 fibers.

The cable length under tension was 145 m and the maximum applied fiber strain 0.5%. Accurate attenuation values at 1.3 µm were therefore difficult to achieve except for MC1 fibers. However, the ratio of 1.55 µm to 1.3 µm microbending loss was found to be around 3, compared to a ratio of about 2 for the sandpaper test and 5 for the split tube winding test.

At low temperatures the cable will contract relative to the fiber causing the fiber to move towards the outer path of the stranded tube. Below a certain threshold temperature the fiber will press against the tube wall and start to buckle. The associated bending losses are mainly of macroscopic nature (random macrobends). Different cable structures may have quite different thermal properties due to different tube dimensions, stranding pitch, effective thermal expansion coefficient etc. It is therefore difficult to compare and evaluate bending losses of non-identical cables as a function of temperature. To obtain a more universal behaviour we have converted the results to loss increase versus excess length, ε_M, according to Eq.(6) with F = 0. In this way both the cable tension and low temperature results can be shown in the same excess length diagram. Some typical results are shown in Figs.5-7. Fig.5 shows the results for a MC1 bending sensitive fiber at both 1.3 µm and 1.55 µm. Under tension the loss increases linearly with the strain while at low temperatures a much sharper and unlinear loss increase is observed. The reason for this is the different bending mechanisms in the two cases.

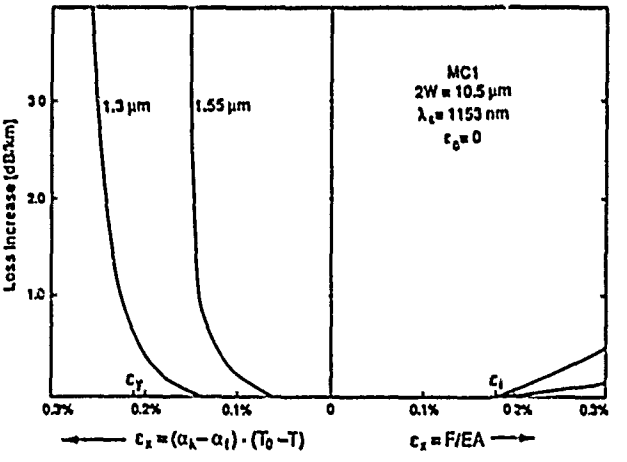

Fig.5: Measured bending losses in a cable at tension (right) and low temperatures (left) for a MC1 fiber at 1.3 and 1.55 µm. ε_M = 0.2% (left) corresponds to T = -32°C for this cable.

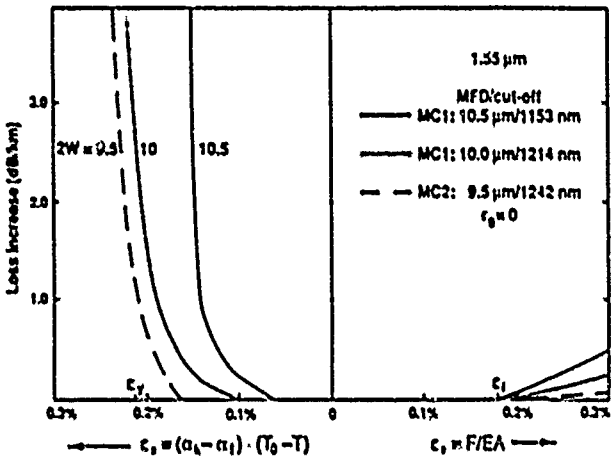

Fig.6: Measured bending losses at 1.55 µm in a cable at tension (right) and low temperatures (left) for MC fibers with different MFD/λ_{cc}.

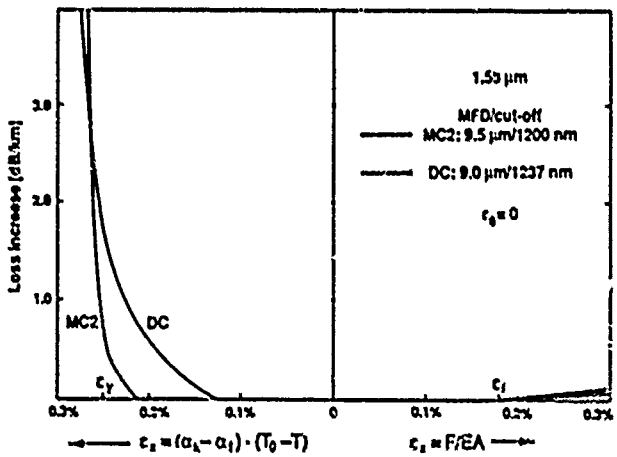

Fig.7: Measured bending losses at 1.55 µm in a cable at tension (right) and low temperatures (left) comparing MC2 and DC fibers.

In Fig.6 MC1 and MC2 fibers are compared at 1.55 µm, and Fig.7 shows the difference between typical MC2 and DC fibers. Here one should note the rather unexpected difference occuring at weak macrobends. For some time now it has been argued strongly in favour of the DC fiber design because of its good bending resistance as demonstrated by pure bending experiments. This is true for strong bending effects, i.e. small bending diameters. In a cable, however, one can not allow such strong bendings. Typically the maximum allowable loss increase at the minimum specified temperature will be 0.1 dB/km. Hence, it is macrobending losses at this level that should be considered when comparing different types of fibers. Our experiments show that from a low temperature boundary point of view DC fibers perform more like MC1 than MC2 fibers. Apart from this divergence the low temperature experiments ranked the fibers similarly to the other tests with DS fiber on top as the most bending resistant of all fibers investigated. The DF fiber turned out to be very bending sensitive at 1.55 µm, but performed excellently at 1.3 µm.

Fig.8 shows an example of spectral attenuation measurements for a bending sensitive MC1 fiber at different temperatures. A theoretical fit to Eq.(1) is shown for the curve at -40°C. The fit appears reasonable and therefore the observed loss indicates a macrobending behaviour. Fits to Eq.(3) yielded unrealistically high p-values which supports the above conclusion.

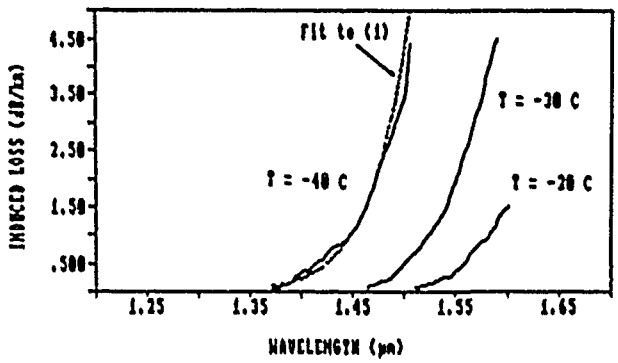

Fig.8: Induced loss vs. wavelength for a MC1 fiber with MFD/λ_{cc} = 10.50 µm/ 1153 nm measured in a test cable at low temperatures (weak macrobending) The broken line shows a fit to the macrobending formula Eq.(1).

CONCLUSIONS

The experiments carried out in this study have provided valuable information on the response of various types of SM fibers to bending phenomena occurring in loose tube cable structures. The tests have also confirmed that microbending losses are dominant in cables at high tension and macrobendings at low temperature.

The bending loss properties of SM fibers in loose tube cables under tension can be qualitatively assessed by microbending tests like the sandpaper and split tube winding test directly on the primary coated fiber. Although they do not reveal the actual situation in a cable, they give a correct qualitative ranking of the fiber bending sensitivity in mutual comparative studies. The random macrobending mechanism which occurs as a result of fiber buckling at low temperatures has on the other hand proved more difficult to assess through such simple tests as e.g. the mandrel

winding test. If such attempts should be made one should concentrate on the weak macrobending effects, i.e. in the order of 0.1 dB/km, when comparing different types of fibers.

Another important result obtained from the experiments is the strong influence that weak macrobending properties have on the low temperature boundary of a cable. Onset of bending losses in the order of 0.1 dB/km may differ as much as 0.1% in fiber excess length between the various fiber types. On the temperature scale this can correspond to 20-50°C depending on the cable structure. This issue is specially important at 1.55 μm where the bending sensitivity of fibers may become the limiting factor in cable design.

The bending sensitivity of SM fibers depends on both the MFD and cut-off wavelength with high MFD/low λ_c as the most and low MFD/high λ_c as the least sensitive combination. This is common to both MC and DC fibers. Microbending losses depend strongly on the MFD and less on λ_c. For macrobendings the dependence on λ_c seems to be somewhat stronger although MFD-dependence still dominates. To ensure proper behaviour of SM fibers in loose tube cables at 1.55 μm it is recommended to restrict the MFD specification to ≤10 μm for MC and ≤9 μm for DC fibers, and to keep $\lambda_c \geq 1.2$μm.

ACKNOWLEDGEMENTS

This work was undertaken as part of the Fiberoptic Submarine Cable development project at EB Cables, supported and partly financed by the Norwegian Telecommunication Administration. The authors are indebted to O. Alm and P. Kummeneje at EB Cables for performing most of the measurements.

REFERENCES

[1] P.Geittner, H.Lydtin, F.Weling, and D.U.Wiechert, "Bend loss characteristics of single mode fibers," Proc. ECOC 1987, Helsinki, vol.2, pp.97-100.

[2] A.B.Sharma, A.H.Al-Ani, and S.J.Halme, "Constant-curvature loss in monomode fibers: an experimental investigation," Appl. Opt. vol.23, 1984, pp.3297-3301.

[3] J.A.Dixon, M.S.Giroux, A.R.Isser, and R.V.Vandewoestine, "Bending and microbending performance of single-mode optical fibers," Proc. OFC/IOOC'87, Reno, Jan. 1987, paper TUA2, p.40.

[4] P.F.Glodis, C.H.Gartside, and J.S. Nobles, "Bending loss resistance in single mode fibers," Proc.OFC/IOOC'87, Reno, Jan. 1987, paper TUA3, p.41.

[5] A.O.Garg and C.K.Eoll,"New measurement technique for measurement of microbend losses in single mode fibers," Tech. Dig. Symp. on Opt. Fiber Measurements, Boulder CO., Sept. 1986, pp. 125-128.

[6] N.Kamikawa and C.-T.Chang, "Predicting microbend losses in single-mode fibers", Tech.Dig. Symp. on Opt. Fiber Measurements, Boulder CO., Sept. 1986, pp. 129-132.

[7] M.Artiglia, G.Coppa, P.Di Vita, M.J. Kalinowski, and M.Potenza, "Bending loss characterization in single-mode fibers," Proc. ECOC 1987, Helsinki, vol.1, 1987, pp. 437-443.

[8] L.Bjerkan, E.Nesset and O.Alm,"Induced losses in strained loose tube fiber cables," Tech. Dig. Symp. on Opt. Fiber Measurements, Boulder CO., Sept. 1988, pp. 89-92.

[9] P.K.Bachmann,"Dispersion flattened and dispersion shifted fibers: worldwide status," Proc. ECOC 1986, Barcelona, vol.II, pp. 17-25.

[10] D.Marcuse, "Curvature loss formula for optical fibers," J. Opt. Soc. Am. vol. 66, 1976, pp. 216-220.

[11] R.Tewari and K.Petermann, "Mode field characteristics of dispersion shifted segmented core fibers," Proc. ECOC 1987, Helsinki, vol.1, pp. 215-218.

[12] K.Petermann, "Fundamental mode microbending loss in graded index and W fibers," Opt. and Quantum Electron. vol.9, 1977, pp. 167-175.

[13] K.Petermann, "Constraints for fundamental mode spot size for broadband dispersion-compensated single-mode fibers," Electron. Lett. vol.19, 1983, pp. 712-713.

[14] K.Petermann and R.Kühne, "Upper and lower limits for the microbending loss in arbitrary single-mode fibers," J. Lightwave Technol. vol.LT-4, 1986, pp. 2-7.

Steinar Stueflotten

EB Cables
Solbråveien 10
N-1370 Asker, Norway

Steinar Stueflotten born in 1949, graduated from the Norwegian Institute of Technology with a Ph.D. degree in physical electronics in 1978. He joined the Central Research Dept. of Elektrisk Bureau in 1978 where he was engaged in fiberoptic systems and cable development. He is presently technical manager at EB Cables.

Leif Bjerkan

EB Cables
Solbråveien 10
N-1370 Asker, Norway

Leif Bjerkan born in 1949, graduated from the Norwegian Institute of Technology with a Ph.D. degree in solid state physics in 1978. Since then he has been involved in research on optical fibers and lasers. He joined EB Cables in 1985 as senior research engineer. Presently he is director of research in solide state physics at ELAB-RUNIT in Trondheim, Norway.

Eivind Nesset

EB Cables
Solbråveien 10
N-1370 Asker, Norway

Eivind Nesset born in 1952, graduated from the Norwegian Institute of Technology with a Ph.D. degree in physical electronics in 1984. He joined EB Cables as a senior research engineer in 1985 and is presently R&D Manager of fiberoptics.

Svend Hopland

Norwegian Telecom. Administration, Cables Division
Munch's gt. 5b
N-0130 Oslo 1, Norway

Svend Hopland graduated from the Norwegian Institute of Technology in 1985 with a Ph.D. on optical fibers. In 1986 he joined the Norwegian Telecommunication Administration, Cables Division. He is presently a senior engineer on fiberoptic cables.

HEAT SHRINKABLE COMPOSITE SPLICE CLOSURES

Michael R. Read

Raychem N.V. Diestsesteenweg 692 - 3200 Kessel-Lo - Belgium

Summary

Heat shrinkable polymers are widely used in joint closure systems to provide effective environmental seals. A new generation of heat shrinkable fibre reinforced composite materials has been developed which allows a wide design fluxibility for closure systems. As splice closures, these heat shrinkable composite closures exhibit many installation and functional benefits such as; split resistance during installation, resistance to mechanical abuse and long term creep resistance. This paper reviews the various designs of the composite closures that have been developed specifically for pressurised and distribution telephone closure systems.

Introduction

Telephone splice closures are used in a wide range of environments around the world which include underground, direct buried and aerial applications. The prime function of a closure is to provide environmental protection to a telephone splice preventing moisture from entering the splice area and hence maintaining the integrity of the telephone system. Throughout their operational lifetime, the closures are subjected to varying chemical environments and physical abuses. These include wide operating temperature variations, exposure to prolonged direct sunlight, immersion in polluted water and mechanical effects like traffic vibration and axial load caused by cable creep.

Conventional non composite heat shrinkable polymeric closures have been used successfully throughout the world since the early 1970's to provide this environmental protection on the telephone network.

With the increasing demand for transmission of high quality and volume of signals on telephone cables, it is important to environmentally protect, with even higher reliability, the telephone network.

In addition, due to the various skill levels of the craft persons and a wide range of torches used to install heat shrinkable closures, installations of variable quality can result. With non composite heat shrinkable closures overheating can cause splitting.

This may tempt the craftsmen to be over cautious and to underheat the closure which then results in poor sealing of the closure to the telephone cable resulting in water ingress.

Advanced composite splice closures have been developed to overcome all installation circumstances and add significant improvement to the performance and lifetime of closures in both the pressurised and distribution network.

This paper covers the design and performance characteristics of the composite material and closure system and includes a comparison with conventional non-composite heat shrinkable polymer closure systems.

Heat shrinkable splice closure for the pressurised network

Effects of pressurisation.

Pressurised splice closures are effectively cylindrical pressure vessels; the internal pressure generates longitudinal and circumferential (hoop) stresses in the walls of the vessel. In particular, the hoop stress (σH) in the material is given by :

$$\sigma H = \frac{Pr}{t}$$

where P = internal pressure
r = radius of vessel
t = wall thickness of vessel

Hoop stresses can give rise to two long term effects in polymeric pressure vessels :

1. Creep deformation. A slow elongation of the material due to the applied stress.

Creep is more significant in a polymeric system than in a metallic one due to the much lower melting points of polymers; creep deformation becomes significant at temperatures typically one-half to two-thirds of the material's absolute melting point.

The effect of creep on a polymer pressure vessel is an increase in its diameter, and consequent reduction of its wall thickness, often referred to as "ballooning".

2. Stress rupture. Susceptibility of the polymer to failure after long time periods at low stresses.

Two possible failure modes can occur : (i) ductile failure at relatively short times and higher applied stresses, and (ii) brittle fracture after longer time periods at lower stress levels. Brittle fracture becomes much more significant at higher temperatures.

There are two ways in which the resistance to creep and stress rupture can be increased :

a. A more "heavily engineered" design. For example, a thicker-walled product, in which the hoop stresses are reduced.

b. The use of an intrinsically "stronger" material which is more resistant to these modes of deformation.
It is this second approach which is described in this paper.

Heat shrinkable composite closure design

The new heat shrinkable closure system consists of a composite material made up of a woven fabric containing crosslinked heat shrinkable polymeric fibres and non shrinking reinforcing fibres, which is coated on both sides with a cross-linked polymeric material. Laminated to the inner surface is an adhesive. A cross-section is shown in Figure 1.

The composite is designed to dimensionally recover in one direction, while maintaining exceptional dimensional stability in the other direction. In order that the composite material can be used as a wraparound closure, a "rail" is formed on the sleeve for closing purposes (see Figure 2). An adhesive layer is extended to provide a complete seal under the closure mechanism.

Temperature indicating paint is coated on the outer surface of the material converting from green to black at a specific temperature to indicate that sufficient heat is applied to closure.

The composite sleeve is used in conjunction with a metal canister which provides the mechanical support to the telephone cable splice connectors.

Three fingered branch-out clips are used to seal to multiple cables at either outlet.

Performance

At installation.

The fibre reinforcement of the composite material ensures that the closure is able to be installed with the wide range of gas torches that exist throughout the world such as gasoline, kerosene, propane, acetylene and modified acetylene - propane torches. On installation the necessary amount of heat is applied to recover the composite closure converting the temperature indicating paint and activating the adhesive to seal the closure to the cables, even in the most difficult outside plant conditions.

The composite material uniformly recovers by 3 to 1, which combined with the minimal longitudinal dimensional change, results in a evenly controlled wall thickness with no reduction of the

sleeve wall thickness even over sharp splice transitions, unlike non composite polymeric material sleeves.

Figure 3 compares the results of a split resistance test of both the composite and the conventional non-composite materials. A sample 100 X 50 mm is placed in an Instron tensile machine at 200°C, and a cut of 5 mm is made in the edge perpendicular to the recovery direction. As the recovery force of the non-composite polymer material develops, a split caused by the cut, propagates across the width of the sleeve. The sample breaks typically within five minutes after starting the test.

The reinforced composite material withstands this split propagation and the sample remains intact even after thirty minutes at 200°C.

This test is designed to simulate the mechanical abuse that the heat shrink able closure might have seen before installation or that can occur when a closure is installed in a confined space such as congested manhole. In such a manhole the hot nozzle of the torch might accidentally touch the sleeve during an installation and potentially damage it, which would lead to the closure splitting. The reinforced composite material can withstand this kind of abuse with the sleeve remaining intact.

Functional performance during life time.

Once installed the high strength of the composite closure together with the adhesive ensures excellent functional performance.

Creep deformation.

The creep behaviour at 60°C of the composite material is compared with that of a conventional non composite closure, see Figure 4.

The conventional non composite material creeps steadily to a strain of about 23 % after around 175 hours, then the closure leaks. In this case, failure was not in the heat shrinkable sleeve material itself, but at the seam where the wraparound was joined; the very high strain caused leakage through the adhesive at this point.

In contrast after initial expansion, the composite sleeve reaches an asymptotic creep level of around 3 % under these test conditions. The initial extension occurs while the fabric in the composite is being put under tension, and there is very little subsequent creep.

Heat shrinkable splice closure for the distribution network

Following the success of the heat shrinkable composite material as a pressurized closure, the technology was used to develop a composite material for a distribution closure.

The additional demands for a distribution closure include a requirement for a recovery ratio of a least 4 to 1, due to wider range of cable configurations, and installations on smaller cables.

The construction of the composite material was modified to accommodate these requirements without sacrificing any of the installation characteristics of the pressurised closure.

An additional aluminium layer has been added between the composite material and adhesive to provide an integrated moisture vapour transmission (MVT) barrier. (See Figure 5).

Once installed this MVT barrier provides resistance to moisture penetration into the splice area, and in effect reconstitutes the MVT barrier of the PE-Aluminium cable sheath, where one is present in a distribution cable.

A comparison of a conventional non-composite polymeric closures, which relies on a separate MVT barrier, versus composite closures containing an

integrated MVT barrier in the sleeve material, is shown in Figure 6.

Functional performance during lifetime.

The functional tests outlined in Table 1 are undertaken to simulate the long term behaviour of installed splice closures. These include a wide range of tests performed between temperatures of -15 and +45°C on extreme cable configurations of both lead and polyethylene sheathed cables. The strength of the composite and the flexibility of the adhesive enables the splice closure to withstand different impact tests at -15°C.

Conventional thermal cycling in air between -40 and +60°C is used to demonstrate the integrity of the installed closure system after accelerated ageing.

Resistance to environmental stress cracking at 50°C in surfactant solution, such as 10 % Igepal in water, and various other aggressive media are performed to demonstrate the environmental resistance of the closure system.

Conclusions

The advanced composite heat shrinkable closures developed, offers significant benefits over conventional non composite heat shrinkable joint closures.

Composite closures eliminate craft sensitivity during installation and offer superior functional benefits once installed.

The material design ensures that the closure is highly split resistant offering excellent torchability when installed with even the fiercest of gas torches available. This ensures that the closures can be reliably installed even in the most demanding of environments.

The closure system design gives superior functional performance over conventional non-composite joint closures. In particular the composite pressurised closure design exhibits outstanding resistance to creep. The composite distribution closures offer significantly improved moisture vapour transmission protection to the splice.

These advanced composite heat shrinkable joint closure systems have been successfully developed to meet the more demanding requirements of todays telephone network.

Acknowledgements

The author wished to acknowledge the many people in Raychem's Telecommunications Division and Corporate R and D in the UK, Belgium and the US who have contributed to the development of the composite closure systems.

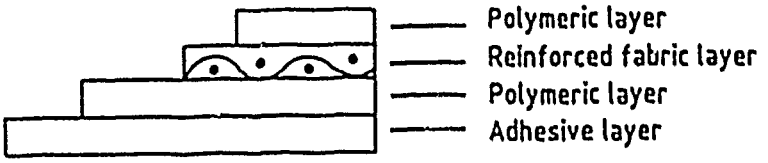

Figure 1 Cross-section of composite heat shrinkable sleeve for pressurised closures.

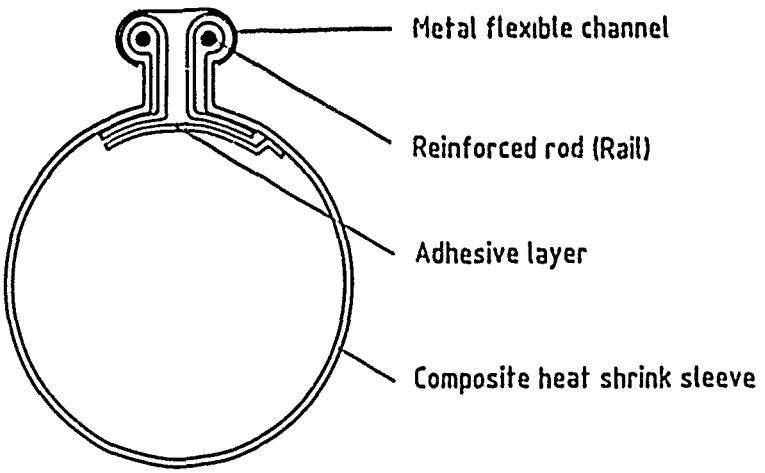

Figure 2 Cross-section of 'Rail and Channel' closure system.

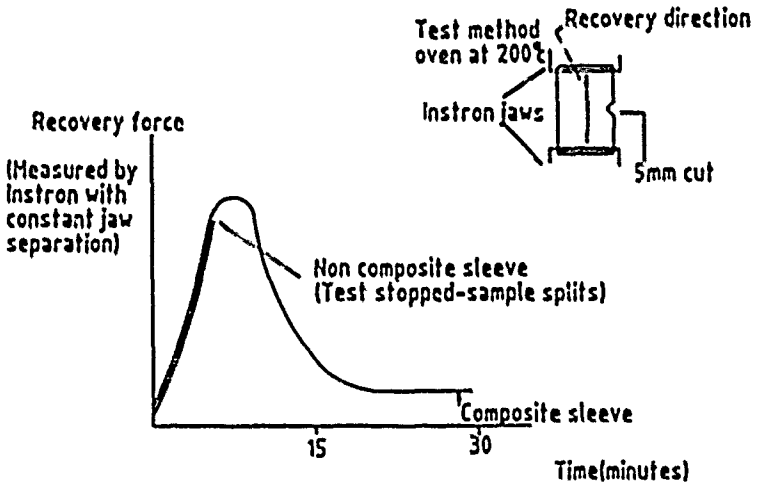

Figure 3 Split resistance test.

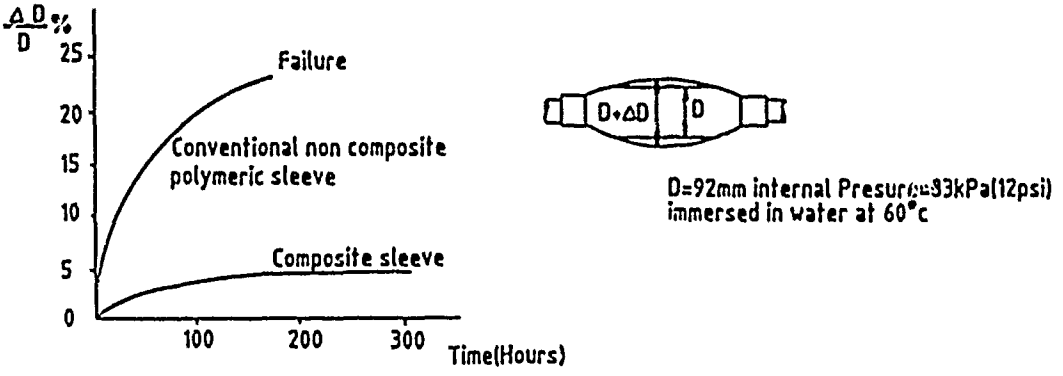

Figure 4 Creep behaviour of composite heat shrinkable sleeve versus conventional non composite sleeve at 60°C.

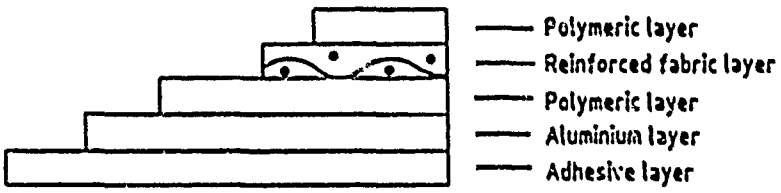

Figure 5 Cross-section of composite heat shrinkable sleeve for distribution closures.

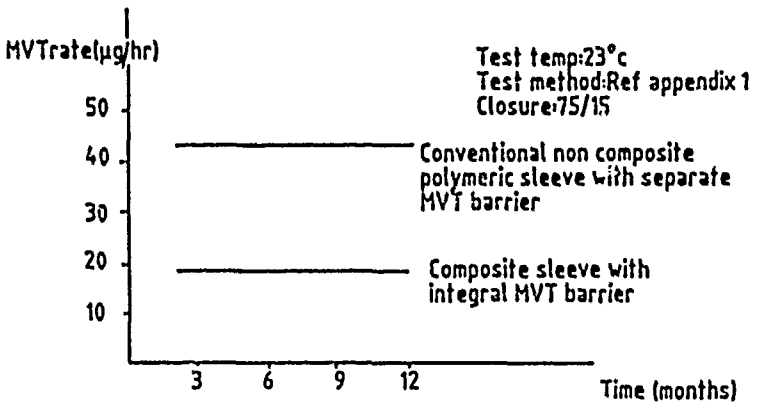

Figure 6 Moisture vapour transmission (MVT) of installed distribution closures.

PROPERTY	TEST CONDITION	REQUIREMENT
Tightness	Water @ 23°C 40 KPa - Internal pressure	15 mins
Static load	Temp. -15°C Load 1000 N Surface area 50mm²	2X5 mins Tightness
Impact	Temp. -15°C 1) 1 kg ball from 2 m 2) Sharp bladed tool 6 kg from 0.3 m	 1 hit 1 hit Tightness
Axial pull	Temp. -15 to 45°C Load 1000 N	8 hours Tightness
Bending	Temp. -5 to 45°C Max 45°C angle or max force 500 N	2X5 mins Tightness
Torsion	Temp. -5 to 45°C Max 90°C angle or 50 Nm torque	2X5 mins Tightness
Vibration	Temp. 10°C Frequency 10 Hz - Amplitude 3 mm	72 hours Tightness
Temperature cycling	-30/+60°C 12 hr cycle - 40 KPa pressure	10 cycles Tightness
Freeze thaw	Ice to water 12 hr cycle - 40 KPa pressure	20 cycles Tightness
Chemical resistance	Temp. 23°C 0.1 N Na 2SO4 0.1 N NaOH 0.1 N H2SO4 0.1 N NaCl Oil ASTM 0396 Petrol Kerosene	30 days Tightness
Moisture vapour transmission	Temp. 10°C 75/15 closure under water (Ref. Appendix 1)	Until stabilisation (3 months)15 µgm/hr
Resistance to stress cracking	Temp. 50°C in a stress crack initiator (e.g. 10% Igepal solution)	168 hrs Tightness

Table 1 : Functional requirements for VASM-2 splice closures for use in the unpressurised network of the German Bundespost (DBP). TL.nr.5975-3006 (Draft May 1989)

Appendix 1

Test method for MVT of installed splice closures.

Sample preparation

The qualification size as specified in the applicable specification sheet shall be installed on aluminium tubes with an outer diameter equivalent to the minimum and maximum cable diameter applicable to that size. The body diameter of the samples shall be in accordance with qualification sample description.

Test procedure

Samples prepared as described shall be connected to the measuring system with suitable stainless steel tubing and connectors and shall be fully immersed in a water bath regulated to 23 ± 1°C. Dry air shall be continuously purged through samples at a constant rate of 10 cc/min for the duration of the test. The sampling gas stream shall be analysed every 24 hours for water content by means of a hygro-meter and flowmeter or other suitable arrangement, until a constant rate of permeation is achieved. This shall be recorded as the moisture vapour transmission rate. The flow diagram is shown in the following section.

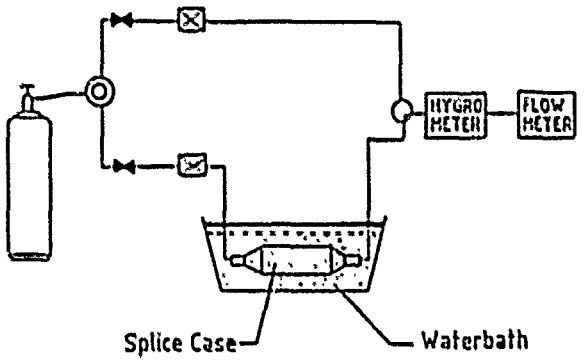

Flow diagram

Michael R. Read

Raychem N.V.
Diesthesteenweg 692
3200 Kessel-Lo

Belgium

Michael Read graduated with an honours degree in Chemistry from the University of Aston in Birmingham (UK) in 1981. He joined Raychem Ltd. in the UK and worked on several research and development projects on high performance materials. In 1984 he was appointed Technical Manager for the Telecommunications Division in the UK. He is currently Development Manager for the Composite Technology Group in Belgium.

FIRE PROPERTIES OF SILICONES FOR THE ELECTRICAL AND OPTICAL FIBER CABLING INDUSTRY

Mr. Robert R. Buch, Dr. William E. Dennis
Mr. Carl M. Monroe, Mr. Roger S. Chaffee

DOW CORNING CORPORATION
Midland, Michigan 48686-0995

ABSTRACT

Fire performance requirements for electrical and optical fiber cabling materials are becoming increasingly demanding and this trend is expected to continue. The fire performance of a material includes a variety of parameters, i.e., heat release, flame spread, yields of smoke, toxic, corrosive combustion products.

In this investigation, these fire parameters were obtained on silicone and several organic materials used in the cabling industry. Recent development efforts have focused on the reduction of smoke yield and flame spread of silicone based materials. Our findings suggest that silicone-based materials offer significant advantages in "fire-sensitive" applications in terms of their heat release, and low yields of smoke, toxic, and corrosive combustion products.

The versatility and utility of the cone calorimeter in the characterization of these fire properties is also demonstrated. Furthermore, the ability of the cone calorimeter to provide guidance in the development of materials and their selection for larger-scale testing is demonstrated.

INTRODUCTION

Since their development in the 1940's, silicones have developed into a multi-billion dollar industry. Initially, products were primarily based on their unique thermo-oxidative stability, electrical properties and capability to perform over a broad range of temperatures. Today, these materials, because of their many unique properties (Figure 1), find applications in industries ranging from electrical, construction, and automotive to cosmetic and medical. The products include fluids, resins, foams, gels, elastomers, and sealants.

In the 1960's, the need for a dielectric fluid to replace Arochlors (PCBs) prompted a thorough study of the fire properties of polydimethylsiloxane (PDMS)[1,2]. In addition to their environmental passivity[3], the unique fire behavior of PDMS was documented.

Silicone rubber has been used as wire and cable insulation since the early 1950's. In subsequent years, performance requirements for coatings have become increasingly stringent. Recently, some of

SILICONES — PROPERTIES

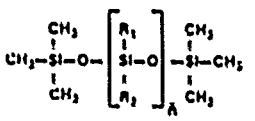

$R_1 = R_2 = CH_3$ (Polydimethylsiloxanes)

- Surface Properties
- Thermophysical Properties
- Oxidative Stability
- Electrical Properties
- Transport Properties
- Optical Properties
- Biologically Inert
- Environmentally Passive
- Fire Properties

(Fluids, Gels, Elastomers, Resins, Foams)

Figure 1. Thermophysical Properties of Silicones

these requirements have focused on the fire performance of cable coating materials. Currently, the most severe test is the Steiner Tunnel Test (E-84/UL 910) directed at the assessment of the flame spread and smoke evolution characteristics of the coatings. Current trends suggest that fire performance requirements will increase. Recently, Factory Mutual proposed a new system for classifying cables based on their ability to resist fire propagation[4]. In December, 1986, New York State enacted legislation requiring the filing of combustion toxicity on certain construction materials used in public buildings. The National Institute of Building Sciences (NIBS) is currently supporting the development of a new combustion toxicity test protocol. The most recent fire performance issue concerns the corrosivity of combustion products[5]. Several laboratories both in the US and Europe are addressing this issue.

In view of these trends, and earlier improvements in the fire performance of silicone cable coatings reported by Cabey[6], this investigation into the further development and characterization of silicone materials for electrical and optical fiber cable was launched. In this study, the measurement of all key fire parameters (Figure 2) was accomplished using a cone calorimeter patterned after the unit developed at the National Bureau of Standards - Center for Fire Research[7].

FACTORS IN CONSIDERING FIRE BEHAVIOR

MATERIAL PROPERTIES
- DENSITY
- TOTAL HEAT CONTENT
- HEAT CAPACITY
- THERMAL CONDUCTIVITY
- CHEMICAL ANALYSIS
- HEAT OF GASIFICATION

BEHAVIOR OF SAMPLES IN FIRE TESTS
- EASE OF IGNITION
- RATE OF HEAT RELEASE
- RATE OF SURFACE FLAME SPREAD
- RATE OF SMOKE RELEASE
- RATE OF TOXIC GAS RELEASE
- CORROSIVE COMBUSTION PRODUCTS

Figure 2. Basic Physical Properties and Fire Parameters of Materials

EXPERIMENTAL

Complete construction details and operating procedures are given elsewhere[8,9]. Two modifications necessary to accommodate the unique fire behavior of silicones are: (1) the stoichiometric ratio relating heat energy release to oxygen consumed is 14560 kJ/kG(O_2) and (2) the load cell readings do not provide a measure of sample mass pyrolysis rate because of the deposition of large quantities of silica ash - a major product of combustion of silicones. Mass burning rate is obtained from the measured rate of heat release and heat of combustion for silicones (PDMS) as follows:

$$M_B = RHR / \Delta H_{Comb.}$$

The materials used in this study were commercial-grade polymers, elastomers, and gels. The elastomers and polymers consisted of four-inch square slabs, 1/4-inch thick. The gel type samples were placed into a round flat dish (14mm x 120mm) for fire testing.

RESULTS AND DISCUSSION

Rate of Heat Release (RHR)

The rate of heat release is a key fire parameter which provides a measure of the rate at which a material will contribute heat to a fire scenario. RHR data for optical fiber cable filling compounds are given in Figure 3 for a range of fire conditions (25, 50, and 75 kW/m²). The RHR for silicone based material is substantially lower than the organic based material. Furthermore, note that the silicone RHR is virtually independent of the applied external heat flux, i.e., fire intensity. In Figure 4, RHR data are given for several organic polymers commonly used in electrical cable coatings. Silicones typically exhibit an RHR in the range of 75 to 150 kW/m² and their RHR is virtually independent of external heat flux. More extensive RHR - external heat flux dependence data for various polymers are given in Figure 5. This unique behavior of silicone based materials is largely attributed to the influence of the silica ash which quickly accumulates on the surface of the burning sample.

OPTICAL FIBER CABLE FILLER COMPOUNDS

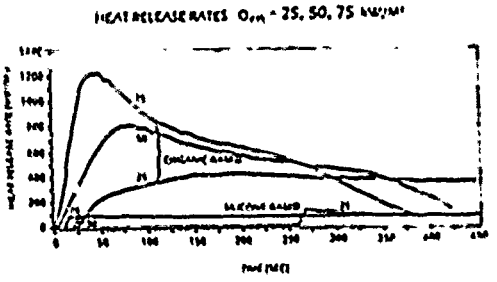

Figure 3. Heat Release Rate Data for Optical Fiber Cable Filler Compounds - Hydrocarbon Based vs. Silicone (PDMS) Based

ELECTRICAL CABLE COATING POLYMERS

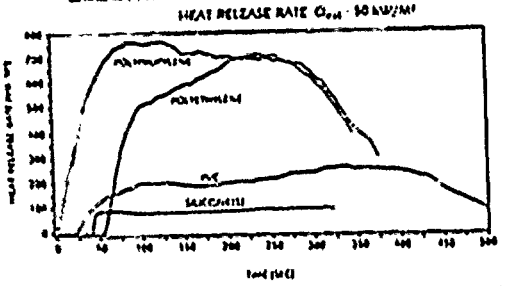

Figure 4. Heat Release Rate Data for Electrical Cable Coating Polymers

HEAT RELEASE RATE—
EXTERNAL HEAT FLUX DEPENDENCE

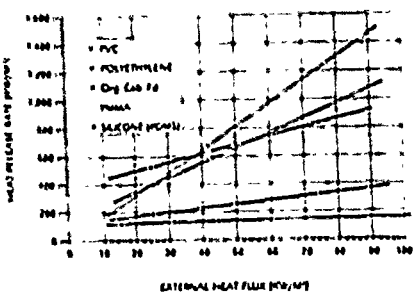

Figure 5. Dependence of RHR on External Heat Flux

Smoke Yield

The yield of smoke from burning electrical cable coatings is a key performance requirement. Quite recently, technology improvements have resulted in the reduction of smoke evolution from both high consistency silicone and liquid silicone (LSR) stocks (Figure 6). It is noteworthy that the smoke suppression technology is based largely on the use of hydrated inorganic oxides. Furthermore, the modest additions of these materials do not significantly compromise electrical and mechanical properties of the coatings. Halogen-based fire

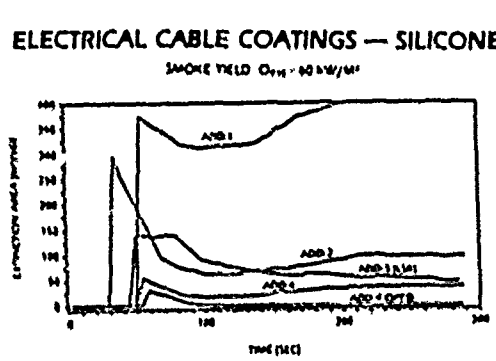

Figure 6. Smoke Yields - Silicone Cable Coating Elastomers with Smoke Suppression Additives

retardants are not used in silicone cable coating stocks. Data for several organic materials are given in Figure 7.

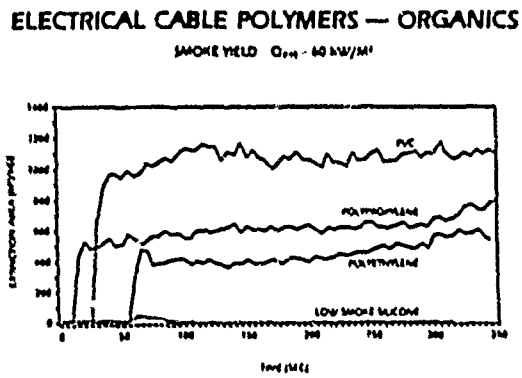

Figure 7. Smoke Yields - Organic Cable Coating Polymers and Optimized Silicone Elastomer (X4188x)

Carbon Monoxide Yield

The principle toxic combustion product is carbon monoxide. Consequently, our assessment of the relative potential toxicity of the combustion products of cable coating and filling compounds is based on the quantitation of carbon monoxide. The cone calorimeter gas analysis system includes on-line infra-red analyzers for both CO_2 and CO. In Figures 8 and 9, carbon monoxide yield data are given for the cable coating and cable filling materials included in this study. These data demonstrate the exceptionally low yield of CO for silicone-based materials in flaming combustion.

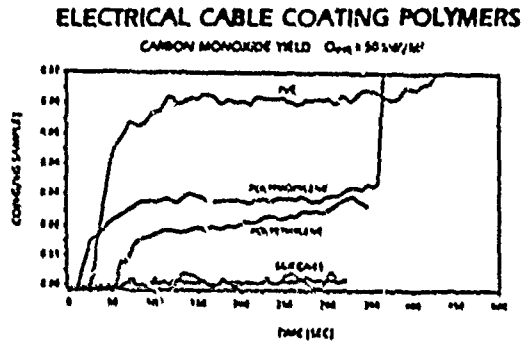

Figure 8. CO Yields - Electrical Cable Coating Polymers

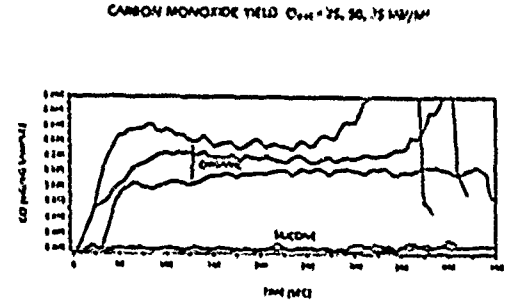

Figure 9. CO Yields - Optical Fiber Cable Filler Compounds - Hydrocarbon Based vs. Silicone (PDMS) Based

Generation Rates of Combustion Products

The various yield parameters (smoke, CO) do not take into account the mass burning rates exhibited by the various materials. The rate of formation of combustion products is dependent upon both the yield of the specific product and the mass burning rate of the material. Thus, the rate of generation is given by the product of the yield times the mass burning rate,

$$(GR)_X = Y_X \cdot M_B$$

The combustion product generation rates (smoke, CO) are summarized in Table 1.

COMBUSTION PRODUCT — GENERATION RATES[1]

OPTICAL CABLE FILLER COMPOUNDS	CO (g/g)	SMOKE (m²/g)
SILICONE	0.96 x 10⁻³	15 x 10⁻³
ORGANIC	4.5 x 10⁻³	196 x 10⁻³
ELECTRICAL CABLE COATINGS/POLYMERS		
POLYETHYLENE	2.4 x 10⁻³	64 x 10⁻³
PVC	18.5 x 10⁻³	150 x 10⁻³
SILICONE	0.34 x 10⁻³	72 x 10⁻³
LOW SMOKE SILICONE	0.80 x 10⁻³	8.4 x 10⁻³

1. G_R = YIELD = MASS BURNING RATE ($\dot{M}_g$)

Table 1. Generation Rates of Smoke and Carbon Monoxide (Over-ventilated and $\dot{q}''_e$ = 40 kW/m²)

Ease of Ignition - Flame Spread

Smoke evolution and flame spread are the two combustion performance parameters assessed in the Steiner Tunnel Test protocols (E-84, UL 910). Whereas the cone calorimeter provides a direct measure of smoke yield, an indirect measure of flame spread must be deduced. The methodology follows test procedures developed by Tewarson[10]. The time to ignition is measured as a function of applied external heat flux ($\dot{q}''_e$) to the test specimen. For this measurement, sample surfaces are blackened by the addition of a light coating of carbon black to minimize surface reflectivity. The reciprocal of ignition energy ($E_{ig} = T_{ig} \cdot \dot{q}''_e$) is plotted as a function of external heat flux. Extrapolation of the curves to $1/E_{ig} = 0$ allows the determination of the critical heat flux ($\dot{q}''_{cr}$) for each material. The greater the value for $\dot{q}''_{cr}$, the lower the expected flame spread for the test material. The data are given in Figure 10 and critical heat flux data are listed in Table 2.

An additional parameter derived from these measurements is that of the reciprocal of the energy of ignition at an external heat flux of 60 kW/m². This heat flux is estimated to represent that in the Steiner Tunnel [11,12]. This parameter is also listed in Table 2 for several materials.

IGNITION/FLAME SPREAD PARAMETERS

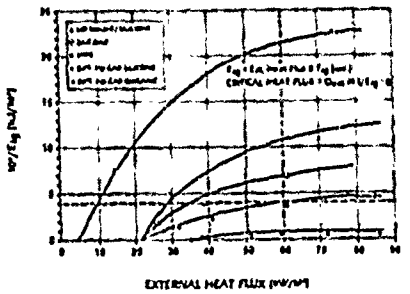

Figure 10. Ignition Time Data - Determination of Critical Heat Flux and Flame Spread Parameter

IGNITION/FLAME SPREAD SUMMARY

CRITICAL HEAT FLUX = Minimum energy flux required for generation of volatiles necessary for ignition.

$(1/E_{ig})_{\dot{q}''=60}$ = "Benchmark" flame spread parameter for UL 910/E-84 (Steiner Tunnel) performance.

MATERIAL	CRITICAL HEAT FLUX (kW/m²)	$(1/E_{ig})_{60}$ (m²/kJ)
OPTICAL FIBER CABLE FILLING COMPOUND		
SILICONE-BASED	21	11
ORGANIC-BASED	5	21
ELECTRICAL CABLE-COATING COMPOUNDS		
SILICONE — GENERAL PURPOSE	21	7
SILICONE — LOW SMOKE/LOW FR	21	3.5
PVC	26	1.3

Table 2 Flame Spread Parameters

Cone Calorimeter - Large Scale Test Correlations

The cone calorimeter, equipped with appropriate accessory apparatus, provides a means for measuring a wide variety of basic fire properties. However, its ultimate success will depend on the correlation of these data with results from large-scale tests and/or real world experiences. To date, correlations of this type are limited in number. In Table 3, suggested parameters for use as guidelines in predicting the performance of cable coatings in the Steiner Tunnel Test are given. In addition to critical heat flux and RHR values, the reciprocal of the energy of ignition measured at an external heat flux of 60kW/m² and a value for the specific extinction of 100 m²/kG are believed to be useful guidelines.

Based on these four parameters [($\dot{q}''_{cr}$), $(1/E_{ig})_{60}$, $(RHR)_{60}$, specific extinction] a high consistency elastomer was selected for testing via the E-84 Steiner Tunnel Test. This material far surpassed the performance requirements of flame spread and smoke development criteria for the Uniform Building Code (Table 3).

CONE CALORIMETER — LARGE SCALE TESTS

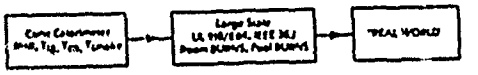

CONE CALORIMETER TEST PARAMETERS	LARGE SCALE E-84/U.B.C. REQUIREMENTS
Low Smoke Silicone Elastomer	Flame Spread Index = 25
$\dot{q}''_{cr}$ = 22 KW/M²	Smoke Development = 50
E_{ig}^{-1} = 3.5 x 10⁻³	Silicone Elastomer Low Smoke
RHR_{60} = 125 KW/M²	FSI = 4
Spec. Extn = 50 M²/KG	SDR = 5

Table 3. Correlation of Cone Calorimeter Fire Test Parameters with Large-Scale Tests

Combustion Model and Fire Properties for Silicones (PDMS)

A model for the degradation/combustion of PDMS as proposed by Lipowitz is given in Figure 11. Details and discussion of this model are given elsewhere[1]. However, this model together with basic thermochemical data is useful for providing insight into the unique fire behavior of PDMS-based silicones. The low rates of heat release are largely attributed to the low heat of combustion for PDMS, its relatively high heat of gasification, and the mediating influence of the substantial yield of silica ash which is deposited on the surface of the fuel source (Figure 11). This silica ash insulates the remaining sample from external radiant and convective energy. Consequently, PDMS based materials exhibit a uniquely low dependence of RHR on external heat flux (fire intensity)[13]. The critical heat flux for PDMS (approximately 22 kW/m^2) is considered to be largely due to the relatively high heat of gasification. The major component of the smoke emanating from combusting silicones is amorphous silica[14]. The reduction of smoke from silicone elastomers largely relies on the use of hydrated inorganic oxides and crosslinking technology to promote char (silica ash) formation. These chars are good electrical insulators thus providing extended retention of electrical integrity in extremely high heat stress scenarios[15]. The combustion products of silicones (CO_2, H_2O, SiO_2) are expected to pose a minimal corrosivity hazard.

SILICONE (PDMS) — COMBUSTION MODEL* — INTRINSIC FIRE PARAMETERS

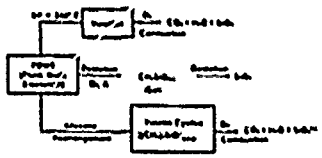

POLYMER		
POLYDIMETHYLSILOXANE	24.8	30 – 35
POLYETHYLENE	43.2	2.2
POLYPROPYLENE	43.2	2.0
PVC	16.8	7.5

* Lipowitz, J., J. Fire and Flamm., 7, 504-529 (1976)

** Babrauskas, V., et al., Combustion Behavior of Selected Substances Adsorbed Onto Fire Retardant Char, Fire and Materials, Vol. 12, 1988, pp. 51-65.

Figure 11 Combustion Model for Silicone (PDMS)

SUMMARY

Silicones encompass a broad range of materials (fluids, gels, resins, elastomers and foams) with fire properties which can offer substantial improvements in fire safety for the electrical and communications industries (Table 4). Recent technology developments demonstrate the capability of these material to meet current fire performance requirements and increasingly stringent requirements anticipated for the future.

SILICONES — FIRE PARAMETERS

- LOW RATE OF HEAT RELEASE
- MINIMAL EXTERNAL HEAT FLUX DEPENDENCE
- LOW FLAME SPREAD RATE
- LOW YIELD OF SMOKE
- LOW YIELD — CARBON MONOXIDE
- LOW CORROSIVITY — COMBUSTION PRODUCTS
- SILICA ASH
  - AMORPHOUS -- PHYSIOLOGICALLY PASSIVE
  - ELECTRICAL INSULATOR

TABLE 4.

The cone calorimeter provides the materials development specialist with a new test capability for the rapid and reliable measurement of a range of basic fire parameters. This information facilitates product optimization and will aid design engineers and regulating agencies in the specification and selection of fire-safe materials.

REFERENCES

1. Lipowitz, J., Flammability of Poly(dimethylsiloxanes). I. A Model for Combustion, J. Fire & Flammability 7, 482-503, (1976)
2. Lipowitz, J. and Ziemelis, M. J., Flammability of Poly(dimethylsiloxanes). II. Flammability and Fire Hazard Properties, J. Fire & Flammability 7, 504-529 (1976).
3. Frye, C. L., The Environmental Chemistry of Liquid Polydimethylsiloxanes: An Overview, 5th International Organosilicon Symposium in Karlsruhe, Germany, August 17, 1978.
4. Major, D., Proposed FMRC Specification Test for Cables, Cable Flammability Conference, Factory Mutual Research Center, June, 1988.
5. "Corrosive Effects of Combustion Products", Fire and Materials Centre, Queen Mary College, U.K., October, 1987.
6. Cabey, M. A., New Silicone Rubber Cable Insulation Promises Circuit Integrity in Flaming Environment, 32nd International Wire & Cable Symposium, 1983.
7. Babrauskas, V., Development of the Cone Calorimeter - A Bench-Scale Heat Release Rate Apparatus Based on Oxygen Consumption, Fire and Materials 8, 81-95 (1984). Also issued as NBS Report NBSIR 82-2611 (1982).

8. Proposed Test Method for Heat and Visible Smoke Release Rates for Materials and Products using an Oxygen Consumption Calorimeter (E-5 Proposal P 190), Annual Book of ASTM Standards, Vol. 04.07, p. 1221-1237, American Society for Testing and Materials, Philadelphia (1986)

9. Construction Drawings for the Cone Calorimeter. Available from the Center for Fire Research. National Bureau of Standards, Gaithersburg, MD 20899.

10. Tewarson, A., Khan, M. M., and Steciak, J., Combustibility of Electrical Wire and Cable for Rail Rapid Transit Systems. Report No. UMTA-MA-06-0025-83-6, May, 1983.

11. Parker, W. J., An Investigation of the Fire Environment in the ASTM E-84 Tunnel Test. NBS Technical Note 945. US Nat. Bureau of Standards (1977).

12. Tewarson, A. and Khan, M. M., Review of Cable Flammability Research at Factory Mutual. FMRC J.i OM2E1.RC, April, 2987.

13. Kanakia, M., Southwest Research Institute. Characterization of Transformer Fluid Pool Fires by Heat Release Rate Calorimetry. SWRI Project No. 03-5344-001 (1979), presented at the 4th International Conference on Fire Safety, U. of San Francisco (1979).

14. Schepers, G., et. al., Biological Action of DeGussa Submicron Amorphous Silica Dust (Dow Corning Silica). Parts I-V Arch. Environ. Health 16, 125, 203, 280, 363, 499 (1957).

15. Noble, M. G., Off. Plast. Caoutch. 22 693 (1975).

Dow Corning Corporation
3901 S. Saginaw Road
Midland, MI 48686

Robert R. Buch

Robert R. Buch joined Dow Corning in 1962 after completing his MS degree (physics) at the University of Wisconsin (Madison). He is aSenior Analytical Specialist currently engaged in studies on fire properties of organosilicon materials. He is a member of the American Chemical Society and the ASTM E5 Committee on Fire Testing and Standards.

Roger G. Chaffee

Roger G. Chaffee received his Bachelor of Science degree in Chemistry from Central Michigan University. He joined Dow Corning Corporation in 1957 and is currently a Senior TS&D Specialist. He is a member of the American Chemical Society.

Carl M. Monroe

Carl Monroe received his BS degree in pulp and paper chemistry from Western Michigan University in 1962. He currently is an Associate Development Scientist at the Dow Corning Corporation in Elastomers Development. He has been involved in a variety of projects, i.e., high green strength rubber, fluorosilicones, silicone liquid polymer systems, blends of silicone rubber with plastics and organic rubbers, low smoke technology, etc. Work experience is all with Dow Corning. He is a member of the American Chemical Society and Rubber Division ACS.

William E. Dennis

William E. Dennis graduated from Alma College in 1962 with a BS degree in Chemistry and from Wayne State University in 1966 with a PHD. degree in synthetic organic chemistry.

He has worked for Dow Corning Corporation since 1966 on a variety of research and development projects including materials for the optical fiber cabling industry. He is presently a Sr. Technical Specialist in the Electronics and Communication Industry of the High Technology Commercialization Unit.

He is a member of the American Chemical Society, Sigma XI, SAMPE and the Optical Society of America.

NEW NITROGEN GAS EXTRUSION PROCESS FOR HIGHLY EXPANDED POLYETHYLENE INSULATED COAXIAL CABLES

M.Ishihara, Y.Suzuki, Y.Ito, S.Kawabata, S.Takaki

Sumitomo Electric Industries, Ltd.
Yokohama, Japan

SUMMARY

Instead of fluorocarbon extrusion process which has a pollution problem, we have developed a new nitrogen gas extrusion process for 80 % expanded polyethylene insulated coaxial cables. This process provides a stable production of cable at a line speed equal to that of conventional extrusion process using fluorocarbon. The extrusion technology is realized with specially designed equipment and the extrusion materials which have been developed. The cables have proved to be satisfactory in all applications. This paper describes the new extrusion process and discusses the cable characteristics.

1. INTRODUCTION

Coaxial cables with 80% expanded polyethylene insulation are widely used for CATV lines due to their excellent transmission characteristics. Up to this time, we developed the high expansion technique by using fluorocarbon and adopted this to actual mass production.

But now a serious pollution problem has become evident; it was found that the fluorocarbon is an air-pollutant. It destroys the ozone layer and increases ultra-violet radiation which damages biological systems including humans. It is a worldwide pollution problem which should be solved as soon as possible.

Besides fluorocarbon, other expansion techniques have utilized fluorocarbon substitute, organic solvent, methane gas, and nitrogen gas as a blowing agent. But there are some disadvantages, as follows;

Fluorocarbon substitute	:	Not commercial
Organic solvent	:	Air-pollutant
Methane gas	:	Dangerous due to its explosiveness and air-pollutant.
Nitrogen gas	:	Non-polluting and safety. But impossible to obtain more than 70 % expansion.

The conventional nitrogen gas extrusion process couldn't be applied to obtain expanded polyethylene insulation over 70%. This is mainly due to difference of expansion mechanism between fluorocarbon and nitrogen gas. In case of fluorocarbon, the advantageous property is that the vaporization just after extruded makes the viscosity of cell wall higher and prevents cell broken. Nitrogen gas doesn't have above effect.

From the viewpoint of environmental conservation, we started to investigate and have succeeded in developing a new nitrogen gas extrusion process, which is based upon our high expansion techniques using fluorocarbon and a chemical blowing agent.

This paper describes the new extrusion process and discusses the cable characteristics.

2. MANUFACTURING PROCESS

2-1.Extrusion line

2-1-1.Schematic diagram

A schematic diagram of the nitrogen gas extrusion line for manufacturing highly expanded polyethylene insulation cores is shown in Fig.1. We remodeled the

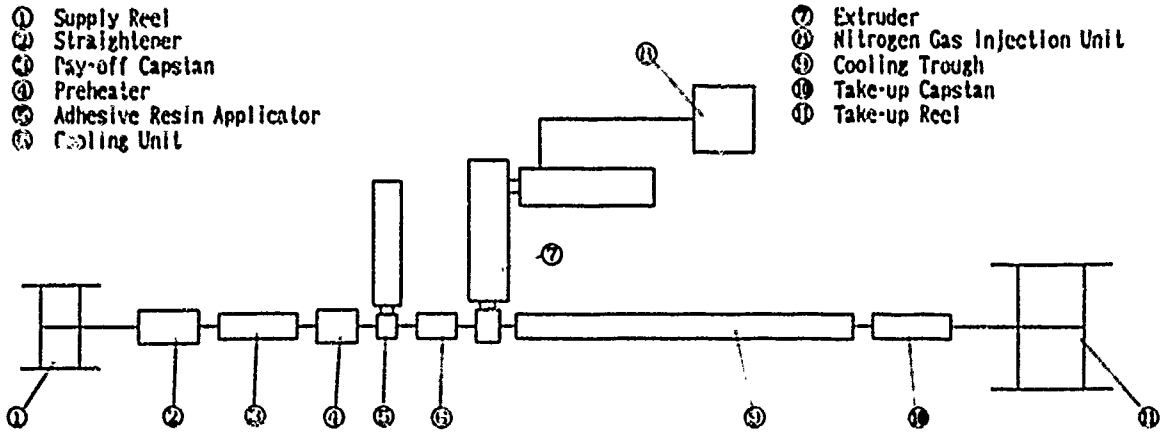

Fig. 1. Extrusion Line

conventional fluorocarbon extrusion line into this new line. The prominent features of this process are as follows:

1)Extrusion facility: It consists of tandem type extruders as before. But the screws are designed to obtain a good mixture of nitrogen gas and polyethylene in injection zone and not cause regular fluctuation.

2)Nitrogen gas injection unit: Instead of fluorocarbon, the nitrogen gas is used as blowing agent. It is continuously supplied to the primary extruder with the injection unit.

3)Adhesive resin applicator: An adhesive coating is applied to the surface of inner conductor so as to provide good adhesion between the inner conductor and insulation layer.

2-1-2. Extrusion facility

The primary extruder functions to melt the polyethylene compounds and throughly mix it with the nitrogen gas blowing agent, which is supplied to primary extruder by the injection unit. The mixture is advanced to the secondary extruder, where additional mixing is accomplished and material is cooled to a temperature which is suitable for making highly expanded polyethylene insulation. After that the mixture is extruded through the die.

In order to make a stable extrusion and uniformity of polyethylene and nitrogen gas, the line is carefully designed. We adopted the two-stage extruder to obtain a stable gas pressure at the injection zone in the primary extruder. The primary extruder's screw is a venting type, which is so designed that its venting zone is located just at the gas inlet and provided with special mixing device. The secondary extruder's screw is a common mixing type and its metering zone is specially designed so as not to cause the regular fluctuation of out-put. In this process extrusion temperature must be strictly controlled and stepless controllers are used for regulating temperature of the cylinder barrel, the cross-head and the extrusion die of the secondary extruder.

2-2-3. Nitrogen gas injection unit

The layout of the injection unit is shown in Fig.2. It consists of the supply tank, compressor, pressure stabilizer and specially designed inlet valve. The gas is taken from the supply tank and it is possible to obtain desirable pressure with the pressure stabilizer.

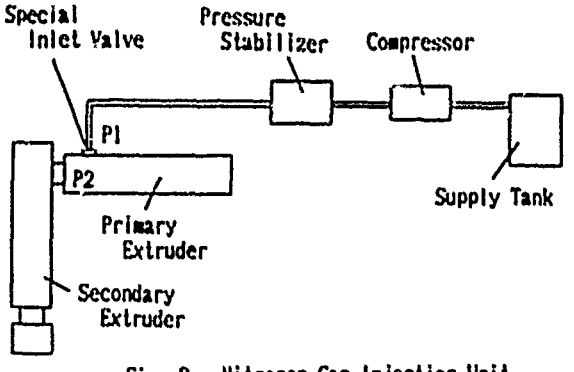

Fig. 2. Nitrogen Gas Injection Unit

We control the mass flow of gas by adjusting the gas pressure at inlet (P1) and molten polyethylene pressure at injection part of primary extruder (P2). Moreover, in order to prevent the fluctuation of flow, we make P1 constant with the pressure stabilizer and P2 with the two-stage extruder.

2-2-4. Adhesive resin applicator

Coatable plastics, such as modified low density polyethylene with a high melt index, are applied to the surface of the conductor at the adhesive resin applicator by a floating die. This process is immediately followed by the extrusion of expanded insulation. The adhesive coating insures good adhesion between the conductor and expanded insulation. If it doesn't have enough adhesion, the expanded polyethylene wouldn't be perfectly insulated and the cable core collapses into the figure eight form such as Fig.3.

2-3. Materials

2-3-1. Insulation materials

Through the investigation of the conventional expanded extrusion techniqus, such as fluorocarbon extrusion and the chemical blowing method, we have obtained the knowledge that the development of material was very important to obtain high expansion rate. From this investigation we developed the new material for nitrogen gas extrusion.

Table 1 shows the result of material evaluation. In Table 1, resin A, resin B are mixture type of low density polyethylene (LDPE) and high density polyethylene (HDPE) and resin C is HDPE which is now used as insulation for telecommunication cables in our company. They all contain a small amount of antioxidant and nucleating agent to obtain fine cells. Resin A is a specially modified compound for new process, which comprises LDPE with unique arrangement of side chain and some amount of special HDPE which provides a high mechanical strength of expanded insulation and improves the extrudability. Resin B is formulated with above LDPE and resin C. Resin A gives the most desirable expansion rate and cell structure, but resin B and resin C didn't show good results.

2-3-2 Adhesive material

Adhesive material is more important for nitrogen gas extrusion than for fluorocarbon extrusion. In case of nitrogen gas extrusion, it's more necessary to keep

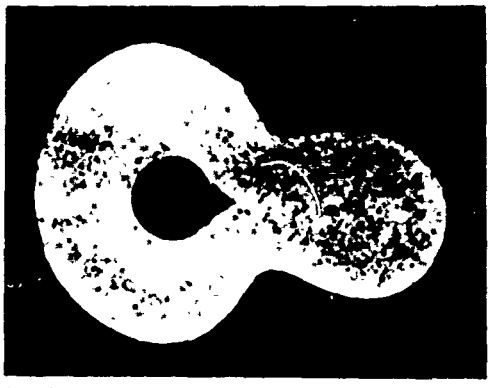

Fig. 3. The Core with the Figure Eight Form

Table 1. Properties of Insulation Materials

Item \ Materials		Resin A (New Material)	Resin B	Resin C	Remarks
Contents	LDPE	Special LDPE	Special LDPE	---	
	HDPE	Special HDPE	Resin C	Resin C	
Density (g/cm3)		0.93	0.93	0.96	
Melt Index (g/10 min.)		2.51	1.60	0.75	
Expansion Rate (%)		81	70	57	Specific Grarity Method
Cell Structure		Fine	Coarse	Coarse	

Note : Conductor diameter : 2.85 mm
Insulation diameter: 11.5 mm
Blowing agent : Nitrogen gas

Table 2. Properties of Adhesive Materials

Item \ Materials	Resin D (New Material)	Resin E (Conventional Material)
Density (g/cm3)	0.92	0.92
Melt Index (g/10min.)	6.35	20.0
Ultimate Strength (kg/mm^2)	1.4	1.3
Elongation (%)	545	550

insulation layer and adhesive layer. Table 2 shows the result of material evaluation. Resin E is used in the conventional fluorocarbon extrusion in our company, but the adhesion is not enough. Therefore, resin D is developed by formulating the resin E with special additive.

2-4.Extursion condition

2-4-1 Nitrogen injection condition

For the purpose of achieving desirable expansion rate, we adjust the gas pressure (P1) and molten polyethylene pressure at the injection zone in the primary extrder (P2) so as to control the mass flow of gas which is injected into primary extruder and mixed with molten polyethylene. Fig.4 shows the relationship among P1,P2 and the expansion rate. P1 will be controlled in the range of 20 ~30 kg/cm^2 higher than P2. Ordinarily P2 is selected within 30 ~80 kg/cm^2 considering safty of high pressure and stability of P2.

2-4-2 Insulating condition

We made the first experiment using the same crosshead tools, adhesive material and insulation condition for fluorocarbon extrusion, but it failed. The expanded polyethylene wasn't insulated perfectly and the cable core collapsed into the figure eight form, such as Fig.3. By observing Fig.3, there is a part of the insulation layer separated from the adhesive layer and it has collapsed. We supposed that bad insulation is caused by the lack of adhesion between the insulation layer and the adhesive layer. Through some trials , it has been clear that the core easily collapses as the expansion rate become higher, especially over 70%.

Therefore, we have developed a suitable cross-head tools and modified adhesive resin and selected the suitable pre-heating temperature and stock temperature in order to achieve enough adhesion. We have succeeded in production of the round and good cores.

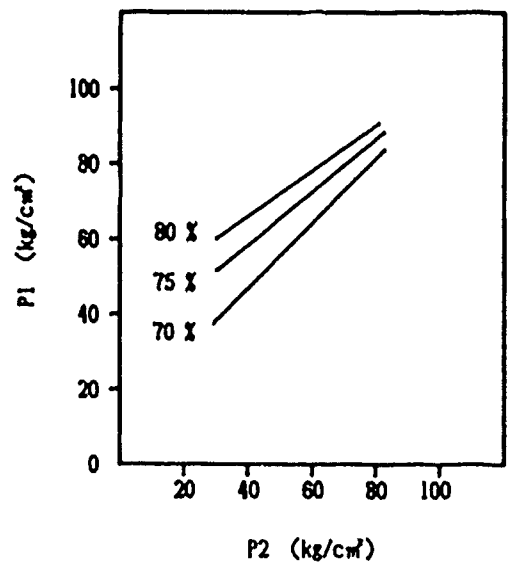

Fig. 4 The Relationship among P1,P2 and the Expansion Rate

2-5. Manufacturing

Two standard sized CATV cables shown in Table 3, with about 80% expanded insulation have been successfully manufactured. The extrusion speeds are approximately equal to those of the conventional process using fluorocarbon. In case of 8C-SA cable the core diameter and capacitance are controlled within ±0.6 % and ±0.4 % . The fluctuations are shown in Fig.5 and Fig.6. Cross-sections of expanded insulations are shown in Fig.7 and Fig.8, illustrating that the both cell structures are excellent and equal to those made by using fluorocarbon.

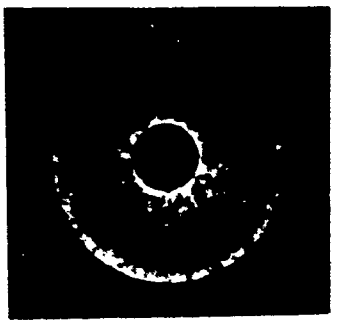

Fig. 7. Cross-Section of 8C-SA Cable

Table 3. Cable Structures

Cable Type	8C-SA	12C-SA
Diameter of Inner Conductor (mm)	2.08	2.85
Diameter of Core (mm)	8.50	11.50
Diameter of Outer Conductor (mm)	9.50	12.70
Diameter of Polyethlene Jacket (mm)	11.90	15.30

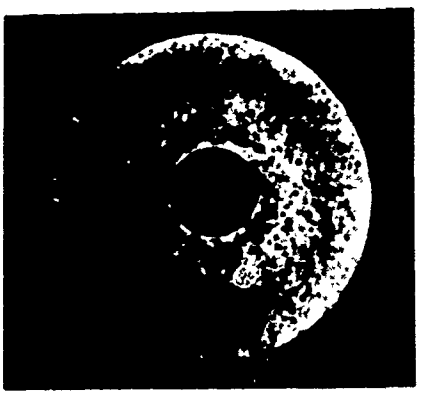

Fig. 8. Cross Section of 12C-SA Cable

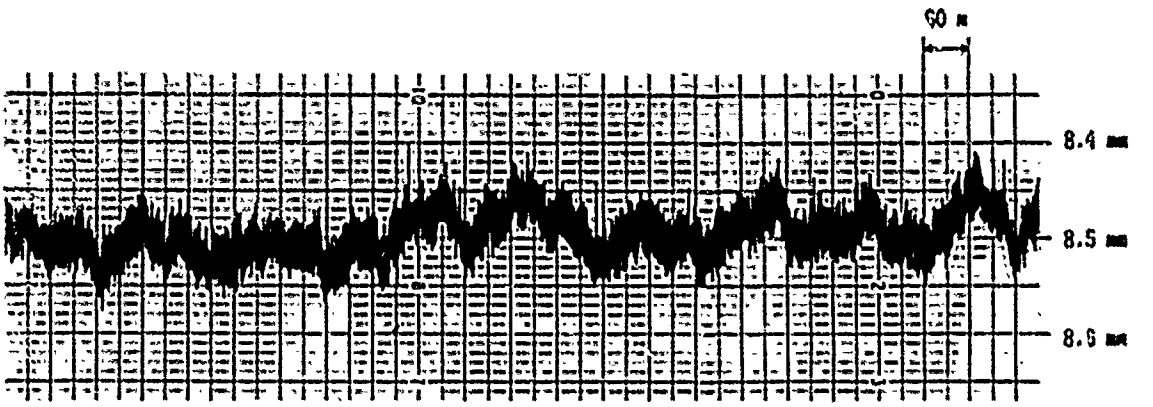

Fig. 5. Diameter Fluctuation of 8C-SA Cable

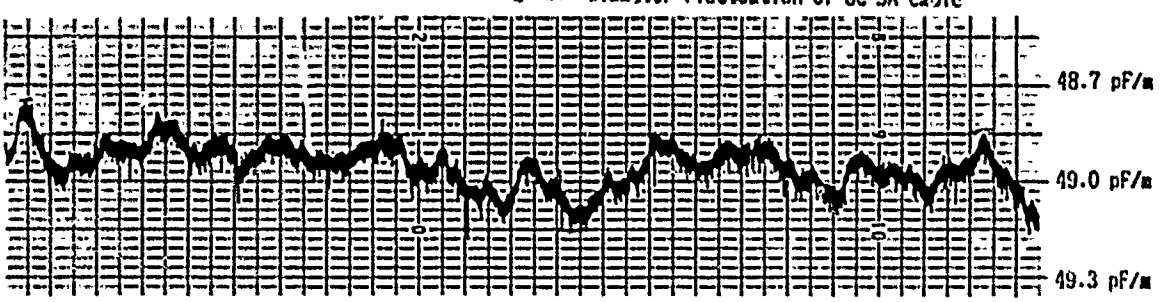

Fig. 6. Capacitance Fluctration of 8C-SA Cable

Table 4. Properties of Cables

Items \ Cable Size		8C-SA	12C-SA
Electrical Properties	Attenuation Constant at 250 MHz (dB/km)	52	35
	Characteristic Impedance at 10 MHz (Ω)	75	75
	Dissipation Factor at 23 ℃	0.7×10^{-4}	0.7×10^{-4}
	Dielectric Constant at 23 ℃	1.24	1.24
Mechanical Properties	Bending Test	No Cracks	No Cracks
	Pull-Out Strength (kg/20cm) Inner Conductor to Insulation Outer Conductor to Insulation	 Over 20 4.5	 Over 20 7.0
	Vibration Test	No Cracks	No Cracks

Note
1) Bending test condition
Bending diameter : 238 mm (8C-SA)
306 mm (12C-SA)
Bending angle : ±180 ° / cycle
Number of bending : 3 cycles

2) Vibration test condition
The cables are fixed as shown in Fig.12
Amplitude : ±5 mm
Cycle : 10 Hz
Number of times : 1 million times

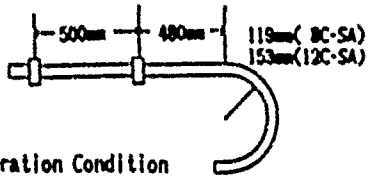

Fig. 12 Vibration Condition

3. PROPERTIES OF CABLES

Table 4 shows the electrical and mechanical properties of CATV cables using this new process.

3-1 Electrical properties

The frequency characteristics of attenuation constants and the VSWR characteristics are shown in Fig.9 through Fig.11. Attenuation constants are equal to those of cables manufactured in conventional fluorocarbon extrusion and the VSWR charts show excellent properties due to stable extrusion and specially designed extrusion line.

3-2 Mechanical properties

Bending test, pull-out strength test and vibration test are carried out and show good results compared to conventional cables.

4. CONCLUSION

An extrusion technique of highly expanded polyethylene by nitrogen gas has been developed and applied to CATV cables instead of conventional fluorocarbon, which causes the air-pollution. Main features of our nitrogen gas extrusion process are as follows.:

(1) Non-polluting and safe high expansion process.
(2) The process uses a specially designed extrusion line and matrials.

- A specially designed two-stage extruder to obtain good uniformity of polyethylene and nitrogen gas.
- A specially designed cross-head tools and a specially modified adhesive material to realize the insulation with round core.
- A specially modified insulation material for high expansion.

5.REFERENCE

1) Mr.Yuto and Mr.Nakahara, et al., "Novel Extrusion Process for Robust Highly Expanded Polyethylen Insulated Coaxial Cables ", 25th International Wire and Cable Symposium.1976.

2) Mr.Suzuki and Mr.Mori,et al., "Microaxial Cables Insulated with Highly Expanded Polyethylene by Chemical Blowing Method ", 27th International Wire and Cable Symposium.1978.

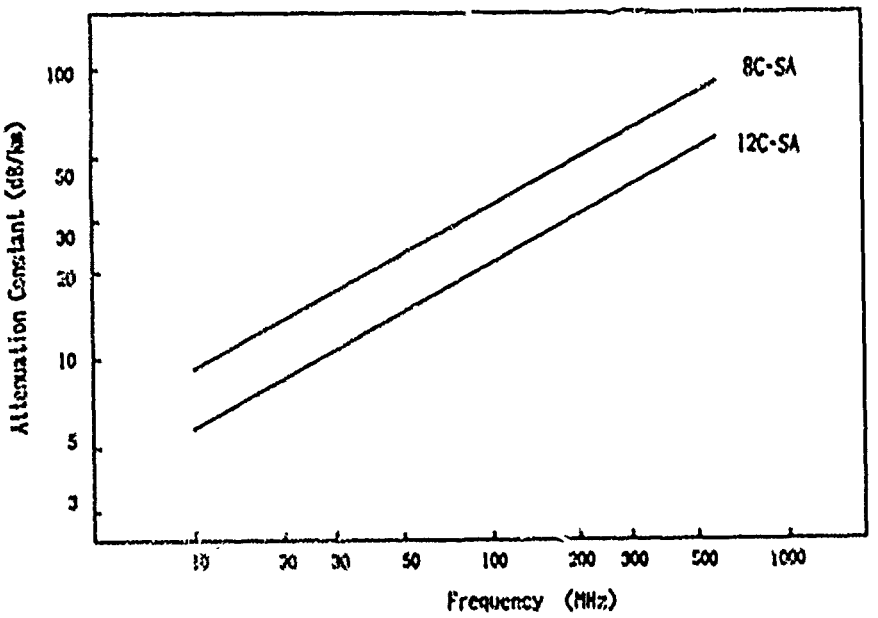

Fig.9 Attenuation Constants vs Frequency Characteristics

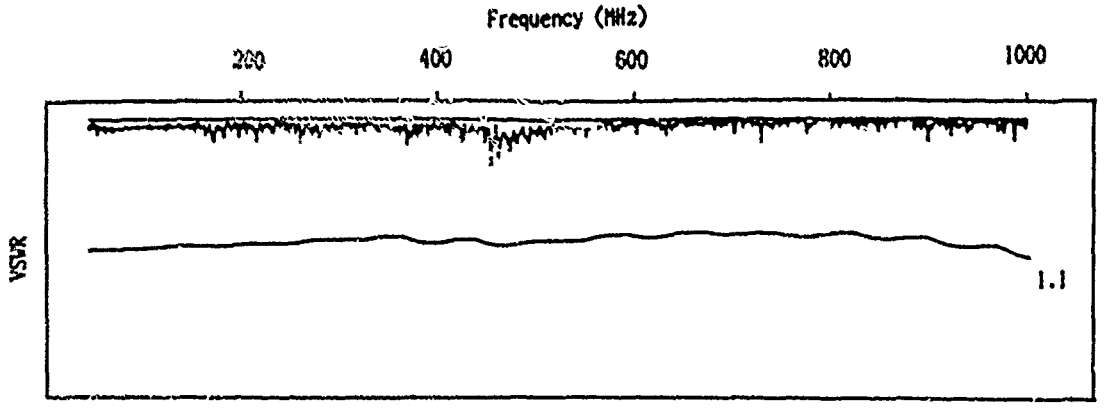

Fig.10. VSWR Characteristics of 8C-SA Cable

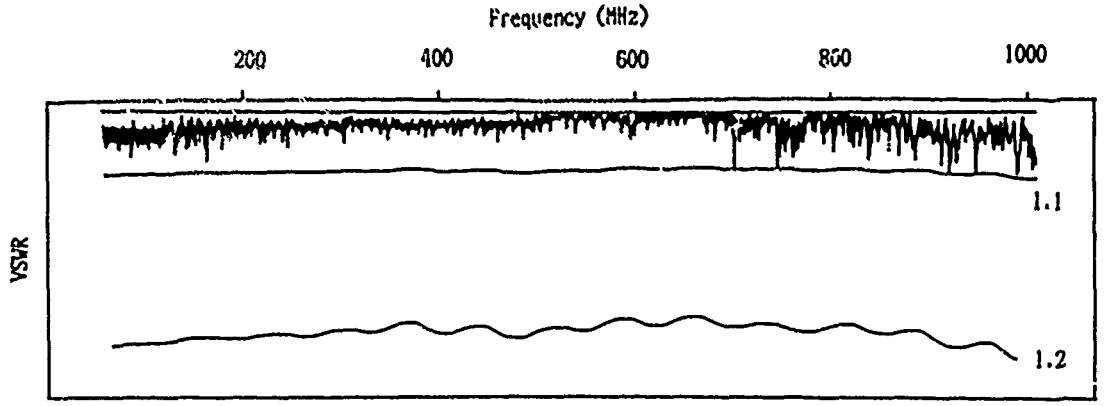

Fig.11. VSWR Characteristics of 12C-SA Cable

Mahito Ishikawa

Sumitomo Electric
Industries, Ltd.
1, Taya-cho
Sakae-ku
Yokohama
Japan

Mahito Ishikawa received his B.S.degree in metal engineering from Tohoku Univ. in 1969. He then joined Sumitomo Electric Industries, Ltd. and has been engaged in communication cable production. He is now a manager of Communications Div..

Saburo Kavabata

Sumitomo Electric
Industries, Ltd.
1, Taya-cho
Sakae-ku
Yokohama
Japan

Saburo Kavabata graduated from Niitsu Industrial High School majoring mechanical engineering in Niigata Prefecture in 1968. He then joined Sumitomo Electric Industries, Ltd. and has been engaged in plant for communication cables and test plant. He is now a member of Communications Div..

Yoichi Suzuki

Sumitomo Electric
Industries, Ltd.
1, Taya-cho
Sakae-ku
Yokohama
Japan

Yoichi Suzuki received his B.S.degree in applied chemical engineering from Tohoku Univ. in 1971. He then joined Sumitomo Electric Industries, Ltd. and has been engaged in research and development of communication cable production. He is now an assistant general manager of Communications Div..

Shigenori Takaki

Sumitomo Electric
Industries, Ltd.
1, Taya-cho
Sakae-ku
Yokohama
Japan

Shigenori Takaki graduated from Tohoku Univ.in 1986 with B.S.degree in mechanical engineering. He then joined Sumitomo Electric Industries, Ltd. and has been engaged in communication cable production. He is now a member of Communications Div..

Yasushi Ito

Sumitomo Electric
Industries, Ltd.
1, Taya-cho
Sakae-ku
Yokohama
Japan

Yasushi Ito received his B.S.degree in mechanical Engineering from Kyusu Institute of Technology in 1977. He then joined Sumitomo Electric Industries, Ltd. and has been engaged in plant engineering for communication cables and test plant. He is now a assistant general manager of Communications Div..

RHEOLOGY OF A POLYMER BLEND FOR CABLE-FILLING COMPOUNDS

Saad A. Khan* and Elliott E. Hershkowitz*

* Bellcore, 331 Newman Springs Road, Red Bank, NJ 07701
* Bellcore, 445 South Street, Morristown, NJ 07960

ABSTRACT

Blends of rubber, polyethylene and mineral oil are used to fill buried telephone cables to limit water intrusion that may adversely affect their performance. Rheological measurements show the material to be resistant to permanent chemical degradation that can occur during processing or prolonged exposure to elevated temperatures. Studies done at 60 °C show the material to exist as a phase separated system with any applied deformation causing structural breakdown and reduction in viscosity and moduli. The structural breakdown is physical because the initial properties are recovered upon heating the sample above its separation temperature. Studies done on individual components (rubber, polyethylene) reveal that the rubber is dissolved in the mineral oil; the polyethylene crystallites act as a suspension forming an incipient network that is disrupted by shear. Room temperature studies indicate a significantly reduced sensitivity of the structure to any applied deformation. The material is much more elastic than viscous, retaining much of its structure to support water pressure heads. The improved elastic properties are a consequence of the rubber existing in a microphase separated state and forming sufficiently strong physical cross-links.

1. INTRODUCTION

Polyolefin insulated telephone cables (PIC) in the buried environment are filled with polymeric compounds to prevent water intrusion that can adversely affect their performance [1, 2]. The original PIC cable in buried plant had an unfilled, air core with polyethylene conductor insulation and a polyethylene outer jacket. In the buried environment, these cables were susceptible to water penetration through pin-holes in the outer jackets, damages caused by the rigors of installation or stress cracking of the polyethylene. Consequently, a petroleum jelly (PJ- oil and wax) was introduced as a filler [3] to limit the void in the core. This material proved to be unsuitable because it flowed in the cable during storage and ran out of it in hot weather.

A high viscosity material, consisting of a mixture of polyethylene and petroleum jelly (PEPJ), was subsequently developed [1, 3]. This material caused handling problems during splicing. In addition, it is brittle at room temperature and produces voids by thermal shrinkage through which water can penetrate. Presently, the PEPJ compounds have mostly been superceded by extended thermoplastic rubbers (ETPR) which are block copolymer solutions in mineral oil [1]. These materials are easy to handle, and are less likely to form voids by thermal shrinkage since they remain rubbery ("soft") at low temperatures.

In this paper, we use rheological techniques to assess the effect of processing on the properties and reliability of the ETPR compound. This is part of an overall study to better understand the water blocking ability of the filling-compound and to provide guidelines for more effective water resistant cables. These are important issues because there have been reports of filling-compound failures arising from oil separation from the bulk material. Furthermore, there is considerable interest in replacing pressurized cables in underground duct systems (urban environments) with filled cables. The high costs associated with new pressurized plant, combined with the splicing advantage of color coded cables make filled systems very attractive. However, the cables in an underground environment are exposed to more severe conditions since they can be under as much as twenty feet of water. The filling compounds must be capable of limiting water intrusion at such pressure heads to prevent degradation of the electrical properties of the cables and splices. The absence of an incipient trouble indicator, such as an air leak, places the burden of cable integrity on the filling compounds and the splice encapsulants.

2. EXPERIMENTS

Materials

The principal components of the filling-compound used in our study consist of a styrene-ethylene/butylene-styrene (S-EB-S) triblock copolymer (Krayton G, manufactured by Shell) with a molecular weight of 54,000 and a S/EB ratio of 29/71, a low molecular weight polyethylene, and mineral oil. These are mixed to obtain the final product with approximately the following weight composition: 88% mineral oil, 6% SEBS rubber, 4% polyethylene, 2% antioxidants and stabilizers [4]. Depending on temperature, this material may exist as a macro- or a combination of macro- and micro-phase separated system. The macro-phase separation

occurs below ~100 °C when the polyethylene crystallites form a suspension. The micro-phase separation depends on the interaction of the solvent with two thermodynamically incompatible phases (PS and PEB) of the rubber. Since the solubility parameter of mineral oil (δ_s=7.4) is not in between that of PS (9.1) and PEB (7.9), but close to that of PEB, it can only solvate this elastomeric mid-block [5]. The PS end-blocks unite to form submicroscopic particles or domains, the shape and size of which are functions of both the concentration and temperature of the system. At our low concentration of 6% SEBS rubber, spherical microdomains [6, 7] may be formed. The microphase separated system undergoes a transition from the ordered to the disordered state, referred to as the microphase separation transition (MST) [6-9], at a certain temperature.

Methods

Rheological techniques were used in this study because the viscoelastic properties are directly related to the processing and water blocking ability of the cable-filling compound. Steady and dynamic shear experiments were used to investigate the properties of the system. The steady shear experiments are useful to simulate flows under processing conditions as they provide viscosity data as a function of shear rate. For complex systems, however, the measurements do not provide sufficient information on the long-range order as shear rate covers the microstructure of the system. On the other hand, the small deformation applied in dynamic tests does not alter the microstructure of a system and is effective in probing any long-range order that may exist. In the dynamic experiments, a sinusoidal strain γ is imposed on the sample at a frequency ω and strain amplitude γ_o.

$$\gamma = \gamma_o \sin \omega t \qquad (1)$$

In the linear viscoelastic (low strain) regime, the resulting stress is also oscillatory and can be decomposed into two parts [10]:

$$\tau_{yx} = \gamma_o [\, G' \sin \omega t + G'' \cos \omega t] \qquad (2)$$

The stress response in-phase with the strain defines the storage or elastic modulus G', and the out-of-phase response defines a loss or viscous modulus, G''. The elastic modulus is sensitive to the structure of the material. The dynamic analog to the steady shear viscosity (η) is the complex viscosity defined as,

$$\eta^* = [G'^2 + G''^2]^{1/2} / \omega$$

A Rheometrics Mechanical Spectrometer (RMS 800) having a cone and plate geometry was used for our measurements. Data were taken at 60 °C and 25 °C because they are typical of the temperatures used in drip and pressure head tests respectively.

3. RESULTS

An important aspect of this study has been to determine the effects of processing/shear and thermal aging on the properties of the filling-compound. Fig. 1 illustrates the effect of shear on the viscosity-shear rate response of the material at 60 °C. The first run (Run 1) was made after putting the sample in the rheometer and heating it to 60 °C. With each subsequent measurement (Runs 2 and 3), we find the viscosity to decrease at low shear rates. This indicates that shear breaks down the long-range microstructural order. The comparable values between Runs 2 and 3 indicate that most of the long-range order has been destroyed by the end of Run 2. After Run 3, we heated the sample in situ in the rheometer to 100 °C (the material is homogeneous and has a Newtonian viscosity at this temperature) and held it there for 20 minutes. Run 4 shows the viscosity of the sample after it has been cooled back to 60 °C. The viscosity of the sample has increased by more than an order of magnitude at low shear rates. We therefore find that the shear induced degradation is reversible and the material recovers its structure when heated above its separation temperature. The big difference in viscosity at low shear rates suggest that the long-range order of the sample is extremely shear sensitive. The convergence of the viscosities at high shear rates, on the other hand, suggests that the short range structure of the material is relatively insensitive to shear history.

Dynamic oscillatory experiments were performed to probe further the shear sensitivity of the cable-filling compound. In Fig. 2, the effect of strain amplitude on dynamic properties are plotted. At the initial strain of 0.5%, the elastic modulus is larger than the viscous modulus by a factor of 3. The rapid decrease of G' with increasing strain is indicative of structural breakdown [11, 12]. At a strain of ~5%, there is a cross-over between G' and G'', and the material becomes more viscous than elastic beyond this strain. The increase in loss tangent (tan δ), defined as G''/G', from ~0.2 (solid-like behavior) to ~3.5 (fluid-like response) by the end of the run indicates structural breakdown. The sharp increase in tan δ for strains up to ~10% clearly reveals the sensitivity of the long-range order to any small deformation. With increasing strains an equilibrium structure is reached as evident by the asymptotic behavior of tan δ and similar steady shear viscosities of different runs (Fig. 1).

The thermal stability of the filling-compound was tested by maintaining it at 140 °C for 58 days, and then measuring its rheological proper-

ties. The viscosity shear-rate data of such a sample is plotted in Fig. 3. Runs 1 and 2 were done sequentially after putting the sample in the rheometer and heating it to 60 °C. The data in Run 3 were taken after the sample had been heated to and cooled back from 100 °C. As in the fresh sample, the aged material shows reversible shear induced degradation. In addition, the viscosity values fall within the envelope defined by that of a fresh sample (lines), indicating that ETPR is unaffected by adverse thermal conditions.

Dynamic measurements were used to study the effect of annealing on the properties of a shear-degraded material. In Fig. 4, we have plotted the loss tangent (tan δ) as a function of frequency(ω). Here, a sample cooled from 100 °C to 60 °C was sheared for 12 minutes at a shear rate of 0.4 s^{-1}. The dynamic properties were then measured at a strain of 10% (Sheared). After maintaining the sample at that temperature for 15.5 hours, we measured its properties again (Annealed). We find the loss tangent to be slightly smaller for the second run at low frequencies. Since the elastic modulus (G') is sensitive to the structure of the material and the loss modulus (G'') to the viscous dissipation, a smaller tan δ indicates the build up of some long-range order with time. This is however much smaller than what is observed when a sample is heated above its separation temperature (Fig. 1, Runs 3 and 4). Note that the high frequency responses of the two samples are similar because we are then probing only very short-range features of the microstructure at this strain amplitude.

The effect of cooling rate on the viscosity of the filling-compound is shown in Fig. 5. Two samples were cooled *in situ* from 100 °C to 60 °C, one in 8 minutes and the other in 2 hours. We find that rapid cooling of the sample results in a higher viscosity at low shear rates. Thus, the long-range features of the microstructure are different in the two cases; rapid cooling gives a kinetically controlled structure whereas slow cooling results in a thermodynamically controlled structure. Fig. 6 shows the time dependent behavior of the kinetically derived structure. In this figure, the dynamic moduli is plotted as a function of time for a sample that was cooled from 100 °C to 60 °C in ~7 minutes. In order to prevent shear induced structural breakdown, we perturbed the sample every 20 minutes instead of applying a continuous sinusoidal deformation. The dynamic properties show little change in the five hours of the experiment, suggesting that the relaxation or transition of the kinetically frozen structure to the thermodynamically favored one requires very long times if it occurs at all.

4. DISCUSSION

Measurements were done on the individual components of the filling compound at 60 °C to better understand its observed behavior. The effect of strain on the dynamic viscoelastic properties of a 12 wt. % rubber in mineral oil is shown in Fig. 7a. Unlike the filling-compound, we find the rubber solution to be strain-independent for relatively large strains. The shape of the curves are similar to polymer solutions and reveal no structural breakdown. The excellent agreement between successive runs also indicates absence of any structure. A plot of the moduli and complex viscosity (η^*) as a function of frequency (Fig. 7b) show presence of a zero-shear η^*, and G', G'' to have slopes approximating 1 and 2 at low frequencies -- behaviors typical of polymers dissolved in a solvent [13]. On the contrary, a plot of the loss tangent versus strain of a 10 wt.% polyethylene in mineral oil (Fig. 8a) reveal the presence of structure (tan δ < 1 at low strains) that is disrupted with increasing strain, similar to that of the filling-compound (Fig. 2). A follow-up to the first run (Run 2) show that most of the long-range order was destroyed in the first experiment because tan δ is greater than unity for all strains. In Fig. 8b, the flat moduli versus frequency curves indicate the material to have an elastic (suspension-like) character, but comparable values of G' and G'' suggest absence of any yield stress. Thus, at 60 °C, ETPR exists as a macrophase separated system. The rubber is solvated by mineral oil; the polyethylene crystallites acts as a suspension that forms some incipient but labile network structure. The extreme shear sensitivity make the filling-compound incapable of supporting any pressure at this temperature.

Dynamic experiments were conducted at room temperature (~25 °C) to assess the reliability of the cable-filling material at lower temperatures. Fig. 9a shows the moduli versus frequency response of the rubber component in mineral oil. At this temperature, the flat-shaped curves along with a substantially larger G' over G'' indicate the presence of a gel-like material [14]. We believe that the rubber exists in a microphase separated state with the polystyrene microdomains forming physical cross-links. These cross-links are sufficiently strong because we observe no structural breakdown with strain (Fig. 9b) and good overlap between the two runs in Fig. 9a, where Run 2 was conducted following the strain sweep.

The frequency dependence of the moduli of the filling-compound are plotted in Fig. 10a. We find a strong similarity between this and the rubber component behavior. In addition, we find the strain and frequency response of the polyethylene component (not shown) to be similar to its behavior at 60 °C (Fig. 8). All these suggest that ETPR at room temperature exists as both a macro- (PE) and micro-phase (SEBS) separated system with the rubber component dictating its behavior. From

Fig. 10b, which plots G', G'' and tan δ as a function of strain, we find a significant reduction in shear-induced breakdown. The loss tangent remains strain invariant at ~0.2 indicating that the material retains much of its elastic structure to support pressure heads.

5. SUMMARY

Rheological studies on a cable filling compound composed of a block copolymer, polyethylene and mineral oil revealed the following:

The cable filling compound is resistant to any permanent chemical degradation that can be caused by processing or prolonged exposure to high temperature. Studies at 60 °C show that the material is extremely shear sensitive and suffers structural breakdown with any applied deformation. Rough handling of the cables could, therefore, lower the viscosity and moduli of the material and make it more susceptible to water penetration. The material does not have a yield stress and will therefore not be able to support any water pressure heads.

The structural breakdown is physical in nature because the initial properties are recovered upon heating the sample above a critical temperature. Annealing also results in a slight recovery of properties. The rate of cooling the material also affects its final properties and possibly its microstructure. During the cable filling process, differences in cooling time may lead to non-uniform materials having variable degrees of water blocking ability.

Studies done on the individual components of the filling-compound reveal that the properties of the material at 60 °C is dominated by the polyethylene component. The rubber is compatible with mineral oil. However, the polyethylene crystallites form a network structure that can be disrupted by shear.

Room temperature results indicate a significantly reduced sensitivity of the structure to any applied deformation, with the material retaining most of its structure to support pressure heads. The improved elastic properties result from the rubber existing in a microphase separated state, and its polystyrene domains forming sufficiently strong physical cross-links.

Acknowledgements

The authors would like to thank S.E. Deering, I.M. Plitz and P.C. Warren for their help during the course of this work.

REFERENCES

1. A.C. Levy and R. Sabia, Proc. 31st International Wire and Cable Symposium (1982), 313.
2. C. Glenlewski and L.L. Blyler, Proc. 30th International Wire and Cable Symposium (1981), 270.
3. J.J. Kaufman and T.E. Luisi, Proc. 23rd International Wire and Cable Symposium (1974), 76.
4. U.S. Patent 4,259,540 (1981).
5. G.C. Hergenberger and M.C. Williams, Macromolecules 21 (1988), 1773.
6. M. Shibayama, T. Hashimoto and H. Kawai, Macromolecules 16 (1983), 16.
7. T. Hashimoto, M. Shibayama and H. Kawai, Macromolecules 16 (1983), 361.
8. F.S. Bates, Macromolecules 17 (1984), 2607.
9. J.L. Jorgensen in **Processing, Structure and Properties of Block Copolymers**, ed. M.J. Folkes (Elsevier Science, New York 1985).
10. R.B. Bird, R.C. Armstrong and O. Hassager, **Dynamics of Polymeric Liquids, Vol. 1: Fluid Mechanics**, 2nd ed. (Wiley, New York 1987).
11. E.M. Chan and R.K. Prud'homme, Rheol. Acta. 27, (in press).
12. S.A. Khan, P. Barboux, B.G. Bagley and F.E. Torres, J. Non-Cryst. Solids., (in press).
13. J.D. Ferry, **Viscoelastic Properties of Polymers**, 3rd ed. (Wiley, New York, 1980).
14. A.H. Clark and S.B. Ross-Murphy, Adv. Polym. Sci. 83 (1987), 60.

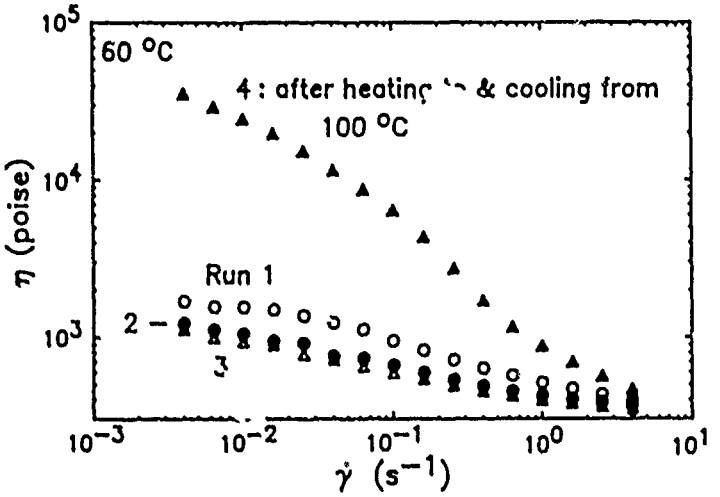

Fig. 1 Effect of shear on the viscosity vs. shear rate behavior of a polymer blend cable-filling compound. Runs 1 through 4 were done sequentially after loading the sample in the rheometer and heating it to 60 °C.

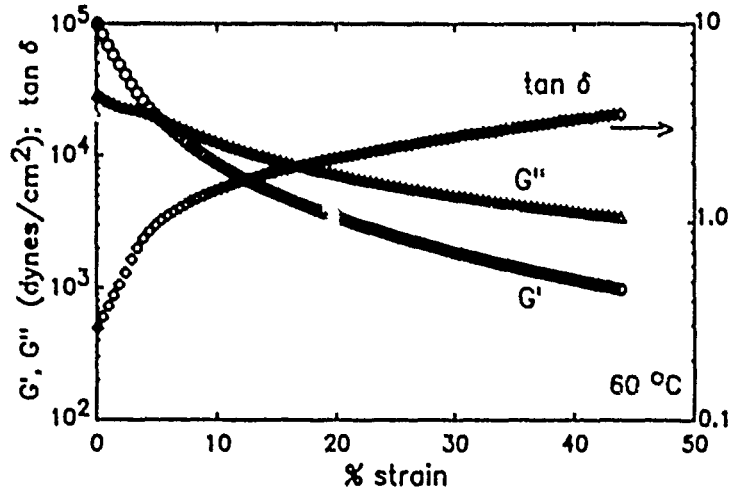

Fig. 2 Effect of strain amplitude on the dynamic viscoelastic functions of a polymer blend. The test was done at 60 °C after cooling the sample from 100 °C. The frequency of oscillation was 2.5 rad/s.

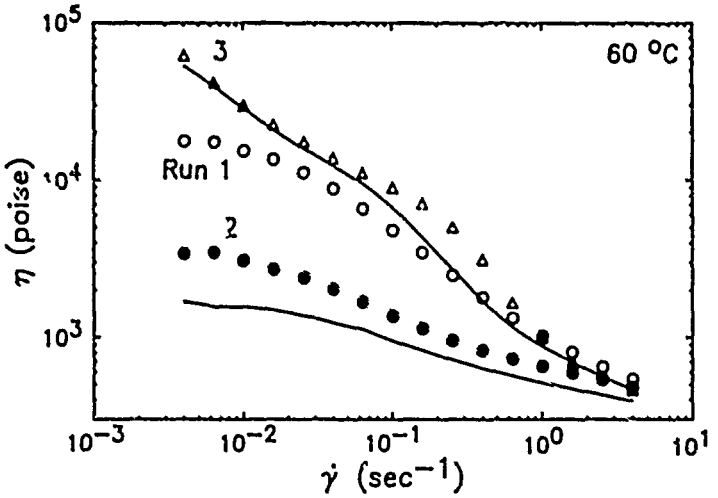

Fig. 3 Viscosity of an aged sample (58 days at 140 °C) are compared to that of fresh samples (lines). The runs were done sequentially at 60 °C; the sample was heated to 100 °C and cooled back again prior to run 3.

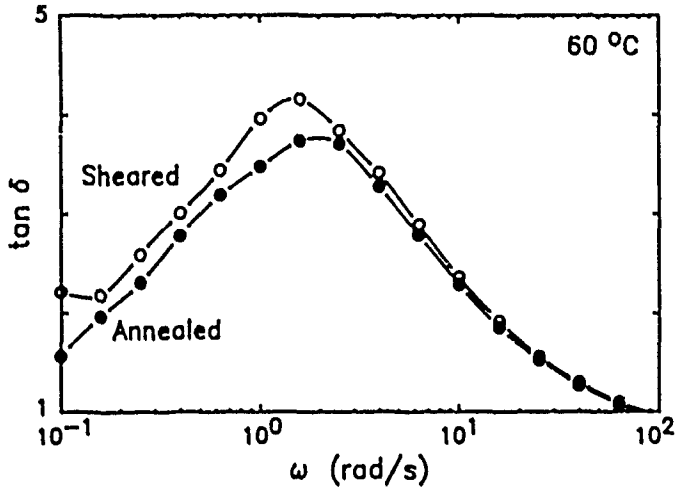

Fig. 4 Effect of annealing on the loss tangent of a polymer blend. The behavior of a sample immediately following shear (0.4 s^{-1} for 12 minutes) and after annealing (15.5 hrs.) are shown at a constant strain of 10%.

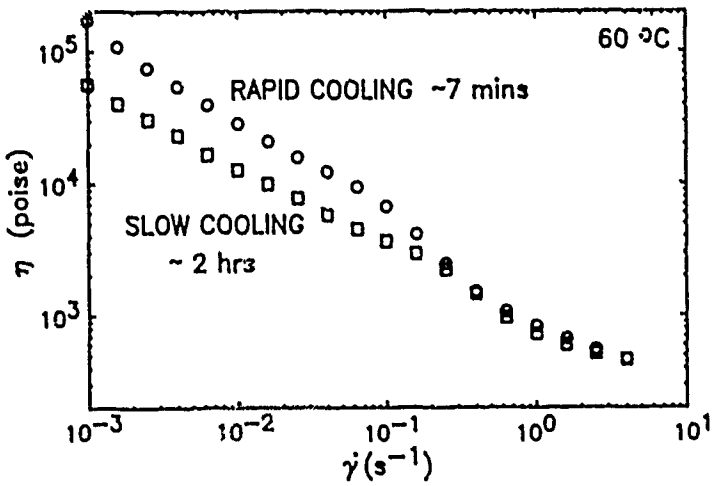

Fig. 5 The influence of cooling rate on the viscosity of a cable-filling compound. The samples were cooled in situ in the rheometer from 100 °C to 60 °C, one in ~7 minutes and the other in ~2 hours.

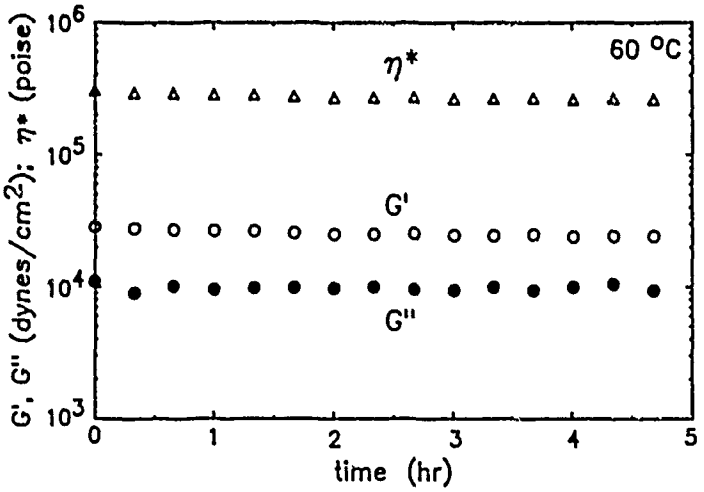

Fig. 6 Dynamic viscoelastic properties as a function of time for a sample cooled from 100 °C to 60 °C in ~7 minutes. The frequency and strain amplitude were 0.1 rad/s and 1.5 % respectively.

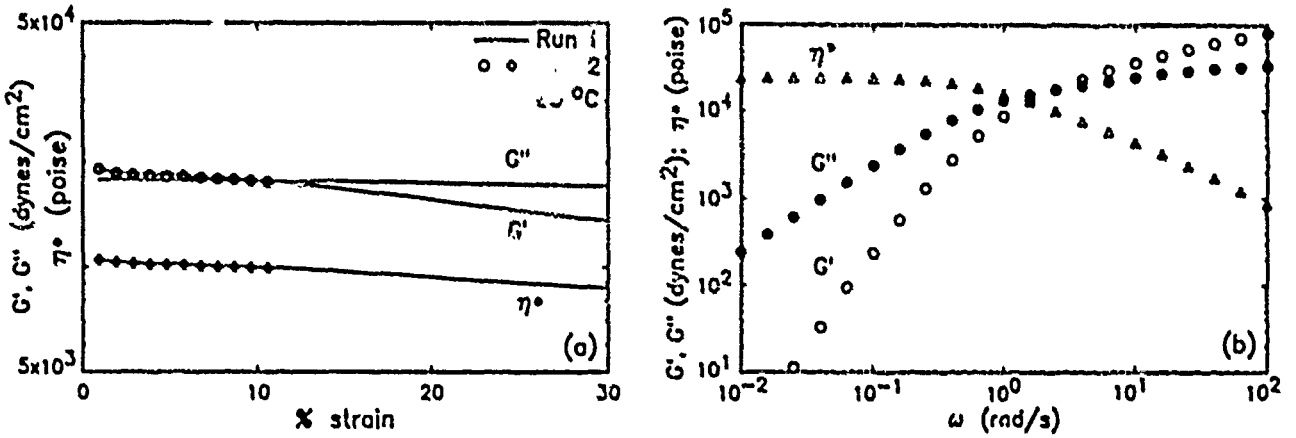

Fig. 7 The dynamic moduli and complex viscosity of the rubber component of the filling-compound (12 wt. % PEB in mineral oil) as a function of (a) strain under a constant frequency of 2.5 rad/s, and, (b) frequency at a constant strain of 8%. The measurements were done at 60 °C.

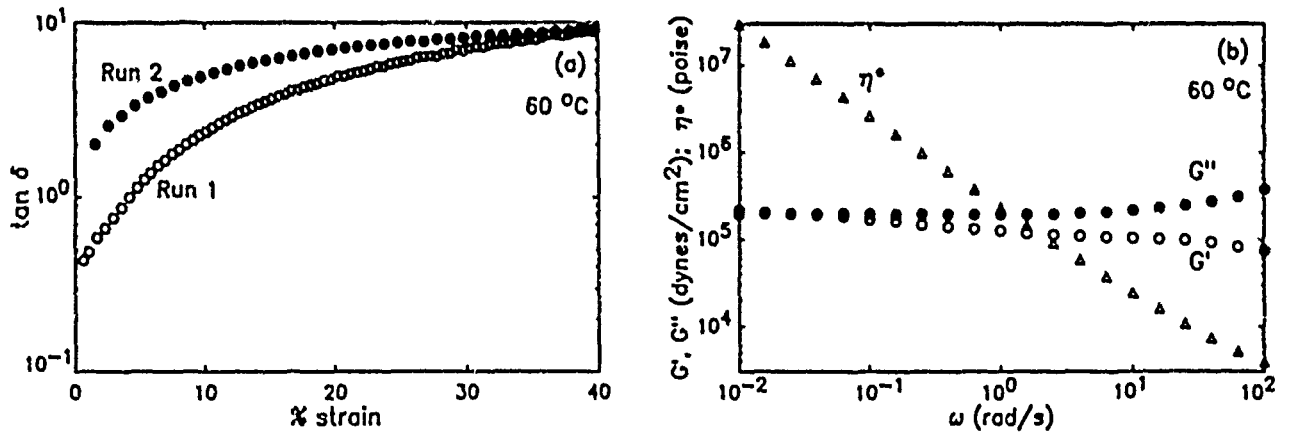

Fig. 8 (a) Effect of strain on the loss tangent of the polyethylene component (10 wt.% in mineral oil) of the cable-filling compound at 60 °C. The frequency was fixed at 2.5 rad/s. (b) Dynamic moduli and complex viscosity as a function of frequency for the same sample at a strain of 1.5%.

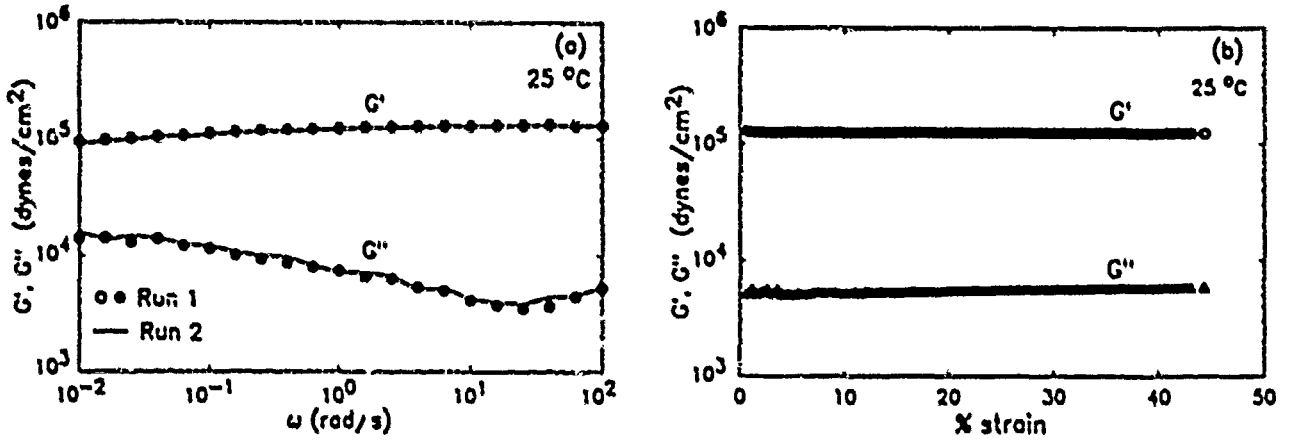

Fig. 9 The elastic and loss moduli of the rubber component at room temperature as a function of (a) frequency, and, (b) strain. The strain in (a) and the frequency in (b) were fixed at 1.5% and 2.5 rad/s respectively.

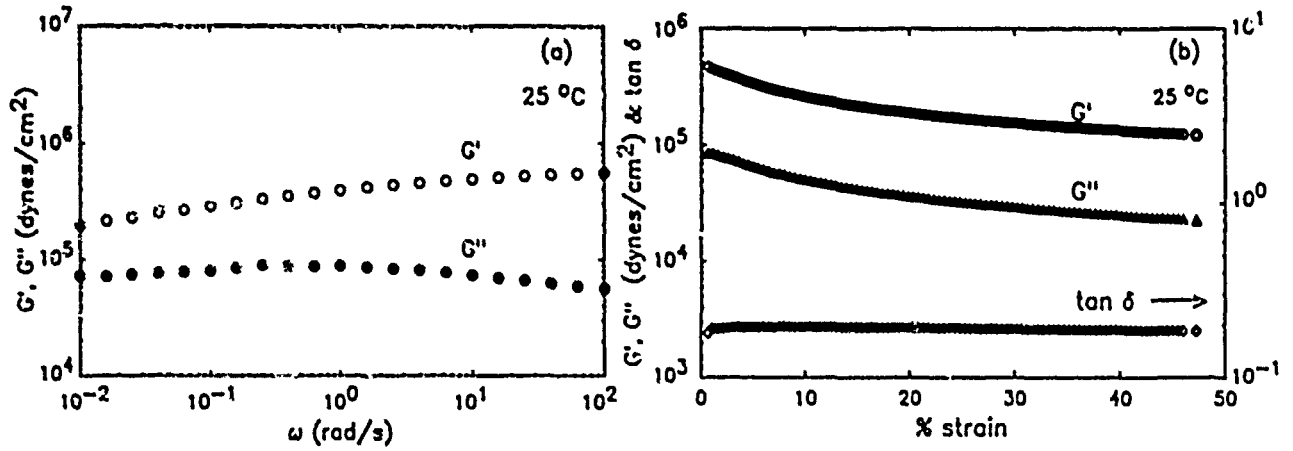

Fig. 10 Dynamic material functions of the polymer blend filling-compound at room temperature as a function of (a) frequency, and, (b) strain. The strain and frequency were kept constant in (a) and (b) respectively at 1.5% and 2.5 rad/s.

REFLECTIONLESS MECHANICAL INTERCONNECTION COMPONENTS FOR ANALOG SYSTEMS

J. A. Aberson, G. A. Alameel, G. F. DeVeau, K. M. Yatsuski

AT&T Bell Laboratories

2600 N.J. Expressway Norcross, GA 30071

ABSTRACT

By polishing 10-degree angles onto Rotary Mechanical Splices and ST® connectors, very low ("reflectionless") levels of return-loss (less than -60 dB) are achieved. Environmental stabilities, and field installation results are given for insertion loss and return loss. Angled Rotary splices are also shown to be tunable to very low (0.05 dB) insertion losses.

The return-losses demonstrated qualify angled Rotarys and ST® connectors [1] for analog video systems where worst-case reflections of less than -40 dB are now deemed necessary.

1. ST® connector is a registered trademark of AT&T.

INTRODUCTION

How and why mechanical splice and connector Fresnel reflections cause intensity noise in lasers and power penalties in digital optical-fiber systems have been vigorously debated questions for the past few years. Recently, standards bodies have come to general agreement that worst-case reflectances that are less than -25 dB or more conservatively -30 dB will have no adverse effect on present and future digital lightguide transmission systems. Most mechanical splices, including the Rotary Mechanical Splice (RMS), and physically contacting ST connectors have worst case reflectances less than -30 dB and are excellent choices for any digital network.[1]

Now the new "reflection" question is how amplitude-modulated (AM) video system performance is affected. First, optical isolators are used on transmitters to limit reflected energy from splices, from connectors and, just as importantly, from the fiber itself (Raleigh backscatter). This leaves, however, the question about affects of re-reflected energy from these same components into the receiver. Although AM analog video systems using LASER LINK™ [2] and standard RMS's are presently performing satisfactorily, a low-reflection angle-polish is available for the RMS if video system operators desire or if future systems demand extremely low splice reflectance. A similar angle-polish on the ST connector could be made available if applications warrant.

BACKGROUND

Reflections from fiber interfaces (mechanical joints) result from refractive index changes; i.e. index matching materials at splices, air or air bubbles, poorly polished surfaces, scratches, glass compaction, debris and to a lesser degree, optical differences between fibers. Various techniques have been employed to reduce these reflectances. These include: careful selection of index matching materials for splices with a refractive index the same as the fiber, selection of polishing media to avoid surface and subsurface damage,[2] fiber-to-fiber contact for connectors, and oblique fiber-end-faces.

For mechanical splices, selection of the proper index matching material is relatively easy, and when fiber end-faces are properly prepared in the laboratory, reflectances for both splices and connectors can be at very low levels. Field preparation, however, may introduce conditions that leave slight imperfections of polished fiber surfaces which cause some reflection. Typical reflectances from field installed standard Rotary splices and standard ST connectors range from about -30 dB to almost unmeasurable levels of about -70 dB with an average of less than -40 dB. These levels of reflected light will have no effect on digital and frequency-modulated (FM) analog systems. AM analog systems, on the other hand, are believed to require a lower maximum value of -40 dB and an average value of less than -50 dB.

2. LASER LINK is a trademark of Anixter

The easiest method of controlling reflectances from mechanical joints to meet AM needs is not to reduce the reflections themselves, but to prevent the reflected and re-reflected light energy from being captured and guided by the fiber back to the laser source or ahead to the receiver. As mentioned, optical isolators stop fiber, connector, and splice reflections from entering transmitters, but do not prevent re-reflected energy from finding it's way into receivers. A second method, and one that is general, is to create oblique end-faces[3] on the fibers at the joint. With end-faces of 6 degrees or more, any reflections from interface are reflected at an angle that is unacceptable by the fibers' mode field and thus the reflected energy is captured by the cladding (Figure 1) and then quickly attenuated.

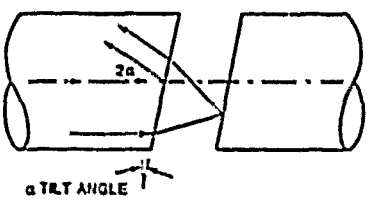

FIGURE 1

Splices and connectors that employ polishing methods for fiber-end preparation can be simply adapted to polish angles across fibers held in connector/splice ferrules.

LOW REFLECTANCE TECHNIQUE

Optical polishing fixtures have been designed to angle polish Rotary splices, Figure 2, and the ST connectors, Figure 3.

FIGURE 2

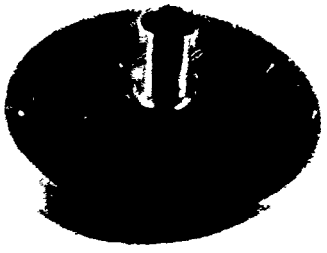

FIGURE 3

The end angle chosen for both Rotary splices and ST connectors is 10 degrees. Although angles of only 6 degrees are sufficient, a margin of 4 degrees was allowed for possible uneven fixture wear, variability, and initial tool tolerances.

To insure low insertion loss of joints, mated angled end-faces must match nearly parallel. To achieve this, the tabs on the Rotary splice are held by the slot in the polishing fixture, Figure 2. Likewise, the bayonnet feature of the ST connector keys into the ST connector polishing fixture. The alignment of the slot relative to the slope on the polishing fixture is such that only one fixture is required to polish both ferrule halves. Figure 4 shows where the angle is relative to the tabs on the Rotary and how the 10 degree angles parallel each other in a completed joint. This same concept is used with ST connectors.

Since mated ferrules are used with Rotary splices, very little rotational movement is usually required to tune standard 0-degree splices to insertion losses of 0.05 dB or less. Generally about 10 degrees of relative rotation between mated ferrules is all that is needed (which is about the width of the tab) to achieve this performance. Even with the 10-degree end-angles, angled Rotarys can be rotated to this amount, and consequently, can be tuned to the same low insertion losses as a standard RMS. ST connectors are, of course, not tuned.

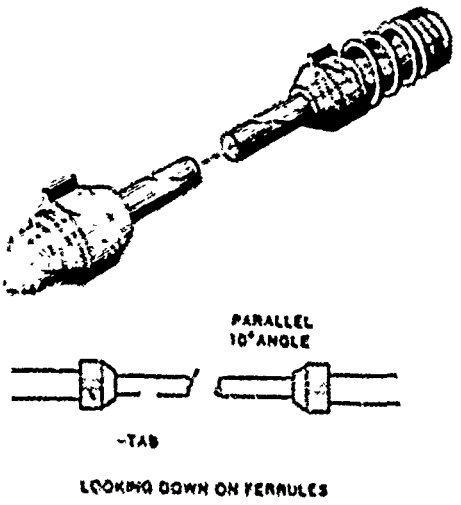

FIGURE 4

LABORATORY RESULTS - ENVIRONMENTAL PERFORMANCE OF ANGLED ROTARY SPLICES

Rotary splices were installed between two twelve-fiber ribbons with unlike fibers and polished with a 10-degree angle. Standard index-matching gel was used between the ferrules. These splices were tuned to an average splice loss of 0.054 dB with a standard deviation of 0.021 dB and set in an environmental chamber and cycled between -40°C and 85°C. Splice loss and reflectance (return loss) was measured at the temperature extremes and at room temperature using an Anritsu MW98A Optical Time Domain Reflectometer (OTDR). Figures 5 and 6 show the bidirectional average splice-loss and

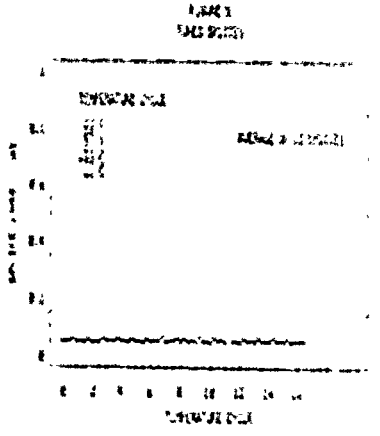

return-loss variations for these splices. These very small splice-loss variations look similar to or somewhat better than those for standard Rotary splices. The average return loss (-68 dB) shown for angled RMS is equivalent to fusion or "reflectionless" splices. When measured with an OTDR, return losses for angled RMS are indistinguishable from fusion splices, but angled RMS splice losses are lower.

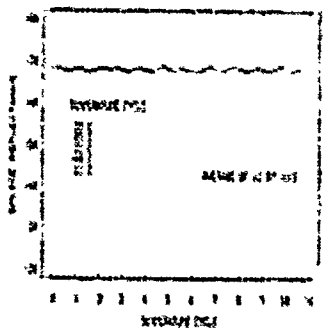

Angle-polished Rotary splices were installed by Southwestern Bell in St. Louis, Missouri in January 1989. A total of 55 splices were installed on a short C.O.-to-C.O. trunk. For this trial, only splices exceeding 0.20 dB (measured unidirectionally with an OTDR) were tuned. Tuning was done with an OTDR and only to the extent of reducing splice losses to less than 0.20 dB. Figures 7 and 8 show the bidirectionally measured splice loss and the reflectances of the 55 Rotary splices. The OTDR's pulse used limits measurements to -59 dB. Except for three splices at -46, -49 and -55 dB, all splices were reflectionless.

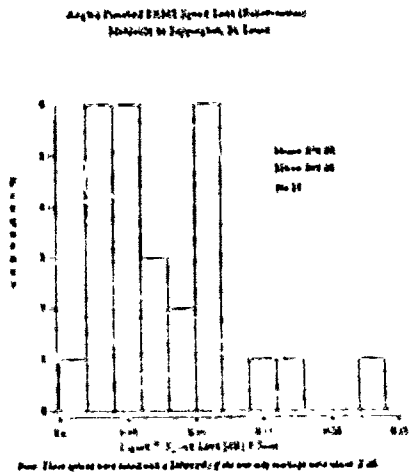

*While all 55 splices were measured with an OTDR unidirectionally from one end of the span or the other, only 27 were measured from both ends. Contrary to splice losses, accurate OTDR measurements for return-loss do not require bidirectional averages. Unidirectional measurements suffice.

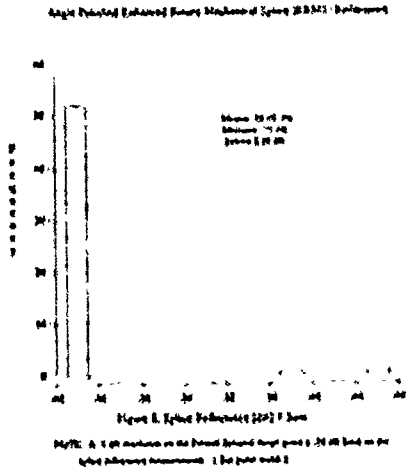

ANGLED ST CONNECTOR, LABORATORY RESULTS

A total of 20, single-mode, ST connectors (field-mountable) were installed using standard field tools and polished with the angled tool. This yielded a total of ten jumper cables. The splitter method for measuring reflectance was used to obtain room temperature data of insertion loss and reflectance. One hundred measurements were made by interconnecting the assembled pigtails. Figures 9 and 10 are histograms showing the distribution of loss and return losses from this study.

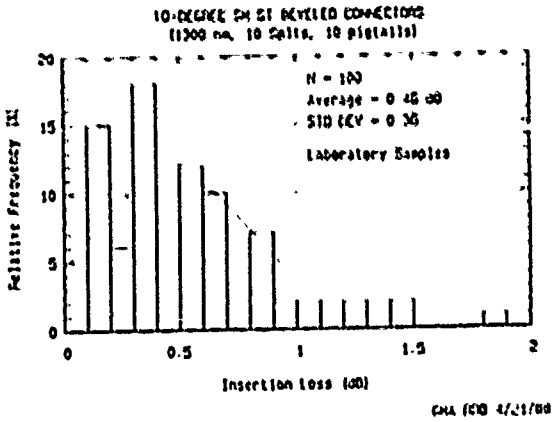

FIGURE 9

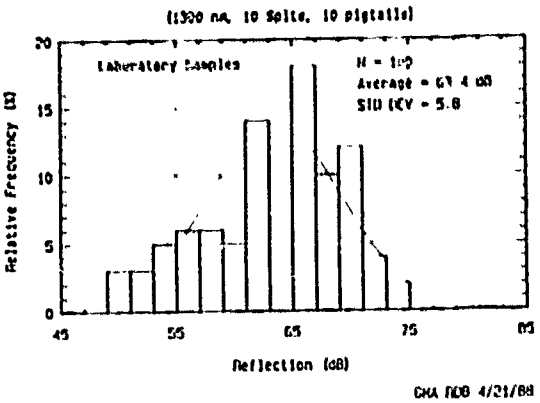

FIGURE 10

In order to do drop tests and environmental tests on the angled-polished ST connectors, four connectors were installed on 1.1 kilometer lengths of fiber so that an OTDR could be used to monitor performance. Drop tests from a height of 14 inches were performed while monitoring insertion loss and reflectance. Figures 11 and 12 show that the dropped joints remained stable.

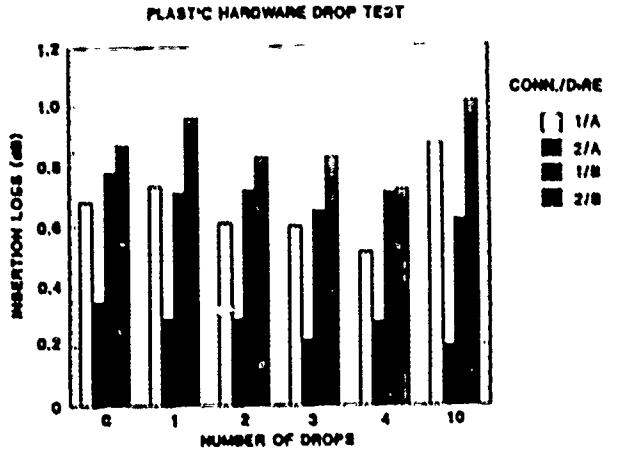

FIGURE 11

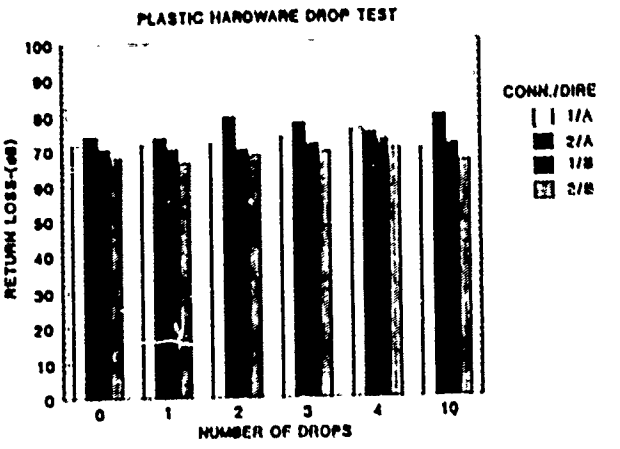

FIGURE 12

Figures 13 and 14 show the environmental performance of the ST connectors when cycled between -40°C and 85°C. Measurements were taken at 1300 nm and the connectors were exposed to each temperature extreme for at least 10 hours over a five day period.

Although the angle-polished ST connector is not currently a product, this effort demonstrates the feasibility of the approach if an application warrants it.

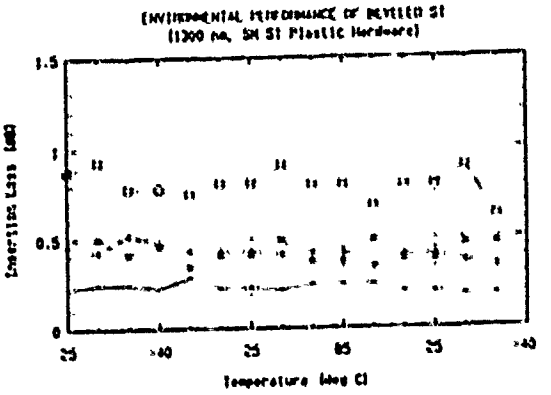

FIGURE 13

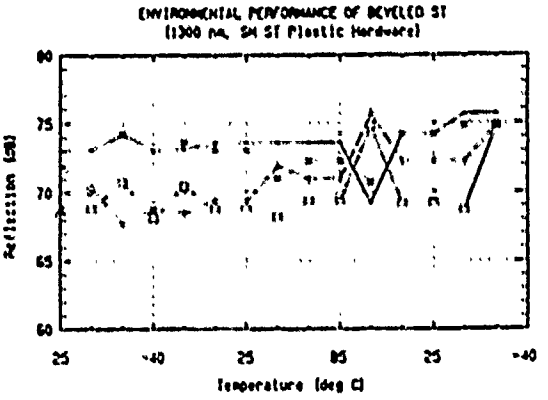

FIGURE 14

CONCLUSIONS AND RECOMMENDATIONS

As the presented lab and field results show, RMS and ST connectors with 10-degree fiber-end-faces achieve return-loss levels that are practically described as "reflectionless" (i.e. OTDR averages of less than -60 dB).

This reflection performance is achieved by substituting simple 10-degree angle polishing fixtures into the standard installation procedures. Moreover, by using the tabs on the splices/connectors, the 10-degree end faces of joined ferrules are made to align parallel to each other, and effects on joint insertion loss are thereby minimized.

Environmental (thermal cycling) and drop tests show stabilities that are at least as good as standard 0-degree RMS and STs.

Overall, the stable insertion-loss and return-loss performance of angled RMS and ST connectors make them completely suitable and recommended for an unrestricted use in any optical fiber system that will use AM analog (video) transmission.

REFERENCES

1. Judy, A. F., Aberson, J. A., DeVeau, G. F., "Field Measurements of Return Loss for Ferrule-Based Mechanical Splices," 37th IWCS, Reno, Nevada, 1988.
2. Clayton, J. B., Alameel, G. M., DeVeau, G. F., Sandahl, C. P., "Low-Reflection Polish for Ferrule-Based Mechanical Splices and Straight-Tip Connectors," OFC '89, Houston, Texas.
3. Young, W. C., Shah, V. S., and Curtis, L., "Optimization of Return Loss Performance of Single-Mode Fiber Mechanical Splices," 37th IWCS, Reno, Nevada, 1988.

James A. Aberson has been at AT&T Bell Laboratories, Norcross, Georgia since 1980, where he has worked principally on analysis and design of fiber splicing methods and devices. Since 1986, he has been Supervisor of the Lightguide Joining Group which is responsible for all fiber splicing methods and recommendations for AT&T and its customers. He holds BS, MS and PH.D. degrees in Structures and Mechanics from North Carolina State University.

Mr. Deveau is a Member of Technical Staff at AT&T Bell Laboratories, Norcross, Georgia. After joining Bell Laboratories in 1967 he was involved with multipair cable design and development. Since 1980 Mr. DeVeau has been engaged in the development of fiber optic splicing systems.

Kenneth M. Yasinski is a Member of Technical Staff at AT&T Bell Laboratories in Norcross, Georgia. After joining AT&T Bell Laboratories in 1981, his main area of responsibility has been in the development of fiber splicing techniques and tools. Mr. Yasinski received his BMET degree from the Southern College of Technology in Marietta, Georgia.

AN ENHANCED RIBBON STRUCTURE FOR HIGH FIBER COUNT CABLES IN THE LOOP

K. W. Jackson, P. D. Patel, M. L. Pearsall, J. R. Petisce
AT&T Bell Laboratories
Norcross, Georgia 30071

G. A. Lochkovic
AT&T Network Systems
Norcross, Georgia 30071

Abstract

Single-mode lightguide installations in the loop and in metropolitan area networks require high fiber count cables that can be placed, spliced, and reconfigured simply and rapidly. We describe the design, process, and performance characteristics of a new compact ribbon structure that meets the critical functional requirements of the loop environment. The new ribbon structure is an enhanced evolution of the Adhesive Sandwich Ribbon (ASR) technology first introduced by AT&T in the Chicago Lightwave Communication Project in 1977. The enhanced ribbon is based on UV coating technology similar to that used for fibers. Twelve coated fibers are colored in line, coated with a UV curable bonding matrix, and cured into a symmetrical compact array of twelve contiguous fibers. The fibers are equally suitable for mass silicon array or individual fiber splicing. Each individual fiber can be rapidly identified and accessed from either the cable end or mid-span. The new ribbons are robust and craft-friendly, yet 40% more compact than the ASR. Cabled ribbons have a simple unique marking identifier and up to 204 fibers can be placed into a compact 0.6 inch diameter sheath. The new ribbon demonstrates excellent cabling, low temperature and installation performance.

Introduction

As optical fiber technology migrates to the loop plant, cable designs must evolve to adapt to the special needs of the user. A tapered network of high fiber count cables with numerous branch points seems a probable feature of loop applications. The complex topology of a branched network requires cables with flexible features and increased quality. Global metrics of installed cost, operating expense, reliability, and compatibility with the existing infrastructure all become important. Several design parameters must simultaneously be considered to achieve an optimal design. This paper describes the design, process, and performance characteristics of a new generation AT&T ribbon structure that is more compact and tailored to the special requirements for loop plant and metropolitan area networks. The new ribbon, Xpress-12 AccuRibbon, is an advanced evolution of AT&T's original Adhesive Sandwich Ribbon (ASR). Figure 1 shows a sectional view of the AccuRibbon structure. AT&T was the first to develop fiber ribbon technology when the ASR structure was introduced in the Chicago Lightwave Project in 1977 (1,2). The new ribbon uses fiber coating technology to bond fibers into a linear symmetrical array instead of laminating them between two tapes.

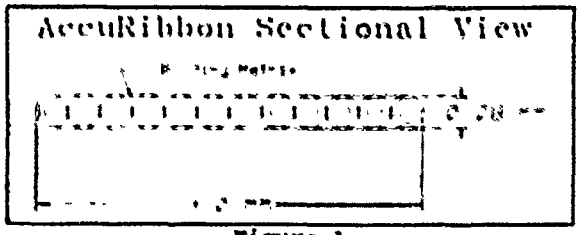

Figure 1

Design

Strategy

Manufacture of ribbons by tape lamination is complex because the tapes must be aligned, tensioned, and juxtaposed with a moving array of fibers and then trimmed to final shape. The enhanced ribbon uses state-of-the-art UV fiber coating process technology to simplify and optimize the manufacture of ribbons, and to provide improved quality. We used the method of robust design to determine optimal values for the ribbon design parameters (3). This technique uses designed experiments to identify settings of design parameters that render the product performance least sensitive to manufacturing, environmental, and use variation. Robust design is an effective strategy for improving product quality because the influence of the sources of variation are controlled in the design stage rather than controlling the sources of variation.

The properties of the material which bonds the fibers into a ribbon (bonding matrix), the ribbon geometry, and the application technique are major categories of design parameters. Performance metrics are cabling loss, low temperature added loss, handling robustness, fiber accessibility and identification, and aging reliability.

Bonding Matrix Material

The performance and manufacturability of fiber ribbons are closely related to the material properties of the bonding matrix materials. Important properties for product performance include modulus, adhesion to color-coded fibers, tear strength and aging reliability. The viscoelastic behavior of the matrix material modulus is important because it affects the deformation mechanics and microbending losses of the ribboned fibers during temperature cycling and aging (4). The time-temperature response of the matrix must be engineered to be compatible with long-term exposure to cable filling compounds and humidity. The chemical natures of these two environments are opposite and a balanced response must be achieved.

We evaluated ribbons made with bonding matrices having room temperature moduli from about 1 to 200 kpsi and different time/temperature behaviors. We found low temperature added loss variation least with matrix materials which give strain-free fibers in the cable. Added loss variation at a low temperature, T_L, after aging at a high temperature, T_H, is related to both the rate and magnitude of the change in matrix modulus over the temperature interval $[T_L, T_H]$. Figure 2 illustrates three typical modulus/temperature behaviors for matrix materials. Using T_o as a reference, ribbons made from Type-A materials typically show small

added loss variation as the temperature is lowered from T_0 to T_L because the modulus change is small and gradual. In contrast, Type-C materials that pass through a sharp glass transition between T_0 and T_L have a larger and steeper modulus change and greater added loss variation. When the ribbon samples are aged at T_H and then

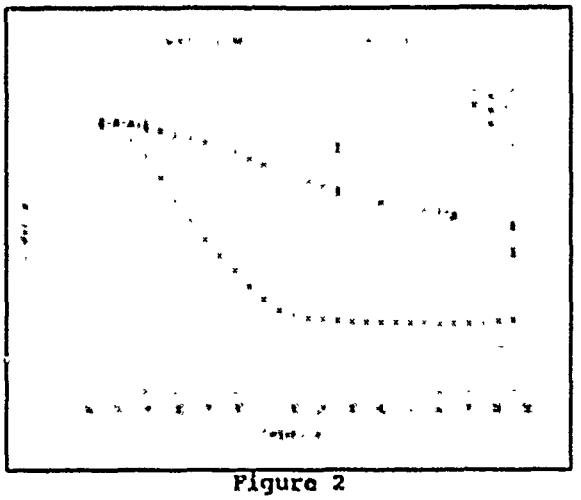

Figure 2

remeasured at T_L the Type-A materials pass through a glass transition and show increased added loss variation whereas the Type-C materials show little additional change in loss variation. We found matrix materials of Type-B behavior with small gradual changes in modulus over $[T_L, T_H]$ to be optimal for ribbons.

Ribbon robustness (the ability of the fibers to stay bonded together with handling) and easy fiber access (the ability of individual fibers to be easily separated from the ribbon) are competing requirements which require balancing interfacial and bulk properties. For example, we find ribbon robustness for cable processing and handling directly related to the room temperature modulus and tear strength of the matrix. In contrast, ease of fiber access is inversely related to room temperature modulus and tear strength. Moreover, ease of fiber access and identification is also strongly influenced by interfacial conditions between the matrix and the colorant on the fiber and between the colorant and the fiber coating. We find optimal fiber access and identification occur with cohesive failure of the matrix between contiguous fibers. Ribbon robustness also depends on long-term chemical compatibility with filling compounds, colorants, and humid air. Accelerated laboratory aging experiments verify long-term stability of the matrix with filling compounds as well as exposure to above ground outside-plant environments.

Production costs are related to line speed which depends on the cure speed of the matrix prepolymer. Rapid cure rates are desirable to make the degree of cure robust to perturbations in line conditions such as speed, UV dose, temperature and alignment.

Bonding Matrix Geometry

Two important structural parameters of a ribbon are the volume and geometry of the bonding matrix. These parameters are largely a function of the application technique and line conditions. Four different ribbon structures as illustrated in Figure 3 can be obtained depending on the application method. We found the symmetrical structure of Figure 3b with relatively flat ribbon surfaces like ASR to give the optimal ribbon performance. The structure of 3a is not optimal because the ribbon is thicker than necessary which can make single fiber access (breakout) difficult and reduce the packing efficiency in cable. A pronounced meniscus

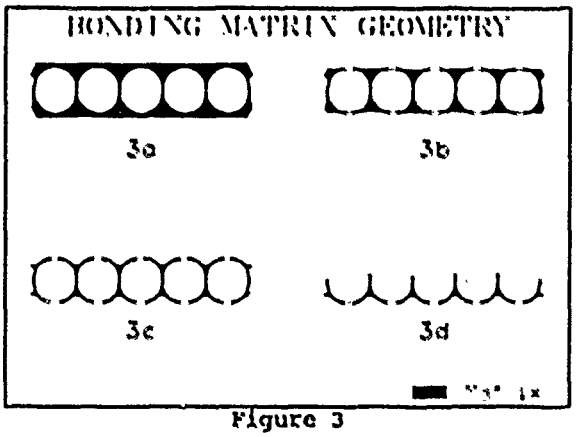

Figure 3

structure as in 3c, although symmetric, can restrict freedom of ribbons to move transversely and relieve cabling and environmentally induced strains. We find the pronounced asymmetrical structure of 3d not to be optimal because of preferential bending strains that can be induced during cure and temperature changes (similar to the bimetallic switch in a thermostat).

A variety of application techniques using rollers, wipers, and dies have been developed to apply coatings to substrates (5). Many of these standard methods have been reported to be applicable to forming fiber ribbons (6,7). Our evaluation of several methods indicate that a die coater operating on principles similar to fiber coating produces the most symmetrical, uniform and mechanically robust ribbon structure (8). Moreover, the die method assures high quality ribbons where no fibers can interchange position (fiber crossover) during manufacture. Disadvantages of roll and wiper application include potential for asymmetric geometries, fiber crossovers and a tendency to form pronounced meniscus-structured ribbons.

Packing Density

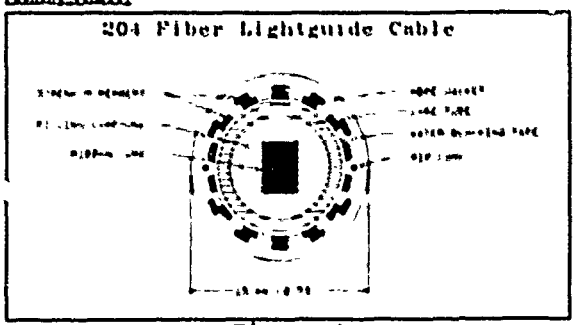

Figure 4

The UV bonded ribbon is about 40 percent smaller than tape ribbons; and, all of the fibers in a ribbon unit are directly accessible. A more compact structure permits higher fiber packing density. The allowable packing density is a function of the fiber's critical bending radius, the clearance between the ribbon stack and the core tube and excess length. With the new, smaller size structure we can accommodate 204 fibers in a 0.6 inch diameter sheath which provides the highest fiber packing density available. The 17 ribbon array in Figure 4 illustrates the increased packing efficiency of an AccuRibbon array cable.

Ribbon Manufacturing Process

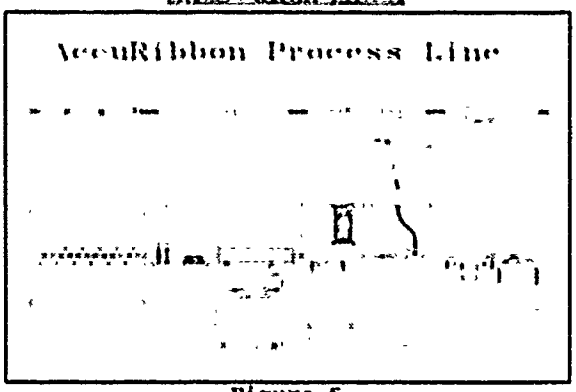

Figure 5

Figure 5 illustrates the ribbon manufacturing process consisting of the following steps: fiber payout under precisely controlled tension, color application and cure, fiber organization, coating application, coating cure, ribbon identification marking and ribbon take-up. Precise tension control minimizes differential stresses between fibers in a ribbon. The fibers are organized into a 12 fiber linear array as they are coated continuously with a matrix free of voids or heterogeneities that can compromise ribbon performance. The organized, matrix-coated fibers are then subjected to uniform UV radiation to cure the matrix. The ribbon is then wound on a spool at controlled tensions providing reliable loss measurement in ribbon form before cabling.

Performance

Ribbon Performance

Mechanical Robustness: Several tests verify the handling robustness of the AccuRibbon structure. In a typical manufacturing quality test, lengths of ribbon under tension must withstand more than 15 twists per meter. Other robustness tests include 90 degree single fiber peel tests, high temperature fiber separation tests, and a long-length, rewind torture test where the ribbons pass through a serpentine path that subjects the ribbon to combined tension, torsion and bending. Adversarial handling tests confirm that individual fibers can be easily accessed and stripped and that the ribbon can be mass-spliced with existing tools, array connectors and methods.

Thermally Induced Microbend Loss: A potential source of added loss in cabled optical fibers is microbending induced by thermal buckling. Buckling results from compressive strain exerted on the glass by the coating which has a much larger coefficient of thermal expansion than the glass. In matrix bonded ribbons, the effective volume of coating that is mechanically coupled to the fiber is increased. This can increase fiber microbending if the matrix properties and geometry are not suitably selected. The strain can be estimated using mechanics of composite materials. The ribbon structure can be modeled as a continuous, unidirectional fiber composite with orthotropic properties. The effective longitudinal modulus, E_L, of the composite can be calculated from the rule of mixtures,

$$E_L = \sum_i E_i V_i \qquad (1)$$

where E_i and V_i are the respective moduli and volume fractions of each constituent. Similarly, the effective longitudinal coefficient of thermal expansion, α_L, can be calculated from Schapery's Equation (9),

$$\alpha_L = \frac{1}{E_L} \sum_i \alpha_i \cdot E_i \cdot V_i \qquad (2)$$

Because constituent properties change substantially with temperature, Equation (2) is integrated with respect to temperature to determine the elongation per unit length, $\Delta l/l$. Thus, the thermal strain is given by

$$\frac{\Delta l}{l} = \int \alpha_L \, dT \qquad (3)$$

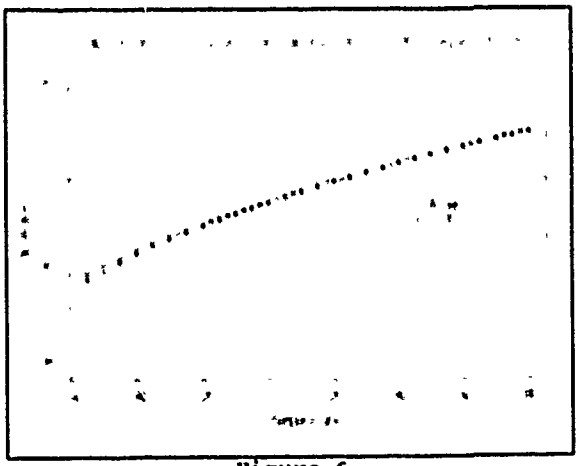

Figure 6

The buckling strain exerted on the glass is found by subtracting the thermal strain on the glass alone from the thermal strain of the composite ribbon. Figure 6 shows that, for the optimal structure of Figure 3b, the incremental buckling strains due to ribboning are pure compression and are negligible because the coated fiber and the ribbon structure have essentially the same thermal strains. Contrasted is the nonoptimal asymmetric structure of Figure 3c, thermal contraction induces a bending moment in addition to axial compression. The asymmetrical loading can cause increased buckling instability.

Cable Performance

Mechanical Performance: We conducted a variety of mechanical endurance tests on AT&T Metallic Crossply and Dielectric Cables containing 12 AccuRibbon arrays. Table I summarizes some of the industry standard EIA (Electronic Industries Association) mechanical tests listed in the associated Bellcore generic cable specification (10). The new ribbon meets or exceeds applicable mechanical and construction tests in the Bellcore generic cable specification. We subjected the prototype cables to a series of field handling, placing and installation trials at the AT&T Bell Laboratories Chester Field Testing Laboratory. Here we reproduce aerial, buried and underground installation using normal and abusive procedures. The new ribbon cables performed excellently with no evidence of sheath or fiber damage, or increase in optical loss.

Mechanical Tests

Test	Specification	Requirement
Tensile Strength	FOTP-33 §5.3.5	600 lb, Bend Radius = 20·Cable O.D.
Compressive Strength	FOTP-41 §5.3.4	1000 lb, total load
Cable Twist	FOTP-85 §5.3.6	±180° Twist, 10 Cycles
Low & High Temperature Bend	FOTP-37 §5.3.2	Bend Radius = 15·Cable O.D., 4 Wraps ea. at -30°C, -60°C
Cyclic Flex	FOTP-104 §5.3.7	Bend Radius = 15·Cable O.D.
Impact Resistance	FOTP-25 §5.3.3	52 ft-lb, Impact, 25 Cycles
External Freezing	FOTP-98 §5.3.8	1 hr. min freeze @ -2°C

FOTP's from EIA Std. RS-455. Section numbers from Bellcore TR-TSY-000020, Issue 3, December 1987.

Table I

Optical Performance: The boxplots of Figure 7 show the loss statistics for 216 ribboned fibers. Both the mean and median loss

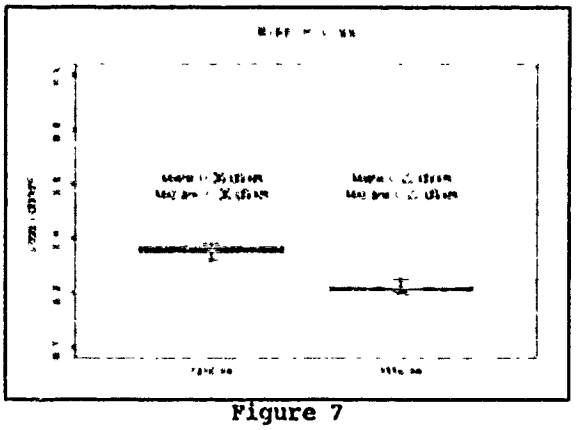

Figure 7

are equal having values of 0.36 dB/km and 0.22 dB/km at wavelengths of 1310 and 1550 nm, respectively. Figure 8 shows typical cabling loss performance of a highly-packed, 144 fiber ribbon cable. Figure 8 shows that the mean and median cable loss for the new ribbon structure are equal with values of 0.36 dB/km and 0.22 dB/km at 1310 and 1550 nm, respectively. The mean loss added to the ribbons in

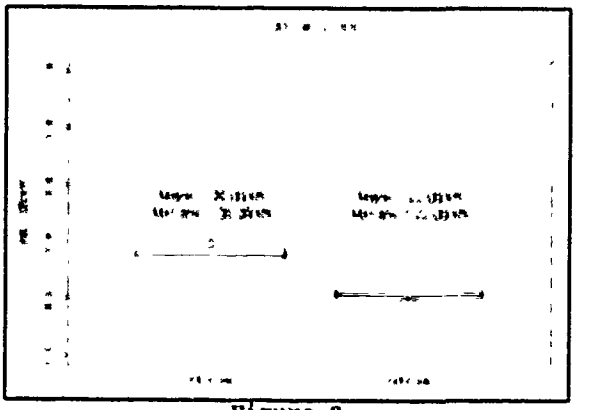

Figure 8

cabling is zero at both 1310 and 1550 nm. Figure 9 shows mean added loss as a function of temperature for the Bellcore environmental cycle. The cycle consists of cycling from -40C to 65C, followed by heat aging for 5 days at 85C, followed by more cycling between -40C and 65C. The mean added loss values at the last -40C exposure after aging for five days at 85C (the most severe point in the cycle) are 0.00 dB/km and 0.04 dB/km at 1310 nm and 1550 nm, respectively. Extending the low temperature exposure of ribbons to -55C, we measured mean values of added loss at 1310 and 1550 to be 0.00 db/km and 0.01 dB/km, respectively.

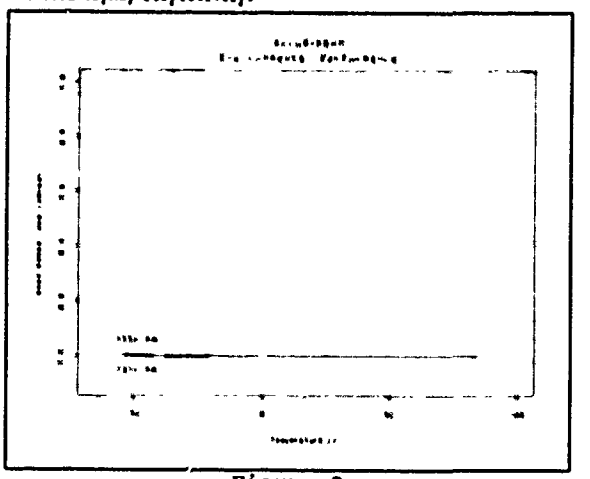

Figure 9

Summary of Enhanced Features

The new AccuRibbon array has several enhanced features that benefit the user. The AccuRibbon structure is 40% more compact and thus can provide the largest number of fibers available in a 0.6 inch sheath. The ribbons are redundantly marked with a simple two digit number and two letter color designator which makes single fiber access in high fiber count cables quick and simple. The fibers in the new AccuRibbon array can be mass-spliced with silicon chip arrays or broken-out individually and spliced individually. The ribbon itself is both mechanically robust for manufacturing and outside plant installation handling by craftsmen and with equipment. The highly uniform fiber coating process technology provides a very uniform ribbon geometry that is consistent for each ribbon produced and the fiber loss can be reliably measured in ribbon form.

Conclusion

Our results demonstrate that ribbons made using UV fiber coating process technology provide a 40% more compact structure that exhibits excellent optical and mechanical performance in cabling, environmental cycling, and installation. The fibers are quickly and easily accessible for mid-span breakouts or for restorations using existing tools and a simple unique ribbon and fiber identification code. The AccuRibbon array provides many advanced features for loop and metropolitan area network applications with cables having up to 17 ribbon units (204 fibers) that are directly accessible from a single core tube contained within a 0.6 inch diameter sheath.

Acknowledgements

We acknowledge the contributions of R.J. Brown, L.C. Hotchkiss, and L.D. Tate.

References

1. Standley, R. D.; "Fiber Ribbon Optical Transmission Lines", B.S.T.J., Vol. 53, No. 6, July-August 1974, pp. 1183-1185.

2. Schwartz, M. I., W. A. Reenstra and J.J. Mullins; "The Chicago Lightwave Project", B.S.T.J., Vol. 57, No. 6, July-August 1978, pp. 1181-1188.

3. Dehnad, D.; Quality Control, Robust Design, and the Taguchi Method, Wadsworth & Brooks/Cole, 1989.

4. Brockway, G. S. and N. R. Santana; "Analysis of Thermally-Induced Loss in Fiber Optic Ribbons", B.S.T.J., Vol. 62, No. 5, Part 1, April 1983, pp. 993-1018.

5. Middleman, S.; Fundamentals of Polymer Processing, McGraw-Hill, 1977, pp. 188-224.

6. Deitelsky, F. T. , R. B. Sprow and F. J. Tolpolski; "Lightguide Packaging", The Western Electric Engineer, Winter 1980, pg. 81.

7. Lackas, W., J. N. Schneider; "New Optic Fiber Ribbon Cable Design"; IWCS Pro. 1986, pp. 4-10.

8. U.S. Patent # 4474830.

9. Schapery, R. A.; "Thermal Expansion Coefficients of Composite Based on Energy Principles", J. Compos. Mater., 2(3), 1968, pp. 280-404.

10. Generic Requirements for Optical Fiber and Optical Fiber Cable, Bellcore TR-TSY-000020, Issue 4, April 1989.

K. W. JACKSON
AT&T Bell Laboratories
Norcross, GA 30071

K. W. Jackson is a Distinguished Member of Technical Staff in the Lightguide Technology Department at AT&T Bell Laboratories, Norcross, GA. He joined the Western Electric Company in 1970 having received a B.S.M.E. from Auburn University. He joined AT&T Bell Laboratories in 1981 having received an M.S.M.E. and PhD from the Georgia Institute of Technology. Since 1981 he has worked in the areas of Lightguide Fiber Fabrication, Lightguide Connectors, Materials Design and Fabrication and Lightguide Cable Design and Development.

P. D. PATEL
AT&T Bell Laboratories
Norcross, GA 30071

P. D. Patel is a Distinguished Member of Technical Staff at AT&T Bell Laboratories, Norcross, Georgia. He joined Bell Laboratories in North Andover, Massachusetts in 1969 after receiving degrees in Mechanical Engineering, including a B.E. from Maharaja Sayajirao University, India, and Engr. Sc. D. degrees from Columbia University. Since 1979 he has worked in the Lightguide Technology Department at Norcross and is currently working in the Exploratory Lightguide Cable Group. He is a member of the American Society of Mechanical Engineers.

M. L. PEARSALL
AT&T Bell Laboratories
Norcross, GA 30071

Michael L. Pearsall is a Member of Technical Staff at AT&T Bell Laboratories, Norcross, GA. He joined Bell Laboratories in 1986. He received a B.S. in Mechanical Engineering from North Carolina A&T State University in 1985 and a M.S. in Applied Mechanics Engineering Science from the University of Michigan in 1987. Currently, he is a member of the Lightguide Cable Group engaged in product development, mechanical analysis and statistical studies.

J. R. PETISCE
AT&T Bell Laboratories
Norcross, GA 30071

James R. Petisce is a Member of Technical Staff in the Mat Engineering Department at AT&T Bell Laboratories in Norcro After receiving a BA/MA in Chemistry from Boston Un 1980, he received a PhD in Organic Chemistry from University (Evanston, IL) in 1984. Since joining Bell L 1984, he has worked on the design and development of coatings, UV curable adhesives, index matching compoun polyimide optical fiber coatings. His present responsibilities inclu design and development of materials for optical fiber and cable.

G. A. LOCHKOVIC
AT&T Network Systems
Norcross, GA 30071

Greg Lochkovic is a Process/Product Development Engineer with AT&T Network Cable Systems, Norcross, GA. He joined AT&T in 1985 after receiving a B.S.M.E. from Purdue University.

New Generation of Self Supporting Optical Fibre Aerial Cables

by Helmut G. Haag, Georg Hög and Peter E. Zamzow

AEG KABEL Aktiengesellschaft
Mönchengladbach, Federal Republic of Germany

0. Abstract

This contribution outlines two new approaches for optical fibre aerial cables with metallic armouring for high tension power lines. A ground wire with a central hollow pipe is described in which in a later stage optical fibre elements can be blown in over some km single length. The fibre element for up to 6 fibres has only a diameter of 1.3 mm but sufficient strength for the blowing-in operation and excellent temperature behaviour. The other approach described here is an optical fibre ground wire with the same diameter, weight, strength, and short circuit current capacity as Al/St 50/30 ground wire used on 110 kV overhead lines. The optical fibre buffer element formed with a steel tube is stranded over a Al profile wire together with Ay and Aw wires.

1. Introduction

The optical transmission technique with optical fibres in self supporting aerial cables is of great interest for power utilities, because the transmission tasks like data transmission, ISDN and protection signals are more and more digital. Moreover for this transmission medium no electromagnetic interference occurs and the broadband characteristics of the optical fibres together with the low attenuation allows fast data transmission, an enormous increase of available transmission channels, and long repeater spacing. This contribution describes new generations of self supporting optical fibre aerial cables. One construction is designed for the later incorporation of optical fibres and the second construction is designed for replacing old earthropes on old and weak power lines by an optical fibre aerial cable.

2. State of the Art

The first optical fibre aerial cables were installed in 1978 on a 110 kV line. The metal armoured aerial cable consisted of 3 star quads and 2 optical fibres. This 1.6 km long length was installed in two pieces at the lower traverse of the towers. Since that time this route is in service without any difficulties. In further projects double armoured aerial cables were installed. Because of torsion problems the lay length of both armour layers were chosen in such a way that the resulting torsion moment becomes negligible. In 1981 a 8 km long route was erected. The cable contains besides 2 optical fibres 8 star quads. The attenuation in a temperature range between -15 and +40 °C as measured during service shows constant temperature independent behaviour. For the 20 kV lines first optical fibre phase ropes were installed in 1985.

Also totally dielectric self supporting aerial cables were installed between the beginning of the eighties and 1984 on 20 kV and also high tension towers up to 380 kV. Even if the optical transmission characteristics behaves constantly over all environmental conditions there is only little future for those cables. By their different me-

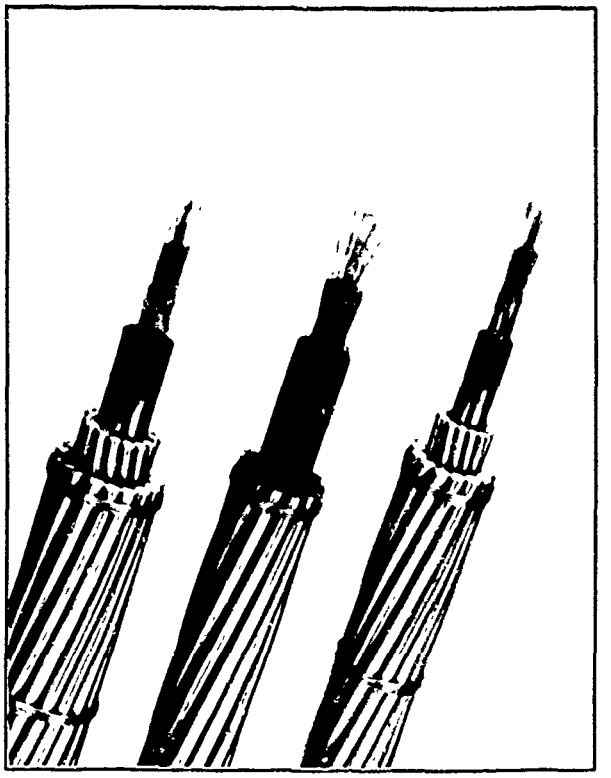

Fig. 1: Standard optical fibre aerial cables

chanical behaviour compared to phase ropes with respect to sag, additional loading, vibration and swinging behaviour these cables are so different that there is only narrow space on the power line poles. That is true, even if the electrical problems of plastics and electrical AC fields is solved [1], [2].

Therefore since 1986 annually some hundred kilometre of optical fibre aerial cables with metallic armouring are laid in the net of the German power utilities [3].

The construction of those optical fibre aerial cables is designed for the wide temperature range and the high forces which acts on the cable during its life. The best possibility to prevent optical fibres from mechanical forces and to give them sufficient place for free movement is the loose tube technique. Depending on the number of fibres per cables one or two fibres are incorporated in a tube of approximately 2 mm diameter. To prevent that humidity comes to the primary coated fibres and to give the fibres a floating surrounding these tubes are filled with a thixotropic jelly. Six of these tubes are stranded around a central strength element made of fibre reinforced plastic (FRP). By the choice of the lay length, the operational range with respect to constrain and elongation can be chosen. Moreover for single mode fibres the effect of microbending which lead to additional attenuation at 1550 nm must be taken into account. The variation of length by lateral forces and temperature are calculated from the formula

Parameter/Type (Ay/Aw)	Dimension	232/44-27.6	75/25-7.5	112/28-11.0
Diameter	mm	24.1	16.4	16.8
Weight	kg/km	1045	450	551
Armouring layers		2	1	2
portion Aw	mm²	44.2	24.9	28.3
portion Ay	mm²	232.1	74.7	111.5
Young's modulus	kN/mm²	75.3	84.5	79.6
Calculated breaking force	kN	118.4	52.0	64.1
Permissible strain	N/mm²	171	202	186
Mean permissible strain (EDS)	N/mm²	71	81	75
Maximum permissible strain	N/mm²	341	412	375
Thermal expansion coefficient	$10^{-6}K^{-1}$	19.5	18.3	18.9
DC resistant	Ω/km	0.138	0.407	0.280
Rated short circuit current	kA·s²	22.6	7.5	11.0

Table 1: Data of standard optical fibre aerial cables

$$\epsilon = \sigma/E+(\theta-20)T_k$$

ϵ = elongation, relative length variation
σ = strain
E = Young's modulus
T_k = thermal expansion coefficient
θ = temperature (°C)

Type of rope		Temperature and additional load (Z)										
		-5+Z/2	-5+Z	-20	-10	-5	+0	+10	+20	+30	+40	+60
Phase rope	Sag m	11.77	12.12	10.84	11.21	11.39	11.57	11.92	12.26	12.60	12.93	13.57
Al/St 265/35	Strain N/mm²	58.6	72.0	46.7	45.2	44.5	43.8	42.5	41.3	40.2	39.2	37.3
Aerial Cable	Sag m	12.48	13.34	10.97	11.29	11.45	11.61	11.92	12.22	12.53	12.82	13.40
Ay/Aw 75/25-7.5	Strain N/mm²	122.5	162.8	80.9	78.6	77.5	76.5	74.5	72.6	70.9	69.2	66.2
Aerial Cable	Sag m	12.08	12.66	10.89	11.24	11.41	11.58	11.92	12.25	12.57	12.89	13.51
Ay/Aw 112/28-11.0	Strain N/mm²	78.9	103.6	54.4	52.8	52.0	51.2	49.8	48.4	47.2	46.0	43.9
Aerial Cable	Sag m	11.80	12.18	10.86	11.22	11.40	11.57	11.92	12.26	12.59	12.92	13.55
Ay/Aw 232/44-27.6	Strain N/mm²	65.3	79.9	52.4	50.7	49.9	49.2	47.7	46.4	45.2	44.1	42.0

Table 2: Comparison of sag for phase rope and different optical fibre aerial cables

For these aerial cables one can calculate more or less independent from the armouring a change of length in the order of a maximum of 2 °/₀₀ in the interesting operational range. To this value an additional elongation of about 1 °/₀₀ must be added which results from the setting of the armouring. By this the cable construction must consider an operational range of about 4 °/₀₀. Over this core a polyethylene sheath is extruded with high precision which is the basis for the one or two layer armouring of aluminium alloy and aluminium clad steel wires. By a ratio of 1 to 4 of these wires the mechanical behaviour and temperature elongation of these aerial cables is comparable to those of the phase ropes. Table 1 and Figure 1 shows the mechanical data respectively the outfit of typical optical fibre aerial cables. As shown in Table 2 these aerial cables can be installed with the same sag over the operational range as conventional phase ropes.

By numerous measurements it was shown that these aerial cables show no change in attenuation over the temperature range of -40 to +70 °C as well as with loading far beyond the permissible strain.
But these standard aerial cables with a diameter in the range of 15 to 25 mm diameter depending on the number of fibres and especially the kind of armouring can be installed only on newer power lines. In case of old towers it is normally not possible to install an additional aerial cable by the strength of the towers. In this case the aerial cable must be installed as earth rope in replacing the existing earth rope. But for those earth ropes normally steel ropes with 50 mm² and a diameter of about 10 mm are in use. In replacing these earth ropes the power utilities normally use Al/St-ropes with 50/30 mm². This rope has a diameter of 11.65 mm and a weight of 378 kg/km. The new generation of optical fibre aerial cables must come as close as possible to these figures if they will be installed on these old lines. The optical fibre aerial cable described in section 3.2 fulfil these requirements. But for this new construction principles have been developed.

On the other hand not on all power lines which will be erected or upgraded or where the earth rope is replaced will need at the moment optical fibre transmission paths. For this purpose the cable described in section 3.1 was developed where in the centre of the earth rope a tube is incorporated in which at a later stage optical fibre elements can be blown in.

3. New Constructions for Optical Fibre Aerial Cables

With the construction for optical fibre aerial cables described in the following two aims with two different cables are envisaged:

1. To create a ground wire in which in a later stage optical fibres can be incorporated.

2. To create an optical fibre ground wire with the lowest possible diameter increase compared to the bare ground wire.

Both cables are intended for the use with power utilities in addition to the existing optical fibre aerial cables.

3.1 Ground wire with central tube

To enable the user of high tension power lines to incorporate optical fibres in a ground wire in a later stage it is necessary to provide a ground wire with this possibility. To protect fibres from environmental conditions it is advantageous to put the optical fibres respectively the optical fibre element inside the armouring. This is normally done by providing a tube inside the ground wire. To be able to pull in the fibres it is necessary to have the tube as straight as possible. Therefore a central tube will be preferred. The dimensions of this tube depend from the element diameter, and the material of the tube should be chosen in such a way that as less friction as possible between the inner tube wall and the fibre element arise. Moreover the tube must be the base for the armouring with steel and aluminium alloy wires. Out of these considerations the central tube will have an inner diameter of 4 mm with a wall thickness of 1 mm and is made of polyamide. Over this a double layer

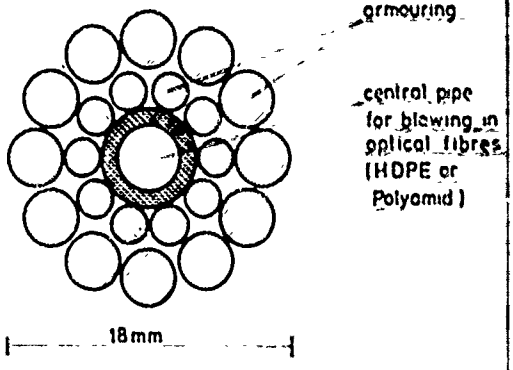

95/55 Earthrope I_s = 17.4 kA /0.6 sec

Construction

Number of fibres	1 - 4	
Central pipe	Inner/Outer diameter = 4/6mm	
Amouring	1 layer 10 × 2,5mm	steel
	2 layer 12 × 3,5mm	ALDREY
Cable diameter	18 mm	
Cable weight	686 kg/km	
Cross section	164,5mm²	
Aluminum cross section	115,45 mm²	
Steel cross section	49,10 mm²	
Ultimate tensile strength	94,3 kN	
Young's modulus	89,4 kN/mm²	
Nominal short time current (t_{in} = 20 °C)	1sec	11,9 kA
	0,6sec	15,3 kA

Fig. 2: Cross-section and data of ground wire with central tube

armouring is applied. To protect the strength bearing aluminium clad steel wires (Aw) from vibration and other forces these wires are put in the first armouring layer and the second layer is made of aluminium alloy (Ay) with a minimum diameter of 3 mm to avoid damage of these wires by lightning. In the here described cable the Ay-wires are chosen with 3.5 mm diameter.

Out of the armouring the short circuit current of this cable will be 12 kA for 1 second respectively 15.3 kA for 0.6 seconds. Figure 2 shows the cross-section of this cable with the relevant mechanical characteristics. In Figure 3 a photograph of this rope is shown. The aerial cable has a diameter of 18.0 mm and is only 2 mm thicker than a comparable rope Ay/St 95/55, the weight is almost the same and this aerial cable can be installed with the same sag as the other phase ropes. By the lower heat capacity of aerial cables by their plastic inner construction the short circuit current capacity is about 10 % lower than this of the comparable ground wire even if the Ay-portion is higher.

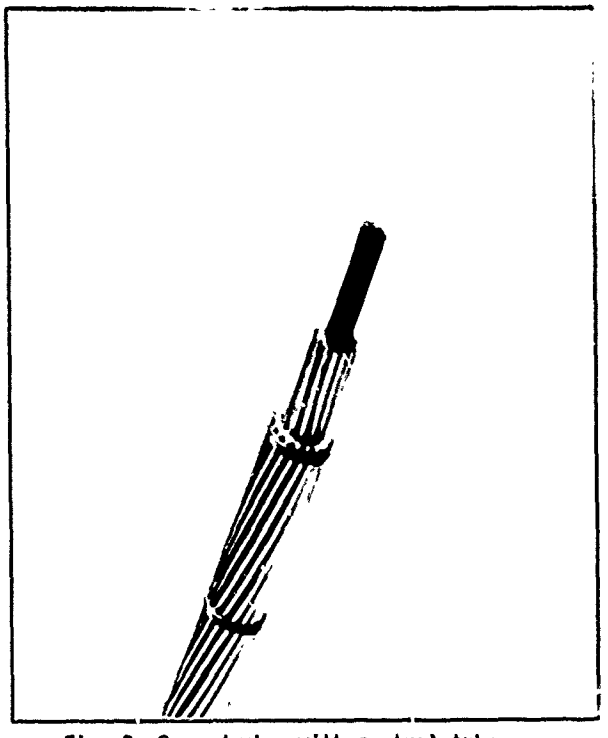

Fig. 3: Ground wire with central tube

This cable is fixed to the towers by spiral armatures to avoid deformation of the inner tube, because such a deformation will disturb the flowing parameters inside the tube severely and the blowing-in will be more difficult.

How does such an optical fibre element look like which can be incorporated in such a tube. It was prefered, that the element will be blown-in instead of pulled-in by a pulling wire. By this the required pulling forces and therefore the strength of the fibre element are limited. But a compression protection for temperature loading will be needed because this element is not fixed to the armouring.

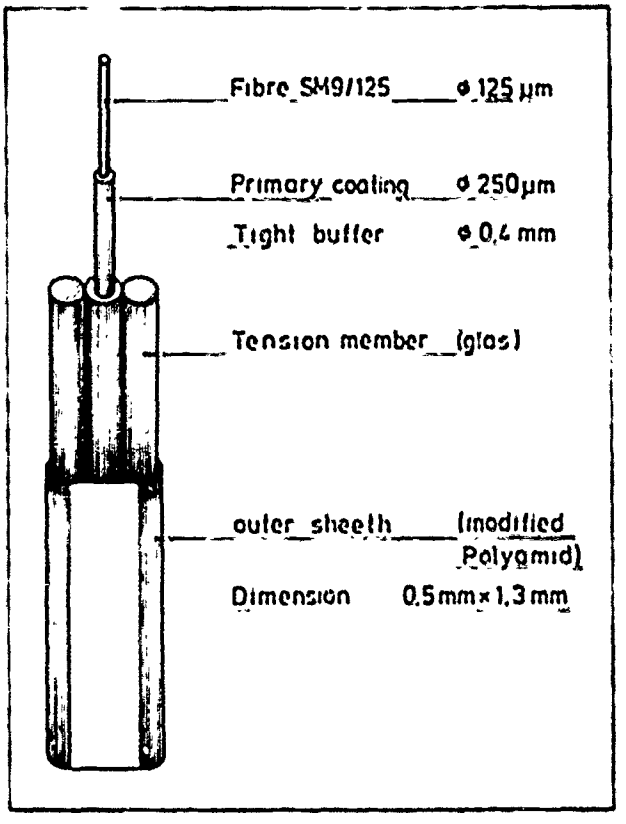

Fig. 4: Single fibre element for blowing-in

The primary coated optical fibre - normally single mode fibre - will be secondary coated by polyamide. For a one fibre element such a fibre is fixed between two FRP members with also 0.4 mm diameter and coated together with a polyamide sheath which leads to a diameter of 1.3 mm (Figure 4). Also a six fibre element will have the same diameter where the FRP member is put in the central and the fibres are stranded around this element. Such an element can be wind on a spool and rewinded for blowing in from this spool (Figure 5 (below)). The other possibility shown in Figure 5 (above) is the cross winding of the element and then allowing the pay-off from the inner side of the spool with no rotation of the whole fibre spool. In the latter case the dynamic force on the fibre in the upwinding process is much lower and independent from the total length of the fibre. Therefore this cross winding technique was chosen. It is possible of cross winding about 5000 m of such an optical fibre element.

The required apparatus to blow-in the fibre element is shown in Figure 6. With a maximum pressure of 30 bar in this attempt 1000 m of a one fibre element are blown-in in an installed ground wire with a central tube. During and after the blowing-in no change in attenuation at 1300 nm and at 1550 nm were observed (Figure 7). Also at pulling forces up to the maximum permissible load of 38 kN no change in attenuation arises. For temperature loading the bare fibre element winded on a cross

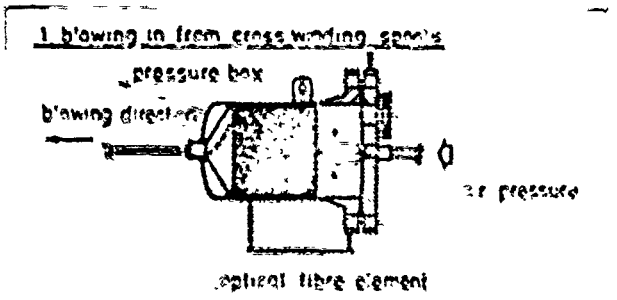

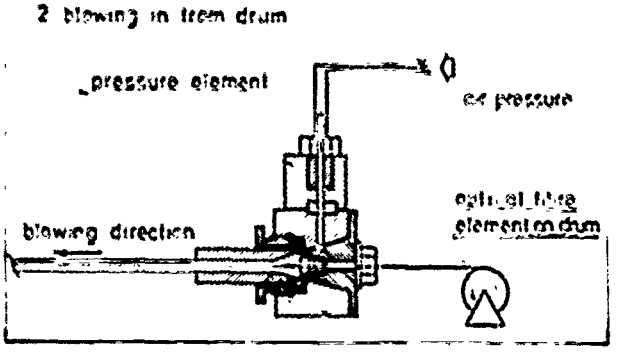

Fig. 5: Principles for the blowing-in apparatus

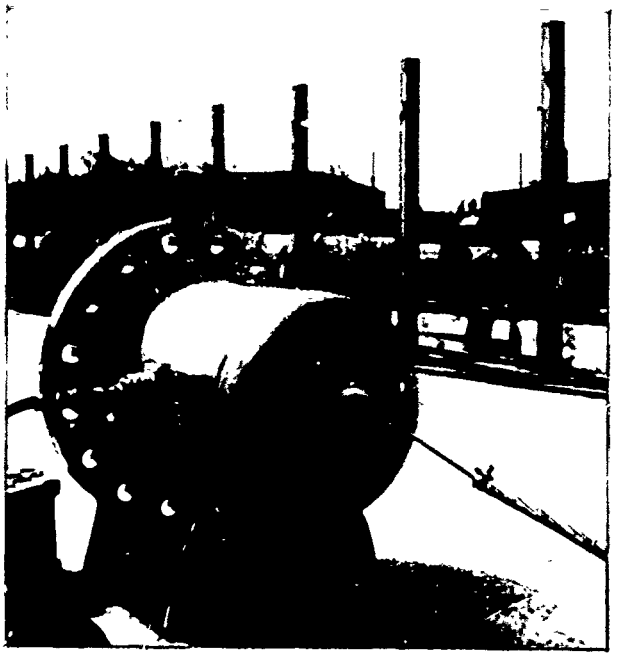

Fig. 6. High pressure blowing-in apparatus for cross winding spools adopted to the ground wire

winding spool were tested. By the lateral forces of the winding pressure such test is even more severe than testing it on an installed cable. The test installation and the results at 1300 and 1550 nm are shown in Figure 8 respectively 9. Only at 1550 nm and -40 °C slight increases in attenuation are seen.

By the promising results of these tests a larger field trial over a length of approximately 12 km will be carried out in 1990 to get experience from real installation and on long term behaviour before those systems will be installed on a regular basis. The armatures and the closures for those cables are identical to those of conventional aerial cables.

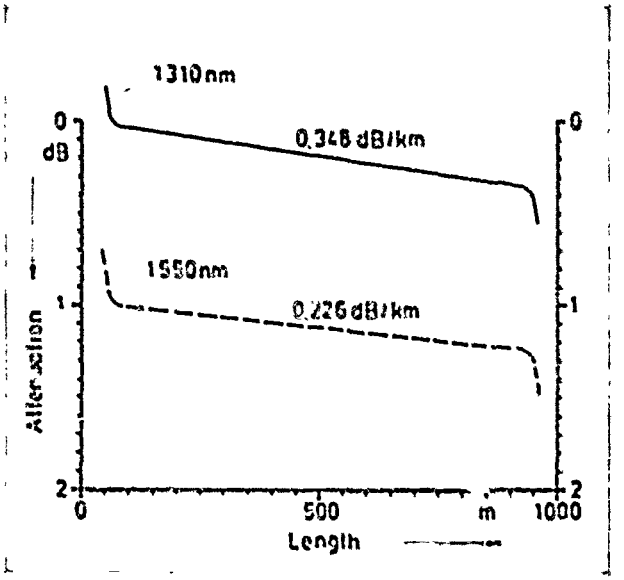

Fig. 7: Attenuation of fibre after being blown-in

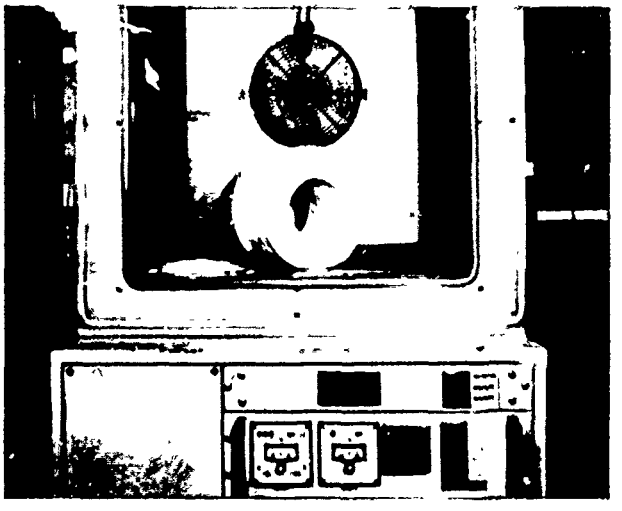

Fig. 8: Test set-up for temperature cycling with cross winding spool

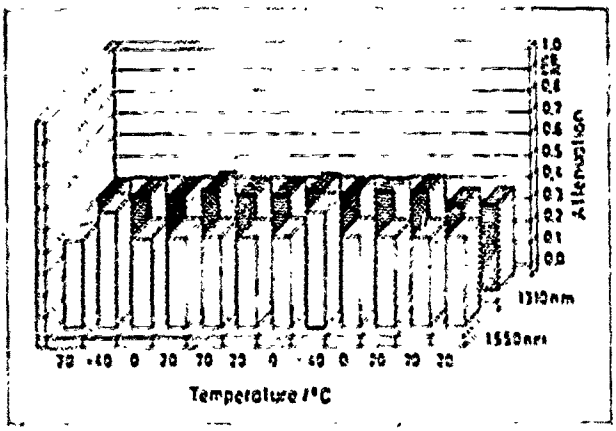

Fig. 9: Results from temperature cycling for cross-winded fibre element

3.2 Optical Fibre Ground Wire

Optical fibre aerial cables up to now consist of a dielectric optical fibre core with polyethylene sheath and a diameter between 7 and 11 mm. An one or double layer armouring is applied over this sheath. This means that optical fibre aerial cables have a diameter over armouring of at least 15 mm independent from the armouring.

On old power lines normally the existing ground wires with 50 mm² steel are replaced by ground wires Ay/St 50/30 or Ay/St 70/12 wit' a diameter of 11.65 mm respectively 11.72 mm. Their weight is 378 kg/km respectively 284 kg/km. To get optical fibre ground wires with diameters in this range the cross-section of the fibre element must be reduced drastically. But the operational range of the fibres must not be reduced because the requirement for a 5 to 4 °/₀₀ operational range still remains. From this point it seems reasonable to replace steel or aluminium alloy wires by optical fibre buffers with the same diameter. But these buffers

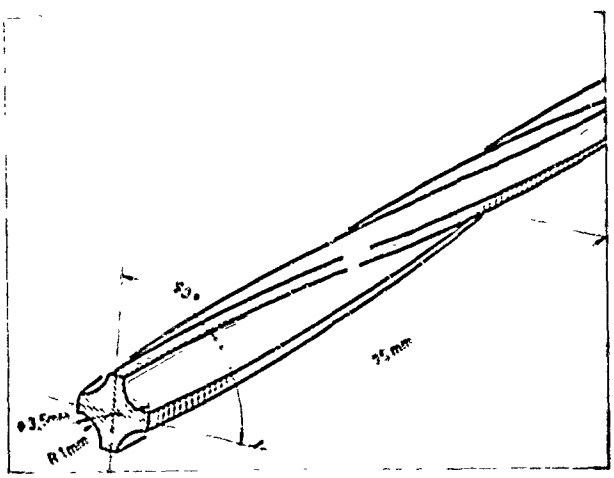

Fig. 10: Profile core for optical fibre ground wire

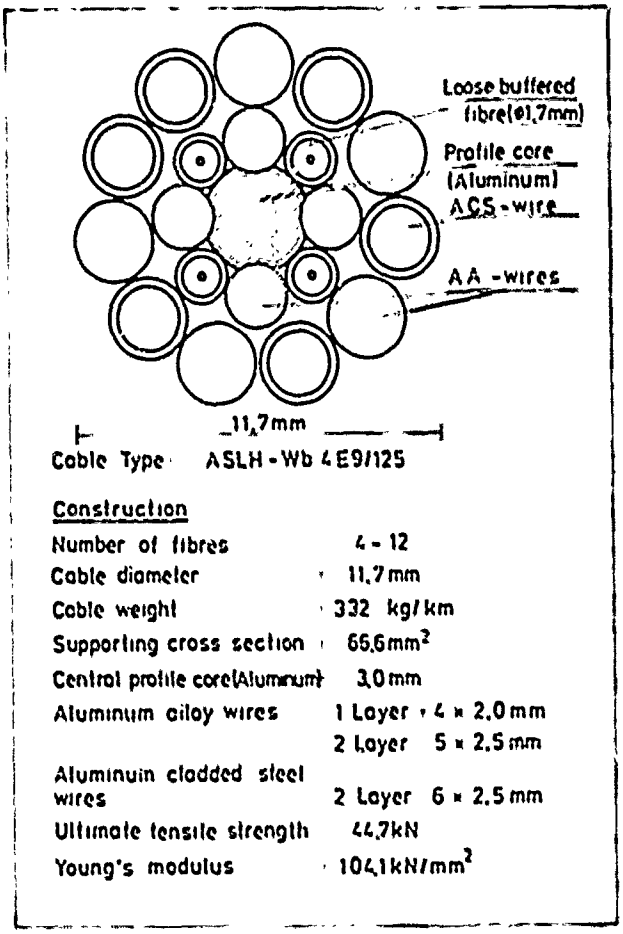

Fig 11: Optical fibre ground wire with profile central element

cannot be arranged centrally because in this case the operational range could not be achieved. As outlined before the laylength of the optical fibre buffer must be in the range of 70 to 80 mm to achieve the required operational range. This is for steel wires to short. Moreover it can be said that the aerial cable must be fixed on the towers with spiral armatures to avoid lateral forces on the fibre element. This means the steel elements should be as far as possible to the outer layers of the armouring.

These considerations led to the new developed optical fibre ground wire in which the central element is the most important element. In the stranding process as central element an aluminium profile is rolled to form hollow grooves (Fig. 10) and in the same process stage the first layer of aluminium alloy wires is stranded in the formed grooves and between these aluminium alloy wires optical fibre buffers are stranded. This construction prevents the optical fibre buffers from dislocation forces. In the same stranding process from a second cage a layer of Ay and Aw wires are stranded in the opposite direction. By this the optical fibre buffers are protected in chambers formed from the aluminium profile, the Ay/Aw wires of the first and second layer.

This cable with 4 optical fibre buffers can keep per buffer a maximum of 4 fibres so that with this construction up to 16 fibre ground wires are possible. And this cable is with 11.7 mm as thick as the bare ground wires Ay/St 50/30 respectively Ay/St 70/12. The weight is with 332 kg/km between the two before-mentioned ground wires. By the cross section of aluminium and aluminium alloy the short circuit current for 1 second reaches 5.7 kA and 7.4 kA for 0.6 seconds.

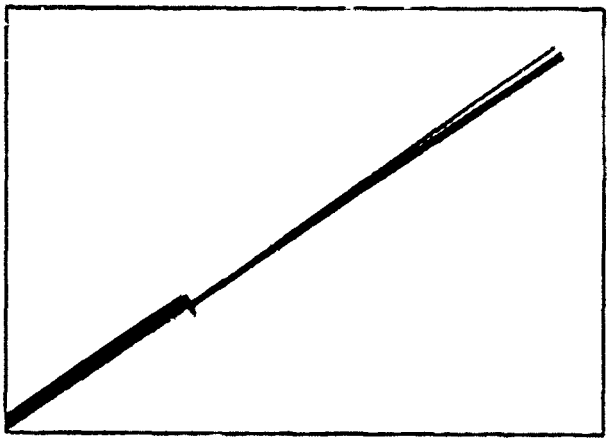

Fig. 12: Steel tube buffer with 4 single mode fibres

Besides forming the central profile wire the construction of the buffers is of primary importance. Up to now normally as buffer material an extruded plastic material is used. For the above-mentioned cable a tube with inner diameter of 1.2 mm and an outer diameter of 1.7 mm is adequate. But on the other hand also steel tubes can be used. Such a steel tube is made in forming a steel tape to a tube and welding it by a laser beam. In this case tapes with 0,15 mm thickness can be used so that a tube of 1.4/1.7 mm can be formed. In both cases the tube will be filled with jelly. By the expected lateral forces during service and the pulling forces during the fabrication on normal steel wire stranding machines the steel tube is preferable. Figure 12 shows such a steel tube with 4 fibres. An additional advantage of this steel tube is the higher inner diameter which leads to a larger operational range for the same laying length or the possibility to have a larger laying length giving the same operational range but with better performances at 1550 nm by a larger bending radius. Figure 13 shows a photograph of the entire cable. During the fabrication process no additional attenuation arises at 1300 and 1550 nm. Further results on this cable will be reported on the symposium.

After tests in the laboratories and the internal test field, field trials are foreseen for 1990. For these field trials some modifications have to be done on the hood closure for the cable inlet to achieve tight closures.

4. Outlook

By these new developed optical fibre ground wires new possibilities for power utilities arise. Now for all overhead power lines adequate ground wires are available. Whereas for 220 and 380 kV lines the standard optical fibre aerial cable with conventional fibre core will be used it will be possible for 110 kV lines to replace the existing earth wire by a thin optical fibre ground wire with no additional loading on the towers or add a separate aerial cable on 20 kV lines. On the other hand it is possible to install on other power lines ground wires with a central tube for cases where at the moment no optical fibres are needed. At the time of need optical fibre elements can be incorporated with less effort.

Also in other countries cable manufacturers and power utilities work in this subject [4].

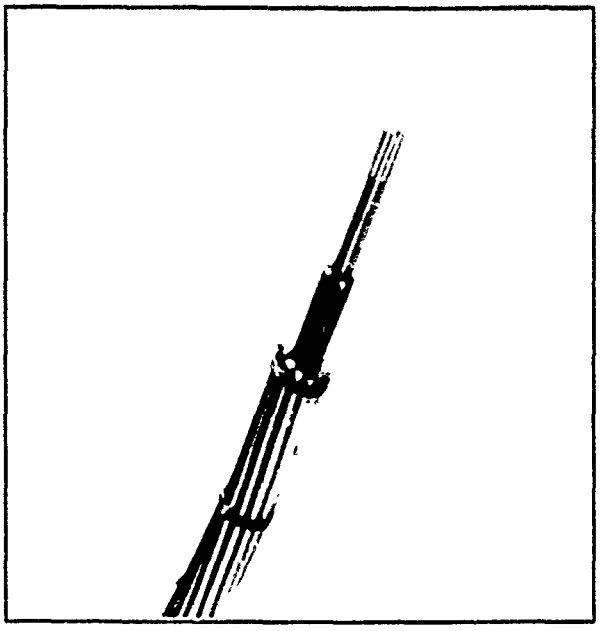

Fig. 13: Optical fibre ground wire

5. Literature

[1] JÜrdens C., H. G. Haag, R. Buchwald, Experience with Optical Fibre Aerial Cables on High Tension Power Lines, CIGRE, Sec. 22-11, Paris 1988

[2] Oestreich U., H. Nassar, Self-Supporting dielectric Fiber Optic Cables in High-Voltage Lines, 37th IWCS 1988, 79 pp

[3] Schneider J.M., J. Schmelter, R. Herff, Optical Ground Wire Design with a Minimum of Dielectrics, 37th IWCS 1988, 83 pp

[4] Kawasaki M., et al., Suitable Design and Characteristics of Optical Ground Wire for 1.55 µm wavelength, 37th IWCS 1988, 93 pp

Helmut G. Haag (Speaker)
AEG KABEL AG
Manager Communication System Techniques
Mönchengladbach, West Germany

Helmut G. Haag (41) is head of the Technical Sales Division for Telecommunications. After reaching his Dipl.-Physiker-degree from the University of Stuttgart he joined AEG KABEL in 1975 for the development of coaxial cables. Later he has been also responsible for the development of optical fibre cables. From 1980 to 1983 he built up the production plant for these cables. In autumn 1983 he took his present position.

Georg F. Hög
AEG KABEL AG
Telecommunications Development
Mönchengladbach, West Germany

Georg F. Hög (39) is head of the Development Group for Optical Fibre Cables. He reached his Dipl.-Ing.-Degree from the University of Aachen and joined AEG KABEL in 1977. After being engaged in the development of symmetrical telecommunications cables he got the responsibility for this group und 1980. Since spring 1985 he covers his present position.

Peter E. Zamzow
AEG KABEL AG
Telecommunication Development
Mönchengladbach, West Germany

Peter E. Zamzow (49) is director of the Telecommunications Development Division. After finishing his postgraduate studies in telecommunications in Munich and Graz as Dipl.-Ing. he joined AEG KABEL in 1970. He has been engaged in development and production of telecommunication cables. In 1980 he became head of the fibre optic division at AEG KABEL and in 1982 he was nominated as a senior engineer. Since 1985 he has covered his present position.

DISPERSION-FLATTENED SINGLE-MODE FIBERS FOR THE SUBSCRIBER LOOP: DESIGN, PROPERTIES, CABLING AND PASSIVE COMPONENTS.

W. Stich and J. Schulte
Kabelmetal Electro GmbH, P.O. Box 260, 3000 Hannover, Fed. Rep. of Germany

T.M. Hauff, W.E. Heinlein, M. Koratzky and A.M. Ochler
University of Kaiserslautern, P.O. Box 3049, 6750 Kaiserslautern, Fed. Rep. of Germany

Summary.

Chromatic dispersion of standard single-mode fibers is a limiting factor for the length and bit rate of an optical transmission line. Dispersion-flattened single-mode (DFSM) fibers have low dispersion in the second and third transmission windows and therefore offer the system designer a considerable increase in possible system configurations. A newly-designed DFSM fiber that can be used in the subscriber loop is presented in this paper. The design has been optimized for low dispersion, low bending loss and low splice loss. A trial production of the fiber confirmed that these goals have been achieved. Cables with DFSM fibers have been fabricated. They pass all standard quality tests without any problem. Connectors with DFSM fibers exhibit good performance. In addition, we fabricated couplers and multiplexers from our DFSM fiber.

Introduction.

The dispersion in an optical transmission line is determined by the dispersion characteristics of the fiber and the spectral width of the light source (laser, LED). The dispersion of a single-mode fiber is given by the chromatic dispersion which is the sum of the material dispersion and the waveguide dispersion. The latter can be modified through proper choice of the refractive index profile. Standard single-mode fibers have a zero dispersion point around 1.3 µm but a high dispersion value in the third transmission window (about 20 ps/(km • nm). For dispersion-shifted fibers the refractive index profile has been designed in such a way that zero dispersion results around 1.55 µm. However, these fibers have high absolute values of dispersion in the second transmission window. The DFSM fiber combines the advantages of both fiber types; it has low dispersion in both the second and third transmission windows (Fig. 1).

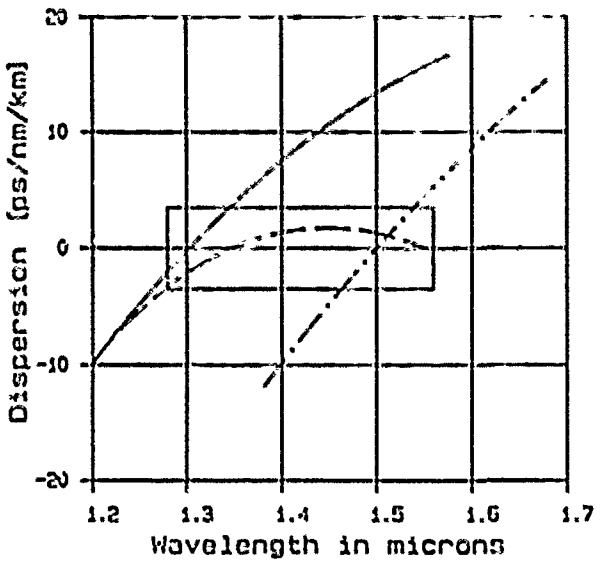

Fig.1.Dispersion of different fiber types: Conventional single-mode fiber:solid line; Dispersion-flattened single-mode fiber (DFSM): dash line; Dispersion-shifted single-mode fiber: dash-dot line.

So far, DFSM fibers have a slightly higher attenuation than standard single-mode fibers. This limits their use in long-haul applications. Nevertheless, the DFSM fiber can be applied in the subscriber loop where distances are shorter than in long-haul applications. The low absolute dispersion value of the DFSM fiber offers new possibilities, such as wavelength division multiplexing at several wavelengths in the second and third windows for high bit rate transmission using LEDs or inexpensive multimode semiconductor laser diodes[1]. We therefore present a new DFSM fiber which has been fabricated in a laboratory trial production with excellent results.

Design goals for DFSM fibers.

The design has been optimized to meet the requirements described hereafter. The absolute values of chromatic dispersion should be less than 3.5 ps/(km·nm) in the 1.29 μm $\leq \lambda \leq$ 1.56 μm wavelength range (Fig. 1) which covers the second and third transmission windows. The cutoff wavelength must be sufficiently small to ensure single-mode operation. The bending loss behavior should be comparable or better than that of standard single-mode fibers in order to make use of standard coating materials and cable designs. The spot sizes should be as large as possible to facilitate low-loss connections (using splices and standard single-mode connectors). The density of dopants in the core region should be as low as possible to minimize their contribution to the attenuation. The design must allow for fabrication tolerances and limitations in order to provide for high fiber production yield. The fabrication of fused couplers from these DFSM fibers should be possible.

DFSM fiber design.

A triple-clad approach was used in our design because the outermost index step is light-guiding. This results in low sensitivity to bending loss. For the analytical description of the DFSM fiber we used the equations given in Ref.[2]. We searched for the best compromise of this optimization problem with six degrees of freedom by varying the refractive indices and radii of the core and its segments. We found the local optima by calculating the chromatic dispersion, bending loss[3] and spot sizes[4] of fundamental and first-order higher modes for different combinations of radii and refractive indices. By comparing the theoretically predicted and practically achieved properties, the optimum DFSM fiber design evolved through fine tuning within the region of local optima. The fiber fabrication process leads to a decrease in the refractive index value near the fiber center. This central dip is taken into consideration in our fiber design (Fig. 2). The calculated absolute maximum value of chromatic dispersion of our fiber design is less than 2.7 ps/(km·nm) within the mentioned wavelength range. This results in a margin for small profile deviations in the fabricated fibers. Therefore, small deviations from the profile should not cause the 3.5ps/(km·nm) absolute value of the chromatic dispersion to be exceeded. Fig.3 shows the theoretically-predicted dispersion and the measured dispersion of a fabricated fiber.

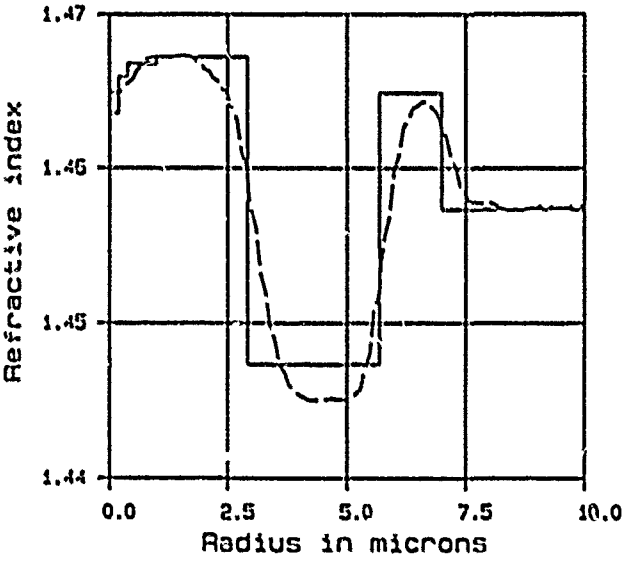

Fig.2. Refractive index profile of the designed DFSM-fiber with typical dip (solid line) and measured profile of a fabricated fiber (dash line).

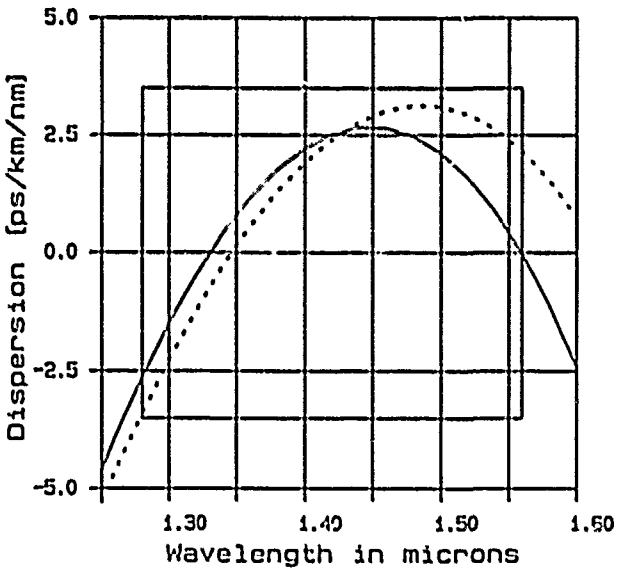

Fig.3. Chromatic dispersion of the designed fiber (solid line) and a typical measurement result (dot line).

Influence of fiber fabrication.

Preform fabrication and fiber drawing generally prompt the refractive index profile to deviate from the theoretically ideal profile. These deviations are caused by the statistically varying fluctuations or systematic changes of radii and refractive indices. A main mechanism that changes the refractive index profile is dopant diffusion during fiber fabrication. Diffusion leads to a smoothed profile. Fig. 2 shows the designed index profile and, as an example, the profile of a fabricated fiber. The latter illustrates the case of imprecise fluorine doping and profile smoothing through diffusion.

Fig. 4 shows the effect of deviations of radii up to ±0.1 µm and deviations of the relative refractive index differences up to ±0.02% on the chromatic dispersion. The minimum and maximum chromatic dispersion values of worst-case combinations of these deviations for each wavelength are shown by the dash-dot lines. However, these worst case combinations are of very low probability. Thus, we calculated the chromatic dispersion for statistically perturbed radii and refractive index differences. The variance of the deviation of the radii is 0.1 µm and the variance of the deviation of the refractive index differences is 0.02%. 68% of the chromatic dispersion curves of all statistically perturbed fibers are within the dashed lines. This shows the partial compensation of the perturbation of one fiber design parameter by other fiber design parameters.

Deviations from the ideal value of the actual refractive index level in the realized preform can be compensated through a suitable drawing ratio. Fig. 5 shows, as an example, the calculated fiber drawing ratios that compensate a deviation of the refractive index of the fluorine-doped part of the fiber. Deviations of the refractive index difference up to 30% can be compensated. However, some simultaneous changes of other fiber parameters must then be taken into account.

The effect of diffusion-generated changes of the refractive index profile on dispersion can also be compensated by a suitable drawing ratio. Fig. 6 shows the chromatic dispersion of a fiber with a diffusion-smoothed profile with and without compensation through the drawing ratio. Typical diffusion can completely be compensated through an adjustment of the drawing ratio.

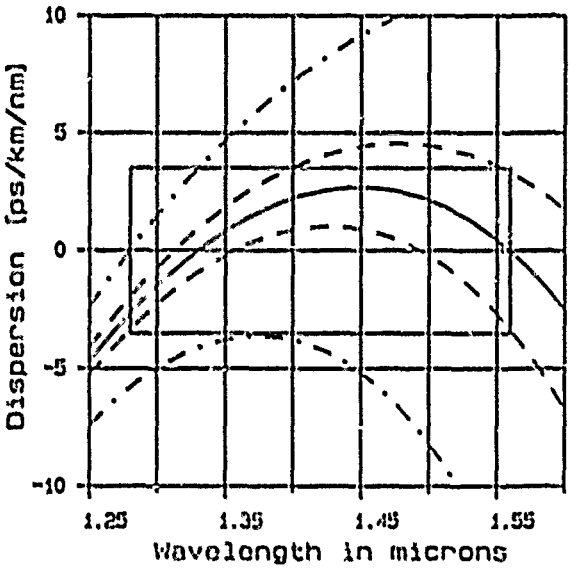

Fig.4. Calculated chromatic dispersion of the designed DFSM-fiber: solid line. For statistical deviations with variances of radii and relative index differences of 0.1 µm and 0.02%, respectively, the chromatic dispersions of 68% of the perturbed fibers are within the dash lines. Chromatic dispersion for worst-case perturbations of radii up to 0.1 µm and of relative refractive index differences up to 0.02%: dash-dot lines.

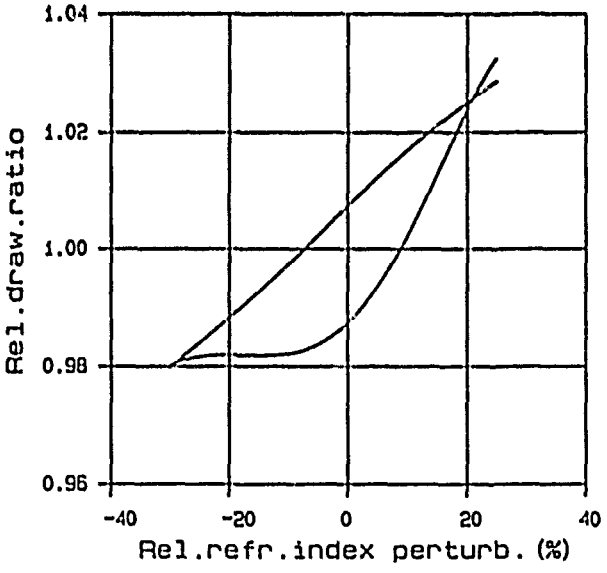

Fig.5. Compensation of the perturbation of the relative refractive index difference of the fluorine-doped cladding of a DFSM fiber by the relative fiber drawing ratio. The absolute value of chromatic dispersion within the lines is < 3.5 ps /(km•nm).

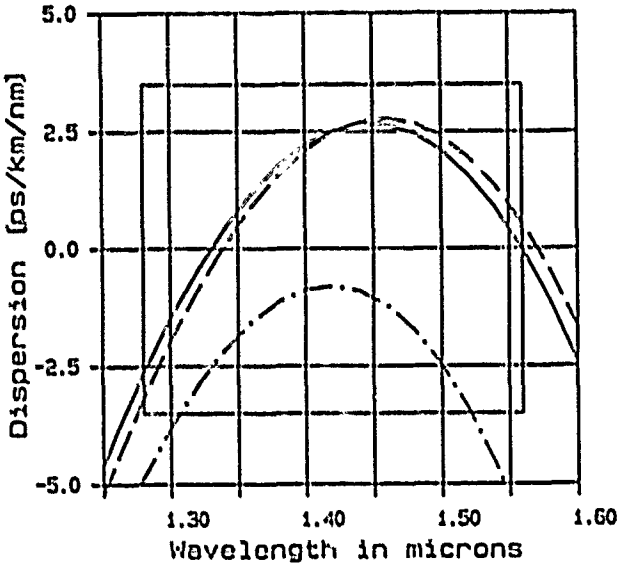

Fig. 6. Calculated chromatic dispersion of the diffusion-smoothed fiber without (dash-dot line) and with (dot line) compensation by the relative fiber drawing ratio.

DFSM fiber trial production.

The DFSM fibers were fabricated using the PICVD (Plasma Impulse Chemical Vapor Deposition) process[5]. They were cut to a length of 2.2 km. Small deviations of the achieved profile with respect to the planned design have led to altered dispersion behavior as a function of wavelength. These may possibly cause the dispersion to exceed the absolute value of 3.5 ps/(km • nm) in portions of the wavelength range. Fig. 7 shows a histogram of the achieved dispersion values for λ = 1.29 µm. These dispersion values are concentrated in the range between 3.0 and 3.5 ps/(km • nm). Fig. 8 illustrates the distribution of the dispersion maximum. Here, too, more than 75% of the fiber samples fall below the 3.5 ps/(km• nm) value. This proves that our goal, which is to keep the absolute dispersion to 3.5 ps/(km•nm) within the 1.29 µm $\leqslant \lambda \leqslant$ 1.56 µm wavelength range, can be achieved with the design of our profile.

The cutoff wavelength was determined in accordance with CCITT through bending tests on short (2 m) samples. The measured cutoff wavelengths are between 1.0 and 1.2 µm. The influence of cabling on the cutoff wavelength was determined by using specially-fabricated fibers with a cutoff wavelength in excess of 1.4 µm. After cabling was completed, the cutoff wavelength was once again measured on a 30 m sample of the cable. All measurement values were found to be below 1.3 µm. Here, too, it was not possible to observe any mode coupling or additional attenuation. Furthermore, we determined the mode field diameter in accordance with the variable aperture method and the data were evaluated according to the "Petermann II Definition". The average field diameter of 5.9 µm for λ = 1.3 µm is in good agreement with the theoretically predicted value. The field diameter of the DFSM fibers is smaller than that of conventional fibers. The effect of this property on splices and connectors will be discussed below.

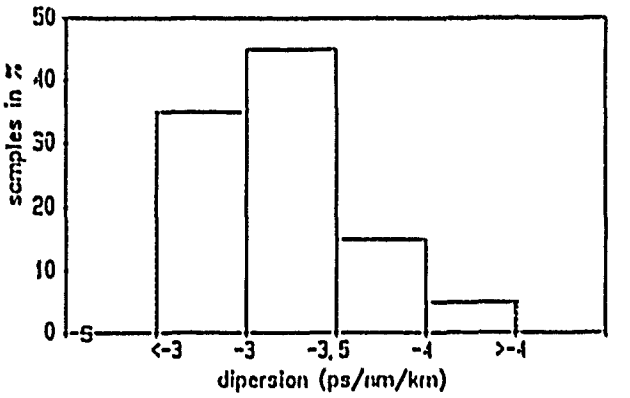

Fig.7. Distribution of dispersion values at 1290 nm measured on 45 km of fiber, cut into 2.2 km long samples.

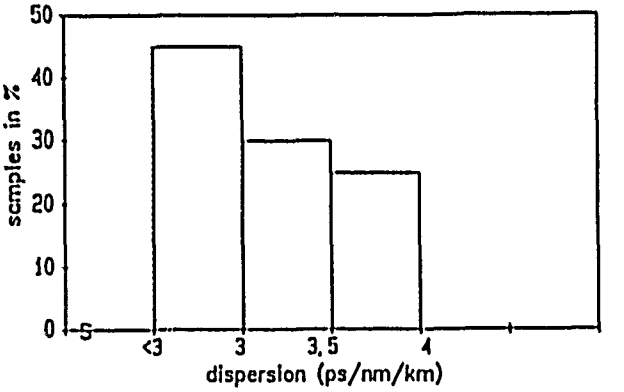

Fig.8. Distribution of maximum dispersion values on the same samples as those in Fig. 7.

The smaller field results in low sensitivity to bending of the fiber. Fig. 9 illustrates the additional attenuation of two DFSM fibers as well as that of a standard matched-cladding single-mode fibers after winding 100 turns on a mandrel with 50 mm diameter. In comparison to standard matched-cladding single-mode fibers, the additional attenuation caused

by bending occurs only at the longer wavelengths in DFSM fibers; i.e. in a range which does not affect the cabling. The tests were conducted on two DFSM fibers with deliberately low cutoff wavelength (< 1.05 μm). Therefore, the average sensitivity to bending of our DFSM fibers is even better because a longer cutoff wavelength causes a correspondingly lower sensitivity to bending.

A standard loose tube cable construction was used to investigate the performance of the DFSM fibers in a cable. There is no measurable increase in attenuation of the DFSM fibers in a cable. This confirms their low sensitivity to macro- and micro-bending.

In addition, we examined the behavior of DFSM fibers as a function of temperature variation. For this the cable was subjected to a continuous heat cycling test for 10 days at reference temperatures of -20°C, 0°C, +20°C and +60°C. The change in attenuation was determined through OTDR measurements at 1.3 μm and 1.55 μm. The maximum deviation measured on all fibers from the +20°C reference value was less than 0.01 dB/km. This value is equal to the resolution capability of the OTDR.

Splice Loss.

In Ref.[6] we have shown that low-loss fusion splices (≤ 0.05 dB) between DFSM fibers can be carried out routinely. We have also shown that low-loss splices between DFSM and standard single-mode fibers can be made. It is therefore possible to use components with standard single-mode pigtails in conjunction with DFSM fibers.

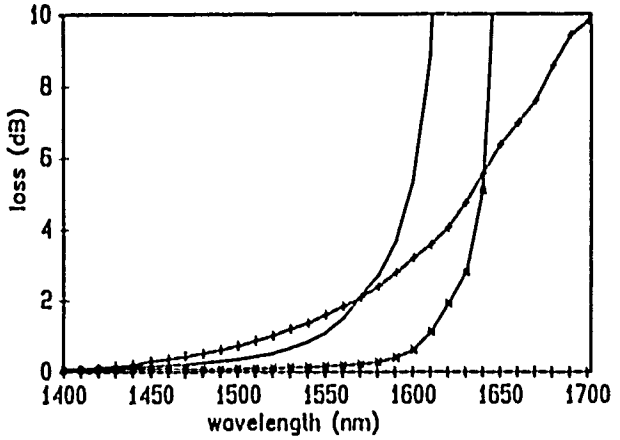

Fig.9. Macro-bending loss (100 turns of fiber on 50 mm diameter):
solid line: DFSM fiber, 1028 nm cutoff wavelength;
***** line: DFSM fiber, 1050 nm cutoff wavelength;
+++++ line: Standard matched-cladding single-mode fiber

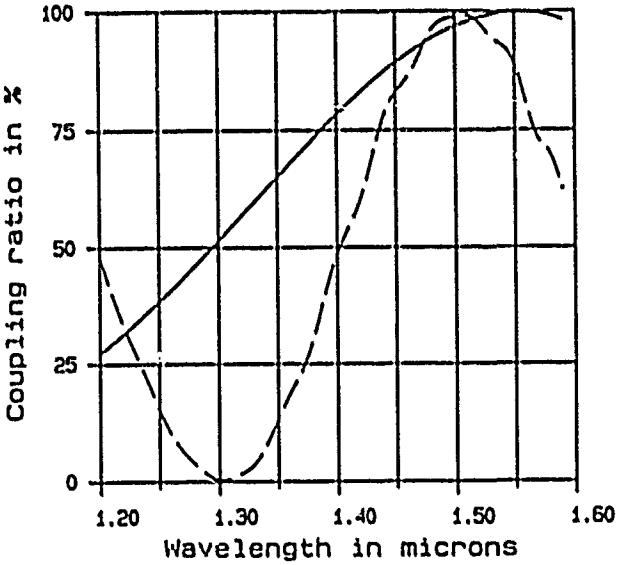

Fig.10. Coupling ratio of single-wavelength DFSM-fiber coupler (solid line) and DFSM-fiber wavelength division multiplexer (dash line).

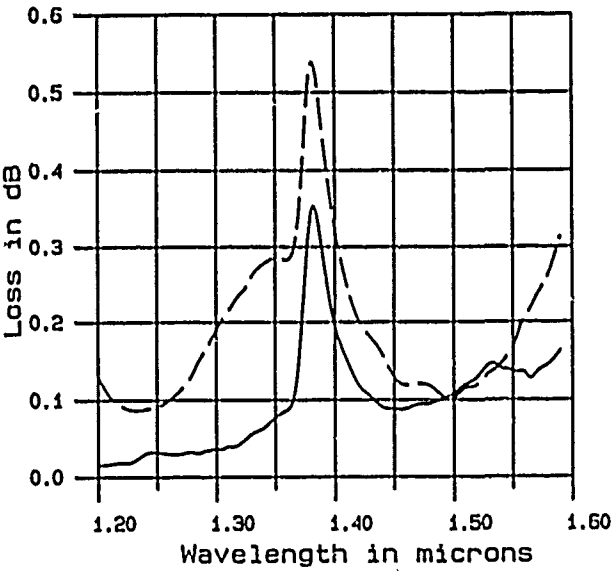

Fig.11. Loss of single-wavelength DFSM-fiber coupler (solid line) and DFSM-fiber wavelength division multiplexer (dash line).

Biconically-tapered DFSM couplers.

Biconically-fused fiber devices like couplers and multiplexers can be made from DFSM fibers in the same manner as from standard single-mode fibers. Typical characteristics of such devices are shown in Figs. 10 and 11. In order to investigate the diffusion processes within the coupler waist we developed a high-contrast, dynamic RNF (Refracted Near-

Field) technique with high spatial resolution by deconvolving the input-focus near-field[3]. Fig. 12 shows the deconvolved refractive index profile of a cross-section within the coupler waist. As a result of diffusion, the multiple claddings of the two cores disappeared. Details, including field calculations and propagation characteristics , i.e. polarization dependence, are given in Ref.[4].

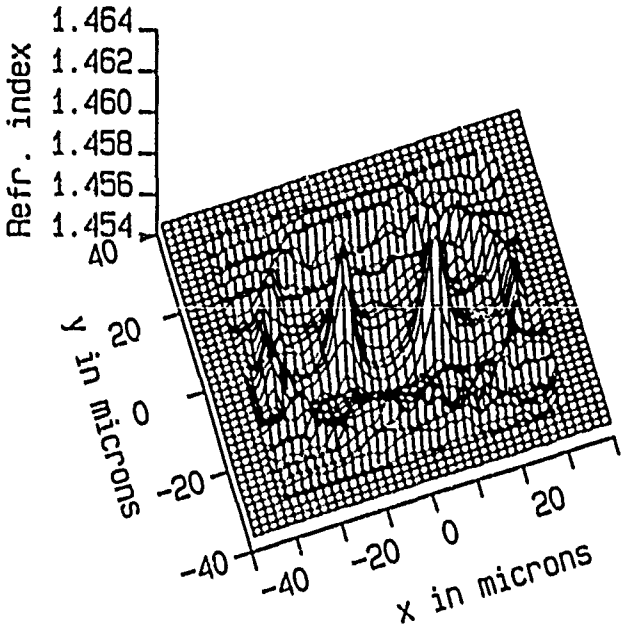

Fig.12. Measured refractive index profile of fused section of DFSM-fiber single-wavelength coupler, deconvolved with the input-focus near-field.

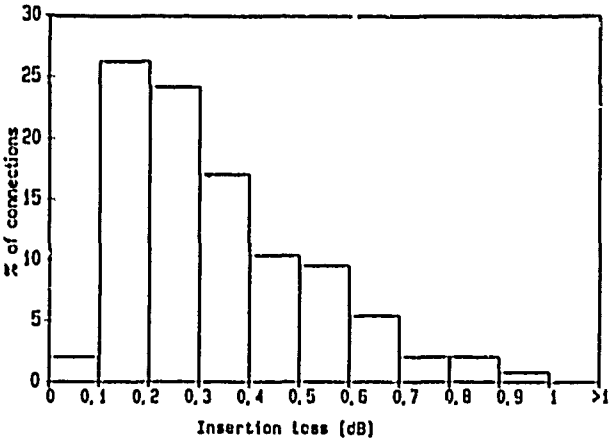

Fig.13. Distribution of insertion losses (DIN type 47 256 connector) with DFSM fibers: 240 connectors randomly oriented against reference connector.

Connectors.

Fig. 13 illustrates a histogram of insertion losses which were measured with DIN type 47256 connectors used between two DFSM fibers. The losses of connectors with DFSM fibers are only slightly higher than those of connectors with standard single-mode fibers. This can be tolerated in the subscriber loop.

Conclusion.

We designed, fabricated and cabled DFSM fibers with a maximum absolute chromatic dispersion of $\leq$ 3.5 ps (km$\cdot$nm) with low bending and splice losses for the 1.29 µm $\leq \lambda \leq$ 1.56 µm wavelength range. This new design takes into account fabrication tolerances and limitations. The fiber behaves well in the cable. All standard quality tests have been satisfactorily completed on cables with DFSM fibers. Connectors with DFSM fibers exhibit proper performance. In addition, we fabricated low-loss fused couplers and multiplexers from the DFSM fibers. Therefore, the designer has at his disposal all necessary components to install the DFSM fiber in the subscriber loop. The characteristics of the DFSM fibers offer the system designer a considerable increase in possible systems configurations.

Acknowledgments.

This project was supported by the German Federal Ministry of Research and Technology, Bonn, Fed. Rep. of Germany. The authors wish to thank Mr. H. Hofheimer of Cable Consultants Corp., Larchmont NY for his valuable assistance in preparing this paper.

References.

1. L. Bosselaar, G. Kuyt, L.L. Kanters, G.D. Khoe, "Properties and Applications of the Dispersion-Flattened Single-Mode Fibre", Proc. E-FOC 1989, Amsterdam, page 173
2. H. Etzkorn, T. Heun, "Highly Accurate Numerical Method for Determination of Propagation Characteristics of Dispersion-Flattened Fibers", Optical & Quantum Electronics, Vol. 18, 1986, p. 1
3. Petermann, K. "Fundamental Mode Microbending Loss in Graded-Index and W-Fibers." Optical and Quantum Electronics, Vol. 9, 1977, p. 167
4. W. A. Snyder, J. D. Love, "Optical Waveguide Theory", Chapman & Hall, London, New York, 1983

5. U. Ackermann, H. Bauch, R. T. Kersten V. Paquet, G. Weidemann, T. Nagg, E. Rauchle, "Physical Processes in a Microwave-Produced Plasma for Preform Fabrication", Proc. OFC, Houston, Feb. 1989, p. 107
6. W. Stieb, J. Schulte, A. M. Oehler, T. M. Hauff, W. E. Heinlein, "Fusion Splices with Low Loss between SM-Fibers of Different Types", Proc. 37th IWCS, Reno, 1988, p. 569-575
7. A. M. Oehler et al., "High-Contrast Refractive Index Measurement of Fused Single-Mode Fibre Couplers with High Spatial Resolution by Deconvolving with the exact Near-Field", to be published
8. A. M. Oehler, T. M. Hauff, W. E. Heinlein, M. Moratzky, W. Stieb, J. Schulte, "Fused Single-Mode Fibre Couplers with Low Polarization Sensitivity: Refractive-Index Profile Measurement, Modelling and Realization", Proc. 15th European Conf. on Optical Communications, Gothenburg, 1989

Werner Stieb
Kabelmetal Electro GmbH
P.O. Box 260
3000 Hannover 1
Fed. Rep. of Germany

Werner Stieb, after receiving his electrical engineering degree from the University of Kaiserslautern in 1986, joined Kabelmetal Electro as a development engineer in the field of telecommunication cables. As a group leader he is responsible for development of passive optical components.

Johann Schulte
Kabelmetal Electro GmbH
P.O. Box 260
3000 Hannover 1
Fed. Rep. of Germany

Johann Schulte received his physics degree in quantum optics in 1981 and his Ph.D. in engineering in 1986 from the Technical University Hannover. After a research fellowship at IBM, Yorktown Heights NY, he joined Kabelmetal Electro in 1987, where he is presently engaged in the development of components for optical communications.

Thomas Hauff
Univ.of Kaiserslautern
Dept. of Theoretical EE & Optical Communic.
P.O. Box 3049
6750 Kaiserslautern
Fed. Rep. of Germany

Thomas Hauff received his Dipl.Ing. degree in electrical engineering from the Univ. of Kaiserslautern in 1986, after which he joined the Dept. of Theoretical EE & Optical Communication to pursue his Ph. D. He is engaged in theoretical studies of propagation characteristics of waveguides and non-linear optics.

W. E. Heinlein
Univ.of Kaiserslautern
Dept. of Theoretical EE & Optical Communic.
P.O. Box 3049
6750 Kaiserslautern
West Germany

Walter Emil Heinlein received his Dipl.Ing. degree in electrical communications engineering in 1955 and his Dr.-Ing. degree in 1958 from the Univ. of Stuttgart. In 1957 he joined Siemens AG., Munich, where, as head of a research laboratory, he performed exploratory development work on microwave applications of semiconductors, active filters and fiber optic transmission systems. Since 1975, he has been a Professor of Theoretical Electrical Engineering at the University of Kaiserslautern, where he is engaged in research on optical communications. Prof. Heinlein is co-author and author of two books. He is a member of the Optical Society of America (OSA) and the Institute of Electrical and Electronics Engineers (IEEE).

Matthias Moratzky
Univ.of Kaiserslautern
Dept. of Theoretical EE & Optical Communic.
P.O. Box 3049
6750 Kaiserslautern
Fed. Rep. of Germany

Matthias Moratzky received his Dipl. Ing. degree in electrical engineering from the University of Kaiserslautern in 1989, after which he joined the Dept. of Theoretical EE & Optical Communication. He is engaged in theoretical studies of propagation and coupling characteristics of single-mode fiber couplers.

Albrecht Oehler
Univ.of Kaiserslautern
Dept. of Theoretical
EE & Optical Communic.
P.O. Box 3049
6750 Kaiserslautern
Fed. Rep. of Germany

Albrecht Oehler received his Dipl.Ing. degree in electrical communications engineering from the University of Kaiserslautern in 1985. Following a fellowship at Siemens AG in Munich, where he was engaged in exploratory development work on fiber optic transmission systems, he joined the Dept. of Theor. EE & Optical Communication to pursue his Ph. D. in fiber optics. He is engaged in theoretical studies of propagation and coupling characteristics of single-mode fiber couplers.

DEVELOPMENT OF THE OPTICAL FIBER CABLE INSTALLED IN THE SEWER PIPE NETWORK

Masayuki NIIJIMA Shintaro SENTSUI Katsuhiko KOMIYAMA

THE FURUKAWA ELECTRIC CO., LTD., TOKYO, JAPAN

Summary

We find the new cable installation duct in metropolitan area. This is a sewer pipe. As severage system look like a network, an intelligence network easily can be introduced through sewer pipe in this case. To satisfy installation in a sewer pipe we introduced stainless pipe fiber units which consisted of thin stainless tubes and contained an optical fiber. Stainless pipe units were stranded Jelly-filled and polyethylene sheath was applied. The cable whose outer diameter and weight were about 10 mm and 100 kg/km, respectively. The test result of the cable was excellent for using stainless pipe units. The damage by rats was limited to only PE sheaeth, metal tubes were not damaged. Further more the cable was installed into the 250 mm sewerpipe, actually in September 1988. The cable was run through in the sewer pipe and anchored to the upside of the sewer pipe by installation robot, successfully. For the result of this installation trial, the new cable shows to have satisfactory performance for practical use.

1. INTRODUCTION

Optical fibers are characterized by them small diameter, light weight, broad-band, non - inductive property. More and more optical fibers are being introduced in Japan. In metropolitan area such as Tokyo, in particular, there is a rapid progress of its introduction. Optical fiber cables are generally installated cable ducts under ground in order not to damage the scenery of towns. As a result of recent progress in informationalization, however, the lack of installation space for new cables has become a problem. Under such circumastances, we focused on other existing pipes to use them as new cable installation space. These pipes include waterworks, sewer systems and gas pipelines. Since they are networks, it is easy to select cable routes. Moreover, being led into all the subscribers' houses, these pipes will be useful once optical fibers are brought into subscribers' use. From the viewpoint of safety, however, with current technology it is impossible to use gas pipelines and waterworks on which pressure is exerted. As a consequence, we investigated sewer systems as the prime candidate.

There are several problems we must solve to install optical cables through sewer systems. Difference of sewer systems from general cable ducts is that water is always running through sewer systems. Water degrade the performance of optical fibers. Moreover, since water running through these pipes is sewage water, member protecting optical fibers must be the one that can be submerged in it. To avoid these problems, optical fibers must be designed so that it will not get wet, and its member must be chemical-proof. There have also been a number of reports stating that rats living in the sewer systems gnawed cables. Cables must protect optical fibers from the attack of rats. If the size of sewer systems is so small that a man cannot go through, water flow will be affected by the diameter of cables. Accordingly, the size of cables as well must be made thinner.

To meet these requirements, we developed cables smaller in diameter using a metal tube made by inserting an optical fiber in a thin stainless tube. In extreme narrow sewer systems, in particular, as an optical fiber cable is installed by a robot, flexibility will become an essential requirement.

2. CABLE DESIGN

When installing optical cables through sewer systems, you must make sure that cables are laid on the upper wall of pipes where possible. Sewer systems may not always but intermittently have a running water. However, water may always stay in the lower part of pipes. Therefore, it is recommended to lay cables as high as possible to prevent the deterioration of cables. The size of sewer systems ranges form 4 m to 25 cm in inside diameter. When laying optical cables on the upper inner wall of pipes, trunk pipes of 2 m in diameter allow a man to work in it, however, it is necessary to use a robot in the thinnest branch pipes of 25 cm in diameter. In the latter case, cables must be about 10 mm in outside diameter and flexible.

Since rats may gnaw cables in sewer systems, tests were actually performed on a variety of cables to see damage by rats' gnawing. Cables used as samples and their results are shown in table 1. According to these results, non-metallic structure is helpless against rats' grawing. General LAP sheath also proved to be useless. The test results shows that it is effective

to insert an optical fiber in a stainless steel tube or use stainless steel braiding to protect optical fibers from rats.

Evaluation was made using 50/125 um standard GI type fiber.

2-1 STAINLESS TUBED FIBER UNIT

Normally plastic and alminum are used to protect optical fibers, however, these materials are not strong enough to protect it from moisture and rats. If outside diameter is not limited, such materials as corrugated sheath can also be used. However, when cables are installed by a robot, these materials are not proper due to its excessive outside diameter and weight and poor flexibility. For that reason, we developed a stainless pipe fiber units which consisted of thin stainless tubes and contained an optical fiber to invent thin cables. Cross section of a metal tube unit is shown in Fig. 1. The outside and inside diameters of the pipe are 1.2 mm and 0.8 mm, respectively, and the outside dimeter of the optical fiber cort is 0.4 mm. These figures are similar to those for the conventional core would not be damaged by rats' gnawing.

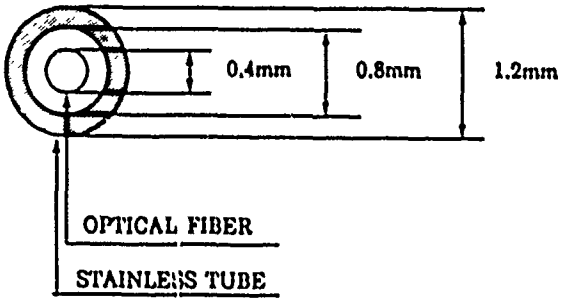

FIG.1 CROSS SECTION OF THE METAL TUBED FIBER UNIT

2-2 CABLE

The cross section of the developed cable was shown in Fig. 2. The cable is made by stranding six cores of the optical fiber unit mentioned in 2-1 around the center tension member and covering it with polyethylene sheath. It is a thin cable with an outside diameter of about 7 mm. Stainless steel and polyethelene are used as cable member since it is thought to be resistant to corrosion by waste water within sewer systems. PH value measured in the actual sewer systems is within a range of 5 to 9. The said materials are strong enough to resist it.

We performed tests on an optical unit and cable to see damage by rat's gnawing. As far as the cable is concerned, although polyethylene sheath was damaged, stainless steel pipe was unharmed. Both the optical fiber and unit were safe.

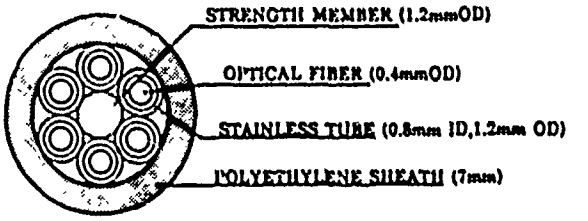

FIG.2 CROSS SECTION OF DEVEROPED CABLE

TABLE 1 GNAWING TEST RESULT

SAMPLE	OUTER DIAMETER	RESULT	DECREASE RASIO OF WEIGHT
NON-METALLIC SLOT CABLE	11.5 mm	THE WHOLE	54.3 %
LAP SHEAETH SLOT CABLE	10.5 mm	THE WHOLE	53.7 %
STAINLESS STEEL BRADING UNIT	12.0 mm	AN IMPRESSION OF TEETH	0 %
STAINLESS STEEL BRADING CABLE	14.5 mm	THE SURFACE	2.0 %
CCP-H CABLE (STEEL CORRUGATED)	15.0 mm	NO DAMAGE	-
CCP-H CABLE (WITH PE SHEATH)	17.0 mm	THE SURFACE	-
METAL TUBED FIBER UNIT	1.2 mm	NO DAMAGE	0 %
METAL TUBUD FIBER UNITS STRANDED CABLE	7.0 mm	THE SURFACE	3.0 %

3.CHARACTERISTICS

3-1 STAINLESS TUBED FIBER UNIT

3-1-1 Elongation

The elongation test results of the stainless tubed fiber unit is shown in Fig. 3. In the elongation test, the elongation of the tube, distortion in tension and elongation of the fiber were measured by exerting tensile force on the tube of 10 m in gauge length.

According to the results, the optical fiber is longer than the stainless tube by 0.05 %, and Young's modulus of the tube which is calculated from load and elongationis about 10,000 kg/mm^2. This proves the material to be well annealed. On the other hand, the Young's modulus of stainless steel is 17,000 kg/mm^2, which is much lower than the past results. This is because the handling of tube was taken into consideration. That is, if stainless steel with a high Young's modulus is used, a tube will not become flexible, making its handling during terminal processing difficult. As a result, workability may drop and fibers may be disconnected.

To avoid such problems, the tube used in this test is annealed to decrease its Young's modulus.

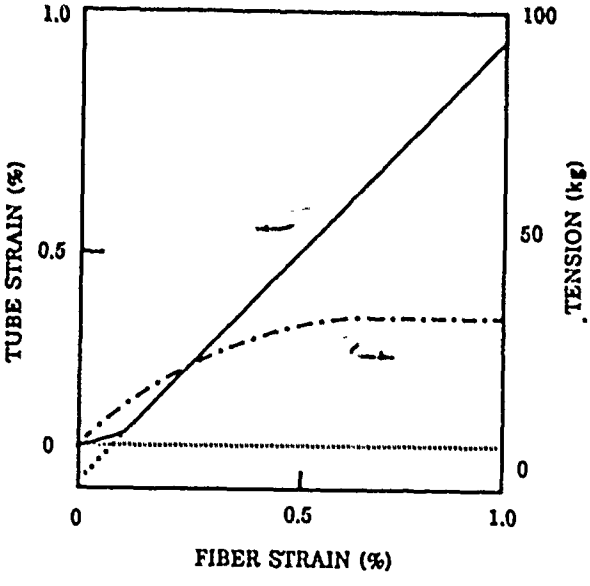

FIG.3 ELONGATION TEST RESULT (METAL TUBED FIBER UNIT)

3-1-2 Other characteristics

Other evaluation results are shown in Table 2.

Lateral pressure: No increase in loss even with a width of 50 mm and a load of 250 kg or over, thus proving the core to be very strong.

Bending : Loss is no greater than nylon core. However, flexibility is less.

Temperature : Favorable changes in loss are obtained within 0.1 dB/km during the measurement at temperatures ranging from -40 to +80 ℃. Possible reasons are that the coefficient of linear expansion of nylon is smaller than that of linear expansion of nylon is smaller than that of stainless steel, and fiber can move within the tube.

TABLE 2 TEST RESULT

ITEM	RESULT
LATERAL PRESSURE	LOSS NO INCREASE OF 250kg/50mm
BENDING	LOSS NO INCREASE OF 50mm DIAMETER
TEMPERATURE	LOSS NO INCREASE OF -40~+80℃

3-2 CABLE

3-2-1 Manufacturing-process loss

Changes in manufacturing-process transmission loss of optical fibers in the form of a cable are shown in fig. 4. Optical fibers in the form of a cable caused no changes in loss, showing favorable results.

3-2-2 Elongation

Elongation test results are shown in Fig. 5. Fiber strain is 0 with a tensile force up to 100 kg, which is the weight for 1 km. A tensile force of 250 kg causes elongation strain by 0.2 %, not increasing transmission loss. This represents that being a thin cable of 7 mm in outside diameter, the optical fiber cable is very strong.

3-2-3 Lateral pressure

In lateral pressure test, applied pressure, transmission loss and deformation were measured by applying load on a cable sandwitched between plates of 50 mm in width. The results are shown in Fig. 6. Transmission loss does not occur with a load of less than 500 kg, thus showing the immense protective effects of metal tube.

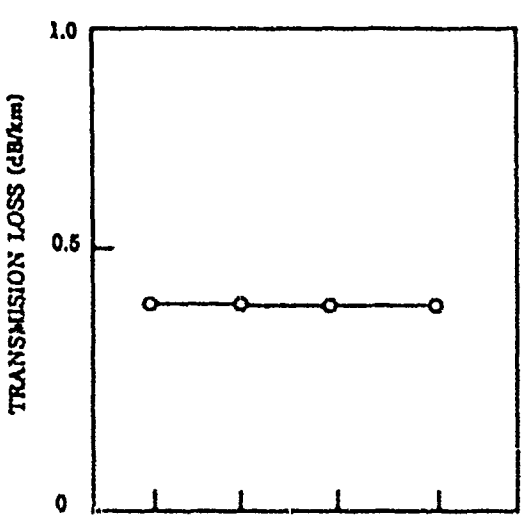

A: OPTICAL FIBER B: METAL TUBED FIBER UNIT
C:STRANDED UNIT D:CABLE

FIG.4 TRANSMISSION LOSS IN MANUFACTURING PROCESS

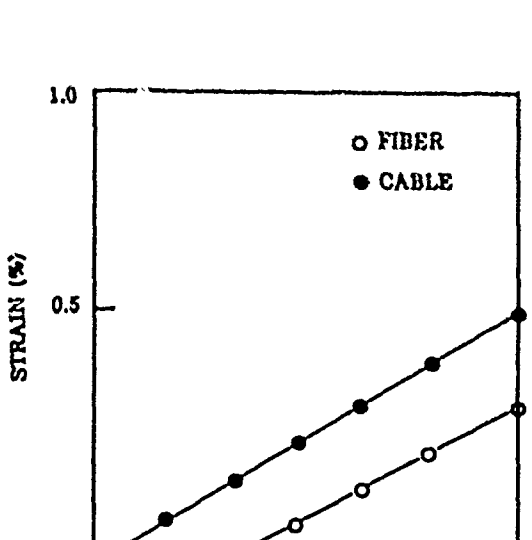

FIG.5 ELONGATION TEST RESULT (CABLE)

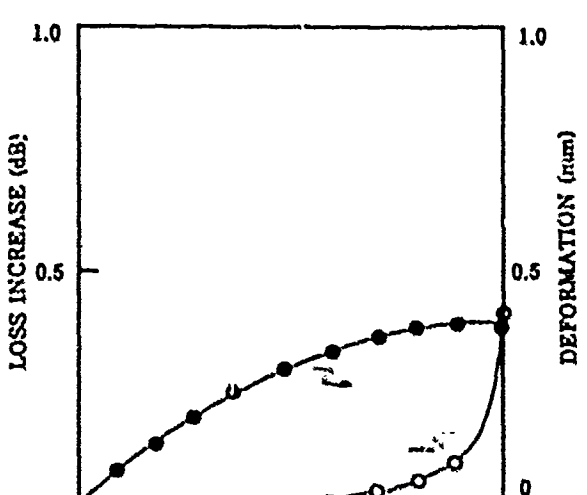

FIG.6 LATERAL PRESSURE TEST RESULT

3-2-4 Flexibility

One end of a cable of 500 mm in length is held and load is applied to the opposite end of the cable to measure the weight of weight and deflection. The results are shown in Fig. 7. When load is 100 g, a deflection of 300 mm occurs. This proves the cable structure to be flexible.

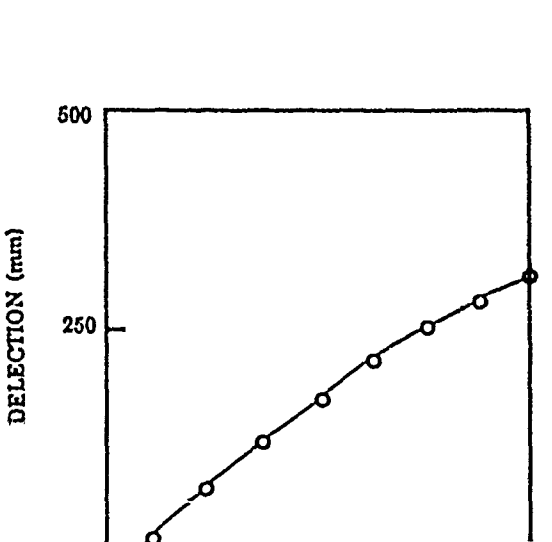

FIG.7 FLEXIBILITY TEST RESULT

3-2-5 Environmental test

As an environmental test, we performed an accelerated corrosion test using solution which is assumed to be in sewer systems. Requirements are shown in Table 3. One kind of alkali solution and three kinds of acid solutions are used in the test. As samples, a collecting unit and stainless tubed unit, from which cable and polyethylene were removed, are used.

Six months have passed since this test as started, however, no abnormalities are found in any of these samples.

4. INSTALLATION TEST

A core which is made by inserting an optical fiber in a metal tube is used to make a cable to be laid through sewer systems. As a result, a cable which is thinner and stronger than the conventional cables is invented. However, this cable has not been actually used. We redesigned it to improve safety prior to the field test. Cross section of the cable used in the test is shown in Fig. 8. Eight optical fiber cores are inserted in a metal tube and stranded, and stainless steel braiding is added. This structure proved to be effective in the test to see damage by rats' gnawing. The outside diameter of the cable is about 10 mm and weight about 100 kg/km.

After having been installed through sewer pipe of 250 mm in inside diameter, the cable was fixed onto the upper wall of the sewer pipes using a cable installation.

The cable installation robot is made up of three cars. The first car raises a cable to the upper part of the pipe, the second car fixes it onto the upper wall with nails, and the third car inspects the work.

A laying test was performed in September, 1988. A cable was laid through the existing sewer pipe of about 3 km in length, which was currently in use. One year has passed since the laying is completed, however, no problems have occurred by now.

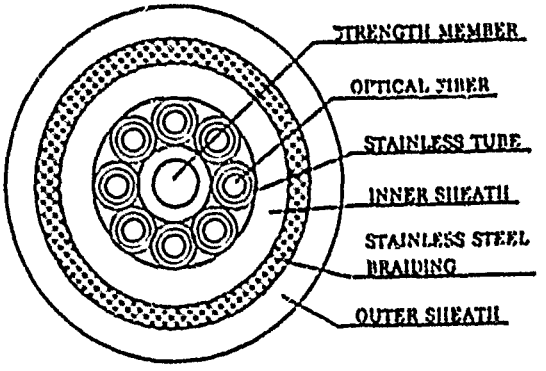

FIG.8 CROSS SECTION OF NEW TYPE CABLE

5.Conclusion

We focused on sewer pipes, developed cables and performed a laying test to remedy the shortage of cable ducts in metropolitan area. As a result, we came to the conclusion that inserting an optical fiber in a stainless steel pipe is effective to protect the optical fiber from waste water or rats. We actually made a cable on an experimental basis and performed a installating test. Cable could be made thinner, stronger and more resistant to corrosion than the conventional cables by inserting the cable in a stainless tube. Installating was completed in September, 1988, and no problems have occurred by now. We will continue to monitor this cable.

Our next goal is to make it possible to increase fibers in a metal tube. We are now developing cables with up to 24 fibers.

6.Acknowledgment

We express our appreciation to Sewage Tokyo Metropolitan Gaverment and Tokyo Metropolitan Sewage Service Company for their useful advice and instructions on the development of the said cable for sewage.

TABLE 3 ENVIRONMENTAL TEST RESULT

		METAL TUBE FIBER UNIT	STRANDED UNIT	CABLE
ALKALI (pH10)	NaOH+SEWAGE	NO DAMAGE	NO DAMAGE	NO DAMAGE
ACID (pH4)	H_2CrO_4+SEWAGE	NO DAMAGE	NO DAMAGE	NO DAMAGE
	HCl+SEWAGE	NO DAMAGE	NO DAMAGE	NO DAMAGE
	H_2SO_4+SEWAGE	NO DAMAGE	NO DAMAGE	NO DAMAGE

Masayuki Niijima
The Furukawa Electric Co.,Ltd
6-1,Marunouchi 2-chome
Chiyoda-ku,Tokyo,100
Japan

Mr. Niijima graduated from Waseda Univ. 1985 with a B.S. in electrical engineering. Then he joined the Furukawa Electric Co., Ltd. and has been engaged in development of optical fiber cables.
Mr. Niijima is now a staff engineer of Marketing & Engineering Department, Fiber Optics & Telecommunication Division at the Furukawa Electric Co., Ltd. and a member of the IEE of Japan.

Katsuhiko Koniyasu
The Furukawa Electric Co.,Ltd
6-1,Marunouchi 2-chome
Chiyoda-ku,Tokyo,100
Japan

Mr. Koniyasu received the B.E. degree in Electric Engineering from Yamanasi University in 1967, then he joined the Furukawa Electric Co., Ltd. and engaged in Cable Engineering and Cable Accessories.
Mr. Koniyasu is now a staff manager of Marketing & Engineering Department, Fiber Optics & Telecommunication Division.
He is a member of the Japan Electric Wire & Cable Maker's association.

Shintaro Sentsui
The Furukawa Electric Co.,Ltd.
6 Yawata-kaigandori,
Ichihara,Chiba,290
Japan

Shintaro Sentsui received his B.S. degree in Physical Engineering from Tokyo University in 1970, and then joined the Furukawa Electric Co., Ltd.
He has been engaged in research and development of superconduction co-axial line, characterization and measurment of optical fiber.
He is now a manager of Optical Fiber Transmission, Chiba Research Laboratory, Research & Development Division.
He is a member of Institute of Electrronics, Information, and Communication engineers of Japan.

On the crest of a new wave in optical submarine cable technology

Wolfgang Giebel

SIEMENS AG, Munich

Abstract

We present here a submarine communication cable system which, when operating at 140 Mbit/s, needs a land-based repeater at the latest every 250 km. The target of the development work that began in 1985 was to introduce a submarine cable system capable of competing with radio relay and overland cable systems, while permitting both national and international traffic.

The result of our development is a smallsized but robust undersea cable with a diameter of about 10 mm, which requires no conventional cable-laying vessel, which can be clad on board the converted supply ship with a double armoring - the so-called protector - and can be plowed into the seabed. The plow, operating on the "constant protection factor" principle, has been tried and tested and is field proven in the Philippines.

The submarine cable system had its initial trials 1987 in Singapore. The first route, with a total length of 93 km, has been in operation since November 1988 in the Philippines.

On the crest of a new wave in optical submarine cable technology

Telegraph cables operated without repeaters. At first they were of small diameter and yet efficient. Kunert (1) writes about a telegraph cable laid in the North Sea in 1859 that had an outside diameter of 13 mm and remained in operation until 1903 (Fig. 1). In the course of these 44 years it was damaged by ice five times and repaired.

Fig. 1
Telegraph cable (1859)

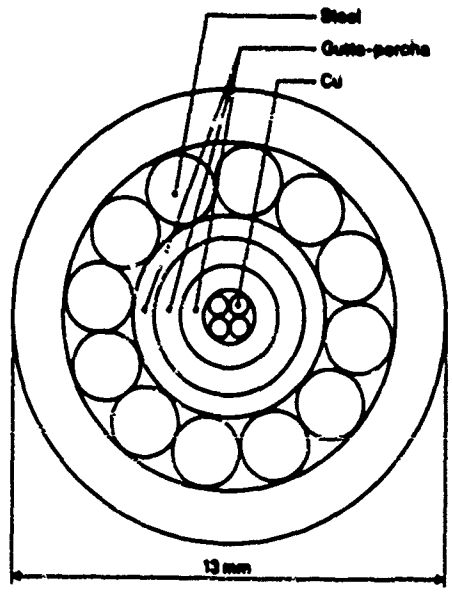

The question is: why do practically all submarine cables today have twice the diameter of this cable of 1859?

The decisive element is certainly not the power feed for the repeaters. We know that in the course of time the telegraph cables became thicker, and that telephone cables for repeaterless operation have diameters of well above 20 mm. The factor that determines the outside diameter is the need for tensile strength. This need increased 100 years ago because of the impossibility of correctly positioning the cable-laying vessel. In the event of a disturbance, the captain had to anchor the ship by the cable. Tensile strength requirements of 20 t were quite justifiable. On the other hand, the submarine cables were damaged by fishing vessels - by so-called otter boards. The obvious answer was to reinforce the cable with an additional layer of armoring wires. The ship owners responded by strengthening their fishing gear. The Danes put an end to this jockeying between cable manufacturers (and operators) and ship owners in

the North Sea area by developing and using a cable plow (11). The logical consequence, i.e. reducing the thickness of the cables, did not occur, however.

If a submarine cable in the coastal area is adequately protected, there is no reason why the outer diameter, depending on core design and handling criteria, should not be less than 10 mm and still guarantee the expected service life of 20 years. Deep water is in itself sufficient protection.

On the basis of these considerations, a submarine cable concept, the MINISUB system, was developed with the following objective:

The cost of the system must be comparable with that of radio relay and overland cable systems, thereby exploiting a niche for submarine application that was hitherto inaccessible to submarine cables.

This requirement could only be met under the following conditions:

* Dispensing with conventional cable laying vessels
  - The cable must be of small diameter. Up to 200 km must be stowed in one standard-size container.
  - The cable can thus be brought to the ship. The ship no longer has to fetch the cable from the works. This saves transport and mobilisation costs.
  - A modular laying concept for adaption to locally available ships is required.
* Favorably priced cable, thoroughly tested.
* Precise protective measures tailored to the individual application (protector, plow) thus ensuring maximum reliability.
* Streamlined laying and repair procedures.
* Large repeater spacings.
* Practical trials in additon to laboratory tests.

There is not sufficient time for a detailed discussion of every point mentioned here, but the chief criteria of our MINISUB system are outlined below.

The MINISUB cable

The cable must be significantly heavier than water, afford mechanical protection for the optical fiber and must not fill up with water if damaged. Moreover, it must be capable of being laid on the seabed and taken up again from on board the ship. For MINISUB we use a buffer that loosely envelops the required number of fibers from 2 to 16 and permits a certain surplus fiber length. A special filling compound prevents the intrusion of water if the cable is damaged, even at a depth of 3000 m. This buffer is surrounded by a metal corset of armoring wires, the interstitial spaces being filled, and the whole is protected by a plastic sheath. This MINISUB design features an outside diameter of about 10 mm, a weight of less than 200 kg/km and a sinking rate of about 0.4 m/s. Conventional submarine cables have a diameter of over 20 mm, weigh more than 1000 kg/km and sink at about 0.5 m/s (Figs. 2,3).

Fig. 2
MINISUB cable
in the container

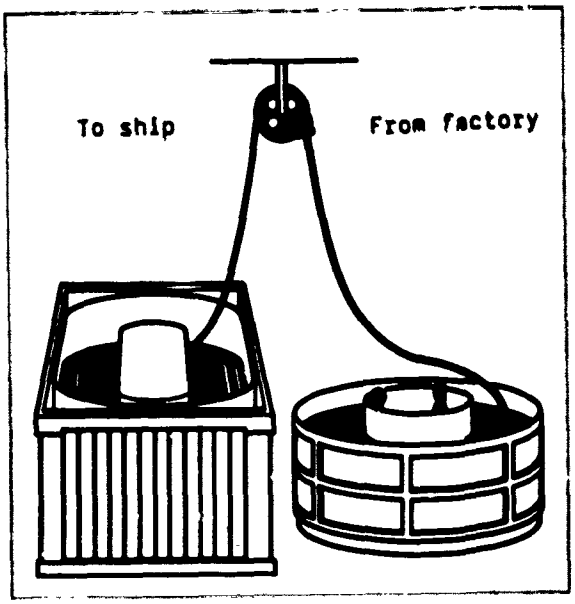

As regards the tests on the cable itself, a four-minute film, shown here today for the first time, will give you an overall picture of the results obtained.

Fig. 3
MINISUB cable

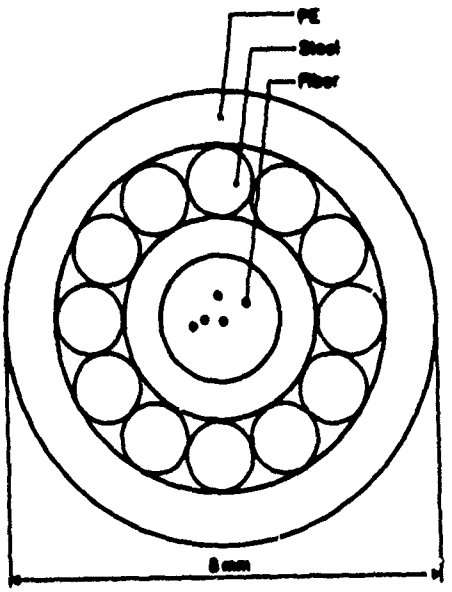

Protection

Like conventional submarine cables, MINISUB requires additional protection in the shore region, on a rocky bottom in some cases, and where there are strong currents.

Fig. 4
The MINISUB cable inserted in its protector by the combiner

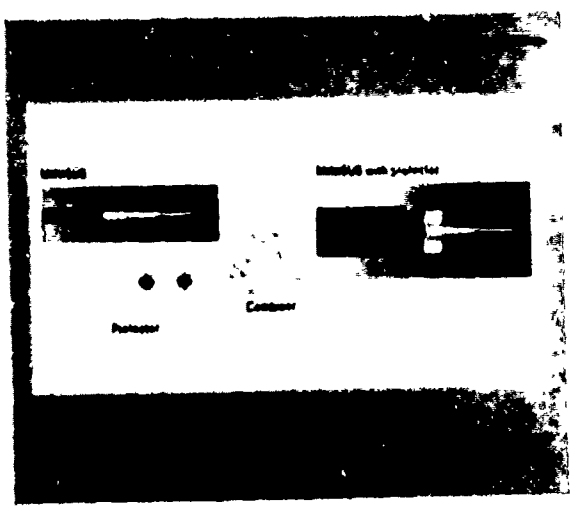

As additional protection, it would be possible, for example, to apply several layers of armoring in the factory. This is cost-intensive. Moreover, transport and logistics problems then arise, and short-notice changes in the cable route are not possible, since matched lengths have already been prepared. We have therefore developed a protector consisting of two plastic-covered steel ropes. Cross-links form a duct, into which the MINISUB cable can be threaded on board the ship with the aid of a combiner (Fig. 4).

As a further protective measure in the shore region, the MINISUB cable is enclosed by a conduit (Fig. 5) that runs from the land-end point (LEP) to the transition point (TP). The conduit is chosen such that it is readily washed into the seabed by a water jet and can be protected by stones or concrete. If several conduits are laid side-by-side in the landing region, this considerably reduces costs if laying of further cables becomes necessary.

The water depth at the transition point (TP) is about 10 m. At this point the cable-laying vessel can anchor safely, and divers can work for long periods under water without the need for decompression when inserting the MINISUB cable that is to be brought ashore.

Fig. 5
Schematic representation
of a MINISUB route

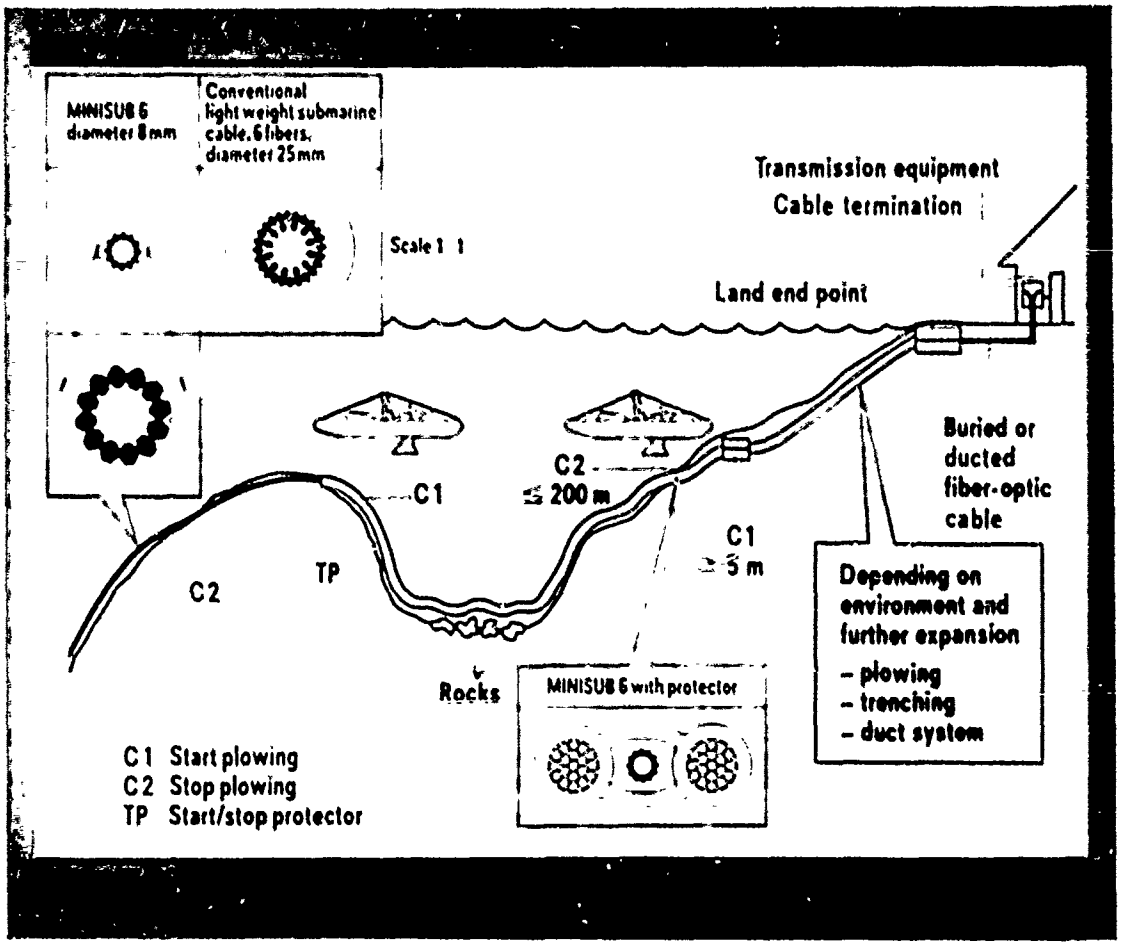

From the TP onward the floatable underwater cable plow developed in the last two years can then be put to work (Fig. 6). Operating on the constant-protection-factor principle, the plow-in depth of the cable varies with the consistency of the seabed. If the plowshare hits an obstacle, the arm carrying the plowshare jumps over it without damaging the cable and digs into the seabed again behind the obstacle. All movements of the plow, which is designed for water depths up to 400 m, are displayed on board the cable-laying vessel and recorded in the measuring container.

Fig. 6
Floatable Plow

Laying technique

According to the route, water and weather conditions, a suitable ship is chosen for cable laying. It is fitted out with the appropriate containers (Fig. 7), such as the measuring equipment, cable and protector containers, and the required laying equipment. After a few days the ship is ready to sail. On completion of cable laying, the ship is stripped down again and returned to its original purpose.

The same applies to all repair work. Specially developed grappling equipment goes on board the ship together with the repair specialist, and the cable is hauled up. It is repaired in the measuring container, which contains all the necessary apparatus for cable repairs.

Fig. 7
Drawing of the ship with containers (2 views)

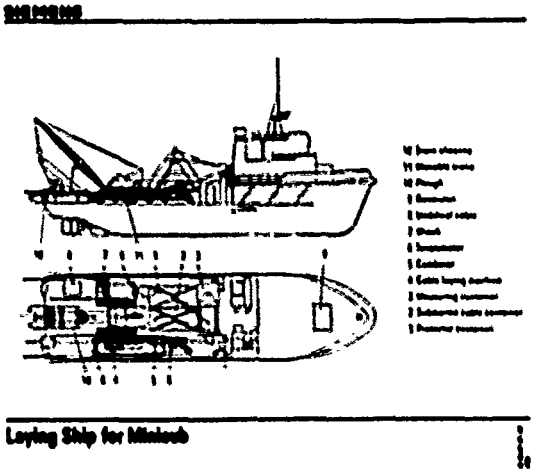

Laying Ship for Minisub

Transmission equipment

The transmission capacity of optical fibers is limited by the presently available transmission equipments, which have been operating reliably on overland lines at 2 Mbit/s to 565 Mbit/s. In the case of unregenerated transmission, the maximum range is the most important feature. This is determind by:

- the fiber attenuation
- the transmit power of the DFB (distributed feedback) laser and
- the sensitivity of the receive diode.

With selected fibers and specially adapted equipment, Siemens is today able to transmit at 140 Mbit/s, using a wavelength of 1550 nm, over a distance of 200 km without repeaters.

A further important consideration is the reliability of the transmission equipment. Obviously, the cost of replacing a module in the land-based system, in terms of down-time and expenditure of resources on repair, is only a fraction of the cost of repairing an underwater repeater.

In the near future, 300 km and more will be spanned without repeaters. If optical repeaters are used, it will certainly become possible to span 600 km, at a conservative estimate, without going ashore. This is also the target of our efforts at present.

Project experience

The MINISUB concept was born in 1986 out of optical fiber applications in security systems; first evaluation modules were produced and the design was developed. In 1987 the research and development results for the cable and protector became available, the production parameters were finalized, and the laying hardware, included the cable plow, was ready.

In order to clarify how all the elements of the system function under practical conditions, a trial was planned in Singapore between the islands Pulau Hantu and Pulau Semakau. We chartered the supply ship "Nanato" in July 1987 and commenced the trials. The results of laying about 2 km of MINISUB cable with protector and partly plowing-in the cable were positive. And so it was decided to complete the range of cables and protectors, to adapt the plow and laying facilities even better to the conditons met with in practice, and to plan a commercial installation for 1988.

In May 1988 a contract was signed with the Philippine Long Distance Telephone Company (PLDT) to link Argao on the island of Cebu with Dumaguete on the island of Negros by a four-fiber MINISUB cable over a distance of about 93 km. The preliminary work on organizing the project had begun in March 1988 and the laying task was completed by October 19. When this paper is presented, the first anniversary of successful operation of the 140-Mbit/s system in 1 + 1 configuration will have been celebrated (Fig. 8).

Fig. 6
PHI MINISUB route Argao-Dumaguete

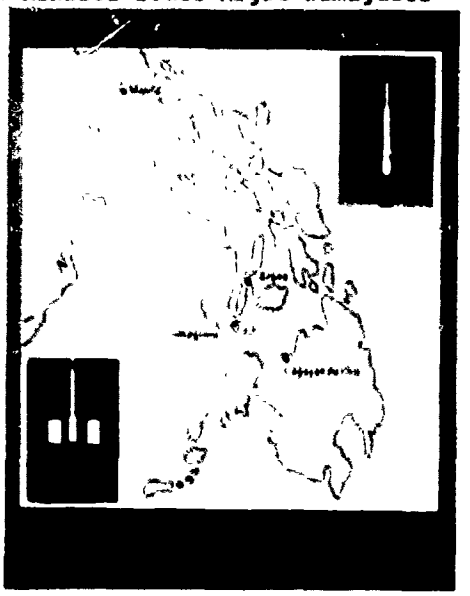

No deterioration of the cable characteristics can be discerned. Typhoons have lashed the landing points; the route is intact.

Introduction of new technology

When something new is created, old specifications must be reconsidered and, if necessary, amended. The simplest course of action for the author of a specification is to accept the new while demanding the old. This cannot be done here. Standards and specifications are certainly indispensable; the space for innovation is dictated by the user.

Literature

(I) Telegraphen-Seehabit 1962
A. Kunert
Karl Glitscher, Buchdruckerei,
Köln-Mülheim

(II) Development of Submarine Cable Plough
G. Ture Jönsson and Jens Kiil,
Telecom Denmark
Teletechnik 1986, No. 1.

Biography

Dipl.-Ing. (FH) Wolfgang Giebel, born in 1941, joined Siemens in 1964; headed several laboratories for design and testing of telecommunication cable accessoiries; marketed this equipment world wide entered the field of heat shrink articles, and is now responsible for submarine cable activities of the Telecommunications Cable Group.

Wolfgang Giebel
SIEMENS AG
Abt. NK VD
P.O. Box 700078
D-8000 Munich 70
Tel.: intern 49-89-72225196

" A ONE-HUNDRED-FIBER SUBMARINE CABLE COMPOSED OF HERMETICALLY COATED FIBER RIBBONS INSERTED INTO SLOTS "

Nobuyuki YOSHIZAWA, Yoshiaki MIYAJIMA and Yutaka KATSUYAMA

NTT TRANSMISSION SYSTEMS LABORATORIES

TOKAI-MURA, IBARAKI-KEN, 319-11, JAPAN

Abstract

A carbon coated fiber with 6.2kgf failure strength is obtained for the first time. Also, a direct-core-monitoring fusion splicing method for carbon coated fibers is developed. Significant problems are solved and carbon coated fiber is proven practically applicable. Consequently, a new type of submarine cable using one hundred carbon coated fibers is proposed and developed. This is a shallow sea cable for non-repeated systems. The simple structure is realized by fully utilizing the advantages of hermetically coated fiber. Results of tests on the manufactured cable revealed excellent optical and mechanical properties.

1. Introduction

Carbon is believed to be an excellent candidate as a hermetic coating material. The use of carbon coating on optical fibers can greatly improve fiber reliability by preventing both mechanical fatigue and hydrogen induced loss increase.[1][2][3] The coating speed of carbon on fiber has been increased to a rate sufficient for commercial use[4]. Carbon coated fiber has been proposed for use in harsh environments such as under the sea where the fiber must withstand high strain levels over long periods of time. However, carbon coated fiber has not been used practically because some problems remain. The initial strength of carbon coated fiber has been lower than that of conventional fiber. Also, the fusion splicing characteristics of carbon coated fiber remain unclear. These problems must be solved before the fiber can be adopted for practical use. From the point of view of cable structure designing, the conventional submarine cable structure is designed to overcome inherent weaknesses in conventional fiber which do not exist in carbon coated fiber. Therefore, a new simplified structure that fully utilizes the many advantages of carbon coated fiber must be designed. However, no new structure has yet been proposed.

In the former half of this manuscript, we report recent technical progress in carbon coated fiber. The two main problems mentioned above have been examined and solved. We describe the process by which we solved these problems. Consequently, no significant technical problem remain for carbon coated fiber and it is now ready for practical application.

In the latter half of this manuscript, we propose a new submarine cable structure which fully utilizes the advantages of carbon coated fiber. The cable structure is designed for a shallow sea non-repeated system. It is a far simpler and more economical cable than conventional cables.

2. Recent progress in carbon coated fiber

The initial failure strength of carbon coated fiber is low, ranging from 4kgf[4] to 5kgf[3], whereas that of conventional non-hermetic fiber is greater than 6kgf. Therefore, we must carefully handle the carbon coated fiber during splicing to avoid fiber failure caused by the low initial strength. Moreover, direct-core-monitoring fusion splicing equipment has been widely used in submarine cable jointing, and a carbon coating on the fiber prevents the monitoring of the fiber core. This is a significant problem in splicing. We examined and solved both the above problems.

2.1 Initial strength improvements of carbon coated fiber

The main factors causing strength degradation have not been reported. In order to attain high strength carbon coated fiber, many factors such as carbon characteristics, carbon thickness, and CVD conditions, must be examined. This complexity has been preventing improvements in this area. We examined the relationship between carbon structure and coated fiber strength. We supposed that amorphous carbon with a fine structure was necessary to attain high strength, and so we examined the surface of carbon coated optical fibers with a scanning tunnel microscope (STM) to ascertain roughness.

Test specimens were Ge-doped silica core fibers for 1.3μm use and were carbon coated using an in-line chemical vapor deposition (CVD) process. Figure 1 shows typical surface images of carbon coated optical fibers measured by the STM. There is a clear difference between the images of samples (A) and (B). The STM can statistically evaluate the surface roughness, which is determined by the height from the minimum value. Measuring accuracy is of the order of one nm. The measured mean surface roughnesses are 4 nm and 68 nm for samples (A) and (B), respectively. Standard deviations are 1 nm and 27 nm, respectively.

Different carbon coated fibers were fabricated under different CVD conditions and the surface roughnesses were measured with the STM. Figure 2 shows the relationship between the surface roughness and tensile failure strength of the fibers. In the failure strength measurement, fifteen specimens of one type of fiber were tensile tested at room temperature and the average failure strength is plotted in Fig.2. The strain rate was 20%/min, and the gage length was 300 mm.

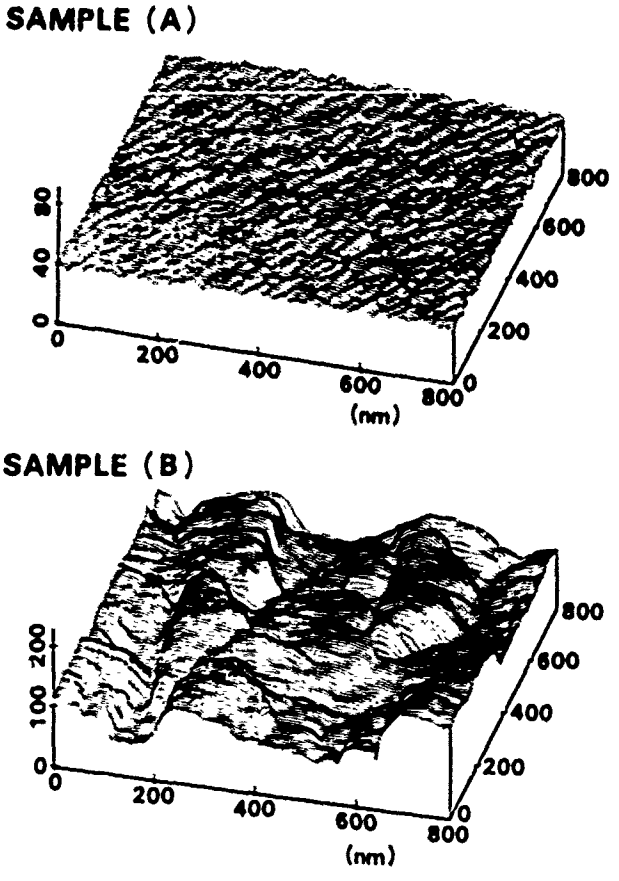

Figure 1. STM images of carbon surfaces.

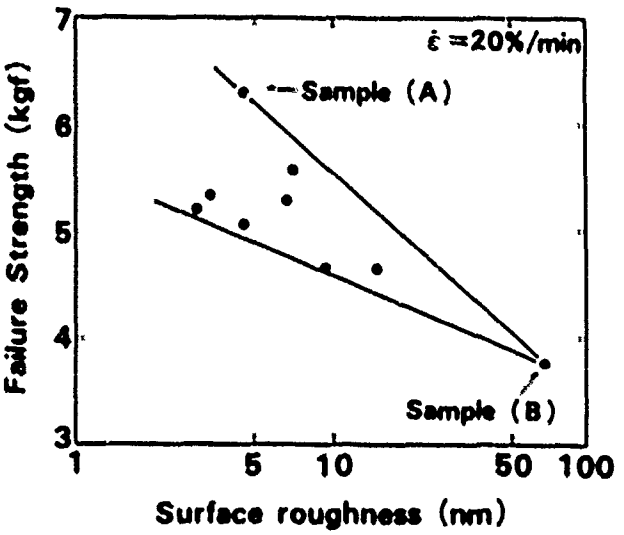

Figure 2. Relationship between carbon surface roughness and failure strength.

It is found that the strength is less than 4kgf when the roughness is greater than 50nm, as in sample (B). When the roughness is less than 5nm, the strength is greater than 5kgf, as in sample (A). This fact indicates that roughness is one essential factor, although a flat surface alone is not sufficient to prevent strength degradation of the fiber resulting from carbon coating.

In order to find other factors, we prepared carbon coated fibers with different carbon thicknesses and measured their tensile strength. It is found that the strength is also dependent on the thickness, and the strongest sample (A) is obtained when the thickness is 35nm. When the thickness is less than 30nm, the strength is low, which may be because water diffusion through the carbon coating causes strength degradation. When the thickness is greater than 70nm, the strength is also low.

Figure 3 shows the Weibull distribution of sample (A). The Weibull plots of sample (A) are in a straight line and there is no low strength distribution. The failure strength at 50% failure probability is as high as 6.2kgf. This value is compatible with conventional silica fiber.

Dynamic fatigue tests were conducted to obtain n-values. Figure 4 shows the relationship between the strain rate and the failure strength of samples (A) and (B). The strain rate was varied from 1 to 100 %/min. In spite of the strain rate change, the strength was nearly constant. The n-value of sample (A) is as large as 670. Sample (A) also has sufficient practical resistance to hydrogen. Optical loss at 1.24μm wavelength was stable for

300 hours at 75℃ in hydrogen at a pressure of 1 atmosphere.

As a result, a hermetically coated fiber whose initial failure strength is compatible with conventional silica fiber is obtained for the first time.

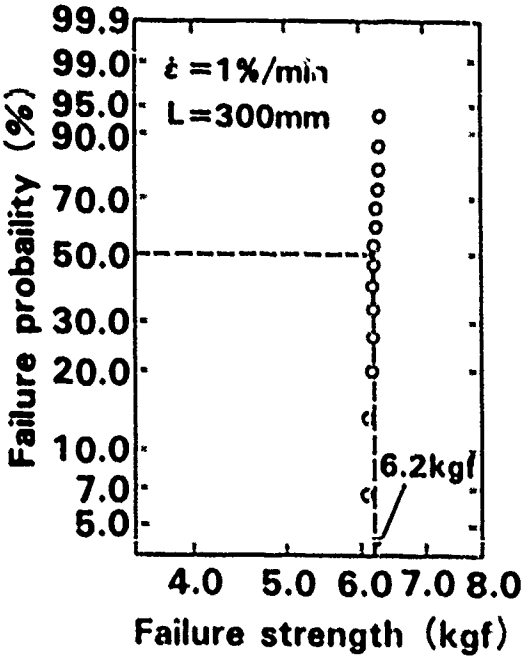

Figure 3. Weibull distribution of the failure strength of Sample (A).

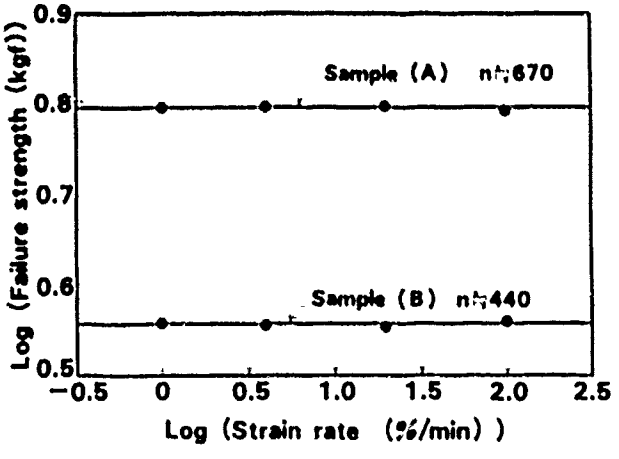

Figure 4. Dynamic fatigue test results.

2.2 Direct-core-monitoring fusion splicing of carbon coated fibers

Direct-core-monitoring fusion splicing equipment can align opposing fiber cores and estimate splice losses by monitoring the fiber core.[8] However, carbon coating on the fiber prevents monitoring. Also, the carbon will invade the fusion spliced points and may degrade both the splice strength and reliability. Therefore, the carbon coating must be removed before fusion splicing. The carbon is resistant to both acid and alkali and cannot be removed by chemical reaction. Also, it is impossible to remove it mechanically without damaging the fiber surface. To overcome these problems, we developed a new way to remove the carbon coating by pyrolysis. Two opposing carbon coated fibers were set between the electrodes of direct-core -monitoring fusion splicing equipment, and the carbon coatings around the splice points were removed by a cleaning discharge. The cleaning discharge removes the carbon coatings without damaging the fiber surfaces. Then, the fiber cores can be monitored and fusion spliced in the conventional way.

The cleaning discharge conditions were examined experimentally. Carbon coated fibers were fusion spliced with various discharge times and discharge currents. Figure 5 shows the experimental results when the electrode gap is 1.5mm and the fiber gap is 110μ m. Region A in the figure shows an area where the discharge power is low and the carbon coatings can not be completely removed. In this region, the splice equipment could not identify the fiber cores. In Region B, the fibers

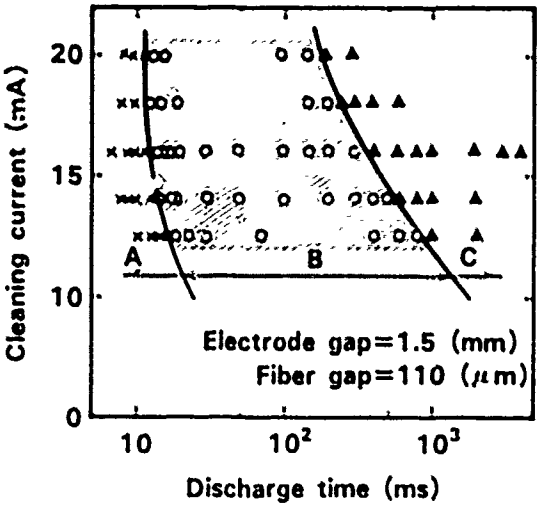

Figure 5. Cleaning discharge power dependence of splice characteristics. A: carbon remained. B: carbon removed. C: Fiber ends deformed.

were effectively cleaned. In this area, the average splice loss was 0.04dB for 20 samples of single-mode fibers for 1.3μm use. In Region C, the discharge power is too strong. This causes fiber-end deformation which reduces the tensile strength at the splice point after fusion.

The tensile strength of arc fusion spliced carbon coated fibers was measured. Figure 6 shows the Weibull distribution of the splice strength for fibers A, B, and C. A shows the results for a fiber which is fusion spliced with its carbon coating in place. The average splice strength was as low as 0.3kgf. Carbon may invade the fusion spliced points and may degrade the splice strength. B shows results for the same carbon coated fiber as A, but which is fusion spliced after a cleaning discharge. The average splice strength is as high as 0.6kgf, this value is compatible with that for conventional silica fiber C.

As a result, a fusion splicing technique has been established for carbon coated fibers.

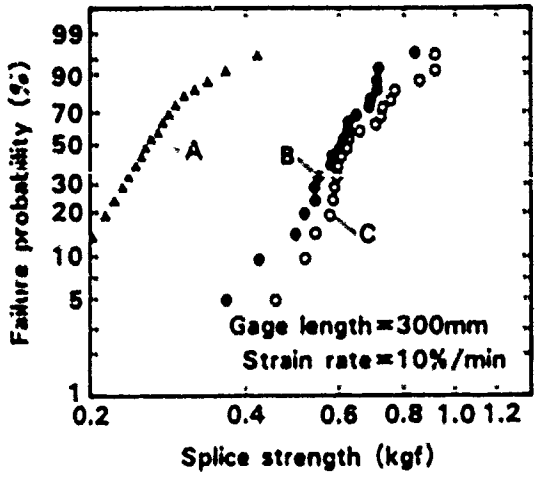

Figure 6. Weibull distribution of the splice strength. A: carbon coated fiber spliced without a cleaning discharge.
B: carbon coated fiber spliced after a cleaning discharge.
C: conventional silica fiber.

3. Design concepts and test results for a submarine cable using carbon coated fibers

The development of a non-repeated submarine cable with a large number of optical fibers has become necessary in order to construct optical fiber links across a channel. However, it is difficult to accommodate a hundred fibers in a conventional submarine cable structure[7] because a welded-pipe structure with a large diameter can not resist required lateral pressure. Recent technical progress in carbon coated fiber has made it possible to design a new one-hundred-fiber submarine cable with a compact and economical structure. The design concepts and test results will be described in this section.

3.1 Design concepts

The advantages of carbon coated fiber from the viewpoint of submarine cable design are summarized in Table 1. They are:

① Carbon coated fiber can withstand high strain levels over long periods of time because its n-value is greater than 200, whereas that of conventional silica fiber is 20[8]. Figure 7 shows calculated results for σ_p/σ_r dependence on the n-value, where σ_p is the fiber strain in proof testing and σ_p is the permanently allowable fiber strain in a cable[9]. For conventional fiber, σ_p/σ_r is about 4, then σ_r must be less than 0.5% even if σ_p is as high as 2%[10]. For carbon coated fiber, σ_p/σ_r is close to 1, then σ_r can be as high as 0.9% when σ_p = 1%. Consequently, a cable structure with both low tensile rigidity and initial elongation is an acceptable structure for carbon coated fiber.

② For carbon coated fiber, the n-value is constant in wet conditions[11] and permeation is acceptable. Therefore, a simple LAP sheath structure is sufficient. For silica fiber, the n-value decreases in wet conditions[12]. Therefore, permeation into the fiber from the sea must be

Table 1 Advantages of a submarine cable using carbon coated fibers

	Carbon coated fiber	Conventional fiber
Allowable strain	0.9% for 1% proofed	0.5% for 2% proofed
Humidity permeation	Acceptable	Not acceptable (Strength reduces)
Cable materials	Any	Special materials (Free from hydrogen)
Watertightness	Not essential	Essential

prevented by adopting a welded metal pipe structure with no pin-holes.

③ Carbon coated fiber is resistant to hydrogen, therefore any economical cable materials are acceptable. On the other hand, silica fiber is very sensitive to hydrogen and cable materials such as tension members and filling compounds must be carefully selected so that they will not generate hydrogen during the lifetime of the cable.[11]

④ For a submarine cable using carbon coated fibers, watertightness is not essential and a simple cable structure similar to that of a land cable is applicable. On the other hand, watertightness is essential for submarine cables using silica fibers. When the cable is damaged on the sea bottom, sea water penetrates into the pressure resistant metal pipe. Then, hydrogen is generated due to metal corrosion and optical loss increases drastically. Also, fiber strength degrades in wet conditions. Therefore, the cable must be carefully manufactured in order to completely fill the air spaces with filling compound[12].

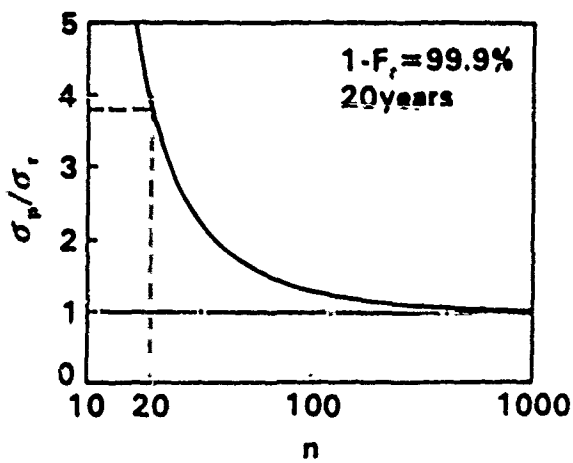

Figure 7. σ_p/σ_r dependence on n-value.

Table 2 Cable specifications

	New cable	Conventional
Fiber	100	6
Allowable depth	500m	8000m
System	non-repeated	repeated
Diameter	18mm	24mm
Weight	0.3kg/m	1.1kg/m

3.2 New cable structure

A one-hundred-fiber cable is designed taking advantage of the carbon coated fiber properties listed in Table 1. Cable specifications are listed in Table 2 together with that of a conventional submarine cable. This is a shallow sea cable for a non-repeated system. The cable structure can be made especially simple in this case because electrical power supply is not required. The cross section of the new cable is shown in Fig. 8. Armoring wires can be incorporated according to need. Carbon coated fiber ribbons are packed into slots arranged helically on a polyethylene rod with a center steel wire. A LAP tape sheath is extruded over the slot. For conventional submarine cable structure, a high-tensile-rigidity, composite-steel-strands-and-welded-metal-pipe structure is indispensable[7]. The new cable enabled drastic cost saving by eliminating the composite structure without degrading

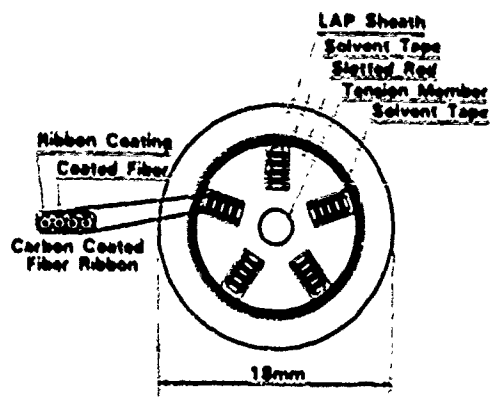

(A) New Cable Structure

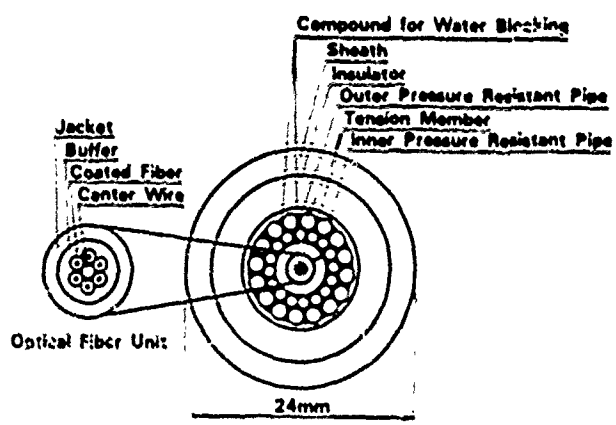

(B) Conventional Cable Structure

Figure 8. Cross sections of (A) new and (B) conventional submarine optical fiber cable.

reliability. The new cable can accommodate 25 fiber ribbons each containing 4 fibers. The new cable structure is simple and economical. The advantages of the slot structure with fiber ribbons include great compactness, suitability for high-speed mass production, ease of fiber identification and simultaneous mass splicing[13]. Mass splicing is important for submarine cables with large numbers of fibers. This is because it allows a broken cable to be repaired within 24 hours, which is necessary because the sea condition is unstable.

3.3 Test results

One kilometer of the new cable was manufactured and the cable characteristics were examined. Single-mode optical fibers for 1.3μm use were used in the cable. Conventional silica fiber ribbons and carbon coated fiber ribbons were packed into slots for comparison.

Optical losses at each stage of the manufacturing process were measured. The losses remained unchanged during the cabling process at both 1.3μm and 1.55μm wavelengths as shown in Fig.9.

A tensile test was conducted using a 150 m length of the cable. The cable tension dependence of the cable strain was measured by monitoring the phase shift change of the optical pulses. In this test, fiber ends were fixed to the cable ends. Figure 10 shows the test results together with optical loss changes due to stretching. The residual fiber strain after 0.5% elongation was about 0.06%. This strain value is far smaller than the allowable permanent strain of carbon coated fiber. The loss changes were less than the measuring accuracy; $\pm$ 0.01dB.

Optical loss changes due to hydraulic pressure were measured. A 200m length of the cable was set in a pressure vessel with the ends out of the vessel and hydraulic pressure was applied. An 800m fiber loop was made by splicing fibers and the wavelength dependence of the optical losses was measured at 0atm , 25atm and 50atm. Figure 11 shows the experimental results. Optical losses were stable at both 1.3μm and 1.55μm wavelengths.

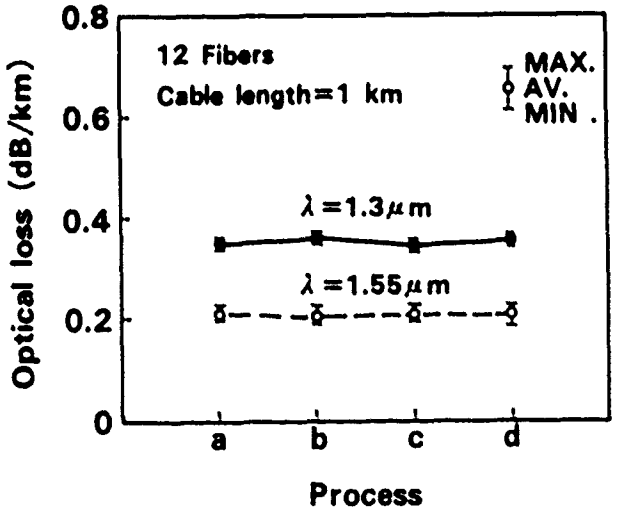

Figure 9. Optical losses in cabling process. a: carbon coated fiber. b:fiber ribbon. C: slot d: cable

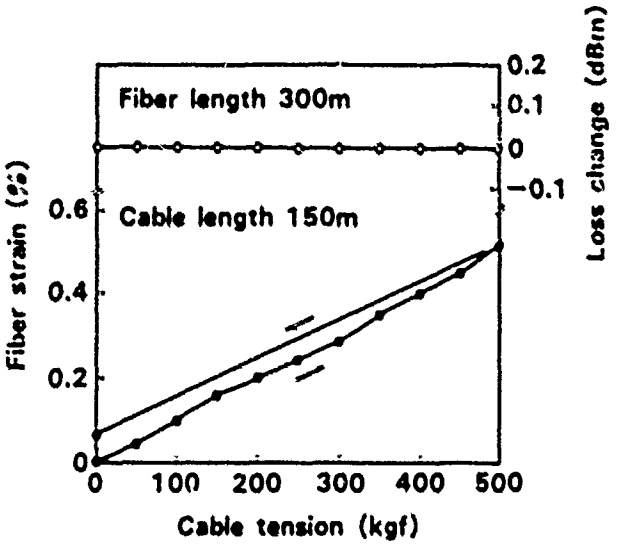

Figure 10. Tensile test results of the new cable.

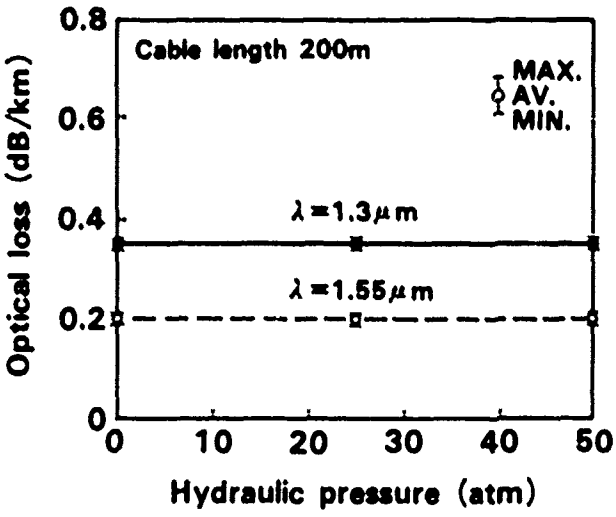

Figure 11.Hydraulic pressure test results.

Optical loss changes due to water penetration were measured. The steel wire in the center of the cable and the aluminum tape of the LAP sheath were connected electrically and the cable was set in a pressure vessel. Water at a pressure of 50 atmospheres was applied to the vessel and the temperature was maintained at 30℃ . The wavelength dependence of optical losses were measured after 1 month. For conventional silica fiber, hydrogen induced optical loss increase was detected as shown in Fig.12. For carbon coated fiber, the wavelength dependence of the optical losses was identical to that before the water penetration test. The hydrogen resistance of the carbon coated fibers is proved in practical conditions.

Furthermore, squeezing tests , bending tests, lateral pressing tests and thermal tests were conducted. The test results are summarized in Table 3 and prove the excellent performance of the cable.

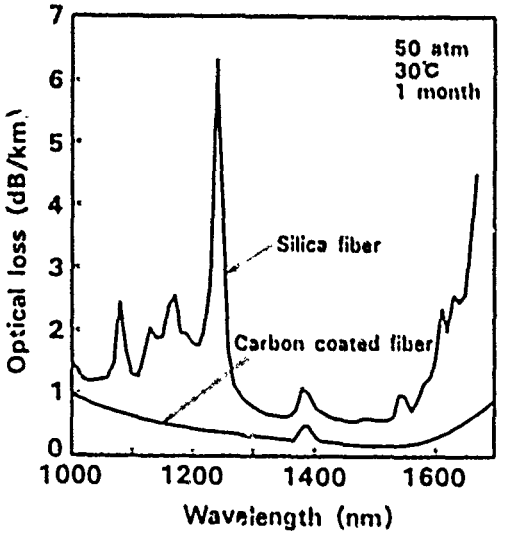

Figure 12. Optical losses after water penetration. The cable remained under water for 1 month.

4. Conclusion

New technologies for carbon coated optical fibers are developed for the first time. They are;

① A hermetically coated fiber is obtained whose initial failure strength is compatible with conventional silica fiber.

② A direct-core-monitoring fusion splicing method for carbon coated fiber is developed.

Based on this technical progress, carbon coated fiber shows great potential for practical application. Consequently,

③ A new type of submarine cable containing one hundred carbon coated fibers is proposed and developed.

The advantages of hermetically coated fiber was examined and fully utilized in the cable. The new cable has many advantages including high-reliability, compactness, ease of fiber identification, simultaneous mass splicing and drastic cost saving. Test results revealed excellent optical and mechanical properties and demonstrated the possibility for practical application in non-repeated submarine systems.

Acknowledgment

The authors would like to thank A. Sakamoto for his encouragement, and thank H. Inoue and H. Tada for their assistance with the experiments.

References

[1] R. HISKES, C. A. SCHANTZ, et al, " High performance hermetic optical fibers ", Technical digest for Optical Fiber Communication Conference, 1984, Paper WI6-1

[2] K. E. LU , M. T. LEE, D. R. POWERS, G. S. GLAESEMANN, " Hermetically coated optical fibers ", Technical digest for Optical Fiber Communication Conference, 1988, Paper PD1-1

Table Test results

	Condition	Loss change
Squeezing	Cable 150m Tension 400kgf Curved guide radius 300mm 3 times	(±0.01dB
Bending	Bar diameter 100mm 10 times	(±0.01dB
Pressing	500kg/50mm	(±0.01dB
Temperature	-20 to 40℃ 1000m fiber loop	(±0.01dB

[3] R. G. HUFF, F. V. DIMARCELLO, and A. C. HART, " Amorphous carbon hermetically coated optical fibers", Technical digest for Optical Fiber Communication Conference, 1988, Paper TUG-2
[4] C.M.G. JOCHEM, H. SCHAPER, M.J.M.J. SWARTS and J.W.M. SMITS," High-speed process for hermetic microcrystalline carbon coating on optical fibers", Technical digest for Optical Fiber Communication Conference, 1989, Paper PD8-1
[5] O. KAWATA, K. HOSHINO, Y. MIYAJIMA, M. OHNISHI and K. ISHIHARA," A splicing and inspection technique for single-mode fibers using direct core monitoring", IEEE, J. Lightwave Technol. LT-2, p 185, 1984
[6] K. E. LU, G. S. GLAESEMANN and G. KAR," Hermetically coated optical fibers ", IWCS Proceedings 1987, p241
[7] N. YOSHIZAWA," Estimation of submarine optical fiber cable elongation", IEEE, J. Lightwave Technol. LT-3, p189, 1985
[8] D. KALISH and K. B. TARIYAL," Static and dynamic fatigue of a polymer-coated fused silica optical fiber", J. Amer. Ceram. Soc., 61, no.11-12, p518, 1978
[9] N. KOJIMA, Y. MIYAJIMA, Y. MURAKAMI, T. YABUTA et all," Studies on designing of submarine optical fiber cable", IEEE, J. Quantum Electron. QE-18, 4, p733, 1982
[10] M. MIYAJIMA," Studies on high-tensile proof tests of optical fibers", IEEE, J. Lightwave technol., LT-1,2, p340, 1983
[11] M. OHNISHI, N. YOSHIZAWA, Y. MIYAJIMA, O. KAWATA and Y. NEGISHI," Loss stability assurance against hydrogen for submarine optical fiber cable", IEEE, J. Lightwave technol., LT-6, 2, p203, 1988
[12] N. YOSHIZAWA, M. OHNISHI, K. ISHIHARA and Y. NEGISHI," Water propagation blocking properties of submarine optical fiber cable", Electronics Letters, 21, 18, p796, 1985
[13] M. TACHIKURA and N. KASHIMA, " Fusion mass-splices for optical fibers using high-frequency discharge ", IEEE, J. Lightwave technol. , LT-2 p25, 1984

Nobuyuki YOSHIZAWA

NTT Transmisson Systems Labs.

He was born in Tokyo, Japan, on March 6, 1954. He received the B.S., M.S. and Ph.D degrees in mechanical engineering, from Waseda University, Tokyo, in 1972, 1974 and 1986, respectively. He joined NTT Electrical Communications Laboratories, Ibaraki, Japan, where he has been engaged in the research and design of submarine optical fiber cable. Dr. Yoshizawa is a member of the Institute of Electronics, Information and Communication Engineers of Japan.

Yoshiaki MIYAJIMA

NTT Transmisson Systems Labs.

He was born in Kagoshima, Japan, on March 2, 1953. He received the B. S., M.S.and Ph. D degrees in electrical engineering, from Kyushu University, Fukuoka, Japan in 1976, 1978 and 1986, respectively. He jointed NTT Electrical Communications Laboratories, Ibaraki, Japan, where he has been engaged in the research on mechanical reliability of optical fibers for submarine cables. Dr. Miyajima is a member of the Institute of Electronics, Information and Communication Engineers of Japan.

Yutaka KATSUYAMA

NTT Transmission Systems Labs.

He was born in Kyouto on February 26, 1949. He received the B. E. degree in mechanical engineering, M. E. degree in physical engineering and Ph. D degree in communication engineering from Kyoto University, Kyoto, in 1971, 1973 and 1981, respectively. He jointed NTT Electrical Communications Laboratories, Ibaraki, Japan, where he has been engaged in the research and developmental work on design and characterization of subscriber optical fiber cables. Dr. Katsuyama is a member of the Optical Society of America and the Institute of Electronics, Information and Communication Engineers of Japan.

POST-MORTEM FAILURE ANALYSIS OF OPTICAL FIBER CABLES

H.H. Yuce, A. DeVito, C. J. Wieczorek W.T. Anderson, J.P. Varachi, Jr., P.E.

Bell Communications Research

Morristown, New Jersey 07960-1910

SUMMARY

This paper documents three different post-mortem analyses of optical fiber cables that caused system failures. The first case was on an optical fiber cable that contained fiber breaks. Examination of the fiber coating and fracture surfaces revealed that the mechanism for these low strength fiber breaks was most probably surface damages introduced during the fiber drawing process. The second analysis documents a service failure caused by a combination of fire damage and a very cold temperature. The examination revealed that the extreme heat had not only caused extensive damage to the external duct and cable sheath but also core components of the optical fiber cable. Although the buffer tubes were deformed, the fibers kept their mechanical integrity. The last case was an examination of an optical cable which failed in an above ground closure. The cable failure was caused by a combination of a broken central strength member and low temperatures.

1.0 INTRODUCTION

In a relatively short time, fiber optic technology has made rapid strides from a state of sheer laboratory curiosity to a multitude of technically and economically successful commercial systems extending to all major areas of communications, sensors, and signal processing applications. Optical fibers have significant advantages for point to point communications compared to metallic media. These advantages include large bandwidth, low transmission losses, a physically small cross section, and freedom from electromagnetic interference. The large communication capacity of an optical fiber cable carries with it a concomitant requirement for high reliability. The mechanical reliability of such a cable and fiber depends upon the stresses and the environment to which the fibers are exposed. Although glass fibers are inherently very strong, the presence of small flaws can lead to large strength reductions. In addition, such flaws can actually increase in size due to stress induced reactions with chemical species in the environment, a process known as static fatigue. Some investigators have shown that fiber strength can decrease with no applied stress if soaked in higher temperature water and some common chemicals. [1,2] There are numerous opportunities to generate flaws during the manufacture of glass fibers especially during the drawing and coating operations. [3] Further reduction of fiber strength may occur during cabling, deploying, or handling such as splicing or connectorization. [4,5]

The long term reliability of the communication media is critical in assuring the long term performance of such systems over their design lifetimes. In addition, as optical fibers are introduced for newer applications and often harsher environments (from long distance transmission to subscriber loops and customer premises installations), it is important to understand phenomena which can degrade their performance, as well as explore means by which these degradation effects can be overcome.

Today, the maximum age of installed cables are: 10 years for multimode (6 years average) and 5 years for single mode (2-3 years average). At the end of 1988, there were 4.7 Million-fiber km (95% interoffice, 5% feeder) in the ground. At first glance, 2 to 10 years of experience with this new optical medium may seem reassuring, but we have great expectations for the longevity of cables. Because the cost of installing and splicing these cables may approach or exceed the cost of the cable itself, an expectation of a 40 year service life is not unreasonable. Our limited experience with optical cables does not yet support this expectation. As with any new technology, each field failure presents us with an opportunity to learn unanticipated modes of failure, and hopefully, the

study of such failures may ultimately lead to improvements in fiber and cable design and testing.

To date, approximately 1900 fiber outages have been reported [6] to Bellcore, and most of these were caused by digups or natural catastrophes. However, the precise cause of many of these outages could not be determined. Occasionally, when the cause of an outage is not understood, Bellcore is asked to investigate. We have studied the cable or fiber remnants from 25 field failures to date. Some of these cases can be summarized as:

- Broken fibers during installation
- Broken fibers after installation (cables and splice cases)
- Fire damage
- Lightning damage to cables (both in duct and directly buried)
- Steam damage
- Hydrogen in submarine cable [7,8]
- Jacket failure during installation

In this paper, we present several "*post mortem*" analyses in detail and describe what we have learned from them.

2.0 BROKEN FIBERS AFTER INSTALLATION

2.1 Introduction

In October 1984, a 16 fiber optical cable was installed in a 1 1/4 inch inner duct, in an underground conduit system. The cable which connected two central offices was 15,326 feet in length and had been placed in one continuous piece in 8 separate pulling operations utilizing seven "figure eights". The cable was shipped with one broken fiber. After installation, splicing, and testing four additional broken fibers were detected. Four transposition splices were made to recover four of the fibers. In August 1988, an increase in attenuation in one fiber in this cable caused a system failure. When the system failure occurred, transmission was switched to a protection fiber, which was the last available good fiber in the cable. As a result, two replacement cable sections were installed to replace the portion of the cable containing the transposition splices. In November 1988, the defective cable sections containing the broken fibers were shipped to Bellcore's facility in Morristown, N.J. so that the authors could conduct a post-mortem examination.

2.2 Initial Inspection

A high resolution OTDR was used to observe the condition of each fiber and to verify that no additional damage had occurred during the removal process. Our initial findings matched the information received from the field which indicated that a break in fiber 15 caused the system failure.

Upon completion of all the initial measurements which located the fiber breaks, the authors examined the cables further to determine, if possible, the causes for the fiber failures. The location of each fiber break was determined from each end of the sample cable and comparing the added length to the length of an unbroken reference fiber and the length determined from the cable footage markings. The cable was cut 30 meters beyond the break, and measurements were taken to reverify the precision of the OTDR by measuring the actual length of removed cable. Using the footage markings, the cable was cut approximately 7 meters beyond the cable break. A helium neon laser was connected to fiber 15 in order to assist in locating the break. All sheath and core wrap over the fibers were removed in short pieces until the fiber break was clearly observed by the presence of the laser light. The end faces of the fibers were approximately 1/8 inch apart. The fibers were removed from the cable and upon further examination it was noted that the coating on fiber 15 appeared to have disintegrated. An examination of the sheath and core materials in the area of the break did not indicate any defects which may have caused the fiber break.

During the cable examination a sheath repair, approximately 1 1/16 inches in diameter and 7 1/2 inches long, was discovered. The region of the jacket that had been repaired was examined, and it was noted that there was an area 1/8 inch x 1/4 inch that was void of jacket material, exposing the corrugated armor. A section of cable approximately 10 feet long was removed for further analysis, which will be presented later in Sec. 2.3.1.

An attempt was now made to locate the defect in fiber 12. The process described above was employed and it was observed that fiber 12 was broken with the end faces separated by approximately 1/8 inch. The sheath and core components were intact and did not contribute to the fiber break. Fiber 12 was removed from the cable and initial examination revealed no unusual bubbles or other coating defects as had been noted on fiber 15. The second cable sample containing the break in fiber 10 was located and the fiber was exposed following the procedure outlined above. After gaining access to fiber 10, it was observed that here again, the fiber was broken with its

end faces separated by approximately 1/8 inch. An examination of the cable showed no imperfections which may have contributed to the fiber failure.

2.3 Failure Analysis of Cable and Fibers

2.3.1 Cable Analysis

The cable sheath damage area was examined to determine the cause of the jacket failure. The cable sample was systematically dissected to ascertain the effect of the jacket failure on the cable core, and to resolve any connection with the failure of fiber 15, 28 feet from this point. The breach in the cable jacket was oval in configuration and measured approximately 1/8 x 1/4 inch (see figure 1). The corrugated armor was visible and the polymer coating on the armor, was for the most part absent.

The absence of corrosion on the unprotected armor can be attributed to the excellent field repair of the cable. The jacket in the area around the hole had a sheen typical of that observed on jacket specimens that were subjected to tensile and elongation testing. The inside of the jacket did not show any imperfections except for the hole. Examination of the armor revealed that the armor was spliced, and the splice was almost directly beneath the jacket hole. The armor splice was mechanically intact, and it appeared to have been fabricated following good commercial practice. The corrugations did not show any imperfections, and as expected; the polymer coating in the splice area was not on the armor because it was removed in preparation for welding. The cable was not stretched beyond the point of recovery in the area of interest. This was verified by a measurement comparison of the corrugation pitch in the section examined with another section of the cable. The core components and fibers were not damaged which indicated that the break of fiber 15 was independent of the jacket defect.

Based on the visual examination of the hole in the jacket and the absence of any markings on the exposed armor, it is highly unlikely that the jacket hole was made during cable installation. In the authors' opinion, the hole in the jacket is not the result of installation damage, but a manufacturing defect. One possible scenario is that the spliced armor was cleaned with a solvent prior to joining, and the residual solvent left on the armor vaporized when the extruded hot polyethylene came in contact with the armor. The vapor was trapped between the armor and the jacket. The jacket ruptured from the gas pressure and the remaining jacket material contracted and adhered to the armor when it cooled.

2.3.2 Fiber Analysis

2.3.2.1 Experimental Procedure

In order to identify the failure mechanisms of the broken fibers, five different types of tests were performed:

Fractographic Analysis- Both faces of the broken fibers (fibers 10, 12, and 15) were examined under a scanning electron microscope. The protective polymer coating on the fibers was removed in the vicinity of the break by using chemical stripping. The fiber ends were carefully cleaned by soaking the fibers in acetone for a short period of time to remove dirt and cable filling compound. The fracture surfaces were coated with a gold deposit of 10-20 angstroms thick, and then examined under a scanning electron microscope. Any particles or inclusions present on the fracture surface were identified with the help of energy dispersion x-ray analysis.

Defect Analysis - In order to identify defects on the coating, the fibers were examined under a stereo microscope.

Dynamic Tensile Strength- The strength tests were performed on a screw driven universal tensile testing machine with a measurement accuracy of ±0.1 N, in a laboratory environment of 22° C ±2° C and relative humidity of 45% ±5%. Samples were gripped on 10 cm (4 inches) diameter capstans covered with a soft elastomeric sleeve. Masking tape was used to hold the fiber samples securely on the capstans. Tensile strength was determined at a strain rate of 5%/min., with a gage length of 50 cm (19.6 inches).

Two-point Bending Strength (Dynamic)- Using the dynamic two-point bending method [9] (see figure 2) fiber strength was measured. This technique is especially useful if there is a problem in handling the fiber, for example, when the coating is defective or damaged. The test consists of bending a fiber sample 180° between two parallel jaws which are driven at such a velocity that the stress rate at the tip of the fiber bend remains constant. The fiber is bent to a continuously smaller radius until it eventually fractures, and by measuring jaw separation at the instant of fracture, the fiber strength can be determined.

Stripping Test - The stripping force of the coating was measured using a commercial stripping tool mounted on a screw driven universal tensile testing machine. The gage length of the stripped section was 3 cm (1.2 inches) and the test was conducted at the rate of 50.8 cm/min (20 inches/min).

2.3.3 Results and Discussion

Fiber 10, which failed at sheath footage marker 9415, was carefully examined around the breakage area. The coating showed no sign of damage or defect. Based on the fractographic analysis [10] (see figure 3), this fiber failed at 27,000 psi. As seen in figure 3, there are a couple of possible locations where a flaw could have started. Fiber 12, which failed at sheath footage marker 12072, was examined around the breakage area under a stereo microscope. The coating did not show any sign of defects or damage. Based on the fractographic analysis of fiber 12 (shown in figure 4), it failed at 32,000 psi. The boundaries of the mirror or mist region are shaped in the form of a circular arc [11]. The flaw where the fracture originated is located at the center of this imaginary arc, as seen in figure 4. Based on the scanning electron microscope analysis, the cause of this low strength failure was probably due to an abrasive surface scratch. The surface of the preform or the fiber may have been scratched by contact with other surfaces, e.g., the top seal, the bottom furnace door or the coating applicator. Sometimes small fiber fragments can be left in the coating applicator during start-up operation; these fragments can subsequently scratch the fiber. A severe abrasion against the bottom furnace door can cause the fiber to have extremely low strength. Some of the factors which can contribute to surface scratches of this type are poor preform handling and transport procedures, crooked preforms, improper preform centering, and poor fiber draw tower alignment.

Fiber 15, which failed at sheath footage marker 13000, was examined around the breakage area under a stereo microscope. Between sheath footage markers 12993 and 13007 coating defects were observed as shown in figures 5-6. Within this 14 foot distance, fiber 15 had apparently experienced difficulties in the coating application procedure. Figure 5 shows the physical evidence of irregularities in the thickness of the coating. In this figure fiber 14 is also shown for comparison. This fiber was in the same cable unit with fiber 15 and did not have any sign of defects within the length of fiber that was analyzed. In some areas of fiber 15 the coating thickness is so thin that the glass fiber is directly exposed to the environment (figure 6). Eccentricity of the coating can also be observed in figure 6. At many locations bubbles were observed in the coating and in some cases these bubbles caused local holes in the coating.

Because fiber 15 exhibited coating problems and there was a defect in the cable jacket 28 feet away from the failure point, further investigations were conducted on fibers in the same unit (unit 4) of sample one, between sheath footage markers 12977 and 13260. The fibers in this unit are designated as fibers 13, 14, 15, and 16. The type of tests that were conducted on all four fibers are summarized in Table 1. Figure 7 shows the strip test results for these four fibers between sheath footage markers 12994 and 12996. Fiber 15 had a 33% lower stripping force compared to fiber 13 and a 42% reduction compared to fiber 14. As mentioned earlier, this location is 4 feet away from the breakage point, where fiber 15 had defects in the coating. Figure 8 summarizes the stripping test results for fiber 15 at 7 different locations, between sheath footage markers 12977 and 13260, including the area of defective coating. The dynamic tensile test results for all fibers are summarized in figure 9. As summarized in Table 1 strength test results for fiber 15 do not cover the defective coating area. As shown in figure 6, coating irregularities made it impossible to grip the samples around the capstans. Therefore, tensile strength tests could not be conducted at the defective coating zone. Within the sheath footage markers that the fibers from the same unit were tested, fiber 15 showed the lowest mean strength. There are three mechanisms which can lower the fiber strength: (a) lower adhesion between glass fiber and coating; (b) higher water permeation (even though all four fibers have exactly the same coating, different colors or dying procedure could affect the coating properties); (c) different preform. The two-point bending test was done at the defective coating location (sheath footage markers 12996 through 13007) and non-defective zone (around sheath footage marker 13260). The results are summarized in figure 10. Since effective gage length is only 0.5 mm (0.02 inches), the probability of measuring a fiber sample containing a flaw is very small and consequently the results tend to be uniform and unimodal as was the case in the non-defective coating area (see figure 10). The bi-modal distribution of strength in the defective coating zone was due to: a) the glass fiber exposed to the environment and probably damaged after it was manufactured (during handling, shipping, cabling, etc.) and/or b) lack of coating protection which will accelerate crack growth during testing. Both ends of the fractured fiber 15 were examined in a scanning electron microscope. The fracture surfaces did not show any "mist" and "hackle" regions. All of the surface was

a mirror area which was due to a very low strength failure. A fracture below 24,500 psi (for 125 µm glass diameter) will be mostly the mirror area and will not display other features. Since this failure happened 47 months after the fiber was put into service, it appears that a low stress static fatigue mechanism was the main reason of this failure. In figure 11, possible flaw starting zones can be seen from a different angle. Figure 11 also shows the damaged fiber surface which was probably caused during manufacturing as explained for fiber 12, or by handling of the fiber in preparation for cabling because of defective coating.

3.0 FIRE DAMAGE

3.1 Introduction

In this case several weeks prior to the failure, a section of a fiber optic cable was damaged by a fire. A combination of fire damage and a very cold night led to the ultimate system failure. The cable route was almost exclusively in duct and connected the downtown central office with a suburban office. The section of the cable which the operating company determined to have caused the failure was suspended under a bridge which crossed railroad tracks. This eight fiber cable carried one working system, using fibers 1 and 2, with a one-to-one protection provided on fibers 3 and 4. Fibers 5 and 6 were unused, and fibers 7 and 8 continued to another town with protection provided on another route. On the evening of December 17, a small frame building close to the tracks and very close to the bridge caught fire and burned to the ground. This fire lead to immediate trouble reports for many of the circuits carried by plastic insulated copper cables, which were placed immediately adjacent to the fiber cable, but the fiber cable continued to function during and after the fire. On the evening of December 30, which was reportedly one of the coldest nights of the winter to that point, the working 405 Mbit system on fibers 1 and 2 switched to protect. Service was transferred to fibers 5 and 6 at that time. On the evening of January 7, which was also very cold, the protect circuit on fibers 3 and 4 went out, and several hours later the system on fibers 7 and 8 also failed. That evening, an emergency restoration was performed by splicing in a temporary cable section which was placed on top of the bridge in a plastic conduit. A permanent restoration had been planned since the fire, involving a new and somewhat longer route which did not use this bridge.

Since this cable carried a large amount of traffic including a number of special circuits, there was concern that an abrupt failure caused by the fire could have been disastrous, and a better understanding of why the cable failed some two weeks after the first damage was desired. The cable was housed in a heavy cement-coated paper conduit which was damaged but mostly intact. Inside the conduit was polyethylene innerduct, which had been heated sufficiently by the fire to deform. Some sections of the corrugated cable sheath could be seen exposed through gaps in the conduit and the innerduct and cable sheath. The external examination indicated that the cable exterior had been extensively damaged by the fire over approximately a 20 foot section. The restoration had been performed between an existing splice point in a manhole several hundred feet north of the bridge and another point, which was not originally a splice point, several hundred feet south of the bridge.

3.2 Initial Inspection

A short wavelength (850 nm) OTDR was used because of its very high resolution (approximately 10 meters). A launch spool of approximately 1 km of single-mode fiber was spliced between the OTDR and the test fiber. All eight fibers were measured from the north end of the cable. All eight were continuous between the two ends, and the cable section was measured to be approximately 530 meters long. Seven of the eight fibers demonstrated increased attenuation in the vicinity of the fire damage, with the 850 nm attenuation increases ranging between 2 and 3 dB. The eighth fiber had no increased attenuation in the vicinity of the fire damage.

The damaged cable was received in Morristown in late February 1988. The cable was transported on a reel, and OTDR measurements were taken. All fibers were continuous, and the attenuation increases due to the fire damage ranged from 0 to 3 dB. Once OTDR measurements had confirmed that no additional damage has resulted from the removal and transportation of the cable, the 13 meter damaged section was dissected. The high density innerduct had melted and bonded to the cable sheath over most of this length and was extremely difficult to remove. Considering this, it was decided to examine smaller sections of the cable. Three one foot sections were removed one from each end and the middle of damage area. The following is a discussion of what was observed as a result of the examination of the cores of each one of the samples.

3.3 Failure Analysis of Cable and Fibers

3.3.1 Cable Analysis

Sample #1

Upon examination of sample #1, it was noted that the cable's outer jacket and the high density innerduct had melted together and became one. The filler tubes had also flowed, and an examination of the sample's cross-section revealed that the steel central strength member had migrated down and was resting upon the corrugated steel armor (See Figure 12). The complete removal of the cable sample from the innerduct, at this point, would be impossible. The only way to examine any damage which may have occurred to the core components was to remove the steel central strength member, via the sample end, then carefully remove both the blue and orange buffer tubes using the same technique. This was successfully accomplished. The buffer tubes were removed intact and the fibers were extracted. Upon examination all fibers appeared to be in good condition, maintaining original appearance in both coating and color. It should be noted that all fibers were easily removed from the buffer tubes. Examination of the buffer tubes revealed that, although the outside polymer material had maintained its original appearance, the inner nylon jacket of the buffer tubes had crystallized and become hard because of the exposure to the heat. The buffer tubes contained "flat" spots along their length which prompted further examination. After further investigation it was concluded that the "flat" spots, which occurred along the length of buffer tube, were caused by the softening of the cable core components during the fire, resulting in their gradual downward movement, thereby exerting pressure on the tubes by the steel central strength member.

Sample #2

This sample appeared to have been exposed to slightly lower temperatures. Only a portion of the outer sheath had flowed and adhered to the innerduct. The entire cable sheath and innerduct had not become one as in the previous sample. One half of the innerduct was cut away to expose the cable and it was immediately noted that the cable identification and length markings were unchanged in their appearance. The outer sheath of sample #2 was removed, followed by the steel armor. Due to the effects of the extreme heat it appeared that the inner jacket had softened and adhered to the steel armor in spots and had also split because of the flowing of the jacket around the ripcord. Also, because of the temperature extremes, the kevlar layer adhered to the inside of the inner jacket preventing its easy removal. After exposing the cable core, it was observed that the filler tubes had softened and flowed in this sample also. Examination of the buffer tubes revealed that although they appeared to be in original condition, the inner nylon jacket had crystallized and become hard similar to what was observed in sample #1. The "flat" spots that had been observed in sample #1 were not noted here. The fibers were easily removed from the buffer tubes and appeared to be in original condition.

Sample #3

The final cable sample was removed and examined. Upon inspection, no damage to the outer sheath was noted and all cable identification and length markings were in original condition. The inner jacket was removed and examined. The flooding compound remained intact and the steel armor retained its original appearance. The inner jacket also retained its original appearance with no evidence of softening. The buffer tubes appeared to have retained their original appearance but upon further investigation it was noted that the jacket on the steel central strength member had softened and started to flow causing the buffer tubes to adhere to it. It should be noted that the buffer tubes were not deformed at this point along the span of cable. Examination of the buffer tubes found that just as in samples #1 and #2, the inner nylon jacket had crystallized and become hard. No "flat" spots were noted as in sample #1. The fibers were easily removed from the tubes and appeared to have retained their original appearance.

After thoroughly examining the cable samples, it is our opinion that the increases in attenuation that caused the system failure are directly linked to the "flat" spots that were observed in the buffer tubes taken from sample #1. When the materials in the cable core began to flow, as a result of the extreme heat, the movement of these components caused pressure to be applied to the buffer tubes. The pressure applied by the steel central strength member directly over the buffer tubes was the main cause of the deformation. Once the source of heat (the fire) was removed, the inner nylon jacket of the buffer tubes crystallized. This process caused the inside diameter of the buffer tubes to decrease. The extreme cold temperatures on the night of the failure caused the entire cable structure to contract, applying additional pressures to the constricted buffer tubes, thereby increasing the attenuation and causing the systems to fail. Had the deformation of the buffer tubes not occurred, this cable may have survived the effects of the fire.

3.1.2 Fiber Analysis

Considering the massive extent of the damage, a very extensive mechanical analysis, as explained in section 2.3.2.1, was conducted on fiber samples which were recovered from the burned cable. Both glass fiber and coating were still in good condition. No considerable degradation on fiber strength could be observed.

3.2 Discussions

The mode of failure observed here (during a period of extremely low temperature, long after damage had occurred) has been observed in several other post-mortem analyses. Optical cables can be damaged in ways which are not immediately apparent - the systems continue to function and no large attenuation increases can be found. However, extremely low temperatures can greatly magnify the effects of the damage and lead to system failure. Considering this delayed mode of failure, it should be noted that an attenuation measurement is not always a reliable indicator of the presence of sufficient damage to the cable to cause future problems.

4.0 CENTRAL STRENGTH MEMBER FAILURE IN CABLE

4.1 Introduction

In this case, the cable route between two towns was directly buried. The cable was installed in August 1987 and was carrying one working system with protection. On an early morning in January 1988, the working system switched to protect. A Central Office technician transferred the working system to a spare fiber, and transmission was restored. The temperature was reported to be very low at the time of failure.

The following morning, a technician attempted to locate the fault. Using an OTDR, they found that the fault was at a point 2053 meters from the Central Office, which corresponded to a splice point on the span records. Technicians then physically examined the splice point. The splice case was stored in an above ground closure. Since the splicing operation was performed in a splicing van, approximately 50 meters of slack cable was also stored in the cabinet, and cable slack was coiled and secured to a bracket in the rear of the cabinet with cable clamps. The splice case was opened and examined, and no problems were found. After the examination, the splice case was closed and the high loss region (2.5 to 3 dB) was still present.

A 300 m reel of restoration cable was spliced to unused fibers so that a short wavelength multimode OTDR could better resolve the fault, and it was found that the fault was within 2 m of the splice. 10 m of cable past the splice was cut out and respliced, which eliminated the fault.

4.2 Failure Analysis of Cable and Fibers

Approximately two feet of sheath was removed between the 12 to 14 foot marks to expose the cable core, and a broken central strength member was found. The cable was loose tube design. A 2 mm diameter fiberglass reinforced epoxy rod is used as a central member to resist buckling when the cable is bent. The cable core is surrounded by a layer of fiberglass and Kevlar™ and an inner jacket of polyethylene, which in turn is surrounded by another layer of Kevlar™ and an outer polyethylene jacket.

Prior to physical examination, a HeNe laser was used to test the continuity of the fibers. All 12 fibers were continuous, and no high loss regions were found. The sample was too short for accurate attenuation measurements to be made.

An additional section of sheath was removed for a distance of approximately 2 meters on either side of the damaged point. No other damage was observed. The unit tubes, stranding lay, and central member and fibers were in good condition except for the short damaged section identified initially. Upon unstranding the core to reveal the condition of the central member, it was observed that the two pieces of broken central strength member had overlapped each other by 20 mm. See Figure 13.

4.3 Discussions

One possible cause to be investigated is that the cable may have been bent to an excessively small diameter. However, there was no sign of small radius bending when the cable was examined, so excessive bending introduced when coiling the slack cable in the pedestal can be eliminated as a probable cause. An undamaged section of the cable section of the sample was bent in the laboratory in an attempt to reproduce the type of damage found. Two types of bends were introduced. First, the sample was bent over the corner of a bench to simulate the type of damage which could have occurred if the loose inside end of the cable were excessively bent while the cable was still on the reel. This might have happened during installation if

the end were loose during the burial. Second, the cable was bent by hand into a small loop until the central member failed. In both cases, it was quite difficult to break the central member, and bend diameters of three to four inches were typically required. The outer jacket of the cable was also quite noticeably buckled, whereas no noticeable buckling was observed in the field.

The increased attenuation at low temperatures is explained by the broken central member. This member provides the only significant resistance to compressive loading along the cable axes, significant compressive forces are generated by the contraction of the jacket and unit tubes at low temperatures. However, central member failures are very rare. The central member could have been damaged prior to or during manufacture, shipping, or installation. a damaged or broken central member would not be immediately detected, and at the moderate temperatures experienced during manufacture and installation, the fault could pass undetected. Since the damage is so close to the terminus of the route, subtile damage could not be distinguished from a nearby splice, but low temperatures would increase the attenuation of the damaged section significantly and ultimately lead to system failure.

5.0 CONCLUSIONS

This paper presents, in detail, three "post mortem" analyses out of twenty five cases that the authors have studied. Some of these cases help to identify modes of failure which were not anticipated earlier. In all three cases, initial OTDR readings taken in the field indicated that the fibers were functioning properly, only to fail sometime later. Considering this delayed mode of failure, it should be noted that an attenuation measurement is not a reliable indicator of the presence of sufficient damage to the cable to cause future problems. If physical damage occurs, it should be considered likely that the cable will fail when exposed to more severe environmental conditions whether or not a measurable attenuation increase is observed at more moderate conditions. Experienced gained from these studies is providing valuable input to Bellcore's generic requirements.

REFERENCES

1. J.T. Krause; *J. Non-Crystal Solids* 38; 1980; 497.
2. H.H. Yuce et al.; *Proceedings of SPIE* 992; 1988; 211.
3. D. Kalish et al.; " Fiber Characterization - Mechanical"; In " *Optical Fiber Telecommunications*" (S. E. Miller and A. G. Chynoweth ed); Academic Press; 1979; 401.
4. W.R. Wagner; In *Fractography of Glasses and Ceramics*; Advances in Ceramics 22; 1988;389
5. T. Wei et al.; To be published in *Proceedings of 35th International Wire and Cable Symposium* ; 1989.
6. R.A Connolly; Bellcore, Red Bank New Jersey; private communications.
7. W.T. Anderson et al.; *Proceedings of 37th International Wire and Cable Symposium* ; 1988; 188.
8. W.T Anderson et al.; To be published in *Proceedings of 38th International Wire and Cable Symposium* ; 1989.
9. H.H. Yuce et al.; *Proceedings of IOOC'89* ; 2; 1989; 44.
10. S.T. Gulati et al.; *Proceedings of 27th International Wire and Cable Symposium* ; 1978; 342.
11. J.J. Mecholsky, et al; Ceram Bull V. 56, No 11; 1977; 1016.

Figure 1. Sheath Damage at Sheath Footage Marker 13028

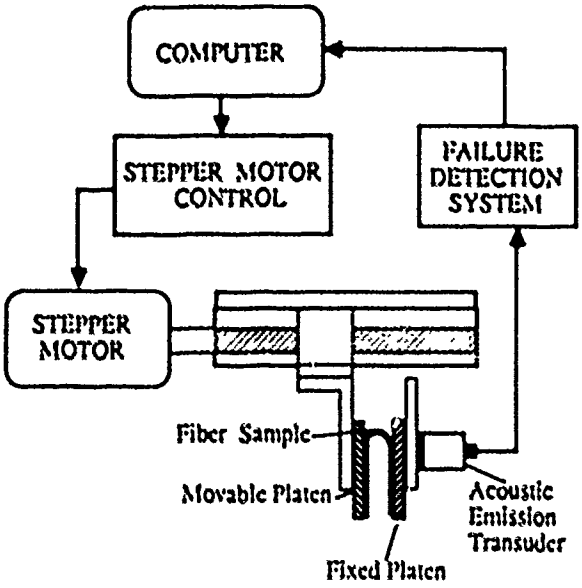

Figure 2. Two-Point Bending Apparatus

Figure 3. Fracture Surface of Fiber 10

Figure 4. Fracture Surface of Fiber 12

Figure 5. Defective Coating

Figure 6. Defective Coating

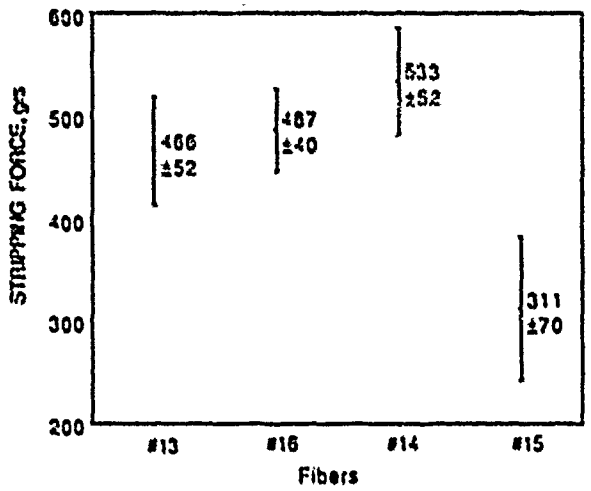

Figure 7. Coating Strip Test Results Between Sheath Footage Markers 12994-12996

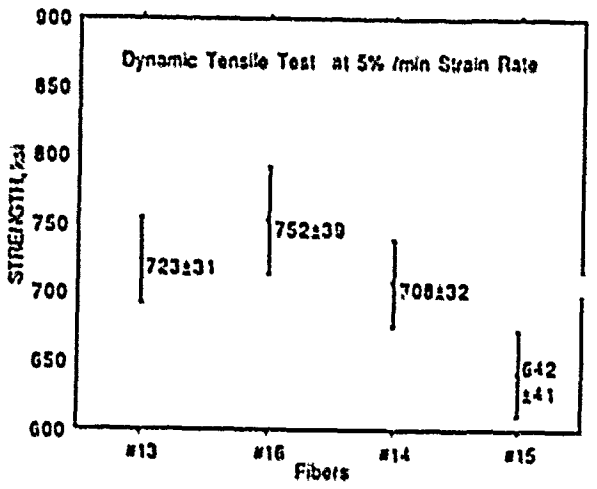

Figure 9. Dynamic Tensile Strength of Fibers From Unit 4

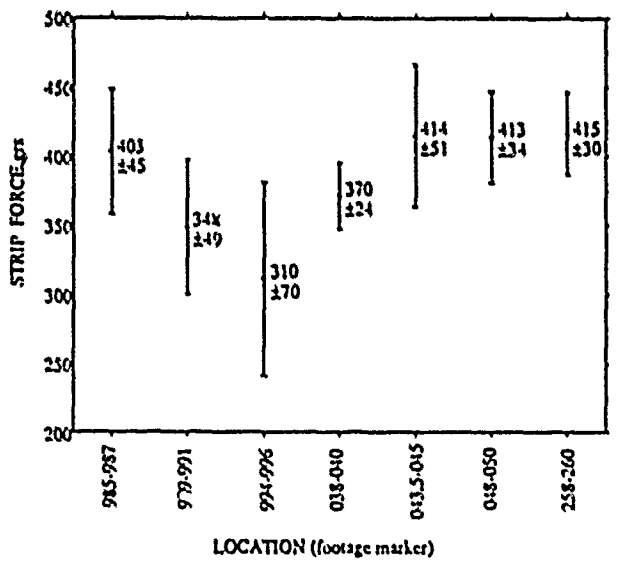

Figure 8. Coating Strip Force Results for Fiber 15 at Different Locations

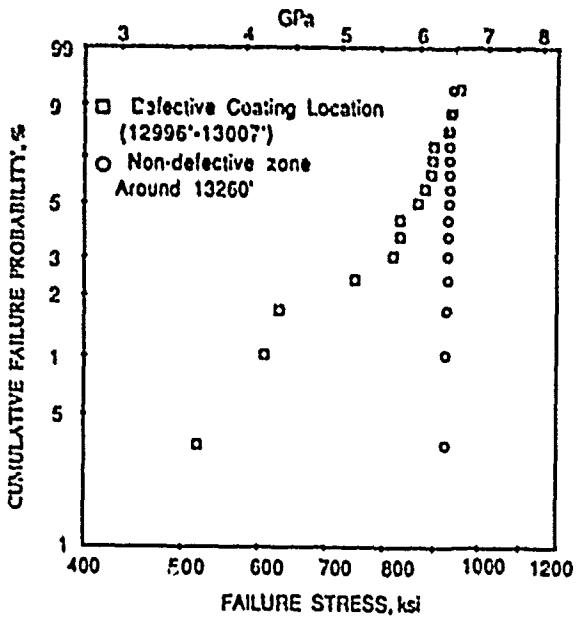

Figure 10. Two-Point Dynamic Strength Test Results at 6 MPa/sec for Fiber 15

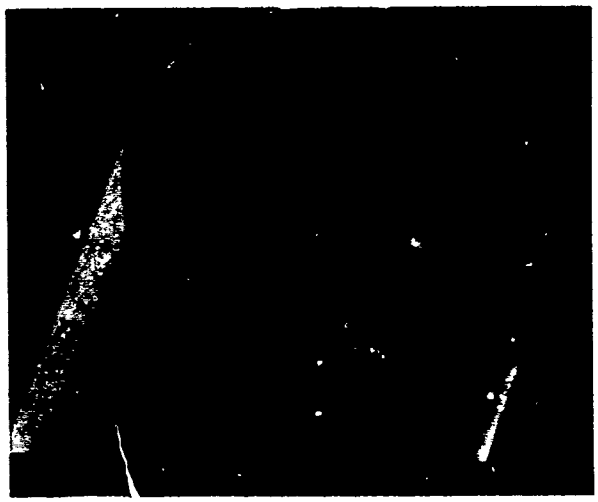

Figure 11. Fracture Surface of Fiber 15

Figure 12. End View of Sample #1

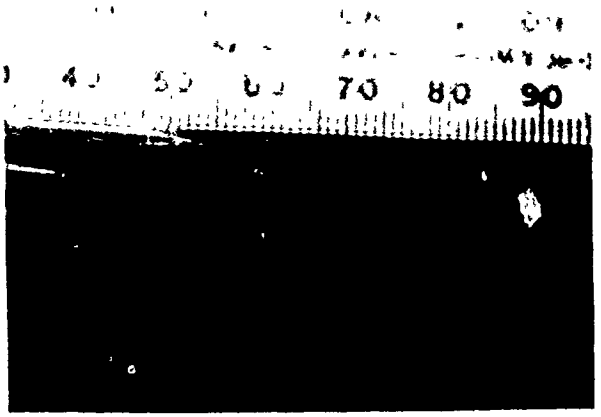

Figure 13. Damage Section Unstranded

Fibers	#13			#14			#15			#16		
Locations	Stripping Test	Tensile Test	Bending Test	Stripping Test	Tensile Test	Bending Test	Stripping Test	Tensile Test	Bending Test	Stripping Test	Tensile Test	Bending Test
12971.0' - 12985.0'		x			x						x	
12985.0' - 12987.0'		x			x		x				x	
12987.0' - 12989.0'		x			x						x	
12989.0' - 12991.0'		x			x		x				x	
12991.0' - 12994.0'		x			x						x	
12994.0' - 12996.0'	x			x			x			x		
12996.0' - 13000.0'		x			x				x		x	
13000.0'							FAILED					
13000.0' - 13012.0'		x			x				x		x	
13012.0' - 13027.5'		x			x						x	
13027.5' - 13028.5'	x			x			x			x		
13028.5' - 13034.0'		x			x						x	
13034.0' - 13038.0'		x			x						x	
13038.0' - 13040.0'		x			x		x				x	
13040.0' - 13043.5'		x			x						x	
13043.5' - 13045.0'		x			x		x				x	
13045.0' - 13048.0'		x			x						x	
13048.0' - 13050.0'	x			x			x			x		
•	•											
13250.0' - 13258.0'		x			x						x	
13258.0' - 13260.0'	x	x		x	x		x			x	x	
13260.0' - 13261.0									x			

Table 1. Locations and Test Types for Four Fibers From Unit 4

Hakan H. Yuce is a Member of Technical Staff in the Fiber Distribution and Reliability Research District at Bellcore in Morristown, New Jersey where he is involved in failure analysis and reliability studies of optical fibers. He received a B.S. in mechanical engineering from the Technical University of Istanbul, Turkey; an M.S. from MIT; and a PhD from Stanford University.

Anthony DeVito joined Bellcore's Optical Cables District, as a Member of Technical Staff, July of 1988. He is currently involved in post-mortem analysis and writing generic requirements for optical fiber cables. Prior to joining Bellcore he worked as a member of the Transmission Product Evaluation Staff at Bell South Services in Birmingham, Alabama. His responsibilities included the technical analysis of fiber optic splicing equipment, test sets and optical cables. He has 18 years experience with the Bell Operating Companies in the area of Outside Plant Construction, Construction Methods, and Fiber Cable Installation and Testing.

Casey J. Wieczorek is a member of the Optical Cable Group in Bellcore, Morristown, N.J. He joined Western Electric in 1967 and worked on various cable designs and manufacturing processes. He is currently responsible for the development of generic requirements and test procedures for optical cables. He holds a B.S. degree in Mechanical Engineering from Fairleigh Dickinson University and did graduate work at Stevens Institute of Technology.

William T. Anderson received the BSEE degree with Highest Honors from Georgia Institute of Technology in 1970, the MS degree in Electrical Engineering from Stanford University in 1971, and the Ph.D. degree in Electrical Engineering from Georgia Institute of Technology in 1979. He worked at Bell Telephone Laboratories from 1970 to 1983 in the areas of transmission and crosstalk in multipair cable and single-mode fiber measurement and design. In 1983, he joined Bell Communications Research, and is presently responsible for optical cable requirements and analysis. Dr. Anderson is a member of the Optical Society of America.

John P. Varachi, Jr, P.E., received the BSME degree from Fairleigh Dickinson University, Rutherford, N.J. in 1976 and the MSME degree from The Polytechnic Institute of New York, Brooklyn, N.Y. in 1978. He is currently District Manager, "Fiber Distribution and Reliability Research" at Bellcore. From 1969 through 1983 he was engaged in exploratory development at Bell Laboratories in mechanical design and analysis for telephone central office and outside plant apparatus. He also performed physical design and systems engineering for copper and optical fiber based digital loop electronic systems for outside plant and customer premises applications.

FIBER OPTIC CONNECTOR GEOMETRY TEST STATION

Zygmunt Pasturczyk, Bennett Wong, and Costas Saravanos

NORTHERN TELECOM CANADA LIMITED, OPTICAL CABLE DIVISION
Saskatoon, Saskatchewan, CANADA

ABSTRACT

A versatile test station for measuring the geometrical parameters of fiber optic connector ferrules was developed. Through the use of non-contacting optical methods, submicron measurement accuracy and repeatability have been achieved. Since close matching between ferrule and fiber diameters is essential to low-loss connectors, the capabilities of this system have proven to be indispensable for qualifying connector components prior to assembly.

INTRODUCTION

Low-loss fiber optic connectors require components which are manufactured with submicron precision. The size and shape of a connector ferrule may have significant impact in the resulting connector's performance. For single mode fibers, two parameters which strongly influence connector loss are axial offset and angular misalignment. The loss dependence in dB from these effects is given by

$$A(dB) = 4.34\ [(d/w_o)^2+(\pi\ n_{cl}\ w_o\ \theta/\lambda)^2]$$

where d is the axial offset, θ is the angular misalignment, n_{cl} is the cladding index of refraction, w_o the mode field radius, and λ the wavelength of operation.

To minimize the above losses, it is necessary to impose stringent controls on the dimensions of the connector. Three parameters of particular importance are: (1) The concentricity of the microhole with respect to the ferrule's outside diameter, (2) the angle of the microhole with respect to ferrule axis, and (3) the inside diameter and ovality of the microhole. Conventional methods for measuring these parameters are at best repeatable to only 0.5 μm. To meet the demand for routine, submicron measurements, a new test system was developed. This connector geometry test station has been used extensively for screening connector parts prior to assembly into connectorized fiber optic cables, and have contributed to a considerable reduction of the average connector insertion loss.

TEST SETUP

A diagram of the equipment setup in shown in Figure 1. The system was constructed on an optical table in order to maintain alignment and to minimize vibrations. A special holder is used to hold the ferrule firmly in place for the measurement. This holder was designed so that uniform radial pressure is applied around the ferrule.

A microscope lens located directly in front of the ferrule delivers a highly magnified image of the ferrule end-face to the CCD camera. The output of the camera is fed into the video frame grabber where it is digitized and then transferred to the computer. A monitor connected to the frame grabber is used to focus and align the image. The ferrule end-face is illuminated through the lens using a fiber optic light bundle and a beam splitter. The camera, illumination optics, and microscope lens are mounted as a single assembly on a micrometer-driven translation stage.

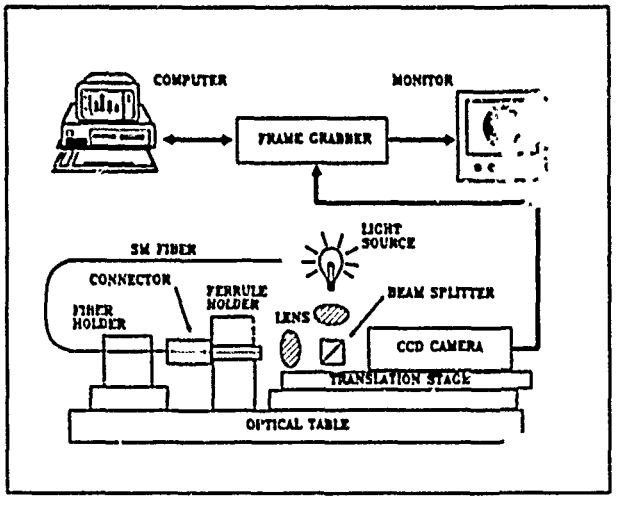

Figure 1. Fiber Optic Connector Geometry Test Station.

Two slightly different equipment configurations are used to illuminate the microhole of the ferrule under test. The choice of illumination depends on which parameter is to be measured. All attachments were designed for quick removal and replacement at

the back of the ferrule. The simplest is a light source which projects a beam through the microhole. The second illumination scheme involves a fiber holder and positioner which is used to precisely manipulate and place an optical fiber inside the ferrule. This fiber end is set at a slight angle to the ferrule axis. The far end of the fiber is coupled to a light source in order to illuminate its core.

Operation of the frame grabber and pacing of the test sequence is controlled by the computer. The custom software performs all the necessary image processing and data conversion of the end-face image to the required geometrical parameters.

MEASUREMENT TECHNIQUES

Two different measurement techniques are supported by the hardware described in the previous section. Each method is used for determining a different set of connector parameters. In the first test, an empty ferrule is measured, while the second method involves placing a loose fiber inside th microcapilary during the measurement.

Connector With Empty Ferrule

This technique is used to measure the *inner diameter* and *ovality* of a microhole, and its *concentricity* with respect to the ferrule axis.

With an empty connector ferrule mounted in the ferrule holder, the translation stage is adjusted to obtain a focused image of the end-face on the camera. The end-face illumination is then removed while the microhole of the ferrule is lit through its back using the second light source. A bright image of the hole at the end-face thus appears at the camera.

Analysis of a single image is sufficient to determine the microhole's diameter and ovality. However, in order to find the concentricity, the ferrule must be rotated 180° and then a second image taken. The location of the center of the microhole is found for each of the two images, and the concentricity of the microhole is simply the displacement between the two centers.

Using this method, the concentricity error of a microhole can be measured in less than 1 minute. Its disadvantage is that it cannot provide any information regarding the angle of the microhole with respect to ferrule axis.

Connector With Loose Fiber

This technique is useful for finding the microhole *angle* with respect to ferrule axis.

With the connector under test mounted firmly in the ferrule holder, one end of a stripped and cleaved single mode fiber is inserted into the microhole. This fiber is held in place by a fiber holder located immediately behind the connector. The other end of the fiber is prepared and aligned to the light source.

The position of the camera stage is adjusted to focus on the ferrule's end-face. Next, the fiber end is brought to the same focus by adjusting its position at the fiber holder. The image obtained at this point shows a brightly illuminated fiber core area surrounded by a darker cladding region. This image can then be used to determine the coordinates of the core center. As in the previous method, the ferrule is rotated by 180° and a second image is taken. The displacement of the fiber core center as a result of rotating the ferrule gives the concentricity of the microhole.

The angle of the microhole with respect to the ferrule axis is found by moving the fiber further into the ferrule by 1.0 mm. This is accomplished by first moving the camera assembly stage away from the ferrule by 1.0 mm, then the fiber is driven toward the camera until the fiber end is again in focus. The high-magnification of the system's optics has a sufficiently shallow depth of field so that focusing errors are in the order of a only a few tens of microns. Again, images of the fiber end-face are taken with a 180° rotation between the two samples. Displacement of the fiber core center due to the rotation is calculated and the actual ferrule concentricity (found in the previous step) is subtracted from the displacement. The residual offset divided by the 1.0 mm fiber protrusion gives the tangent of twice the microhole angle.

With this technique, a typical measurement of a microhole angle requires approximately 5 minutes.

System Calibration

There are two calibrations required for the test set. The first corrects for distortions introduced by the optics and the CCD camera pixels. The second calibration establishes the scaling of the image as seen by the system. While the later is easily found by measuring an object of known dimensions, correcting for optical non-linearities requires characterizing the camera on a pixel level. As most CCD cameras contain over 200,000 pixels in the sensing area, a point-wise calibration would be extremely inefficient. Fortunately, the objects to be measured are all similar in size and shape, so only the regions around where the object will appear need to be characterized. This can be accomplished by measuring an object similar in size (such as a fiber) to a microhole and with a known ovality.

TEST RESULTS

The capabilities and limitations of the test station were verified experimentally by measuring a small number of ferrules several times. The mean and standard deviation were calculated for each

ferrule separately, then a combined standard deviation was calculated for each ferrule parameter. These results are summarized in Table 1.

Parameter	S.D. (1S)
Microhole Concentricity	0.05 Mm
Connector Concentricity	0.03 Mm
Microhole Angle	0.01 deg
Microhole Diameter	0.1 Mm
Microhole Ovality	0.15 %
Ferrule Length	1.0 Mm

TABLE 1. Measurement accuracy for Connector Geometry Test Station.

Concentricity results obtained for finished connectors are affected differently by the two test methods described. In the case of the empty ferrule, the primary source of error is the imperfections at the edge of the microhole. With the loose fiber method, errors can result from interactions between the fiber and ferrule during the rotation.

CONCLUSIONS

A versatile test station for characterizing fiber optic connector geometric parameters has been developed. Based on non-contacting optical methods, the system is capable of testing microhole concentricity, angle, diameter, and ovality with submicron accuracy and precision.

Northern Telecom Canada Limited
Optical Cable Division
P.O. Box 807
Saskatoon, Saskatchewan
Canada S7K 3L7

Zygmunt Pasturczyk received the M.Sc. degree in physics from the Warsaw Technical University in 1976. In 1977, at the Warsaw Technical University, he was engaged in optical waveguides and integrated optics research. He joined SED Systems in 1982, where he was involved with optical instrumentation for upper atmosphere research. Since 1988 he has been a Research Scientist with Northern Telecom Optical Cable Division, working in the development of fiber optics installation products.

Bennett Wong was born in Hong Kong in 1956. He received the B.ASc. degree in electrical engineering from the University of British Columbia in 1980. From 1980 to 1984, he worked as a Development Engineer at Phillips Cables. Bennett joined the Optical Cable Division of Northern Telecom in 1984, and is currently the Senior Project Engineer in the Optical Fiber Testing Development department.

Costas Saravanos was born in Makrakomi, Greece, in 1951. He received the B.Sc. degree in physics from the University of Athens in 1973, and the M.Sc. degree in solid-state physics from the South Dakota School of Mines and Technology in 1980 and is currently completing the Ph.D. degree in electrical engineering at the University of Ottawa.

Following a year with the Digital Transmission Division of Northern Telecom, Canada, he joined the Optical Cable Division in 1982 where he was engaged in single mode fiber process optimization. Since 1985 he has been a Manager in the Fiber Research Laboratories in Ottawa and Saskatoon responsible for fiber design optimization, fiber characterization and installation products development.

CORE FILLING ASSESSMENT AND PERFORMANCE OF FILLED CABLES IN DUCT INSTALLATIONS

J. A. Olszewski and R. Rossi

General Cable Company
South Plainfield, N.J.

DIGEST:

A study of a derived water propagation model for small bore tubes which utilized an electrical transmission line analog, has shown that the water ingress failures in currently produced filled cables is caused by a plastic flow of cable sheaths and, possibly, an inadequate design of the filling compounds. High water pressures involved in the underground environment, coupled with the existence of faults in the polyethylene insulation, makes the use of filled cables as a replacement for pressurized links in ducts highly questionable.

INTRODUCTION:

It has been shown that water propagation in a narrow channel, and its pressure, is analogous to an electrical transmission line and its potential distribution. The derived equations are adapted herein to water flow in imperfectly filled telephone cables, enabling estimates of the time to failure versus the applied water pressure and/or the cable length. These relationships, when combined with an earlier work, also allow predictions of the transmission degradation of repeater spans employing cables of a given filling compound type and process versus the service time of a desired 40 years duration. The paper contains a few theoretical scenario examples and proposes water penetration test criteria which will yield results more applicable to the practical service environment. In addition, the work addresses a possible use of filled cables in ducts, where water head pressures can be considerably higher than the 3 ft normally taken for buried installations. The experimental evidence, however, of the industry wide variation in the degree of cable filling, combined with insulation imperfections in the form of pin-holes, raises questions as to the wisdom of the placement of currently designed filled cables in ducts.

THEORY - WATER FLOW IN SMALL HORIZONTAL TUBES:

The work on the water propagation in small-bore horizontal tubes[1] yielded the following relationships:

$$P(x) = P(o)\, e^{-r\, L(x) \sqrt{R / t\, P_{wf}}} \qquad \text{--------(1)}$$

where, in British units of lb, ft, and s, currently preferred by the industry

- $L(x)$ = distance from input point x along flow channel, ft
- $P(o)$ = water input pressure, lb/ft^2
- $P(x)$ = water pressure at point x along flow channel, lb/ft^2
  - $\geq P_{wf}$ (since P(x) cannot extend beyond water wavefront)
- P_{wf} = water wavefront pressure, lb/ft^2
- r = inside radius of flow channel, ft
- R = hydraulic resistance per unit channel length $lb \cdot s/ft^6$
- t = time of water pressure application, s

Equation (1) can be used to yield the water pressure distribution along the channel length, the time to traverse a given length, and therefore also the velocity of the water wavefront.

The hydraulic resistance R per unit length is defined as

$$R = \frac{P(o) - P_{wf}}{Q\, L} \qquad \text{----------(2)}$$

where, L = test length in flow test, ft and Q = flow rate in channel length L, ft^3/s

while the pressure drop $P(o) - P_{wf}$ is given by Poiseuille's equation, since the values of the estimated Reynolds numbers imply laminar flow in channel sizes and pressures normally expected in the installed telephone cables, i.e.

$$P_{in} - P_{out} = P(o) - P_{wf} = \frac{8\, Q\, L\, n}{\pi\, r^4} \qquad \text{---------(3)}$$

where n = water viscosity
= 1.002cP @ 68°F (or 0.95cP @ 72°F)
= 2.093×10^{-5}, $lb \cdot s/ft^2$ @ 68°F in British units[2]

The flow rate Q is given by a classical relationship, namely

$$Q = vA \qquad \text{----------(4)}$$

where v = water wavefront velocity at end of any given channel length L, ft/s
and A = flow channel cross-section, ft^2

and since since it has been experimentally established[1] that the flow rate Q' is inversely proportional to the channel length of interest L',

$$Q = \frac{Q\ L}{L'} \qquad \text{----------(5)}$$

Another form of the flow rate relationship for L = 3 ft, empirically established from experiments on horizontal capillary tubes, is of the following form:

$$Q(3') = 2570\ P(o)\ d^{4.3}\ ,\ ft/s \qquad \text{--------(6)}$$

where d = 2r

An additional fact of importance, indicated by equation (1), is the direct proportion between the water velocity v and the square root of time t.

PRACTICAL FIELD WATER PRESSURES:

Superior performance of plastic insulated filled telephone cables in buried service environment[3] has prompted the users to consider their suitability for pressurised cable links, or in other words, their use in the ducts. Buried cables however, typically experience low water pressures since they are installed at a 3 ft depth. Their testing at the cable manufacturing plants, designed for verification of the integrity of the filling is, therefore, conducted with a 3 ft water head pressure applied to the end of a 3 ft cable sample length, with the requirement that no water leakage occurs for one hour of water pressure application. Duct cables, on the other hand, are normally pressurized with dry air to 10 psig, but working pressures of 6 to 8 psig are common[4]. Simple calculations of expected water pressures, in the two operating environments discussed, show the following for standard 68°F temperature:

Buried: 3 ft head = 3 (28,316.85 x.9982/453.59
= 186.95 lb/ ft^2
= 1.30 psig

Duct : 7 psig ave. = 7 (144)
= 1,008 lb/ft^2
= (3) 1,008/186.95
= 16.2 ft head

10 psig max. = 1,440 lb/ft^2
= 23.1 ft head

Note: The above constants are: 28,316.85 cc/ft^3
.9982 water density @ 68°F[5]
453.59 g/lb
and 144 in^2/ft^2

The above figures attest to the severity of the underground environment, but the incentives for the use of filled cables are many, the major being the lower maintenance cost and the elimination of capital outlay for the construction of the pressure plant.

It should be noted that the water pressures acting on the cores of damaged installed cables are essentially the same as those acting on the outside of the cable sheaths. Factory testing of short cable samples, however, consists of applying a given water column height to the core with sheath being at atmospheric pressure. This test proceedure, therefore, results in pressure differences, departure from practical field reality, and more pessimistic results, especially if

i. Polyethylene jacket is not bonded to shield or armor
ii. Test pressures are high
iii. Test duration is long
iv. Test temperature is higher than that of operating environment
v. Cable sample diameters are large

In general, General Cable Company test data confirm the above. It appears that the jackets cold flow and balloon, creating water channels, enlarging built-in paths due to imperfect filling. This issue has to be addressed by the industry, or the test data has to be put into a proper perspective, or new evaluation techniques will have to be developed.

BURIED CABLE AND WATER FLOW RESISTANCE PARAMETERS:

One of the most important and currently underrated parameters of the water flow resistance in filled cables is the water flow rate Q at failure. Besides the time to failure and the applied pressure, the flow rate is determined by the channel size, and thus in turn, the degree of cable core filling, or jacket expansion.
The flow rate in cc/hr, the units used by the industry for three foot cable lengths, was empirically established in the experimental work on miniature tubes, and based on equation (6), is given by

$$Q(3') = 2.62 \times 10^{11}\ P(o)\ d^{4.3}\ ,cc/hr \qquad \text{----(6a)}$$

or, the equivalent flow channel diameter

$$d = 2r$$

$$= \left[\frac{Q(3')}{2.62\times10^{11}\ P(o)}\right]^{.233}, \text{ ft} \quad \text{----(6b)}$$

Utilizing the above, together with the experience gained in current cable testing of three foot long cable samples under three foot water head and typical flow rates at failure ranging from .001 to 10 cc/hr, Table 1 below yields a rather informative range of hypothetical flow resistance parameters.

Table 1

Open Channel Water Flow Resistance Parameters for 3 ft Length Under 3 ft Water Head Pressure

Q(3')	d	$P(o)-P_{wf}$	P_{wf}	R	t
cc/hr	ft	lb/ft^2	lb/ft^2	$lb\cdot s/ft^6$	hr
10.	.001105	168.42	18.53	$.572\times10^9$	.00441
1.	.0006460	144.18	42.77	4.899 "	.01373
.1	.0003778	123.25	63.70	41.88 "	.05060
.01	.0002209	105.45	81.50	358.3 "	.1945
.001	.0001292	90.11	96.84	3062. "	.7624

The values of Table 1 show that for a given applied pressure, the higher the flow rate, the larger the channel size, the higher the pressure differential between the input and the output, the lower the water wavefront propagation pressure, the lower the hydraulic resistance, the shorter the time to failure, and vice versa.

It should be noted that the failure times for current design cables are considerably longer than those computed in Table 1, assuming the existence of flow channels. This leads to a conclusion that these cables have either randomly interrupted channels, or no built-in channels. The degree of deviation between the practical water penetration times and the theoretical results also precludes, in most cases, the existence of non-linear continuous channels. Thus, the derived theoretical model per equation (1), or for that matter Poiseuille's law equation (3), developed for open channels, have to be augmented by the fact that the continuous channels in cable cores are being created on application of pressure.
This basically implies that the water wavefront propagation pressure inside the core, becomes a channel forming, or channel boring pressure, and is higher than that associated with the open channel. This takes time, as shown in Figure 1, especially if the distance between the flow blocks and the pressure application point increases. It should be noted that Figure 1 shows the pressure distribution along an

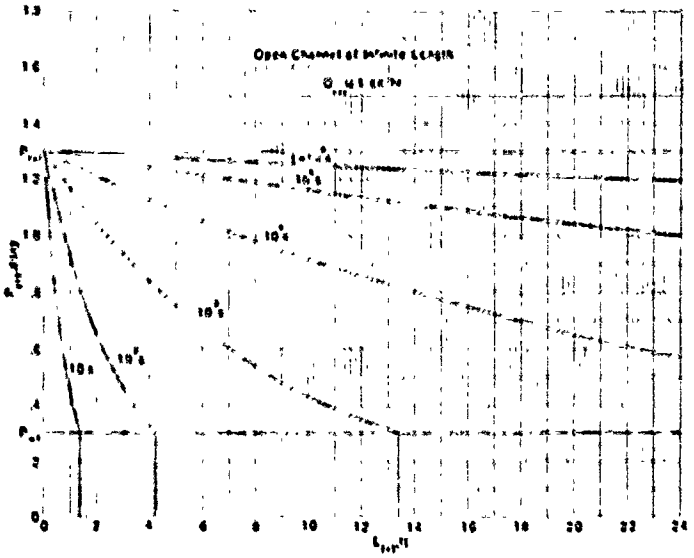

Figure 1

open channel of Q(3') = 1 cc/hr at different times, ranging from 10 to 10^6 seconds after the application of pressure.
Observation of numerous cable samples in production testing has shown that the flow rate at the moment of failure often decreases almost instantaneously and in some cases stops completely for a considerable time. The peculiarity of this behavior is believed to be caused by the pressure drop at the output the instant the failure occurs. This is then followed by a decrease in channel cross-section, or its complete closure, by the memory in the stressed cable components, especially that of polyethylene jacket. It takes time to build up the pressure again at the failure end, if it is closed, or to open up the flow channel. If, on the other hand, the channel at the failure point remains partially open, the pressure there will be lower than that just before the failure, and new flow conditions will eventually be established.

Water temperature is expected to have a measurable effect on the pressure gradient, flow rate, time to failure, etc. This is apparent from equation (3), where water viscosity parameter n is temperature dependent. Higher temperature geographic regions will have somewhat more acute water flow problems than the cooler northern regions.

The most important parameter, from the viewpoint of cable performance, is the time to failure t, and is given by equation (1) or its rearrangement, that is:

$$t = \frac{R\ r^2\ L(x)^2}{[\ln P(x)/P(o)]^2\ P_{wf}}, \text{ s} \quad \text{--------(1a)}$$

where at the time of failure $P(x) = P_{wf}$.

Most of the flow parameters are interrelated, but certainly for a given cable quality and applied pressure, the time to failure t is directly proportional to the cable length squared. In other words, doubling the length will quadruple the time to failure, and so on.
At first glance equation (1a) appears to have an error, inasmuch as the failure time is shown to be also directly proportional to the square of the flow channel's equivalent radius r. This is not so, as the channel radius has a larger effect on the hydraulic resistance R and the wavefront pressure P_{wf}. Figures of Table 1 confirm this assertion.

The effect of another test variable, the applied pressure P(o), on the time to failure, is more complex, but can be determined from equation (1a). In general though, it can be stated that higher pressures will reduce the failure times, provided that no shifts of filler mass take place. The theory suggests the following relationship:

$$t \propto \left[\frac{P'(o)}{P(o)}\right]^{y} \qquad \text{----------(7)}$$

where P'(o) = applied reference pressure
and P(o) = applied pressure of interest

with the exponent $y \approx 1$ when cable cores are poorly filled, and $y > 1$ and increasing with improved core filling. In the latter case, y attains a maximum value when the wavefront propagation pressure P_{wf} approaches the value of P(o) for $P(o) < P'(o)$, or when P_{wf} approaches the value of P'(o) for $P'(o) < P(o)$.

The value of the wavefront propagation pressure is critically important. $P_{wf}/P(o)$ ratio >1, or at least tending to unity, is most desirable for any value of P(o). The importance of this relationship is depicted in Figure 2; the higher the $P_{wf}/P(o)$ the longer is the time to failure. However, although theoretically ratios of $P_{wf}/P(o) > 1$ are possible, in which case the cable should never fail, in practice this appears to be valid only at the start, since the time of the pressure application continuously reduces this ratio to less than unity through cold flow of the filler and the cable sheath. The whole issue of water penetration failures appears to reduce to that of time under pressure.
The above statements, of course, are not meant to imply the unimportance of a high degree of cable core filling. Well filled cores will tend to have smaller flow channels, and in turn, higher required wavefront pressures for slower water penetration. What is questioned, is the ability of current design cables to block water ingress at high field pressures.

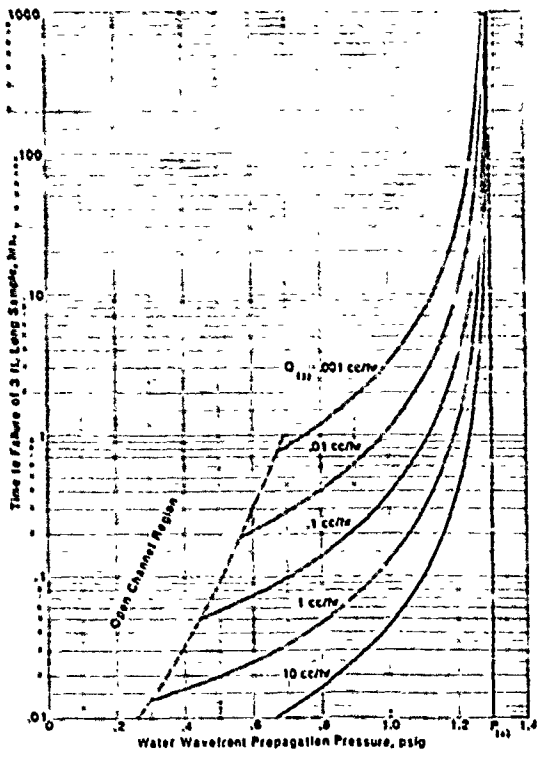

Figure 2

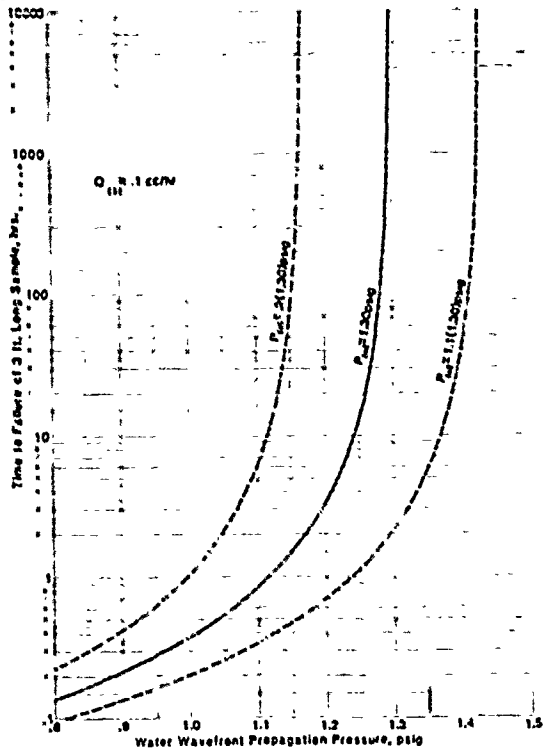

Figure 3

Analysis of plots in Figure 2, representing the predicted performance of current design filled cables for buried use, and taking into account the fact that 3 ft long samples of these cables under a 3 ft water head (1.30 psig) fail on the average after about 50 hours, the typical theoretical water propagation pressure P_{wf} is 1.24 to 1.30 psig. This curiously narrow range seems to confirm earlier statements on the importance of time. The plots also suggest a high spread in time to failure, which is supported by the test data.

Another source of sample to sample failure time scatter is shown by the plots of Figure 3, that is, when small errors are made in the prescribed test pressure. For example, when a 3 ft sample is tested at a 3 ft high water head (1.30 psig) and the propagation pressure is 1.15 psig, such sample will theoretically fail at best after 1.5 hours, but when P(o) is mistakenly set at 10% higher value, and 1.15 psig remains the channel forming pressure, the sample will be expected to fail after about 0.48 hours. On the other hand, 10% lower than 1.30 psig nominal test pressure, could be expected to produce a failure after about 85 hours. Similarly, at P_{wf} = 0.90 psig, the corresponding theoretical failure times become only 0.22, 0.13 and 0.42 hours respectively.

The above estimates do not take into account so far undetermined jacket expansion rates.

The parameter of hydraulic resistance R was introduced as a convenience and in order to avoid the need to use water physical properties, such as surface tension. Its value, per equation (1a), is directly proportional to failure time. It determines the rate of exponential decay of pressure along the cable.

FILLED CABLE FOR DUCT INSTALLATIONS:

Given the scenario described in the preceding section, the increase in pressure from 186.9 lb/ft^2, applicable to buried cable, to 1,000 lb/ft^2, or as high as 1,400 lb/ft^2, applicable to underground cables, spells out problems unless the water entry is quickly detected and the fault is repaired. High strength cable sheath and highly compacted filling free of voids with properly designed filler, are the keys to success. The current technology filled cables in duct installations, even if made under the greatest of care, will allow water entry into their cores as projected in Figure 4, for a 40 year span of service. Combining the above with earlier determined changes[8] in 1 kHz mutual capacitance versus time for a variety of filled cables with 1/4" diameter holes in their sheaths, 1 ft apart, and each rotated 90 degrees from the preceding, that were immersed in

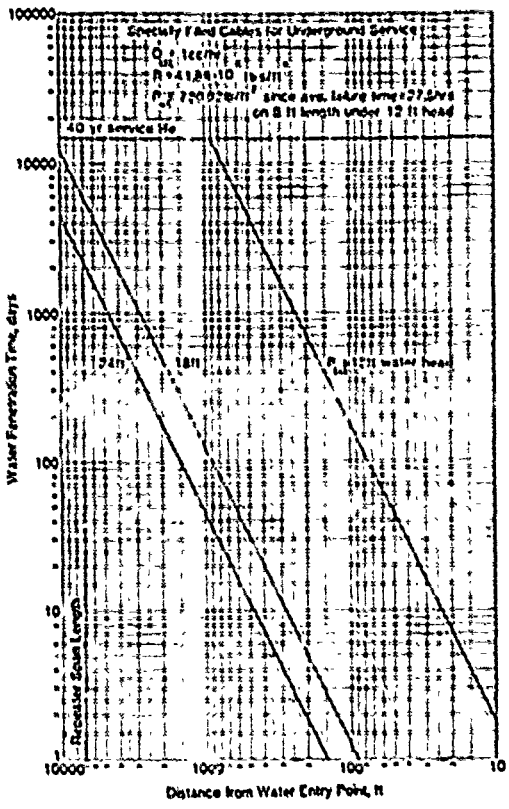

Figure 4

water at room temperature - see Figure 5 taken from reference 6 - the predicted mutual capacitance changes in duct cables after 40 years of service will be as shown in Figure 6, for 12, 18 and 24 water head pressures and the most immune filling compound labeled Q9. Its absorption of water was found to be similar to that of ETPR compound.

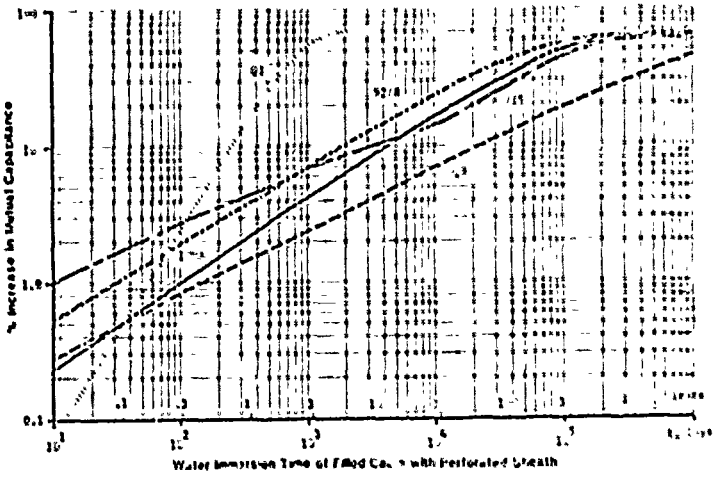

Figure 5

The expected increases in mutual capacitance were estimated at 8%, which translates to about 4% increase in voice frequency attenuation, and roughly about the same per cent increase in T-carrier attenuation, as the presence of water in the core is not expected to affect the dissipation factor at high carrier frequencies.

The water entry into the long lengths of duct cable links however, will expose insulation faults, and therefore will result in low resistances to ground, high crosstalk, shorts and in time open-circuits due to the corrosion of conductors. As an example, a 7,000 ft repeater span length employing 3,000 pair, No. 26 AWG, foam-skin insulated cable with one insulation fault (pin-hole) per 40,000 ft minimum of conductor, can possibly end up with 7(3,000)2/40 = 1,050 uninterrupted circuits at the end

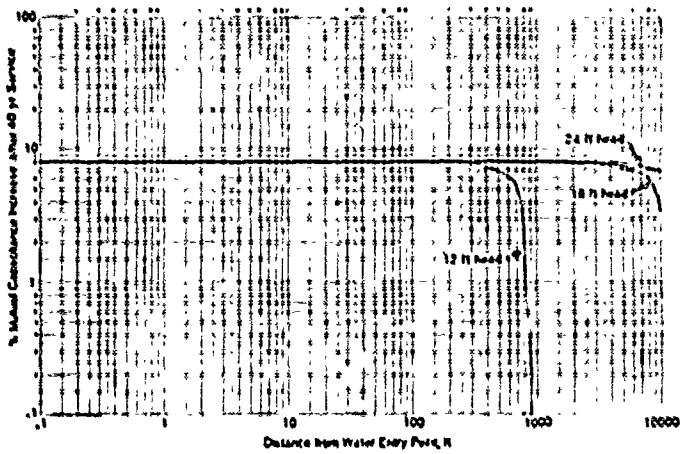

Figure 6

of its 40 year service, when it is acted upon by a 24 ft water head. A 12 ft water head pressure on the same repeater link, per Figure 6, will have 1(3,000)2/40 = 150 faulty circuits. In either case though, the situation is intolerable, especially if a cable sheath fault is located in the span away from the repeater, or if more than one sheath fault develops. An assumption of lesser "duty cycle" or time under water pressure, also will not change the situation drastically.

CONCLUSIONS:

Assuming the validity of the developed water propagation model, the work described herein leads to the following conclusions:

1. Current water flow testing methods may be inadequate in properly evaluating future designs.
2. The flow rate at failure is an important parameter which characterises the efficiency of the cable core filling.
3. Current filled cables typically have no contineous open channels, although core wrap and/or shield-armor tape overlaps remain the weaknesses of the design.
4. The water penetration failures of filled telephone cables appear to be those of time at a given pressure. The cable sheaths cold flow and balloon and, with time, water channels are created.
5. High spread in sample to sample failure time of reasonably well filled cables is theoretically due to small deviations in channel producing pressure. Small errors in setting the test pressure also contribute to the failure time variability.
6. While damaged buried filled cables, typically operating under a 3 ft water head pressure, can be penetrated by water for a few hundred feet within their 40 year service life, the filled duct cables, even of most careful manufacture, operating at up to 24 ft water head pressure, can be penetrated by water for distances in excess of a typical PCM carrier repeater span. The presence of insulation faults precludes the use of current design filled cables in the underground environment.
7. Currently employed cable sheaths in filled cables appear to be the weakest link requiring correction, but also a possible need for redesign of the filling compounds cannot be discounted.

REFERENCES:

1. J. A. Olszewski, "Transient Water Filling of Small Diameter Horizontal Tubes", 4th Symposium on Fluid Transients in Fluid-Structure Interaction, ASME Winter Annual Meeting, San Francisco, December 11 - 14, 1989.
2. F. J. Bueche, "Theory and Problems of College Physics", 7th Edition, Schaum Outline Series, McGraw-Hill Book Co., 1973.
3. N. E. Hardwick, "Buried Cable Comparisons", Telephone Engineer & Management, September, 1978.
4. Bell Communications Research, "Statistical Analysis of Water Resistance in ETPR and Experimental Filled Cables", Special Report SR - TSY -000794, Issue 1, June, 1988.
5. R. C. Weast, "CRC Handbook of Chemistry and Physics", CRC Press Inc., Boca Raton, Florida, 1985.
6. J. A. Olszewski, "Capacitance Relationships in Filled Telephone Cables and Equilibrium Prediction from Water Immersion Tests", 24th International Wire & Cable Symposium, 1975.

R. Rossi joined General Cable Co. in 1963. Since that time he has worked in Product Engineering, Quality Control, and Application Engineering. With a B.S. in Engineering Sciences, he is currently Director of Application Engineering.

J. A. Olszewski joined General Cable Co. in 1955 and is currently Transmission Research Specialist. He has also held positions in International Operations. He holds an M.Sc. in Electrical Engineering.

STRENGTH AND STATIC FATIGUE OF OPTICAL FIBERS AT DIFFERENT TEMPERATURES

Dipak R. Biswas

SpecTran Corporation, Sturbridge, MA 01566

ABSTRACT

Optical fiber coatings play an important role in fiber strength, static fatigue, attenuation and performance at different temperatures. Various coatings are available for diverse applications. No single coating is available to fulfill the requirements. The major function of a coating is to protect the glass surface from external abrasion and environment, and to preserve strength. The polymeric coatings such as ultraviolet cured epoxy acrylate, silicones and polyimides are commonly used. The operating temperatures of the above coatings are 80°C, 200°C and 300°C respectively. For even higher temperatures, metallic coated fibers are being considered. The strength and fatigue of high temperature coated fibers such as silicone, polyimide and aluminum are discussed.

1. Introduction

There is considerable interest in high temperature coatings for the automobile and aircraft industries. Most standard telecommunication optical fiber uses ultraviolet (UV) cured epoxy acrylate coatings. The maximum safe operating temperature is nearly 100°C, but for applications which require temperatures in excess of 100°C, there are various polymeric and metallic coatings available. Silicone coatings are extensively used for optical fiber ground wire which experiences ambient temperatures above 100°C. Silicone coated fibers can be used safely up to 200°C. A new polymer for fibers based on ladder siloxane polymer (LSP)[1,2], demonstrating good heat resistant properties has been shown to perform quite well above 200°C exposure. Polyimide coating on optical fiber, however, can withstand temperature up to 350°C. Research work is continuing for the development of polymers capable of withstanding temperatures of nearly 400°C. Currently, for temperature applications greater than 350°C, metallic coated fibers are being used. Aluminum coating on fiber can withstand temperatures up to 500°C whereas gold coated fibers can withstand 900°C. Investigation is ongoing for copper and nickel coatings for possible higher temperature applications. The purpose of this paper is to present strength and fatigue data on fibers coated with silicone and aluminum, together with recent experimental data on high temperature strength of polyimide coated fibers.

2. Experimental Procedure

The fibers used in this study were drawn from a silica preform to a diameter of 140μm and were coated with a polyimide coating to 170μm. The coating was applied by dip coating and cured thermally. Dynamic tensile strength was determined at room temperature and at 300°C in air. 0.7m gage length with a strain rate of 4%/minute was used to measure the strengths. Mandrel testing of polyimide coated fibers is continuing in water at 80°C.

3. Results and Discussions

A. Silicone Coated Optical Fibers

The determination of strength of silicone coated optical fiber by using dynamic tensile testing is quite difficult as the polymer is soft and difficult to grip. In addition, the coating stretches considerably during tensile testing. Therefore, mandrel testing and two-point bend testing are being used to generate static and dynamic fatigue data at different temperatures.

A 400μm silicone coated 50/125μm graded index fibers was used by Wade et.al.[3] to generate static fatigue data at room temperature, 150°C, 220°C and 300°C. The fibers were wrapped on different size mandrels, placed in an oven and the time to failure recorded. A plot of time to failure vs strength is shown in Figure 1.

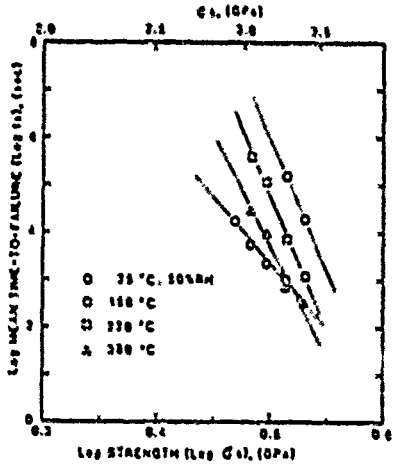

Figure 1. Time to failure vs applied stress on silicone coated fibers at different temperatures (Ref 3).

The slope of the straight line gave the static fatigue parameter 'n_g'-value of 27 for room temperature testing. The 'n_g'- values were increased to nearly 50 at higher temperatures. This higher n_g-value indicates that silicone coated fiber has an excellent static fatigue resistance at high temperature applications. In a different experiment, Cueller et. al.[4] performed the static fatigue experiment on silicone coated fibers by using a two-point bend apparatus. Approximately six inch long large core fibers (480μm core/625μm clad) were placed in a two-point bending fixture, the fixture was submerged in water at 80°C and the time to failure monitored. Figure 2 shows the static fatigue data for silicone coated fibers compared with uv-acrylate coated fibers. A significant improvement in static fatigue resistance was observed in silicone coated fiber compared to acrylate coated fiber in water at 80°C.

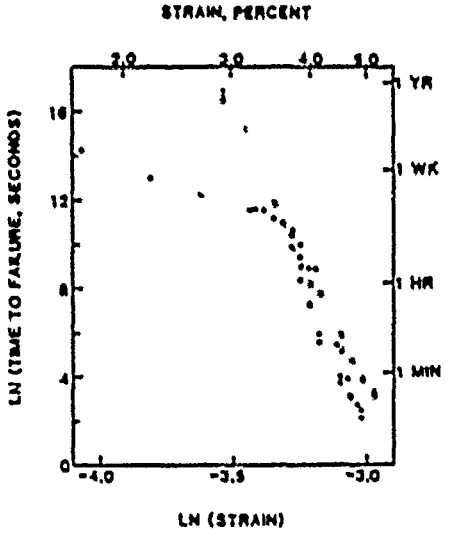

Figure 2. Time to failure vs applied stress on silicone coated fibers (open circle) and uv-acrylate coated fibers (close circles) in water at 80°C (Ref 4).

B. Polyimide Coated Optical Fibers

Polyimide coating has an excellent thermal stability and chemical resistance together with good dielectric properties. The dynamic tensile strength was determined at room temperature and at 300°C. The fibers were kept at 300°C for 15 minutes before the tensile testing was done at 4%/minute strain rate. The results are summarized in Table 1.

Table 1. Dynamic Tensile Strength of Polyimide Coated Fibers

Temp. (°C)	Dynamic Tensile Strength (Kpsi) Max.	Min	Med	St. Dev.
Room Temp	683.1	412.2	632.8	63
300	694.1	338.1	613.5	99

It appears that the strength does not degrade when testing was performed at 300°C. Static fatigue testing in water at 80°C is underway. Preliminary results indicate that the n_s - value is above 30 which indicates[5] that the polyimide coated fibers are quite resistant to slow crack growth or static fatigue compared to uv-acrylate coated fibers.

C. Aluminum Coated Optical Fibers

For applications that are in excess of 350°C, metallic coated fibers are preferred. Aluminum coating on optical fibers is extensively studied[5,6]. Aluminum coating on optical fibers can be applied by the dip coating process. Pinnow et.al.[5] studied the fatigue of 80μm diameter silica fibers with 15 - 20μm thick aluminum coating. Both dynamic and static fatigue results were reported. The average strength of aluminum coated fiber was 520 Kpsi at 4%/minute strain rate. The dynamic tensile strength did not change with different strain rates indicating a high fatigue resistance. In static fatigue measurement, it was reported that aluminum coated fibers can survive five orders of magnitude higher than conventional polymer coated optical fibers.

Tanaka et.al.[6] reported the static fatigue data of aluminum coated optical fibers at high temperatures up to 400°C. The static fatigue results are shown in Figure 3.

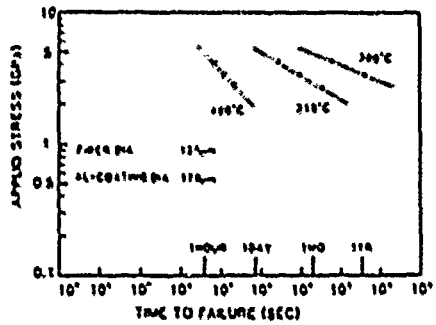

Figure 3. Static fatigue data of aluminum coated fibers at high temperatures (Ref 6).

It was found that aluminum coated fibers had sufficient lifetime at 350°C. At higher temperatures and under the service loading condition, aluminum coating degraded due to creep phenomenon.

4. Summary and Conclusions

When optical fibers are used in an environment exceeding 100°C, uv-cured epoxy acrylate coatings are not preferred. Silicone, ladder siloxane polymer and polyimide coatings are generally used from 200°C to 350°C. Since the silicone coating is very soft, it is difficult to determine the accurate strength by tensile testing. Strength and fatigue of silicone coated fibers can be determined by two-point bending and mandrel testing. Silicone coated fibers show an excellent fatigue resistance in water at 80°C and also at 100 to 300°C. The polyimide coated fiber, in contrast, is hard and has a slick appearance. It can retain its original strength when exposed to 300°C. The preliminary static fatigue data for polyimide coated fiber showed a good fatigue resistance in water at 80°C. For higher temperature applications, metal coated fibers are being used. Aluminum coated fiber has a strength of nearly 500 Kpsi at room temperature. The coated fiber showed excellent fatigue performances at room temperature and at high temperatures. Thus, the different high temperature coatings on fiber are showing good performances at their application temperatures. More data is needed for a reliable lifetime prediction of these high temperature coated fibers.

REFERENCES

1. B. Bagley, C. Kurkjian and W. Quinn, Mat. Res. Soc. Symp., 88, 35 (1987).

2. S. Araki, T. Shimomichi and H. Suzuki, 37th IWCS, proceedings, 745 (1988).

3. A. Wada, H. Ishi, S. Araki, T. Kobayashi and R. Yamauchi, OFC Tech Digest, TUI5, 42 (1986).

4. E. Cueller, D. Roberts and L. Middleman, OFC Tech Digest, TUQ 6, (1987).

5. D. Pinnow, G. Robertson and J. Wysocki, Appl. Phys. Lett., 34 (1) 17 (1979).

6. S. Tanaka, T. Shiota, R. Yamauchi and K. Inada, OFC Tech Digest, TUQ 25 (1985).

Dipak R. Biswas received his Ph.D. from the University of California, Berkeley in 1976. After working at Lawrence Berkeley Laboratory, University of Utah and Institute of Gas Technology, he joined ITT Electro-Optical Products Division. At ITT and Alcatel Cable Systems he worked on optical fiber strength and coating developments for different commercial and military applications until 1988. Currently, as Director of Research and Development at SpecTran Corportion, he is working on strength and reliability of silica and fluoride fibers, hermetic coatings, sensors and high temperature coating developments.

HIGH STRENGTH, FATIGUE RESISTANT, SINGLEMODE OPTICAL FIBERS WITH UNIQUE THIN HARD COATINGS FOR SPECIAL/SEVERE APPLICATIONS

B. J. Skutnik, M. H. Hodge, J. P. Clarkin

Ensign-Bickford Optics Company, Avon, CT 06001

Abstract

The enhanced mechanical properties of fibers with silica core and thin, bonded, hard polymeric cladding have been well documented over the past six years. These step-index large core fibers, however, are bandwidth limited and are not suitable for systems with high data rates or long lengths. This paper describes the extension of this technology to coat all-silica, multicomponent singlemode fibers during the draw process. The resulting fibers can be proof tested at very high levels, have high Weibull strength and slope parameters, and are highly fatigue resistant. The coating has little measurable effect on the basic attenuation or microbend induced attenuation of the singlemode fiber. These coated fibers represent a true "new generation" in singlemode fiber technology.

Summary

In earlier work Hard Clad Silica (HCS®) optical fibers have been shown to have high strength and to be highly fatigue resistant in moist or wet environments. Recent tests, described here, have proven that HCS technology can be extended to all silica optical fibers including singlemode fibers. This demonstrates that the reliability, survivability of singlemode fiber is enhanced by employing HCS technology. Singlemode fiber lengths of >10 km have been achieved at proof test levels of 400 ksi (2.76 GPa). Combined with their high Weibull strength, ~700 ksi, slope, m >50, and good fatigue resistance, N ≈26, these fibers are strong candidates for all high reliability, high strength, long-haul application; e.g. fiber guided missiles, tethers and subscriber loop applications.

Introduction

In recent years the reliability of optical fibers has become of great concern due to military, medical and other specialty high performance applications. With the nearing promise of fiber-to-the-home and its inherent requirements for a robust optical fiber, the telcom market has come to value stronger, more fatigue resistant fibers, too.

The original HCS optical fibers were designed[1,2] to be strong, relatively insensitive to environmental conditions and easily terminated[3]. These fibers have high values for initial strength and Weibull slope. Typical mean strengths are above 780 ksi (5.4 GPa) and "m" values range from 60 to >>100.

In previous reports[2,4-8], HCS fibers were shown to have high strength and excellent static/dynamic fatigue resistance in high humidity and water environments, especially at elevated temperatures. Their insensitivity to moisture exposure, even at moderate stresses prior to testing, exemplify their enhanced reliability.

The overall strength and fatigue properties of HCS fibers are due to the passivating nature of the hard cladding[9,10]. It was designed to bond to the pristine freshly drawn silica surface and has low water absorption and low water vapor permeability properties. It deactivates (passivates) the silica surface and over time protects silica fiber core from attack by moisture. These fibers do not exhibit zero-stress aging degradation of strength[11]. With their high initial strengths and with moderate but very predictable fatigue resistance, HCS fibers have been shown to behave more reliably than most currently available hermetic optical fibers[11,12].

More recently the HCS technology has been extended to all-silica type fibers[13,14], where the coating does not need to serve as a cladding. The improvements in strength, fatigue resistance and reliability for the all-silica fibers are essentially the same as the HCS optical fibers. A new singlemode fiber (SMF) structure has been developed with enhanced reliability. A thin, hard, adhesive, polymeric coating is placed between the silica cladding and the usual combination buffer coating. See Figure 1.

This paper presents results on the properties of this new SMF and compares them with results for commercially available SMFs. Dynamic strength, fatigue resistance, including zero-stress aging in boiling water and extensive long gage dynamic testing are used to illustrate the reliability of this new fiber. Proof testing at high stresses, up to 400 ksi (2.76 GPa), has yielded long lengths of failure free fiber.

Experimental Details

The SMF fibers were drawn using a conventional silica fiber draw tower. The fiber was drawn directly from preforms which yielded the standard 8/125 core/clad silica dimensions. When employed, the proprietary hard polymer was applied via a specially designed applicator and delivery system. The polymer was cured on-line and the fiber prevented from solid contact until the coating was fully cured.

All fibers had a common DeSoto uv-curable acrylate single buffer coating applied and cured on-line using standard application and cure equipment.

Dynamic tensile strength testing was performed using a universal tensile testing machine with specially designed grips for optical fiber. Test samples were tested at ambient conditions - 23°C, ~65% RH - with a 9 meter gage length and 0.9 cm/sec (5% /min) strain rate. Typically 20 samples were tested per sample fiber, except for the special experiment where 100 samples were tested.

Static fatigue testing was performed via the mandrel wrap technique[9,15]. In this technique ~1.1 meters of fiber are wrapped around mandrels of various diameters. The diameters of the mandrel and of the silica fiber determine the stress the fiber experiences[16]. Fiber samples wrapped on the mandrels were immersed in ambient water. The time to the first break (failure) was measured. The mandrel sizes were selected to yield failure times covering 4 to 6 orders of magnitude.

To evaluate the effects of zero-stress aging, sections of fiber were exposed to boiling water for 24 hours and then ~1.1 meter samples prepared on appropriate mandrel sizes. The wrapped aged samples were immersed in ambient water and their failure times measured.

Dynamic Strength

To demonstrate the strength enhancement, single-mode fibers were drawn from a single preform with and without the HCS-type coating. All fibers had standard buffer coatings on them. The results are shown in Figure 2. The ultimate strength is slightly higher for the coated samples, but much more significantly, the low values in the tail section are greatly shifted to higher strengths.

Since the development of the HCS-type coating for SMF is still in its start-up period, a comparison of standard HCS fiber strength and the HCS coated SMF will illustrate the level of strength enhancement that can be expected in the future. This is done in Figure 3. The standard HCS fiber has a slightly higher mean strength, and even more significantly, a single line describes its Weibull plot, i.e. it doesn't display a low strength tail like the SMF fiber. This is important for reliability prediction as is discussed later.

In this figure the strength measurements for one of the best commercial telcom SMF fibers is also plotted. The silica diameters for all three fibers are nominally the same, 125μ. The two HCS coated fibers were proof tested at 100 ksi (0.69 GPa), while the commercial fiber was probably proof tested at 50 ksi (0.35 GPa). The two HCS coated fibers have higher mean strengths than the commercial fiber. While the HCS coated plot does cross the commercial SMF plot, the former has a much higher strength tail which tightens up rather than spreading out at the lowest failure strengths. This feature predicts a better probability of high strength for long lengths. This is verified later when the results of off-line proof testing are presented.

The preform used to produce the fibers with and without the HCS coating appeared to have some internal flaws, which were thought to lead to the residual lower strength tail observed in Figures 2 and 3. A more carefully selected preform was obtained and drawn into another HCS coated SMF. Approximately 1.2 km of this fiber was cut up into 100 ~1m samples, randomized in sets of 20, and the dynamic strength tested with 9 meter gage lengths. The results of this experiment are given in Figure 4. This is a fascinating and unusual plot. Not only are all the failure strengths above 600 ksi under a moderately slow (5%/min) strain rate in a highly humid environment (65% RH), but also there is no low strength tail in this specific fiber lot. We thus confirmed the initial suspicion that for a good preform the HCS coated SMF can have a unimodal Weibull plot with a high median strength even under adverse, though realistic, environmental conditions. The result also predicts a higher probability of long length high strength fibers.

Fatigue/Zero-Stress Aging

It should be noted that for the dynamic strength testing reported in Figures 2-4, the gage length (9m) is long and the strain rate (0.1%/sec., 5%/min) is moderately slow. In the high humidity of the test environment, sufficient time is thus available for fatigue to occur. The fatigue behavior of the new SMF structure is the other significant advantage it has over conventional SMF.

The fatigue behavior of the new HCS coated SMF and that of conventional SMF was measured. The results for fiber samples tested in ambient water are given in Figure 5, where the Charles[17] power law plot is employed. Also plotted in this figure are the results for fibers subjected to 24 hours of zero-stress aging in boiling water.

First, the conventional SMF is weaker but its initial fatigue, slope for filled squares line, is quite similar to that of the new HCS SMF. After aging, however, the conventional fiber has significantly lost strength and fatigue resistance.

On the other hand, the new HCS-type fiber shows no discernable difference in its strength or fatigue behavior. The importance of this result is that it predicts no transition in their static fatigue behavior for the new HCS SMF but does indicate one for the conventional SMF, which will occur at indeterminate times at different operational temperatures[11].

More concretely, after zero-stress aging in boiling water for 24 hours, the conventional (commercial) fibers break in <1 sec at stresses above 290 ksi (2.0 GPa), while the new HCS-type fibers would still have expected lifetimes at 290 ksi stress of >9 years, or about 10^8 times longer. The consequences on fiber reliability are thus great.

Proof Testing

To confirm the strength results and to demonstrate the practical advantages of the new HCS style singlemode fiber construction for the specialty applications of SMF that require strong, reliable, long lengths of fiber, two representative fibers were produced from different preforms. The two case studies are summarized in Table I and II.

Table I

Case A: 8/125/140 — 220 um Buffer

Step	Proof Test (ksi-GPa)	Length (m)
Fiber Draw	200 - 1.4	4300*
Re-Proof	200 - 1.4	4300
Re-Proof	300 - 2.1	4100
Re-Proof	400 - 2.8	3300

*Proof Tested On-Line

Table II

Case B: 8/125/140 — 230 um Buffer

Step	Proof Test (ksi-GPa)	Length (m)
Fiber Draw	300 - 2.1	11,000*
Re-Proof	400 - 2.8	11,000

*Proof Tested On-Line

These results prove that the sharpening of the Weibull curve for the new HCS-type SMF in Figure 2 is real and also reinforce the unimodal Weibull observed for the large test sample case in Figure 4. More importantly they establish that the new construction can indeed be drawn into high strength, long length fibers which should have predictable fatigue behavior and excellent reliability. For those applications requiring ultra-high proof testing, these new fibers have proven their ability to be tested off line to very high strength levels.

Application Implications

The new structure HCS-type singlemode fibers with their high initial strength, relative insensitivity to environmental conditions and zero-stress aging, and very good and predictable fatigue resistance have outperformed hermetic-coated fibers in test simulating stringent operating conditions[11,12]. Their ability to yield long lengths at high proof test levels is promising in terms of cost efficiency and predictability.

Such high strength, fatigue resistant fibers are desirable for applications where high stress will be encountered, such as fiber guided missiles, delay line bobbins, tethers and tight bend radius deployment.

This fiber construction may provide substantially higher and more predictable reliability in high stress, high temperature, small bend radius cabling or subscriber loop applications where installation restrictions and practices may require a more robust, fatigue resistant "hook-up" fiber.

Finally the robust strength and fatigue properties of these fibers may permit the design and installation of new cable structures taking full advantage of the small size and weight of optical fibers. Even greater savings in weight or size or increased reliability will be possible for these special situations such as avioptic or space applications.

References

1. W. B. Beck, "Hard Clad Silica (HCS®) Fibers for Data and Power Transmission", in EFOC/LAN 85 Proc., 146 (1985).
2. B. J. Skutnik, M. H. Hodge and D. K. Nath, "High Strength, Reliable, Hard Clad Silica Fibers", in FOC/LAN 85 Proc., 232 (1985).
3. B. J. Skutnik and B. D. Munsey, "The Connector Connection in Fiber Optics", in Seventeenth Annual Connectors and Interconnection Technology Symposium Proc., 262 (1984).
4. B. J. Skutnik and R. E. Hille, SPIE Vol. 506, 184 (1984).
5. B. J. Skutnik, M. H. Hodge and D. K. Nath, paper 83-G-86 Am. Ceram. Soc. Annual Meeting Abstracts, p. 348, April 1986.
6. B. J. Skutnik, M. H. Hodge and J. P. Clarkin, SPIE Vol. 842, 162 (1987).
7. B. J. Skutnik and M. H. Hodge, "Passivated Optical Fibers for Adverse Environments", in OPTO 88 Proc. 159 (1988).
8. B. J. Skutnik, M. H. Hodge, J. P. Clarkin, SPIE Vol. 906, 244 (1988).
9. B. J. Skutnik, B. D. Munsey and C. T. Brucker, Mat. Res. Soc. Proc. Vol. 88, 27 (1987).
10. T. S. Wei and B. J. Skutnik, J. Non-Cryst. Solids 102, 100 (1988).
11. J. E. Ritter, T. H. Service and K. Jakus, J. Am. Ceram. Soc. 71, 988 (1988).
12. G. D. Leatherman, paper Am. Ceram. Soc. Fall Glass Division Meeting Abstracts, Nov. 1988.
13. J. P. Clarkin, B. J. Skutnik, B. D. Munsey, J. Non-Cryst. Solids 102, 106 (1988).
14. J. P. Clarkin and B. J. Skutnik, SPIE Vol. 992, 204 (1988).
15. B. J. Skutnik and T. S. Wei, SPIE Vol. 842, 41 (1987).
16. B. J. Skutnik, W. B. Beck and M. H. Hodge, SPIE Vol. 787, 8 (1987).
17. R. J. Charles, J. Appl. Phys. 29, 1547, 1554, 1657 (1958).

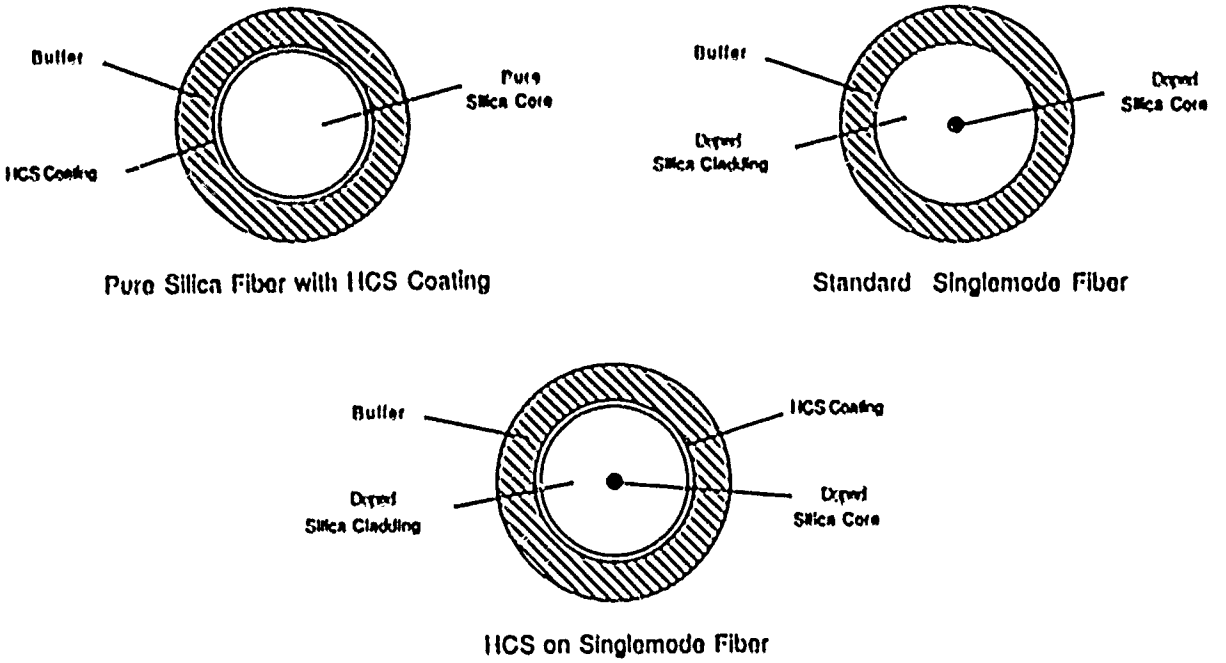

Figure 1

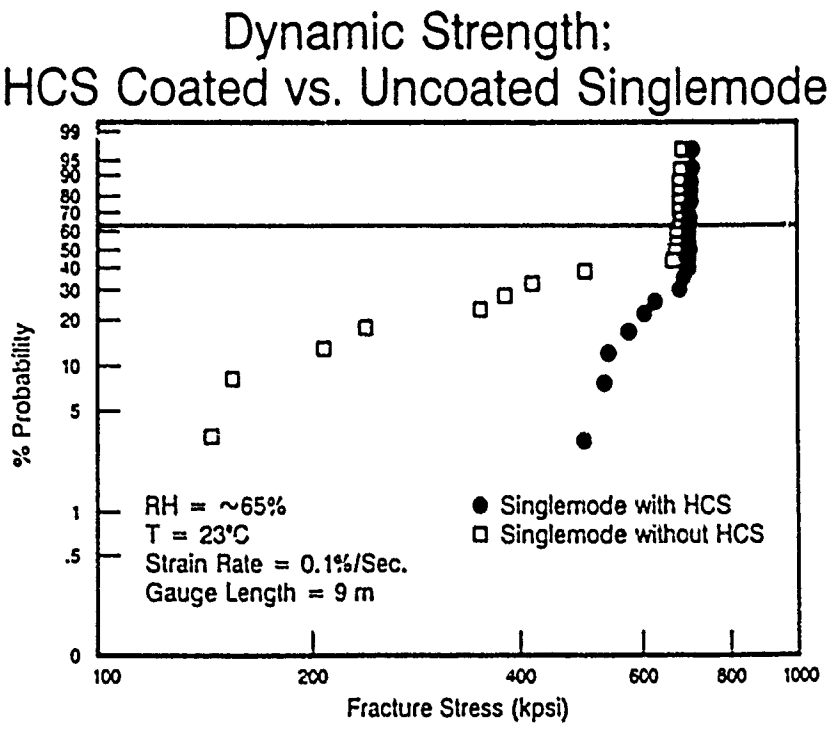

Figure 2

Dynamic Strength: Standard HCS vs. HCS on Singlemode

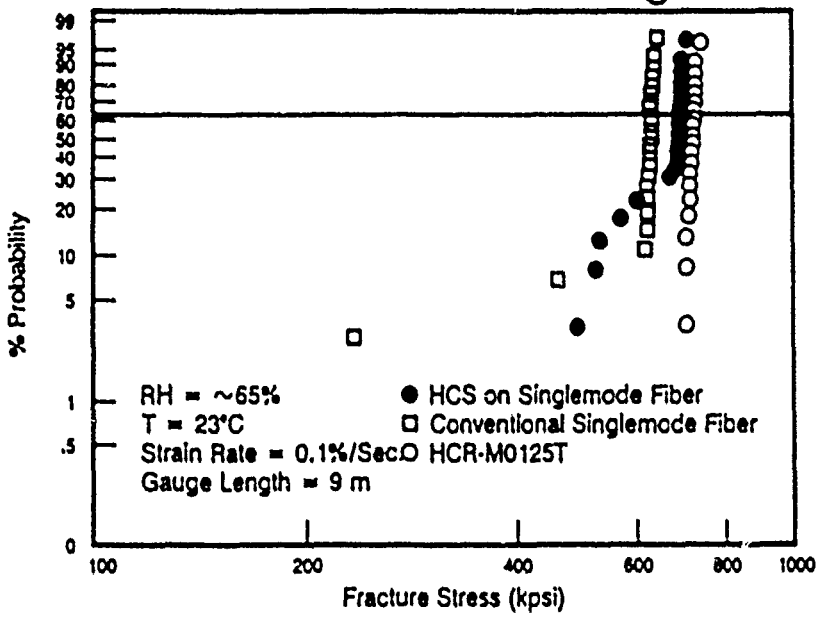

Figure 3

Dynamic Strength: HCS Coated Singlemode vs. Standard HCS

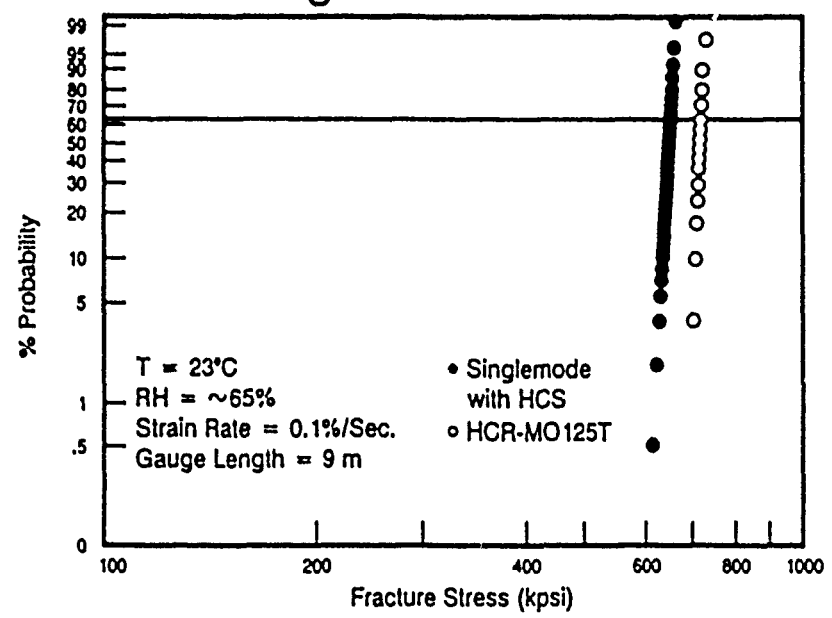

Figure 4

Static Fatigue Resistance: Zero Stress Aging

- ● HCS on Singlemode
- ○ HCS on Singlemode Zero Stress Aging - 24 Hr. in Boiling Water
- ■ Conventional Singlemode
- □ Conventional Singlemode Zero Stress Aging - 24 Hr. in Boiling Water

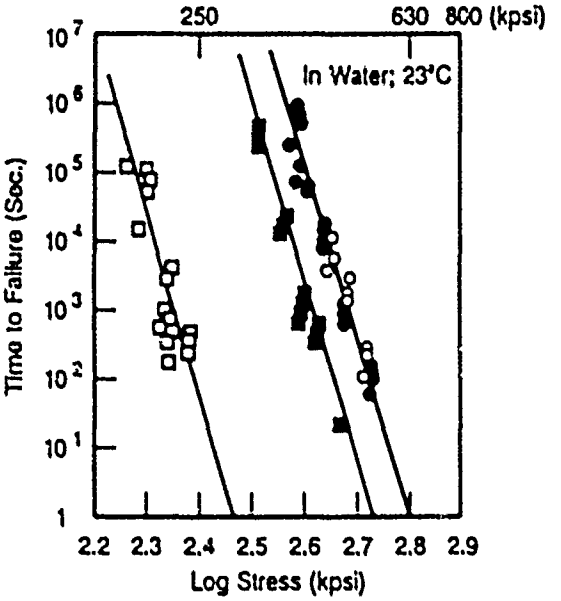

Figure 5

AN OVERVIEW OF THE DEVELOPMENT OF A NEW GENERATION OF AEROSPACE WIRE AND CABLE INSULATION SYSTEMS

Richard E. Hawkins

Champlain Cable Corporation
Winooski, Vermont

ABSTRACT

Recent publicity highlighting potential problems with Kapton[1] and other polyimide based insulations has created a need for an improved insulation system to take its place.

This paper endeavors to provide background about the concerns and a summary of efforts currently taking place to create hybrid insulations providing the superior mechanical durability of polyimide insulations with the arc track and environmental performance of fluorocarbon insulations.

INTRODUCTION

Polyimide based insulations as described in MIL W 81381 and similar specifications have been in use since the mid 1960s. These high performance insulations have been used extensively in aerospace applications because their excellent thermal, mechanical and dielectric properties allow space and weight savings over other insulation systems offering comparable performance. Over the years polyimide based insulation systems have been used extensively in most major military and commercial aircraft programs.

The usual construction technique for these insulations involves wrapping a polyimide film around the conductor in two or more layers. Because polyimide is a thermoset material the film is coated with a thin layer of FEP, a thermoplastic fluoropolymer, which acts as a heat sealable adhesive to bond the layers together and form a continuous insulation.

The basic cause for concern has come from an unusual phenomenon called carbon arc tracking, whereby a damaged bundle of polyimide insulated wires stressed with an overload current can form a conductive carbon path in the insulation and cause a short circuit. While a great deal of disagreement still exists as to whether arc tracking is a real world problem, the fact remains that the Navy and Marines have banned polyimide insulated wire or cable for new aircraft construction including the F-14, F-18 and the AV-8B. The Air Force has taken a more moderate position by allowing polyimide on current programs including the F-15 and F-16 but new programs may only use polyimide insulations where specifically justified.

Currently the only reasonable alternative to polyimide based insulations is cross-linked Tefzel[1] (XL-ETFE) as described in MIL W 22759/32-35,41-46 and related specifications. XL-ETFE is acknowledged to have advantages over polyimide in arc track resistance, handling and resistance to some fluids but the high temperature properties of XL-ETFE may be too marginal to be a direct replacement for polyimide even though both are rated at 200°C. Since, however, XL-ETFE is the closest in size, weight and performance that has military approval it is being used in all new Navy aircraft and is the only realistic candidate for other military aircraft forced away from polyimide based insulations.

Because of the gap in performance between these insulations it quickly became apparent that a new insulation design offering an improved balance of performance would be highly desirable. To date, hybrid insulation systems have been considered the most practical approach to this development since a breakthrough in material chemistry is believed to be necessary to produce a single material insulation capable of the necessary performance.

Hybrid insulation systems are not a new idea. There are composites or hybrids specified in MIL W 22759, 25038, 81044, and large gauge 81381. What is new about the combinations currently being evaluated are the specific materials and insulation thicknesses along with the performance gains being sought.

DESIGN GOAL - IMPROVED BALANCE OF PROPERTIES

A combination of efforts by airframe manufacturers, material manufacturers and wire processors have generated several candidate insulation systems likely to yield a more ideal balance of performance. These constructions generally consist of multiple layers of polyimide film and fluoroplastics like PFA, TFE or XL-ETFE. They are intended to combine the best properties of the polyimide with the arc track resistance and other advantages of the fluoropolymers.

The common goal for all development programs is to eliminate the potential of carbon arc tracking. Secondary goals include performance improvements in the following areas:

* environmental - forced hydrolysis
* environmental - UV resistance
* stiffness/springback
* topcoat chipping and peeling

Areas of improvement over the following XL-ETFE performance areas are being sought in:

* weight
* diameter
* elevated temperature performance
  - cut through
  - deformation

The insulation systems under development generally consist of multiple layers of polyimide film and fluoropolymers such as PFA, TFE or XL-ETFE. The approaches being taken are varied and the resulting insulations yield somewhat different handling and performance characteristics. All of the insulations currently being evaluated at this time, however, are substantially more arc track resistant than MIL W 81381 type polyimide insulations and offer improved durability over XL-ETFE insulations.

It has been found that an insulation containing polyimide can be as arc track resistant as an all fluorocarbon insulation if it contains the correct percentage of fluorocarbon. The type of fluorocarbon used in an insulation combined with the relative thickness and placement of the layers can also affect its arc track resistance. It is generally theorized that the fluorocarbon layer(s) tend to quench an arc in the polyimide. Fluoropolymers such as FEP or non cross-linked ETFE are considered less desirable because they are more apt to melt during the process of arcing thus exposing more polyimide as fuel for the arc tracking.

While the inclusion of a polyimide layer will tend to increase insulation stiffness it greatly increases mechanical toughness. Dynamic cut through resistance is significantly improved throughout the rated temperature range of the wire. The relative placement of this layer can affect the performance of a particular insulation design however as a group the polyimide/fluorocarbon hybrid insulations are several times more cut through resistant at 150 and 200°C than equivalent XL-ETFE insulations. To add perspective to this level of performance these hybrids generate approximately 50-75% of the cut through resistance of the very tough MIL W 81381 polyimide insulations throughout the rated temperature range.

CURRENT DEVELOPMENT PROGRAMS

There are several activities currently underway whose purpose it is to define more ideal insulation systems for aircraft applications. They include the following.

NEMA Task Force

This group is a subcommittee of the High Temperature Insulations Committee of the National Electrical Manufacturers Association. Its membership includes wire and cable producers as well as material manufacturers. The purpose of the NEMA task force is to design and test new constructions and write military specifications for the best insulation candidate(s). Only materials used in current military specifications are being considered because their known thermal aging and other long term performance characteristics will make them more acceptable in the short term. The group's activities are sanctioned by the Air Force who recognizes an immediate need for an alternative.

During the design phase several candidate constructions were generated. These were then reduced to three on the basis of reproducability in manufacture and overall anticipated performance. Two of the insulations are two layer polyimide/fluorocarbon constructions (Figure 1). The third insulation system is a three layer fluorocarbon/polyimide/fluorocarbon construction (Figure 2).

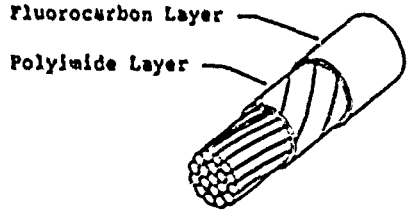

Figure 1 - Polyimide/Fluorocarbon Insulation

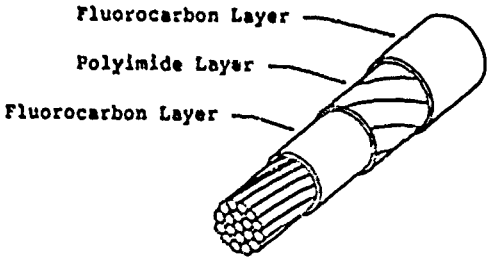

Figure 2 - Fluorocarbon/Polyimide/Fluorocarbon Insulation

The three candidates, as well as baseline samples of MIL W 81381 (polyimide) and MIL W 22759 (cross-linked ETFE), were produced by at least two participants and entered into a five laboratory round robin test program.

The evaluation will be performed on thin and medium wall thickness versions of each design.

Tests involving critical performance areas included:

* Diameter
* Weight
* Wall Thickness and Concentricity
* Dry Arc Resistance
* Insulation Shrinkage
* Abrasion Resistance
* Cold Bend
* Dynamic Cut Through
* Notch Propagation
* Stiffness and Springback
* Heat Aging
* Cross-link Proof

At the time of the writing of this paper the round robin testing was not yet completed. It is anticipated that the participants will have finished their round robin testing and reported the test results to the Air Force by the time it is published.

The testing done in this program will be particularly important because it is the first time this type of hybrid insulation system will have had the benefit of round robin testing. Single lab bias will be eliminated and the credibility of the resulting test data will be enhanced.

Lockheed Test Program

Several months ago Lockheed ran a test program to evaluate hybrid insulation samples of various designs from several manufacturers. Arc track resistance and the ability to pass a stringent hot air impingement test were key. For this phase of the program the dry arc track testing was performed on a qualitative basis. From the initial round they selected the following design (Figure 3):

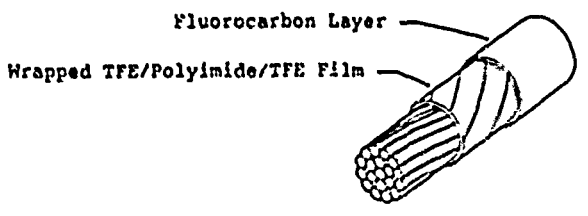

Figure 3 - TFE/Polyimide Film + Fluorocarbon Insulation

To test the reproducability of the the design and its performance Lockheed asked all of the participating processors to manufacture the selected design. A second round of testing is under way to evaluate the repeatability of the results. In this case dry arc track testing is being performed on a quantitative basis. The relative arc track resistance of an insulation system will be given strong consideration in the design optimization process.

Air Force Test Program

The Air Force has appropriated $750,000 to fund a comprehensive airframe wire and cable test program. McDonnell Aircraft was selected from several candidates to run the extensive analysis. The program will test ten of the most promising hybrid constructions against XL-ETFE and polyimide baseline insulations over a period of twenty months.

Constructions were selected for testing from candidates presented at an insulators conference held at McDonnell Aircraft in February of this year. Participants included Champlain Cable, Marcel, Brand Rex, DuPont, Gore, Independent, NEMA, Teledyne Thermatics and Tensolite. Champlain was fortunate enough to have a candidate selected. We also produced one of the two NEMA candidate insulations selected for the test program.

Most of the selected constructions are similar to those illustrated for the NEMA and Lockheed programs. Additionally two newly developed materials will participate in the evaluation. The first is a high strength, crush resistant TFE insulation. The second new material is a polyimide insulation whose chemistry has been modified to be arc track resistant.

As in the NEMA program thin and medium wall thickness versions of each design will be evaluated. Additionally, cables manufactured with the thin wall version of these constructions will be tested. MIL W 81381 and 22759 wire as well as related cables are also included to provide baseline performance information.

This evaluation will take place in two stages. The first stage will include a battery of screening tests to narrow the field of new constructions from ten to four. These tests are expected include most of those present in the NEMA program and may include additional tests such as flex life, flammability, toxicity and fluid immersion.

The second stage will compare the final four candidates against the baseline constructions in a much more exhaustive battery of tests.

In addition to the tests carried out in the screening portion of the program the following tests are among those planned:

* Thermal Index
* Corona Inception and Extinction
* Surface Resistance
* Time/Current to Smoke
* Wet Arc Tracking
* Hydrolysis
* Humidity Resistance
* Propellent Resistance
* Impact and Crush Resistance
* Wire Surface Markability

Prior to the initiation of the testing McDonnell Aircraft and the Air Force are working to define and justify minimum performance criteria for each of the tests.

They are also developing a comprehensive system of ranking the insulation candidates based upon the relative importance of each performance attribute.

Because of the stature of this test program and because it seems to include the best efforts of other programs it may overshadow the Lockheed and NEMA efforts. It is getting considerable attention and the results will probably be instrumental in the determination of the next generation of military aerospace wiring.

CONCLUSION

The ground rules for designing aircraft wiring insulation systems are evolving. More and more critical performance areas are being identified which are changing the balance of properties required for today's wire and cable. Significant design and test efforts by wire and cable producers as well as the Air Force, McDonnell Douglas, Lockheed and others are aimed at developing the next generation of aircraft wire. The leading contenders are arc track resistant hybrid insulations combining layers of fluoropolymer and polyimide as well as a newly developed chemically modified arc track resistant polyimide.

REFERENCES

[1] Reg. Trademark of E. I. DuPont

Richard E. Hawkins
Champlain Cable Corp.
P.O. Box 7
Winooski, VT 05404

Richard Hawkins is the Advanced Applications Engineering manager at Champlain Cable Corp. in Winooski, VT. He has worked in the wire industry for 15 years, 12 of which have been with Champlain Cable in various manufacturing management and engineering positions. He is a 1971 graduate of Northeastern University with a degree in Industrial Engineering.

SINGLE AND MULTIMODE TACTICAL CABLE ASSEMBLIES

B. V. Darden, K. Kathiresan, B. G. LeFevre
AT&T Bell Laboratories, Norcross, GA 30071

J. B. Fluevog
AT&T Network Systems, Norcross, GA 30071

V. E. Kalomiris
U. S. Army CECOM, Ft. Monmouth, NJ 07703-5202

ABSTRACT

The design and development of tactical duplex fiber optic cable assemblies, for both multimode and single-mode systems operations, have been completed. Development effort was guided by detailed design criteria supplied by the contracting organization, the U. S. Army CECOM. A completed cable assembly consists of a 1-km cable containing two tightly buffered multimode or single-mode fibers terminated with duplex, hermaphroditic connectors. A radiation-hardened multimode fiber was developed for optimal operation at the 1300 nm wavelength region. The Single-mode fiber is a standard depressed-clad design. Both cable assemblies are identical except for the fiber, increased precision of the biconic components for single-mode, sleeve retainer, and dust-cover and end cap colors. The cable has a 8-mm O.D. and a 1780-newton tensile rating. The connector, whether multimode or single-mode, is less than 4 cm. in diameter and a mated pair weights less than 600 grams, including dust covers. Both cable assemblies are rated for operation at temperatures ranging from -55 °C to 85 °C.

INTRODUCTION

The development of multimode and single-mode duplex cable assemblies for use in severe tactical field environments has been completed. Multimode assemblies, known as Tactical Fiber Optic Cable Assemblies (TFOCA) will be used in the Fiber Optic Transmission System-Long Haul (FOTS-LH) program. Single-mode assemblies are being used in the Single-Mode Fiber Optic Communications System (SIMFOCS). Technical guidance and funding were provided by the U. S. Army Communications- Electronics Command (CECOM) and the U. S. Air Force. Each cable assembly was designed to meet stringent specifications imposed by the contracting agency. A completed cable assembly consists of a 1-km cable containing two tightly buffered multimode or single-mode fibers terminated with duplex, hermaphroditic connectors. A radiation-hard multimode fiber was developed for optimal operation at the 1300 nm wavelength region. The single-mode fiber is a standard depressed-clad design. Both all-dielectric cable designs are identical except for the fiber. The cable has a 8-mm O.D. and a 1780-newton tensile rating. The connector, whether multimode or single-mode, is less than 4 cm in diameter and a mated pair weighs less than 600 grams, including dust covers. Both cable assemblies are rated and tested for operation at temperatures ranging from -55 °C to 85 °C.

CABLE ASSEMBLY DESIGN

The cable assemblies were designed to meet stringent environmental and mechanical test requirements (given in Table I) specified by the contracting agency. Both cable assembly designs are similar except for the fiber and some design improvements for single-mode connectors. TFOCA uses a 50/125 μm radiation-hardened multimode fiber and the SIMFOCS assembly uses standard depressed-cladding single-mode fiber.[1] [2] These assemblies are designed for use in tactical environments. While the primary operational wavelength for both assemblies is the 1300 nm region, TFOCA assemblies can be operated at 850 nm and 1300 nm, and SIMFOCS assemblies at 1310 nm and 1550 nm wavelengths. [3] [4] For both applications, the fibers were proof tested to 690 MPa (100 ksi). A completed cable assembly is illustrated in Figure 1. A cross-sectional view of the cable and an illustration of the connector are given in Figures 2 and 3, respectively.

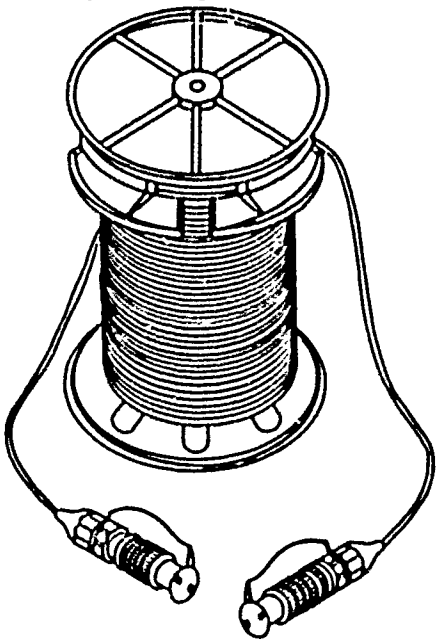

Figure 1. Tactical Cable Assembly

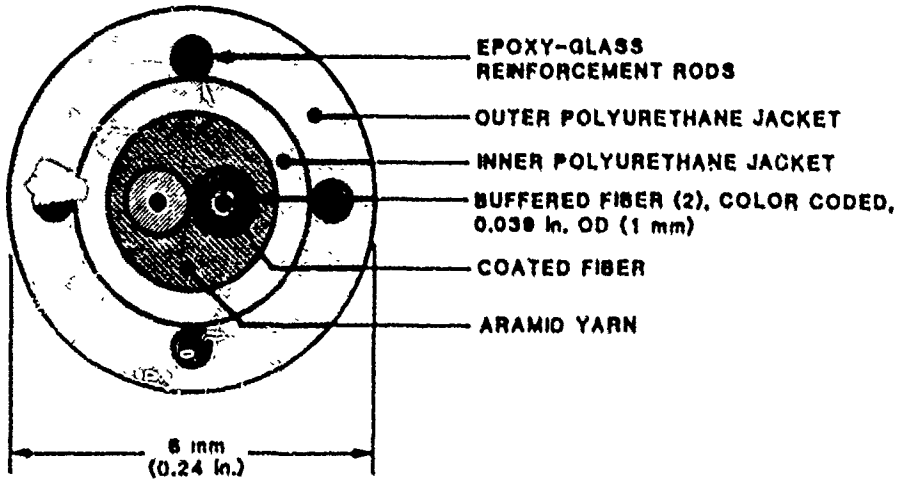

Figure 2. Tactical Cable Cross Section

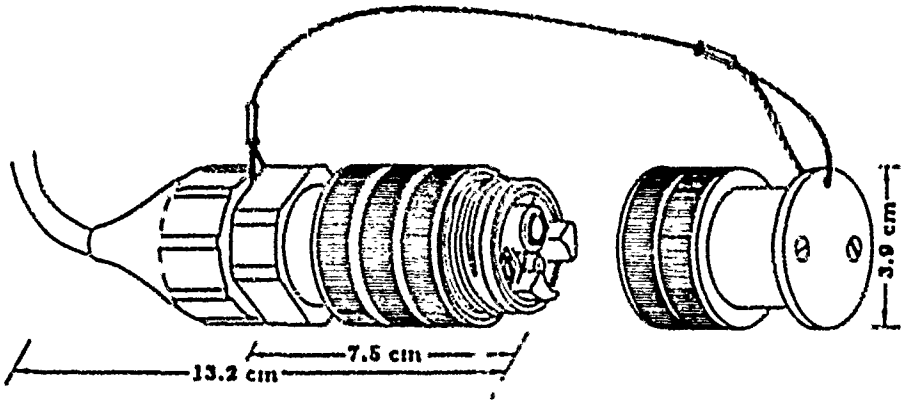

Figure 3. Tactical Connector

TABLE I. LIST OF TESTS FOR ASSEMBLY

- ATTENUATION
- TEMPERATURE CYCLING
- HUMIDITY
- STORAGE/TRANSIT
- ALTITUDE
- SALT FOG
- WATER IMMERSION
- TENSILE STRENGTH
- FUNGUS
- VIBRATION
- SHOCK

OPTICAL FIBER

The multimode fiber developed for TFOCA is a conventional graded-index design, modified for radiation hardness. The nominal characteristics of the fiber are as follows:

Fiber outer diameter:	125 μm
Core diameter:	50 μm
Numerical aperture:	0.23
Attenuation at 850 nm:	$\leq$ 2.8 dB/km
at 1300 nm:	$\leq$ 0.8 dB/km
Bandwidth 1300 nm:	$\geq$ 400 MHz-km
Proof test level:	100 ksi

The radiation-hardened fiber meets the specification for operation under the environmental conditions required for the Fiber Optic Transmission System-Long Haul Program. The multimode assemblies were tested at both 850 nm and 1320 nm wavelengths.

The single-mode fiber used in the SIMFOCS cable assembly is a standard depressed-cladding design which has been shown to have exceptional microbending and macrobending performance. For this application, the fibers were proof tested to 690 MPa (100 ksi). Tests were conducted and the results are presented only at 1310 nm wavelength.

Both multimode and single-mode fiber are coated with dual acrylate coatings which are mechanically strippable. These fibers are then tight-buffered to a 1.0 mm (.039 inch) diameter with a polyester elastomer. The buffering material is also mechanically strippable in order to facilitate termination and repair in the field. The buffering material was chosen to minimize microbending losses induced by exposure of the cable to temperature extremes required by the design criteria.

Fiber Performance

All the fibers were tested for their optical and dimensional requirements before being used in the cable. These tests listed in Table II, include attenuation, attenuation uniformity, cut-off wavelength, mode-field radius, clad and coating diameters, core eccentricity, etc. Though not required under the development program, the fibers were tested for response to environmental temperature cycling. The temperature cycle used was:

- baseline the loss measurements through multiple measurements at room temperature, 25°C,
- reduce the temperature to -40°C and dwell at least 24 hours before measurement,
- reduce the temperature to -55°C and dwell at least 12 hours before measurement,
- return to room temperature, 25°C, and dwell at least 12 hours before measurement,
- increase the temperature to 71°C and dwell at least 12 hours before measurement,
- increase the temperature to 85°C and dwell at least 24 hours before measurement,
- return to room temperature, 25°C, and dwell at least 12 hours before measurement.

TABLE II. LIST OF TESTS FOR FIBER

- ATTENUATION
- BANDWIDTH
- FIBER PROOF STRENGTH
- CORE/MODE-FIELD DIAMETER
- CUT-OFF WAVELENGTH
- CORE-CLADDING INDEX DIFFERENCE
- CORE ECCENTRICITY
- CORE OVALITY
- CLADDING OUTER DIAMETER
- COATING OUTER DIAMETER
- TEMPERATURE CYCLING

The contracts required that the assemblies and components be subjected to three temperature cycles described above. Instead, the samples were subjected to five temperature cycles. The design requirement of temperature extremes is from -40°C to 71°C. The temperature range was extended to -55°C and 85°C to investigate the performance at more stringent temperatures. The performance of the single-mode fibers for the temperature cycles is presented in Figure 4. The fibers show excellent performance with a maximum added loss of 0.05 dB/km.

Buffered Fiber Performance

Requirements for buffered fibers included dimensional requirements on the outer diameter and concentricity of the fiber. Every buffered fiber used in the cables was screened for these dimensional requirements. Though not required, the buffered fibers were also tested for response to temperature cycling. The results of this test, which uses the same cycle described in the fiber section, are given in Figure 5. The buffered fibers were also subjected to an accelerated-aging test which simulates the use of this buffered fiber (and the cable in general) at 85°C for the design life of 30 years. The accelerated aging test consists of exposure of the materials to 110°C for 10 days. This time-temperature relationship was arrived at by using viscoelastic principles. The excellent accelerated-aging performance of the buffered fibers is illustrated in Figure 6. After the completion of the accelerated-aging test, further testing was continued with temperature cycling between -75°C and 100°C. The results of this temperature cycling are also presented in Figure 6 and again show the excellent performance of the buffered fibers.

CABLE DESIGN

The cable structure provides a range of physical characteristics required for tactical deployment while maintaining the optical performance detailed above. Optical, mechanical, and environmental cable test requirements are listed in Table III.

The cable design is all-dielectric, 6 mm in diameter, and weighs about 32 kg/km. It has a 1780-Newton tensile load rating. The design evolved through a program of prototyping and testing in which key parameters were varied in order to meet or surpass the requirements.

The cable construction consists of two fibers, either radiation-hardened multimode or single-mode, buffered to a diameter of 1.0 mm as shown in Figure 2. The buffering material is a polyester elastomer and is color coded for fiber identification purposes. Two fibers are stranded together, forming the center core of the cable. Around the two fibers, two layers of aramid yarn are applied with opposite lay directions. The jacket is formed directly over the yarn from two extrusions of polyurethane with four embedded epoxy-glass rods. The final cable diameter is 6.0 mm.

Cable Performance

The multimode cable was designed to operate over the range -40°C to 71°C with less than 0.5 dB/km increase in attenuation at either 850 or 1300 nm. This performance of the cable over the required temperature range using the temperature cycle previously described is shown in Figure 7. As the figure shows, the cable not

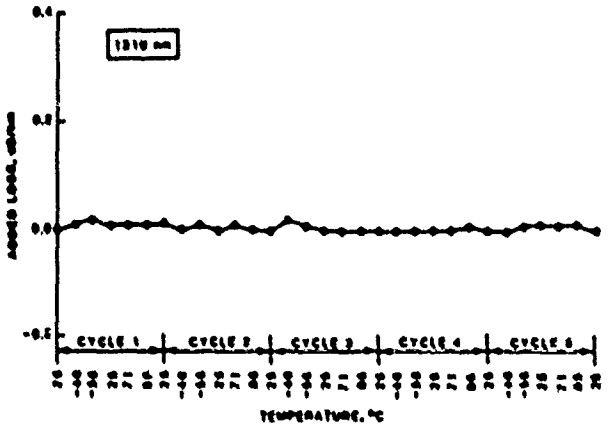

Figure 4. SIMFOCS Fiber Temperature Cycling Test Result

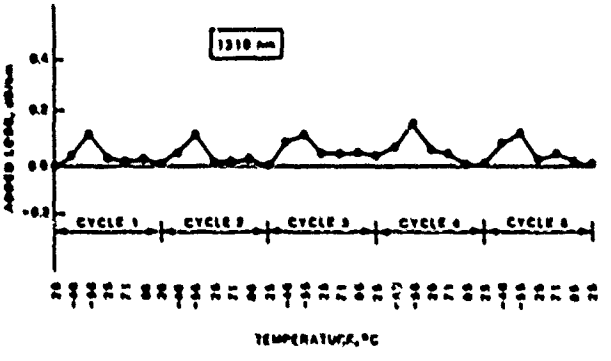

Figure 5. SIMFOCS Buffered Fiber Temperature Cycling Test Result

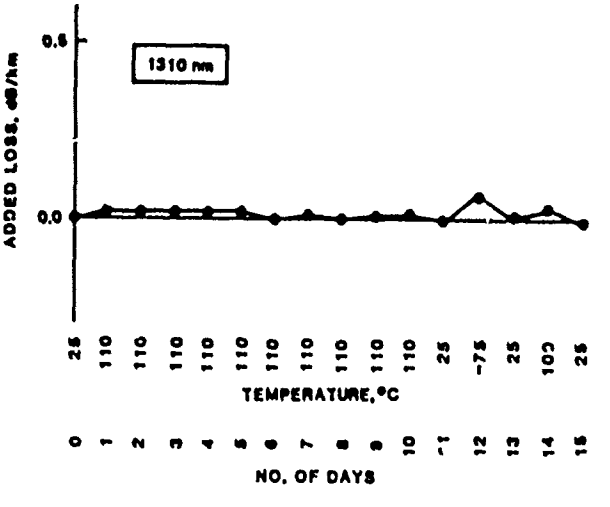

Figure 6. SIMFOCS Buffered Fiber Accelerated Aging Test Result

TABLE III. LIST OF TESTS FOR CABLE

- ATTENUATION
- ALL-DIELECTRIC
- TIGHT BUFFERED
- CABLE DIAMETER
- CABLE DIAMETER
- CABLE WEIGHT
- TEMPERATURE CYCLING
- LONG TERM AGING
- FLAMMABILITY
- RADIANT HEAT
- OPERATING TENSILE LOADING
- TENSILE STRENGTH
- COLD BEND
- IMPACT
- KNOT
- COMPRESSION
- CYCLIC FLEXING
- TWIST BEND
- FREEZING WATER IMMERSION
- CORNER BEND

only performs for the required -46 °C to 71 °C range, but also for the extended range of -55 °C to 85 °C.

Single-mode cables, as a component of the SIMFOCS assembly, were also subjected to a battery of optical, environmental, and mechanical tests. The mean optical loss was 0.4 dB/km at 1310 nm, showing that there was basically no added loss due to the buffering and cabling processes for these cables. The cable was designed for a temperature range of -46 °C to 71 °C, and the evaluation was extended to -55 °C and 85 °C as mentioned before. The results of temperature cycling of three samples of 1-km lengths are presented in Figure 8. The cables pass the requirement of 0.3 dB/km maximum added loss for three temperature cycles between -46 °C and 71 °C. The cable also passes the requirement for five temperature cycles between -55 °C and 85 °C. The maximum of mean added loss was at -55 °C and was less than 0.15 dB/km. As a comparison, the multimode TFOCA cable had an added mean loss of less than 0.2 dB/km as opposed to the requirement of 0.5 dB/km between -55 °C and 85 °C. This establishes that the basic cable design is applicable for both multimode and single-mode fibers.

The results of accelerated aging testing of three 0.5 km lengths of single-mode cables are presented in Figure 9. This figure, again, shows excellent performance of the cable not only for the accelerated aging test, but also for the unrequired temperature cycling between -75 °C and 100 °C. The temperature cycling between -75 °C and 100 °C was added to this aging test just to study the performance beyond the cable's design limits.

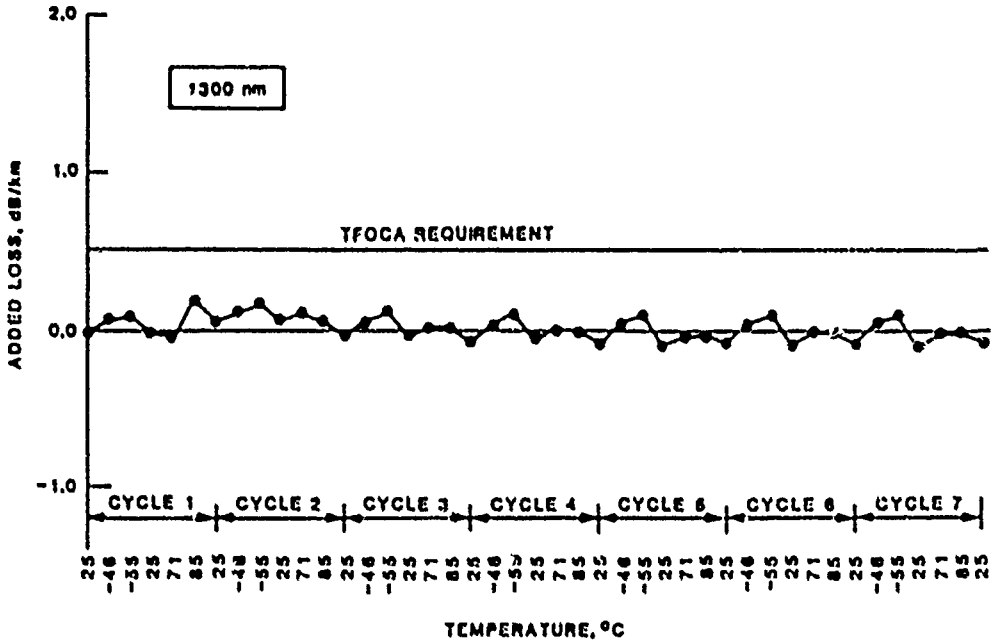

Figure 7. TFOCA Cable Temperature Cycling Test Result

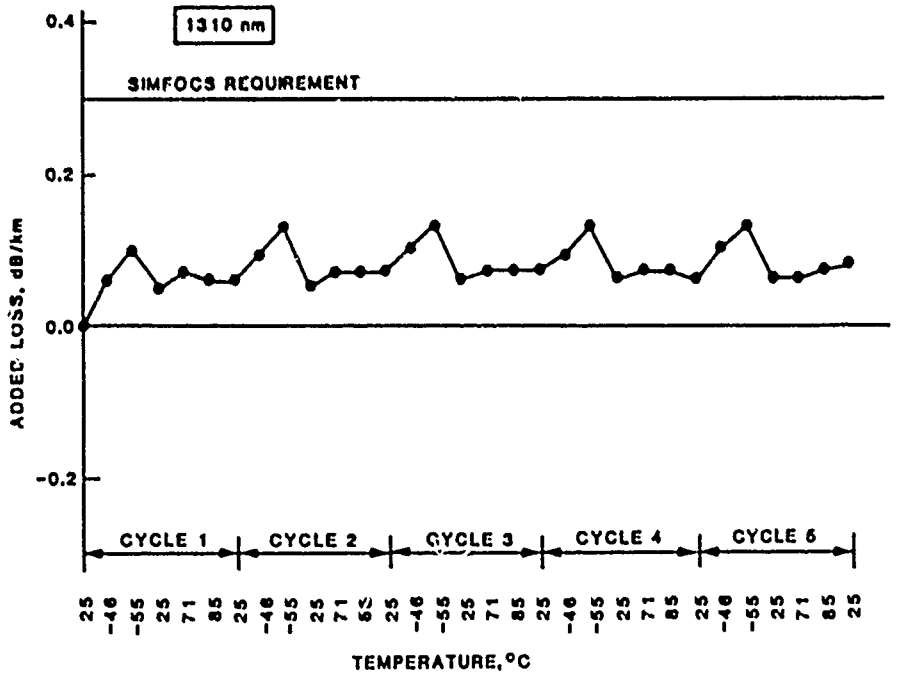

Figure 8. SIMFOCS Cable Temperature Cycling Test Result

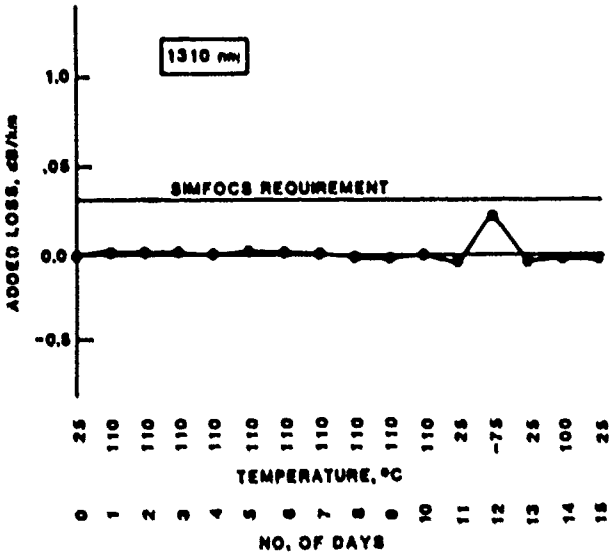

Figure 9. SIMFOCS Cable Accelerated Aging Test Result

The multimode and single-mode cables were also subjected to an extensive list of mechanical tests. Results of the mechanical tests can be found in References 3 and 4.

DUPLEX CONNECTOR DESIGN

The tactical connector is a hermaphroditic duplex embodiment of AT&T's biconic connector. Large-scale manufacture and installation of the biconic connector in several simplex configurations began in 1979. Since then it has been used to join about three million cable ends. Many connectors have been in stable continuous operation with consistent performance since 1979 in a variety of environmental circumstances.

In the duplex-configured connector,[5] one of the two fiber channels terminates with a biconic alignment sleeve and the other with a plug. The connector is rugged, waterproof, and resistant to the stringent environment typical of tactical military applications. It meets the mechanical and environmental requirements supplied by the U. S. Army CECOM in the contractual statements of work. The requirements are listed in Table IV.

The connector, shown in Figure 3, is less than 4 cm. in diameter, and a mated pair weighs under 600 grams, including dust covers. A companion bulkhead receptacle, EMI-rated for frequencies from 10 kHz to 12 GHz, was developed for the system and shares a common hermaphroditic interface. Hence, any cable end will mate with any other or with a receptacle. Geometric alignment and orientation features on the front face preclude mismating connectors, provide a hermaphroditic profile, and protect the biconic components during impact.

The connector is joined to a cable by capturing the aramid yarn used in cables with a special steel retention assembly easily put together without special tools. No adhesive is used in the cable termination operation. At final connector assembly, the cable-retainer is sandwiched between the connector shell and end cap. Thus, any subsequent cable tension is transferred to the metal shell.

A metal shell encloses the fiber termini assembly. It also provides storage space for slack fiber and retains the cable-termination hardware. A free-turning, threaded coupling nut tightens the joint between two connectors or between a connector and receptacle. The connector shell and coupling nut are designed to elastically withstand 400-pounds tension across a connection.

All possible water leak paths into the connector are blocked by elastomeric seals, and a hermaphroditic dust cover prevents water or dust entry into an unmated connector.

Cleanliness is essential to a repeatable low-loss lightguide connection, and a significant attribute of the duplex connector is that it is easy to clean. After soaking an uncovered connector in mud, it is necessary merely to rinse it in a pail of water and to wipe the biconic components dry in order to restore unaffected optical transmission. No special cleaning kit is required.

A dust cover is provided to prevent water or dust entry into an unmated connector. The cover is also hermaphroditic so that when two connectors are mated, their respective dust covers can be similarly mated to prevent contamination. A lanyard prevents inadvertent separation of the connector and cover. All outer metal components of the connector and receptacle are either die-cast or wrought aluminum with an olive drab cadmium finish for appearance and corrosion resistance.

TABLE IV. LIST OF TESTS FOR CONNECTOR

- ATTENUATION
- SIZE
- WEIGHT
- HIGH TEMPERATURE
- LOW TEMPERATURE
- THERMAL SHOCK
- CROSSTALK
- HUMIDITY
- ROTATION
- SHOCK DROP
- SHOCK
- VIBRATION
- MATING DURABILITY
- SALT FOG
- WATER IMMERSION
- DUST
- CABLE RETENSION
- FLEX LIFE
- TWIST
- MUD

The dust-cover shell and end cap of the SIMFOCS unit are yellow to visually distinguish it from the all-olive drab TFOCA connector. The single-mode front face differs intentionally from the corresponding TFOCA part to mechanically prevent the inadvertent mating of single-mode and multimode connectors. Another crucial but somewhat imperceptible difference between the designs is the increased precision of the biconic components required for the single-mode application.

Except for the sleeve retainer and the two yellow parts mentioned above, all hardware is common between the TFOCA and SIMFOCS designs.

Connector Performance

The primary design objectives of the duplex connector are low coupling loss and field ruggedness. The unit is required to remain optically and mechanically functional under environmental and mechanical exposures typical of tactical field applications. Tests were conducted to evaluate performance with respect to the requirements listed in Table IV. Some of the tests are reviewed and the results summarized in the following paragraphs.

Multimode Coupling Loss

Coupling-loss measurements were made by concatenating pairs of plug terminated 1-km cables randomly selected from a group of 24. The coupling loss was derived by subtracting the cabled-fiber attenuation from that of the measured assembly. For 32 couplings (64 channels) the mean loss and standard deviation were 0.66 dB and 0.19 dB, respectively.

Single-mode Coupling Loss

Using the same technique as for multimode, for 60 couplings (120 channels) the mean loss and standard deviation were 0.67 dB and 0.24 dB, respectively, as shown in Figure 10.

Connector-loss measurements were also made using the cut-and-insert method per EIA Fiber Optic Test Procedure No. 34 on four 12-m long cables. Average loss was 0.55 dB with standard deviation of 0.11 dB.

Single-Mode Mating Durability

This test was conducted to determine the mechanical durability of the connector assemblies as a result of 1000 coupling cycles. The failure criteria includes visible physical damage as well as optical malfunction. Loss readings were made at increments of 50 matings. At the conclusion of the test, the loss in each channel was within 0.09 dB of the initial baseline readings. The maximum loss increase observed during the test was 0.24 dB. The connectors were cleaned once after 750 matings.

Single-Mode Mud Immersion

The connector was designed to allow quick access to the biconic components so they can be easily cleaned after mud immersion. This aspect of the design was evaluated by subjecting a connector pair to 10 cycles of the following sequence:

a. decouple and immerse each end in a mud bath for 5 minutes

b. water rinse, wipe clean, and air dry

c. recouple and measure loss

The maximum observed loss change was 0.13 dB.

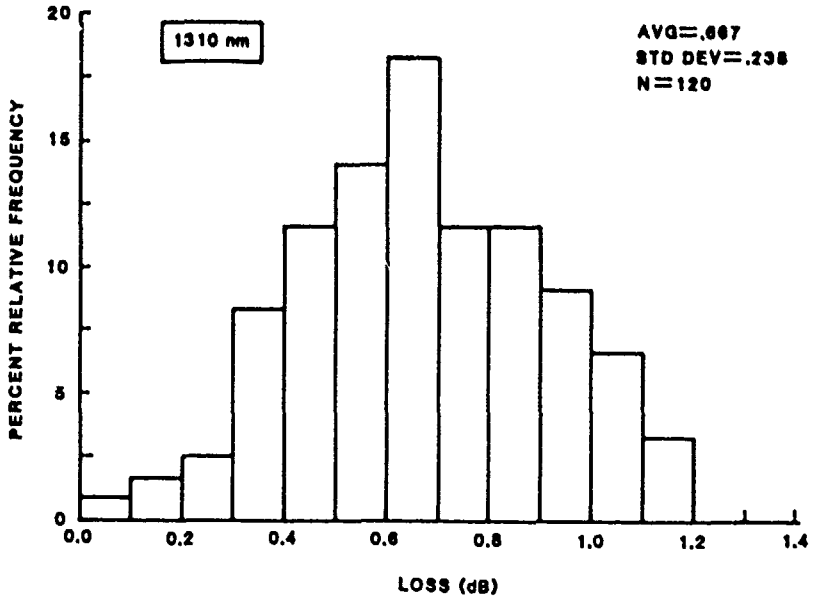

Figure 10. SIMFOCS Connector Coupling Loss

CABLE ASSEMBLY PERFORMANCE

The 1-km long cable assemblies, including connectors, are required to be subjected to a battery of environmental and mechanical tests to insure reliable performance in the tactical field environment. Table I lists the tests. Some of the results are summarized below.

Attenuation

Attenuation measurements by concatenation of TFOCA and SIMFOCS assemblies were made and the results are presented in Figures 11 and 12.

TFOCA - Pairs of 1-km cables were randomly selected and concatenated. For 72 bidirectional couplings (144 channels) the mean loss and standard deviation at 1300 nm wavelength were 1.35 dB and 0.33 dB, respectively, as shown in Figure 11.

SIMFOCS - Pairs of 1-km cables were randomly selected from a group of 16 and concatenated. Figure 12 shows that for 64 couplings (128 channels) the mean loss and standard deviation at 1310 nm wavelength were 1.08 dB and 0.23 dB, respectively.

For comparative purposes, design transmission loss targets were 2.8 dB for multimode and 1.4 dB for single-mode cable assemblies.

SIMFOCS Storage and Transit Temperature

The cable assembly was exposed to temperature extremes from -55°C to 85°C to determine whether adverse effects would result from storage and transit environments. Maximum loss increase observed was 0.09 dB.

Immersion

The TFOCA and SIMFOCS cable assemblies were immersed in a tank with one meter of water covering the units for 120 hours, and no leakage was observed.

CONCLUSIONS

The duplex tactical cable assemblies described herein meet the requirements prescribed by the project sponsor, the U. S. Army CECOM. At the 1300 nm wavelength region, average cable assembly loss of 1.35 dB and 1.08 dB for multimode and single-mode, respectively, are well below the transmission loss targets. Low-loss fiber, cable, and connector designs have been integrated successfully into the assemblies.

By designing the basic cable assembly to accommodate both types of fiber, 50/125 μm multimode and single-mode, considerable development time and expense was conserved.

ACKNOWLEDGEMENTS

The authors gratefully acknowledge the support and contributions of several members of AT&T Bell Laboratories and AT&T Network Systems.

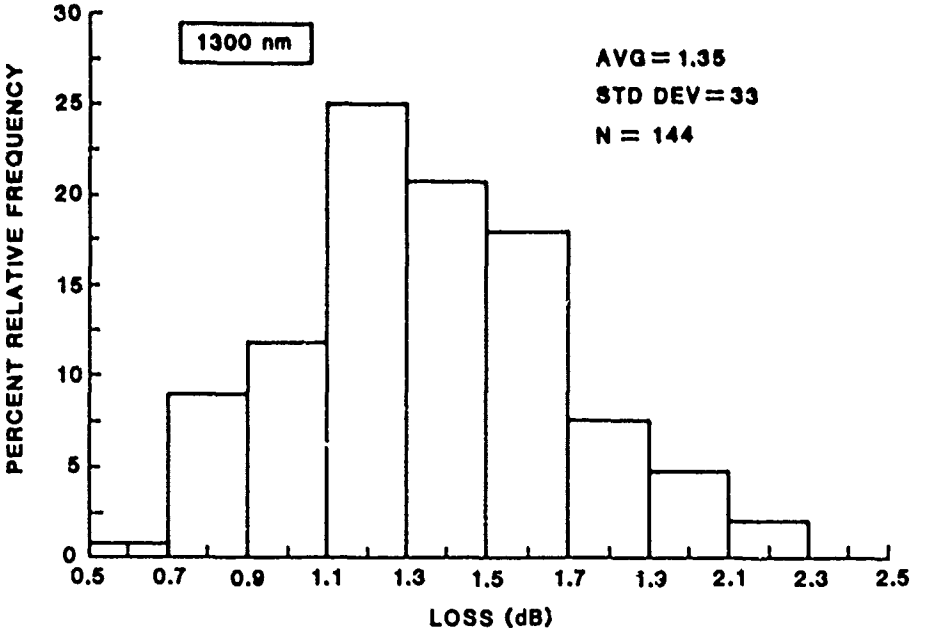

Figure 11. TFOCA Cable Assembly Attenuation

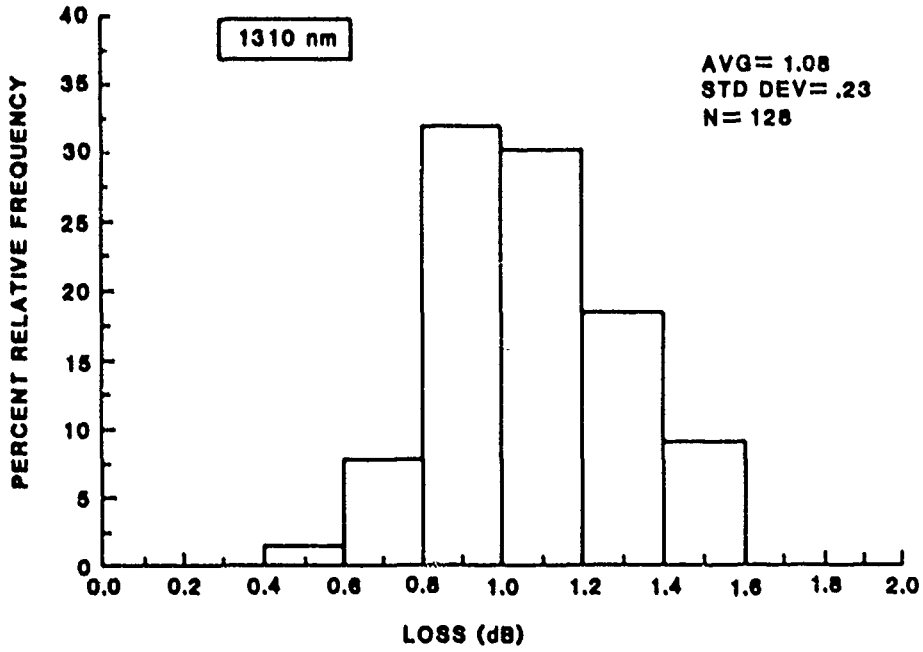

Figure 12. SIMFOCS Cable Assembly Attenuation

REFERENCES

1. "Tactical Fiber Optic Cable Assembly," U. S. Army CECOM Contract No. DAAB07-84-C-K565, August, 1984.
2. "Single-Mode Fiber Optic Communications System," U. S. Army CECOM Contract No. DAAB07-85-C-K551, September, 1985.
3. J. M. Anderson, B. V. Darden, A. C. Jenkins, B. G. LeFevre, M. R. Reynolds, A. J. Ritger, V. E. Kalomiris, "Tactical Fiber Optic Cable Assemblies," 1985 IEEE Military Communications Conference, Boston, Mass.
4. B. V. Darden, K. Kathiresan, V. E. Kalomiris, "Single-Mode Tactical Fiber Optic Cable Assemblies," International Wire and Cable Symposium Proceedings, 1987, pp.108-115.
5. J. M. Anderson, B. V. Darden, B. G. LeFevre, and V. E. Kalomiris, "A Two-Fiber Tactical Fiber-Optic Connector," International Wire and Cable Symposium Proceedings, 1985, pp. 286-292.

Bruce V. Darden is a Member of Technical Staff at AT&T Bell Laboratories, Norcross, Georgia. He received a B. S. degree in Engineering from North Carolina State University in 1951, and held engineering positions with Western Electric until 1960 when he joined AT&T Bell Laboratories. He is currently a member of the Connector System Development Group.

Kris Kathiresan is a Member of Technical Staff in the Lightguide Technology Department at AT&T Bell Laboratories in Norcross, Georgia. He is responsible for the design and development of specialty cables, including military applications.

Dr. Kathiresan joined AT&T Bell Laboratories in 1985. He has a B. E. Hons in Mechanical Engineering from University of Madras, India, an M. E. in Aerospace Engineering from Indian Institute of Science, India, and a Ph. D. in Engineering Science and Mechanics from Georgia Institute of Technology, Atlanta, Georgia.

Dr. Kathiresan is a Senior Member of American Institute of Aeronautics and Astronautics and a Member of American Society of Mechanical Engineers. He is a registered Professional Engineer (Mechanical) in States of Georgia and Florida.

Bruce G. LeFevre is a Member of Technical Staff at AT&T Bell Laboratories, Norcross, Georgia. He received his B. S. (Colorado School of Mines) and Ph. D. (University of Florida) in Physical Metallurgy. He joined AT&T Bell Laboratories in 1976 after ten years on the faculty of Georgia Institute of Technology. He has been involved in the study of metals and alloys used in the manufacture of cables and connectors, and is currently working with fiber-optic connectors.

Jill B. Fluevog is a Development Engineer in the Lightguide Cable Engineering Department at AT&T Network Systems, Norcross, Georgia. She joined AT&T in 1985 after receiving a Bachelors Degree in Chemical Engineering from Georgia Institute of Technology. She is responsible for the development of lightguide cable products and processes for military applications. Ms. Fluevog is a member of American Institute of Chemical Engineers, Institute of Electrical and Electronics Engineers and Society of Plastic Engineers.

Vasilios E. Kalomiris is currently acting branch chief for Local Area Networks and Fiber Optics at CECOM. Previously he was a project leader responsible for fiber optic cables, connectors, and fiber optic systems development. Prior to joining CECOM, he worked for ITT-EOPD as a project engineer for the air-layable fiber optic cable program. He also worked for General Cable Corp. R&D as a research engineer where he was involved with the design, development and manufacture of a prototype super-conductive power cable with flexible core.

Education : B. A. in Mathematics, B. S. in Electrical Engineering, and M. S. in Electrical Engineering, all from the New York University, and an M. B. A. from Fairleigh Dickinson University. He is a member of AFCEA, IEEE and the Technical Chamber of Greece (Society of Professional Engineers). He received the 3rd Annual Engineering Excellence Award for 1986 from CECOM; served for three years as chairman of the Tri-Service Group on fibers, cables and connectors; currently is chairing the point-to-point systems group.

Fiber Optic LAN for Military Applications

R. Hausmayer and L. A. Bergman
Jet Propulsion Laboratory
California Institute of Technology
Pasadena, California 91109

F. Halloran and J. Martinez
U. S. Army Communications Electronics-Command
Fort Monmouth, New Jersey 07703

ABSTRACT

An asynchronous high-speed fiber optic local area network is described that supports ordinary data packet traffic simultaneously with synchronous T1 voice traffic over a common FDDI token ring channel. A voice interface module was developed that parses, buffers, and resynchronizes the voice data to the packet network. The transmission medium consisted of ruggedized 50/125-μm multimode optical fiber cables and connectors. 1.3-μm optical components were used for data transmission and multiplexing.

I. INTRODUCTION

Many different protocol strategies have been proposed over the past few years for combining data, voice, video, and other forms of real-time traffic onto one local area network (LAN). These range from highly synchronous protocols dedicating isolated channels for the real-time service via TDM [1] and Wavelength Division Multiplexing (WDM) [2,3] to complex reservation bit schemes using a single common packet channel [4]. However, most real-time services, such as voice or video, require bandwidth significantly beyond the few Mbit/s capacity of most of these LANs, and furthermore, few of these protocols will provide high efficiency at higher data rates [5] should technology permit futher growth in the future. The proposed Fiber (Optic) Distributed Data Interface (FDDI) standard [6], which has a highly deterministic dual-counter-rotating token ring topology, possesses enough bandwidth to support up to 800 voice channels or perhaps 1-2 digitized video channels, and is therefore one promising candidate for real-time networks. A surrogate commercially available token ring running at 80 Mbit/s [7] was used for an initial proof-of-concept laboratory demonstration. The fiber optic components were based on 1.3-μm technology, including 50/125-μm multi-mode optical fiber, dual-fiber ruggedized connectors, and LED sources and PIN photodiode detectors. The network voice interface was designed to be compatible with standard T1 transmission channels, using private automatic branch exchange (PABX) equipment for telephone call setup and switching functions.

II. NETWORK ARCHITECTURE

A. Voice Transmission Strategy

The network voice interface module (VIM) is based on *double elastic buffering*, at both the network input and output ports. This approach is illustrated in Fig. 1, by drawing an analogy to a fire bucket brigate between two rain barrels. The input/output barrels are in turn being continuously filled/emptied, respectively, by two identical pipes. As long as the net volume of water (bits) that is passed through the system remains constant (Nri = Np = Nro), no information will be lost. Equilibrium will be guaranteed if the packet arrival rate is bounded (deterministic). Many system configurations exist that satisfy this boundary condition; for example, the buckets may be made larger and passed with less frequency, or the barrels may be made larger to tolerate greater fluctuations in load. Generally, the double elastic buffer can be configured to minimize latency or maximally smooth network load variations—but not both.

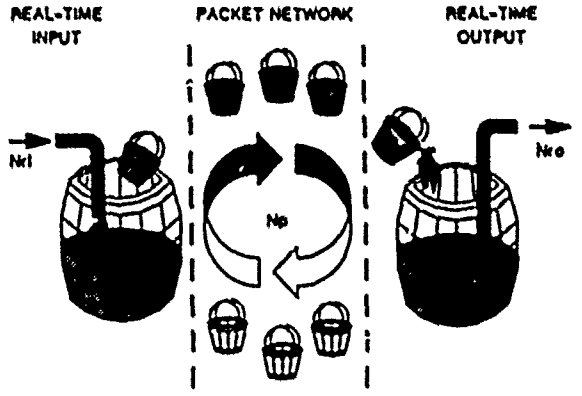

Fig. 1
Double elastic buffering for transporting real-time voice traffic across asynchronous local networks. Note that for steady state operation: Nri = Nrp = Nro.

B. Testbed Topology

The computer, PABX, and gateway stations in the network are connected in a dual-counter-rotating ring topology (Fig. 2), operating at 80 Mbit/s. Six network interface units (NIU) were configured into the testbed initially. Each of three 68020-based workstations have an NIU integrated into the computer VME backplane. The PABX's T1 interface to the network through a voice interface module (VIM) that contains an NIU and double elastic buffers described earlier. The uni-directional coax ring topology is extended to an optical fiber dual-counter-rotating ring topology by means of a media access box (MAB). In addition to fiber optic transceivers, each MAB includes an 8-port wire center and a microprocessor controller to probe the continuity of each ring and maximally configure the network. A 68010-based gateway provides

backbone service to lower speed (<20 Mbit/s) sub-nets, such as IEEE 802.3 [8] and IEEE 802.5 [9]. All fiber optic components are based on 1.3-μm technology. The fibers between each pair of stations are packaged in one militarized cable with equally ruggedized dual-fiber connectors. The one exception is one link in the ring that maintains full-duplex operation by multiplexing both ring directions into one fiber using wavelength division multiplexing at 0.8-μm and 1.3-μm.

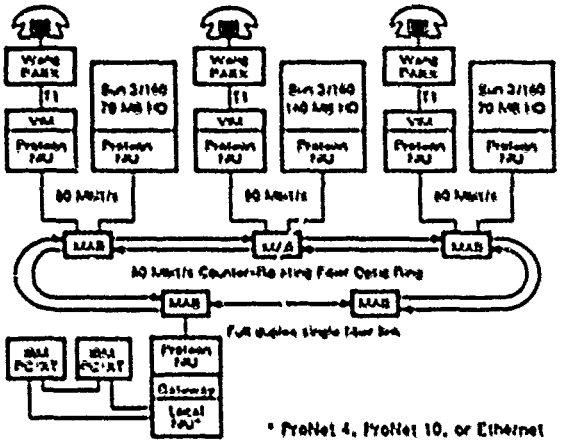

Fig. 2
Fiber optic local network testbed.

C. Network Interface Unit (NIU)

Each NIU consists of a control (CTL) and host specific board (HSB) [7,10]. The CTL board implements the networks transmission function such as repeater, address recognition, serial to parallel conversion, token management, bit stuffing and error timeout. The HSB manages all the communication processing such as buffering, sequencing and controlling. This gives the host a low software overhead. The VME interface allows the host to gather or scatter operation, and it also makes transmission of multiple packets without intervention possible. A message experiences two time delays between two nodes: a propagation delay of the transmitting medium, which for a fiber-optic link is about 5 μsec/km, and the station latency at each node. Due to the special format of the addressed message, the NIU has a station delay of 50 bits. The sum of the station latencies plus the sum of the propagation delays is called the *ring latency*. The NIU uses a 4 into 6 bit blocking coding technique to combine the clock with the data—making the effective signal rate on the fiber 120 Mbit/s. This coding scheme reduces the bandwidth compared to Manchester coding and it is still balanced over every six bits.

D. Voice Interface Module

The voice interface module (VIM) implements in physical hardware the rain barrel analogy depicted in Fig. 1. The overall process of sending voice over a high speed (80 Mb/s) packet oriented token driven fiber optics local area network represents a design challenge, because the isosynchronous nature the voice data has to be matched to the asynchronous nature of the packet data, which is subject to the availability of the token, before it can be sent to the dual counter rotating fiber optics ring. This means blocks of digital samples (μ255 or "A" law) must be accummulated and dispatched rapidly enough to maintain an average pool of data in a reservoir sufficient to supply the real time demand at the receiving site or node. The design was distributed over two custom built cards (Fig. 3), one interfacing to the digital T1 stream (FIFO/T1 card), and the other to the packet VME bus over which DMA packet transactions are conducted (Bus/Mux card). Both cards are bi-directional, to support a telephone conversation.

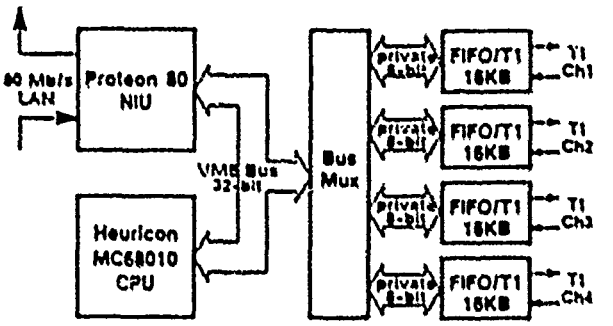

Fig. 3
Block diagram of voice interface module (VIM).

The Bus/Mux card's function is to provide the interface between the 32 bit VME bus and the 8 bit storage reservoirs (FIFOs). To do this a controller was custom built to orchestrate the data flow and latching between the 32-bit DMA transaction requests and the 8 bit FIFOs. The First In First Out (FIFO) memory in the VIM are used as elastic buffers to interface the asynchronous controlling computer system to the T1 voice data traffic.

E. Fiber Optics

The fiber optic portion of the testbed consists of the Media Access Boxes and the dual optical fiber counterclockwise rotating ring network, of which one link is to be converted into a single fiber bi-directional channel. The performance requirements of the network were a maximum transmission distance of two kilometers at a data rate of 125 Mb/s, having a BER of less than 10^{-9}.

1. *Media Access Box (MAB).* The MABs convert the digital data streams arriving from voice interface modules (VIM) and computer work stations, into optical signals to be transmitted over optical fibers. Each MAB includes a wire center [11], a fiber optic interface [12] and two dual-fiber fiber optic bulkhead connectors [13], as shown in Fig. 4.

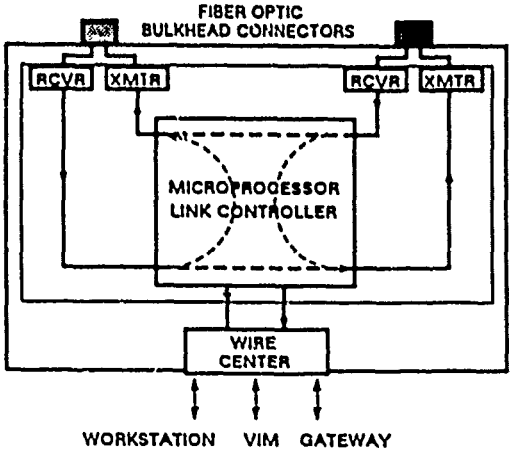

Fig. 4
Media Access Box.

The wire center is an eight-port device that connects electrically up to seven NIUs using twin shielded twisted pair cables. These may be VIMs, computer hosts, or gateways. The eighth port connects the wire center to the fiber optic ring. The wire center passes signals from one node to the next. If a port is unused, the cable breaks, or a host computer is powered down, the port is bypassed by a relay in the wire center. LED indicators, one at each port, indicate whether the specific port is in the ring or not. The fiber optic interface attaches the wire center to the fiber optic counter rotating ring network through four fibers, two transmitting and two receiving. The heart of each unit is a one chip microprocessor, which provides all of the fault tolerance and switching features, and controls nine front panel LED indicators, which display the link status. When first powered on, each unit resets the microprocessor and begins running an operating program. The microprocessor then asserts a signaling carrier onto its fiber optic transmitters, and begins monitoring the signal quality outputs of its fiber optic receivers. In the first phase, the four paths that directly interface to each unit are tested. Each unit tries to handshake with its adjacent units, by probing with the transmitters and acknowledging messages received. If a probe is received, the receiver is declared good and an acknowledge is sent. If an acknowledge is received, the transmitter is declared good. In the second phase of operation the global connections are tested. Each unit tries to determine if there is a complete loop available on either the primary or secondary path. After this phase each unit knows which of the paths are available, and sets the indicator LEDs accordingly. If the primary and secondary loops are both unoperational, the network enters the wrap mode, which makes the most of the available interconnections, decomposing the network into two or more fully functional but disconnected networks. If both optical transmitters or receivers are inoperable, the unit has no way of forming a duplex link with other ring members, and will enter loopback mode. The fiber optic transceivers are hybrid modules [14], packaged in 24-pin DIP carrier and designed for direct printed circuit board mounting. The transmitter utilizes an edge emitting InGaAsP LED, having a rise/fall time of 2 ns. The optical output power is -22dBm, at a wavelength of 1310 nm with a spectral width of 150 nm (FWHM). The receiver utilizes an InGaAs PIN photodiode, and has a sensitivity of -32dBm and a NEP of -42dBm [15]. The transceivers operate at data rates of 125 Mb/s NRZ, using differential emitter coupled logic (ECL). They also possess integral fiber optic mini-BNC connectors, which in turn are connected to the dual-fiber bulkhead connectors, which link the MAB to the ring network. The two-fiber tactical fiber optic bulkhead connector utilizes two biconic connectors, in an hermaphroditic arrangement as shown in Fig. 5 [25]. The insertion loss from plug to bulkhead is less than 1 dB. It and its companion dual-fiber cable [16] are fully militarized and designed to withstand the stringent environmental and mechanical needs of a tactical field environment.

2. *Dual Fiber Optic Network.* The fiber optic link connecting the MABs consists of a ruggedized two-fiber tactical fiber optic cable, containing two tightly buffered 50/125 μm multi-mode optical fibers. The cables are terminated with hermaphroditic connectors, which facilitate field deployment and retrieval without physical or optical degradation. The fibers are radiation hard, with dual wavelength capability, and a numerical aperture of 0.22. Their attenuation is 3.5 dB/km at 850 nm, and 1.0 dB/km at 1300 nm and their bandwidth at 1300 nm is greater than 400 MHz-km. The optical fibers are cabled in a ruggedized all dielectric structure, embedded in kevlar yarns and surrounded by reinforcing elements and an outer jacket as shown in Fig. 6 [25]. The cable's outside diameter is 6 mm, and its weight is 30 kg/km. Using the model shown in Fig. 7, the power budget of a typical link of the ring network may be calculated as shown in Table 1. A transmission distance of 3 km is estimated.

- 1.1 dB average cable assembly loss (1.3 um)
- DOD-STD-1678 testing: impact, compression and tensile strength

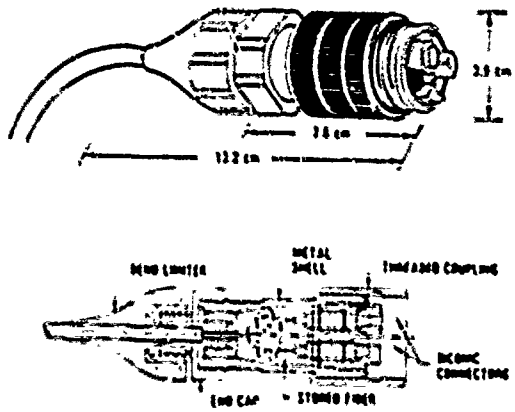

Fig. 5
Fiber optic cable assembly.

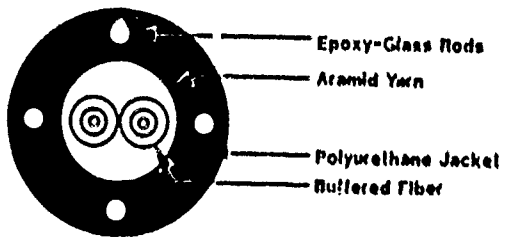

Fig. 6
Tactical fiber optic cable.

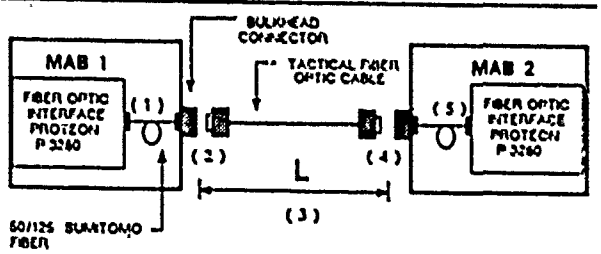

Fig. 7
Optical power budget test setup.

3. *Single Optical Fiber, Dual-Channel Link.* In order to further decrease the complexity and cost of the fiber optic network, wavelength division multiplexing (WDM) was used in order to combine the two counter rotating network channels on one single fiber. One of the transceiver pairs of the fiber optic interface has been replaced with modules, operating at 850 nm. The WDMs [17] employ a grating structure, having 50/125-μm fiber pigtails and terminated with biconic connectors. The cable, as before, is the dual-

fiber tactical fiber optic cable, which will eventually be replaced with a single fiber cable, being lighter and less costly. The WDMs, various connectors, and increased fiber attenuation at 820 nm (3.5 dB/km), introduce additional losses in the network thereby reducing the overall power budget—and the maximum MAB/MAB separation distance. The test setup and the power budget calculations for the modified link, are shown Fig. 8 and Table 1, respectively. A single fiber length of about 0.5 km is estimated. Longer ranges could be achieved by replacing the LED modules with more powerful laser diode transmitters.

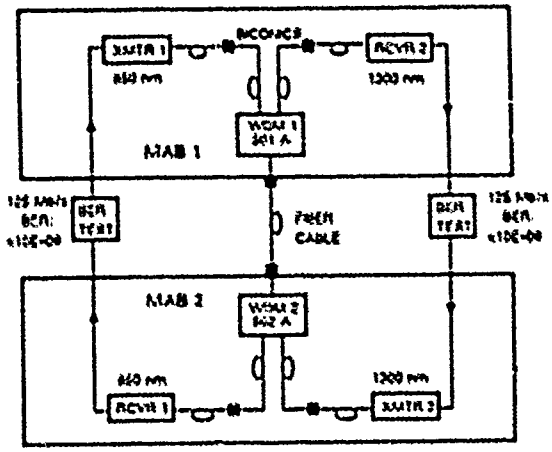

Fig. 8
WDM measurement setup

Table 1
Fiber power budget calculation

WAVELENGTH	850 nm	1300 nm
XMTR AVERAGE OPTICAL OUTPUT (1). (includes 10m splice to 2 BNC connectors)	-13 dBm	-22 dBm
RCVR SENSITIVITY (5)	-24 dBm	-32 dBm
POWER AVAILABLE FOR LOSS	11 dB	10 dB
WDM INSERTION & CONNECTOR LOSSES	2 dB	2 dB
BULKHEAD CONNECTOR LOSS (1.5 db per connector)	3 dB	3 dB
MISC ADDITIONAL L[illegible]SES	1 dB	1 dB
SYSTEM MARGIN	3 dB	3 dB
REMAINING POWER	2 dB	1 dB
CABLE ATTENUATION	3.5 dB/Km	1 dB/Km
MAXIMUM LINK SPACING:		
SINGLE FIBER	L = 0.57 Km	L = 1.0 Km
DUAL FIBER (without WDM)		L = 3.0 Km

F. Peripherals

The testbed includes three computer workstations and two PCs. These serve several functions: a) act as a source and sink of data traffic, b) provide a platform to develop VIM software, c) perform gateway functions between the 80 Mbit/s token ring and IEEE 802.3 and 802.5 subnets, and d) act as a network monitor and controller for the VIM modules. The workstations possess a 68020 processor operating at 16.7 MHz, 4Mbyte RAM, 140MB disk storage, and a built-in 802.3 interface. The operating system is a partially converged version of BSD 4.2 and AT&T System V UNIX, and includes utilities for implementing network file system access [18]. Two IBM PCs are also used to exercise the sub-net (Fig. 2). Three Private Automatic Branch Exchange (PABX) telephone switches are configured into the testbed. Each PABX possesses two T1 ports—one to each of the other two switches. When the packet network and VIMs are inserted in these three T1 links, the logical T1 connection topology remains the same although the voice is now exchanged in the form of packets. The fully-digital PABX system built on a non-blocking distributed architecture, capable of handling simultaneous voice and data traffic over standard two-pair telephone wire [19]. A 1m³ module houses the main processor, disc drives, power supply, and interface units (IUs).

III. PERFORMANCE

A. Theory

The network performance is illustrated in Fig. 9 and 10 [20]. Fig. 9 shows time delay versus throughput for several token protocols. Observe that FDDI offers about 20% greater capacity (768 voice channels) than the 80 Mbit/s LAN (624 channels) at time delays of ~1 ms or more. In practice, fewer voice channels

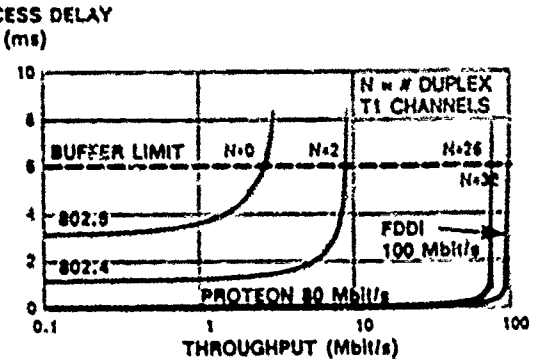

Fig. 9
Access time delay is plotted as a function of throughput for four different types of token ring LANs.

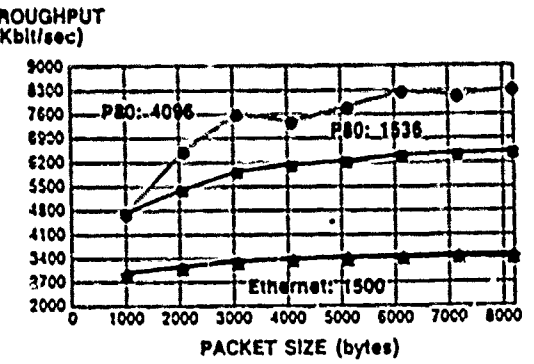

Fig. 10
Measured throughput between two Sun computers using UDP and aligning data to 1K byte boundaries. Message length in bytes follows LAN NIU type.

would be used to give reasonable access delays for data-only packets. For example, in network file system service an access delay of <250 μs would be desired thereby restricting the throughput to about 30 Mbit/s or 240 voice channels. The capacity of low-speed LANs is too low to support T1 traffic. However, single voice channels might be supported using the same technique.

B. Measurements

1. *Workstation Throughput.* Throughput was measured with the User Datagram Protocol (UDP) and Transmission Control Protocol/Internet Protocol (TCP/IP) of the workstations [21]. UDP is considerably more efficient but does not perform flow control, acknowledgments, and error checking. The test software generated long blocks of random data in RAM and directly sent this to the network, bypassing the disk subsystem. At the receiving workstation, the same data was discarded on a byte-by-byte basis. For a TCP/IP protocol and unloaded LAN, the throughput between two workstations was measured to be 2.2 Mbit/s for the 50 Mbit/s LAN and 1.8 Mbit/s for Ethernet. The 20% improvement is limited by the TCP/IP software overhead. For the simpler UDP protocol (Fig. 10), the token ring provides a two to three-fold improvement over Ethernet (depending on packet size). Still, the throughput is much less than expected from theory — a limitation imposed by the operating system overhead. A typical test set-up is depicted in Fig. 11.

Fig. 11
Workstation throughput test set-up.

2. *Voice.* Bit error rate (BER) tests were performed at the T1 interface of two VIM units attached to the ring. Less than 4 errors in 10^{12} transmitted bits were recorded over a 48-hour period. Error injection tests indicate that BERs on the order of 10^{-4} were not discernible. With the oversized FIFOs described previously, the delay from one PABX to the second PABX was measured to be 30 ms. This may require T1 echo cancellation equipment.

IV. APPLICATIONS

The overall purpose in developing the testbed is to determine the feasibility of using one type of LAN for high speed voice/data communications to serve a variety of Command, Control, and Communication (C^3) applications for the tactical Army [22]. An important concept in the Army's Airland Battle 2000 doctrine is the concept of the dispersed command post. Distributing the command post over a greater area increases survivability by removing a single point of failure—if one shelter is destroyed the command post can still operate. By using a LAN as described in this paper, shelters can be dispersed over a greater area then what is possible with today's metallic based LANs. Such integrated services as voice, data, graphics, and map updates would be provided in the command post over a single medium. This would greatly increase the mobility of the command post by reducing the cabling requirements. One potential application for the LAN in today's Army would be in the Standard Integrated Command Post System (SICPS) program. The LAN would be used as a high speed backbone to allow interconnection of the lower speed LANs in the shelter. A LAN interface into the Mobile Subscriber Equipment (MSE) could be developed allowing voice and data to be transported between shelters and the Army's backbone communications network. The LAN would provide benefits to the command post in rapid deployment time, increased mobility, and integrated services. The testbed gives the Army the capability of doing experimentation that would aid in achieving the goal of a distributed command post. The areas of modular network concepts, interconnecting lower speed LANs through a high speed backbone, demonstration of rapid deployment capability using fiber optics, and interfacing Army communication equipment to a LAN will be investigated to try to meet the Army's goal.

V. FUTURE DIRECTIONS

With the emergence of FDDI type components, the existing MABs will eventually be replaced. A new FDDI card, in its developmental stage, includes a chipset [23] that invokes the physical and data link layers, and the station management as outlined by the FDDI standard. The fiber optic transmitters and receivers will be replaced by a single transceiver module, operating at a wavelength of 1300 nm, at 100 Mb/s. All the electronic and fiber optic components will reside on one single PCB card which will be attached to the backplane of a workstation, eliminating the VIMs and MABs altogether. The fiber optic cable will be connected directly to the workstation. In the future design, voice, data and video signals will all be transmitted over the fiber network. A new network node, 20 Km away from the other nodes, will be intregrated into the existing network. Because of the great distance, laser diode transmitters are going to be deployed. If sufficient power remains, optical bypass switches may be incorporated into the network ring, resulting in greater flexibility and fault tolerance.

VI. CONCLUSIONS

While a synchronous version of FDDI may ultimately emerge with more efficient voice interfaces [24], the testbed presented here demonstrates that high-capacity high-quality voice traffic may also be transmitted over *asynchronous deterministic* LANs, such as FDDI. Counter to most other LAN voice transmission schemes, we allow voice and data stations to compete on an equal basis for network bandwidth. The advantages are that voice and data nodes may now run different protocols and that data nodes or gateways can be added to the network at will without negotiating with the voice transactions. Future enhancements will include upgrading the NIUs to meet the forthcoming FDDI standard and adding laser diode fiber optic transmitters for longer spans between nodes.

VII. ACKNOWLEDGEMENTS

The research described in this paper was carried out at the Jet Propulsion Laboratory, California Institute of Technology, and was sponsored by the U. S. Army CECOM through an agreement with

the National Aeronautics and Space Administration. Reference herein to any specific commercial product, process, or service by trade name, trademark, manufacturer, or otherwise, does not constitute or imply its endorsement by the United States Government, the U.S. Army CECOM, or the Jet Propulsion Laboratory, California Institute of Technology.

VIII. REFERENCES

[1] L. A. Bergman and S. T. Eng, "A Synchronous Fiber Optic Ring Local Area Network for Multigigabit/s Mixed-Traffic Communication," IEEE Journal on Selected Areas in Communications, Vol. SAC-3, No. 6, pp. 842-848, Nov 1985.

[2] A.A. Lazar, A. Patir, T. Takahashi, and M. El Zarki, "Magnet: Columbia's Integrated Network Testbed," IEEE Journal on Selected Areas in Communications, Vol. SAC-3, No. 6, pp 859-871, 1985.

[3] A. Patir, T. Takahashi, Y. Tamura, M. El Zarki, and A. A. Lazar, "An Optical Fiber-Based Integrated LAN for MAGNET's Testbed Environment," *IEEE Journal of Selected Areas in Communications*, Vol. SAC-4, No. 6, pp. 872-881, Sept 1986.

[4] H. R. Muller, H. Keller, and H. Meyr, "Transmission in a Synchronous Token Ring," in Local Computer Networks, P. C. Ravasio, G. Hopkins, and N. Naffah (editors), North-Holland Pub. Co., pp. 125-147, 1982.

[5] J. O. Limb, "Performance of Local Area Networks at High Speed," IEEE Communications Magazine, Vol. 22, No. 8, pp. 41-45, Aug. 1984.

[6] F. E. Ross, "Fiber Distributed Data Interface," *OFC/IOOC '87*, Reno, Nevada, 19-22 Jan. 1987, WJ1.

[7] H. Salwen, A. C. Marshall and N. K. Salwen, "ProNet, An 80 MBIT/s Token Ring for High-Speed LAN Applications," Proteon information sheets.

[8] ANSI/IEEE Std 802.3-1985 ISO Draft Proposal 8802/3, Carrier Sense Multiple Access with Collision Detection (CSMA/CD): Access Method and Physical Layer Specifications, ISBN 0-471-82749-5, John Wiley & Sons, Inc., 1985.

[9] ANSI/IEEE Std 802.5-1985 ISO Draft Proposal 8802/5, *Token Ring Access Method and Physical Layer Specifications*, ISBN 0-471-82996-X, John Wiley & Sons, Inc., 1985.

[10] Proteon 1580 NIU for VME bus.

[11] Proteon p2400 wire center.

[12] Proteon p3250 fiber optic modem for counter rotating ring.

[13] AT&T Model 105243596 dual-fiber bulkhead connectors.

[14] Sumitomo DM-54 fiber optic transceiver modules.

[15] Note: transceiver characteristics are typical values measured through a 50/125 µm, 10 m, Sumitomo optical fiber.

[16] AT&T Model 10524331 tactical dual-fiber cable.

[17] AT&T 501A/502A wavelength division multiplexer.

[18] Sun Microsystems, Inc., Model 3/160M.

[19] Wang WBX public automatic branch exchange (PABX)

[20] L. A. Bergman, R. Hartmayer, S. Marelid, W. H. Wu, G Edgar, P. Cassell, R. Mancini, J. Kiernicki, L. J. Paul, J. Jeng, C Pardo, F. Halloran, and J. Martinez, "A Fiber Optic Tactical Voice/Data Network Based on FDDI," *IEEE INFOCOM'88*, New Orleans, March 27-31, pp. 45-54, 1988.

[21] Sun Microsystems, Inc., 3/160M.

[22] M. S. Frankel, C. J. Graff, L. U. Dworkin, T. J. Klein, and R. L. desJardins, "An Overview of the Army/DARPA Distributed Communications and Processing Experiment," IEEE Journal on Selected Areas in Communications, Vol. SAC-4, No. 2, pp. 207-215, Mar 1986.

[23] AMD SuperNet FDDI chipset.

[24] FDDI 2 (X3T9.5) Working Paper, Feb.1, 1987.

[25] CECOM Research and Development Technical Report TR-84-K551-F "Tactical Fiber Optic Cable Assemblies", AT&T Technology Systems, Sep 1987.

Ron Hartmayer received the B.S and M.S. degree in electrical engineering from the University of California in Los-Angeles, in 1956 and 1958 respectively. In 1956 he joined the Opto-Electronics Systems Technology Group at the Jet Propulsion Laboratory in Pasadena, CA. He is currently working on high-speed fiber optic networks for FDDI, and on optical image processing.

Larry A. Bergman received the B.S. degree in electronic engineering from the California Polytechnic State University, San Luis Obispo, in 1973, the M.S. degree in electrical engineering from the California Institute of Technology, Pasadena, in 1974, and the Ph.D. degree in electrical engineering from Chalmers University of Technology , Gothenburg, Sweden, in 1983. In 1975, he joined the Information Systems Division at NASA's Jet Propulsion Laboratory, Pasadena, where he worked on multi-fault tolerant power conditioning systems and spacecraft data buses. In 1977, he joined the fiber optics research group at JPL where he worked on the development of a low power fiber optic spacecraft data bus, and designed a Space Shuttle optical fiber experiment. In 1981, he initiated advanced high-speed fiber optic LAN development efforts for spacecraft applications. Presently, he is a group leader, conducting research on multi-gigabit/s fiber optic LANs for supercomputer communications, real-time FDDI networks for spacecraft and tactical applications, and holographic optical interconnects for VLSI chips.

Mr Frank Halloran is currently employed as an Electronic Engineer for the US Army CECOM at Ft. Monmouth, NJ. Mr Halloran recieved a Bachelor of Science Degree in Electrical Engineering from Rutgers University in 1981, he has completed his coursework requirements for a Masters Degree in Computer Science at Monmouth College, NJ. Mr Halloran is currently assigned to the Local Area Networks/Fiber Optics group where he is the project leader of the Fiber Optic Tactical Local Area Network Project.

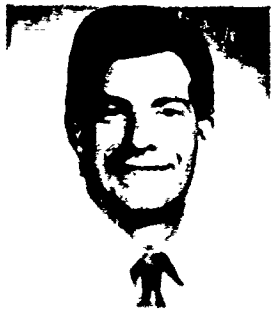

James Martinez received the BS degree in computer science from the University of Dayton, OH in 1985 and has completed his course work requirements for a MS in computer science at Monmouth College, NJ. He is currently employed by the US Army CECOM at Fort Monmouth, NJ. His projects include assisting on the Fiber Optic Tactical Local Area Network program and project leader of the Miniaturized Fiber Optic Telephone Switch.

A SMALL DIAMETER, HIGH STRENGTH, SINGLE CHANNEL FIBER OPTIC AIRCRAFT CABLE FAMILY FOR USE WITH 38999 CONTACTS

W. B. Beck, R. E. Hille, P. O. Scadding

Ensign-Bickford Optics Company, Avon, Connecticut 06001

Abstract

Nearly all available specialty fiber optic cabling systems are merely extensions of telecommunications fiber technology developed in the late '70s. The aircraft and mobile platform environments present the most difficult challenge to the fiber optic cable designer. A combination of very severe and dynamic environmental conditions, ultra-high reliability requirements, diameter limitations imposed by existing contact designs and high density interconnection makes for very difficult design trade-offs. This paper will discuss these design trade-offs in-depth and present a fully integrated "systems approach" to the design of a family of high reliability, simplex optical cables that can be used in data links, sensor networks and laser ordnance cabling for airframe and platform applications. This family of cables is designed around ultra-high strength and proof tested fibers with large core diameters for extremely high coupled power levels, high numerical aperture for extremely low bending induced attenuation, radiation hard core materials for application in strategic and tactical systems, very flat spectral attenuation for use in wideband sensor systems and a unique hard coating for use with no epoxy, no polish single-channel or pin contact interconnection systems. This cable is currently being flown in operational avionic and missile systems, and is being considered for several more programs in the near future.

Introduction

Fiber optic cable designers face a triple challenge. First, they must design a product that will provide the utmost reliability in the most difficult and dynamic of environments. Second, they have virtually no control over the fiber design, being at the mercy of telco fiber manufacturers. And third, they must wait 5 to 10 years before their development efforts are paid back, often tying a design to a specific Defense Program with uncertain future prospects. Unfortunately, these three challenges have impeded the development of even adequate optical fiber cables for the Aerospace industry. This paper will describe in detail the trade-offs and design challenges, as well as present a family of 3 lightweight, high strength cables that address the majority of known applications of fiber optics in avionics. The cables were developed using an overall systems approach in the hopes of anticipating both data and power delivery applications. These cables were developed with concerns for fiber reliability, cable installability, connectorization with existing pin contact envelope, easy and rapid termination and reconfiguration, and with an eye on future "tappability" for networking. Nearly all of the key issues have been resolved and production cabling now exists and is flying in a variety of systems and platforms.

The Problem

Unlike a telecommunication system, a fiber optic link or network in an aircraft does not have to transmit tens of kilometers at Gigabit digital transmission rates. All but the most advanced networks operate at 100 Mbits/sec and most at 10 Mbits or less. Furthermore, with typical path lengths of 100 meters or less, extremely low attenuation per kilometer is also not critical. For this reason, use of telecom fibers is not the optimum solution. By beginning with the most appropriate fiber for the job, the cable design problem is simplified.

The four primary design goals for an aircraft cable are as follows:

1. Optical Functionality - the optical system must "play"
2. Physical Robustness - the cable/interconnect must stand up to installation
3. Long-term Reliability - the cable must last the design lifetime
4. Small Size/Weight - the cable system must save space & weight

Optical functionality requirements are relaxed somewhat due to the reduced data rates and distances of most Avionic systems. This allows more flexibility in meeting the other three design objectives. The one aspect of optical functionality that is unique to the Avionics world is the need for a (relatively) large number of production bulkheads. This is particularly true as more complex systems are combinations of "building blocks" produced by separate subcontractors, (e.g. the Space Station or the next generation Airbus). Production breaks mean bulkhead connectors and additional optical "loss" and points of failure in a link. Reducing the loss of the cable per kilometer does very little to improve system margins. The only ways to increase the power level at the receiver are to increase the power level coupled into the

link from the transmitter and to reduce connector and bend-induced losses in between.

Physical robustness is normally assured by "burying" the fiber under layers of buffers and tubes, strength members and jackets. This approach may suffice for telecom, datacom or even shipboard applications, but two factors preclude this approach for aircraft cabling. First, the overall diameter of an avionic cable must be compatible with existing Size 16 pin contacts. Many interconnect systems (e.g. LRU "blind mate" connectors) must accommodate both fiber optic and electrical contacts. It is not likely that the Aerospace industry is going to throw away 25 years of connector development investment for the sake of fiber optics. Second, adding more protective layers increases the weight of the cable. For fiber to pay its way in new systems, it must reduce overall system weight, not increase it.

Long-term reliability is the biggest hurdle for any new technology in the Aerospace world and this is no exception for optical fiber cable. It is very difficult and expensive to try out fiber optics in production airframe systems. There have been several trial links reported in the literature by Boeing, Douglas and Aerospatiale[1,2,3]. Results from these few trials have been encouraging but only emphasize the need to test long term reliability in the laboratory even more. Moreover, fiber optic test procedures must be utilized, not those developed for copper wire. This point is extremely important. Optical fiber cables have different deterioration and failure modes. The blind use of existing wire cable specifications and tests is not prudent.

Small size and weight is of paramount importance in avionics systems. As fly-by-wire and fly-by-light systems get more complex, individual components must get progressively smaller and lighter. Optical fiber cables must fit the envelope of a typical 38999 size 16 pin. This is one of the most limiting specifications but compatibility with existing interconnect designs is key to adoption of the technology.

Design Goals

Table 1 lists general design goals common to this family of aircraft cables. (All specifications are based on a standard one kilometer test length.)

Table 2 lists additional design targets that are "application-specific".

Design Approach

Several guiding principles are common to the design of this family of Airframe Cables. First, large core, "step-index" fibers are used in all cables. Second, these fibers are screen or "proof" tested at very high levels to insure survival of the cabling, installation and application environments. Third, well characterized materials such as DuPont's Kevlar® are used, taking advantage of the extensive development, testing, processing and real world experience associated with these materials. Finally, only hard polymer clad or coated fibers are used. This insures that the reliability associated with a high proof test level is preserved throughout the cabling, harnessing, installation, fiber stripping and terminating processes via the preservation of the inherent strength of pristine silica.

Cable Matrix

See Table 3.

Discussion

General

The three cables are essentially the same design. A very high strength, fatigue resistant, high proof test fiber is buffered with an extruded, mechanically removable DuPont Tefzel® buffer. No silicone primary buffer is used. This eliminates the problems associated with silicone residue, i.e. unreliable termination. A penalty is paid in terms of low temperature attenuation change but in the context of high NA fiber and short haul systems, this penalty is very small. Braided Kevlar® is used because of the small diameter and thin wall of the outer jacket. The braid keeps the jacket round and kink resistant. An outer jacket of modified ETFE is used to provide good chemical and abrasion resistance as well as good thermal stability and flame retardancy.

Fiber Selection

There is currently a debate in the Avionics "Community" on the subject of fiber choice. Some believe that 100/140um fiber is best for Aircraft cables because it allows for a smaller "minimum long-term installed bend radius". This conclusion is based on the erroneous assumptions that 100um fibers are as strong and as fatigue resistant as 200um hard clad or hard coat fibers. Figure 1 shows a Weibull Failure Probability Graph comparing 100/140um fiber to 200um hard clad type fiber used in the tappable datacom cable described in Table 3.

It can be seen from Table 4 that on the basis of average tensile strength, proof test level, and static fatigue over time, the 200um fiber actually has a smaller long term minimum bend radius than the 100/140um fiber. Furthermore, the inherent tensile strength of the larger 200um fiber adds to the strength of the cable and allows for crimp on fiber attachment strengths as high as 5 kg. Table 4 summarizes the comparison between 200um hard clad fiber and 100um commercial fiber.

Several tactical and strategic programs require higher operating temperature range and an increased resistance to EMP environments. In order to achieve these goals and provide most of the advantages of the hard clad fiber, a "hard coat", all-silica 200um fiber is used. In this fiber design, numerical aperture and bend radius are traded-off for extremely high resistance to EMP (rapid recovery) and higher temperature range. The tensile strength is nearly as high as the hard clad type but the slightly increased silica diameter increases the long-term minimum bend radius of this cable 12 to

16mm. The lower numerical aperture of this fiber (0.22 vs 0.37) makes the cable more sensitive to bend-induced attenuation and more sensitive to low temperature induced attenuation. For this reason, an extremely small cross-section jacket is used to compensate.

The Laser Ordnance Cable uses a 400um hard clad fiber. In this cable, reliability, EMP resistance, small bend radius and high power handling dominate the design goal. The fiber has been subjected to a series of classified strength and radiation tests and has been selected for the Laser Ordnance Initiation (LOI) system for the SICBM program. This cable is very specialized in the world of Avionics but is extremely versatile for LOI and wideband sensor systems.

Cable Design

The primary cable design challenge with all three of these cables is one of thermomechanical stability. Optical fibers are sensitive to a phenomenon known as "microbend" induced attenuation. When an optical fiber is bent or stressed nonuniformly, optical power "leaks" out of the fiber. The sensitivity of a fiber to this type of attenuation is given by the following formula:

$$\Delta \text{ Attenuation} \propto 1/(NA^3)$$

This bend induced attenuation may manifest itself in several ways. First, if the cable is bent around another cable in a harness or loaded around a sharp edge, the attenuation of that point of cable will increase. Figures 2 and 3 show the sensitivity of various cables to this type of "macro-bend" induced attenuation.

If fibers in a cable jacket are bent nonuniformly on a micro scale due to thermomechanically induced stresses or point pressure (e.g. tie-wrapped) attenuation will also increase. Use of a high numerical aperture fiber reduces sensitivity; use of a stable, small cross-section jacket reduces thermomechanically induced stresses.

When thin wall jackets are used, especially with higher modulus materials such as Tefzel, care must be taken to prevent kinking of the tube. Use of a larger diameter fiber and a Kevlar braid combine to mitigate this tendency. In the 400um LOI cable, the fiber prevents small radius kinking and adds substantialy to cable tensile strength.

Connectorization

The Aerospace industry uses a wide variety of connector formats developed and tested over the years. It would be extremely beneficial if optical fiber cables could be terminated with the same type of pin and shell interconnect systems as electrical wire. So far, a great deal of effort has gone into conversion of existing pins, in particular size 16 pins, to fit the popular 38999 family of circular connectors already in use in a number of platforms. The key to a simple and reliable interconnect system lies in the cable and more importantly, fiber design.

When cable jacketing materials change length in different environments, the fiber does not. This difference in thermal coefficient of expansion causes tremendous pressure on fibers in the cable and also on the fiber/pin interface. When commercial fibers are terminated, their protective buffers are removed. With no protection on the surface of the silica, the strength of the fiber drops to 3% of its normal strength. (This phenomenon can be observed by stripping a fiber and bending it.) Any time a fiber is terminated after its protective buffer has been removed, it is nearly impossible to guarantee the reliability of the termination. Add to this, the pressures a large jacket can exert on a small cross-sectional area fiber, and the problem becomes worse.

The cable family described above is specifically designed for high reliability terminations. The small cross-section jacket combined with the large cross-section but high strength fiber reduces stresses at the termination. The hard cladding or coatings left on the fiber during termination preserve the high reliability level assured by the initial fiber proof test. Furthermore, with a thin-film bonded coating left on the fiber, crimp-on pin contacts, the norm for wire interconnect, are now achievable. This type of termination practice is absolutely necessary for fiber to be used extensively in avionics. (Pin contacts are under development by several companies that take full advantage of the design features of these cables.)

"Tappability"

As avionic systems grow more complex, fly-by-light will become essential not merely desirable. The interconnection of subsystems and LRUs via databus will become an important capability[4]. By using hard clad fiber for aircraft cables, future tappability is assured. Both head-end driven or regenerated and all passive, bi-directional systems can be implemented with the hard clad, tappable cable[5]. Tappability is useful in LOI systems as well. A smaller, low power on-tap can be used to inject a signal into the high power (400um) line for (non-destructive) system path verification.

Applications

The cables described above are not prototypes. They have been tested, flight tested and in the case of the standard datacom cable are used in production aircraft and other platforms. The LOI cable was used on the SICBM flight test. Both single channel MIL-Std SMA and 38999 pin contacts are used. Table 5 summarizes most of the current and future uses of these type of cables.

Summary

A family of production optical fiber cables has been developed for existing and anticipated applications of lightwave technology. The central design goals for all three types are robustness in installation and termination; reliability in use. Large core fibers are used to provide strength and rigidity. Hard coat/clad fibers are used for tensile strength and fatigue resistance. Small dia-

meter jackets are used for pin contact compatibility and to mitigate thermomechanical stressing of fibers. All cables are designed to extremely high tensile strength, insensitivity to bend induced attenuation and very small long-term minimum bend radius. These cables have been systems-engineered from the fiber to the termination, specifically for avionic applications.

References

1. William R. Little, "A Review of Fiber Optic Flight Experience; Past Problems, Future Direction", SPIE, Vol 989, pg 11 (1988).
2. John J. Arcin, SAE ASD Committee AS-3: Fiber Optics, April 18-21, 1988.
3. J. P. Domergue, "Aerospatiale Investigations on Aircraft Behaviour of Optical Technology", EMFOC-89, 5.2.3, pg 99.
4. W. H. Hall, D. R. Brown, J. W. Burgess, "The Requirement for IFABUS Laboratory Equipment and the Development of the British Aerospace/Plessey IFABUS Demonstration", EMFOC-89, 5.2.2, pg 98.
5. W. D. Beck, M. H. Hodge, R. T. Dillon, "An Optical Tapping System for Avionics Databussing", EMFOC-89, 5.2.4, pg 105.

Optical Throughput	<10 dB/km @ 820 nm
Optical Bandwidth (3 dB)	>10 MHz-km
Temperature Envelope	-65 to +125 °C (or +150 °C)
Overall Diameter	≤ 1.8 mm
Minimum bend radius	< 12 mm (0.5 inches)
Weight	< 3 kg / km
Tensile Strength	> 50 kg @ 2% elongation

Table 1.

Tappability	Requirement for bus networks
Radiation Resistance	Resistance to EMP or Cumulative dose
High Optical Damage Threshold	Requirement for Laser Ordnance Cable
Broad, Flat Spectral Response	Needed for broad-band sensors
Higher Temperature Range	Requirement for Tactical Systems
Vibration Reliabilitiy	Helicopter Applications

Table 2.

Cable type	Datacom, Rad Hard Tappable, Crimpable	Datacom, Rad Hard (EMP-Pulsed)	Laser Ordnance
Cross-Section	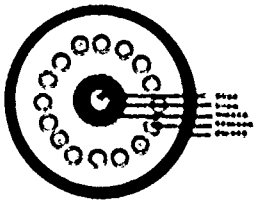	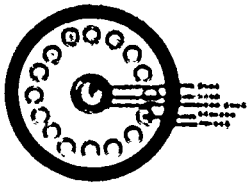	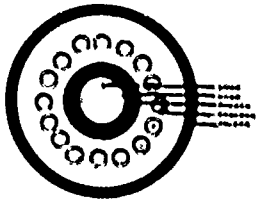
Specification			
Fiber (µm)	200 / 230 / 500	200 / 240 / 260 / 375	400 / 430 / 730
Buffer	Tefzel®	Tefzel®	Tefzel®
Strength member	Kevlar® 49 Braid	Kevlar® 49 Braid	Kevlar® 49 Braid
Outer Jacket	Modified ETFE	Modified ETFE	Modified ETFE
Diameter	1.8 mm	1.65 mm	1.8 mm
Weight (kg/km)	2.8	2.6	3.2
Attenuation (dB/km)	≤ 10 @ 820nm	≤ 10 @ 820nm	≤ 10 @ 1.06µm
Bandwidth (MHz-km)	≥ 15	≥ 20	N.A.
Proof Test (KPSI)	200	200	250
Fiber Tensile (KPSI)	720	700	680
Fiber Tensile (kg)	17	22	60
Cable Tensile (kg)	80	80	100
Elongation (%@80kg)	2%	2%	2%
Temp Range (°C)	-65 /+125	-65 /+150	-65 /+125
Flammability	Self-extinguishing	Self-extinguishing	Self-extinguishing
Fluid Immersion	Very Resistant	Very Resistant	Very Resistant
Radiation	long term gamma	pulsed gamma	pulsed gamma
Power (Nd:YAG)	> 20 Watts CW	> 1MWatt/cm²	>0.5 joule pulse
Tappable	yes	no	yes
Crimpable	yes	no	yes
Min Bend Rad.(mm)	12	16	21
Flex life (FOTP-1)	>25,000	>25,000	>25,000
Impact (FOTP-25)	50 @ 0.5 kg	50 @ 0.5 kg	50 @ 0.5 kg

Table 3.

FIBER SELECTION COMPARISON

200/230 µm HCS vs. 100/140 µm ALL-SILICA

FIBER	200/230	100/140
COUPLED POWER	0 dBm	-6dBm
µBEND SENSITIVITY	LOW	MEDIUM
AVERAGE TENSILE (KPSI)	780	550
MINIMUM BEND RADIUS (mm)*	12	42
BEND RADIUS AT BREAK (mm)+	1.28	1.27

* BASED ON PROOF TEST LEVEL AND TYPICAL STATIC FATIGUE RATE

\+ BASED ON AVERAGE WEIBULL FAILURE PROBABILITIES

Table 4.

Cable Type	Application	Function
Standard	Remote LRU	Noise free interconnect
	Sensor Cable	Sensor / transducer interconnect
	Data bus	Multifunction LRU linear bus interconnect
	Audio-Video bus	Entertainment distribution
Tactical	Datalinks	Noise free, rad-hard channels
	Sensor Cable	Position, temperature, flow, pressure, damage, laser, strain sensor interconnect
	Data b·	High speed integration of subsystems
	Con·	·tuation and signalling
	·	·el to CPU datahandling
LOI	La··	·ket motor ignition
		·age separation
		Stores release
		Crew Safety
	Laser Transmission	Free Space Communication
		Laser tracking

Table 5.

WEIBULL FAILURE PROBABILITY:

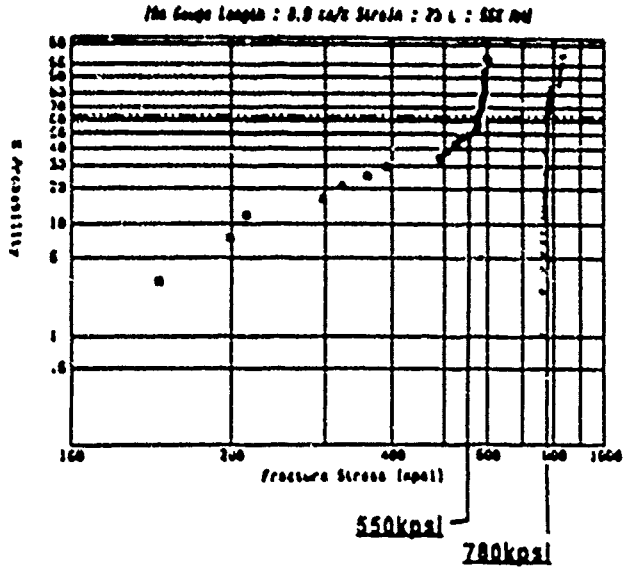

+ =200/230 µm HCS®
■ =100/140 µm All-Silica

Figure 1.

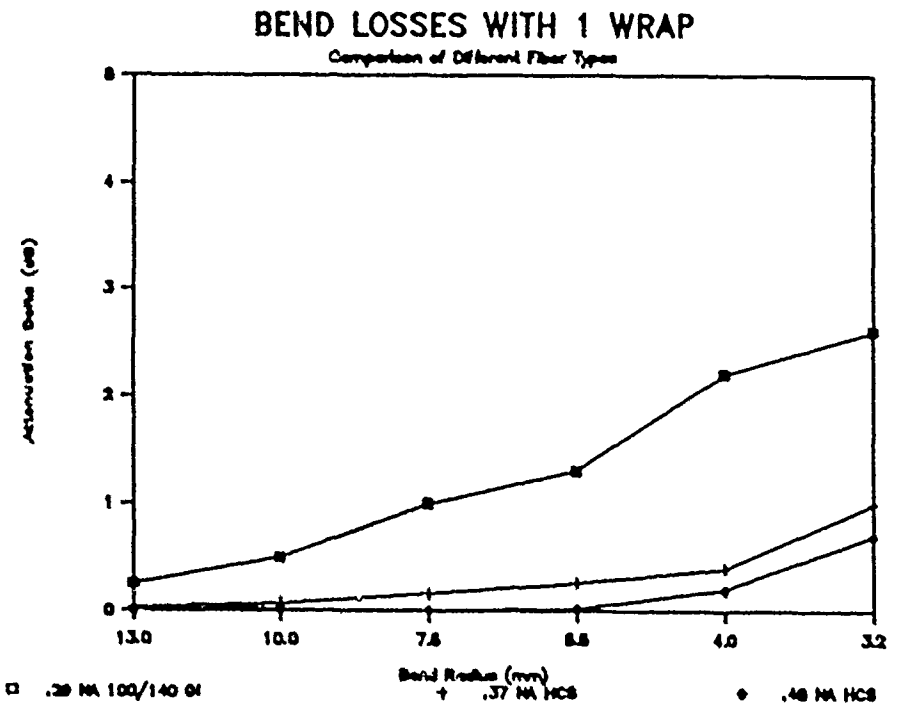

Figure 2.

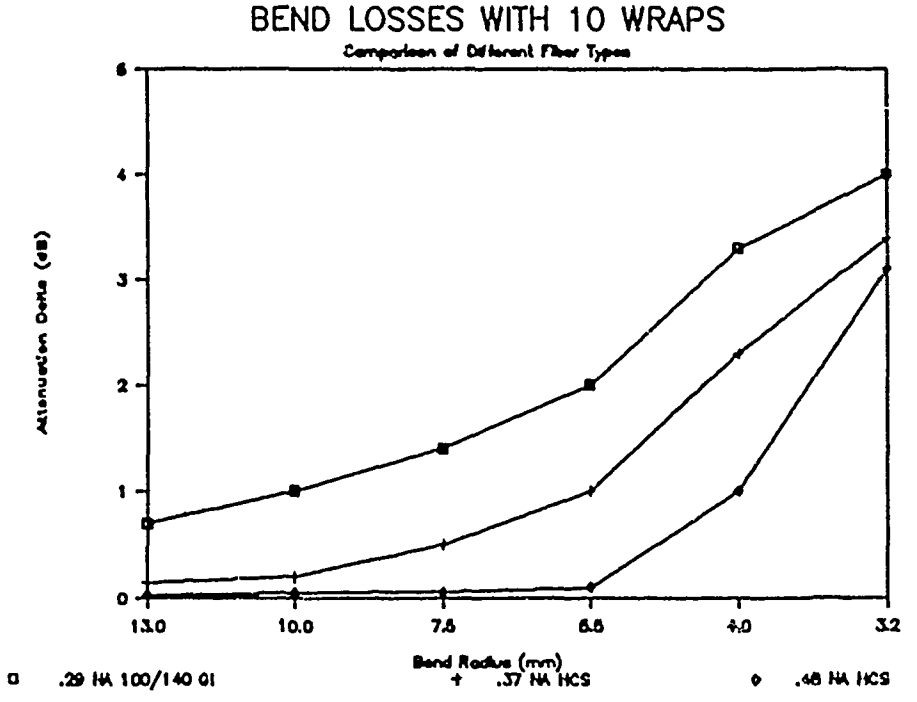

Figure 3.

INTERFACE COMPONENTS FOR HIGH PERFORMANCE BIDIRECTIONAL TRANSMISSION OVER SINGLE FIBER CABLE

Ted Leonard, John Eide, Chip Mueller

Alcatel Cable Systems, Inc. C/S #19000 Roanoke, VA 24019

ABSTRACT

Recent advances in active and passive fiber optic components design have resulted in dramatic performance improvements as well as significant cost reductions. These two factors have opened the way for new system implementations for single fiber cables,especially in the areas of avionics data bus and in remotely piloted vehicles.

This paper describes the development of passive couplers and interconnect modules that enable, for example, the transmission of multiple video channels in one direction and control signals in the opposite direction through a single fiber. The significance of this work is that through new packaging techniques the interface size, weight, and cost have dropped significantly, which make fiber optic bus and control systems cost effective.

Included in the paper will be physical descriptions of some new innovative modules, along with test data illustrating optical performance and environmental compatibility.

SUMMARY

Fiber optic transceivers, which incorporate a coupler, active devices, and a fiber pigtail or connector into a single small package, can improve system performance and reduce both component cost and size. This is critical for fiber optic system implementation which is rapidly becoming system cost limited rather than technology limited. Transceivers can be built in both single mode and multimode forms for a wide variety of single and bidirectional fiber data links. These modules have been built, packaged, and tested in single and multimode forms for variety of applications. Larger systems combining many wavelengths into single fiber links utilizing large numbers of modules and couplers can also be realized.

SINGLE FIBER SYSTEMS AND REQUIREMENTS

Two of the largest potential applications of fiber optic transceivers, fiber tethered vehicles, and fiber-to-the-subscriber (FTTS), are evolving as bidirectional systems operating over a single fiber. For example, the fiber-guided missile will be a major market in itself and will share many basic requirements with FTTS links: both systems will likely utilize bidirectional single-mode links capable of carrying video in one direction and lower speed digital traffic in the opposite direction with wavelength division multiplexing (WDM).

Another high volume application of transceivers requiring two separate wavelengths on a single fiber is sensor links for advanced avionics systems. In this case, a reference channel is often sent along with the modulated channel on separate wavelengths over multimode fiber. The two sources are combined with a WDM coupler for unidirectional transmission over a single fiber.

Designs being developed for each of these high volume applications are driven by similar constraints on size, environmental extremes, performance, and cost. A primary requirement is that the optical transceiver occupy as little board space as possible and be rugged enough to be easily handled. One approach is to package the active and passive optical components together in a common package so there are no external fibers except the link fiber itself. This "module" concept not only enhances the ruggedness and decreases the size, but it also allows for optimum component selection to meet overall assembly specifications. The result is higher performance assemblies and increased yield resulting in higher quality, and lower cost compared with individually packaged components.

SINGLE MODE MODULE DESIGN

Single mode fiber is the driving requirement for FTTS modules. Module development is currently limited by the available variety of single mode couplers. Currently, high performance couplers are fabricated using fused biconic taper (FBT) technology for single mode power splitters and wavelength division multiplexers (WDM). These couplers are typically 1-2 inches in length and less than 1/4 inches in diameter. Single mode modules must also utilize the most efficient methods known to couple optical power into and out of fiber. Most single mode modules therefore utilize an FBT coupler in combination with single mode pigtailed active devices and short fiber lengths all contained within a single package.

MULTIMODE MODULE DESIGN

The LED combiner module is an example of recent developments in multimode transceivers. In this particular case two LEDs with different wavelengths are optically coupled into a single optical fiber link with a high coupling efficiency. This module is based on proven coupler principles used in the standard wavelength division multiplexer product line. In the module the two LEDs are an integral part of the coupler and all are contained in the same package.

The basic layout of the LED combiner module is shown in Figure 1. Starting on the left side, the short wavelength light from a 730nm surface emitting LED is collected and collimated by a microlens. The collimated light passes through a short wavelength pass filter. A GRIN lens focuses the collimated beam into the link fiber placed inside the capillary tube. On the right side, a GRIN lens captures the light emitted from an 865nm LED and focuses the beam into a short length of fiber. The short length of fiber is attached to the lens. The lens collimates this beam on to the filter. The filter acts as a reflector for this wavelength and reflects the beam back. The lens then refocuses this reflected beam into the link fiber. The entire assembly described above is attached to a metal heat sink plate. This total assembly is cast molded into a single unit.

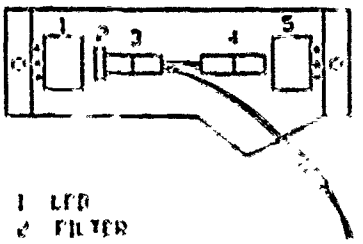

Figure 1 - Multimode LED Combiner Module

SINGLE MODE MODULE DEVELOPMENT

Single mode 1200/1300 nm WDM bidirectional modules have demonstrated LED output power of 4 microwatts(-24 dBm) and PIN responsivities of 0.5 A/W at the package ST connector interface. The modules incorporate a single mode ST style connector, a fused biconic taper 1200/1300 nm WDM coupler, a 1200 nm or 1300 nm edge emitting LED, and an InGaAs PIN photodiode, in a single molded package. The package dimensions are 0.5" x 0.7" x 5.25" with only the single ST connector optical connection and the necessary LED and PIN electrical leads visible on the package exterior (see Figure 2).

Figure 2 - Single Mode Module

Module operation was tested over a -20 to +70°C temperature range. The signal crosstalk isolation between the LED and PIN is <5nA at a full LED bias of 100 milliamperes. Typical link loss budgets were examined for three possible module uses (see Table 1). The values clearly show that simple LED/PIN/coupler modules can be used for a variety of applications. Systems requiring a greater value for overall gain could be satisfied by using a laser source.

Single mode bidirectional modules were also fabricated using a variety of power splitting couplers. The LED/PIN/coupler modules incorporate either an integral ST or FC style connector in the package. The performance of these modules varies directly with the coupler split ratio. The module splitting ratio is designed around the systems operating characteristics to best utilize the available link loss budget. The package and performance characteristics were identical to those for the WDM module (except for signal crosstalk isolation which was found to be >17dB).

MULTIMODE MODULE DEVELOPMENT

Multimode modules have been fabricated to combine LED outputs of different wavelengths onto a single fiber. The LEDs are short wavelength surface emitters and the WDM coupler is based on an existing bulk optics design utilizing a dichroic filter. The module operating temperature range is limited to -30° to +80°C by the LEDs, the coupler is rated for operation from -55° to +125°C. Output power variation with temperature was found to be less than 0.4% per degree C. The modules achieved in excess of 1 mW (0 dBm) output power from the 200/230 micron link fiber at 100 milliampere LED drive current.

The package for the multimode module is 1.6" x 0.6" x 0.3" with only a single fiber pigtail and the required LED electrical leads external. (Figure 1). The package size is determined mainly by the bulk optics coupler. Alternative coupler varieties show promising reductions in module size (as high as 50%) and potential improvements in performance and ease in fabrication.

The multimode approach easily applies itself to larger system designs where a number of modules and/or couplers can be used to efficiently couple many different wavelengths onto a single fiber link. The same combination can be used with PIN or APD detectors to demodulate the signals off this single fiber link. This approach is also feasible with single mode modules and couplers.

EXAMPLE WDM LINK LOSS BUDGETS

	POTS 192KB/s	OC-3 155MB/s	ANALOG 6MHz
XCVR OUTPUT POWER (2mW AVERAGE)	-27dBm	-27dBm	-27dBm
RX SENSITIVITY	-49dBm	-49dBm	-49dBm
DUPLEXER LOSS	2dB	2dB	2dB
SYSTEM GAIN	29dB	11dB	11dB
CABLE SPLICE LOSS 6 @ 0.2dB EA	1.2dB	1.2dB	1.2dB
REPAIR SPLICE LOSS 6 @ 0.2dB EA	1.2dB	1.2dB	1.2dB
OPTICAL RACK & DROP CONNECTOR 2 @ 0.6dB EA	1.2dB	1.2dB	1.2dB
TEMPERATURE & AGING MARGIN -20°C TO +70°C	3.0dB	3.0dB	3.0dB
TOTAL LINK LOSSES (LESS CABLE)	6.6dB	6.6dB	6.6dB
AVAILABLE CABLE LOSS	22.4dB	4.4dB	4.4dB
MAXIMUM LINK LENGTH:			
1300nm 0.5dB/km	44.8km	8.8km	8.8km
1200nm 0.7dB/km	32.0km	6.3km	6.3km

TABLE 1

Mr. Chip Mueller received his BS and MS degrees in Electrical Engineering from the University of Delaware in 1984 and 1986 respectively. He joined Alcatel Cable Systems in 1986 and is currently a senior engineer engaged in the development and production of Fiber Optic Components and Modules.

Mr. John Eide holds a BS degree in Math, Astronomy and Physics from the University of Oslo. In 1961 the same university awarded him an MS degree in Physics. Mr. Eide is presently holding a staff scientist position with Alcatel in the III-V Device group. He has numerous publications in the area of solid state devices and holds patent on Thin Magnetic Film Storage Device.

Mr. Ted Leonard received the BSEE degree from North Carolina State University and the MSEE degree from Florida Institute of Technology. He is currently Department Manager, Fiber Optic Components and Manager, Military and Commercial Business Development at Alcatel Cable Systems in Roanoke, VA. Prior to his employment at Alcatel he was a Senior Principal Scientist at ITT Electro-Optical Products Division in fiber optic systems and a Lead Engineer at Harris Corporation. Mr. Leonard is a Senior Member of the IEEE and a member of SPIE.

Field Measurements of the Effects of Hydrogen Gas on Installed Submarine Single-Mode Fiber Cables

W. T. Anderson, A. J. Johnson, and A. DeVito

Bellcore, Morristown, New Jersey

Summary

Measurements for the presence of molecular hydrogen on 23 submarine cables are reported. These measurements were made using an Optical Time Domain Reflectometer (OTDR) operating at 1240 nm, a wavelength at which the hydrogen-induced attenuation is very large. 19 of the 23 submarine cables measured were clearly degraded by molecular hydrogen. In 3 of the 19 cases where hydrogen was found, the amount of hydrogen present was not uniformly distributed along the submarine cable. The source of the hydrogen is probably corrosion of the galvanized steel armor wires. Placing an hermetic barrier, such as a formed layer of lead, between the armor and the cable core appears to be an effective means of protecting the fiber from the degrading effects of hydrogen.

1. Introduction

It is well known that hydrogen gas increases the attenuation of optical fibers.[1,2] In multimode fibers, hydrogen bonds chemically to the dopants in the glass, leading to a large and irreversible increase in the attenuation at and above 1300 nm. In single-mode fibers, with their lower dopant concentrations, the hydrogen does not bond but remains in the molecular state. This molecular hydrogen produces an easily identifiable series of sharp absorption peaks, most notably at 1240 nm. The lack of significant chemical bonding in single-mode fibers makes them relatively insensitive to the effects of hydrogen, and until recently, hydrogen was not thought to be a problem for cables which contain single-mode fibers. To produce a significant increase in attenuation for single-mode fibers, several tenths of an atmosphere partial pressure of hydrogen are required, while only several hundredths of an atmosphere produces a significant increase in attenuation for multimode fibers.

One type of environment which has implicated in the generation of hydrogen is the submarine environment. Submarine cables are commonly used to cross rivers, bays, and lakes. Layers of armor wire are often added to otherwise conventional optical cables used in duct and buried applications to provide additional mechanical protection and sufficient weight to facilitate installation. Four factors make submarine cables potentially vulnerable to the effects of hydrogen:

- Armoring the cable increases the amount of metal which is subject to corrosion, both galvanic corrosion between the armor wires and other dissimilar metals in the cable and also self-corrosion of the galvanized steel armor wires
- The higher pressure at the depths encountered in submarine installations permits higher partial pressures of hydrogen than at atmospheric pressure
- The submarine environment is highly conducive to corrosion, both galvanic and bacterial
- Stray current pickup by the armor wire may produce hydrogen

Because of these concerns, a series of diagnostic measurements of installed submarine cables was begun in 1986. At the 1988 International Wire and Cable Symposium, we reported results from the first phase of these measurements, and significant amounts of hydrogen were found in all three of the single-mode submarine cables which were measured.[3] This conclusion was based upon spectral attenuation measurements performed in the field environment, and the distinctive spectral shape of molecular hydrogen was observed in all three cases. An example of one of these measurements is shown in Figure 1. The partial pressures of hydrogen found ranged from 0.3 to 0.7 atmospheres, a surprisingly large amount, and these pressures were fairly well correlated with the average depth of the cables.

Measurements of one of the cables four times over a 14 month period revealed that the amount of hydrogen present, and therefore the attenuation, was slowly increasing with time.

These three cables were of similar designs and were located in a similar environment, so additional measurements are needed to study the dependence of the hydrogen effect on cable design and environment. However, field spectral attenuation measurements are difficult to perform, and the equipment is bulky and fragile. For the next phase of the study, an easier and more readily transported test set was needed so that a larger number of cables, of different designs and in different locations, could be measured. In this paper, we report on the use of an OTDR to measure 23 installed submarine cables.

In the next section, the measurement of the hydrogen effect in the field is discussed, and the motivation for the use of an OTDR is explained. In Section 3, the data taken with this set on 23 different submarine cables is summarized. In Section 4, the highly nonuniform length dependence of the hydrogen effect observed for 3 of the cables is discussed. In Section 5, additional measurements of the time dependence of the hydrogen effect are presented Finally, in Section 6, conclusions are drawn.

2. Measurements of the Hydrogen Effect

2.1 *The Characteristic Signature of Hydrogen*

When hydrogen is generated in a cable, it diffuses readily into the glass fibers, either remaining in a molecular state or dissociating and chemically bonding to the glass. At the relatively low temperatures encountered in the submarine environment, the extent of chemical bonding in single-mode fibers should be negligible.[2] In the molecular state, hydrogen causes a series of readily observable absorption peaks in the 1100 to 1600 nm region including one particularly strong, narrow peak at 1240 nm.[1,2] A typical spectral attenuation plot showing the effects of hydrogen is shown in Figure 1. Any measurement of an installed cable to determine whether hydrogen is present should look for this characteristic molecular hydrogen absorption peak. This distinct peak is unique to the molecular hydrogen effect and unlikely to be confused with most other loss-increasing mechanisms, such as microbending or macrobending, which have different spectral signatures. One other loss mechanism, absorption due to OH^-, can be present at 1240 nm, but OH^- absorption at 1240 nm will generally be much less than .1 dB/km while hydrogen present in significant quantities will produce losses much larger.

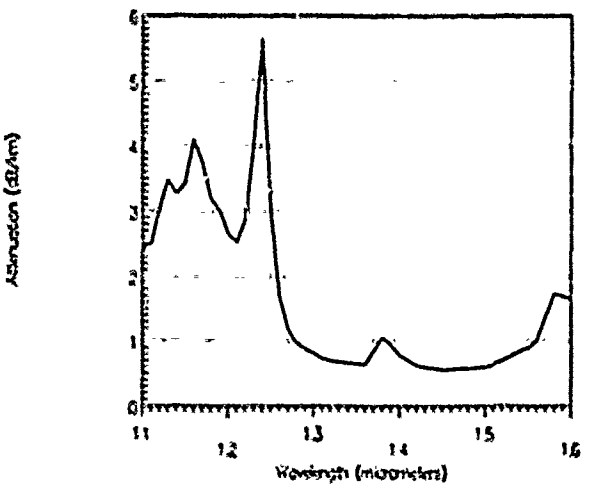

Figure 1. Spectral Attenuation, Hydrogen Present

The height of the prominent 1240 nm hydrogen peak is proportional to the partial pressure of hydrogen present so that a measurement of the height of this peak can be used to estimate the amount, or partial pressure, of hydrogen present. One atmosphere partial pressure of hydrogen produces an added loss at 1240 nm of approximately 7 dB/km.

2.2 *Spectral Attenuation Measurements*

The most straightforward method for measuring the height of the 1240 nm absorption peak is to perform a spectral scan. Spectral attenuation test sets are commonly used in factories and laboratories, but the relative fragility of the equipment makes it ill suited to field applications. The cutback method[4] is commonly used and is generally considered the most accurate attenuation measurement. Since cutback is destructive, for a field measurement a similar method, attenuation by substitution or insertion loss, has been used with little loss in accuracy. However, either of these spectral methods have other disadvantages. First, they measure only end-to-end attenuation and give no resolution of the attenuation variation along the cable. This is a major disadvantage since the type of submarine cable used in the trunk network usually represents only a small part of the span, and the effect of hydrogen on a one or two kilometer submarine cable is easily lost in the measurement of 20 or 30 kilometers of cable between Central Offices. Second, commercially available test sets require that the launch and detect fibers be at the same location,

which requires a loopback to measure installed cables. This limitation can be overcome by building a test set with remote-end capability, but this increases the cost and difficulty of the measurement.

Because of these disadvantages to the use of spectral attenuation as a diagnostic tool for measuring the effects of hydrogen on installed cables, the use of OTDRs for this purpose was investigated.

2.3 Optical Time Domain Reflectometry

The use of OTDRs is well established, as are their advantages and disadvantages. The OTDR performs a single-ended measurement. However, unless the fiber is perfectly uniform along its length, the attenuation readings of the OTDR can be in error due to the differences in backscatter capture along the fiber. In practice, this disadvantage can be overcome by performing the measurement from both directions, but this eliminates one of the major advantages of the OTDR.

Another advantage to the use of an OTDR is its ability to resolve the variation of attenuation along the length of the cable. This is a major advantage in this work since the submarine cable is typically only a small portion of a much longer cable section, and the use of an OTDR permits the attenuation of the submarine cable to be isolated from the attenuation of the rest of the section. Also, if the submarine cable is sufficiently long, the variation of the hydrogen effect along it, perhaps due to depth or local environment, can be studied.

OTDRs are commonly used to measure single-mode fibers at 1310 nm and at 1550 nm. 1310 nm is relatively insensitive to hydrogen, but 1550 nm is somewhat more sensitive. However, since added attenuation at 1550 nm could be caused by a number of factors, including hydrogen, a measurement at 1550 nm is not a conclusive indicator of the presence of hydrogen. For a conclusive measurement of the hydrogen effect, an OTDR should operate at 1240 nm, a wavelength which is not commonly used in OTDRs. As a baseline, from which the added attenuation due to hydrogen can be calculated, a dual wavelength OTDR, operating at 1310 nm in addition to 1240 nm, is needed. Since variations in backscatter along the fiber are not highly wavelength-dependent, bidirectional measurements are not needed to determine the difference in attenuation at these two wavelengths. Bidirectional measurements would be needed if the absolute attenuation at either wavelength were desired.

The OTDR used for the measurements reported in this paper has a dual wavelength source plug-in operating nominally at 1240 nm and 1310 nm. The actual operating wavelengths were found to be 1236 nm and 1313 nm. Since the center wavelength of the "1240 nm" laser does not correspond exactly to the center of the hydrogen peak (which we have measured to be near 1238 nm), the measurements made with this OTDR may slightly underestimate the amount of hydrogen present. Comparisons of spectral scans to OTDR measurements has given agreement to within 20% at 1240 nm. To calculate a hydrogen indicator in a manner consistent with that in the previous paper,[3] the attenuation measured at these two wavelengths are subtracted, and the difference in the Rayleigh scattering loss expected at these two wavelengths is also subtracted so that the hydrogen indicator represents only the attenuation attributable to hydrogen at the peak near 1240 nm. The scattering loss is well approximated over this limited wavelength range as $\alpha_{scat} = \lambda^{-4}$, where λ is the wavelength in μm. Between the measurement wavelengths of 1236 nm and 1313 nm, scattering loss then would be expected to decrease by 0.092 dB/km, leaving for the hydrogen indicator

$$h_{indic} = \alpha_{1236nm} - \alpha_{1313nm} - 0.092$$

This hydrogen indicator should be zero if there is no hydrogen present, but the presence of OH^- absorption will typically give a hydrogen indicator of a few hundredths of a dB. The indicator is proportional to the partial pressure present, and a value of 7 dB/km would imply a partial pressure of approximately 1 atm of hydrogen.

To automate the analysis of the data and to automate the measurement, a portable computer was interfaced to the OTDR. The computer set the OTDR parameters and recorded traces at both wavelengths for later analysis.

3. Detailed Results of Measurements

3.1 Summary

23 submarine cables from the Northeast, South, and Western regions of the continental United States were measured with the OTDR. Each cable was given a one letter code for identification. Since Bellcore was asked not to disclose the exact location of these cables, the code is not intended to be mnemonic. 21 of the 23 were armored with one or more layers of galvanized steel wires (cable N was unarmored, and cable X was armored with stainless steel wires rather than galvanized steel wires).

Data was analyzed, as described in the previous section, to compute a hydrogen indicator. From marine charts, bottom surveys, or information provided by the local engineers, the average depths were estimated. Any significant departure from uniform attenuation in the submarine section was noted, and three cables which had such nonuniform behavior are discussed further in the next section. The hydrogen indicators for these 23 cables are summarized in Figure 2.

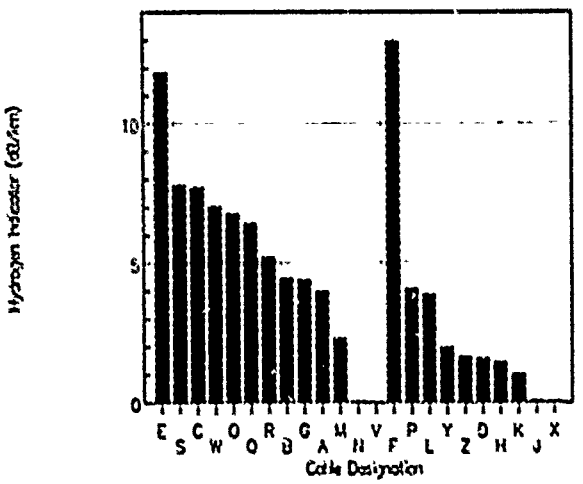

Figure 2. Summary of Hydrogen Measurements

The first 13 cables (E through V) were placed in salt water environments, typically bays or tidal rivers. The remaining 10 cables (F through J) were placed in fresh water, typically inland lakes or rivers. The hydrogen indicators measured range from nearly zero (for cables N, V, J, and X) to 13.0 dB/km for cable F (a fresh water crossing!). In absolute terms, the levels of hydrogen indicators plotted in Figure 2 correspond, at 7 dB/km per atmosphere, to partial pressures as large as 1.9 atmospheres, or about 27 psi!

3.2 Depth Dependence

Some of the variability from cable to cable may be explained by the differing depths of the cables. An upper limit to the amount of hydrogen present can be calculated based upon the fact that these cables will not support pressurization. The maximum partial pressure of hydrogen is then limited by the ambient pressure, which is a function of the depth of the cable. The upper limit to the hydrogen indicator is then

$$h_{indic} < 7(1 + \frac{d}{33}) \text{ dB/km}$$

where d is the average depth of the cable in feet. The hydrogen indicators presented in Figure 2 can be expressed in terms of a percentage of this predicted worst-case value for each of the cables, as shown in Figure 3.

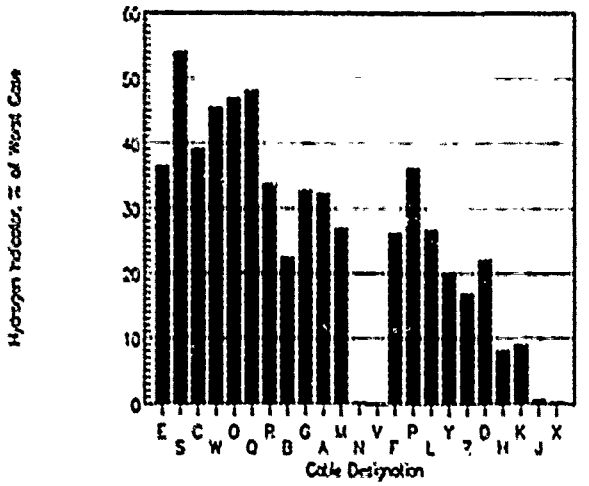

Figure 3. Hydrogen Indicators, Percent of Worst Case

Accounting for depth differences in this manner explains some, but not all, of the variability in the hydrogen indicator measured for these cables, as can be seen from the greater uniformity from cable to cable shown in Figure 3 as compared to Figure 2. However, other factors, such as differences in cable design or the local environment, cannot be neglected. Also, it should be pointed out that, for several of these cables, the average depths are at best rough estimates since marine surveys or accurate charts were not always available.

To further study the dependence of the hydrogen indicator on depth, Figure 4 plots one against the other for the 19 cables which were affected by hydrogen (excluding hydrogen-free cables N, V, J, and X, which will be discussed in more detail later). Cables installed in fresh water are plotted with an "F" on this plot, and salt water installations are plotted with an "S". Linear regression was applied to the fresh and the salt water cables separately, and the two best fit lines are plotted in Figure 4. The higher of the two is the best fit for salt water, and the lower is the best fit for fresh water. Correlation coefficients are 0.67 for salt water and 0.89 for fresh water. Eliminating the one outlier at 60 ft (cable B) improves the correlation for salt water cables to 0.81. Cable B was unusual in several respects, as will be

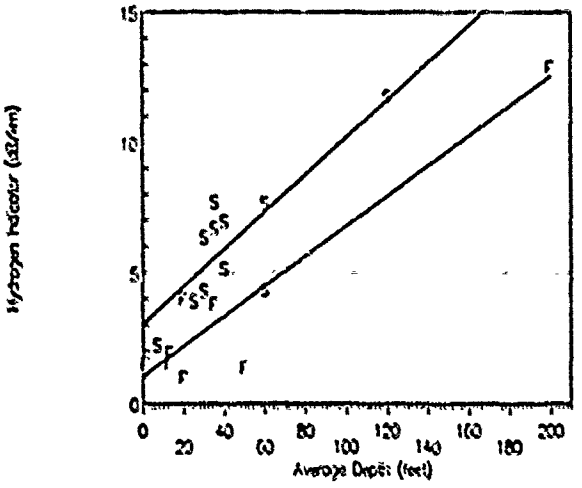

Figure 4. Depth Dependence of Hydrogen Indicator

discussed further in Section 4. From Figure 4, it is clear that salt water is a harsher environment, and the levels of hydrogen observed are consistently higher in salt water than in fresh water.

While the dependence of the hydrogen indicator on depth is important, this one factor alone does not explain the amount of hydrogen present in these cables. It is also interesting to note that the y-intercept of the best-fit lines are not zero. The linear models predict that a submarine cable placed at the surface would have a hydrogen indicator of about 3 dB/km in salt water or about 1 dB/km in fresh water. This prediction was well tested by cable D, which was placed in a shallow fresh-water swamp. The hydrogen indicator for cable D was 1.6 dB/km.

3.3 Cables with no Measurable Hydrogen Effect

While 19 of the 23 cables are clearly degraded by hydrogen, and the levels of hydrogen encountered are extremely large, four cables are clearly unaffected by hydrogen- cables N, V, J, and X. These four cables will be discussed in some detail.

Cable N is significantly different from the others in that it has no armor wires. The cable has a conventional poly-steel-poly jacket and was installed across a salt water bay. This cable was buried several feet into a soft bottom soil, and since there was no significant boat traffic in this area, armor was not needed. Armored submarine cables installed in similar environments in the same area were affected by hydrogen. The absence of hydrogen in this unarmored cable points to the corrosion of the armor wires as the probable source of hydrogen in the other armored cables.

Cable X was also armored, but with stainless steel wires rather than galvanized steel wires. Unfortunately, cable X was installed only 7 months prior to the measurement, so the absence of hydrogen after only 7 months is not conclusive. Hydrogen-generating corrosion and diffusion of hydrogen into the core of the cable may not yet have reached equilibrium, and additional measurements are needed.

Cables V and J, on the other hand, are armored. Cable V is installed in salt water across a bay, and cable J is installed in a fresh water river. However, in one significant regard, the construction of these cables differs from most of the other armored cables. A 3 mm layer of lead was formed between the armor wires and the cable core, and this lead evidently formed a barrier to the entry of hydrogen into the cable core.

4. Nonuniform Distributions of Hydrogen

Three of the cables measured had significantly nonuniform distributions of hydrogen. That is, the amount of hydrogen varied considerably from one part of the cable to another. This might be expected if, for example, the depth of the cable also varied considerably, or if the bottom conditions were more conducive to corrosion at one end of the cable than at the other.

First, consider cables Y and Z. These two cables, which cross the same bay a few hundred feet apart, start in relatively deep water (40 to 45 feet) in a navigation channel at the end nearest the point where the OTDR was located, and then rise to a relatively shallow shelf, 8 to 10 feet deep, for the remainder of the crossing. In Figure 5, the OTDR traces for cable Y are shown. The submarine crossing begins approximately 1.6 km from the Central Office where the OTDR was located, and it ends approximately 6.7 km away. The deep water section lies between 1.6 and 2.4 km, where the slope of the 1240 nm trace is noticeably steeper than before 1.6 km. However, the steepest section begins at 2.4 km, continuing to approximately 4.4 km, where the slope once again becomes relatively shallow. This behavior is not well correlated with the depth along the cable. OTDR traces for Cable Z are similar, except that the route which cable Z follows is slightly shorter. Traces are shown in Figure 6.

Breaking these two traces into three regions, over which the traces are well characterized by a straight line, and applying linear regression, the hydrogen

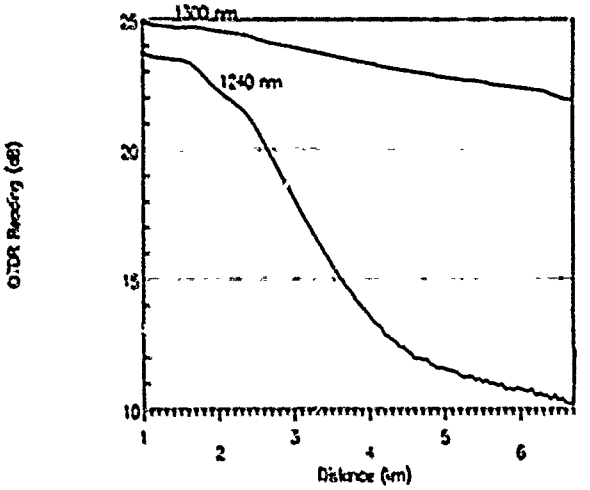

Figure 5. OTDR Traces, Cable Y

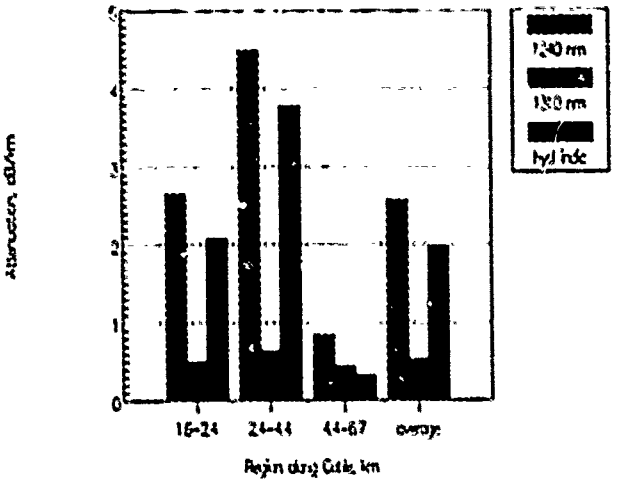

Figure 7. Length Dependence, Cable Y

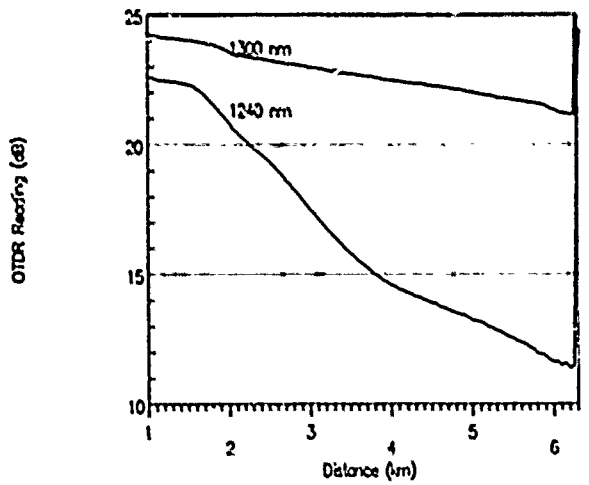

Figure 6. OTDR Traces- Cable Z

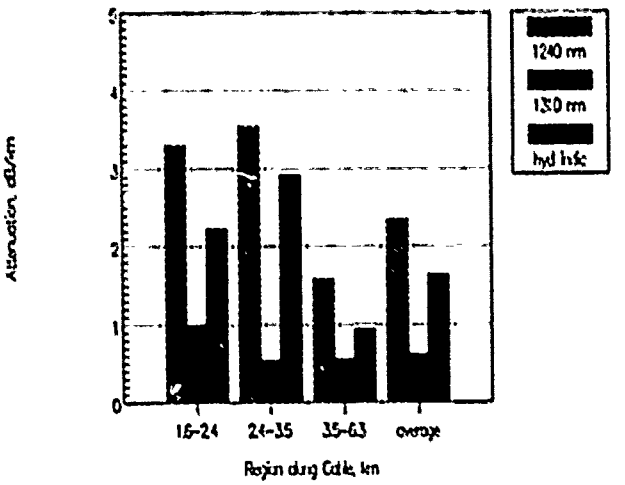

Figure 8. Length Dependence, Cable Z

indicator in each of the three regions for the two cables can be computed. These are plotted along with the attenuations at 1310 nm and at 1240 nm in Figures 7 and 8.

In the previous paper,[3] spectral attenuation measurements for these two cables (which were then called Cable 2), revealed that the levels of hydrogen were significantly different between the two cables. This difference between two identical cables installed in the same environment remains a mystery.

Finally, consider cable B. In Figure 9, the OTDR traces are plotted, and in Figure 10, the depth profile is plotted.

Cable B has three distinct regions where the hydrogen indicator is well characterized by a straight line-between 0.2 and 0.6 km, between 0.6 and 1.6 km, and from 1.6 km to the end of the cable at 1.9 km. The hydrogen indicators resulting from linear fits in each of these three regions are plotted in Figure 11. If depth were the dominant environmental factor, then the middle region, which is the deepest, would have the most hydrogen. In fact, it has the least. The relatively shallow region between 0.2 and 0.6 km, where the depth varies from 30 to 70 feet, has by far the most hydrogen, with a hydrogen indicator of just under 14 dB/km. This corresponds to a partial pressure of just under 2 atmospheres, which is still

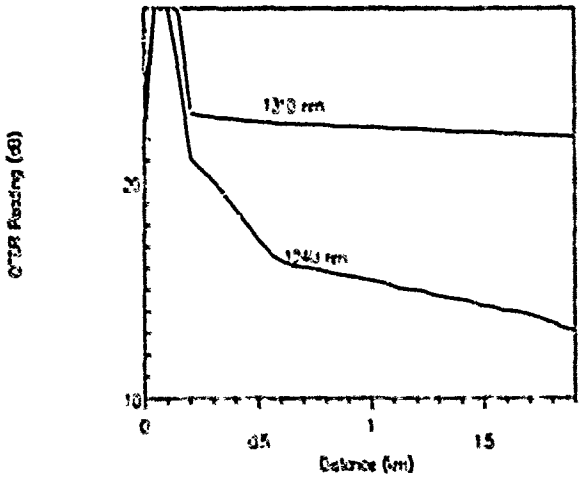

Figure 9. OTDR Traces, Cable B

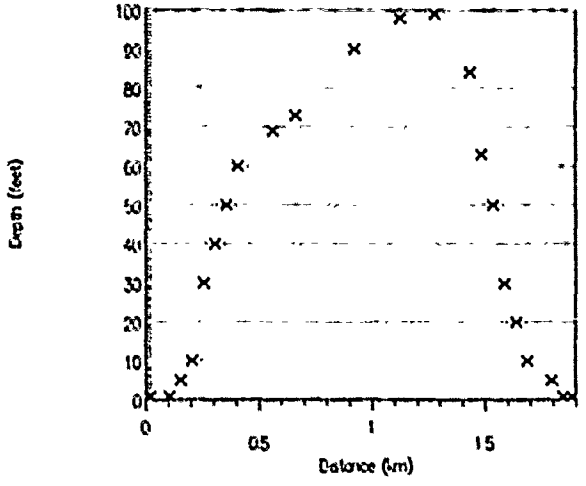

Figure 10. Depth Profile of Cable B

slightly below the predicted worst-case value for this region of the cable, which has an average depth of 50 feet.

In these three cases, the variation of the hydrogen indicator along the cable is poorly correlated with the depth. Other unknown factors, such as environmental variations or variations in cable construction, must account for this anomaly.

5. Time Dependence of Cable B

In the previous paper[3], the time dependence of one cable was studied over a 14 month period, and a power law model for the observed hydrogen indicator

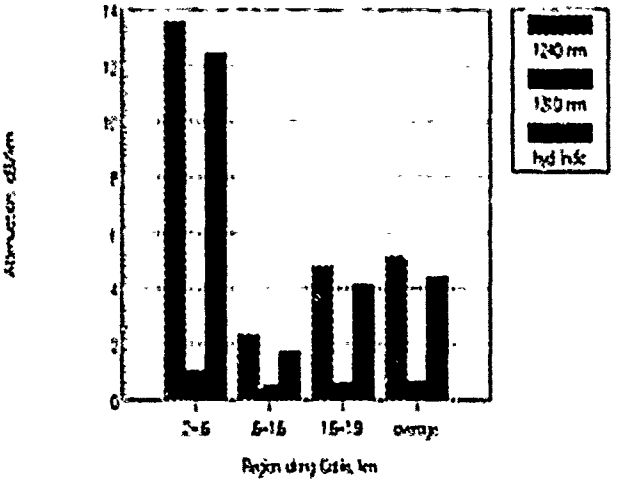

Figure 11. Length Dependence, Cable B

was postulated (this cable was "Cable Number 1" in the previous paper). A power law exponent of 0.24 gave a correlation coefficient of 0.99. One additional spectral measurement of this cable was performed, and the time dependence is shown in Figure 12. With this additional measurement, the best fit power law exponent is now 0.18, which is significantly lower. However, the correlation has dropped to 0.96.

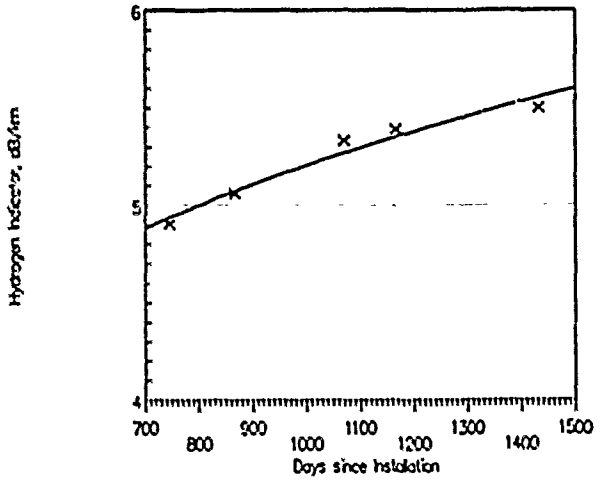

Figure 12. Time Dependence of Cable B

In spite of the change in the power law exponent, the conclusion reached in the previous paper that the rate of increase in the hydrogen indicator with time is slowing is still valid. One possible explanation for this slowing can be found in the length dependence of the hydrogen indicator, as presented in the previous

section. Since most of the hydrogen is isolated in one small section of the cable, where the partial pressure of hydrogen is approaching the ambient pressure, significant diffusion of hydrogen out of this cable section is undoubtedly significant, and this diffusion may limit further increases.

6. Conclusions

We have reported that almost all armored cables in either fresh or salt water submarine environments are affected to some degree by the effects of molecular hydrogen. Only four cables were unaffected. Two had a layer of lead under the armor wires providing an hermetic barrier to the entry of hydrogen generated by the corrosion of the armor wires. We expect that all submarine cables containing laters of galvanized armor wires will be impaired to some extent by molecular hydrogen unless some hermetic barrier to the hydrogen is present.

The levels of hydrogen encountered depend upon the depth and upon the salinity of the water, but other local environmental and cable design factors also have a significant effect. In three cases, the variation of the level of hydrogen encountered along the submarine cable varied significantly and in a fashion which was not correlated to the depth of the cable. Also, two cables of identical designs installed across the same body of water but several hundred feet apart behaved significantly differently. We conclude from these observations that local variations in the environment, such as the nature of the sediment or depth of burial, play an important role in determining the amount of hydrogen generated.

In the previous paper, we recommended that users leave sufficient margin in span designs for the worst-case loss increase, which can be predicted from the average depth d in meters and the length L in kilometers as follows:

$$0.3\,L\left(\frac{d}{10}+1\right)\text{ dB between 1290nm and 1330nm}$$

$$0.8\,L\left(\frac{d}{10}+1\right)\text{ dB between 1525nm and 1575nm}$$

This paper has reinforced that conclusion. Loss increases of as much as 54% of these worst-case values have been observed.

To avoid the effects of hydrogen in submarine cables, two alternative design paths should be considered. First, using existing armor designs, some hermetic barrier to the entry of hydrogen should be provided. This could take the form of a metallic tube protecting the cable core, and may be of formed lead or other impermeable metal with a soldered or welded seam. An overlapped seam, which was present in many of the cables tested, is not sufficient to prevent the entry of hydrogen. Alternatively, hermetically coated optical fibers could be used to prevent the entry of hydrogen. Such coatings must be optimized for resistance to the entry of hydrogen rather than for a reduction in susceptibility to static fatigue, as is commonly done.

A second possible design path for the prevention of deterioration due to hydrogen is to avoid generating hydrogen in the armor wires. This might be accomplished by using corrosion-resistant metals in the armor wires or by coating the armor wires with a protective polymer. However, stray current pickup could still lead to the generation of hydrogen. Additional measurements of installed cables containing corrosion-resistant metals are needed to determine whether this approach is effective.

The nature of the corrosion which provides the source of the hydrogen found in these cables has not yet been positively identified. Both bacterial and galvanic corrosion are consistent with these observations. Work continues at Bellcore toward a better understanding of the nature of this corrosion.

Acknowledgements

The authors are greatly indebted to several engineers in the telephone companies, without whose assistance these measurements could not have been made. Unfortunately, this acknowledgement must be given anonymously. The authors also acknowledge contributions by Bellcore colleagues George Schick and Karen Tellefsen toward a better understanding of the corrosion mechanisms responsible for the generation of hydrogen.

References

[1] K. Noguchi, Y. Murakami, and K, Ishihara, "Infrared Loss Spectrum of Hydrogen Molecules in a Silica Fiber," *Electronics Letters*, Vol. 19, No. 24, P. 1045, November 24, 1983.

[2] J. D. Rush, K. J. Beales, D. M. Cooper, W. J. Duncan, and N. H. Rabone, "Hydrogen Related Degradation in Optical Fibers-Implications and Practical Solutions," *Br. Telecom Technol. J.*, Vol. 2, No. 4, p. 84, September 1984.

[3] W. T. Anderson, A. J. Johnson, J. P. Kilmer, and R. M. Kanen, "Hydrogen Gas Effects on Installed Submarine Single-Mode Fiber Cables," *Proceedings of the 37th International Wire and Cable Symposium*, p. 188, November 1988.

[4] EIA/TIA-455-78, FOTP-78, "Spectral Attenuation Cutback Measurement for Single-Mode Optical Fibers"

Authors

William T. Anderson was born in Buckhannon, West Virginia, in 1948. The received the B.S.E.E degree with Highest Honors from Georgia Institute of Technology in 1970, the M.S. degree in Electrical Engineering from Stanford University in 1971, and the Ph.D. degree in Electrical Engineering from Georgia Institute of Technology in 1979. He worked at Bell Telephone Laboratories from 1970 to 1983 in the areas of transmission and crosstalk in multipair cable and single-mode fiber measurement and design. In 1983, he joined Bell Communications Research, and is presently responsible for optical cable requirements and analysis. Dr. Anderson is a member of the Optical Society of America.

Aaron J. Johnson was born in Washington, DC, in 1958. He received the B.S. degree in Electrical Engineering and Economics from Carnegie-Mellon University in 1980 and the M.S. degree in Electrical Engineering from Georgia Institute of Technology in 1981. He worked for IIT Research Institute from 1982 to 1984, where he was engaged in electromagnetic compatibility analysis. Since 1984, he has been with Bell Communications Research where he has been developing novel optical fiber measurements and writing generic requirements for optical fibers and optical fiber cables. Mr. Johnson is a member of the Optical Society of America.

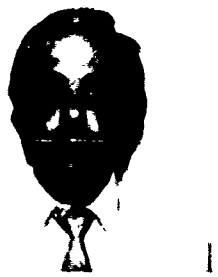

Anthony DeVito joined Bellcore's Optical Cables District, as a Member of Technical Staff, in July, 1988. He is currently involved in post-mortem analysis and writing of generic requirements for optical fiber cables. Prior to joining Bellcore he worked as a member of the Transmission Product Evaluation Staff at BellSouth Services in Birmingham, Alabama. Mr. DeVito's responsibilities included the technical analysis of fiber optic splicing equipment, test sets and optical cables. Mr. DeVito has 18 years experience with the Bell Operating Companies in the area of Outside Plant Construction, Construction Methods, and Fiber Cable Installation and Testing.

INVESTIGATION OF TOTAL AND DISTRIBUTED HYDROGEN LEVELS IN INSTALLED FIBEROPTIC SUBMARINE CABLES

S. Hopland

Norwegian Telecommunications Administration
Cables Division,
Oslo, NORWAY.

ABSTRACT

In this paper we present new data for hydrogen induced attenuation in installed fiberoptic submarine cables in which no hydrogen barrier was used. We have performed both spectral measurements and used a 1238 nm OTDR module to examine the hydrogen induced loss. We have shown that the hydrogen levels within 2.5 years after installation are much lower than reported by others. A trend for a small increase in hydrogen induced loss at 1244 nm with time have been observed. No evident hydrogen induced loss dependancy on sea depth was found. Enhanced hydrogen evolution was registered in a small region near a damage on the outer jacket of the cable. We believe that a corrosion process is responsible for the observed hydrogen evoluton.

1. INTRODUCTION

In recent years, a lot of attention has been focused on the effects of hydrogen in fiberoptic cables . The evolution of hydrogen gas (H_2) inside or outside the cable will, if H_2 is allowed to diffuse into the fibre core, cause attenuation increases which may impair the signal transmission.

The presence of molecular hydrogen (H_2) in the core of an optical fibre causes attenuation increases with characteristic spectral features. The most evident is a strong and narrow absorption peak near 1240 nm [1]. At the transmission wavelengths 1300 nm and 1550 nm the loss increase is much smaller, but generally increases with increasing wavelength [1]. A small absorption peak appears at 1590 nm [1]. If the hydrogen in the fiber core has reached equilibrium with the hydrogen source, the induced loss at the 1240 nm peak wavelength is directly related to the hydrogen partial pressure at the fiber surface [2], and thus an indicator of the hydrogen level in the cable core. From the height of the 1240 nm peak we can also estimate the induced losses at other wavelengths.

In single mode fibres, losses can also be induced by reactions of H_2 with hydroxyl (OH^-); thereby increasing the absorption peak at 1380 nm [3]. Also, a broadbanded attenuation will be induced [4]. The magnitude of these losses are dependant on hydrogen level, time, temperature and fiber type. It can be shown, however, that in a submarine cable life time (30 years) at + 3-5 °C, these losses are negligible compared to the H_2 induced losses for all relevant hydrogen levels at the transmission wavelengths 1300 nm and 1550 nm [5].

In some submarine cable constructions a hermetic metal tube encloses the cable core and forms a hydrogen barrier. Here, the hydrogen generated outside the tube is prevented from diffusing into the cable core. On the other hand, hydrogen from inside the tube is not allowed to diffuse out. Another method of preventing hydrogen to reach the fibers, is the use of hydrogen absorbing filling compounds. Other constructions, like the ones used by the Norwegian Telecommunications Administration (N.T.A), do not use any hydrogen barriers, which allows for hydrogen to diffuse freely in and out of the cable structure. In this case, extra precaution must be taken in selecting proper materials in the cable construction to avoid hydrogen evolution.

So far, few data about hydrogen levels in installed submarine cables have been reported. Recently, alarming levels of hydrogen were observed in some installed submarine cables of the "open " type, which severely restricted their use [6].

In this work, we have examined the hydrogen levels in a number of our installed submarine cables. We present new data of the hydrogen induced attenuation and offer some indications of the reasons for the hydrogen evolution.

2. CABLE CONSTRUCTION AND MARINE ENVIRONMENT

The N.T.A. uses cables from two different manufacturers. The cable construction consist of a metal free cable core which may be of the slotted core or the loose tube design. The cable core is surrounded by a jacket of polyethylene, and then follows an armour consisting of one or two layers of galvanized steel wires. Two layers of steel wires are applied if extra tensile strength is needed for protection. A bitumen or asfalt filling compound is used around the steel wires to prevent longitudinal water intrusion and corrosion. Finally, an outer jacket of high density polyethylene forms an extre protection against water corrosion. The cable construction for one layer of steel wires is shown in Fig. 1.

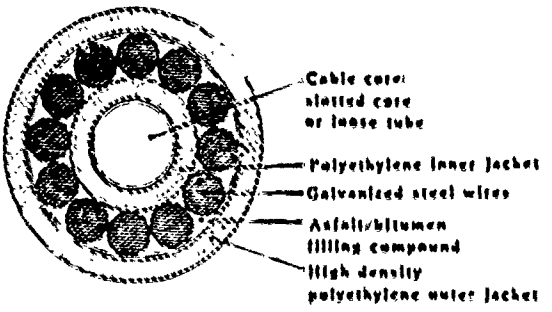

Figure 1: Submarine cable construction.

We have installed several submarine cables along the N.rwegian coastline as parts of our regional and trunk network. The cables are usually laid directly on the bottom of the sea. The sea floor conditions are not known in details. Typically, the bottom may be rocky, or it may consist of clay and sand. The depths may vary between 20 and 1000 meters and the water condtions are salt.

3. HYDROGEN SOURCE

In our submarine cables, potential hydrogen sources are degradation of polymer materials and outgassing or selfcorrosion of metal members.

All the materials used in the cables from the two manufacturers were tested individually for hydrogen outgassing (in dry atmosphere) at elevated temperatures by means of gas chromotography. Only negligable hydrogen evolution was observed in these experiments.

However, in an ageing test, where a long length of cable was kept at + 70° C for 7 days, an absorption peak near 1240 nm was detected; showing the presence of hydrogen. When this ageing test was performed on a duct cable, which is essentially identical to the inner part of the submarine cable except for the armour and the asfalt/bitumen filling, no traces of hydrogen was found.

This suggested that hydrogen was generated from the combination of steel wires and asfalt/bitumen, probably as a result of a corrosion process assisted by remnants of water in the filling compound.

4. MEASUREMENTS

4.1 Spectral measurements

Spectral measurements were performed using a spectrum analyzer with a wavelenght accuracy of ± 0.5 nm. A stabilized white light source was placed in the far end of the measured cable section. The sections consisted of partly submarine cable and partly land cable. Typically, the submarine cable constituted 50 -100 % of the measured cable section.

Initially, spectral loss curves were compared with loss curves taken with a standard laboratory equipment, and very good agreement was found.

The peak wavelenght of the H_2 absorption was found to be 1244 nm.

4.2 OTDR measurements

In addition to the spectral measurements, an OTDR with a laser source operating at 1238 nm wavelength was used . This is a 6 nm offset from the H_2 peak wavelength. Therefore, the observed loss increase at 1238 nm is only half of the loss increase at 1244 nm [7]. From the OTDR traces, we could reveal possible variations of the hydrogen induced loss along the individual submarine cable lengths.

Standard OTDR equipments at 1318 nm and 1550 nm were used for control measurements.

4.3 Measured cables

We have measured 11 different submarine cables with single armour from two different manufacturers. The cables had been in the sea environment for a time period of 0.5 - 2 years, and the average sea depth were ranging from 20 to 800 meters as shown in Table 1.

Submarine cable	Length (km)	Time after installation (months)	Average sea depth (m)
1 *	11.4	15	100-150
2	5.7	19	450-500
3 **	8.9	15.5	50
4	10.8	6	225
5	10.6	6.5	100
6	13.4	6.5	700-900
7	11.8	15	10-20
8	10.7	15	100-150
9	11.1	11.5	100-150
10 ***	7.1	24	500
11	5.4	19	400-500

Number of steel wires in the armour: 9-11.

* This cable has 13 steel wires in the armour.
** Cable has damage on outer jacket (see 5.2.2).
*** This cable has asfalt/polypropylene yarn as outer jacket.

Table 1: Measured submarine cables

Smaller lenghts of cable (leftovers) from some of the cables listed in Table 1, which were stored dry on land at approximately + 10 ° C, were also measured. Long lenghts of fiber were provided by looping fibers in each cable sample.

5. MEASUREMENT RESULTS

5.1 Spectral measurements

Since the installed cables were measured after at least 6 months in the sea, we can assume that the hydrogen diffusion has reached stationary condition, and that the induced losses at 1244 nm reflect the hydrogen level in the cable core.

The hydrogen induced loss at 1244 nm was calculated from the spectral loss curve. A correction was made for the contribution of the 1380 nm peak [4]. The latter is usually negligible, but will play a role when the hydrogen induced losses becomes small. We measured routinely 3 fibers in each cable, and average values were used in the calculations.

The hydrogen induced losses of the installed cables at 1244 nm are plotted versus average sea depth as shown in Fig. 2, and versus time after installation as shown in Fig. 3. Also included in Fig. 3 are the hydrogen induced losses at 1244 nm of corresponding cable lenghts stored dry on land for the same time period.

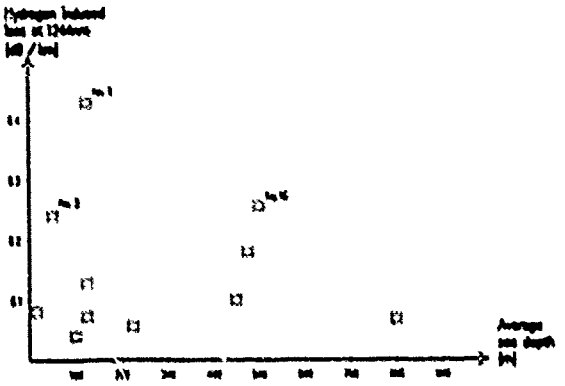

Figure 2: Hydrogen induced loss versus average sea depth for different cables.

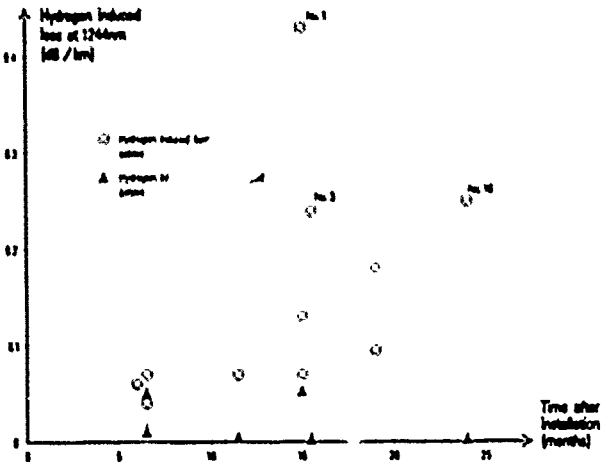

Figure 3: Hydrogen induced loss versus time after installation for different cables.

From Fig. 2, there are no evident indications of any depth dependance of the hydrogen induced loss. This was further investigated by means of the 1238 nm module (see section 5.2.1).

The observed hydrogen induced losses of the installed cables are approximately one order of magnitude lower than reported earlier [4]. No attenuation increases attributable to hydrogen at 1318 nm and 1550 nm could be detected in the cables.

The hydrogen induced losses in the dry stored cable samples are systematically lower than in the corresponding installed cables. The corrotion process which is dependant on small amounts of water, have decreased, possibly as a result of a drying effect of the long term storage of the cable samples.

Cable no. 10 has a different outer protection (asfalt/polypropylene yarn) than the other cables. This seems not to affect the hydrogen evolution in the cable significantly, at least at this time of observation (see Fig. 3).

All the measurements have been made on different cables, which have been in the sea for different durations, and the data indicate a slight increase in the hydrogen induced loss with time. To further investigate this, some of the cables have been remeasured 6 months later, and the results are shown in Fig. 4.

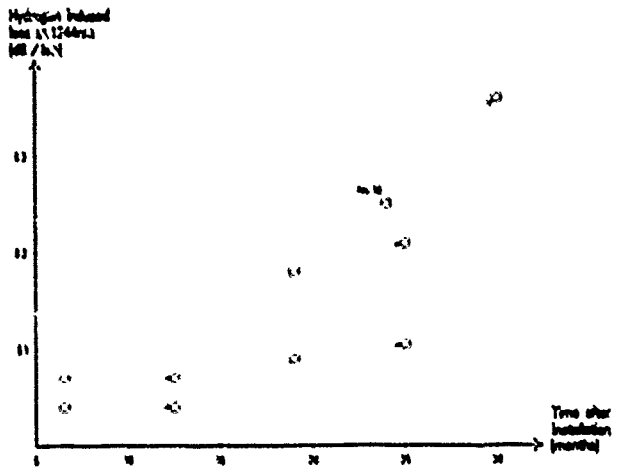

Figure 4: Hydrogen evolution versus time on individual cables.

A small attenuation increase with time have been registered on cables with high density polyethylene jackets. An interesting observation was that the attenuation increase in the cable with asfalt/-polypropylene yarn was more pronounced than in cables with high density polyethylene (see Fig. 4). In the cables with the lowest hydrogen levels, it becomes generally difficult to detect small changes, and here more time and further measurements are needed to detect possible changes in

hydrogen levels. However, the repeated measurements indicates a trend for a small increase in hydrogen induced loss with time.

Obviously, for the installed cables no drying effect will take place. On the contrary, water may slowly penetrate the outer jacket, and increase the water content in the vincinity of the armour steel wires. This would tend to increase the corrotion and hence the hydrogen evolution on a long term basis, which have been observed in our measurements. On the other hand, it is well known that corrotion decreases with time. Therefore, it is difficult to predict any time dependance of the hydrogen evolution at this point of investigation. More data from the installed cables over a longer time period are required in addition to data from relevant laboratory experiments.

5.2 1238 nm OTDR measurements

The 1238 nm OTDR was used as a supplement to the spectral measurements. In cases where it was not possible to obtain spectral loss curves, the 1238 nm OTDR readings were used to calculate the hydrogen induced loss at 1244 nm [7]. We measured routinely 3 fibers in each cable, and average values were used in the calculations. The OTDR module was also used to reveal possible variations of the hydrogen induced loss along the cable lenghts. Possible variations due to depth and local hydrogen sources could readily be registered with the OTDR module.

5.2.1 Depth dependance of hydrogen induced loss

The 1238 nm OTDR traces were examined and compared to the sea depth profiles of the installed cables. In general, many of the OTDR traces were essentially straight lines. In some cables, small variations in the slope of the traces were observed. However, there were no systematic correlation between these variations and the corresponding depth profiles. The variations may be attributable to parameters in the armouring process during fabrication. A typical example of an OTDR trace is shown in Fig. 5. The sea depth profile is also shown.

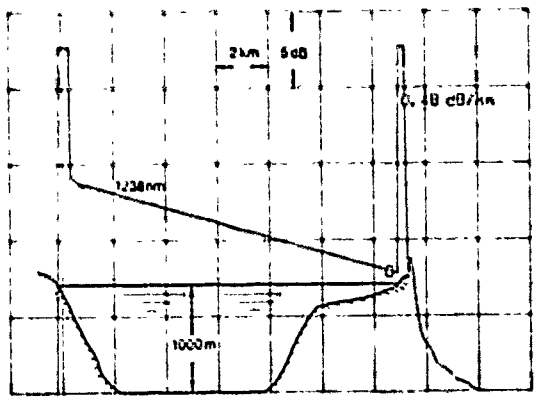

Figure 5: Typical 1238 nm OTDR trace with corresponding sea depth profile.

In summary, our data show no evident dependance on depth of the hydrogen induced losses. This is in contrast to an earlier report [6].

5.2.2 Local hydrogen source

For one of the submarine cables (cable no. 3: loose tube design) we had to change the cable route after the cable had been laid. Part of the cable was retrieved, and relaid in a different route. During the retrieval, the cable jacket was slightly damaged on two locations due to some unintended friction with rocks on the sea bottom. The cable was measured after 21 months with OTDR. The 1238 nm and 1310 nm OTDR traces are shown in Fig. 6. At the damaged points, the traces revealed small regions (200-300 meters) with high hydrogen induced losses. Here, the hydrogen induced loss was estimated to be approximately one order of magnitude higher than the rest of the cable. Longitudinal water intrusion and increased hydrogen evolution due to corrosion explains this effect.

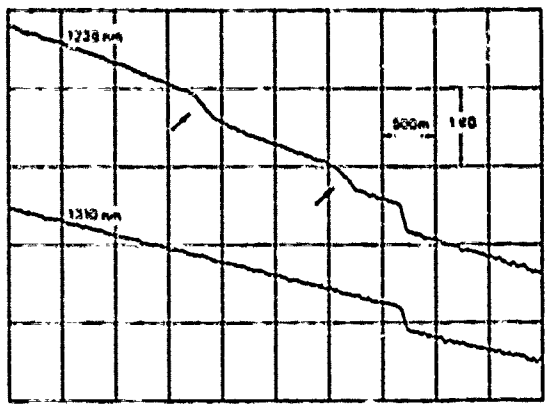

Figure 6: Increased local hydrogen evolution caused by damaged outer jacket.

On a test cable, the time evolution of the local hydrogen source due to damage on the outer jacket was studied [7]. The hydrogen evolution inceased rather quickly (in a few months), but seems not to increase significantly with time in a time scale of 1-2 years.

The "steps" in the OTDR traces attributable to the local hydrogen sources were typically 0.1-0.2 dB at 1238 nm after 1-2 years. For a cable lenght of 10 km, this corresponds to an increase of 0.01-0.02 dB/km in the overall hydrogen induced loss at 1238 nm. From the viewpiont of increased attenuation, this is not crucial. However, a short cable length near the jacket damage is exposed to a high corrosion level, and this could degrade the tensile strength of the armour wires on a long time scale.

Only these two incidents of local hydrogen sources attributable to damaged outer jackets, caused by recovery of submarine cable, were observed.

6. CONCLUDING REMARKS

We have in this investigation supplied at new set of data of hydrogen induced losses in hydrogen barrier-free installed submarine cables which are more optimistic than reported earlier. By spectral and 1238 nm OTDR measurements we have shown that the hydrogen levels within 2.5 years after installation on cables with one layer of armour wires are low. We have not been able to detect attenuation increases attributable to hydrogen at the transmission wavelenghts 1318 nm and 1550 nm. The evidence indicates that corrosion is the hydrogen generating mechanism. We have so far observed a trend for a small increase in hydrogen levels with time for cables with a high density polyethylene outer jacket. A more pronounced attenuation increase was registered when an outer jacket of asfalt/polypropylene yarn was used, probably as a result of poorer corrosion resistance of the outer jacket. No evident dependance of hydrogen induced loss on sea depth was found.

Increased corrotion and hydrogen evolution have been observed locally when the cable outer jacket was damaged and sea water was allowed to penetrate along the armouring wires. However, if the number of such damages are kept low, it will only impose small increase in the overall hydrogen induced attenuation.

7. ACKNOWLEDGEMENT

The author would like to thank I. Gangsø and P. Berglund for assistance in collecting the field data. Also thanks to our cable manufacturers Alcatel STK and EB Cables, for valuable discussions.

8. REFERENCES

1. "Interactions of Hydrogen and Deuterium with Silica Optical Fibers; A Review". J. Stone, Journal of Lightwave Technology, Vol LT-5, pp. 712-733, May 1987.

2. "Hydrogen Susceptibility Studies Pertaining to Optical Fiber Cables". E. W. Mies, D. L. Philen, W. D. Reents and D. A. Meade. Presented at OFC 84, paper WI3.

3. "Transmission Loss Increase in Optical Fibres due to Hydrogen Permeation". K. Mochizuki, Y. Namihira, H. Yamamoto, Electronics Letters 19, pp. 743-745, 1983.

4. "Long Term Loss Stability of Single - Mode Optical Fibers Exposed to Hydrogen". N. J. Pitt, A. Marshall, Electronics Letters 20, pp. 512-514, 1984.

5. Audun Nordvik, A/S Optoplan (Trondheim). Private Communications.

6. "Hydrogen Gas Effects on Installed Submarine Single- Mode Fiber Cables ". W. T. Anderson, A. J. Johnson, J. P. Kilmer, and R. M. Kanen. International Wire and Cable Symposium, 1988.

7. "Measurements on hydrogen evolution in fiber-optic cables by 1240 nm OTDR". S. Hopland and L. Djerkan. SPIE symposium, OE/FIBERS 89. Boston Sept. 89.

8. "On the Ultimate lower Limit of Attenuation in Glass Optical Fibres". D. B. Keck, R. D. Maurer, P. C. Shultz, Applied Physics Letters 22, pp. 307-309, 1973.

Svend Hopland

Norwegian Telecommunications Administration
Cables Division
Munch's gate 5b
N-0130 Oslo 1, Norway

Svend Hopland graduated from the Norwegian Institute of Technology in 1985 with Ph. D. on optical fibers. In 1986 he joined the Norwegian Telecommunications Administration, Cables Division. He is presently a senior engineer on fiberoptic cables.

CORROSION-RESISTANT ARMOR TO PREVENT H_2-INDUCED LOSS IN UNDERWATER (WIRE-ARMORED) FIBER OPTIC CABLE

N. E. Hardwick, III, L. C. Hotchkiss, J. J. Blee and D. L. Philen

AT&T Bell Laboratories
Norcross, Georgia 30071

ABSTRACT

The increasing number of fiber optic routes being installed leads to an increasing number of underwater installations. Expensive right-of-way considerations have led to additional planned "water crossings" in which optical fiber cables are installed across rivers, lakes, and bays. Added loss due to hydrogen generation has been observed in underwater optical fiber cable installations using conventional galvanized steel armor wire. The effect has been observed in different cable designs from multiple suppliers. Extensive on-site measurements and tank testing of wire armor cable immersed in sea water has confirmed these phenomena. Long haul, undersea (transoceanic) type cables (where fibers are contained in a hermetically sealed tube) have not experienced similar H_2 problems.

A new Corrosion-Resistant Armor design is introduced that uses stainless steel armor wires in conjunction with plastic coatings as a superior corrosion preventive measure and to prevent the H_2 effects. This paper introduces the new armor design, discusses the H_2-generation mechanisms, and presents over a year of test data that verify that the improved armor structure eliminates the H_2-induced cable problems.

1.0 INTRODUCTION

Over the last decade, optical fiber cable has experienced a meteoric rise as the predominant means of transmission media in new voice and data communications. Because of the increasing number of optical fiber cable miles being installed in recent years, an increasing number of underwater installations have been necessary. In many instances, these so-called water crossings have been made to effect the most economical right-of-way acquisition.

A recent paper by W. T. Anderson et. al.[1] reported spectral attenuation measurements of installed armored "submarine" cables from several suppliers that contain single mode fibers showing increased attenuation because of the presence of molecular hydrogen. The submarine (i.e., underwater) environment typically requires armoring the optical fiber cable with one or more layers of armor wire, both for mechanical protection from marine traffic as well as to provide sufficient weight for the cable to remain at the water bottom. The Anderson paper[1] suggested a number of possible sources for the hydrogen generation, including corrosion of the galvanized steel wires typically used in wire-armored optical fiber cable, but did not draw a conclusion about the H_2-generation mechanism. This paper discusses the H_2-generation mechanism in detail and presents supporting test data. An improved armor structure is introduced that eliminates the H_2-induced cable problems.

The Improved Corrosion-Resistant Armor design solves the H_2 problem by eliminating the H_2 generation source. This differs from the approach of long haul, undersea (transoceanic) type cables which employ hermetically-sealed tubes[2] to block H_2 ingress to the fiber areas. Another H_2-blocking approach is to use hermetically-coated fibers to stop the H_2 diffusion at the fiber surface.[3] Hermetically-coated fibers can also be used with the H_2-resistant sheath approaches as an extra measure of protection.

2.0 H_2-GENERATION DUE TO GALVANIZED STEEL ARMOR WIRE CORROSION

Typically an underwater cable (other than specially-designed cable for long undersea routes) includes a core portion comprising terrestrial optical fiber cable. This core is protected in water crossings by an oversheath with layers of metallic strength members and twine bedding as well as a tar-impregnated twine outer protective wrap as shown in Figure 1. In conventional practice, the strength members of the armor layer of the cable are made of galvanized steel wire.

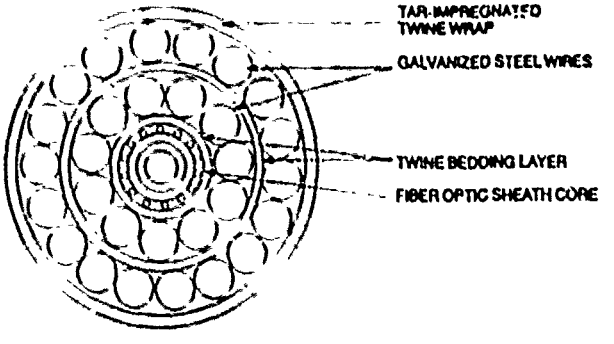

Figure 1. Typical Oversheath Design Using Galvanized Steel Armor Wire for Fiber Optic Underwater Cable

When an underwater cable is deployed, water enters the twine layer and migrates to the interstices of the cable armoring wires because the tar coating on the protective twine wrap does not form an integral water blocking sheath. With the water in contact with the galvanized steel armor wires, self-corrosion and hydrogen generation may occur.

Hydrogen-induced attenuation at both the 1310 and 1550 nm operating wavelengths has been observed in installed, armored underwater optical fiber cables that include the conventional galvanized armor wires. Test data show that even when the core portion of the underwater cable generates no hydrogen, added loss can occur because of the armor wire corrosion.

All metals, except the noble metal gold, have some finite corrosion rate in natural environments. When a metal corrodes, the surface is covered by micro/macroscopic cells where an anodic (oxidation) reaction occurs, i.e., corrosion of the metal, but the surface also is covered by micro/macroscopic cells where a cathodic (reduction) reaction takes place. In acidic and neutral waters this cathodic reaction can produce the deleterious hydrogen molecules. In order for corrosion to occur, a cathodic reaction must occur to consume the electrons liberated in a corrosion reaction, otherwise the corrosion reaction cannot take place. Metals characterized by a relatively high electrochemical reactivity are referred to as active metals, and will be more likely to produce hydrogen than a metal characterized by a relatively low electrochemical reactivity.

2.1 Hydrogen Entrapment in Vicinity of Fibers

In the original traditional armored cable designs, it was thought that because the outer sheathing of the cable was comprised of twine with an application of tar material to the twine, that any hydrogen which was generated would migrate out of the cable and thus no added loss would occur. This has been found to be an incorrect assumption.

Unfortunately, hydrogen does not diffuse readily or completely out of the armored cable structure. The induced H_2 loss scenario is as follows. Water, in the vicinity of the wire outer strength members interacts with the zinc coated, i.e., galvanized, wire and causes corrosion. Corrosion causes hydrogen gas to be given off. The hydrogen that is generated inside the cable occupies the interstices in the cable. Bubbles form, but these may be microscopic in size. The only way for the hydrogen to escape from the cable is as relatively large bubbles. Although the twine-tar layer allows water to enter the cable, it does not readily allow the hydrogen bubbles to coalesce into bubbles which are sufficiently large to escape the cable unless hydrogen generation is very high. Because hydrogen is not highly soluble in water, it remains in the cable until the outside pressure is overcome. (See Figure 2 for a sketch of H_2 entrapment mechanisms.) At 32 feet of water, an additional atmosphere is required to overcome the water pressure.

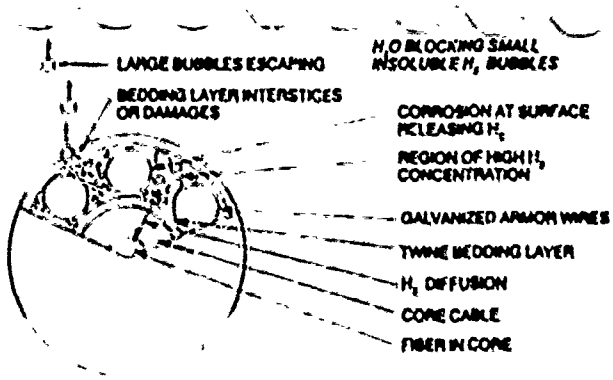

Figure 2. H_2 Generation, Bubble Entrapment and H_2 Inner Diffusion Mechanisms

2.2 Hydrogen Diffusion Into Cable Core

Diffusion is a partial pressure (concentration) driven effect. The partial pressure of hydrogen in the optical fiber cable core is essentially zero, i.e., 10^{-6} atmosphere ambient, and hydrogen cannot readily diffuse into the water because of its low solubility. As a result, the hydrogen diffuses into the cable core, and hence into the fibers, until the partial pressure inside the optical fiber cable equilibrates with that in the outer twine layer. The magnitude of partial pressure will show a depth dependence because the concentration (molecules/cc or partial pressure) will be greater with increasing depth. Hence, added loss in the optical fiber will be in direct proportion to the depth of the cable in the water. (Measurements reported in the Anderson paper[1] support the dependence of H_2-induced loss on depth.)

3.0 CORROSION RESISTANT SHEATH TO PREVENT H_2-GENERATION

An improved Corrosion-Resistant Armor structure that eliminates H_2-induced loss problems due to corrosion is shown in Figure 3. The core cable shown is a Lightpack® cable with Primary RL sheath that was used in the tests. (Table I lists the specifications for single wire, double wire, and triple wire oversheaths for small fiber count core cables.)

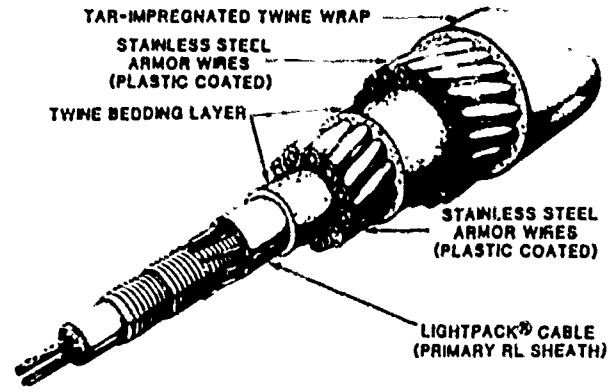

Figure 3. AT&T Double Wire Armored Lightguide Cable with Corrosion-Resistant Armor

Concentrating on the oversheath, an important design consideration was to eliminate the problem areas while not changing the traditional construction, handling characteristics, and manufacturing processes. Therefore, the galvanized armor wires were replaced by a highly corrosion-resistant grade of stainless steel wire. In the improved design, these armor wires are also coated with a plastic layer to prevent liquid water from reaching these wires. These seemingly redundant protection mechanisms are important in avoiding hydrogen generation because of metallic corrosion as well as electrical disturbances which will be discussed later.

Table I

	SINGLE WIRE	DOUBLE WIRE	TRIPLE WIRE
LG Cable O.D. for up to 48 fibers*	.42"	.42"	.42"
Armor Wire Material	SS	SS	SS
Number of Armor Wires			
Layer 1	11	11	11
Layer 2	-	18	18
Layer 3	-	-	24
UBL of Armor (lbs)	10,000	26,000	46,000
Cable Tension to Produce 0.33% Strain (lbs	5,400	14,300	26,100
Final Diameter of the Armored Cable	1.00"	1.50"	2.00"
Final Weight (lbs/1000')	640	1450	2500
Weight in Water (lbs/1000')	380	900	1500
Minimum Bend Diameter	32"	36"	42"

*Additional sizes are available for fiber counts greater than 48.

4.0 SALT WATER TANK TESTS TO VERIFY H_2-GENERATION MECHANISMS AND PREVENTION

A number of fiber optic cables were placed in 500-gallon polyethylene tanks containing ASTM-D-1141 artificial sea water to verify the hydrogen generating mechanisms and evaluate the hydrogen prevention methods of the Corrosion-Resistant Armor. A schematic of the test setup is shown in Figure 4. Approximately 250 feet of double wire armored cable was coiled in each tank. The fibers were "loop-back" spliced using the AT&T Rotary Mechanical Splice so as to provide a long length of fiber (~ 1000 meters). The fiber ends were then spliced to master fibers that were brought into the laboratory for spectral analysis. Detailed spectral loss measurements were made over the range from 1200 nm to 1600 nm. Particular attention was made to the hydrogen signature wavelength of 1240 nm. If any gaseous hydrogen is present in the cable, its effects will be seen here first. (The comparable loss magnitudes at 1310 nm and 1550 nm will be much lower—by a factor on the order of 30.)

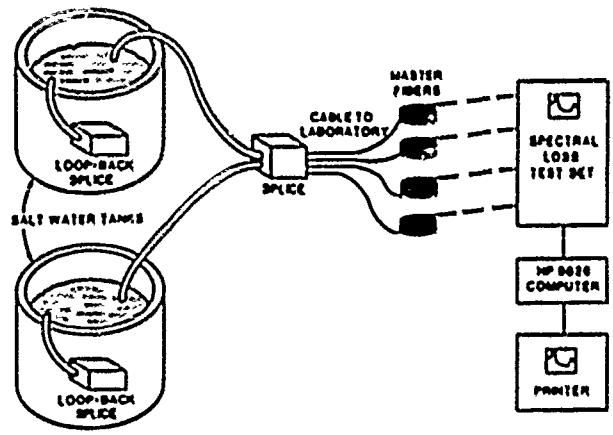

Figure 4. Schematic of Loss Measurement Setup for Salt Water Tank Tests

The plot of the added loss at 1240 nm for an underwater cable (core is Lightpack cable with Primary RL sheath) with the traditional galvanized steel oversheath is shown in Figure 5. This plot shows the difference in added loss between 1240 nm and 1310 nm to eliminate any minor fluctuations in the test setup. Although this test was terminated after 120 days, the added cable loss due to hydrogen is apparently approaching the 1 atmosphere pressure level of about 7 dB/km. On the other hand, the improved Corrosion-Resistant Armor design (with the same core cable) exhibits no added loss in exactly the same tank environment after almost a year.

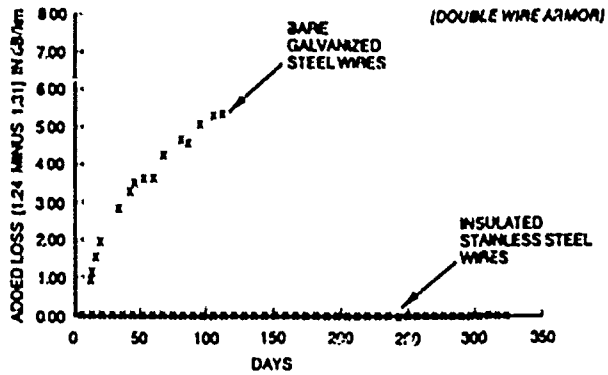

Figure 5. H_2 Induced Loss (1240 nm) in SM Fibers Due to Armor Layer Corrosion in Sea Water

To confirm the theory that H_2 generation reported in armored underwater cables is attributable to galvanized wire corrosion, an armored oversheath (with the same core cable) was manufactured with the galvanized wires coated with an identical plastic coating. The tank tests using this design revealed almost as low added loss as the improved design for the tank conditions corresponding to Figure 5. This result strongly supports the conclusion that galvanized steel corrosion is the hydrogen source in the high loss cables reported by Anderson et al[1]. To further confirm the hydrogen entrapment hypothesis, the entire twine wrap as well as the plastic coating was removed from a long section of the galvanized armor wires. This "damaged" condition permits galvanized steel corrosion to occur and hydrogen to be generated but the twine wrap is not there to trap the bubbles. With the cable in the salt water tank in this condition, no measurable loss occurred and this result supports the hydrogen entrapment hypothesis.

5.0 A CAVEAT TO ONLY PROTECTING AGAINST H_2-GENERATION DUE TO CORROSION

Hydrogen can be generated not only through self-corrosion of a metal, but also through forced corrosion by electrical disturbances. An electrical disturbance can induce currents on a cable and cause that cable to corrode by making the cable anodic or cause the cable to generate hydrogen by making the cable cathodic. These disturbances can take the form of:

1. Corrosion mitigation measures such as cathodic protection used on the cable itself to protect it from corrosion,
2. Electrical interference from other cathodic protection systems and,
3. Stray currents picked up from power ground return arrangements.
4. Galvanic cells set up between the involved metals,
5. Long cells in which the anode and cathode are separated by long distances and which occur naturally in the environment,

Electrical disturbances are commonplace. In accordance with today's government regulations, any potentially polluting source is required to have environmental protection. An underwater pipeline, cable, mothballed ship, bridge support or pier, or fuel storage facility, for example, may be anodic and corrode. In order to prevent corrosion of the above structures, the corrosion process is reversed by applying cathodic protection to that structure. The effected structure is made cathodic to an anode or string of anodes placed nearby in the water or ground. This is accomplished by using consumable anodes which have a significantly more anodic potential than the affected structure or by using a rectifier and nonconsumable anodes to shift the potential of the affected structure to a more cathodic potential than the anodes. Because of the proximity of the cable in question to that cathodically protected structure or because of electrical bonding, i.e. grounding, of the cable and the protected structure, currents can be induced on the cable causing the cable to either corrode or produce hydrogen. Measures to mitigate the cathodic protection interference involve electrical bonding to make the cable cathodic like the interfering structure and produce hydrogen, or applying an additional cathodic protection system to the cable which would make the cable separately cathodic, but also producing hydrogen.

An electrical disturbance also can appear as electrical currents picked up by the cable which can be a lower resistance path for an electrical power substation return. These currents can emanate from direct current traction systems, from substantial welding activity in shipyards, and from poorly grounded electrical equipment. The lengths of cable involved in power pickup would produce the hydrogen while the lengths involved in power loss would experience corrosion. Mitigation measures involve either electrical bonding at the power loss point or the use of a cathodic protection system on the cable, causing that cable to be cathodic and produce hydrogen.

The problem of electrical disturbances can occur in both fresh water and salt water and is quite common. For example, when a cable is routed into a manhole, exposed metals must be grounded to the grounding system in the manhole. Since flooded manholes are common and commonly corrosive to telephone plant, cathodic protection of telephone plant is also common. The bonding system in manholes means that the cathodic protection of one cable will cause interference (an electrical disturbance) to the other structures bonded together in the flooded manhole.

Using a metal of low electrochemical reactivity is not sufficient in itself to prevent hydrogen generation where electrical disturbances are present. Since it is extremely difficult to prevent electrical pickup on the armor wires, electrical isolation of the metal from the environment in interference areas is also necessary to prevent the metal from corroding and generating hydrogen. The use of insulation over the armor wires serves to prevent the discharge of the stray currents that could generate the deleterious hydrogen molecules.

6.0 POWERED, SALT WATER TESTS TO CONFIRM CORROSION-RESISTANT SHEATH RESISTANCE TO ELECTRICAL DISTURBANCES

To investigate the effects of electrical disturbances on the new enhanced design wire armor oversheath configurations, cables were powered in the salt water tanks. More specifically, a new condition was added wherein an electrical disturbance was created on the wire armor by making that armor cathodic.

This electrical disturbance was created by polarizing the wire armor using a DC power supply. The cable's armor was connected to the negative side of the power supply and a stainless steel anode rod was connected to the positive side (see Figure 6). The polarity resulted in the cable's armor

producing hydrogen and the anode rod corroding. The rate of hydrogen generation (directly related to impressed current flow in the circuit) was approximately seven times the equivalent corrosion current calculated via Faraday's Law for the free corrosion of zinc in sea water. A galvanized steel wire armor potential of approximately -2.0 volts (± 0.1 volts) vs. a $Cu/CuSO_4$ halfcell was found necessary to produce that high rate of hydrogen generation (current flow). This artificially high disturbance current imposed on the test cable's armor could create up to seven times the unpowered rate of hydrogen generation of undisturbed cables and an anticipated significant increase in the growth of the 1240 nm peak; i.e., this is a very severe test.

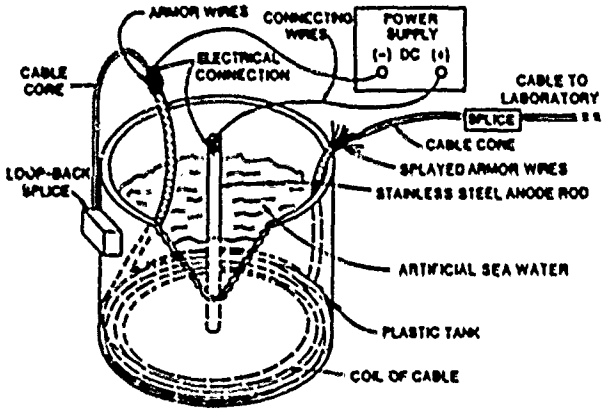

Figure 6. Test Setup with a Power Supply to Create an Electrical Disturbance

The results of tank tests using powered wire armor are plotted in Figure 7. Note first that the fiber optic cable with the traditional galvanized steel armor wire reaches its saturation loss level (~ 7 dB/km added loss @ 1240 nm) in 25 days. This compares to a loss increase rate approximately four times as rapid as the unpowered galvanized-steel armor cable. Also observe that the added loss for the cable with plastic-coated galvanized steel armor wire increases at a less rapid but alarming rate when the armor wires are powered.

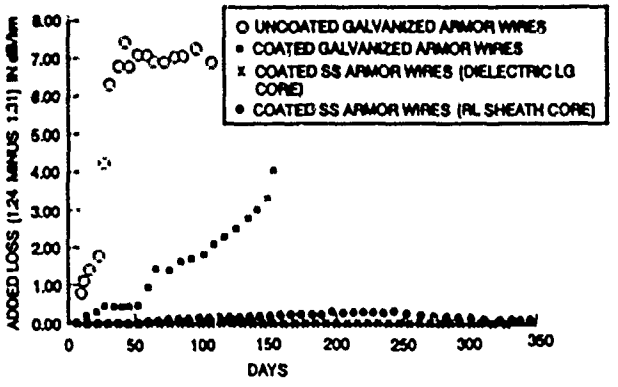

Figure 7. H_2 Induced Loss (1240 nm) with Powered Armor Wire (SM Fibers) in Sea Water

The two lower curves in Figure 7 represent powered fiber optic cables with the new Corrosion-Resistant Armor oversheath (i.e., stainless steel armor wires with plastic coatings). The curve with the slight rise in added loss after 100 days (to a level almost discernible at 1310 nm and 1550 nm) that then falls to insignificant added loss has a Lightpack cable with RL sheath as the core like all samples discussed to this point. The lowest curve which exhibits no added loss for over a year has the same new Corrosion-Resistant Armor but has an all dielectric Lightguide cable as the core. The authors believe that the type of core cable is coincidental and the only reason that the Corrosion-Resistant Armor test cable with RL sheath core has a very slight added loss is because an excessive number of pinholes were created in the plastic layer of the stainless steel armor wires during production. The large H_2-induced loss in the powered, coated galvanized wire test cable (discussed in the paragraph above) also resulted because of pinholes in the plastic coating. Ground fault screening tests confirmed the pinhole conditions and checks of the powering current indicate three orders of magnitude greater current flow in the armor wires of the cable with the RL sheath core (vs the cable with the all dielectric cable core).

The tests using excessively powered armor wires reveal that the new Corrosion-Resistant Armor design prevents serious hydrogen generation from both armor wire corrosion as well as electrical disturbances. On the other hand, an underwater oversheath using traditional bare galvanized steel armor wires encounters rapid loss increases even in the absence of electrical disturbances. Furthermore, the added loss increases much more dramatically when the armor wires are powered and increases at a fast rate even when the galvanized wires are plastic coated. Recall that these powered tests represent very severe conditions with a large safety factor over conditions expected in actual installations.

7.0 IMPLICATIONS OF THE TEST RESULTS

The tank test results vividly demonstrate that oversheaths using galvanized steel armor wires can encounter large hydrogen-induced fiber attenuation in a short time even in benign underwater environments. The experimental results also demonstrate that because the Corrosion-Resistant Armor design utilizes insulated armor wires made of a material with low or electrochemical reactivity the hydrogen-generated loss levels are inconsequential even in the harsh salt water environments with severe electrical disturbances. The electrochemical reactivity of the stainless steel armor wires appears to be sufficiently low that relatively large pinholes can be tolerated without serious hydrogen problems even with severely overdriven power conditions. In contrast, the galvanized steel armor wires encounter severe hydrogen degradation under the same conditions despite having plastic coatings.

8.0 CONCLUSIONS

A detailed hypothesis for the hydrogen generation mechanisms in traditional wire-armored underwater cable was presented and supported by test data. The salt water tank tests clearly demonstrated that the galvanized armor wires were the hydrogen generation culprits. Since rapid increase in fiber loss occurred in salt water tests with no electrical disturbances, the self-corrosion of bare galvanized armor wire dominates (in previously installed wire-armored traditional cables) and thus suggests a large spectrum of potential underwater problem areas. For high reliability and minimum long term cost (repair of underwater cable is expensive), the authors recommend that all future armored cable water crossings using optical fiber cables employ H_2-resistant oversheath armor and/or hermetic fibers.

A new Corrosion Resistant Armor has been designed to prevent detrimental hydrogen-induced loss in underwater fiber optic cable. (Table II lists some of the key features of this wire-armor oversheath design.) Extensive tank testing has confirmed the ability of the new oversheath to dramatically reduce the 1240 nm H_2-induced added loss that occurs in traditional armored underwater cable that use galvanized steel armor wire. With the new Corrosion-Resistant Armor, transmission properties at the 1310 nm and 1550 nm windows remain essentially unchanged even during severe testing.

Table II

- New Underwater Armor Oversheath
- Plastic Coated, Stainless Steel Armor Wires
- H_2-Induced Attenuation Eliminated (Long-Term Tests Conducted In Sea Water)
- Stainless Steel Armor Provides Maximum Long-Term Mechanical and Corrosion Protection
- Protects Against Galvanic and Electrolytic Corrosion
- Armor Design Provides Excellent Tensile Strength
- Tough Underwater Oversheath with Excellent Abrasion Resistance
- Proven Exceptional Handling Characteristics
- Good Underwater Weight Properties

REFERENCES

1. W. T. Anderson, A. J. Johnson, J. P. Kilmer, and R. M. Kanen, "Hydrogen Gas Effects on Installed Submarine Single-Mode Fiber Cables, Proceedings of the 37th *International Wire and Cable Symposium*, Reno, Nevada, November 15-17, 1988, pp. 188-199.
2. A. Adl, T.-M. Chien, and T. C. Chu, "Design and Testing of the SL Cable," *Journal of Lightwave Technology*, Volume LT-2, No. 6, December, 1984, pp. 824-832.
3. R. J. Huff, F. V. DiMarcello, and A. C. Hart, Jr., "Amorphorus Carbon Hermetically Coated Optical Fibers," in *Optical Fiber Communication Conference, 1988 Technical Digest Series, Vol. 1*, (Optical Society of America, Washington, D.C., 1988), paper TUG2.

NATHAN E. HARDWICK, III
AT&T Bell Laboratories
Norcross, Georgia 30071

Nathan E. Hardwick, III is a Distinguished Member of Technical Staff in the Lightguide Media Department at AT&T Bell Laboratories, Norcross, Georgia. He has received B.S. and M.S. Degrees in Mechanical Engineering from the University of South Carolina and a Ph.D. in Mechanical Engineering from Lehigh University. After joining Bell Laboratories in 1965, Dr. Hardwick initially designed and thermally characterized integrated circuit packages. Later work included responsibility for the design and the initial installation of the outside plant hardware system for FT3 lightguide cable. More recently, Nate has worked on SM multifiber splicing, splice mechanisms analyses, and designing optical fiber cables. Dr. Hardwick spent one year as a Bell Laboratories Visiting Professor at N.C. A&T State University.

L. C. HOTCHKISS
AT&T Bell Laboratories
Norcross, Georgia 30071

L. C. Hotchkiss is a Distinguished Member of Technical Staff in Lightguide Technology Department at AT&T Bell Laboratories, Norcross, Georgia. He earned a Bachelors Degree in Electrical Engineering from University of Wisconsin and a Masters Degree in Electrical Engineering from Stevens Institute of Technology. He has 30 years of experience, primarily in the design of test equipment, and is presently responsible for the design and programming of fiber optic environmental loss measuring test sets.

JOHN J. BLEE
AT&T Bell Laboratories
Norcross, GA 30071

John J. Blee was educated at Rutgers College, Rensselaer Polytechnic Institute, and Georgia Institute of Technology with his master's degree work in metallurgy and corrosion. He has been with Bell Laboratories since 1970. Mr. Blee's current work encompasses the physical metallurgy, finishing, and corrosion responsibilities for the metallic components in optical fiber and copper cables, closures, and connectors.

DAN L. PHILEN
AT&T Bell Laboratories
Norcross, GA 30071

Dan L. Philen received a B.S. degree in chemistry from Auburn University, Auburn, AL, in 1968, and a Ph.D. degree in physical chemistry from Texas A&M University, College Station, TX, in 1975. During 1969 and 1970, he was an instructor in oxygen and acetylene production for the U.S. Army, and was a Robert A. Welch Postdoctoral Fellow in electrical engineering in 1975 at Rice University, Houston, TX. From 1976 to 1979 he was with Georgia Institute of Technology, Atlanta, GA, engaged, in measurements of trace pollutants in the upper atmosphere by laser induced fluorescence. Since 1979 he has been with AT&T Bell Laboratories, Atlanta, GA, working in exploratory and factory measurements on optical fibers. He is the Laser Safety Officer for Bell Laboratories in Atlanta. He is the author of numerous publications on measurements of optical fiber properties. He is listed in "Who's Who in Optical Science And Engineering", "Who's Who In Technology Today", "Who's Who in The South and Southwest", and "Men of Achievement - Fourteenth Edition". He is a member of The American Chemical Society, The Optical Society of America, Sigma Xi - The Research Society of North America, Sigma Pi Sigma - Physics Honorary, and Phi Lambda Upsilon - Chemistry Honorary.

FIBRE RELIABILITY CONSIDERATIONS IN FUTURE LOW COST SUBMARINE SYSTEMS

E S R Sikora, C A Gould, J V Wright and J M Scott

British Telecom Research Laboratories, Martlesham, UK

1. ABSTRACT

First generation undersea optical fibre cables are operating at 1.3μm with repeater spacings of approximately 50km. Second generation systems utilise the lower loss window at 1.55μm where the repeater spacing can be greater than 100km. Consequently fewer repeaters are needed and therefore the cost of the cable becomes a greater proportion of the total system cost. As a number of fibre submarine systems have been successfully installed it is appropriate to examine whether fibres could be used more effectively in future submarine cable designs.

2. INTRODUCTION

Deep water cables have been designed to withstand a continuous strain of typically 0.35% with a maximum strain up to typically 0.87% [1]. New fibre claddings and coatings are being developed with the aim of reducing the sensitivity of the fibre to hydrogen or to improve its static and dynamic fatigue performance. For example, N values greater than 150 are being measured for hermetic fibres. Improvements in quality control have also led to fibre proof strains of 2% being commercially available.

In this paper we show that, given realistic assumptions concerning the maximum stress levels during service, carbon coated hermetic fibres or surface modified high strength fibres are not necessary where maximum cable strains are of the order of 1.0% or less. It is suggested that the reduction in hydrogen permeation claimed for hermetically coated fibres is likely to be more important in reducing cable costs than an increased resistance to static fatigue. It is also suggested that the fibre crack distribution becomes significantly more important as the mean strength of the fibre is increased.

The use of strong, lightweight materials for future submarine cables is also examined with an emphasis on fibre reliability requirements and possible cable cost reductions.

3. CABLE COSTS

The costs of a submarine system attributable to the cable and marine installation is dependant upon system length. The costs are highest for a short haul shallow lay system which requires protection from ship damage by the use of armouring or cable burial techniques. Typically the cable costs will account for 45% and the marine installation for 25% of the total system costs. Longer haul systems are laid predominantly in the deep-sea using armourless cable; ship protection is only required for a relatively short distance at the shore ends. Consequently cable and marine installation costs are reduced, see Table 1 for a typical transoceanic system. However they still account for 50% of the total system cost.

TABLE 1. SYSTEM COST BREAKDOWN

	Cost %
Cable	42.4
Repeaters	27.9
Installation	8
Terminal	7.7
Others	14.1

4. CURRENT CABLE DESIGNS

Cables for deep-sea use are generally lightweight employing no external armouring and the fibres within the cables may be tight jacketed or allowed to move within a groove.

A typical tight jacketed structure, Fig 4.1, [2] consists of an optical unit surrounded by helically laid steel wire strand strength members, a copper tube and an outer sheath of low density polyethylene. The optical unit is a nylon tube which contains a number of fibres laid around a kingwire and embedded in an elastomer.

fig 4.1 TIGHT JACKETED DESIGN, Ref.2.

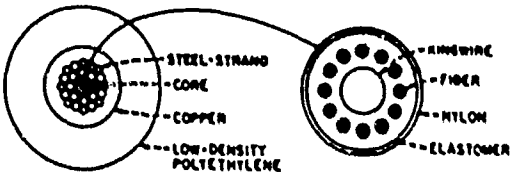

fig 4.2 TIGHT JACKETED DESIGN, Ref.3

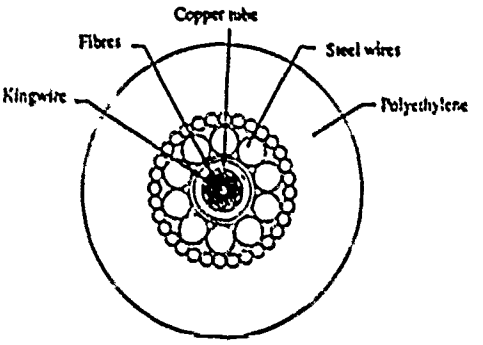

fig 4.3 V-GROOVE DESIGN, Ref.4.

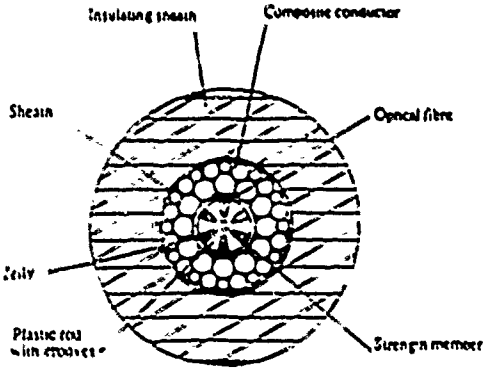

In this type of design the fibre strain is essentially the same as the cable strain. Another approach, Fig 4.2, [3] may be to have the steel wires outside the copper tube and a number of secondary coated fibres laid helically around the king wire. The 'V-groove' type cable, Fig 4.3, [4] has a similar construction except that the optical unit comprises a grooved plastic rod with a steel king wire through its centre, the fibre being inserted in the helical grooves. After insertion of the fibres a tape is usually wrapped around the rod and a polymer sheath is extruded over the tapes. The length of fibre within each groove is such that as the cable is strained the fibre moves from the top to the bottom of each groove before experiencing any strain. The movement of the fibre is reversed when the load is removed. This allows the cable to be strained by up to about 0.9% before the fibre is strained.

In both types of cable the tensile strength characteristics are governed by the grade, the size and the lay of the steel wire. The copper tube is used to reduce hydrogen permeation into the optical unit and to act as a power feed conductor for the high voltage supply to each repeater.

The fibres have to withstand the strains involved in cable laying and recovery as well as any residual strain the fibre may experience while on the sea bed. As the 'V groove' type cable structure has a significant strain relief which minimises the problem of fibre survival, this paper will only deal with fibre survival in tight jacketed structures. The largest cable and hence fibre strains occur during laying and recovery. Typical strains for a transatlantic cable are given in Table 2 [5].

5. *ASSESSMENT OF FIBRE LIFETIMES*

Fibre reliability during the cable life is estimated using models describing the crack growth in the silica during service. All the models or theories are based on the same crack velocity function but thereafter differ in the

TABLE 2. EXPECTED SERVICE CONDITIONS FOR FIBRE

Operation	Strain %	Time
Installation	0.44	6 hours
Cable as installed	0.04	25 years
Recovery, Lift	0.87	5 hours
Hold	0.54	48 hours
Relay	0.44	6 hours
Cable after recovery and relaying	0.24	25 years

assumptions used. A commonly used estimation of the minimum fibre life is:

$$t = \left[\frac{\sigma_p}{\sigma_w}\right]^N \frac{B(N+1)}{\sigma_p^2} \qquad 5.1$$

Where σ_p is the proof stress, σ_w is the maximum dynamic stress generated by a constant stress rate, N is the stress corrosion susceptibility constant and B is a constant describing the material and environment. Alternatively, if σ_w is taken as the static stress then the factor N+1 must be omitted. A variation [1] which takes into account the strain history of the fibre during service and estimates the value of the proof stress needed for the fibre to survive is:

$$\sigma_p = \frac{K_{IC}}{Y a_p^{1/2}} \qquad 5.2$$

Where: $a_p^M = \sum_i A M E^N Y^N \int_0^{t_i} \epsilon_i(t)^N dt$

and $M = (N-2)/2$

K_{IC} is the stress intensity factor at failure, a is the crack depth, Y is a constant depending on the geometry of the crack, A is a constant in the crack velocity equation, E is the Youngs Modulus and $\epsilon(t)$ is the time dependent strain. The derivation of 5.1 does not take into account any crack distribution in the fibre. One example [6] of a fibre lifetime theory which takes into account the crack distribution, the mean fibre strength and the effects of the proof test on the fibre is:

$$t = \frac{\sigma_d^{N+1}}{\sigma_w^N (N+1)\dot{\sigma}} \qquad 5.3$$

where

$$\left[\frac{\sigma_d}{\sigma_o}\right]^{N+1} = \Psi^{\frac{N+1}{m}} - \left[\frac{\sigma_p}{\sigma_o}\right]^{N+1} + \frac{B(N+1)\dot{\sigma}}{\sigma_o^3} \Psi^{\frac{N-2}{m}}$$

and

$$\Psi = \ln\left[\frac{1}{1-F}\right] + \left[\frac{\sigma_p}{\sigma_o}\right]^m$$

F is the failure probability, $\dot{\sigma}$ is the stress rate, σ_o the Weibull mean failure stress, and m the crack distribution parameter. Variations in the fibre stress history can be taken into account by normalising all the expected static service stresses σ_i and maximum dynamic stresses σ_j (assuming a constant stress rate) to a given static stress σ_{norm} and calculating the time t_{norm} spent at the normalised stress.

$$t_{norm} = \sum_i \left[\frac{\sigma_i}{\sigma_{norm}}\right]^N t_i + \sum_j \left[\frac{\sigma_j}{\sigma_{norm}}\right]^N \frac{t_j}{(N+1)} \qquad 5.4$$

Thus if $t_{norm} < t$ when $\sigma_w = \sigma_{norm}$ the fibre can be expected to survive with a probability greater than that used to calculate the expected failure time t. Calculation of the failure time using equation 5.1 or 5.3 requires knowledge of the stress corrosion constants N and B. Various values have been published recently and are listed in Table 3.

Given the service conditions suggested in Table 2 and normalising the strains to 0.87%, using an N value of 20, it is obvious that the recovery lift is the most critical service condition. If the fibre survives the recovery lift then it is expected to survive the other service conditions.

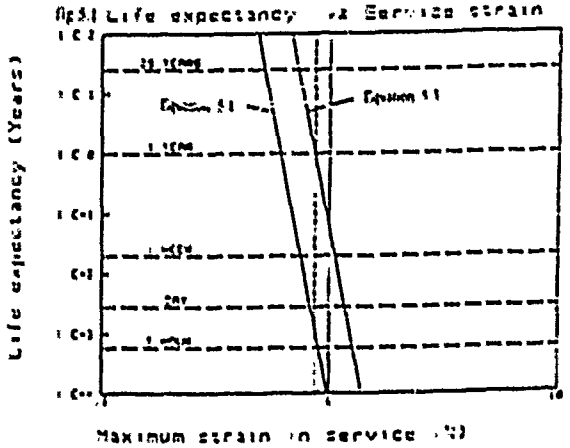

Fig 5.1 Life expectancy vs Service strain

TABLE 3. RANGE OF VALUES FOR N and B

	N		B
	Dynamic	Static	Pa^2sec
Double acrylate coated fibre	20 to 30	20 to 23	10^{10} to 10^{18}
Hermetic fibre	>100	>100	
Surface modified fibre	20	35 to 130	

The fibre lifetimes have been calculated for different values of stress, Fig 5.1, using equations 5.1 and 5.3 for the values of the constants given in Table 4. Variations in N and B with time have not been considered in this paper, (equation 5.4 can be modified to take into account changes in N), as current deep sea cable design practice assumes N and B to be constant with time. There is, at present, some evidence to suggest that even at 3 °C there is a transition in the value of N and hence B with time [7]. Further work is still required to define more clearly the onset of any transition and the likely values of N and B after the transition before any changes in N and B can sensibly be taken into account in deep sea water cables.

Fig 5.1 shows that the fibre will survive the expected service conditions (see Table 2) using either equation 5.1 or 5.3. The estimated failure time for the fibre at a maximum dynamic strain of 0.87% for equation 5.1 is approximately 10 hours while for a continuous strain of 0.87% equation 5.3 estimates the fibre life to be approximately 1 year.

6. *RELATIVE MERITS OF THEORIES*

The failure time at the Weibull mean failure probability (63.28%) using a crack distribution described by the

TABLE 4. CONTANTS USED TO DETERMINE FIBRE LIFETIMES

		EQUATION 5.1	EQUATION 5.3
N		20	20
B	Pa^2sec	2×10^{14}	2×10^{14}
ϵ_p	%	2	2
ϵ_w	%	0.87	0.87
ϵ_o	%		3.5
$\dot{\epsilon}$	%/sec		0.4
m			4
F			0.05
E	GPa	72	72

Weibull slope m can be shown to be:

$$t = \left[\frac{\sigma_o}{\sigma_w}\right]^N \frac{B(N+1)}{\sigma_o^2} \qquad 6.1$$

Although equation 6.1 is less complicated than equation 5.3, for obvious reasons, it is instructive to compare it to equation 5.1 which describes the time to failure neglecting any crack distribution. The two equations have the same form but in equation 5.1 the proof stress replaces the mean strength. It follows therefore that if $\sigma_o > \sigma_p$ equation 5.1 will predict a shorter lifetime than equation 6.1.

Figure 6.1 shows an idealised set of results from a dynamic fatigue test. The majority of the failures of plot A occur at about a strain of 5.5% with a small number of failures below this giving rise to a broader crack distribution described by an m value of about 4. Line B is a hypothetical set of results described by equation 5.1 with a mean strength equal to the proof strain. The vertical line C is the proof test value cutting both the low strength tail of plot A and line B. Line B can therefore be seen as the low strength tail of plot A which has been shifted to the left to give a mean strength equal to the proof strain. This shift to the left can be related to an increase in fibre length by:

$$L_1 = L_0 \left[\frac{\sigma_0}{\sigma_1}\right]^m \qquad 6.2$$

It can be argued therefore that equation 5.1 is simply a special case of the crack distribution theory.

Fig 6.1 CUMULATIVE PROBABILITY OF FAILURE TIME

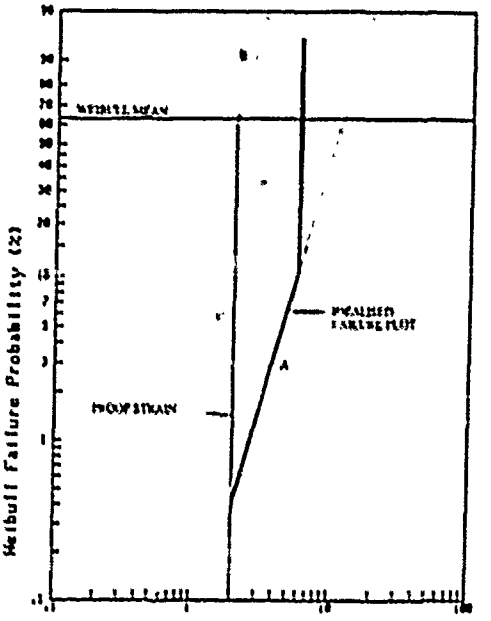

The mean failure strain for the low strength tail of plot A is approximately 11%, the test length being 1km. Using equation 6.2 the fibre length for a mean failure strain of 2% is 900km. The cable tension during recovery lift depends to a certain extent on the ship's speed. Recovery from a depth of 5.5km may induce significant strain for approximately 8km either side of the recovery point. This suggests that, assuming a six fibre cable, approximately 96km of fibre may be under a significant strain. Using equation 6.2 the mean failure strain, (ie. the strain at which the probability of failure is 63.2%), for a 96km length of fibre is about 3.5%. The use of a mean failure strain of 2% would therefore seem to be unduly pessimistic.

The effect of different crack distributions, as described by the parameter m, and mean strengths on the fibre life is shown in Fig 6.2. It can be seen that as the mean strength is increased the crack distribution becomes more important as it has a greater effect on the fibre life.

Equation 5.1 and the theory which considers the crack distribution, the probability of failure and the effects of the proof stress suggest that the fibre will survive the recovery lift, given the constants in Table 4. The weakness of equation 5.1, it may be argued, is that it takes no account of the crack distribution and that it

uses too low a value of the 'mean fibre strength' thus neglecting any improvement in quality control during the fibre and cable manufacture. The use of fibre life models which are too pessimistic may also inhibit cable design and encourage work in areas which may not be required.

fig 6.2 Life expectancy vs Weibull parameters

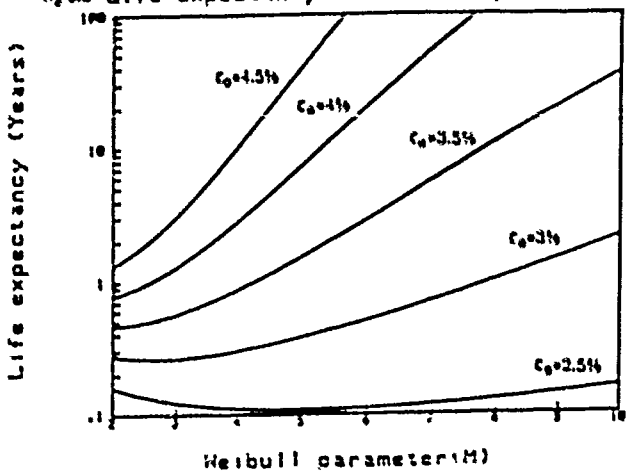

Other fibre life theories have been published, for example reference [8], which take into account the crack distribution, the mean fibre strength and the effects of proof testing. Work is still required to determine which of the probabilistic theories is the most accurate.

7. *LIMITS TO PRESENT CABLE STRAIN*

Present cable strains are limited by the estimated fibre lifetimes calculated using equations 5.1 & 5.2. If estimations of fibre life, on the other hand, were to take into account the crack distribution and use a realistic value of the mean strength the present cables rather than being fibre strain limited may well be cable strain limited, see Fig 5.1. The drive to reduce cable costs will tend to generate cable designs that utilise more fully the strength characteristics of the fibre, or a more realistic or more generous interpretation of them.

8. *FUTURE CABLE DESIGNS*

The main requirement of future cable design is to minimise the total cost to the owner operator over the life of the system. This includes the manufactured purchase cost, the installation cost and the unknown liability for consequential service recovery and repair. For a short unrepeated system the cable cost and marine installation cost could be 60% and 15% of the system cost respectivly. Neglecting inflation, maintenance could cost a further 2% per repair. Clearly there needs to be a balance between high initial capital cost of say a maximum metal design with good reliability and the savings made on a minimum metal design but at the expense of lowered reliability and higher future maintenance costs.

Present deep water cables have an operational cable safety factor approaching 2. It may therefore be possible to reduce the safety factor while still maintaining the required fibre reliability. Operational experience with the first dozen or so optical cables may also indicate undue pessimism with the new optical technology. Hindsight may indicate that in order to generate success and acceptance of this new technology the design was unduly cautious. Not only can a realistic cable design be tailored to each application, but also the reliability performance enhanced due to a fibre reassessment.

Typical constructions contain a significant amount of copper to supply electrical power to all the repeaters and to reduce hydrogen permeation to the optical unit. Use of hermetic fibres would eliminate the need for the copper as a hydrogen barrier. Aluminium could be used instead for power transmission to repeaters. The cable self modulus (ratio of strength to wet weight) would be improved as the wet weight is reduced. This would allow the steel content of the cable to be reduced. Any reduction in cable diameter would reduce the hydrodynamic drag load and any seabed peelout load during the lift stage of a cable recovery, both aspects tending to reduce the maximum tension.

8.1 *Maximum Metal Cable*

Figures 8.1, 8.2 & 8.3 indicate a typical deep water cable, its load elongation curve and peak cable strain during recovery. The example design gives a 200kN strength, self modulus of 20+km and a power feed DC resistance of about 1Ω/km, allowing a recovery speed of about 1.5 knots at less than 1% fibre strain for the conditions given at a tension of about 80% UTS.

fig 8.1 MAXIMUM METAL CABLE

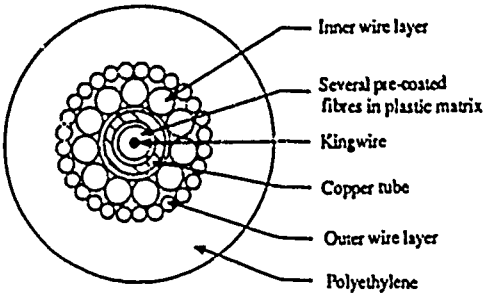

8.2 Minimum Metal Cable

Figures 8.2 & 8.3 also show the characteristics of a cable Fig 8.4 with half the strength of the maximum metal design. This can be done with a single wire lay construction and thereby the possibility of contralay strand wires and torsional balance lost. However, for a strength of say 100kN, the self modulus is still 20+km and the power feed DC resistance still about 1Ω/km,

Fig 8.2 LOAD / ELONGATION CHARACTERISTICS

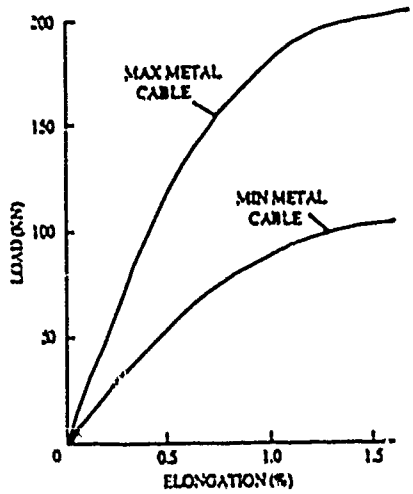

Fig 8.3 CABLE STRAIN DURING WORST TRANSATLANTIC RECOVERY

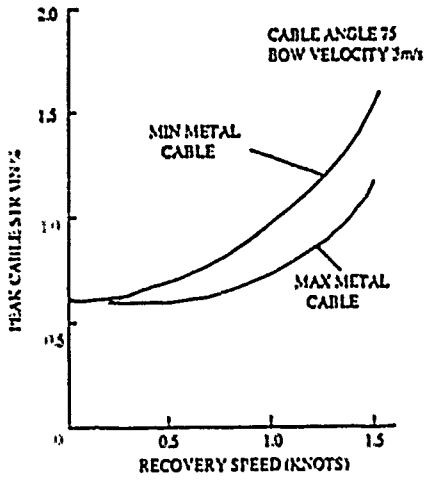

Fig 8.4 MINIMUM METAL CABLE

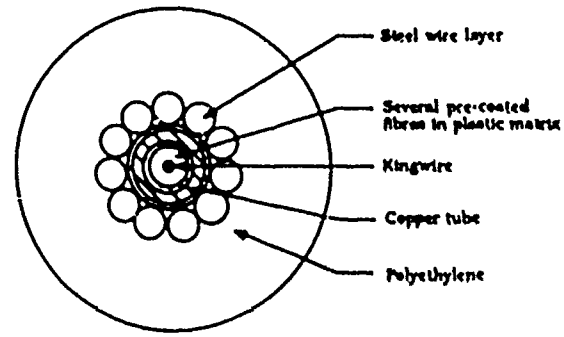

allowing a recovery speed of just over 1 knot at less than 1% fibre strain for the same marine conditions at about 80% UTS. For bad weather conditions in deepwater the dynamic loads can be high, and the margin between UTS and actual tension seen at the bow could be less than desired. Thus the cable could be viewed as on the limit of marine handling ability, but at a possible cost of about 60% of that of the maximum metal case above.

8.3 Plastic Cable Design

The above metal construction comprises the steel content for strength and the copper content for radial pressure resistance, resistance to hydrogen, and electrical power feed. For an unrepeatered system or one with only a couple of repeaters a plastic cable can be constructed with a pair of wires for power feed and electroding detection purposes. For example, 1mm diameter copper gives a resistance of about 10Ω/km. A 500km, two repeater system would thus require a system voltage of 2.7kV. It may be preferable to place the fibre package within a copper tube and abandon load wires to simplify manufacture, Fig 8.5.

Pultrusion techniques could be used to form a final cable product tube where fibre and a filling compound are inserted during the pultrusion operation. Alternatively Kevlar impregnated resin yarns or ultra high modulus yarns or a combination may be suitable. The typical Youngs Moduli of Kevlar 29 and 49 yarns are 29GPa and 49GPa, at many times the price of Ultra High Modulus Polyethylene (UHMP) at say 39GPa, Fig 8.5 gives a possible tubular UHMP pultrusion of say 19GPa. Assuming inner and outer radii of 5mm and 25mm, the 471 mm area at a maximum working strain of 0.87% would give a working cable strength of 78kN. Using the allowable fibre fatigue model with a working fibre strain of 1.2% the working cable strength could easily be 107kN, Fig 8.6. Assuming positive weighting by means of a thin mineral impact protective sheathing

Fig. 8.5(a) PLASTIC CABLE DESIGN

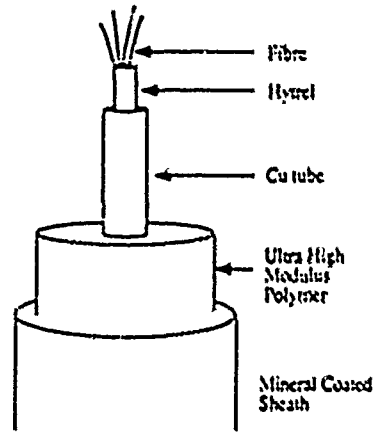

Fig 8.5(b)

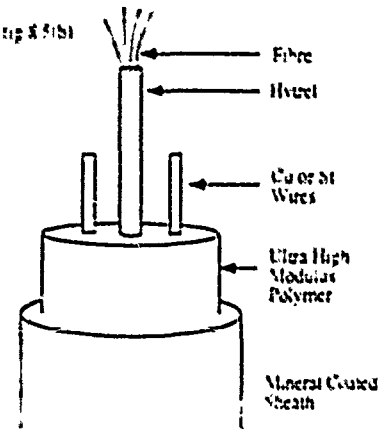

the wet weight could be 0.1 tonnes/km or 0.2 tonnes/km giving a more than adequate wet cable self modulus. Recovery load would then be predominantly

Fig.8.6 LOAD / ELONGATION CHARACTERISTICS

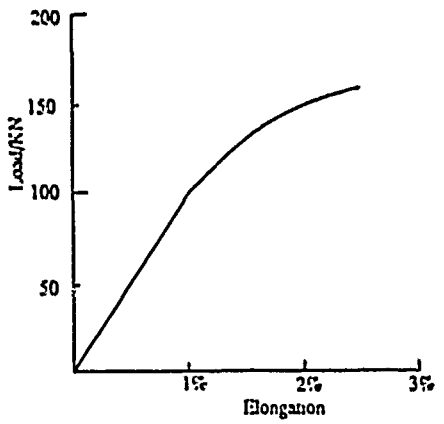

due to hydrodynamic drag resistance with a trivial wet weight, compared with a metallic cable where the steel content creates the majority of the recovery tension, Fig 8.7. The cost of such a cable would be approximately 20% of the maximum metal case.

Fig.8.7 CABLE STRAIN DURING WORST TRANSATLANTIC RECOVERY

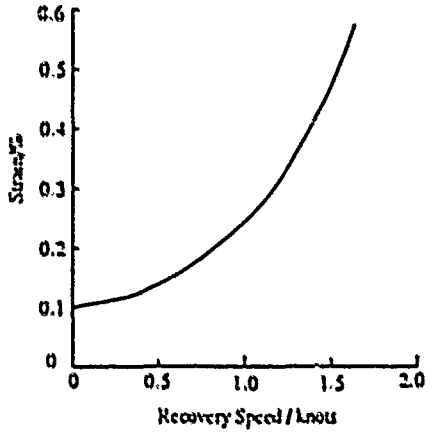

8.4 Fibre Strength Aspects

The above indicates that the maximum and minimum metal cables are basically cable strain limited if equation 5.3 is used to estimate the fibre lifetimes. For the plastic design it is clear that the recovery strain is significantly less than either of the two metal cables thus short term creep during recovery is unlikely to be a problem. A rough estimate of the maximum allowable creep can be made as follows. Equation 6.2 is used to estimate the mean failure strain (ϵ_a) for 25000km of fibre, say $\epsilon_a = 0.875\%$. A linear creep rate of say $4.7\times10^{-6}\%/hr$ is assumed. A failure probability F of 10^{-4} is also assumed giving approximately 2 failures over 25 years for an 6 fibre 4000km cable. The static failure strain for a 25 year lifetime, given the above probability of failure, calculated using equation 5.3 is approximately 1.2%. The maximum dynamic strain due to linear creep that the fibre can withstand over the 25 years is estimated, using equation 5.4 to be 1.4%.

It is clear though that using the probabilistic fibre survival analysis fibres with N values between 20 and 30 are likely to survive. This suggests that fibres with hermetic coatings will be useful owing to their reduced sensitivity to hydrogen rather than to their higher N values.

9. CONCLUSIONS

A number of factors affecting the fibre reliability in present and possible future deep sea cable designs have

been examined.

- The current practice of neglecting the fibre crack distribution and mean failure strain in fibre reliability analysis for deep sea cable design does not take into account the many improvements in fibre coating technology and in the fibre and cable manufacture thus significantly under-utilising the mechanical strength properties of the fibre.
- A number of probabilistic fibre reliability models have been published which include the fibre crack distribution and the mean fibre strength. Some work remains to be done to determine which model gives the most accurate fibre life extrapolation.
- It is argued that (5.1) is a special case of the more detailed probabilistic model in which the proof strain is assumed to be equal to the mean failure strain of the fibre. The estimates of fibre reliability therefore tend to be unduly pessimistic.
- If the fibre crack distribution and mean failure strain are taken into account the present tight jacketed cable designs would tend to be cable strain limited rather than fibre strain limited.
- The minimum metal cable design would cost approximately 60% of the maximum metal cable design. Calculations suggest that the minimum metal type designs would also be cable strain limited.
- Initial calculations suggest that the cost of a 'polymer' cable would be approximately 20% of the cost of the maximum metal cable. Short term creep is not thought to be a problem as recovery strains would be small.
- Present evidence indicates that the N values of current fibres (20 to 30) would be adequate for future low cost cable designs. Hermetic fibres would be used for their reduced sensitivity to hydrogen rather than any increased resistance to stress corrosion.

10. ACKNOWLEDGEMENTS

Acknowledgement is made to the Director Network Technology, British Telecom Research and Technology for permission to publish this paper.

11. REFERENCES

[1] Determination of Fibre Proof Test Stress for Undersea Lightguide Cable. T C Chu, H C Chandan. AT&T Technical Journal, Vol 64, No.4, April 1985.

[2] HAW-4/TPC-3:System planning and progress. I Yasuhisa and G M Jeffcoat. International Conference on Optical Fibre Submarine Telecommunication Systems, February 1986 France.

[3] Undersea Lightwave Communications, page 253. Edited by P K Runge and P R Trischitta. Published by IEEE Press.

[4] The existing French systems: S280 - S140 - SR and CELTIC. J Godeluck. International Conference on Optical Fibre Submarine Telecommunition Systems, February 1986 France.

[5] Undersea Lightwave Communications, page 57. Edited by P K Runge and P R Trischitta. Published by IEEE Press.

[6] Proof Testing of Optical Glass Fibres. P W France and W J Duncan. Advances in Ceramics, Vol. 2, Physics of Fibre Optics, The American Ceramics Society 1981.

[7] Temperature Dependence of the Transition in Static Fatigue of Fused Silica Optical Fibre. J T Krause and C J Shute. Advanced Ceramic Materials, Vol. 3, No. 2, 1988.

[8] Studies in High Tensile Proof Tests of Optical Fibres. Y Miyajima. Journal of Lightwave Technology, Vol. LT(2), June 1983.

Jennifer Scott received the B.Sc. in Physics from the University of Birmingham in 1988. Since then she has been working at the British Telecom Research Laboratories in Suffolk, UK. Her work is based on fibre studies with a view to future submerged systems.

Ed Sikora obtained a degree in Mechanical Engineering from Middlesex Polytechnic in 1979 and an M.Sc. in Advanced Mechanical Engineering from Imperial College in 1980. From 1980 to 1989 he worked for GEC at The Hirst Research Centre on various aspects of optical fibre manufacture, testing and reliability. In 1989 he joined the Future Submerged Systems Group at BTRL and is currently involved in assessing fibre for submarine systems.

John Wright was born in London and read Natural Sciences at the University of Cambridge, receiving his degree in 1970. Subsequently he worked at the Cavendish Laboratory and at Imperial College on infra-red emission studies of the atmosphere. In 1974, he joined the optical communications division of British Telecom Research Laboratories (then Post Office Research Centre) where he has worked on many aspects of fibre characterisation and waveguide propagation theory. He currently heads a group with responsibility for future submarine systems.

Tony Gould gradu[illegible] from Leeds University in 1972 with a B.Sc. in Mech[illegible]al Engineering. That year he joined British Telecom working on the theoretical aspects of coaxial, and later optical-fibre, submarine cable design. In 1984, he assumed responsibility for all aspects of optical-fibre submarine cable, jointing, terminations and associated technology.

WILL A REDUCED BEND LOSS SENSITIVITY AFFECT THE LIFETIME OF OPTICAL FIBER?

Torbjörn Svensson
Swedish Telecom
Technology Department
Material Laboratory
S-123 86 Farsta Sweden

Abstract

The strive for low transmission losses in communication systems based on optical fibers has lead to fibers which are quite insensitive to bending losses caused by mechanisms as radiation loss and transition loss. Thus, bending of the fiber down to small diameters will not have a disastrous influence on the transmission of light. However, the lack of readily observable losses also implies that local deformation of the fiber sometimes will pass the OTDR check of the installed cable. This fact might imply a danger to the system, since the long-time durability relies upon the fiber strength, which will be degraded by permanent stress on fiber bends. This paper may serve as a guidance to the determination of the risk for long-time failure in strongly deformed parts of a cable, where the attenuation caused by fiber bends is on the limit of what can be detected by OTDR (optical time domain reflectometer) measurements.

Introduction

The design and performance of transmission system based on optical fibers are strongly dependent on the magnitude of transmission losses, and also the long time strength of the fiber. Today, the attenuation caused by intrinsic absorption has come close to the theoretical limits, about 0.3 dB/km at 1300 nm and 0.17 dB/km at 1550 nm wavelength in a silica based optical fiber. The minimum strength of optical fiber is ensured by the screen test, the strain of which is steadily increasing. A screen test strain between 0.7% and 1.0% is readily applied without excessive losses of the yield at fiber drawing. The knowledge of making good fiber is thereby well established.

However, another important cause of transmission losses is due to bend losses. Large losses are unwanted, of course, but the bend loss may also be useful as an indicator of, equally unwanted, deformation of the fiber, which degrades its long-time strength. The design of fibers with suitable bending sensitivity is not readily manageable without excessive understanding, due to a large number of optical and geometrical variables[1]. A good portion of knowledge is also required to define the limits of allowed stress on fiber. This is based on environment-dependent fatigue of the glass fiber, and, in some cases, on the flaw distribution along the fiber[2]. It is the author's hope, that this paper will be a short path to a quantitative understanding of the bend losses and the mechanical lifetime of optical fibres.

Bend losses

The total bend loss is assumed to be composed by pure bend loss and transition loss. Both the pure bend loss and the transition loss increase when longer operating wavelengths are used. According to the name, small bend radii also imply large losses. The pure bend loss is caused by radiation losses along the bent fiber. The pure bend loss depends negatively on the core radius (and the mode field diameter), i.e smaller core radii imply larger losses. This type of loss dominates a carefully performed wrapping test of optical fibers.

Transition loss occurs at changes of the curvature of the fiber. The transition loss does not lose its power as rapidly with larger bend radii as does the pure bend loss. Thus, it dominates the bend losses in fibers with varying, large bend radii. Contrary to the pure bend loss, the transition loss depends positively on the core radius, i.e larger core radii imply larger transition losses.

The transition loss may be important at short wavelengths in tests of optical fibers, where surface roughness plays an important role, due to the frequent occurence of changes of curvature. The importance of transition loss caused by the stress

inducing fiber bends regarded in the following is limited, however.

Loss equations

Some useful expressions for estimating bend losses of different origins in step-index fibers will be briefly reviewed below. The attenuation caused by pure bend loss, α_b, in a step-index fiber bent to a *constant radius* R_0 has been shown to equal[3]

$$\alpha_b = \frac{A_c}{\sqrt{R_0}} \exp(-D \cdot R_0) \quad [dB/m] \qquad ...(1)$$

$$\text{where } D = 0.852 \frac{n_2 \Delta^{3/2}}{\lambda} (2.748 - 0.996 \frac{\lambda}{\lambda_c})^3 \quad [1/m]$$

$$\text{and } A_c = \frac{30 \cdot (n_1 - n_2)^{1/4}}{\sqrt{\lambda}} (\frac{\lambda_c}{\lambda})^{3/2} \quad [dB \cdot m^{1/2}]$$

The expressions for D and A_c are valid for $1 < \frac{\lambda}{\lambda_c} < 2$.

The relative refractive index $\Delta = (n_1 - n_2)/n_2$, the refractive indices in core and cladding are n_1 and n_2, and the vacuum wavelength is λ [m]. The radius of the core and the bend radius are a [m] and R_0 [m], respectively. The core radius and the refractive indices determine the theoretical cut-off wavelength, which for the LP_{11} mode is $\lambda_c = \frac{2\pi \cdot a}{2.405} \cdot \sqrt{n_1^2 - n_2^2}$

For *randomized bends* has also been shown, that the pure bend loss may be described by

$$<\alpha_b> [dB/m] =$$

$$A_c \sqrt{\pi D} \left(1 + \frac{1}{2 \cdot \sqrt{D \cdot <r>}}\right) \cdot \exp\left(-2 \cdot \sqrt{D \cdot <r>}\right) \qquad ...(2)$$

where $<r>$, in [m], is the average screw radius which depend on available space and compressive strain in the fiber.

Attenuation caused by transition losses, α_t, only occurs in splice-free fiber when there are changes of the curvature along the fiber. Such changes occur, when cooling a coated fiber, due to contraction of the coating. It also occurs at cooling a slotted core, or a loose tube, surrounding the fiber. The contractive forces give the fiber roughly the shape of a screw. The mean bend radius, $<r>$, of the screw is determined by the compressive strain, ε, along the fiber ($\varepsilon = -dl/l$, where dl is the length increment of the fiber length l at tension), and the available space for lateral movements of the fiber. In a loose tube- or a slotted core cable the allowed space for displacement of the fiber, is the radius, r_s, of a straight tube or slot with an assumedly circular cross section.

For energetic reasons, one will find the relation $<r> \approx <r_s>/(2 \cdot \varepsilon)$. The magnitude of the compressive strain ε depends on an eventual fiber excess, and the different thermal expansion coefficients in the materials involved, and is easily calculated as a function of temperature. Also needed is an empirically determined coefficient, η, which depends on the strain confinement on the fiber. For a nylon coated fiber, $\eta \approx 1.5$, and for a fiber loosely enclosed in a tube, $\eta \approx 1.0$. From this, the transition loss can be described by[3]

$$<\alpha_t> = \frac{4.343}{4} \frac{\varepsilon^{2+\eta}}{(<r_s>)^3} (k_0 n_1)^4 \cdot w_0^6 \quad [dB/m] \qquad ...(3)$$

where w_0 is the mode field radius (or "spot size"),

$w_0 = a \cdot [0.65 + 0.434 \cdot (\frac{\lambda_c}{\lambda})^{3/2} + 0.01496 \cdot (\frac{\lambda_c}{\lambda})^6]$, and $k_0 = \frac{2\pi}{\lambda}$.

The mode field radius w_0, the slot radius r_s, and the wavelength λ are all in [m].

To estimate the thermally induced total bend losses of a fiber in a cable (or just a coated fiber) the pure bend loss and the transition loss according to the equations (2) and (3) are added:

$$<\alpha_{tot}> = <\alpha_b> + <\alpha_t> =$$

$$A_c \sqrt{\pi D} \left(1 + \frac{1}{2 \cdot \sqrt{D \cdot <r>}}\right) \cdot \exp\left(-2 \cdot \sqrt{D \cdot <r>}\right)$$

$$\frac{4.343}{4} \frac{\varepsilon^{2+\eta}}{(<r_s>)^3} (k_0 n_1)^4 \cdot w_0^6 \quad [dB/m] \qquad ...(4)$$

In the above formula, the effective value of ε depends on cable design, materials and temperature.

Local bends

At an OTDR check of an installed cable, points of severe bending of the fiber may be observed as local attenuation. When a maximal risk for failure is to be estimated, it is sufficient to consider the attenuation being caused by pure bend loss only. Therefore, equation (1) makes reasonable account for the observable bend attenuation. From this equation, and the observed attenuation, the bend radius and the corresponding failure risk can be estimated.

Accidental bending to small diameters may occur at strongly deformed parts of a cable, e.g at unexpected displacements of rocky ground, in tight indoor installations, etc. Since bends of

this origin probably will be quite sparsely distributed along a cable, there is just a small probability for them to coincide with the fragile parts of the fiber, which have survived the screen test. Thus, this hazard is different from the threat of permanent, long-distance stresses that may be built-in during installation.

Using a fiber with optimal strength and bending sensitivity, it should be possible to localize the deformed part of the cable by OTDR, and release the strain before any fracture occurs. In this way the expenses for repair can be saved.

Fiber strain in bends

Some simple geometry shows that the maximal tensile strain ε in an optical fiber with the diameter ϕ_g of the glass and stress-free wrapped on a cylinder with a diameter 2·R equals

$$\varepsilon = \ln\left(\frac{1}{1-\phi_g/(2\cdot R)}\right)$$

Assuming that $\phi_g/(2R) << 1$, a Taylor transformation simplifies the expression $\varepsilon \approx \phi_g/(2\cdot R)$. When the bend diameter is much larger than the diameter of the fiber, one can write

$$\varepsilon \approx \phi_g/\phi_b \qquad ...(5)$$

where ϕ_b is the bend diameter of the glass fiber. For a coated fiber, the value of ϕ_b is slightly larger than the diameter 2·R of the cylinder on which the fiber is wrapped.

Applying equation (5), using the dimensions of a singel-mode fiber, ϕ_g = 125 µm, and a wrapping diameter, ϕ_b = 20 mm, yields a maximal strain equal to ε = 0.0062, i.e 0.62%. For an assumedly bend-sensitive fiber, a singel turn of this diameter may imply an attenuation of 0.1 dB, which is near the limit of what can be detected by usual OTDR instruments. If one compare the strain in this fiber bend with the strain applied in ordinary screen tests, about 0.7%, a conclusion will be that for[illegible] a hardly-detectable bend implies an obvious risk [illegible]acture, at first sight.

Lifetime estimation

There are two ways to estimate the lifetime of stressed optical fiber, which are described in Swedish Telecom Documents no 1521-A103 and 1521-A104[4,5]. In short, one of the methods is based on the failure frequency statistics at fiber drawing, which can be related to the expected failure frequency at long-time static load of the fiber. The other method is based on complete knowledge of the fatigue parameters, which enables the estimation of an absolute minimum risk for failure.

In this paper, the lifetime will be estimated using the latter, inert strength technique. The instrumental requirements are described in the litterature[2]. This technique is used when no risk for failure is allowed, irrespective of the length of fiber. For this purpose, the most relevant part of the document 1521-A104 is recaptured below.

---

2 INERT STRENGTH TECHNIQUE

In case of expecting a failure-free operation at static (constant) load one is able to show that, provided the B-parameter is known, the minimum lifetime t_{min} for an unlimited length of fibre is given by the equation

$$t_{min} = B\cdot \frac{\sigma_p^{n-2}}{\sigma_s^{n}}$$

where σ_s is the static stress, σ_p is the proof- or screen stress, n is the stress corrosion susceptibility parameter (or stress corrosion factor) and B is the inert strength factor. The proof stress is related to the proof strain ε_p by Young's modulus E for the glass due to the expression $\sigma_p = E\cdot\varepsilon_p$. The inert strength factor B and the stress corrosion factor n are evaluated from a plot of the logarithm of the median strength σ of the fibres versus the logarithm of the stress rate $d\sigma/dt$ at a series of tensile tests of the fibers.

According to the formula in the testing instructions above, the minimal time-to-fracture t_{min} at a static stress σ_s on a fiber with a minimum initial strength σ_p can be calculated when the fatigue parameters B and n are known. By dividing the stresses σ_s och σ_p with the Young's modulus E the stress can be substituted by strain, i.e ε_s och ε_p. Thus, the formula will be written

$$t_{min} = \frac{B}{E^2}\cdot\frac{\varepsilon_p^{n-2}}{\varepsilon_s^{n}} \qquad ...(6)$$

The well-known equation for fiber fatigue at tensile test;

$$\sigma^{n-2} = \sigma_i^{n-2} - \frac{\sigma^{n+1}}{B\cdot(n+1)\cdot d\sigma/dt} \qquad ...(7)$$

can be used to evaluate the fatigue parameters B and n from a series of tensile tests at constant stress rate, $d\sigma/dt$. This is done by fitting to the measured average tensile strength the theoretical

strength, σ, over a wide range including very high values on the stress rate. The initial, inert, strength σ_i will be degraded by the currently applied stress. The slower the tensile speed, the worse will be the degradation of the strength because more time is available for crack propagation[2].

Some examples of fitting the equation (7) to the tensile strength data on optical fibers are shown in the figure below;

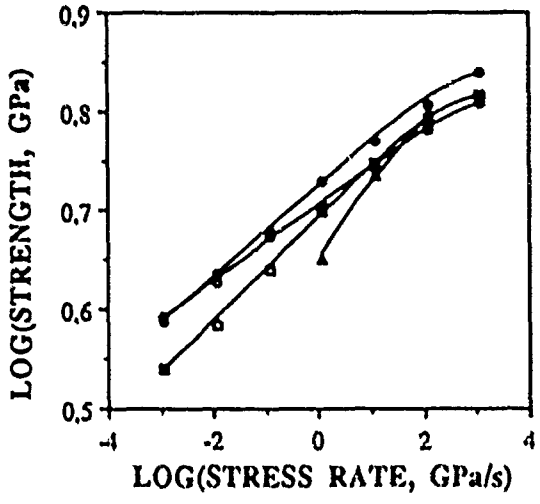

Figure 1. Strength of singel-mode fibers from different vendors. Measured values (symbols) and theoretical curves.

The fibers tested due to Figure 1 are all silica-based single-mode fibers, but having different coatings. Parameters corresponding to the curves in Figure 1 are shown in Table 1 below;

Fiber	σ_i	B	n
	GPa	$(GPa)^2 \cdot s$	
A	7.0	0.040	20.5
B	6.6	0.0115	24.9
C	6.7	0.050	18.0
D	6.62	0.185	11.35

23°C, 55%RH, 500 mm fully loaded length

Table 1. Fatigue parameters for single-mode silica fibers.

The temperature and humidity at conditioning and testing were 23 °C and 50% RH. For each vendor's fiber, A to D, a series of tensile tests were made on 30 samples at each tensile speed. The calculation of σ_i and B was based on the measured median fracture stresses and equation (7), assuming that E= 70 GPa.

Obviously, the coating properties influence the strength of the glass, so when making a lifetime estimation on a certain fiber, one should not rely upon fatigue properties of different optical fibers.

Limited length

Because of the limited length involved in the local bends, the risk for stress-induced fatigue and fracture should be based on the average strength of short lengths of fiber, rather than the screening strength. Normally, all fibers have a substantial strength as measured on short-length samples (see Table 1). They also have a narrow strength distribution. For the high-strength mode typical for 500 mm samples, the weibull modulus is often better than 80 (corresponding to 80% chance that the strength of an arbitrary sample is within ±2% from the expected mean value). The small number of bends along a cable line, and the extension of each bend, a few centimeters in a multi-fiber cable, makes a negligible chance for an abnormally weak point to coincide with any of the local bends.

Owing to the above arguments, the lifetime of the bent fiber can be calculated from equation (6) if the screen strain is replaced by $\varepsilon_p = \sigma_i/E$. The static strain, ε_s, induced by bending is given by equation (5). Combining all expressions yields the allowed bend diameter, ϕ_b, for the expected lifetime, t_{exp}, of the bend,

$$\phi_b = \phi_g \cdot \left[\frac{t_{exp} \cdot E^2}{B \cdot (\sigma_i/E)^{n-2}}\right]^{1/n} \qquad ..(8)$$

Inserting the values for a typical fiber, C in Table 1, yields an allowed minimum bend diameter of 6.1 mm, for an expected lifetime of 40 years. For the fibers A to D the corresponding values are given in Table 2.

A	B	C	D
4.91 mm	4.28 mm	6.10 mm	13.6 mm

23°C, 55%RH, a limited number of bends

Table 2 Minimum bend diameter at 40 years failure-free service

A priori, the bending sensitivity of the fiber should be such, that one turn, or a part hereof, with minimum bend diameter

above, should respond with an attenuation that is possible to detect with an OTDR instrument. A larger bending sensitivity than this, simplifies the use of an OTDR for bend localization. In fact, commercial single-mode fibers usually are quite bend sensitive, their values of detectable bend diameter at 1550 nm wavelength may range from 25 mm to 60 mm.

Of course, the detectable bend radius of a certain fiber can be readily measured, but adjusting the sensitivity of the fiber is not an easy matter. The refractive index of the core and the cladding, and the core radius are probably the most suitable parameters for adjustments, but the refractive index profile is also important. For step-index single-mode fibers the required values on core radius and refactive index are available through equation (1). Designing a more bend-sensitive fiber by decreasing the core radius may partly compensate the increase of the total loss by reducing the transition sensitivity due to equation (4).

Improvements

The process of fiber drawing offers few possibilities to further improve the maximal strength of silica based optical fibers, since an improvement of the long-length fiber strength by a substantially increased screen strain also degrades the maximal strength (of short-length fibers). The fatigue properties may still be improved by elaborate coatings, but have to compete with requirements on e.g strippability for easy splicing of the fibers. More sensitive OTDR instruments may be expected in a future, but probably the presently available instruments will be sufficient for detecting bends.

As the OTDR-detectable bend diameter for many available fibers substantially exceeds the minimum allowed bend diameter for 40 years failure-free operation, there is still room for reducing the bend loss sensitivity, without affecting the lifetime of optical fiber.

Conclusion

For fibers with good fatigue properties, the critical diameter for excessive fatigue in fiber bends is so small, that probably it will "never" appear in a carefully installed armoured or duct cable. However, the topic is still interesting for special cables, installations and low-grade fiber where the fiber's deformation is extreme or its fatigue properties for various reasons cannot meet usual requirements. The superior means to avoid future problems with fiber bends are a suitable design of the fiber, in order to achieve an optimal bending sensitivity, and a cable design which can resist local deformation without straining the fibers.

References

1. E.-G. Neumann (ed.), *Single-Mode Fibers, Fundamentals*, Springer-Verlag, ISBN 3-540-18745-6. (1988)
2. T. Svensson, "High Strain-Rate Testing of Optical Fibers", *Proc of the 37th IWCS symposium*, Reno, USA, nov 15-17 1988, p 217-24
3. S. Zhou et al., "Transmission loss in deformed optical Fibers", *Televerket Rapport Plm 88 177* (1988), a shortened version published in *Tele* (English ed.) 2/88 p17-26 (1988)
4. "Lifetime Estimation of Optical Fibre, Failure Frequency Technique", *Televerket Testing Instructions 1521-A103 Ue* (1988)
5. "Lifetime Estimation of Optical Fibre, Inert Strength Technique", *Televerket Testing Instructions 1521-A104 Ue* (1988)

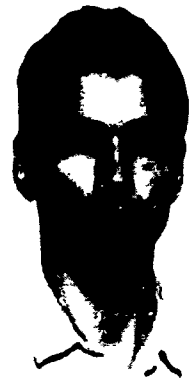

Torbjörn Svensson received his M.Sc. degree from the Royal Institute of Technology, Stockholm, Sweden in 1977.
He joined the Dept of Physical Metallurgy at the RIT where he worked on mechanisms of plastic deformation of solids. In 1979 he joined the Dept of Materials at the National Defence Research Institute of Sweden, where he studied the influence of shock wave propagation on material properties, and developed instruments for high strain rate testing of materials. In 1985 he joined the Material Laboratory at the Swedish Telecom Technology Dept, where he is engaged in quality assurance and development of methods for testing fibers and cables.

AUTHORS INDEX

Name	Page
Aberson, J. A.	564
Aida, F.	318
Akasaka, N.	295
Akers, F. I.	188
Alameel, G. A.	564
Amano, T.	76
Anderson, G. B.	500
Anderson, T. W.	675
Anderson, W. T.	611
Arakawa, K.	88
Asano, Y.	205
Beck, W. B.	665
Becker, J. A.	212
Beltz, L.	123
Bensel, W. H.	149
Bergman, L. A.	658
Bernard, W.	233, 402
Bhattacharyya, A.	306
Bhowmick, A. K.	306
Biswas, D.	634
Bjerkan, L.	526
Blanco, C.	6
Blee, J. J.	689
Boinet, JP.	132
Bonicel, JP.	326
Bow, K. E.	427
Bucaro, J.	179
Buch, R. R.	542
Busch, W. F.	427
Camara, S.	6
Cannell, G. J.	518
Chaffee, R. G.	542
Chan, M. G.	98
Chang, C. T.	357
Chang, T.-C.	475
Chein, C. K.	509
Chiu, W.-J.	274
Clarkin, J.P.	638
Cobb, G.	149
Conner, M. E.	408
Cortines, C. G.	6
Couvrie, G.	326
Dandridge, A.	179
Darden, B. V.	648
De, P. P.	306
DeBruycker, E.	513
Dennis, W. E.	542
Desroches, L.	27
Deusser, P.	212
DeVeau, G. F.	564
de Vecchis, M.	132, 326
DeVito, A.	675
Dixit, M.	149
Drouet, D.	94
Dye, K. S.	98
Effenberger, J. A.	434
Eickholt, J.	120
Eide, J.	672
Ekroth, C.-G.	486
Esposito, E.	56
Eutin, W.	212
Fedor, A.	183
Felske, N. E.	505
Ferguson, D. A.	94
Finzel, L.	390
Fluevog, J. B.	162, 648
Fukui, K.	38
Fukuma, M.	205
Giebel, W.	597
Girbig, R.	480
Gould, C. A.	696
Grant, S.	233
Grant, S. C.	402
Guilbert, P. A.	27
Haag, H. G.	575
Haber, J. B.	149
Haibara, T.	225
Halloran, F.	658
Halvarsson, S.	486
Hardwirk, N. E., III	689
Hartmayer, R.	658
Hasegawa, S.	76
Hassett, S. L.	408
Hasz, C. H.	199
Hauff, M. T.	583
Hawkins, R. E.	644
Hayakawa, T.	155
Hayashi, K.	69
Heckmann, S.	374
Heier, M.	390
Heinlein, W. E.	583
Hershkowitz, E. E.	556
Hickman, T. R.	179
Hille, R. E.	665
Hirao, H.	218
Hiramatsu, H.	463
Hodge, M. H.	638
Hoffart, M.	480
Hög, G.	575
Hopland, S.	526, 684
Hore, L.	46
Horima, H.	76, 251, 295, 331, 338
Hosokawa, E.	318
Hosoya, H.	218
Hotchkiss, L. C.	689
Hsu, H.	172
Huang, Y. J.	357
Huber, J. C.	420
Hulbert, P.	64
Hwang, W.-K.	274
Igarashi, H.	251, 338
Ikeya, H.	88
Inoue, H.	111
Ishi, N.	463
Ishida, H.	444
Ishikawa, K.	251
Ishikawa, M.	549
Ishizaki, N.	38

Name	Page
Ito, K.	318
Ito, Y.	549
Iwano, S.	492
Jackson, K. W.	569
James, S. M.	94
Johnson, A. J.	675
Kakii, T.	444
Kalomiris, V.	172
Kalomiris, V. E.	648
Kanayama, K.	492
Kathiresan, K.	162, 648
Katsuyama, Y.	603
Kaufman, S.	301
Kawabata, S.	549
Kawase, M.	225
Kawazoe, H.	456
Keith, R. H.	422
Key, P.	199
Khan, S. A.	556
Kihara, Y.	456
Kikuchi, K.	344
Kikuchi, Y.	240
Kobayashi, H.	191
Kobayashi, K.	240
Koerber, K. G.	434
Komiyama, K.	591
Komura, K.	438
Konno, S.	344
Kouteynikoff, P.	326
Kuck, V. J.	98
Kurki, J.	380
Kurokawa, M.	155
Kurosawa, A.	251
Kuwata, K.	338
Lagakos, N.	179
Lai, T. S.	357
LaTorra, M. N.	434
LeFevre, B.	648
Leino, E.	380
Leonard, T.	672
Lin, J.-C.	475
Liu, Y.	475
Loan, L. D.	98
Lochkovic, G. A.	569
Luh, G.-F.	274
Lupton, E. C.	434
MacGregor, T.	141
Maeda, K.	469
Martinez, J.	658
Masuda, Y.	69
Matsuda, Y.	438
Matsumoto, M.	225
Matsuno, S.	331
McCarter, J.	141
McKiterick, M.	64
Meisenheimer, H.	351
Menze, B.	368
Mikami, M.	469
Misono, M.	240
Misono, N.	155
Miyazaki, M.	155
Miyazima, Y.	603
Mogi, A.	155
Monroe, C. M.	542
Moratzky, M.	583
Mori, A.	21
Morikawa, G.	344
Morrison, S.	84
Mueller, C.	672
Mukherjee, B.	306
Nagai, K.	463
Nagase, R.	492
Nakamura, A.	21
Nakano, K.	492
Narcisco, R.	136
Nesset, E.	526
Nicholson, G.	141
Niijima, M.	591
Niikura, K.	155, 251, 295, 331
Nilsson, E.	486
Oehler, A.	583
Ogata, K.	251, 331, 338
Ohira, S.	251
Ohta, T.	456
Okada, M.	331
Okada, N.	155, 240
Okagawa, S.	469
Oksanen, L.	380
Olszewski, J.	627
Ona, A.	344
Osaka, K.	205
Parris, D. R.	105
Pasturczyk, Z.	623
Patel, P. D.	569
Pearsall, M. L.	569
Pegge, C. S.	246
Peng, H. K.	357
Pepe, R. C.	259
Petisce, J. R.	569
Petriello, J.	434
Philen, D. L.	689
Phoenix, A.	450
Pikula, D. G.	427
Pinyan, J.	513
Plasse, M.	27
Poulsen, J.	259
Räsänen, T.	380
Read, M. R.	533
Rebers, K.	395
Rees, D.	450
Riech, V.	374
Roberts, J. L. L.	450
Rossi, R.	627
Rozental, S.	141
Russell, J. N.	518
Ryuto, M.	344
Saito, A.	331, 338
Saito, K.	444
Sanghi, L. K.	306
Sano, H.	69
Santos, F.	6
Saravanos, C.	84, 623
Sasatani, Y.	21
Sato, N.	240

Name	Page
Sato, T.	438
Sawada, H.	76
Sawano, H.	240
Scadding, P. O.	665
Schilling, F. C.	98
Schneider, J. M.	212
Schulte, J.	368, 583
Schuster, R.	64
Scott, J. M.	696
Semple, G. J.	141
Sen, A.	306
Sentsui, S.	469, 591
Shaikhzadeh, F.	38
Sherrets, L.	162
Shimirak, G.	513
Shimizu, M.	191
Shimizu, S.	438
Shishido, T.	338
Sigematsu, T.	456
Sikora, E. S. R.	696
Skutnik, B. J.	638
Smith, B.	141
Smith, R. J.	505
Souza, J. C.	38
Spedding, S. T.	246
Stieb, W.	583
Stormbom, L.	380
Stueflotten, S.	526
Sugita, E.	492
Summers, A. T.	450
Sutton, P. A.	450
Suzuki, H.	240
Suzuki, S.	444
Suzuki, Y.	549
Svensson, T.	705
Takaki, S.	549
Takenaka, K.	21
Tamamoto, Y.	318
Tanaka, S.	69
Tatat, O.	326
Terasawa, Y.	69
Thambythurai, G.	246
Thomas, W. W.	246
Togo, S.	218
Toler, R. J.	509
Tzeng, G. T.	357
Ueda, S.	21
Varachi, J. P.	611
Vergez, C.	132
Wagman, R.	408
Walker, D. J.	246
Watanabe, I.	191
Watanabe, T.	205
Wei, T.	199
Wenski, W.	368
Wieczorek, C. J.	611
Wilson, T. E.	188
Wong, B.	623
Wong, D.	136
Worthington, P.	518
Wright, J. V.	696
Wu, M.-J.	274
Yamanishi, T.	295
Yamashita, K.	344
Yasinski, K.	564
Yoki, K.	21
Yokosuka, H.	218
Yoshida, K.	88
Yoshida, S.	318
Yoshizawa, N.	603
Yuce, H. H.	199, 611
Zamzow, P. E.	575
Zell, W.	212

IWCS

International Wire & Cable Symposium

SPONSORED BY U.S. ARMY COMMUNICATIONS-ELECTRONICS COMMAND (CECOM)
FORT MONMOUTH, NEW JERSEY
13, 14 and 15 November 1990
Bally's Reno Hotel, Reno, Nevada

Please provide a 300-500 word abstract (25 copies) of proposed technical paper on such subjects as design, application, materials, and manufacturing of communications and electronics wire and cable of interest to the commercial and military electronics industries. Such offers should be submitted no later than 15 March 1990 to the Headquarters, US Army Communications-Electronics Command, ATTN: AMSEL-RD-C3-PB, Fort Monmouth, New Jersey 17703-5202.

TITLE: _____

AUTHORS: _____

COMPANY: _____

ADDRESS: _____

AUTHOR(S): _____

CONTACT FOR CORRESPONDENCE: _____

ADDRESS AND TELEPHONE: _____

_____

I. PAPER TITLE: _____

_____

II. BACKGROUND (Why was work undertaken?):

III. PRIMARY CONCLUSION OR RESULT:

IV. DESCRIBE THE NOVELTY AND HOW THIS WORK ADVANCES THEORY OR TECHNOLOGY:

V. 300-500 WORD COMPREHENSIVE SUMMARY, INCLUDING METHODOLOGY IN REACHING CONCLUSION OR RESULT:

Fold here

Stamp

Commander
US Army Communications-Electronics Command
Attn: AMSEL-RD-C³-PB
Fort Monmouth, NJ 07703-5202

Fold here